Laboratory Testing of Nonlinear Soil Properties: I & II

Donald G. Anderson
CH2M HILL
P.O. Box 91500
Bellevue, WA 98009-2050

Lifelines Research Program
Pacific Earthquake Engineering Research Center
University of California at Berkeley
December 2003

Abstract

A laboratory testing program involving 15 dual specimen direct simple shear (DSDSS) tests and 25 combined resonant column/cyclic torsional shear (RC/TS) tests was carried out on intact samples of soil collected as part of the ROSRINE (Resolution of Site Response Issues from the Northridge Earthquake) project. The DSDSS and combined RC/TS tests were conducted at the University of California at Los Angeles (UCLA) under the direction of Professor Mladen Vucetic and at the University of Texas at Austin (UT) under the direction of Professor Kenneth Stokoe, respectively. The purpose of these laboratory tests was to characterize the dynamic stiffness and damping properties of soils collected from a number of sites where ground motions were measured during the 1994 Northridge Earthquake. This summary report provides an overview of the results from the testing programs conducted at UCLA and UT. The summary includes limited comparisons of the results to field measurements of shear wave velocity and shear modulus, as well as comparisons between results obtained by DSDSS and combined RC/TS tests for seven sets of companion samples. The similarity of these results to existing soil models is also discussed. Complete documentation of the UCLA and UT testing programs is provided in attachments to this summary report.

Keywords: Modulus, damping, cyclic, ROSRINE

Acknowledgements

This work made use of the Earthquake Engineering Research Centers Shared Facilities supported by the National Science Foundation, under award number EEC-9701568 through the Pacific Earthquake Engineering Research Center. Any opinions, findings and conclusions or recommendations expressed in this material are those of the authors and do not necessarily reflect those of the National Science Foundation.

Funding for the laboratory testing program described in this summary report was provided through the Lifeline Research Program of the Pacific Earthquake Engineering Research Center. The sponsors of the Lifeline Research Program include the California Department of Transportation (Caltrans), the Pacific Gas & Electric Company (PG&E), the California Energy Commission (CEC), and the Pacific Earthquake Engineering Research (PEER) Center. In addition to direct funding, the project has been supported by extensive collaboration with the U.S. Geological Survey (USGS), the California Geological Survey (CGS – formerly called the California Division of Mines and Geology – CDMG), the Southern California Earthquake Center (SCEC), the University of California at Santa Barbara, the Nuclear Power Engineering Corporation (NUPEC) of Japan, and Kajima Corporation of Japan.

Table of Contents

Attachments

List of Figures

List of Tables

1. Introduction

This report summarizes the results of cyclic laboratory tests conducted on intact soil samples collected as part of the ROSRINE (Resolution of Site Response Issues from the Northridge Earthquake) field sampling and testing program. The cyclic tests were conducted to characterize the stiffness and damping properties of soils at a number of strong motion recording sites. Two methods of testing were used during the completion of the program: (1) dual specimen direct simple shear (DSDSS) tests, and (2) combined resonant column/cyclic torsional shear (RC/TS) tests. The DSDSS tests were conducted at the University of California at Los Angeles (UCLA) under the direction of Professor Mladen Vucetic, while the combined RC/TS tests were conducted at the University of Texas at Austin (UT) under the direction of Professor Kenneth Stokoe. Results of both cyclic testing programs are reviewed in this summary report. Complete documentation for each program, including detailed test results, is included in two companion reports that are attached to this summary report.

1.1 Purpose

The purpose of this testing program was to evaluate the shear modulus and material damping properties of intact soil samples at small to large shearing strains and from low to high confining pressures. The modulus and material damping information was of interest for several reasons:

- The information will assist in completing the characterization of sites where in situ shear wave velocities have been collected, and where site response calculations are planned as part of a post-Northridge earthquake ground response study;
- The modulus and damping properties will provide information for calibrating existing soil models used to estimate the stiffness and damping characteristics of soil; and

- Direct comparisons of shear modulus and material damping properties can be made for a limited number of companion specimens tested with DSDSS and RC/TS testing equipment.

The overall objective of the ROSRINE program is to improve the profession's ability to estimate ground response during seismic events. Previous phases of the ROSRINE program have involved cyclic laboratory tests and in situ shear wave velocity measurements at strong motion recording sites. The locations and characteristics of sites investigated to date can be found on the ROSRINE website (http://geoinfo.usc.edu/gees/rosrine/). As additional sites were added to the ROSRINE program and as the extent of previous ROSRINE laboratory testing programs was reviewed, particularly relative to material type and laboratory test conditions, the need for the additional testing described in this summary report was identified.

1.2 Scope of Work

The scope of work for this phase of the ROSRINE testing program involved the following activities:

- *Selection of samples from an inventory of samples collected as part of the ROSRINE program:* The sample selection process specifically focused on identifying high-quality samples that would fill in gaps from previous phases of the ROSRINE testing program or provide information where no information existed.
- *Distribution of selected samples to each university:* Selected samples were transported to UT and UCLA. In several cases samples were split between the two universities, so that testing could be conducted on similar soil samples at each institution.
- *Coordinating conduct of 15 DSDSS tests at UCLA and 25 combined RC/TS tests at UT:* As part of this effort, it was necessary to reach consensus on the soil unit weights, the coefficients of earth pressure at rest, and the groundwater table locations to use in computing the effective test pressures for each test setup.
- *Evaluating the results of each program and comparing them to each other where possible:* Although this was not the primary objective of the program, preliminary

comparisons of results were made to field velocity measurements, to a limited number of cases where companion soil samples were tested using the DSDSS and RC/TS test equipment, and to published modulus and damping models.

- *Presenting the results of the two testing programs:* This effort included preparing this summary report and posting the results of the laboratory testing programs on the ROSRINE website (http://geoinfo.usc.edu/gees/rosrine/), where all ROSRINE information is being presented.

The work described in this report was carried out between the Spring of 2001 and the Fall of 2003. Interim results of the laboratory testing were presented at quarterly progress meetings of the Lifeline Research Group of the Pacific Earthquake Engineering Research (PEER) Center, as the results became available.

1.3 Background

The ROSRINE program was initiated in the mid-1990s through joint funding from the National Science Foundation (NSF), the Electric Power Research Institute (EPRI), and the California Department of Transportation (Caltrans). Since the initial program, a number of other organizations have added to the funding for the project, including the Pacific Gas & Electric Company (PG&E) and the California Energy Commission (CEC). In addition to direct funding, the project has been supported by extensive collaboration with the U.S. Geological Survey (USGS), the California Geological Survey (CGS – formerly called the California Division of Mines and Geology – CDMG), the Pacific Earthquake Engineering Research (PEER) Center, the Southern California Earthquake Center (SCEC), the University of California at Santa Barbara, the Nuclear Power Engineering Corporation (NUPEC) of Japan, and Kajima Corporation of Japan.

The motivation for the ROSRINE program was that a large number of accelerograph records were collected at the ground surface throughout the Los Angeles area during the 1994 Northridge earthquake. Many of these records were obtained at sites underlain by shallow-to-deep deposits of soil or soft rock. Under the levels of ground motion produced during the Northridge earthquake, it was anticipated that the soil and soft rock would have modified the ground motions as they propagated from bedrock to the ground surface through the inherent

nonlinearity of soil and soft rock. The characteristics of the source motion during the Northridge earthquake are reasonably well established by a number of records obtained on rock. With the availability of both the soil and rock records, an opportunity was available for evaluating the adequacy of current analytical methods used when estimating the effects of soil nonlinearity on wave propagation. This evaluation could be accomplished by characterizing the dynamic properties of soils at selected recording sites, conducting numerical analyses to estimate ground motions at the recording sites, and then evaluating the predicted versus measured ground motions. The key soil characteristics required for the numerical modeling were the low-strain amplitude shear wave velocity measured in situ and the manner in which soil stiffness (measured in terms of shear modulus) and material damping ratio varied with shearing strain amplitude.

The initial ROSRINE laboratory testing program involved collecting and testing soil and soft rock samples from seven strong motion recording sites located in the Los Angeles area. Shear wave velocities had been measured in situ for each of the sites. Thirty-five soil samples were tested to determine the variation in shear modulus and material damping with shearing strain amplitude. These tests were conducted at UCLA and UT using DSDSS and combined RC/TS test methods, respectively, at estimated in situ effective confining stresses. Depths of the samples ranged from near-surface to over 250 meters (m) below the ground surface. The product of this initial laboratory testing program was sets of shear modulus (G) and material damping (D) versus shearing strain amplitude (γ) curves and tabulations for each sample. Additionally, the effects of confining stress and frequency of cyclic loading were investigated for some samples. These results are posted on the ROSRINE website.

Subsequent phases of the ROSRINE program have resulted in additional site characterization efforts involving both in situ measurements and laboratory testing. A third cyclic testing method involving cyclic triaxial testing was added to the program. This program was conducted at the University of California at Berkeley (UCB) under the direction of Dr. Michael Riemer. Over 50 strong motion recording sites have now been characterized. The location of each of the sites, with the available data, can be found on the ROSRINE website.

The analytical phase of the ROSRINE program is still underway. Results of the numerical modeling effort will be used as a basis for improving engineering models currently being applied during site response analyses. These improvements include quantifying the uncertainties and biases introduced from the field and laboratory testing process, as well as the

uncertainties and biases associated with commonly used empirical soil models for representing the change in shear modulus and material damping with shearing strain amplitude.

1.4 Project Organization

The contract for the current phase of the ROSRINE test program was administered through the PEER Lifeline Research Program. This laboratory testing work is part of ***Topic 2 – Site Response*** within the PEER Lifeline Program. The title of the research effort is Task 2B01/2B02 – *Laboratory Testing of Nonlinear Soil Properties: I and II.* This program was originally referred to as the PEARL program, which is the acronym for Program of Earthquake-Applied Research for Lifelines.

The laboratory testing programs conducted for this project were led by two university professors: Dr. Mladen Vucetic at UCLA and Dr. Kenneth Stokoe at UT. Professors Vucetic and Stokoe were selected to conduct these tests because of their past experience on the ROSRINE program and, most importantly, their international recognition as being amongst the foremost laboratory testers of seismic soil properties. Professors Vucetic and Stokoe were assisted by research associates and graduate students from their respective academic institutions. Additional information about the testing facilities and support used by each institution can be found in Attachment B and Attachment C, which contain the reports prepared by each group.

Several other individuals served in key roles during the testing program:

- Dr. Clifford Roblee from Caltrans oversaw the coordination with previous phases of the ROSRINE program, including the identification of priority samples to test;
- Dr. Robert Nigbor from the University of Southern California (USC) was responsible for the drilling and sampling programs and for the downhole shear wave velocity measurements using the OYO P-S suspension logging device; and
- Dr. Michael Riemer of UCB served as the Lifeline Program Coordinator for the PEER Center.

Dr. Donald Anderson of CH2M HILL was the project manager for this project. Both UCLA and UT were subcontractors to CH2M HILL for the laboratory work, and CH2M HILL was contracted the PEER Center to provide the test information.

2. Laboratory Test Programs

The following paragraphs provide a summary of the test programs carried out at UCLA and UT. The summary describes the method used for selecting and distributing samples for testing and the basis of the unit weights and groundwater elevations used in effective confining pressure determinations. These discussions are followed by separate subsections for UCLA and UT summarizing information about the testing method, the assigned samples, and the test results for each program. Complete documentation for the UCLA and UT programs is provided in Attachments B and C to this summary report.

2.1 Sample Selection and Test Parameters

The initial step in the laboratory testing program involved identification of samples for testing and the determination of unit weights and groundwater locations at each of the strong motion recording sites of interest. The procedures for accomplishing these tasks are summarized in the following three subsections.

2.1.1 Sample inventory and storage

Samples were selected from a large inventory of samples that were available from drilling and sampling efforts carried out by GEOVision Geophysical Services of Corona, California and by the United States Geological Survey in Menlo Park, California, as part of the ROSRINE research program. Additional samples were also obtained from drilling and sampling operations that were carried out by Kajima/NUPEC, as part of a cooperative effort with the PEER Lifeline Research Program.

Sample were initially delivered to UCLA by Dr. Robert Nigbor of USC, who coordinated the field sampling program through GEOVision. The documentation for the samples included boring logs for each site, and the results of classification tests conducted in the laboratory. The boring logs and laboratory classification data can be found on the ROSRINE website. An inventory of the available samples is included in Attachment A to this summary report.

Samples were stored in UCLA's humidity room for the initial portion of the program. However, midway through the testing program, all samples were transported to UT when UCLA had to vacate their facilities for remodeling. A vehicle was used to transport the samples to UT. Cushioning material was used to protect the samples from excessive vibration during transport. All samples that have not been tested currently reside at UT.

2.1.2 Sample selection

When selecting samples for testing, consideration was given to the following constraints and test program goals:

- *Quality of Sample:* Samples that appeared to be of high quality were selected for possible testing. This requirement usually precluded testing of liner samples that were available from some of the sites, as these samples were considered to be too disturbed to meet the needs of this phase of the ROSRINE program.
- *Type of Material:* The existing database of cohesionless soils was relatively large, and therefore more focus was placed on testing fine-grained soils.
- *Available Data:* An effort was made to fill-in data gaps where obvious need existed. For example, if shear modulus and material damping ratio information was not available within a certain depth interval that appeared critical for ground response modeling, a specific effort was made to conduct either a DSDSS or a combined RC/TS test on samples from the depth interval.
- *Test Equipment Capabilities:* The equipment used by UCLA and UT had different test capabilities. For instance, the DSDSS device was capable of testing to shearing strains in excess of 5 percent, but it was limited to a confining stress that was equivalent to approximately 35 m in depth. Therefore DSDSS samples were selected from the upper 35 m of soil profile. The combined RC/TS device could test samples at very high confining stresses, but was more limited by the shearing strain amplitudes that could be applied.
- *Comparison of Results from Different Equipment:* Though of lower priority, comparisons between shear modulus and damping ratio data from the DSDSS and RC/TS test equipment were of interest. Several samples were split so that testing could be conducted with both devices on essentially the same sample.

Using the above criteria and testing program goals, 15 samples were selected for testing at UCLA, and 25 samples were selected for testing at UT by Drs. Clifford Roblee and Donald Anderson during a meeting at Caltrans in June of 2001.

2.1.3 Groundwater location and soil unit weights

The groundwater location at each site and the unit weights of soil were estimated for use in effective confining pressure calculations. These values are summarized in Table 2-1.

Table 2-1. Groundwater and Unit Weight Information

Location	Depth to Groundwater (m)	Overburden Pressure		Comments
		Depth Interval (m)	Total Unit Weight (kg/m^3)	
Meloland	2	0-bottom of hole	2003	Groundwater location based on P-wave velocity. Unit weight interpreted from UCLA tests.
Tarzana	18.3	0-12.2	1763	Groundwater location based on P-wave velocity. Unit weight interpreted from UCLA tests.
Lake Hughes	8.5	0-bottom of hole	1843	Groundwater location based on P-wave velocity. Unit weight estimated from soil type
Dayton	7.6	0-bottom of hole	1923	Groundwater location based on P-wave velocity. Unit weight estimated from soil type and summary of index tests.
Obregon Park	6.1	0-38.1	2003	Groundwater location based on P-wave velocity. Unit weight interpreted from UCLA lab tests.
Saturn	9.1	0-15.2	2163	Groundwater location based on P-wave velocity. Upper location may be perched on clay layer at 15.2 m below the ground surface. Unit weight interpreted from laboratory tests.
	25.9	15.2-bottom of hole	2003	

Location	Depth to Groundwater (m)	Overburden Pressure		Comments
		Depth Interval (m)	Total Unit Weight (kg/m^3)	
LA Bulk Mail	41.2	0-bottom of hole	1843	Groundwater location based on P-wave velocity. Unit weight estimated from soil type, water contents, and estimated saturation
Yermo	41.2	0-bottom of hole	2003	Groundwater location based on P-wave velocity. Unit weight estimated from soil type, water contents, and estimated saturation
Joshua Tree	>100.6	0-bottom of hole	2163	P-wave velocities < 1500 mps to bottom of hole. Unit weight estimated from soil type, water contents, and estimated saturation
Gilroy #3	10.7	0-24.4	1923	Groundwater location based on P-wave velocity. Unit weight estimated from soil type and summary of index tests.
		24.4-bottom of hole	2163	
Halls Valley	19.8	0-45.7	1923	Groundwater location based on P-wave velocity. Unit weight estimated from soil type and summary of index tests.
		45.7-bottom of hole	2163	

As noted in the comments column of Table 2-1, groundwater levels were estimated from the compressional (P-) wave velocities shown in velocity plots for each site. The P-wave velocity plots are presented on the ROSRINE website. This method of defining the top of the groundwater surface is approximate and can result in groundwater elevations that are too high in geologically old, fine-grained soils. In such soils capillarity can result in fully saturated conditions (and P-wave velocities equal to 1,500 meters per second – mps) above the true groundwater elevation.[1] In the absence of groundwater monitoring wells, the potential for this

[1] Capillarity can result in fully saturated conditions (B-values close to 1.0) many meters above the point of zero capillarity – where the phreatic surface occurs. As the degree of saturation approaches 100 percent, the P-wave velocity reaches 1,500 mps.

situation occurring could not be determined. However, the boring logs indicate that the soil profiles at many of the sites include interlayers of cohesionless soils, and it was reasoned that these would limit the capillary rise – making the P-wave velocity a reasonable method of determining the groundwater elevation. As will be pointed out later in this report, the potential for variations in the groundwater elevation should be considered during the use of the material damping data obtained from the DSDSS and combined RC/TS testing program.

Where P-wave velocities were questionable or did not reach 1,500 mps, depth of groundwater was inferred from information reported in the boring log for the site. The boring logs are also found on the ROSRINE website. Unit weights of samples were estimated on the basis of soil type and laboratory tests conducted on nearby samples.

2.2 UCLA Test Program

The UCLA test program involved 15 tests on intact, high-quality soil samples. Each sample was tested at the estimated in situ effective confining stress. Testing involved application of cycles of horizontal load to a platen located at one end of the test specimen, and this load resulted in repeated cycles of a predetermined level of shearing strain. The following three subsection provide summaries of the test method used by UCLA, the assigned samples, and the test results. Complete documentation of the UCLA test program, including results, can be found in Attachment B.

2.2.1 Test method

The UCLA tests were conducted with a dual-specimen, direct simple shear (DSDSS) test device. This device was designed and built by Professor Vucetic and Dr. Doroudian [Doroudian and Vucetic, 1995]. Two specimens are tested in parallel during each set of tests. Each sample is retained in a wire-reinforced membrane to limit lateral expansion of the test specimen under vertical load. The wire-reinforced membrane in combination with the vertical load is intended to re-create the in situ state of stress. The device has been specifically developed to allow testing from small shearing strains (e.g., less than 0.001 percent) to shearing strains greater than 5 percent.

If the degree of saturation drops below 100 percent (e.g., B-values less than 0.95), the P-wave velocity rapidly drops below 1,500 mps.

Test specimens had diameters of approximately 67 millimeters (mm) and heights of approximately 18 to 19 mm. The following test parameters were controlled during each test:

- *Confining Stress.* Each specimen was consolidated before cyclic loading under the estimated effective vertical stress.
- *Time of Confinement.* Samples were consolidated until the end of primary consolidation before cyclic testing.
- *Cyclic Shearing Strain Amplitude.* Cyclic shearing strains varied from about 0.0003 to 3.2 percent.
- *Number of Cycles of Load.* Approximately 7 cycles of controlled cyclic strain were applied during each load sequence.
- *Frequency of Loading.* The rate of loading ranged from 5 to 10 seconds (sec) per full cycle.

On all but Meloland S-2, Meloland S-3, and Meloland S-5 tests, some type of monotonic loading to failure was performed at the end of the test. For the monotonic tests failure was defined when no further increase in shearing resistance occurred with increases in shearing strain. The level of shearing strain at the completion of monotonic loading was typically 3 to 4 percent. Often a number of these high-strain cycles was applied to evaluate the degradation in stiffness with cycles of large-strain loading.

2.2.2 Assigned samples

The sample number, depth, and soil type tested by UCLA are summarized in Table 2-2. The type of soil was determined by UCLA by conducting classification tests on the test samples. Results of the classification tests are provided in Attachment B for each set of test results.

Table 2-2. Inventory of Samples Tested by UCLA

Site Location	Sample No.	Depth (m)	Soil Type
Meloland	S-2	5.5-6.1	ML
	S-3	8.5-9.1	CH
	S-5	18.0-18.6	CL
	S-7	29.9-30.5	CL

Site Location	Sample No.	Depth (m)	Soil Type
Obregon Park	P-5	15.2-16.2	CH
	P-7	21.3-22.3	ML
	P-9	27.4-28.4	CL
LA Bulk Mail	P-1	4.6-5.5	CL
	P-3	15.2-16.2	ML
Halls Valley	P-1	1.8-2.7	CL
	P-2	4.6-5.5	CL
	P-3	15.2-16.2	CH
Yermo	P-4	24.4-25.3	SM
Joshua Tree	P-3	12.2-13.1	SM-SC
Gilroy #3	P-1	4.6-5.5	CL

Notes:
P = Pitcher tube sample; S = Shelby tube sample.
Soil descriptions based on Unified Soil Classification System (USCS)

2.2.3 UCLA test results

Results of the test conducted by UCLA are presented in detail in Attachment B for each sample tested. Each set of results includes the following information:

- *Classification Data:* USCS classification, Atterberg limits, void ratio, degree of saturation, unit weight, and water content are tabulated for each sample. Plots are also provided showing results of grain-size analyses (e.g., sieve and hydrometer) and results of specific gravity tests.
- *Modulus and Damping Plots:* Individual plots show shearing stress and shearing strain for each cycle of load. Hysteresis loops showing shearing stress versus shearing strain for representative cycles at different levels of shearing strain are also given. These plots identify the secant shear modulus and the material damping ratio for the selected cycle of loading. Typically shear modulus and damping ratio values were determined to a shearing strain amplitude of 0.1 to 0.3 percent. For a few tests the modulus and damping ratio values were tabulated or shown to shearing strains of

2 to 3 percent. The normalized shear modulus and material damping ratio results are also compared to the Vucetic and Dobry [1991] soil model.

- *Tabulated Modulus and Damping Data:* Tabulations giving the shear modulus (G), the normalized shear modulus (G/G_{max}), and material damping ratio (D) are provided as a function of shearing strain amplitude (γ).
- *Monotonic Loading Results:* On most tests (i.e., all but Meloland S-2, Meloland S-3, and Meloland S-5) results from monotonic loading to failure conducted at the end of the test are given. For these tests failure was defined when no further increase in shearing resistance occurred with increases in shearing strain. The level of shearing strain at the completion of monotonic loading was typically 3 to 4 percent. Often a number of these high-strain cycles was applied to evaluate the degradation in stiffness with cycles of loading. Damping ratios were not determined for these tests.

The UCLA report presents results from each test specimen as a separate set of data.

2.3 UT Test Program

The UT test program involved 25 tests on intact, high quality soil samples. Each sample was tested at multiple confining stresses – typically ranging from 25 percent of the mean in situ effective stress to four times the mean in situ effective stress. Testing involved application of cycles of load using both resonant column and cyclic torsional shear testing methods to produce cyclic response at increasing levels of shearing strain. The following three subsection provide summaries of the test methods used at UT, the assigned samples, and the test results. Complete documentation of the UT test program, including results, can be found in Attachment C.

2.3.1 Test method

The UT tests were conducted with the combined resonant column/cyclic torsional shear (RC/TS) device. This type of testing device was designed by Professor Stokoe and his students at UT. The RC/TS device is used to apply torsional loading to the top of a cylindrical soil sample. Each sample is enclosed within a rubber membrane to enable application of an isotropic confining pressure to the sample. The device has been specifically developed to allow accurate testing from very small shearing strains (e.g., less than 0.001 percent) to shearing strains up to

approximately 0.5 percent (depending on the stiffness of the soil) at hydrostatic confining pressures as high as 3,500 kPa.

Test specimens had diameters of approximately 38 to 71 mm and nominal heights of twice the corresponding diameters. The following test parameters were controlled during each test:

- *Confining Stress.* Each specimen was tested at five isotropic confining pressures. These pressures ranged from 25 percent of the estimated mean effective confining pressure [$\sigma_m' = \sigma_v'(1 + 2k_o)/3$ where σ_m' is the mean isotropic confining stress, σ_v' is the vertical effective stress, and k_o is the lateral earth pressure coefficient] to four times the estimated mean confining stress.
- *Time of Confinement.* Time of confinement was at least 1,000 minutes (min) at each pressure.
- *Shearing Strain Amplitude.* Cyclic shearing strains varied from about 0.005 percent to about 0.1 percent.
- *Number of Cycles of Load.* Ten cycles of load were applied during torsional shear tests and approximately 1,000 for resonant column tests.
- *Frequency of Loading.* Cyclic torsional shear tests were conducted at 0.1 to 5 Hz; resonant column tests typically varied from 25 to 250 Hz.

2.3.2 Assigned samples

The sample number, depth, and soil type tested by UT are summarized in Table 2-3. Results of the classification tests are provided in Attachment C for each set of test results.

Table 2-3. Inventory of Samples Tested by UT

Site Location	Sample No.	Depth (m)	Soil Type
Tarzana	P-3	9.1-10.1	MH
	P-4	12.8-13.1	CH
Meloland	S-2	5.5-6.1	CH
	S-3	8.5-9.1	CH

Site Location	Sample No.	Depth (m)	Soil Type
	WS-1	36.0-36.6	CH
	WS-3	60.4-61.0	CH
	WS-4	79.0-79.6	CH
	WS-6	115.2-115.9	CL
	WS-7	133.5-134.1	CH
Obregon Park	P-8	30.5-31.4	CH
LA Bulk Mail	P-1	4.6-5.5	CL
	P-3	15.2-16.2	CL
	P-5	50.3-51.2	CL
LA Bulk Mail	P-6	62.5-63.4	SM
	P-7	80.8-81.7	SP
Halls Valley	P-1	1.8-2.7	CL
	P-3	15.2-16.2	CH
Yermo	P-6	61.0-61.9	SM
	P-7	80.8-81.7	SP
Joshua Tree	P-7	71.6-72.6	SP
	P-8	99.7-100.6	SW
Gilroy #3	P-4	54.9-55.8	CL
	P-5	108.2-109.1	ML
Saturn	P-4	30.5-31.4	CH
Lake Hughes	P-1	1.8-2.4	SW-SM

Notes:
P = Pitcher tube sample; S = Shelby tube sample; WS = wireline Shelby tube sample.
Soil descriptions based on Unified Soil Classification System (USCS).

2.3.3 UT test results

Results of the tests conducted at UT are presented in detail in Attachment C for each sample tested. Each set of results includes the following information:

- *Classification Data:* Tabulated information for each sample includes the USCS classification, water content, dry density, percent passing the No. 200 sieve, Atterberg limits, void ratio, assumed specific gravity, degree of saturation, and grain-size distribution.
- *Confining Pressure Plots:* Plots showing the effects of confining pressure on shear wave velocity, shear modulus, and material damping ratio at low shearing levels are presented. Comparisons have been made to show the confining pressure effects for plastic and nonplastic soils. For the plastic soils, results are separated into three confining pressure groups: i.e., low (~27 to 199 kPa), medium (~242 to 551 kPa), and high (~769 to 898 kPa). The variations of low-strain shear modulus and material damping with excitation frequency (i.e., resonant column versus cyclic torsion) are also provided for plastic and nonplastic soils.
- *Shear Modulus Versus Shearing Strain Plots:* Composite plots show the variation in shear modulus (G) and normalized shear modulus (G/G_{max}) with shearing strain amplitude (γ) from both the resonant column and cyclic torsional shear tests. For plastic soils the modulus and normalized shear modulus plots are further separated to show the effects of shearing strain amplitude at low, medium, and high confining pressures. Results of the resonant column and torsional shear testing are also compared to empirical models suggested by Seed et al. [1986], Vucetic and Dobry [1991], and Darendeli [2001].
- *Material Damping Versus Shearing Strain Plots:* Composite plots showing the variation of material damping ratio with shearing strain amplitude – similar to those described above for shear modulus and normalized shear modulus – are provided. Similar to the modulus plots, information is separated according to whether results are for plastic or nonplastic soils, and for plastic soils, whether the confining pressure was low, medium, or high. Comparisons are also shown for resonant column and cyclic torsional shear for the same samples and shearing strain levels. Results of the resonant column and torsional shear testing are also compared to empirical models suggested by Seed et al. [1986], Vucetic and Dobry [1991], and Darendeli [2001].

The results summarized above are supported within the UT report by separate appendices for each test specimen. The appendices show the variation in properties with time of confinement, isotropic confining pressure, shearing strain level, and frequency of loading. Tabulations of key data are also presented.

3. Evaluation of Results

Only a limited evaluation of the laboratory test results obtained by UCLA and UT is included in this summary report, as the primary intent of this phase of the ROSRINE laboratory testing program was to extend the database of ROSRINE test information, rather than to evaluate the specific laboratory test results. Each of the university researchers performed an analysis of their results. The reader is referred to the UCLA report in Attachment B and to Volume I of the UT report in Attachment C for these evaluations. Future evaluations are planned for the full ROSRINE database; however, this work will be conducted as a separate project. As noted in the background discussions, a large number of DSDSS, combined RC/TS, and cyclic triaxial tests were conducted during previous phases of the ROSRINE project, and these results also need to be brought into the final evaluation of the ROSRINE laboratory test results.

3.1 Comparisons to Field Velocities

A comparison was made between the shear wave velocities recorded during the field geophysical program conducted at the ROSRINE sites and those measured or computed from the laboratory tests conducted at UCLA and UT during this testing program. This comparison was made for two reasons. First, the ratio of laboratory-to-field velocity is assumed to give some indication of sample disturbance, and second, a procedure has been suggested recently for adjusting the shapes of the modulus and damping ratio versus shearing strain curves by the ratio of laboratory-to-field velocity.

With regard to the first reason given above, the comparison of field- and laboratory-derived shear wave velocities is assumed to be an indication of the disturbance that has occurred during the sampling process from a combination of effects, including:

- the process of drilling and sampling,
- the inevitable stress relief that occurs when the sample is removed from the earth,

- disturbance during setup of the sample in the laboratory test device, and
- boundary conditions imposed during the test, such as the choice and application of confining pressures.

Usually, the ratio of laboratory-to-field velocity is less than 1.0 and can range from 0.8 to less than 0.5. Samples of soil that are geologically older generally have a lower ratio than geologically young samples, and samples with a significant stress history, say from glacial overconsolidation, will often have a lower ratio.

Until recently, the ratio of laboratory-to-field velocity was of greater academic interest than practical, as the common method of adjusting for "disturbance" effects was to multiply the normalized shear modulus (G/G_{max}) curve from the laboratory test, or empirical relationship, by the shear modulus calculated from in situ shear wave velocity measurements. However, recently a modification to this normal procedure has been suggested by Drs. Robert Pyke and Clifford Roblee (personal communications, 2001), where the shear modulus and damping ratio curves for a location are adjusted by the ratio of laboratory derived shear wave velocity (V_{slab}) to field measurement (V_{sfield}). This adjustment is intended to account for the possible effects of disturbance on the shape of the G/G_{max} and damping ratio (D) versus shearing strain amplitude curves.

Figure 3-1 shows a plot of velocity ratio versus depth from the UCLA and UT test programs. The field velocity values for each site were obtained from the ROSRINE website. When selecting the field shear wave velocity, the velocity value at the closest depth to the sample tested was used. Velocity values above and below the selected field velocity were considered during the selection of the velocity to check for significant velocity variations. If a significant variation did occur, the average velocity within 1.5 to 3 m was used. The laboratory velocity was reported by UT, but the UCLA value had to be calculated based on the mass density of the soil.

Typical velocity ratios in Figure 3-1 range from values of approximately 1.0 to approximately 0.5 at the deepest depths. It appears that the velocity ratios for the UCLA tests in the upper 30 m are, on the average, somewhat lower than those obtained by UT, but the difference may not be particularly significant relative to some of the uncertainties in the methods used to determine and compare the velocities.

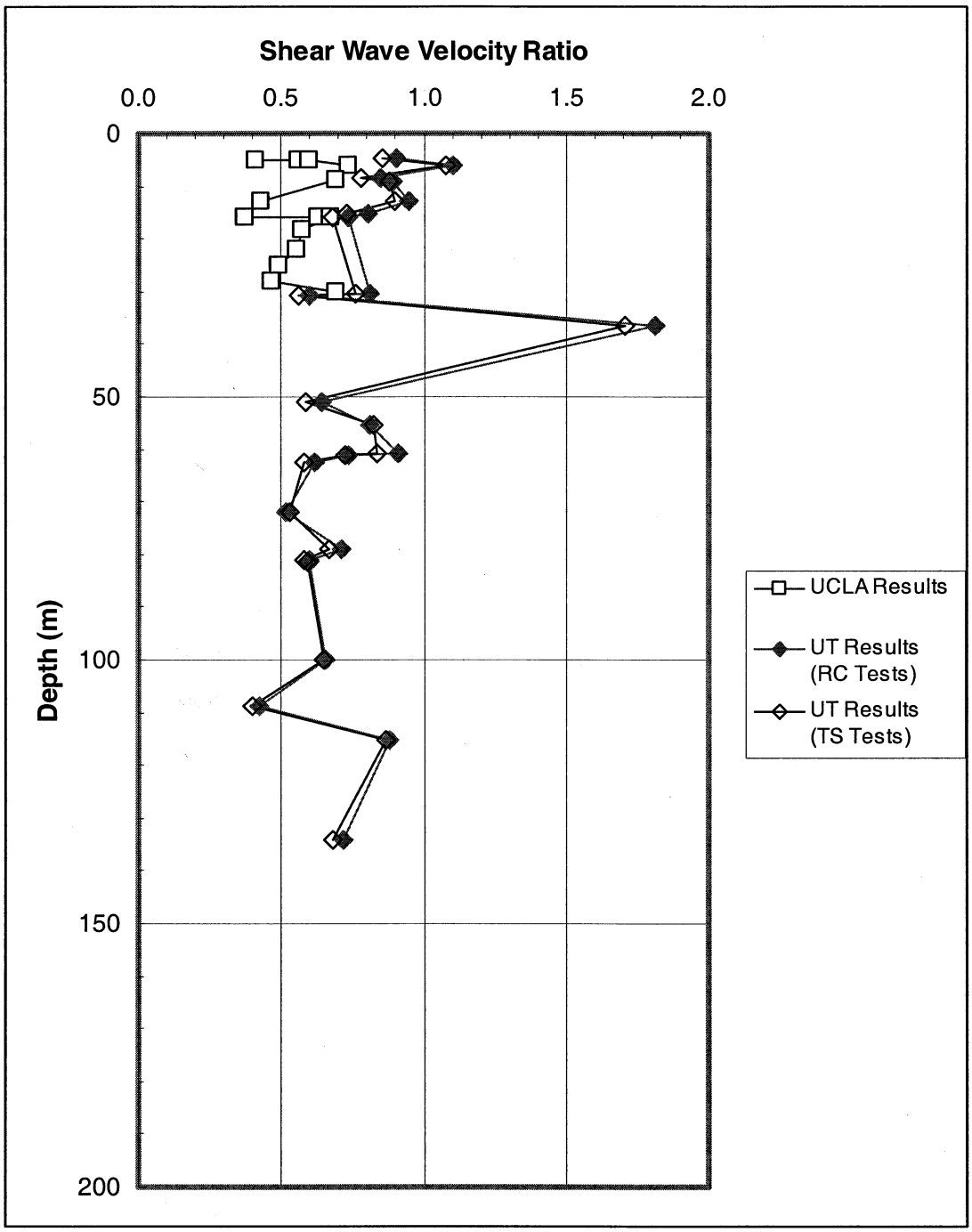

Fig. 3-1 **Comparison of In Situ and UT and UCLA Laboratory Measurements in terms of Velocity Ratio**

The sources of uncertainty in the velocity ratio determinations shown in Figure 3-1 include the following:

- *The selection of the shear wave velocity from the field records.* Velocity measurements were typically available at 0.5-m intervals. Often there was significant variation between values within each interval. For the comparison in Figure 3-1, velocities were averaged within the soil sample interval. For a specific depth this variation could be 50 mps or more, and such a variation could affect the velocity-ratio comparison.
- *The conversion of the UCLA laboratory results to shear wave velocities.* The UCLA data were obtained as hysteresis loops showing stress versus strain. The secant modulus for the loop was converted to an equivalent shear wave velocity using the equation

$$V_s = [G_{max} / \rho]^{0.5} \quad (1)$$

  Where V_s is the shear wave velocity, G_{max} is the low-strain shear modulus, and ρ is the mass density of the soil. The mass density is defined as γ_t/g where γ_t is the soil total unit weight and g is gravitational acceleration (980 cm/sec^2). Some variation in the ratio could have occurred from the variation in modulus values at low shearing strains during the UCLA tests. The fourth cycle of loading in the first strain series was used in this determination, as it seemed to be somewhat more consistent from test-to-test.
- *The frequency of loading during the UCLA tests.* In the case of the UCLA data, the testing frequency was much lower than the frequency of seismic waves in the field. The effects of strain rate in the DSDSS device have been shown to be more significant for cohesive soils than cohesionless [Matesic and Vucetic, 2003]. If a rate effect were included in the comparison, the difference would have been smaller.
- *The confining pressure used during the UCLA tests.* Another possible source of uncertainty was the confining pressure used in the test conducted by UCLA. As noted previously, the groundwater elevation was selected on the basis of P-wave velocities, and this method could have introduced uncertainties. If the assumed groundwater elevation were too high, the resulting effective stress during testing

would have resulted in a modulus value that was too low relative to the in situ stress state. If lower groundwater elevations had been used, the fit to the field velocity value would generally improve.

- *The selection of the velocity from the UT test results.* The UT velocity value was selected at the closest stress to the estimated mean confining pressure. Uncertainties in estimating the mean effective in situ confining pressure would, therefore, lead to inaccuracies in the estimated shear wave velocity values. One of these uncertainties involved the assumption on groundwater table elevation at each site. As noted previously, the groundwater elevation was selected on the basis of P-wave velocity, and this method could have resulted in groundwater elevations that were too high.

The anomalously high ratio from the UT data at approximately 40 m below the ground surface was discussed with Professor Stokoe. Professor Stokoe confirmed that this test result appeared to be good, and hence, the high velocity measured in the laboratory may represent a thin, very stiff interlayer of soil that was not recorded in the field test. Since the field velocity is averaged over a travel path, the average of the field measurement could easily be lower than what would represent a thin layer.

Overall, the comparisons shown in Figure 3-1 are reasonably consistent with what is normally found when comparing laboratory and field velocity values. These inevitable difference emphasize the need for high-caliber in situ measurements whenever characterizing the dynamic properties at a site.

3.2 Low-Strain Modulus and Material Damping

The UCLA and UT test results were obtained for a range of shearing strain amplitudes – typically from less that 0.001 percent and extending to over 0.1 percent. The low-strain results were reviewed to determine how they varied with confining pressure, including how they compared to published shear modulus and material damping relationships, and how they compared to each other.

3.2.1 Effects of confining pressure

The UT program produced an extensive amount of information about the variation of low-strain shear modulus and material damping with confining pressure. Test results were

typically obtained at five pressures: $0.25\sigma_m'$, $0.50\sigma_m'$, $1.0\sigma_m'$, $2.0\sigma_m'$, and $4.0\sigma_m'$, where σ_m' is the mean effective in situ confining pressure. The UT report compares these results for the following different soil types and estimated in situ confining pressure conditions:

- All cohesionless test results, of which there were eight sets, and
- Cohesive soils at low (~27 to 199 kPa), medium (~242 to 551 kPa), and high (~769 to 898 kPa) in situ confining pressures.

Modulus results from the tests on eight cohesionless soil samples show a linear increase in shear modulus with the increase in confining pressure when plotted on a log-log basis. The slopes of the modulus-confining pressure lines are approximately 0.5, similar to the slope that is often cited for soils. Discussions in the UT report mention that the similarity of the recorded slopes to the slope in the original Hardin equation [Hardin, 1978] indicates that no overconsolidation effects seem to exist in situ, or possibly more importantly, if these effects once existed, they are not preserved in the sampling process. This observation is in contrast to the results from tests on cohesive soils, where it is evident from many of the laboratory test results that some stress history effect is preserved and recorded during testing. Similar to what was noted for the cohesionless soils, the normally consolidated portion of the modulus-confining pressure relationship for cohesive soils has a slope of approximately 0.5.

The UT material damping data are plotted in a similar log-log basis to show the effect of confining pressure on material damping. These plots indicate that cohesionless soil has a relatively linear decrease in damping with confining pressure with a typical slope of from negative 0.1 to negative 0.2. The corresponding log damping versus log confining pressure plots for cohesive soils are also relatively linear, but the slope of the relationship varies significantly. While there appears to be some correlation between the reduced slope and overconsolidation, it is not nearly as evident as the change in slope for the log modulus versus log confining pressure plots. This observation is consistent with previous observations made by Professor Stokoe, who noted during review of this summary report that the effects of mean confining pressure are typically much less on the low-strain damping value than on the low-strain shear modulus.

Another observation from the UT data is that the variation in material damping value is much greater for any confining pressure than the variation in shear modulus at the same pressure.

Typically, the modulus variation is less than half an order of magnitude while the damping variation is nearly an order of magnitude. This variation suggests that it will likely be more difficult developing a generic soil model that accurately predicts material damping at low shearing strain levels than developing a model for shear modulus at the same shearing strains. In other words, the fit to modulus data will likely be much better than the fit to damping data for any confining pressure.

3.2.2 Comparison of results from DSDSS and RC/TS methods

As noted in the introductory paragraph, the primary intent of this program was not to compare the results of the DSDSS test results with the combined RC/TS test results. Rather, the intent was to fill in data gaps in the previous characterization programs or for the characterization of new strong motion recording sites. This meant that many of the UT tests were conducted at higher confining pressures, say beyond 30-m sample depth. The UCLA tests were focused on obtaining high-strain data in the upper 30 m of soil profile. A limited number of companion tests were, however, conducted by UCLA and UT on samples from the same depth interval, and it is instructive to observe the comparison of results for these samples.

Figure 3-2 shows the ratio of low-strain shear modulus and low-strain material damping for seven pairs of samples that were tested by UCLA and UT. The ratios in these plots are the UCLA modulus or damping value divided by the modulus or damping value from the test conducted by UT on the companion sample. The following observations are made from this plot:

- The results confirm the observations made previously from Figure 3-1 which suggest that, on the average, the UCLA modulus values are lower than the comparable UT values. The greatest difference appears to be at shallow depths, and the difference seems to decrease with increasing depth.
- The ratio of damping values indicates that the UCLA low-strain damping values are higher than the low-strain damping values from UT measured in the TS test at frequencies of approximately 0.5 Hz. This trend is expected because as the stiffness decreases, the material damping normally increases. Therefore the observed trend follows the expectations; i.e., the damping from UCLA at low strain should be greater than the equivalent damping from UT.

- This trend in damping is reversed, when the RC damping values (frequencies of 25 to 250 Hz) were used in the comparison. The reversal was due to the significant frequency effects that occurred in the RC testing method. This comparison points out an important observation: that the RC testing method can result in material damping values at low shearing strain levels that are too high, relative to results at lower frequencies. This observation needs to be recognized when conducting site-response analyses based only on RC testing method.

As with the velocity comparisons in the previous section, there are a number of factors that could have contributed to the trends shown in Figure 3-2. The most significant involves defining a common confining pressure at which to make the comparisons. The UCLA tests were conducted at a specified vertical stress condition, while the UT tests were conducted at a mean stress condition. For the comparisons shown in Figure 3-2, the vertical stress applied during the UCLA test was converted to an equivalent mean stress using the following equation:

$$\sigma_m' = \sigma_v' \, (1 + 2k_o)/3 \qquad (2)$$

Where σ_m' and σ_v' are the mean and vertical effective stress, respectively, and k_o is the coefficient of earth pressure at rest. A value of 0.5 was assumed for k_o. It is possible that a different value of k_o may have been more appropriate – though higher values would have accentuated the pressure difference by producing a higher σ_m' which would have resulted in a higher value of low-strain modulus and a lower value of low-strain material damping ratio from the UT tests. The comparison for material damping ratio would, however, have improved.

The difference in shear modulus and material damping values from the DSDSS and combined RC/TS test devices at low shearing strains has been observed previously, and it continues to be an issue that warrants further evaluation.

3.3 High-Strain Modulus and Material Damping

The results from UCLA and UT include plots of shear modulus and material damping versus shearing strain. The shear modulus data are plotted as a function of both absolute shear modulus (G) and normalized shear modulus, where the modulus was normalized by the low-strain modulus (i.e., G/G_{max}). Conventional practice is to use the normalized shear modulus with the field measurement of shear modulus (from shear wave velocity) to define the in situ

modulus-strain curve for the soil. These field adjustments are not currently made for material damping, partly because of the difficulty in estimating material damping in situ. Additional observations from each of the high-strain portions of the testing programs are summarized below.

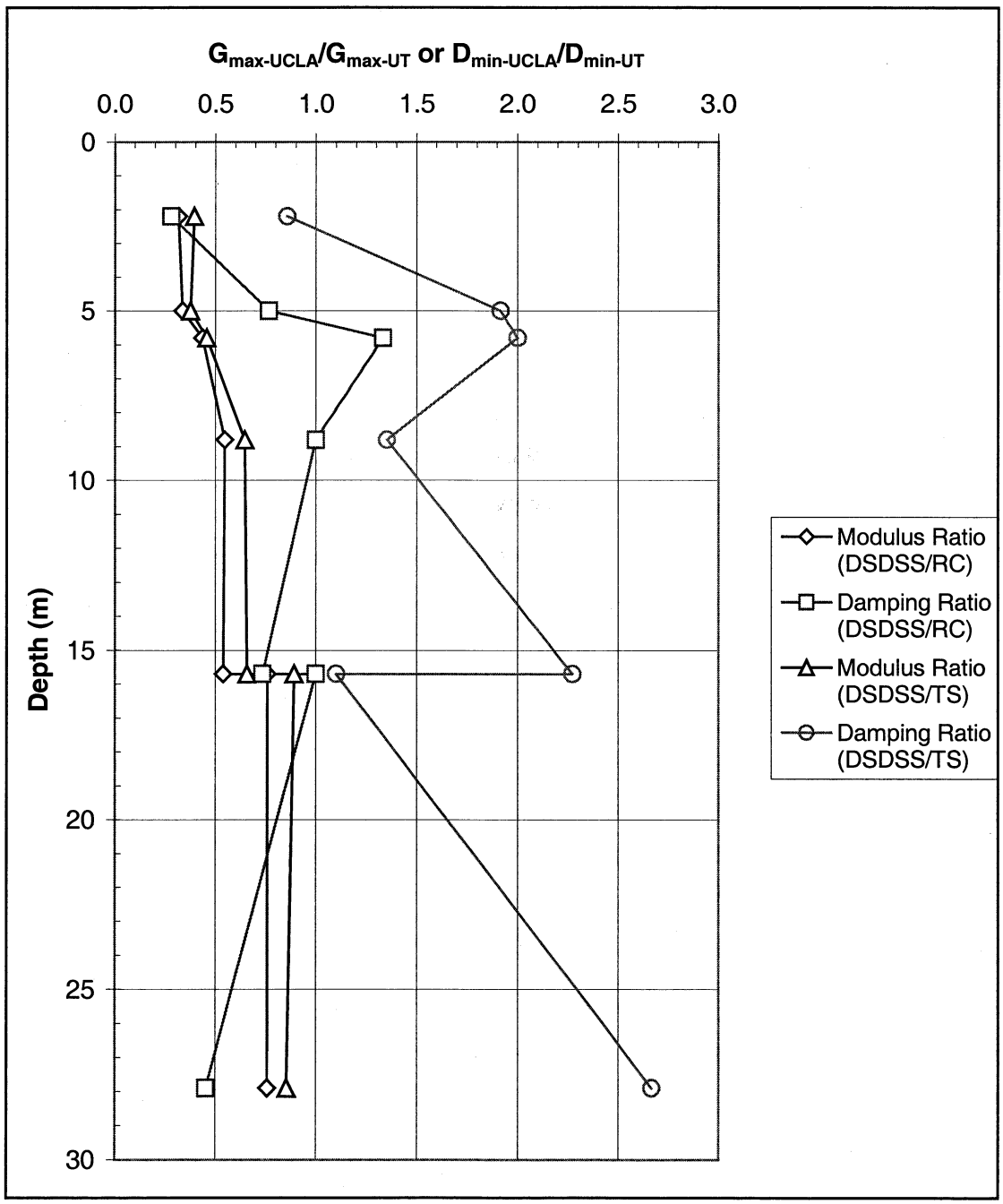

Fig. 3-2 Low-Strain Modulus and Damping Ratio Comparisons

3.3.1 Shear modulus versus shearing strain

Attachments B and C include plots of shear modulus values as a function of the logarithm of the shearing strain level. These plots show that as shearing strain increased, the shear modulus decreased once a threshold strain was exceeded. The threshold strain ranges from 0.001 percent to 0.01 percent with the UT data showing an increase in the threshold strain with increasing confining pressure. The range of confining pressures was much smaller in the UCLA tests – probably explaining why this same trend was not evident for the UCLA samples.

A clear observation from the UCLA set of data is that higher shearing strains were achieved during the test. A number of tests were conducted to shearing strains of nearly 3 percent allowing a secant shear modulus to be determined. Material damping measurements were made up to approximately 0.1 to 0.3 percent shearing strain. According to Professor Vucetic, the shape of the hysteresis loop above 0.1 to 0.3 percent shearing strain sometimes precluded consistent determination of material damping at higher levels of shearing strain. Rather than interpreting damping for these cases, readers who are interested in using the data should carefully review the shapes of the hysteresis loops and decide on the best way of interpreting damping values for each set of data. Generally, the combined RC/TS tests conducted at UT were limited to approximately 0.1 percent shearing strain.

As noted in Section 3.2, the low strain moduli (G_{max}) obtained from the UCLA program were typically 50 to 80 percent of the modulus values obtained by UT for the limited set of data that could be compared. This difference meant that the shear modulus versus shearing strain curves were typically higher from UT by a factor of 50 to 100 percent, as shown in Figure 3-3 through 3-9. However, as will be discussed in the next section, the G/G_{max} curves for each testing group were very similar, indicating that whatever affected the absolute value of shear modulus, did not seem to have the same effect on the change in the normalized shear modulus versus shearing strain.

3.3.2 Normalized shear modulus versus shearing strain

The normalized shear modulus versus the logarithm of the shearing strain was also plotted by UCLA and UT for each test specimen. These plots are presented in the UCLA and UT reports in Attachments B and C, respectively. The plots show the characteristic normalized shear modulus versus shearing strain shape, where the normalized shear modulus (G/G_{max}) is 1.0 until a threshold strain of 0.001 to 0.01 percent occurs, at which point the normalized shear

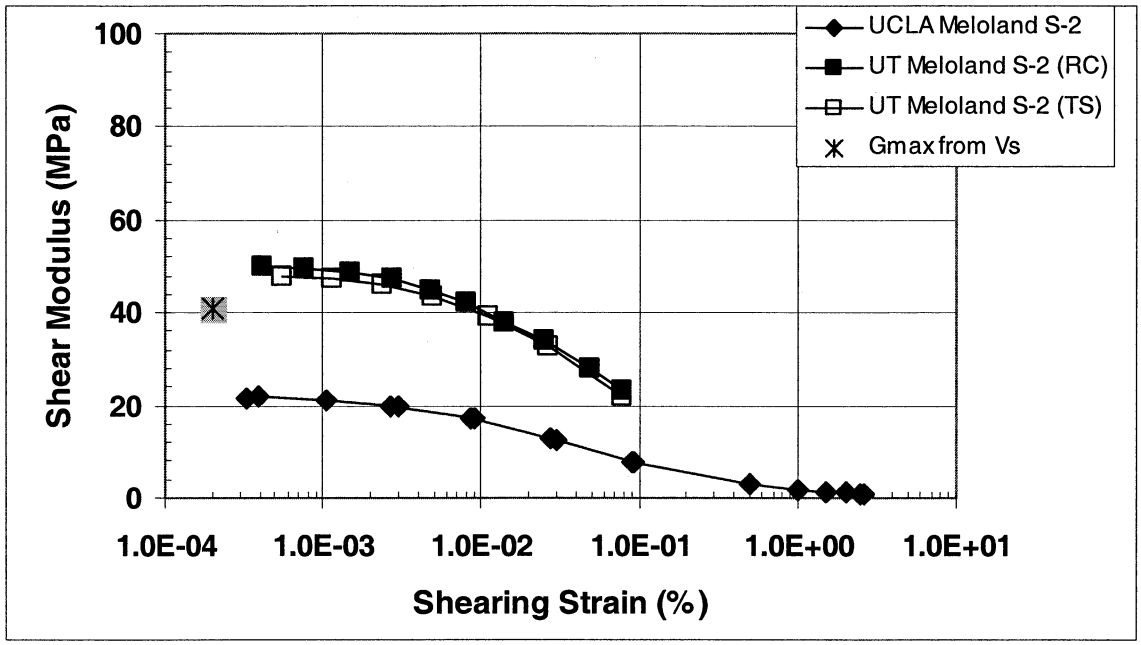

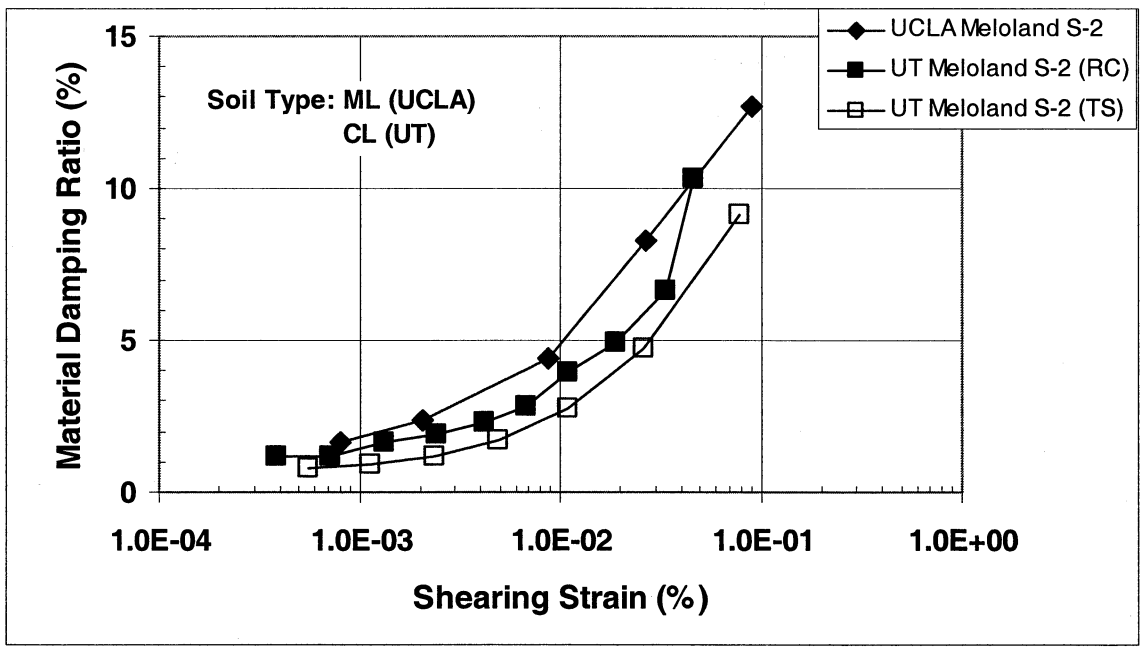

Fig. 3-3 Modulus and Damping Comparisons (Meloland S-2)

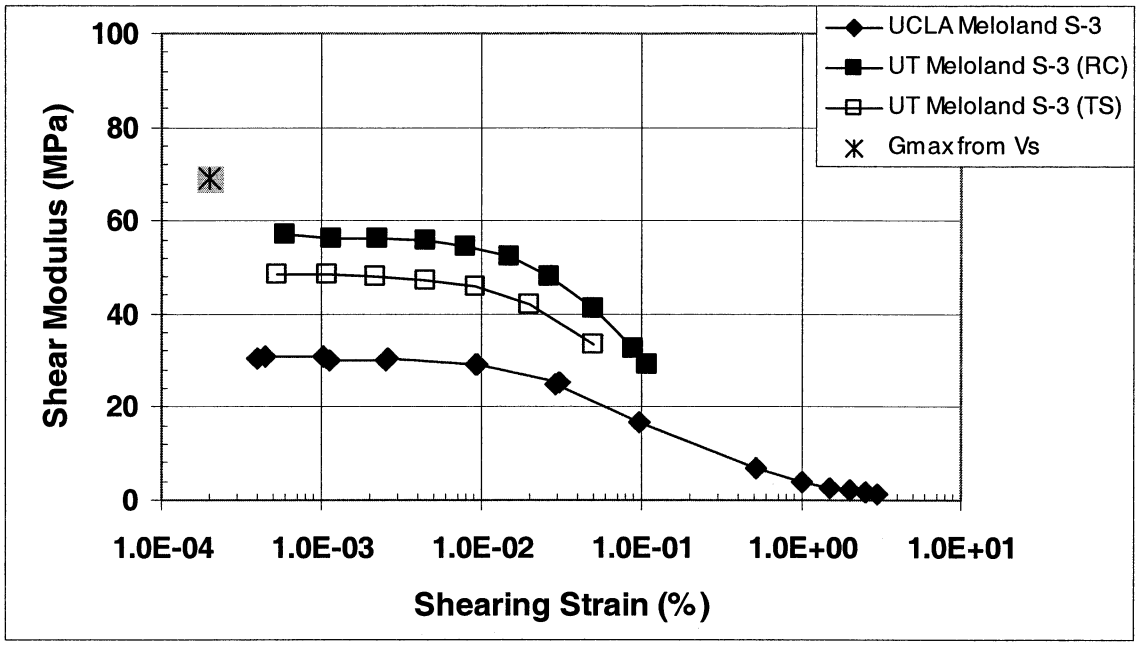

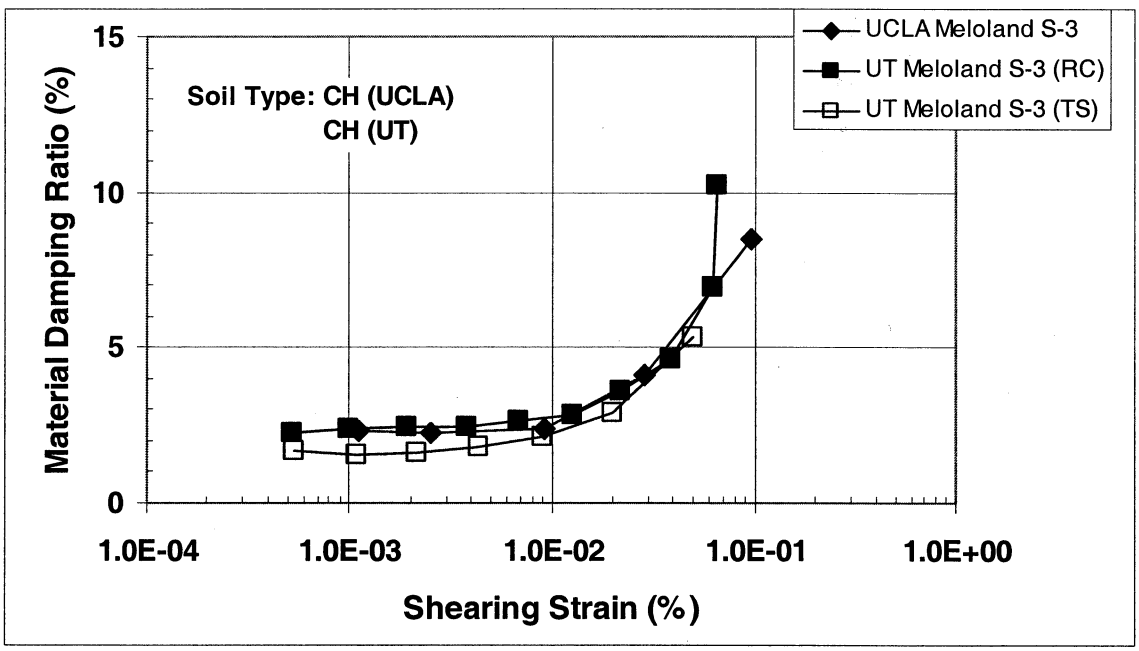

Fig. 3-4 Modulus and Damping Comparisons (Meloland S-3)

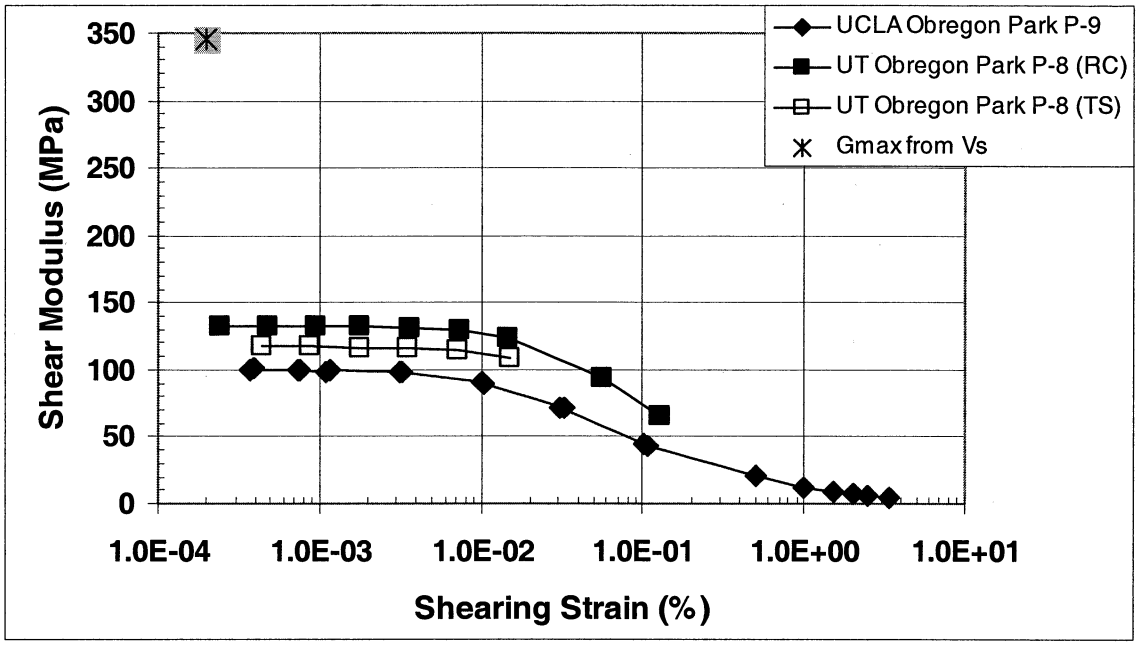

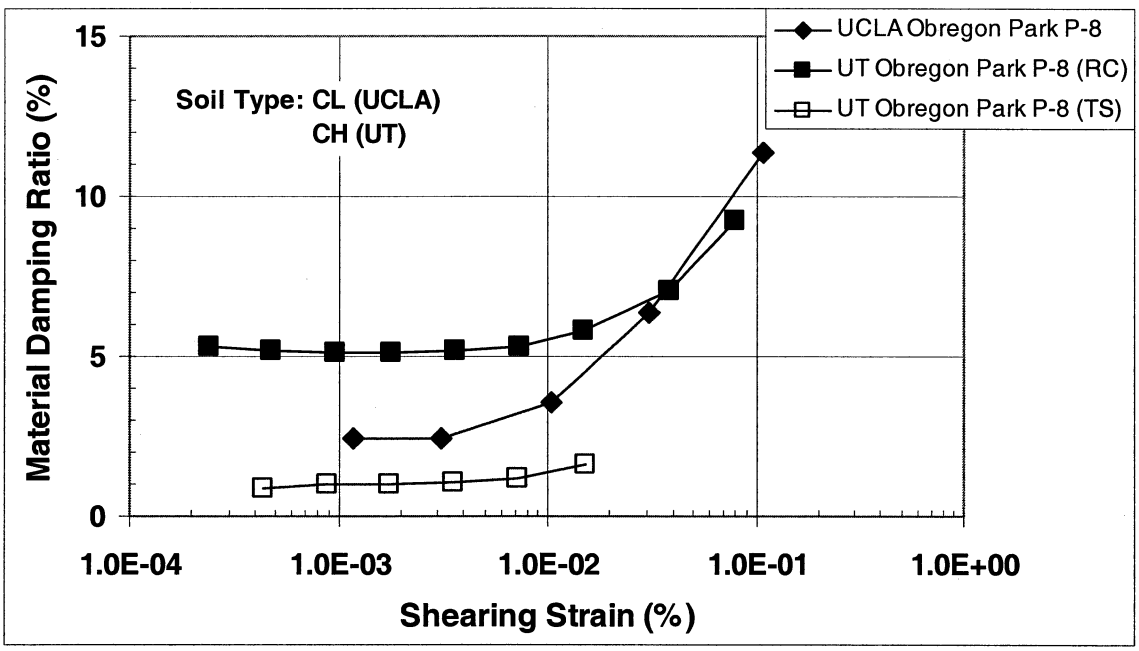

Fig. 3-5 Modulus and Damping Comparisons (Obregon Park)

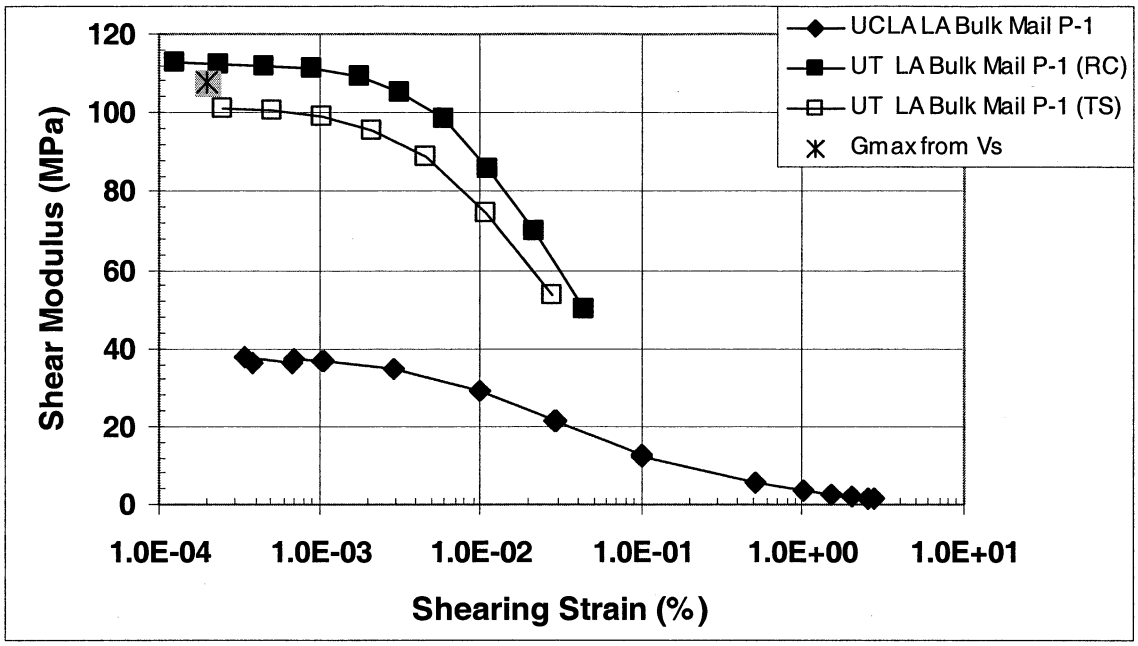

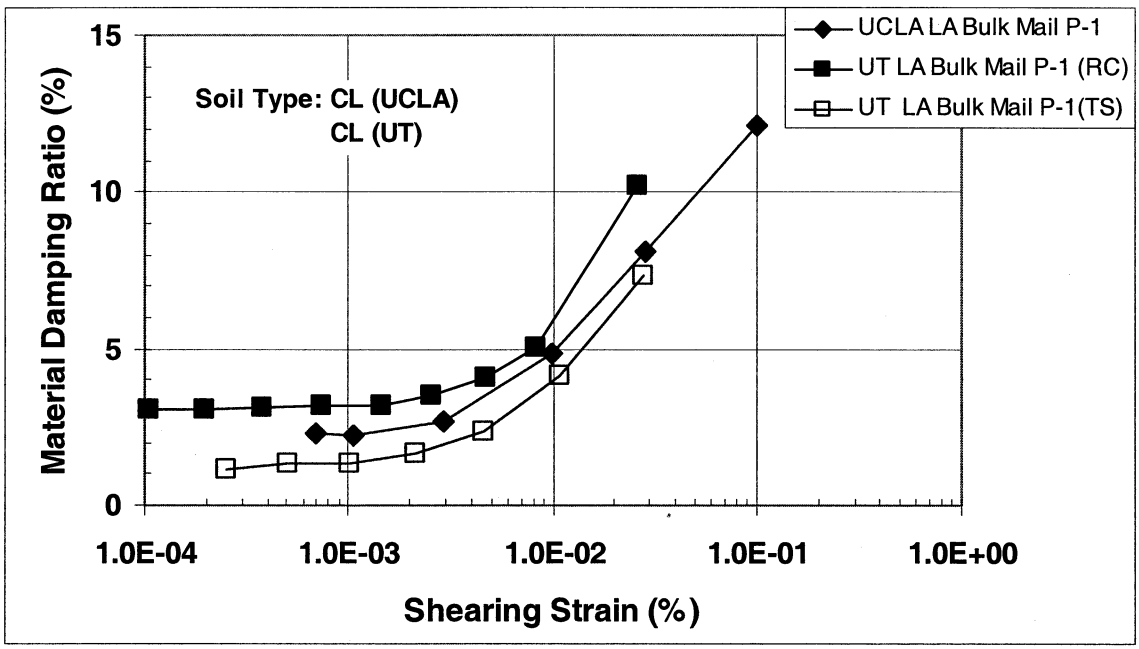

Fig. 3-6 Modulus and Damping Comparisons (LA Bulk Mail P-1)

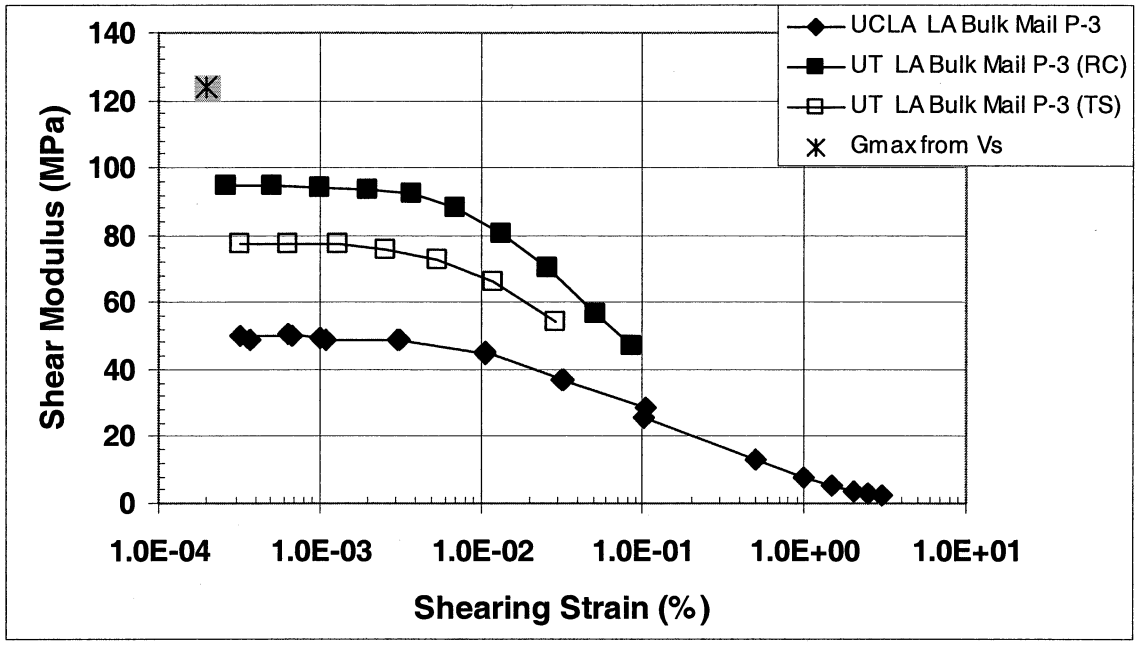

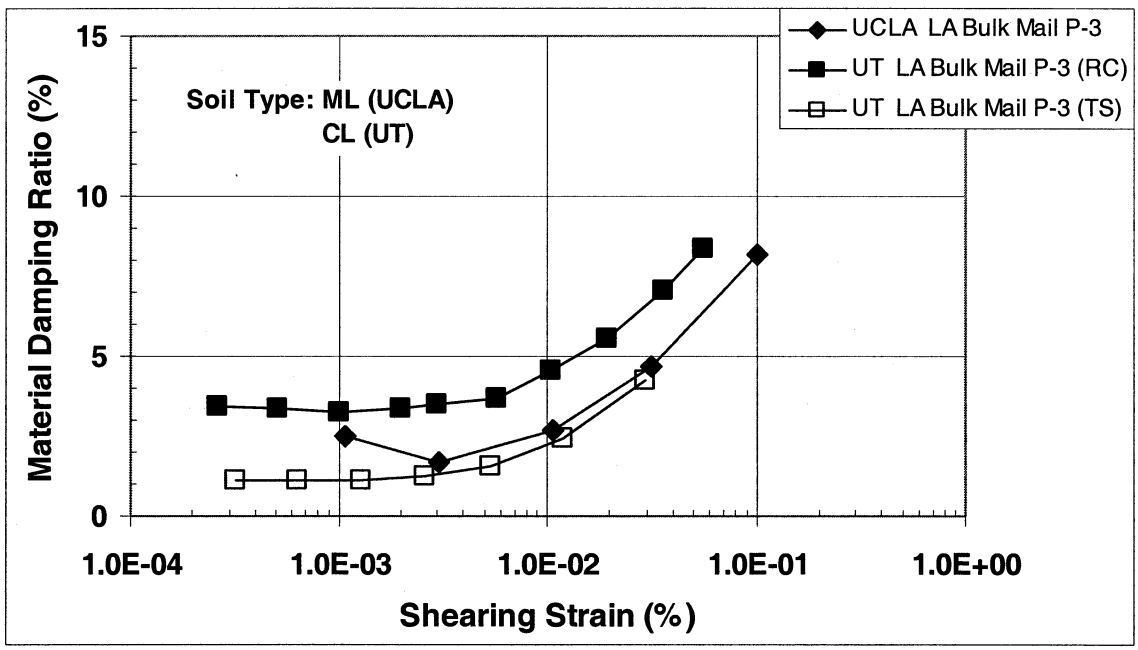

Fig. 3-7 Modulus and Damping Comparisons (LA Bulk Mail P-3)

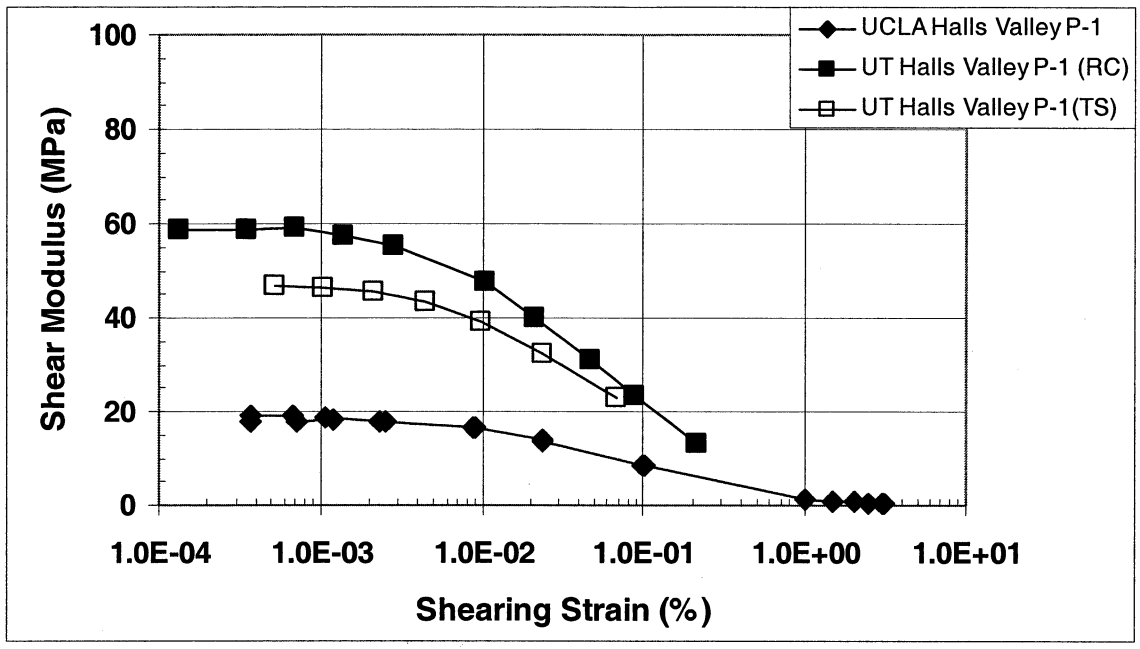

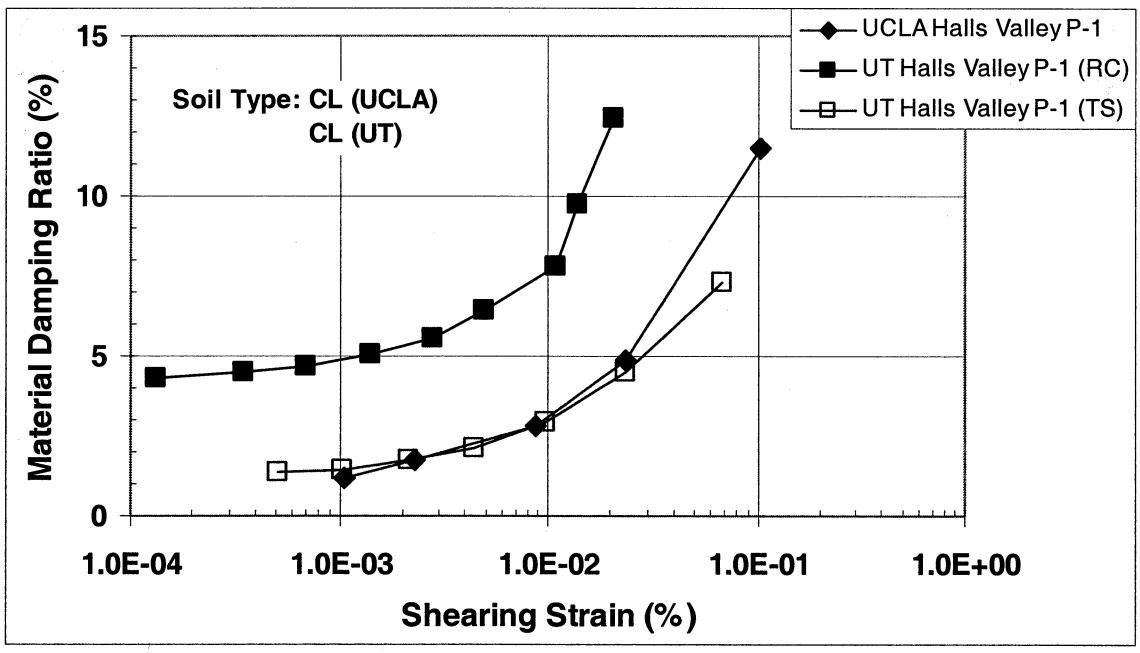

Fig. 3-8 Modulus and Damping Comparisons (Halls Valley P-1)

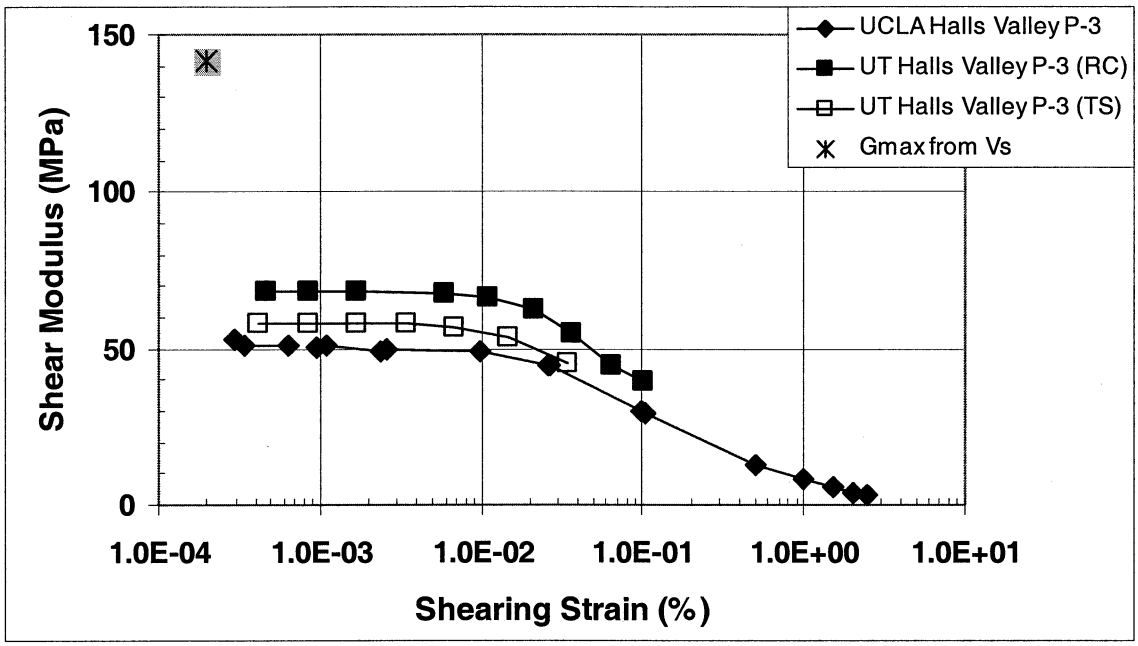

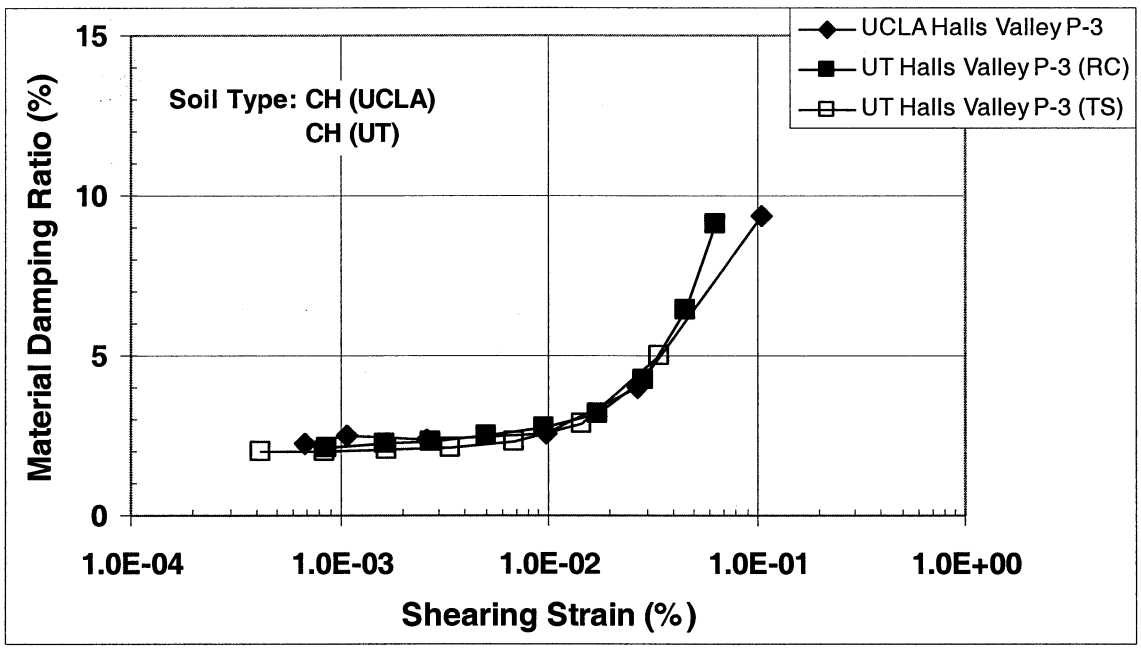

Fig. 3-9 Modulus and Damping Comparisons (Halls Valley P-3)

modulus decreases with increasing shearing strain. At strains of 1 percent, the normalized shear modulus is typically 0.1 or less. Results from the UCLA and UT tests are consistent with these normal observations.

Figures 3-10 through 3-16 show the comparisons of the normalized shear modulus versus shearing strain curves for the seven tests that were conducted on companion samples. While the shear modulus values obtained for similar samples by UCLA and UT differed significantly, the G/G_{max} values are very similar as shown in Figures 3-10 through 3-16. This similarity occurs when the modulus reduction curves have both a relatively flat break at the threshold strain[2] and a sharp break.

As will be noted in the next section of this summary report, the shapes of the normalized shear modulus versus shearing strain curves are also consistent with published relationships by Seed et al. [1986], Vucetic and Dobry [1991], and Darendeli [2001] – where little modulus reduction occurs below a shearing strain of approximately 0.001 to 0.01 percent, after which a significant reduction occurs. All of the samples for these comparisons originated within 30 m of the ground surface, and therefore the influence of confining pressure on the shapes of these curves is not particularly noticeable.

The fact that the normalized shear modulus curves are relatively similar even though the modulus strain curves between the two testing methods differ significantly could have several important implications. The obvious conclusion is that the inherent modulus-strain behavior of soils is preserved relative to the low-strain modulus. However, as noted by Stokoe in a discussion of these test results, it could mean that the unavoidable disturbance that occurs during the sampling and sample setup process masks any difference that could result from different testing methods. The fact that the shapes of the curves differ consistently for each testing method suggests, however, that some structure must be preserved during sampling and measured during each cyclic test.

---

[2] Threshold strain is normally defined as the point at which the normalized shear modulus curve becomes less than 1.0. The location of the threshold strain is usually assumed to vary with soil type and confining pressure, and could potentially vary with frequency of loading.

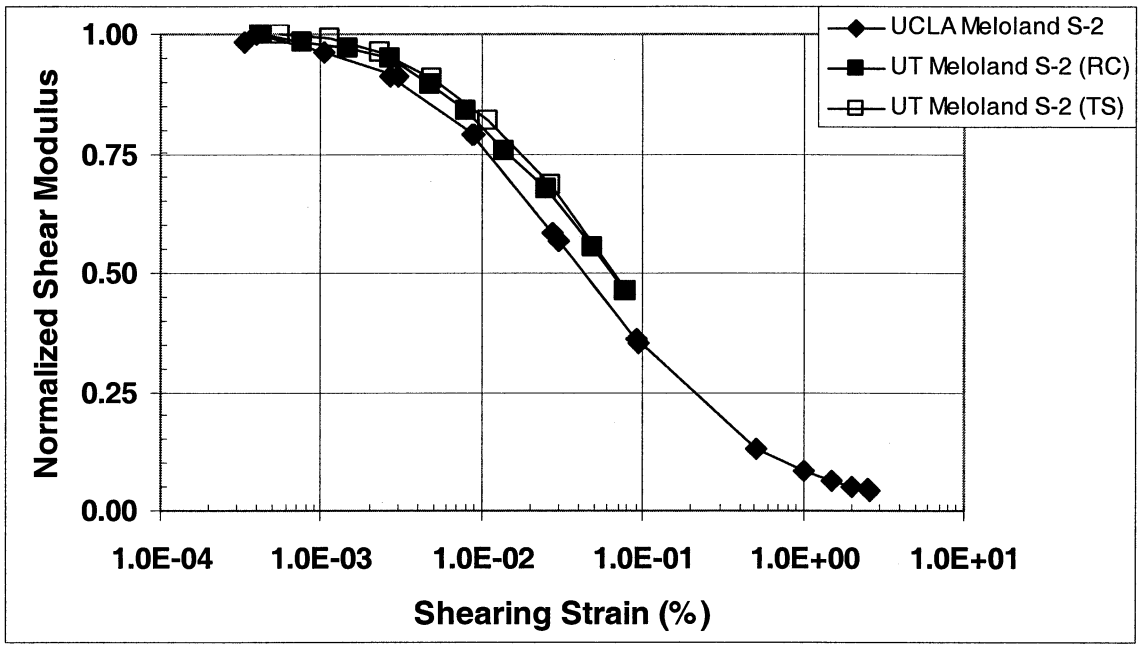

Fig. 3-10 Normalized Shear Modulus Ratio Comparisons (Meloland S-2)

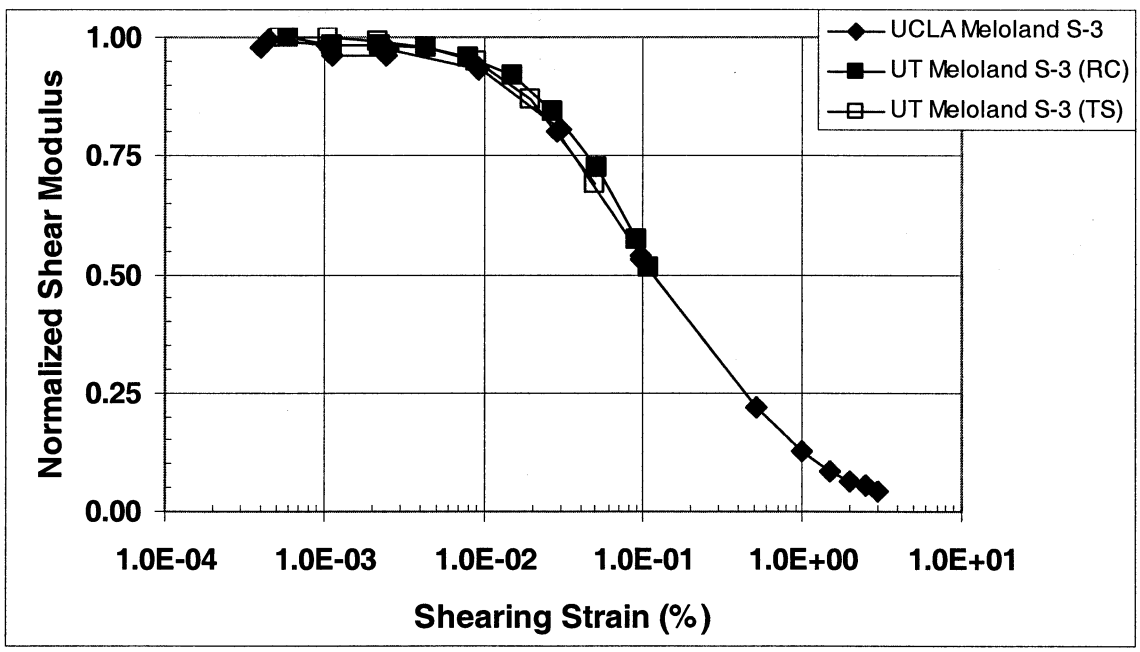

Fig. 3-11 Normalized Shear Modulus Ratio Comparisons (Meloland S-3)

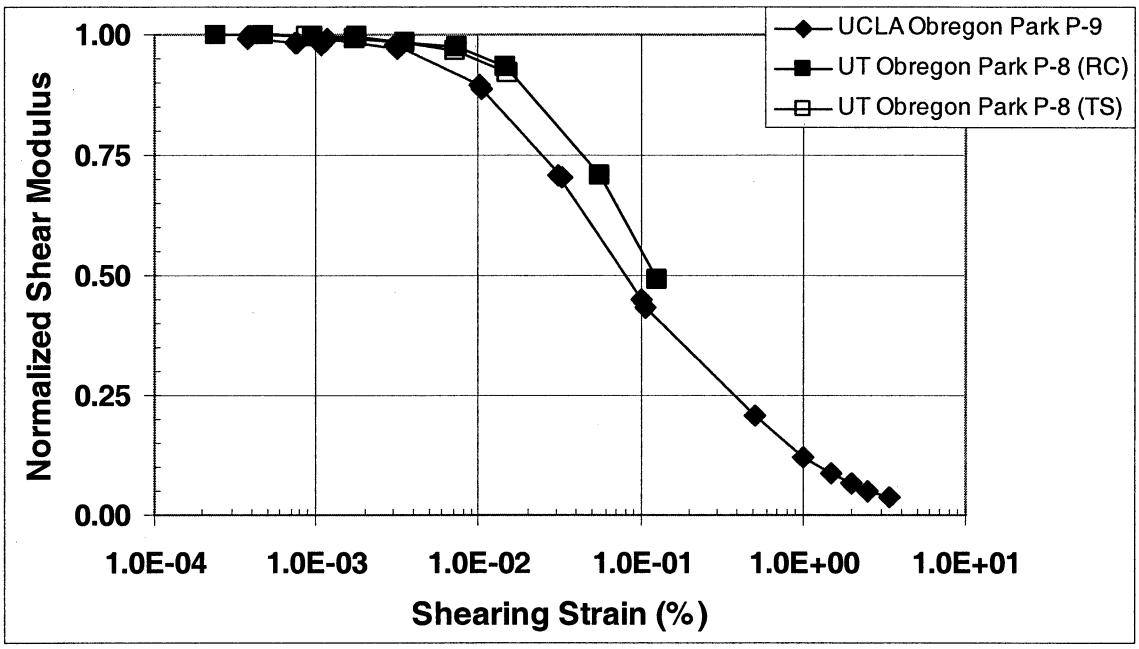

Fig. 3-12 Normalized Shear Modulus Ratio Comparisons (Obregon Park)

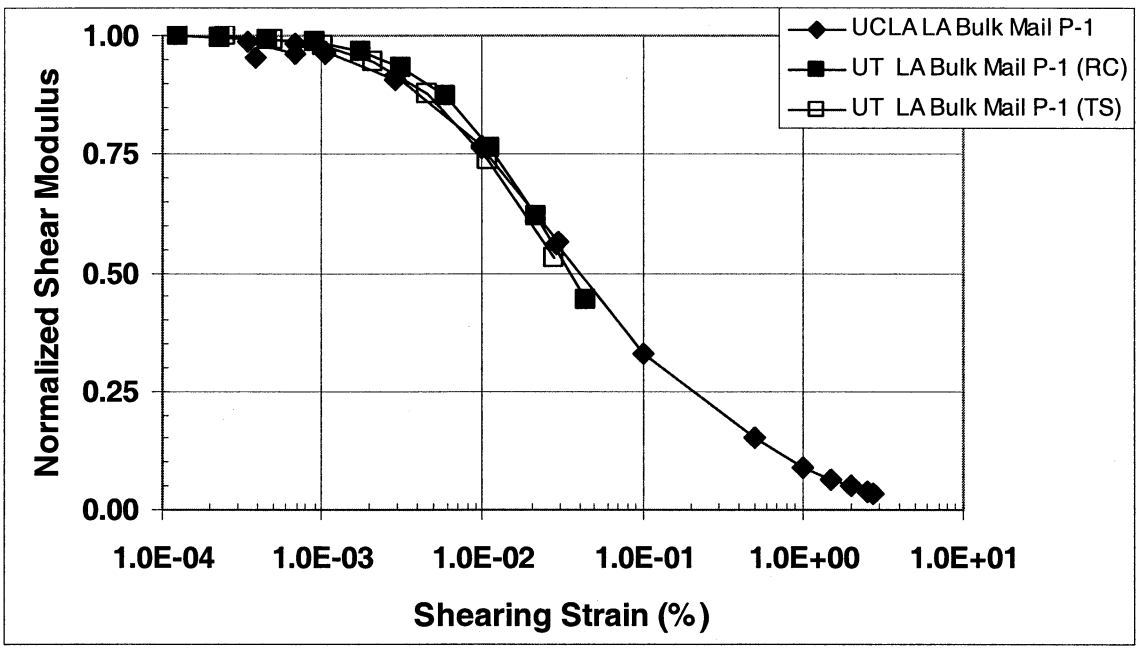

Fig. 3-13 Normalized Shear Modulus Ratio Comparisons (LA Bulk Mail P-1)

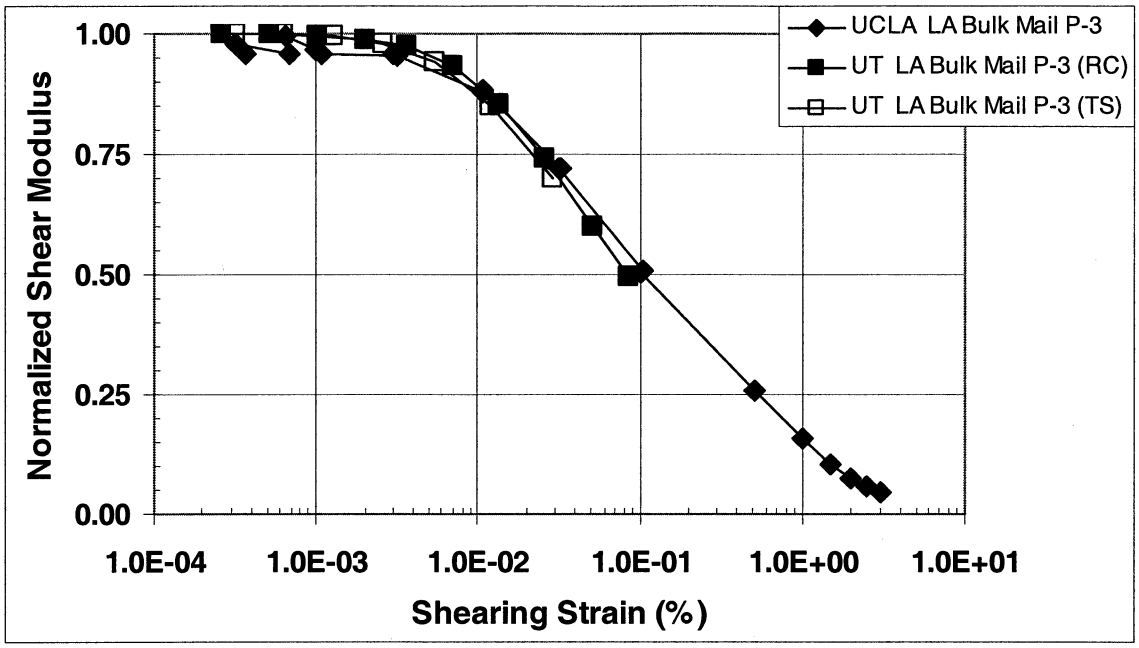

Fig. 3-14 Normalized Shear Modulus Ratio Comparisons (LA Bulk Mail P-3)

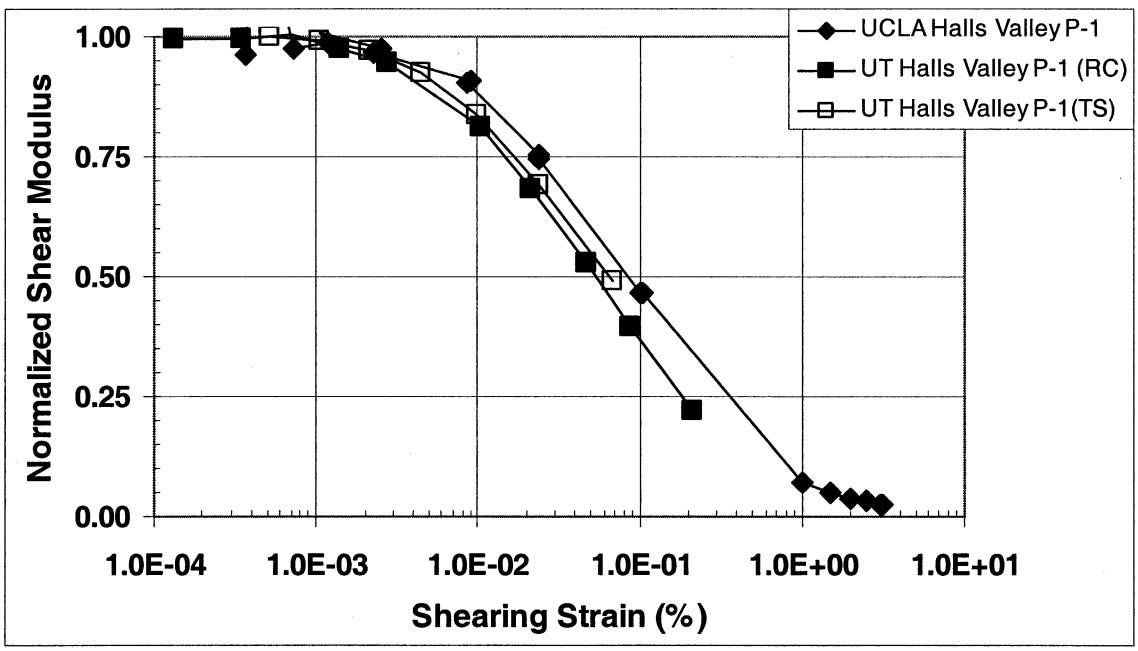

Fig. 3-15 Normalized Shear Modulus Ratio Comparisons (Halls Valley P-1)

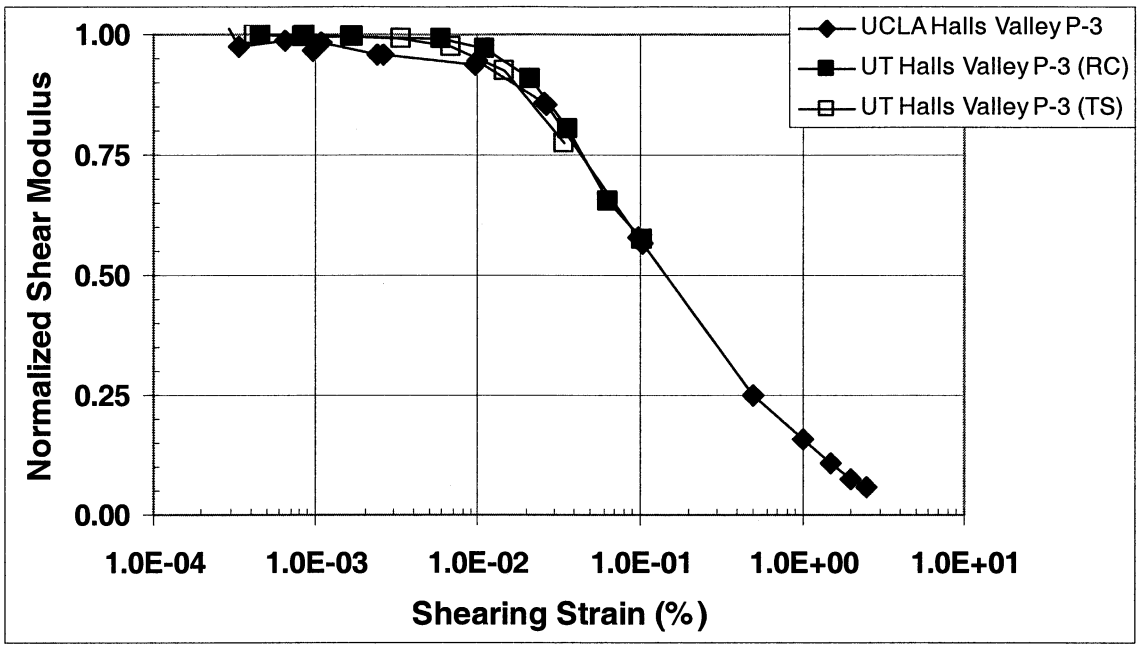

Fig. 3-16 Normalized Shear Modulus Ratio Comparisons (Halls Valley P-3)

3.3.4 Material damping versus shearing strain

Each university program determined the variation of material damping with shearing strain amplitude. The results of these measurements are consistent with normal observations in laboratory testing programs – where the material damping value is low at low shearing strain levels, for example less than 5 percent, and increases with shearing strain once the threshold strain of 0.001 to 0.01 percent is exceeded. The maximum material damping value is typically from 15 to 20 percent at shearing strains of 1 percent. Results of the testing at the UCLA and UT are consistent with these observations.

As shown in Figures 3-3 through 3-9, the comparison between damping results obtained for similar samples by UCLA and UT are reasonably similar, particularly considering the significant differences in shear modulus values for the same comparisons. The UCLA results are consistently above those obtained by the UT when compared to the TS results. This difference is most likely due to the effects of sample disturbance or the state of confining stress. The UCLA damping results are below those from UT when the comparison is made for the RC tests. In most cases the results are within a few percent or less at low shearing strain levels and tend to be even closer at high shearing strain levels.

While these damping comparisons are within a few percent in absolute value at low shearing strain amplitudes, these differences can have a noticeable effect on wave propagation

studies. Other than the method for adjusting for sample disturbance mentioned in Section 3.1, no corrections are typically made to material damping to adjust to field damping values – though there is an increasing awareness that the material damping versus shearing strain curve needs to be lower. Various methods have been recommended for measuring material damping in situ; however, generally, no single method has been agreed upon within the profession for making in situ damping measurements. Those methods that have been proposed have an accuracy that is probably within the few percent difference between the UT and UCLA results.

It was apparent from these results that the UCLA DSDSS device has overcome some of its original problems in obtaining stable damping values at very low-to-intermediate shearing strain levels. The shapes of the hysteresis loops measured in the DSDSS device also are consistent with the expected shape up to a shearing strain of 0.1 percent. At higher strains, the "banana shape" of the hysteresis loop precluded consistent material damping measurements. It is often assumed that the "banana shape" is due to dilation of the test specimen at higher shearing strains. However, these shapes could also be caused by the testing method. Additional evaluation of this behavior is probably warranted.

3.4 Comparison to Empirical Models

Both the UCLA and UT programs include comparisons to published empirical relationships for normalized shear modulus and material damping ratio versus shearing strain level. UCLA's comparisons are made with the relationship recommended by Vucetic and Dobry [1991], while the UT program includes comparisons to relationships proposed by Seed et al. [1986], Vucetic and Dobry [1991], and a new model proposed by Darendeli [2001].

3.4.1 Vucetic and Dobry model

The Vucetic and Dobry model correlates the shape of the normalized shear modulus and material damping ratio relationships with plasticity index (PI) where the threshold shearing strain tends to increase with PI – indicating that the modulus remains linear for higher strains. On the other hand, material damping tends to decrease at higher shearing strain levels with increasing PI. The Vucetic and Dobry model was developed from testing results conducted at low confining pressures, and therefore it is expected to be more suitable for tests conducted on samples from shallow depths.

Both the UCLA and UT programs show that the Vucetic and Dobry model provides a reasonable estimate of the shear modulus reduction curve as the PI varied over low confining pressures. The UT program involves a wider confining pressure range than the UCLA program, and results suggest more departure from the empirical correlation at higher confining pressures. As noted in the previous paragraph, this is not surprising given the understanding that there is a confining pressure dependence in the shape of the normalized shear modulus curve.

The UCLA and UT programs also provide a comparison of their results to the material damping ratio curves in the Vucetic and Dobry model. The general conclusion from these comparisons is that variations occurred, particularly at low shearing strain levels where at times the measured material damping ratio is several percentages higher in absolute terms than the value estimated by the Vucetic and Dobry model. However, overall the damping estimates from the Vucetic and Dobry model appear to give a reasonable representation of the laboratory test results for soils with a plasticity index greater than 5 percent. The discussion in the UT report specifically notes, however, that the results of the current testing program extend to lower shearing strains than are given in the Vucetic and Dobry model and that the UT results exhibit more linearity at high levels of confining pressure – similar to what is observed for the normalized shear modulus curve comparison. At low shearing strain levels, it is unclear whether this difference represents a limitation in the testing equipment for both programs or the Vucetic and Dobry model.

3.4.2 Seed et al. model

The UT program includes specific comparisons to the Seed et al. [1986] correlation for cohesionless soils. Though not explicitly stated, the UCLA tests on cohesionless soils are also compared to the Seed et al. model in that the Vucetic and Dobry curve at a PI of 0 is similar to the Seed et al. model for cohesionless soils.

Both the UCLA and the UT programs find that the Seed et al. model provides a reasonable estimate of shear modulus reduction curve for cohesionless soils. According to the UT interpretations, some variation occurs at higher confining pressures, and this difference is attributed to the effects of confining pressure that are not included in the Seed et al. model. Only three tests were conducted by UCLA at PI $\leq$ 5 percent, and the results of these seem to be more inconsistent. The shape of the normalized shear modulus curve at PI = 3.5 percent is consistent

with the cohesionless curve while the other two curves are significantly stiffer than would have been expected from the Seed et al. model.

The UT damping ratio measurements correspond to the lower bound of the range that Seed et al. [1986] provide for sands. As with the normalized shear modulus comparisons, the UCLA tests at a PI ≤ 5 percent seem to be scattered. This may be the results of the method used by the DSDSS device to develop horizontal stress. In cohesionless soil the horizontal stress develops after some lateral soil expansion, which could alter the form of the material damping versus shearing strain curve.

3.4.3 Darendeli model

The UT program also includes comparison of their results to a model recently developed at UT by Darendeli [2001]. The Darendeli model is described in more detail in Section 4.1.4 of Attachment C. Generally it is a modified version of the hyperbolic model originally recommended by Hardin and Drnevich [1972]. The reference strain is defined as the shearing strain at which the G/G_{max} equals 0.5 and can be estimated based on the PI, overconsolidation ratio (OCR), the mean confining stress (σ_m'), and a series of parameters obtained by curve fitting with a large database maintained at UT. For this testing program, the Darendeli model provides good comparisons to the laboratory values of normalized shear modulus and material damping ratio variation with shearing strain amplitude. One of the unique features of the Darendeli model is that it is able to account for the changes in normalized shear modulus and damping ratio shapes at high confining pressures.

While the Darendeli model is not compared to the results of the UCLA tests, the ability of the Derendeli model to approximate the Vucetic and Dobry model results suggests that it would provide reasonable comparisons overall with the UCLA results. Since the UCLA tests were conducted at lower confining pressures, the additional benefits of the confining pressure term in the Derendeli model would not have been as significant as it was for the UT test comparisons.

3.4.4 Other models

Several other models representing the change in shear modulus and material damping with shearing strain amplitude have been developed or are in the process of being developed. These models include those proposed by the Electric Power Research Institute (EPRI) in the early 1990s [EPRI, 1993] and a model currently under development at Caltrans by Dr. Clifford

Roblee [personal communications, 2001]. The EPRI model shows modulus and material damping ratio versus shearing strain curves that vary with depth, thereby accounting for confining pressure effects. The Roblee model has some of the same features as the Derendeli model, but makes an adjustment to the reference shearing strain for soil sample disturbance.

With regard to the Roblee model, the disturbance adjustment factor is based on the ratio of shear wave velocity measured in the laboratory at low shearing strain amplitudes relative to the in situ velocity. The results of this testing program shown in Figures 3-10 through 3-16 do not appear to support the disturbance factor adjustment, as the normalized shear modulus curves for these comparisons are approximately the same even though the ratio of laboratory-to-field shear wave velocity differed. It is difficult to say from this limited database whether the disturbance adjustment method is incorrect or compensating factors masked these effects in the laboratory testing program.

A worthwhile future evaluation would be to include these other models, as well as those described above, in a complete evaluation of the ROSRINE laboratory test database. As noted previously, such an evaluation was not part of this testing program.

4. Conclusions and Recommendations

This report provides a summary of the results from a series of laboratory tests conducted by UCLA and UT as part of the PEER Lifeline Research Program. These tests were conducted on samples recovered at strong motion recording sites where in situ shear wave velocity measurements have been made. The laboratory and field test results are within the overall site characterization objective of the ROSRINE research effort. The following conclusions and recommendations can be made from the results of the laboratory testing program described in this summary report.

4.1 Conclusions

The laboratory tests conducted by UCLA and UT extend the current ROSRINE database by providing additional high-quality cyclic test results for cohesionless and cohesive soils obtained from depths up to 134 m below the ground surface and tested at shearing strain amplitudes from less than 0.001 percent to more than 1 percent. Each set of test results is completely documented in Attachments B and C to this summary report, and electronic copies of the laboratory test information can be found on the ROSRINE website. Individuals who are developing soil models and conducting site response analyses for the ROSRINE research program should benefit from the data provided by the UCLA and UT tests.

Results of the UCLA and UT testing programs are consistent with expected shear modulus and material damping versus shearing strain relationships. Shear modulus values are relatively constant until a threshold shearing strain of 0.001 to 0.01 percent is reached, after which shear modulus decreases significantly with increasing shearing strain. At shearing strains of 1.0 percent and higher, the shear modulus is usually less 10 percent of its initial value. Material damping values are also consistent with published data – with damping increasing from less than 5 percent below the threshold strain to value of 10 percent or more at high stains.

Some caution should be taken when using the low-strain material damping values obtained from the UCLA and UT testing programs in numerical modeling efforts. Effective confining pressures used during this testing program where based on groundwater elevations determined on the basis of P-wave velocity measurements. This method of determining the groundwater elevation can result in elevations that are too high if the site comprises thick deposits of geologically old fine-grained soils. While this potential is thought to be limited for this program, it cannot be ruled out. If the groundwater elevation for a site were too high, the confining pressure would have been underestimated. As the confining pressure increases, material damping decreases – suggesting that the material damping could be lower than given by the laboratory test results. This same problem will not exist for shear modulus as long as the shear modulus is determined by multiplying the shear modulus from the in situ measurement by the normalized shear modulus. If absolute value values of shear modulus from the laboratory tests are being used in the numerical modeling, then the absolute shear modulus could be too low.

Preliminary comparisons of the UCLA and UT test results to field velocities, to each other, and to published correlations reveal the following important trends.

- A difference exists between the low-strain shear wave velocity measured in the field and the low-strain velocity determined during the laboratory testing program. The ratio of the laboratory-to-field velocity ranges from 50 to 80 percent, which is consistent with previously reported comparisons. This difference between field and laboratory velocities emphasizes the need to consider both the field and laboratory modulus data when developing a soil model for the ROSRINE site response evaluations.
- There continues to be significant variation in the absolute value of shear modulus obtained by DSDSS and combined RC/TS testing methods. However, both the normalized shear modulus and the material damping ratio are much more similar for the two testing methods. Likewise, the normalized shear modulus and damping ratio results from DSDSS and RC/TS tests are consistent with empirical relationships commonly used to define the variation in normalized shear modulus and material damping with shearing strain.

- Significant differences between the nonlinear properties from each test method and from the empirically-derived nonlinear properties can occur for individual samples – even though the overall trends in data are consistent with each other and with published empirical correlations. These differences result from sample disturbance that is inevitable with current sampling and testing methods and the heterogeneity of soil. In the absence of in situ testing methods that provide modulus and damping over a complete range of shearing strains, these variations have to be accounted for when conducting site response evaluations through the use of different realizations of properties and soil layer boundaries.

4.2 Recommendations

A number of recommendations were identified based on a review of the results of this testing program and on the interaction that occurred with Professors Stokoe and Vucetic and with Dr. Cliff Roblee during the course of this project. These recommendations are listed below.

- A comprehensive evaluation of the entire ROSRINE laboratory database is needed. This evaluation should be focused on identifying soil parameters and test conditions that affect the variation in shear modulus and material damping. A detail review of the ability of current soil models (e.g., Vucetic and Dobry, Seed et al., Darendeli, EPRI, Caltrans, etc.) to represent laboratory and in situ behavior of soil during cyclic loading should be included in this evaluation.
- Additional laboratory testing programs are needed to quantify the effects of soil disturbance and to resolve uncertainties that may be caused by boundary conditions imposed by current testing methods and equipment. These future evaluations should include an evaluation of methods for adjusting laboratory-derived modulus and damping properties to field conditions. The studies should also include comprehensive evaluations of the effects of the frequency of loading and corresponding average rate of loading on the shear modulus and material damping ratio versus shearing strain curves.

- A need continues to exist for an in situ test device that can determine the shear modulus and material damping characteristics of soil at levels of shearing strain, or deformation, consistent with what occurs in the ground during a strong ground shaking. Until such a method is available, many of the current uncertainties associated with laboratory testing methods will remain.
- The importance of uncertainties in material property characterization on site response predictions is not fully appreciated. It is assumed that current uncertainties in material property characterization directly affect site response calculations. Further effort needs to be made to quantify these effects by conducting numerical analyses that systematically evaluate the effects of material property variation. Results of these evaluations should be used to determine soil properties or conditions which involve the most uncertainty and types of tests or evaluations that might be used to lessen the uncertainties.
- Conclusions reached during the National Science Foundation workshop titled *International Workshop on the Uncertainties in Nonlinear Soil Properties and Their Impact on Modeling Dynamic Soil Response*, which is planned for March of 2004 at the PEER Center, should provide a basis for deciding where the priorities for future cyclic testing programs might best be directed.

5. References

Darendeli, B.M. (2001). "Development of a New Family of Normalized Modulus Reduction and Material Damping Curves," PhD. Dissertation, University of Texas at Austin, 362 p.

Doroudian, M. and M. Vucetic (1995). "A Direct Simple Shear Device for Measuring Small-Strain Behavior," ASTM Geotechnical Testing Journal, Vol. 18, No. 1, pp. 69-85.

EPRI (1993). "Guidelines for Determining Design Basis Ground Motions – Volume 1: Method and Guidelines for Estimating Earthquake Ground Motion in Eastern North America." Electric Power Research Institute, Report TR-102293.

Hardin, B.O. (1978). "The Nature of Stress-Strain Behavior for Soils," *Proceedings, Earthquake Engineering and Soil Dynamics – Volume I*, ASCE Geotechnical Engineering Division Specialty Conference, Pasadena, June, pp. 3-90.

Hardin, B.O. and V.P. Drnevich (1972). "Shear Modulus and Damping in Soils: Design Equations and Curves," Journal of the Soil Mechanics and Foundations Division, ASCE, Vol. 98, No. SM6, July, pp. 667-692.

Matesic, L. and M. Vucetic (2003). "Strain-Rate Effect on Soil Secant Shear Modulus at Small Cyclic Strains," Journal of Geotechnical and Geoenvironmental Engineering, ASCE, Vol. 129, No. 6, pp. 536-549.

Seed, H.B., R.T. Wong, I.M. Idriss, and K. Tokimatsu (1986), "Moduli and Damping Factors for Dynamic Analyses of Cohesionless Soils," Journal of the Soil Mechanics and Foundations Division, ASCE, Vol. 112, No. SM11, November, pp. 1016-1032.

Vucetic, M. and R. Dobry (1991). "Effect of Soil Plasticity on Cyclic Response," Journal of Geotechnical Engineering, Vol. 117, No. 1, January, pp. 89-107.

Attachment A
Inventory of ROSRINE Samples

Table A-1 Sample Inventory

Site Name	Sample Label	Sample Type	Cored Interval (ft)		Sample Description/Soil Type	Sample Distribution		Comments
			From	To		UCLA	UT	
Meloland	S-1	Shelby	8	10.5	Recovery: 18". Lost bottom 7" of core and top 9". Sand		X	Disturbed Sample
Meloland	S-2	Shelby	18	20	Recovery: 14". Silt (ML)	1/2	1/2	Dark yellowish brown. UCS=0.7tsf
Meloland	S-3	Shelby	28	30	Recovery: 20". Brown clay; sticky, plastic (CL). UCS=3.0 tsf. Silty Clay (CL)	1/2	1/2	Brown clay; sticky, plastic (CL). UCS=3.0 tsf
Meloland	S-4	Shelby	38	40	Recovery: 20". Pushed 20" to refusal; prob. slough in tube. Fine Sand		X	Probably disturbed sample
Meloland	S-5	Shelby	59	61	Recovery: 12". Sandy Silt (ML)	X, c		UCS=1.4 tsf
Meloland	S-6	Shelby	78	79.5	Recovery: 18".Yellowish brown, well-sorted vf running sand (SP) w/ tr silt; probably disturbed in core. Silty Sand (SP)		X	Yellowish brown, well-sorted vf running sand (SP) w/ tr silt
Meloland	S-7	Shelby	98	99.5	Recovery: 18". Silty Sand (SP/SM)	X		UCS 1.0 tsf (after draining)
Meloland	WS-1	Wireline Shelby	118	119.5	Recovery: 18". Greyish brown clay; stiff, mod sticky and plastic (CL). Clay (CL)		X	Greyish brown clay; stiff, mod sticky and plastic

Site Name	Sample Label	Sample Type	Cored Interval (ft)		Sample Description/Soil Type	Sample Distribution		Comments
			From	To		UCLA	UT	
Meloland	WS-3	Wireline Shelby	198	200	Recovery: 20". Dark greyish brown silt loam (CL); sl. sticky and plastic; tr. coal ?		X	
Meloland	WS-4	Wireline Shelby	259	261	Recovery: 13". Grey clay w/ lighter grey silt partings; bedding may be inclined.		X	
Meloland	WS-6	Wireline Shelby	378	380	Recovery: 13". Greyish brown clay; UCS >4.8 tsf. Tube end crumpled.		X	
Meloland	WS-7	Wireline Shelby	438	440	Recovery: 13". Dark grey clay; UCS >4.8 tsf. Tube end crumpled.		X	
Meloland	C-1	USGS core sample	555	560	Recovery: 33". Brown clay, v. sticky and plastic (CL-CH?), stiff; effervescent.		X	
Meloland	C-2	USGS core sample	615	620	Recovery: 46". Dark greyish brown clay, sticky and plastic (CL); firm; viol. effervescence; salty taste		X	
Meloland	C-3	USGS core sample	735	740	Recovery: 40". Dark yellowish brown f-vf sandy loam, non-sticky; v. sl. plastic (ML); sl. effervescence		X	

Site Name	Sample Label	Sample Type	Cored Interval (ft)		Sample Description/Soil Type	Sample Distribution		Comments
			From	To		UCLA	UT	
Meloland	C-4	USGS core sample	795	800	Recovery: 4". Not found 02/26/01 D. Ponti	-	X	
Arleta	P-1	Pitcher/ 2.8	20	22.5	Current Soil Length as of Jan. 18, 2001 Inventory: 24"		X	
Arleta	P-2		15					
Arleta	P-3	Pitcher/ 2.8	81	82.5	Current Soil Length as of Jan. 18, 2001 Inventory: all	X		
Arleta	P-4		31					
Arleta	P-5	Pitcher/ 2.8	141	142.5	Current Soil Length as of Jan. 18, 2001 Inventory: all		X	
Kagel	T-1	Brass Tube/1.9	12.5	13.8	Current Soil Length as of Jan. 18, 2001 Inventory: all		X	
Kagel	T-2	Brass Tube/1.9	17.5	18.5	Current Soil Length as of Jan. 18, 2001 Inventory: all		X	
Kagel	T-3	Brass Tube/1.9	25	27.5	Current Soil Length as of Jan. 18, 2001 Inventory: all		X	
Kagel	T-4	Brass Tube/1.9	40	42.5	Current Soil Length as of Jan. 18, 2001 Inventory: all		X	
Kagel	T-4	Brass Tube/1.9	42.5	45	Current Soil Length as of Jan. 18, 2001 Inventory: all		X	

Site Name	Sample Label	Sample Type	Cored Interval (ft)		Sample Description/Soil Type	Sample Distribution		Comments
			From	To		UCLA	UT	
Kagel	T-5	Brass Tube/1.9	62.5	65	Current Soil Length as of Jan. 18, 2001 Inventory: all		X	
Kagel	T-6	Brass Tube/1.9	82.5	85	Current Soil Length as of Jan. 18, 2001 Inventory: all		X	
Kagel	T-7		31					
Kagel	T-8	Brass Tube/1.9	152.5	155	Current Soil Length as of Jan. 18, 2001 Inventory: all		X	
Kagel	T-9	Brass Tube/1.9	202.5	205	Current Soil Length as of Jan. 18, 2001 Inventory: all		X	
Kagel	T-10	Brass Tube/1.9	210	212.5	Current Soil Length as of Jan. 18, 2001 Inventory: all		X	
Kagel	T-11	Brass Tube/1.9	257.5	260	Current Soil Length as of Jan. 18, 2001 Inventory: all		X	
Kagel	T-12							
La Cienega	S-1	Pitcher/ 2.8	5	7.5	Current Soil Length as of Jan. 18, 2001 Inventory: all		X	
La Cienega	S-2	Pitcher/ 2.8	10	12.5	Current Soil Length as of Jan. 18, 2001 Inventory: all		X	
La Cienega	S-3(b)	Pitcher/ 2.8	15	17.5	Current Soil Length as of Jan. 18, 2001 Inventory: 6"	c		
La Cienega	S-4(a)	Pitcher/ 2.8	20	22.5	Current Soil Length as of Jan. 18, 2001 Inventory: 15"	c		

Site Name	Sample Label	Sample Type	Cored Interval (ft)		Sample Description/Soil Type	Sample Distribution		Comments
			From	To		UCLA	UT	
La Cienega	S-5(a)	Pitcher/ 2.8	25	27.5	Current Soil Length as of Jan. 18, 2001 Inventory: 15"	c		
La Cienega	S-6	Pitcher/ 2.8	30	32.5	Current Soil Length as of Jan. 18, 2001 Inventory: 12"		X	
La Cienega	S-7	Pitcher/ 2.8	35	37.5	Current Soil Length as of Jan. 18, 2001 Inventory: all		X	
La Cienega	S-8	Pitcher/ 2.8	45	47.5	Current Soil Length as of Jan. 18, 2001 Inventory: all		X	
La Cienega	S-9	Pitcher/ 2.8	55.5	58	Current Soil Length as of Jan. 18, 2001 Inventory: all		X	
La Cienega	S-11		34					
La Cienega	T-4a		28					
La Cienega	T-6a		36					
La Cienega	T-9a		52					
La Cienega	T-16a		95					
La Cienega	T-18a		107					
La Cienega	T-21a		125					
La Cienega	T-25a		150					
La Cienega	T-31a		186					
La Cienega	T-36a		218					

Site Name	Sample Label	Sample Type	Cored Interval (ft)		Sample Description/Soil Type	Sample Distribution		Comments
			From	To		UCLA	UT	
La Cienega	T-38a		241					
La Cienega	L1-1		4.9					
La Cienega	L2-1		6.1					
La Cienega	L2-2b		6.4					
La Cienega	L3-1		7.9					
La Cienega	L5-1		25.9					
La Cienega	L6-1		33.6					
La Cienega	UTS2-1		3.4					
Newhall	P-2	Pitcher/ 2.8	55	57.5	Current Soil Length as of Jan. 18, 2001 Inventory: 24"	X, c		
Newhall	P-3		21					
Newhall	P-4	Pitcher/ 2.8	90	92.5	Current Soil Length as of Jan. 18, 2001 Inventory: all		X	
Newhall	P-5		62					
Newhall	P-6	Pitcher/ 2.8	255	257.5	Current Soil Length as of Jan. 18, 2001 Inventory: all		X	
Newhall	T-4	Brass Tube/1.9	163.6	165	Current Soil Length as of Jan. 18, 2001 Inventory: all		X	
Newhall	T-5	Brass Tube/1.9	122.5	125	Current Soil Length as of Jan. 18, 2001 Inventory: all		X	

Site Name	Sample Label	Sample Type	Cored Interval (ft)		Sample Description/Soil Type	Sample Distribution		Comments
			From	To		UCLA	UT	
Pacoima	C-2	ABS 3" Tube	95	100	Current Soil Length as of Jan. 18, 2001 Inventory: all		X	
Tarzana	P-1	Pitcher/ 2.8	10	12.5	Current Soil Length as of Jan. 18, 2001 Inventory: 19"		X	
Tarzana	P-2	Pitcher/ 2.8	20	22	Current Soil Length as of Jan. 18, 2001 Inventory: 8"	c		
Tarzana	P-3	Pitcher/ 2.8	30	32	Current Soil Length as of Jan. 18, 2001 Inventory: 18"		X	
Tarzana	P-4	Pitcher/ 2.8	40	42	Current Soil Length as of Jan. 18, 2001 Inventory: 18"		X	
Tarzana	P-5	Pitcher/ 2.8	100	101.5	Current Soil Length as of Jan. 18, 2001 Inventory: all - 24" - should check/revise depth interval from original log	c		
Tarzana	P-6	Pitcher/ 2.8	196	198	Current Soil Length as of Jan. 18, 2001 Inventory: all		X	
Baldwin Hills	P-1	Pitcher/ 2.8	41	43	Current Soil Length as of Jan. 18, 2001 Inventory: all		X	
Dayton	P-1	Pitcher/ 2.8	10	13	Current Soil Length as of Jan. 18, 2001 Inventory: all		X	
Dayton	P-2	Pitcher/ 2.8	25.0	28	Current Soil Length as of Jan. 18, 2001 Inventory: all	X, c		

Site Name	Sample Label	Sample Type	Cored Interval (ft)		Sample Description/Soil Type	Sample Distribution		Comments
			From	To		UCLA	UT	
Dayton	P-3	Pitcher/ 2.8	50.0	53	Current Soil Length as of Jan. 18, 2001 Inventory: all	Split	X	
Dayton	P-4	Pitcher/ 2.8	70.0	73	Current Soil Length as of Jan. 18, 2001 Inventory: all		X	
Dayton	P-5	Pitcher/ 2.8	100.0	103	Current Soil Length as of Jan. 18, 2001 Inventory: all		X	
ESC #4	Tube-1	Pitcher/ 2.8	10	11.9	Current Soil Length as of Jan. 18, 2001 Inventory: 12"		X	
ESC #11	Tube-4	Pitcher/ 2.8	22.5	24.5	Current Soil Length as of Jan. 18, 2001 Inventory: 6"	c		
ESC #22	Tube-8	Pitcher/ 2.8	52.5	55	Current Soil Length as of Jan. 18, 2001 Inventory: 20"	c		
LA00	-	Pitcher/ 2.8	8.0	11	Could not find during Jan. 18, 2001 Inventory	-	-	
Lake Hughes #9	P-1	Pitcher/ 2.8	6.0	6-8	Current Soil Length as of Jan. 18, 2001 Inventory: 18"		X	
Lake Hughes #9	P-2	Pitcher/ 2.8	70	70.8	Current Soil Length as of Jan. 18, 2001 Inventory: all		X	
Obregon Park	P-2	Pitcher/ 2.8	5.0	8	Current Soil Length as of Jan. 18, 2001 Inventory: 17"	X		
Obregon Park	-	Pitcher/ 2.8	20	23	Current Soil Length as of Jan. 18, 2001 Inventory: 4"	Split	X	

Site Name	Sample Label	Sample Type	Cored Interval (ft)		Sample Description/Soil Type	Sample Distribution		Comments
			From	To		UCLA	UT	
Obregon Park	-	Pitcher/ 2.8	50	53	Current Soil Length as of Jan. 18, 2001 Inventory: 22"	X, c		
Obregon Park	-	Pitcher/ 2.8	60	63	Current Soil Length as of Jan. 18, 2001 Inventory: 16"	Split	X	
Obregon Park	-	Pitcher/ 2.8	70	73	Current Soil Length as of Jan. 18, 2001 Inventory: all	X		
Obregon Park	-	Pitcher/ 2.8	90	93	Current Soil Length as of Jan. 18, 2001 Inventory: all	X		
Obregon Park	-	Pitcher/ 2.8	100	103	Current Soil Length as of Jan. 18, 2001 Inventory: all		X	
Potrero Canyon P-3	S1-1	Shelby/ 2.8	6	8.5	Current Soil Length as of Jan. 18, 2001 Inventory: all		X	
Potrero Canyon P-3	S2-5	Shelby/ 2.8	25	27.5	Current Soil Length as of Jan. 18, 2001 Inventory: all		X	
Potrero Canyon P-3	P1-S2		2.4					
Potrero Canyon P-3	P1-10	Pitcher/ 2.8	115	117.5	Current Soil Length as of Jan. 18, 2001 Inventory: all		X	
Potrero Canyon P-3	P2-S7		8.5					
Potrero Canyon P-3	P4-S12		16					

Site Name	Sample Label	Sample Type	Cored Interval (ft)		Sample Description/Soil Type	Sample Distribution		Comments
			From	To		UCLA	UT	
Potrero Canyon P-3	P6-S18		31					
Rinaldi 2	P-1	Pitcher/ 2.8	5	6.9	Current Soil Length as of Jan. 18, 2001 Inventory: 12"	c		
Rinaldi 2	P-2		2.4					
Rinaldi 2	P-3	Pitcher/ 2.8	15	16.3	Current Soil Length as of Jan. 18, 2001 Inventory: 6"	c		
Rinaldi 2	P-5		7.6					
Rinaldi 2	P-7	Pitcher/ 2.8	32	33.3	Current Soil Length as of Jan. 18, 2001 Inventory: all		X	
Rinaldi 2	P-8		11					
Rinaldi 2	P-9	Pitcher/ 2.8	37.5	39	Current Soil Length as of Jan. 18, 2001 Inventory: all		X	
Rinaldi 2	P-10		15					
Rinaldi 2	P-11	Pitcher/ 2.8	60	61	Current Soil Length as of Jan. 18, 2001 Inventory: all		X	
Rinaldi 2	P-12		21					
Saturn	P-1	Pitcher/ 2.8	10.0	13	Current Soil Length as of Jan. 18, 2001 Inventory: 24"	X		

Site Name	Sample Label	Sample Type	Cored Interval (ft)		Sample Description/Soil Type	Sample Distribution		Comments
			From	To		UCLA	UT	
Saturn	P-2	Pitcher/ 2.8	25.0	28	Current Soil Length as of Jan. 18, 2001 Inventory: 3"		X	
Saturn	P-3	Pitcher/ 2.8	50.0	53	Current Soil Length as of Jan. 18, 2001 Inventory: 24"	X, c		
Saturn	P-4	Pitcher/ 2.8	100	103	Current Soil Length as of Jan. 18, 2001 Inventory: all		X	
LA Bulk Mail	P-1	Pitcher	15	18	Recovery: 25". Silt and clay.	X		
LA Bulk Mail	P-2	Pitcher	20	23	Recovery: 27.5". Silt and clay.		X	
LA Bulk Mail	P-3	Pitcher	50	53	Recovery: 27.5". Silt.	X		
LA Bulk Mail	P-4	Pitcher	100	103	Recovery: 36". Silt and clay.		X	
LA Bulk Mail	P-5	Pitcher	165	168	Recovery: 36". Silt.		X	
LA Bulk Mail	P-6	Pitcher	205	208	Recovery: 26". Sand and silt.		X	
LA Bulk Mail	P-7	Pitcher	265	268	Recovery: 28". Sand and silt.		X	
LA Bulk Mail	P-8	Pitcher	325	328	Recovery: 24". Eroded bed rock contact.		X	

Site Name	Sample Label	Sample Type	Cored Interval (ft)		Sample Description/Soil Type	Sample Distribution		Comments
			From	To		UCLA	UT	
Yermo	P-1	Pitcher	10	13	Recovery: 18.5". Sand.	X		
Yermo	P-3	Pitcher	40	43	Recovery: 30". Silt.		X	
Yermo	P-4	Pitcher	80	83	Recovery: 22.5". Sand.	X		
Yermo	P-5	Pitcher	153	156	Recovery: 18". Sand.		X	
Yermo	P-6	Pitcher	200	203	Recovery: 25". Fine sand and silt.		X	
Yermo	P-7	Pitcher	265	268	Recovery: 36". Fine sand.		X	
Yermo	P-8	Pitcher	325	328	Recovery: 15". Sand and gravel.		X	
Joshua Tree	P-2	Pitcher	20	23	Recovery: 20.5". Sand.		X	
Joshua Tree	P-3	Pitcher	40	43	Recovery: 36". Sand.	X		
Joshua Tree	P-4	Pitcher	75	78	Recovery: 21". Sand.		X	
Joshua Tree	P-5	Pitcher	160	163	Recovery: 12". Sand.		X	
Joshua Tree	P-7	Pitcher	235	238	Recovery: 32". Sand.		X	
Joshua Tree	P-8	Pitcher	327	330	Recovery: 18". Sand.		X	

Site Name	Sample Label	Sample Type	Cored Interval (ft)		Sample Description/Soil Type	Sample Distribution		Comments
			From	To		UCLA	UT	
Gilroy #3	P-1	Pitcher	15	18	Recovery: 36". Silt and sand.	X		
Gilroy #3	P-2	Pitcher	50	53	Recovery: 16". Gravel.		X	
Gilroy #3	P-3	Pitcher	80	83	Recovery: 29". Silt and gravel.		X	
Gilroy #3	P-4	Pitcher	180	183	Recovery: 29". Silt and sand, some gravel.		X	
Gilroy #3	P-5	Pitcher	355	358	Recovery: 19". Silt and sand, some gravel.		X	
Halls Valley	P-1	Pitcher	6	9	Recovery: 22". Silty clay.		X	
Halls Valley	P-2	Pitcher	15	18	Recovery: 36". Silty clay.	X		
Halls Valley	P-3	Pitcher	50	53	Recovery: 36". Clay.		X	
Halls Valley	P-4	Pitcher	110	113	Recovery: 23". Clay and greenstone.		X	
Sepulveda	S-1		2.4					
Sepulveda	S2-1		3.1					
Sepulveda	S2-2		3.4					
Sepulveda	T-1		14					
Sepulveda	T-2		17					

Site Name	Sample Label	Sample Type	Cored Interval (ft)		Sample Description/Soil Type	Sample Distribution		Comments
			From	To		UCLA	UT	
Sepulveda	T-4		37					
Sepulveda	T-5		59					
Sepulveda	T-6		86					

Attachment B
University of California at Los Angeles
Report for DSDSS Testing

RESULTS OF CYCLIC SIMPLE SHEAR TESTS ON FIFTEEN SOILS CONDUCTED FOR *PEARL* PROJECT AND OTHER RESEARCH PURPOSES

by

Kentaro Tabata[1] and Mladen Vucetic[2]

Civil and Environmental Engineering Department
University of California, Los Angeles
Los Angeles, CA 90095-1593

UCLA Research Report No. UCLA-Eng 02-233

November 2002

[1] Ph.D. candidate, Civil and Environmental Engineering Department, University of California, Los Angeles, CA 90095-1593.
[2] Professor, Civil and Environmental Engineering Department, University of California, Los Angeles, CA 90095-1593.

ABSTRACT

The report contains results of fifteen cyclic (repetitive loading) tests conducted in cyclic strain-controlled stages in a Norwegian Geotechnical Institute (NGI) type of direct simple shear (DSS) apparatus designed specifically for the small-strain testing. The DSS specimens were trimmed from the well-preserved intact soil samples retrieved at seven different seismically active locations in Southern California. From each test, the following cyclic soil relationships and properties are obtained and presented in the report: (i) strain-time history, (ii) stress-time history, (iii) stress-strain cyclic loops, (iv) secant shear modulus reduction with cyclic shear strain amplitude, (v) the variation of the equivalent viscous damping ratio with cyclic shear strain amplitude and (vi) the soil classification properties. The range of applied cyclic shear strain amplitudes was wide, from very small of approximately 0.0003 % to relatively large of 3.2 %.

The testing was done as a part of the research project "Program of Earthquake-Applied Research for Lifelines", abbreviated as PEARL. The PEARL project is a collaborative project focused on obtaining high-quality nonlinear properties of different soils relevant for the estimation and understanding of the near-fault ground motions during strong earthquakes. PEARL is a component of the Lifeline Program at the Pacific Earthquake Engineering Research (PEER) Center.

ACKNOWLEDGEMENTS

The tests and investigation described in this report were conducted at the UCLA Soil Dynamics Laboratory. The research was done as a part of the project "Program of Earthquake-Applied Research for Lifelines", abbreviated as PEARL, which is a component of the Lifeline Program at the Pacific Earthquake Engineering Research (PEER) Center. PEARL is a collaborative research project between the University of Texas at Austin research team lead by Professor Kenneth Stokoe, UCLA team lead by the second author of this report, the California Department of Transportation from Sacramento represented by Dr Clifford Roblee, and the CH2M HILL company from Bellevue, Washington, represented by Dr. Donald Anderson who was the manager of the project.

The financial support was provided by the California Department of Transportation, the Pacific Gas & Electric Company, California Energy Commission and the Pacific Earthquake Engineering Research (PEER) Center. Additional valuable support came from the Okinawa International Exchange and Human Resources Development Foundation (OIHF) which covered the costs of the Ph.D. studies of the first author. The above supports are gratefully acknowledged. The authors also wish to thank Dr. Chu-Chung Hsu, lecturer and researcher at UCLA, for his help in conducting the testing.

TABLE OF CONTENTS

1 INTRODUCTION

1.1 PEARL project

Project "Program of Earthquake-Applied Research for Lifelines" abbreviated as PEARL is a collaborative project focused on obtaining high-quality nonlinear properties of different soils relevant for the estimation and understanding of the near-fault ground motions during strong earthquakes. It is a component of the Lifeline Program at the Pacific Earthquake Engineering Research (PEER) Center. Such properties can improve existing engineering methods and models for the estimation of the near-fault earthquake ground motions which are often responsible for significant portion of earthquake damages. The relevant properties investigated in PEARL are: (1) maximum shear modulus, G_{max}, (2) variation of the secant shear modulus, G_s, with cyclic shear strain, γ_c, (3) variation of the normalized secant shear modulus G_s/G_{max} with cyclic shear strain, γ_c, and (4) variation of the equivalent viscous damping ratio, λ, with cyclic shear strain amplitude, γ_c.

PEARL project has been coordinated through the Pacific Earthquake Engineering Research (PEER) Center headquartered at UC Berkeley. It included two cyclic testing laboratory teams, one at the University of Texas (UT) at Austin supervised by Professor Kenneth Stokoe and the other at UCLA supervised by Professor Mladen Vucetic. The UT team conducted resonant column/torsional shear cyclic tests, while the UCLA team conducted cyclic simple shear tests. The manager of the project was Dr. Donald Anderson from the CH2M HILL company from Bellevue, Washington, while Dr Clifford Roblee from the California Department

of Transportation, Sacramento, California, coordinated the activities and provided technical input on behalf of the project sponsors.

1.2 Previous similar investigations at the UCLA Soil Dynamics Laboratory

Before this investigation, four similar investigations were conducted at the UCLA Soil Dynamics Laboratory. They were all the parts of the project "Resolution of Site Response Issues from the Northridge Earthquake" abbreviated as ROSRINE which was also a collaborative research project focused on improving existing engineering methods and models for the estimation of earthquake ground motions. ROSRINE project has been coordinated through the Southern California Earthquake Center (SCEC), bringing together under one umbrella a highly organized and structured group of geologists, geophysicists, geotechnical engineers and engineering seismologists to address long-standing geotechnical site characterization and ground motion response issues which resurfaced during the 1994 Northridge earthquake (Nigbor et al., 1997; Roblee, et al., 1998; Schneider. et al., 1997). These four previous investigations are described in the following reports:

1. Hsu, C.-C. and Vucetic, M. (1998): Results of classification tests for ROSRINE project, *UCLA Research Report*, No. ENG-98-199, Civil and Environmental Engineering Department, University of California, Los Angles, 260 p.

2. Vucetic, M., Hsu, C.-C., and Doroudian, M. (1998): Results of cyclic and dynamic simple shear tests on soils from La Cienega site conducted for ROSRINE project and other research purposes, *UCLA Research Report*, No. ENG-98-200, Civil and Environmental Engineering Department, University of California, Los Angles, 440 p.

3. Hsu, C.-C. and Vucetic, M. (1999): Results of cyclic and dynamic simple shear tests on soils from Tarzana and Rinaldi sites conducted for ROSRINE project and other research purposes, *UCLA Research Report*, No. ENG-99-205, Civil and Environmental Engineering Department, University of California, Los Angles, 263 p.

4. Tabata, K. and Vucetic, M. (2000): Results of cyclic simple shear tests on thirteen soils from Los Angeles basin conducted for ROSRINE project and other research purposes, *UCLA Research Report*, No. ENG-00-219, Civil and Environmental Engineering Department, University of California, Los Angles, 284 p.

The tests presented in this report were conducted in the similar manner as the tests presented in the above reports.

1.3 Objectives of the investigation

The investigation described in this report had two main objectives, as explained below.

1.3.1 Primary objective

The primary objective was to determine the dynamic and cyclic properties of soils from seven seismically-active Southern California sites in the Norwegian Geotechnical Institute (NGI) type of direct simple shear (DSS) testing apparatus for the purposes of the PEARL project. These seven sites, named after their locations, are: Meloland, Obregon Park, LA Bulk Mail, Halls Valley, Yermo, Joshua Tree, and Gilroy #3. The scope of the testing covering this primary objective was determined by the PEARL sponsors and technical staff.

1.3.2 Secondary objective

The secondary objective was to investigate certain general aspects of the dynamic and cyclic soil behavior that have not been well understood or investigated to a satisfactory extent, along the lines of the research that has been conducted at the UCLA Soil Dynamics Laboratory for a number of years. These aspects are, for example, the effect of the shape of cyclic loading on cyclic response, the effects of frequency and strain rate on cyclic properties, and the values of the cyclic threshold shear strain in clayey soils. The investigation of these and some other aspects of cyclic loading behavior was facilitated by extending the original scope of the testing prescribed by the PEARL project.

1.4 Scope of the investigation

A total of fifteen cyclic direct simple shear (DSS) tests of the Norwegian Geotechnical Institute (NGI) type were conducted in several cyclic strain-controlled stages in a unique DSS device designed specifically for small-strain testing. The following parameters and relationships have been derived from the test results and are presented in this report:

- applied shear strain, γ, time histories,
- obtained shear stress, τ, time histories,
- stress-strain cyclic loops,
- variation of secant shear modulus, G_s, with cyclic shear strain amplitude, γ_c, commonly called the secant shear modulus reduction curve, or simply the modulus reduction curve,

- maximum secant shear modulus, G_{max}, estimated at the cyclic shear strain amplitude $\gamma_c = 0.0001$ % by extrapolation of the secant shear modulus reduction curve,

- variation of the normalized secant shear modulus, G_s/G_{max}, with γ_c commonly called the normalized modulus reduction curve, and

- variation of the equivalent viscous damping ratio, λ, with γ_c.

The range of the applied cyclic shear strain amplitudes, γ_c, was wide, from very small of approximately 0.0003 % to 3.2 %. For each specimen tested, the geotechnical classification tests were performed as well. They included specific gravity test, wet sieve analysis, hydrometer test, Atterberg plastic limit test and Atterberg liquid limit test.

The testing program is summarized below in Table 1.4.1.

1.5 Types of soil samples delivered for testing

The soil samples were delivered in the standard thin-wall tubes, which are 2.8 inches in diameter. The sampling was done with either pitcher sampler or Shelby tube sampler. The 2.8-inch samples seemed to be intact, i.e., well preserved "undisturbed" samples.

Table 1.4.1 Summary of testing program.

Test No.	Site location	Sample label	Depth (ft)	Classification symbol	Liquid limit LL (%)	Plasticity index PI	Void ratio e	Degree of saturation S_r (%)	Unit weight (kN/m^3)	Water content w (%)	Vertical stress σ_{vc} (kPa)
1	Meloland	S-2	18-20	ML	26.6	3.5	0.62	99.6	19.7	23.4	55
2		S-3	28-30	CH	60.8	29.8	0.78	90.9	19.0	25.9	101
3		S-5	59-61	CL	29.5	15.8	0.67	96.6	19.6	24.0	187
4		S-7	98-100	CL	41.0	21.2	0.69	95.2	19.2	24.9	308
5	Obregon Park	P-5	50-53	CH	50.5	22.9	0.61	95.3	19.9	22.4	211
6		P-7	70-73	ML	37.7	11.6	0.55		19.9	19.3	281
7		P-9	90-93	CL	41.0	21.2	0.48	90.7	20.8	16.6	361
8	LA Bulk Mail	P-1	15-18	CL	26.3	8.1	0.51	94.4	20.8	17.8	94
9		P-3	50-53	ML	47.5	18.0	0.70	99.7	19.7	25.7	289
10	Halls Valley	P-1	6-9	CL	42.1	26.1	0.75	93.5	18.9	26.4	37
11		P-2	15-18	CL	38.2	24.6	0.87	95.2	18.4	32.5	105
12		P-3	50-53	CH	84.7	47.2	1.08		17.7	42.7	274
13	Yermo	P-4	80-83	SM	NP	NP	0.59	55.2	18.6	12.5	480
14	Joshua Tree	P-3	40-43	SM-SC	15.5	5.7	0.44	84.2	21.0	13.7	276
15	Gilroy #3	P-1	15-18	CL	28.9	14.6	0.57	98.8	20.1	22.9	108

2 DESCRIPTION OF CYCLIC DIRECT SIMPLE SHEAR AND CLASSIFICATION TESTS CONDUCTED

2.1 Direct simple shear testing

2.1.1 Simple shear testing concept

Simple shear testing has become increasingly relevant because of both the greater awareness of the importance of stress-strain anisotropy in geotechnical problems and its simplicity relative to triaxial and hollow-cylinder testing. Since the development of early simple shear device prototypes, including the cylindrical Swedish Geotechnical Institute (SGI) type (Kjellman, 1951), the rectangular Cambridge type (Roscoe, 1953) and the cylindrical Norwegian Geotechnical Institute (NGI) type (Bjerrum and Landva, 1966), the interest in the test has grown. The simple shear apparatuses are designed for the testing of soil specimens under the conditions of simple shear strains, which can reasonably well simulate pure shear stress conditions. These conditions cannot be obtained directly with other standard laboratory tests, and yet they are applicable to a number of common field situations (e.g., horizontal segment of the slope failure surface and foundation bearing capacity failure surface, behavior of soil surrounding vertically loaded piles, etc.). In soil dynamics, the role of simple shear testing is particularly significant. In the cyclic simple shear test, the stress-strain conditions correspond rather closely to those occurring during the propagation of shear waves through soil deposits. A typical example of the utilization of simple shear conditions in geotechnical earthquake engineering is shown on Fig. 2.1.1.1, where an idealized case of vertically propagating seismic shear waves commonly considered in practice is presented. In the analysis of seismic site response, the *vertically* propagating shear waves are considered extremely important, because the resulting *horizontal shaking* of ground surface causes major damage to civil engineering structures.

2.1.2 UCLA dual-specimen direct simple shear (DSDSS) test

The tests presented in this report were conducted in a unique DSS device designed specially for the small-strain cyclic testing. The device was designed at the UCLA Soil Dynamics Laboratory by Doroudian and Vucetic (1995) and was named the dual-specimen direct simple shear (DSDSS) device. The device has been already used for the investigations of several important cyclic soil properties at very small cyclic shear strain amplitudes (Doroudian and Vucetic, 1998; Lanzo et al., 1997; Vucetic et al., 1998b; 1998c). The key features of the DSDSS device, which are relevant for the understanding of the test results presented in this report, are summarized below. A full, detailed description of the DSDSS device can be found in Doroudian and Vucetic (1995)

The DSDSS device is illustrated in Fig. 2.1.2.1, while the principles of the testing are shown in Fig. 2.1.2.2. It can be seen in Fig. 2.1.2.2 that the most unique feature of the apparatus is that two parallel specimens of the same soil are tested simultaneously, instead of just one. Such a special configuration, in conjunction with very stiff components of the device and high-precision non-contact displacement transducer, enables almost complete elimination of problems associated with false deformations, system compliance and friction. As a result of such a design, very small strains and stresses can be applied and measured accurately in a controlled manner.

2.1.3 Specifics of the tests presented in this report

The tests presented in this report were conducted under the constant volume conditions, which are equivalent to undrained conditions (Bjerrum and Landva, 1966). In general, such tests are appropriate for the testing of fully saturated soils. As shown in Table 1.4.1, the specimens tested in the present investigation were not fully saturated, although the degree of saturation in

almost all of them was high. However, at very small cyclic shear strain amplitudes, γ_c, smaller than the volumetric cyclic threshold shear strain, γ_{tv}, the volume changes in partially saturated and dry soils are negligible. As described by Dobry et al. (1982) and Vucetic (1994b), if γ_c smaller than γ_{tv} is applied, soil microstructure practically does not change. Hence the constant volume testing can be used to describe the cyclic behavior of partially saturated soils at small cyclic strains. The tests presented in this report have been conducted mainly in the domain of small γ_c below γ_{tv}.

The specimens tested had the diameter of 66.7 mm and height of approximately 18 to 19 mm. For their trimming, a special NGI DSS trimming apparatus, shown in Fig. 2.1.3.1, was used. In the NGI DSS trimming apparatus the specimen is always confined and supported during the trimming within a steel ring knife, which reduces the specimen disturbance during trimming to a minimum.

Each specimen was consolidated to the estimated total vertical stress, σ_{vc}, before the application of cyclic shear loading. The values of the applied σ_{vc} are listed in Table 1.4.1. These values were estimated from the unit weights of specimens and the ground water table levels provided by other PEARL researchers. It should be noted from the individual test results in Chapter 3 below that in some cases the ground water table level estimates and specimen moisture contents are not in agreement.

In the investigation described in this report, the DSDSS cyclic tests had multiple cyclic stages. The cyclic shear strain amplitude, γ_c, was approximately constant in each stage, but larger in each consecutive stage, varying generally from 0.0003 % to 3.2 %. Each test had

typically seven consecutive cyclic strain-controlled stages with the following levels of γ_c: 0.0003 %, 0.001 %, 0.003 %, 0.01 %, 0.03 %, 0.1 % and 3.2 %.

It should be noted that γ_c of approximately 0.1 % applied in the sixth stage is larger than the volumetric cyclic threshold shear strain, γ_{tv}, of the non-plastic and low-plasticity soils tested, and probably larger than γ_{tv} of some high-plasticity soils tested. In the seventh stage, $\gamma_c \approx 3.2\%$ was well beyond γ_{tv} of any type of soil. As described by Dobry et al. (1982) and Vucetic (1994b), if $\gamma_c > \gamma_{tv}$ is applied, the soil microstructure is permanently changed, resulting in the change of shear stiffness, permanent pore water pressure change in fully-saturated soils, and volume change (cyclic settlement) in partially-saturated and dry soils. Consequently, the effects of such changes should be considered when using the test data obtained in this investigation at $\gamma_c \gg \gamma_{tv}$, in particular the effects that changes in the sixth stage might have had on the results obtained in the seventh stage.

The recorded data were processed with a modern data acquisition system.

2.2 Soil classification testing

2.2.1 Introduction

As already mentioned, on all fifteen soil specimens the following classification tests were conducted, if applicable: wet sieve analysis test, hydrometer test, Atterberg liquid limit test, Atterberg plastic limit test, and specific gravity test.

Sieve analysis and hydrometer tests were conducted to construct the grain size distribution curves. The specific gravity test results were used to interpret the hydrometer test

results. The Atterberg limits tests were conducted on the fines passing sieve #40 with the diameter of openings of 0.425 mm, and were used to determine the locations of the fines in the Unified Soil Classification System (USCS) plasticity chart. The grain size distributions and the results of Atterberg limits tests were used jointly to determine the classification symbols of the soils tested according to the USCS. The color of samples was also identified.

For convenience, the classification tests and USCS are described below for those readers whose background is not geotechnical engineering.

2.2.2 Unified Soil Classification System - USCS

Classification of soils was determined according to the American Society for Testing Materials (ASTM) standard ASTM D 2487-90 (1992), titled "Standard Test Method for Classification of Soils for Engineering Purposes." The ASTM D 421-85 (1992) standard titled "Standard Practice for Dry Preparation of Soil Samples for Particle-Size Analysis and Determination of Soil Constants" was also taken into consideration throughout the classification testing.

2.2.3 Wet sieve analysis test

Wet sieve analysis tests were done according to the standard ASTM D 422-63 (1992), titled "Standard Test Method for Particle-Size Analysis of Soil." The wet sieve analysis tests were conducted instead of the dry sieve analyses in order to obtain more appropriate grain size distribution curves. In a dry sieve analysis test, many soil particles, in particular the small size particles, are held together by inter-granular forces throughout the process of sieving. This causes such bonded particles to act as if they are large size particles. The sieve analysis test was

conducted to construct the grain size distribution curve for the range of grains from large to small which are retained on the sieve #200. The #200 sieve has the openings of 0.075 mm. For the smaller particles passing the #200 sieve, the grain size distribution was determined with the help of the hydrometer test.

2.2.4 Hydrometer test

Hydrometer tests were done according to the ASTM D 422-63 (1992) standard titled "Standard Test Method for Particle-Size Analysis of Soil." In the test, the density of a mixture of soil and water in a glass sedimentation cylinder of standard dimensions is recorded with time. Due to the continuous falling of the particles to the bottom of the cylinder the density of the mixture changes with time. Larger particles are falling faster than smaller, which allows a derivation of a correlation between the relative amounts of certain particle sizes and the change of the density of the mixture. The test is conducted with approximately 50 grams of soil passing the #200 sieve. The results of the wet sieve analysis and hydrometer analysis are combined to obtain the grain size distribution curve for the entire range of soil particle sizes present in the soil sample.

2.2.5 Atterberg liquid limit and plastic limit tests and USCS plasticity chart

Atterberg limits tests were done according to the ASTM D 4318-84 (1992) standard, titled "Standard Test Method for Liquid Limit, Plastic Limit and Plasticity Index of Soils." Atterberg limits, named after Swedish soil scientist A. Atterberg, are water content values at which notable changes in soil behavior occur.

The *liquid limit*, denoted LL, marks transition between liquid and plastic behavior. At water content above LL the soil behaves as a viscous liquid, while below LL the soil behaves as a plastic solid. LL is determined in the geotechnical laboratory by partly filling a standard brass cup with thoroughly mixed wet soil (with a depth of about 10 mm at its deepest point) and cutting a groove of a standard dimensions in the soil. The value of LL is taken as the water content at which the groove closes over the length of 13 mm (1/2 inch) when the cup is dropped 10 mm exactly 25 times at a rate of 1.9 to 2.1 drops per second.

The *plastic limit*, denoted PL, is the transition between plastic and brittle behavior. It is determined in the geotechnical laboratory as the water content at which a thread of soil having the diameter of 3.2 mm (1/8 inch) begins to crumble when rolled under the palm of the hand.

From the liquid limit and plastic limit test results, the *plasticity index*, PI = LL – PL, can be determined. PI shows how much water must be added to the soil at plastic limit to bring it to the liquid limit. In other words, PI corresponds to the minimum amount of water required to transform the soil from brittle to liquid, or the water content over which the soil behaves as a plastic material. PI depends on the size and shape of the grains, mineralogy of the grains and chemistry of water.

2.2.6 Relation between soil's plasticity index and cyclic soil properties

Plasticity index, PI, can be conveniently related to several fundamental dynamic and cyclic soil properties used in nonlinear site response analyses. The charts and tables describing the relations between the PI values and cyclic soil properties can be found, among others, in the following papers: Dobry and Vucetic (1987), Vucetic and Dobry, (1991) and Vucetic (1994a; 1994b).

In this report, the normalized modulus reduction curves, $G_s/G_{\max}$ vs. $\log\gamma_c$, and the equivalent viscous damping ratio curves, λ vs. $\log\gamma_c$, are compared to the same type of average curves for different soils plasticity indices, PI, proposed by Vucetic and Dobry (1991).

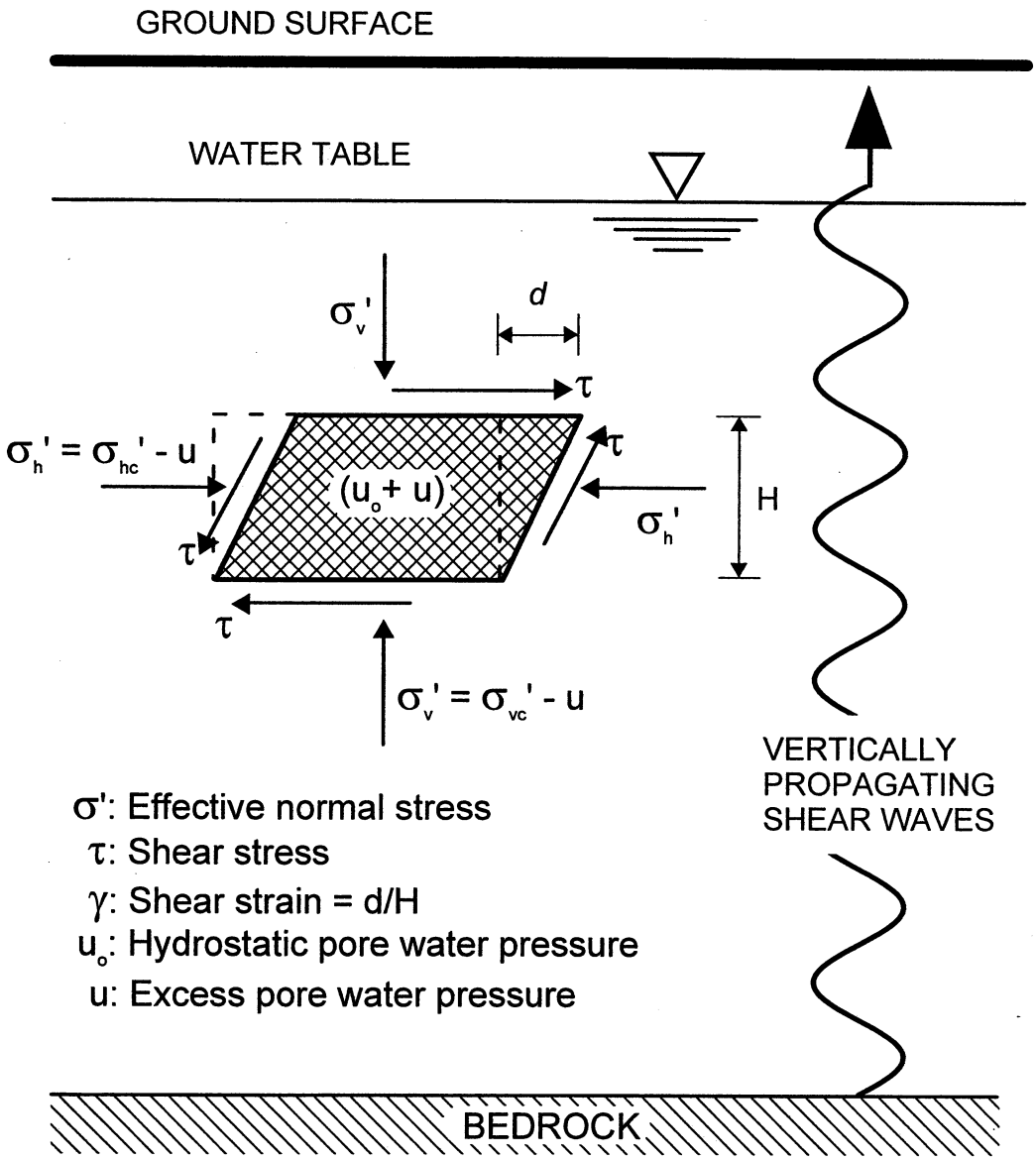

Fig. 2.1.1.1 Idealized stress-strain conditions of a soil element at level ground during earthquakes

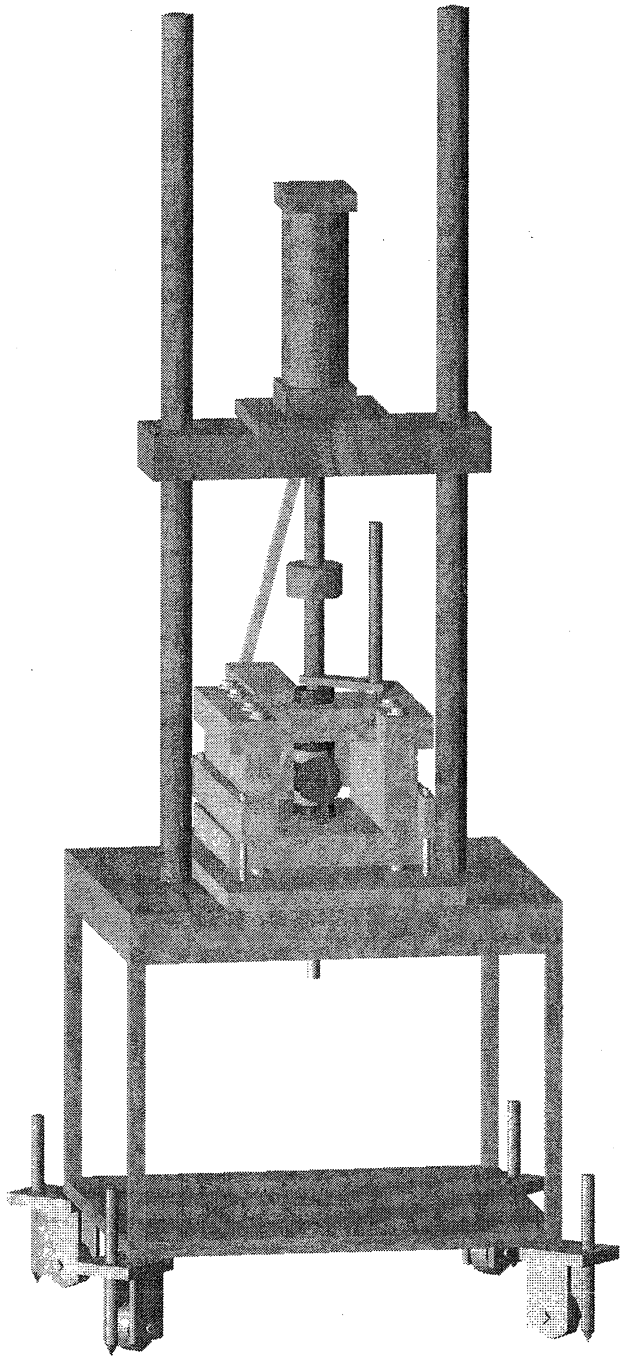

Fig. 2.1.2.1 Dual-specimen direct simple shear (DSDSS) device (after Doroudian and Vucetic, 1995)

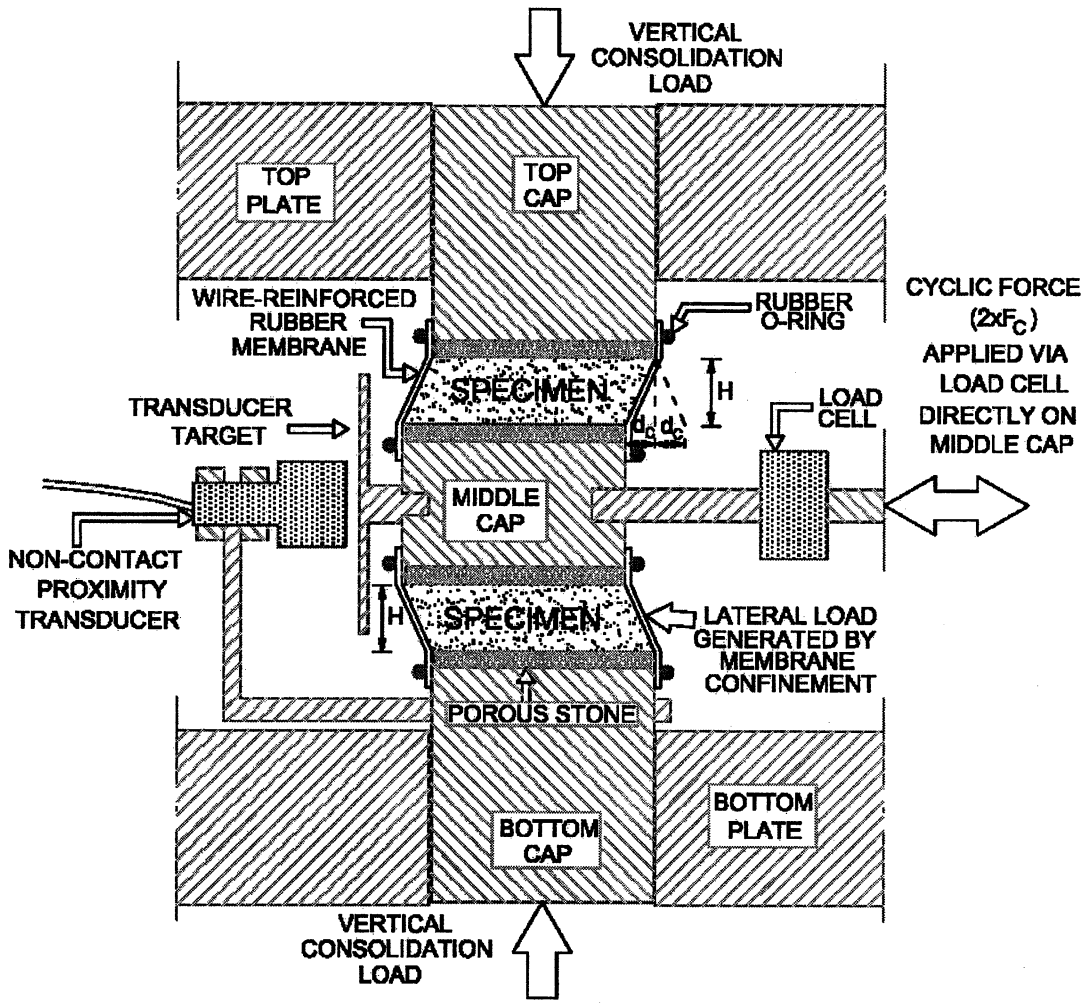

d_C = horizontal cyclic displacement amplitude
F_C = horizontal cyclic shear force
H = height of specimen
A = area of specimen
$\gamma_C = d_C / H$ = horizontal cyclic shear strain amplitude
$\tau_C = F_C / A$ = horizontal cyclic shear stress amplitude

Fig. 2.1.2.2 Illustration of the principles of testing with the dual-specimen direct simple shear (DSDSS) device (Doroudian and Vucetic, 1995)

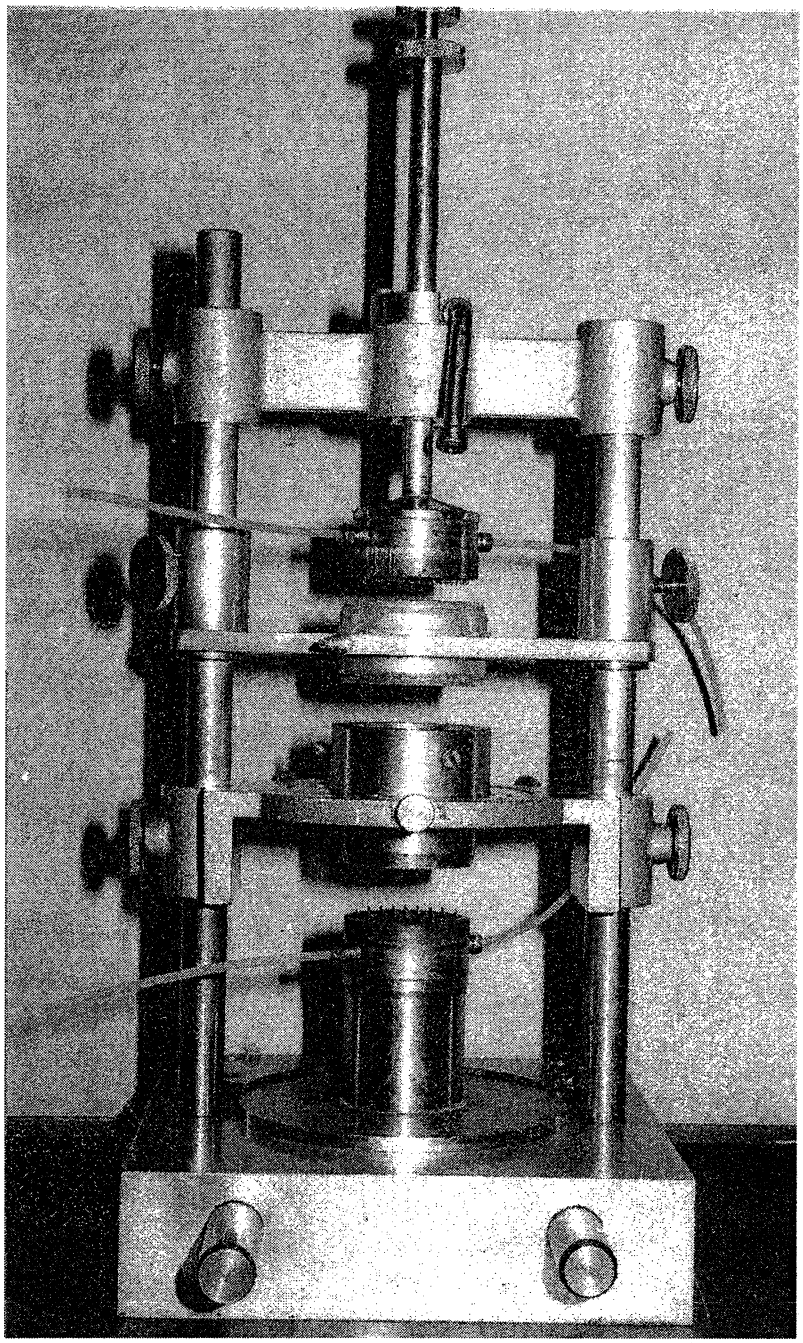

Fig. 2.1.3.1 NGI DSS trimming apparatus

3 TEST RESULTS

3.1 Test data interpretation

In order to understand the test results presented in this chapter, the parameters and relationships that are employed to describe them are defined below.

3.1.1 Definition of parameters

In Figure 3.1.1.1, an idealized cyclic stress-strain loop representative of the loops typically obtained in a cyclic simple shear test is presented. As shown in the figure, such cyclic behavior can be characterized with the following parameters:

$\tau =$ shear stress,

$\gamma =$ shear strain,

$\tau_c =$ cyclic shear stress amplitude,

$\gamma_c =$ cyclic shear strain amplitude,

$G_{max} =$ maximum shear modulus, and

$G_s =$ secant shear modulus corresponding to τ_c and γ_c.

From such a loop, the parameter called the equivalent viscous damping ratio, λ, can be determined as well. The definition of λ used in this report is illustrated in Fig. 3.1.1.2. The ratio λ is expressed by the equation:

$$\lambda = \frac{1}{4\pi}\frac{\Delta W}{\frac{\gamma_c \tau_c}{2}} = \quad \text{equivalent viscous damping ratio, where}$$

$\Delta W =$ area of loop.

In soil dynamics and geotechnical earthquake engineering practice, the cyclic soil behavior is conveniently characterized by several relationships that combine above parameters. These relationships are described below and are developed for the fifteen specimens tested in this investigation.

3.1.2 Modulus reduction curve, G_s versus γ_c, presented in a semi-logarithmic format

The evaluation of secant shear modulus, G_s, is very important in soil dynamics. Secant shear modulus, G_s, is often used as a constant shear modulus in linear wave propagation and lumped parameter system dynamic analyses.

In Fig 3.1.2.1a, an example of such a modulus reduction curve is presented. Seed and Idriss (1970) originally suggested such presentation in a semi-logarithmic format. The semi-log presentation emphasizes modulus reduction in the range of small strains that are usually dominant in the soil dynamics and geotechnical earthquake engineering problems.

3.1.3 Normalized modulus reduction curve, G_s/G_{max} versus γ_c, presented in a semi-logarithmic format

Considering that variation of both G_s and G_{max} depends on more or less the same parameters, such as the confining or vertical stress, σ_{vc}, overconsolidation ratio, OCR, and void ratio (see Dobry and Vucetic, 1987), in particular in the range of small γ_c, it is convenient to present the reduction of G_s modulus with γ_c in the normalized form with respect to G_{max}, i.e., in

the G_s/G_{max} versus γ_c format. Consequently, the shape of the normalized modulus reduction curve, G_s/G_{max} versus $\log\gamma_c$, depends predominantly on the type of soil, instead of the parameters listed above. An example of the G_s/G_{max} versus $\log\gamma_c$ modulus reduction curve is presented in Fig. 3.1.2.1b.

3.1.4 Equivalent viscous damping ratio curve, λ versus γ_c, presented in a semi-logarithmic format

The evaluation of the variation of the equivalent viscous damping ratio, λ, with γ_c is also very important in soil dynamics. Just like the secant shear modulus, G_s, damping ratio λ is often used in the wave propagation and lumped parameter system dynamic analyses. The equivalent viscous damping ratio, λ, describes approximately the critical damping ratio, β, of a one-degree-of-freedom system subjected to a harmonic forcing function having the frequency equal to the natural frequency of the system. The definition of the ratio β in terms of the area of the cyclic loop, ΔW, was derived by Jacobsen (1930) and is illustrated in Fig. 3.1.4.1. In Fig 3.1.2.1c, an example of the λ versus $\log\gamma_c$ curve is presented. Again, as shown, this relationship between λ and γ_c is customarily presented in design practice in a semi-log format.

3.1.5 Specifics of the data interpretation in this investigation

In the first six cyclic strain-controlled stages of each test, the values of G_s and λ were derived from the results obtained in the first two to four cycles. In the last seventh stage of each test, the values of G_s were derived from the first quarter of the first cycle, considering that the corresponding stress-strain loading curve is essentially a monotonic loading curve. In some tests, the seventh stage consisted of only half a cycle, or just the monotonic loading part.

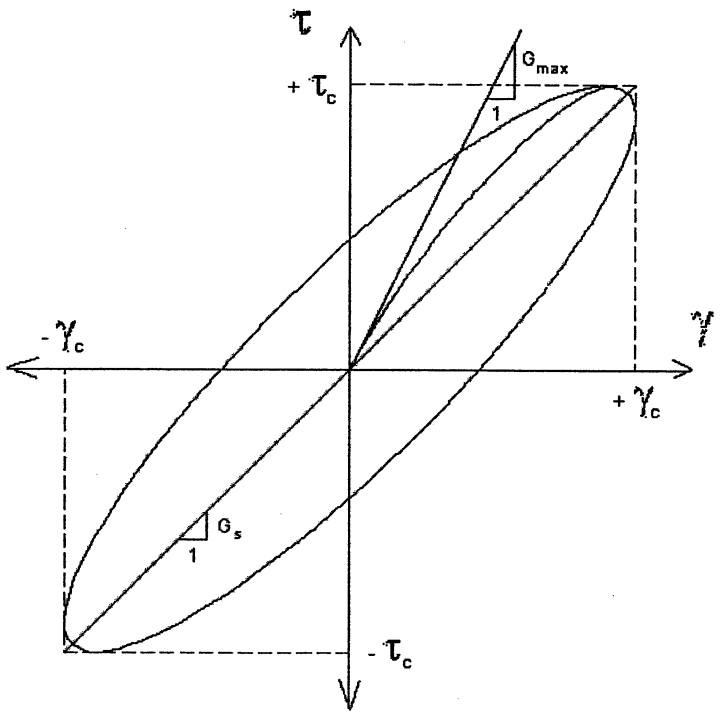

Fig. 3.1.1.1 Idealized cyclic stress-strain loop with relevant parameters

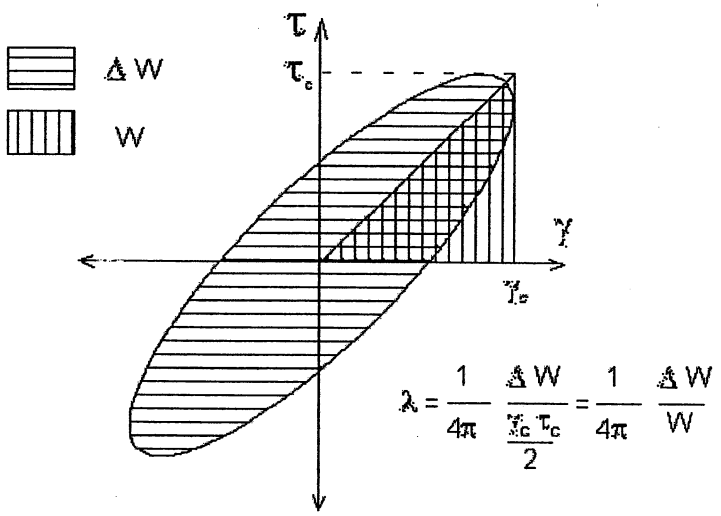

Fig. 3.1.1.2 Definition of the equivalent viscous damping ratio, λ, used in this report

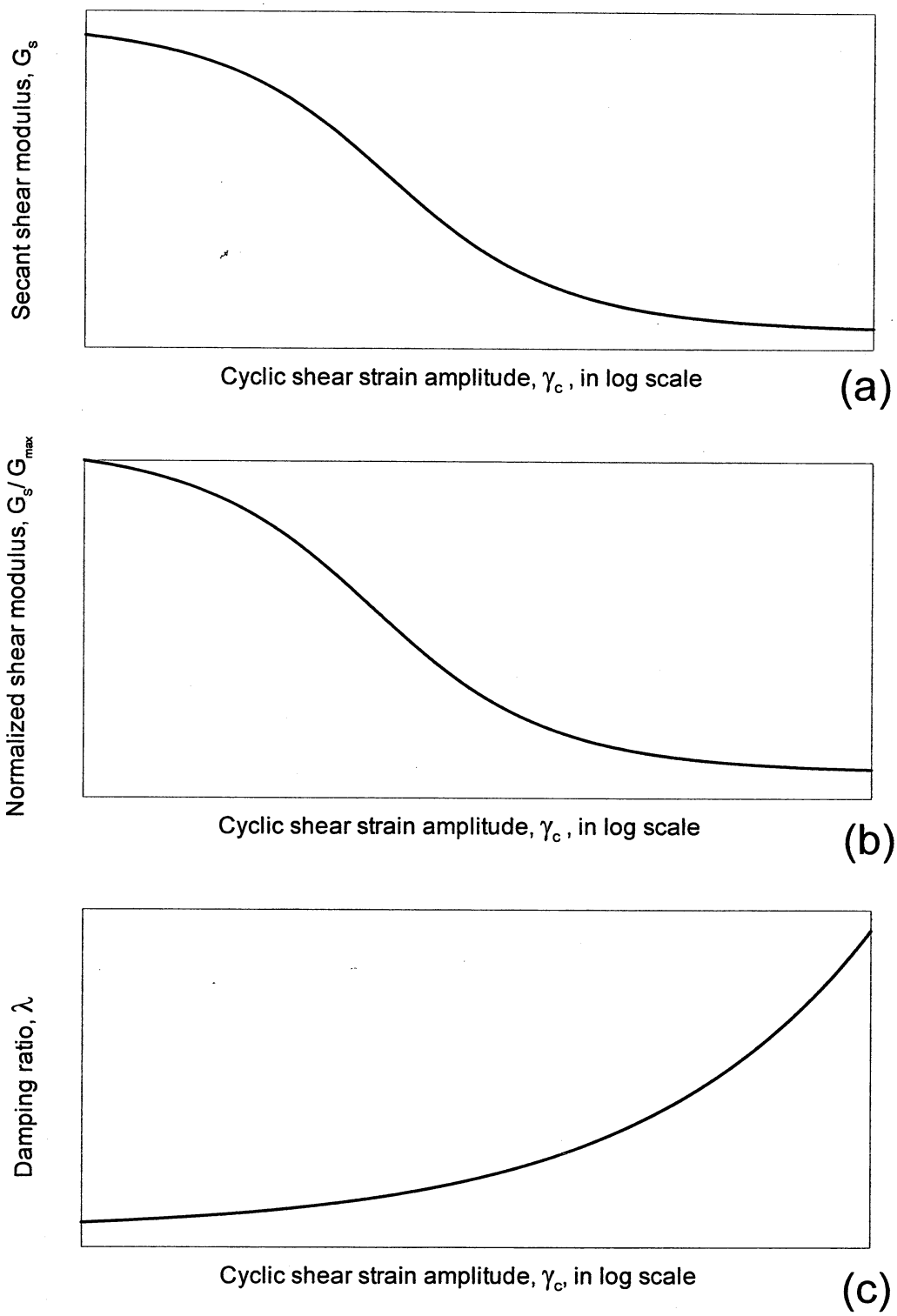

Fig. 3.1.2.1 Examples of modulus reduction and damping curves

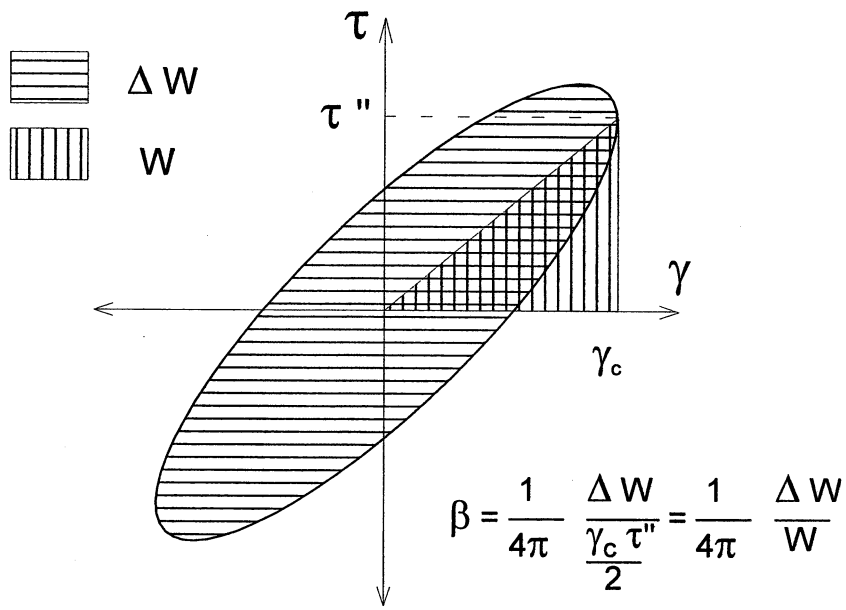

Fig. 3.1.4.1 Definition of the critical damping ratio, β, based on the area of the cyclic loop derived by Jacobsen (1930)

3.2 Test 1: MELOLAND S-2

UCLA Soil Dynamics Laboratory

Double Specimen Direct Simple Shear (DSDSS) Test

Principal investigator: Mladen Vucetic, Professor

Test performed by: Kentaro Tabata Test No.: 1

Project:	PEARL			Date:	5/28/2001
Boring:	Meloland				
Tube No.:	S-2	Depth (ft):	18.0 -19.7	GWT (ft):	6.5 (reported by others)
Comments:	Dark yellowish brown silt. Specimen obtained from the bottom of the tube (specimen depth ~ 19 ft).				

FORM 1: SPECIMEN PREPARATION

WATER CONTENT, SPECIFIC GRAVITY

	Before consol.	After shearing	
Container No.	ST-23	MT-17	MT-23
Cont+wet soil (g)	40.20	185.24	186.12
Cont+dry soil (g)	38.37	158.77	160.67
Container (g)	30.56	50.20	49.65
Water (g)	1.83	26.47	25.45
Dry soil (g)	7.81	108.57	111.02
Water content(%)	23.43	24.38	22.92
Avg. water cont. (%)	23.43		23.65
Spceific gravity			2.65

UNIT WEIGHT, VOID RATIO, SATURATION

	Before consol.	Before shearing	After shearing
Average weight (g)	136.74	136.74	
Height (cm)	1.965	1.948	
Area (cm^2)	34.84	34.84	
Volume (cm^3)	68.45	67.86	
Unit weight (g/cm^3)	1.998	2.015	
Unit weight (kN/m^3)	19.58	19.75	
Void ratio	0.64	0.62	
Saturation (%)	97.4	99.6	

HEIGHT OF SPECIMEN

	Before consol.		Before shearing	After shearing		
	Top	Bottom	Average	Average		
Height (cm)	1.965	1.965	1.948	1.948		

AREA OF SPECIMEN

Initial diameter (cm			6.660	Initial area (cm^2)		34.837
Load (kg)	Stress (kg/cm^2)	Stress (kN/m^2)	Diameter (cm)	Membrane (cm)	Corrected diameter (cm)	Area (cm^2)

Meloland S-2					
DSDSS TEST - Step 2b					
Type of soil: ML					
LL	26.6	PI	3.5	%Silt	53.9
e_0	0.63	S_0 (%)	99.6	%Clay	12.0
σ_v (kPa)	55	OCR	n/a	w (%)	23.7
γ_c (%)	~0.0004	H_0 (mm)	19.48	Spec. Gr.	2.65

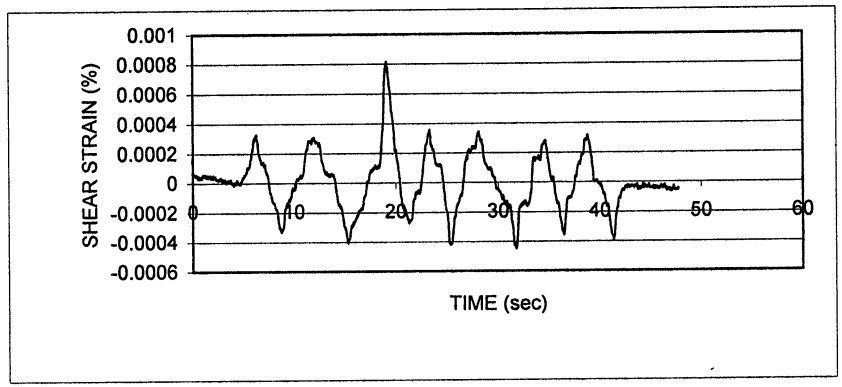

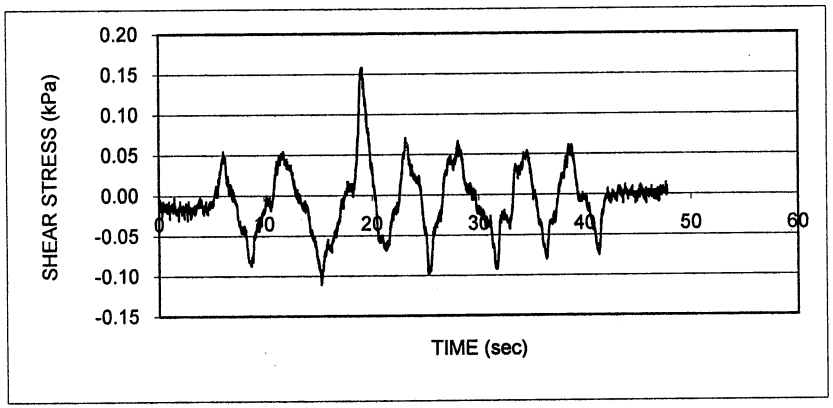

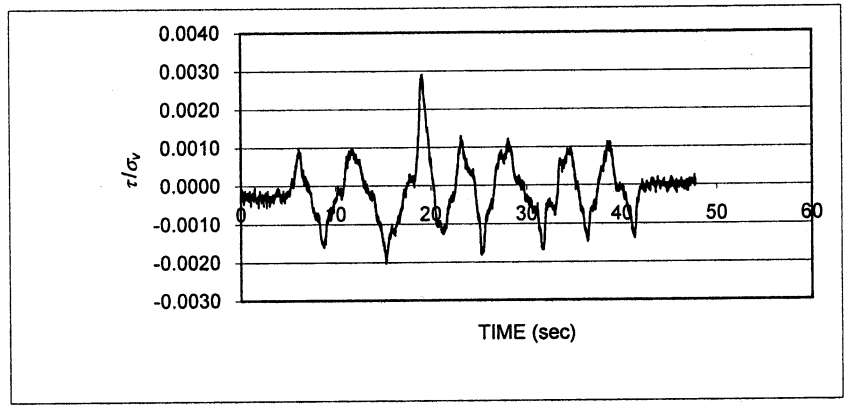

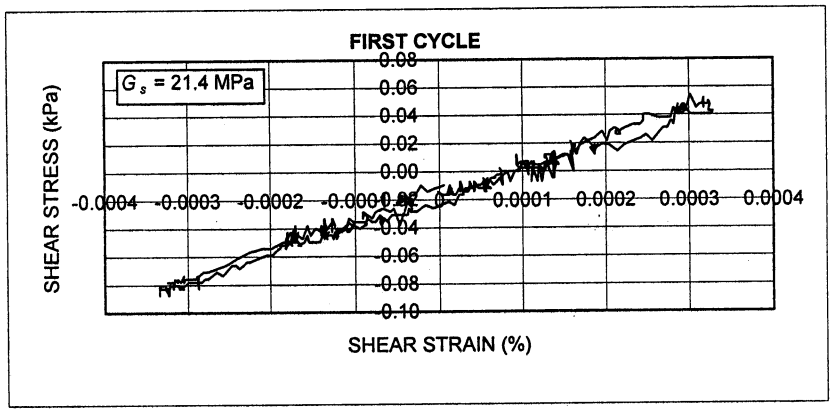

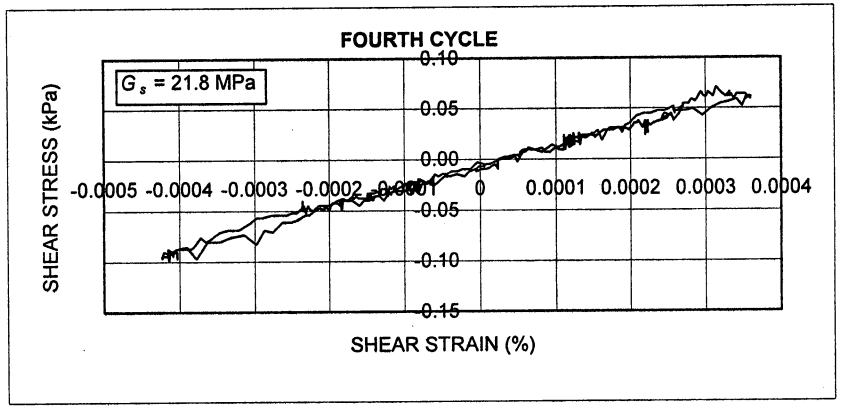

Meloland S-2					
DSDSS TEST - Step 3b					
Type of soil: ML					
LL	26.6	PI	3.5	%Silt	53.9
e_0	0.63	S_0 (%)	99.6	%Clay	12.0
σ_v (kPa)	55	OCR	n/a	w (%)	23.7
γ_c (%)	~0.0009	H_0 (mm)	19.48	Spec. Gr.	2.65

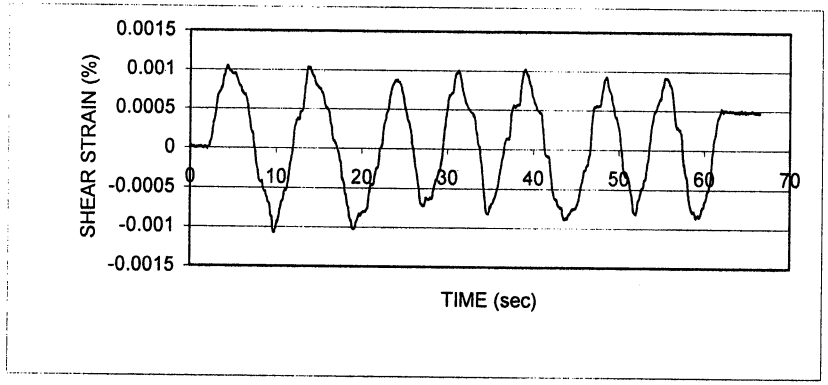

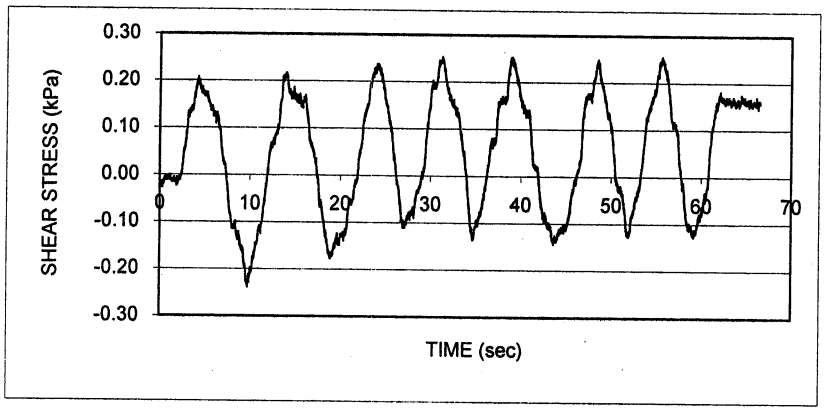

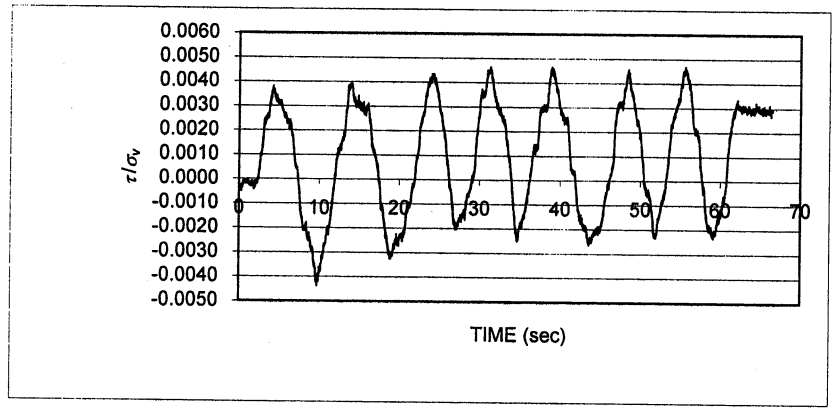

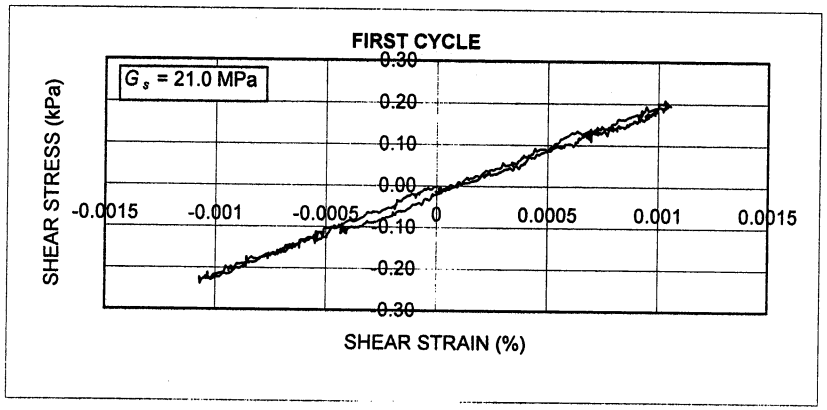

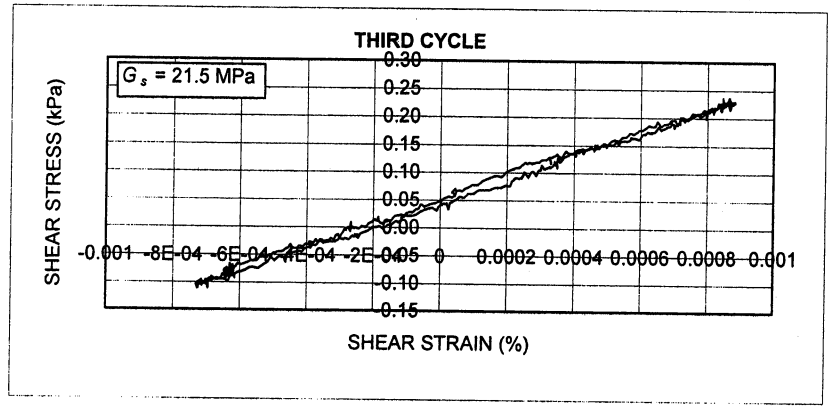

Meloland S-2					
DSDSS TEST - Step 4b					
Type of soil: ML					
LL	26.6	PI	3.5	%Silt	53.9
e_0	0.63	S_0 (%)	99.6	%Clay	12.0
σ_v (kPa)	55	OCR	n/a	w (%)	23.7
γ_c (%)	~0.0027	H_0 (mm)	19.48	Spec. Gr.	2.65

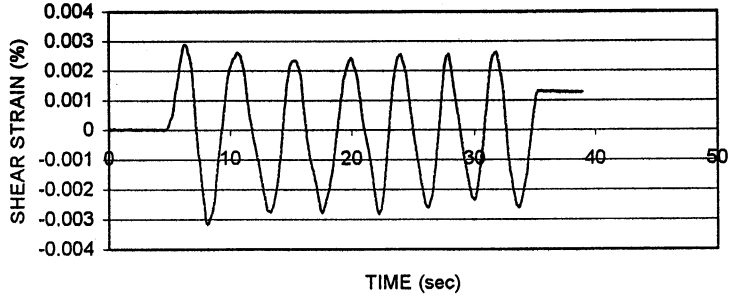

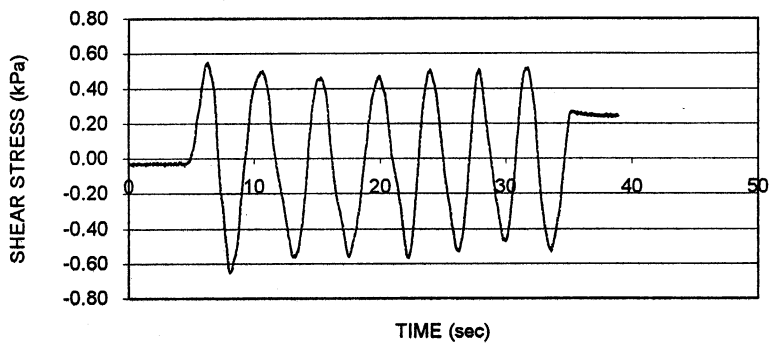

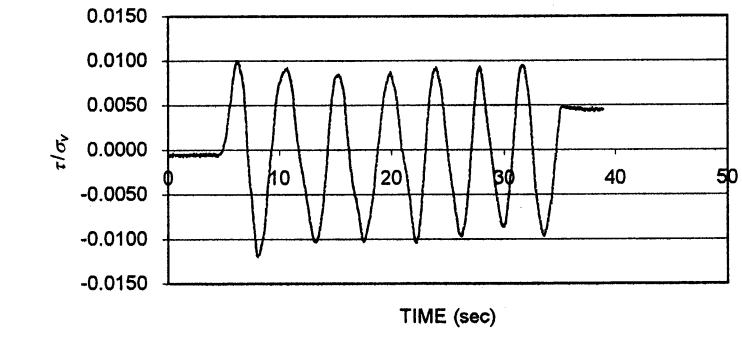

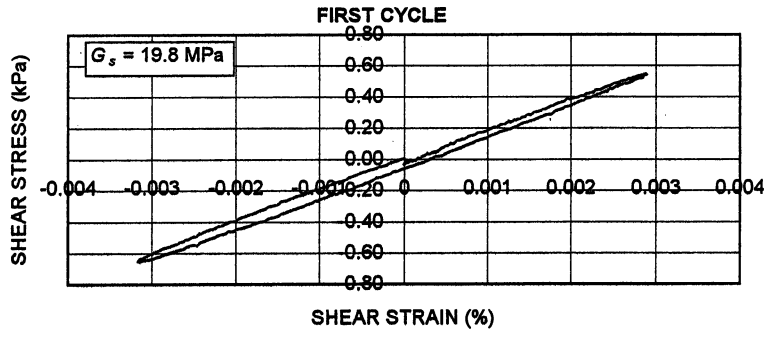

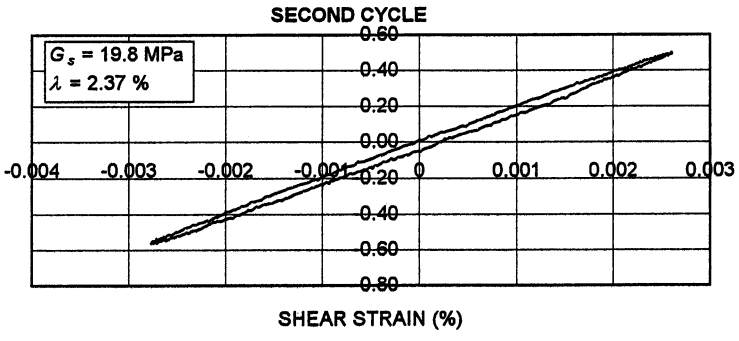

Meloland S-2					
DSDSS TEST - Step 5b					
Type of soil: ML					
LL	26.6	PI	3.5	%Silt	53.9
e_0	0.63	S_0 (%)	99.6	%Clay	12.0
σ_v (kPa)	55	OCR	n/a	w (%)	23.7
γ_c (%)	~0.009	H_0 (mm)	19.48	Spec. Gr.	2.65

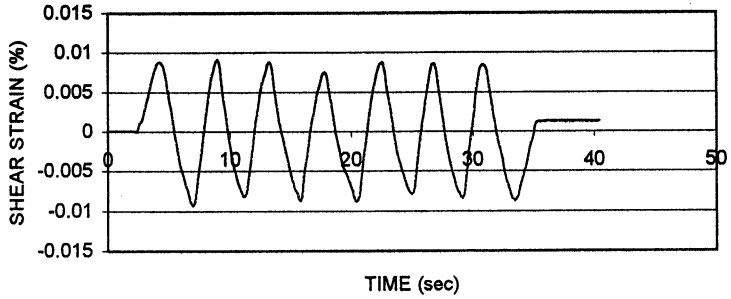

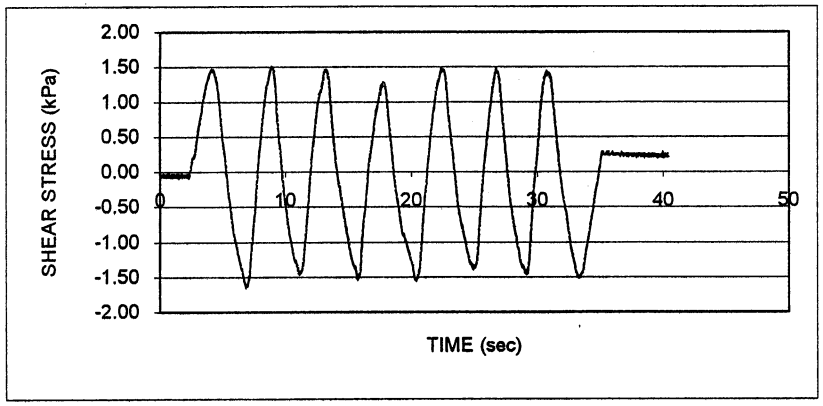

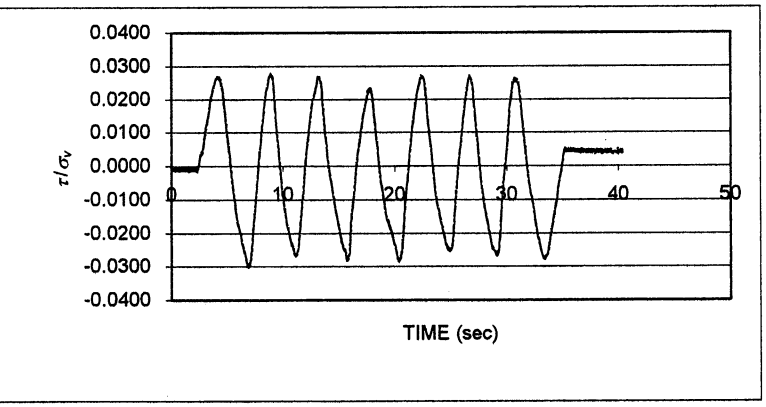

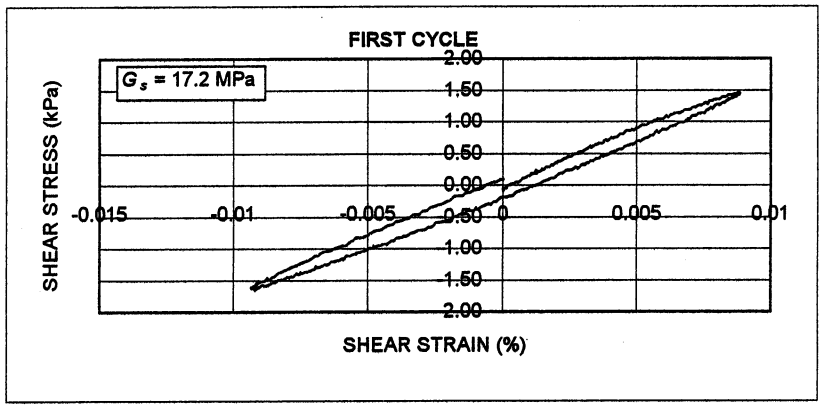

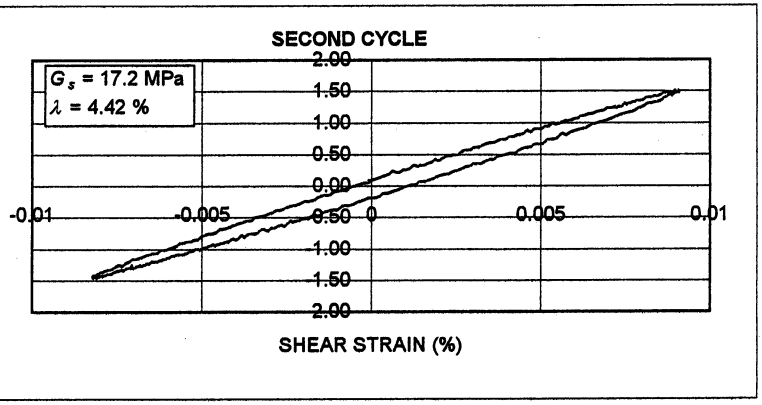

Meloland S-2					
DSDSS TEST - Step 6b					
Type of soil: ML					
LL	26.6	PI	3.5	%Silt	53.9
e_0	0.63	S_0 (%)	99.6	%Clay	12.0
σ_v (kPa)	55	OCR	n/a	w (%)	23.7
γ_c (%)	~0.028	H_0 (mm)	19.48	Spec. Gr.	2.65

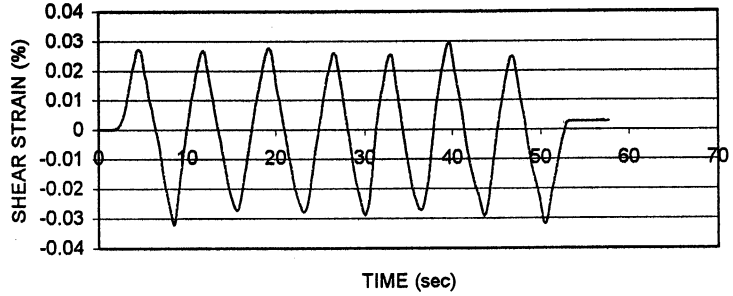

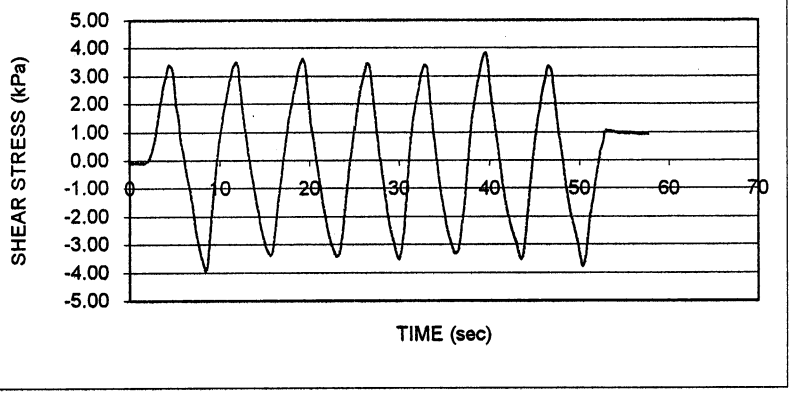

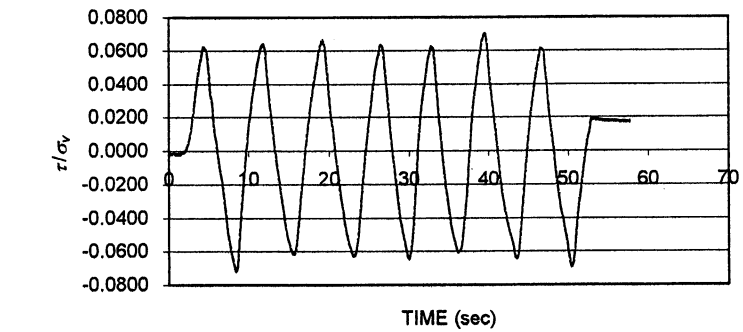

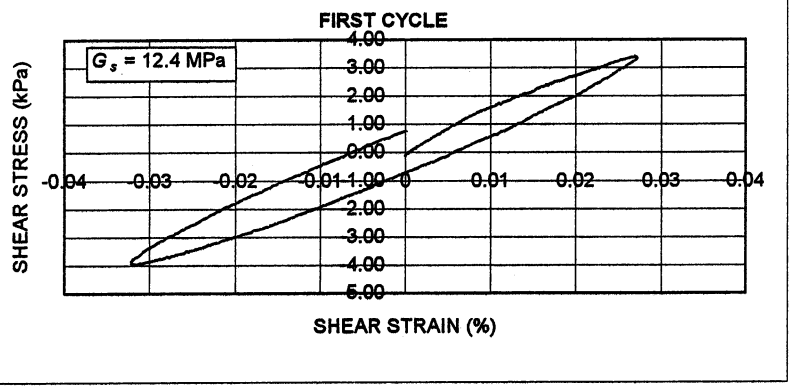

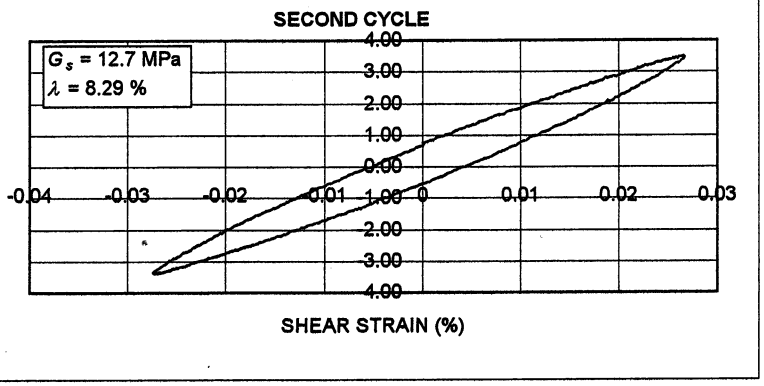

Meloland S-2					
DSDSS TEST - Step 7b					
Type of soil: ML					
LL	26.6	PI	3.5	%Silt	53.9
e_0	0.63	S_0 (%)	99.6	%Clay	12.0
σ_v (kPa)	55	OCR	n/a	w (%)	23.7
γ_c (%)	~0.09	H_0 (mm)	19.48	Spec. Gr.	2.65

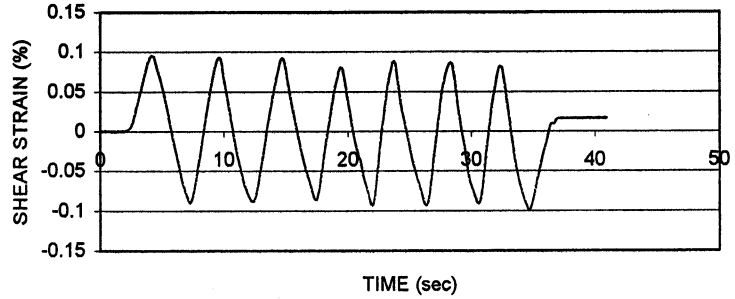

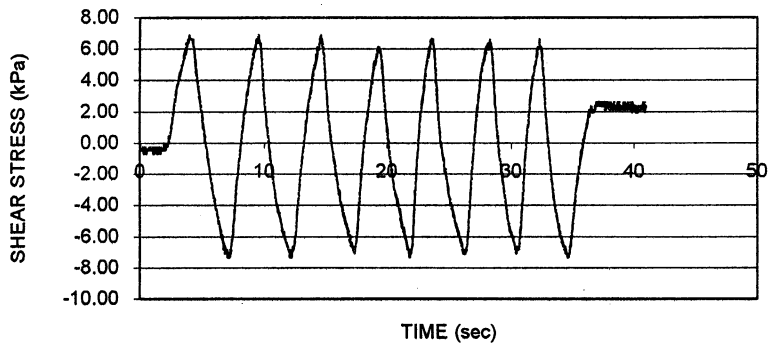

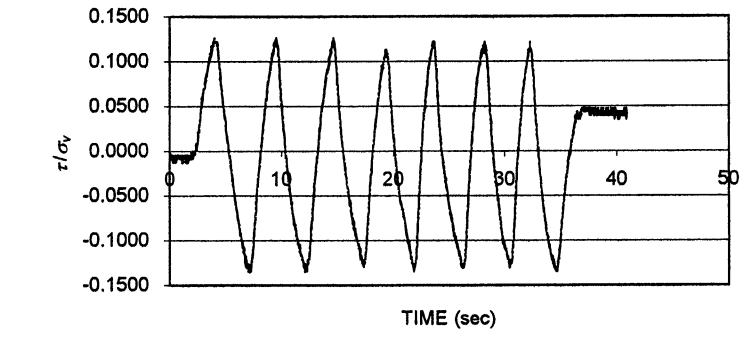

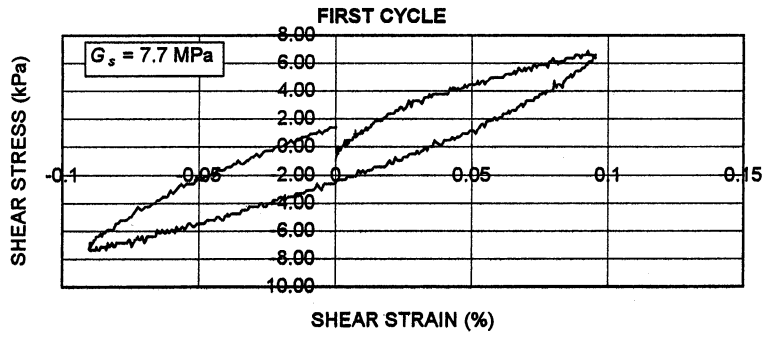

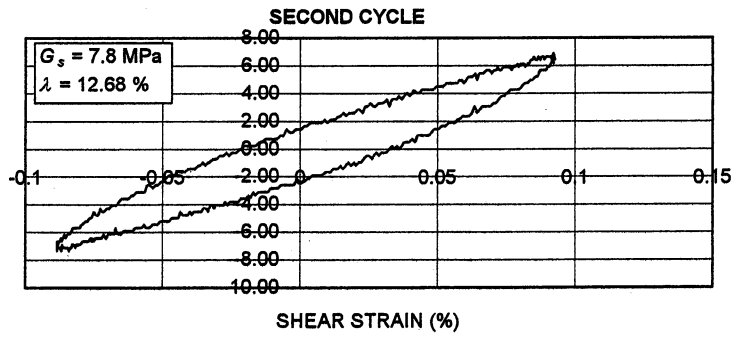

Meloland S-2					
DSDSS TEST - Step 8					
Type of soil: ML					
LL	26.6	PI	3.5	%Silt	53.9
e_0	0.63	S_0 (%)	99.6	%Clay	12.0
σ_v (kPa)	55	OCR	n/a	w (%)	23.7
γ_c (%)	~3.0	H_0 (mm)	19.48	Spec. Gr.	2.65

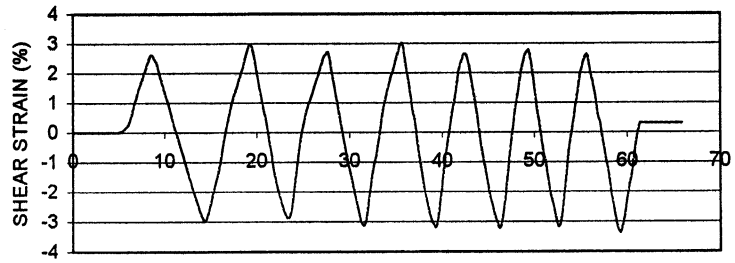

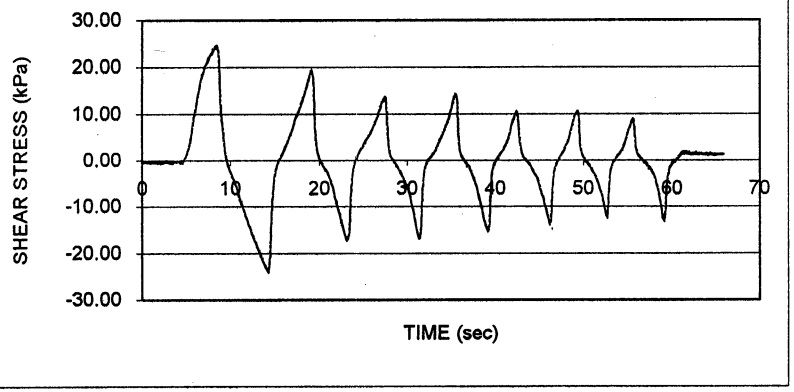

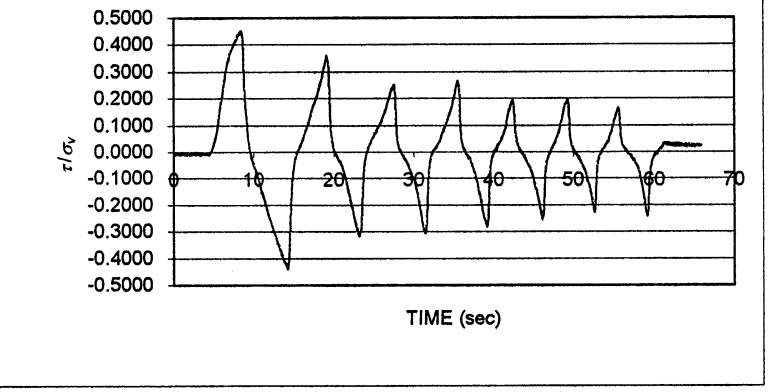

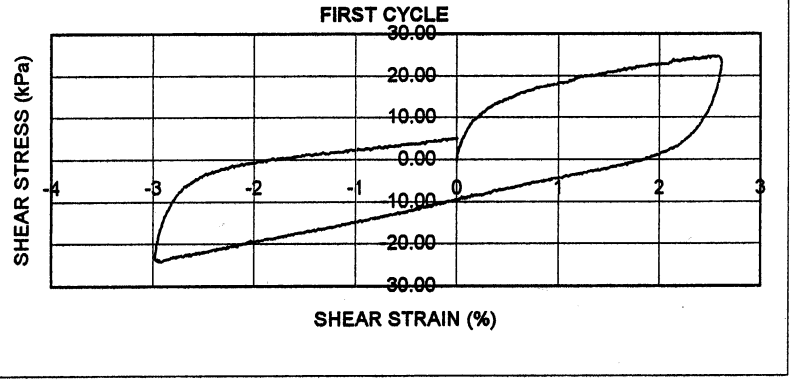

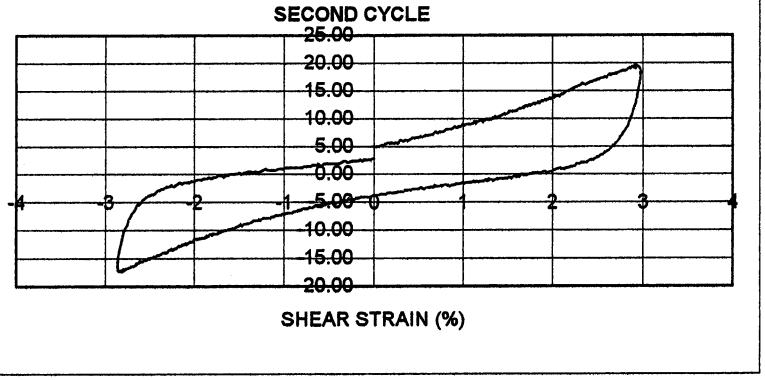

UCLA Soil Dynamics Laboratory

Double Specimen Direct Simple Shear (DSDSS) Test

Principal investigator: Mladen Vucetic, Professor

Test performed by: Kentaro Tabata Test No.: 1

Project:	PEARL			Date:	5/28/2001
Boring:	Meloland				
Tube No.:	S-2			Depth (ft):	18.0-19.7
Specific gravity	2.65	LL (%):	26.6	PI:	3.5
Group symbol:	ML	Silt (%):	53.9	Clay (%):	12.0
Comments:	Dark yellowish brown silt.				

MODULUS REDUCTION			DAMPING		
γ_c (%)	G_s (MPa)	G_s/G_{max}	γ_c (%)	λ (%)	
0.00033	21.434	0.983			
0.00039	21.781	0.999			
0.00106	21.012	0.964	0.00081	1.625	
0.00081	21.541	0.988	0.00269	2.373	
0.00303	19.828	0.910	0.00865	4.417	
0.00269	19.836	0.910	0.02705	8.285	
0.00909	17.180	0.788	0.09058	12.685	
0.00865	17.241	0.791			
0.02971	12.391	0.568			
0.02705	12.735	0.584			
0.09284	7.650	0.351			
0.09058	7.842	0.360			
0.50279	2.872	0.132			
1.00015	1.823	0.084			
1.50295	1.386	0.064			
2.00394	1.134	0.052			
2.50673	0.982	0.045			
2.61563	0.896	0.041			

Estimated G_{max} (MPa)	21.8

Meloland, S-2, Depth = 18-19.7 feet, PI = 3.5,
Vertical stress = 55 kPa.

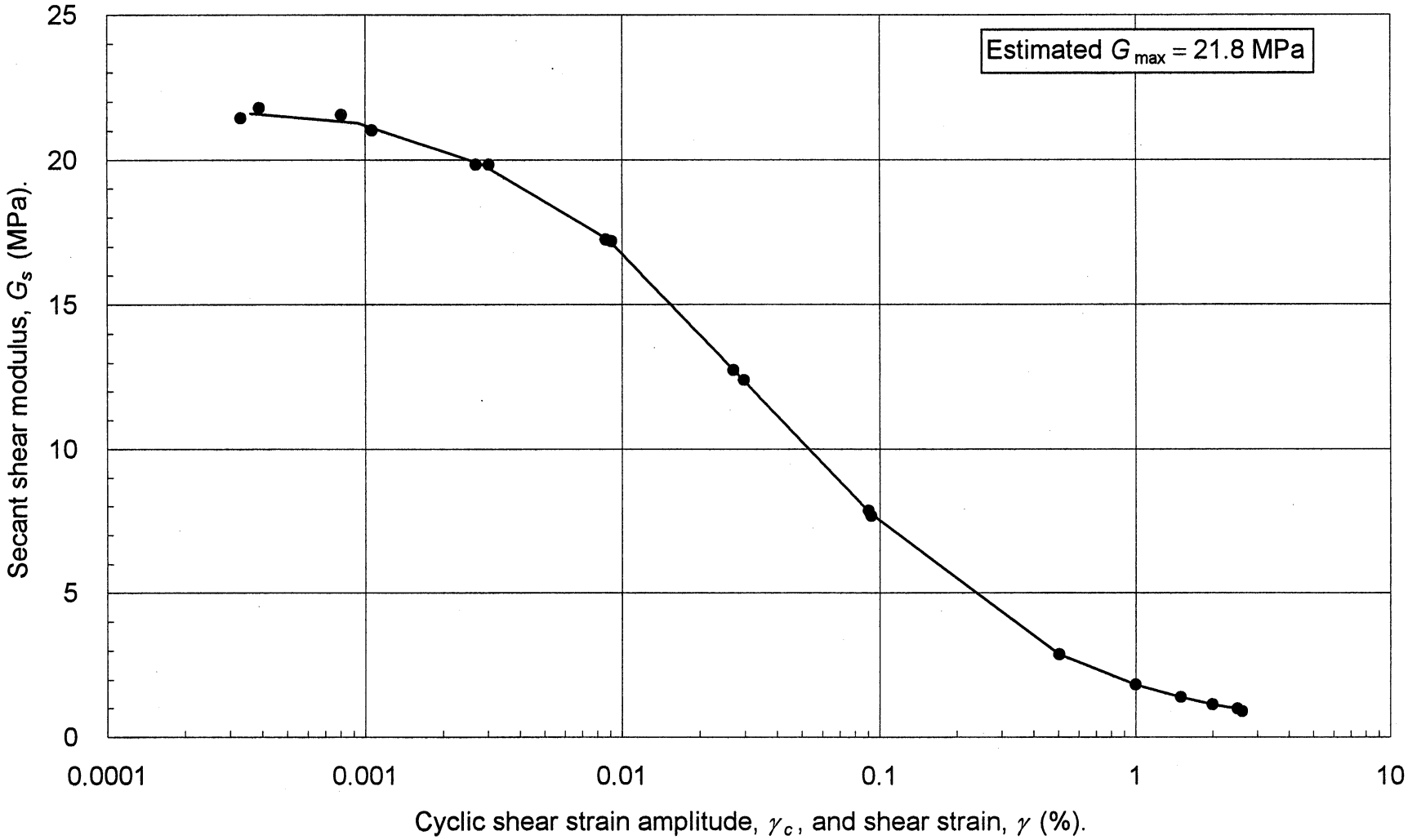

Meloland, S-2, Depth = 18-19.7 feet, PI = 3.5,
Vertical stress = 55 kPa.

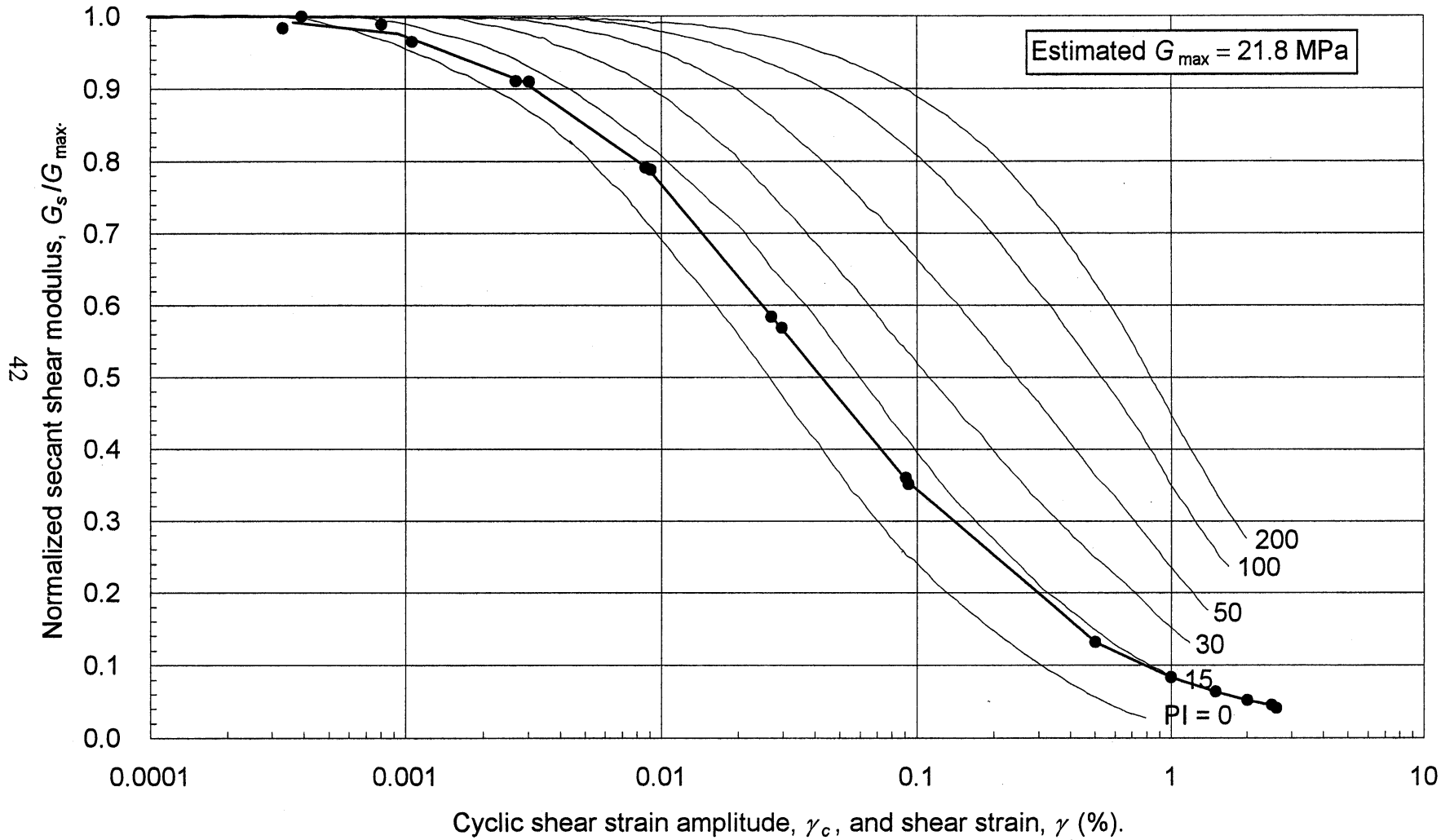

Meloland, S-2, Depth = 18-19.7 feet, PI = 3.5,
Vertical stress = 55 kPa.

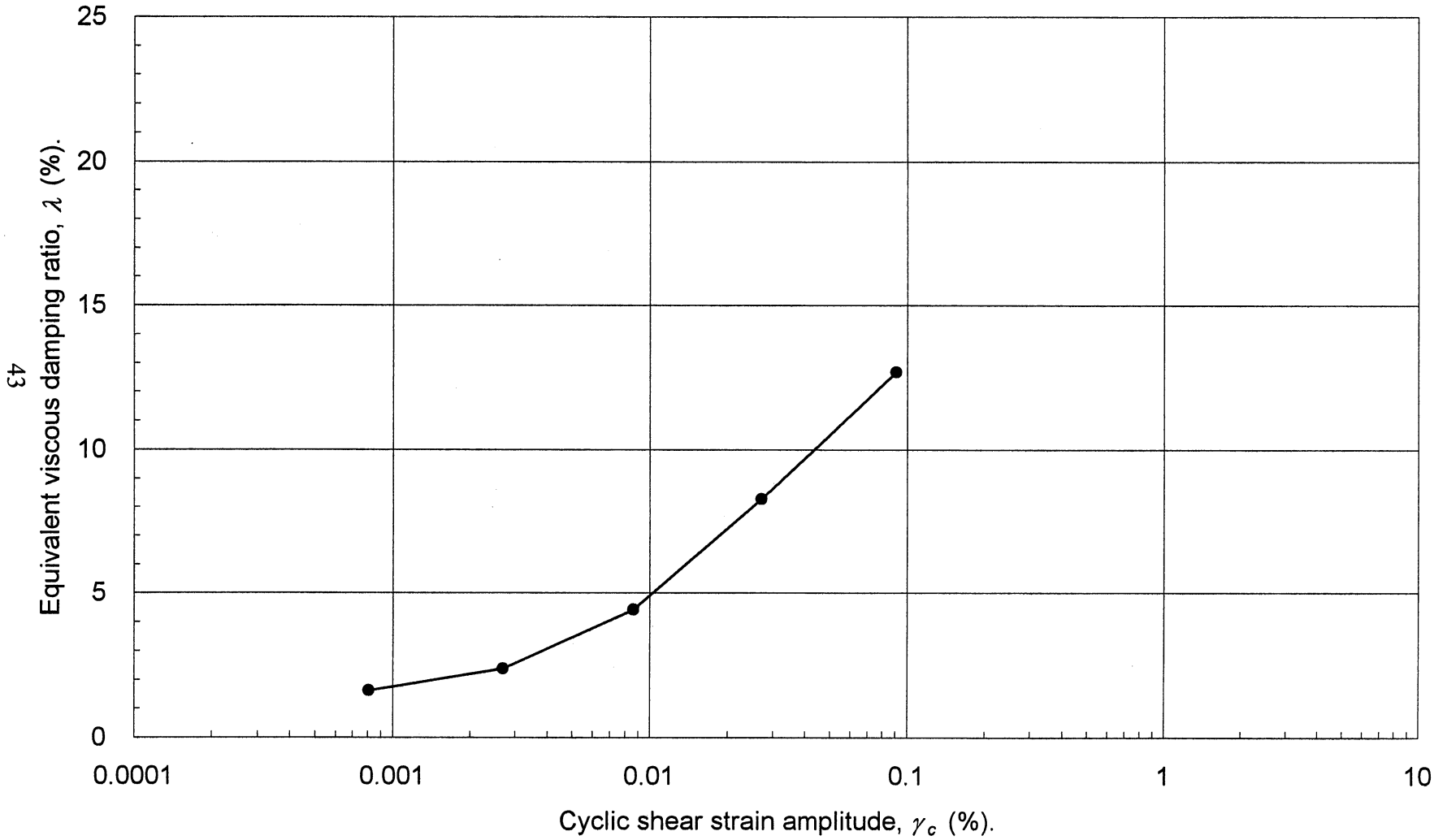

Meloland, S-2, Depth = 18-19.7 feet, PI = 3.5,
Vertical stress = 55 kPa.

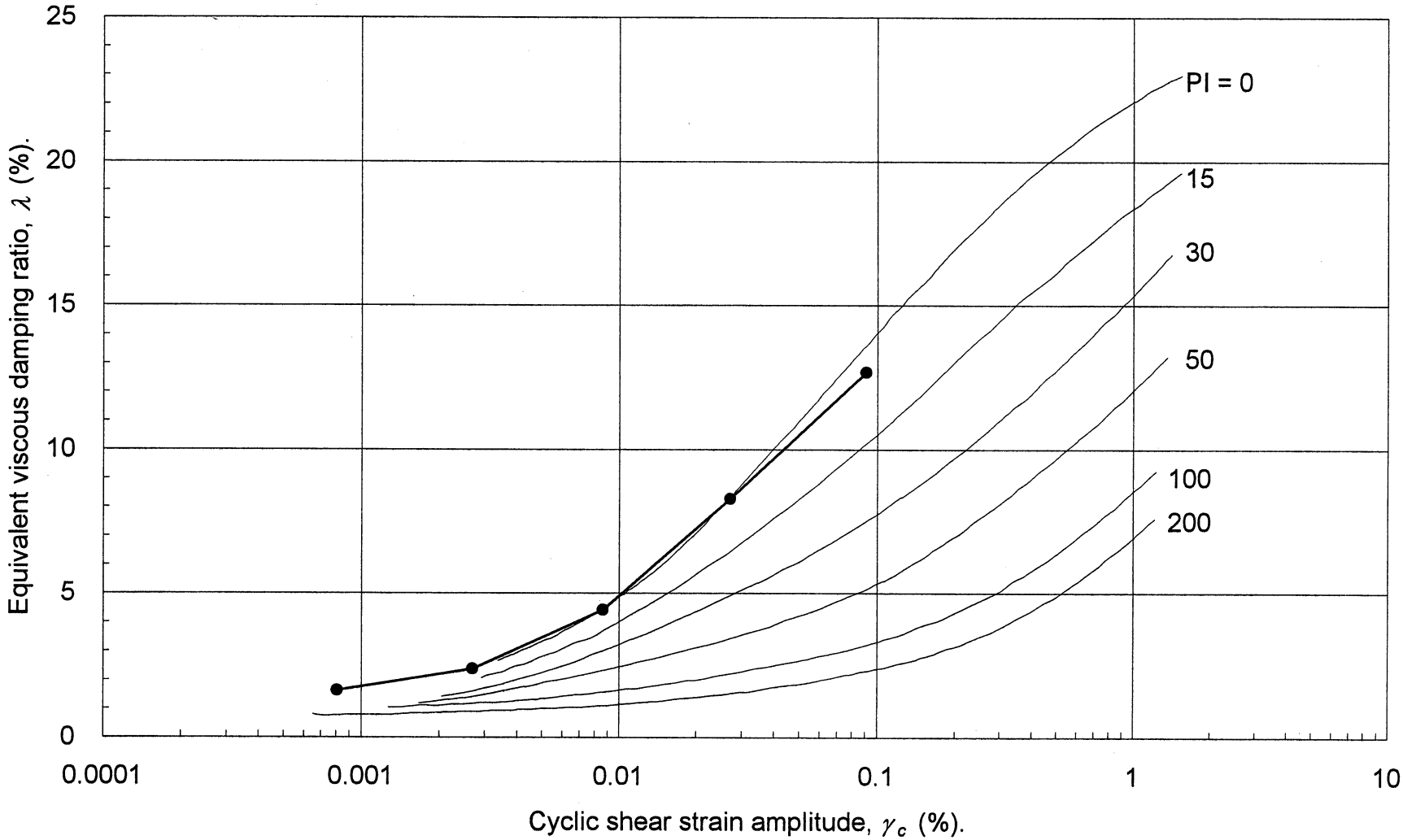

UCLA Soil Dynamics Laboratory

Specific Gravity Test

Principal investigator: Mladen Vucetic, Professor

Test performed by: Kentaro Tabata Test No.: 1

Project:	PEARL			Date:	5/28/2001
Boring:	Meloland				
Tube No.:	S-2	Depth (ft):	18.0 -19.7	GWT (ft):	6.5
Comments:	Dark yellowish brown silt.				

SPECIFIC GRAVITY TEST

Test No.	1		
Bottle No.	3		
Wt. of bottle (g)	178.46		
Volume of bottle (cm^3)	500		
Wt. of bottle+water+soil (g)	694.33		
Temperature (°C)	24.0		
Wt. of bottle+water (g)	675.55		
Evaporating dish No.	BB-2		
Weight of dish (g)	862.78		
Wt. of dish+dry soil (g)	892.92		
Wt. of dry soil (g)	30.14		
Specific gravity of water	0.9973		
Specific gravity of soil	**2.65**		

UCLA Soil Dynamics Laboratory

Grain Size Distribution

Principal investigator: Mladen Vucetic, Professor

Test performed by: Kentaro Tabata Test No.: 1

Project:	PEARL				
Boring:	Meloland				
Tube No.:	S-2	Depth (ft):	18.0 -19.7	GWT (ft):	6.5
Comments:	Dark yellowish brown silt.				

GRAIN SIZE DISTRIBUTION

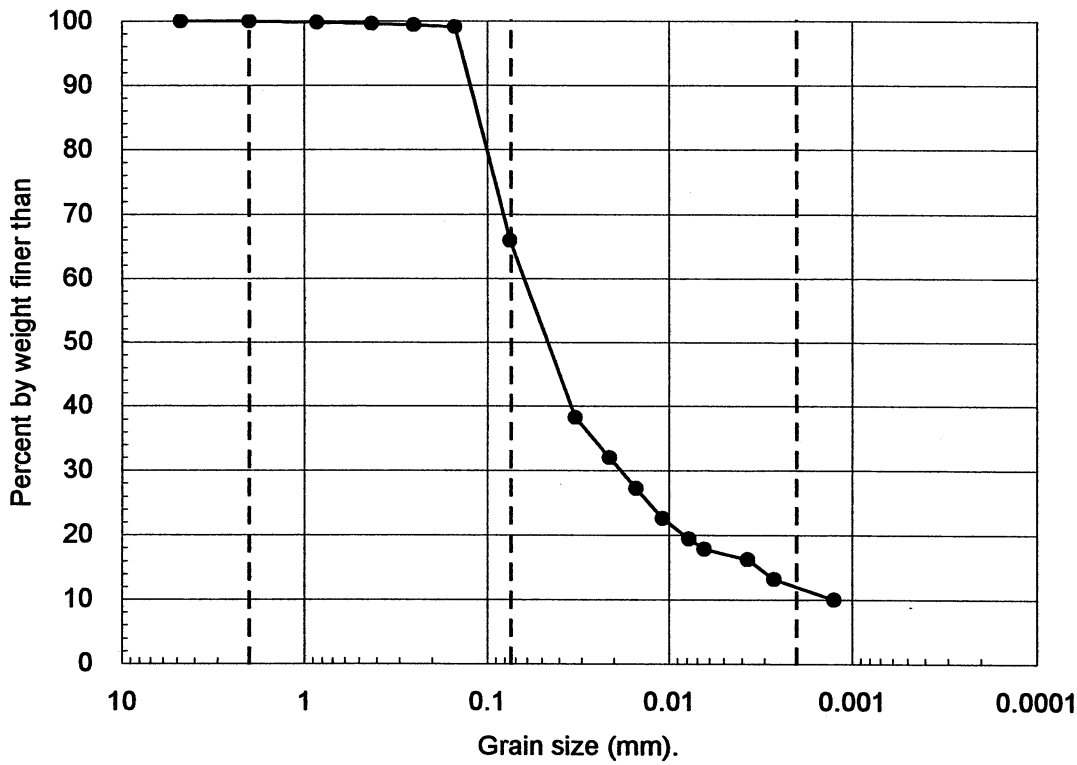

Clay (%)	Silt (%)	Sand (%)	Gravel (%)
12.0	53.9	34.1	0.0

UCLA Soil Dynamics Laboratory

Hydrometer Analysis

Principal investigator: Mladen Vucetic, Professor

Test performed by: Kentaro Tabata Test No.: 1

Project:	PEARL			Date:	5/30/2001
Boring:	Meloland				
Tube No.:	S-2	Depth (ft):	18.0 -19.7	GWT (ft):	6.5
Comments:	Dark yellowish brown silt.				

HYDROMETER TEST

Time	Elapsed time t (sec)	Temp. T (°C)	Reading R'_T	Corr. reading $R_T=R'_T+c_m$	Depth H (cm)	Grain diameter D (mm)	Temp. corr. m_T	Corr. depth $R_T+m_T-c_d$	% by wt. finer than W_D (%)
9:39:57	0								
9:41:57	120	21.0	1014.0	1014.5	12.64	0.0328	0.700	1012.2	38.23
9:44:57	300	21.0	1012.0	1012.5	13.18	0.0212	0.700	1010.2	31.96
9:49:57	600	21.0	1010.5	1011.0	13.58	0.0152	0.700	1008.7	27.26
9:59:57	1200	21.0	1009.0	1009.5	13.98	0.0109	0.700	1007.2	22.56
10:19:57	2400	21.0	1008.0	1008.5	14.25	0.0078	0.700	1006.2	19.43
10:39:57	3600	21.0	1007.5	1008.0	14.38	0.0064	0.700	1005.7	17.86
12:39:57	10800	21.0	1007.0	1007.5	14.52	0.0037	0.700	1005.2	16.29
15:39:57	21600	21.0	1006.0	1006.5	14.78	0.0026	0.700	1004.2	13.16
12:51:00	97863	21.0	1005.0	1005.5	15.05	0.0013	0.700	1003.2	10.03

APPARATUS

Hydrometer no.:	88-18587	a_0	284.03	a_1	-0.2675
Graduate no.:	2				

FACTORS

Meniscus corr., c_m:	0.5	
Disp. agent corr, c_d:	3.0	
Visc. of water, η.	21.0 °C	9.320E-06 g sec/cm^2
	°C	g sec/cm^3

WEIGHT

Dry soil (g)	33.82
Percent by wt (%)	65.93
Dry soil for sieve (g)	17.48
Total (g)	51.30

UNIT WEIGHT

Specific gravity:		2.65
T	γ_w	γ_s
(°C)	(g/cm^3)	(g/cm^3)
21.0	0.9980	2.6407

UCLA Soil Dynamics Laboratory

Sieve Analysis

Principal investigator: Mladen Vucetic, Professor

Test performed by: Kentaro Tabata Test No.: 1

Project:	PEARL			Date:	5/31/2001
Boring:	Meloland				
Tube No.:	S-2	Depth (ft):	18.0 -19.7	GWT (ft):	6.5
Comments:	Dark yellowish brown silt.				

SIEVE ANALYSIS

Sieve No.	Diameter (mm)	Sieve (g)	S+wet (g)	S+dry (g)	Retained (g)	Retained (%)	Cumulated (g)	Cumulated (%)	Passing (%)
4	4.750	461.69		461.69	0.00	0.00	0.00	0.00	100.00
10	2.000	422.44		422.44	0.00	0.00	0.00	0.00	100.00
20	0.850	407.36		407.46	0.10	0.19	0.10	0.19	99.81
40	0.425	337.90		338.01	0.11	0.21	0.21	0.41	99.59
60	0.250	351.56		351.67	0.11	0.21	0.32	0.62	99.38
100	0.150	342.19		342.32	0.13	0.25	0.45	0.88	99.12
200	0.075	299.81		316.84	17.03	33.20	17.48	34.07	65.93
Total					17.48	34.07			

WEIGHT

Dry soil for sieve (g)	17.48
Dry soil for hydr. (g)	33.82
Total (g)	51.30
Percent coaser (%)	34.07

UCLA Soil Dynamics Laboratory

Atterberg Limit Determination

Principal investigator: Mladen Vucetic, Professor

Test performed by: Kentaro Tabata Test No.: 1

Project:	PEARL			Date:	6/22/2001
Boring:	Meloland				
Tube No.:	S-2	Depth (ft):	18.0 -19.7	GWT (ft):	6.5
Comments:	Dark yellowish brown silt.				

LIQUID LIMIT TEST

Test No.	1	2	3	4				
Number of blows	27	20	14	9				
Container No.	T-6	ST-8	ST-5	ST-19				
Container (g)	30.11	30.06	30.12	29.99				
Cont+wet soil (g)	38.41	38.01	40.39	39.44				
Cont+dry soil (g)	36.69	36.29	38.07	37.21				
Water (g)	1.72	1.72	2.32	2.23				
Dry soil (g)	6.58	6.23	7.95	7.22				
Water content (%)	26.14	27.61	29.18	30.89				

PLASTIC LIMIT TEST

Test No.	1	2	3
Container No.	ST-2	ST-6	ST-12
Container (g)	30.27	30.10	30.29
Cont+wet soil (g)	33.01	32.16	31.80
Cont+dry soil (g)	32.49	31.76	31.53
Water (g)	0.52	0.40	0.27
Dry soil (g)	2.22	1.66	1.24
Water content (%)	23.42	24.10	21.77

ATTERBERG LIMITS

Liquid limit (%)	**26.6**
Plastic limit (%)	**23.1**
Plasticity index	**3.5**

CLASSIFICATION

ML

FLOW CHART

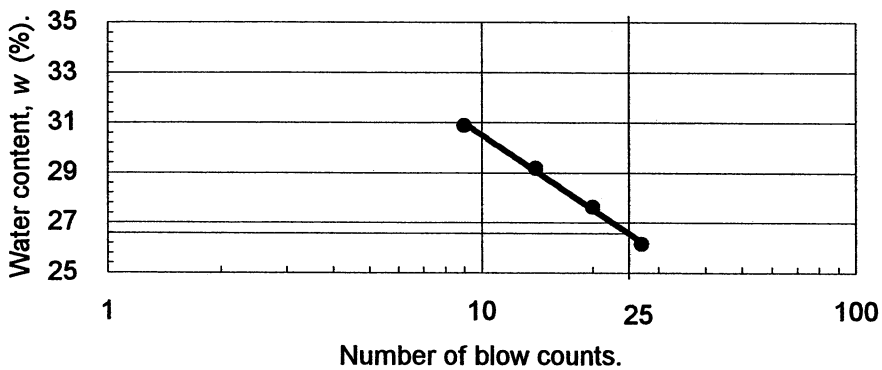

UCLA Soil Dynamics Laboratory

Atterberg Limit Determination

Principal investigator: Mladen Vucetic, Professor

Test performed by: Kentaro Tabata Test No.: 1

Project:	PEARL			Date:	6/22/2001
Boring:	Meloland				
Tube No.:	S-2	Depth (ft):	18.0 -19.7	GWT (ft):	6.5
Comments:	Dark yellowish brown silt.				

PLASTICITY CHART

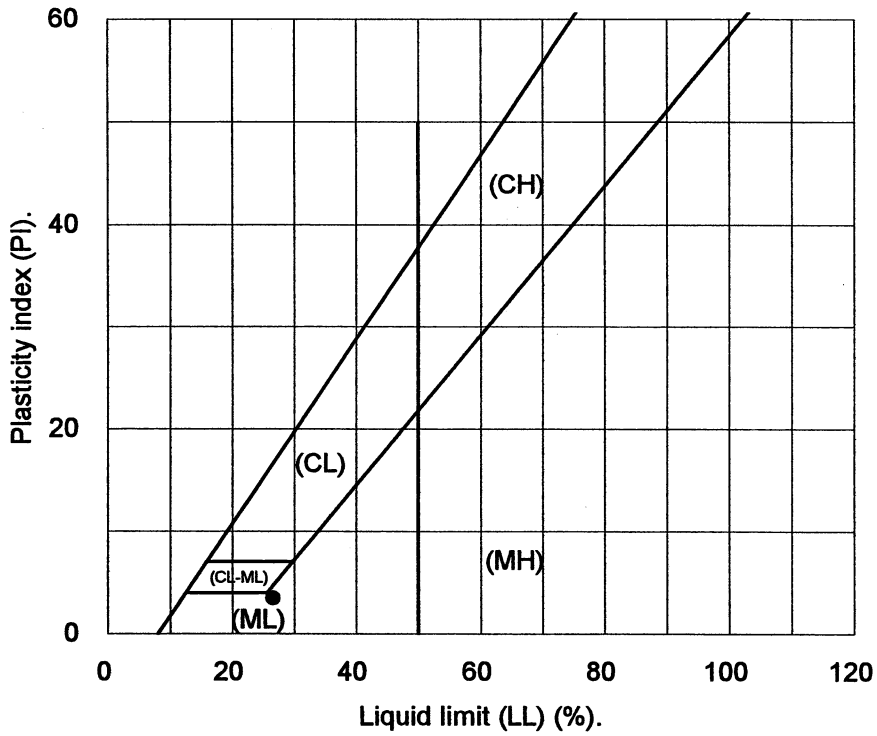

3.3 Test 2: MELOLAND S-3

UCLA Soil Dynamics Laboratory

Double Specimen Direct Simple Shear (DSDSS) Test

Principal investigator: Mladen Vucetic, Professor

Test performed by: Kentaro Tabata Test No.: 2

Project:	PEARL			Date:	6/2/2001
Boring:	Meloland				
Tube No.:	S-3	Depth (ft):	28.0 -29.6	GWT (ft):	6.5 (reported by others)
Comments:	Brown clay. Sticky, plastic soil. Specimen obtained from the bottom of the tube (specimen depth ~ 29ft).				

FORM 1: SPECIMEN PREPARATION

WATER CONTENT, SPECIFIC GRAVITY

	Before consol.	After shearing	
Container No.	ST-12	MT-17	DISH
Cont+wet soil (g)	37.83	182.78	136.49
Cont+dry soil (g)	36.28	155.62	108.88
Container (g)	30.29	50.20	10.82
Water (g)	1.55	27.16	27.61
Dry soil (g)	5.99	105.42	98.06
Water content(%)	25.88	25.76	28.16
Avg. water cont. (%)	25.88		26.96
Spceific gravity			2.74

UNIT WEIGHT, VOID RATIO, SATURATION

	Before consol.	Before shearing	After shearing
Average weight (g)	129.40	129.40	
Height (cm)	1.965	1.917	
Area (cm^2)	34.84	34.84	
Volume (cm^3)	68.45	66.78	
Unit weight (g/cm^3)	1.890	1.938	
Unit weight (kN/m^3)	18.52	18.99	
Void ratio	0.82	0.78	
Saturation (%)	86.0	90.9	

HEIGHT OF SPECIMEN

	Before consol.		Before shearing	After shearing		
	Top	Bottom	Average	Average		
Height (cm)	1.965	1.965	1.917	1.917		

AREA OF SPECIMEN

Initial diameter (cm): 6.660 Initial area (cm^2): 34.837

Load (kg)	Stress (kg/cm^2)	Stress (kN/m^2)	Diameter (cm)	Membrane (cm)	Corrected diameter (cm)	Area (cm^2)

Meloland S-3					
DSDSS TEST - Step 2b					
Type of soil: CH					
LL	60.8	PI	29.8	%Silt	42.8
e_0	0.78	S_0 (%)	90.9	%Clay	56.0
σ_v (kPa)	101	OCR	n/a	w (%)	25.9
γ_c (%)	~0.00042	H_0 (mm)	19.17	Spec. Gr.	2.74

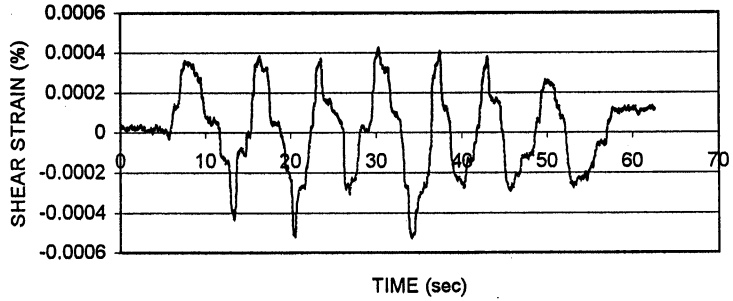

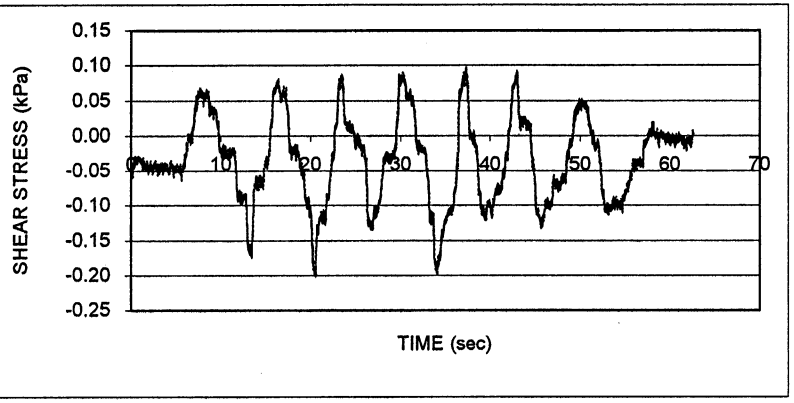

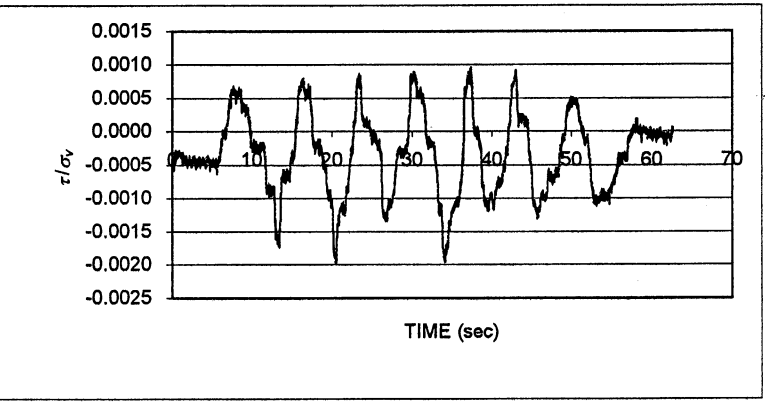

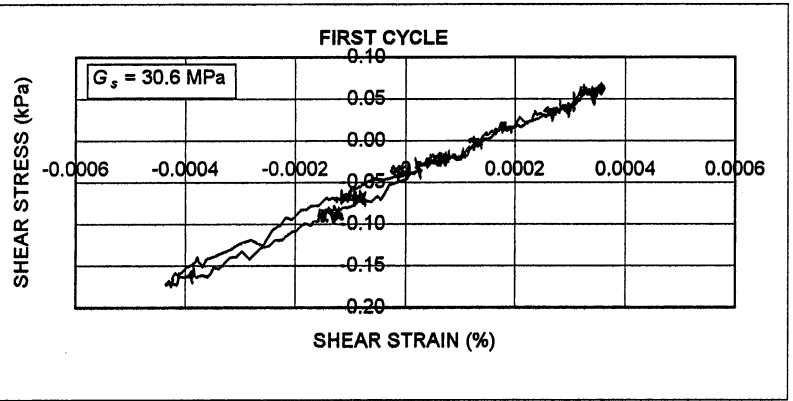

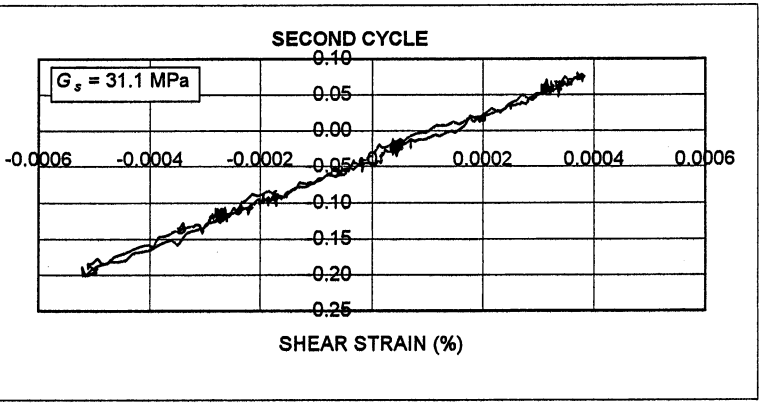

Meloland S-3					
DSDSS TEST - Step 3b					
Type of soil: CH					
LL	60.8	PI	29.8	%Silt	42.8
e_0	0.78	S_0 (%)	90.9	%Clay	56.0
σ_v (kPa)	101	OCR	n/a	w (%)	25.9
γ_c (%)	~0.001	H_0 (mm)	19.17	Spec. Gr.	2.74

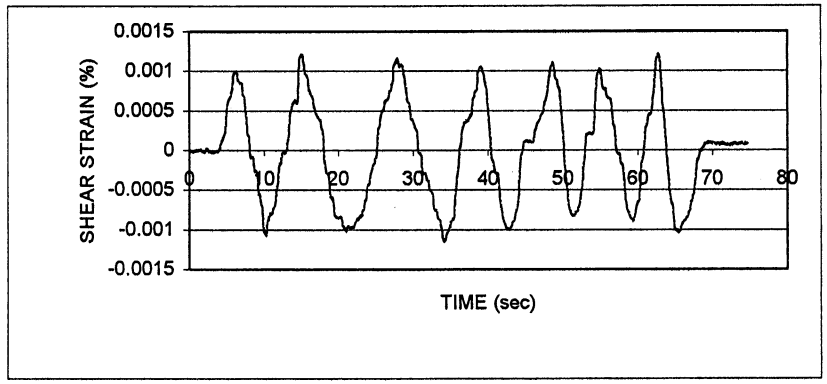

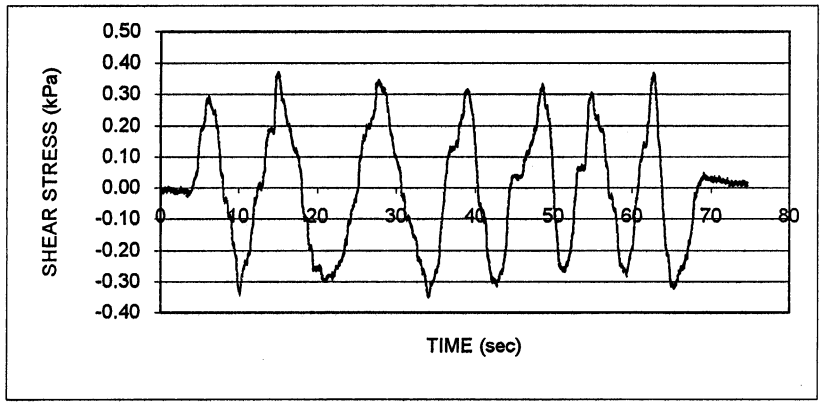

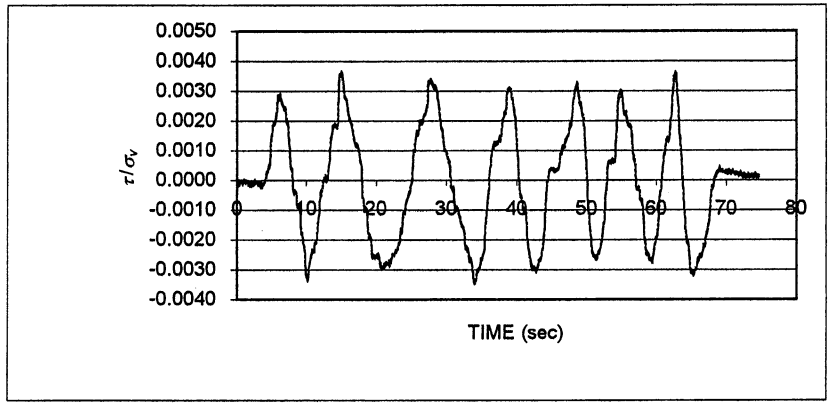

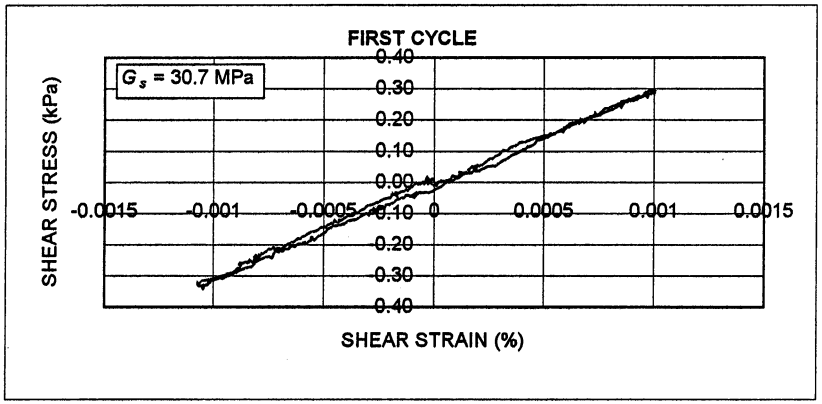

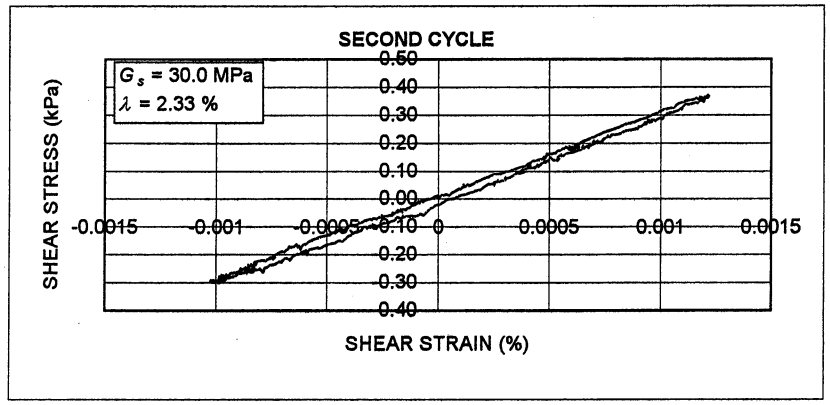

Meloland S-3					
DSDSS TEST - Step 4b					
Type of soil: CH					
LL	60.8	PI	29.8	%Silt	42.8
e_0	0.78	S_0 (%)	90.9	%Clay	56.0
σ_v (kPa)	101	OCR	n/a	w (%)	25.9
γ_c (%)	~0.0025	H_0 (mm)	19.17	Spec. Gr.	2.74

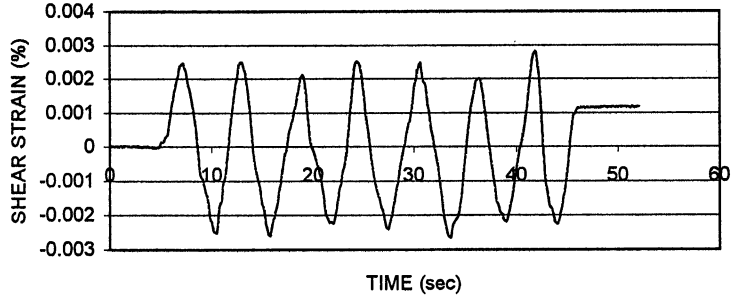

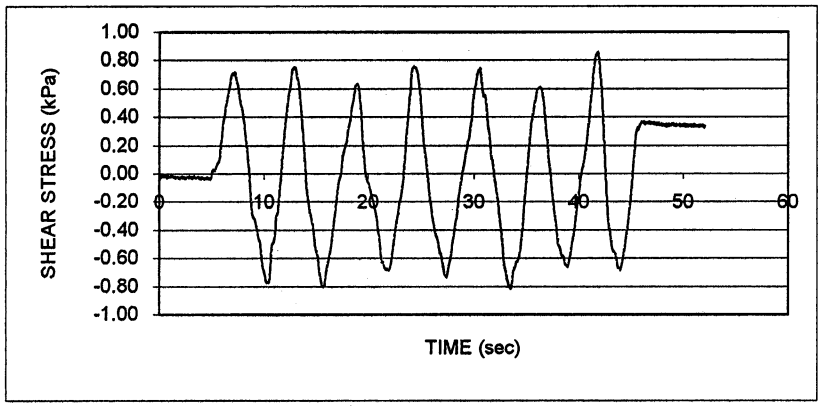

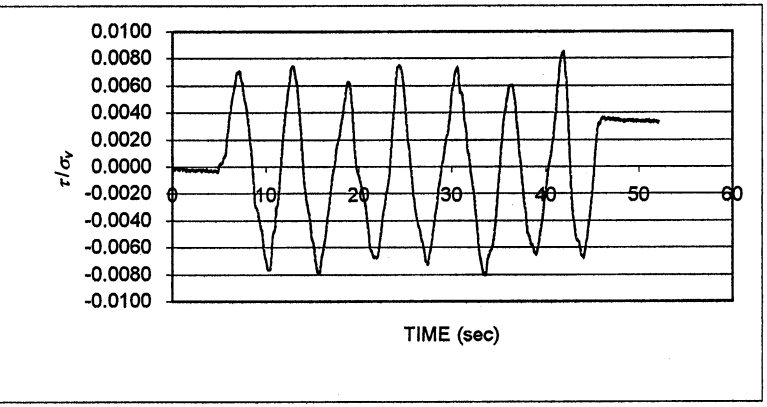

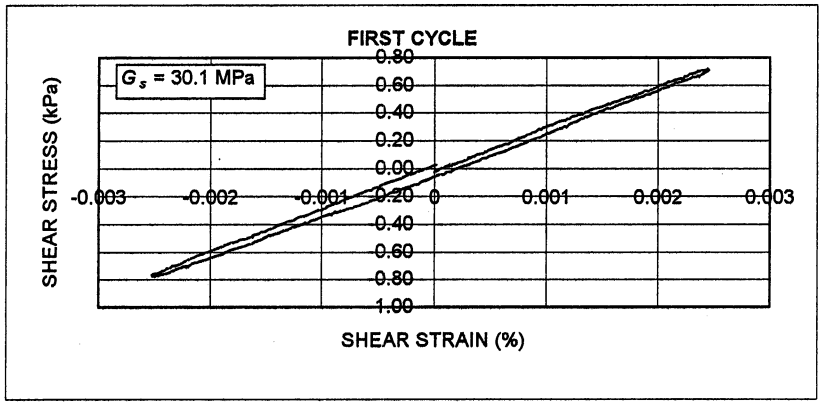

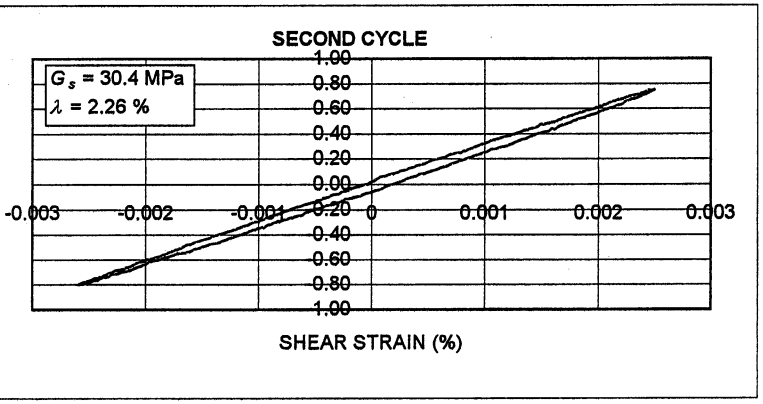

Meloland S-3					
DSDSS TEST - Step 5b					
Type of soil: CH					
LL	60.8	PI	29.8	%Silt	42.8
e_0	0.78	S_0 (%)	90.9	%Clay	56.0
σ_v (kPa)	101	OCR	n/a	w (%)	25.9
γ_c (%)	~0.0095	H_0 (mm)	19.17	Spec. Gr.	2.74

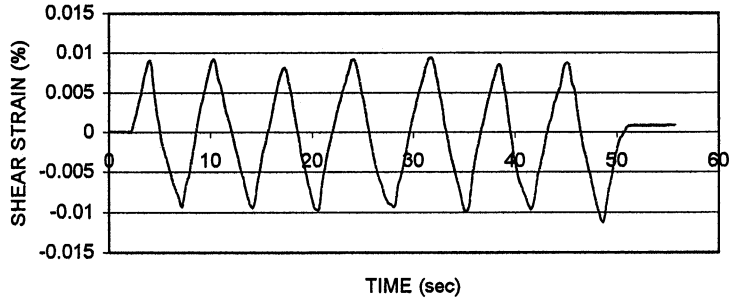

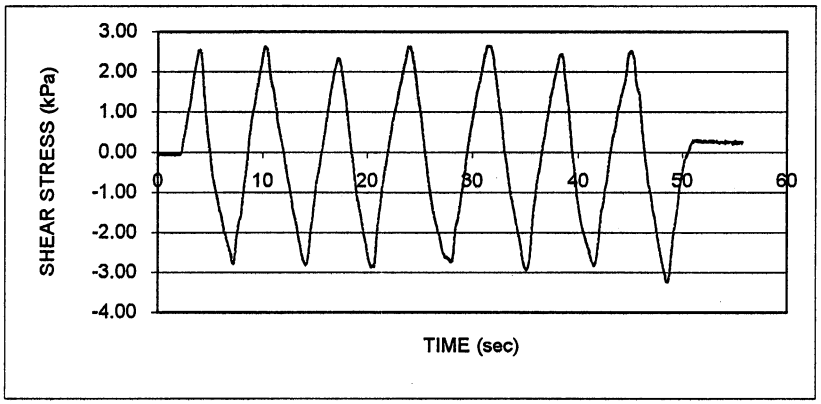

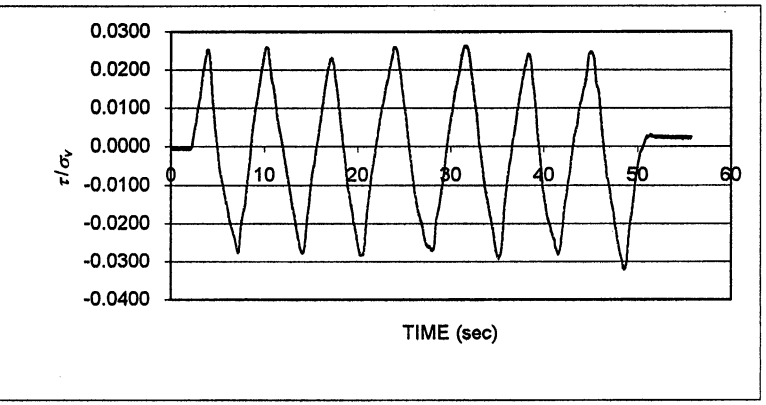

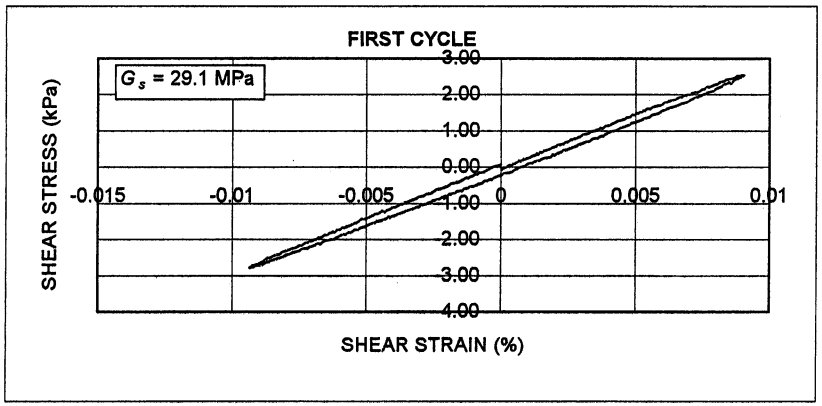

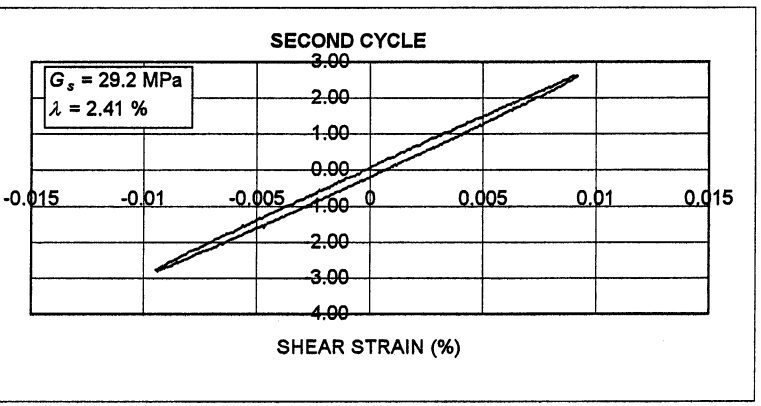

Meloland S-3					
DSDSS TEST - Step 6b					
Type of soil: CH					
LL	60.8	PI	29.8	%Silt	42.8
e_0	0.78	S_0 (%)	90.9	%Clay	56.0
σ_v (kPa)	101	OCR	n/a	w (%)	25.9
γ_c (%)	~0.03	H_0 (mm)	19.17	Spec. Gr.	2.74

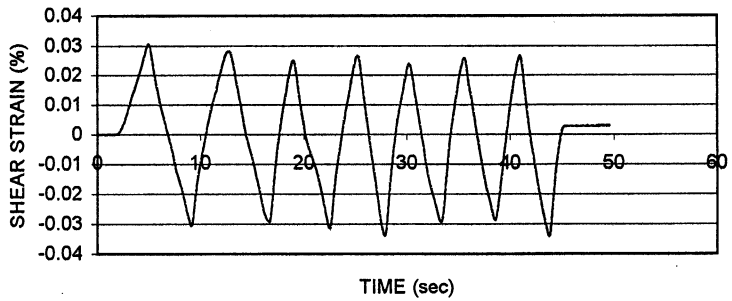

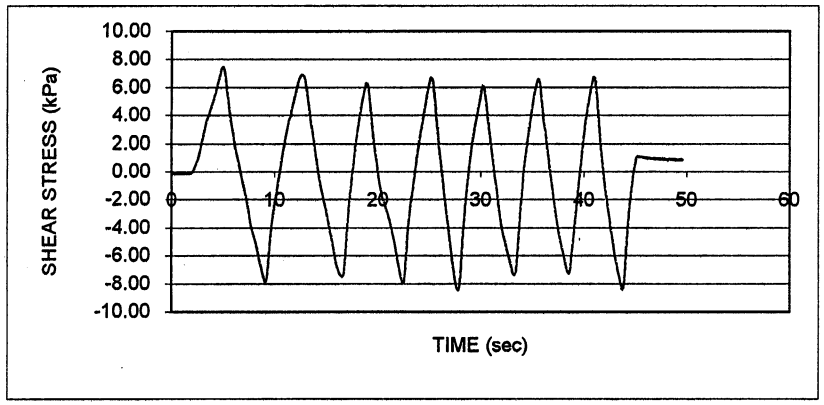

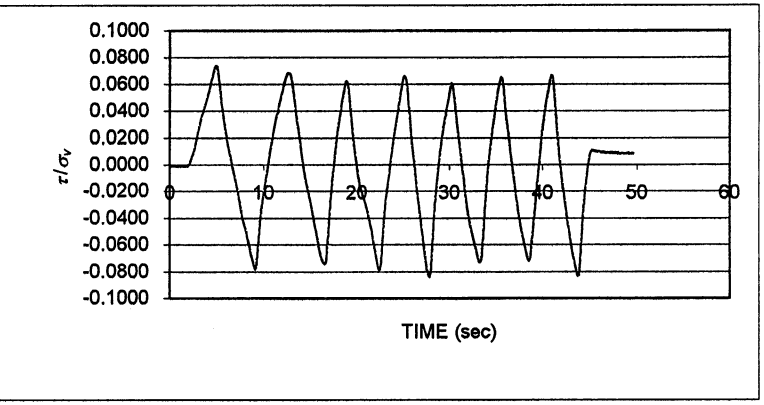

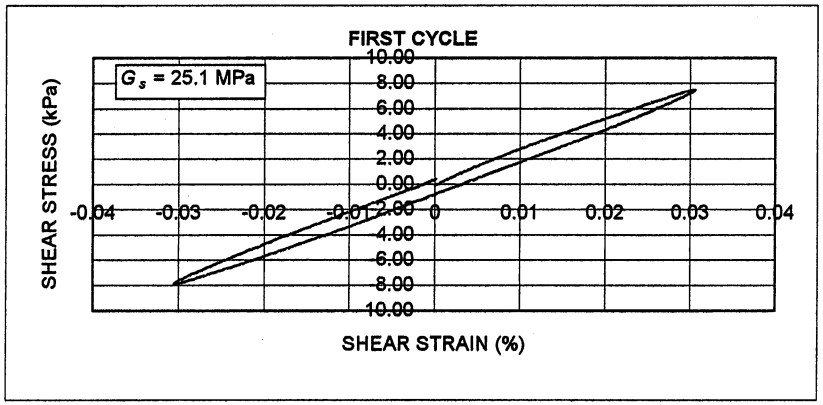

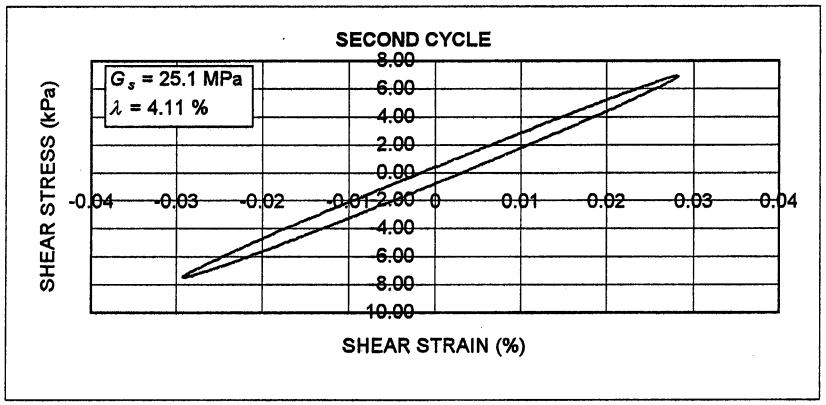

Meloland S-3					
DSDSS TEST - Step 7b					
Type of soil: CH					
LL	60.8	PI	29.8	%Silt	42.8
e_0	0.78	S_0 (%)	90.9	%Clay	56.0
σ_v (kPa)	101	OCR	n/a	w (%)	25.9
γ_c (%)	~0.1	H_0 (mm)	19.17	Spec. Gr.	2.74

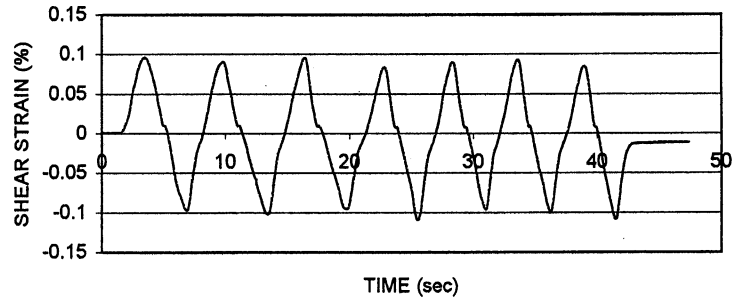

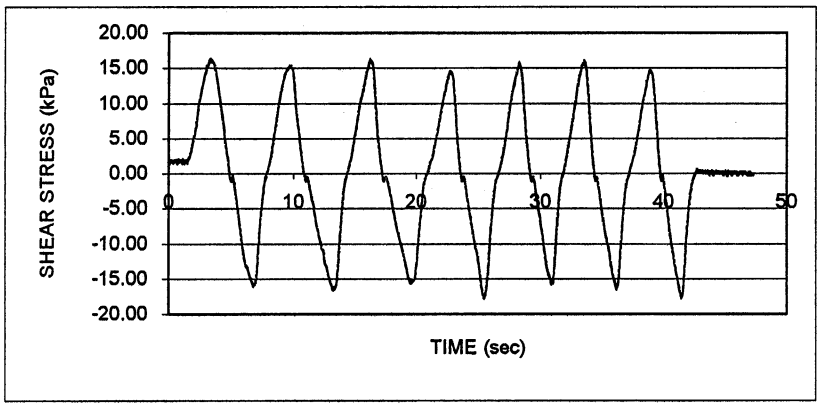

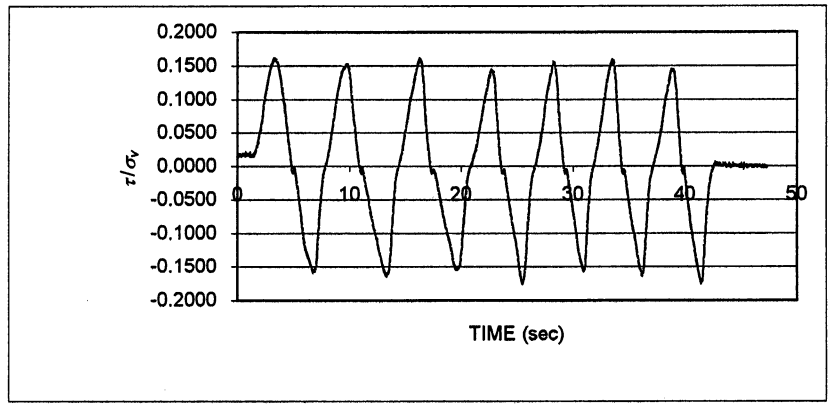

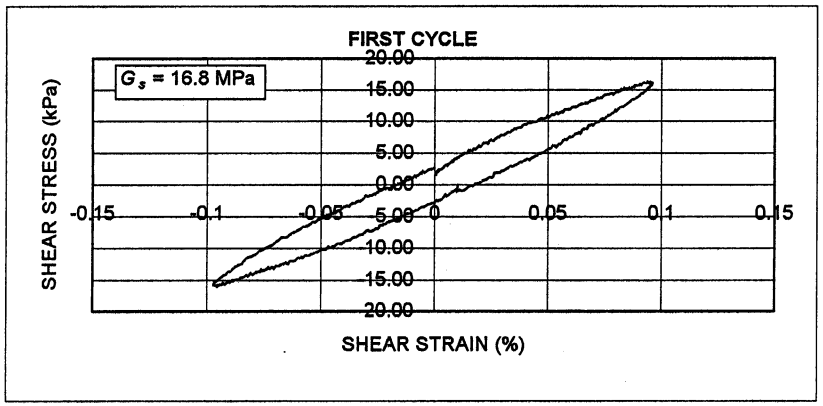

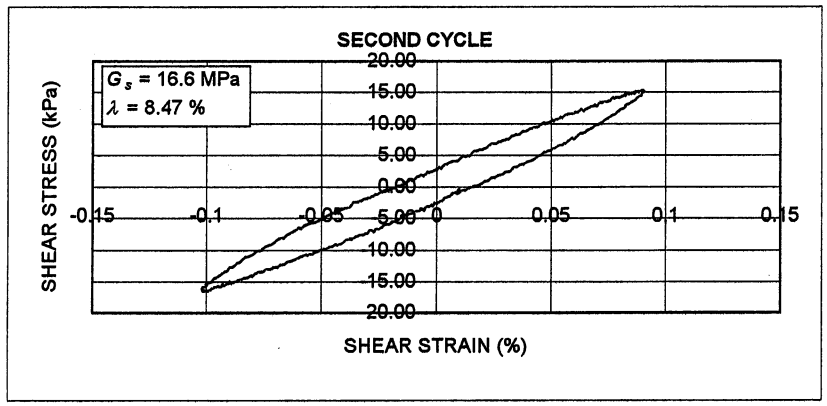

Meloland S-3					
DSDSS TEST - Step 8					
Type of soil: CH					
LL	60.8	PI	29.8	%Silt	42.8
e_0	0.78	S_0 (%)	90.9	%Clay	56.0
σ_v (kPa)	101	OCR	n/a	w (%)	25.9
γ_c (%)	~3.0	H_0 (mm)	19.17	Spec. Gr.	2.74

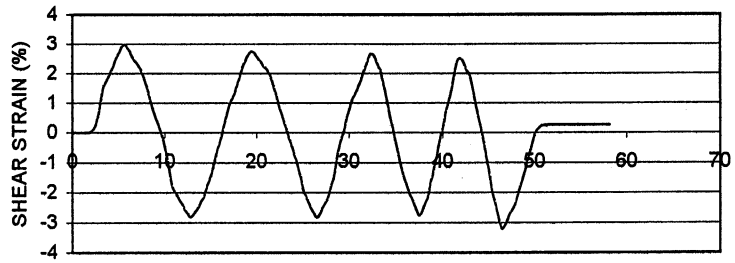

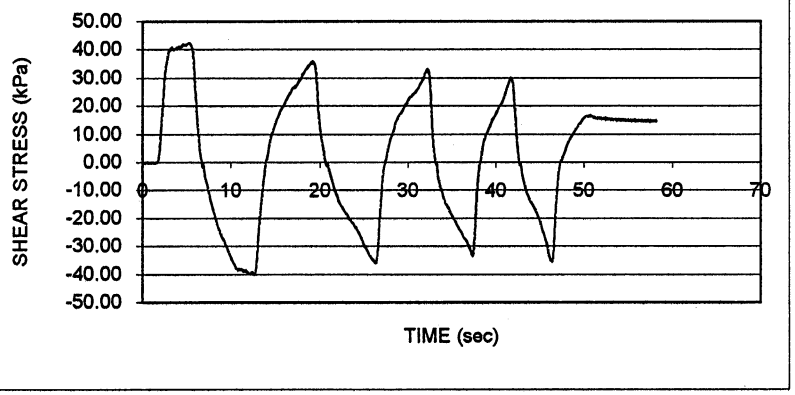

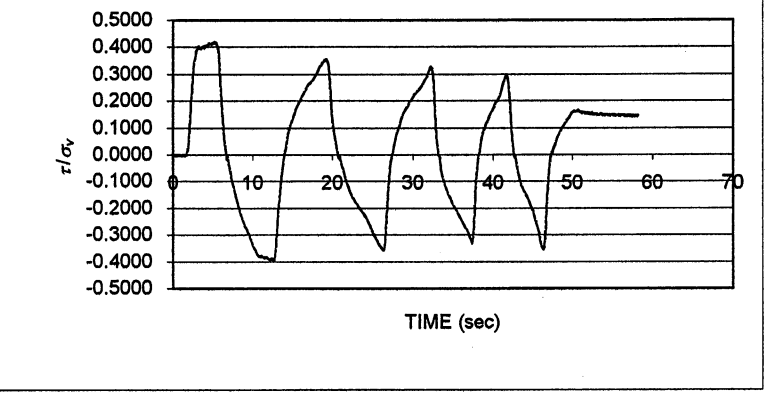

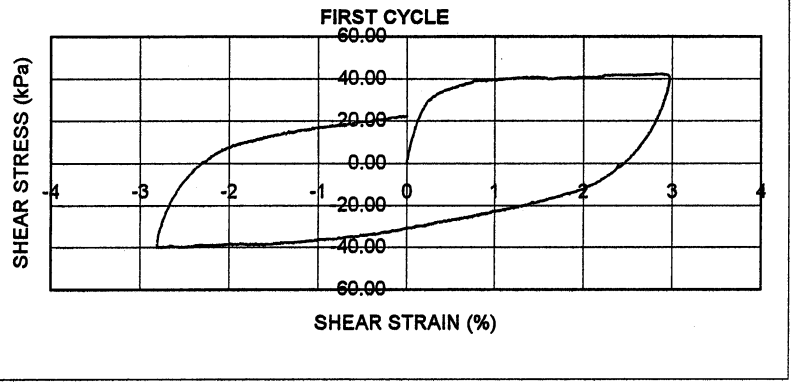

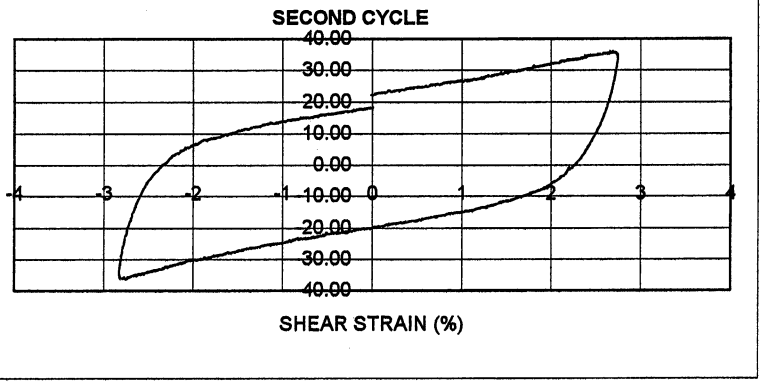

UCLA Soil Dynamics Laboratory

Double Specimen Direct Simple Shear (DSDSS) Test

Principal investigator: Mladen Vucetic, Professor

Test performed by: Kentaro Tabata Test No.: 2

Project:	PEARL			Date:	6/2/2001
Boring:	Meloland				
Tube No.:	S-3			Depth (ft):	28.0-29.6
Specific gravity	2.74	LL (%):	60.8	PI:	29.8
Group symbol:	CH	Silt (%):	42.8	Clay (%):	56.0
Comments:	Brown clay. Sticky, plastic soil.				

MODULUS REDUCTION			DAMPING		
γ_c (%)	G_s (MPa)	G_s/G_{max}	γ_c (%)	λ (%)	
0.00040	30.597	0.981			
0.00045	31.102	0.997			
0.00104	30.744	0.985	0.00112	2.332	
0.00112	29.973	0.961	0.00255	2.265	
0.00249	30.062	0.964	0.00932	2.413	
0.00255	30.400	0.974	0.02877	4.107	
0.00919	29.090	0.932	0.09628	8.470	
0.00932	29.196	0.936			
0.03059	25.109	0.805			
0.02877	25.058	0.803			
0.09647	16.808	0.539			
0.09628	16.594	0.532			
0.51092	6.903	0.221			
1.00159	3.923	0.126			
1.50330	2.693	0.086			
2.00131	2.034	0.065			
2.50115	1.666	0.053			
2.96783	1.372	0.044			

Estimated G_{max} (MPa)	31.2

Meloland, S-3, Depth = 28-29.6 feet, PI = 29.8,
Vertical stress = 101 kPa.

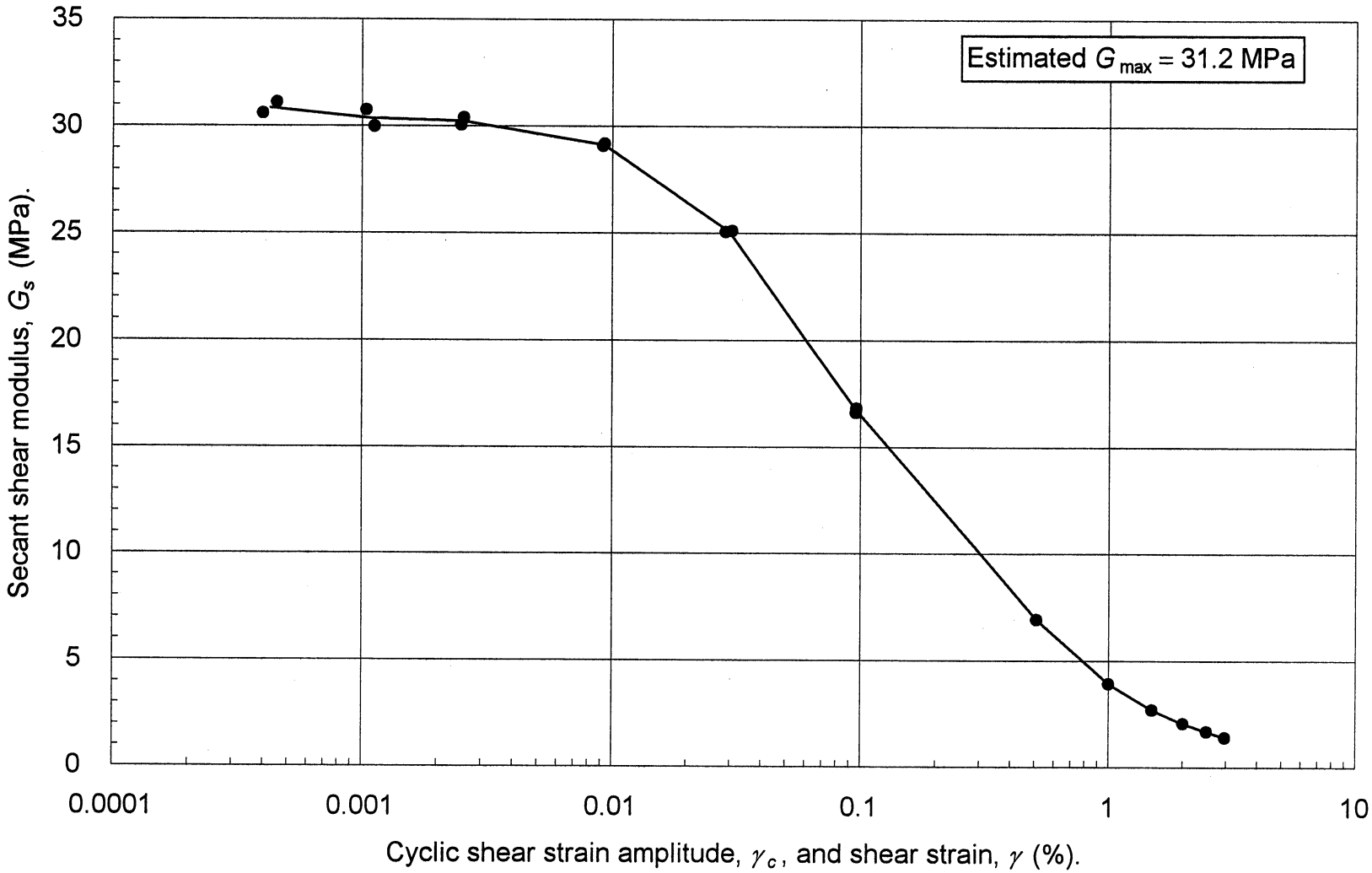

Meloland, S-3, Depth = 28-29.6 feet, PI = 29.8,
Vertical stress = 101 kPa.

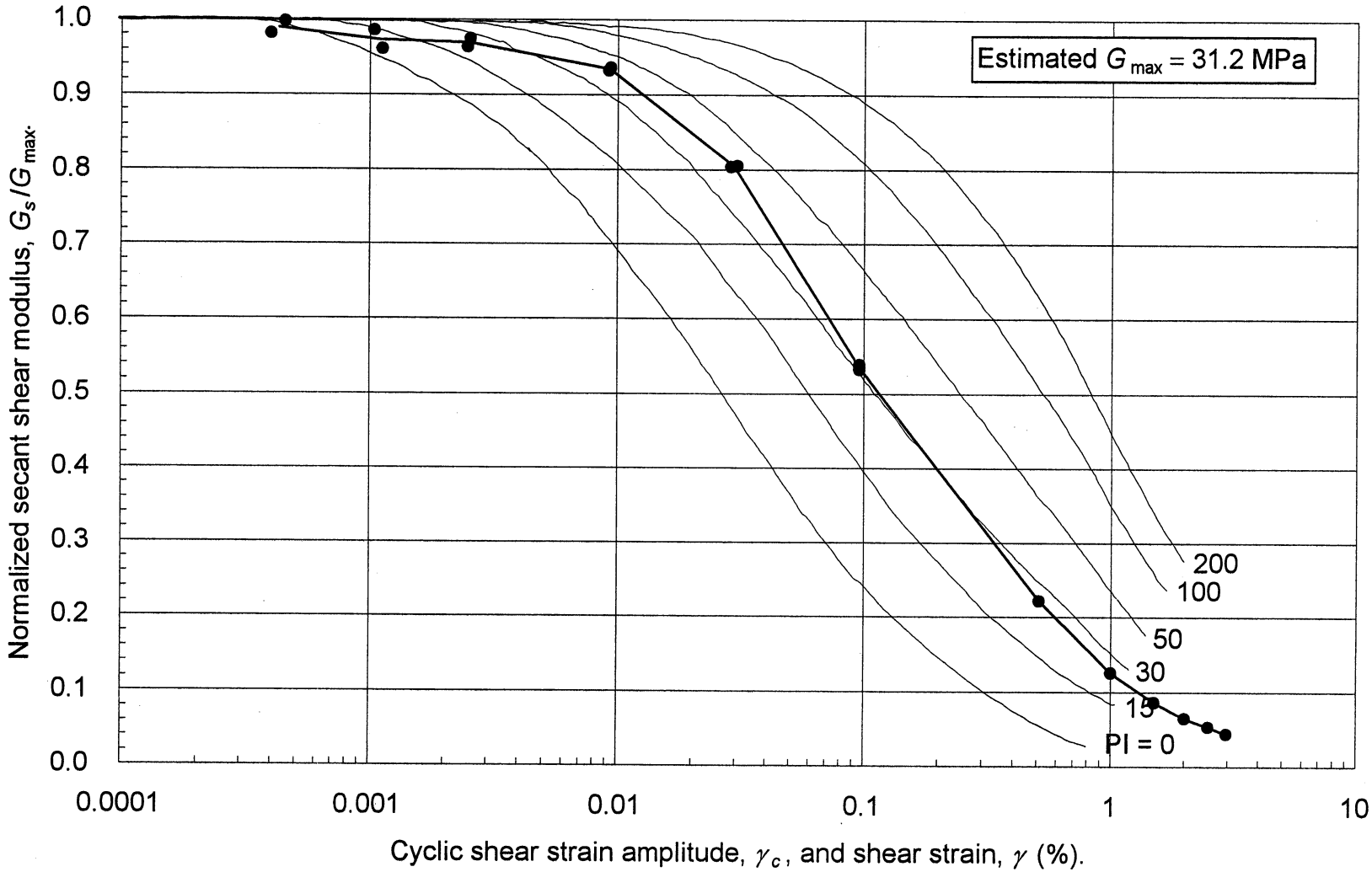

Meloland, S-3, Depth = 28-29.6 feet, PI = 29.8,
Vertical stress = 101 kPa.

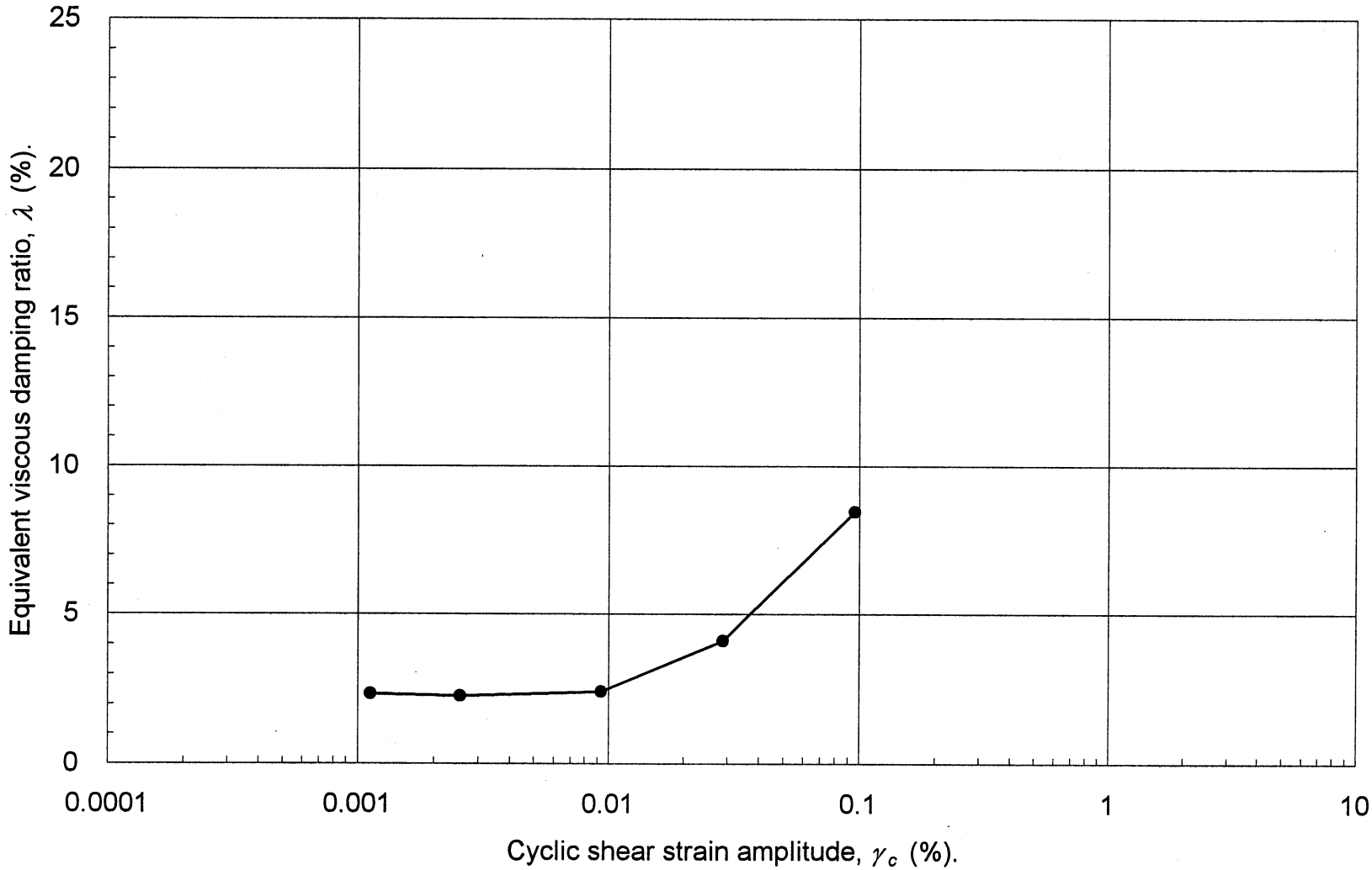

Meloland, S-3, Depth = 28-29.6 feet, PI = 29.8,
Vertical stress = 101 kPa.

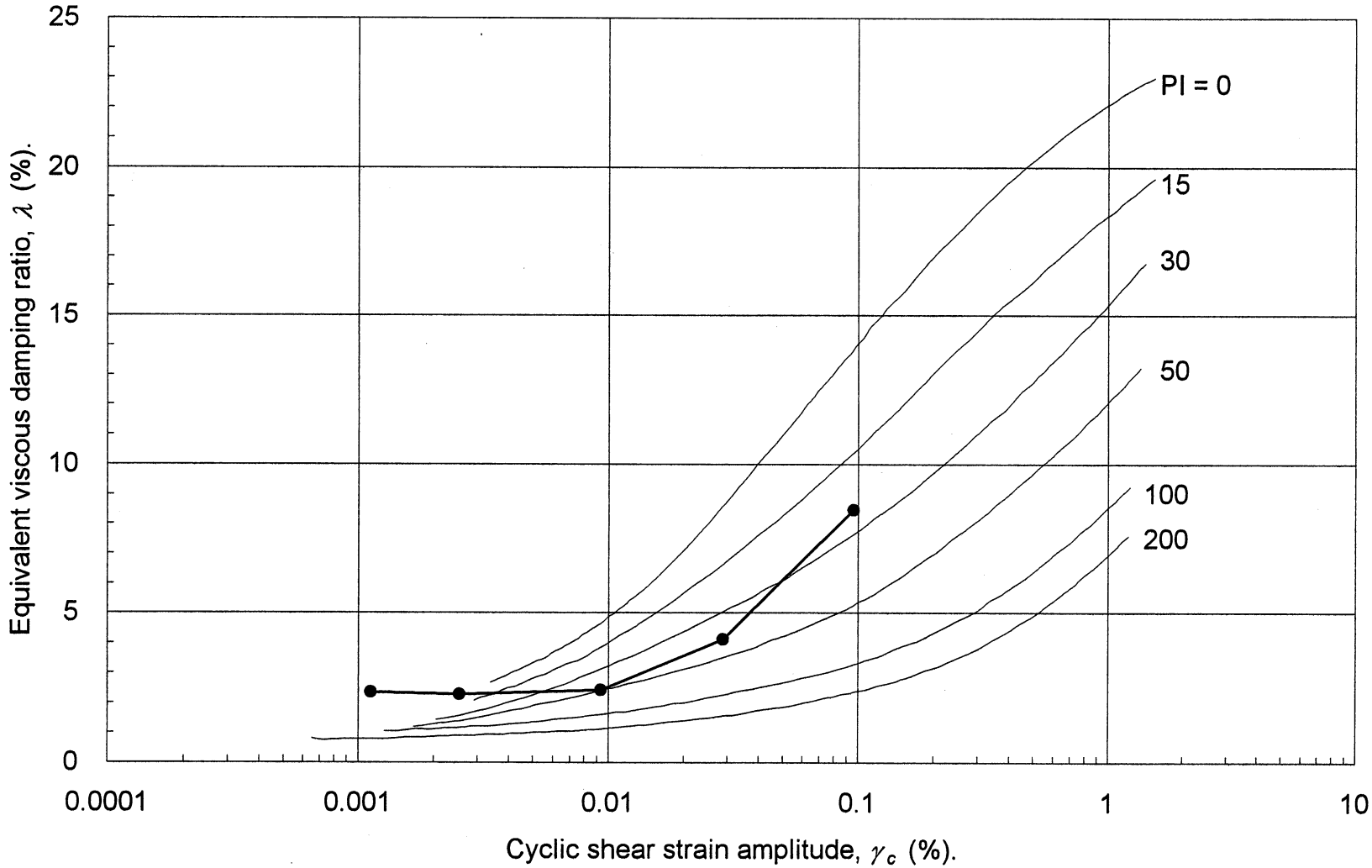

UCLA Soil Dynamics Laboratory

Specific Gravity Test

Principal investigator: Mladen Vucetic, Professor

Test performed by: Kentaro Tabata Test No.: 2

Project:	PEARL			Date:	6/6/2001
Boring:	Meloland				
Tube No.:	S-3	Depth (ft):	28.0 -29.6	GWT (ft):	6.5
Comments:	Brown clay. Sticky, plastic soil.				

SPECIFIC GRAVITY TEST

Test No.	1		
Bottle No.	3		
Wt. of bottle (g)	178.46		
Volume of bottle (cm^3)	500		
Wt. of bottle+water+soil (g)	688.27		
Temperature (°C)	24.0		
Wt. of bottle+water (g)	675.55		
Evaporating dish No.	B-13		
Weight of dish (g)	482.91		
Wt. of dish+dry soil (g)	502.92		
Wt. of dry soil (g)	20.01		
Specific gravity of water	0.9973		
Specific gravity of soil	**2.74**		

UCLA Soil Dynamics Laboratory

Grain Size Distribution

Principal investigator: Mladen Vucetic, Professor

Test performed by: Kentaro Tabata Test No.: 2

Project:	PEARL				
Boring:	Meloland				
Tube No.:	S-3	Depth (ft):	28.0 -29.6	GWT (ft):	6.5
Comments:	Brown clay. Sticky, plastic soil.				

GRAIN SIZE DISTRIBUTION

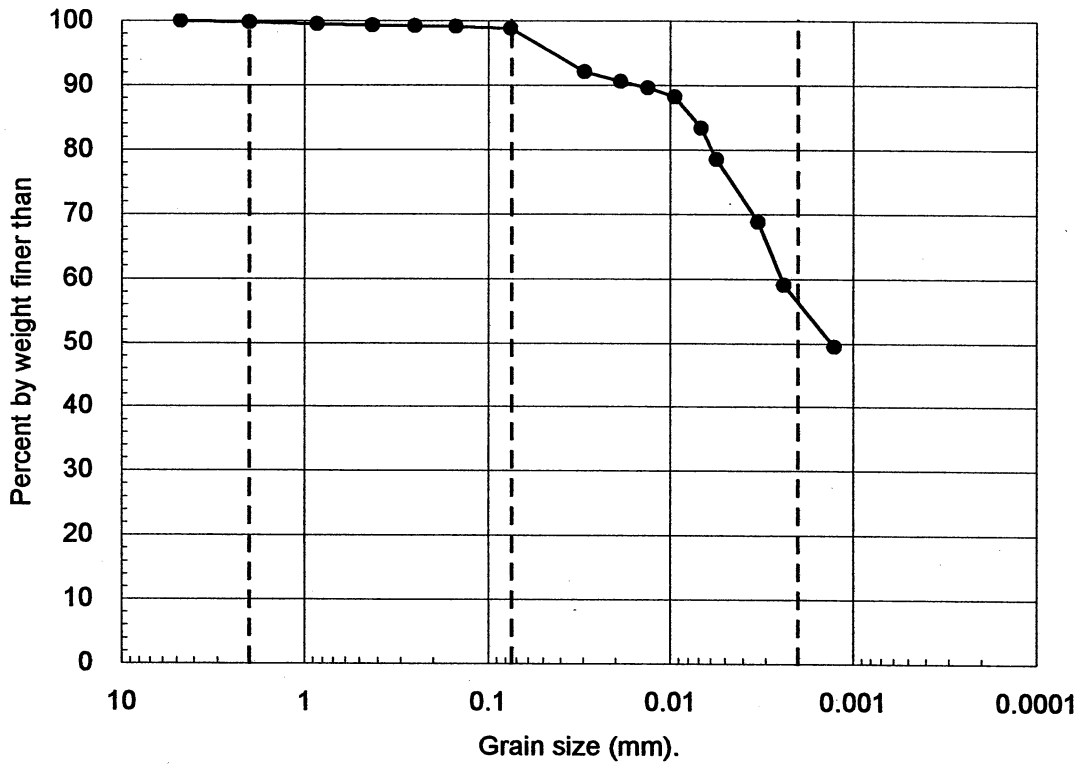

Clay (%)	Silt (%)	Sand (%)	Gravel (%)
56.0	42.8	1.0	0.2

UCLA Soil Dynamics Laboratory

Hydrometer Analysis

Principal investigator: Mladen Vucetic, Professor

Test performed by: Kentaro Tabata Test No.: 2

Project:	PEARL			Date:	6/4/2001
Boring:	Meloland				
Tube No.:	S-3	Depth (ft):	28.0 -29.6	GWT (ft):	6.5
Comments:	Brown clay. Sticky, plastic soil.				

HYDROMETER TEST

Time	Elapsed time t (sec)	Temp. T (°C)	Reading R'_T	Corr. reading $R_T=R'_T+c_m$	Depth H (cm)	Grain diameter D (mm)	Temp. corr. m_T	Corr. depth $R_T+m_T-c_d$	% by wt. finer than W_D (%)
10:44:05	0								
10:46:05	120	21.0	1020.8	1021.3	10.82	0.0295	0.700	1019.0	92.06
10:49:05	300	21.0	1020.5	1021.0	10.90	0.0188	0.700	1018.7	90.60
10:54:05	600	21.0	1020.3	1020.8	10.96	0.0133	0.700	1018.5	89.63
11:04:05	1200	21.0	1020.0	1020.5	11.04	0.0094	0.700	1018.2	88.18
11:24:05	2400	21.0	1019.0	1019.5	11.30	0.0068	0.700	1017.2	83.33
11:44:05	3600	21.0	1018.0	1018.5	11.57	0.0056	0.700	1016.2	78.49
13:44:05	10800	21.0	1016.0	1016.5	12.11	0.0033	0.700	1014.2	68.80
16:40:00	21355	21.0	1014.0	1014.5	12.64	0.0024	0.700	1012.2	59.11
9:00:00	80155	21.0	1012.0	1012.5	13.18	0.0013	0.700	1010.2	49.42
11:30:00	175555	21.0	1010.5	1011.0	13.58	0.0009	0.700	1008.7	42.15

APPARATUS

Hydrometer no.:	88-18587	a_0	284.03	a_1	-0.2675
Graduate no.:	2				

FACTORS

Meniscus corr., c_m:	0.5	
Disp. agent corr, c_d:	3.0	
Visc. of water, η.	21.0 °C	9.320E-06 g sec/cm^2
	°C	g sec/cm^3

WEIGHT

Dry soil (g)	32.14
Percent by wt (%)	98.83
Dry soil for sieve (g)	0.38
Total (g)	32.52

UNIT WEIGHT

Specific gravity:		2.74
T	γ_w	γ_s
(°C)	(g/cm^3)	(g/cm^3)
21.0	0.9980	2.7318

UCLA Soil Dynamics Laboratory

Sieve Analysis

Principal investigator: Mladen Vucetic, Professor

Test performed by: Kentaro Tabata Test No.: 2

Project:	PEARL			Date:	6/6/2001
Boring:	Meloland				
Tube No.:	S-3	Depth (ft):	28.0 -29.6	GWT (ft):	6.5
Comments:	Brown clay. Sticky, plastic soil.				

SIEVE ANALYSIS

Sieve No.	Diameter (mm)	Sieve (g)	S+wet (g)	S+dry (g)	Retained (g)	Retained (%)	Cumulated (g)	Cumulated (%)	Passing (%)
4	4.750	463.40		463.40	0.00	0.00	0.00	0.00	100.00
10	2.000	432.93		432.99	0.06	0.18	0.06	0.18	99.82
20	0.850	407.30		407.39	0.09	0.28	0.15	0.46	99.54
40	0.425	337.87		337.94	0.07	0.22	0.22	0.68	99.32
60	0.250	351.50		351.53	0.03	0.09	0.25	0.77	99.23
100	0.150	342.16		342.20	0.04	0.12	0.29	0.89	99.11
200	0.075	299.82		299.91	0.09	0.28	0.38	1.17	98.83
Total					0.38	1.17			

WEIGHT

Dry soil for sieve (g)	0.38
Dry soil for hydr. (g)	32.14
Total (g)	32.52
Percent coaser (%)	1.17

UCLA Soil Dynamics Laboratory

Atterberg Limit Determination

Principal investigator: Mladen Vucetic, Professor

Test performed by: Kentaro Tabata Test No.: 2

Project:	PEARL			Date:	6/14/2001
Boring:	Meloland				
Tube No.:	S-3	Depth (ft):	28.0 -29.6	GWT (ft):	6.5
Comments:	Brown clay. Sticky, plastic soil.				

LIQUID LIMIT TEST

Test No.	1	2	3	4	5			
Number of blows	31	29	18	12	9			
Container No.	ST-11	ST-7	ST-13	ST-10	ST-15			
Container (g)	30.26	30.35	30.19	30.32	30.26			
Cont+wet soil (g)	35.85	37.31	37.33	37.31	37.39			
Cont+dry soil (g)	33.76	34.72	34.57	34.53	34.49			
Water (g)	2.09	2.59	2.76	2.78	2.90			
Dry soil (g)	3.50	4.37	4.38	4.21	4.23			
Water content (%)	59.71	59.27	63.01	66.03	68.56			

PLASTIC LIMIT TEST

Test No.	1	2	3
Container No.	ST-24	ST-21	ST-18
Container (g)	29.98	30.29	30.13
Cont+wet soil (g)	32.01	33.07	32.78
Cont+dry soil (g)	31.52	32.42	32.16
Water (g)	0.49	0.65	0.62
Dry soil (g)	1.54	2.13	2.03
Water content (%)	31.82	30.52	30.54

ATTERBERG LIMITS

Liquid limit (%)	**60.8**
Plastic limit (%)	**31.0**
Plasticity index	**29.8**

CLASSIFICATION

CH

FLOW CHART

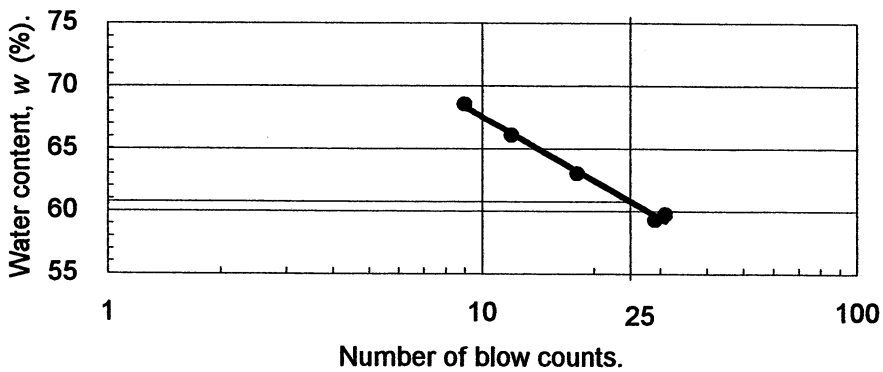

UCLA Soil Dynamics Laboratory

Atterberg Limit Determination

Principal investigator: Mladen Vucetic, Professor

Test performed by: Kentaro Tabata Test No.: 2

Project:	PEARL			Date:	6/14/2001
Boring:	Meloland				
Tube No.:	S-3	Depth (ft):	28.0 -29.6	GWT (ft):	6.5
Comments:	Brown clay. Sticky, plastic soil.				

PLASTICITY CHART

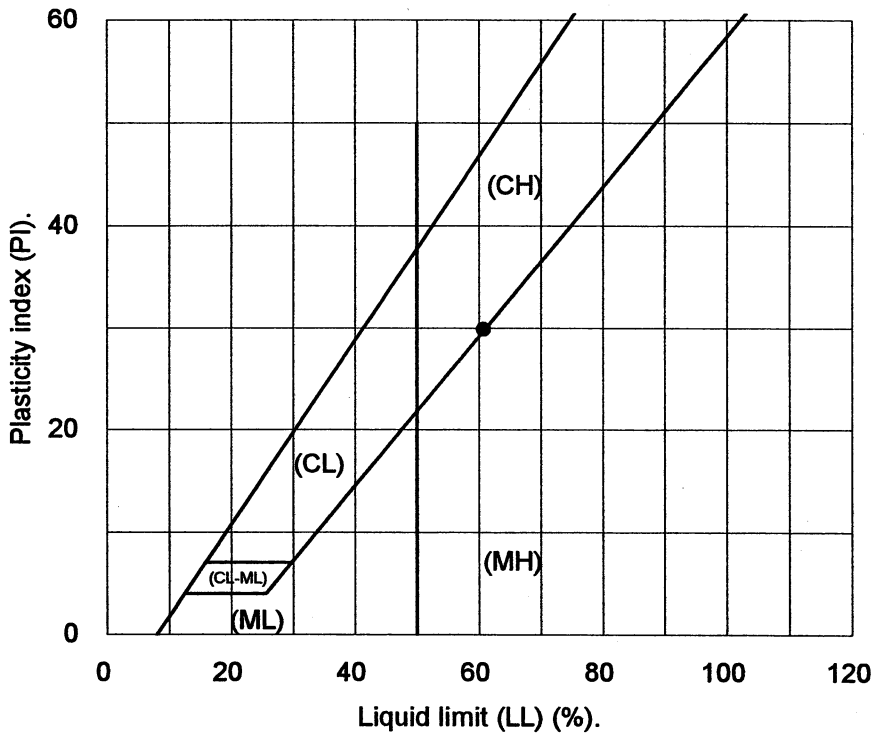

3.4 Test 3: MELOLAND S-5

UCLA Soil Dynamics Laboratory

Double Specimen Direct Simple Shear (DSDSS) Test

Principal investigator: Mladen Vucetic, Professor

Test performed by: Kentaro Tabata Test No.: 3

Project:	PEARL			Date:	5/31/2001
Boring:	Meloland				
Tube No.:	S-5	Depth (ft):	59.0 -60.0	GWT (ft):	6.5 (reported by others)
Comments:	Brown sandy silt. Specimen obtained from the bottom of the tube (specimen depth ~ 59.5 ft).				

FORM 1: SPECIMEN PREPARATION

WATER CONTENT, SPECIFIC GRAVITY

	Before consol.	After shearing	
Container No.	ST-11	ST-13	DISH
Cont+wet soil (g)	38.22	181.09	145.26
Cont+dry soil (g)	36.68	152.64	120.55
Container (g)	30.25	49.56	10.87
Water (g)	1.54	28.45	24.71
Dry soil (g)	6.43	103.08	109.68
Water content(%)	23.95	27.60	22.53
Avg. water cont. (%)	23.95		25.06
Spceific gravity			2.68

UNIT WEIGHT, VOID RATIO, SATURATION

	Before consol.	Before shearing	After shearing
Average weight (g)	133.30	133.30	
Height (cm)	1.965	1.918	
Area (cm^2)	34.84	34.84	
Volume (cm^3)	68.45	66.80	
Unit weight (g/cm^3)	1.947	1.995	
Unit weight (kN/m^3)	19.08	19.55	
Void ratio	0.71	0.66	
Saturation (%)	90.9	96.6	

HEIGHT OF SPECIMEN

	Before consol.		Before shearing	After shearing		
	Top	Bottom	Average	Average		
Height (cm)	1.965	1.965	1.918	1.918		

AREA OF SPECIMEN

Initial diameter (cm): 6.660 Initial area (cm^2): 34.837

Load (kg)	Stress (kg/cm^2)	Stress (kN/m^2)	Diameter (cm)	Membrane (cm)	Corrected diameter (cm)	Area (cm^2)

Meloland S-5					
DSDSS TEST - Step 2b					
Type of soil: CL					
LL	29.5	PI	15.8	%Silt	86.2
e_0	0.66	S_0 (%)	96.6	%Clay	9.6
σ_v (kPa)	187	OCR	n/a	w (%)	24.0
γ_c (%)	~0.00038	H_0 (mm)	19.18	Spec. Gr.	2.68

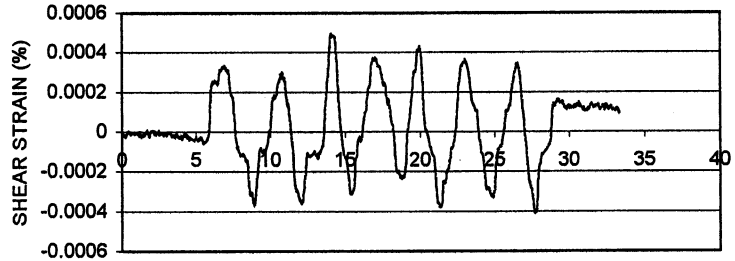

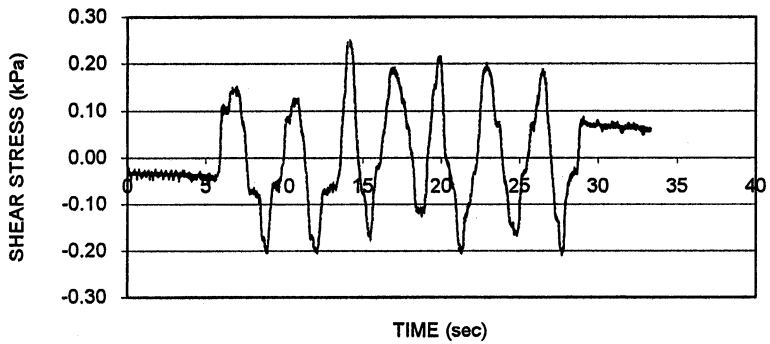

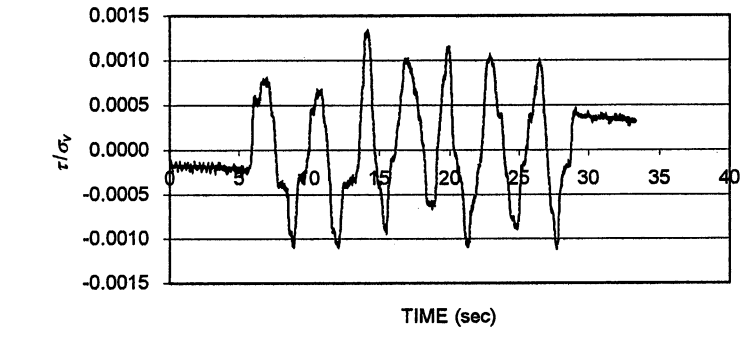

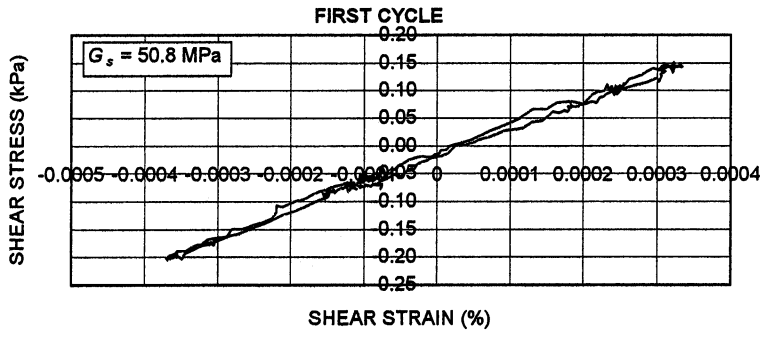

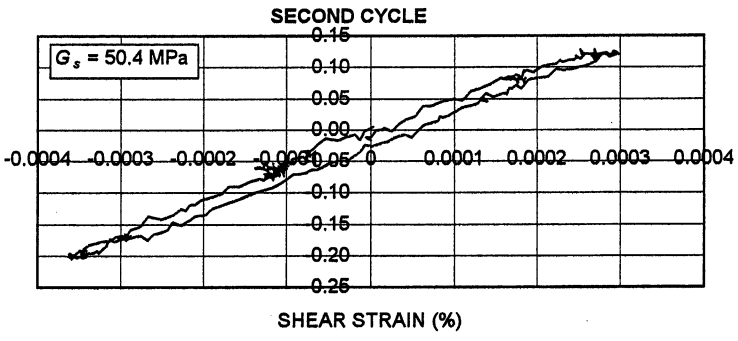

Meloland S-5					
DSDSS TEST - Step 3b					
Type of soil: CL					
LL	29.5	PI	15.8	%Silt	86.2
e_0	0.66	S_0 (%)	96.6	%Clay	9.6
σ_v (kPa)	187	OCR	n/a	w (%)	24.0
γ_c (%)	~0.001	H_0 (mm)	19.18	Spec. Gr.	2.68

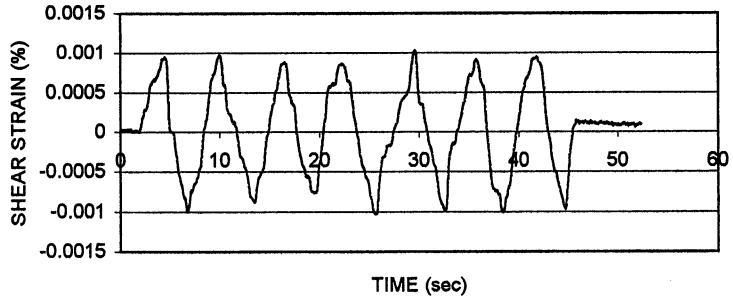

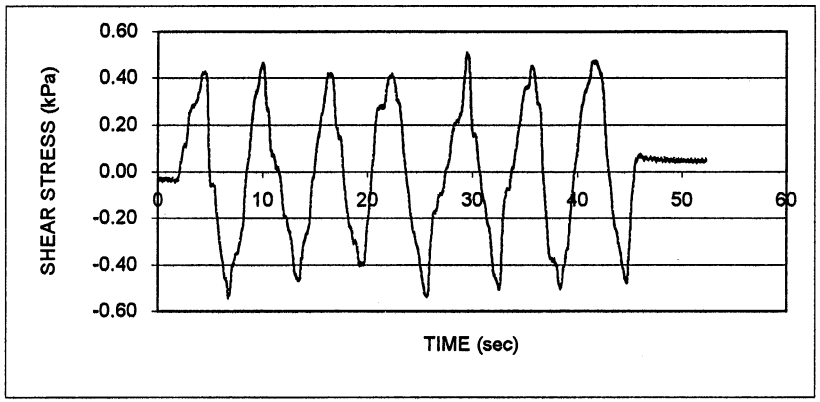

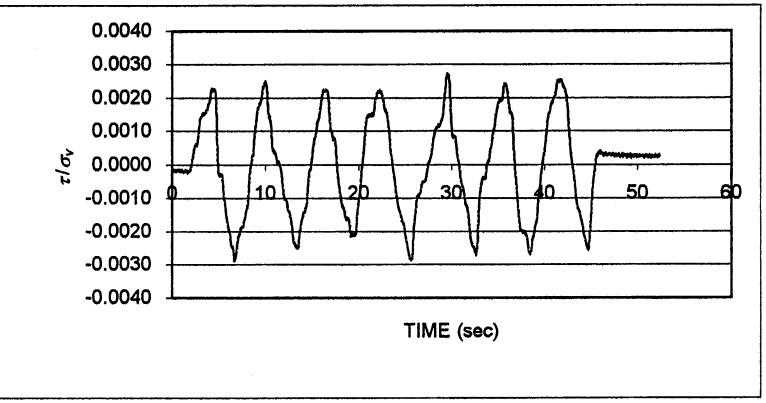

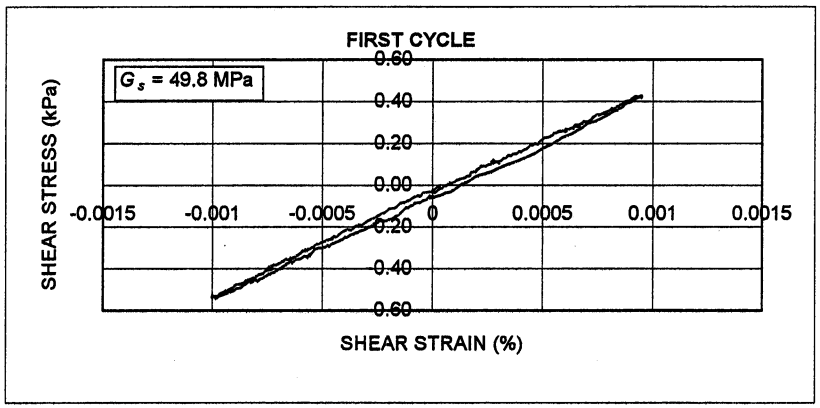

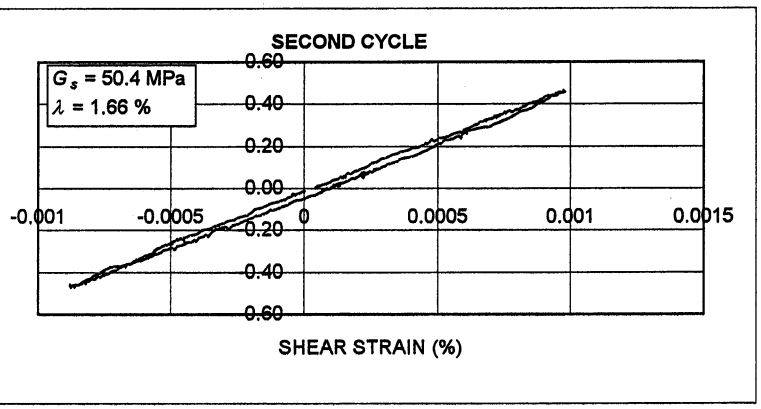

Meloland S-5					
DSDSS TEST - Step 4b					
Type of soil: CL					
LL	29.5	PI	15.8	%Silt	86.2
e_0	0.66	S_0 (%)	96.6	%Clay	9.6
σ_v (kPa)	187	OCR	n/a	w (%)	24.0
γ_c (%)	~0.0029	H_0 (mm)	19.18	Spec. Gr.	2.68

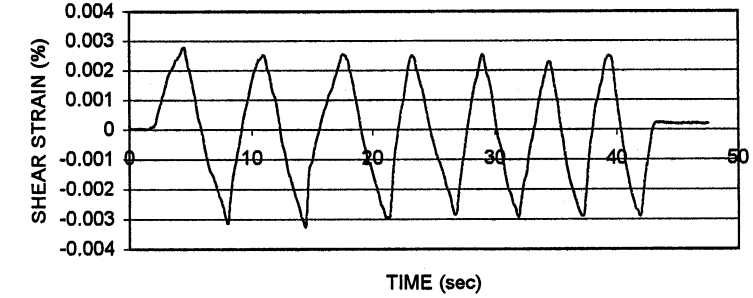

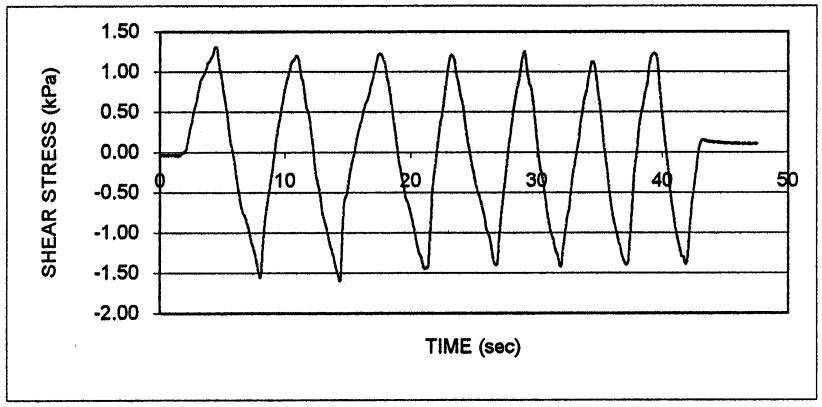

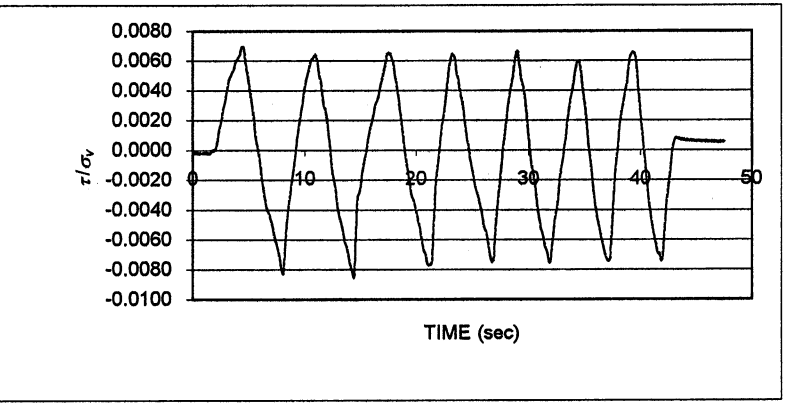

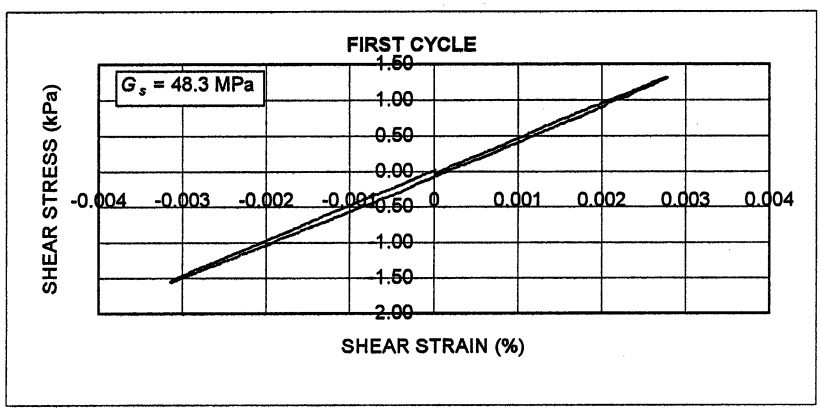

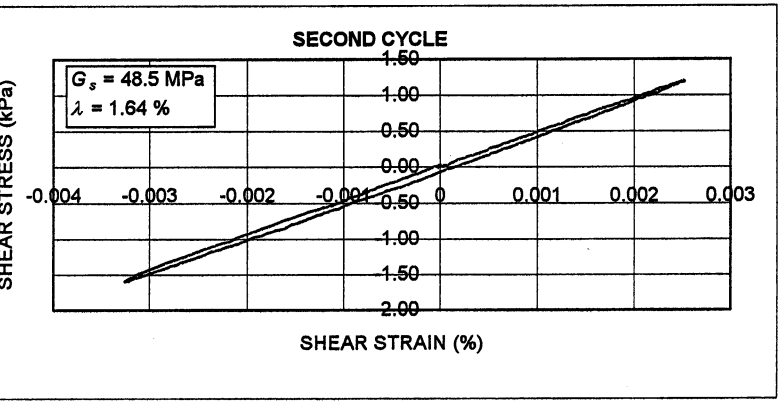

Meloland S-5					
DSDSS TEST - Step 5b					
Type of soil: CL					
LL	29.5	PI	15.8	%Silt	86.2
e_0	0.66	S_0 (%)	96.6	%Clay	9.6
σ_v (kPa)	187	OCR	n/a	w (%)	24.0
γ_c (%)	~0.01	H_0 (mm)	19.18	Spec. Gr.	2.68

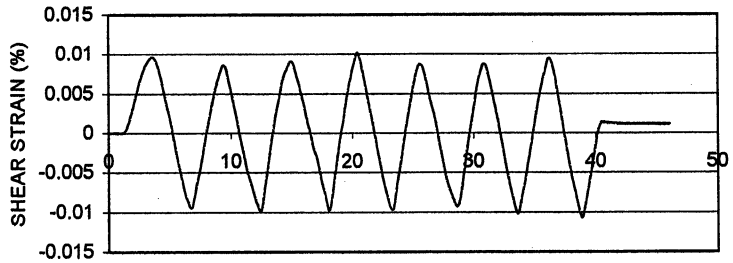

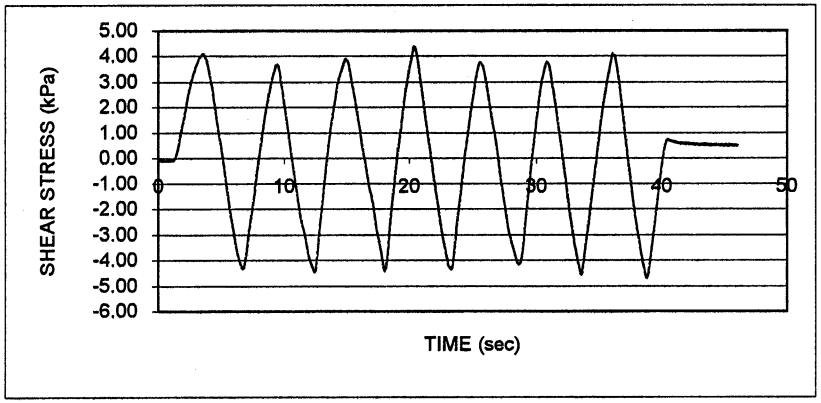

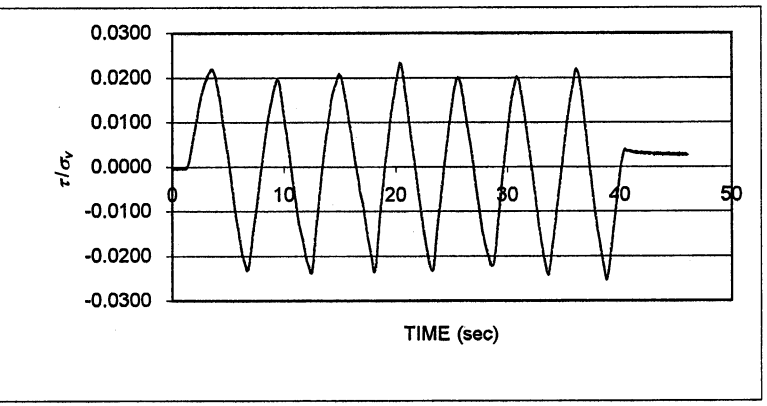

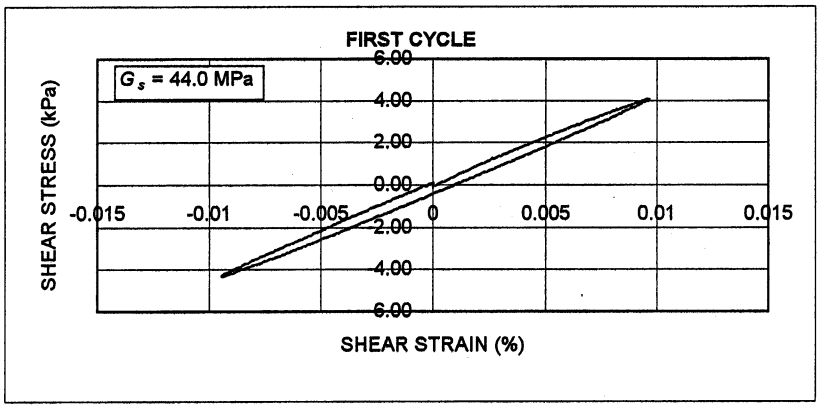

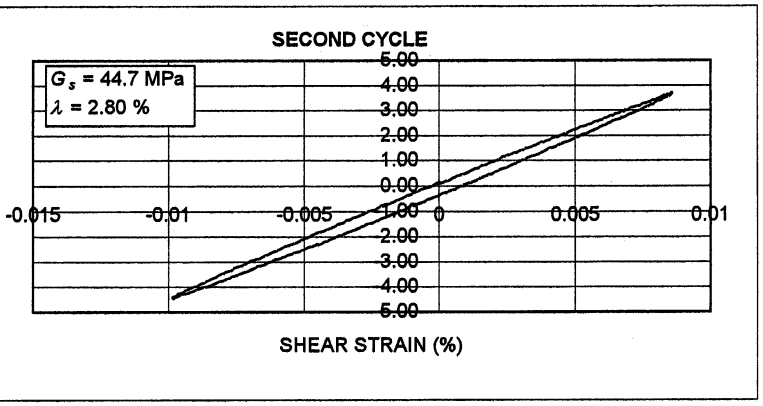

Meloland S-5					
DSDSS TEST - Step 6b					
Type of soil: CL					
LL	29.5	PI	15.8	%Silt	86.2
e_0	0.66	S_0 (%)	96.6	%Clay	9.6
σ_v (kPa)	187	OCR	n/a	w (%)	24.0
γ_c (%)	~0.028	H_0 (mm)	19.18	Spec. Gr.	2.68

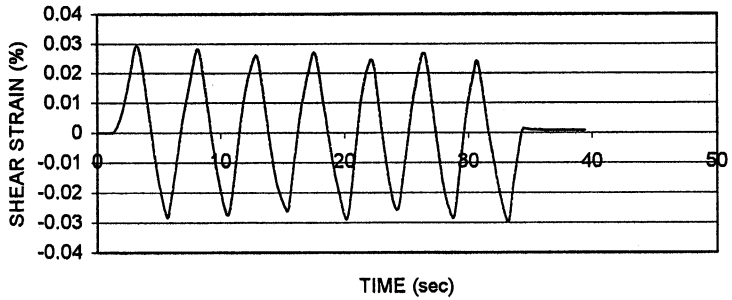

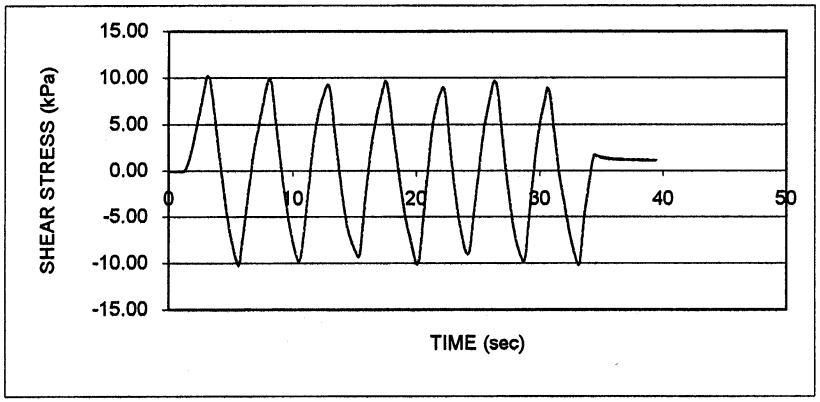

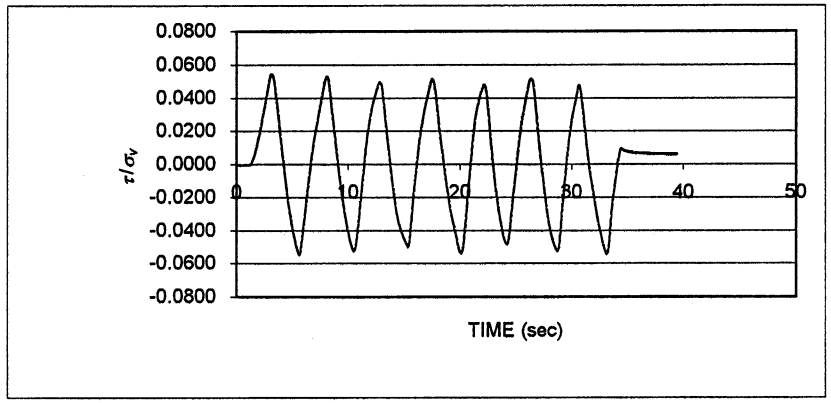

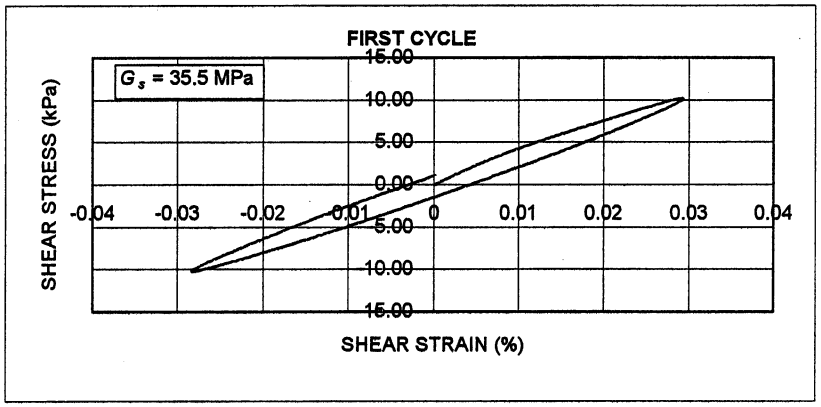

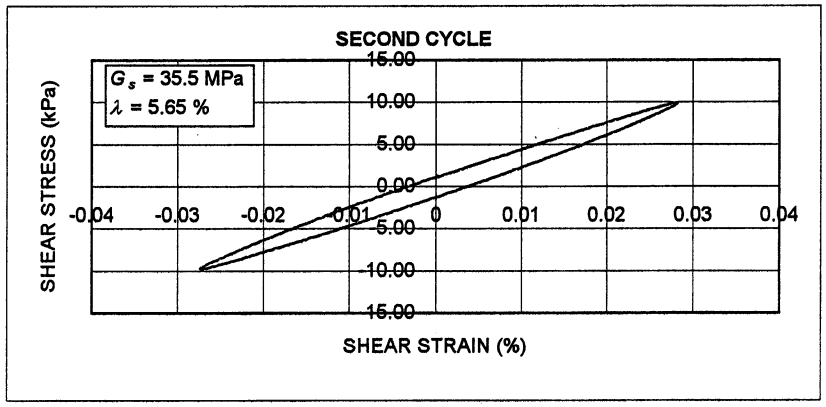

Meloland S-5					
DSDSS TEST - Step 7b					
Type of soil: CL					
LL	29.5	PI	15.8	%Silt	86.2
e_0	0.66	S_0 (%)	96.6	%Clay	9.6
σ_v (kPa)	187	OCR	n/a	w (%)	24.0
γ_c (%)	~0.1	H_0 (mm)	19.18	Spec. Gr.	2.68

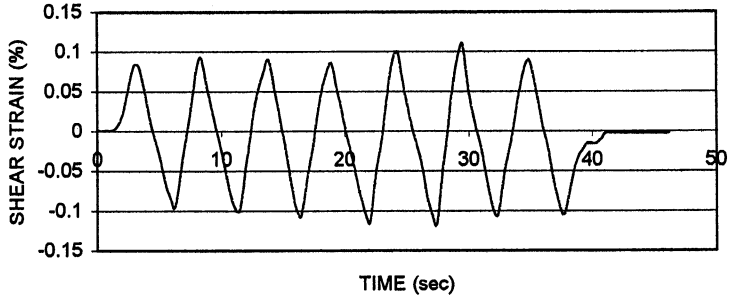

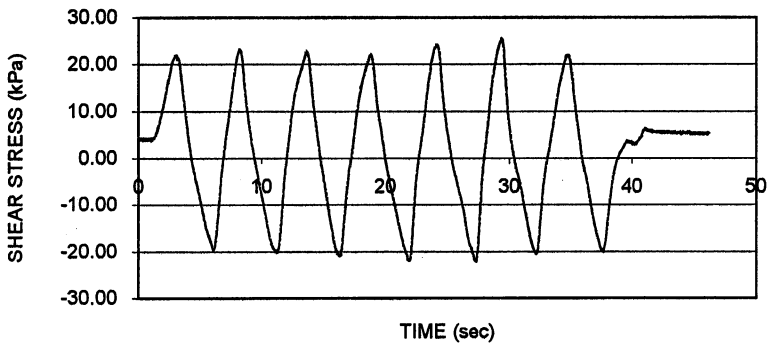

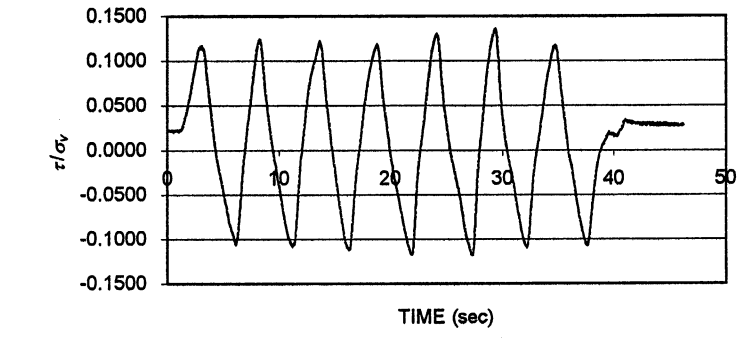

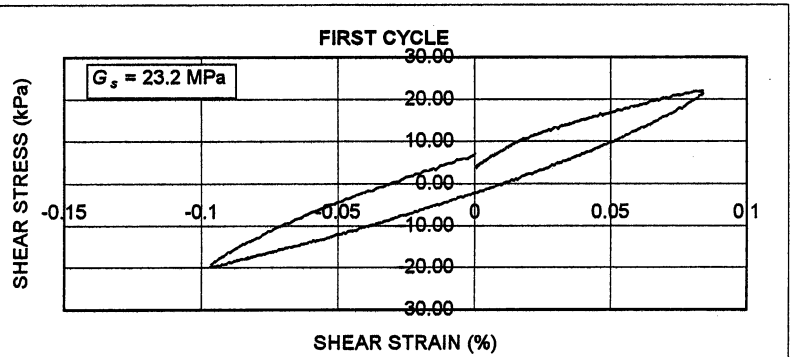

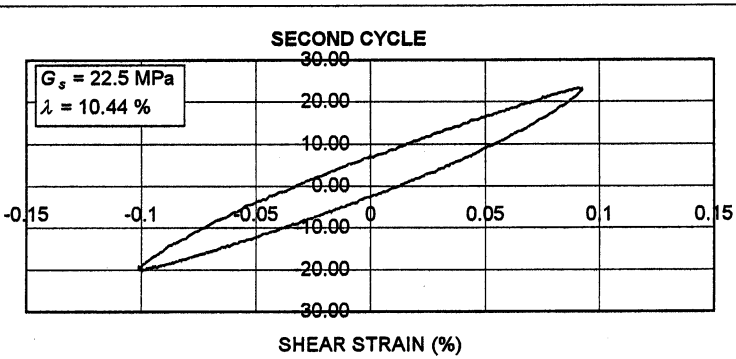

Meloland S-5					
DSDSS TEST - Step 8					
Type of soil: CL					
LL	29.5	PI	15.8	%Silt	86.2
e_0	0.66	S_0 (%)	96.6	%Clay	9.6
σ_v (kPa)	187	OCR	n/a	w (%)	24.0
γ_c (%)	~3.0	H_0 (mm)	19.18	Spec. Gr.	2.68

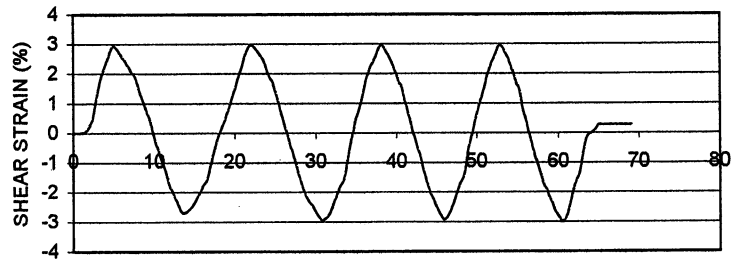

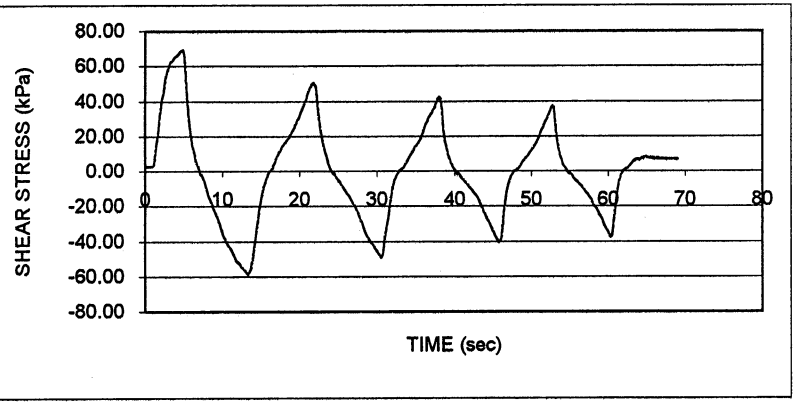

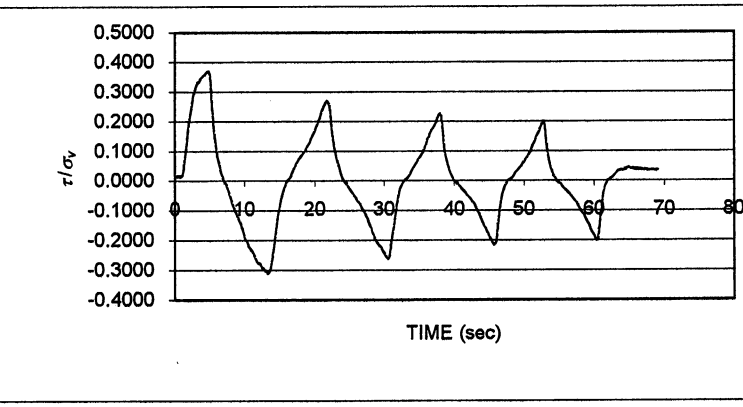

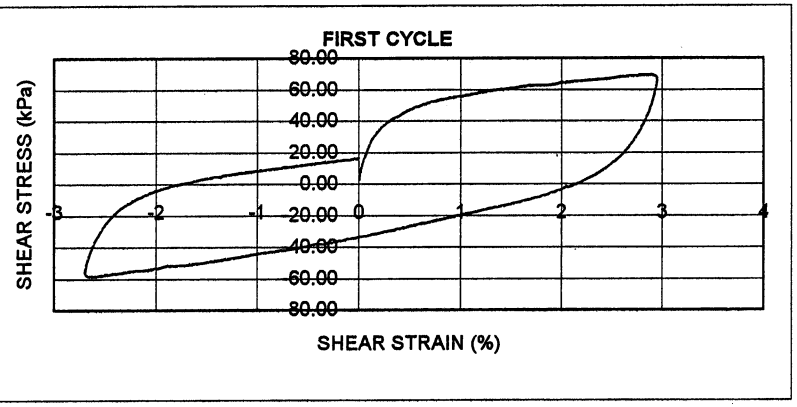

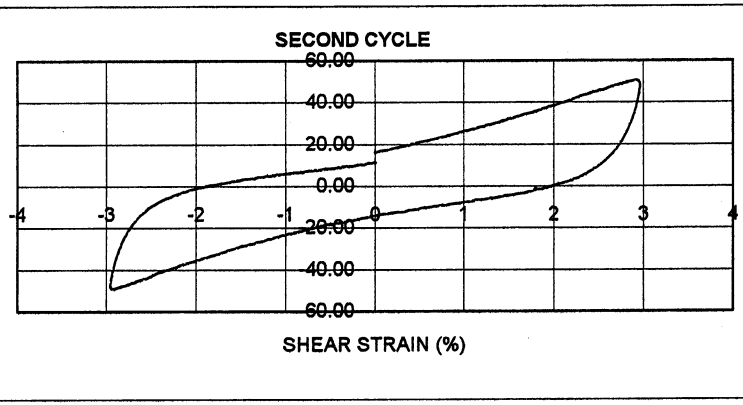

UCLA Soil Dynamics Laboratory

Double Specimen Direct Simple Shear (DSDSS) Test

Principal investigator: Mladen Vucetic, Professor

Test performed by: Kentaro Tabata Test No.: 3

Project:	PEARL			Date:	5/31/2001
Boring:	Meloland				
Tube No.:	S-5			Depth (ft):	59.0-60.0
Specific gravity	2.68	LL (%):	29.5	PI:	15.8
Group symbol:	CL	Silt (%):	86.2	Clay (%):	9.6
Comments:	Brown sandy silt.				

MODULUS REDUCTION			DAMPING		
γ_c (%)	G_s (MPa)	G_s/G_{max}	γ_c (%)	λ (%)	
0.00035	50.754	0.995			
0.00033	50.431	0.989			
0.00098	49.784	0.976	0.00093	1.659	
0.00093	50.391	0.988	0.00289	1.643	
0.00297	48.263	0.946	0.00922	2.802	
0.00289	48.461	0.950	0.02784	5.653	
0.00957	44.037	0.863	0.09688	10.439	
0.00922	44.168	0.866			
0.02890	35.468	0.695			
0.02784	35.501	0.696			
0.09043	23.168	0.454			
0.09688	22.480	0.441			
0.50697	9.385	0.184			
1.00107	5.557	0.109			
1.51172	4.024	0.079			
2.00210	3.204	0.063			
2.50172	2.678	0.053			
2.94600	2.282	0.045			

Estimated G_{max} (MPa)	51.0

Meloland, S-5, Depth = 59-60 feet, PI = 15.8,
Vertical stress = 187 kPa.

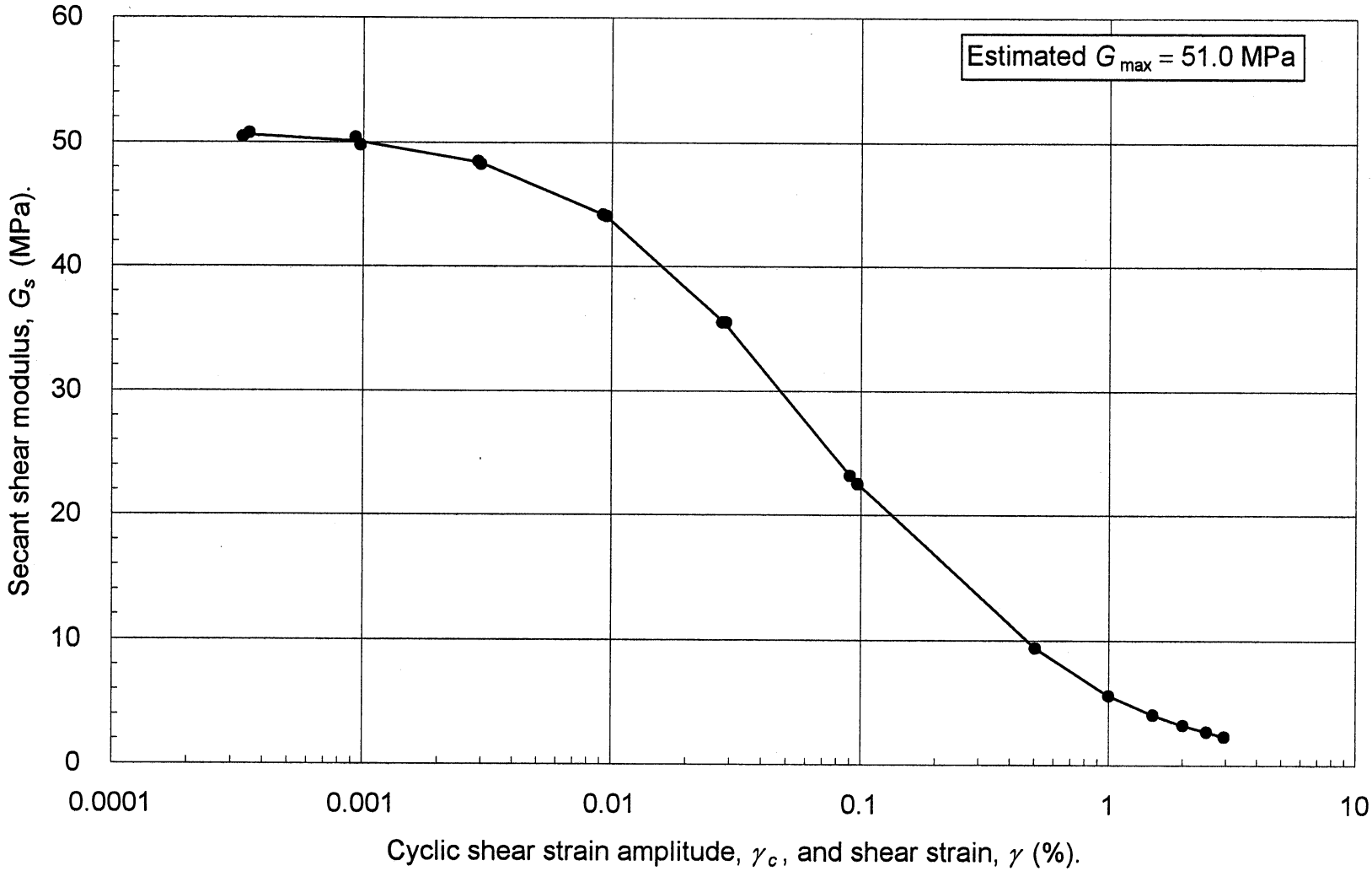

Meloland, S-5, Depth = 59-60 feet, PI = 15.8,
Vertical stress = 187 kPa.

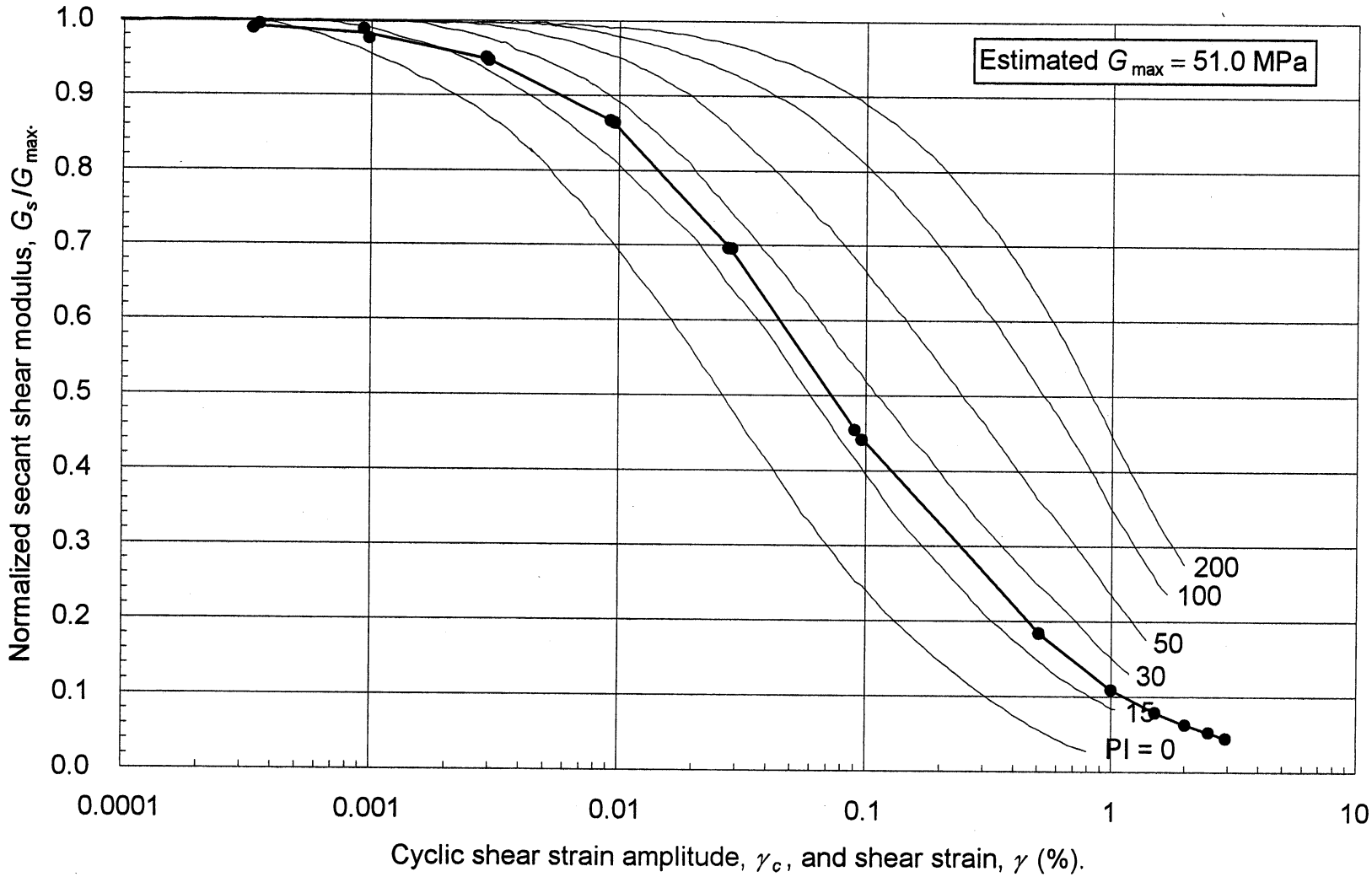

Meloland, S-5, Depth = 59-60 feet, PI = 15.8,
Vertical stress = 187 kPa.

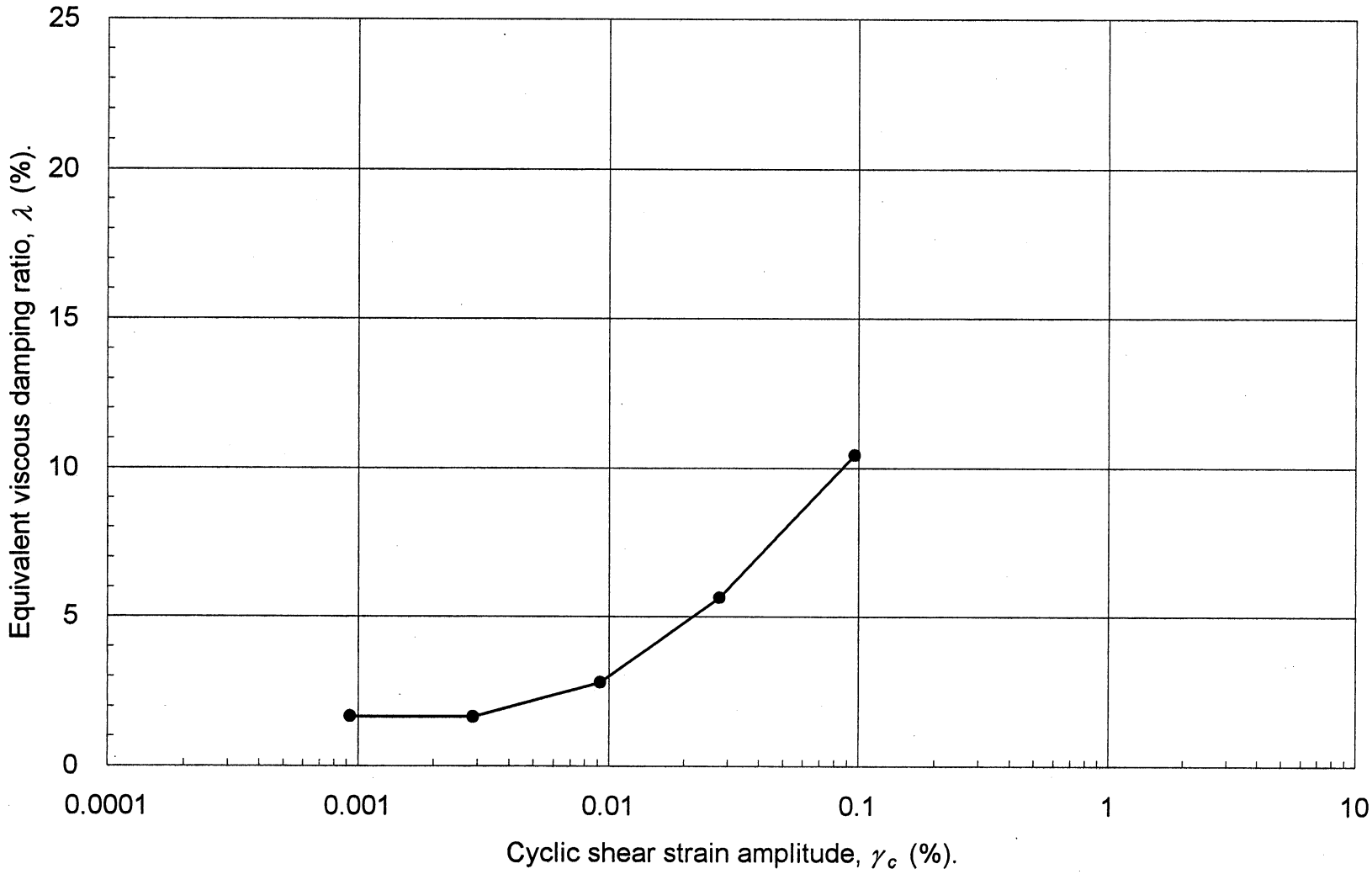

Meloland, S-5, Depth = 59-60 feet, PI = 15.8,
Vertical stress = 187 kPa.

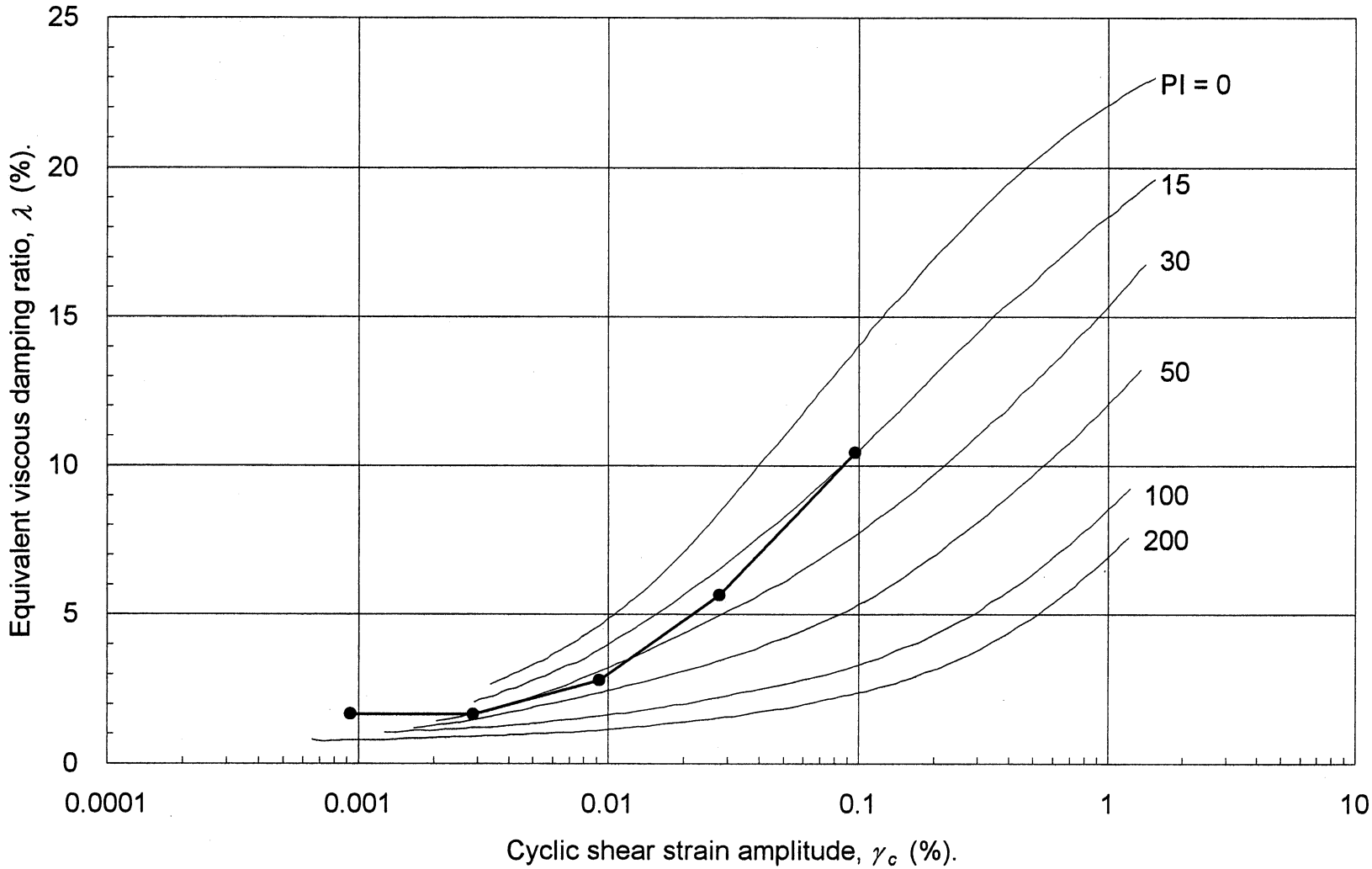

UCLA Soil Dynamics Laboratory

Specific Gravity Test

Principal investigator: Mladen Vucetic, Professor

Test performed by: Kentaro Tabata Test No.: 3

Project:	PEARL			Date:	5/31/2001
Boring:	Meloland				
Tube No.:	S-5	Depth (ft):	59.0 -60.0	GWT (ft):	6.5
Comments:	Brown sandy silt.				

SPECIFIC GRAVITY TEST

Test No.	1		
Bottle No.	3		
Wt. of bottle (g)	178.46		
Volume of bottle (cm^3)	500		
Wt. of bottle+water+soil (g)	689.64		
Temperature (°C)	24.0		
Wt. of bottle+water (g)	675.55		
Evaporating dish No.	B-2		
Weight of dish (g)	537.20		
Wt. of dish+dry soil (g)	559.63		
Wt. of dry soil (g)	22.43		
Specific gravity of water	0.9973		
Specific gravity of soil	**2.68**		

UCLA Soil Dynamics Laboratory

Grain Size Distribution

Principal investigator: Mladen Vucetic, Professor

Test performed by: Kentaro Tabata Test No.: 3

Project:	PEARL				
Boring:	Meloland				
Tube No.:	S-5	Depth (ft):	59.0 -60.0	GWT (ft):	6.5
Comments:	Brown sandy silt.				

GRAIN SIZE DISTRIBUTION

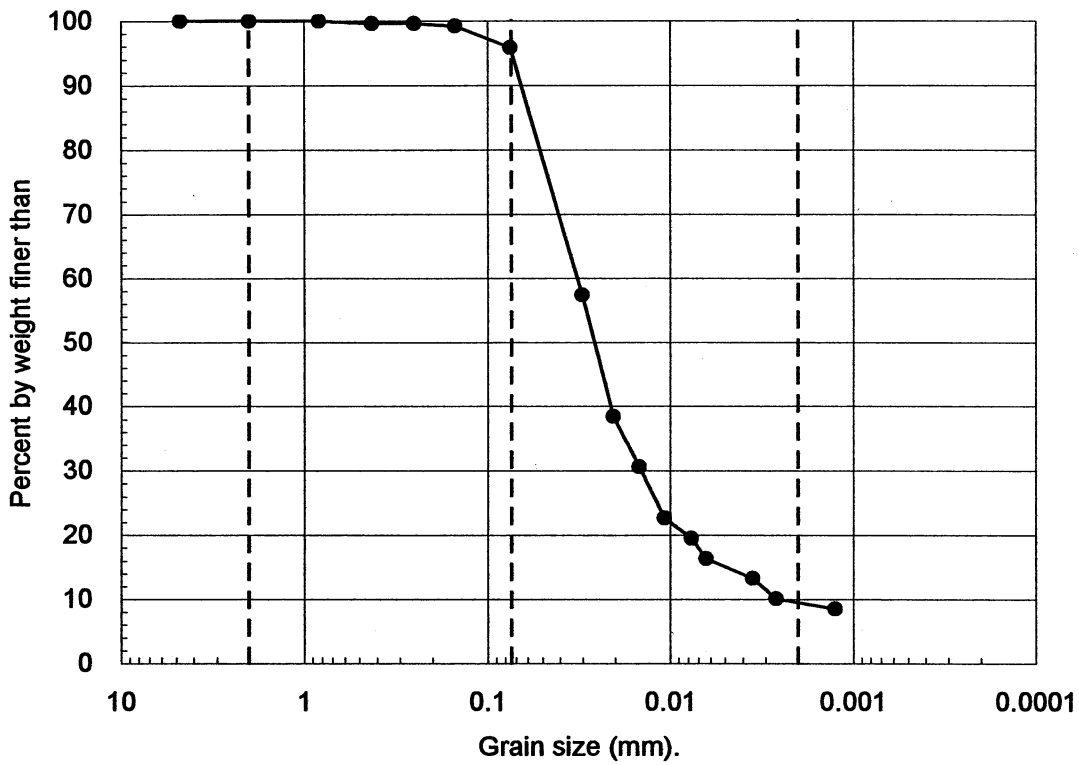

Clay (%)	Silt (%)	Sand (%)	Gravel (%)
9.6	86.2	4.2	0.0

UCLA Soil Dynamics Laboratory

Hydrometer Analysis

Principal investigator: Mladen Vucetic, Professor

Test performed by: Kentaro Tabata Test No.: 3

Project:	PEARL			Date:	5/30/2001
Boring:	Meloland				
Tube No.:	S-5	Depth (ft):	59.0 -60.0	GWT (ft):	6.5
Comments:	Brown sandy silt.				

HYDROMETER TEST

Time	Elapsed time t (sec)	Temp. T (°C)	Reading R'_T	Corr. reading $R_T=R'_T+c_m$	Depth H (cm)	Grain diameter D (mm)	Temp. corr. m_T	Corr. depth $R_T+m_T-c_d$	% by wt. finer than W_D (%)
10:15:13	0								
10:17:13	120	21.0	1020.0	1020.5	10.98	0.0302	0.700	1018.2	57.37
10:20:13	300	21.0	1014.0	1014.5	12.58	0.0205	0.700	1012.2	38.46
10:25:13	600	21.0	1011.5	1012.0	13.25	0.0149	0.700	1009.7	30.58
10:35:13	1200	21.0	1009.0	1009.5	13.92	0.0108	0.700	1007.2	22.70
10:55:13	2400	21.0	1008.0	1008.5	14.18	0.0077	0.700	1006.2	19.54
11:15:13	3600	21.0	1007.0	1007.5	14.45	0.0063	0.700	1005.2	16.39
13:33:00	11867	21.0	1006.0	1006.5	14.72	0.0035	0.700	1004.2	13.24
16:15:13	21600	21.0	1005.0	1005.5	14.98	0.0026	0.700	1003.2	10.09
12:53:00	95867	21.0	1004.5	1005.0	15.12	0.0013	0.700	1002.7	8.51

APPARATUS

Hydrometer no.:	88-18634	a_0	283.24	a_1	-0.2668
Graduate no.:	4				

FACTORS

Meniscus corr., c_m:	0.5	
Disp. agent corr, c_d:	3.0	
Visc. of water, η.	21.0 °C	9.320E-06 g sec/cm^2
	°C	g sec/cm^3

WEIGHT

Dry soil (g)	48.45
Percent by wt (%)	95.79
Dry soil for sieve (g)	2.13
Total (g)	50.58

UNIT WEIGHT

Specific gravity:		2.68
T	γ_w	γ_s
(°C)	(g/cm^3)	(g/cm^3)
21.0	0.9980	2.6768

UCLA Soil Dynamics Laboratory

Sieve Analysis

Principal investigator: Mladen Vucetic, Professor

Test performed by: Kentaro Tabata Test No.: 3

Project:	PEARL			Date:	5/31/2001
Boring:	Meloland				
Tube No.:	S-5	Depth (ft):	59.0 -60.0	GWT (ft):	6.5
Comments:	Brown sandy silt.				

SIEVE ANALYSIS

Sieve No.	Diameter (mm)	Sieve (g)	S+wet (g)	S+dry (g)	Retained (g)	Retained (%)	Cumulated (g)	Cumulated (%)	Passing (%)
4	4.750	461.69		461.69	0.00	0.00	0.00	0.00	100.00
10	2.000	432.93		432.93	0.00	0.00	0.00	0.00	100.00
20	0.833	422.34		422.36	0.02	0.04	0.02	0.04	99.96
40	0.425	379.72		379.88	0.16	0.32	0.18	0.36	99.64
60	0.250	325.97		326.01	0.04	0.08	0.22	0.43	99.57
100	0.150	334.69		334.87	0.18	0.36	0.40	0.79	99.21
200	0.075	338.73		340.46	1.73	3.42	2.13	4.21	95.79
Total					2.13	4.21			

WEIGHT

Dry soil for sieve (g)	2.13
Dry soil for hydr. (g)	48.45
Total (g)	50.58
Percent coaser (%)	4.21

UCLA Soil Dynamics Laboratory

Atterberg Limit Determination

Principal investigator: Mladen Vucetic, Professor

Test performed by: Kentaro Tabata Test No.: 3

Project:	PEARL			Date:	6/16/2001
Boring:	Meloland				
Tube No.:	S-5	Depth (ft):	59.0 -60.0	GWT (ft):	6.5
Comments:	Brown sandy silt.				

LIQUID LIMIT TEST

Test No.	1	2	3	4				
Number of blows	29	20	14	10				
Container No.	ST-20	ST-22	ST-4	ST-23				
Container (g)	30.36	30.06	30.17	30.57				
Cont+wet soil (g)	37.64	39.27	41.04	39.84				
Cont+dry soil (g)	36.00	37.14	38.42	37.52				
Water (g)	1.64	2.13	2.62	2.32				
Dry soil (g)	5.64	7.08	8.25	6.95				
Water content (%)	29.08	30.08	31.76	33.38				

PLASTIC LIMIT TEST

Test No.	1	2	3
Container No.	ST-3	ST-1	ST-14
Container (g)	30.18	30.37	30.45
Cont+wet soil (g)	32.25	33.08	33.17
Cont+dry soil (g)	31.99	32.76	32.85
Water (g)	0.26	0.32	0.32
Dry soil (g)	1.81	2.39	2.40
Water content (%)	14.36	13.39	13.33

ATTERBERG LIMITS

Liquid limit (%)	**29.5**
Plastic limit (%)	**13.7**
Plasticity index	**15.8**

CLASSIFICATION

CL

FLOW CHART

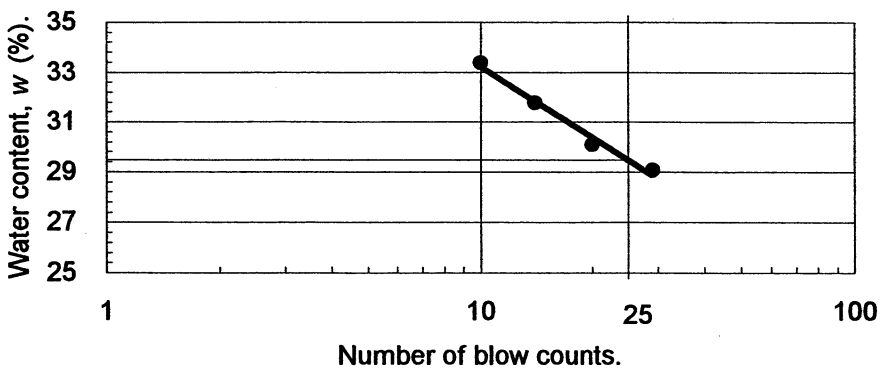

UCLA Soil Dynamics Laboratory

Atterberg Limit Determination

Principal investigator: Mladen Vucetic, Professor

Test performed by: Kentaro Tabata Test No.: 3

Project:	PEARL			Date:	6/16/2001
Boring:	Meloland				
Tube No.:	S-5	Depth (ft):	59.0 -60.0	GWT (ft):	6.5
Comments:	Brown sandy silt.				

PLASTICITY CHART

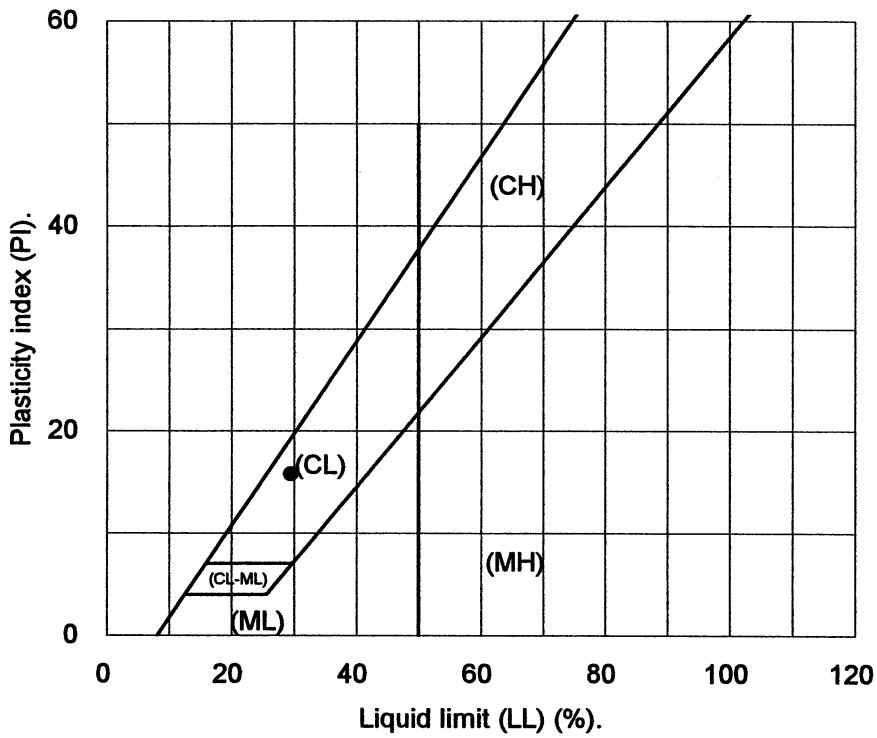

3.5 Test 4: MELOLAND S-7

UCLA Soil Dynamics Laboratory

Double Specimen Direct Simple Shear (DSDSS) Test

Principal investigator: Mladen Vucetic, Professor

Test performed by: Kentaro Tabata Test No.: 4

Project:	PEARL			Date:	4/9/2002
Boring:	Meloland				
Tube No.:	S-7	Depth (ft):	98.0 -100.0	GWT (ft):	6.5 (reported by others)
Comments:	Silty sand. Specimen obtained from the bottom of the tube (specimen depth ~ 99.5 ft).				

FORM 1: SPECIMEN PREPARATION

WATER CONTENT, SPECIFIC GRAVITY				UNIT WEIGHT, VOID RATIO, SATURATION			
	Before consol.	After shearing			Before consol.	Before shearing	After shearing
Container No.	ST-8	MT-13	MT-20	Average weight (g)	133.00	133.00	
Cont+wet soil (g)	54.86	182.03	183.48	Height (cm)	1.960	1.951	
Cont+dry soil (g)	49.92	155.89	157.00	Area (cm^2)	34.84	34.84	
Container (g)	30.06	49.55	50.26	Volume (cm^3)	68.28	67.98	
Water (g)	4.94	26.14	26.48	Unit weight (g/cm^3)	1.948	1.956	
Dry soil (g)	19.86	106.34	106.74	Unit weight (kN/m^3)	19.09	19.17	
Water content(%)	24.87	24.58	24.81	Void ratio	0.69	0.69	
Avg. water cont. (%)	24.87		24.69	Saturation (%)	94.8	95.2	
Spceific gravity			2.64				

HEIGHT OF SPECIMEN						
	Before consol.		Before shearing	After shearing		
	Top	Bottom	Average	Average		
Height (cm)	1.960	1.960	1.951	1.951		

AREA OF SPECIMEN						
Initial diameter (cm)			6.660	Initial area (cm^2)		34.837
Load (kg)	Stress (kg/cm^2)	Stress (kN/m^2)	Diameter (cm)	Membrane (cm)	Corrected diameter (cm)	Area (cm^2)

Meloland S-7					
DSDSS TEST - Step 2					
Type of soil: SM					
LL	NP	PI	NP	%Silt	3.1
e_0	0.68	S_0 (%)	95.2	%Clay	4.0
σ_v (kPa)	308	OCR	n/a	w (%)	24.7
γ_c (%)	~0.00038	H_0 (mm)	19.51	Spec. Gr.	2.64

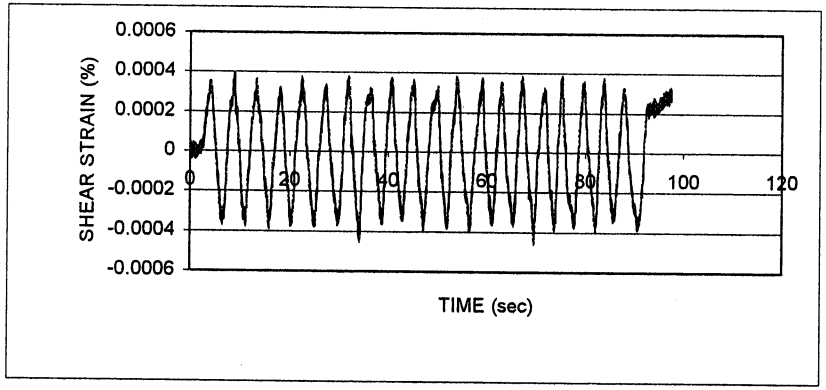

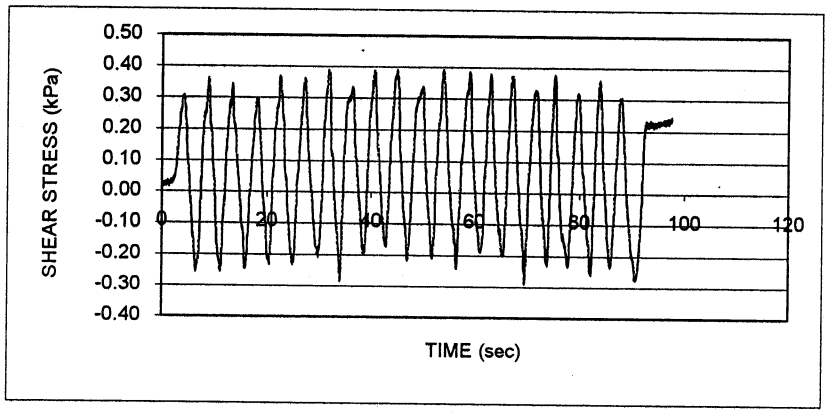

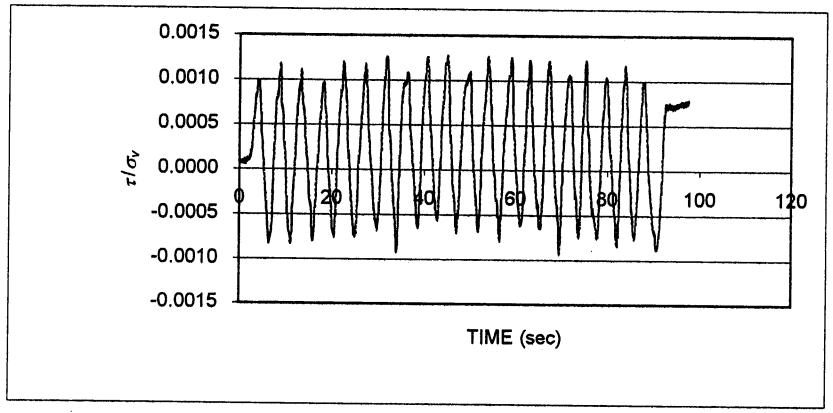

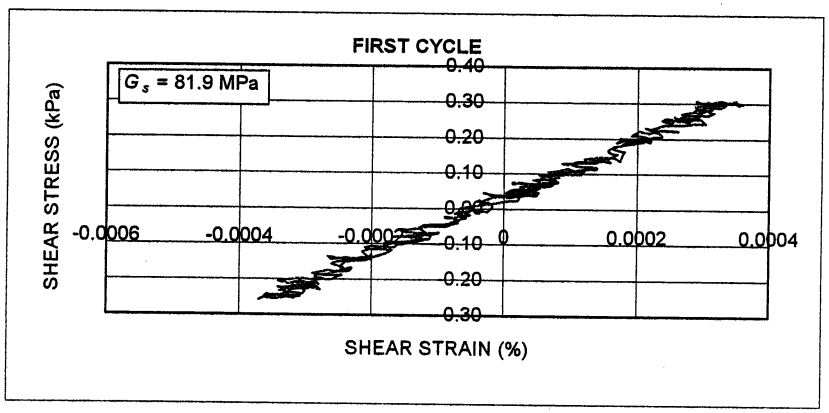

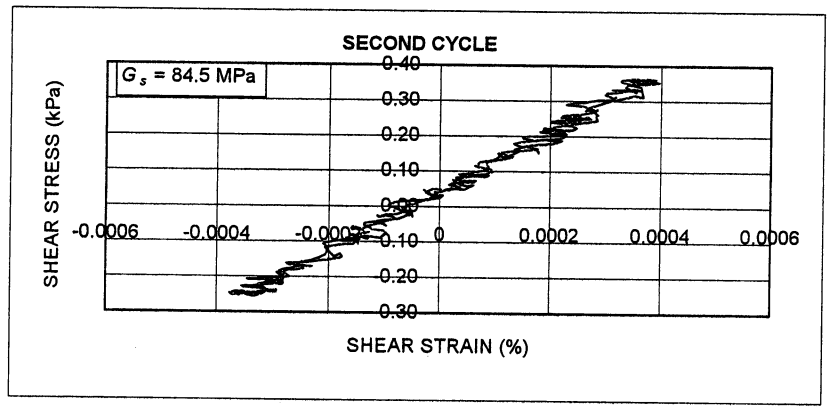

Meloland S-7					
DSDSS TEST - Step 26					
Type of soil: SM					
LL	NP	PI	NP	%Silt	3.1
e_0	0.68	S_0 (%)	95.2	%Clay	4.0
σ_v (kPa)	308	OCR	n/a	w (%)	24.7
γ_c (%)	~0.0007	H_0 (mm)	19.51	Spec. Gr.	2.64

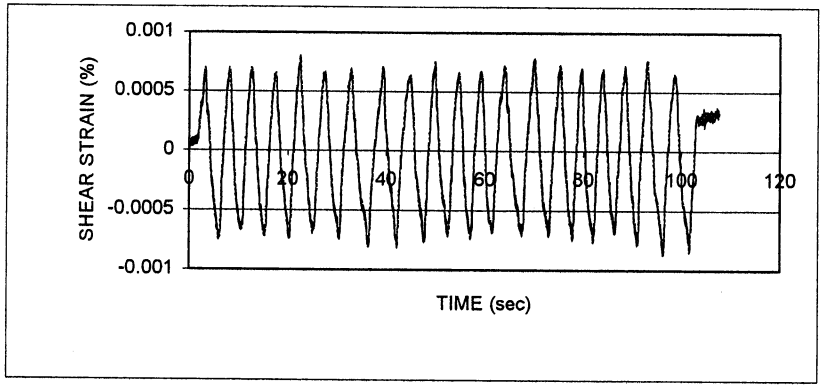

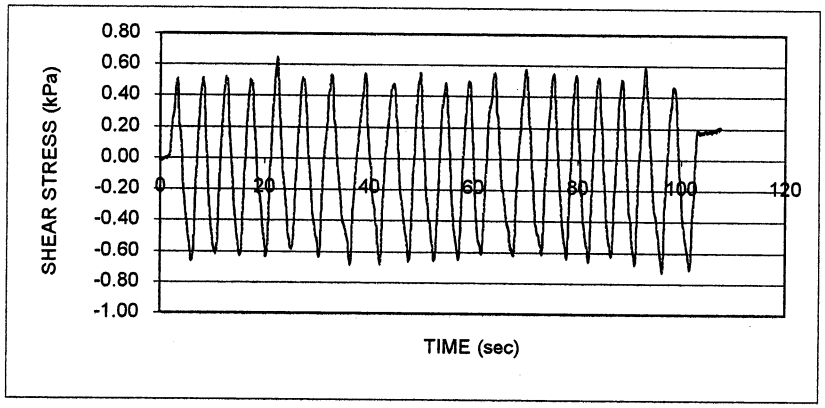

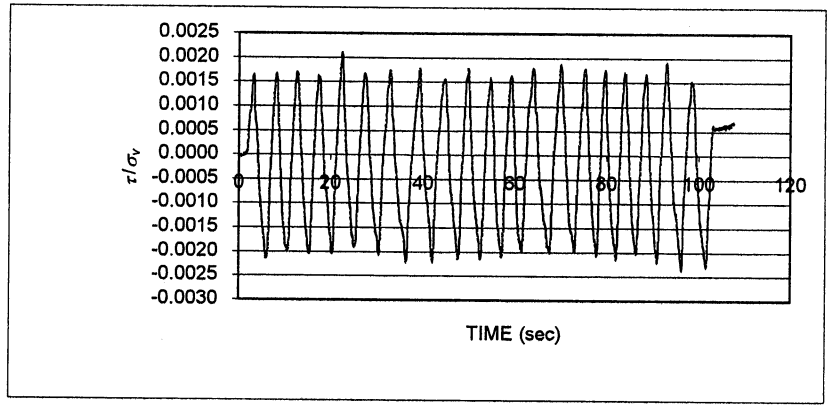

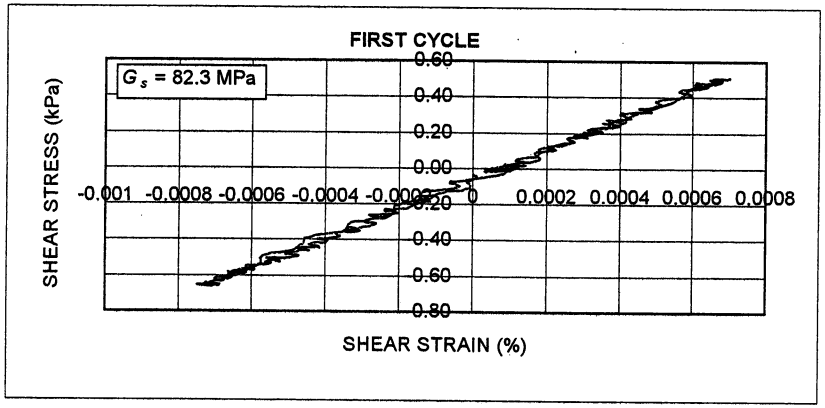

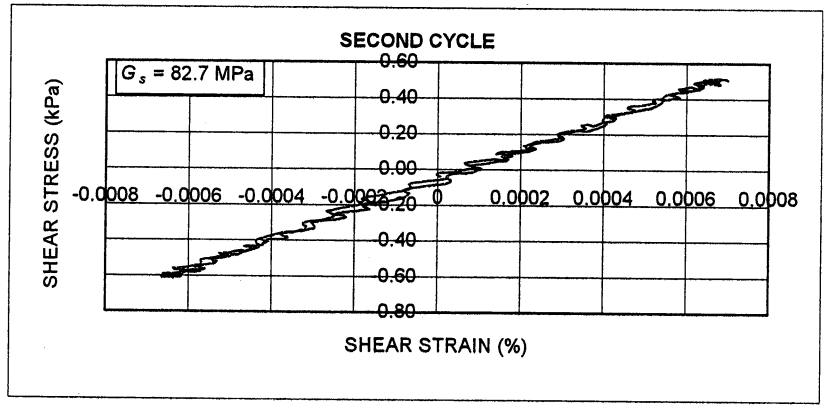

Meloland S-7					
DSDSS TEST - Step 3					
Type of soil: SM					
LL	NP	PI	NP	%Silt	3.1
e_0	0.68	S_0 (%)	95.2	%Clay	4.0
σ_v (kPa)	308	OCR	n/a	w (%)	24.7
γ_c (%)	~0.0011	H_0 (mm)	19.51	Spec. Gr.	2.64

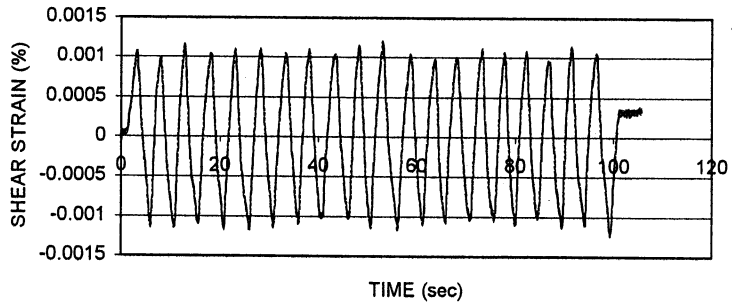

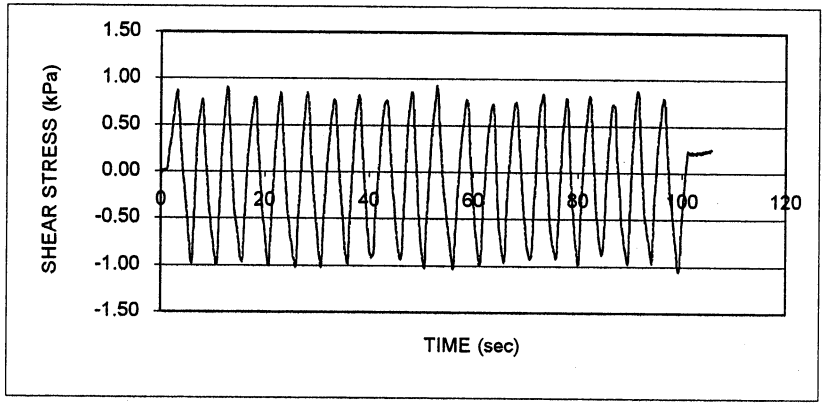

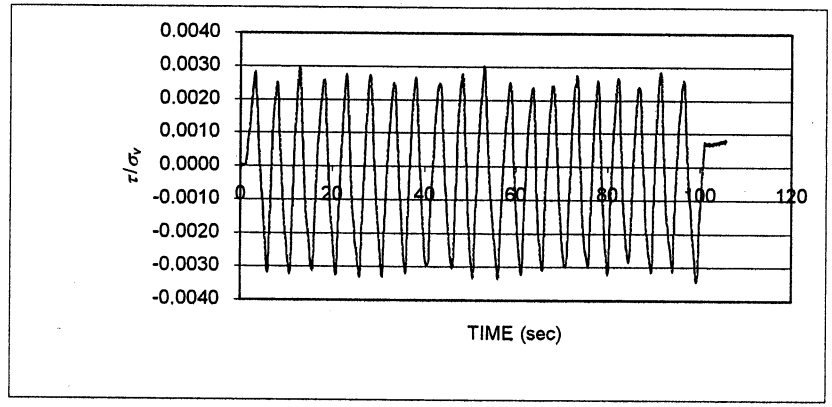

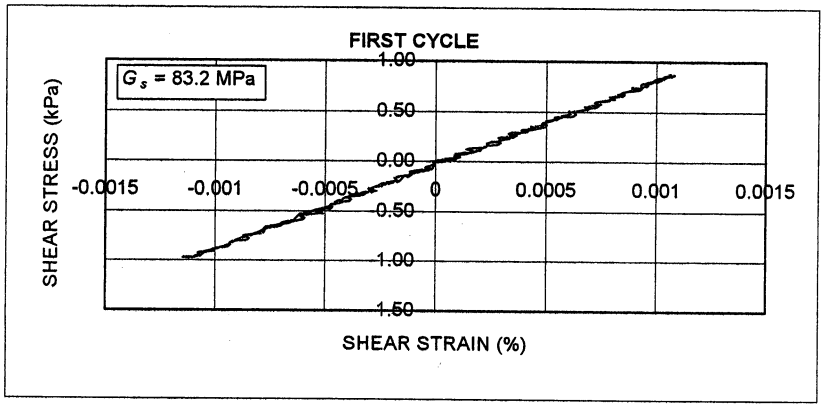

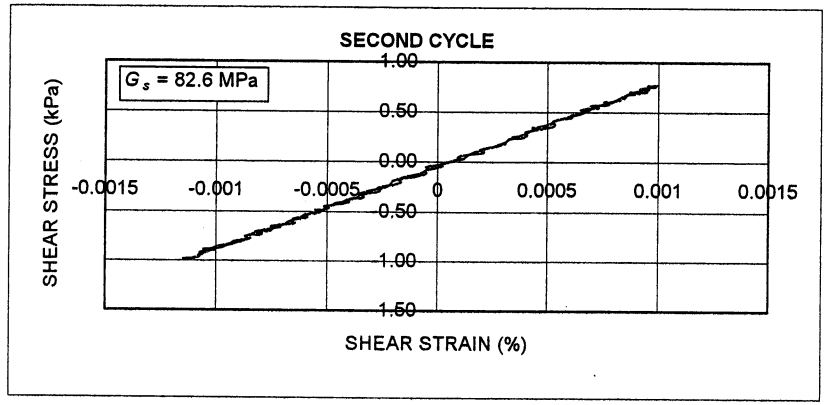

Meloland S-7					
DSDSS TEST - Step 4					
Type of soil: SM					
LL	NP	PI	NP	%Silt	3.1
e_0	0.68	S_0 (%)	95.2	%Clay	4.0
σ_v (kPa)	308	OCR	n/a	w (%)	24.7
γ_c (%)	~0.0032	H_0 (mm)	19.51	Spec. Gr.	2.64

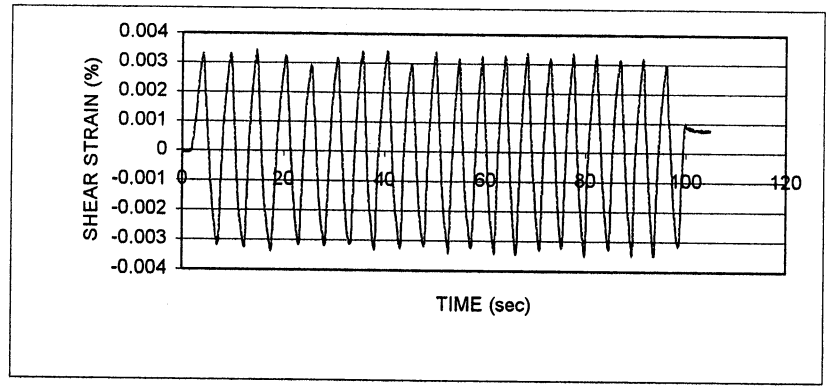

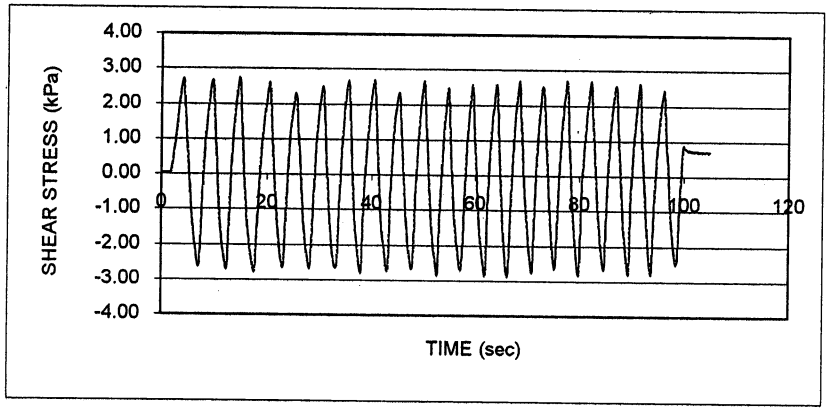

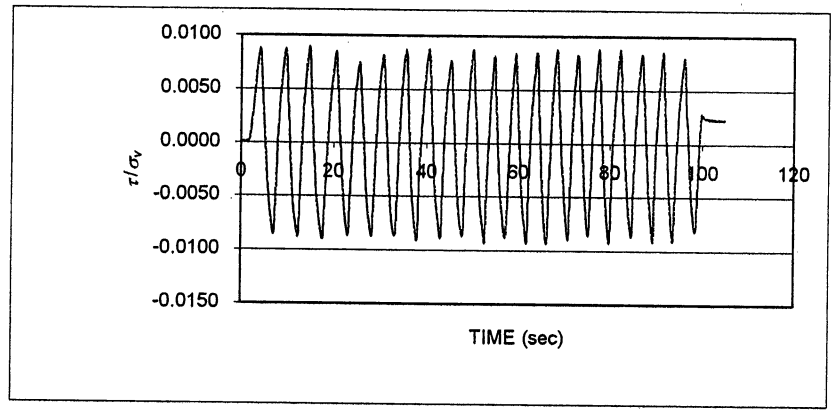

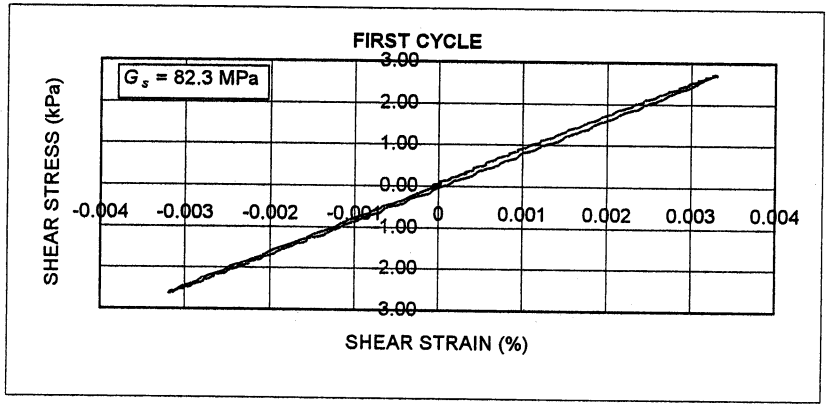

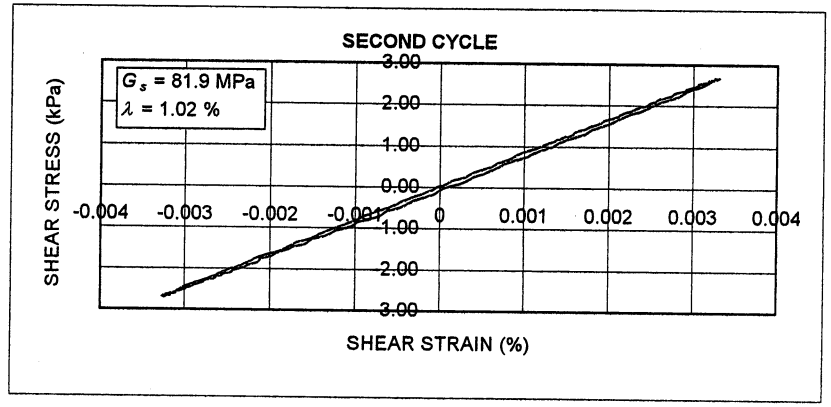

Meloland S-7					
DSDSS TEST - Step 5					
Type of soil: SM					
LL	NP	PI	NP	%Silt	3.1
e_0	0.68	S_0 (%)	95.2	%Clay	4.0
σ_v (kPa)	308	OCR	n/a	w (%)	24.7
γ_c (%)	~0.011	H_0 (mm)	19.51	Spec. Gr.	2.64

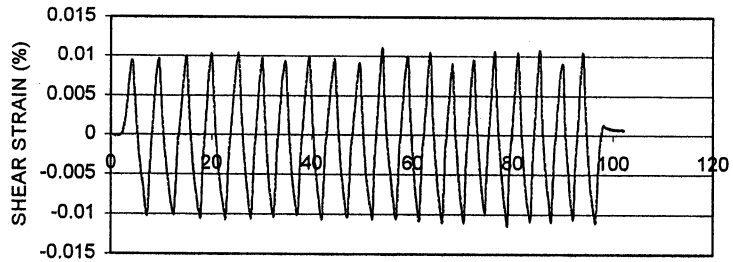

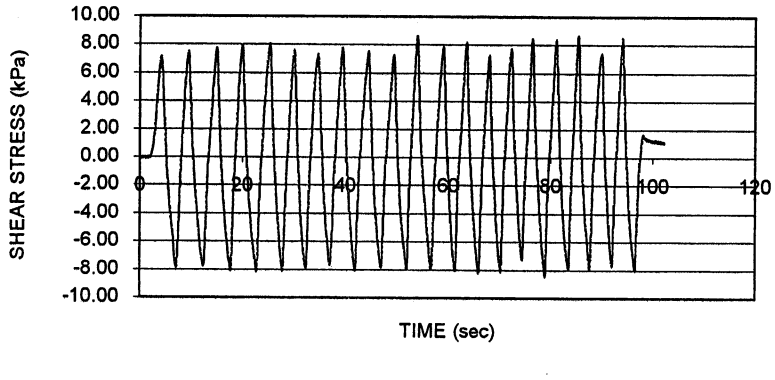

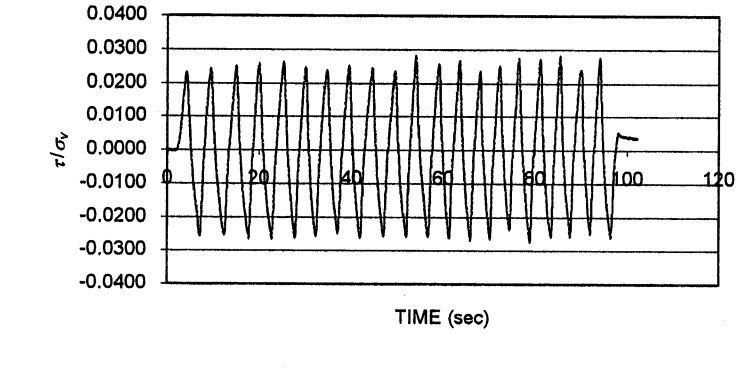

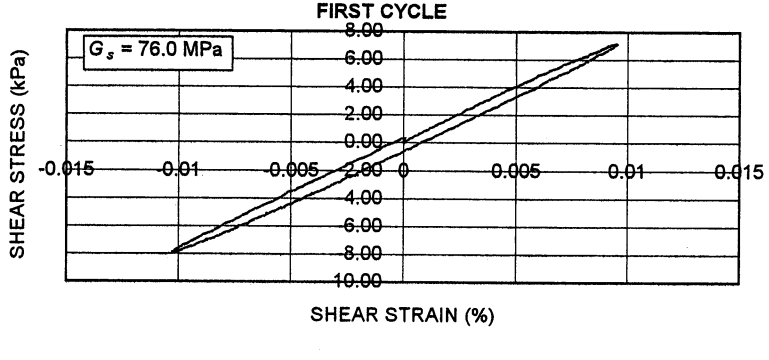

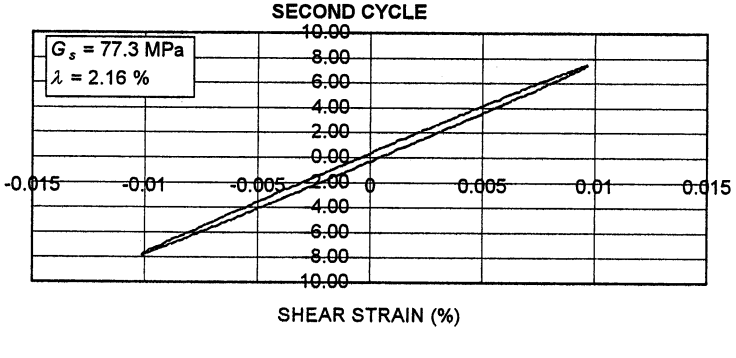

Meloland S-7					
DSDSS TEST - Step 6					
Type of soil: SM					
LL	NP	PI	NP	%Silt	3.1
e_0	0.68	S_0 (%)	95.2	%Clay	4.0
σ_v (kPa)	308	OCR	n/a	w (%)	24.7
γ_c (%)	~0.033	H_0 (mm)	19.51	Spec. Gr.	2.64

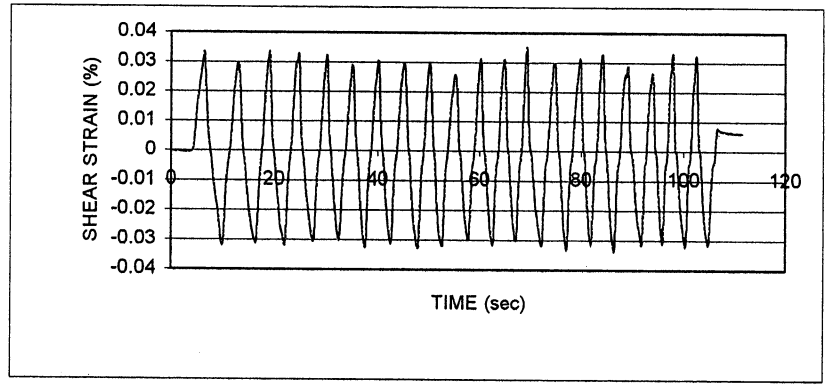

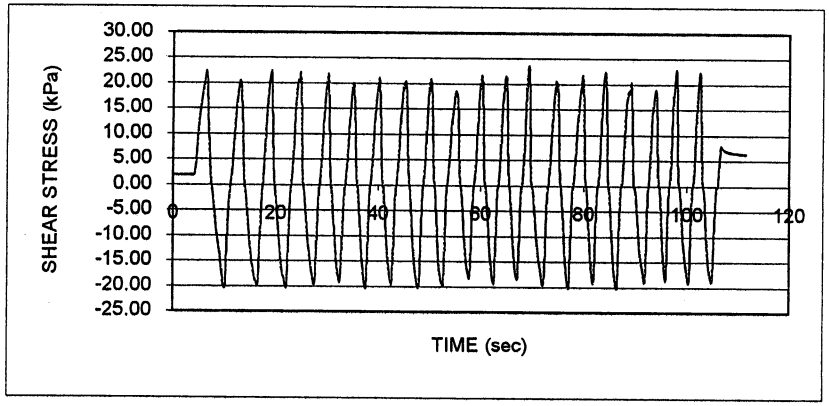

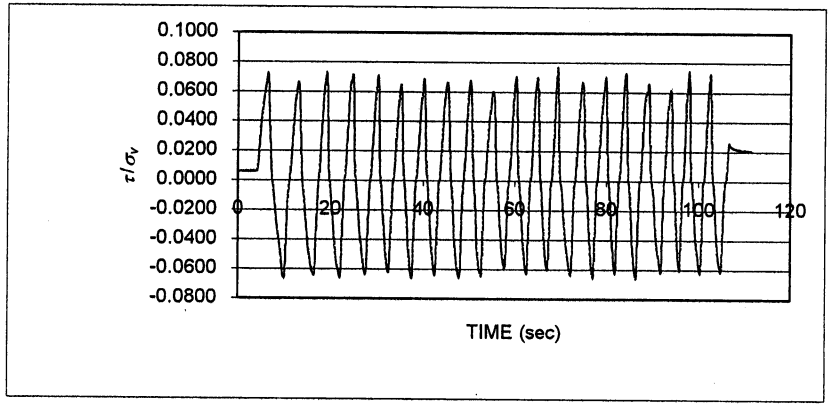

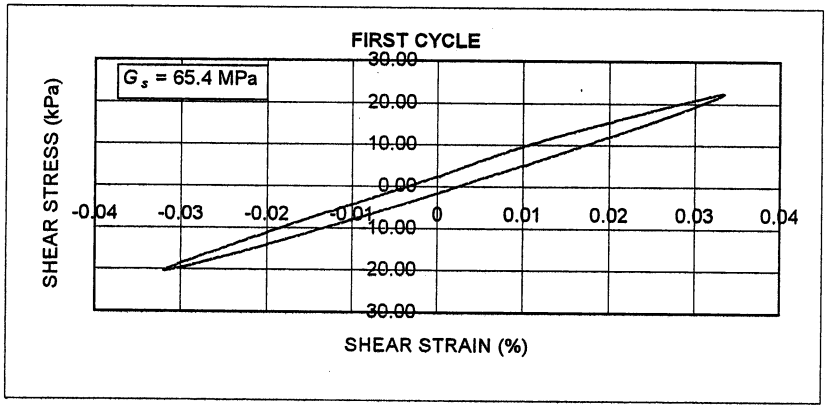

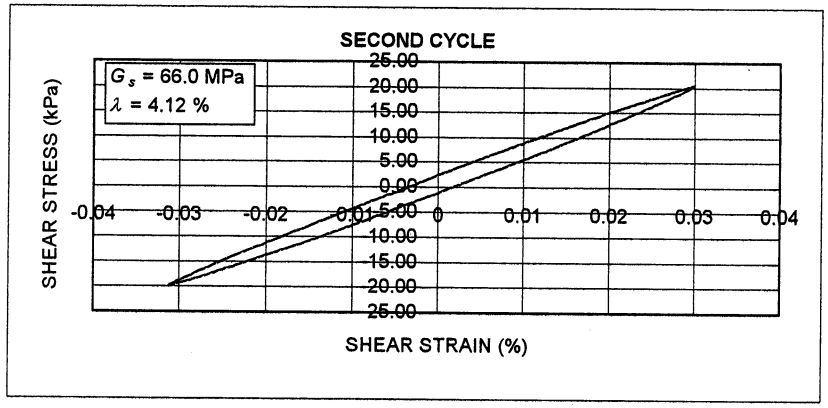

Meloland S-7					
DSDSS TEST - Step 7					
Type of soil: SM					
LL	NP	PI	NP	%Silt	3.1
e_0	0.68	S_0 (%)	95.2	%Clay	4.0
σ_v (kPa)	308	OCR	n/a	w (%)	24.7
γ_c (%)	~0.11	H_0 (mm)	19.51	Spec. Gr.	2.64

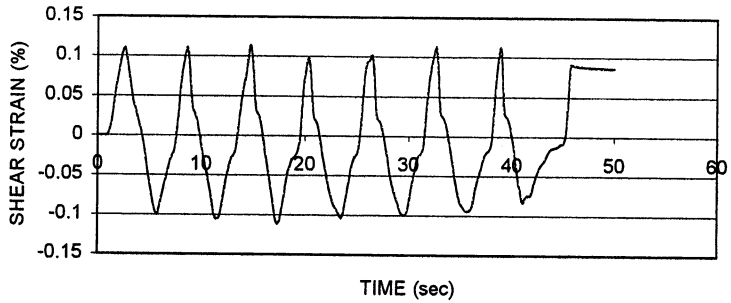

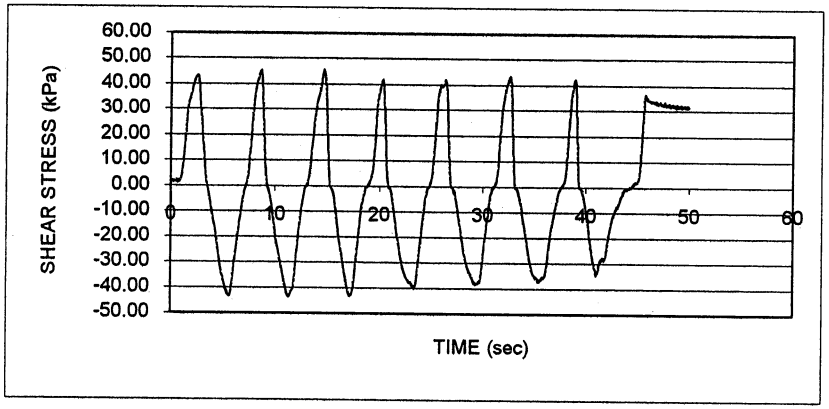

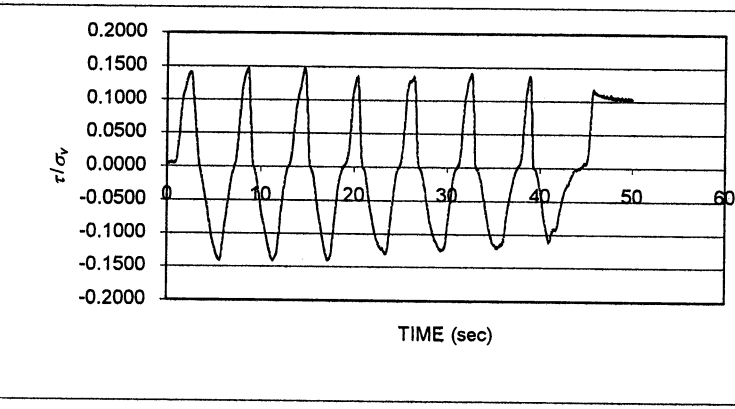

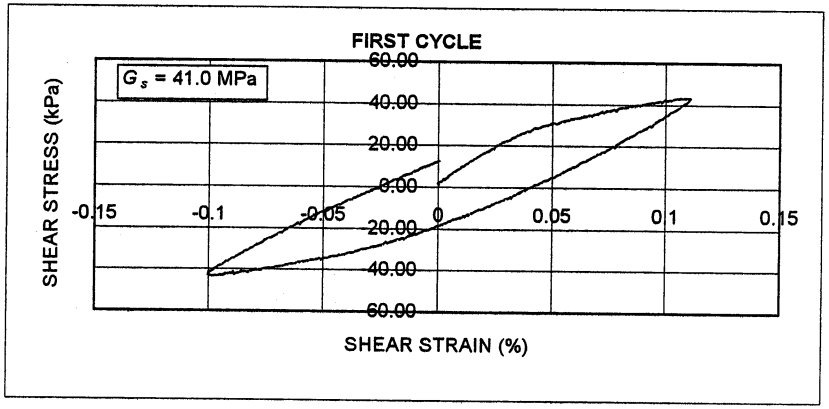

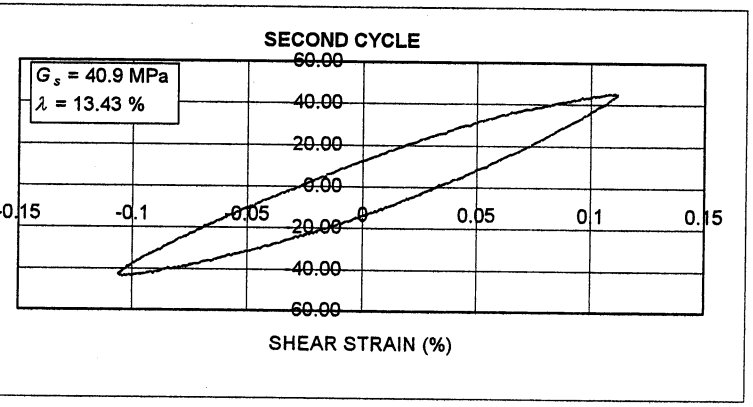

Meloland S-7					
DSDSS TEST - Step 8					
Type of soil: SM					
LL	NP	PI	NP	%Silt	3.1
e_0	0.68	S_0 (%)	95.2	%Clay	4.0
σ_v (kPa)	308	OCR	n/a	w (%)	24.7
γ_c (%)	~3.2	H_0 (mm)	19.51	Spec. Gr.	2.64

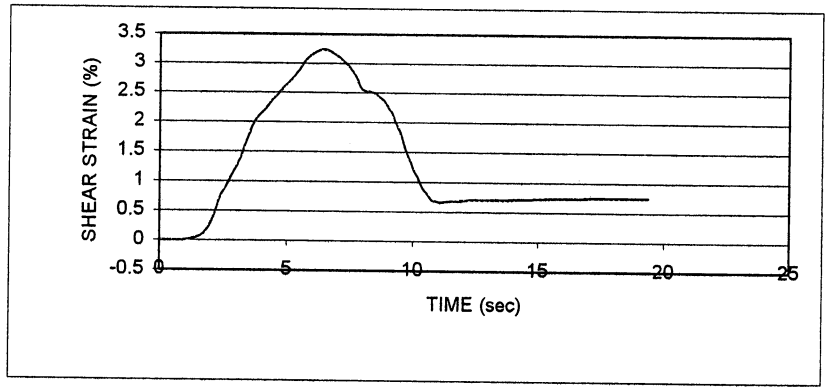

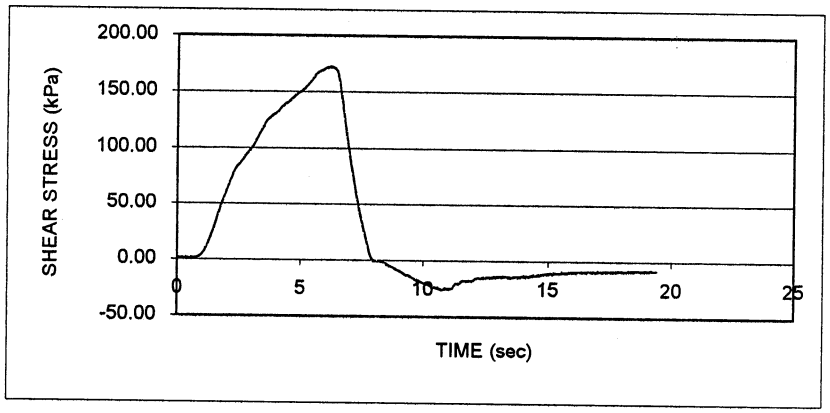

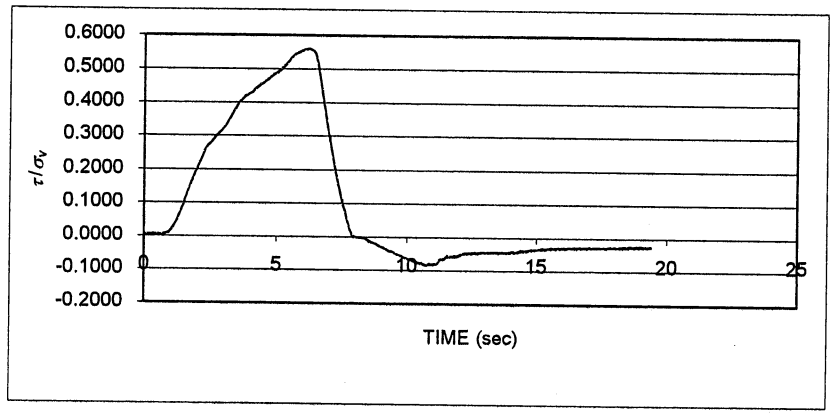

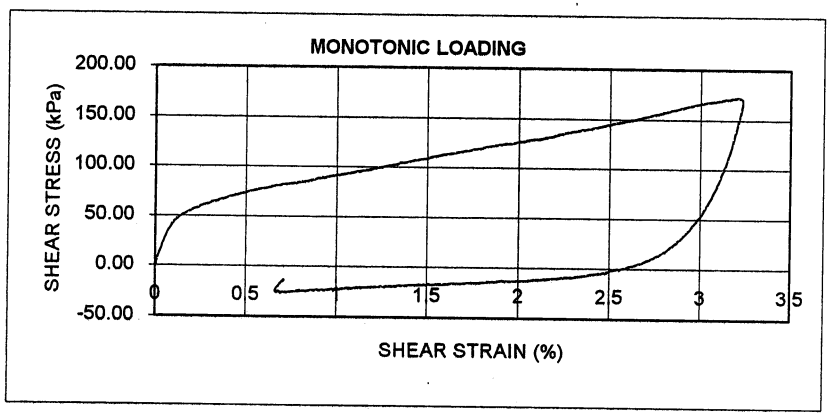

UCLA Soil Dynamics Laboratory

Double Specimen Direct Simple Shear (DSDSS) Test

Principal investigator: Mladen Vucetic, Professor

Test performed by Kentaro Tabata

Test no: 4

Project:	PEARL			Date:	4/9/2002
Sample name:	Meloland (S-7)			Depth (ft):	98.0
Symbol:	SM	LL (%):	0.0	Silt content (%):	3.1
Specific gravity:	2.64	PI:	0.0	Clay content (%):	4.0
Comments:					

Estimated G_{max} (MPa):	84.0

	SHEAR MODULUS			DAMPING RATIO	
Step	γ_c (%)	G_s (MPa)	G_s/G_{max}	γ_c (%)	λ (%)
2x	0.000365	81.86	0.975		
2x	0.000387	84.49	1.006		
26x	0.000725	82.29	0.980		
26x	0.000682	82.66	0.984	0.003287	1.02
3x	0.001115	83.16	0.990	0.009905	2.16
3x	0.001071	82.57	0.983	0.030575	4.12
4x	0.003250	82.26	0.979	0.108834	13.44
4x	0.003287	81.91	0.975		
5x	0.009905	75.97	0.904		
5x	0.009905	77.26	0.920		
6x	0.032759	65.35	0.778		
6x	0.030575	66.02	0.786		
7x	0.105571	41.04	0.489		
7x	0.108834	40.88	0.487		
	γ (%)				
(Monotonic loading)	0.503853	14.61	0.174		
	1.002244	9.13	0.109		
	1.502468	7.26	0.086		
	2.004488	6.30	0.075		
	2.501083	5.79	0.069		
	3.233253	5.27	0.063		

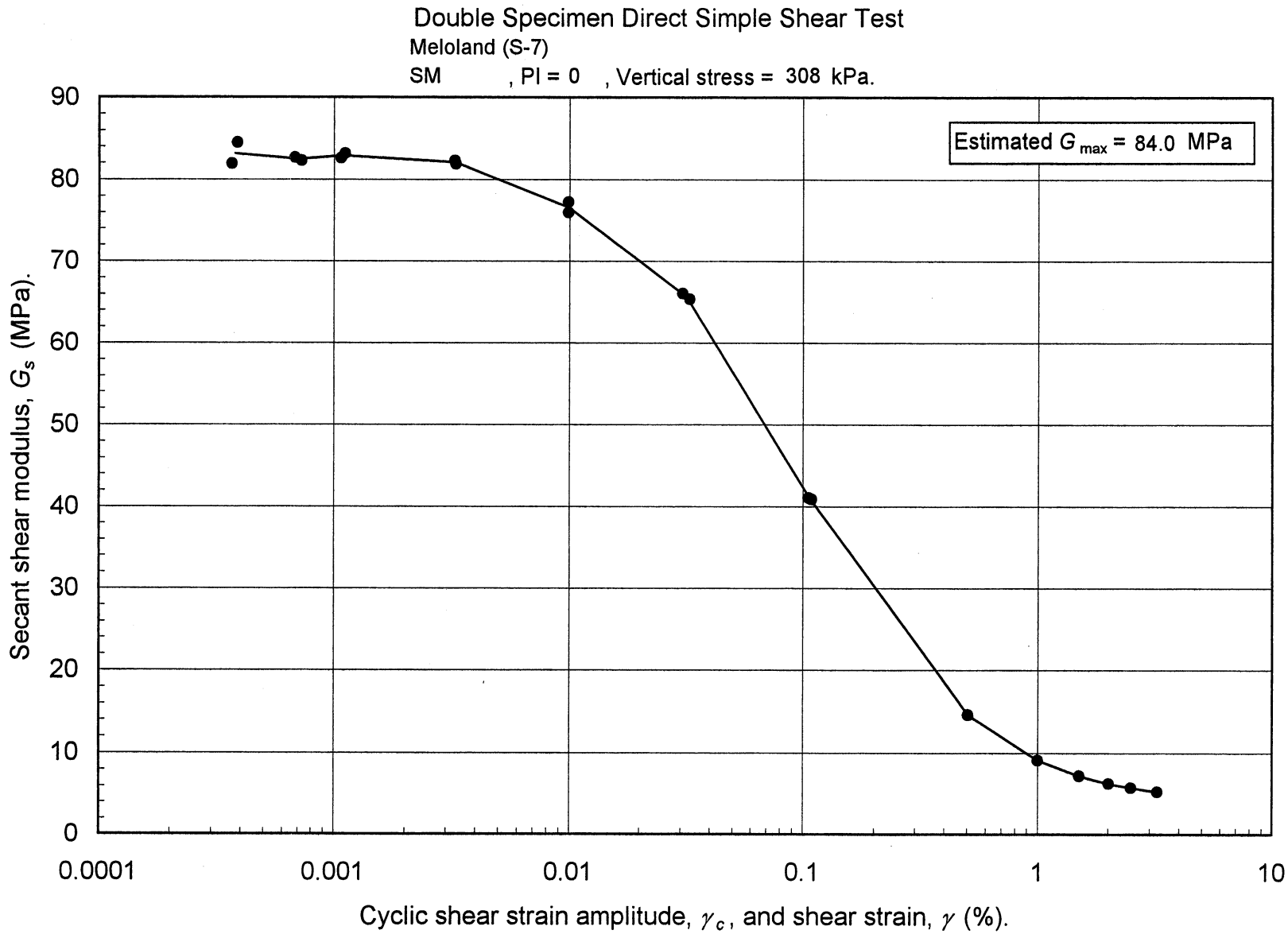
Double Specimen Direct Simple Shear Test
Meloland (S-7)
SM , PI = 0 , Vertical stress = 308 kPa.
Estimated G_{max} = 84.0 MPa
Secant shear modulus, G_s (MPa).
90
80
70
60
50
40
30
20
10
0
0.0001
0.001
0.01
0.1
1
10
Cyclic shear strain amplitude, γ_c, and shear strain, γ (%).

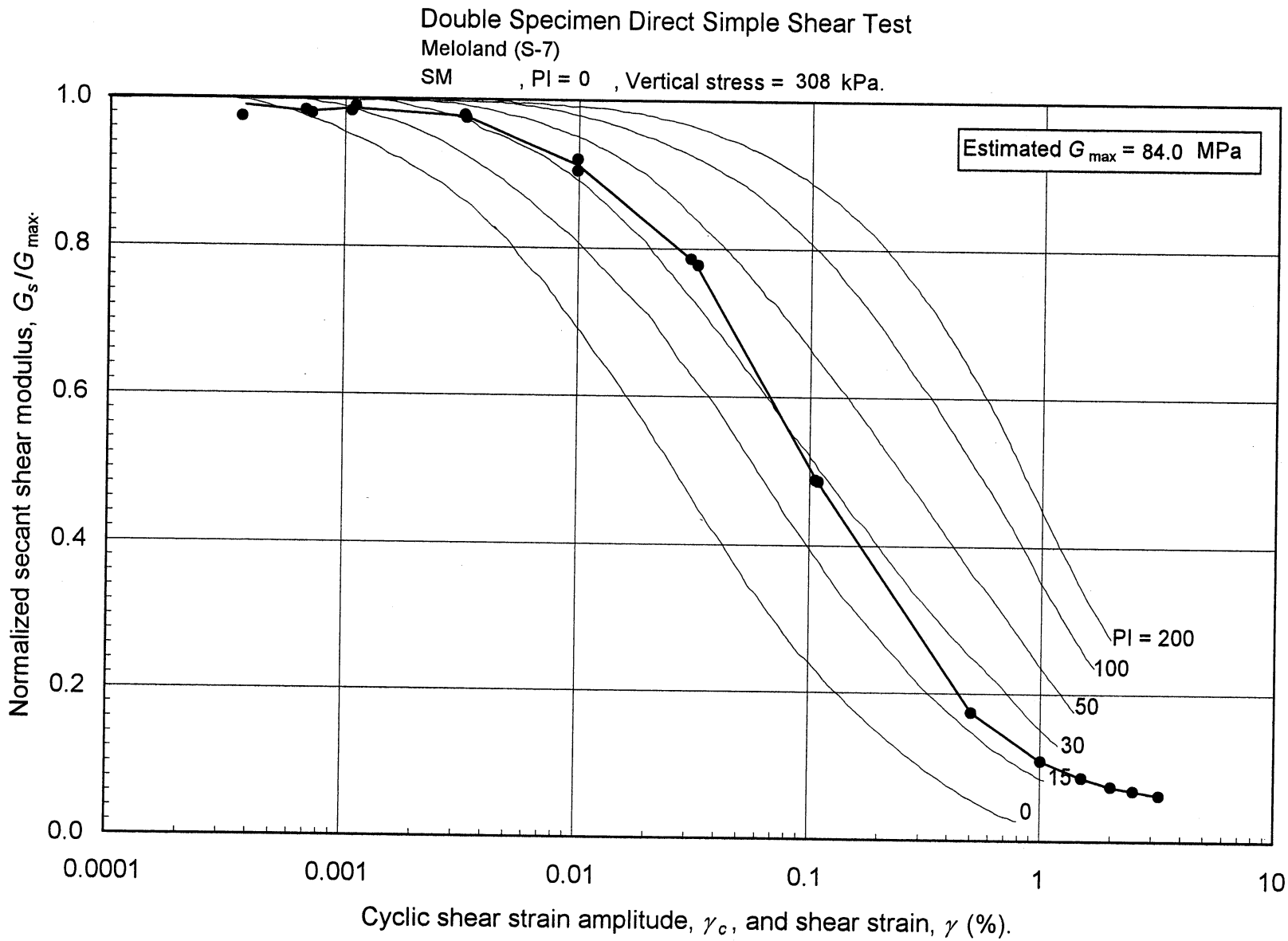
Double Specimen Direct Simple Shear Test
Meloland (S-7)
SM , PI = 0 , Vertical stress = 308 kPa.
Estimated G_{max} = 84.0 MPa
PI = 200
100
50
30
15
0
Normalized secant shear modulus, G_s/G_{max}.
1.0
0.8
0.6
0.4
0.2
0.0
0.0001
0.001
0.01
0.1
1
10
Cyclic shear strain amplitude, γ_c, and shear strain, γ (%).

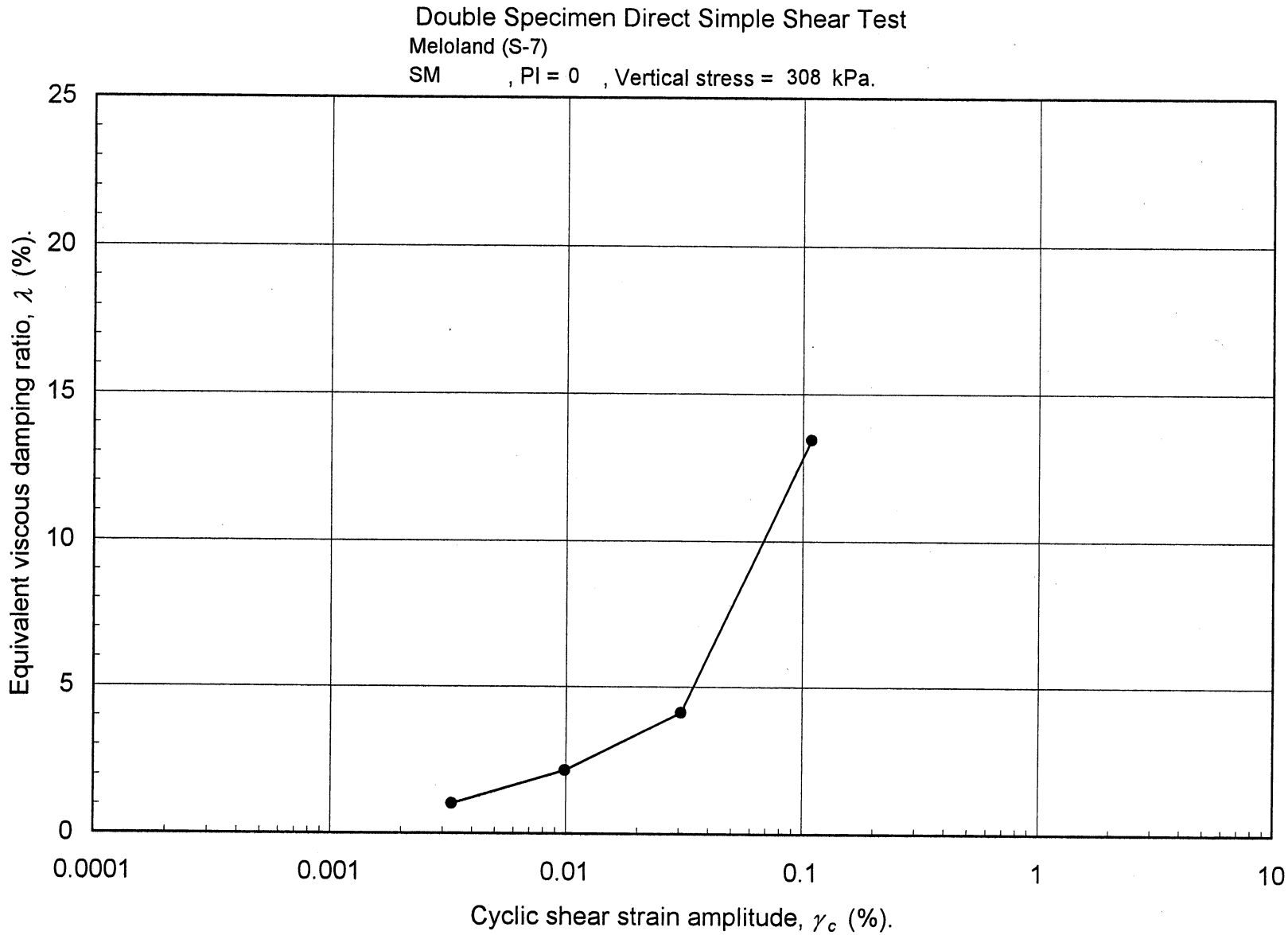
Double Specimen Direct Simple Shear Test
Meloland (S-7)
SM , PI = 0 , Vertical stress = 308 kPa.
Equivalent viscous damping ratio, λ (%).
25
20
15
10
5
0
0.0001
0.001
0.01
0.1
1
10
Cyclic shear strain amplitude, γc (%).

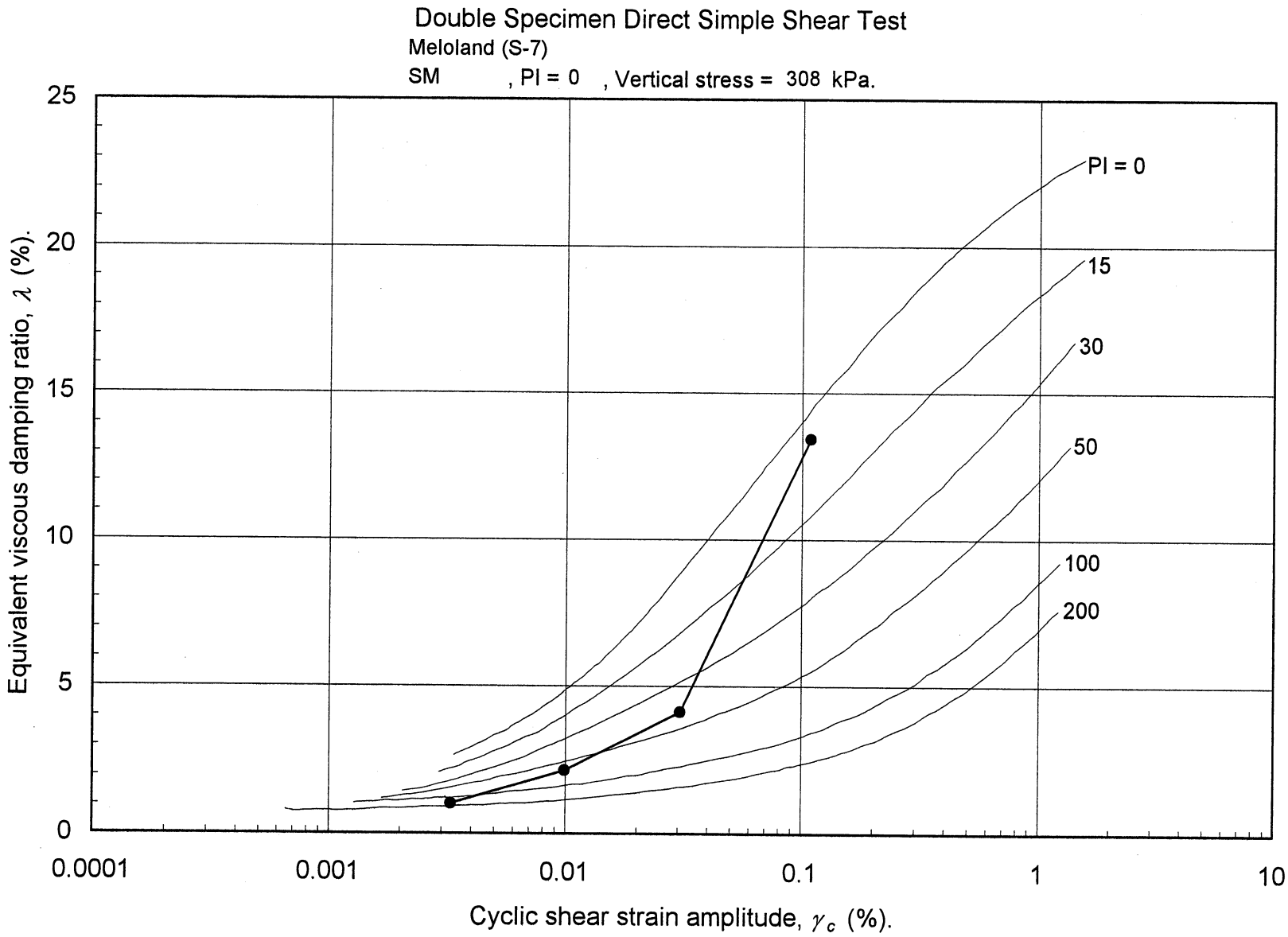
Double Specimen Direct Simple Shear Test
Meloland (S-7)
SM , PI = 0 , Vertical stress = 308 kPa.
Equivalent viscous damping ratio, λ (%).
Cyclic shear strain amplitude, γc (%).
0
5
10
15
20
25
0.0001
0.001
0.01
0.1
1
10
PI = 0
15
30
50
100
200

UCLA Soil Dynamics Laboratory

Specific Gravity Test

Principal investigator: Mladen Vucetic, Professor

Test performed by: Kentaro Tabata Test No.: 4

Project:	PEARL			Date:	4/17/2002
Boring:	Meloland				
Tube No.:	S-7	Depth (ft):	98.0 -100.0	GWT (ft):	6.5
Comments:	Silty sand. Total unit weight: 125 pcf.				

SPECIFIC GRAVITY TEST

Test No.	1		
Bottle No.	3		
Wt. of bottle (g)	178.27		
Volume of bottle (cm^3)	500		
Wt. of bottle+water+soil (g)	694.62		
Temperature (°C)	22.0		
Wt. of bottle+water (g)	676.27		
Evaporating dish No.	B-5		
Weight of dish (g)	507.41		
Wt. of dish+dry soil (g)	536.91		
Wt. of dry soil (g)	29.50		
Specific gravity of water	0.9978		
Specific gravity of soil	**2.64**		

UCLA Soil Dynamics Laboratory

Grain Size Distribution

Principal investigator: Mladen Vucetic, Professor

Test performed by: Kentaro Tabata Test No.: 4

Project:	PEARL				
Boring:	Meloland				
Tube No.:	S-7	Depth (ft):	98.0 -100.0	GWT (ft):	6.5
Comments:	Silty sand. Total unit weight: 125 pcf.				

GRAIN SIZE DISTRIBUTION

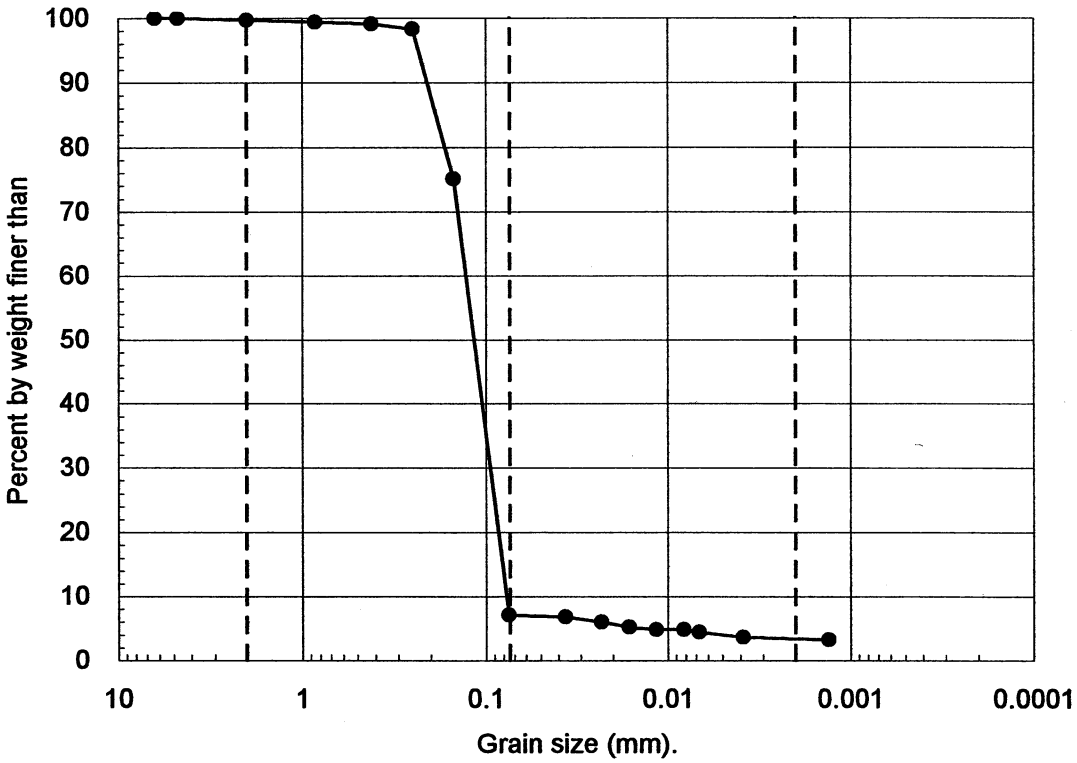

Clay (%)	Silt (%)	Sand (%)	Gravel (%)
4.0	3.1	92.5	0.3

UCLA Soil Dynamics Laboratory

Hydrometer Analysis

Principal investigator: Mladen Vucetic, Professor

Test performed by: Kentaro Tabata Test No.: 4

Project:	PEARL			Date:	4/10/2002
Boring:	Meloland				
Tube No.:	S-7	Depth (ft):	98.0 -100.0	GWT (ft):	6.5
Comments:	Silty sand. Total unit weight: 125 pcf.				

HYDROMETER TEST

Time	Elapsed time t (sec)	Temp. T (°C)	Reading R'_T	Corr. reading $R_T=R'_T+c_m$	Depth H (cm)	Grain diameter D (mm)	Temp. corr. m_T	Corr. depth $R_T+m_T-c_d$	% by wt. finer than W_D (%)
13:15:53	0								
13:17:53	120	23.0	1004.5	1005.0	15.18	0.0365	0.700	1001.7	6.85
13:20:53	300	23.0	1004.3	1004.8	15.24	0.0231	0.700	1001.5	6.04
13:25:53	600	23.0	1004.1	1004.6	15.29	0.0164	0.700	1001.3	5.24
13:35:53	1200	23.0	1004.0	1004.5	15.32	0.0116	0.700	1001.2	4.83
13:55:53	2400	23.0	1004.0	1004.5	15.32	0.0082	0.700	1001.2	4.83
14:15:53	3600	23.0	1003.9	1004.4	15.34	0.0067	0.700	1001.1	4.43
16:15:53	10800	23.0	1003.7	1004.2	15.40	0.0039	0.700	1000.9	3.63
15:15:00	93547	23.0	1003.6	1004.1	15.42	0.0013	0.700	1000.8	3.22

APPARATUS

Hydrometer no.:	88-18587	a_0	284.03	a_1	-0.2675
Graduate no.:	3				

FACTORS

Meniscus corr., c_m:	0.5	
Disp. agent corr, c_d:	4.0	
Visc. of water, η.	23.0 °C	9.565E-06 g sec/cm^2
	°C	g sec/cm^3

WEIGHT

Dry soil (g)	2.85
Percent by wt (%)	7.13
Dry soil for sieve (g)	37.11
Total (g)	39.96

UNIT WEIGHT

Specific gravity:		2.64
T	γ_w	γ_s
(°C)	(g/cm^3)	(g/cm^3)
23.0	0.9976	2.6343

UCLA Soil Dynamics Laboratory

Sieve Analysis

Principal investigator: Mladen Vucetic, Professor

Test performed by: Kentaro Tabata Test No.: 4

Project:	PEARL			Date:	4/17/2002
Boring:	Meloland				
Tube No.:	S-7	Depth (ft):	98.0 -100.0	GWT (ft):	6.5
Comments:	Silty sand. Total unit weight: 125 pcf.				

SIEVE ANALYSIS

Sieve No.	Diameter (mm)	Sieve (g)	S+wet (g)	S+dry (g)	Retained (g)	Retained (%)	Cumulated (g)	Cumulated (%)	Passing (%)
3	6.350	485.05		485.05	0.00	0.00	0.00	0.00	100.00
4	4.750	463.11		463.11	0.00	0.00	0.00	0.00	100.00
10	2.000	422.40		422.53	0.13	0.33	0.13	0.33	99.67
20	0.850	375.43		375.55	0.12	0.30	0.25	0.63	99.37
40	0.420	375.59		375.71	0.12	0.30	0.37	0.93	99.07
60	0.250	323.90		324.19	0.29	0.73	0.66	1.65	98.35
100	0.150	342.15		351.45	9.30	23.27	9.96	24.93	75.07
200	0.075	676.86		704.01	27.15	67.94	37.11	92.87	7.13
Total					37.11	92.87			

WEIGHT

Dry soil for sieve (g)	37.11
Dry soil for hydr. (g)	2.85
Total (g)	39.96
Percent coaser (%)	92.87

3.6 Test 5: OBREGON PARK P-5

UCLA Soil Dynamics Laboratory

Double Specimen Direct Simple Shear (DSDSS) Test

Principal investigator: Mladen Vucetic, Professor

Test performed by: Kentaro Tabata Test No.: 5

Project:	PEARL			Date:	7/6/2002
Boring:	Obregon Park				
Tube No.:	P-5	Depth (ft):	50.0 -53.0	GWT (ft):	20.0 (reported by others)
Comments:	Stiff clay. Specimen obtained from the bottom of the tube (specimen depth ~ 52.5 ft).				

FORM 1: SPECIMEN PREPARATION

WATER CONTENT, SPECIFIC GRAVITY				UNIT WEIGHT, VOID RATIO, SATURATION			
	Before consol.	After shearing			Before consol.	Before shearing	After shearing
Container No.	ST-2	MT-20	MT-17	Average weight (g)	135.99	135.99	
Cont+wet soil (g)	49.08	186.65	183.97	Height (cm)	1.960	1.920	
Cont+dry soil (g)	45.63	163.07	159.07	Area (cm^2)	34.84	34.84	
Container (g)	30.25	50.28	49.56	Volume (cm^3)	68.28	66.88	
Water (g)	3.45	23.58	24.90	Unit weight (g/cm^3)	1.992	2.033	
Dry soil (g)	15.38	112.79	109.51	Unit weight (kN/m^3)	19.52	19.93	
Water content(%)	22.43	20.91	22.74	Void ratio	0.65	0.61	
Avg. water cont. (%)	22.43		21.82	Saturation (%)	92.8	95.3	
Spceific gravity			2.68				

HEIGHT OF SPECIMEN						
	Before consol.		Before shearing	After shearing		
	Top	Bottom	Average	Average		
Height (cm)	1.960	1.960	1.920	1.920		

AREA OF SPECIMEN						
Initial diameter (cm)			6.660	Initial area (cm^2)		34.837
Load (kg)	Stress (kg/cm^2)	Stress (kN/m^2)	Diameter (cm)	Membrane (cm)	Corrected diameter (cm)	Area (cm^2)

Obregon Park P-5					
DSDSS TEST - Step 2b					
Type of soil: CH					
LL	50.5	PI	22.9	%Silt	44.0
e_0	0.61	S_0 (%)	95.3	%Clay	47.0
σ_v (kPa)	211	OCR	n/a	w (%)	21.8
γ_c (%)	~0.0004	H_0 (mm)	19.20	Spec. Gr.	2.68

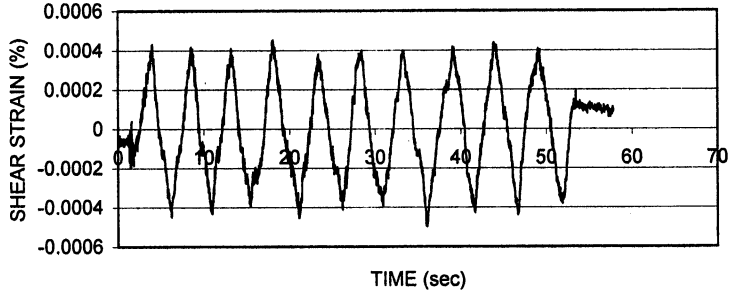

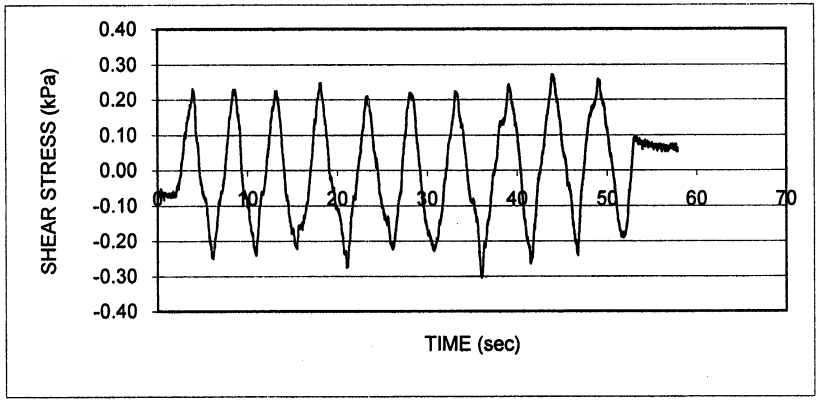

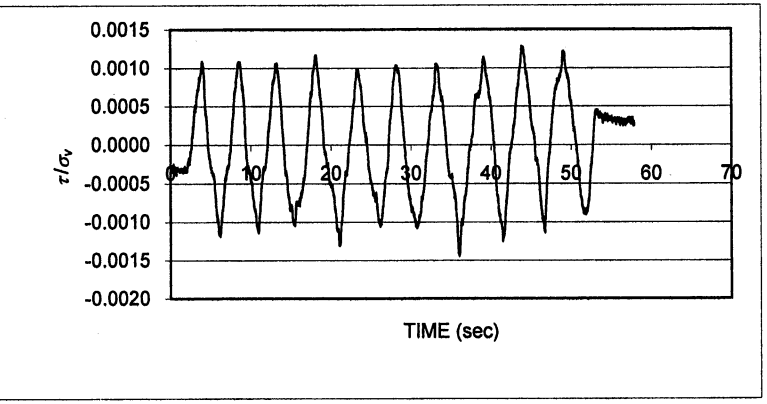

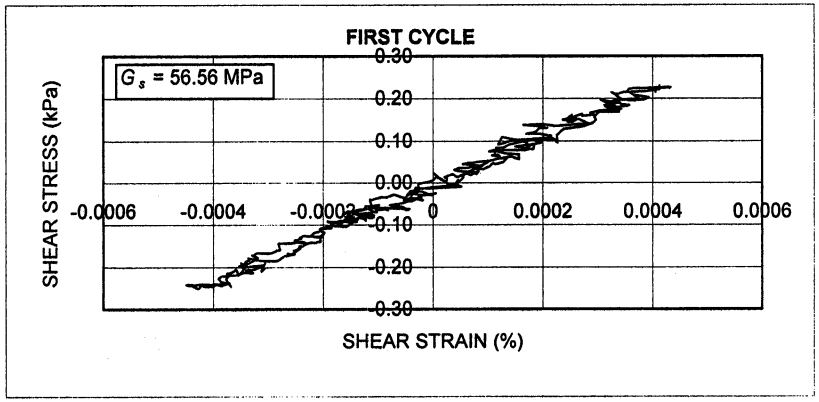

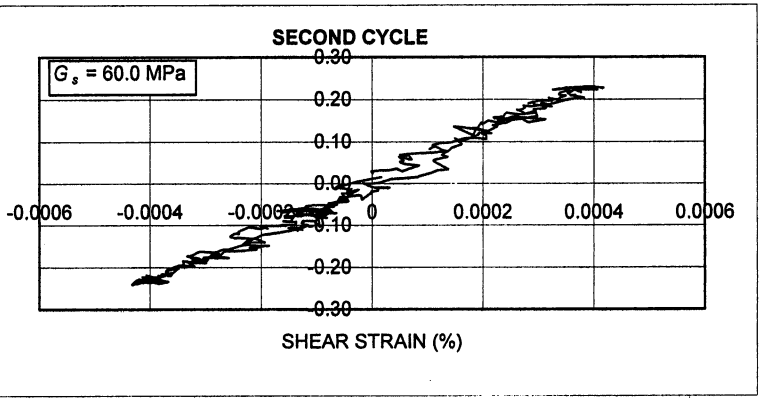

Obregon Park P-5					
DSDSS TEST - Step 26b					
Type of soil: CH					
LL	50.5	PI	22.9	%Silt	44.0
e_0	0.61	S_0 (%)	95.3	%Clay	47.0
σ_v (kPa)	211	OCR	n/a	w (%)	21.8
γ_c (%)	~0.0008	H_0 (mm)	19.20	Spec. Gr.	2.68

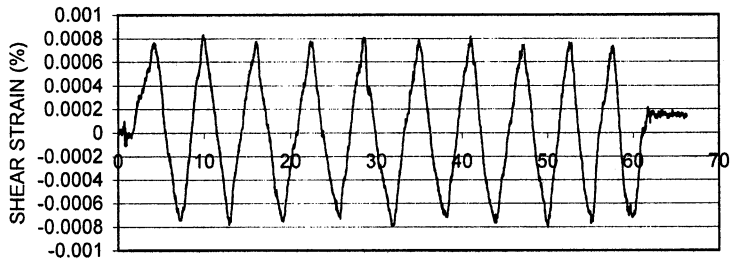

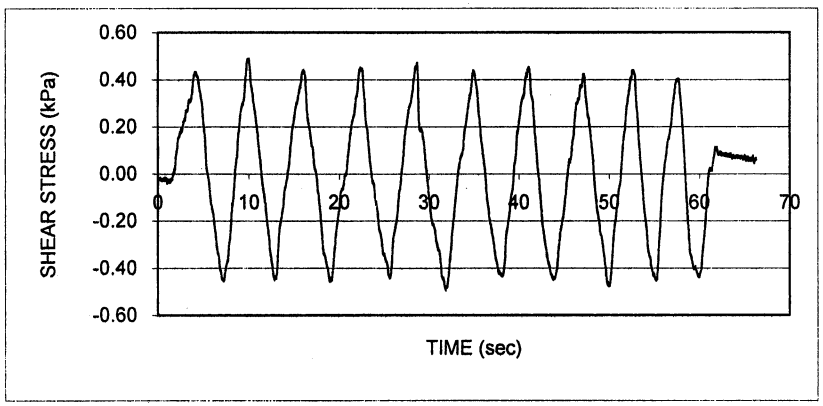

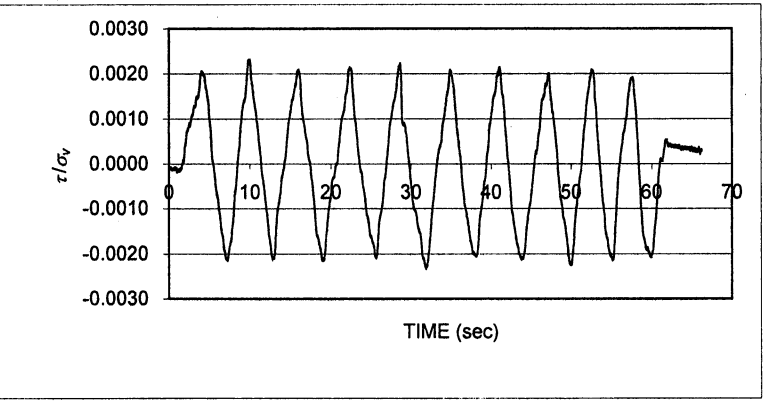

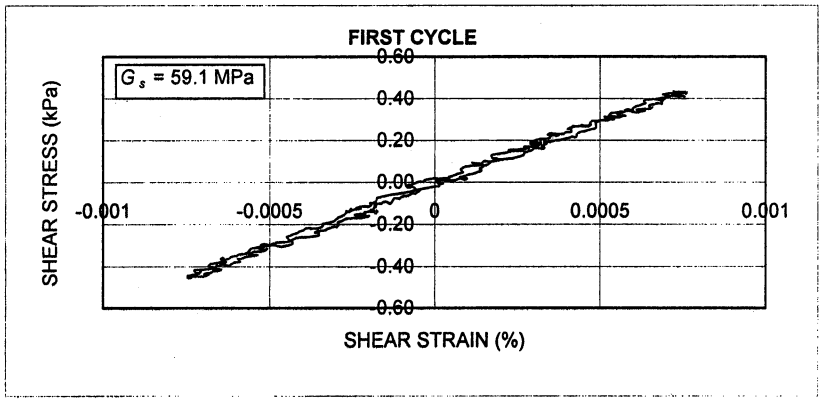

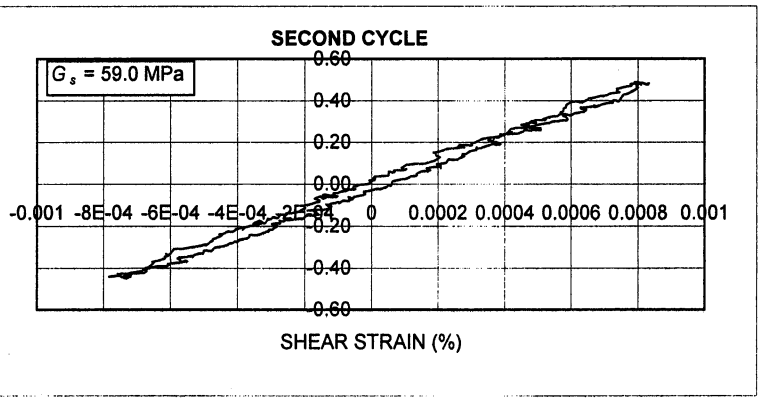

Obregon Park P-5					
DSDSS TEST - Step 3b					
Type of soil: CH					
LL	50.5	PI	22.9	%Silt	44.0
e_0	0.61	S_0 (%)	95.3	%Clay	47.0
σ_v (kPa)	211	OCR	n/a	w (%)	21.8
γ_c (%)	~0.0012	H_0 (mm)	19.20	Spec. Gr.	2.68

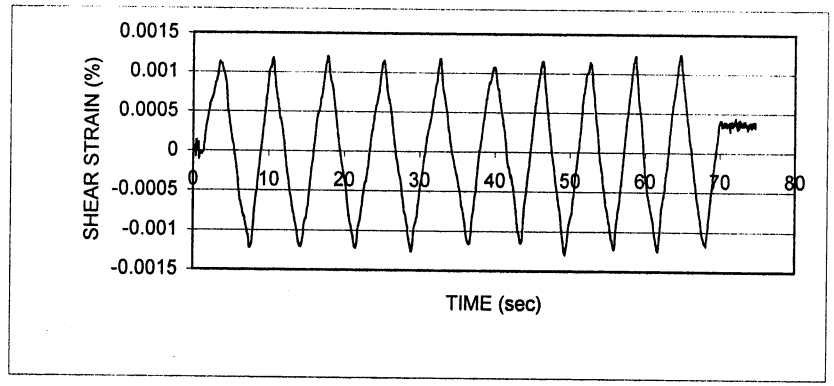

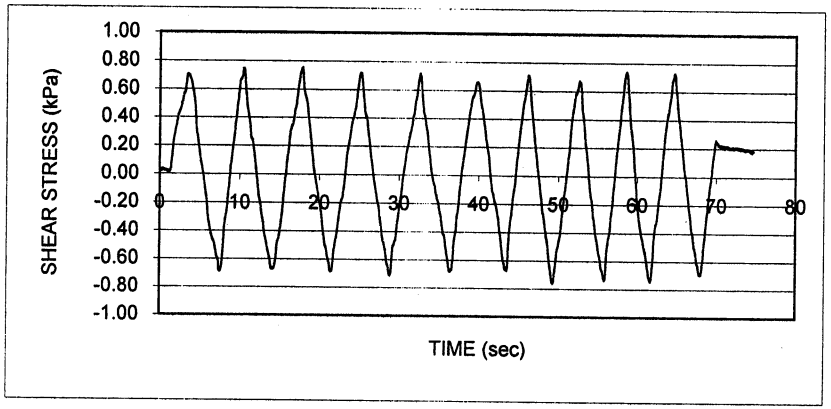

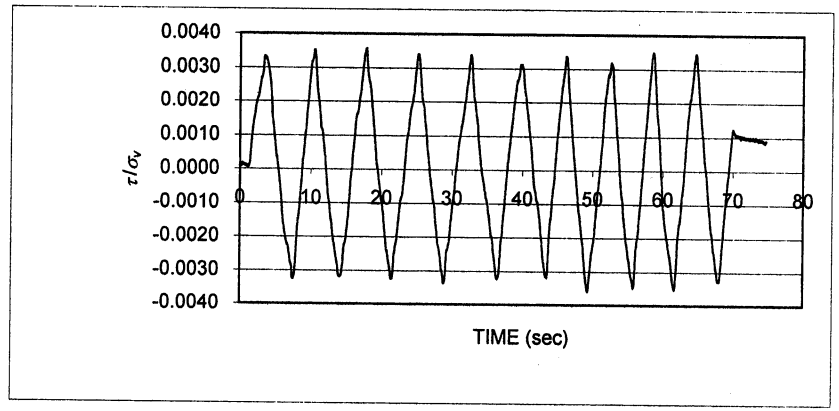

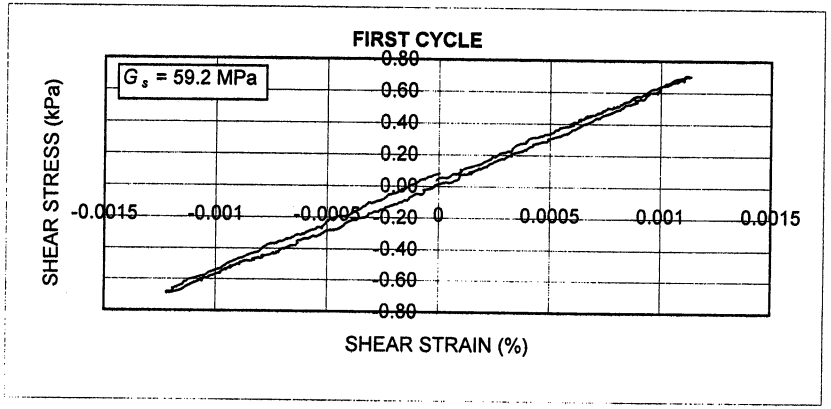

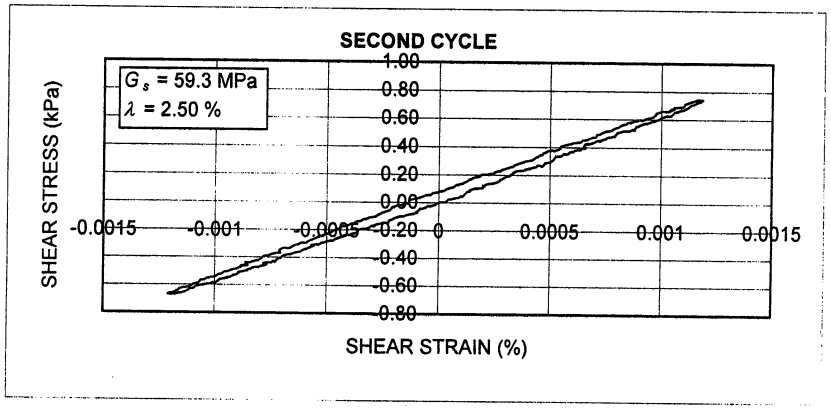

Obregon Park P-5					
DSDSS TEST - Step 4b					
Type of soil: CH					
LL	50.5	PI	22.9	%Silt	44.0
e_0	0.61	S_0 (%)	95.3	%Clay	47.0
σ_v (kPa)	211	OCR	n/a	w (%)	21.8
γ_c (%)	~0.0032	H_0 (mm)	19.20	Spec. Gr.	2.68

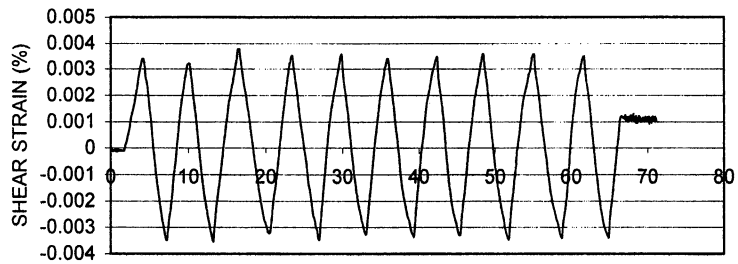

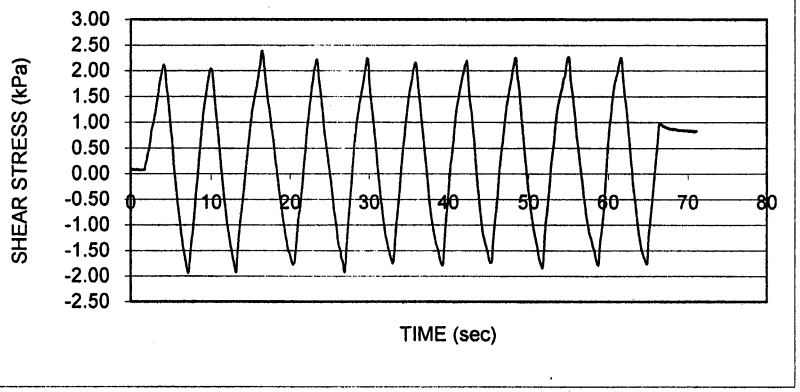

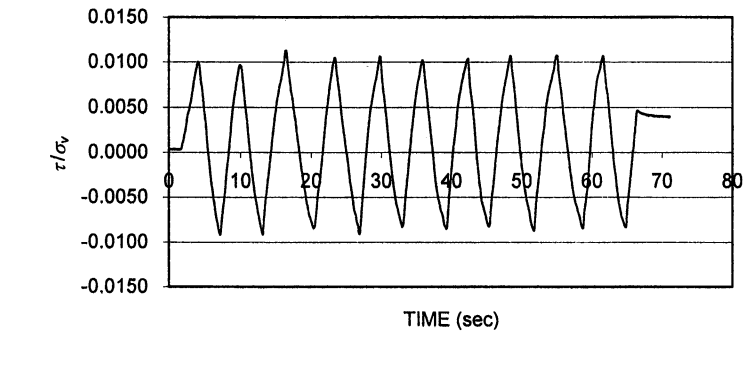

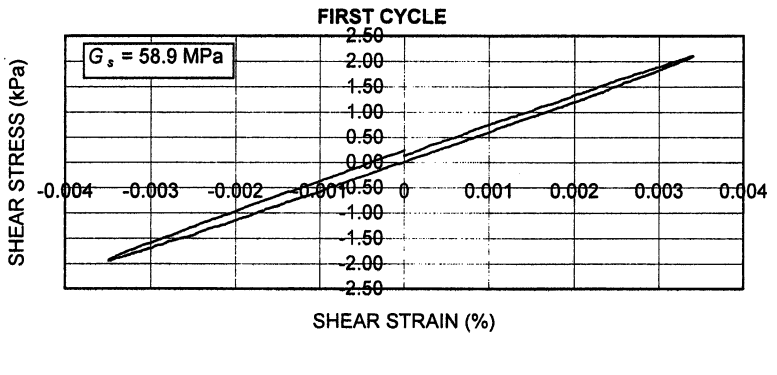

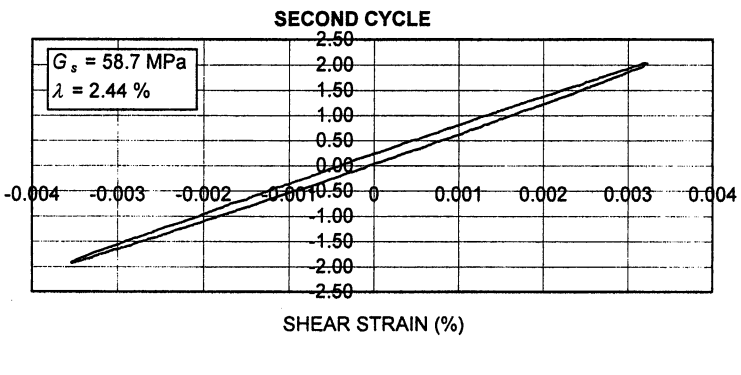

Obregon Park P-5					
DSDSS TEST - Step 5b					
Type of soil: CH					
LL	50.5	PI	22.9	%Silt	44.0
e_0	0.61	S_0 (%)	95.3	%Clay	47.0
σ_v (kPa)	211	OCR	n/a	w (%)	21.8
γ_c (%)	~0.011	H_0 (mm)	19.20	Spec. Gr.	2.68

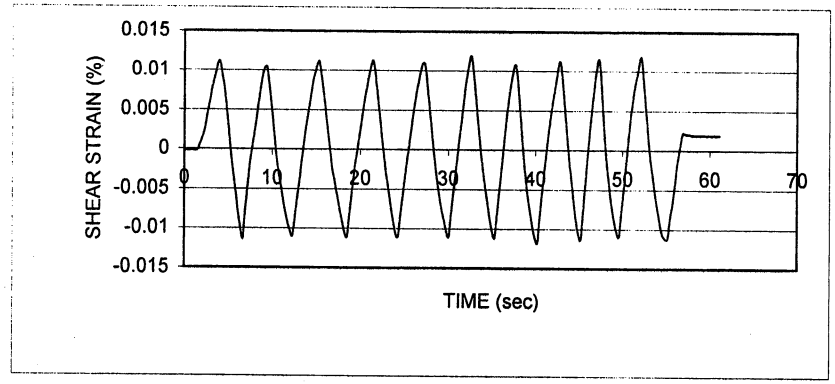

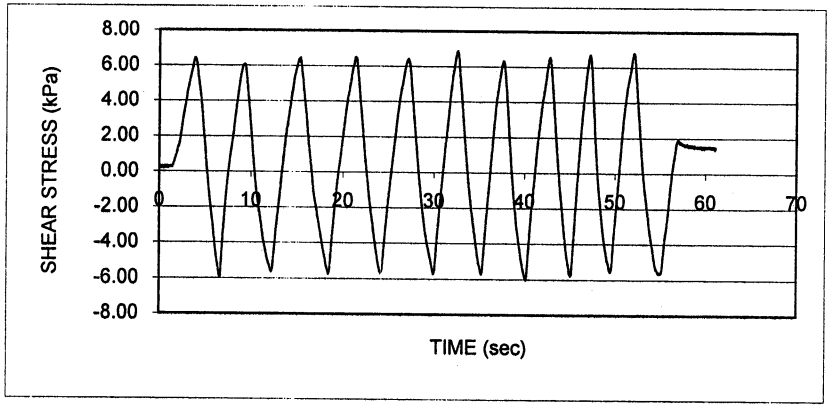

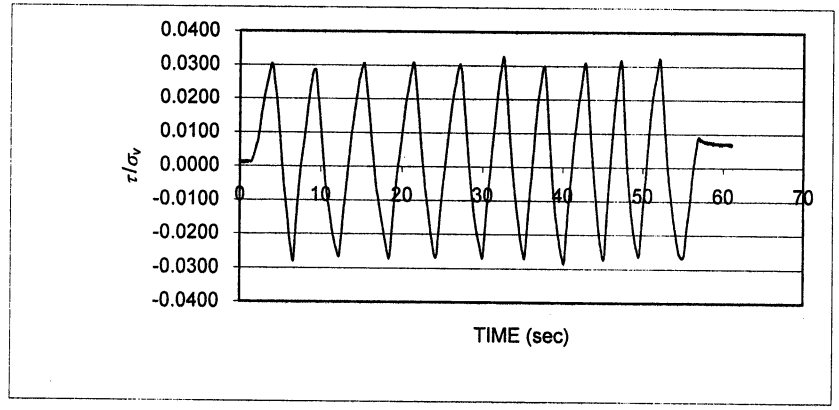

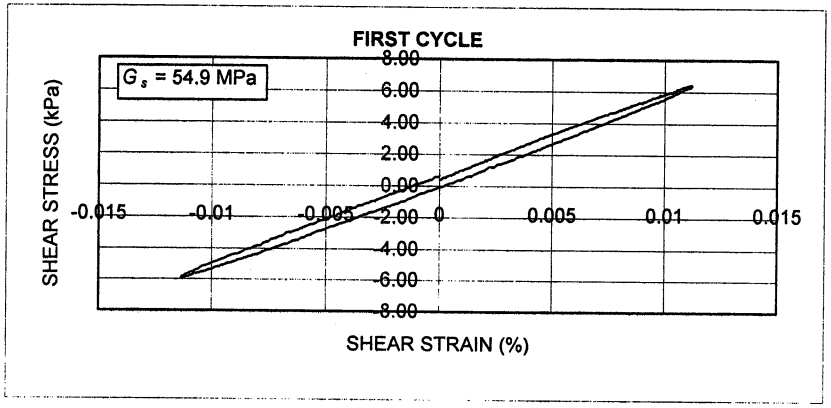

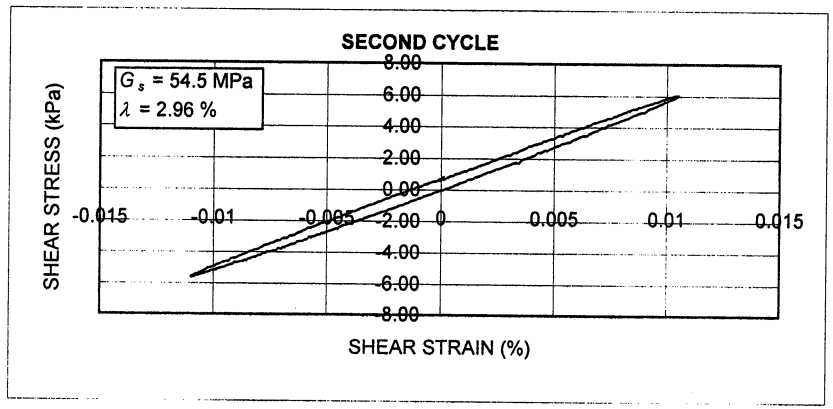

Obregon Park P-5					
DSDSS TEST - Step 6b					
Type of soil: CH					
LL	50.5	PI	22.9	%Silt	44.0
e_0	0.61	S_0 (%)	95.3	%Clay	47.0
σ_v (kPa)	211	OCR	n/a	w (%)	21.8
γ_c (%)	~0.032	H_0 (mm)	19.20	Spec. Gr.	2.68

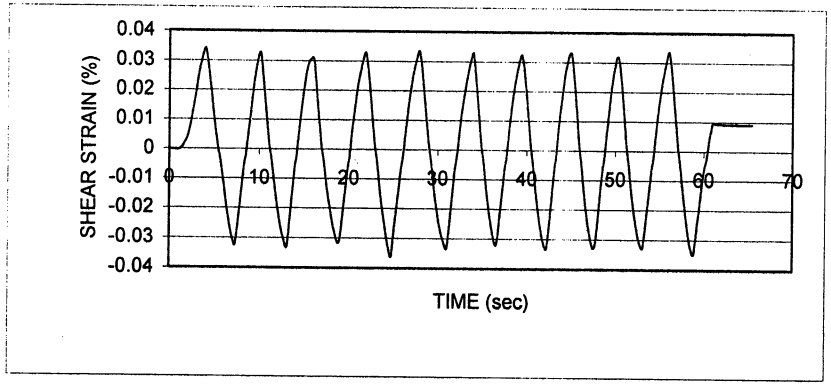

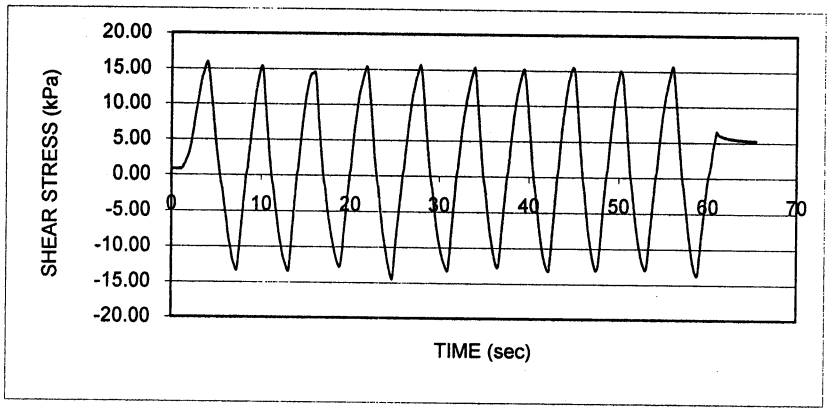

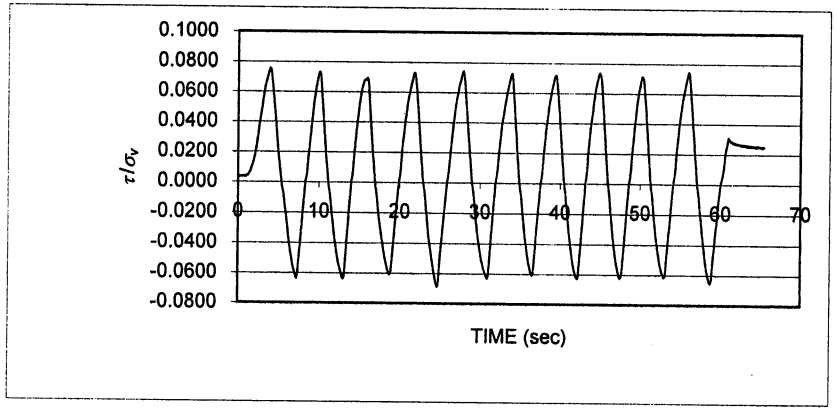

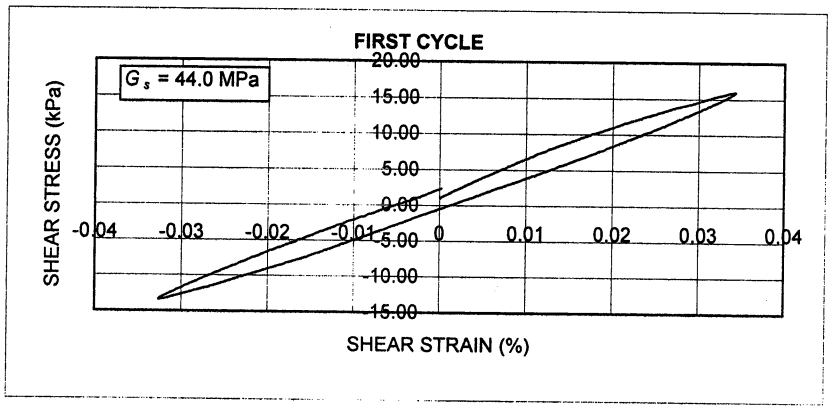

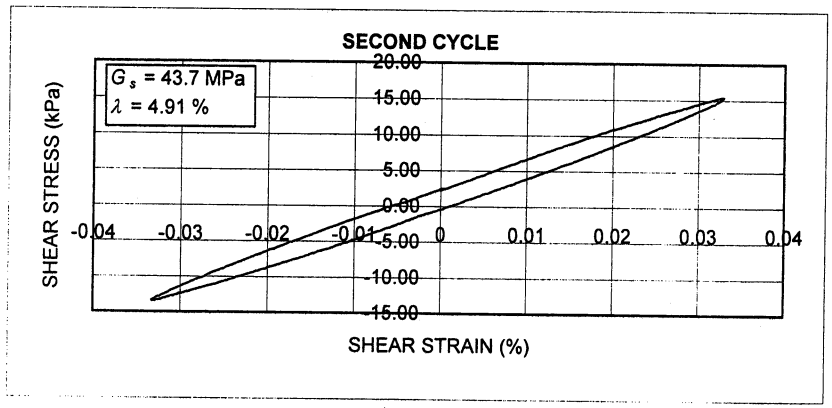

Obregon Park P-5					
DSDSS TEST - Step 7					
Type of soil: CH					
LL	50.5	PI	22.9	%Silt	44.0
e_0	0.61	S_0 (%)	95.3	%Clay	47.0
σ_v (kPa)	211	OCR	n/a	w (%)	21.8
γ_c (%)	~0.11	H_0 (mm)	19.20	Spec. Gr.	2.68

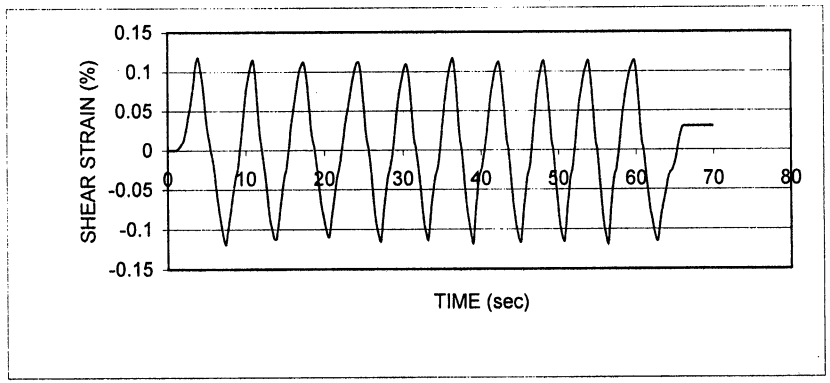

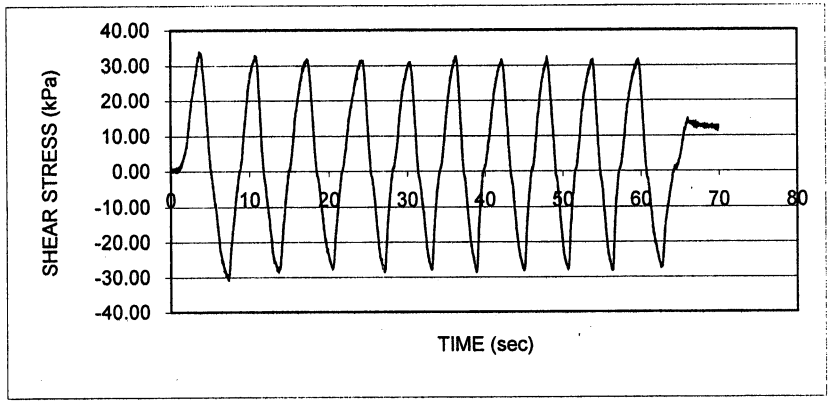

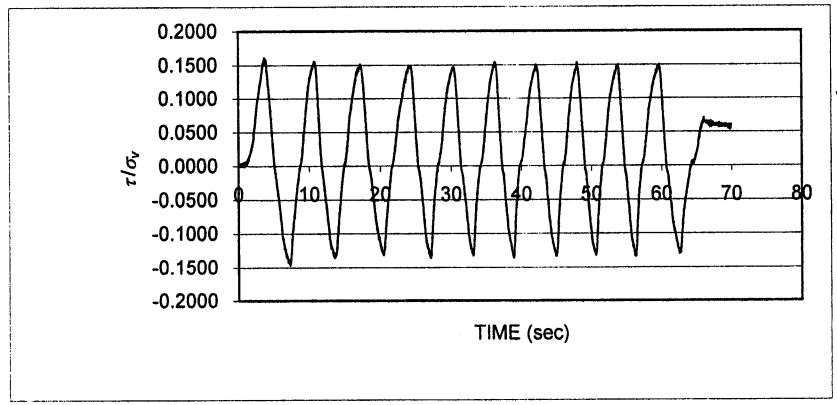

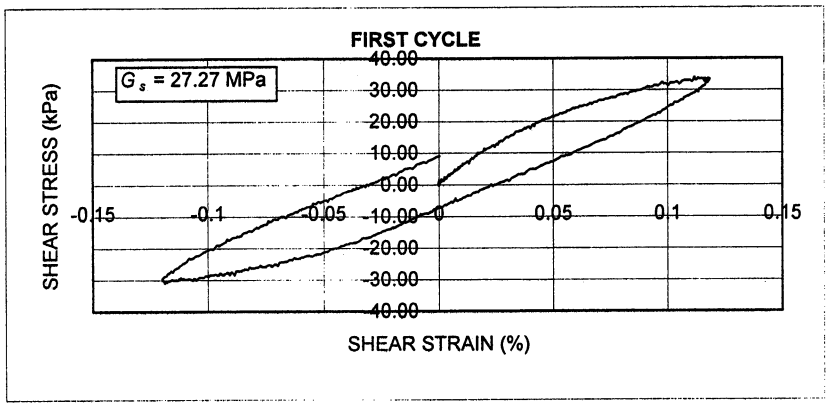

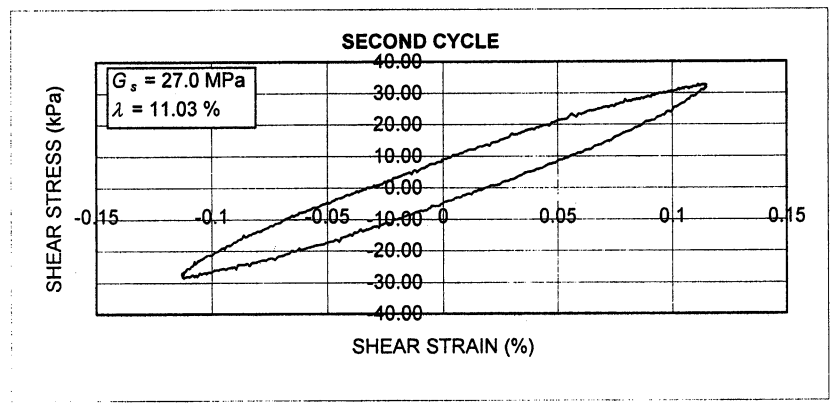

Obregon Park P-5					
DSDSS TEST - Step 8					
Type of soil: CH					
LL	50.5	PI	22.9	%Silt	44.0
e_0	0.61	S_0 (%)	95.3	%Clay	47.0
σ_v (kPa)	211	OCR	n/a	w (%)	21.8
γ_c (%)	~3.5	H_0 (mm)	19.20	Spec. Gr.	2.68

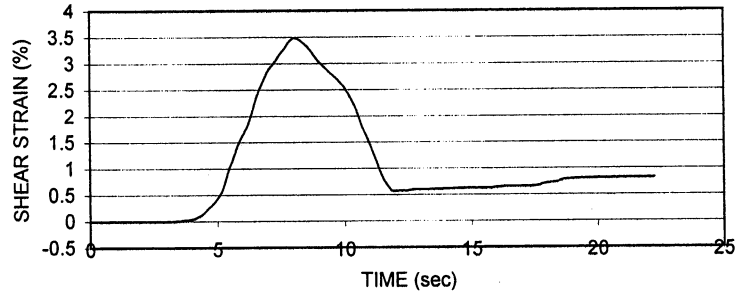

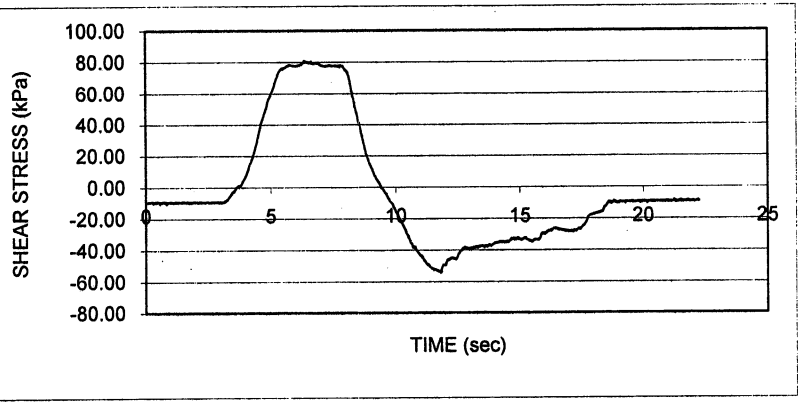

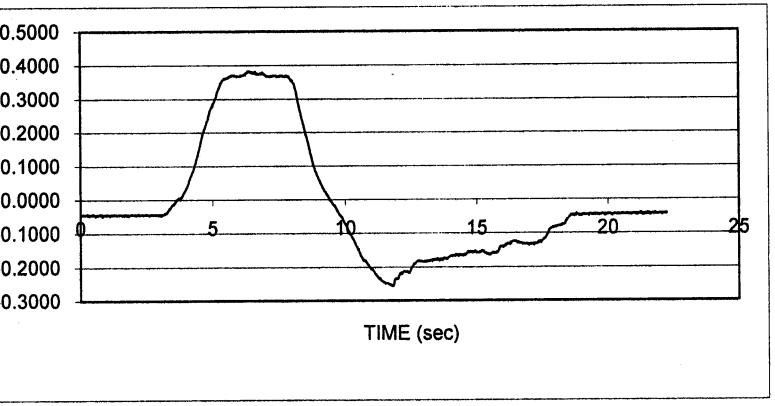

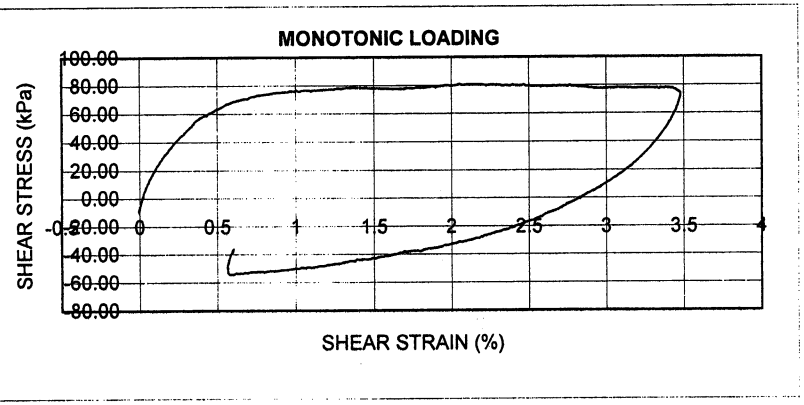

UCLA Soil Dynamics Laboratory

Double Specimen Direct Simple Shear (DSDSS) Test

Principal investigator: Mladen Vucetic, Professor

Test performed by Kentaro Tabata

Test no: 5

Project:	PEARL			Date:	7/6/2002
Sample name:	Obregon Park (P-5)			Depth (ft):	52.5
Symbol:	CL	LL (%):	50.5	Silt content (%):	44.0
Specific gravity:	2.68	PI:	22.9	Clay content (%):	47.0
Comments:					

Estimated G_{max} (MPa):	61.0

SHEAR MODULUS				DAMPING RATIO	
Step	γ_c (%)	G_s (MPa)	G_s/G_{max}	γ_c (%)	λ (%)
2b	0.000441	56.56	0.927		
2b	0.000425	59.99	0.983		
26b	0.000755	59.06	0.968	0.001198	2.50
26b	0.000808	58.95	0.966	0.003385	2.44
3b	0.001180	59.21	0.971	0.010746	2.96
3b	0.001198	59.25	0.971	0.033103	4.91
4b	0.003447	58.90	0.966	0.113996	11.03
4b	0.003385	58.67	0.962		
5b	0.011271	54.88	0.900		
5b	0.010746	54.52	0.894		
6b	0.033444	43.99	0.721		
6b	0.033103	43.70	0.716		
7x	0.119153	27.27	0.447		
7x	0.113996	26.98	0.442		
	γ (%)				
(Monotonic loading)	0.506438	12.51	0.205		
	1.007362	7.59	0.124		
	1.508286	5.16	0.085		
	2.001873	3.98	0.065		
	2.500934	3.19	0.052		
	3.473317	2.15	0.035		

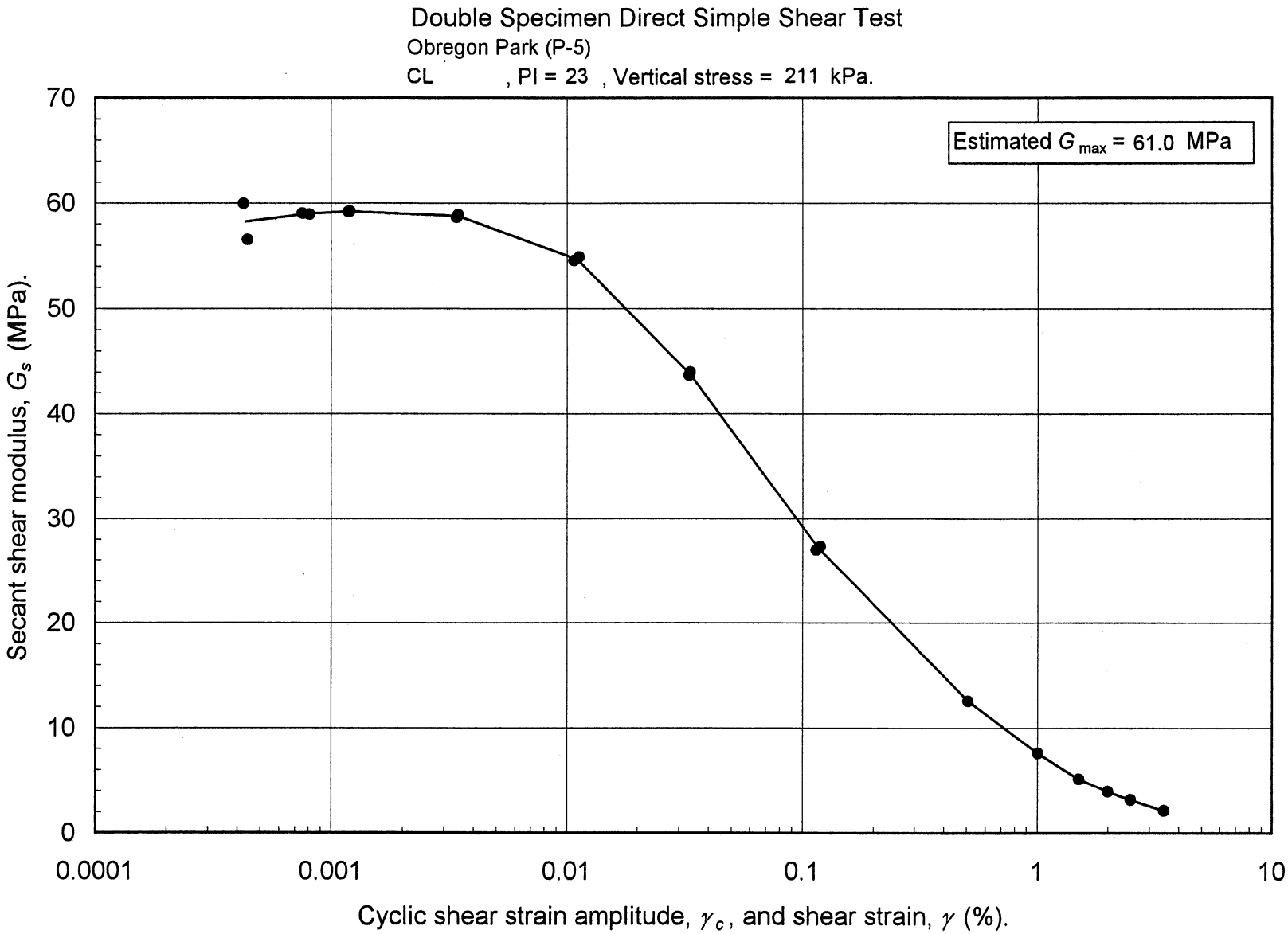
Double Specimen Direct Simple Shear Test
Obregon Park (P-5)
CL , PI = 23 , Vertical stress = 211 kPa.
Estimated G_{max} = 61.0 MPa
Secant shear modulus, G_s (MPa).
70
60
50
40
30
20
10
0
0.0001
0.001
0.01
0.1
1
10
Cyclic shear strain amplitude, γ_c, and shear strain, γ (%).

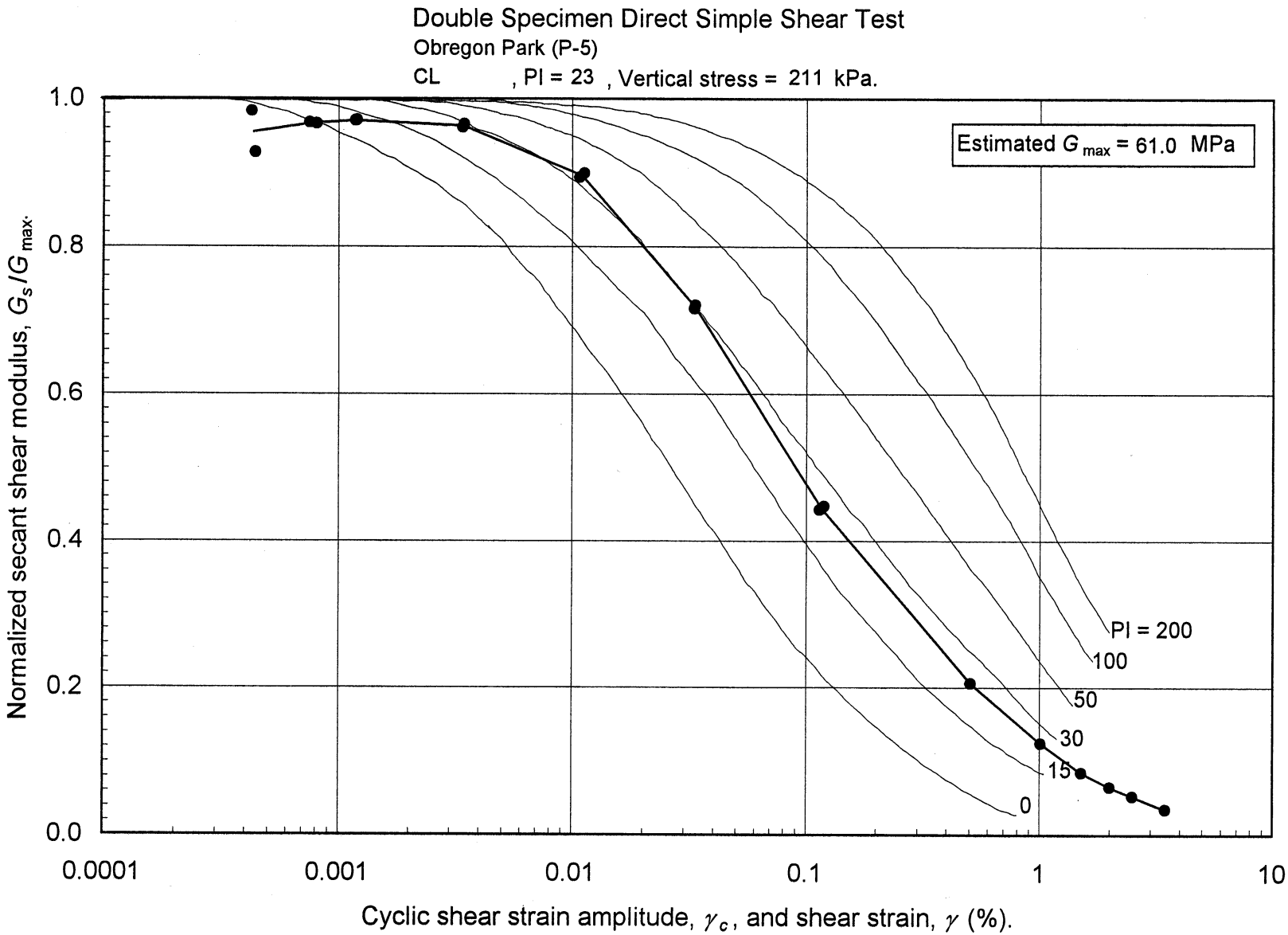
Double Specimen Direct Simple Shear Test
Obregon Park (P-5)
CL , PI = 23 , Vertical stress = 211 kPa.
Estimated G_{max} = 61.0 MPa
PI = 200
100
50
30
15
0
Normalized secant shear modulus, G_s/G_{max}.
1.0
0.8
0.6
0.4
0.2
0.0
0.0001
0.001
0.01
0.1
1
10
Cyclic shear strain amplitude, γ_c, and shear strain, γ (%).

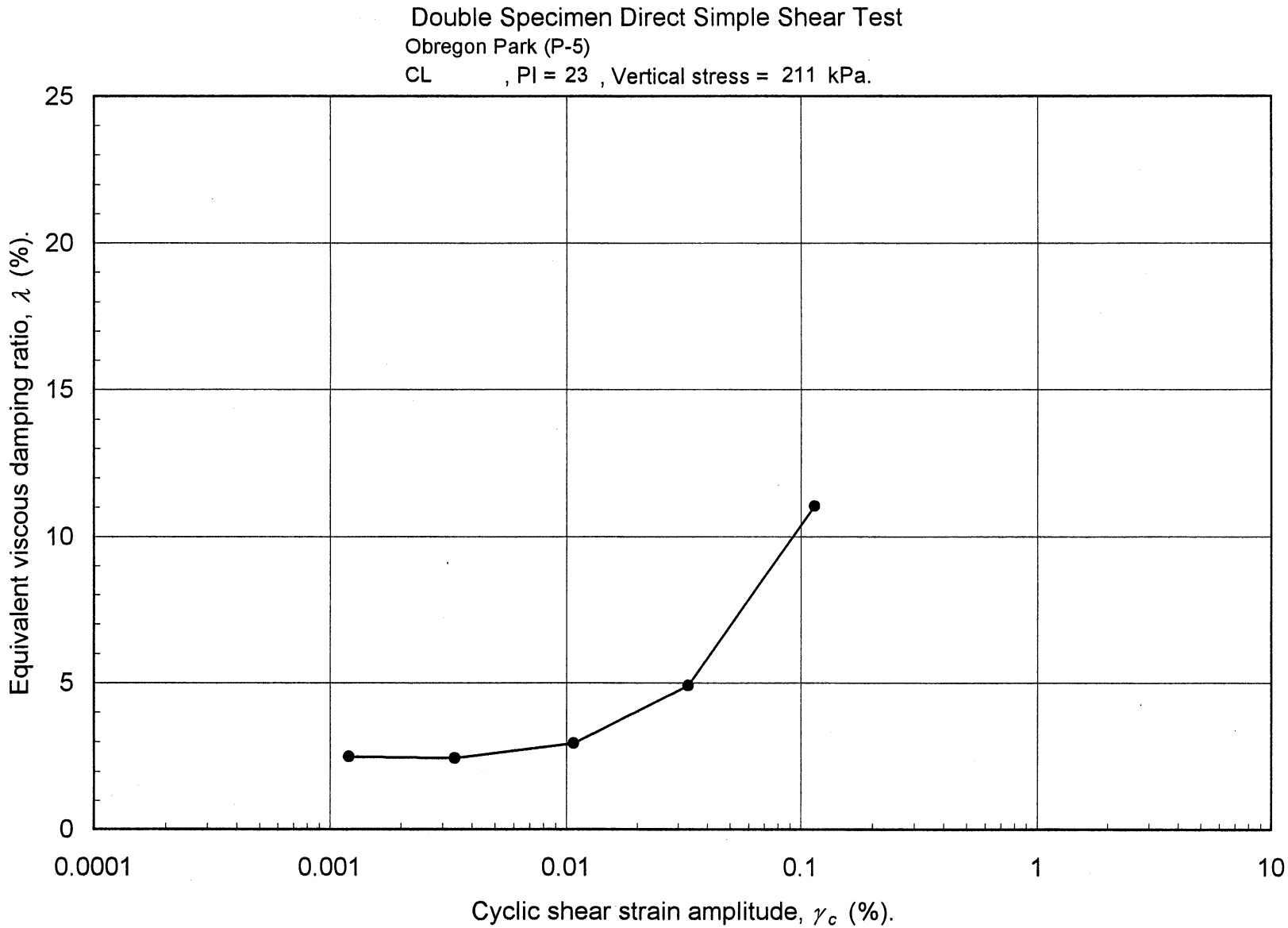
Double Specimen Direct Simple Shear Test
Obregon Park (P-5)
CL , PI = 23 , Vertical stress = 211 kPa.
Equivalent viscous damping ratio, λ (%).
25
20
15
10
5
0
0.0001
0.001
0.01
0.1
1
10
Cyclic shear strain amplitude, γc (%).

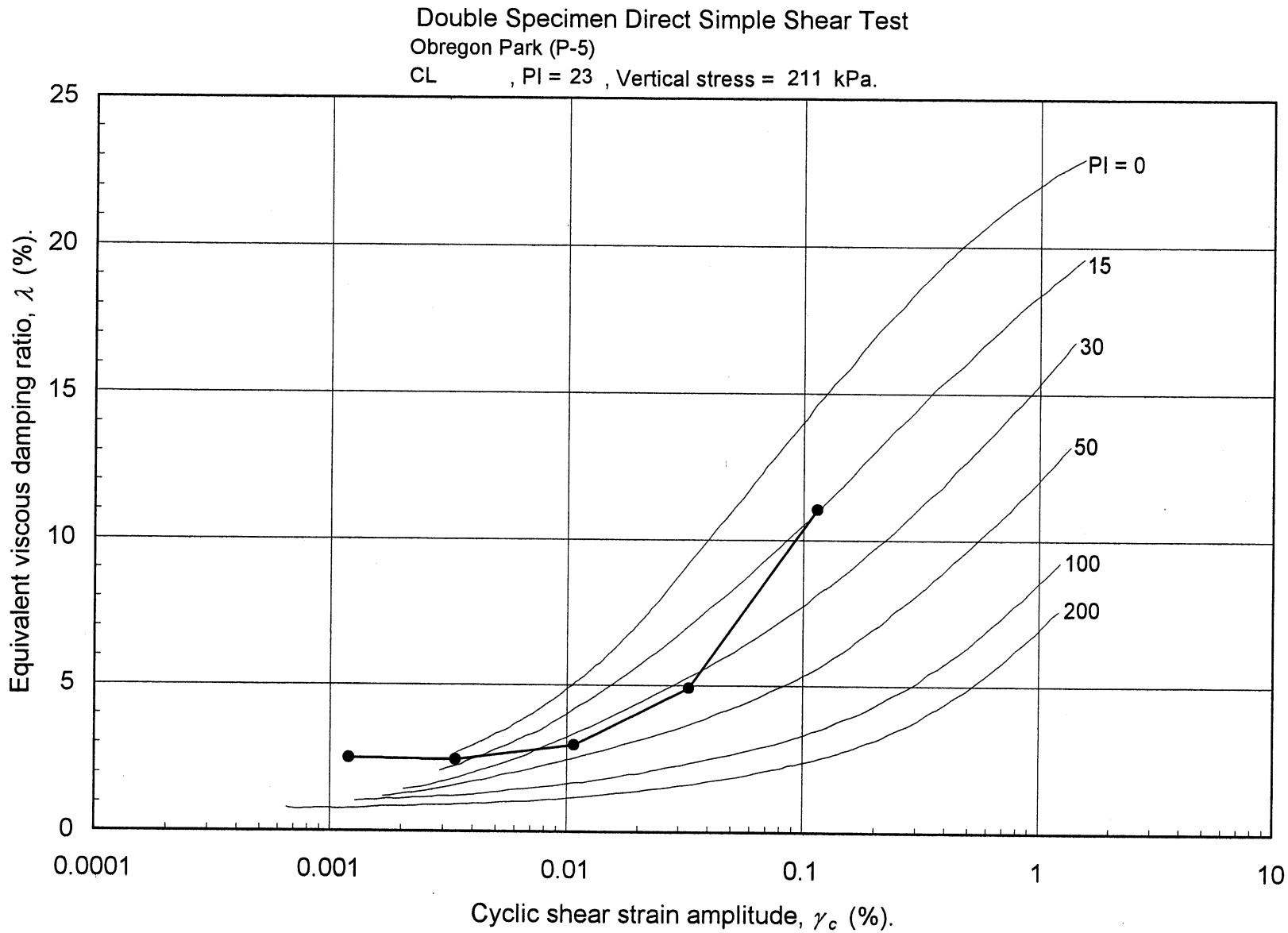
Double Specimen Direct Simple Shear Test
Obregon Park (P-5)
CL , PI = 23 , Vertical stress = 211 kPa.
Equivalent viscous damping ratio, λ (%).
Cyclic shear strain amplitude, γc (%).
0
5
10
15
20
25
0.0001
0.001
0.01
0.1
1
10
PI = 0
15
30
50
100
200

UCLA Soil Dynamics Laboratory

Specific Gravity Test

Principal investigator: Mladen Vucetic, Professor

Test performed by: Kentaro Tabata Test No.: 5

Project:	PEARL			Date:	7/11/2002
Boring:	Obregon Park				
Tube No.:	P-5	Depth (ft):	50.0 -53.0	GWT (ft):	20.0
Comments:	Stiff clay.				

SPECIFIC GRAVITY TEST

Test No.	1		
Bottle No.	3		
Wt. of bottle (g)	178.28		
Volume of bottle (cm^3)	500		
Wt. of bottle+water+soil (g)	702.32		
Temperature (°C)	22.0		
Wt. of bottle+water (g)	676.27		
Evaporating dish No.	B-2		
Weight of dish (g)	537.19		
Wt. of dish+dry soil (g)	578.71		
Wt. of dry soil (g)	41.52		
Specific gravity of water	0.9978		
Specific gravity of soil	**2.68**		

UCLA Soil Dynamics Laboratory

Grain Size Distribution

Principal investigator: Mladen Vucetic, Professor

Test performed by: Kentaro Tabata Test No.: 5

Project:	PEARL				
Boring:	Obregon Park				
Tube No.:	P-5	Depth (ft):	50.0 -53.0	GWT (ft):	20.0
Comments:	Stiff clay.				

GRAIN SIZE DISTRIBUTION

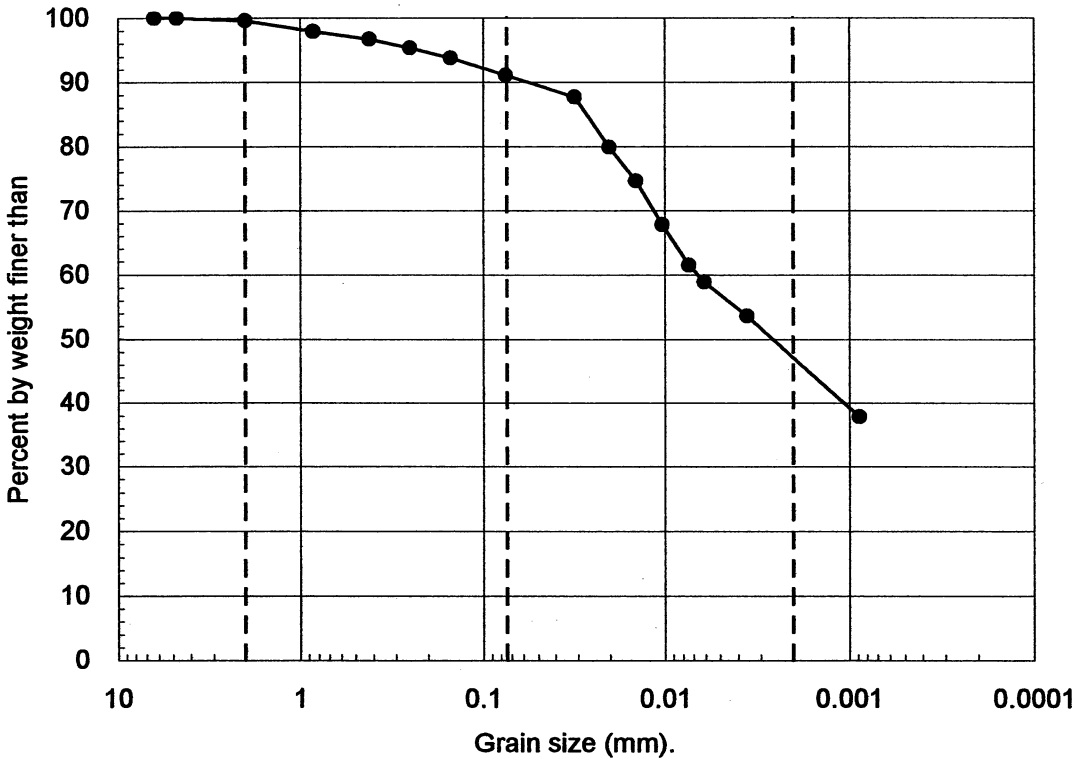

Clay (%)	Silt (%)	Sand (%)	Gravel (%)
47.0	44.0	8.5	0.4

UCLA Soil Dynamics Laboratory

Hydrometer Analysis

Principal investigator: Mladen Vucetic, Professor

Test performed by: Kentaro Tabata Test No.: 5

Project:	PEARL			Date:	7/11/2002
Boring:	Obregon Park				
Tube No.:	P-5	Depth (ft):	50.0 -53.0	GWT (ft):	20.0
Comments:	Stiff clay.				

HYDROMETER TEST

Time	Elapsed time t (sec)	Temp. T (°C)	Reading R'_T	Corr. reading $R_T=R'_T+c_m$	Depth H (cm)	Grain diameter D (mm)	Temp. corr. m_T	Corr. depth $R_T+m_T-c_d$	% by wt. finer than W_D (%)
10:25:43	0								
10:27:43	120	23.0	1018.5	1019.0	11.44	0.0313	0.700	1016.7	87.72
10:30:43	300	23.0	1017.0	1017.5	11.84	0.0201	0.700	1015.2	79.84
10:35:43	600	23.0	1016.0	1016.5	12.11	0.0144	0.700	1014.2	74.59
10:45:43	1200	23.0	1014.7	1015.2	12.45	0.0103	0.700	1012.9	67.76
11:05:43	2400	23.0	1013.5	1014.0	12.78	0.0074	0.700	1011.7	61.46
11:25:43	3600	23.0	1013.0	1013.5	12.91	0.0061	0.700	1011.2	58.83
13:25:43	10800	23.0	1012.0	1012.5	13.18	0.0035	0.700	1010.2	53.58
14:00:00	185657	23.0	1009.0	1009.5	13.98	0.0009	0.700	1007.2	37.82

APPARATUS

Hydrometer no.:	88-18587	a_0	284.03	a_1	-0.2675
Graduate no.:	3				

FACTORS

Meniscus corr., c_m:	0.5	
Disp. agent corr, c_d:	3.0	
Visc. of water, η.	23.0 °C	9.565E-06 g sec/cm^2
	°C	g sec/cm^3

WEIGHT

Dry soil (g)	27.66
Percent by wt (%)	91.05
Dry soil for sieve (g)	2.72
Total (g)	30.38

UNIT WEIGHT

Specific gravity:		2.68
T	γ_w	γ_s
(°C)	(g/cm^3)	(g/cm^3)
23.0	0.9976	2.6721

UCLA Soil Dynamics Laboratory

Sieve Analysis

Principal investigator: Mladen Vucetic, Professor

Test performed by: Kentaro Tabata Test No.: 5

Project:	PEARL			Date:	7/12/2002
Boring:	Obregon Park				
Tube No.:	P-5	Depth (ft):	50.0 -53.0	GWT (ft):	20.0
Comments:	Stiff clay.				

SIEVE ANALYSIS

Sieve No.	Diameter (mm)	Sieve (g)	S+wet (g)	S+dry (g)	Retained (g)	Retained (%)	Cumulated (g)	Cumulated (%)	Passing (%)
3	6.350	485.05		485.05	0.00	0.00	0.00	0.00	100.00
4	4.750	463.11		463.11	0.00	0.00	0.00	0.00	100.00
10	2.000	422.43		422.56	0.13	0.43	0.13	0.43	99.57
20	0.850	375.41		375.90	0.49	1.61	0.62	2.04	97.96
40	0.420	375.61		375.97	0.36	1.18	0.98	3.23	96.77
60	0.250	323.88		324.32	0.44	1.45	1.42	4.67	95.33
100	0.150	342.26		342.74	0.48	1.58	1.90	6.25	93.75
200	0.075	676.91		677.73	0.82	2.70	2.72	8.95	91.05
Total					2.72	8.95			

WEIGHT

Dry soil for sieve (g)	2.72
Dry soil for hydr. (g)	27.66
Total (g)	30.38
Percent coaser (%)	8.95

UCLA Soil Dynamics Laboratory

Atterberg Limit Determination

Principal investigator: Mladen Vucetic, Professor

Test performed by: Kentaro Tabata Test No.: 5

Project:	PEARL			Date:	4/5/2002
Boring:	Obregon Park				
Tube No.:	P-5	Depth (ft):	50.0 -53.0	GWT (ft):	20.0
Comments:	Stiff clay.				

LIQUID LIMIT TEST

Test No.	1	2	3	4	5			
Number of blows	47	36	24	15	8			
Container No.	ST-13	ST-10	ST-3	ST-14	ST-5			
Container (g)	30.21	30.42	30.21	30.46	30.19			
Cont+wet soil (g)	40.15	39.38	37.36	38.55	41.75			
Cont+dry soil (g)	37.02	36.52	34.92	35.66	37.56			
Water (g)	3.13	2.86	2.44	2.89	4.19			
Dry soil (g)	6.81	6.10	4.71	5.20	7.37			
Water content (%)	45.96	46.89	51.80	55.58	56.85			

PLASTIC LIMIT TEST

Test No.	1	2	3
Container No.	ST-12	ST-18	ST-11
Container (g)	30.31	30.15	30.28
Cont+wet soil (g)	32.64	33.81	33.52
Cont+dry soil (g)	32.16	32.97	32.83
Water (g)	0.48	0.84	0.69
Dry soil (g)	1.85	2.82	2.55
Water content (%)	25.95	29.79	27.06

ATTERBERG LIMITS

Liquid limit (%)	**50.5**
Plastic limit (%)	**27.6**
Plasticity index	**22.9**

CLASSIFICATION

CH

FLOW CHART

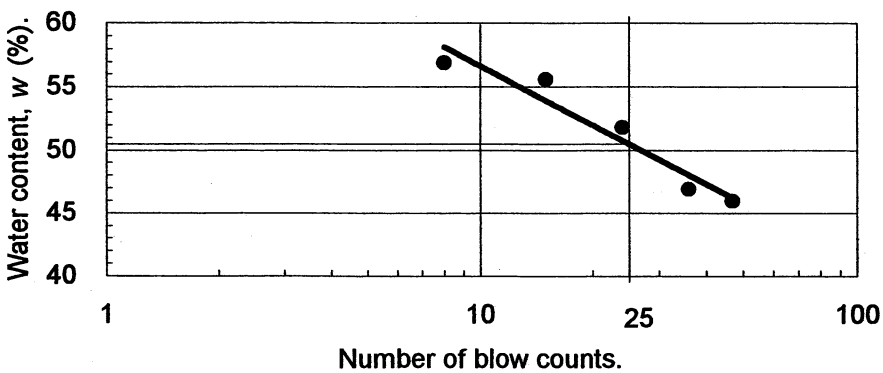

UCLA Soil Dynamics Laboratory

Atterberg Limit Determination

Principal investigator: Mladen Vucetic, Professor

Test performed by: Kentaro Tabata Test No.: 5

Project:	PEARL			Date:	4/5/2002
Boring:	Obregon Park				
Tube No.:	P-5	Depth (ft):	50.0 -53.0	GWT (ft):	20.0
Comments:	Stiff clay.				

PLASTICITY CHART

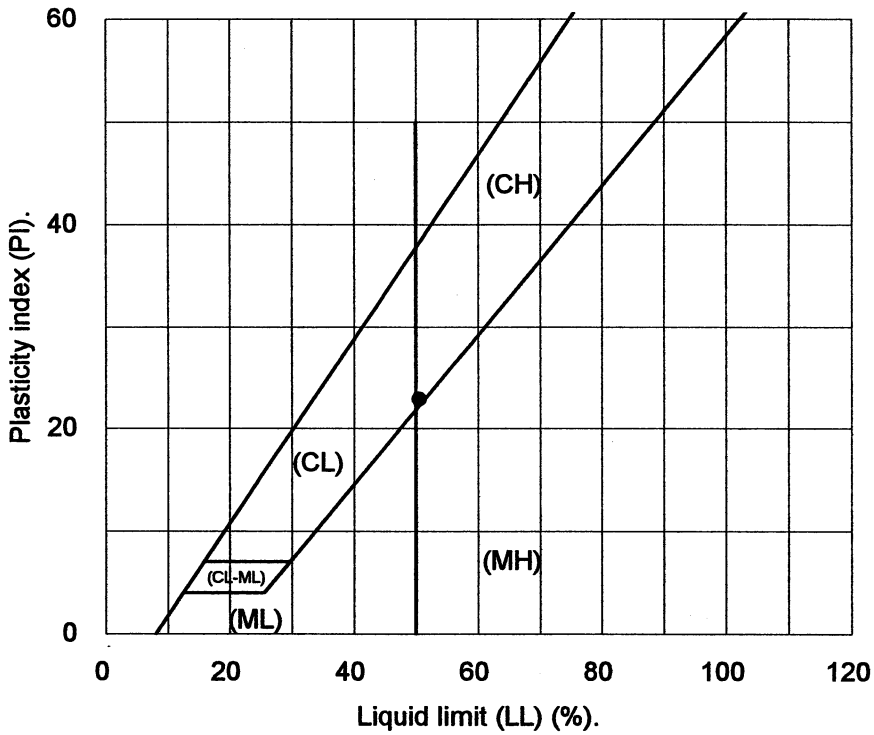

3.7 Test 6: OBREGON PARK P-7

UCLA Soil Dynamics Laboratory

Double Specimen Direct Simple Shear (DSDSS) Test

Principal investigator: Mladen Vucetic, Professor

Test performed by: Kentaro Tabata Test No.: 6

Project:	PEARL			Date:	3/8/2002
Boring:	Obregon Park				
Tube No.:	P-7	Depth (ft):	70.0 -73.0	GWT (ft):	20.0 (reported by others)
Comments:	Silt. Specimen obtained from the bottom of the tube (specimen depth ~ 72.5 ft).				

FORM 1: SPECIMEN PREPARATION

WATER CONTENT, SPECIFIC GRAVITY

	Before consol.	After shearing	
Container No.	ST-13	MT-7	MT-17
Cont+wet soil (g)	40.96	190.84	184.54
Cont+dry soil (g)	39.22	168.09	166.69
Container (g)	30.20	50.77	50.23
Water (g)	1.74	22.75	17.85
Dry soil (g)	9.02	117.32	116.46
Water content(%)	19.29	19.39	15.33
Avg. water cont. (%)	19.29		17.36
Spceific gravity			2.64

UNIT WEIGHT, VOID RATIO, SATURATION

	Before consol.	Before shearing	After shearing
Average weight (g)	136.23	136.23	
Height (cm)	1.960	1.929	
Area (cm^2)	34.84	34.84	
Volume (cm^3)	68.28	67.21	
Unit weight (g/cm^3)	1.995	2.027	
Unit weight (kN/m^3)	19.55	19.86	
Void ratio	0.58	0.55	
Saturation (%)	88.0		

HEIGHT OF SPECIMEN

	Before consol.		Before shearing	After shearing		
	Top	Bottom	Average	Average		
Height (cm)	1.960	1.960	1.929	1.929		

AREA OF SPECIMEN

Initial diameter (cm)	6.660	Initial area (cm^2)	34.837

Load (kg)	Stress (kg/cm^2)	Stress (kN/m^2)	Diameter (cm)	Membrane (cm)	Corrected diameter (cm)	Area (cm^2)

Obregon Park P-7					
DSDSS TEST - Step 2					
Type of soil: ML					
LL	37.7	PI	11.6	%Silt	55.7
e_0	0.55	S_0 (%)		%Clay	29.5
σ_v (kPa)	281	OCR	n/a	w (%)	
γ_c (%)	~0.00038	H_0 (mm)	19.29	Spec. Gr.	2.67

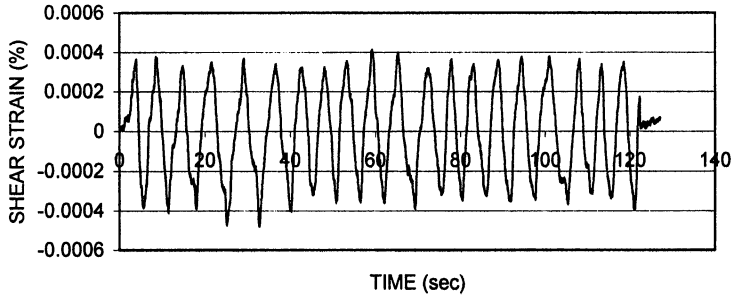

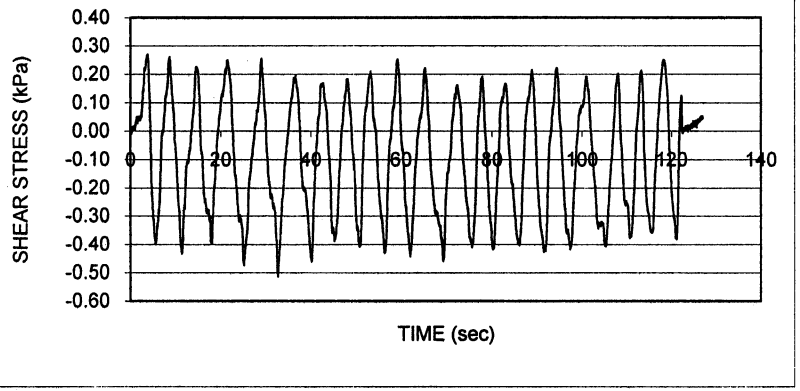

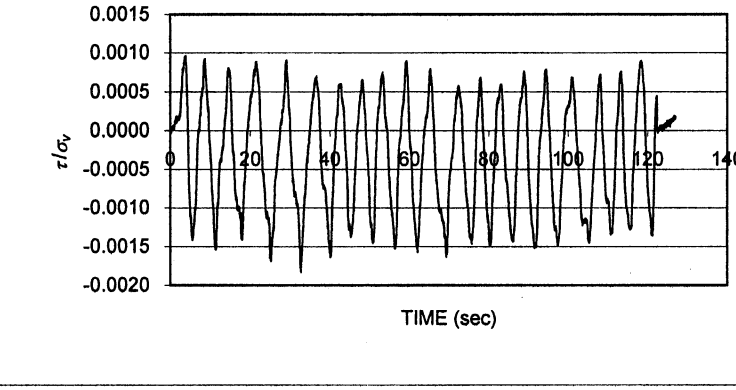

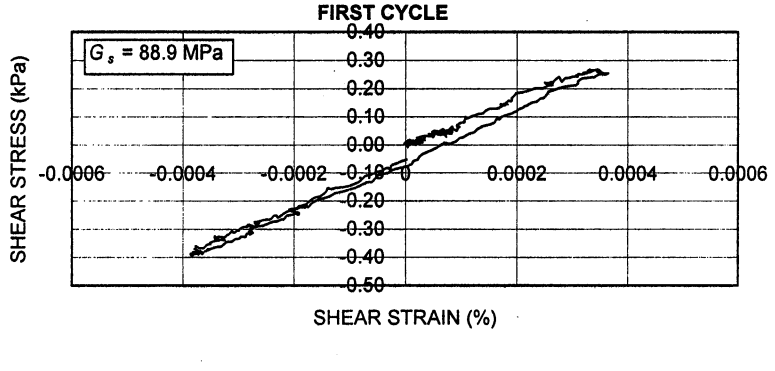

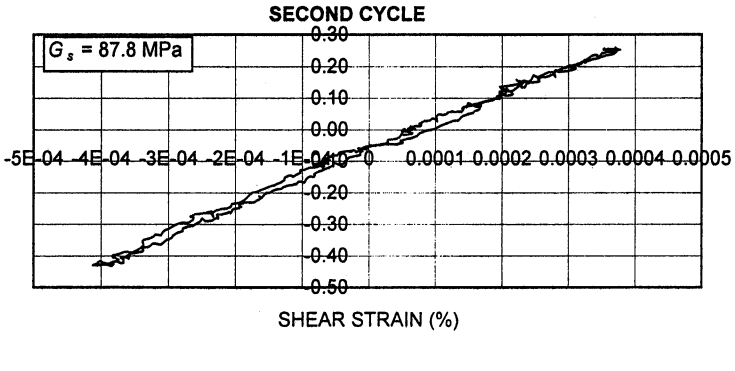

Obregon Park P-7					
DSDSS TEST - Step 26					
Type of soil: ML					
LL	37.7	PI	11.6	%Silt	55.7
e_0	0.55	S_0 (%)		%Clay	29.5
σ_v (kPa)	281	OCR	n/a	w (%)	
γ_c (%)	~0.0007	H_0 (mm)	19.29	Spec. Gr.	2.67

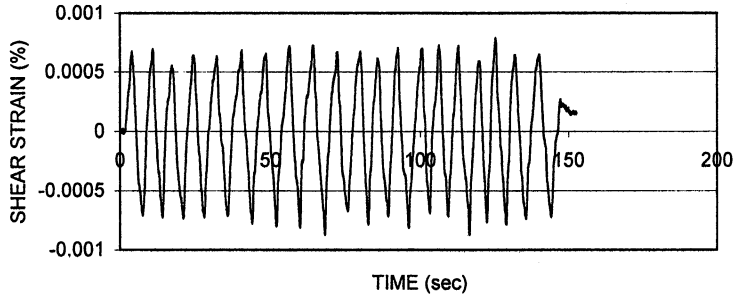

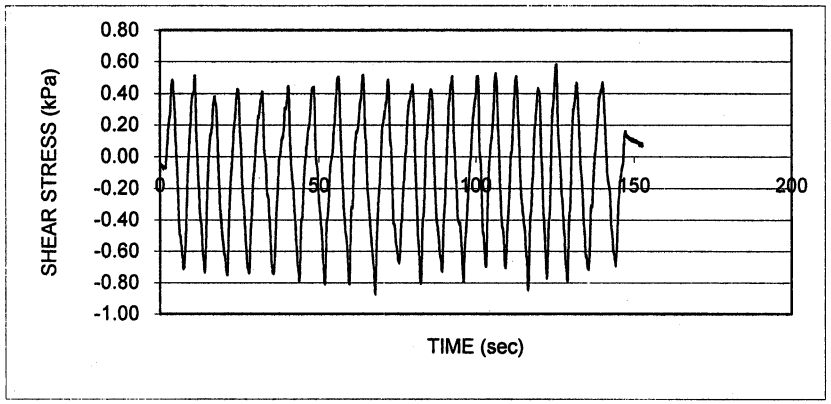

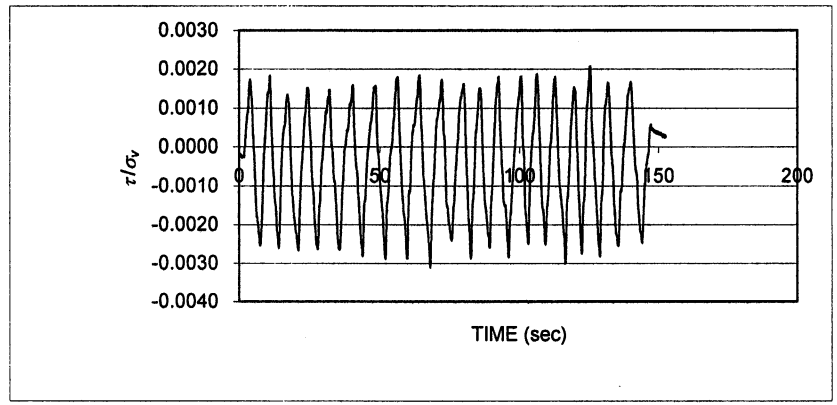

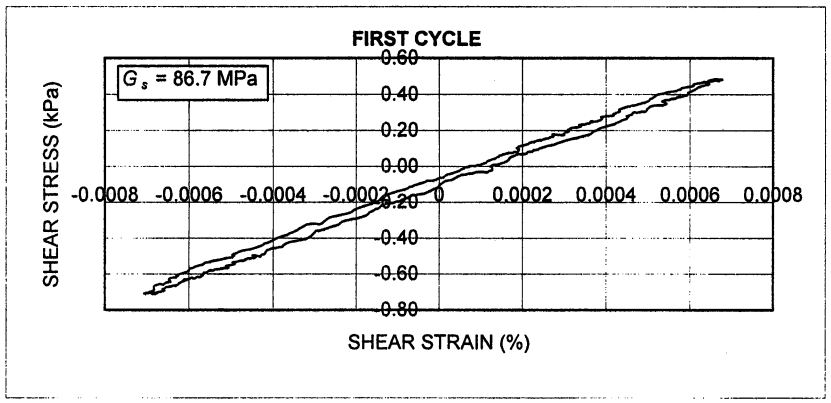

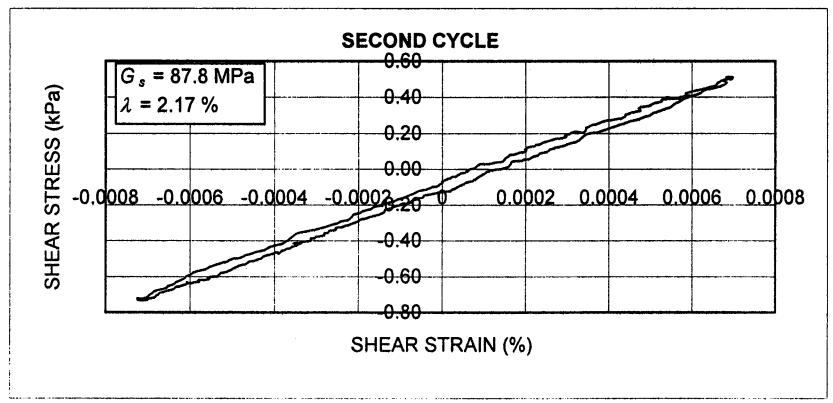

Obregon Park P-7					
DSDSS TEST - Step 3					
Type of soil: ML					
LL	37.7	PI	11.6	%Silt	55.7
e_0	0.55	S_0 (%)		%Clay	29.5
σ_v (kPa)	281	OCR	n/a	w (%)	
γ_c (%)	~0.0011	H_0 (mm)	19.29	Spec. Gr.	2.67

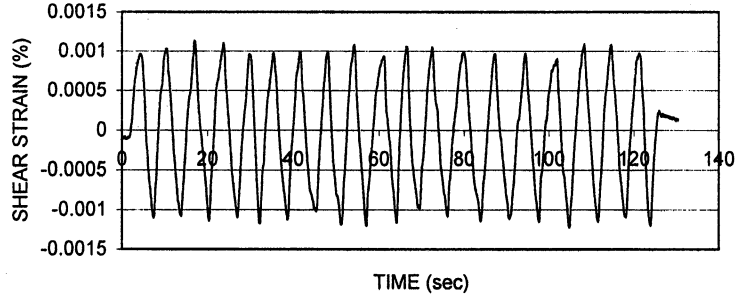

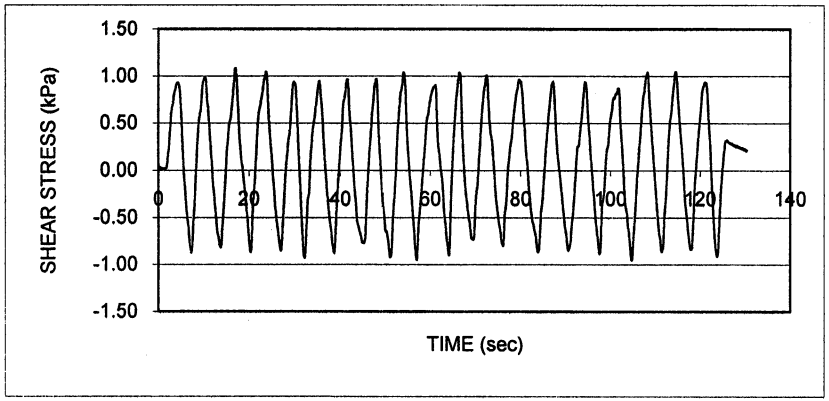

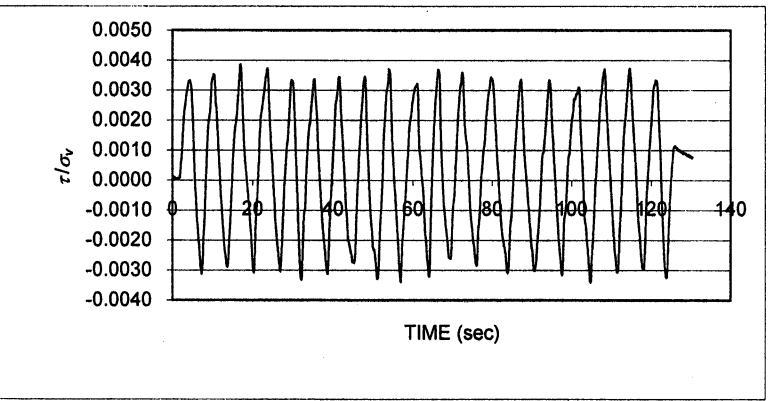

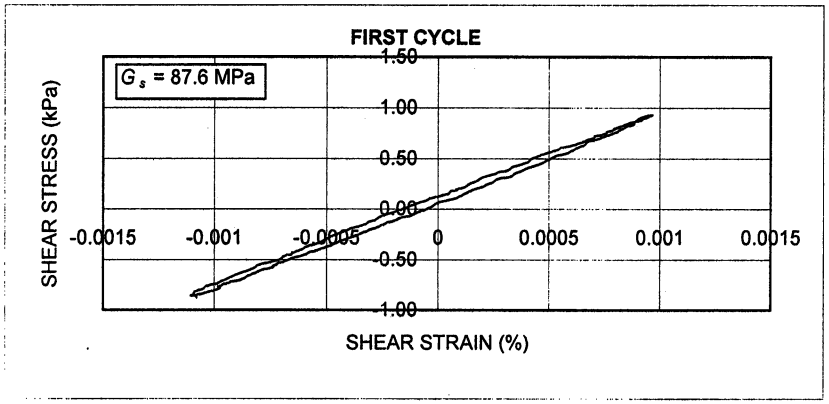

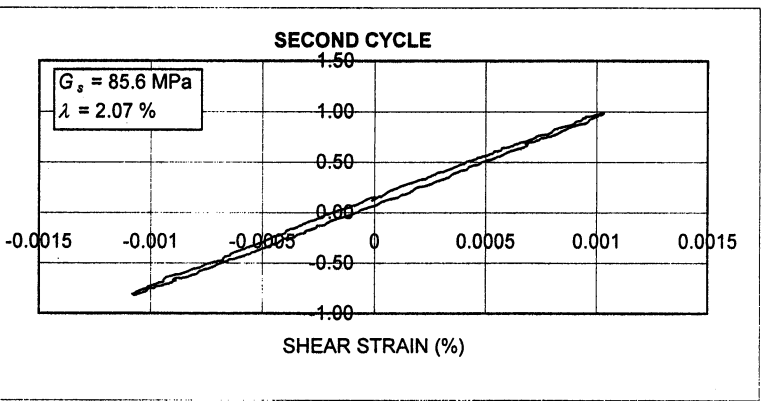

Obregon Park P-7					
DSDSS TEST - Step 4					
Type of soil: ML					
LL	37.7	PI	11.6	%Silt	55.7
e_0	0.55	S_0 (%)		%Clay	29.5
σ_v (kPa)	281	OCR	n/a	w (%)	
γ_c (%)	~0.0031	H_0 (mm)	19.29	Spec. Gr.	2.67

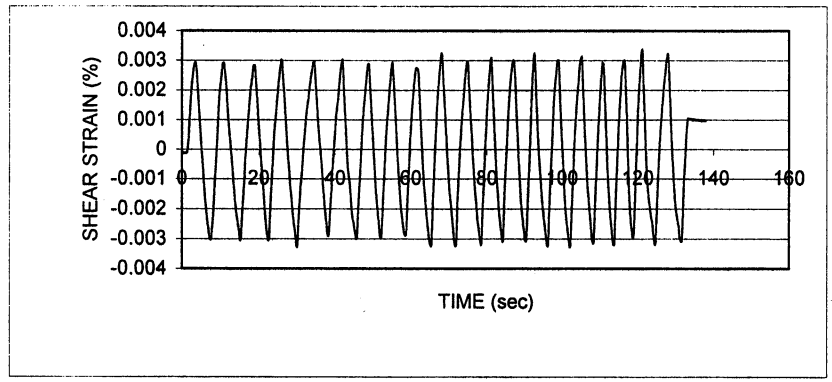

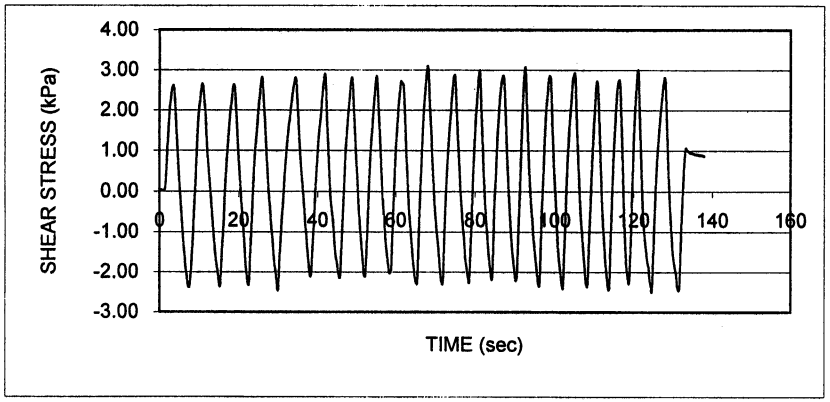

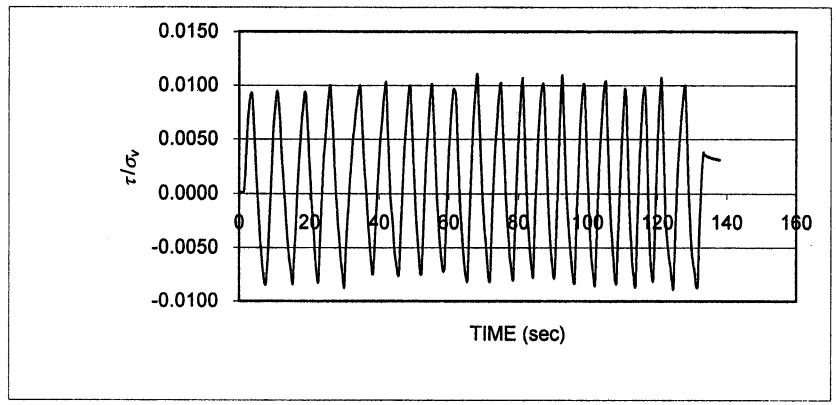

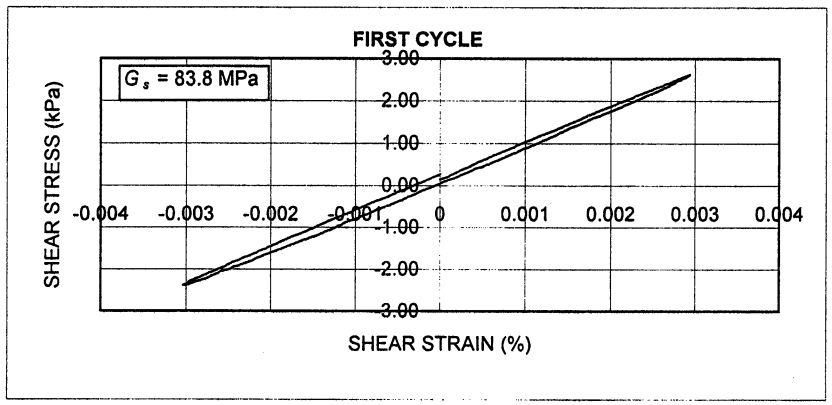

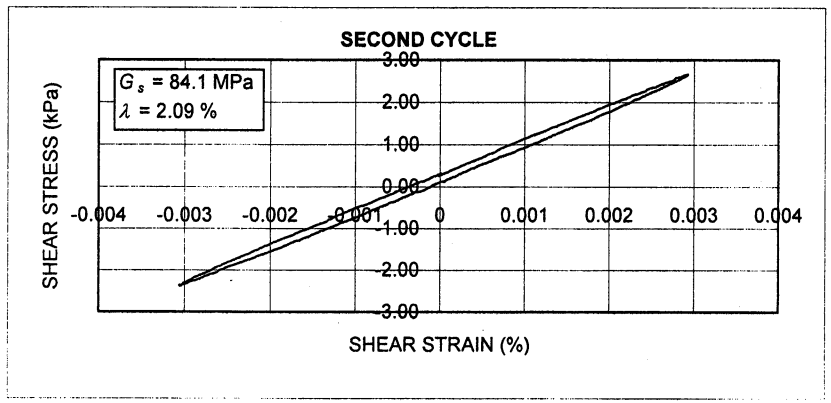

Obregon Park P-7					
DSDSS TEST - Step 5					
Type of soil: ML					
LL	37.7	PI	11.6	%Silt	55.7
e_0	0.55	S_0 (%)		%Clay	29.5
σ_v (kPa)	281	OCR	n/a	w (%)	
γ_c (%)	~0.011	H_0 (mm)	19.29	Spec. Gr.	2.67

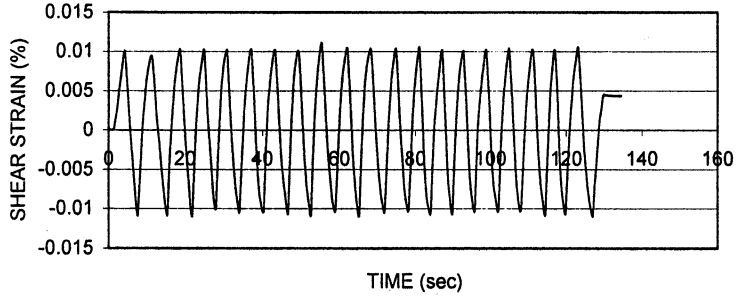

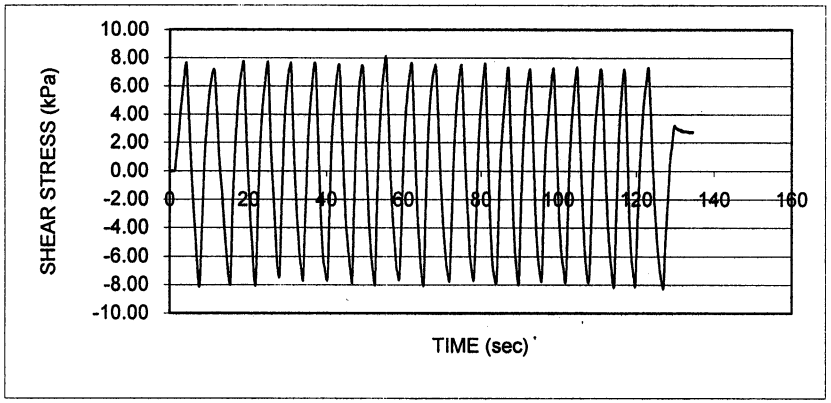

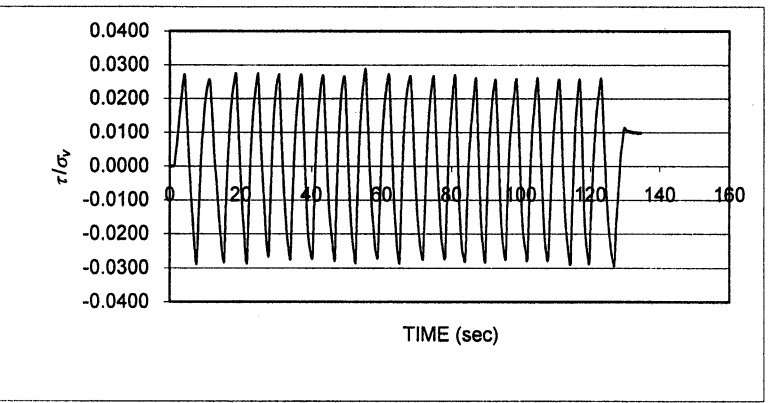

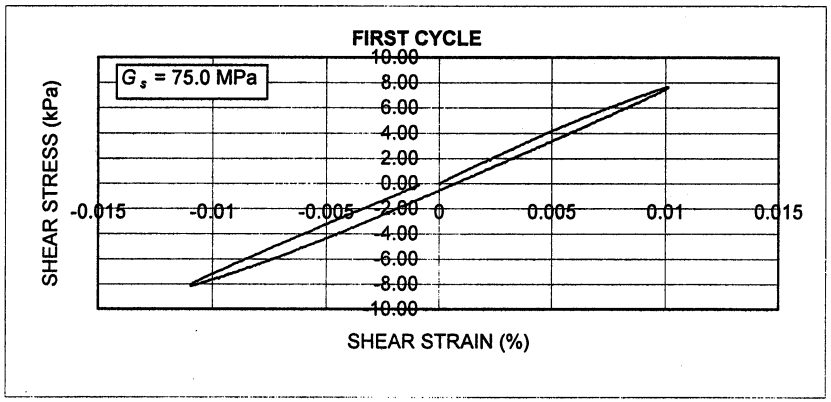

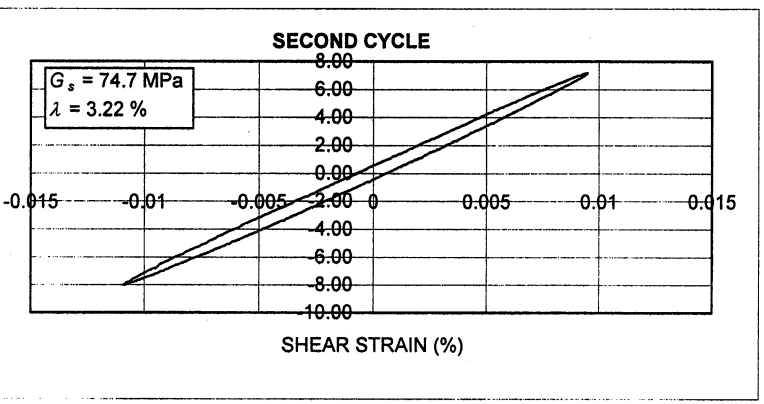

Obregon Park P-7					
DSDSS TEST - Step 6					
Type of soil: ML					
LL	37.7	PI	11.6	%Silt	55.7
e_0	0.55	S_0 (%)		%Clay	29.5
σ_v (kPa)	281	OCR	n/a	w (%)	
γ_c (%)	~0.031	H_0 (mm)	19.29	Spec. Gr.	2.67

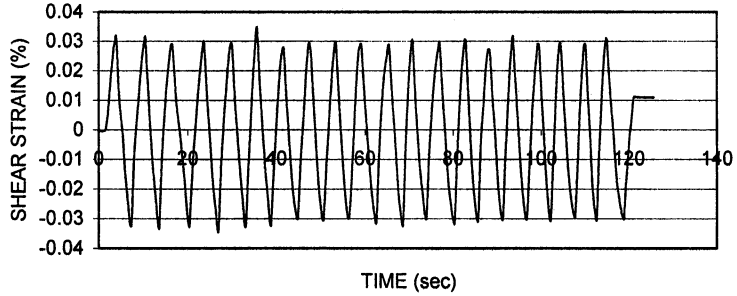

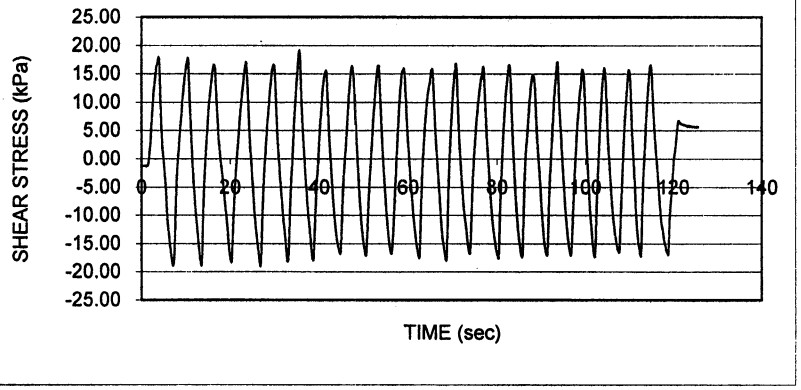

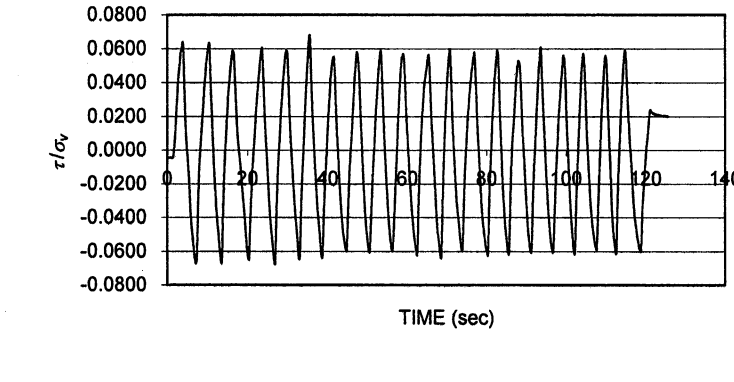

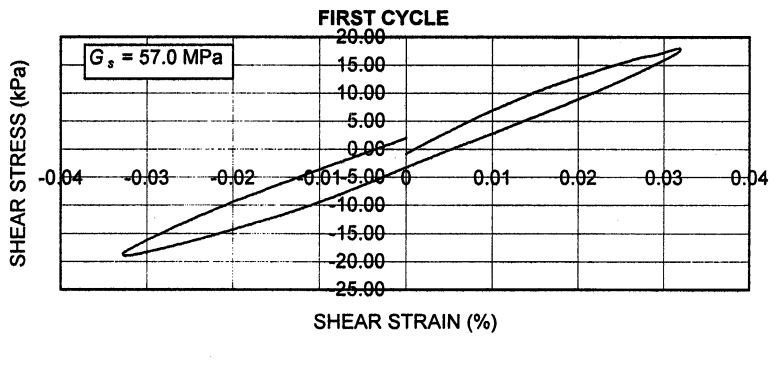

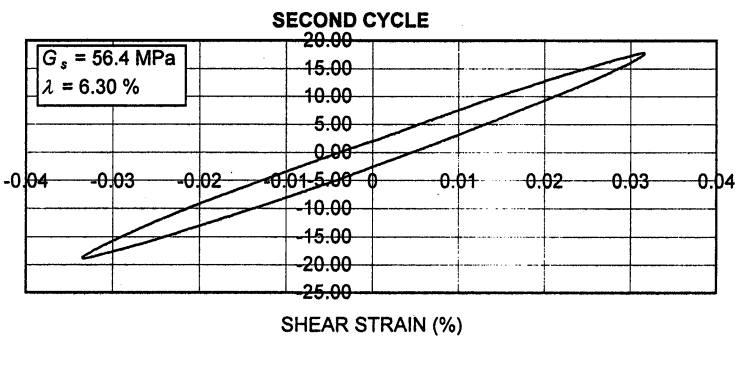

Obregon Park P-7					
DSDSS TEST - Step 7					
Type of soil: ML					
LL	37.7	PI	11.6	%Silt	55.7
e_0	0.55	S_0 (%)		%Clay	29.5
σ_v (kPa)	281	OCR	n/a	w (%)	
γ_c (%)	~0.11	H_0 (mm)	19.29	Spec. Gr.	2.67

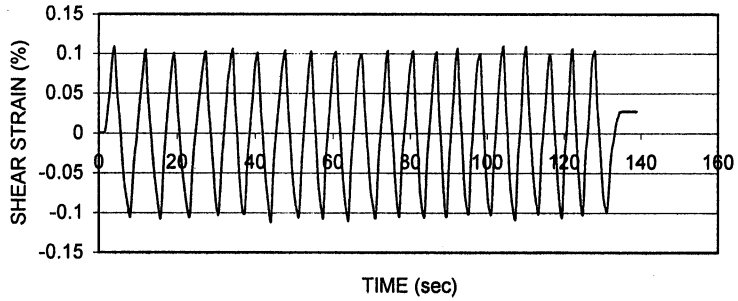

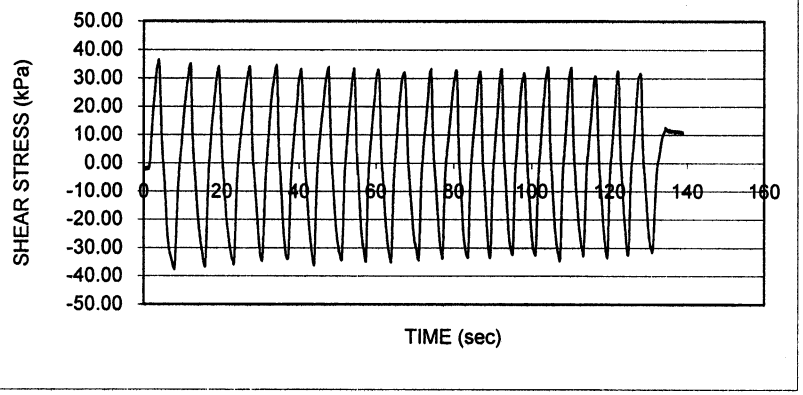

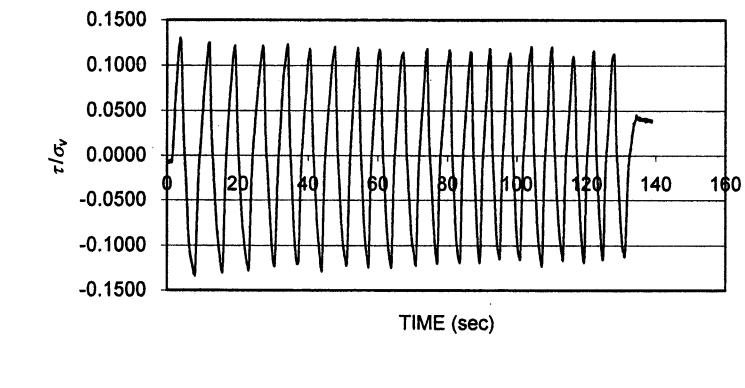

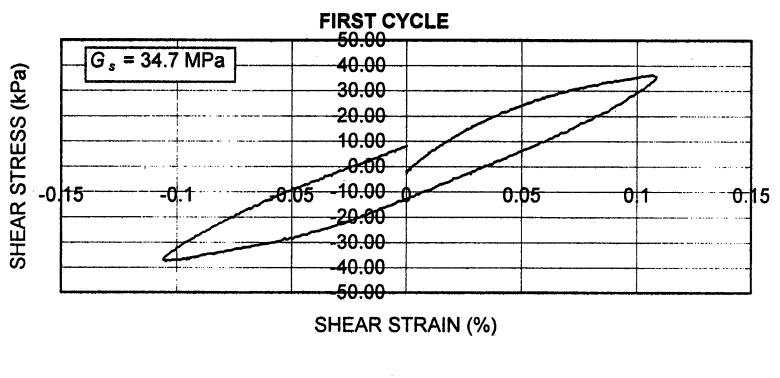

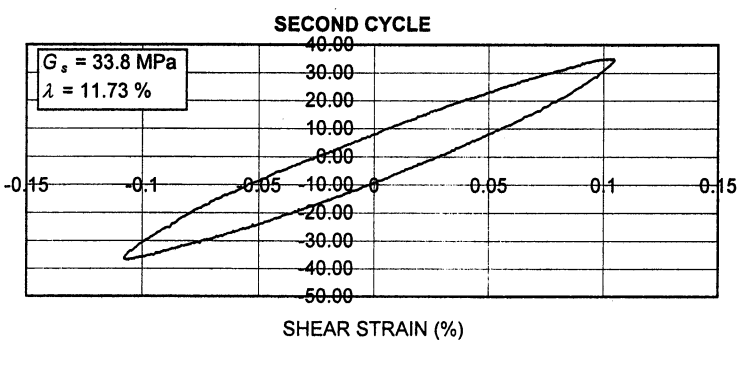

Obregon Park P-7					
DSDSS TEST - Step 8					
Type of soil: ML					
LL	37.7	PI	11.6	%Silt	55.7
e_0	0.55	S_0 (%)		%Clay	29.5
σ_v (kPa)	281	OCR	n/a	w (%)	
γ_c (%)	~3	H_0 (mm)	19.29	Spec. Gr.	2.67

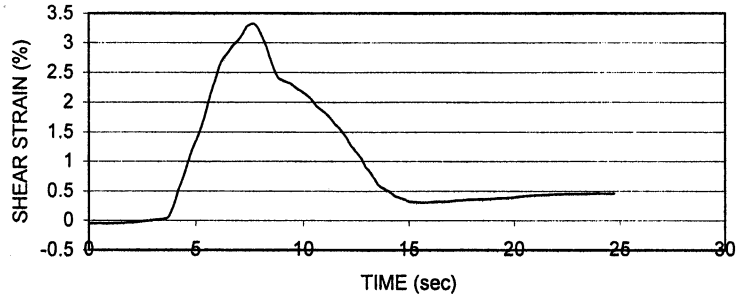

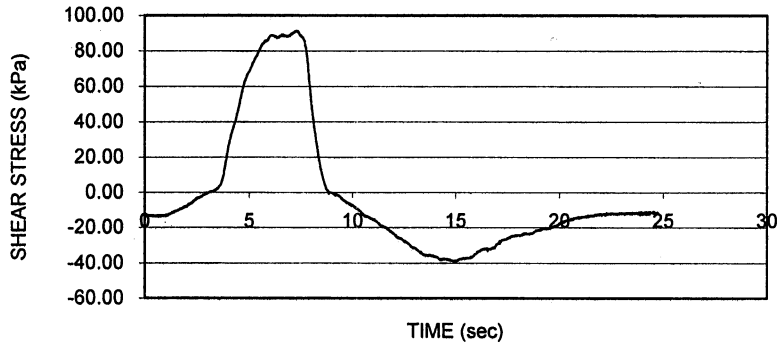

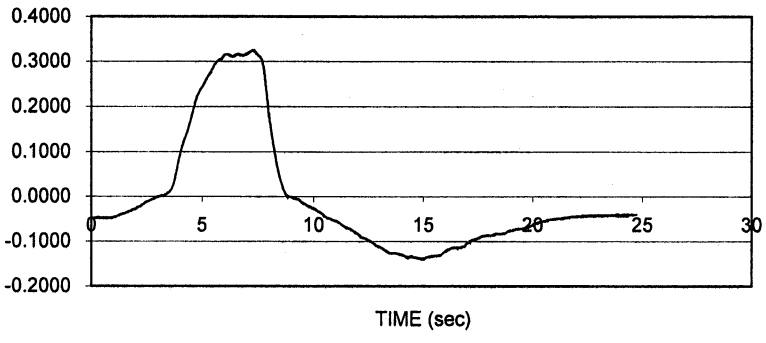

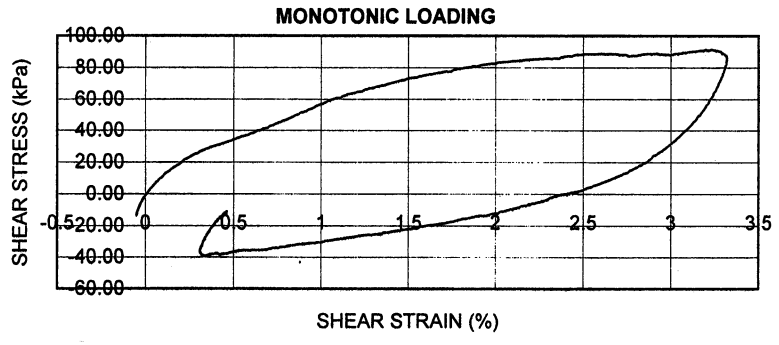

UCLA Soil Dynamics Laboratory

Double Specimen Direct Simple Shear (DSDSS) Test

Principal investigator: Mladen Vucetic, Professor

Test performed by Kentaro Tabata

Test no: 6

Project:	PEARL			Date:	3/8/2002
Sample name:	Obregon Park (P-7)			Depth (ft):	70.0
Symbol:	ML	LL (%):	37.7	Silt content (%):	55.7
Specific gravity:	2.67	PI:	11.6	Clay content (%):	29.5
Comments:					

Estimated G_{max} (MPa):	90.0

SHEAR MODULUS				DAMPING RATIO	
Step	γ_c (%)	G_s (MPa)	G_s/G_{max}	γ_c (%)	λ (%)
2x	0.000376	88.94	0.988		
2x	0.000395	87.83	0.976	0.000711	2.17
26x	0.000693	86.69	0.963	0.001058	2.07
26x	0.000711	87.80	0.976	0.002994	2.09
3x	0.001036	87.57	0.973	0.010201	3.22
3x	0.001058	85.64	0.952	0.032582	6.30
4x	0.002990	83.81	0.931	0.106408	11.73
4x	0.002994	84.10	0.934		
5x	0.010540	75.04	0.834		
5x	0.010201	74.68	0.830		
6x	0.032362	57.05	0.634		
6x	0.032582	56.45	0.627		
7x	0.107233	34.65	0.385		
7x	0.106408	33.82	0.376		
	γ (%)				
(Monotonic loading)	1.000846	5.68	0.063		
	1.504920	4.86	0.054		
	2.010849	4.14	0.046		
	2.507620	3.53	0.039		
	3.000682	2.93	0.033		
	3.310469	2.65	0.029		

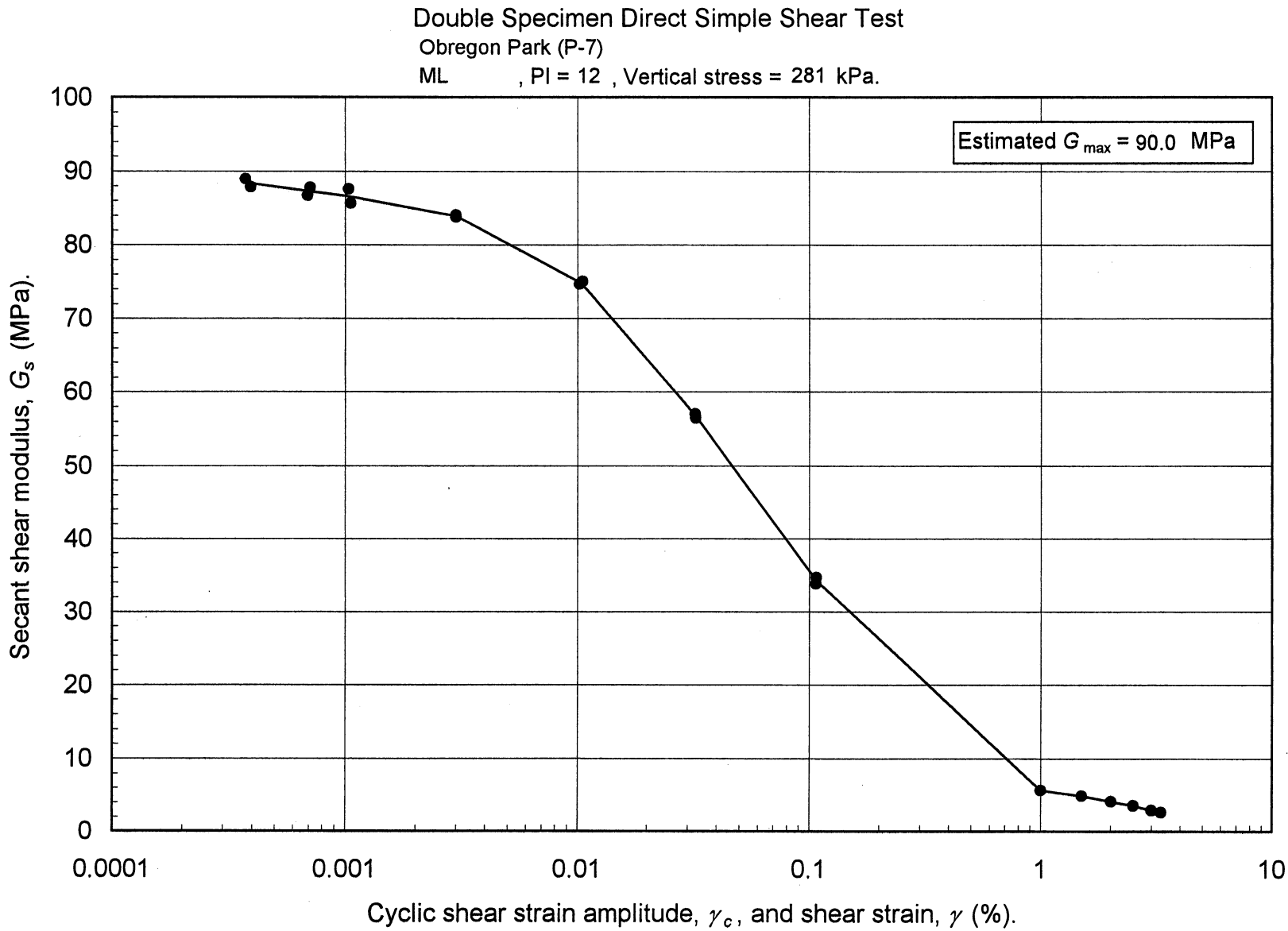
Double Specimen Direct Simple Shear Test
Obregon Park (P-7)
ML , PI = 12 , Vertical stress = 281 kPa.
Estimated G_{max} = 90.0 MPa
Secant shear modulus, G_s (MPa).
100
90
80
70
60
50
40
30
20
10
0
0.0001
0.001
0.01
0.1
1
10
Cyclic shear strain amplitude, γ_c, and shear strain, γ (%).

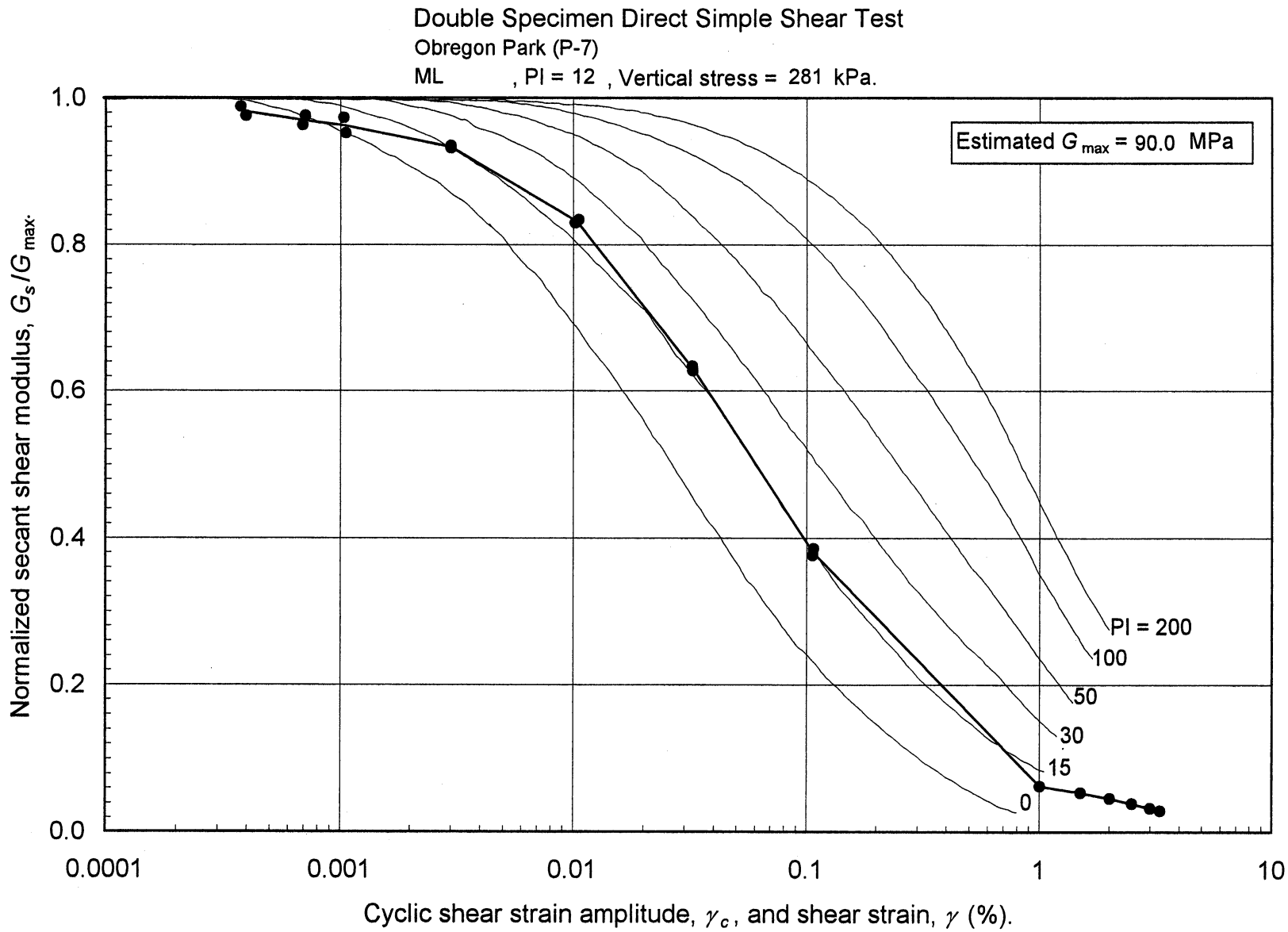
Double Specimen Direct Simple Shear Test
Obregon Park (P-7)
ML , PI = 12 , Vertical stress = 281 kPa.
Estimated G_{max} = 90.0 MPa
PI = 200
100
50
30
15
0
Normalized secant shear modulus, G_s/G_{max}.
1.0
0.8
0.6
0.4
0.2
0.0
0.0001
0.001
0.01
0.1
1
10
Cyclic shear strain amplitude, γ_c, and shear strain, γ (%).

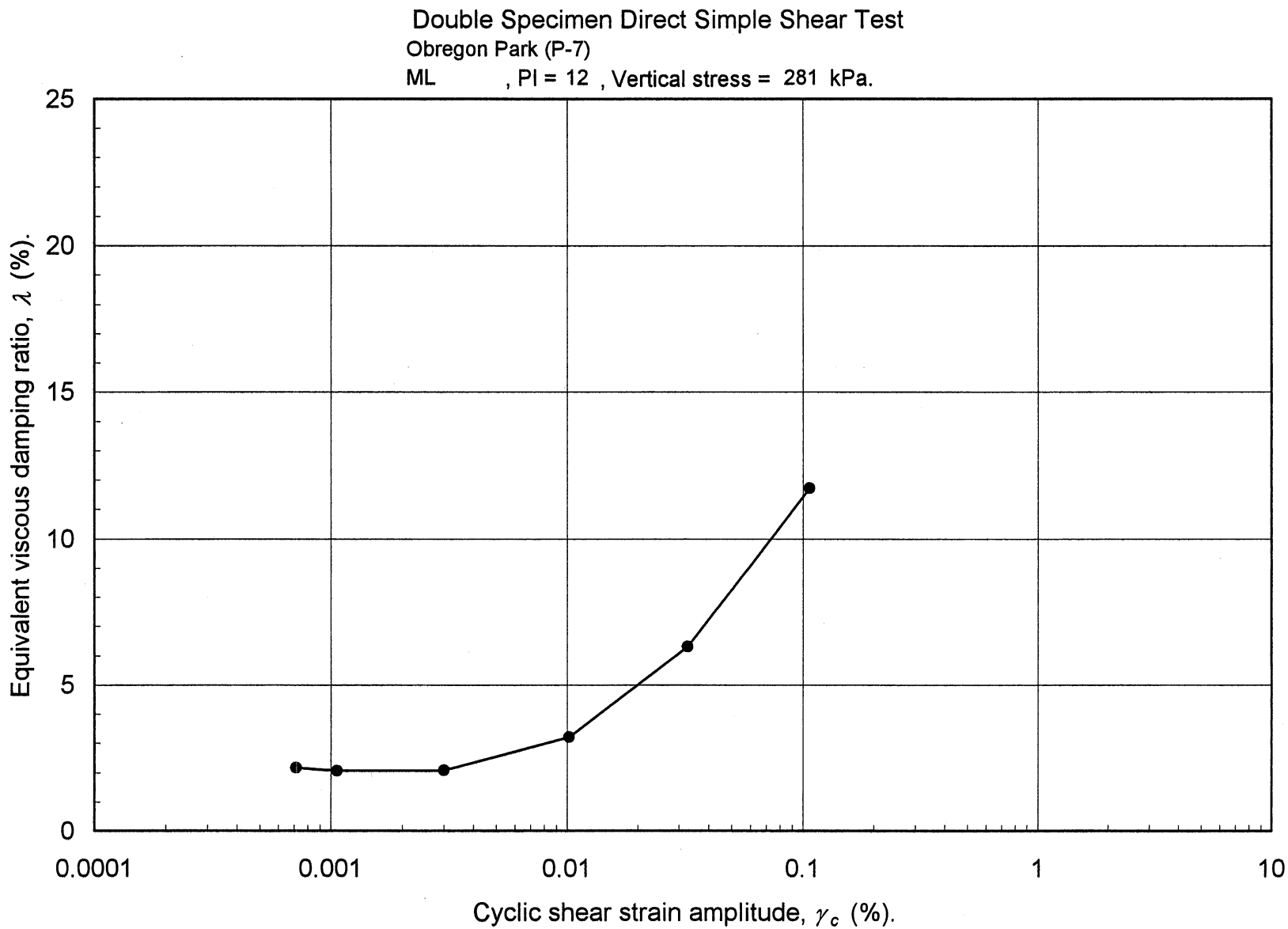
Double Specimen Direct Simple Shear Test
Obregon Park (P-7)
ML , PI = 12 , Vertical stress = 281 kPa.
Equivalent viscous damping ratio, λ (%).
25
20
15
10
5
0
0.0001
0.001
0.01
0.1
1
10
Cyclic shear strain amplitude, γc (%).

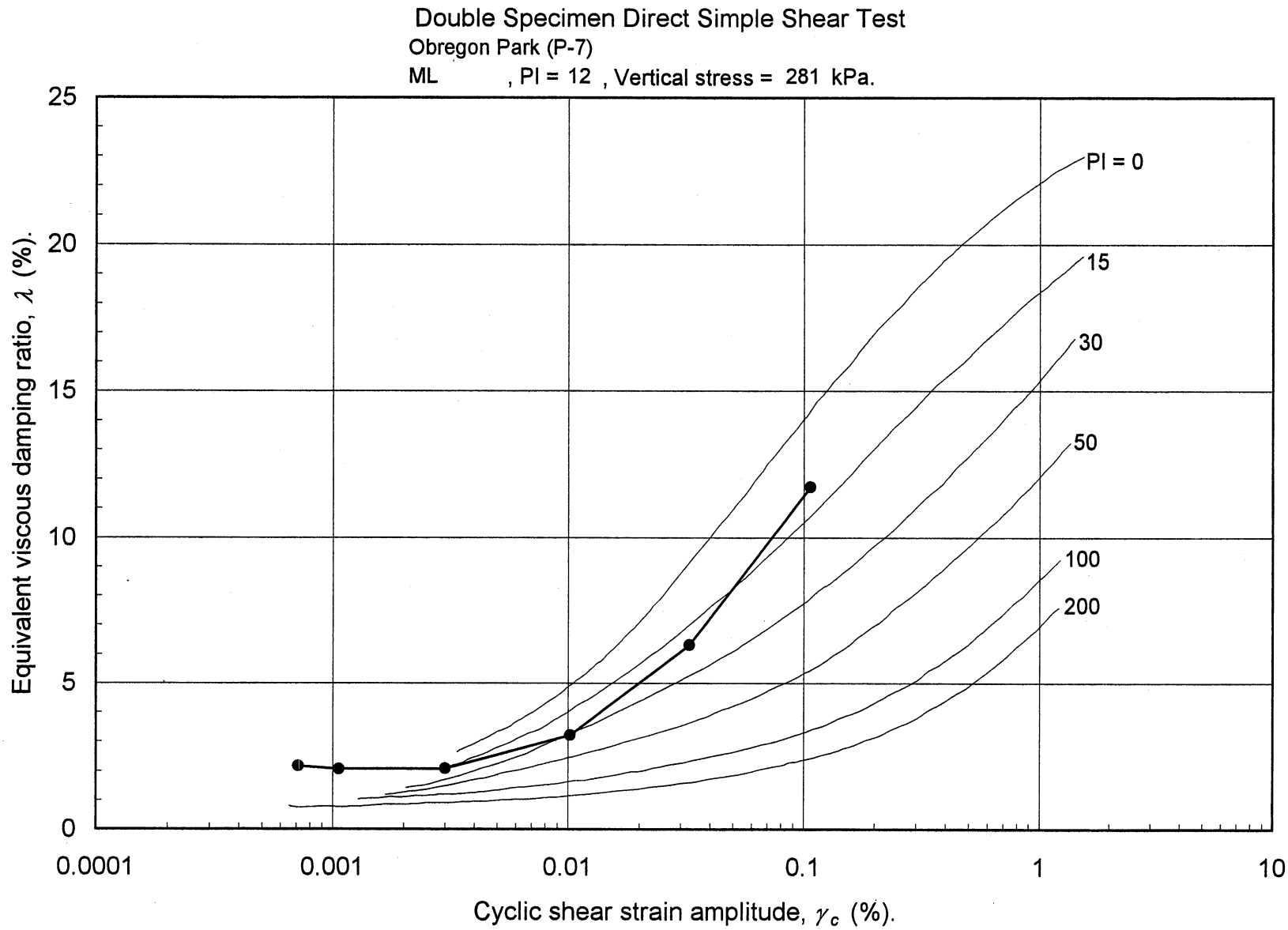
Double Specimen Direct Simple Shear Test
Obregon Park (P-7)
ML , PI = 12 , Vertical stress = 281 kPa.
Equivalent viscous damping ratio, λ (%).
Cyclic shear strain amplitude, γc (%).
0
5
10
15
20
25
0.0001
0.001
0.01
0.1
1
10
PI = 0
15
30
50
100
200

UCLA Soil Dynamics Laboratory

Specific Gravity Test

Principal investigator: Mladen Vucetic, Professor

Test performed by: Kentaro Tabata Test No.: 6

Project:	PEARL			Date:	3/20/2002
Boring:	Obregon Park				
Tube No.:	P-7	Depth (ft):	70.0 -73.0	GWT (ft):	20.0
Comments:	Silt.				

SPECIFIC GRAVITY TEST

Test No.	1		
Bottle No.	3		
Wt. of bottle (g)	178.27		
Volume of bottle (cm^3)	500		
Wt. of bottle+water+soil (g)	688.27		
Temperature (°C)	24.0		
Wt. of bottle+water (g)	676.00		
Evaporating dish No.	B-2		
Weight of dish (g)	537.22		
Wt. of dish+dry soil (g)	556.80		
Wt. of dry soil (g)	19.58		
Specific gravity of water	0.9973		
Specific gravity of soil	**2.67**		

UCLA Soil Dynamics Laboratory

Grain Size Distribution

Principal investigator: Mladen Vucetic, Professor

Test performed by: Kentaro Tabata Test No.: 6

Project:	PEARL				
Boring:	Obregon Park				
Tube No.:	P-7	Depth (ft):	70.0 -73.0	GWT (ft):	20.0
Comments:	Silt.				

GRAIN SIZE DISTRIBUTION

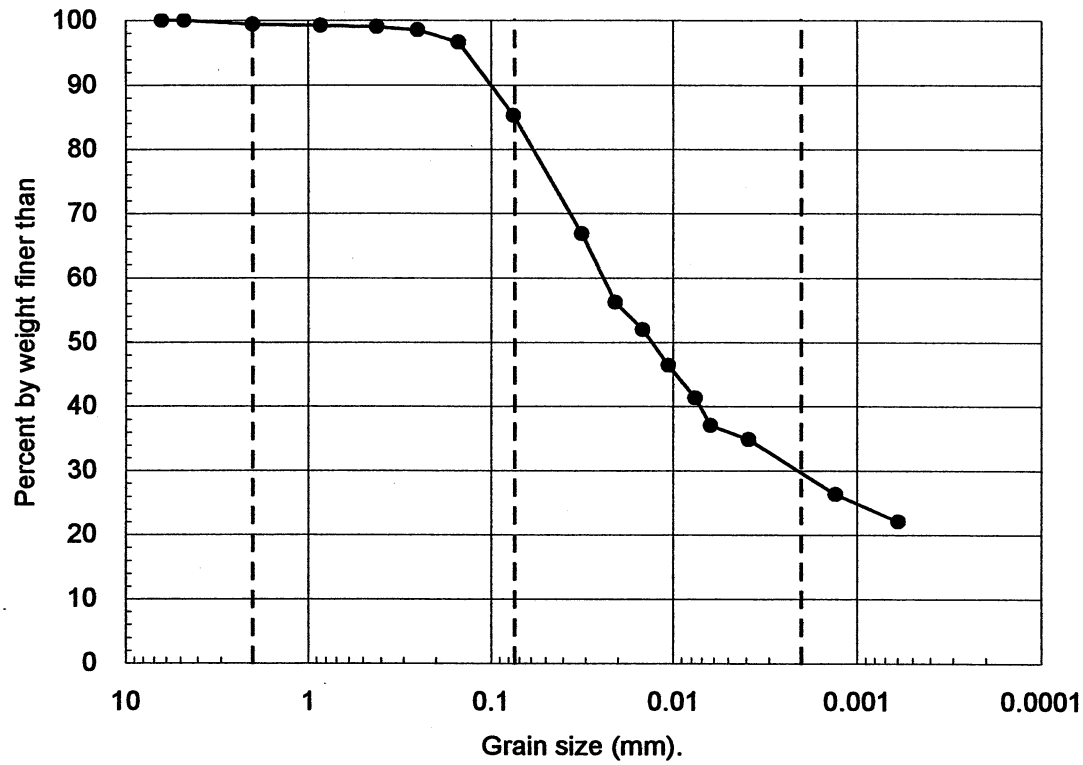

Clay (%)	Silt (%)	Sand (%)	Gravel (%)
29.5	55.7	14.1	0.6

UCLA Soil Dynamics Laboratory

Hydrometer Analysis

Principal investigator: Mladen Vucetic, Professor

Test performed by: Kentaro Tabata Test No.: 6

Project:	PEARL			Date:	3/20/2002
Boring:	Obregon Park				
Tube No.:	P-7	Depth (ft):	70.0 -73.0	GWT (ft):	20.0
Comments:	Silt.				

HYDROMETER TEST

Time	Elapsed time t (sec)	Temp. T (°C)	Reading R'_T	Corr. reading $R_T=R'_T+c_m$	Depth H (cm)	Grain diameter D (mm)	Temp. corr. m_T	Corr. depth $R_T+m_T-c_d$	% by wt. finer than W_D (%)
17:01:24	0								
17:03:24	120	23.0	1017.5	1018.0	11.71	0.0317	0.700	1015.7	66.81
17:06:24	300	23.0	1015.0	1015.5	12.37	0.0206	0.700	1013.2	56.17
17:11:24	600	23.0	1014.0	1014.5	12.64	0.0147	0.700	1012.2	51.92
17:21:24	1200	23.0	1012.7	1013.2	12.99	0.0106	0.700	1010.9	46.39
17:41:24	2400	23.0	1011.5	1012.0	13.31	0.0076	0.700	1009.7	41.28
18:01:24	3600	23.0	1010.5	1011.0	13.58	0.0062	0.700	1008.7	37.02
19:39:00	9456	23.0	1010.0	1010.5	13.71	0.0039	0.700	1008.2	34.90
17:00:00	86316	23.0	1008.0	1008.5	14.25	0.0013	0.700	1006.2	26.38
14:00:00	421116	23.0	1007.0	1007.5	14.51	0.0006	0.700	1005.2	22.13

APPARATUS

Hydrometer no.:	88-18587	a_0	284.03	a_1	-0.2675
Graduate no.:	3				

FACTORS

Meniscus corr., c_m:	0.5	
Disp. agent corr, c_d:	3.0	
Visc. of water, η.	23.0 °C	9.565E-06 g sec/cm^2
	°C	g sec/cm^3

WEIGHT

Dry soil (g)	32.01
Percent by wt (%)	85.25
Dry soil for sieve (g)	5.54
Total (g)	37.55

UNIT WEIGHT

Specific gravity:		2.67
T	γ_w	γ_s
(°C)	(g/cm^3)	(g/cm^3)
23.0	0.9976	2.6660

UCLA Soil Dynamics Laboratory

Sieve Analysis

Principal investigator: Mladen Vucetic, Professor

Test performed by: Kentaro Tabata Test No.: 6

Project:	PEARL			Date:	3/26/2002
Boring:	Obregon Park				
Tube No.:	P-7	Depth (ft):	70.0 -73.0	GWT (ft):	20.0
Comments:	Silt.				

SIEVE ANALYSIS

Sieve No.	Diameter (mm)	Sieve (g)	S+wet (g)	S+dry (g)	Retained (g)	Retained (%)	Cumulated (g)	Cumulated (%)	Passing (%)
3	6.350	485.05		485.05	0.00	0.00	0.00	0.00	100.00
4	4.750	463.08		463.08	0.00	0.00	0.00	0.00	100.00
10	2.000	422.40		422.64	0.24	0.64	0.24	0.64	99.36
20	0.850	375.43		375.50	0.07	0.19	0.31	0.83	99.17
40	0.420	375.66		375.72	0.06	0.16	0.37	0.99	99.01
60	0.250	323.90		324.07	0.17	0.45	0.54	1.44	98.56
100	0.150	342.17		342.90	0.73	1.94	1.27	3.38	96.62
200	0.075	676.84		681.11	4.27	11.37	5.54	14.75	85.25
Total					5.54	14.75			

WEIGHT

Dry soil for sieve (g)	5.54
Dry soil for hydr. (g)	32.01
Total (g)	37.55
Percent coaser (%)	14.75

UCLA Soil Dynamics Laboratory

Atterberg Limit Determination

Principal investigator: Mladen Vucetic, Professor

Test performed by: Kentaro Tabata Test No.: 6

Project:	PEARL			Date:	3/26/2002
Boring:	Obregon Park				
Tube No.:	P-7	Depth (ft):	70.0 -73.0	GWT (ft):	20.0
Comments:	Silt.				

LIQUID LIMIT TEST

Test No.	1	2	3	4	5			
Number of blows	31	27	23	19	14			
Container No.	ST-6	ST-20	ST-8	ST-4	ST-11			
Container (g)	30.10	30.36	30.14	30.18	30.27			
Cont+wet soil (g)	37.58	36.32	35.49	37.49	39.35			
Cont+dry soil (g)	35.59	34.71	33.99	35.45	36.67			
Water (g)	1.99	1.61	1.50	2.04	2.68			
Dry soil (g)	5.49	4.35	3.85	5.27	6.40			
Water content (%)	36.25	37.01	38.96	38.71	41.88			

PLASTIC LIMIT TEST

Test No.	1	2	3
Container No.	ST-5	ST-3	ST-7
Container (g)	30.13	30.18	30.35
Cont+wet soil (g)	33.27	33.46	32.91
Cont+dry soil (g)	32.61	32.78	32.39
Water (g)	0.66	0.68	0.52
Dry soil (g)	2.48	2.60	2.04
Water content (%)	26.61	26.15	25.49

ATTERBERG LIMITS

Liquid limit (%)	**37.7**
Plastic limit (%)	**26.1**
Plasticity index	**11.6**

CLASSIFICATION

ML

FLOW CHART

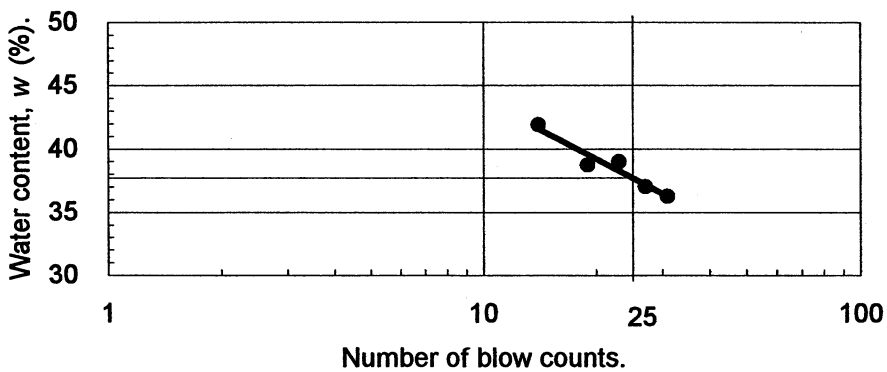

UCLA Soil Dynamics Laboratory

Atterberg Limit Determination

Principal investigator: Mladen Vucetic, Professor

Test performed by: Kentaro Tabata Test No.: 6

Project:	PEARL			Date:	3/26/2002
Boring:	Obregon Park				
Tube No.:	P-7	Depth (ft):	70.0 -73.0	GWT (ft):	20.0
Comments:	Silt.				

PLASTICITY CHART

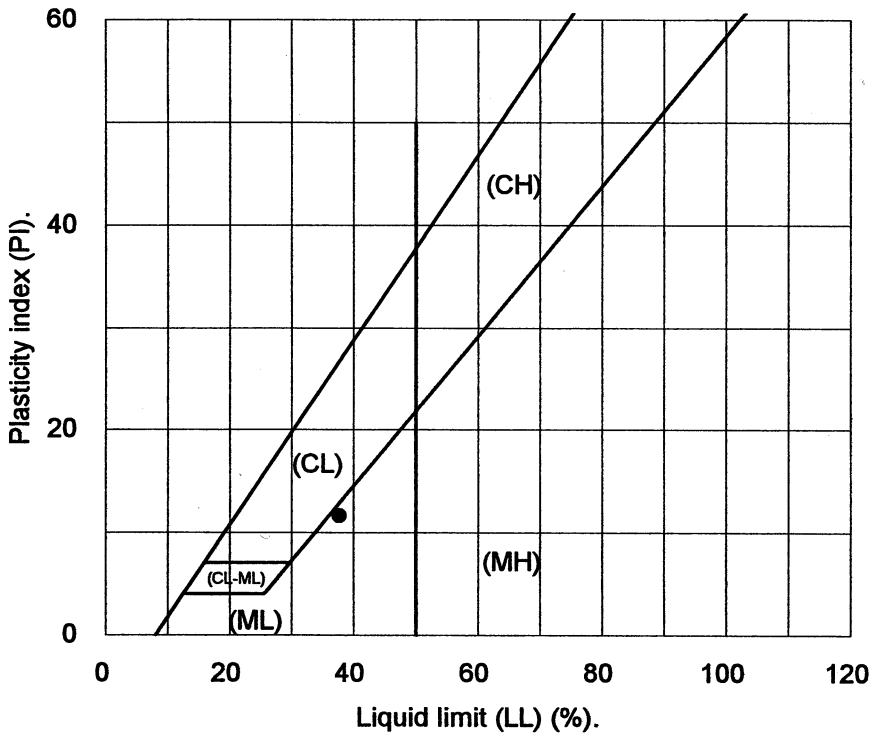

3.8 Test 7: OBREGON PARK P-9

UCLA Soil Dynamics Laboratory

Double Specimen Direct Simple Shear (DSDSS) Test

Principal investigator: Mladen Vucetic, Professor

Test performed by: Kentaro Tabata Test No.: 7

Project:	PEARL			Date:	4/3/2002
Boring:	Obregon Park				
Tube No.:	P-9	Depth (ft):	90.0 -93.0	GWT (ft):	20.0 (reported by others)
Comments:	Clay. Specimen obtained from the bottom of the tube (specimen depth ~ 92.5 ft).				

FORM 1: SPECIMEN PREPARATION

WATER CONTENT, SPECIFIC GRAVITY				UNIT WEIGHT, VOID RATIO, SATURATION			
	Before consol.	After shearing			Before consol.	Before shearing	After shearing
Container No.	ST-5	MT-23	MT-17	Average weight (g)	141.52	141.52	
Cont+wet soil (g)	39.27	192.18	189.83	Height (cm)	1.960	1.919	
Cont+dry soil (g)	37.97	172.40	170.48	Area (cm^2)	34.84	34.84	
Container (g)	30.13	49.65	50.19	Volume (cm^3)	68.28	66.85	
Water (g)	1.30	19.78	19.35	Unit weight (g/cm^3)	2.073	2.117	
Dry soil (g)	7.84	122.75	120.29	Unit weight (kN/m^3)	20.31	20.75	
Water content(%)	16.58	16.11	16.09	Void ratio	0.51	0.48	
Avg. water cont. (%)	16.58		16.10	Saturation (%)	87.6	90.7	
Spceific gravity			2.68				

HEIGHT OF SPECIMEN						
	Before consol.		Before shearing	After shearing		
	Top	Bottom	Average	Average		
Height (cm)	1.960	1.960	1.919	1.919		

AREA OF SPECIMEN						
Initial diameter (cm)			6.660	Initial area (cm^2)		34.837
Load (kg)	Stress (kg/cm^2)	Stress (kN/m^2)	Diameter (cm)	Membrane (cm)	Corrected diameter (cm)	Area (cm^2)

Obregon Park P-9					
DSDSS TEST - Step 2					
Type of soil: CL					
LL	41.0	PI	21.2	%Silt	37.6
e_0	0.48	S_0 (%)	90.7	%Clay	37.0
σ_v (kPa)	361	OCR	n/a	w (%)	16.1
γ_c (%)	~0.0004	H_0 (mm)	19.19	Spec. Gr.	2.68

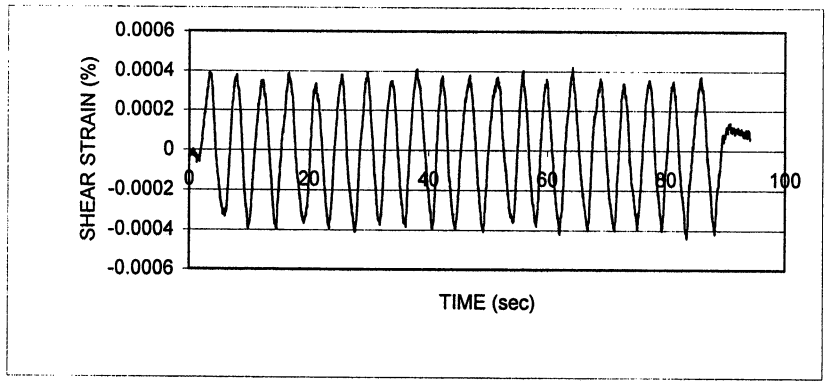

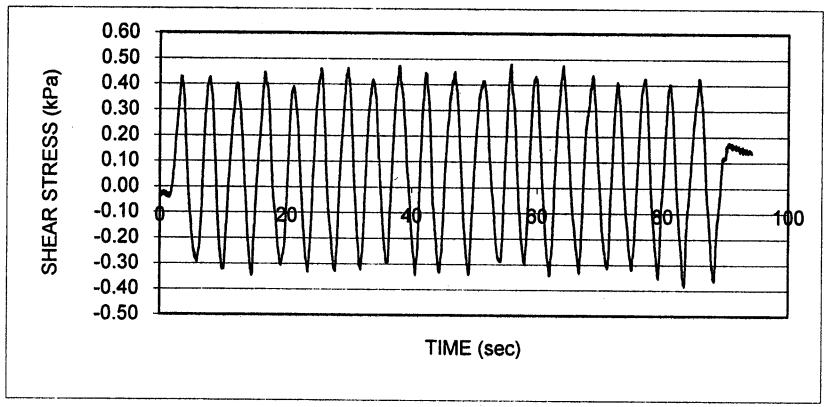

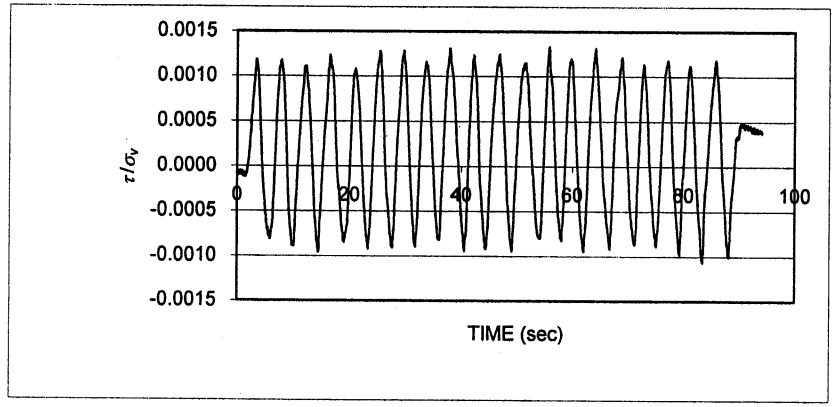

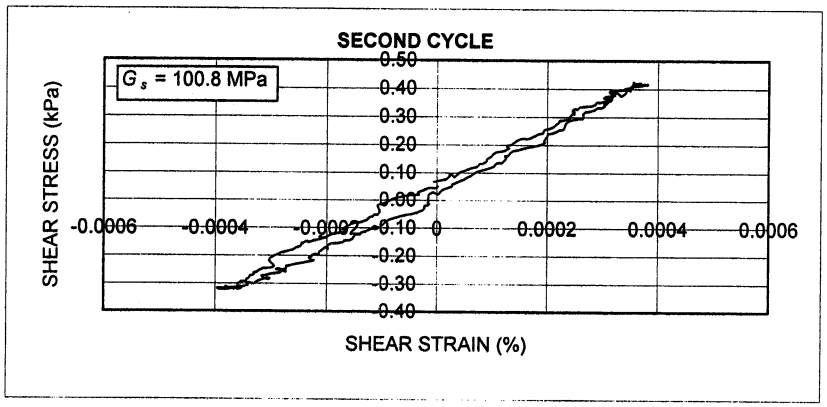

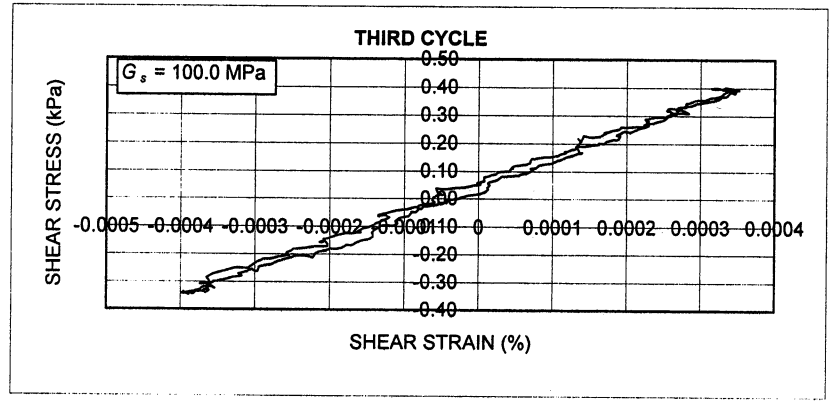

Obregon Park P-9					
DSDSS TEST - Step 26					
Type of soil: CL					
LL	41.0	PI	21.2	%Silt	37.6
e_0	0.48	S_0 (%)	90.7	%Clay	37.0
σ_v (kPa)	361	OCR	n/a	w (%)	16.1
γ_c (%)	~0.00078	H_0 (mm)	19.19	Spec. Gr.	2.68

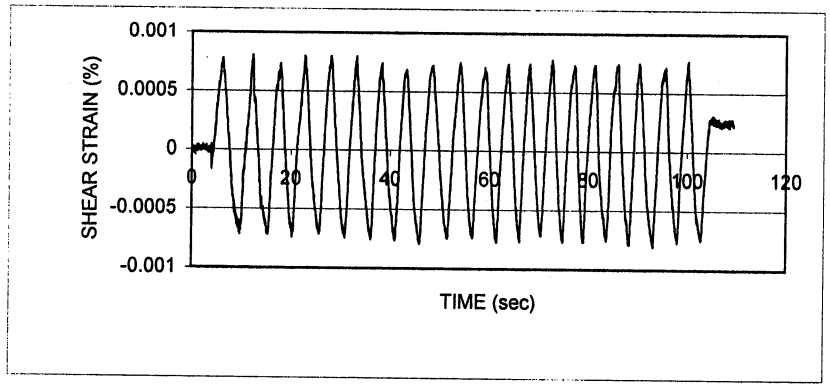

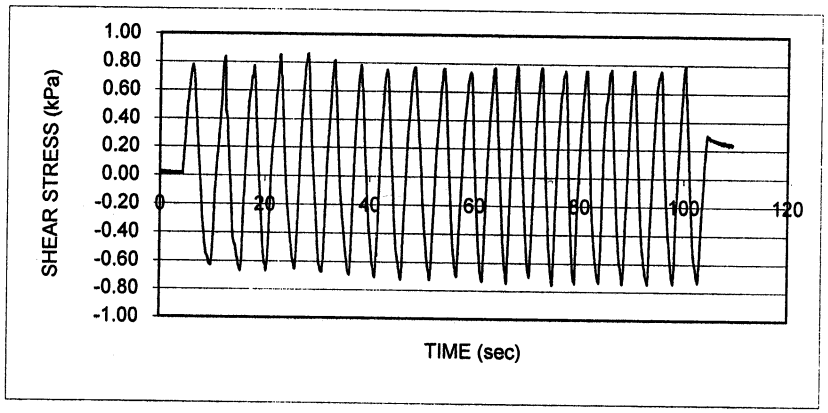

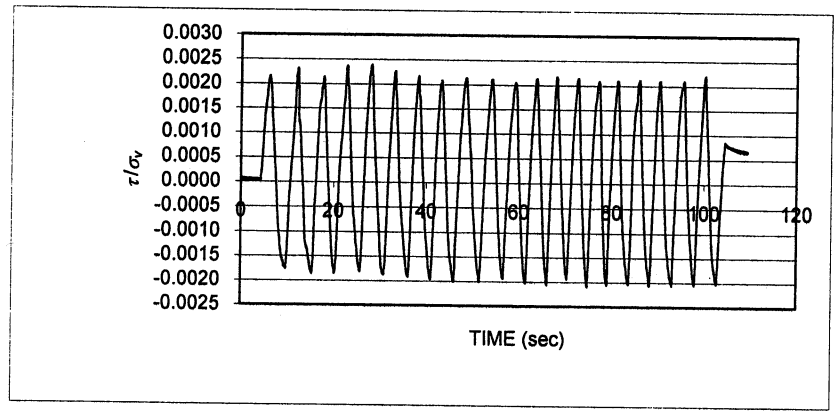

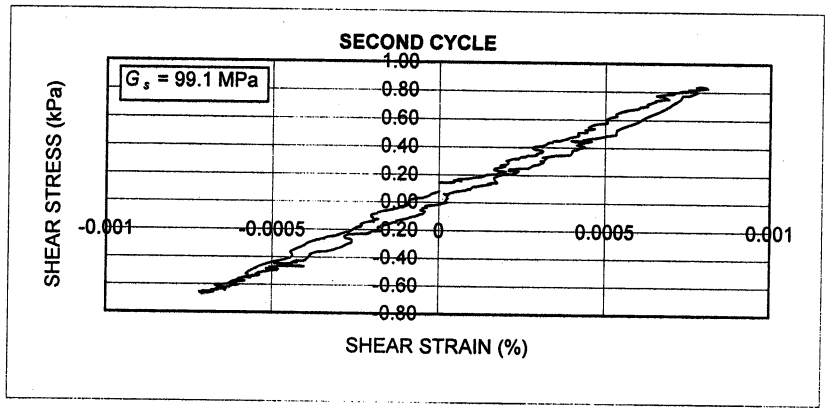

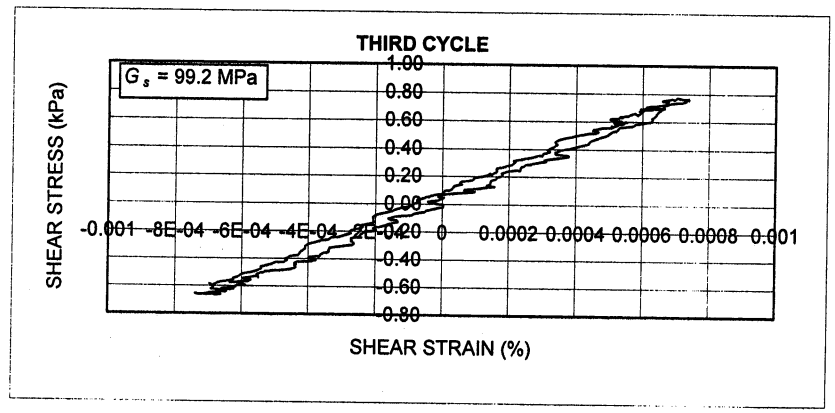

Obregon Park P-9					
DSDSS TEST - Step 3					
Type of soil: CL					
LL	41.0	PI	21.2	%Silt	37.6
e_0	0.48	S_0 (%)	90.7	%Clay	37.0
σ_v (kPa)	361	OCR	n/a	w (%)	16.1
γ_c (%)	~0.0011	H_0 (mm)	19.19	Spec. Gr.	2.68

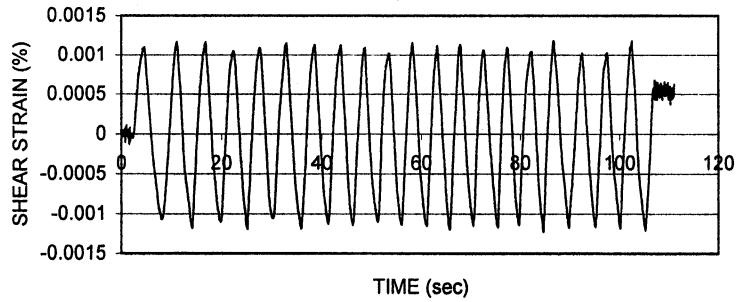

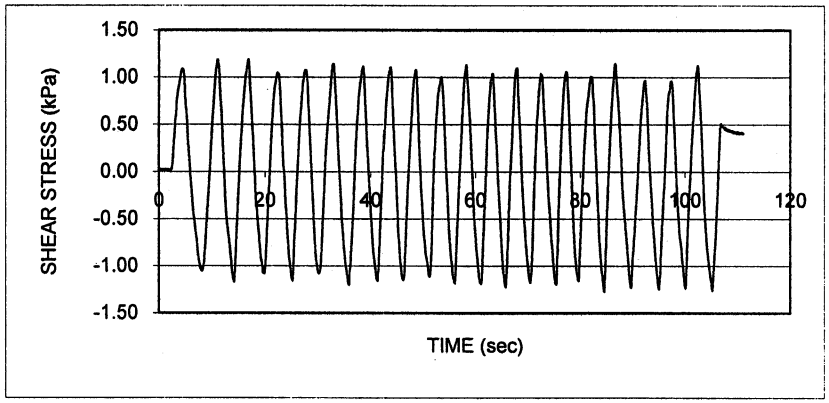

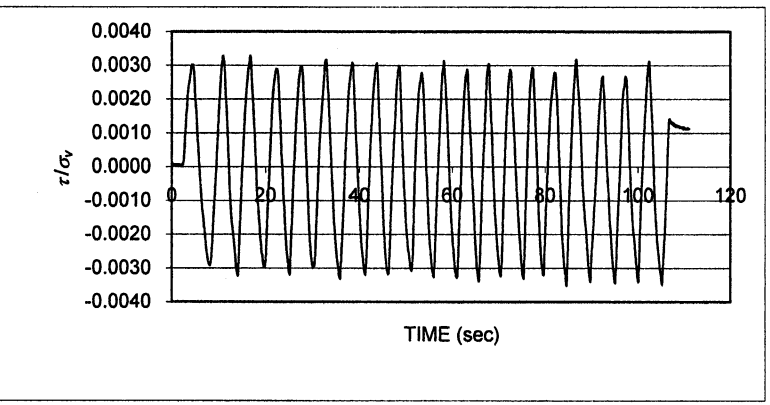

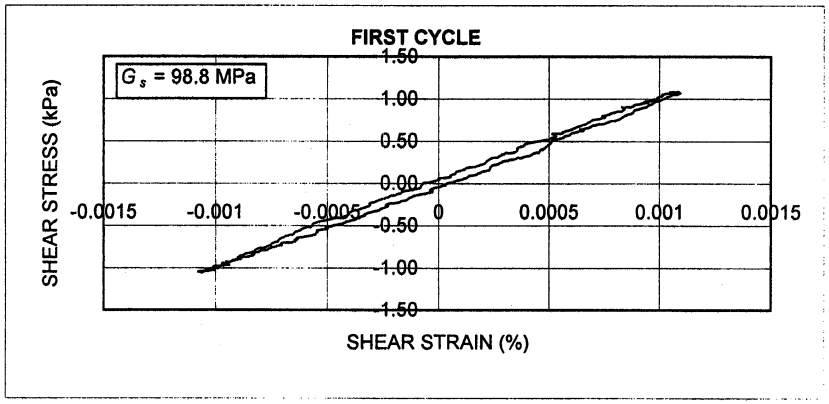

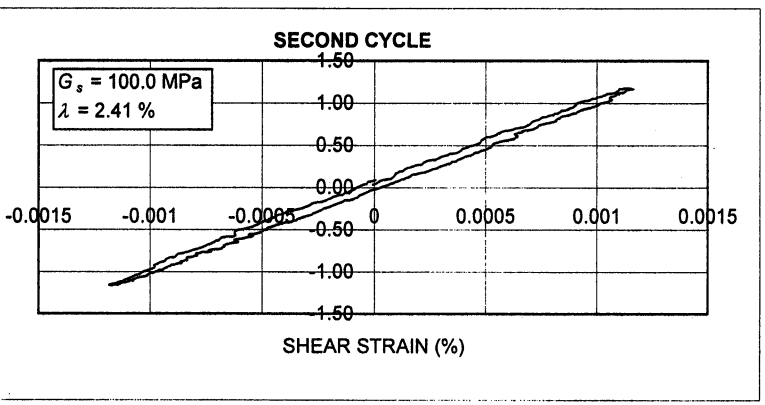

Obregon Park P-9					
DSDSS TEST - Step 4					
Type of soil: CL					
LL	41.0	PI	21.2	%Silt	37.6
e_0	0.48	S_0 (%)	90.7	%Clay	37.0
σ_v (kPa)	361	OCR	n/a	w (%)	16.1
γ_c (%)	~0.0032	H_0 (mm)	19.19	Spec. Gr.	2.68

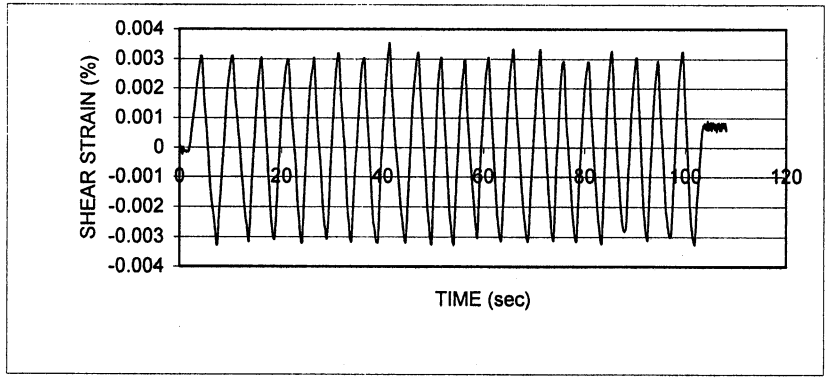

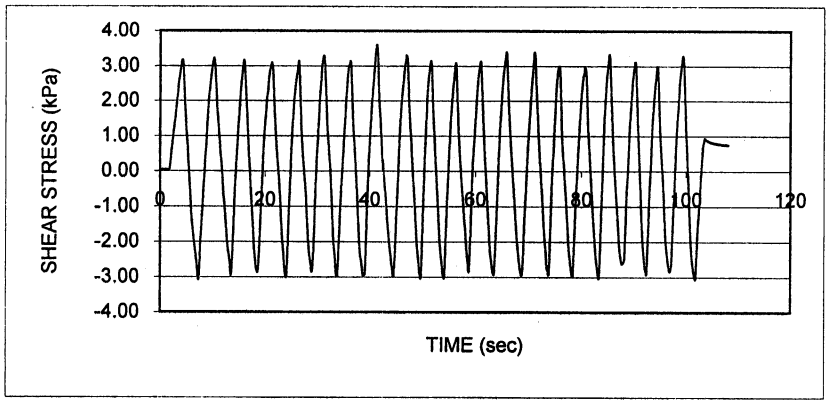

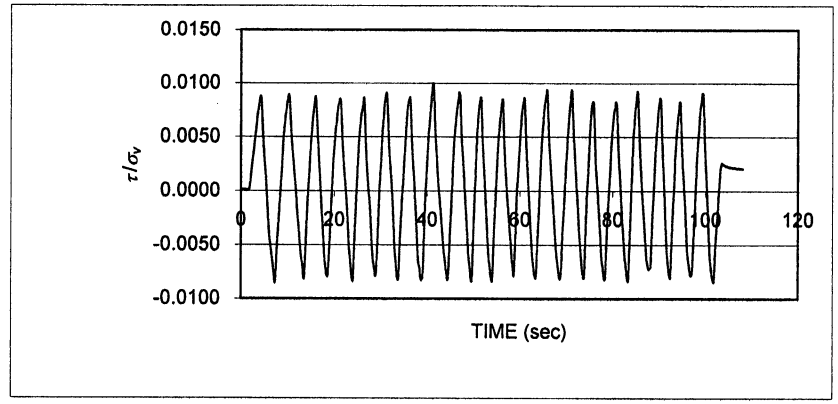

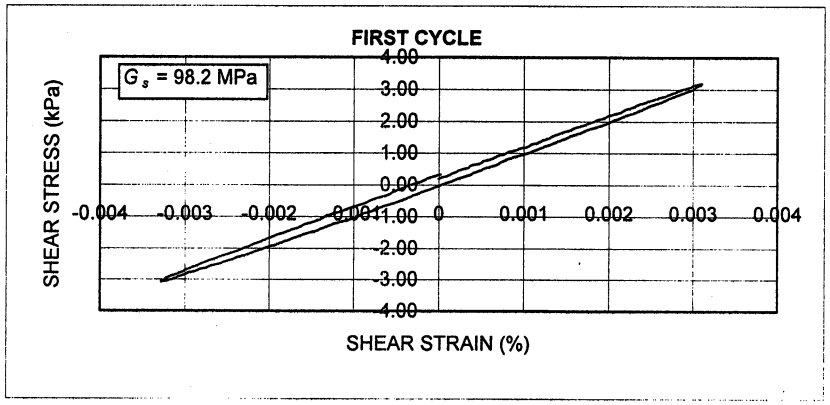

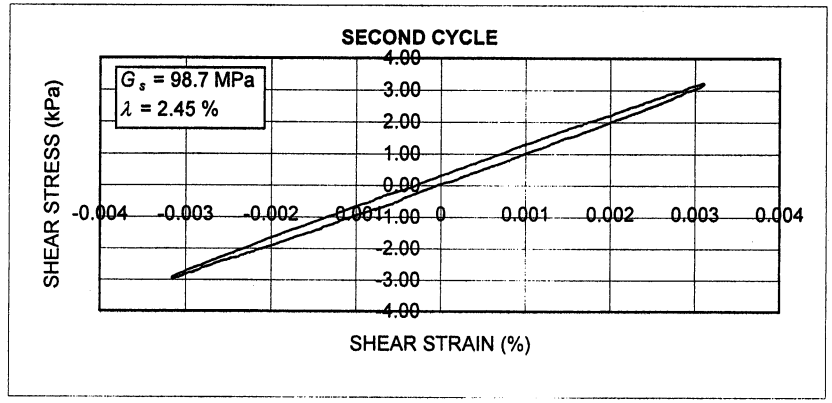

Obregon Park P-9					
DSDSS TEST - Step 5					
Type of soil: CL					
LL	41.0	PI	21.2	%Silt	37.6
e_0	0.48	S_0 (%)	90.7	%Clay	37.0
σ_v (kPa)	361	OCR	n/a	w (%)	16.1
γ_c (%)	~0.011	H_0 (mm)	19.19	Spec. Gr.	2.68

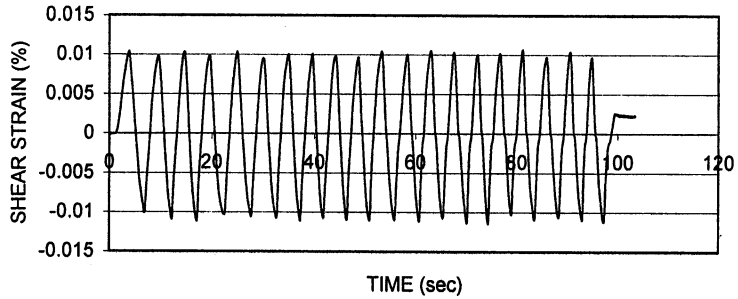

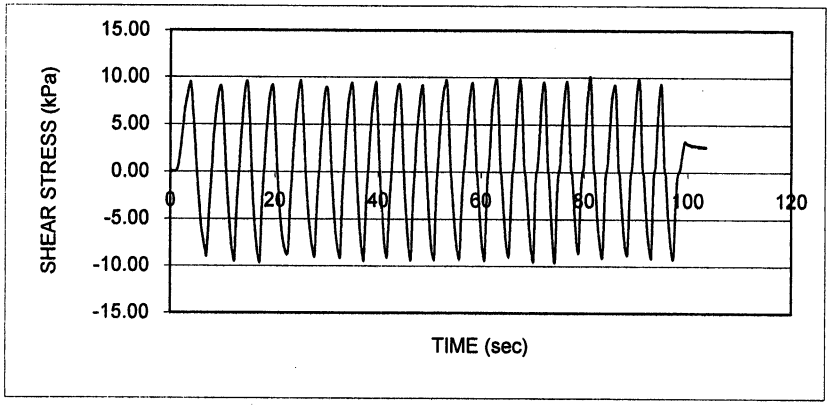

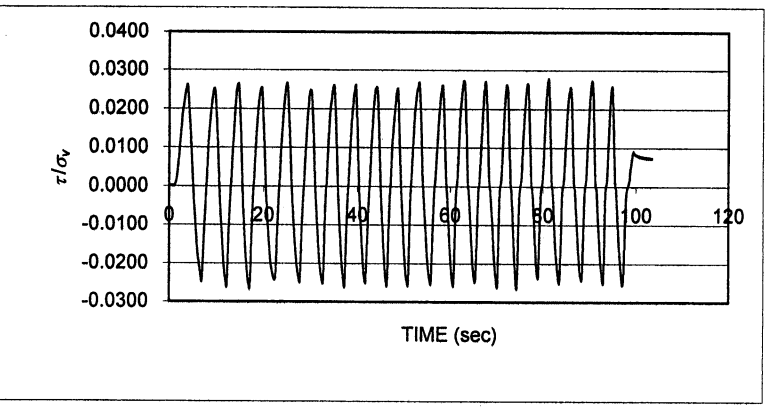

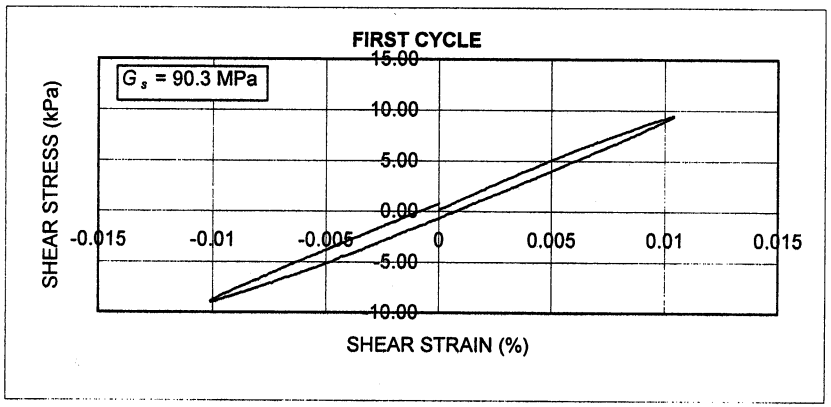

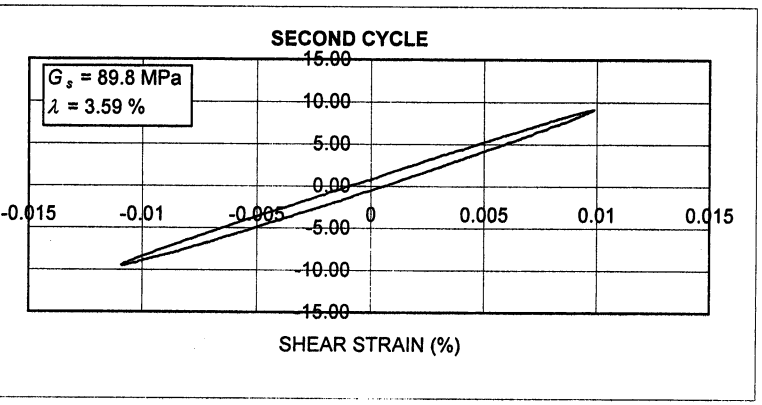

Obregon Park P-9					
DSDSS TEST - Step 6					
Type of soil: CL					
LL	41.0	PI	21.2	%Silt	37.6
e_0	0.48	S_0 (%)	90.7	%Clay	37.0
σ_v (kPa)	361	OCR	n/a	w (%)	16.1
γ_c (%)	~0.033	H_0 (mm)	19.19	Spec. Gr.	2.68

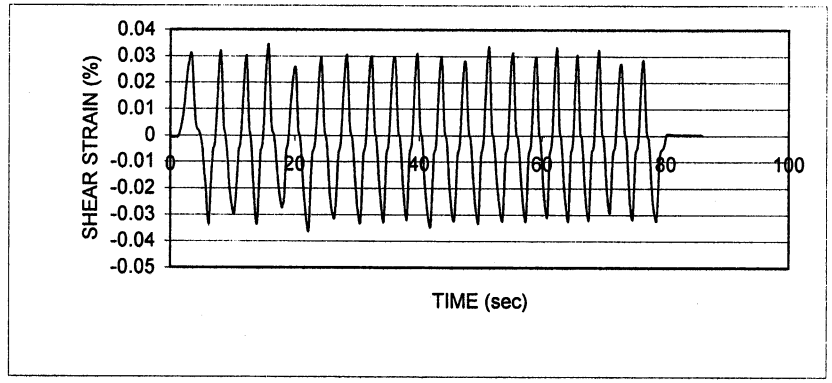

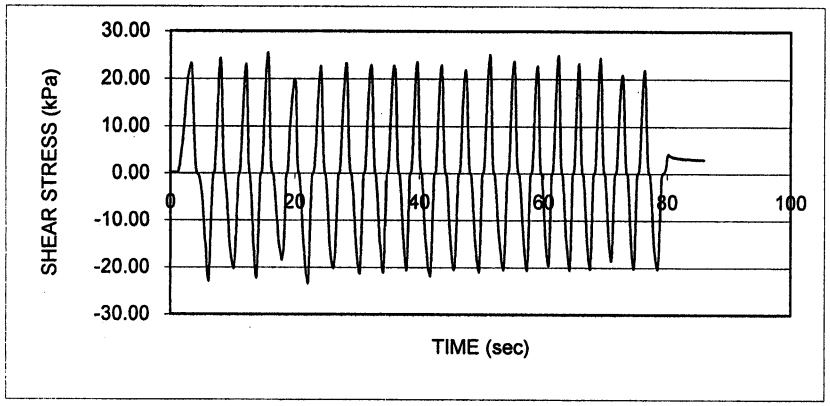

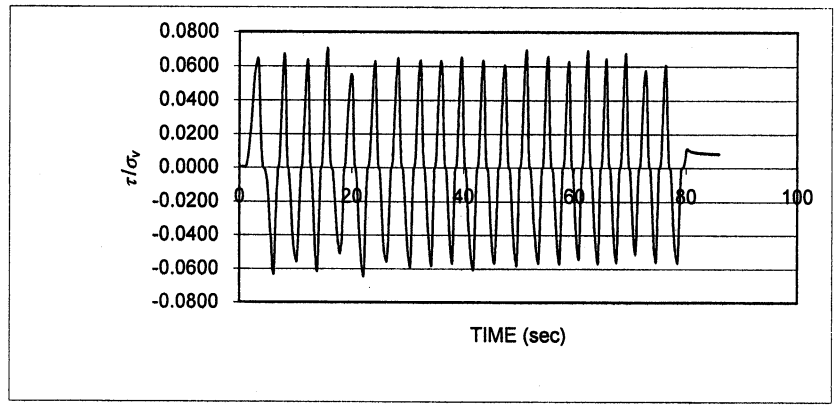

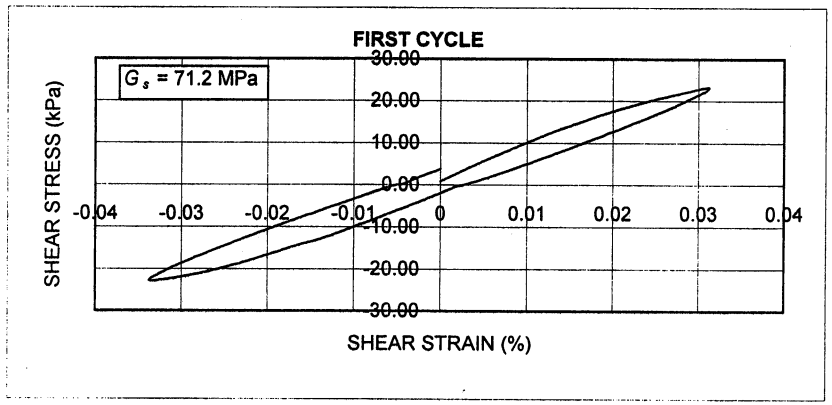

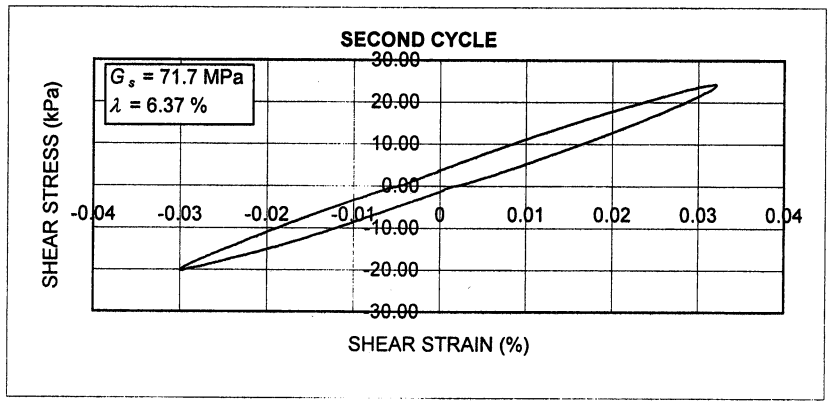

Obregon Park P-9					
DSDSS TEST - Step 7					
Type of soil: CL					
LL	41.0	PI	21.2	%Silt	37.6
e_0	0.48	S_0 (%)	90.7	%Clay	37.0
σ_v (kPa)	361	OCR	n/a	w (%)	16.1
γ_c (%)	~0.11	H_0 (mm)	19.19	Spec. Gr.	2.68

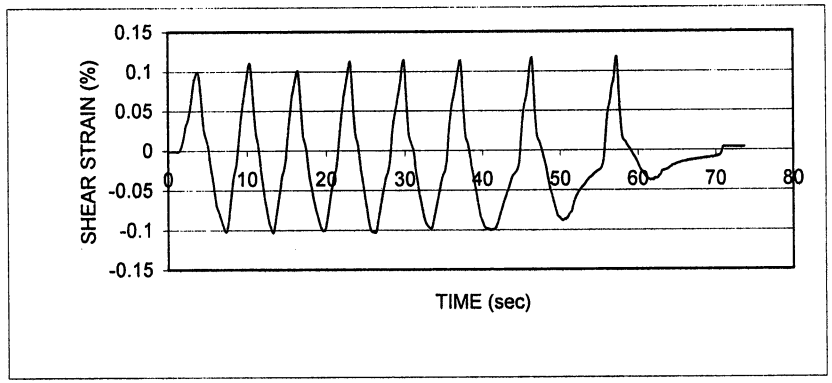

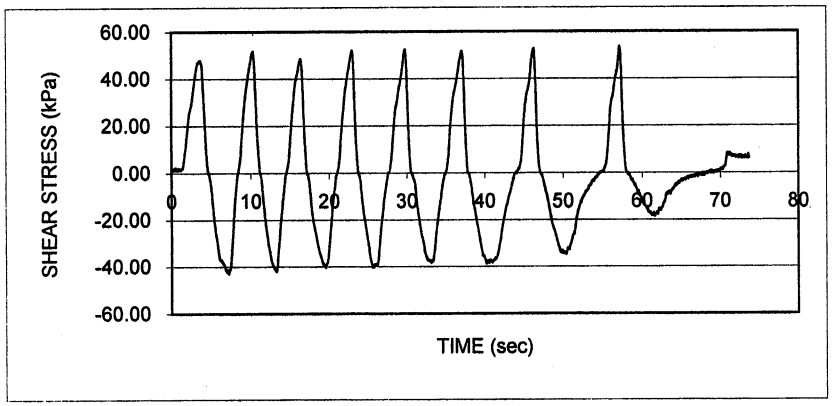

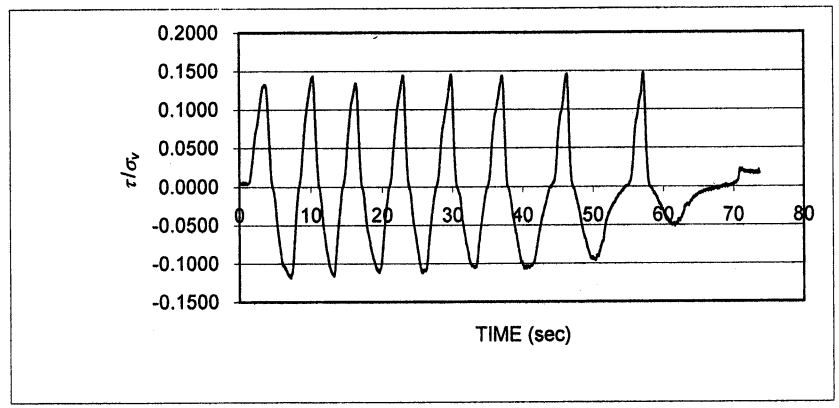

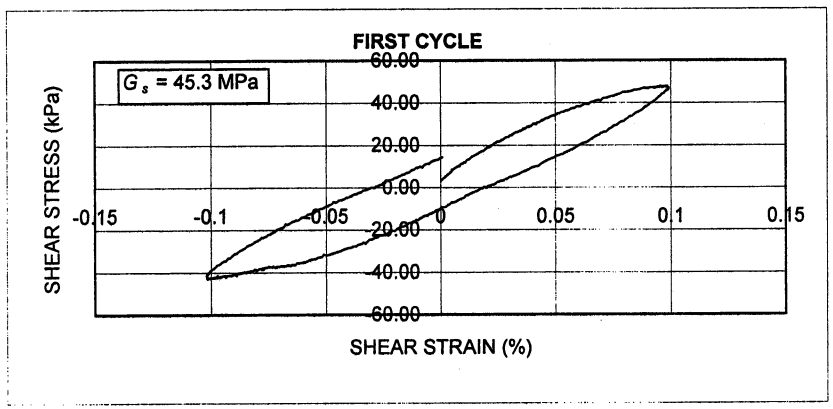

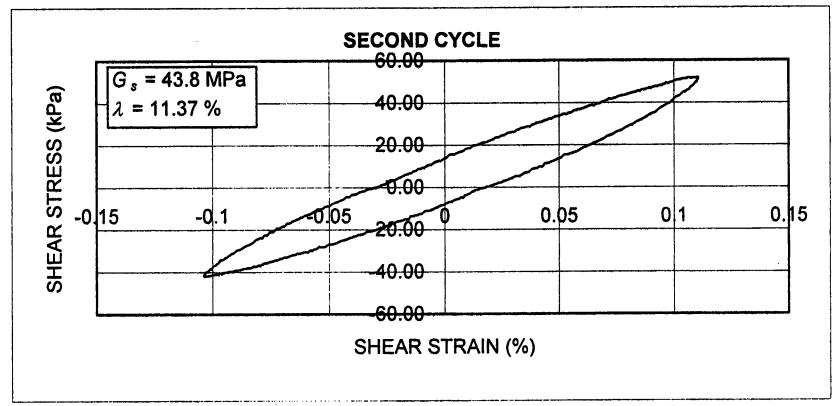

Obregon Park P-9					
DSDSS TEST - Step 8					
Type of soil: CL					
LL	41.0	PI	21.2	%Silt	37.6
e_0	0.48	S_0 (%)	90.7	%Clay	37.0
σ_v (kPa)	361	OCR	n/a	w (%)	16.1
γ_c (%)	~3.4	H_0 (mm)	19.19	Spec. Gr.	2.68

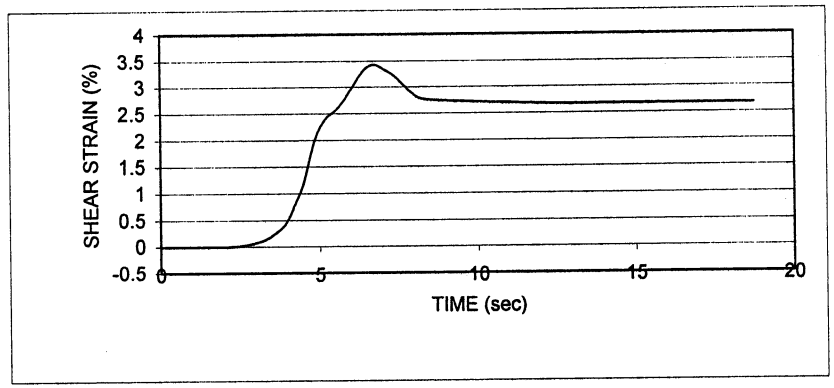

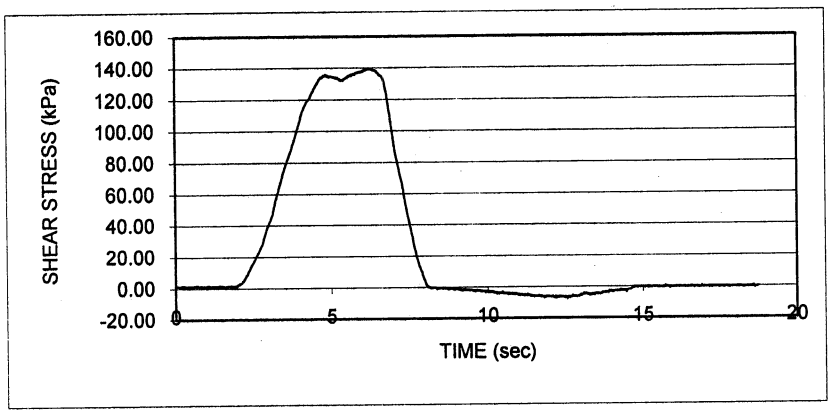

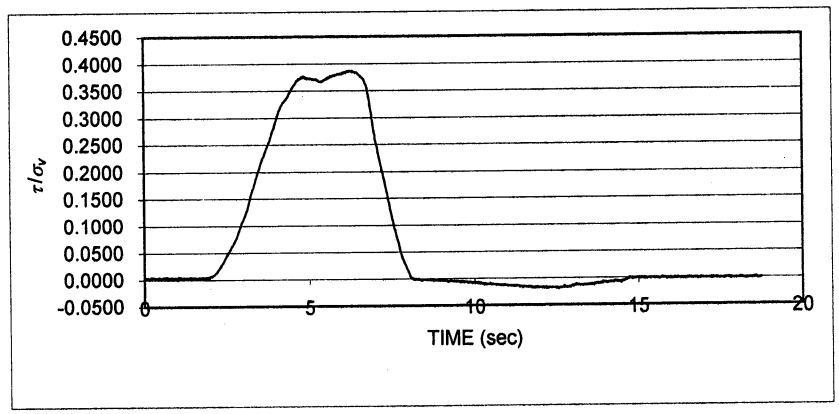

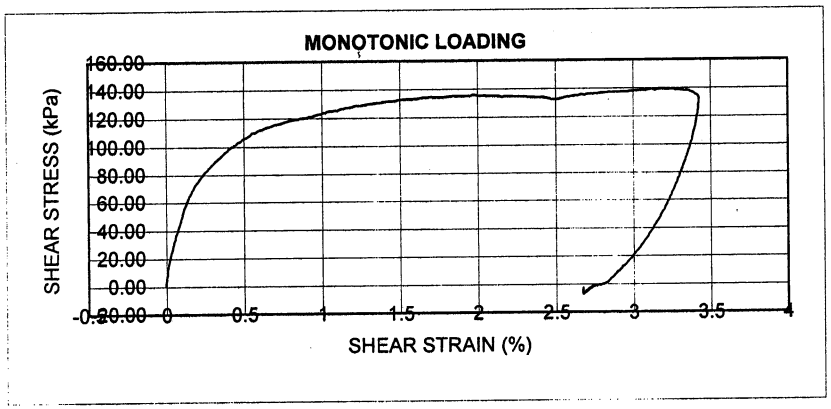

UCLA Soil Dynamics Laboratory
Double Specimen Direct Simple Shear (DSDSS) Test

Principal investigator: Mladen Vucetic, Professor
Test performed by Kentaro Tabata

Test no: 7

Project:	PEARL			Date:	4/3/2002
Sample name:	Obregon Park (P-9)			Depth (ft):	90.0
Symbol:	CL	LL (%):	41.0	Silt content (%):	37.6
Specific gravity:	2.68	PI:	21.2	Clay content (%):	37.0
Comments:					

Estimated G_{max} (MPa):	101.0

SHEAR MODULUS				DAMPING RATIO	
Step	γ_c (%)	G_s (MPa)	G_s/G_{max}	γ_c (%)	λ (%)
2x	0.000389	100.75	0.998		
2x	0.000375	100.03	0.990		
26x	0.000764	99.14	0.982	0.001174	2.41
26x	0.000739	99.24	0.983	0.003134	2.45
3x	0.001085	98.77	0.978	0.010392	3.59
3x	0.001174	99.99	0.990	0.031066	6.37
4x	0.003193	98.22	0.972	0.107332	11.37
4x	0.003134	98.73	0.978		
5x	0.010254	90.31	0.894		
5x	0.010392	89.78	0.889		
6x	0.032494	71.19	0.705		
6x	0.031066	71.73	0.710		
7x	0.100604	45.27	0.448		
7x	0.107332	43.84	0.434		
	γ (%)				
(Monotonic loading)	0.506701	20.97	0.208		
	1.004197	12.32	0.122		
	1.512762	8.78	0.087		
	2.008432	6.73	0.067		
	2.504102	5.27	0.052		
	3.425370	3.86	0.038		

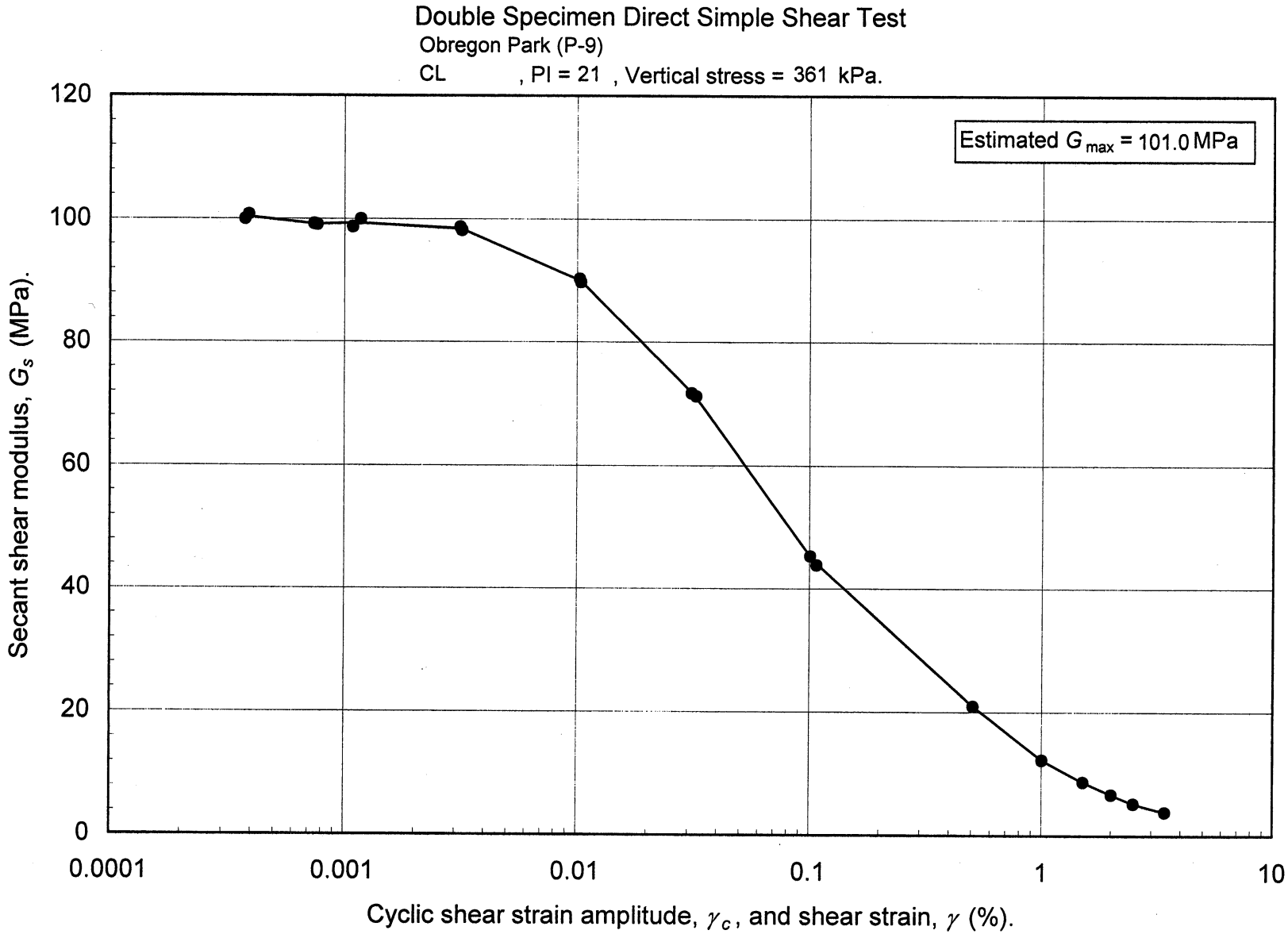
Double Specimen Direct Simple Shear Test
Obregon Park (P-9)
CL , PI = 21 , Vertical stress = 361 kPa.
Estimated G_{max} = 101.0 MPa
Secant shear modulus, G_s (MPa).
120
100
80
60
40
20
0
0.0001
0.001
0.01
0.1
1
10
Cyclic shear strain amplitude, γ_c, and shear strain, γ (%).

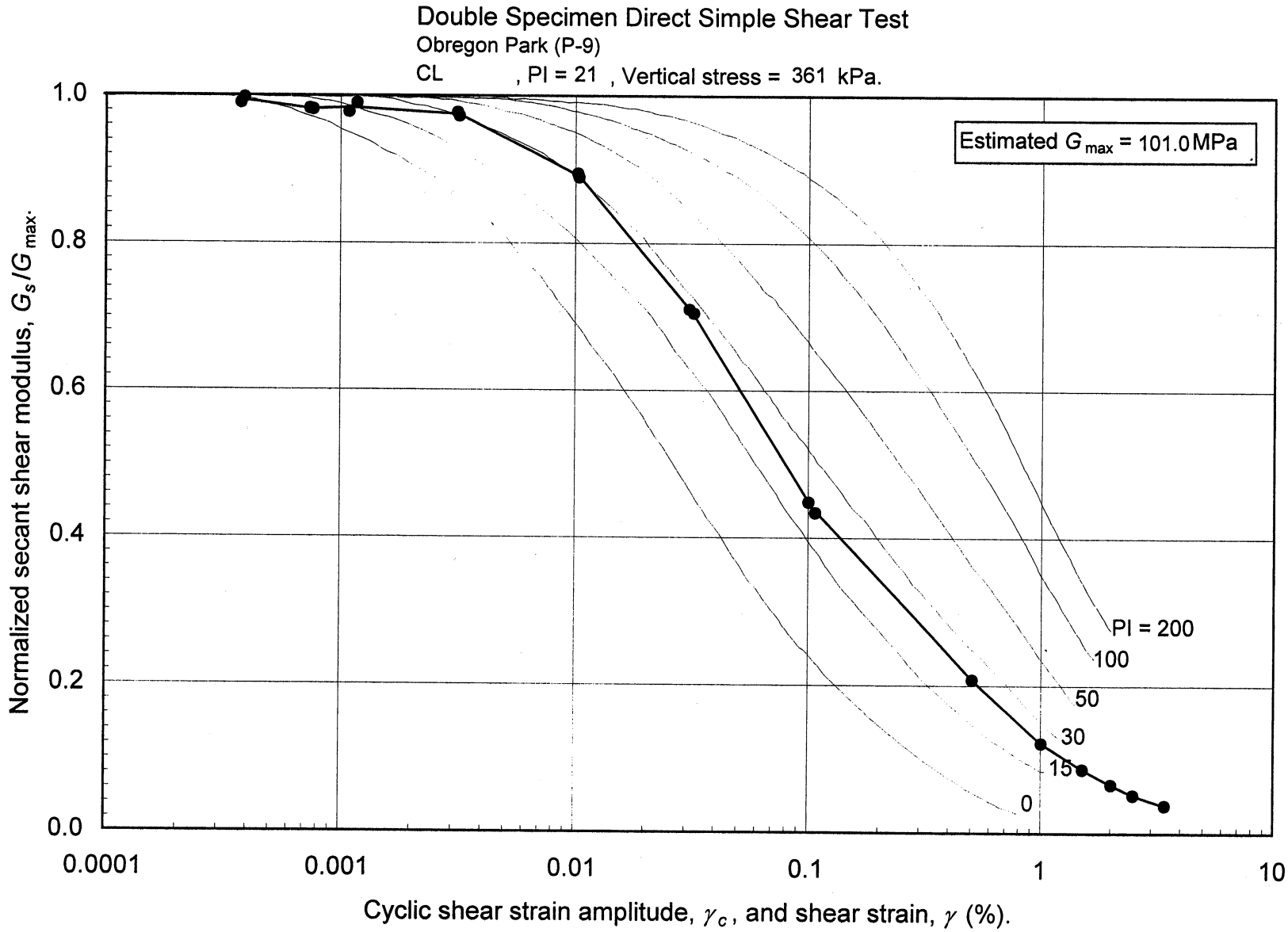
Double Specimen Direct Simple Shear Test
Obregon Park (P-9)
CL , PI = 21 , Vertical stress = 361 kPa.
Estimated G_{max} = 101.0 MPa
PI = 200
100
50
30
15
0
Normalized secant shear modulus, G_s/G_{max}
1.0
0.8
0.6
0.4
0.2
0.0
0.0001
0.001
0.01
0.1
1
10
Cyclic shear strain amplitude, γ_c, and shear strain, γ (%).

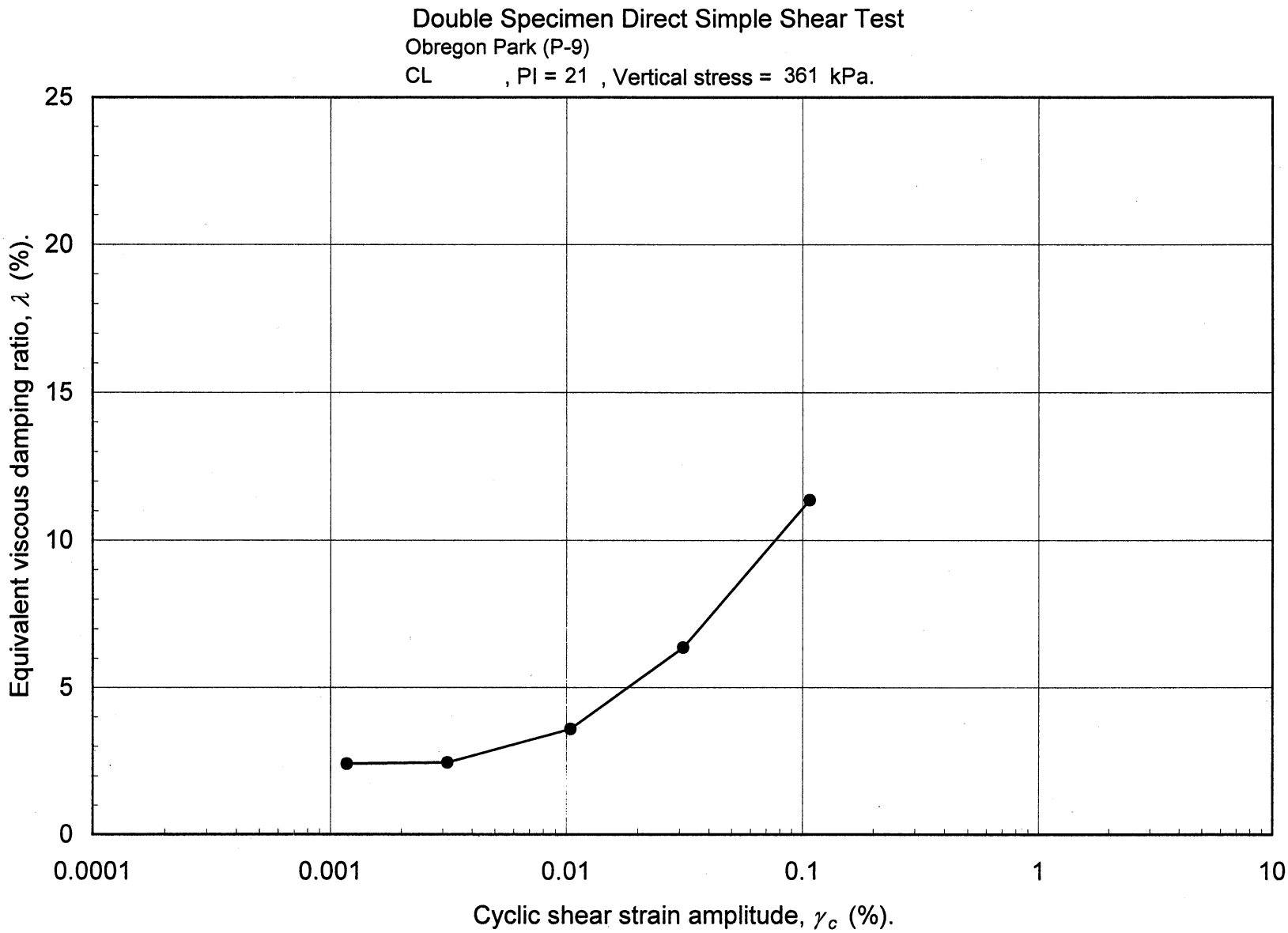
Double Specimen Direct Simple Shear Test
Obregon Park (P-9)
CL , PI = 21 , Vertical stress = 361 kPa.
Equivalent viscous damping ratio, λ (%).
Cyclic shear strain amplitude, γc (%).
0
5
10
15
20
25
0.0001
0.001
0.01
0.1
1
10

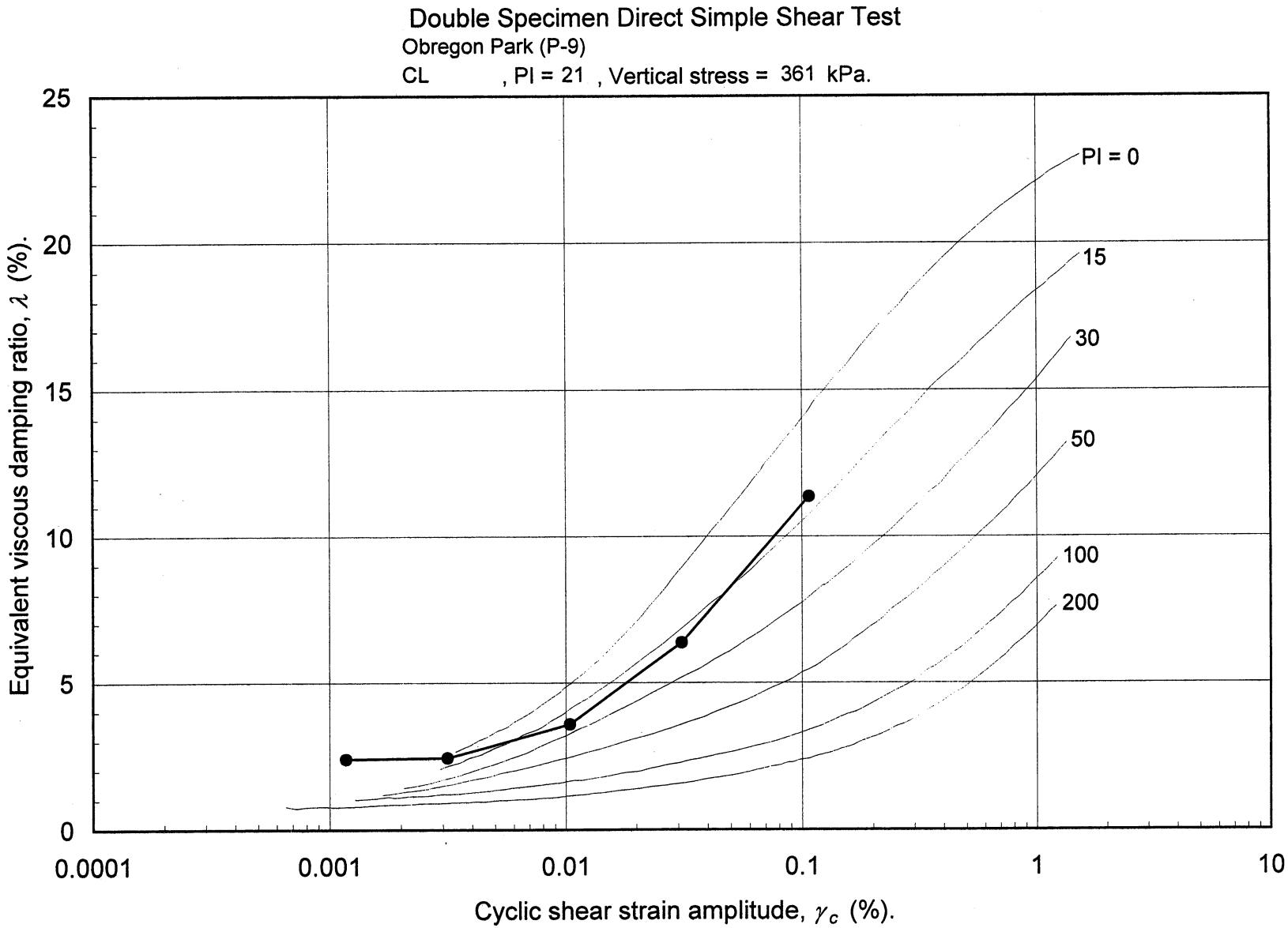
Double Specimen Direct Simple Shear Test
Obregon Park (P-9)
CL , PI = 21 , Vertical stress = 361 kPa.
Equivalent viscous damping ratio, λ (%).
Cyclic shear strain amplitude, γc (%).
25
20
15
10
5
0
0.0001
0.001
0.01
0.1
1
10
PI = 0
15
30
50
100
200

UCLA Soil Dynamics Laboratory

Specific Gravity Test

Principal investigator: Mladen Vucetic, Professor

Test performed by: Kentaro Tabata Test No.: 7

Project:	PEARL			Date:	4/5/2002
Boring:	Obregon Park				
Tube No.:	P-9	Depth (ft):	90.0 93.0	GWT (ft):	20.0
Comments:	Clay.				

SPECIFIC GRAVITY TEST

Test No.	1		
Bottle No.	3		
Wt. of bottle (g)	178.27		
Volume of bottle (cm^3)	500		
Wt. of bottle+water+soil (g)	694.36		
Temperature (°C)	22.0		
Wt. of bottle+water (g)	676.27		
Evaporating dish No.	B-2		
Weight of dish (g)	537.26		
Wt. of dish+dry soil (g)	566.07		
Wt. of dry soil (g)	28.81		
Specific gravity of water	0.9978		
Specific gravity of soil	**2.68**		

UCLA Soil Dynamics Laboratory

Grain Size Distribution

Principal investigator: Mladen Vucetic, Professor

Test performed by: Kentaro Tabata Test No.: 7

Project:	PEARL				
Boring:	Obregon Park				
Tube No.:	P-9	Depth (ft):	90.0 93.0	GWT (ft):	20.0
Comments:	Clay.				

GRAIN SIZE DISTRIBUTION

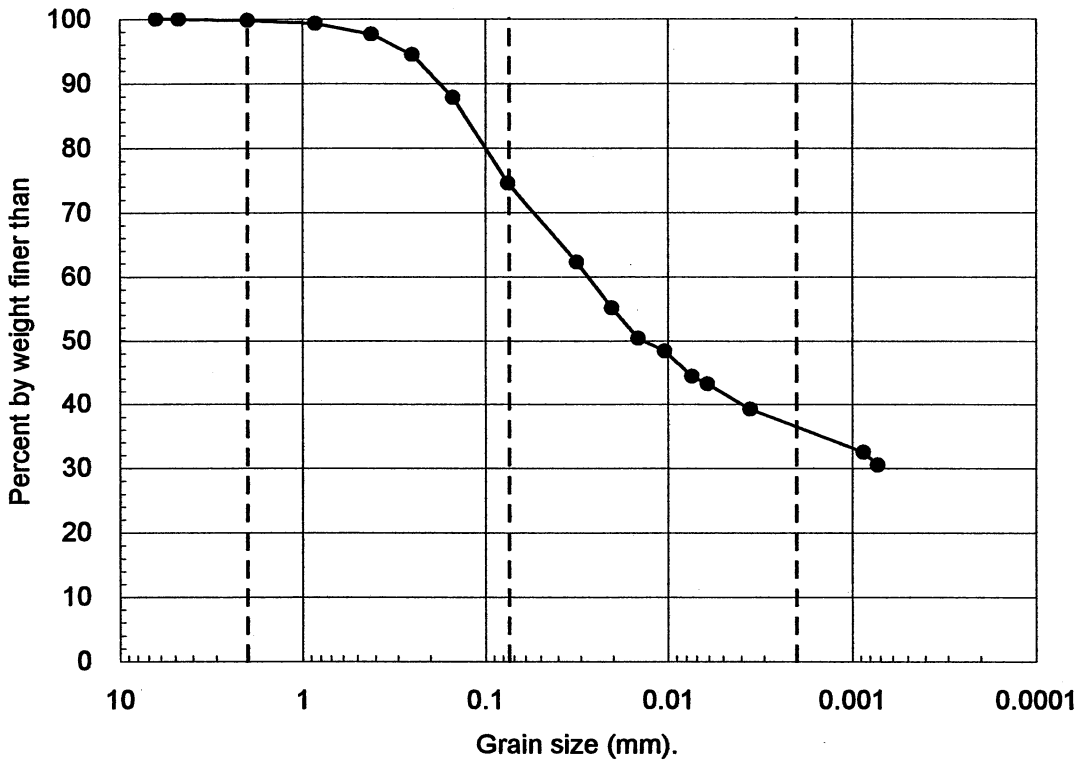

Clay (%)	Silt (%)	Sand (%)	Gravel (%)
37.0	37.6	25.3	0.2

UCLA Soil Dynamics Laboratory

Hydrometer Analysis

Principal investigator: Mladen Vucetic, Professor

Test performed by: Kentaro Tabata Test No.: 7

Project:	PEARL			Date:	4/5/2002
Boring:	Obregon Park				
Tube No.:	P-9	Depth (ft):	90.0 93.0	GWT (ft):	20.0
Comments:	Clay.				

HYDROMETER TEST

Time	Elapsed time t (sec)	Temp. T (°C)	Reading R'_T	Corr. reading $R_T=R'_T+c_m$	Depth H (cm)	Grain diameter D (mm)	Temp. corr. m_T	Corr. depth $R_T+m_T-c_d$	% by wt. finer than W_D (%)
11:31:20	0								
11:33:20	120	23.0	1017.5	1018.0	11.71	0.0316	0.700	1015.7	62.21
11:36:20	300	23.0	1015.7	1016.2	12.19	0.0204	0.700	1013.9	55.08
11:41:20	600	23.0	1014.5	1015.0	12.51	0.0146	0.700	1012.7	50.32
11:51:20	1200	23.0	1014.0	1014.5	12.64	0.0104	0.700	1012.2	48.34
12:11:20	2400	23.0	1013.0	1013.5	12.91	0.0074	0.700	1011.2	44.38
12:31:20	3600	23.0	1012.7	1013.2	12.99	0.0061	0.700	1010.9	43.19
14:31:20	10800	23.0	1011.7	1012.2	13.26	0.0035	0.700	1009.9	39.23
15:10:00	185920	23.0	1010.0	1010.5	13.71	0.0009	0.700	1008.2	32.49
14:10:00	268720	23.0	1009.5	1010.0	13.85	0.0007	0.700	1007.7	30.51

APPARATUS

Hydrometer no.:	88-18587	a_0	284.03	a_1	-0.2675
Graduate no.:	3				

FACTORS

Meniscus corr., c_m:	0.5	
Disp. agent corr, c_d:	3.0	
Visc. of water, η.	23.0 °C	9.565E-06 g sec/cm^2
	°C	g sec/cm^3

WEIGHT

Dry soil (g)	30.00
Percent by wt (%)	74.55
Dry soil for sieve (g)	10.24
Total (g)	40.24

UNIT WEIGHT

Specific gravity:		2.68
T	γ_w	γ_s
(°C)	(g/cm^3)	(g/cm^3)
23.0	0.9976	2.6759

UCLA Soil Dynamics Laboratory

Sieve Analysis

Principal investigator: Mladen Vucetic, Professor

Test performed by: Kentaro Tabata Test No.: 7

Project:	PEARL			Date:	4/9/2002
Boring:	Obregon Park				
Tube No.:	P-9	Depth (ft):	90.0 93.0	GWT (ft):	20.0
Comments:	Clay.				

SIEVE ANALYSIS

Sieve No.	Diameter (mm)	Sieve (g)	S+wet (g)	S+dry (g)	Retained (g)	Retained (%)	Cumulated (g)	Cumulated (%)	Passing (%)
3	6.350	485.05		485.05	0.00	0.00	0.00	0.00	100.00
4	4.750	463.08		463.08	0.00	0.00	0.00	0.00	100.00
10	2.000	422.40		422.47	0.07	0.17	0.07	0.17	99.83
20	0.850	375.43		375.64	0.21	0.52	0.28	0.70	99.30
40	0.420	375.60		376.27	0.67	1.67	0.95	2.36	97.64
60	0.250	323.90		325.18	1.28	3.18	2.23	5.54	94.46
100	0.150	342.17		344.86	2.69	6.68	4.92	12.23	87.77
200	0.075	676.86		682.18	5.32	13.22	10.24	25.45	74.55
Total					10.24	25.45			

WEIGHT

Dry soil for sieve (g)	10.24
Dry soil for hydr. (g)	30.00
Total (g)	40.24
Percent coaser (%)	25.45

UCLA Soil Dynamics Laboratory

Atterberg Limit Determination

Principal investigator: Mladen Vucetic, Professor

Test performed by: Kentaro Tabata Test No.: 7

Project:	PEARL			Date:	4/5/2002
Boring:	Obregon Park				
Tube No.:	P-9	Depth (ft):	90.0 93.0	GWT (ft):	20.0
Comments:	Clay.				

LIQUID LIMIT TEST

Test No.	1	2	3	4	5			
Number of blows	43	34	27	18	9			
Container No.	ST-23	ST-4	ST-21	ST-6	ST-1			
Container (g)	30.57	30.18	30.29	30.10	30.37			
Cont+wet soil (g)	39.75	40.57	37.98	39.64	41.55			
Cont+dry soil (g)	37.28	37.71	35.73	36.70	37.96			
Water (g)	2.47	2.86	2.25	2.94	3.59			
Dry soil (g)	6.71	7.53	5.44	6.60	7.59			
Water content (%)	36.81	37.98	41.36	44.55	47.30			

PLASTIC LIMIT TEST

Test No.	1	2	3
Container No.	ST-19	ST-20	ST-11
Container (g)	29.99	30.36	30.25
Cont+wet soil (g)	32.43	32.68	32.80
Cont+dry soil (g)	32.03	32.30	32.37
Water (g)	0.40	0.38	0.43
Dry soil (g)	2.04	1.94	2.12
Water content (%)	19.61	19.59	20.28

ATTERBERG LIMITS

Liquid limit (%)	**41.0**
Plastic limit (%)	**19.8**
Plasticity index	**21.2**

CLASSIFICATION

CL

FLOW CHART

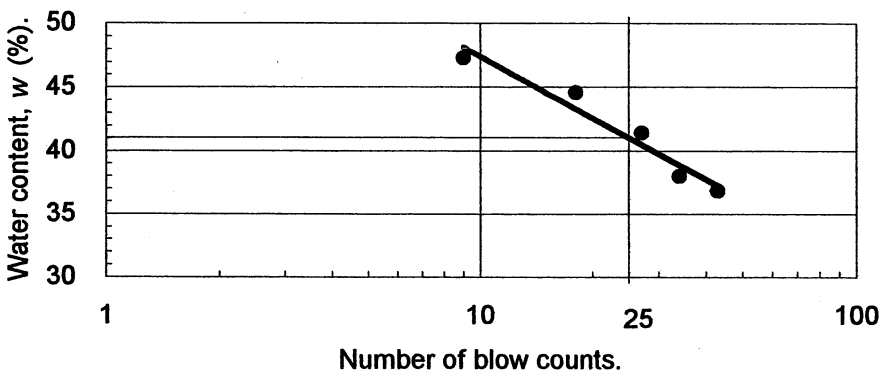

UCLA Soil Dynamics Laboratory

Atterberg Limit Determination

Principal investigator: Mladen Vucetic, Professor

Test performed by: Kentaro Tabata Test No.: 7

Project:	PEARL			Date:	4/5/2002
Boring:	Obregon Park				
Tube No.:	P-9	Depth (ft):	90.0 93.0	GWT (ft):	20.0
Comments:	Clay.				

PLASTICITY CHART

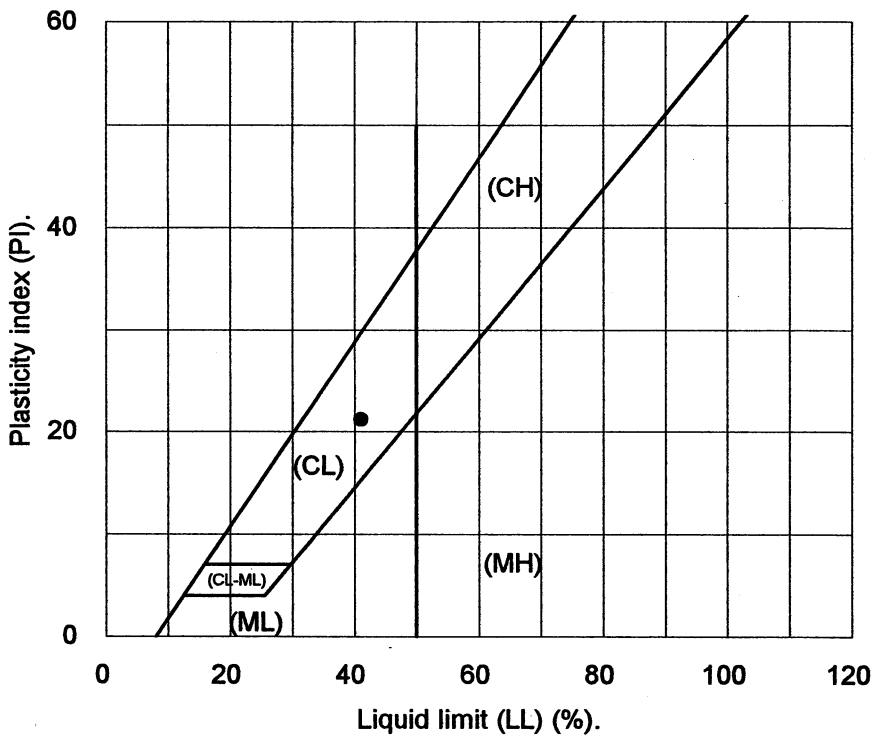

3.9 Test 8: LA BULK MAIL P-1

UCLA Soil Dynamics Laboratory

Double Specimen Direct Simple Shear (DSDSS) Test

Principal investigator: Mladen Vucetic, Professor

Test performed by: Kentaro Tabata Test No.: 8

Project:	PEARL			Date:	11/30/2001
Boring:	LA Bulk Mail				
Tube No.:	P-1	Depth (ft):	15.0 -18.0	GWT (ft):	135.0 (reported by others)
Comments:	Dark brown silt. Specimen obtained from the bottom of the tube (specimen depth ~ 17.5 ft).				

FORM 1: SPECIMEN PREPARATION

WATER CONTENT, SPECIFIC GRAVITY

	Before consol.	After shearing	
Container No.	ST-19	MT-7	MT-20
Cont+wet soil (g)	54.49	192.83	190.98
Cont+dry soil (g)	50.79	172.30	170.49
Container (g)	30.00	50.75	50.26
Water (g)	3.70	20.53	20.49
Dry soil (g)	20.79	121.55	120.23
Water content(%)	17.80	16.89	17.04
Avg. water cont. (%)	17.80		16.97
Spceific gravity			2.73

UNIT WEIGHT, VOID RATIO, SATURATION

	Before consol.	Before shearing	After shearing
Average weight (g)	141.89	141.89	
Height (cm)	1.965	1.912	
Area (cm^2)	34.94	34.94	
Volume (cm^3)	68.66	66.82	
Unit weight (g/cm^3)	2.066	2.123	
Unit weight (kN/m^3)	20.25	20.81	
Void ratio	0.56	0.51	
Saturation (%)	87.4	94.4	

HEIGHT OF SPECIMEN

	Before consol.		Before shearing	After shearing		
	Top	Bottom	Average	Average		
Height (cm)	1.965	1.965	1.912	1.912		

AREA OF SPECIMEN

Initial diameter (cm)	6.670	Initial area (cm^2)	34.942

Load (kg)	Stress (kg/cm^2)	Stress (kN/m^2)	Diameter (cm)	Membrane (cm)	Corrected diameter (cm)	Area (cm^2)

LA Bulk Mail P-1					
DSDSS TEST - Step 2b2					
Type of soil: CL					
LL	26.3	PI	8.1	%Silt	44.8
e_0	0.51	S_0 (%)	94.4	%Clay	26.0
σ_v (kPa)	94	OCR	n/a	w (%)	17.8
γ_c (%)	~0.00038	H_0 (mm)	19.12	Spec. Gr.	2.73

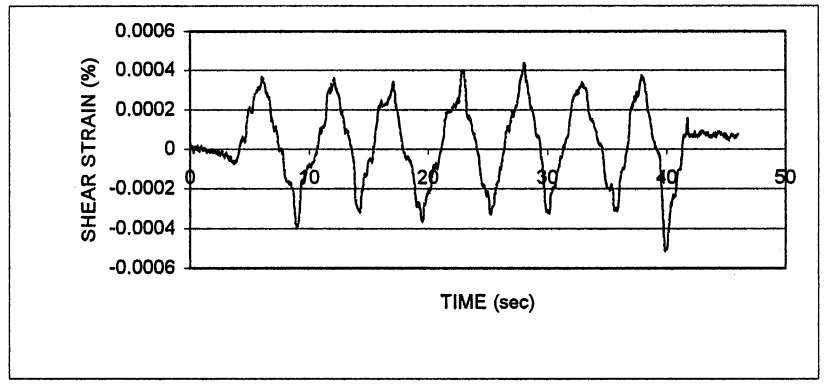

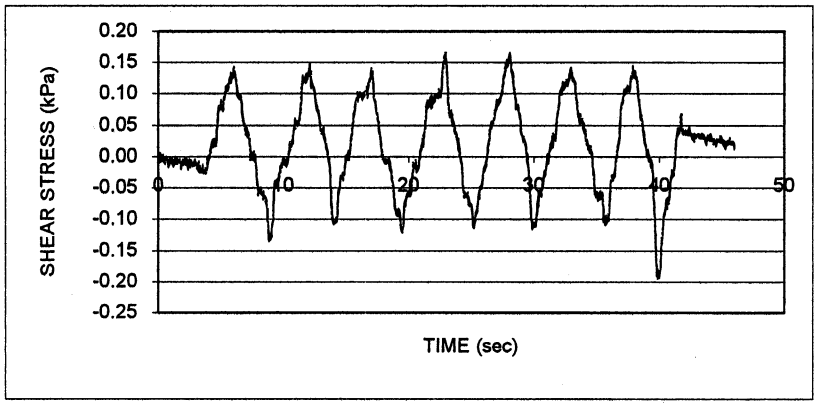

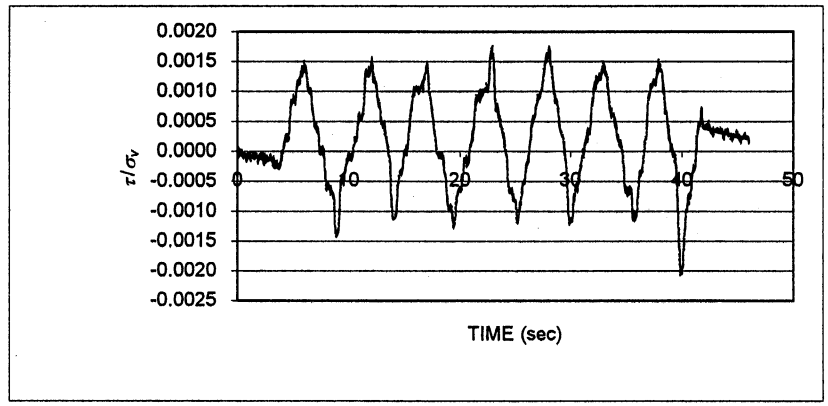

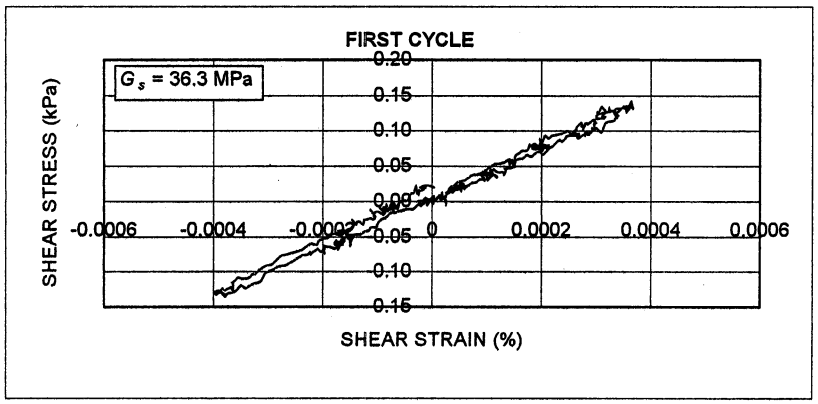

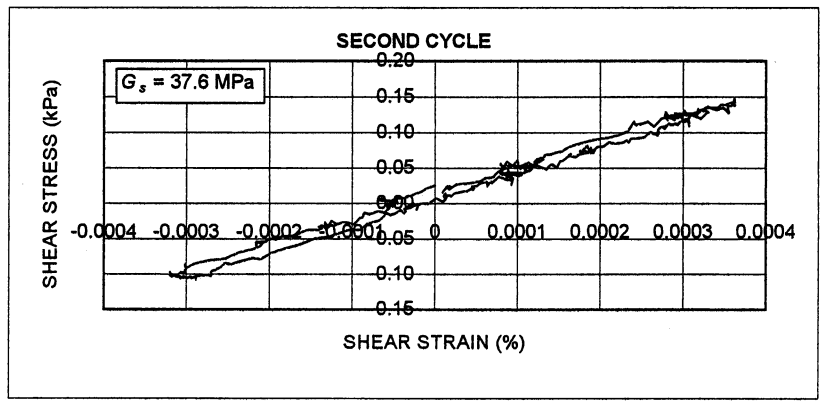

LA Bulk Mail P-1					
DSDSS TEST - Step 26b2					
Type of soil: CL					
LL	26.3	PI	8.1	%Silt	44.8
e_0	0.51	S_0 (%)	94.4	%Clay	26.0
σ_v (kPa)	94	OCR	n/a	w (%)	17.8
γ_c (%)	~0.00075	H_0 (mm)	19.12	Spec. Gr.	2.73

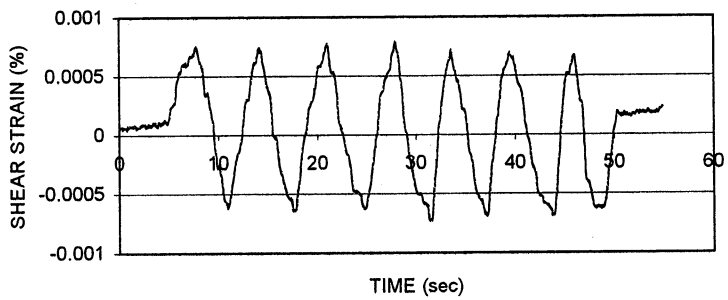

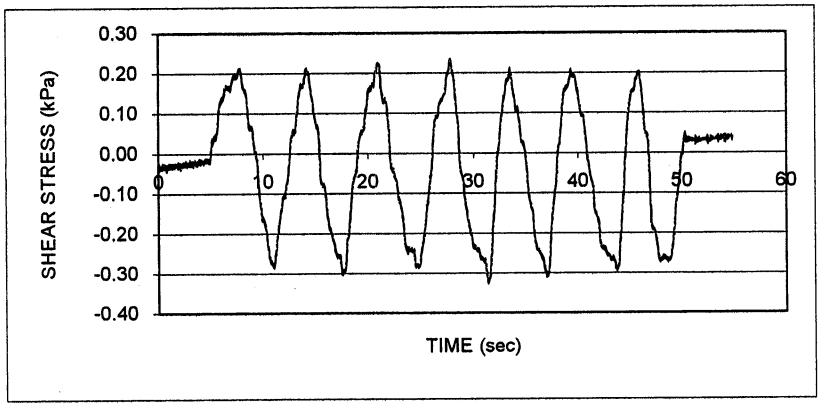

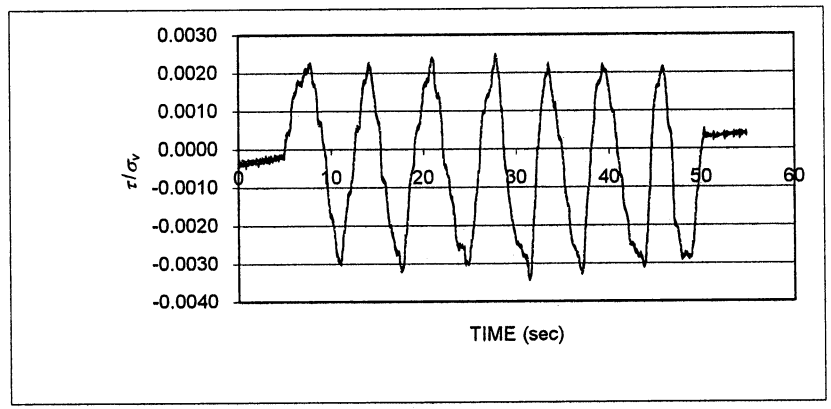

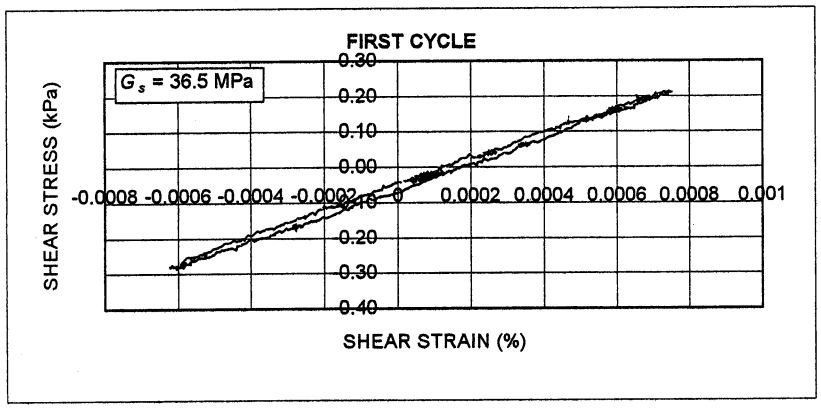

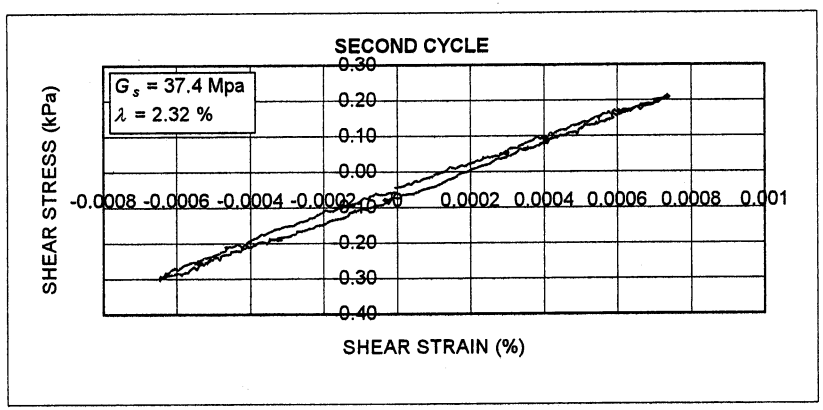

LA Bulk Mail P-1					
DSDSS TEST - Step 3b					
Type of soil: CL					
LL	26.3	PI	8.1	%Silt	44.8
e_0	0.51	S_0 (%)	94.4	%Clay	26.0
σ_v (kPa)	94	OCR	n/a	w (%)	17.8
γ_c (%)	~0.0011	H_0 (mm)	19.12	Spec. Gr.	2.73

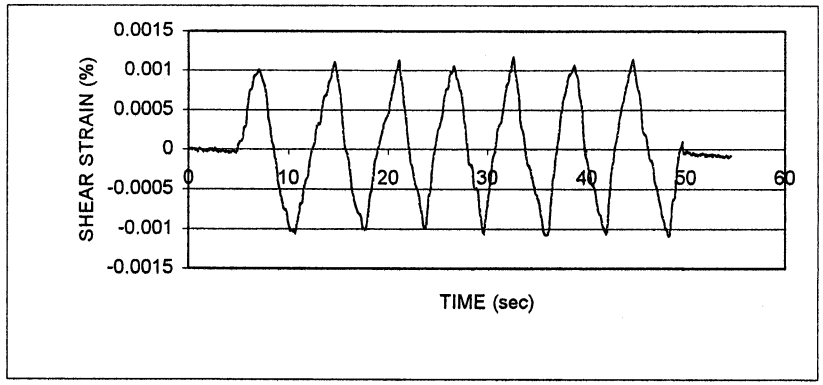

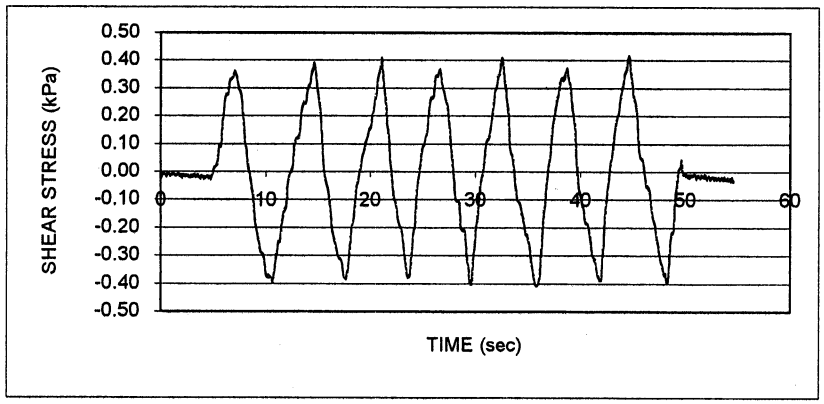

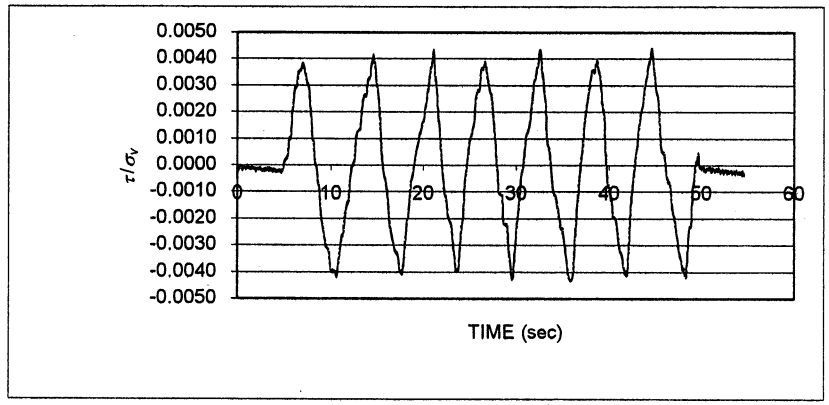

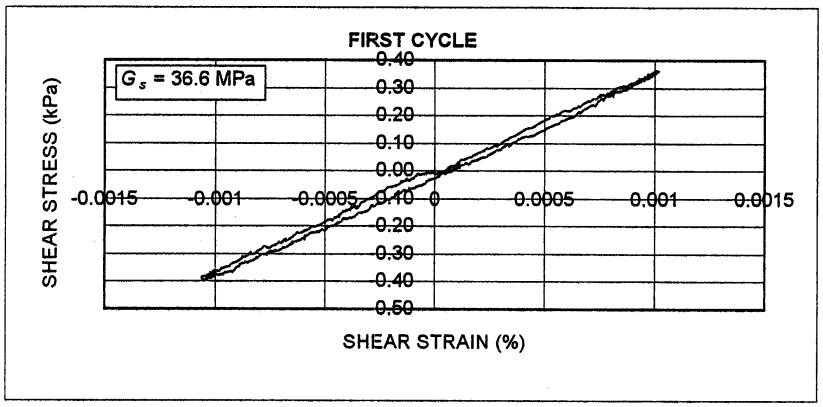

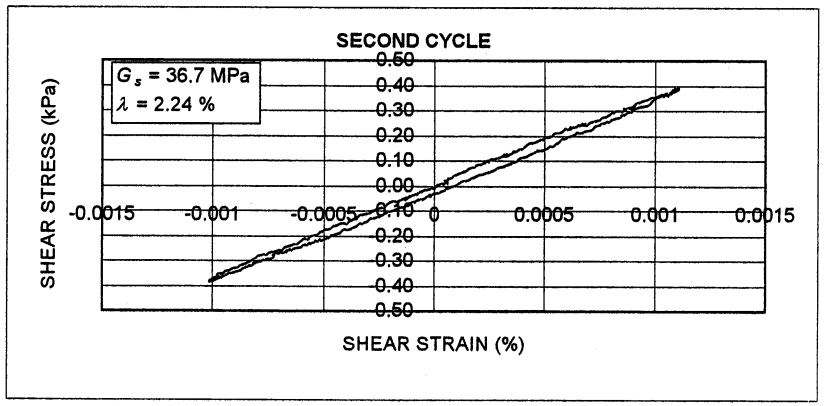

LA Bulk Mail P-1					
DSDSS TEST - Step 4b					
Type of soil: CL					
LL	26.3	PI	8.1	%Silt	44.8
e_0	0.51	S_0 (%)	94.4	%Clay	26.0
σ_v (kPa)	94	OCR	n/a	w (%)	17.8
γ_c (%)	~0.003	H_0 (mm)	19.12	Spec. Gr.	2.73

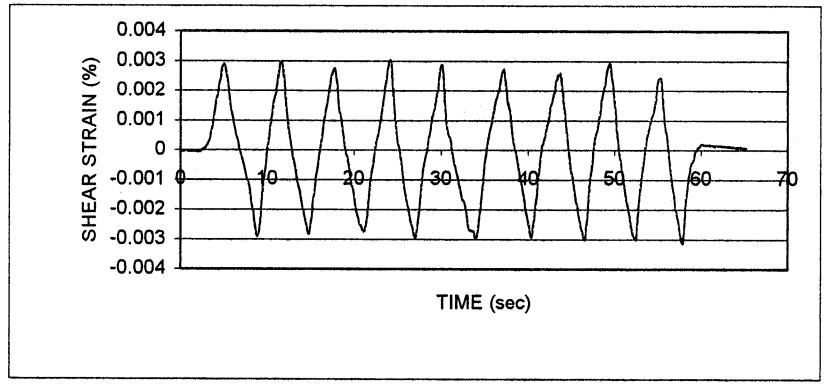

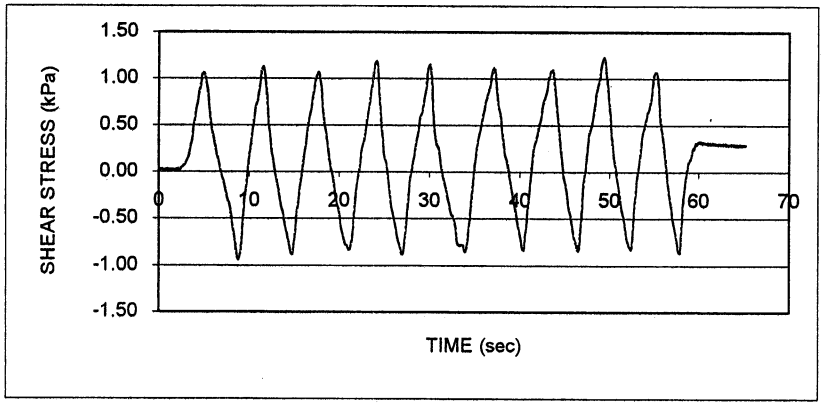

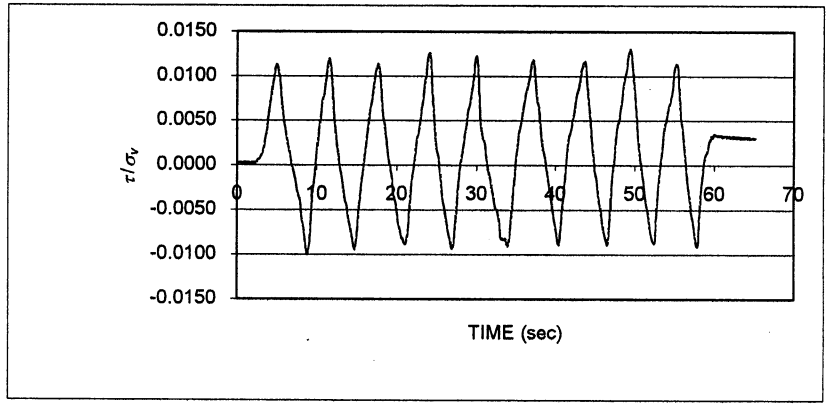

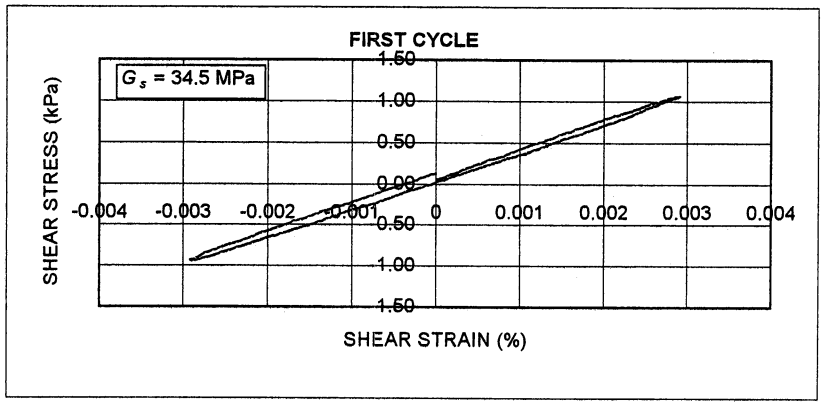

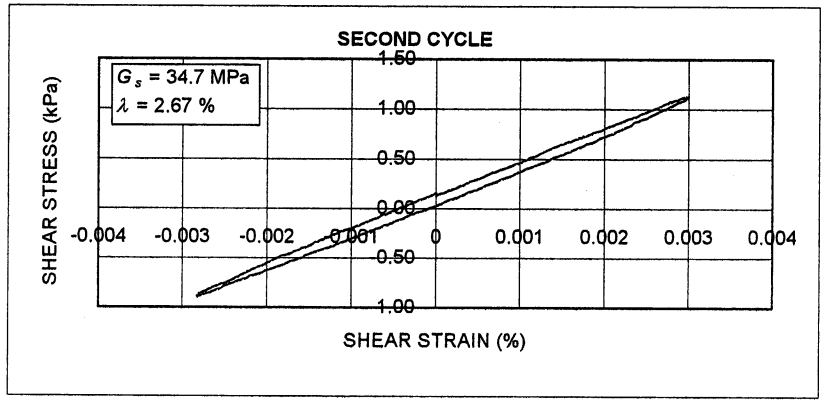

LA Bulk Mail P-1					
DSDSS TEST - Step 5b					
Type of soil: CL					
LL	26.3	PI	8.1	%Silt	44.8
e_0	0.51	S_0 (%)	94.4	%Clay	26.0
σ_v (kPa)	94	OCR	n/a	w (%)	17.8
γ_c (%)	~0.01	H_0 (mm)	19.12	Spec. Gr.	2.73

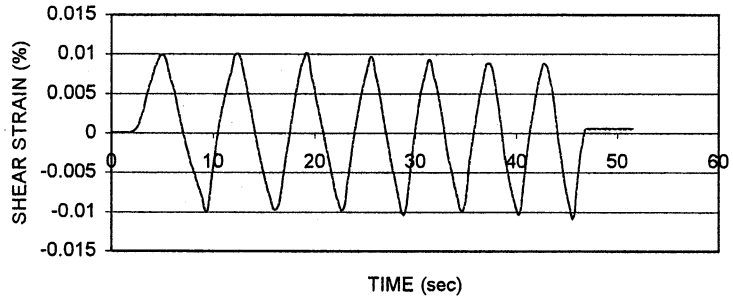

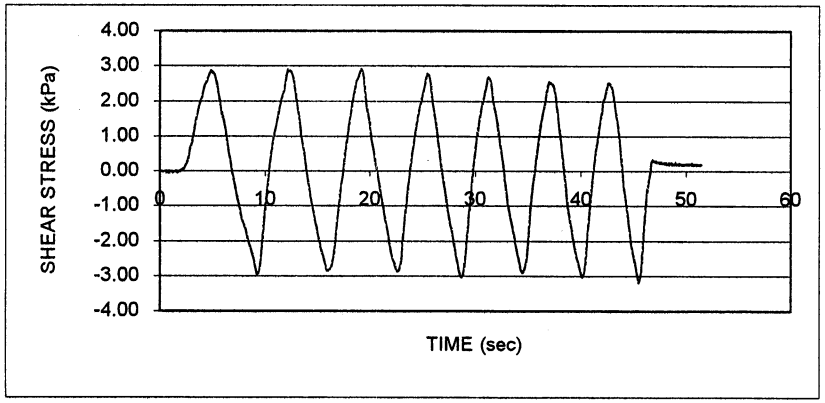

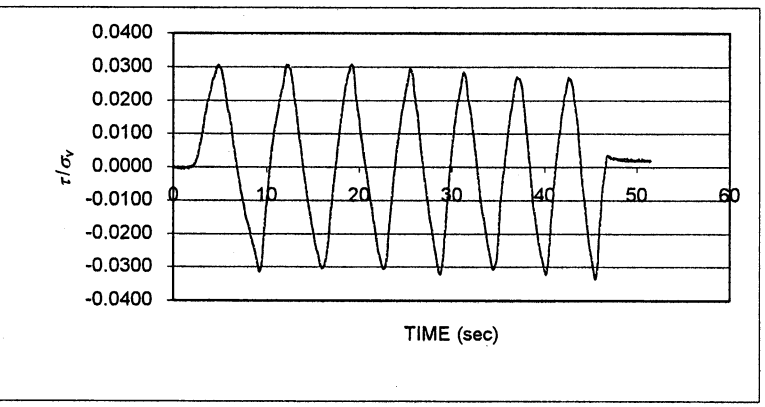

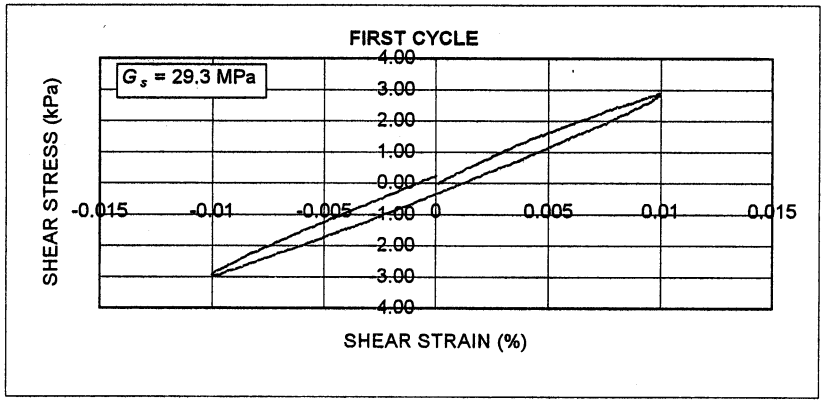

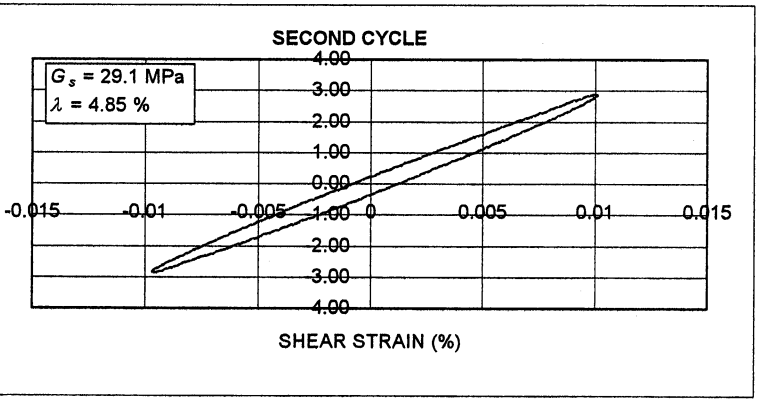

LA Bulk Mail P-1					
DSDSS TEST - Step 6b					
Type of soil: CL					
LL	26.3	PI	8.1	%Silt	44.8
e_0	0.51	S_0 (%)	94.4	%Clay	26.0
σ_v (kPa)	94	OCR	n/a	w (%)	17.8
γ_c (%)	~0.029	H_0 (mm)	19.12	Spec. Gr.	2.73

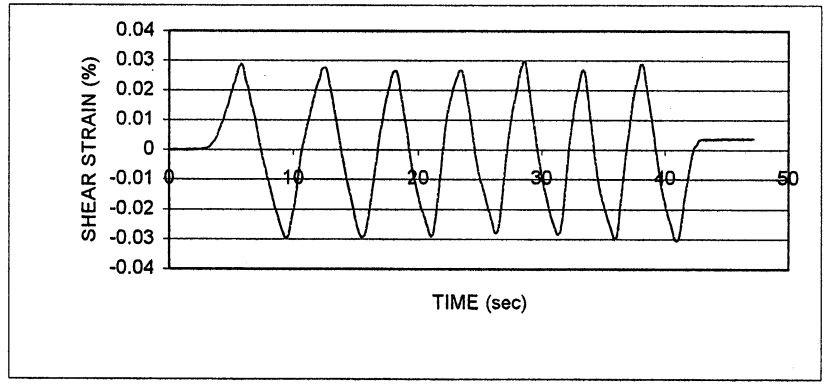

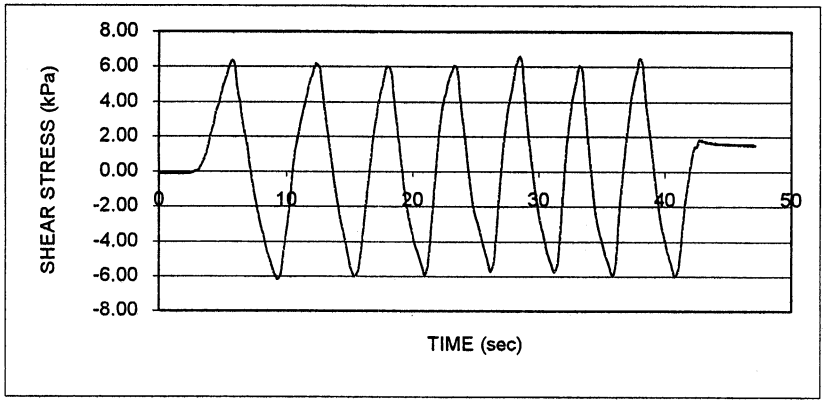

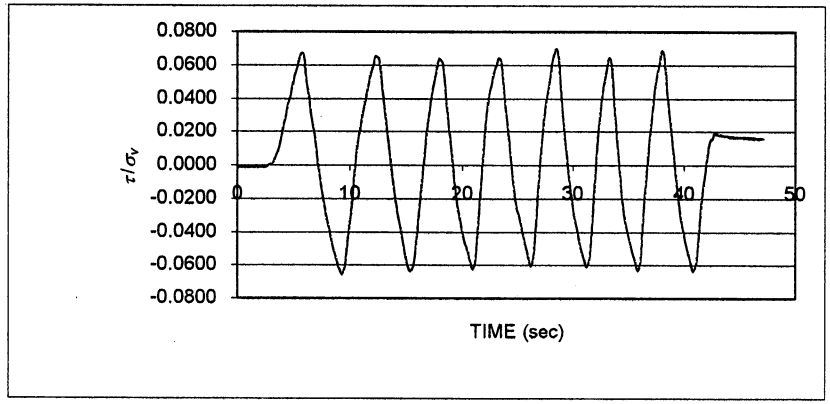

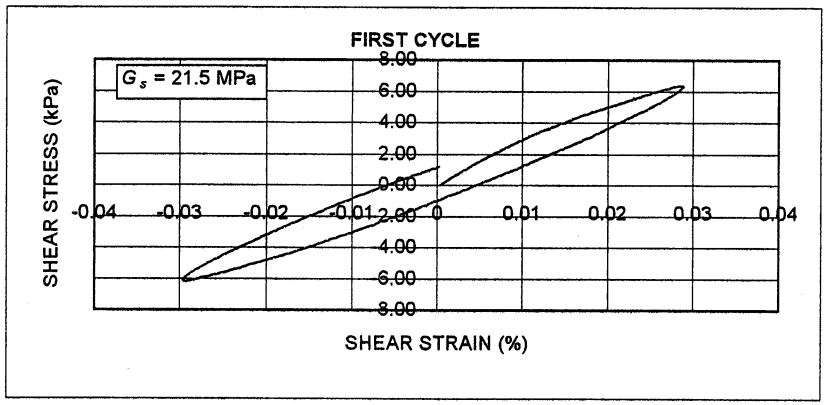

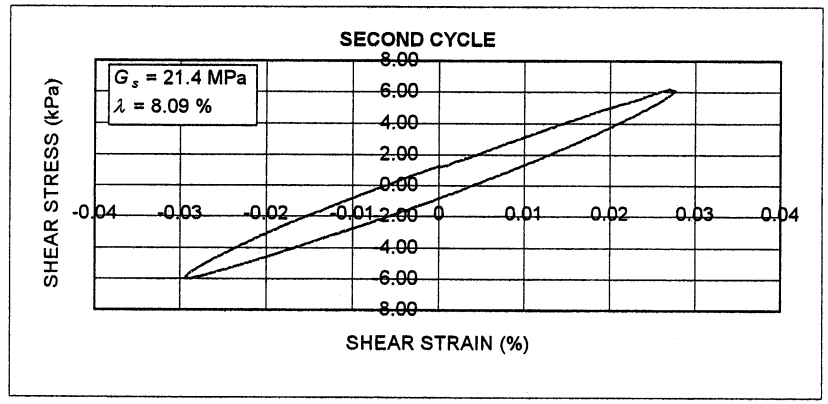

LA Bulk Mail P-1					
DSDSS TEST - Step 7b					
Type of soil: CL					
LL	26.3	PI	8.1	%Silt	44.8
e_0	0.51	S_0 (%)	94.4	%Clay	26.0
σ_v (kPa)	94	OCR	n/a	w (%)	17.8
γ_c (%)	~0.1	H_0 (mm)	19.12	Spec. Gr.	2.73

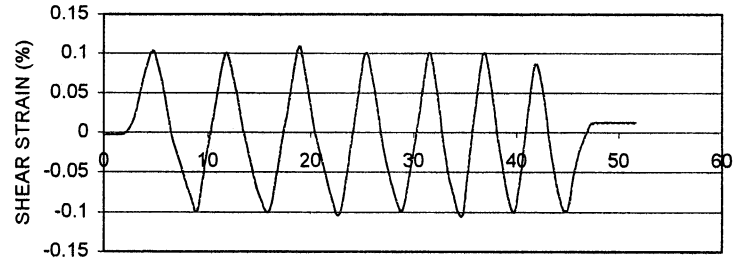

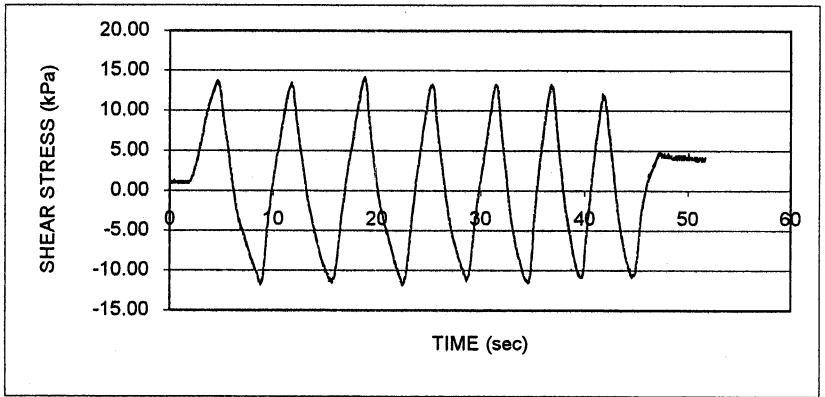

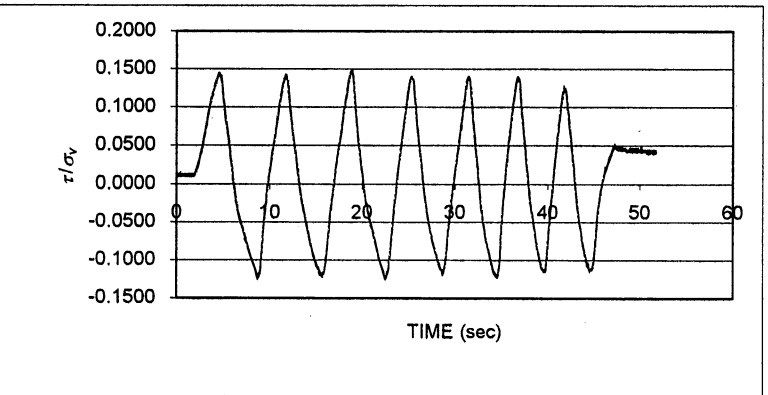

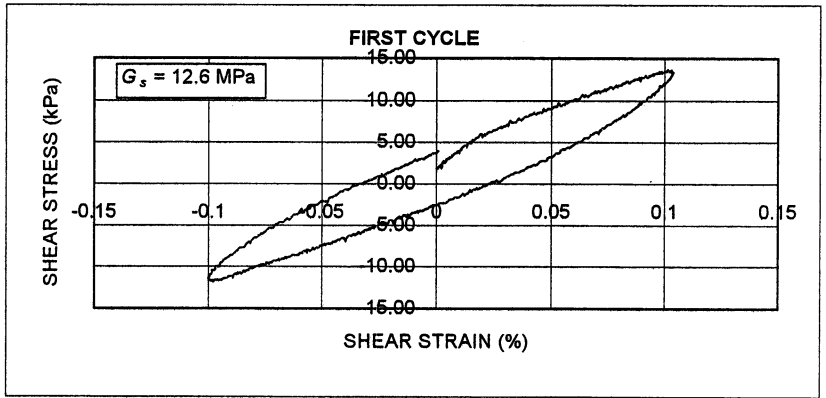

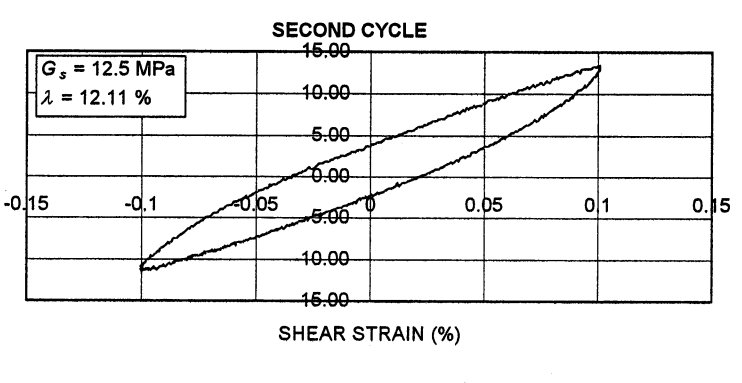

LA Bulk Mail P-1					
DSDSS TEST - Step 8					
Type of soil: CL					
LL	26.3	PI	8.1	%Silt	44.8
e_0	0.51	S_0 (%)	94.4	%Clay	26.0
σ_v (kPa)	94	OCR	n/a	w (%)	17.8
γ_c (%)	~3.0	H_0 (mm)	19.12	Spec. Gr.	2.73

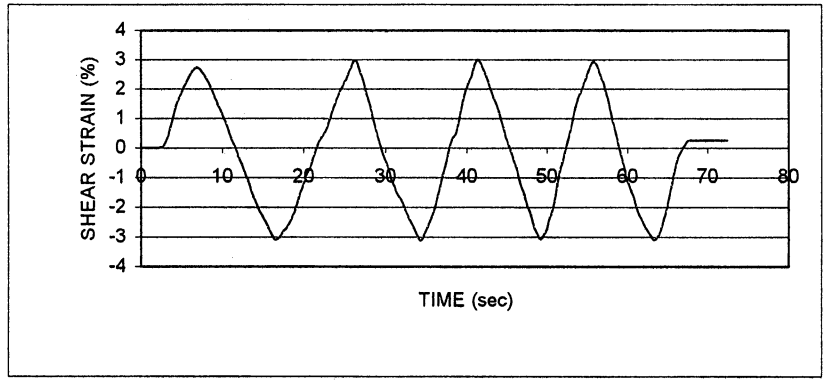

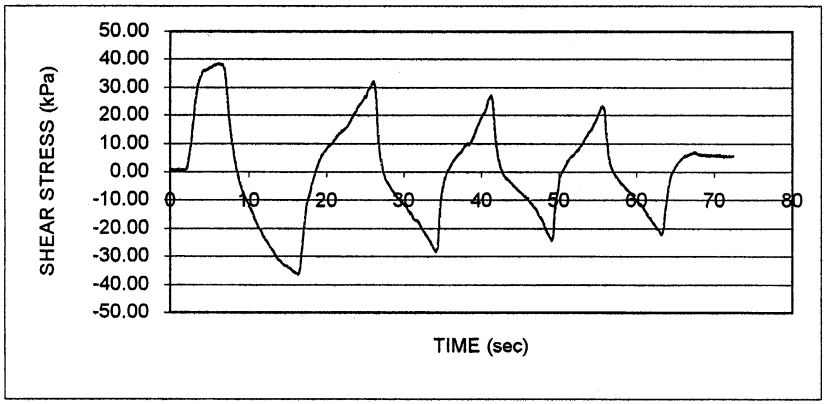

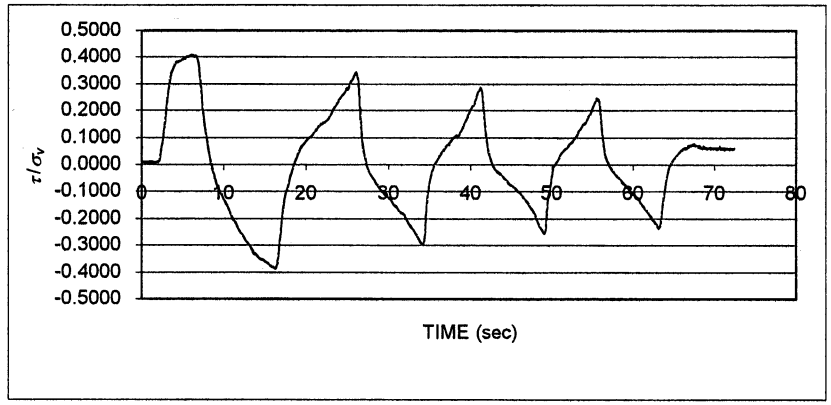

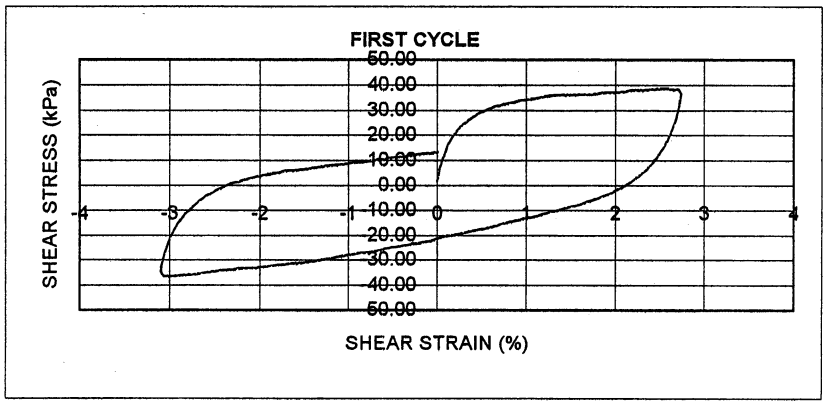

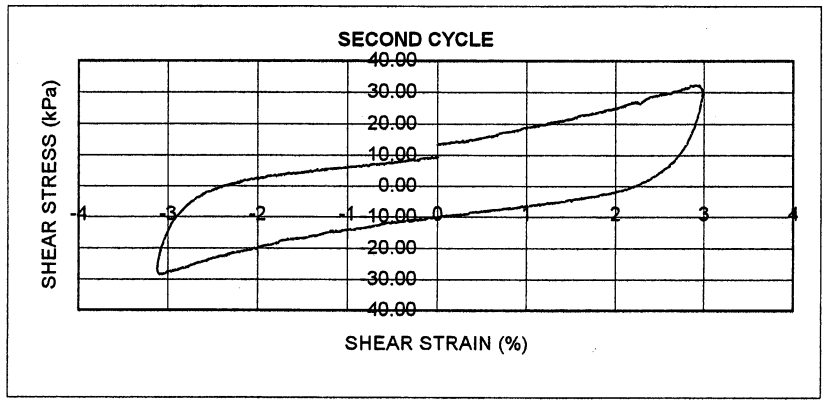

UCLA Soil Dynamics Laboratory

Double Specimen Direct Simple Shear (DSDSS) Test

Principal investigator: Mladen Vucetic, Professor

Test performed by Kentaro Tabata

Test no: 8

Project:	PEARL			Date:	11/30/2001
Sample name:	LA Bulk Mail (P-1)			Depth (ft):	17.5
Symbol:	CL	LL (%):	26.3	Silt content (%):	44.8
Specific gravity:	2.73	PI:	8.1	Clay content (%):	26.0
Comments:					

Estimated G_{max} (MPa):	38.0

SHEAR MODULUS				DAMPING RATIO	
Step	γ_c (%)	G_s (MPa)	G_s/G_{max}	γ_c (%)	λ (%)
2b	0.000383	36.26	0.954		
2b	0.000341	37.56	0.988	0.000694	2.32
26b	0.000687	36.48	0.960	0.001062	2.24
26b	0.000694	37.39	0.984	0.002915	2.67
3b	0.001039	36.56	0.962	0.009912	4.85
3b	0.001062	36.71	0.966	0.028535	8.09
4b	0.002917	34.48	0.907	0.100604	12.11
4b	0.002915	34.73	0.914		
5b	0.010005	29.25	0.770		
5b	0.009912	29.06	0.765		
6b	0.029257	21.48	0.565		
6b	0.028535	21.41	0.563		
7b	0.101805	12.55	0.330		
7b	0.100604	12.47	0.328		
	γ (%)				
(Monotonic loading)	0.506724	5.78	0.152		
	1.009744	3.40	0.090		
	1.503525	2.39	0.063		
	2.004675	1.85	0.049		
	2.503992	1.53	0.040		
	2.735171	1.34	0.035		

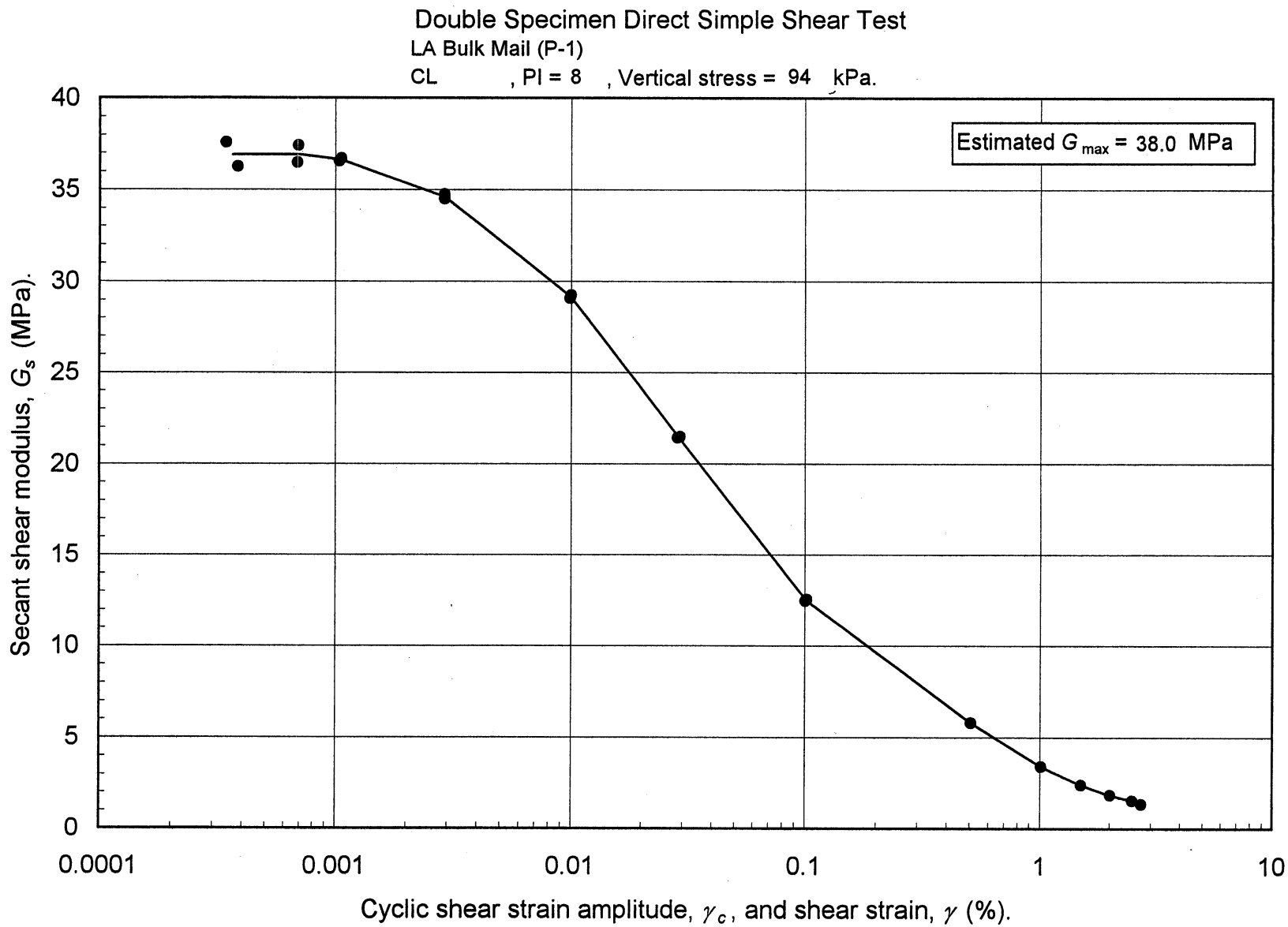
Double Specimen Direct Simple Shear Test
LA Bulk Mail (P-1)
CL , PI = 8 , Vertical stress = 94 kPa.
Estimated G_{max} = 38.0 MPa
Secant shear modulus, G_s (MPa).
40
35
30
25
20
15
10
5
0
0.0001
0.001
0.01
0.1
1
10
Cyclic shear strain amplitude, γ_c, and shear strain, γ (%).

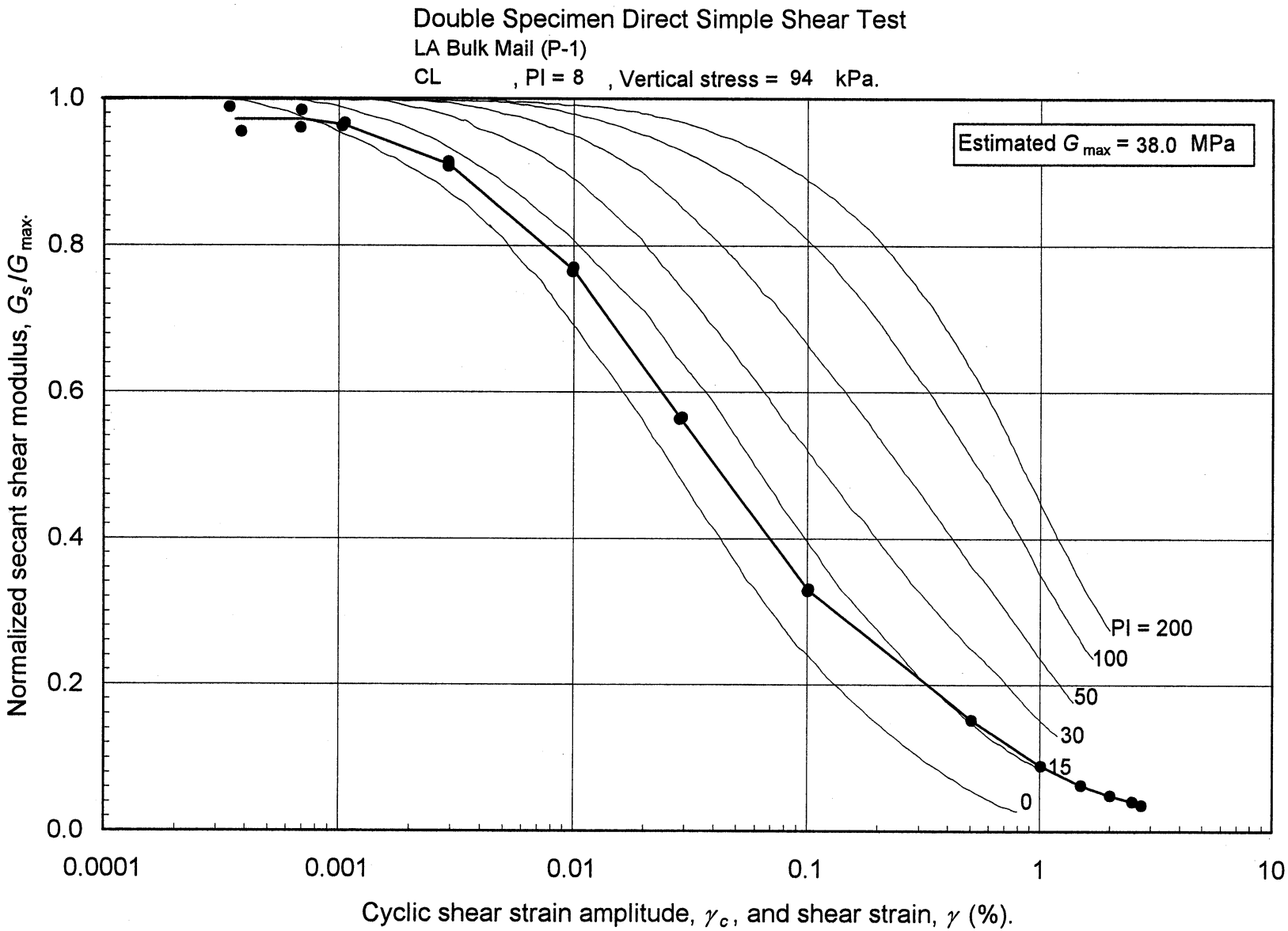
Double Specimen Direct Simple Shear Test
LA Bulk Mail (P-1)
CL , PI = 8 , Vertical stress = 94 kPa.
Estimated G_{max} = 38.0 MPa
PI = 200
100
50
30
15
0
Normalized secant shear modulus, G_s/G_{max}.
1.0
0.8
0.6
0.4
0.2
0.0
0.0001
0.001
0.01
0.1
1
10
Cyclic shear strain amplitude, γ_c, and shear strain, γ (%).

Double Specimen Direct Simple Shear Test

LA Bulk Mail (P-1)

CL , PI = 8 , Vertical stress = 94 kPa.

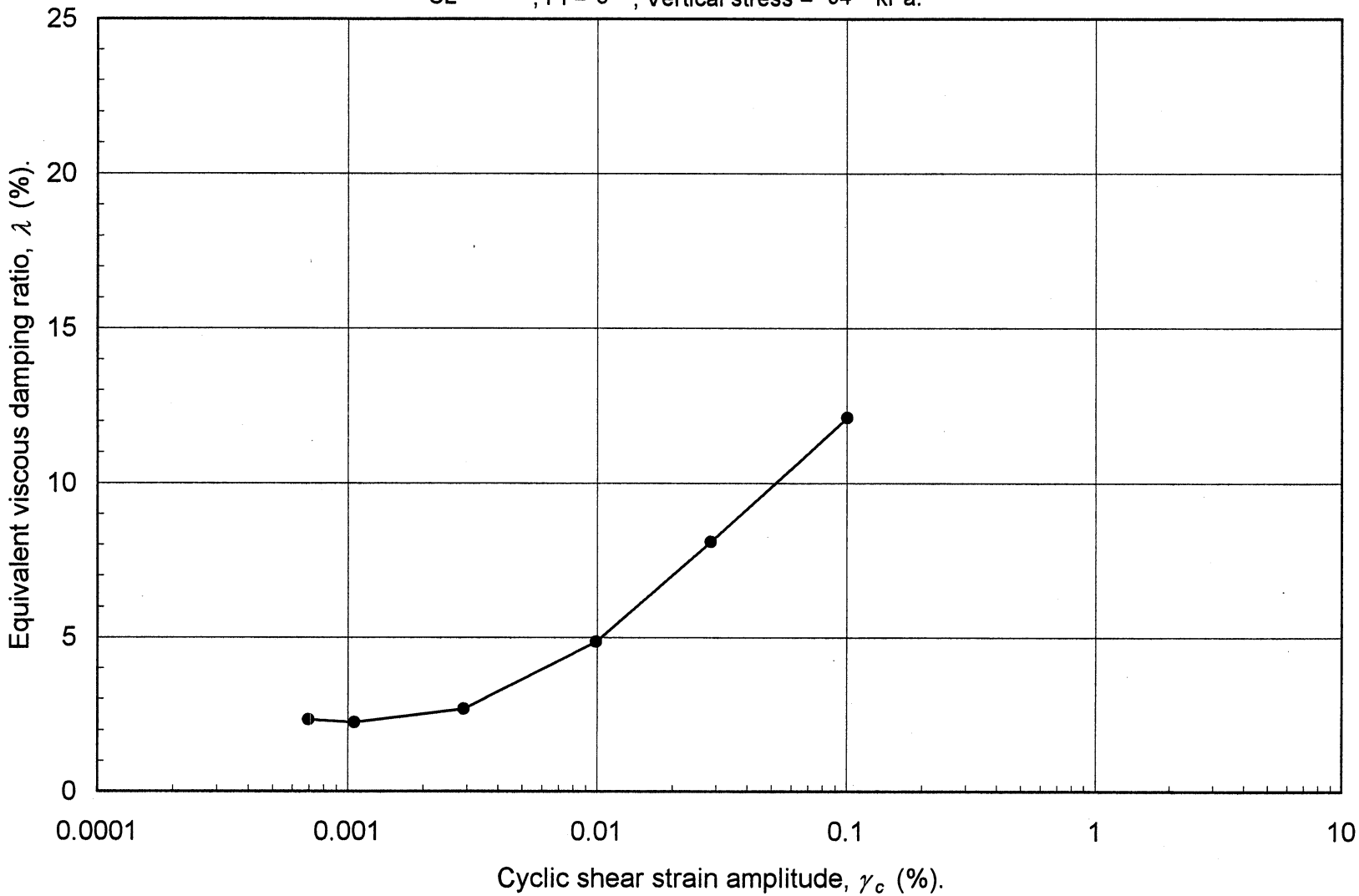

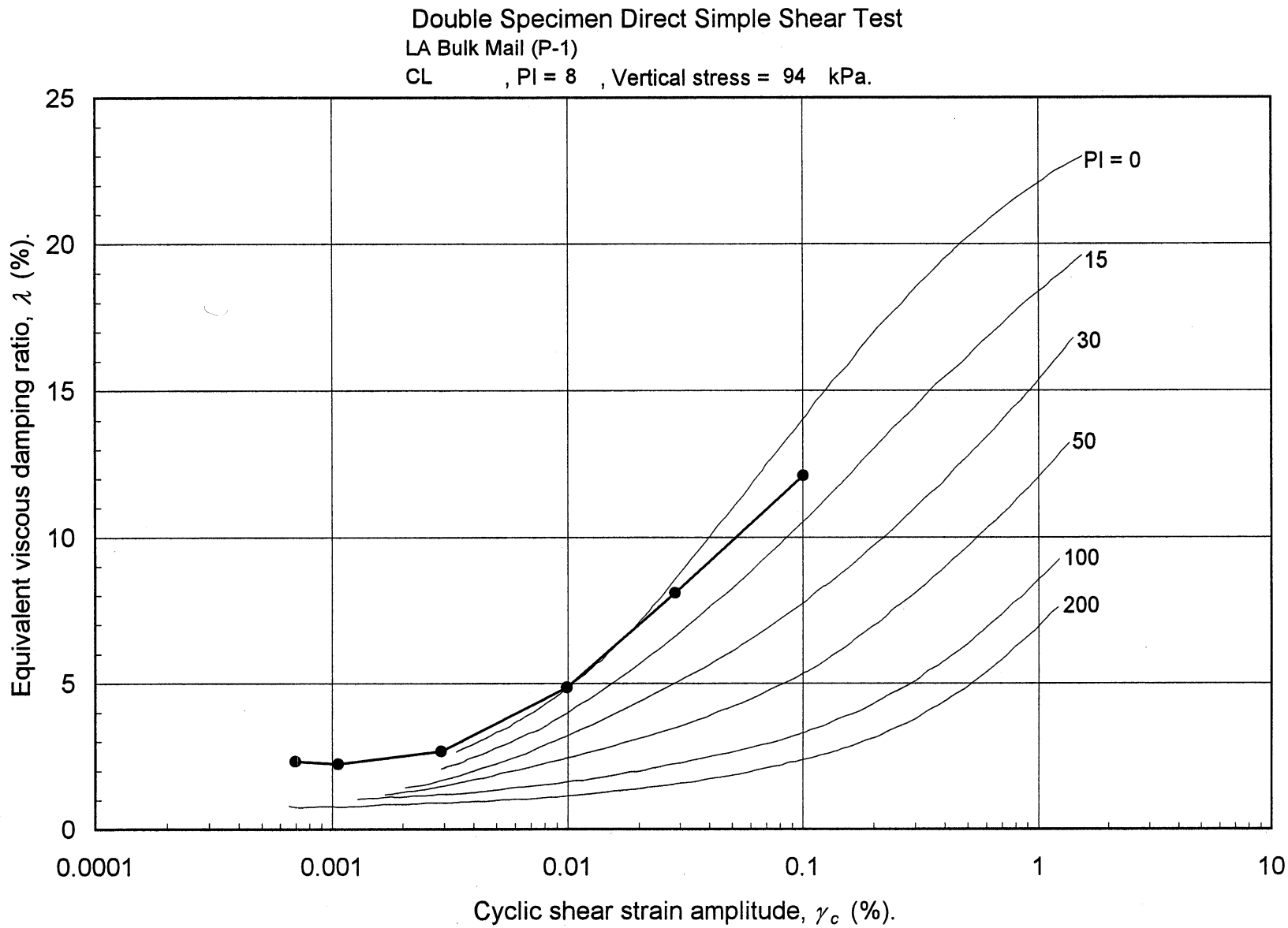
Double Specimen Direct Simple Shear Test
LA Bulk Mail (P-1)
CL , PI = 8 , Vertical stress = 94 kPa.
Equivalent viscous damping ratio, λ (%).
Cyclic shear strain amplitude, γc (%).
0
5
10
15
20
25
0.0001
0.001
0.01
0.1
1
10
PI = 0
15
30
50
100
200

UCLA Soil Dynamics Laboratory

Specific Gravity Test

Principal investigator: Mladen Vucetic, Professor

Test performed by: Kentaro Tabata Test No.: 8

Project:	PEARL			Date:	12/1/2001
Boring:	LA Bulk Mail				
Tube No.:	P-1	Depth (ft):	15.0 -18.0	GWT (ft):	135.0
Comments:	Dark brown silt.				

SPECIFIC GRAVITY TEST

Test No.	1		
Bottle No.	3		
Wt. of bottle (g)	178.08		
Volume of bottle (cm^3)	500		
Wt. of bottle+water+soil (g)	706.04		
Temperature (°C)	21.0		
Wt. of bottle+water (g)	676.40		
Evaporating dish No.	B-13		
Weight of dish (g)	482.86		
Wt. of dish+dry soil (g)	529.55		
Wt. of dry soil (g)	46.69		
Specific gravity of water	0.9980		
Specific gravity of soil	**2.73**		

UCLA Soil Dynamics Laboratory

Grain Size Distribution

Principal investigator: Mladen Vucetic, Professor

Test performed by: Kentaro Tabata Test No.: 8

Project:	PEARL				
Boring:	LA Bulk Mail				
Tube No.:	P-1	Depth (ft):	15.0 -18.0	GWT (ft):	135.0
Comments:	Dark brown silt.				

GRAIN SIZE DISTRIBUTION

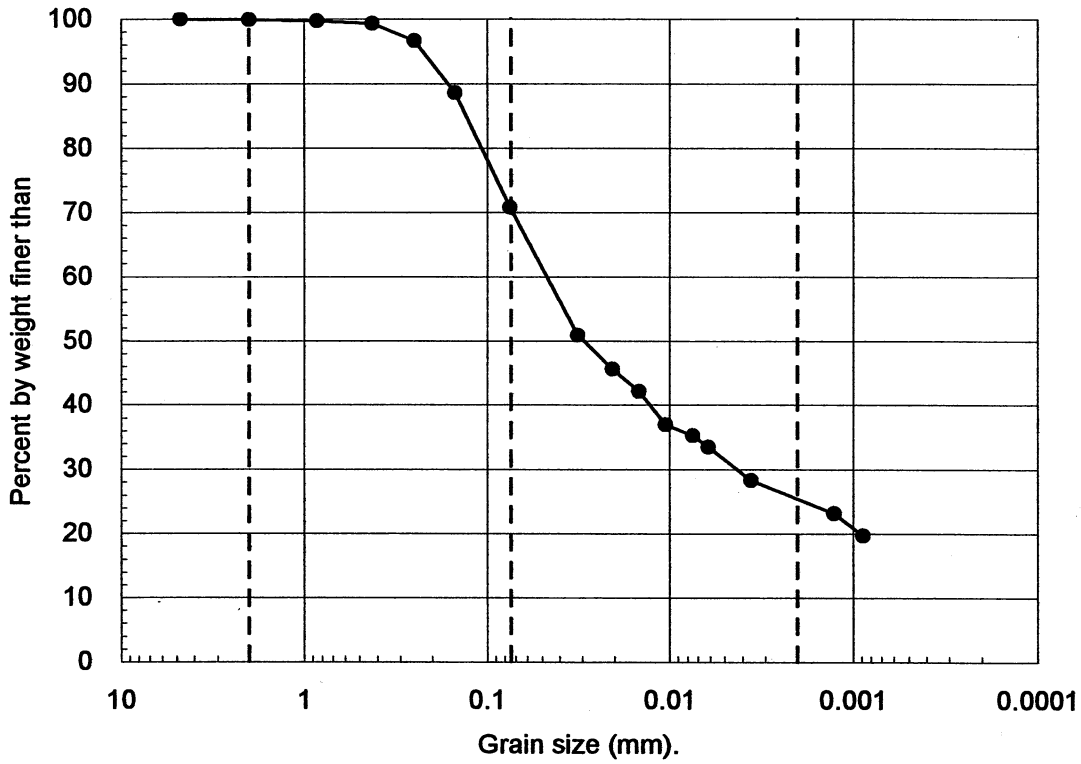

Clay (%)	Silt (%)	Sand (%)	Gravel (%)
26.0	44.8	29.1	0.1

UCLA Soil Dynamics Laboratory

Hydrometer Analysis

Principal investigator: Mladen Vucetic, Professor

Test performed by: Kentaro Tabata Test No.: 8

Project:	PEARL			Date:	1/15/2002
Boring:	LA Bulk Mail				
Tube No.:	P-1	Depth (ft):	15.0 -18.0	GWT (ft):	135.0
Comments:	Dark brown silt.				

HYDROMETER TEST

Time	Elapsed time t (sec)	Temp. T (°C)	Reading R'_T	Corr. reading $R_T=R'_T+c_m$	Depth H (cm)	Grain diameter D (mm)	Temp. corr. m_T	Corr. depth $R_T+m_T-c_d$	% by wt. finer than W_D (%)
11:56:24	0								
11:58:24	120	22.0	1016.5	1017.0	11.97	0.0319	0.700	1014.7	50.81
12:01:24	300	22.0	1015.0	1015.5	12.37	0.0205	0.700	1013.2	45.62
12:06:24	600	22.0	1014.0	1014.5	12.64	0.0147	0.700	1012.2	42.17
12:16:24	1200	22.0	1012.5	1013.0	13.04	0.0105	0.700	1010.7	36.98
12:36:24	2400	22.0	1012.0	1012.5	13.18	0.0075	0.700	1010.2	35.25
12:56:24	3600	22.0	1011.5	1012.0	13.31	0.0061	0.700	1009.7	33.52
14:56:24	10800	22.0	1010.0	1010.5	13.71	0.0036	0.700	1008.2	28.34
13:03:00	90396	22.0	1008.5	1009.0	14.11	0.0013	0.700	1006.7	23.16
16:20:00	188616	22.0	1007.5	1008.0	14.38	0.0009	0.700	1005.7	19.70

APPARATUS

Hydrometer no.:	88-18587	a_0	284.03	a_1	-0.2675
Graduate no.:	3				

FACTORS

Meniscus corr., c_m:	0.5	
Disp. agent corr, c_d:	3.0	
Visc. of water, η.	22.0 °C	9.799E-06 g sec/cm^2
	°C	g sec/cm^3

WEIGHT

Dry soil (g)	32.31
Percent by wt (%)	70.81
Dry soil for sieve (g)	13.32
Total (g)	45.63

UNIT WEIGHT

Specific gravity:		2.73
T	γ_w	γ_s
(°C)	(g/cm^3)	(g/cm^3)
22.0	0.9978	2.7266

UCLA Soil Dynamics Laboratory

Sieve Analysis

Principal investigator: Mladen Vucetic, Professor

Test performed by: Kentaro Tabata Test No.: 8

Project:	PEARL			Date:	1/17/2001
Boring:	LA Bulk Mail				
Tube No.:	P-1	Depth (ft):	15.0 -18.0	GWT (ft):	135.0
Comments:	Dark brown silt.				

SIEVE ANALYSIS

Sieve No.	Diameter (mm)	Sieve (g)	S+wet (g)	S+dry (g)	Retained (g)	Retained (%)	Cumulated (g)	Cumulated (%)	Passing (%)
4	4.750	463.13		463.13	0.00	0.00	0.00	0.00	100.00
10	2.000	422.41		422.46	0.05	0.11	0.05	0.11	99.89
20	0.850	375.42		375.50	0.08	0.18	0.13	0.28	99.72
40	0.425	457.61		457.78	0.17	0.37	0.30	0.66	99.34
60	0.250	323.87		325.13	1.26	2.76	1.56	3.42	96.58
100	0.150	342.15		345.80	3.65	8.00	5.21	11.42	88.58
200	0.075	676.89		685.00	8.11	17.77	13.32	29.19	70.81
Total					13.32	29.19			

WEIGHT

Dry soil for sieve (g)	13.32
Dry soil for hydr. (g)	32.31
Total (g)	45.63
Percent coaser (%)	29.19

UCLA Soil Dynamics Laboratory

Atterberg Limit Determination

Principal investigator: Mladen Vucetic, Professor

Test performed by: Kentaro Tabata Test No.: 8

Project:	PEARL			Date:	1/25/2002
Boring:	LA Bulk Mail				
Tube No.:	P-1	Depth (ft):	15.0 -18.0	GWT (ft):	135.0
Comments:	Dark brown silt.				

LIQUID LIMIT TEST

Test No.	1	2	3	4	5			
Number of blows	48	32	28	17	10			
Container No.	ST-7	ST-6	ST-19	ST-2	ST-20			
Container (g)	30.36	30.11	29.99	30.26	30.37			
Cont+wet soil (g)	36.26	36.56	36.11	37.05	37.61			
Cont+dry soil (g)	35.10	35.28	34.84	35.56	35.98			
Water (g)	1.16	1.28	1.27	1.49	1.63			
Dry soil (g)	4.74	5.17	4.85	5.30	5.61			
Water content (%)	24.47	24.76	26.19	28.11	29.06			

PLASTIC LIMIT TEST

Test No.	1	2	3
Container No.	ST-23	ST-4	ST-13
Container (g)	30.57	30.18	30.20
Cont+wet soil (g)	33.47	32.65	33.89
Cont+dry soil (g)	33.02	32.26	33.34
Water (g)	0.45	0.39	0.55
Dry soil (g)	2.45	2.08	3.14
Water content (%)	18.37	18.75	17.52

ATTERBERG LIMITS

Liquid limit (%)	**26.3**
Plastic limit (%)	**18.2**
Plasticity index	**8.1**

CLASSIFICATION

CL

FLOW CHART

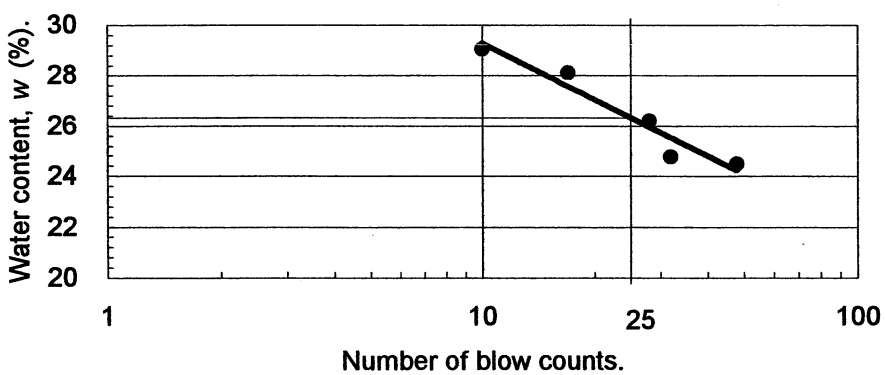

UCLA Soil Dynamics Laboratory

Atterberg Limit Determination

Principal investigator: Mladen Vucetic, Professor

Test performed by: Kentaro Tabata Test No.: 8

Project:	PEARL			Date:	1/25/2002
Boring:	LA Bulk Mail				
Tube No.:	P-1	Depth (ft):	15.0 -18.0	GWT (ft):	135.0
Comments:	Dark brown silt.				

PLASTICITY CHART

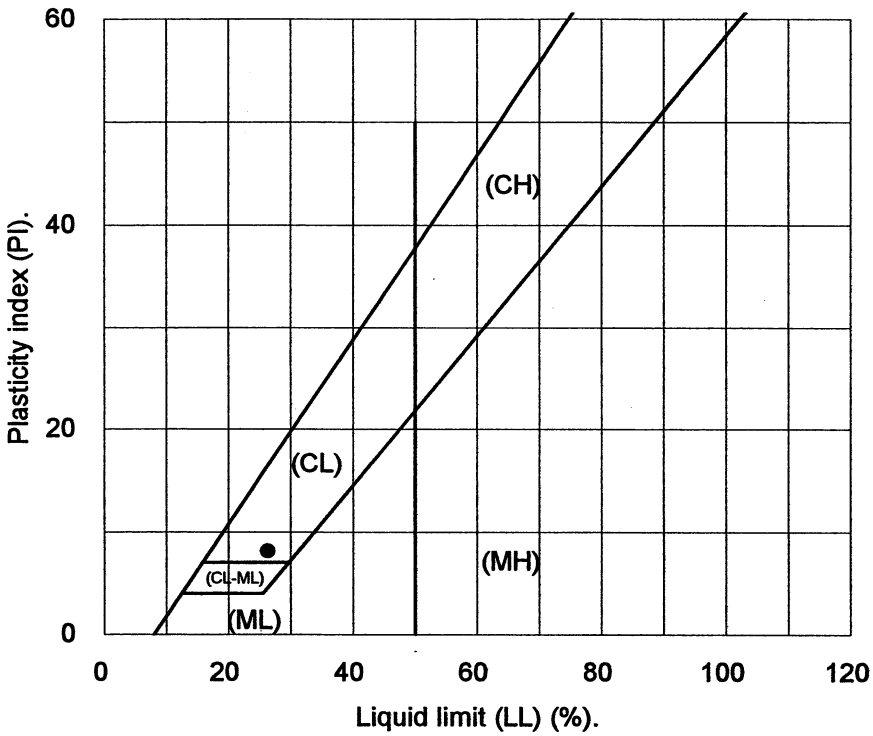

3.10 Test 9: LA BULK MAIL P-3

UCLA Soil Dynamics Laboratory

Double Specimen Direct Simple Shear (DSDSS) Test

Principal investigator: Mladen Vucetic, Professor

Test performed by: Kentaro Tabata Test No.: 9

Project:	PEARL			Date:	12/1/2001
Boring:	LA Bulk Mail				
Tube No.:	P-3	Depth (ft):	50.0 -53.0	GWT (ft):	135.0 (reported by others)
Comments:	Greenish grey silt. Specimen obtained from the bottom of the tube (specimen depth ~ 52.5 ft).				

FORM 1: SPECIMEN PREPARATION

WATER CONTENT, SPECIFIC GRAVITY				UNIT WEIGHT, VOID RATIO, SATURATION			
	Before consol.	After shearing			Before consol.	Before shearing	After shearing
Container No.	ST-15	MT-13	MT-19	Average weight (g)	132.26	132.26	
Cont+wet soil (g)	51.57	180.78	182.29	Height (cm)	1.965	1.879	
Cont+dry soil (g)	47.21	154.50	155.69	Area (cm^2)	34.94	34.94	
Container (g)	30.26	49.58	50.17	Volume (cm^3)	68.66	65.67	
Water (g)	4.36	26.28	26.60	Unit weight (g/cm^3)	1.926	2.014	
Dry soil (g)	16.95	104.92	105.52	Unit weight (kN/m^3)	18.88	19.74	
Water content(%)	25.72	25.05	25.21	Void ratio	0.78	0.70	
Avg. water cont. (%)	25.72		25.13	Saturation (%)	89.8	99.7	
Spceific gravity			2.73				

HEIGHT OF SPECIMEN						
	Before consol.		Before shearing	After shearing		
	Top	Bottom	Average	Average		
Height (cm)	1.965	1.965	1.879	1.879		

AREA OF SPECIMEN						
Initial diameter (cm)			6.670	Initial area (cm^2)		34.942
Load (kg)	Stress (kg/cm^2)	Stress (kN/m^2)	Diameter (cm)	Membrane (cm)	Corrected diameter (cm)	Area (cm^2)

LA Bulk Mail P-3					
DSDSS TEST - Step 2b2					
Type of soil: ML					
LL	47.5	PI	18.0	%Silt	54.9
e_0	0.70	S_0 (%)	99.7	%Clay	38.0
σ_v (kPa)	289	OCR	n/a	w (%)	25.7
γ_c (%)	~0.00038	H_0 (mm)	18.79	Spec. Gr.	2.73

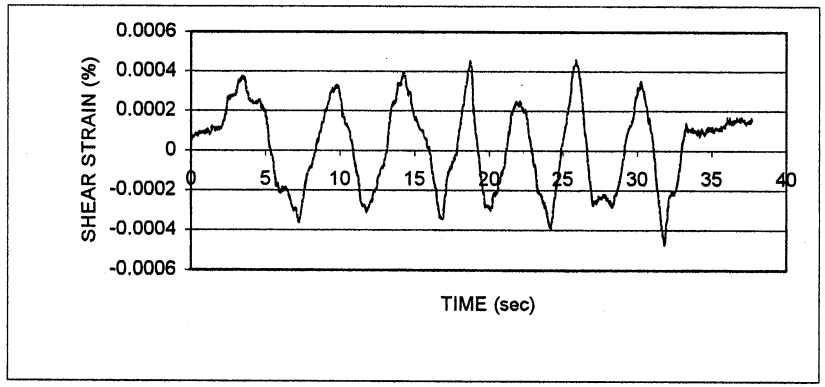

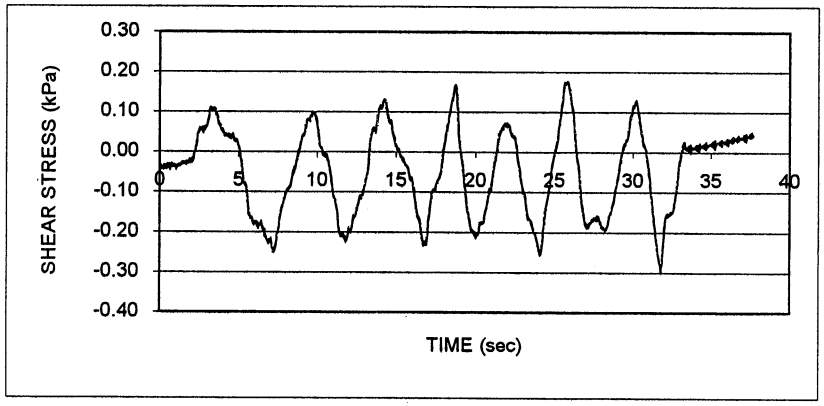

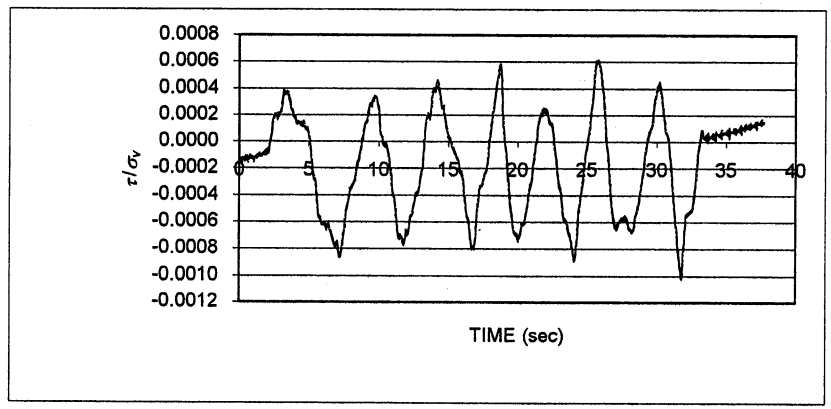

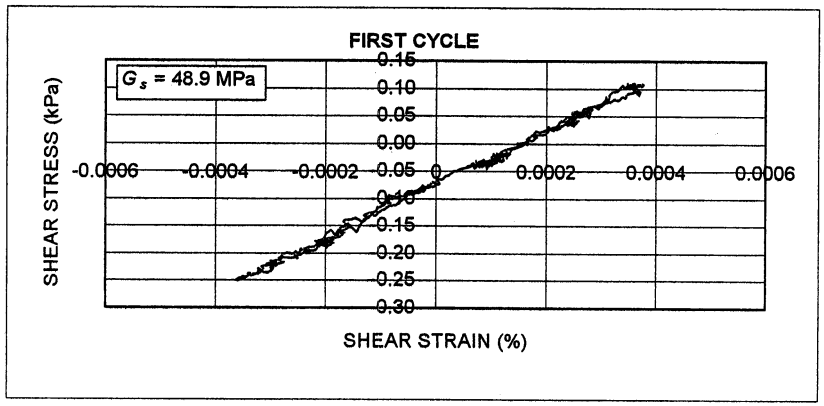

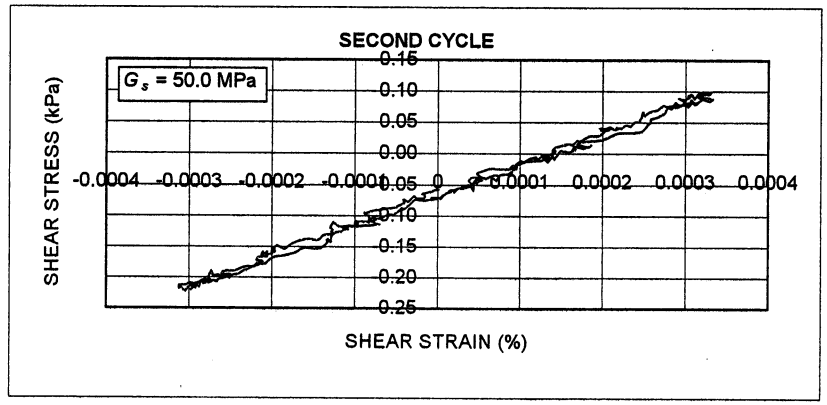

LA Bulk Mail P-3					
DSDSS TEST - Step 26b2					
Type of soil: ML					
LL	47.5	PI	18.0	%Silt	54.9
e_0	0.70	S_0 (%)	99.7	%Clay	38.0
σ_v (kPa)	289	OCR	n/a	w (%)	25.7
γ_c (%)	~0.00075	H_0 (mm)	18.79	Spec. Gr.	2.73

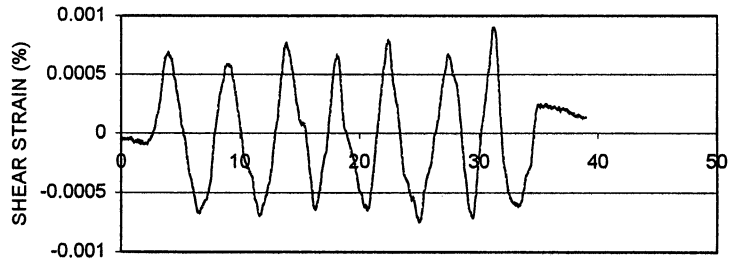

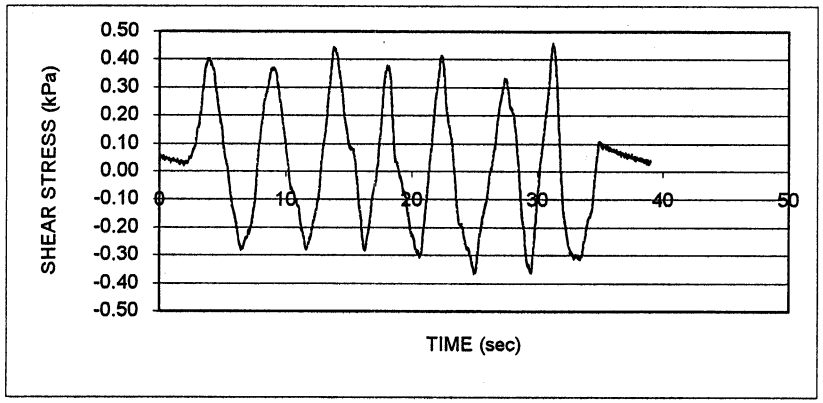

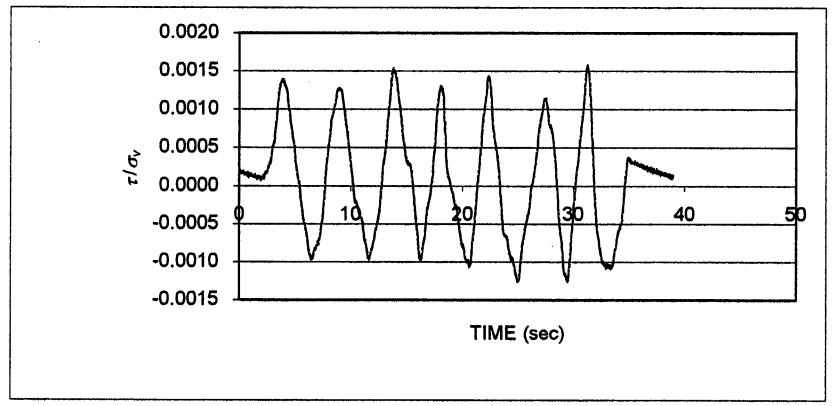

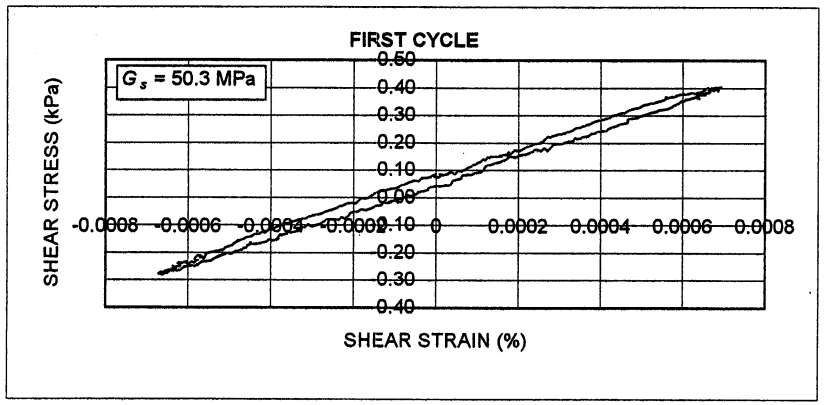

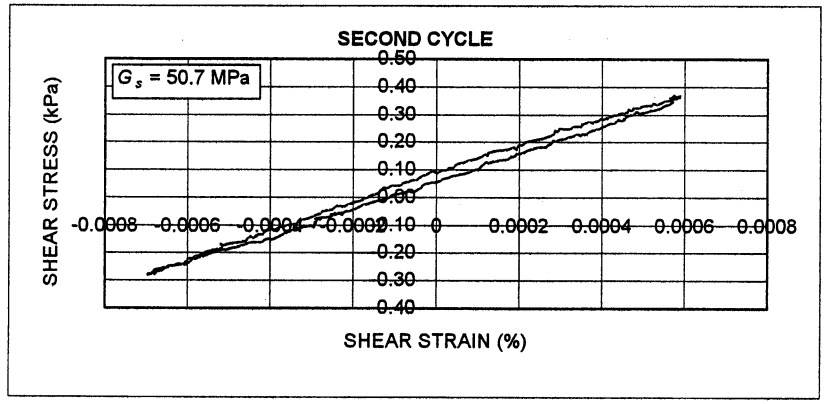

LA Bulk Mail P-3					
DSDSS TEST - Step 3b					
Type of soil: ML					
LL	47.5	PI	18.0	%Silt	54.9
e_0	0.70	S_0 (%)	99.7	%Clay	38.0
σ_v (kPa)	289	OCR	n/a	w (%)	25.7
γ_c (%)	~0.001	H_0 (mm)	18.79	Spec. Gr.	2.73

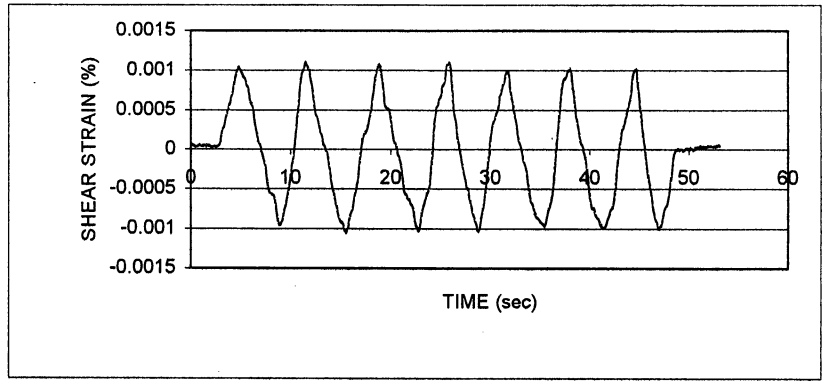

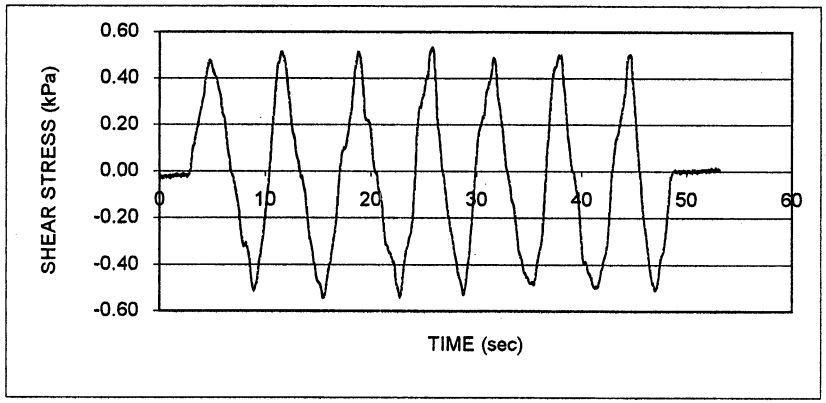

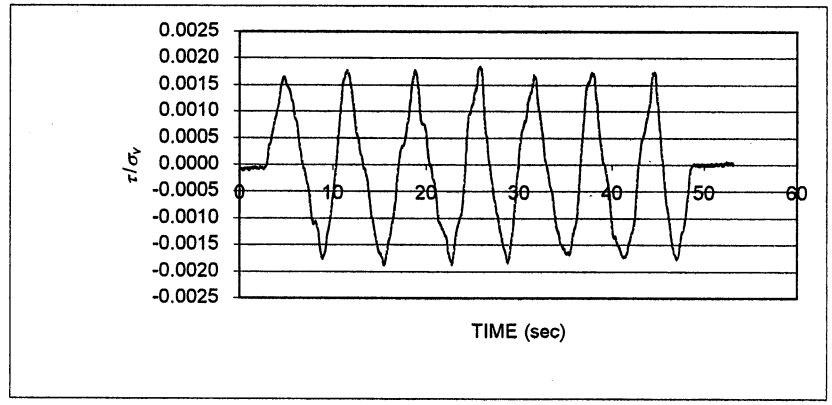

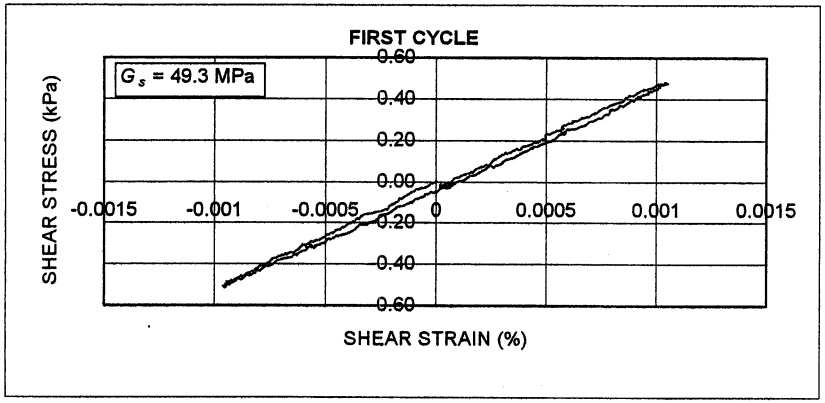

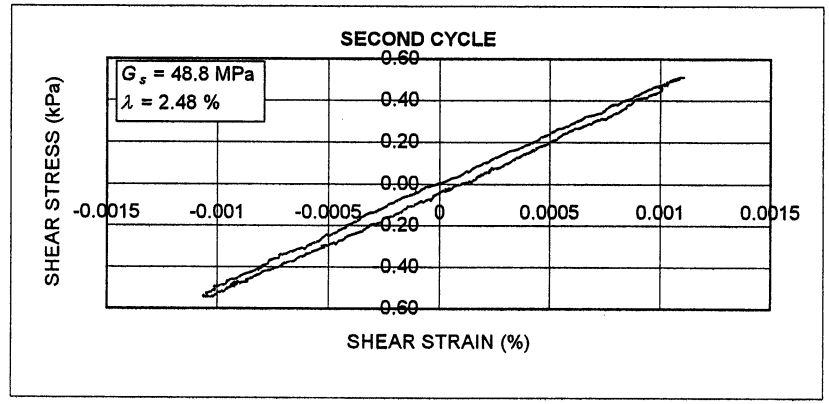

LA Bulk Mail P-3					
DSDSS TEST - Step 4b					
Type of soil: ML					
LL	47.5	PI	18.0	%Silt	54.9
e_0	0.70	S_0 (%)	99.7	%Clay	38.0
σ_v (kPa)	289	OCR	n/a	w (%)	25.7
γ_c (%)	~0.0022	H_0 (mm)	18.79	Spec. Gr.	2.73

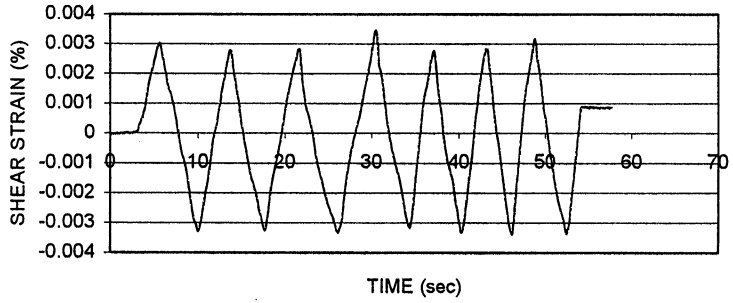

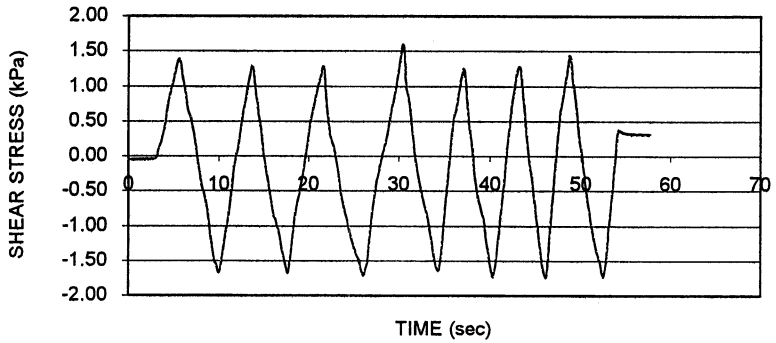

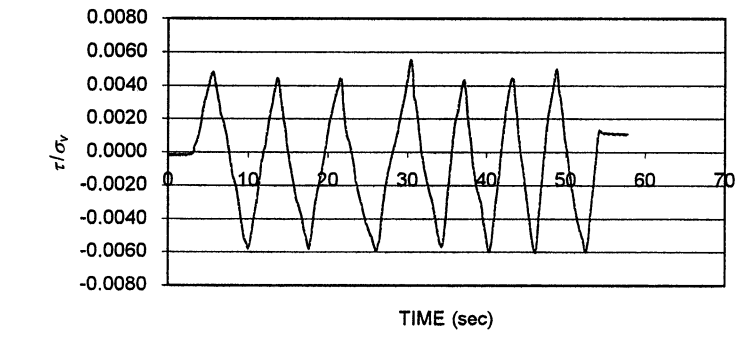

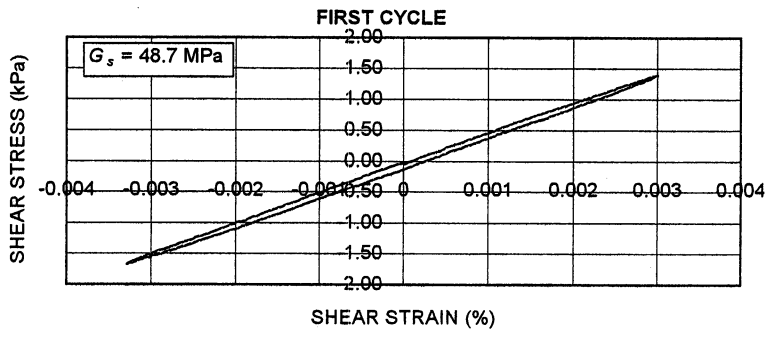

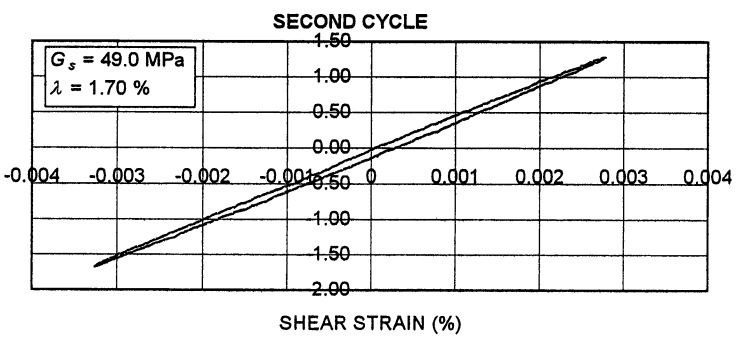

LA Bulk Mail P-3					
DSDSS TEST - Step 5b					
Type of soil: ML					
LL	47.5	PI	18.0	%Silt	54.9
e_0	0.70	S_0 (%)	99.7	%Clay	38.0
σ_v (kPa)	289	OCR	n/a	w (%)	25.7
γ_c (%)	~0.011	H_0 (mm)	18.79	Spec. Gr.	2.73

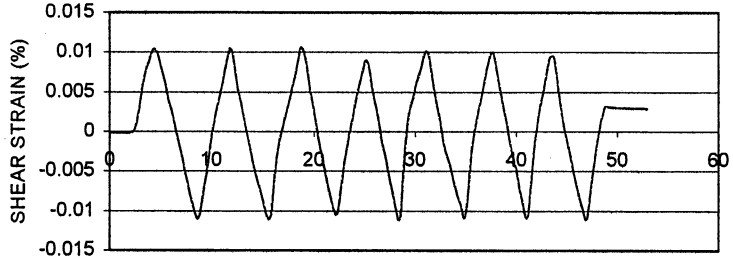

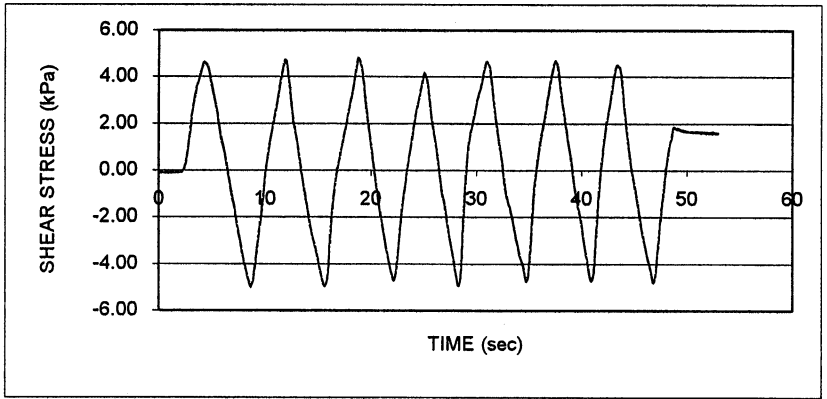

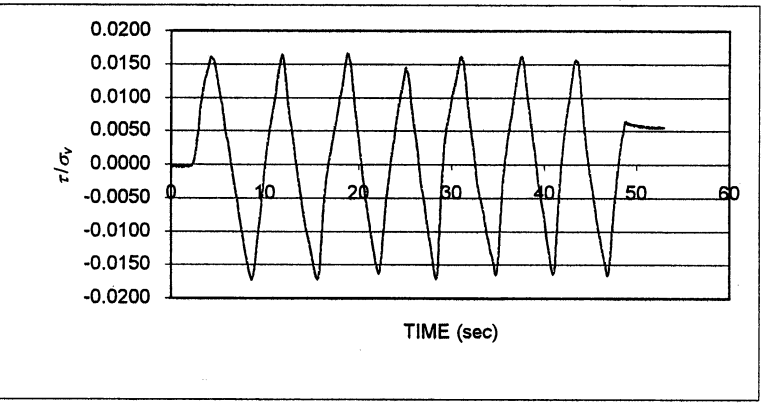

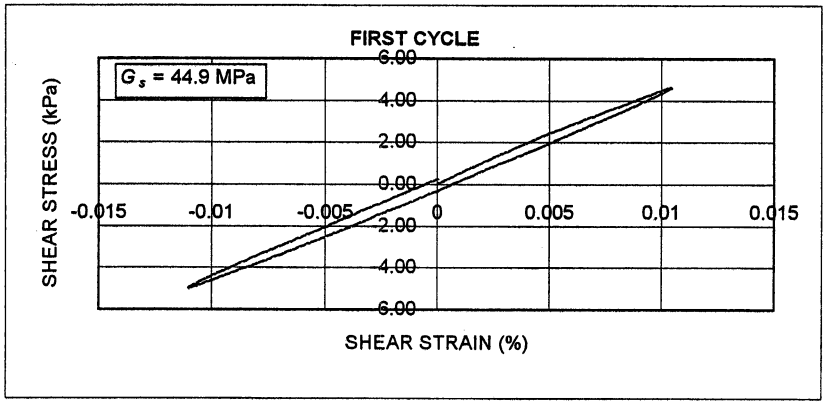

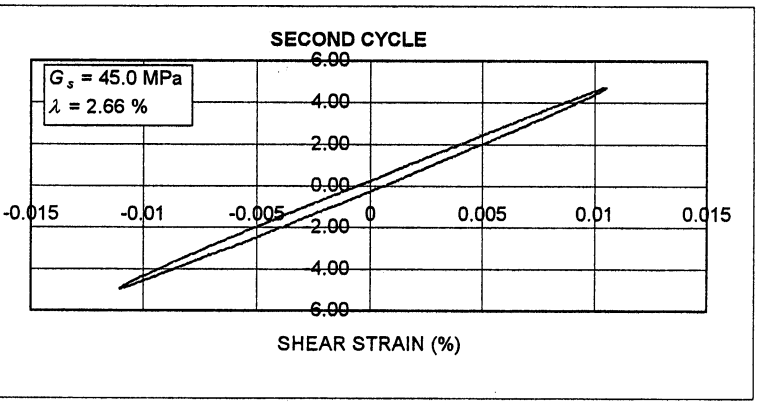

LA Bulk Mail P-3					
DSDSS TEST - Step 6b					
Type of soil: ML					
LL	47.5	PI	18.0	%Silt	54.9
e_0	0.70	S_0 (%)	99.7	%Clay	38.0
σ_v (kPa)	289	OCR	n/a	w (%)	25.7
γ_c (%)	~0.032	H_0 (mm)	18.79	Spec. Gr.	2.73

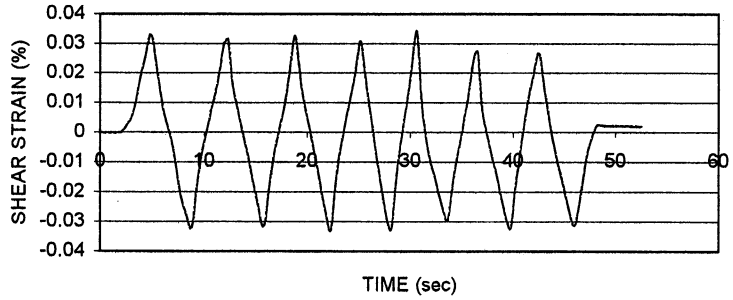

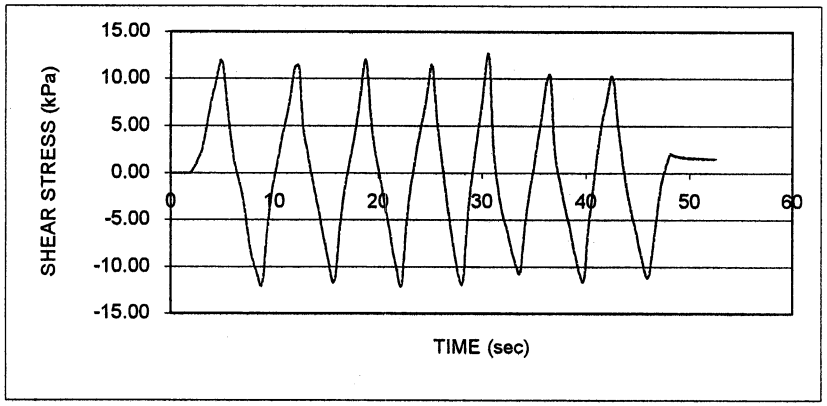

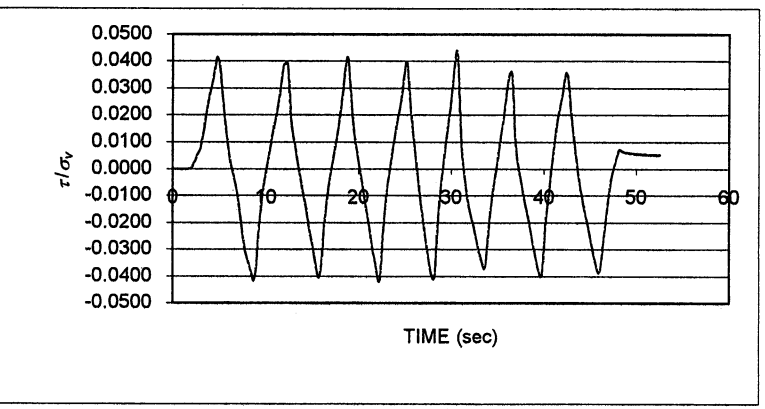

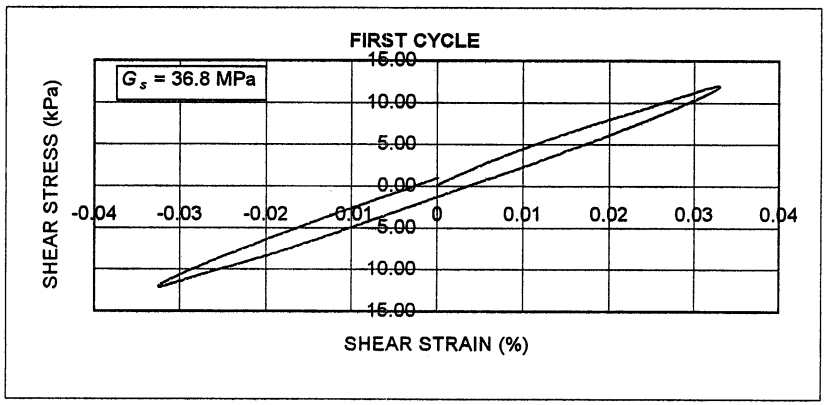

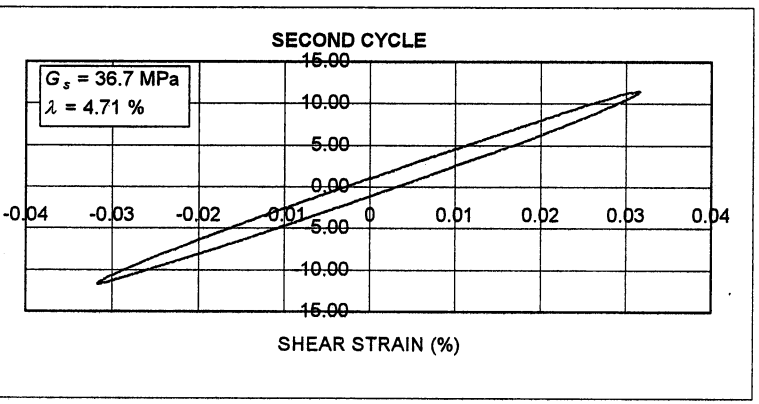

LA Bulk Mail P-3					
DSDSS TEST - Step 7b					
Type of soil: ML					
LL	47.5	PI	18.0	%Silt	54.9
e_0	0.70	S_0 (%)	99.7	%Clay	38.0
σ_v (kPa)	289	OCR	n/a	w (%)	25.7
γ_c (%)	~0.1	H_0 (mm)	18.79	Spec. Gr.	2.73

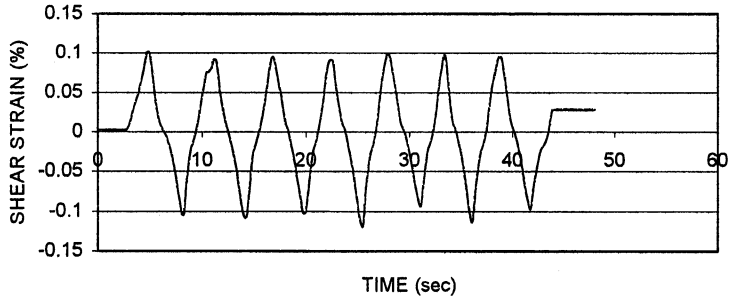

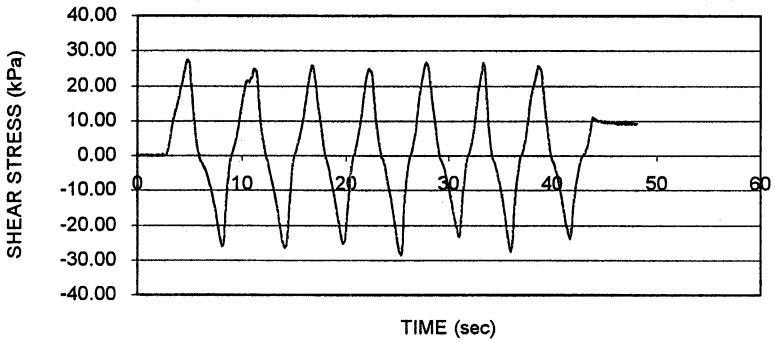

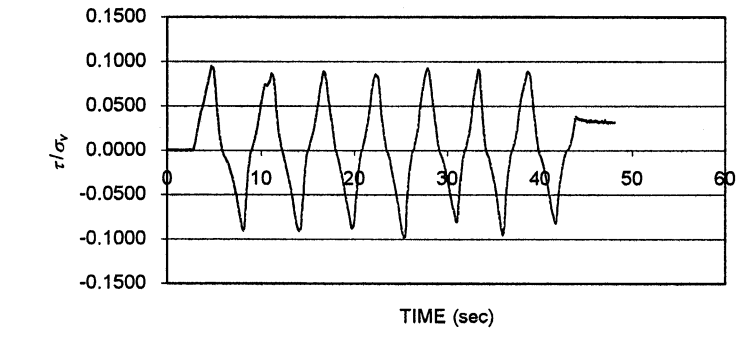

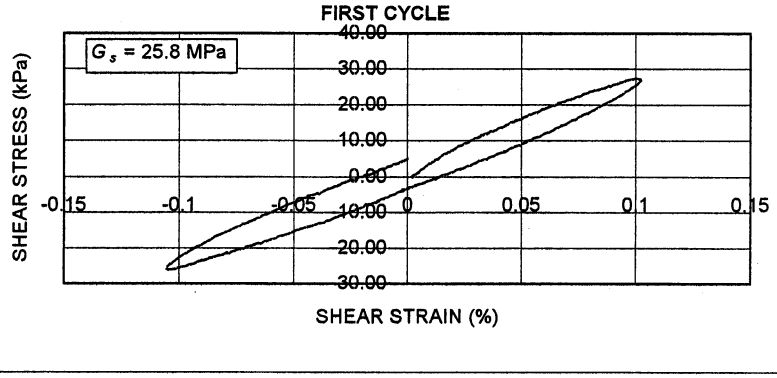

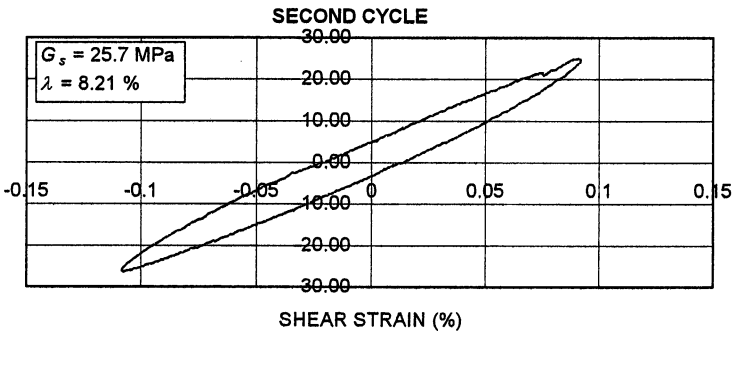

LA Bulk Mail P-3					
DSDSS TEST - Step 8					
Type of soil: ML					
LL	47.5	PI	18.0	%Silt	54.9
e_0	0.70	S_0 (%)	99.7	%Clay	38.0
σ_v (kPa)	289	OCR	n/a	w (%)	25.7
γ_c (%)	~3.0	H_0 (mm)	18.79	Spec. Gr.	2.73

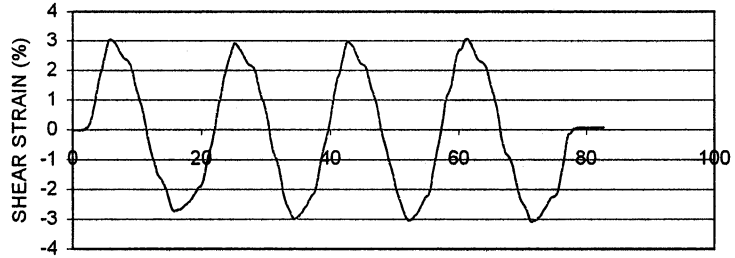

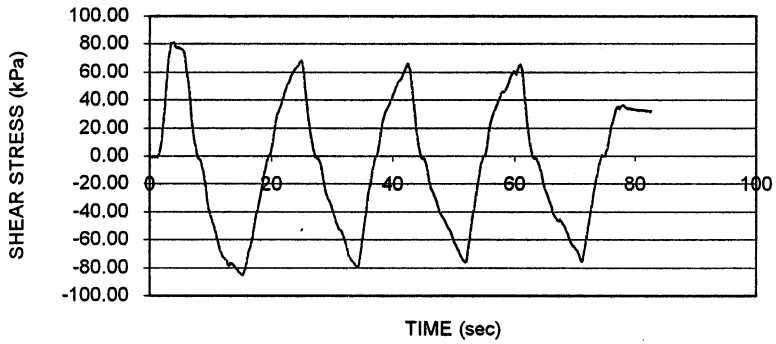

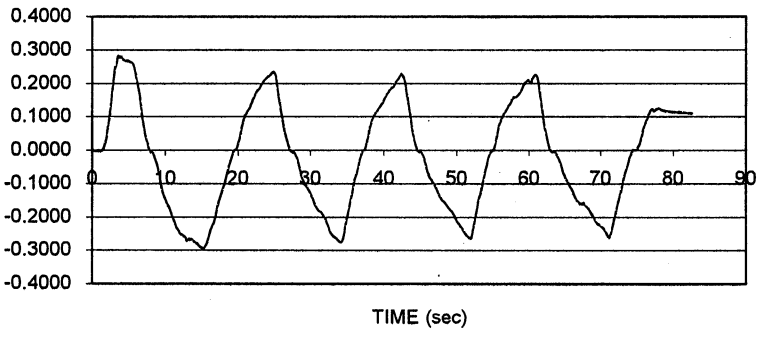

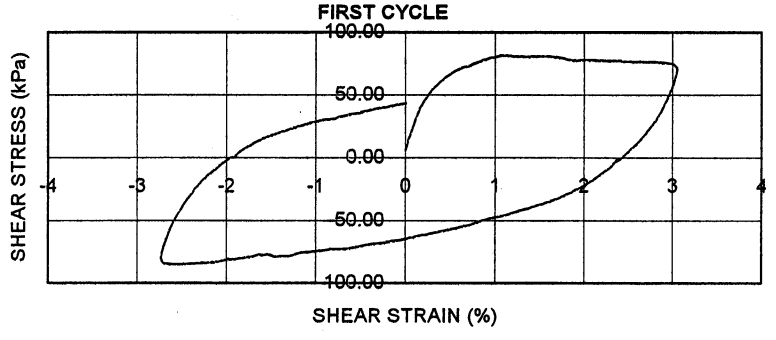

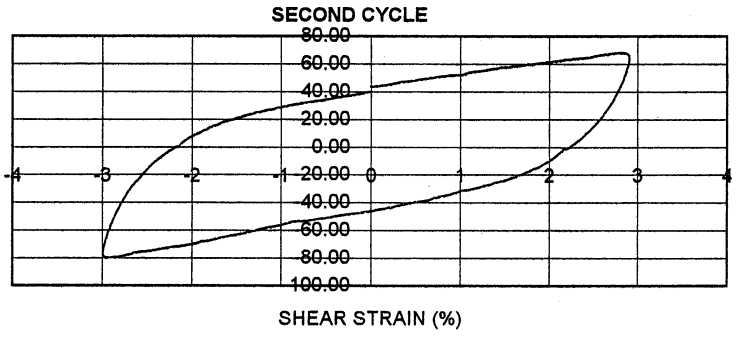

UCLA Soil Dynamics Laboratory

Double Specimen Direct Simple Shear (DSDSS) Test

Principal investigator: Mladen Vucetic, Professor

Test performed by Kentaro Tabata

Test no: 9

Project:	PEARL			Date:	12/1/2001
Sample name:	LA Bulk Mail (P-3)			Depth (ft):	52.5
Symbol:	ML	LL (%):	47.5	Silt content (%):	54.9
Specific gravity:	2.73	PI:	18.0	Clay content (%):	38.0
Comments:					

Estimated G_{max} (MPa):	51.0

SHEAR MODULUS				DAMPING RATIO	
Step	γ_c (%)	G_s (MPa)	G_s/G_{max}	γ_c (%)	λ (%)
2b	0.000370	48.92	0.959		
2b	0.000323	50.01	0.981		
26b	0.000682	50.28	0.986	0.001086	2.48
26b	0.000643	50.72	0.994	0.003024	1.70
3b	0.001008	49.29	0.966	0.010792	2.66
3b	0.001086	48.79	0.957	0.031671	4.71
4b	0.003151	48.74	0.956	0.100300	8.21
4b	0.003024	48.97	0.960		
5b	0.010736	44.90	0.880		
5b	0.010792	44.98	0.882		
6b	0.032763	36.76	0.721		
6b	0.031671	36.67	0.719		
7b	0.103783	25.85	0.507		
7b	0.100300	25.71	0.504		
	γ (%)				
(Monotonic loading)	0.506221	13.21	0.259		
	1.006771	8.01	0.157		
	1.501687	5.38	0.106		
	2.002236	3.87	0.076		
	2.508457	3.06	0.060		
	3.048556	2.35	0.046		

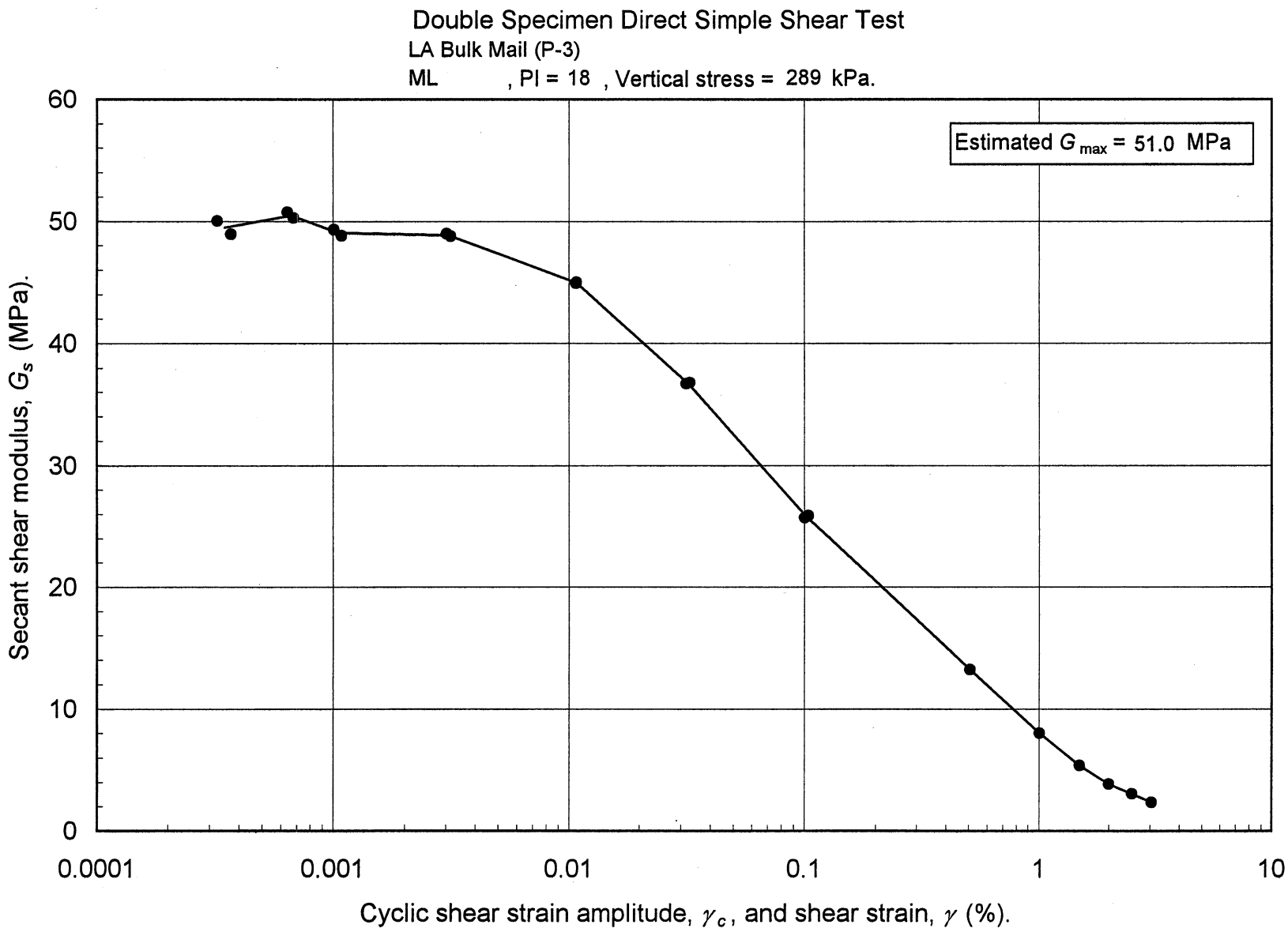
Double Specimen Direct Simple Shear Test
LA Bulk Mail (P-3)
ML , PI = 18 , Vertical stress = 289 kPa.
Estimated G_{max} = 51.0 MPa
Secant shear modulus, G_s (MPa).
60
50
40
30
20
10
0
0.0001
0.001
0.01
0.1
1
10
Cyclic shear strain amplitude, γ_c, and shear strain, γ (%).

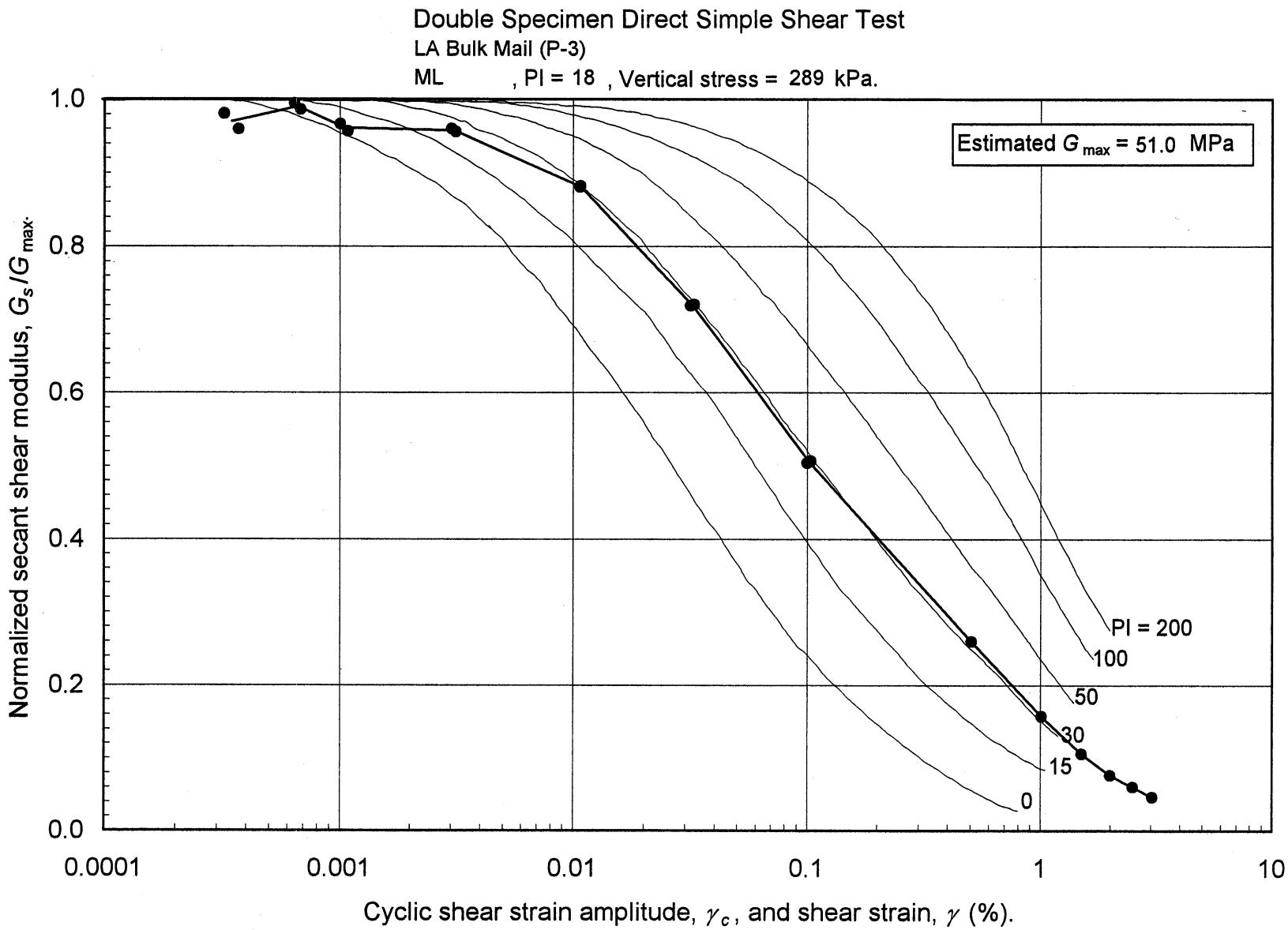
Double Specimen Direct Simple Shear Test
LA Bulk Mail (P-3)
ML , PI = 18 , Vertical stress = 289 kPa.
Estimated G_{max} = 51.0 MPa
Normalized secant shear modulus, G_s/G_{max}
1.0
0.8
0.6
0.4
0.2
0.0
PI = 200
100
50
30
15
0
0.0001
0.001
0.01
0.1
1
10
Cyclic shear strain amplitude, γ_c, and shear strain, γ (%).

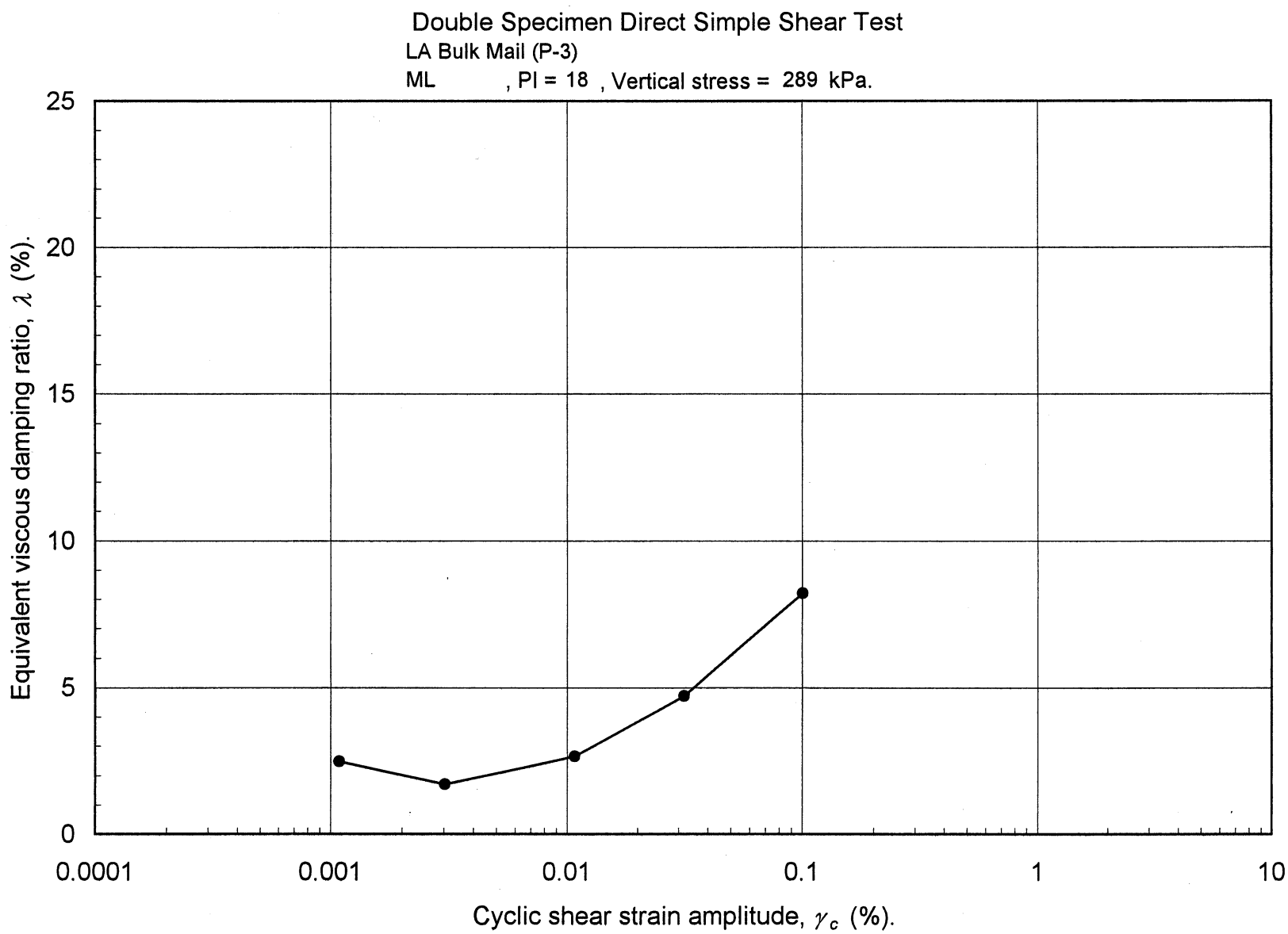
Double Specimen Direct Simple Shear Test
LA Bulk Mail (P-3)
ML , PI = 18 , Vertical stress = 289 kPa.
Equivalent viscous damping ratio, λ (%).
25
20
15
10
5
0
0.0001
0.001
0.01
0.1
1
10
Cyclic shear strain amplitude, γc (%).

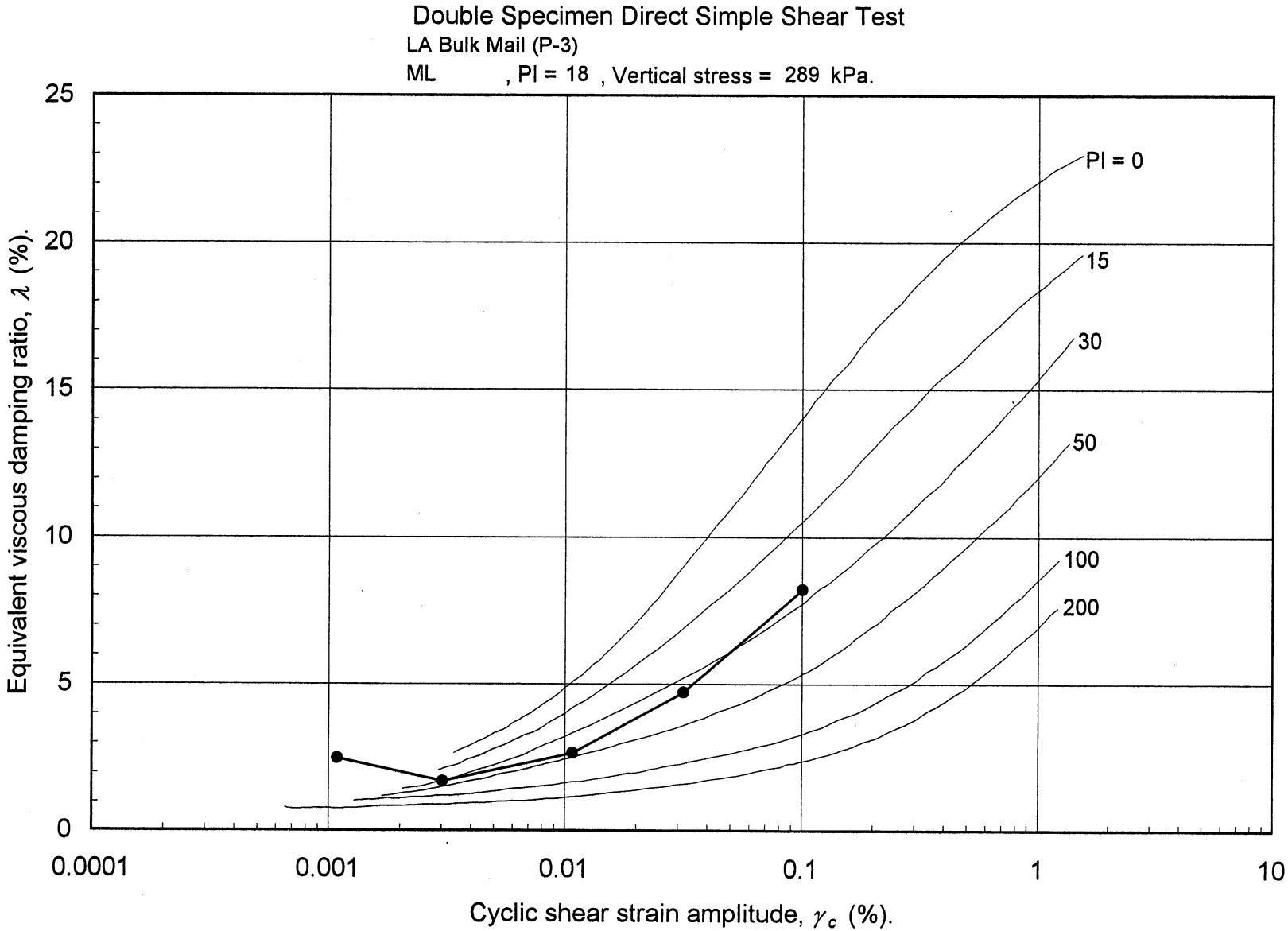
Double Specimen Direct Simple Shear Test
LA Bulk Mail (P-3)
ML , PI = 18 , Vertical stress = 289 kPa.
Equivalent viscous damping ratio, λ (%).
Cyclic shear strain amplitude, γc (%).
0
5
10
15
20
25
0.0001
0.001
0.01
0.1
1
10
PI = 0
15
30
50
100
200

UCLA Soil Dynamics Laboratory

Specific Gravity Test

Principal investigator: Mladen Vucetic, Professor

Test performed by: Kentaro Tabata Test No.: 9

Project:	PEARL			Date:	12/3/2001
Boring:	LA Bulk Mail				
Tube No.:	P-3	Depth (ft):	50.0 -53.0	GWT (ft):	135.0
Comments:	Greenish grey silt.				

SPECIFIC GRAVITY TEST

Test No.	1		
Bottle No.	3		
Wt. of bottle (g)	178.08		
Volume of bottle (cm^3)	500		
Wt. of bottle+water+soil (g)	705.03		
Temperature (°C)	23.0		
Wt. of bottle+water (g)	676.13		
Evaporating dish No.	B-5		
Weight of dish (g)	507.42		
Wt. of dish+dry soil (g)	553.00		
Wt. of dry soil (g)	45.58		
Specific gravity of water	0.9976		
Specific gravity of soil	**2.73**		

UCLA Soil Dynamics Laboratory

Grain Size Distribution

Principal investigator: Mladen Vucetic, Professor

Test performed by: Kentaro Tabata Test No.: 9

Project:	PEARL				
Boring:	LA Bulk Mail				
Tube No.:	P-3	Depth (ft):	50.0 -53.0	GWT (ft):	135.0
Comments:	Greenish grey silt.				

GRAIN SIZE DISTRIBUTION

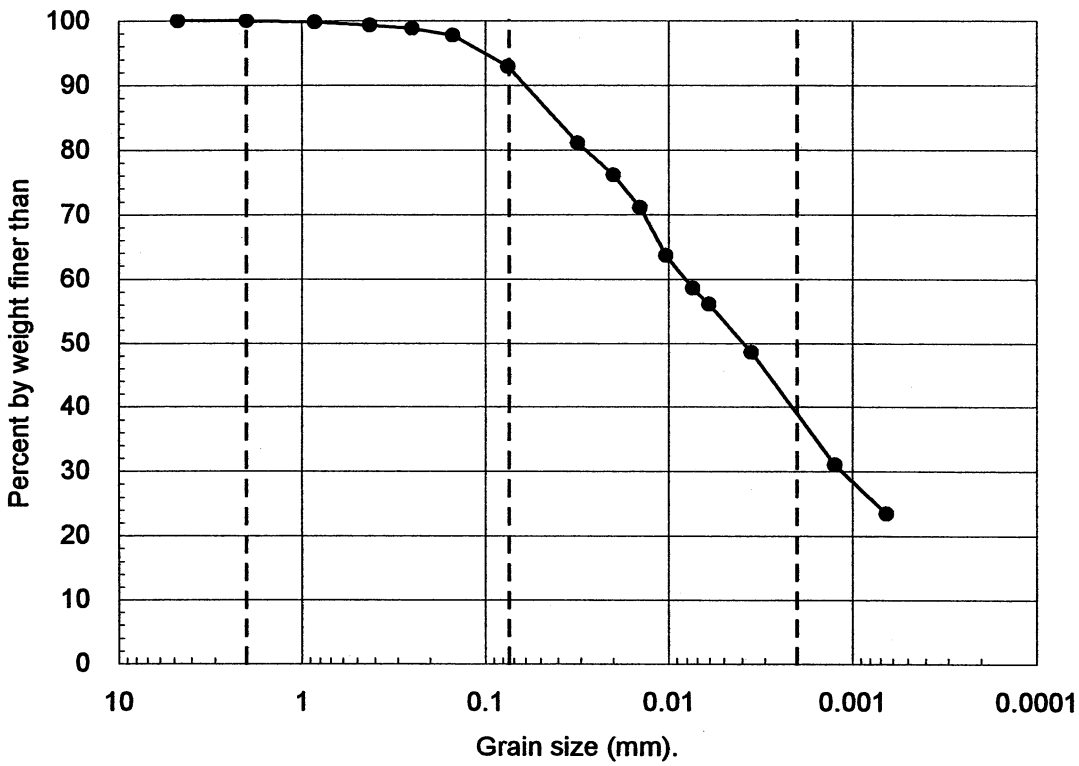

Clay (%)	Silt (%)	Sand (%)	Gravel (%)
38.0	54.9	7.1	0.0

UCLA Soil Dynamics Laboratory

Hydrometer Analysis

Principal investigator: Mladen Vucetic, Professor

Test performed by: Kentaro Tabata Test No.: 9

Project:	PEARL			Date:	1/19/2002
Boring:	LA Bulk Mail				
Tube No.:	P-3	Depth (ft):	50.0 -53.0	GWT (ft):	135.0
Comments:	Greenish grey silt.				

HYDROMETER TEST

Time	Elapsed time t (sec)	Temp. T (°C)	Reading R'_T	Corr. reading $R_T=R'_T+c_m$	Depth H (cm)	Grain diameter D (mm)	Temp. corr. m_T	Corr. depth $R_T+m_T-c_d$	% by wt. finer than W_D (%)
11:54:04	0								
11:56:04	120	22.0	1018.0	1018.5	11.57	0.0314	0.700	1016.2	81.10
11:59:04	300	22.0	1017.0	1017.5	11.84	0.0201	0.700	1015.2	76.09
12:04:04	600	22.0	1016.0	1016.5	12.11	0.0144	0.700	1014.2	71.09
12:14:04	1200	22.0	1014.5	1015.0	12.51	0.0103	0.700	1012.7	63.58
12:34:04	2400	22.0	1013.5	1014.0	12.78	0.0074	0.700	1011.7	58.57
12:54:04	3600	22.0	1013.0	1013.5	12.91	0.0061	0.700	1011.2	56.07
14:54:04	10800	22.0	1011.5	1012.0	13.31	0.0036	0.700	1009.7	48.56
14:00:00	93956	22.0	1008.0	1008.5	14.25	0.0012	0.700	1006.2	31.04
13:05:00	349856	22.0	1006.5	1007.0	14.65	0.0007	0.700	1004.7	23.53

APPARATUS

Hydrometer no.:	88-18587	a_0	284.03	a_1	-0.2675
Graduate no.:	1				

FACTORS

Meniscus corr., c_m:	0.5	
Disp. agent corr, c_d:	3.0	
Visc. of water, η.	22.0 °C	9.799E-06 g sec/cm^2
	°C	g sec/cm^3

WEIGHT

Dry soil (g)	29.30
Percent by wt (%)	92.87
Dry soil for sieve (g)	2.25
Total (g)	31.55

UNIT WEIGHT

Specific gravity:		2.73
T	γ_w	γ_s
(°C)	(g/cm^3)	(g/cm^3)
21.0	0.9978	2.7197

UCLA Soil Dynamics Laboratory

Sieve Analysis

Principal investigator: Mladen Vucetic, Professor

Test performed by: Kentaro Tabata Test No.: 9

Project:	PEARL			Date:	1/22/2002
Boring:	LA Bulk Mail				
Tube No.:	P-3	Depth (ft):	50.0 -53.0	GWT (ft):	135.0
Comments:	Greenish grey silt.				

SIEVE ANALYSIS

Sieve No.	Diameter (mm)	Sieve (g)	S+wet (g)	S+dry (g)	Retained (g)	Retained (%)	Cumulated (g)	Cumulated (%)	Passing (%)
4	4.750	463.14		463.14	0.00	0.00	0.00	0.00	100.00
10	2.000	422.41		422.41	0.00	0.00	0.00	0.00	100.00
20	0.850	375.41		375.48	0.07	0.22	0.07	0.22	99.78
40	0.425	457.57		457.73	0.16	0.51	0.23	0.73	99.27
60	0.250	323.86		324.00	0.14	0.44	0.37	1.17	98.83
100	0.150	342.14		342.48	0.34	1.08	0.71	2.25	97.75
200	0.075	676.89		678.43	1.54	4.88	2.25	7.13	92.87
Total					2.25	7.13			

WEIGHT

Dry soil for sieve (g)	2.25
Dry soil for hydr. (g)	29.30
Total (g)	31.55
Percent coaser (%)	7.13

UCLA Soil Dynamics Laboratory

Atterberg Limit Determination

Principal investigator: Mladen Vucetic, Professor

Test performed by: Kentaro Tabata Test No.: 9

Project:	PEARL			Date:	1/25/2002
Boring:	LA Bulk Mail				
Tube No.:	P-3	Depth (ft):	50.0 -53.0	GWT (ft):	135.0
Comments:	Greenish grey silt.				

LIQUID LIMIT TEST

Test No.	1	2	3	4	5			
Number of blows	34	29	23	19	13			
Container No.	ST-22	ST-18	ST-3	ST-5	ST-14			
Container (g)	30.07	30.14	30.18	30.12	30.46			
Cont+wet soil (g)	36.64	37.23	36.29	37.80	38.28			
Cont+dry soil (g)	34.60	34.97	34.29	35.28	35.61			
Water (g)	2.04	2.26	2.00	2.52	2.67			
Dry soil (g)	4.53	4.83	4.11	5.16	5.15			
Water content (%)	45.03	46.79	48.66	48.84	51.84			

PLASTIC LIMIT TEST

Test No.	1	2	3
Container No.	ST-15	ST-24	ST-12
Container (g)	30.26	29.98	30.29
Cont+wet soil (g)	31.45	31.56	32.93
Cont+dry soil (g)	31.17	31.20	32.35
Water (g)	0.28	0.36	0.58
Dry soil (g)	0.91	1.22	2.06
Water content (%)	30.77	29.51	28.16

ATTERBERG LIMITS

Liquid limit (%)	**47.5**
Plastic limit (%)	**29.5**
Plasticity index	**18.0**

CLASSIFICATION

ML

FLOW CHART

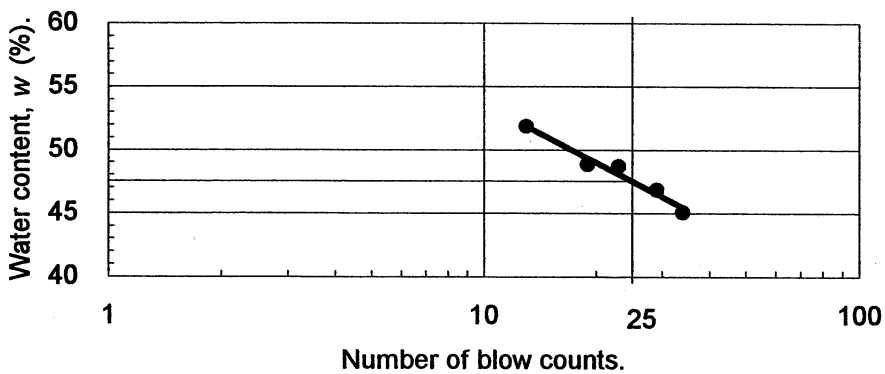

UCLA Soil Dynamics Laboratory

Atterberg Limit Determination

Principal investigator: Mladen Vucetic, Professor

Test performed by: Kentaro Tabata Test No.: 9

Project:	PEARL			Date:	1/25/2002
Boring:	LA Bulk Mail				
Tube No.:	P-3	Depth (ft):	50.0 -53.0	GWT (ft):	135.0
Comments:	Greenish grey silt.				

PLASTICITY CHART

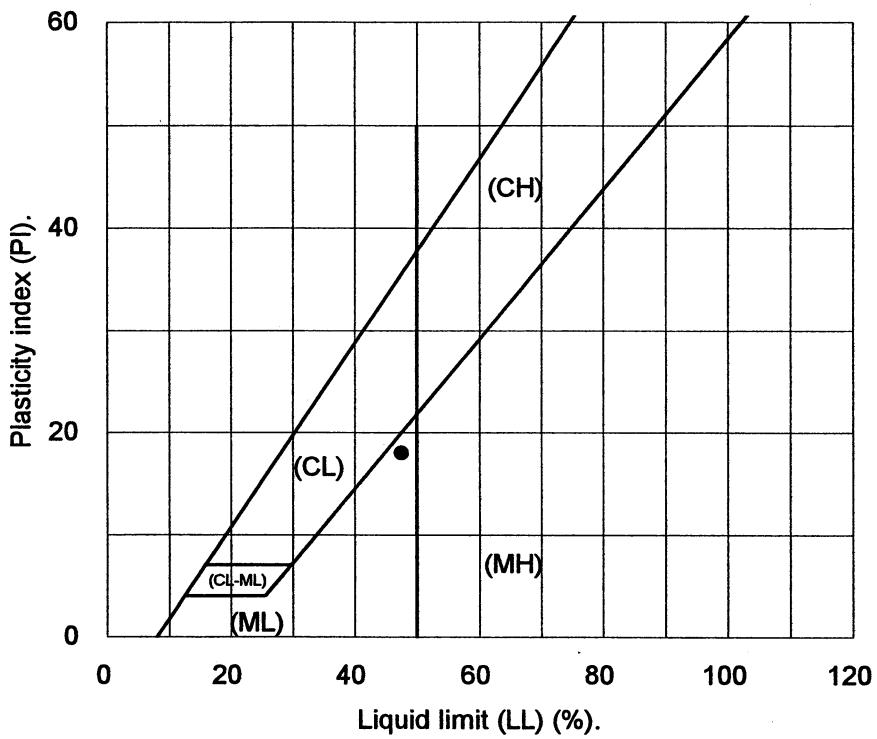

3.11 Test 10: HALLS VALLEY P-1

UCLA Soil Dynamics Laboratory

Double Specimen Direct Simple Shear (DSDSS) Test

Principal investigator: Mladen Vucetic, Professor

Test performed by: Kentaro Tabata Test No.: 10

Project:	PEARL			Date:	2/12/2002
Boring:	Halls Valley				
Tube No.:	P-1	Depth (ft):	6.0 -9.0	GWT (ft):	65.0 (reported by others)
Comments:	Silty clay. Specimen obtained from the top of the tube (specimen depth ~ 6 ft).				

FORM 1: SPECIMEN PREPARATION

WATER CONTENT, SPECIFIC GRAVITY				UNIT WEIGHT, VOID RATIO, SATURATION			
	Before consol.	After shearing			Before consol.	Before shearing	After shearing
Container No.	ST-23	MT-7	MT-14	Average weight (g)	130.35	130.35	
Cont+wet soil (g)	41.12	181.36	179.45	Height (cm)	1.960	1.943	
Cont+dry soil (g)	38.92	154.79	152.06	Area (cm^2)	34.84	34.84	
Container (g)	30.58	50.76	50.22	Volume (cm^3)	68.28	67.69	
Water (g)	2.20	26.57	27.39	Unit weight (g/cm^3)	1.909	1.926	
Dry soil (g)	8.34	104.03	101.84	Unit weight (kN/m^3)	18.71	18.87	
Water content(%)	26.38	25.54	26.90	Void ratio	0.76	0.75	
Avg. water cont. (%)	26.38		26.22	Saturation (%)	92.2	93.5	
Spceific gravity			2.66				

HEIGHT OF SPECIMEN						
	Before consol.		Before shearing	After shearing		
	Top	Bottom	Average	Average		
Height (cm)	1.960	1.960	1.943	1.943		

AREA OF SPECIMEN						
Initial diameter (cm)	6.660			Initial area (cm^2)	34.837	
Load (kg)	Stress (kg/cm^2)	Stress (kN/m^2)	Diameter (cm)	Membrane (cm)	Corrected diameter (cm)	Area (cm^2)

Halls Valley P-1					
DSDSS TEST - Step 2					
Type of soil: CL					
LL	42.1	PI	26.1	%Silt	36.1
e_0	0.75	S_0 (%)	93.5	%Clay	35.0
σ_v (kPa)	37	OCR	n/a	w (%)	26.2
γ_c (%)	~0.0004	H_0 (mm)	19.43	Spec. Gr.	2.66

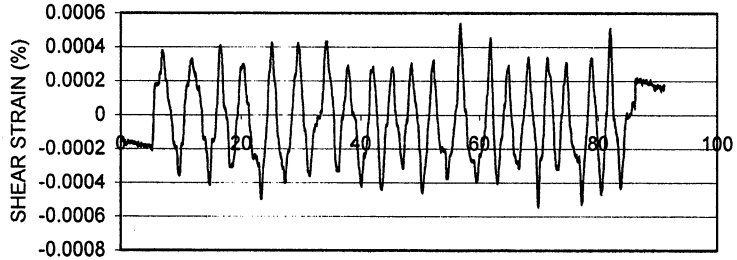

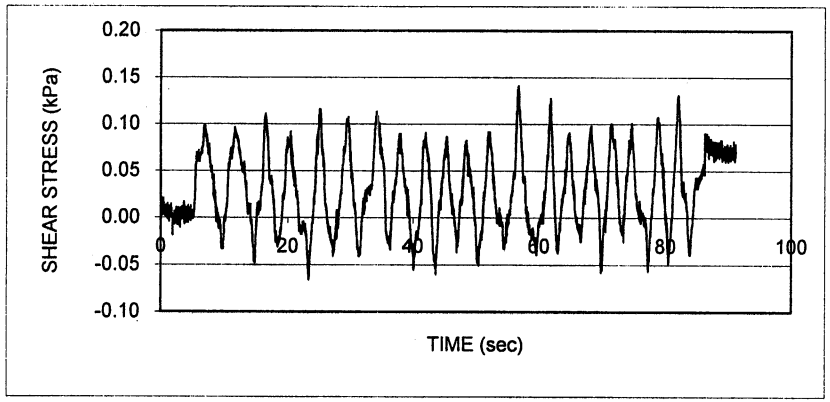

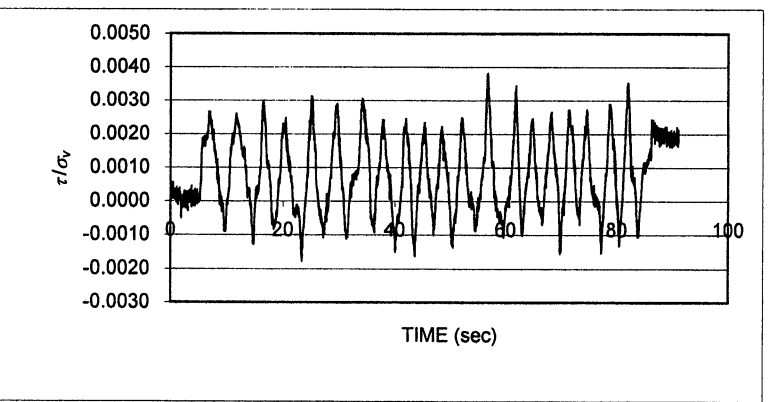

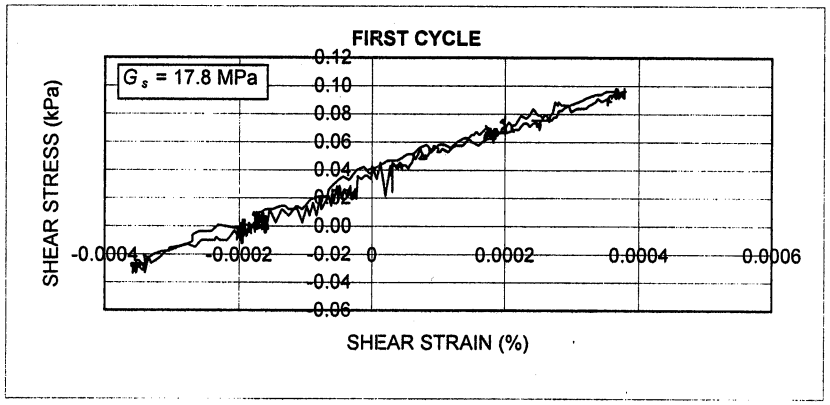

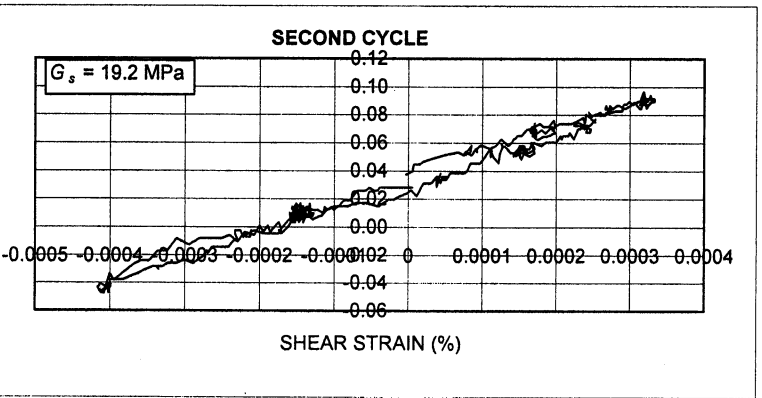

Halls Valley P-1					
DSDSS TEST - Step 26					
Type of soil: CL					
LL	42.1	PI	26.1	%Silt	36.1
e_0	0.75	S_0 (%)	93.5	%Clay	35.0
σ_v (kPa)	37	OCR	n/a	w (%)	26.2
γ_c (%)	~0.00075	H_0 (mm)	19.43	Spec. Gr.	2.66

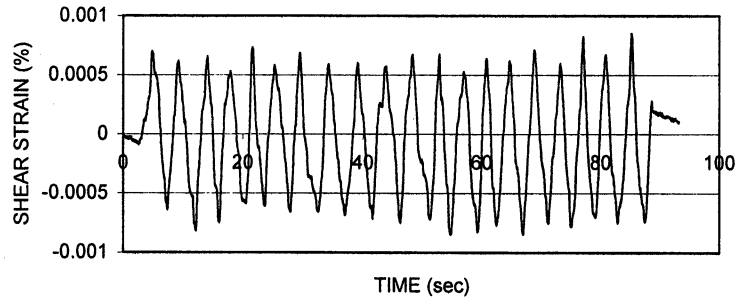

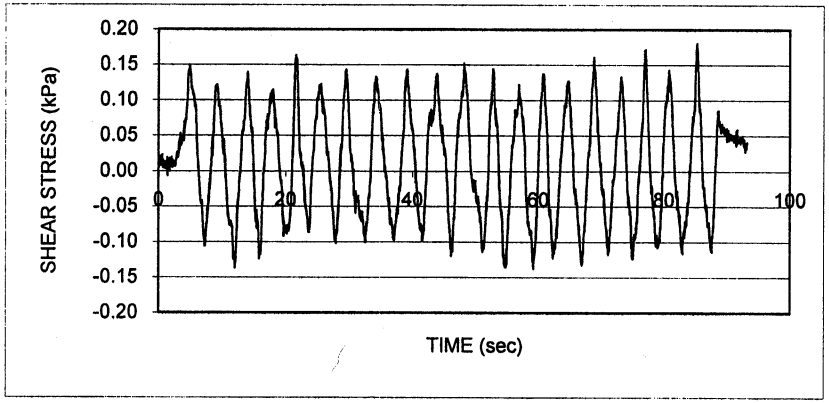

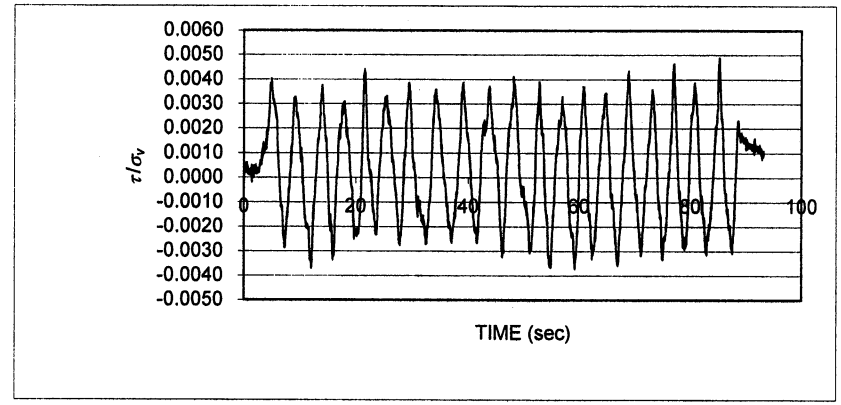

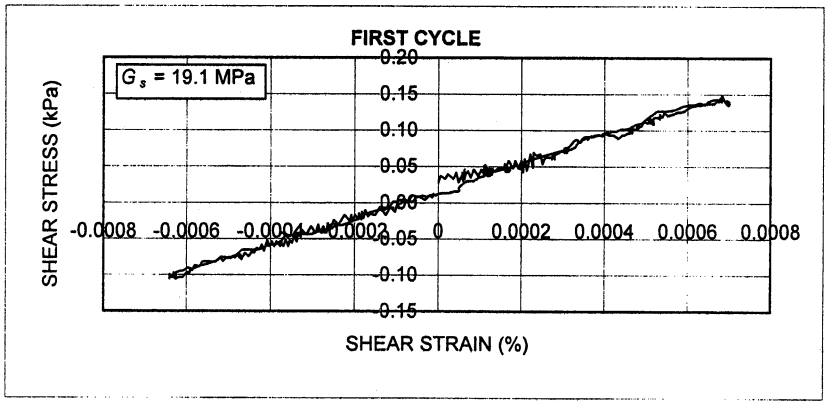

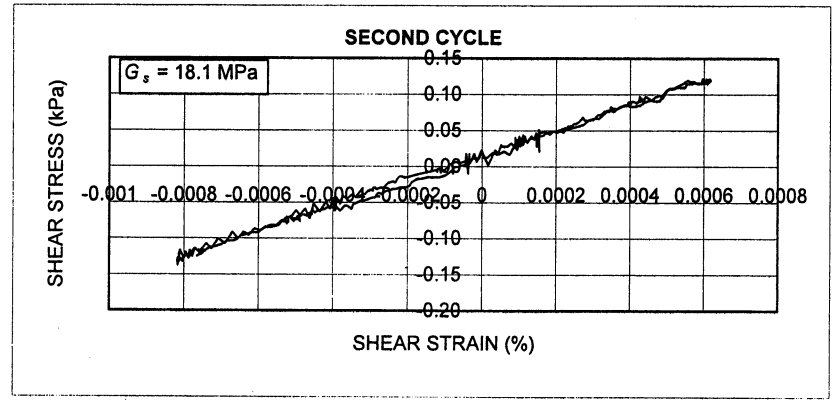

Halls Valley P-1					
DSDSS TEST - Step 3					
Type of soil: CL					
LL	42.1	PI	26.1	%Silt	36.1
e_0	0.75	S_0 (%)	93.5	%Clay	35.0
σ_v (kPa)	37	OCR	n/a	w (%)	26.2
γ_c (%)	~0.001	H_0 (mm)	19.43	Spec. Gr.	2.66

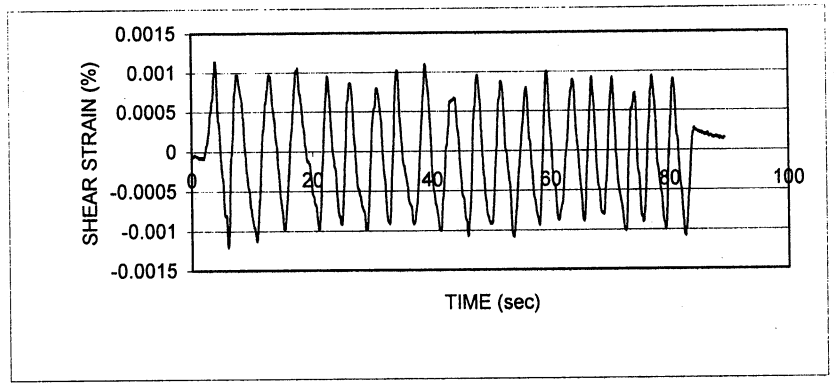

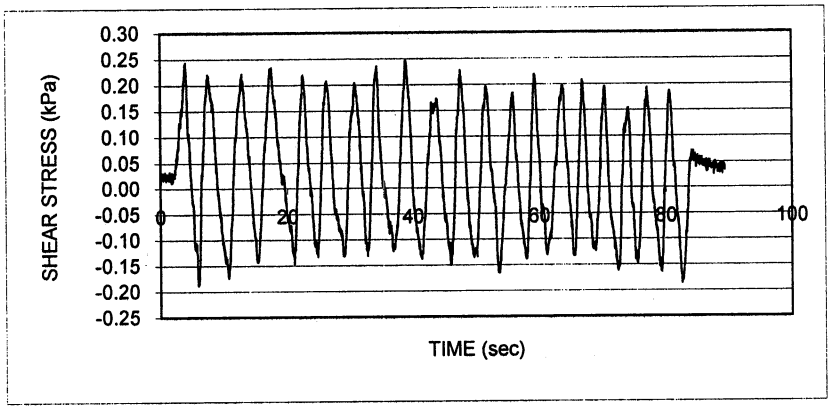

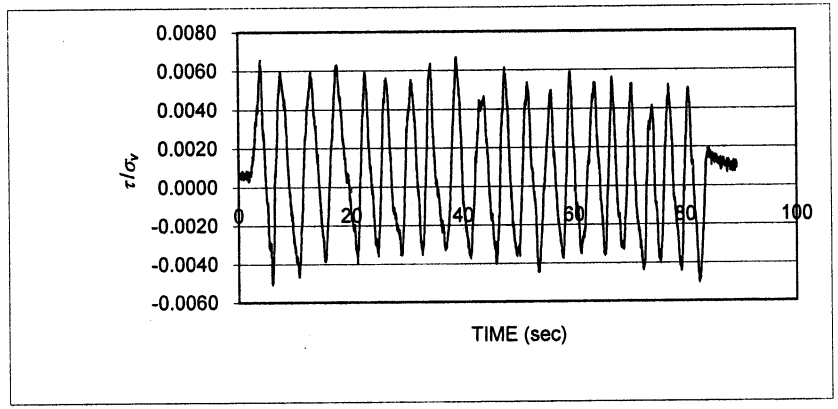

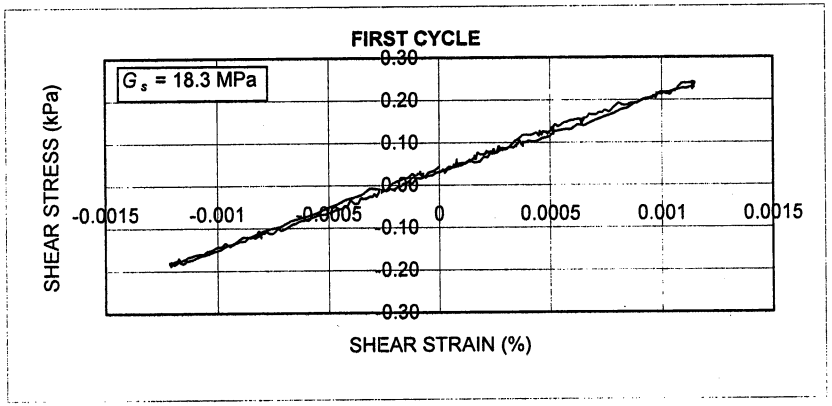

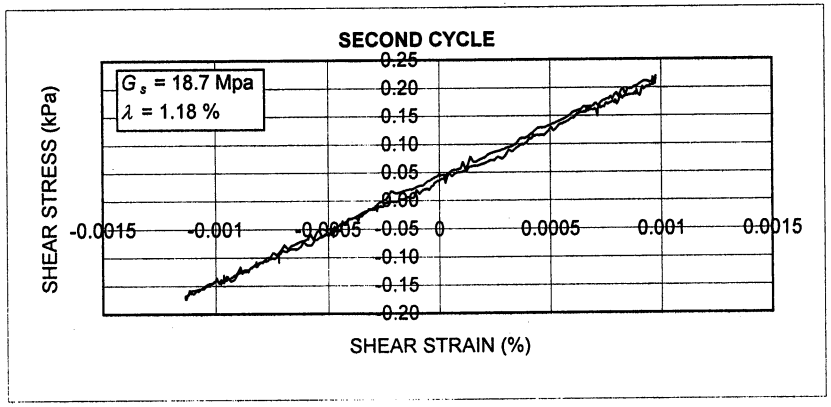

Halls Valley P-1					
DSDSS TEST - Step 4					
Type of soil: CL					
LL	42.1	PI	26.1	%Silt	36.1
e_0	0.75	S_0 (%)	93.5	%Clay	35.0
σ_v (kPa)	37	OCR	n/a	w (%)	26.2
γ_c (%)	~0.0026	H_0 (mm)	19.43	Spec. Gr.	2.66

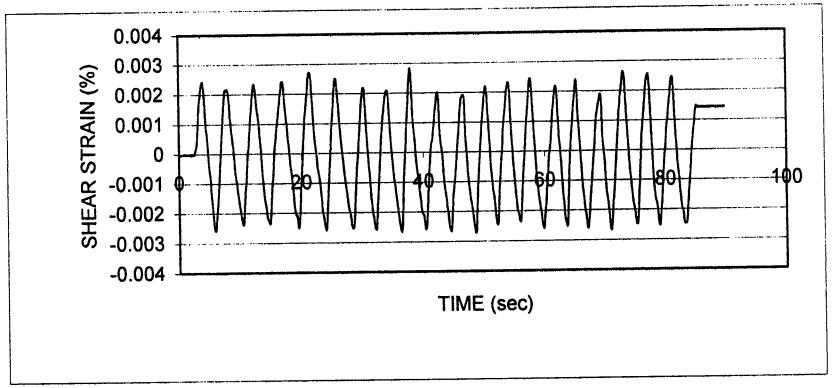

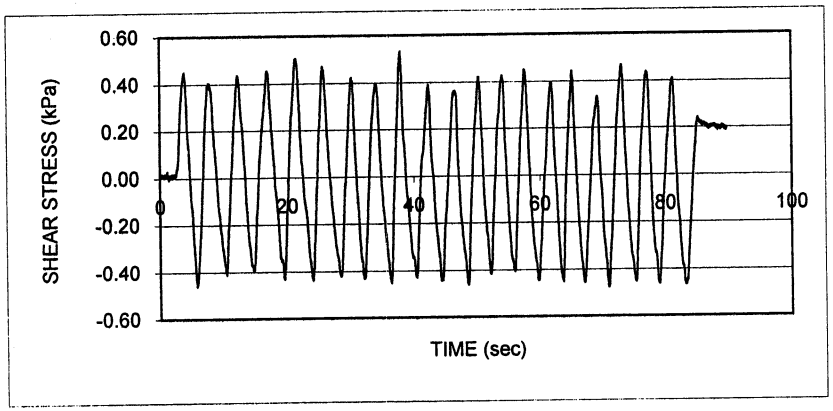

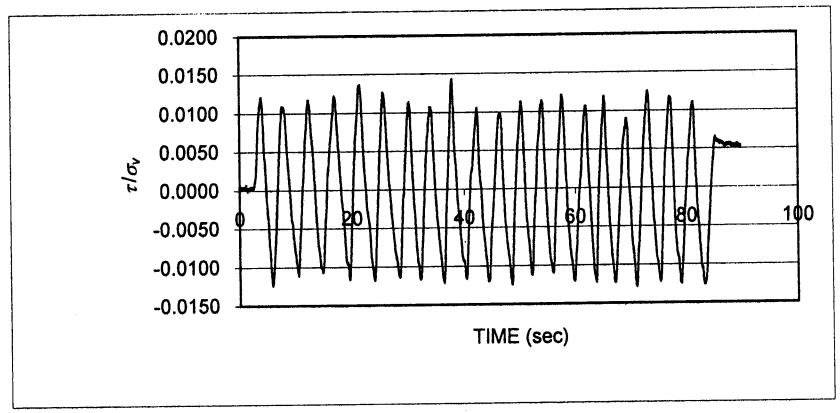

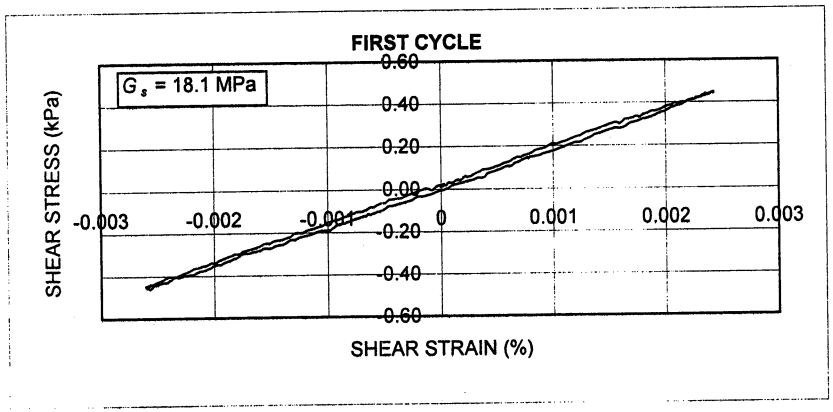

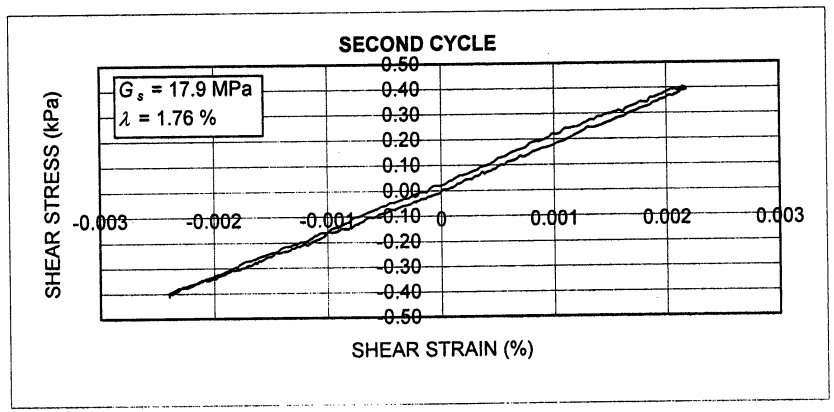

Halls Valley P-1					
DSDSS TEST - Step 5					
Type of soil: CL					
LL	42.1	PI	26.1	%Silt	36.1
e_0	0.75	S_0 (%)	93.5	%Clay	35.0
σ_v (kPa)	37	OCR	n/a	w (%)	26.2
γ_c (%)	~0.008	H_0 (mm)	19.43	Spec. Gr.	2.66

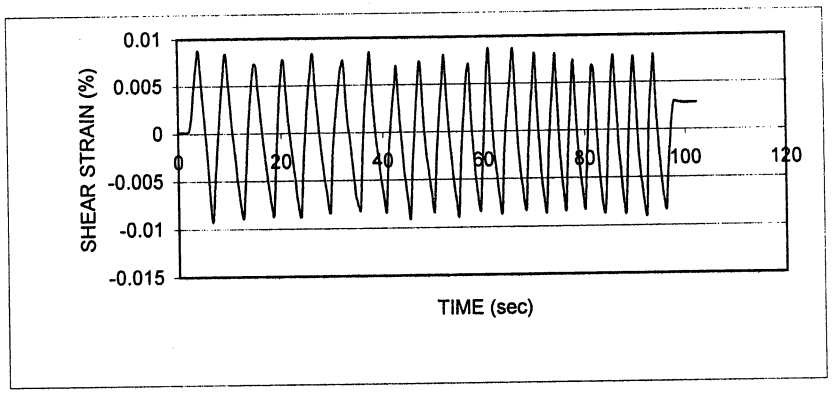

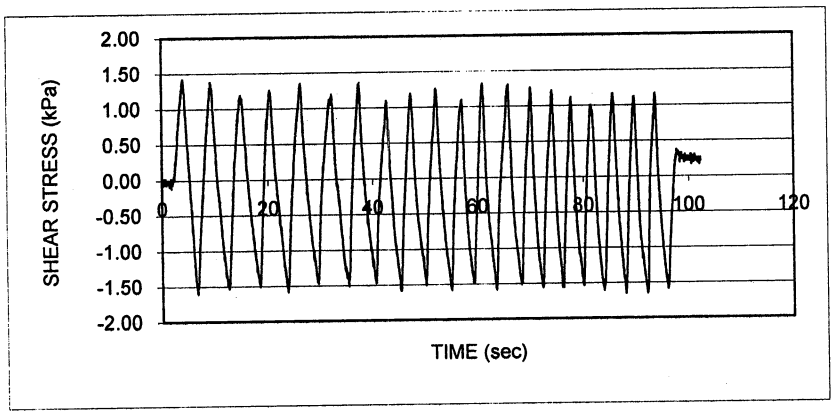

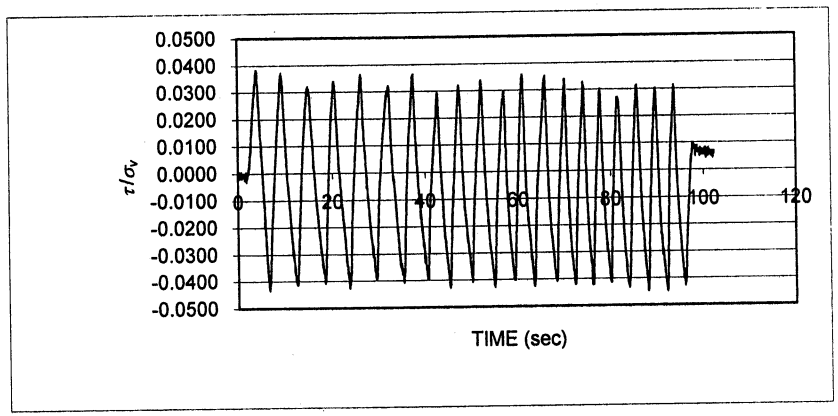

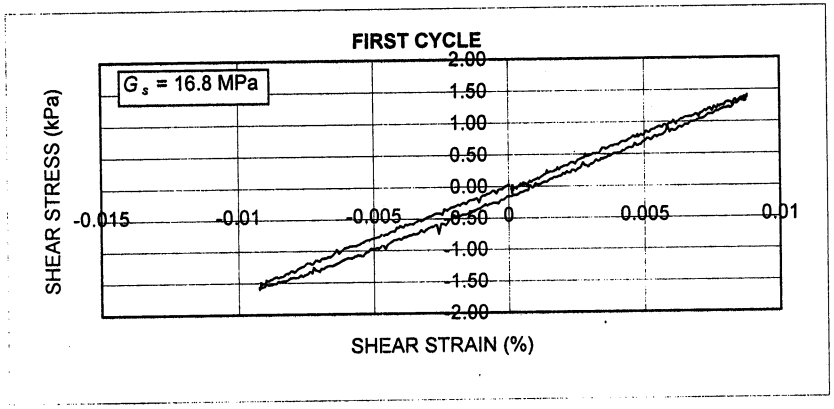

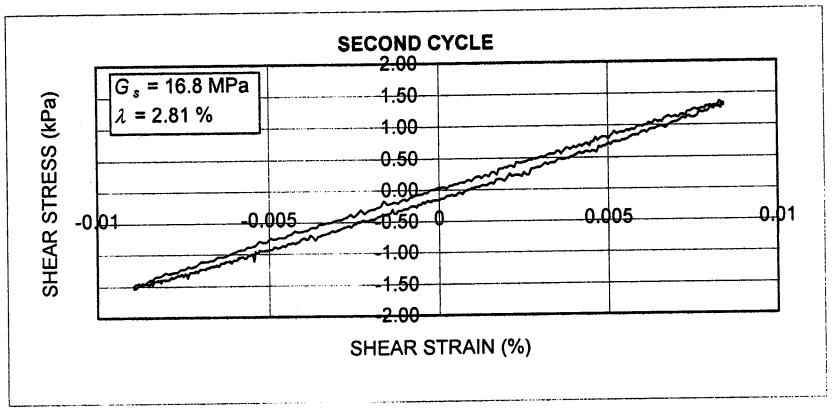

Halls Valley P-1					
DSDSS TEST - Step 6					
Type of soil: CL					
LL	42.1	PI	26.1	%Silt	36.1
e_0	0.75	S_0 (%)	93.5	%Clay	35.0
σ_v (kPa)	37	OCR	n/a	w (%)	26.2
γ_c (%)	~0.025	H_0 (mm)	19.43	Spec. Gr.	2.66

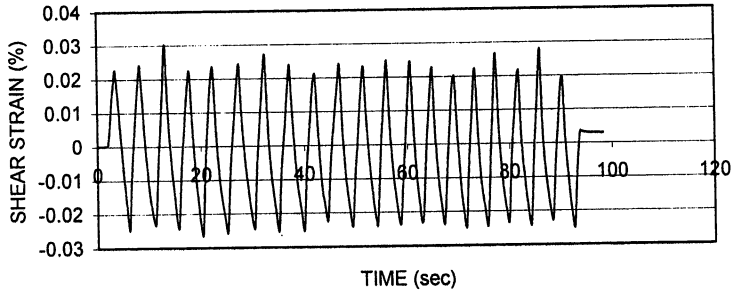

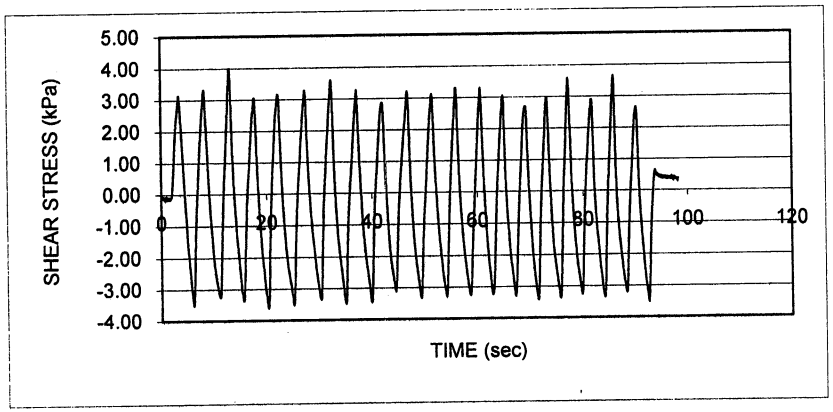

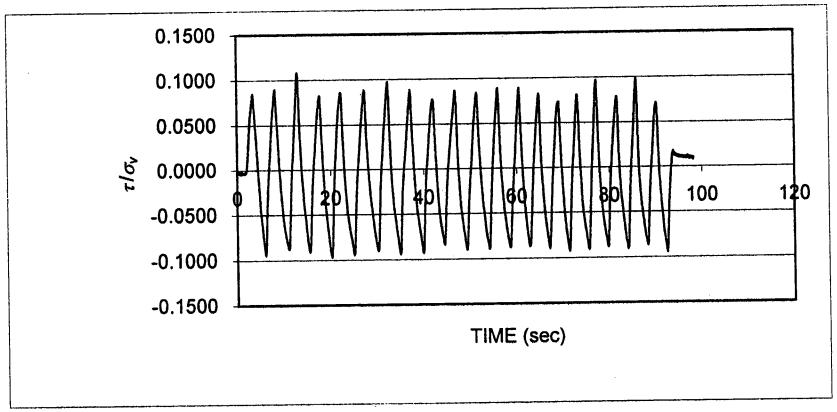

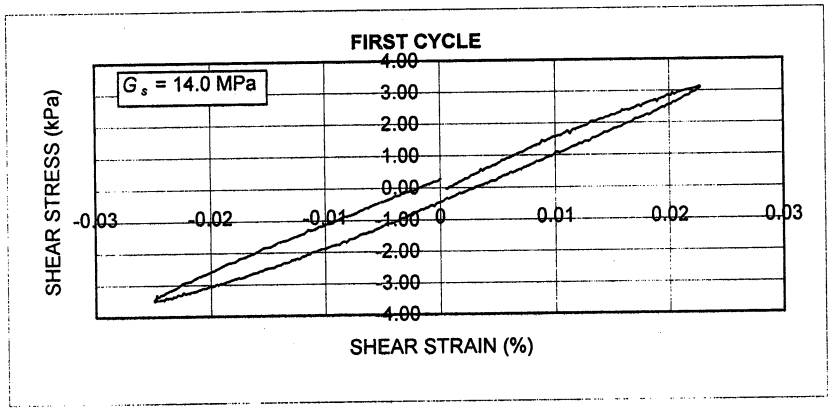

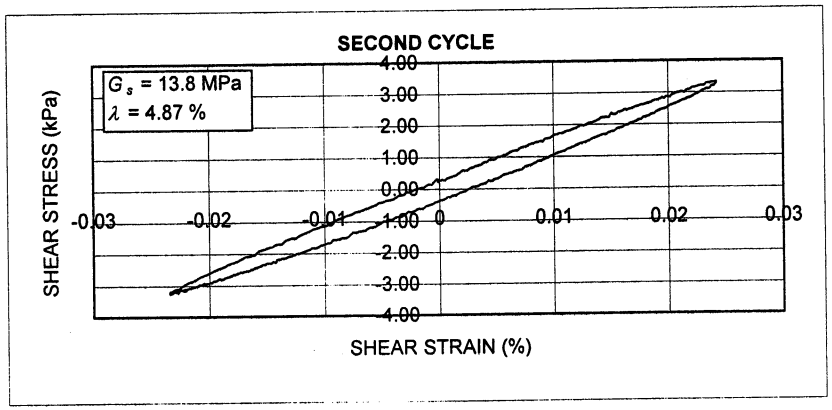

Halls Valley P-1					
DSDSS TEST - Step 7					
Type of soil: CL					
LL	42.1	PI	26.1	%Silt	36.1
e_0	0.75	S_0 (%)	93.5	%Clay	35.0
σ_v (kPa)	37	OCR	n/a	w (%)	26.2
γ_c (%)	~0.11	H_0 (mm)	19.43	Spec. Gr.	2.66

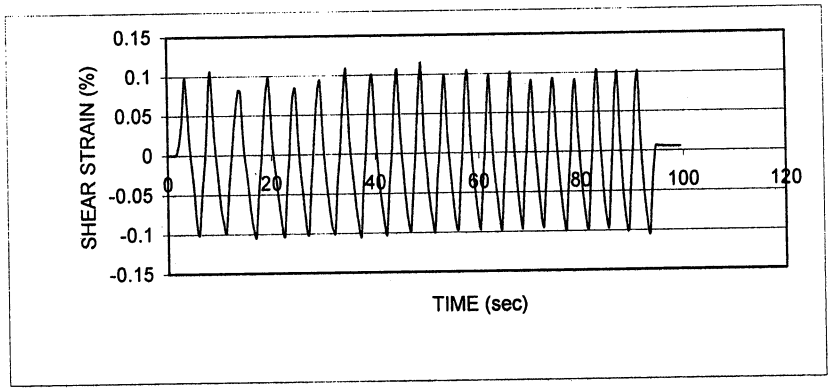

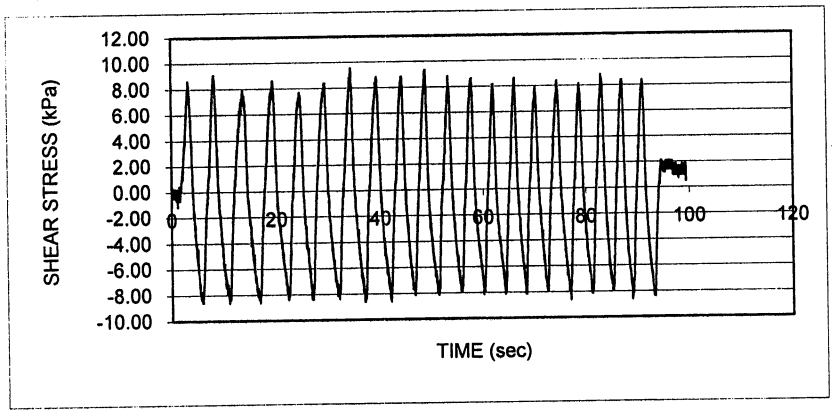

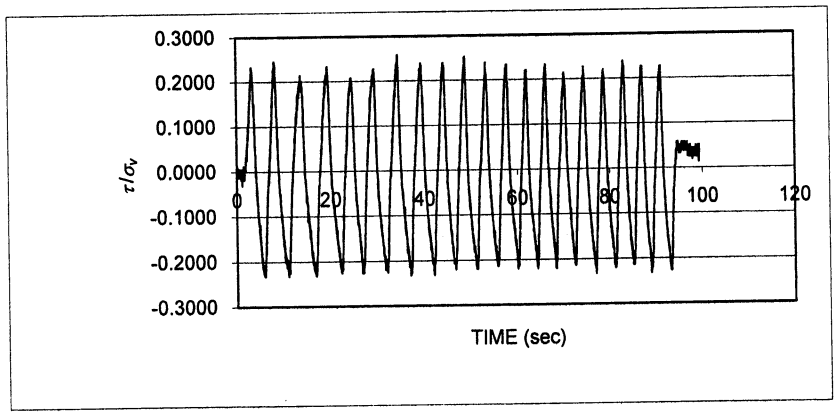

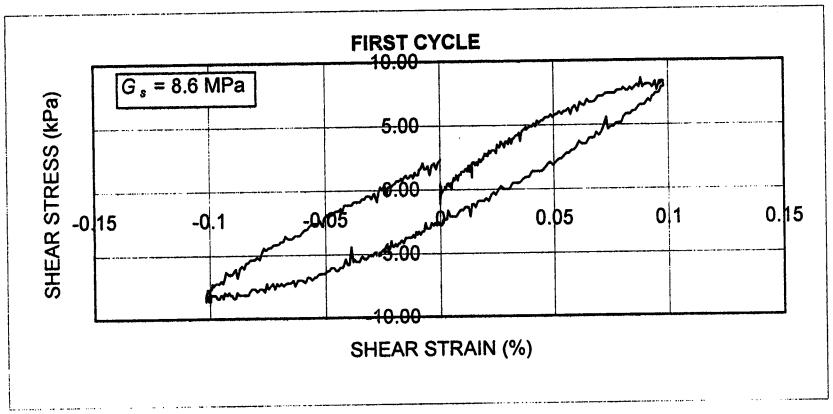

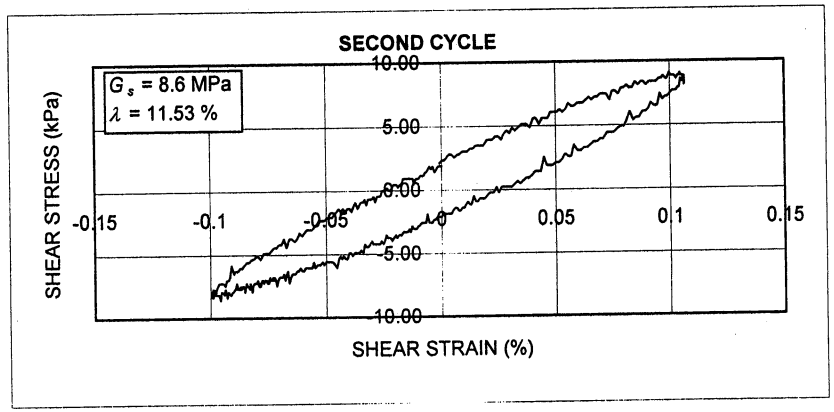

Halls Valley P-1					
DSDSS TEST - Step 8					
Type of soil: CL					
LL	42.1	PI	26.1	%Silt	36.1
e_0	0.75	S_0 (%)	93.5	%Clay	35.0
σ_v (kPa)	37	OCR	n/a	w (%)	26.2
γ_c (%)	~3.1	H_0 (mm)	19.43	Spec. Gr.	2.66

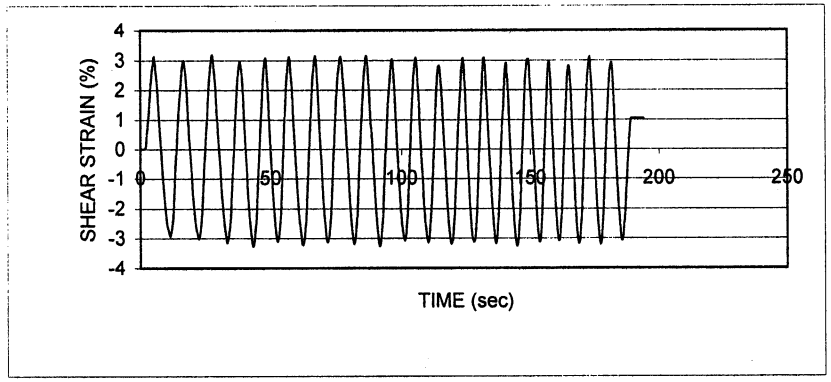

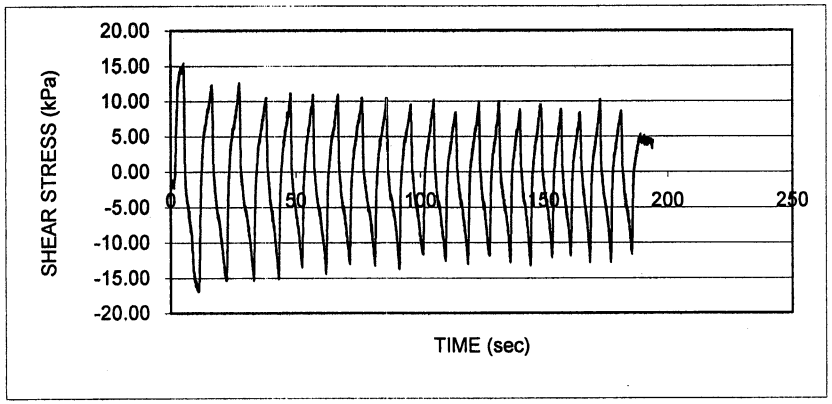

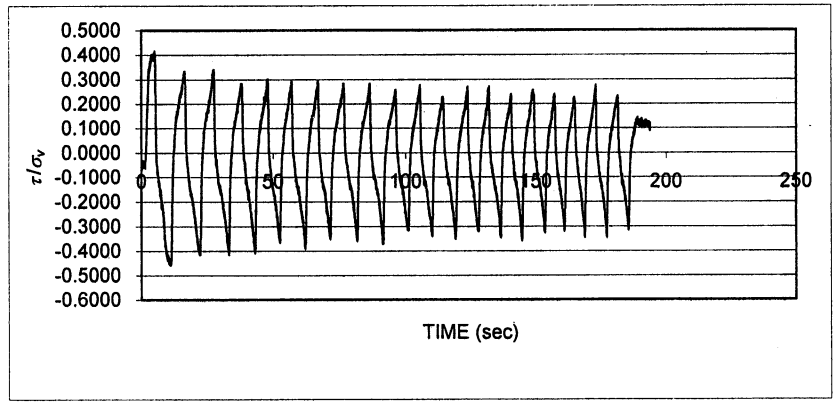

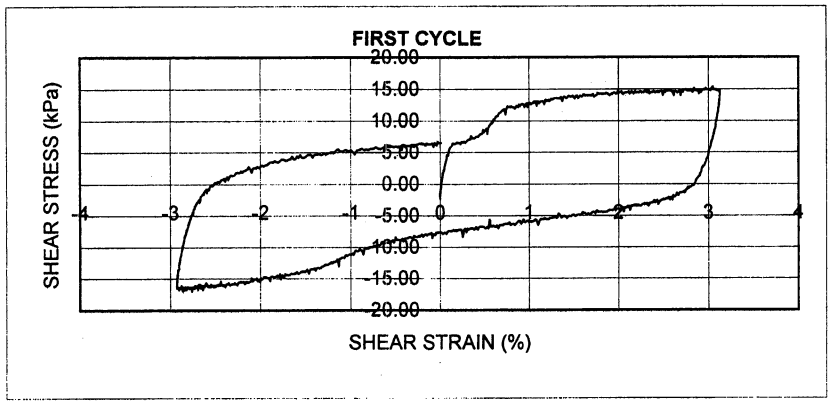

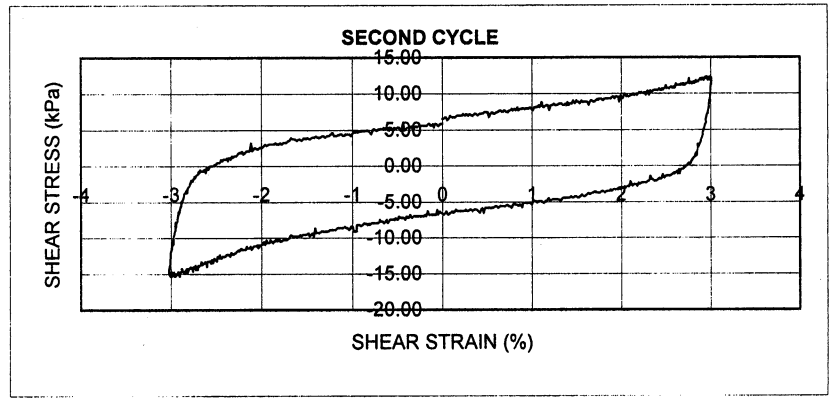

UCLA Soil Dynamics Laboratory
Double Specimen Direct Simple Shear (DSDSS) Test

Principal investigator: Mladen Vucetic, Professor
Test performed by Kentaro Tabata

Test no: 10

Project:	PEARL			Date:	2/12/2002
Sample name:	Halls Valley (P-1)			Depth (ft):	6.0
Symbol:	CL	LL (%):	42.1	Silt content (%):	36.1
Specific gravity:	2.66	PI:	26.1	Clay content (%):	35.0
Comments:					

Estimated G_{max} (MPa):	18.5

SHEAR MODULUS				DAMPING RATIO	
Step	γ_c (%)	G_s (MPa)	G_s/G_{max}	γ_c (%)	λ (%)
2x	0.000370	17.83	0.964		
2x	0.000375	19.21	1.039		
26x	0.000671	19.06	1.030	0.001056	1.18
26x	0.000718	18.06	0.976	0.002288	1.76
3x	0.001181	18.25	0.986	0.008690	2.81
3x	0.001056	18.68	1.010	0.023858	4.87
4x	0.002519	18.08	0.977	0.102912	11.53
4x	0.002288	17.86	0.966		
5x	0.009026	16.78	0.907		
5x	0.008690	16.76	0.906		
6x	0.023849	13.97	0.755		
6x	0.023858	13.82	0.747		
7x	0.100000	8.62	0.466		
7x	0.102912	8.60	0.465		
	γ (%)				
(Monotonic loading)	1.006371	1.27	0.069		
	1.501365	0.92	0.049		
	2.009097	0.72	0.039		
	2.502288	0.59	0.032		
	3.006375	0.50	0.027		
	3.126489	0.48	0.026		

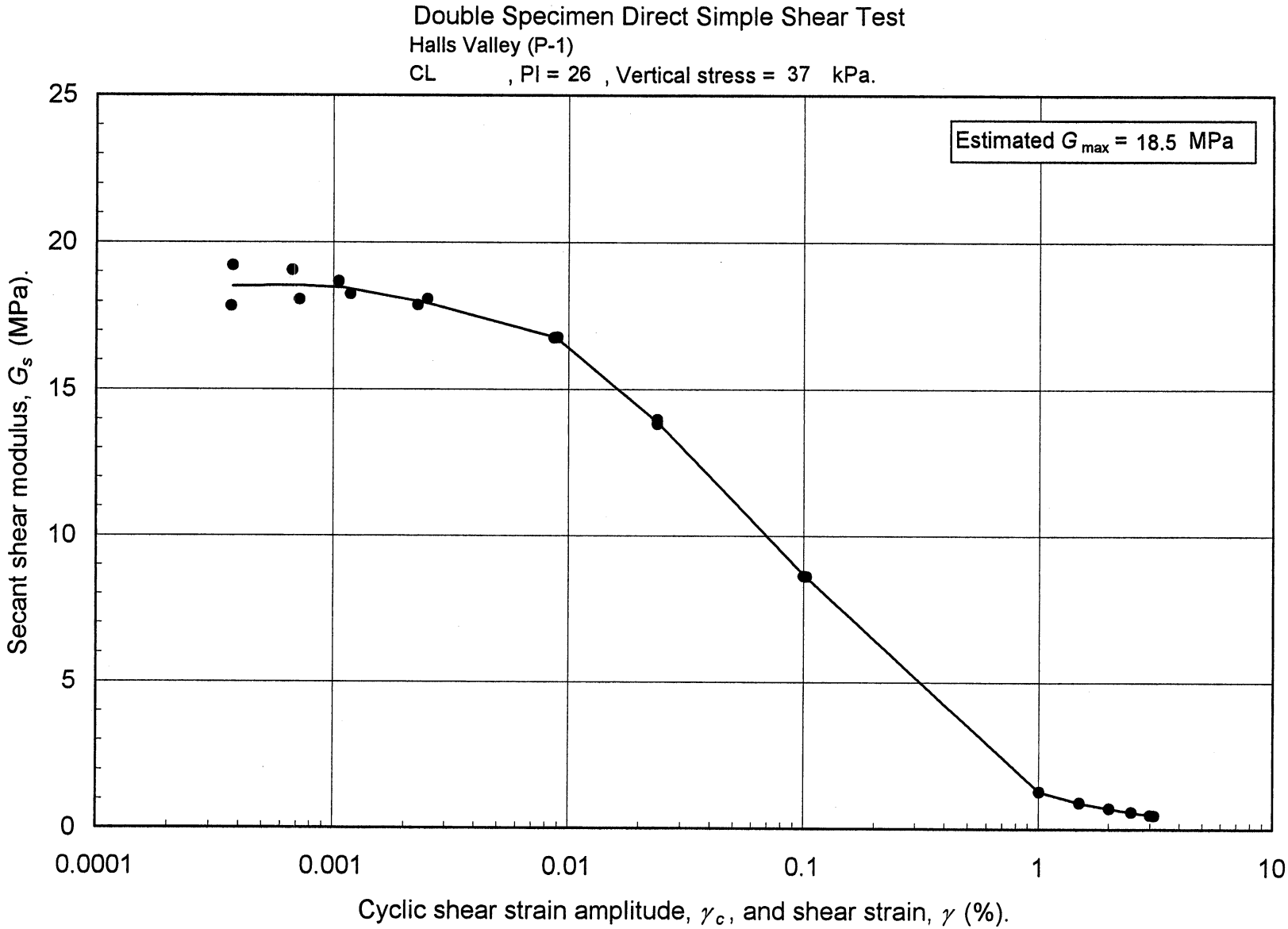
Double Specimen Direct Simple Shear Test
Halls Valley (P-1)
CL , PI = 26 , Vertical stress = 37 kPa.
Estimated G_{max} = 18.5 MPa
Secant shear modulus, G_s (MPa).
25
20
15
10
5
0
0.0001
0.001
0.01
0.1
1
10
Cyclic shear strain amplitude, γ_c, and shear strain, γ (%).

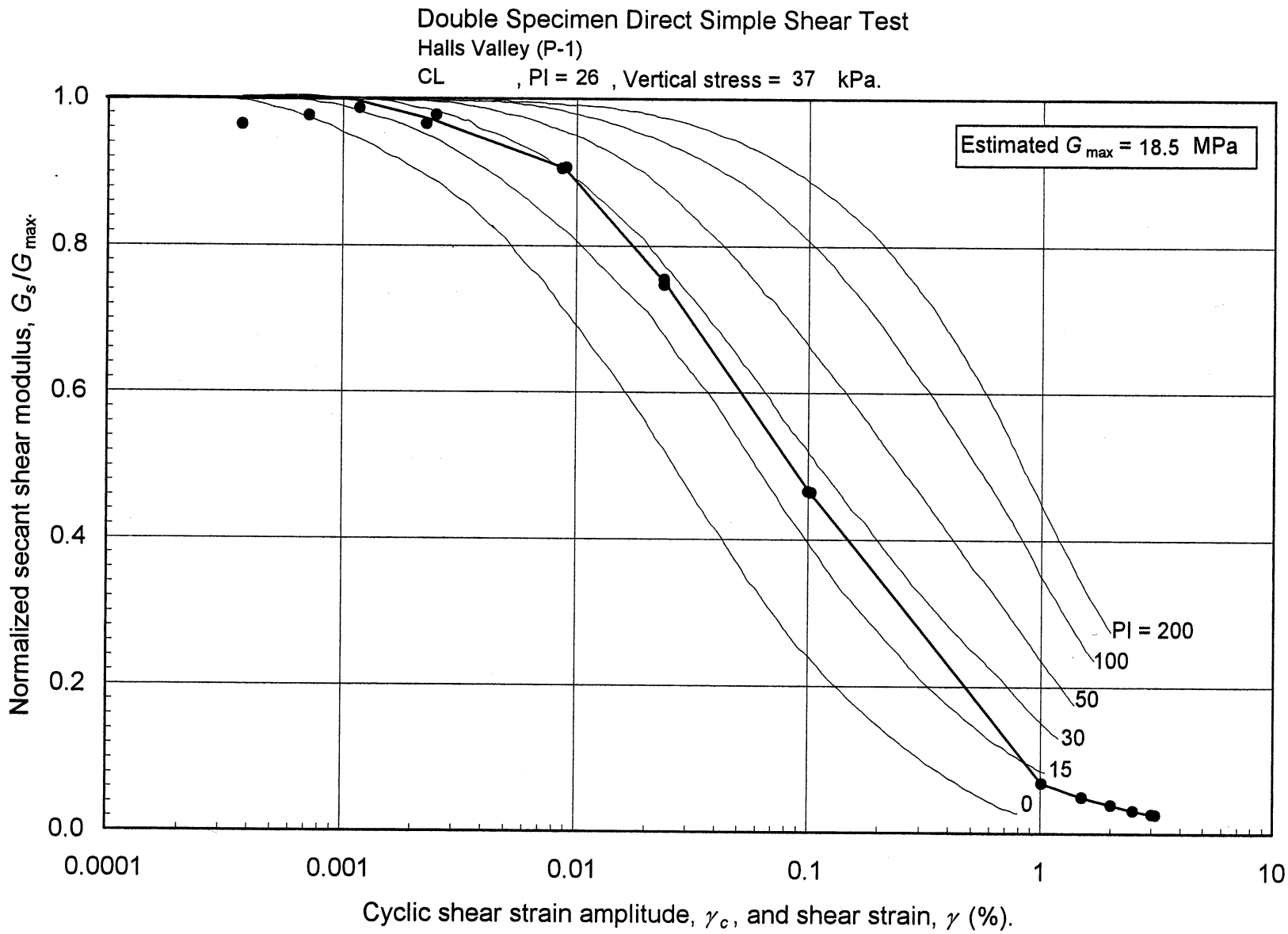
Double Specimen Direct Simple Shear Test
Halls Valley (P-1)
CL , PI = 26 , Vertical stress = 37 kPa.
Estimated G_{max} = 18.5 MPa
PI = 200
100
50
30
15
0
Normalized secant shear modulus, G_s/G_{max}
1.0
0.8
0.6
0.4
0.2
0.0
0.0001
0.001
0.01
0.1
1
10
Cyclic shear strain amplitude, γ_c, and shear strain, γ (%).

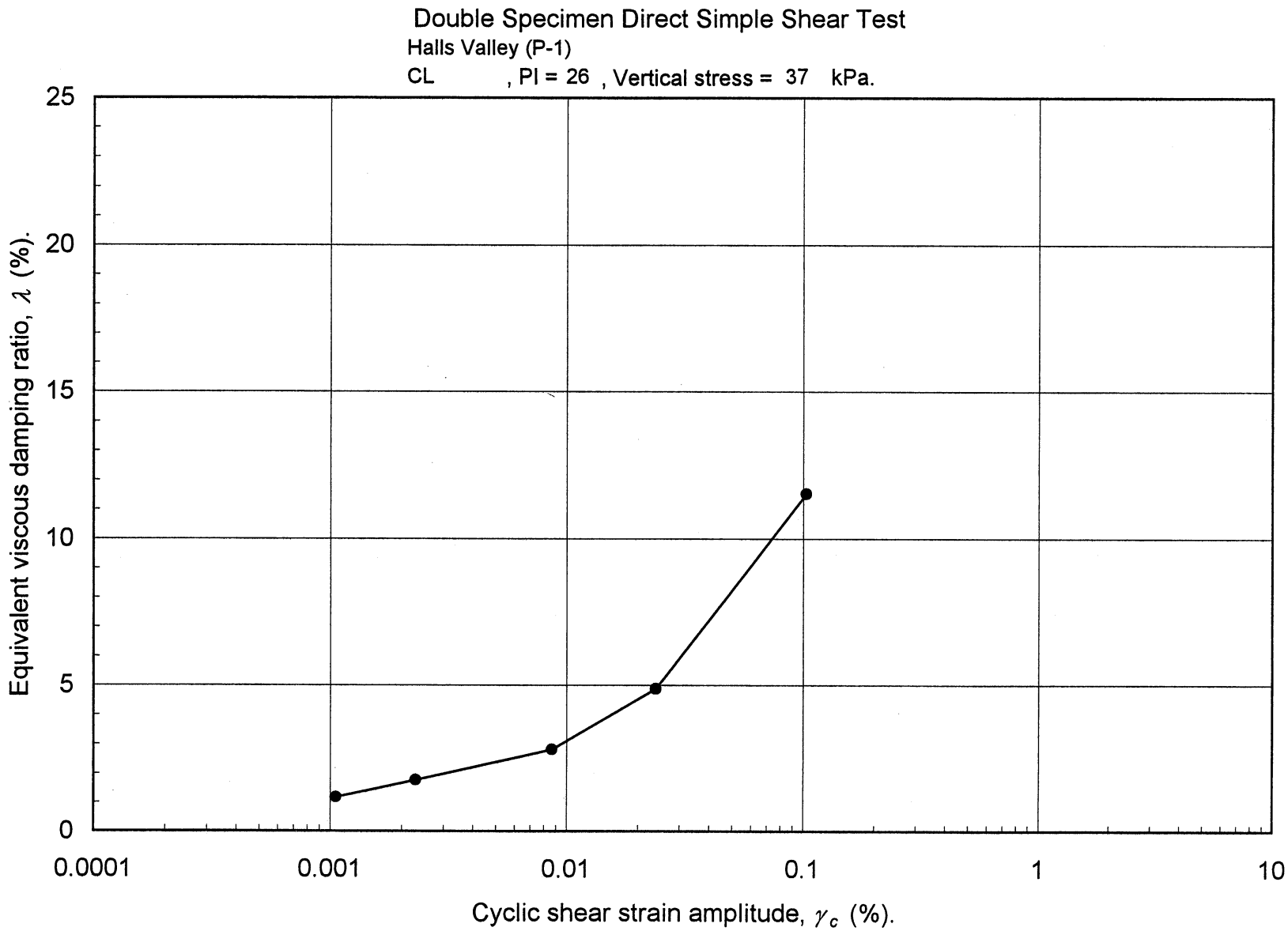
Double Specimen Direct Simple Shear Test
Halls Valley (P-1)
CL , PI = 26 , Vertical stress = 37 kPa.
Equivalent viscous damping ratio, λ (%).
25
20
15
10
5
0
0.0001
0.001
0.01
0.1
1
10
Cyclic shear strain amplitude, γc (%).

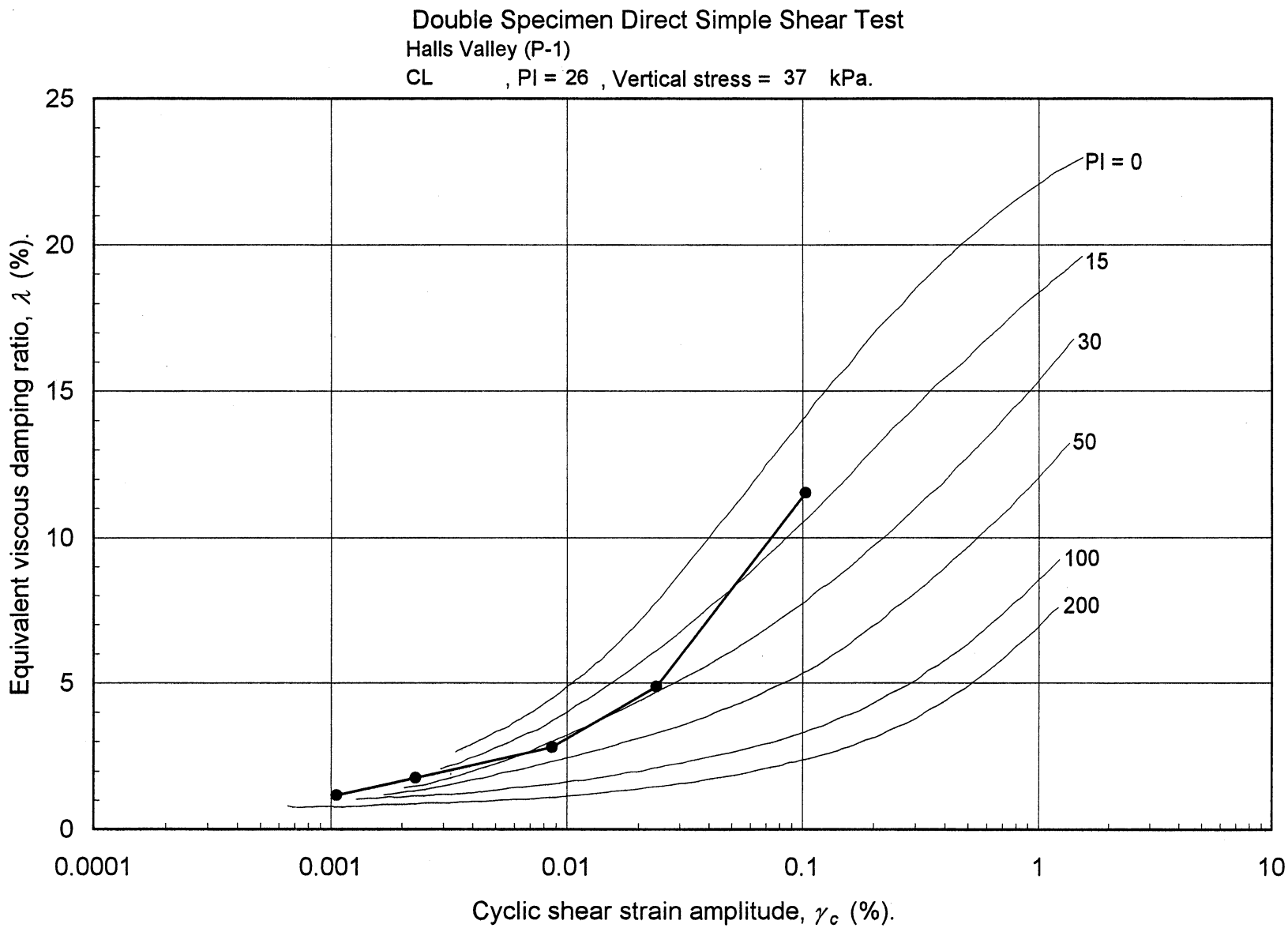
Double Specimen Direct Simple Shear Test
Halls Valley (P-1)
CL , PI = 26 , Vertical stress = 37 kPa.
Equivalent viscous damping ratio, λ (%).
Cyclic shear strain amplitude, γc (%).
0
5
10
15
20
25
0.0001
0.001
0.01
0.1
1
10
PI = 0
15
30
50
100
200

UCLA Soil Dynamics Laboratory

Specific Gravity Test

Principal investigator: Mladen Vucetic, Professor

Test performed by: Kentaro Tabata Test No.: 10

Project:	PEARL			Date:	2/19/2002
Boring:	Halls Valley				
Tube No.:	P-1	Depth (ft):	6.0 -9.0	GWT (ft):	65.0
Comments:	Silty clay.				

SPECIFIC GRAVITY TEST

Test No.	1		
Bottle No.	3		
Wt. of bottle (g)	178.27		
Volume of bottle (cm^3)	500		
Wt. of bottle+water+soil (g)	693.57		
Temperature (°C)	22.0		
Wt. of bottle+water (g)	676.27		
Evaporating dish No.	B-3		
Weight of dish (g)	482.85		
Wt. of dish+dry soil (g)	510.53		
Wt. of dry soil (g)	27.68		
Specific gravity of water	0.9978		
Specific gravity of soil	**2.66**		

UCLA Soil Dynamics Laboratory

Grain Size Distribution

Principal investigator: Mladen Vucetic, Professor

Test performed by: Kentaro Tabata Test No.: 10

Project:	PEARL				
Boring:	Halls Valley				
Tube No.:	P-1	Depth (ft):	6.0 -9.0	GWT (ft):	65.0
Comments:	Silty clay.				

GRAIN SIZE DISTRIBUTION

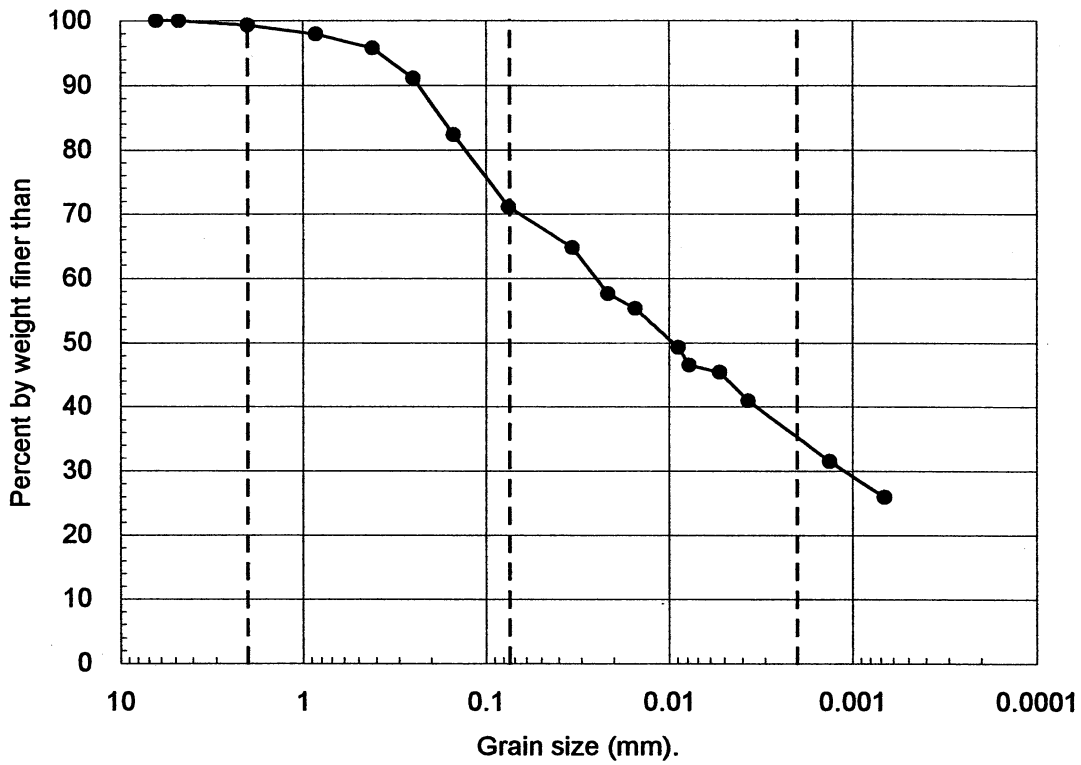

Clay (%)	Silt (%)	Sand (%)	Gravel (%)
35.0	36.1	28.2	0.7

UCLA Soil Dynamics Laboratory

Hydrometer Analysis

Principal investigator: Mladen Vucetic, Professor

Test performed by: Kentaro Tabata Test No.: 10

Project:	PEARL			Date:	2/21/2002
Boring:	Halls Valley				
Tube No.:	P-1	Depth (ft):	6.0 -9.0	GWT (ft):	65.0
Comments:	Silty clay.				

HYDROMETER TEST

Time	Elapsed time t (sec)	Temp. T (°C)	Reading R'_T	Corr. reading $R_T=R'_T+c_m$	Depth H (cm)	Grain diameter D (mm)	Temp. corr. m_T	Corr. depth $R_T+m_T-c_d$	% by wt. finer than W_D (%)
15:33:48	0								
15:35:48	120	22.0	1013.5	1014.0	12.78	0.0337	0.700	1011.7	64.74
15:38:48	300	22.0	1012.2	1012.7	13.12	0.0216	0.700	1010.4	57.54
15:43:48	600	22.0	1011.8	1012.3	13.23	0.0153	0.700	1010.0	55.33
16:03:48	1800	22.0	1010.7	1011.2	13.52	0.0089	0.700	1008.9	49.24
16:13:48	2400	22.0	1010.2	1010.7	13.66	0.0078	0.700	1008.4	46.48
17:00:00	5172	22.0	1010.0	1010.5	13.71	0.0053	0.700	1008.2	45.37
18:33:48	10800	22.0	1009.2	1009.7	13.93	0.0037	0.700	1007.4	40.95
15:38:00	86652	22.0	1007.5	1008.0	14.38	0.0013	0.700	1005.7	31.54
15:45:00	346272	22.0	1006.5	1007.0	14.65	0.0007	0.700	1004.7	26.01

APPARATUS

Hydrometer no.:	88-18587	a_0	284.03	a_1	-0.2675
Graduate no.:	1				

FACTORS

Meniscus corr., c_m:	0.5	
Disp. agent corr, c_d:	3.0	
Visc. of water, η.	22.0 °C	9.799E-06 g sec/cm^2
	°C	g sec/cm^3

WEIGHT

Dry soil (g)	20.58
Percent by wt (%)	71.09
Dry soil for sieve (g)	8.37
Total (g)	28.95

UNIT WEIGHT

Specific gravity:		2.66
T	γ_w	γ_s
(°C)	(g/cm^3)	(g/cm^3)
22.0	0.9978	2.6557

UCLA Soil Dynamics Laboratory

Sieve Analysis

Principal investigator: Mladen Vucetic, Professor

Test performed by: Kentaro Tabata Test No.: 10

Project:	PEARL			Date:	2/25/2002
Boring:	Halls Valley				
Tube No.:	P-1	Depth (ft):	6.0 -9.0	GWT (ft):	65.0
Comments:	Silty clay.				

SIEVE ANALYSIS

Sieve No.	Diameter (mm)	Sieve (g)	S+wet (g)	S+dry (g)	Retained (g)	Retained (%)	Cumulated (g)	Cumulated (%)	Passing (%)
3	6.350	485.05		485.05	0.00	0.00	0.00	0.00	100.00
4	4.750	463.10		463.10	0.00	0.00	0.00	0.00	100.00
10	2.000	422.39		422.60	0.21	0.73	0.21	0.73	99.27
20	0.850	375.43		375.81	0.38	1.31	0.59	2.04	97.96
40	0.420	457.60		458.23	0.63	2.18	1.22	4.21	95.79
60	0.250	323.93		325.28	1.35	4.66	2.57	8.88	91.12
100	0.150	342.18		344.72	2.54	8.77	5.11	17.65	82.35
200	0.075	676.87		680.13	3.26	11.26	8.37	28.91	71.09
Total					8.37	28.91			

WEIGHT

Dry soil for sieve (g)	8.37
Dry soil for hydr. (g)	20.58
Total (g)	28.95
Percent coaser (%)	28.91

UCLA Soil Dynamics Laboratory

Atterberg Limit Determination

Principal investigator: Mladen Vucetic, Professor

Test performed by: Kentaro Tabata Test No.: 10

Project:	PEARL			Date:	2/26/2002
Boring:	Halls Valley				
Tube No.:	P-1	Depth (ft):	6.0 -9.0	GWT (ft):	65.0
Comments:	Silty clay.				

LIQUID LIMIT TEST

Test No.	1	2	3	4	5			
Number of blows	45	30	27	17	12			
Container No.	ST-24	ST-3	ST-6	ST-22	ST-20			
Container (g)	29.98	30.18	30.11	30.06	30.36			
Cont+wet soil (g)	37.72	38.02	38.72	37.67	38.58			
Cont+dry soil (g)	35.56	35.74	36.16	35.37	35.96			
Water (g)	2.16	2.28	2.56	2.30	2.62			
Dry soil (g)	5.58	5.56	6.05	5.31	5.60			
Water content (%)	38.71	41.01	42.31	43.31	46.79			

PLASTIC LIMIT TEST

Test No.	1	2	3
Container No.	ST-7	ST-5	ST-11
Container (g)	30.36	30.12	30.26
Cont+wet soil (g)	33.75	32.87	32.81
Cont+dry soil (g)	33.28	32.49	32.46
Water (g)	0.47	0.38	0.35
Dry soil (g)	2.92	2.37	2.20
Water content (%)	16.10	16.03	15.91

ATTERBERG LIMITS

Liquid limit (%)	**42.1**
Plastic limit (%)	**16.0**
Plasticity index	**26.1**

CLASSIFICATION

CL

FLOW CHART

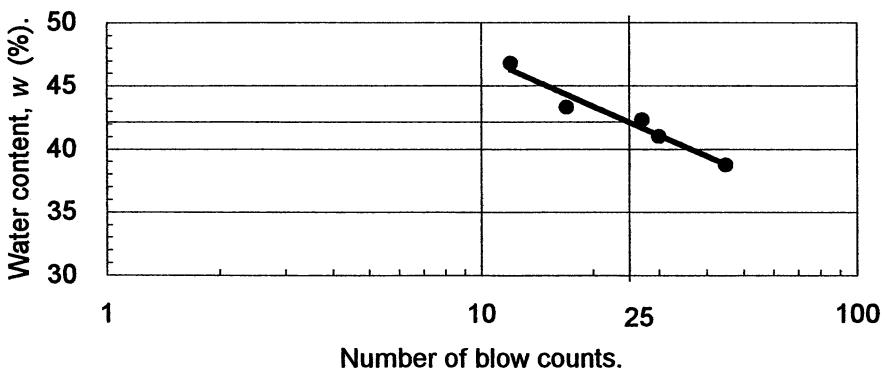

UCLA Soil Dynamics Laboratory

Atterberg Limit Determination

Principal investigator: Mladen Vucetic, Professor

Test performed by: Kentaro Tabata Test No.: 10

Project:	PEARL			Date:	2/26/2002
Boring:	Halls Valley				
Tube No.:	P-1	Depth (ft):	6.0 -9.0	GWT (ft):	65.0
Comments:	Silty clay.				

PLASTICITY CHART

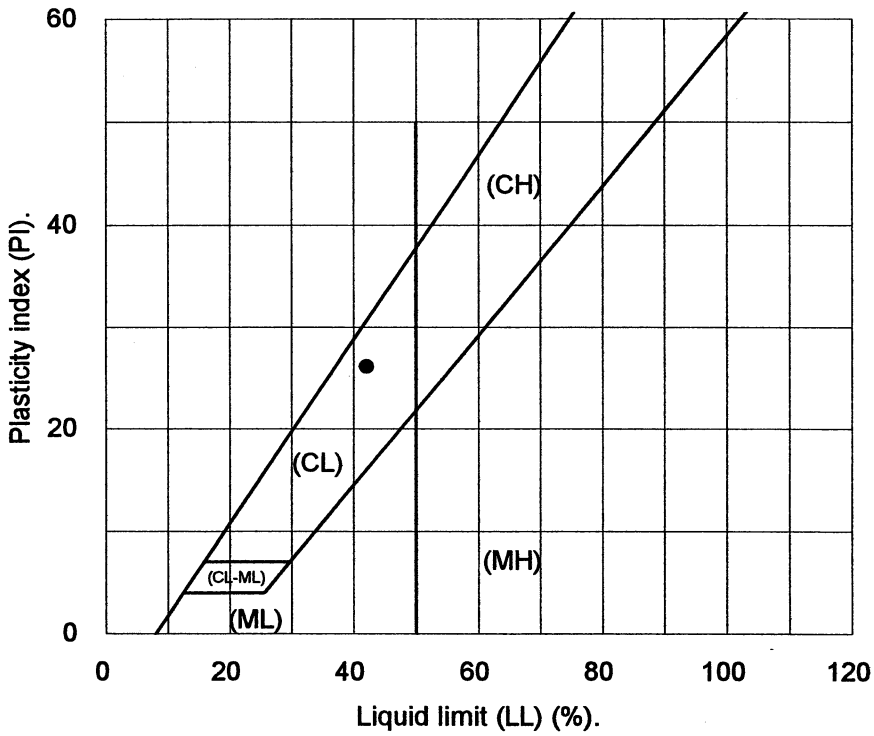

3.12 Test 11: HALLS VALLEY P-2

UCLA Soil Dynamics Laboratory

Double Specimen Direct Simple Shear (DSDSS) Test

Principal investigator: Mladen Vucetic, Professor

Test performed by: Kentaro Tabata Test No.: 11

Project:	PEARL			Date:	1/11/2002
Boring:	Halls Valley				
Tube No.:	P-2	Depth (ft):	15.0 -18.0	GWT (ft):	65.0 (reported by others)
Comments:	Dark grayish brown silty clay. Specimen obtained from the bottom of the tube (specimen depth ~ 17.5 ft).				

FORM 1: SPECIMEN PREPARATION

WATER CONTENT, SPECIFIC GRAVITY				UNIT WEIGHT, VOID RATIO, SATURATION			
	Before consol.	After shearing			Before consol.	Before shearing	After shearing
Container No.	ST-13	MT-14	DISH	Average weight (g)	126.16	126.16	
Cont+wet soil (g)	42.42	175.34	136.24	Height (cm)	1.960	1.926	
Cont+dry soil (g)	39.42	146.18	105.85	Area (cm^2)	34.84	34.84	
Container (g)	30.20	50.22	10.85	Volume (cm^3)	68.28	67.11	
Water (g)	3.00	29.16	30.39	Unit weight (g/cm^3)	1.848	1.880	
Dry soil (g)	9.22	95.96	95.00	Unit weight (kN/m^3)	18.11	18.42	
Water content(%)	32.54	30.39	31.99	Void ratio	0.90	0.87	
Avg. water cont. (%)	32.54		31.19	Saturation (%)	95.7	95.2	
Spceific gravity			2.65				

HEIGHT OF SPECIMEN						
	Before consol.		Before shearing	After shearing		
	Top	Bottom	Average	Average		
Height (cm)	1.960	1.960	1.926	1.926		

AREA OF SPECIMEN						
Initial diameter (cm)			6.660	Initial area (cm^2)		34.837
Load (kg)	Stress (kg/cm^2)	Stress (kN/m^2)	Diameter (cm)	Membrane (cm)	Corrected diameter (cm)	Area (cm^2)

Halls Valley P-2					
DSDSS TEST - Step 26					
Type of soil: CL					
LL	38.2	PI	24.6	%Silt	37.1
e_0	0.87	S_0 (%)	99.3	%Clay	34.0
σ_v (kPa)	105	OCR	n/a	w (%)	32.5
γ_c (%)	~0.0007	H_0 (mm)	19.26	Spec. Gr.	2.65

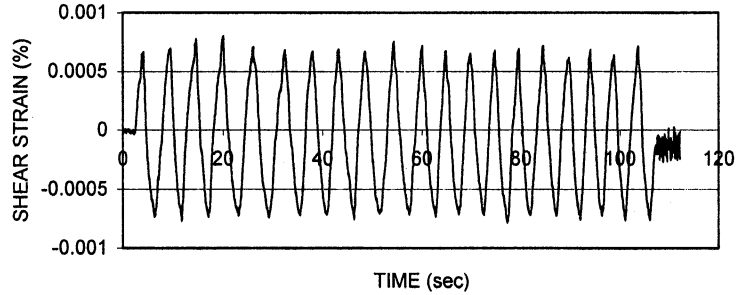

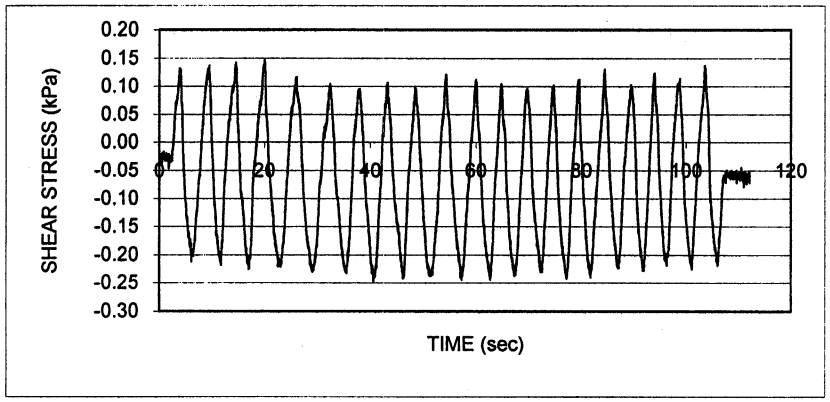

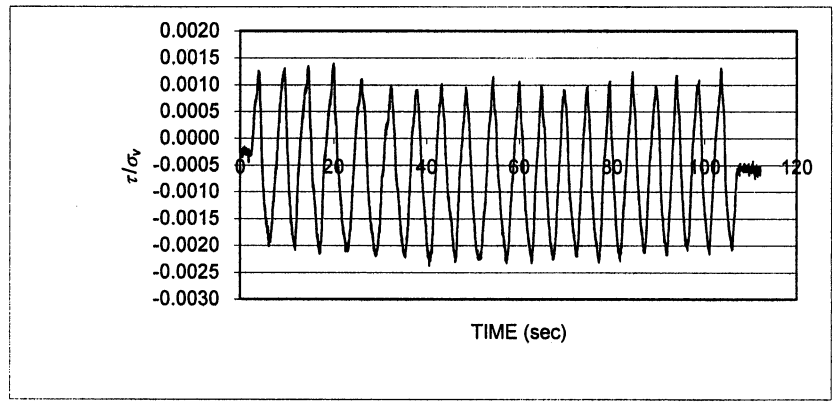

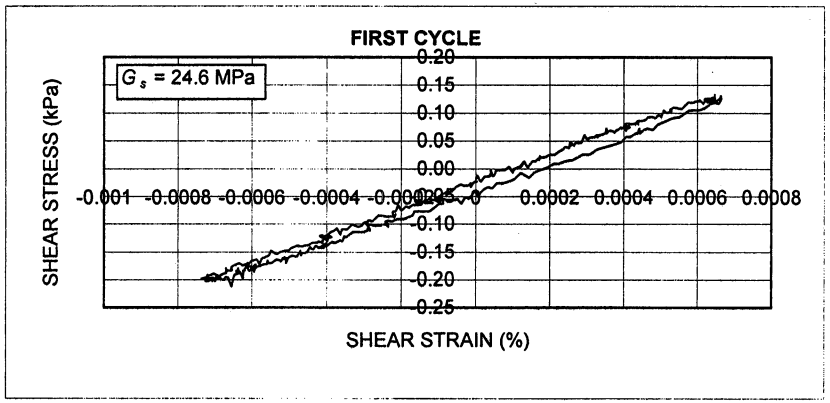

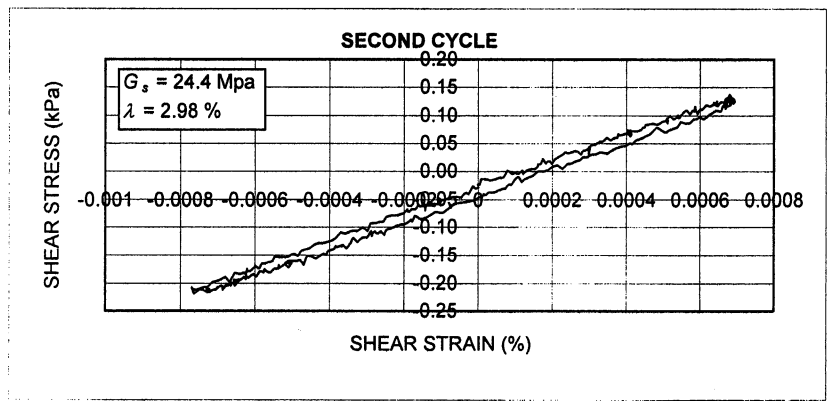

Halls Valley P-2					
DSDSS TEST - Step 3					
Type of soil: CL					
LL	38.2	PI	24.6	%Silt	37.1
e_0	0.87	S_0 (%)	99.3	%Clay	34.0
σ_v (kPa)	105	OCR	n/a	w (%)	32.5
γ_c (%)	~0.001	H_0 (mm)	19.26	Spec. Gr.	2.65

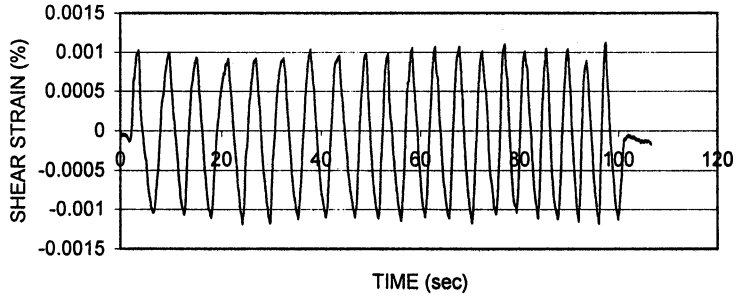

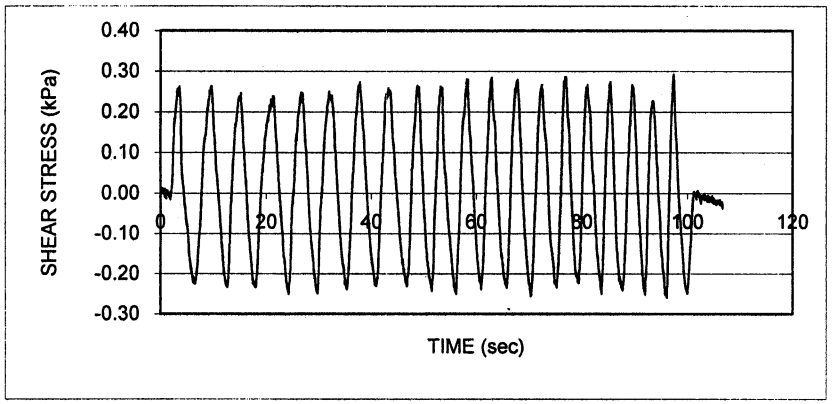

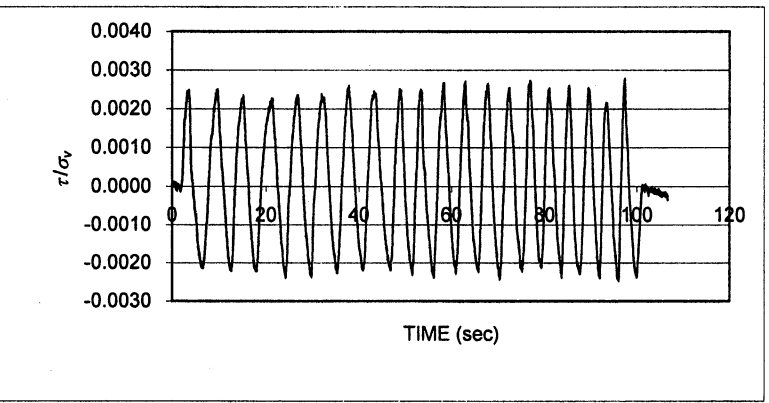

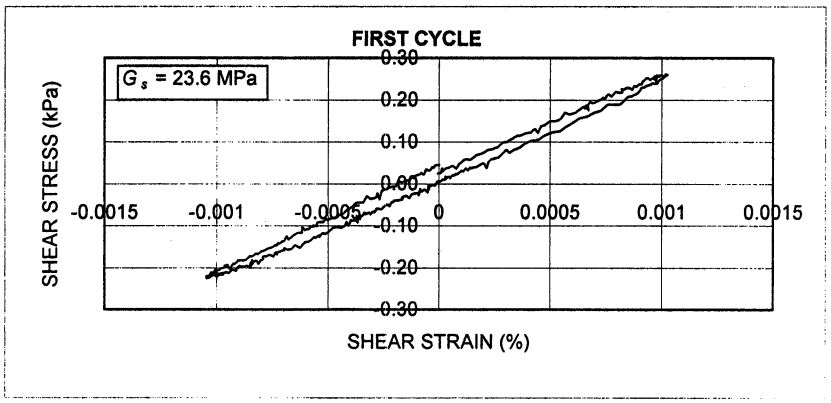

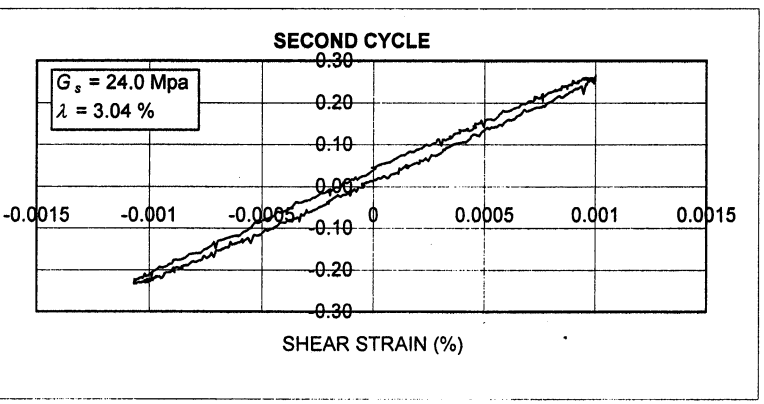

Halls Valley P-2					
DSDSS TEST - Step 4					
Type of soil: CL					
LL	38.2	PI	24.6	%Silt	37.1
e_0	0.87	S_0 (%)	99.3	%Clay	34.0
σ_v (kPa)	105	OCR	n/a	w (%)	32.5
γ_c (%)	~0.0028	H_0 (mm)	19.26	Spec. Gr.	2.65

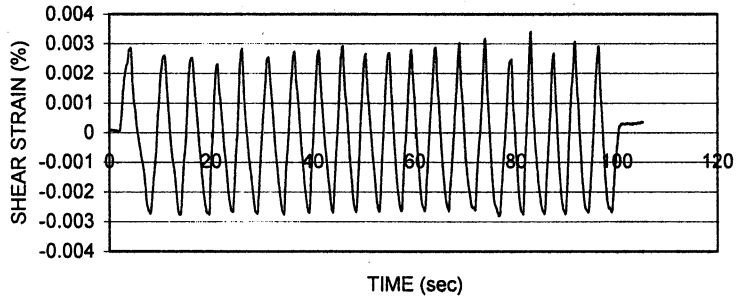

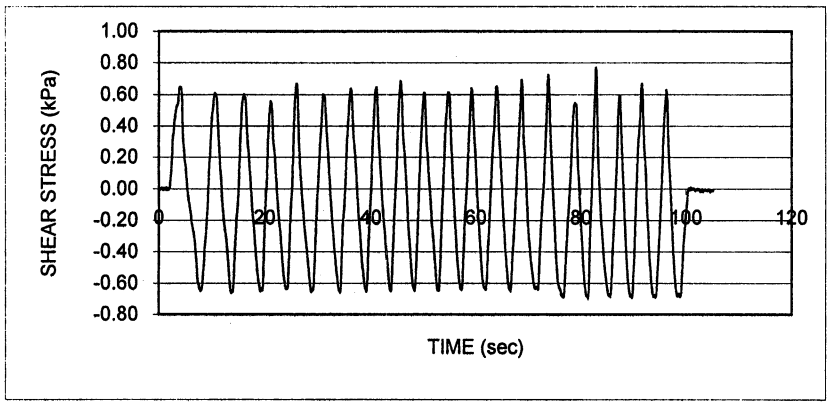

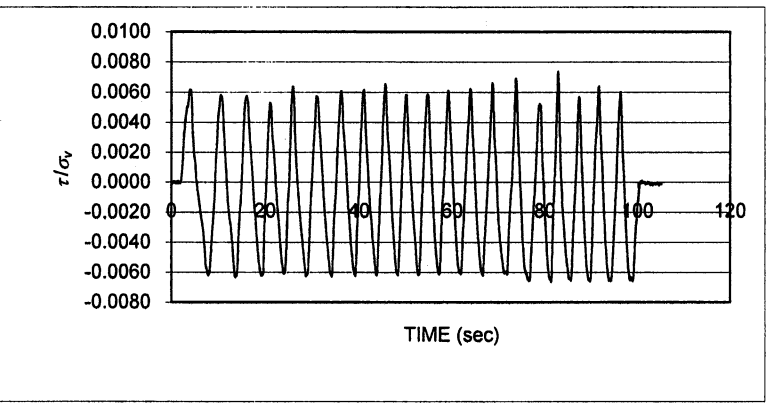

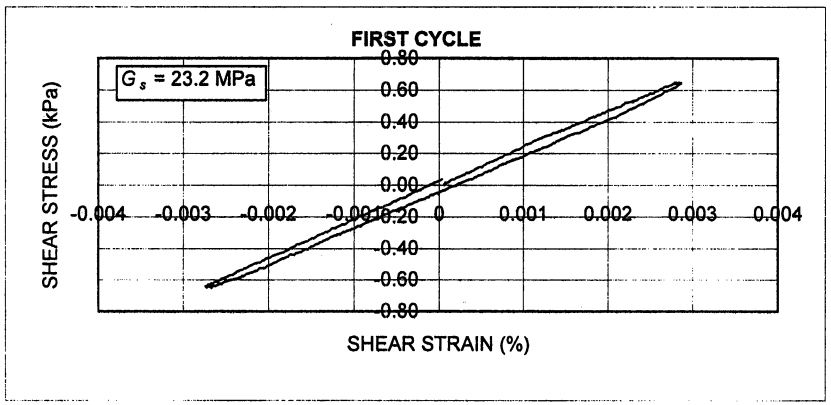

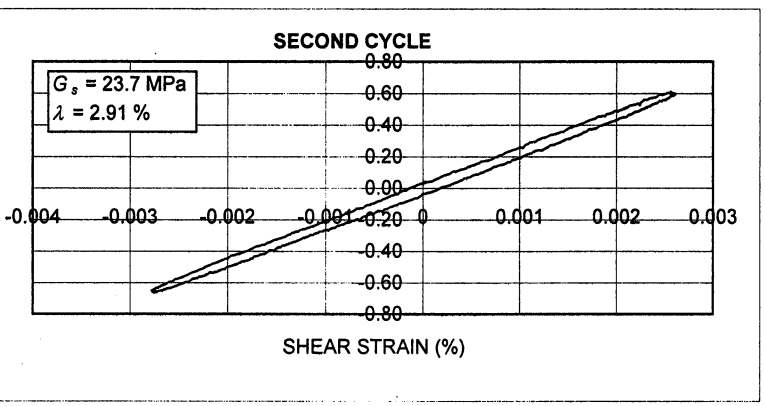

Halls Valley P-2					
DSDSS TEST - Step 5					
Type of soil: CL					
LL	38.2	PI	24.6	%Silt	37.1
e_0	0.87	S_0 (%)	99.3	%Clay	34.0
σ_v (kPa)	105	OCR	n/a	w (%)	32.5
γ_c (%)	~0.009	H_0 (mm)	19.26	Spec. Gr.	2.65

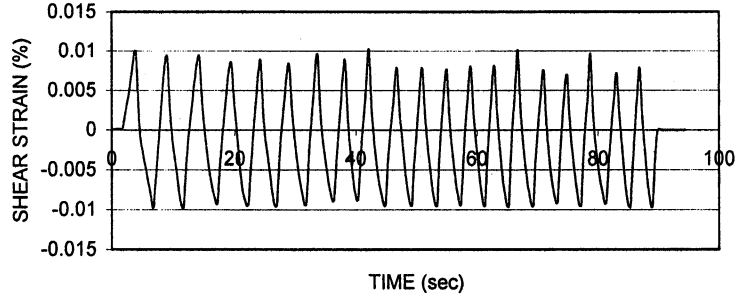

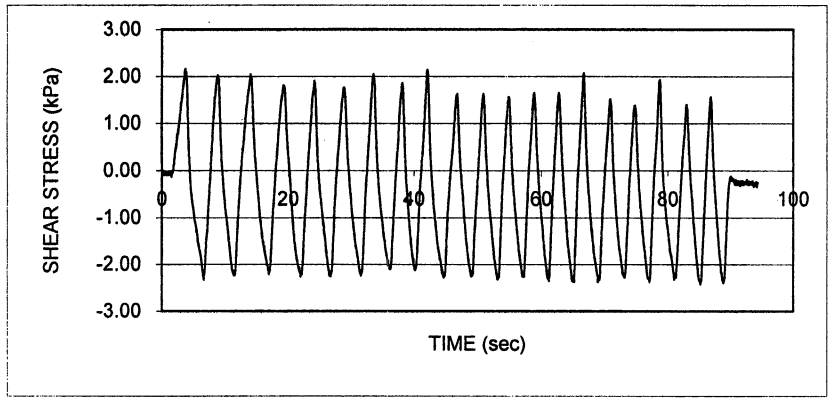

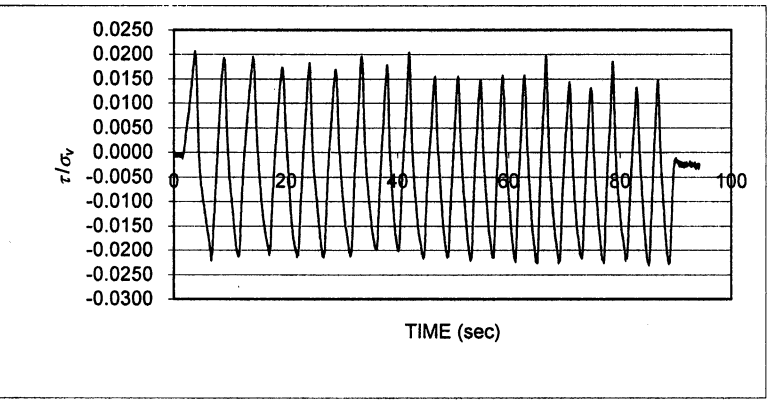

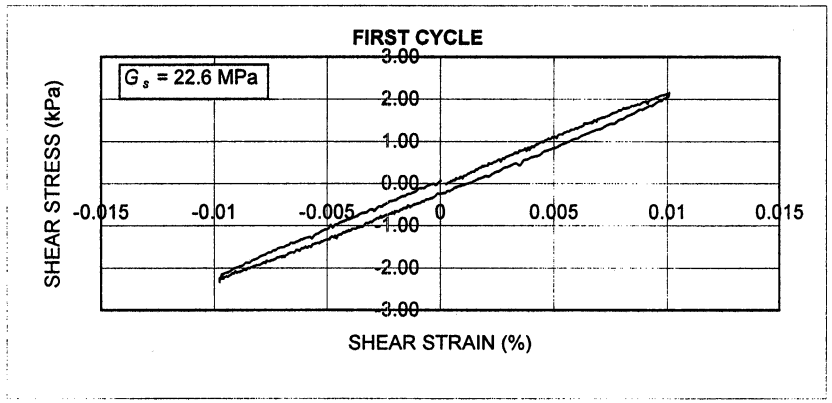

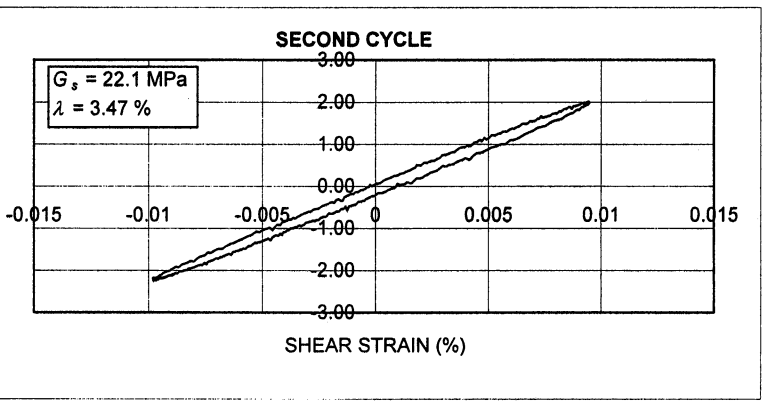

Halls Valley P-2					
DSDSS TEST - Step 6					
Type of soil: CL					
LL	38.2	PI	24.6	%Silt	37.1
e_0	0.87	S_0 (%)	99.3	%Clay	34.0
σ_v (kPa)	105	OCR	n/a	w (%)	32.5
γ_c (%)	~0.03	H_0 (mm)	19.26	Spec. Gr.	2.65

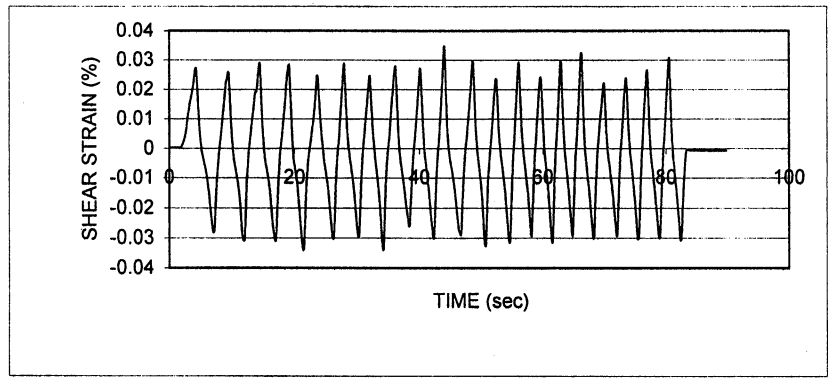

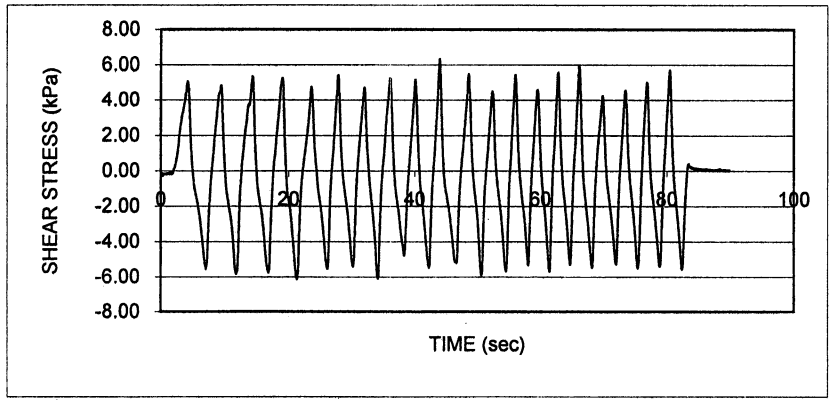

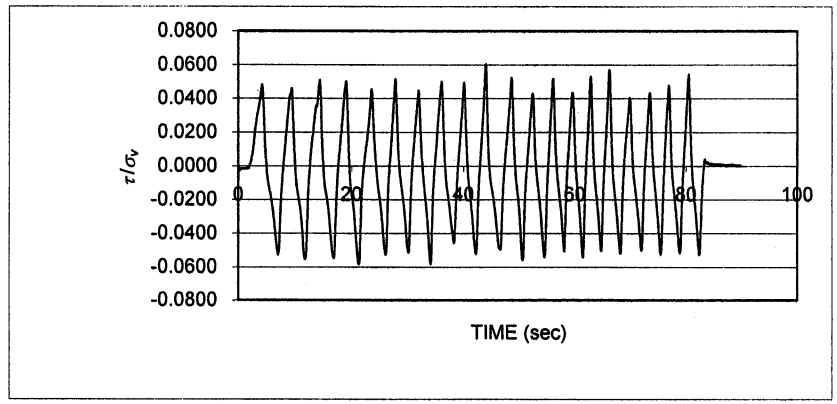

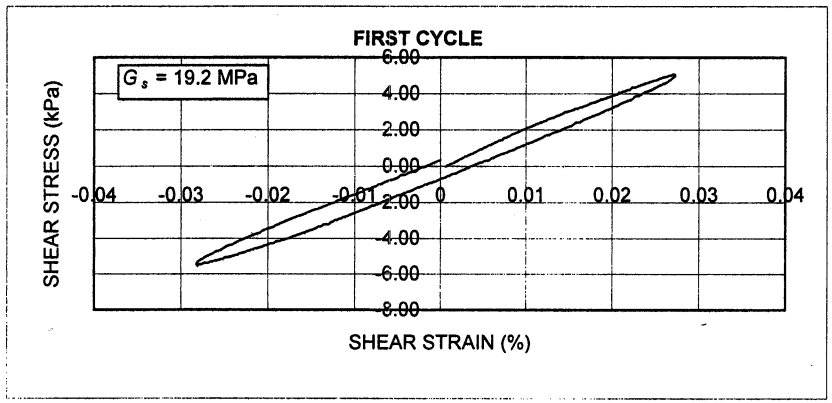

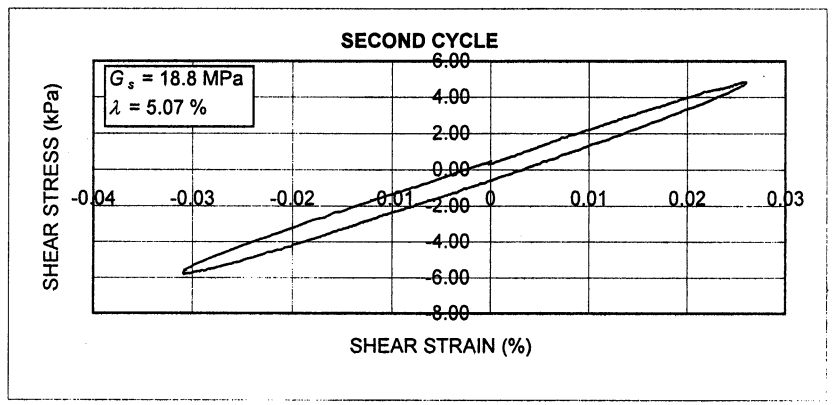

Halls Valley P-2					
DSDSS TEST - Step 7					
Type of soil: CL					
LL	38.2	PI	24.6	%Silt	37.1
e_0	0.87	S_0 (%)	99.3	%Clay	34.0
σ_v (kPa)	105	OCR	n/a	w (%)	32.5
γ_c (%)	~0.12	H_0 (mm)	19.26	Spec. Gr.	2.65

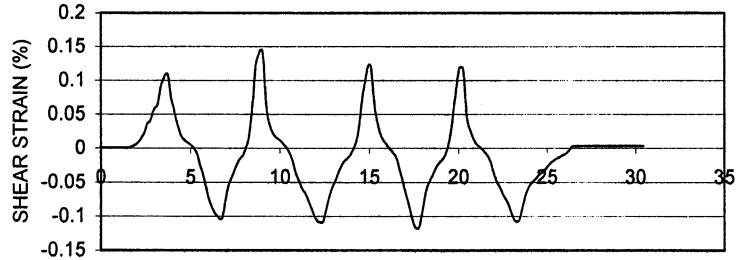

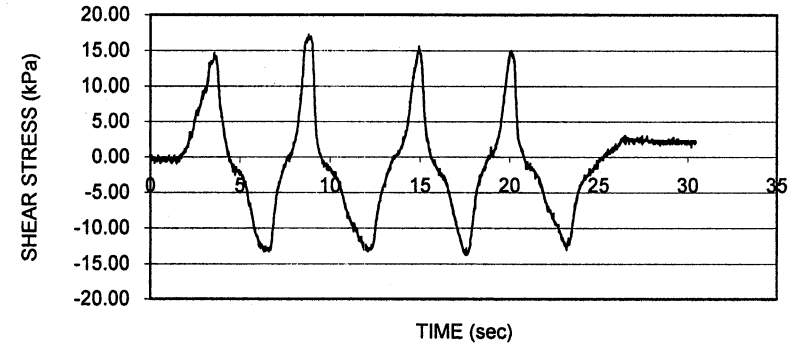

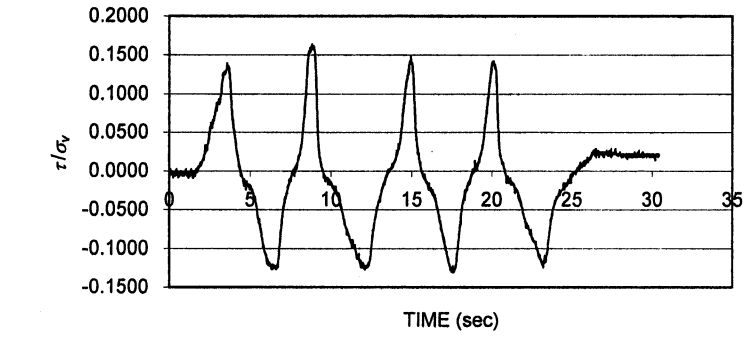

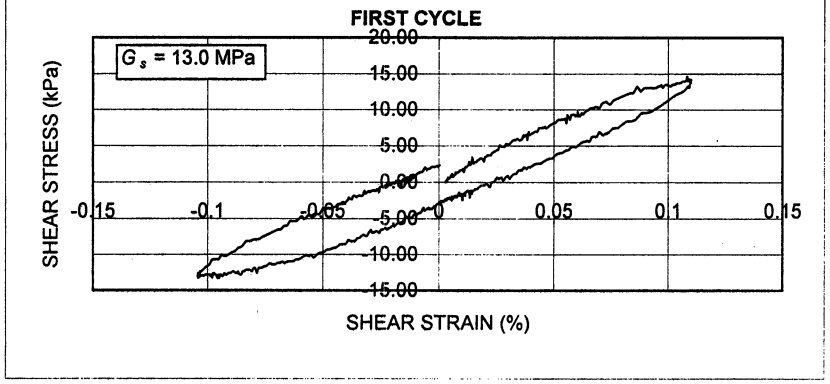

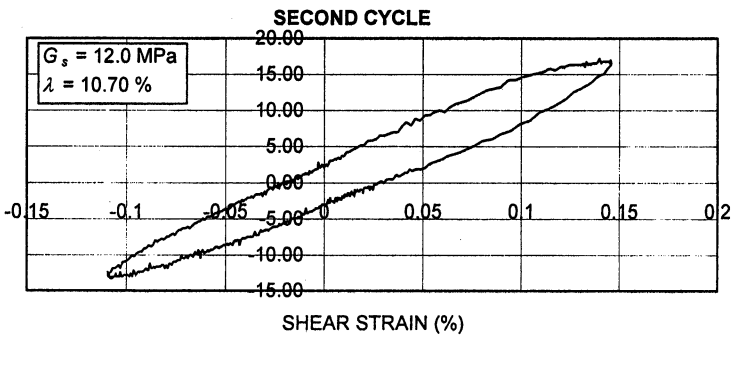

Halls Valley P-2					
DSDSS TEST - Step 76					
Type of soil: CL					
LL	38.2	PI	24.6	%Silt	37.1
e_0	0.87	S_0 (%)	99.3	%Clay	34.0
σ_v (kPa)	105	OCR	n/a	w (%)	32.5
γ_c (%)	~0.3	H_0 (mm)	19.26	Spec. Gr.	2.65

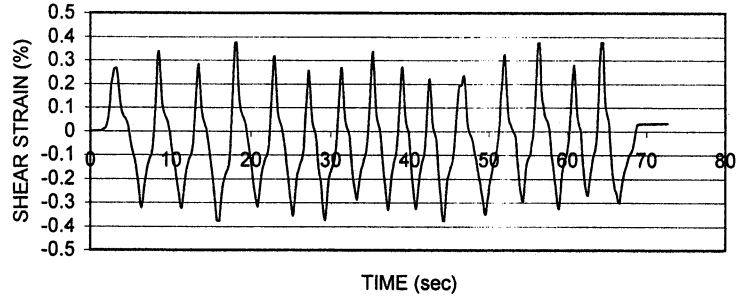

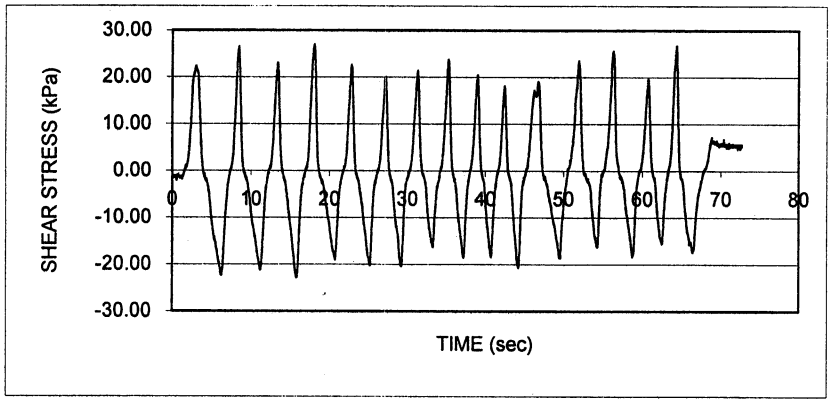

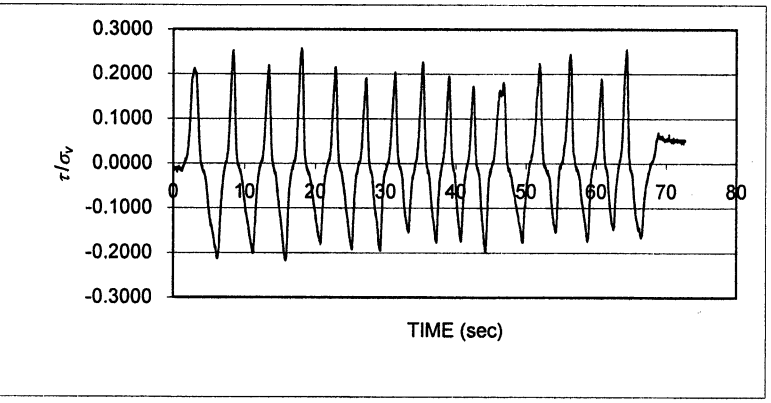

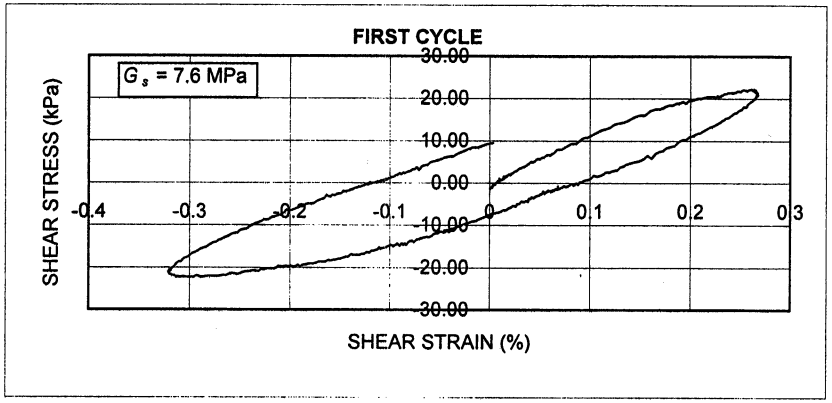

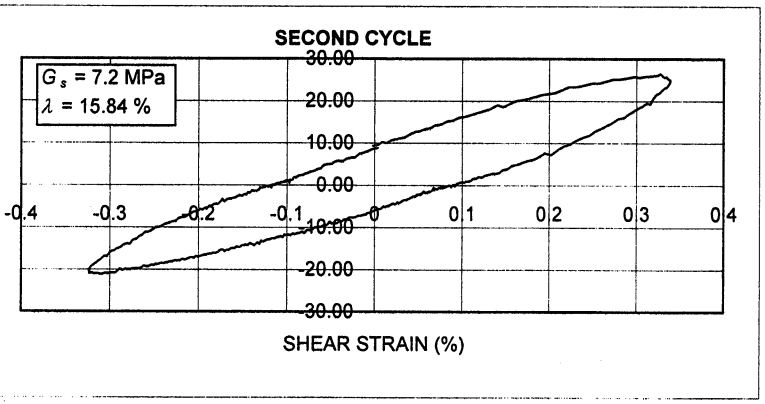

Halls Valley P-2					
DSDSS TEST - Step 8					
Type of soil: CL					
LL	38.2	PI	24.6	%Silt	37.1
e_0	0.87	S_0 (%)	99.3	%Clay	34.0
σ_v (kPa)	105	OCR	n/a	w (%)	32.5
γ_c (%)	~2.8	H_0 (mm)	19.26	Spec. Gr.	2.65

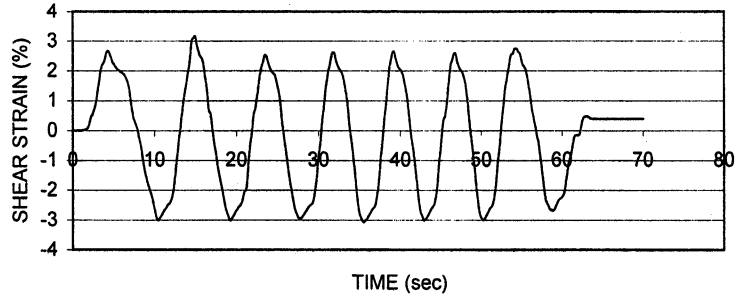

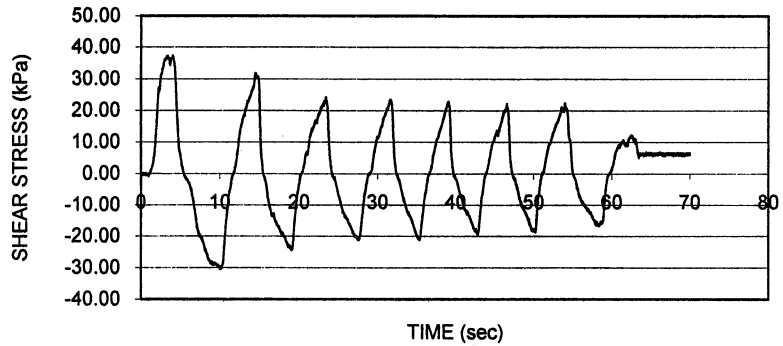

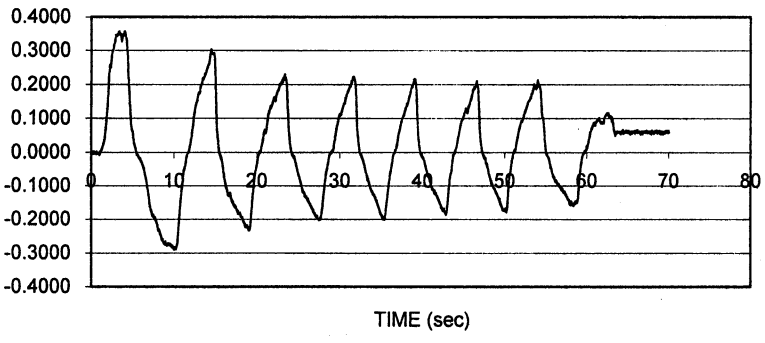

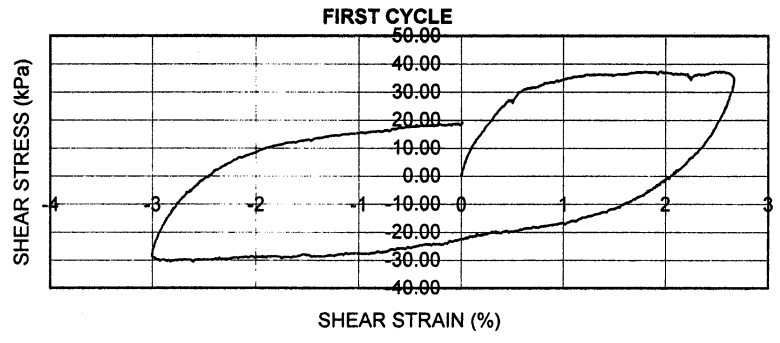

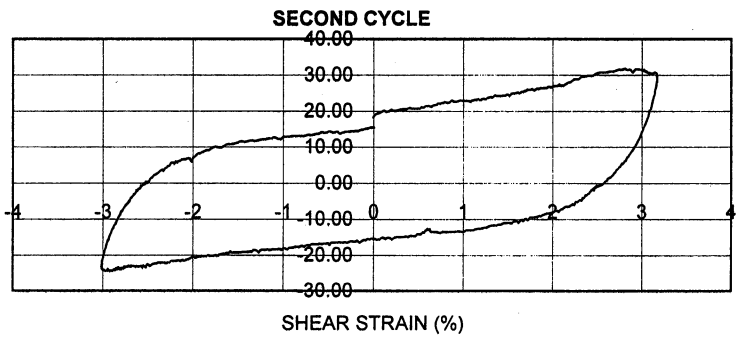

UCLA Soil Dynamics Laboratory

Double Specimen Direct Simple Shear (DSDSS) Test

Principal investigator: Mladen Vucetic, Professor

Test performed by Kentaro Tabata

Test no: 11

Project:	PEARL			Date:	1/11/2002
Sample name:	Halls Valley (P-2)			Depth (ft):	17.5
Symbol:	CL	LL (%):	38.2	Silt content (%):	37.1
Specific gravity:	2.65	PI:	24.6	Clay content (%):	34.0
Comments:					

Estimated G_{max} (MPa):	25.0

SHEAR MODULUS				DAMPING RATIO	
Step	γ_c (%)	G_s (MPa)	G_s/G_{max}	γ_c (%)	λ (%)
26x	0.000700	24.61	0.985	0.000732	2.98
26x	0.000732	24.36	0.974	0.001035	3.04
3x	0.001035	23.57	0.943	0.002694	2.91
3x	0.001035	24.05	0.962	0.009639	3.47
4x	0.002803	23.25	0.930	0.028456	5.07
4x	0.002694	23.69	0.948	0.127595	10.70
5x	0.009932	22.63	0.905	0.331104	15.84
5x	0.009639	22.11	0.885		
6x	0.027759	19.18	0.767		
6x	0.028456	18.79	0.752		
7x	0.107218	13.04	0.522		
7x	0.127595	11.96	0.478		
76x	0.294386	7.60	0.304		
76x	0.331104	7.21	0.288		
	γ (%)				
(Monotonic loading)	0.501183	5.35	0.214		
	1.006081	3.43	0.137		
	1.503588	2.40	0.096		
	2.004809	1.84	0.073		
	2.500496	1.49	0.060		
	2.663894	1.32	0.053		

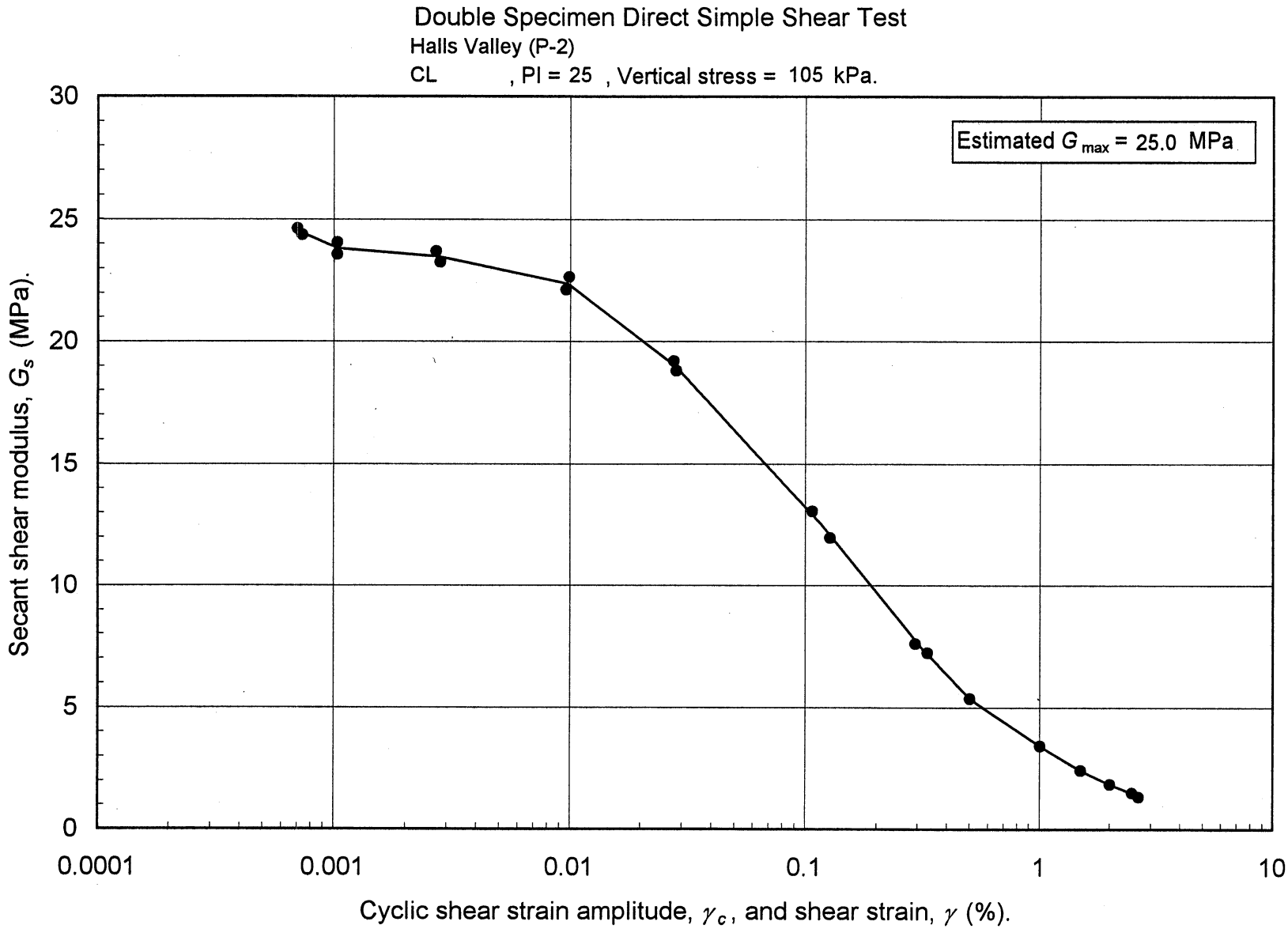
Double Specimen Direct Simple Shear Test
Halls Valley (P-2)
CL , PI = 25 , Vertical stress = 105 kPa.
Estimated G_{max} = 25.0 MPa
Secant shear modulus, G_s (MPa).
30
25
20
15
10
5
0
0.0001
0.001
0.01
0.1
1
10
Cyclic shear strain amplitude, γ_c, and shear strain, γ (%).

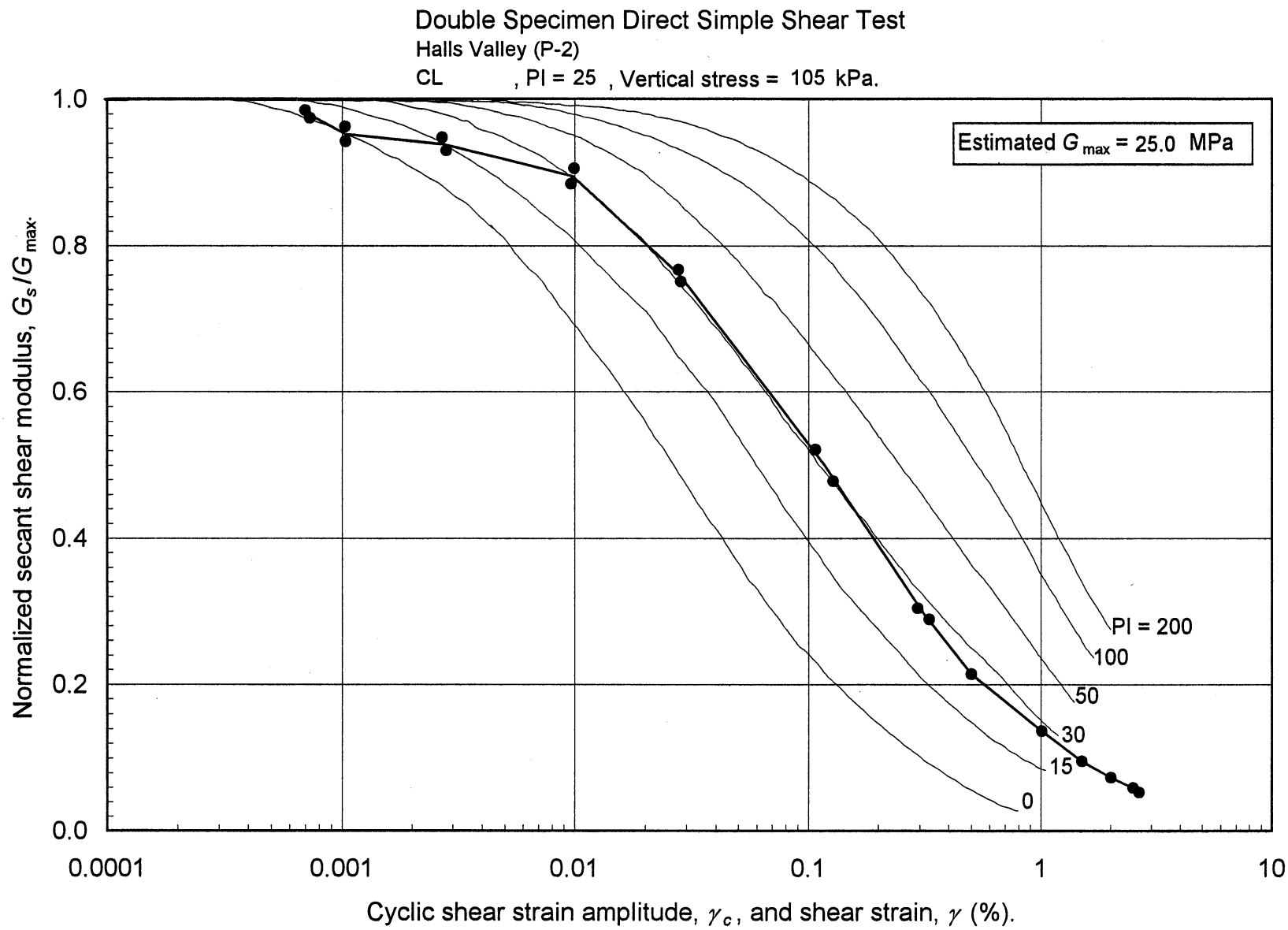
Double Specimen Direct Simple Shear Test
Halls Valley (P-2)
CL , PI = 25 , Vertical stress = 105 kPa.
Estimated G_{max} = 25.0 MPa
Normalized secant shear modulus, G_s/G_{max}
1.0
0.8
0.6
0.4
0.2
0.0
0.0001
0.001
0.01
0.1
1
10
PI = 200
100
50
30
15
0
Cyclic shear strain amplitude, γ_c, and shear strain, γ (%).

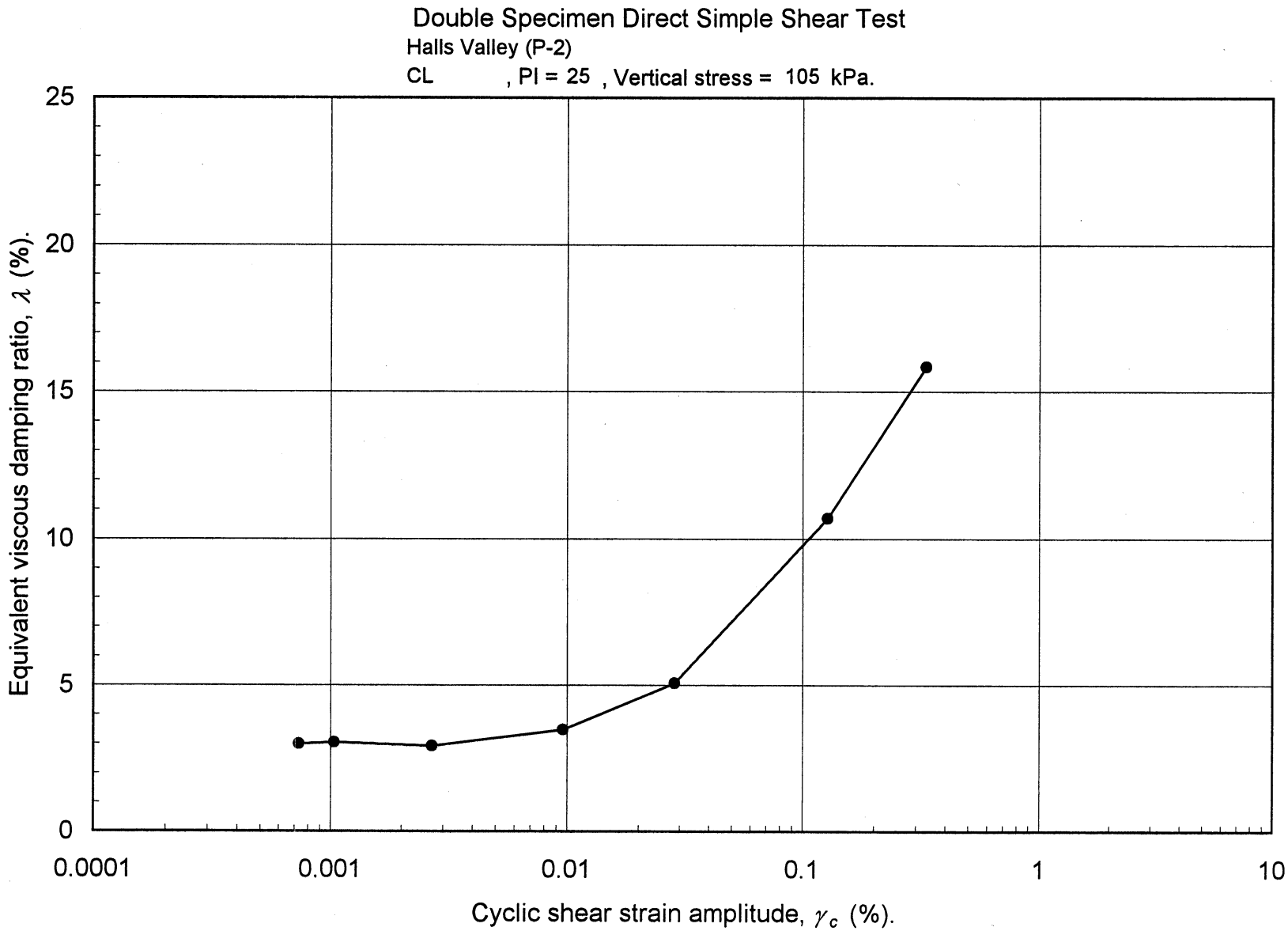
Double Specimen Direct Simple Shear Test
Halls Valley (P-2)
CL , PI = 25 , Vertical stress = 105 kPa.
Equivalent viscous damping ratio, λ (%).
25
20
15
10
5
0
0.0001
0.001
0.01
0.1
1
10
Cyclic shear strain amplitude, γc (%).

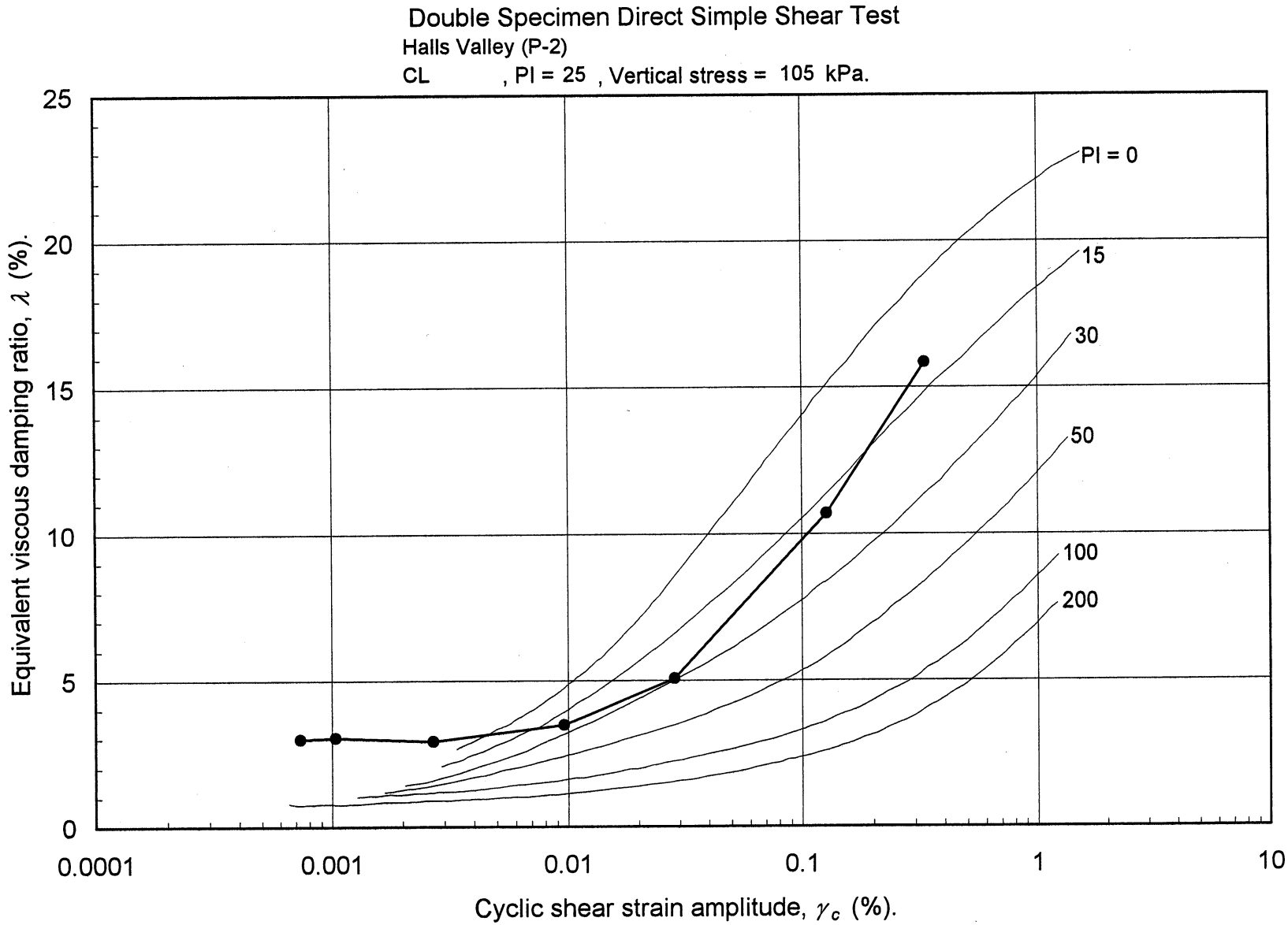
Double Specimen Direct Simple Shear Test
Halls Valley (P-2)
CL , PI = 25 , Vertical stress = 105 kPa.
Equivalent viscous damping ratio, λ (%).
Cyclic shear strain amplitude, γc (%).
0
5
10
15
20
25
0.0001
0.001
0.01
0.1
1
10
PI = 0
15
30
50
100
200

UCLA Soil Dynamics Laboratory

Specific Gravity Test

Principal investigator: Mladen Vucetic, Professor

Test performed by: Kentaro Tabata Test No.: 11

Project:	PEARL			Date:	1/21/2002
Boring:	Halls Valley				
Tube No.:	P-2	Depth (ft):	15.0 -18.0	GWT (ft):	65.0
Comments:	Dark grayish brown silty clay.				

SPECIFIC GRAVITY TEST

Test No.	1		
Bottle No.	3		
Wt. of bottle (g)	178.27		
Volume of bottle (cm^3)	500		
Wt. of bottle+water+soil (g)	693.60		
Temperature (°C)	21.0		
Wt. of bottle+water (g)	676.40		
Evaporating dish No.	B-2		
Weight of dish (g)	537.20		
Wt. of dish+dry soil (g)	564.76		
Wt. of dry soil (g)	27.56		
Specific gravity of water	0.9980		
Specific gravity of soil	**2.65**		

UCLA Soil Dynamics Laboratory

Grain Size Distribution

Principal investigator: Mladen Vucetic, Professor

Test performed by: Kentaro Tabata Test No.: 11

Project:	PEARL				
Boring:	Halls Valley				
Tube No.:	P-2	Depth (ft):	15.0 -18.0	GWT (ft):	65.0
Comments:	Dark grayish brown silty clay.				

GRAIN SIZE DISTRIBUTION

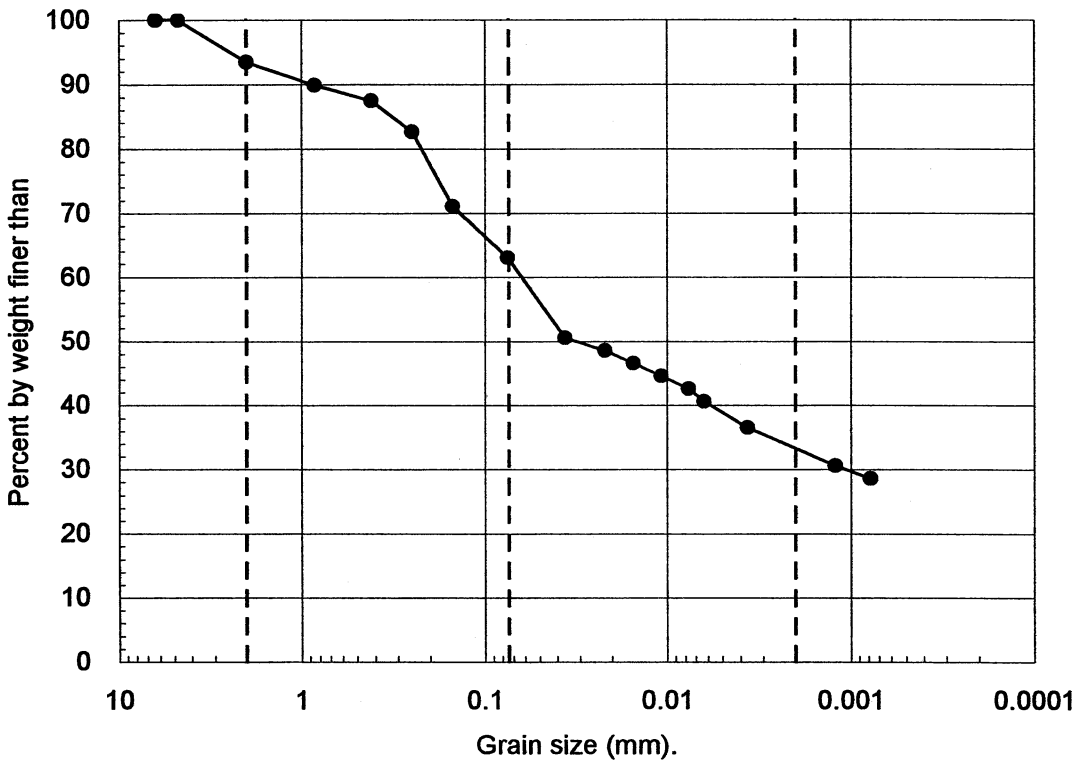

Clay (%)	Silt (%)	Sand (%)	Gravel (%)
34.0	37.1	22.3	6.6

UCLA Soil Dynamics Laboratory

Hydrometer Analysis

Principal investigator: Mladen Vucetic, Professor

Test performed by: Kentaro Tabata Test No.: 11

Project:	PEARL			Date:	1/22/2002
Boring:	Halls Valley				
Tube No.:	P-2	Depth (ft):	15.0 -18.0	GWT (ft):	65.0
Comments:	Dark grayish brown silty clay.				

HYDROMETER TEST

Time	Elapsed time t (sec)	Temp. T (°C)	Reading R'_T	Corr. reading $R_T=R'_T+c_m$	Depth H (cm)	Grain diameter D (mm)	Temp. corr. m_T	Corr. depth $R_T+m_T-c_d$	% by wt. finer than W_D (%)
15:05:20	0								
15:07:02	102	22.0	1014.5	1015.0	12.51	0.0362	0.700	1012.7	50.54
15:10:02	282	22.0	1014.0	1014.5	12.64	0.0219	0.700	1012.2	48.55
15:15:02	582	22.0	1013.5	1014.0	12.78	0.0153	0.700	1011.7	46.56
15:25:02	1182	22.0	1013.0	1013.5	12.91	0.0108	0.700	1011.2	44.57
15:45:02	2382	22.0	1012.5	1013.0	13.04	0.0076	0.700	1010.7	42.58
16:05:02	3582	22.0	1012.0	1012.5	13.18	0.0063	0.700	1010.2	40.59
18:05:02	10782	22.0	1011.0	1011.5	13.44	0.0037	0.700	1009.2	36.61
18:54:00	100120	22.0	1009.5	1010.0	13.85	0.0012	0.700	1007.7	30.64
11:27:00	246100	22.0	1009.0	1009.5	13.98	0.0008	0.700	1007.2	28.65

APPARATUS

Hydrometer no.:	88-18587	a_0	284.03	a_1	-0.2675
Graduate no.:	3				

FACTORS

Meniscus corr., c_m:	0.5	
Disp. agent corr, c_d:	3.0	
Visc. of water, η.	22.0 °C	9.799E-06 g sec/cm^2
	°C	g sec/cm^3

WEIGHT

Dry soil (g)	25.43
Percent by wt (%)	63.07
Dry soil for sieve (g)	14.89
Total (g)	40.32

UNIT WEIGHT

Specific gravity:		2.65
T	γ_w	γ_s
(°C)	(g/cm^3)	(g/cm^3)
22.0	0.9978	2.6486

UCLA Soil Dynamics Laboratory

Sieve Analysis

Principal investigator: Mladen Vucetic, Professor

Test performed by: Kentaro Tabata Test No.: 11

Project:	PEARL			Date:	1/25/2002
Boring:	Halls Valley				
Tube No.:	P-2	Depth (ft):	15.0 -18.0	GWT (ft):	65.0
Comments:	Dark grayish brown silty clay.				

SIEVE ANALYSIS

Sieve No.	Diameter (mm)	Sieve (g)	S+wet (g)	S+dry (g)	Retained (g)	Retained (%)	Cumulated (g)	Cumulated (%)	Passing (%)
3	6.350	485.05		485.05	0.00	0.00	0.00	0.00	100.00
4	4.750	463.13		463.13	0.00	0.00	0.00	0.00	100.00
10	2.000	422.88		425.53	2.65	6.57	2.65	6.57	93.43
20	0.850	375.68		377.09	1.41	3.50	4.06	10.07	89.93
40	0.420	457.72		458.69	0.97	2.41	5.03	12.48	87.52
60	0.250	324.39		326.36	1.97	4.89	7.00	17.36	82.64
100	0.150	342.16		346.82	4.66	11.56	11.66	28.92	71.08
200	0.075	676.91		680.14	3.23	8.01	14.89	36.93	63.07
Total					14.89	36.93			

WEIGHT

Dry soil for sieve (g)	14.89
Dry soil for hydr. (g)	25.43
Total (g)	40.32
Percent coaser (%)	36.93

UCLA Soil Dynamics Laboratory

Atterberg Limit Determination

Principal investigator: Mladen Vucetic, Professor

Test performed by: Kentaro Tabata Test No.: 11

Project:	PEARL			Date:	1/22/2002
Boring:	Halls Valley				
Tube No.:	P-2	Depth (ft):	15.0 -18.0	GWT (ft):	65.0
Comments:	Dark grayish brown silty clay.				

LIQUID LIMIT TEST

Test No.	1	2	3	4	5			
Number of blows	37	22	15	12	9			
Container No.	ST-22	ST-15	ST-3	ST-5	ST-11			
Container (g)	30.08	30.27	30.18	30.13	30.26			
Cont+wet soil (g)	37.17	36.95	36.23	36.35	36.99			
Cont+dry soil (g)	35.25	35.11	34.50	34.55	35.00			
Water (g)	1.92	1.84	1.73	1.80	1.99			
Dry soil (g)	5.17	4.84	4.32	4.42	4.74			
Water content (%)	37.14	38.02	40.05	40.72	41.98			

PLASTIC LIMIT TEST

Test No.	1	2	3
Container No.	ST-8	ST-24	ST-12
Container (g)	30.07	29.98	30.29
Cont+wet soil (g)	33.17	32.31	32.62
Cont+dry soil (g)	32.75	32.05	32.36
Water (g)	0.42	0.26	0.26
Dry soil (g)	2.68	2.07	2.07
Water content (%)	15.67	12.56	12.56

ATTERBERG LIMITS

Liquid limit (%)	**38.2**
Plastic limit (%)	**13.6**
Plasticity index	**24.6**

CLASSIFICATION

CL

FLOW CHART

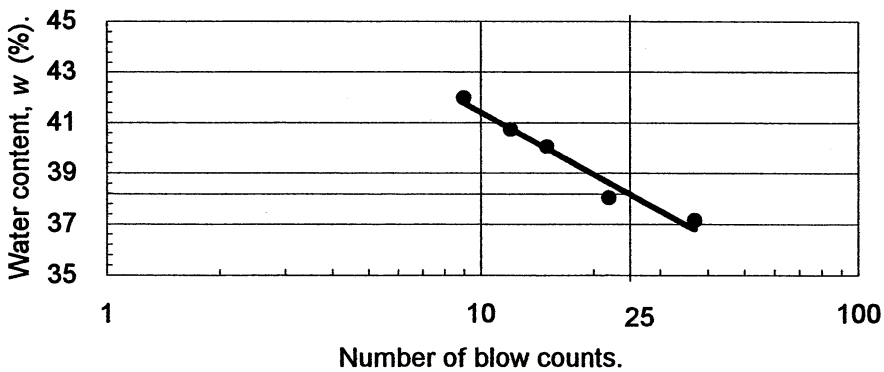

UCLA Soil Dynamics Laboratory

Atterberg Limit Determination

Principal investigator: Mladen Vucetic, Professor

Test performed by: Kentaro Tabata Test No.: 11

Project:	PEARL			Date:	1/22/2002
Boring:	Halls Valley				
Tube No.:	P-2	Depth (ft):	15.0 -18.0	GWT (ft):	65.0
Comments:	Dark grayish brown silty clay.				

PLASTICITY CHART

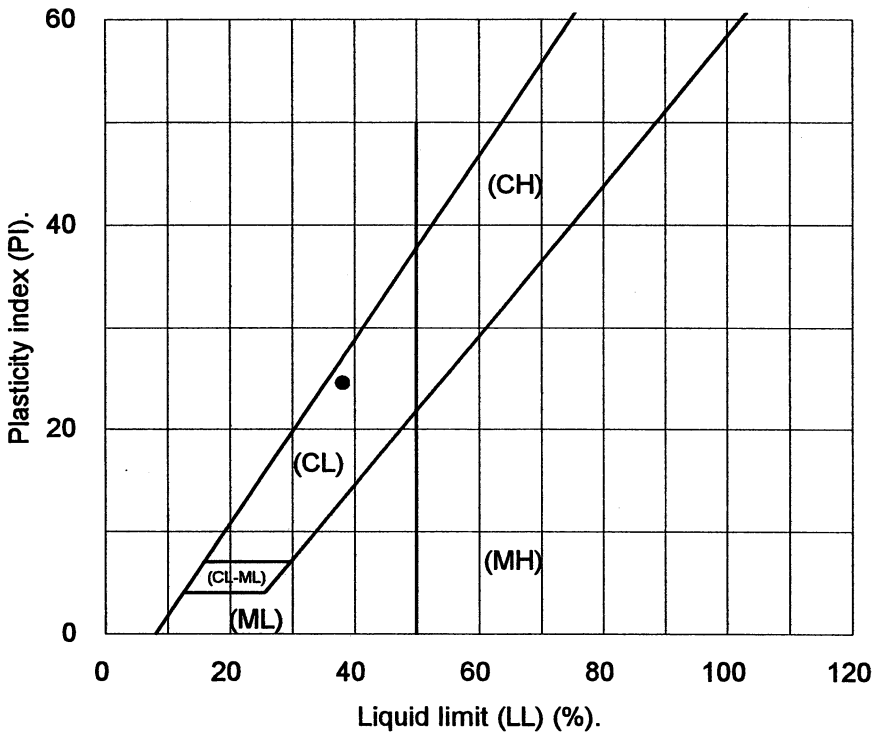

3.13 Test 12: HALLS VALLEY P-3

UCLA Soil Dynamics Laboratory

Double Specimen Direct Simple Shear (DSDSS) Test

Principal investigator: Mladen Vucetic, Professor

Test performed by: Kentaro Tabata Test No.: 12

Project:	PEARL			Date:	2/21/2002
Boring:	Halls Valley				
Tube No.:	P-3	Depth (ft):	50.0 -53.0	GWT (ft):	65.0 (reported by others)
Comments:	Dark greenish gray clay. Specimen obtained from the top of the tube (specimen depth ~ 50 ft).				

FORM 1: SPECIMEN PREPARATION

WATER CONTENT, SPECIFIC GRAVITY

	Before consol.	After shearing	
Container No.	ST-18	MT-17	MT-23
Cont+wet soil (g)	38.40	164.52	165.48
Cont+dry soil (g)	35.93	132.64	133.93
Container (g)	30.14	50.20	49.65
Water (g)	2.47	31.88	31.55
Dry soil (g)	5.79	82.44	84.28
Water content(%)	42.66	38.67	37.43
Avg. water cont. (%)	42.66		38.05
Spceific gravity			2.64

UNIT WEIGHT, VOID RATIO, SATURATION

	Before consol.	Before shearing	After shearing
Average weight (g)	118.62	118.62	
Height (cm)	1.960	1.882	
Area (cm^2)	34.84	34.84	
Volume (cm^3)	68.28	65.56	
Unit weight (g/cm^3)	1.737	1.809	
Unit weight (kN/m^3)	17.02	17.73	
Void ratio	1.17	1.08	
Saturation (%)	96.4		

HEIGHT OF SPECIMEN

	Before consol.		Before shearing	After shearing		
	Top	Bottom	Average	Average		
Height (cm)	1.960	1.960	1.882	1.882		

AREA OF SPECIMEN

Initial diameter (cm)			6.660	Initial area (cm^2)		34.837
Load (kg)	Stress (kg/cm^2)	Stress (kN/m^2)	Diameter (cm)	Membrane (cm)	Corrected diameter (cm)	Area (cm^2)

Halls Valley P-3					
DSDSS TEST - Step 2b					
Type of soil: CH					
LL	84.7	PI	47.2	%Silt	32.5
e_0	1.08	S_0 (%)		%Clay	63.0
σ_v (kPa)	274	OCR	n/a	w (%)	38.1
γ_c (%)	~0.0004	H_0 (mm)	18.82	Spec. Gr.	2.64

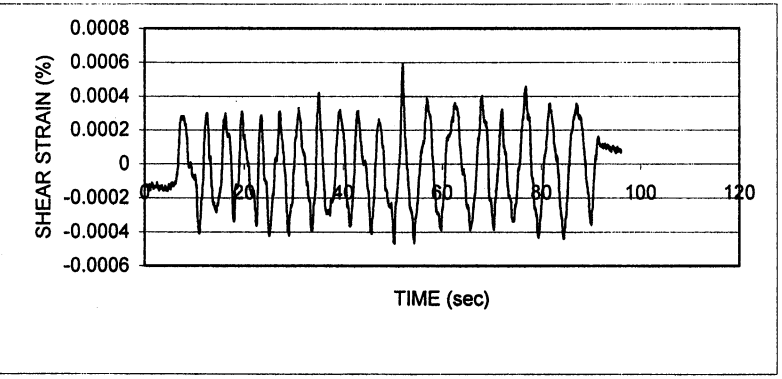

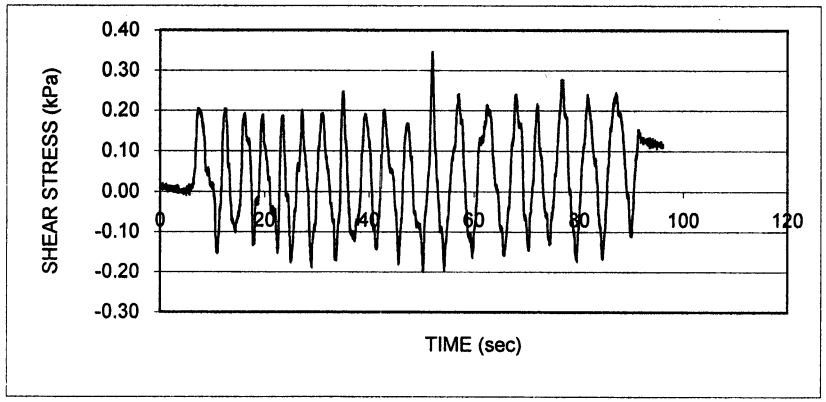

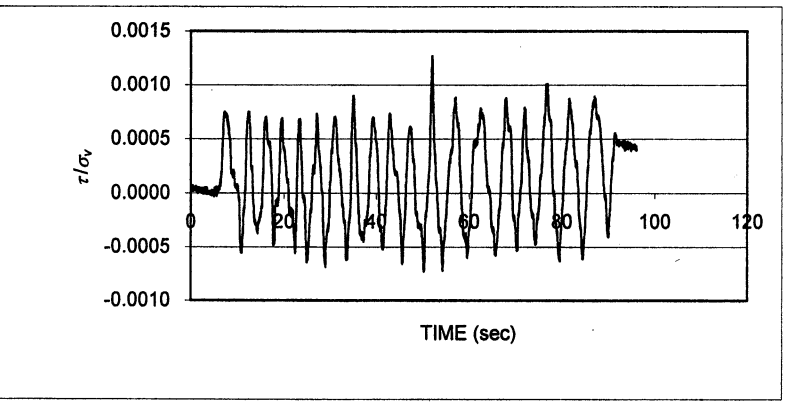

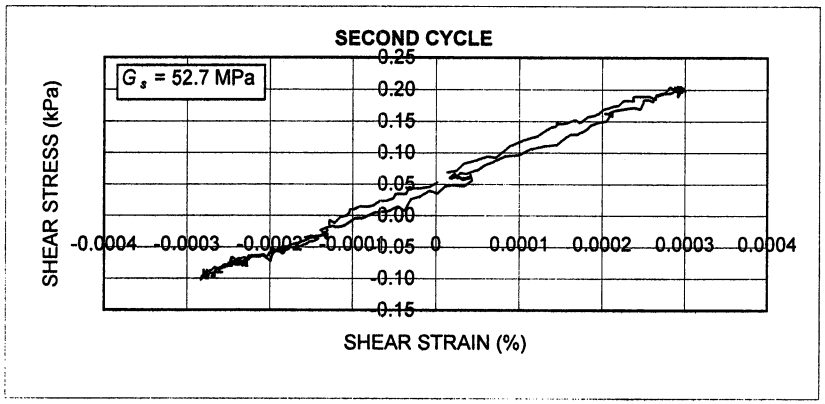

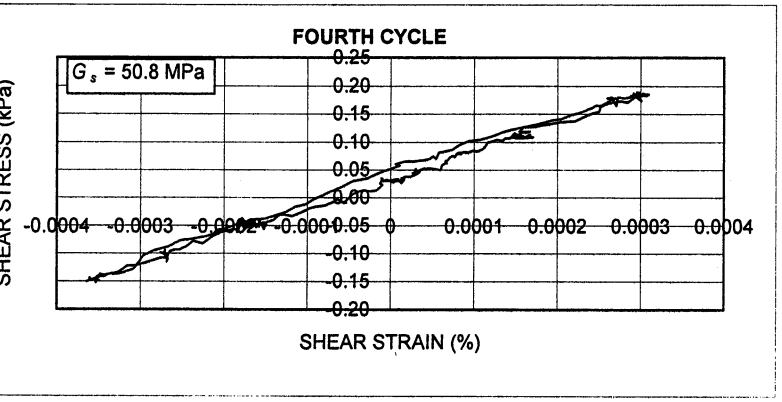

Halls Valley P-3					
DSDSS TEST - Step 26					
Type of soil: CH					
LL	84.7	PI	47.2	%Silt	32.5
e_0	1.08	S_0 (%)		%Clay	63.0
σ_v (kPa)	274	OCR	n/a	w (%)	38.1
γ_c (%)	~0.00075	H_0 (mm)	18.82	Spec. Gr.	2.64

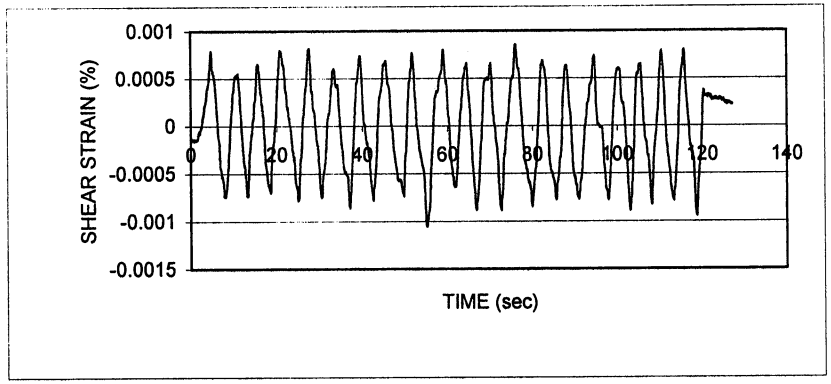

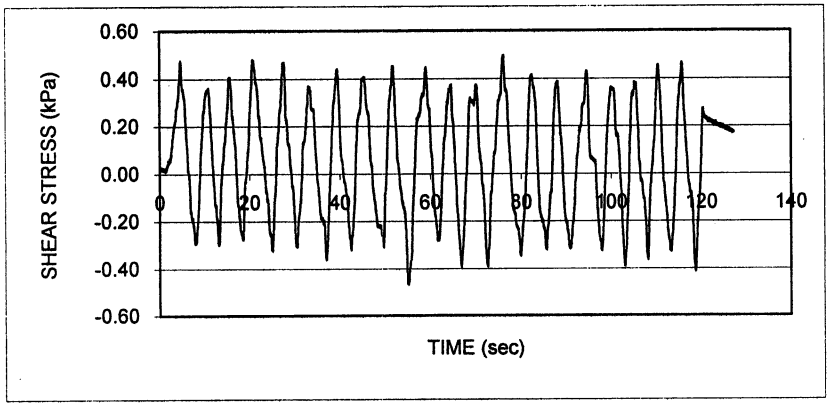

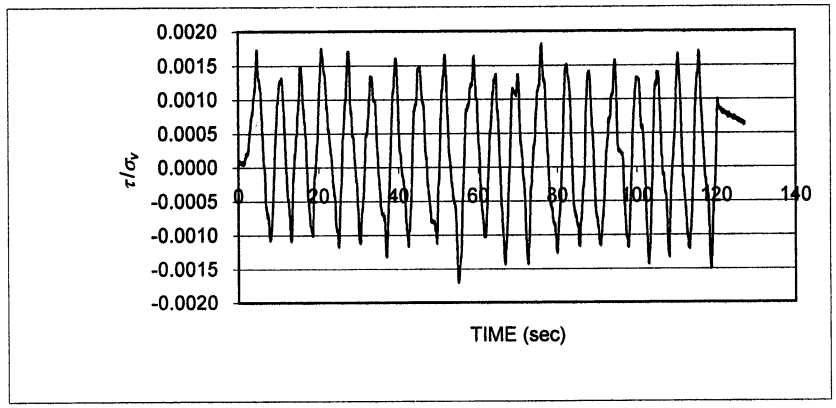

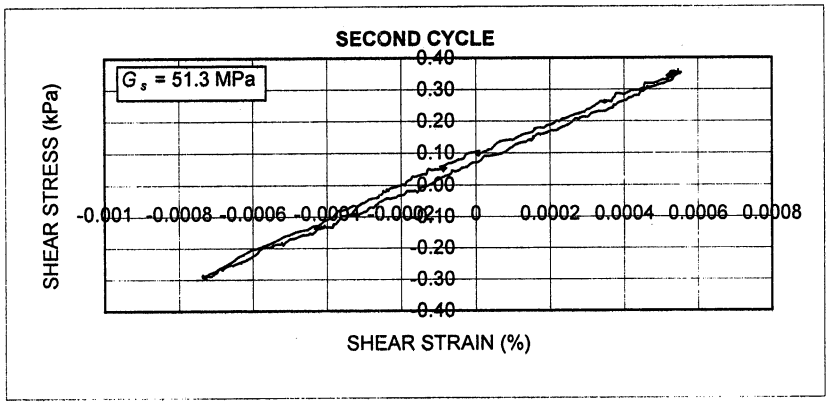

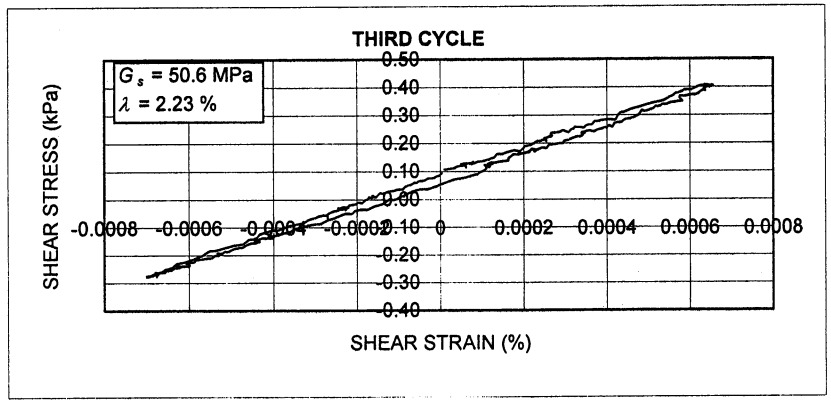

Halls Valley P-3					
DSDSS TEST - Step 3					
Type of soil: CH					
LL	84.7	PI	47.2	%Silt	32.5
e_0	1.08	S_0 (%)		%Clay	63.0
σ_v (kPa)	274	OCR	n/a	w (%)	38.1
γ_c (%)	~0.0012	H_0 (mm)	18.82	Spec. Gr.	2.64

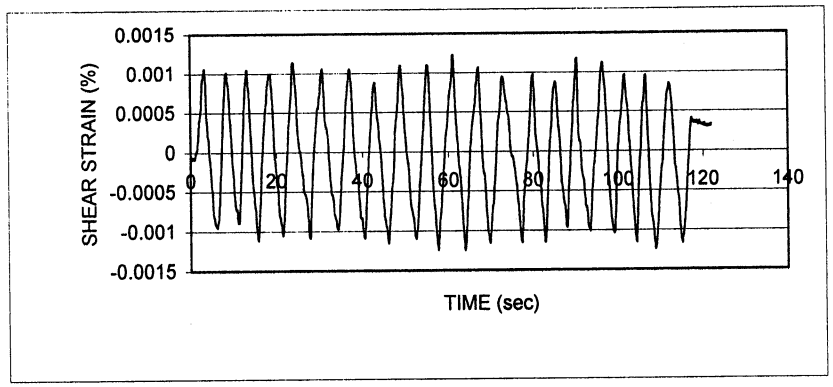

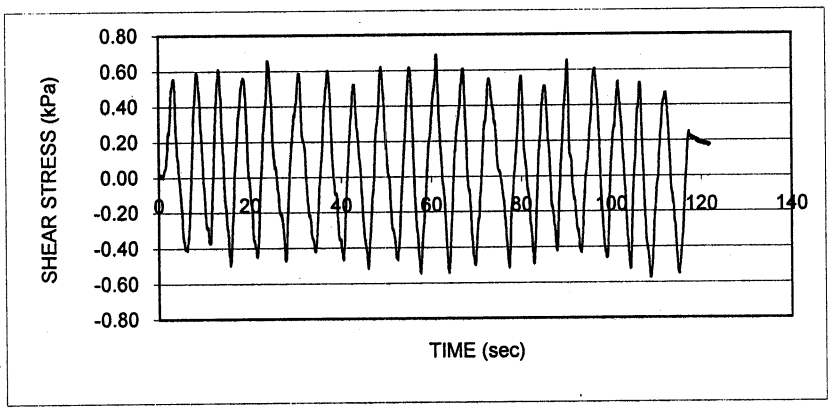

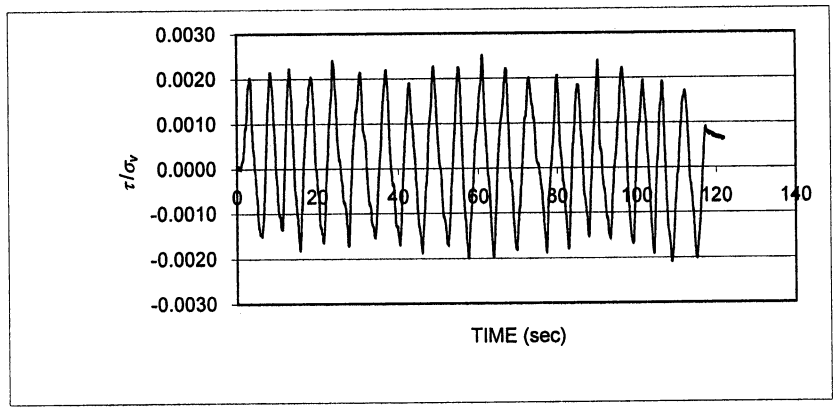

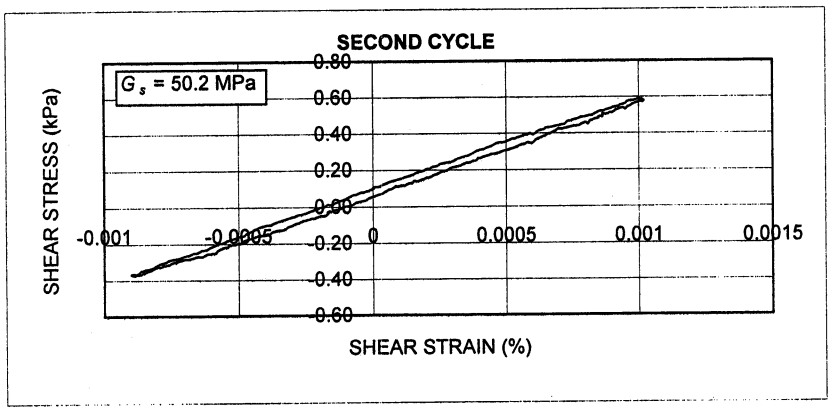

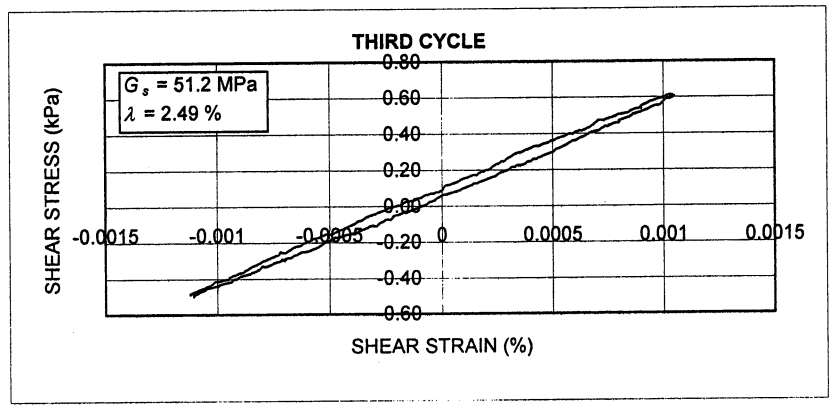

Halls Valley P-3					
DSDSS TEST - Step 4					
Type of soil: CH					
LL	84.7	PI	47.2	%Silt	32.5
e_0	1.08	S_0 (%)		%Clay	63.0
σ_v (kPa)	274	OCR	n/a	w (%)	38.1
γ_c (%)	~0.0026	H_0 (mm)	18.82	Spec. Gr.	2.64

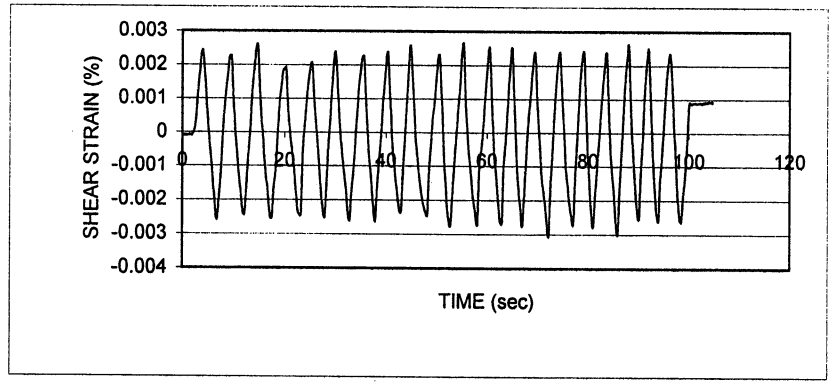

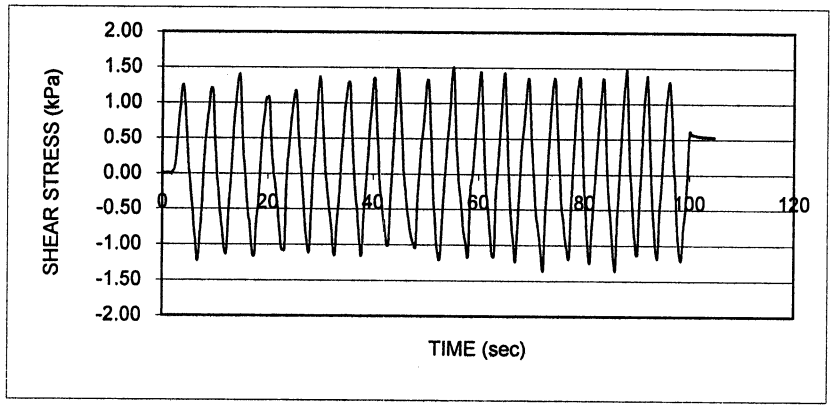

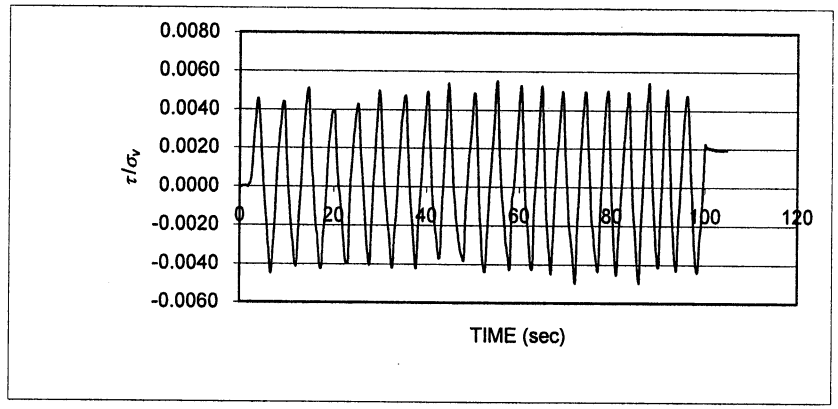

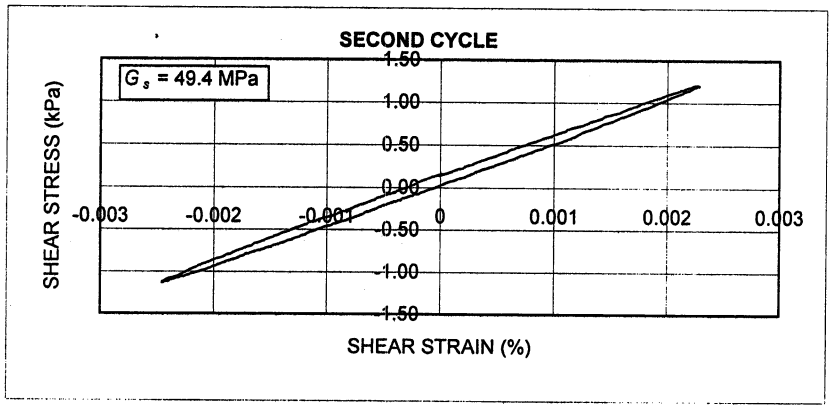

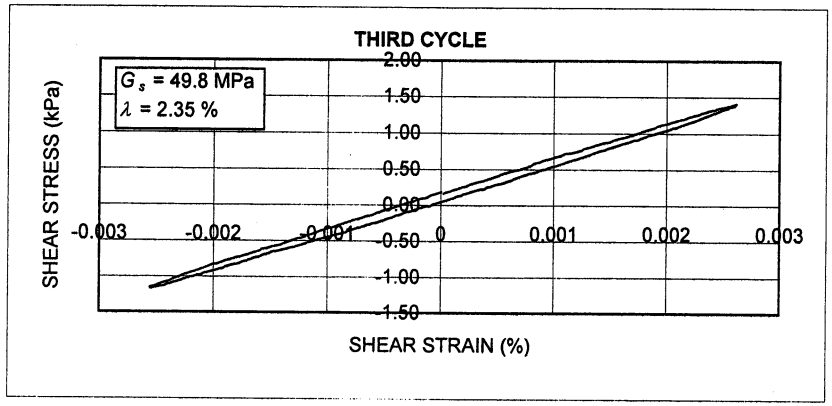

Halls Valley P-3					
DSDSS TEST - Step 5					
Type of soil: CH					
LL	84.7	PI	47.2	%Silt	32.5
e_0	1.08	S_0 (%)		%Clay	63.0
σ_v (kPa)	274	OCR	n/a	w (%)	38.1
γ_c (%)	~0.01	H_0 (mm)	18.82	Spec. Gr.	2.64

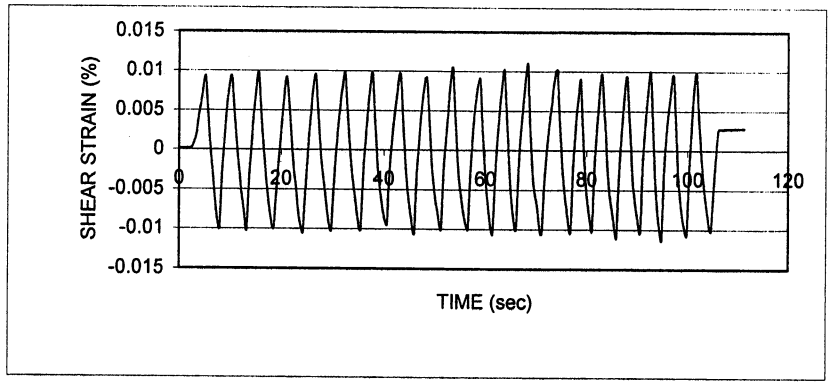

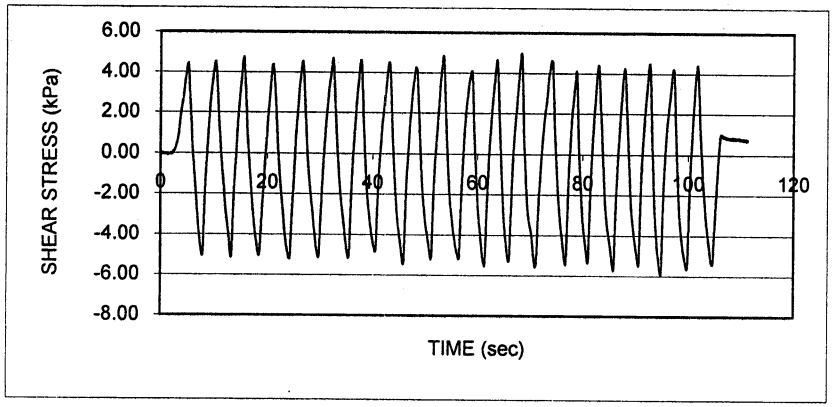

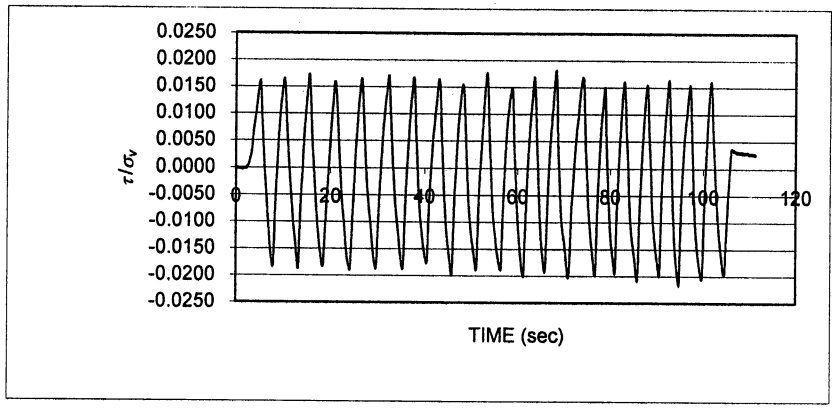

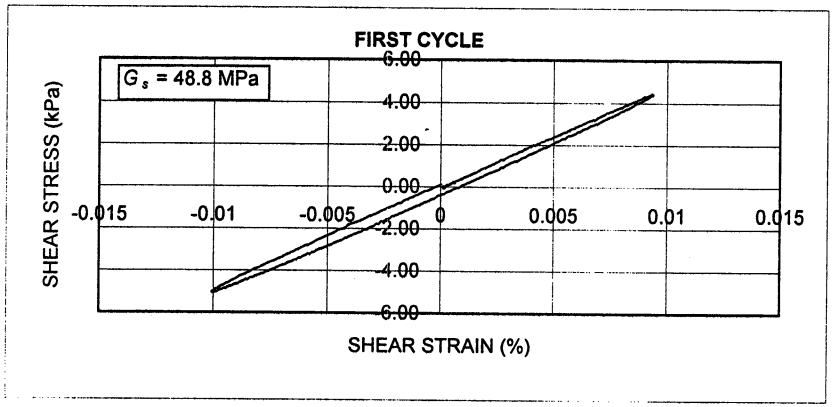

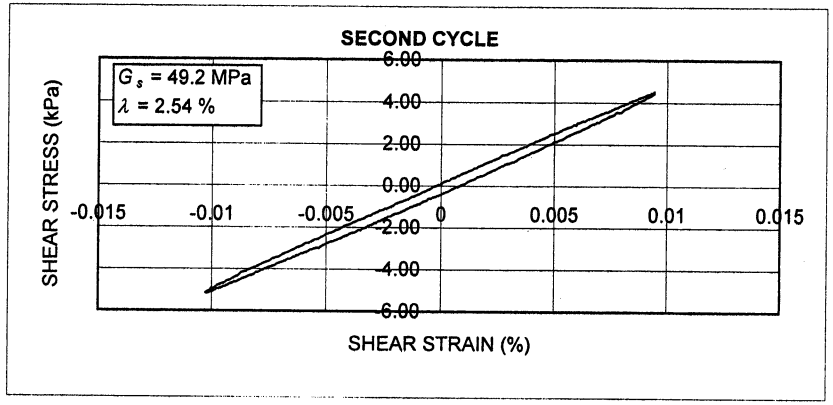

Halls Valley P-3					
DSDSS TEST - Step 6					
Type of soil: CH					
LL	84.7	PI	47.2	%Silt	32.5
e_0	1.08	S_0 (%)		%Clay	63.0
σ_v (kPa)	274	OCR	n/a	w (%)	38.1
γ_c (%)	~0.027	H_0 (mm)	18.82	Spec. Gr.	2.64

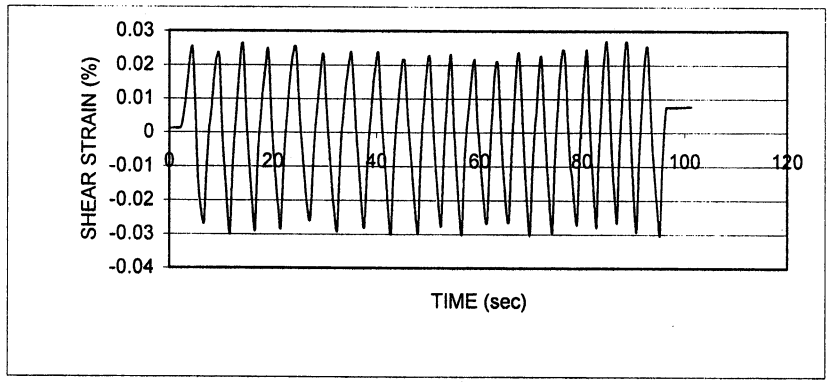

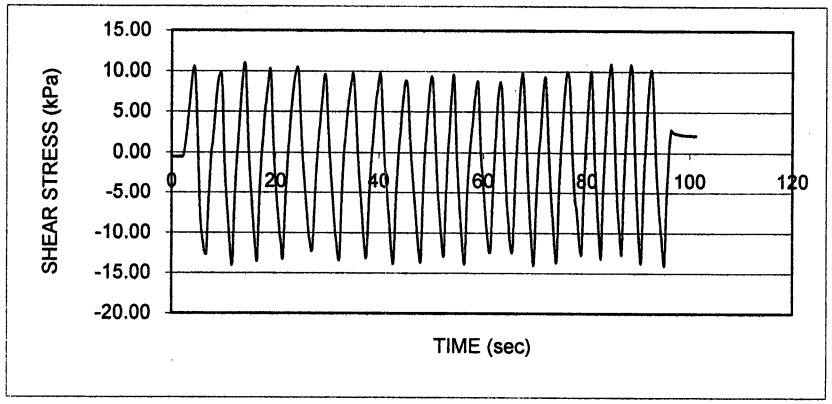

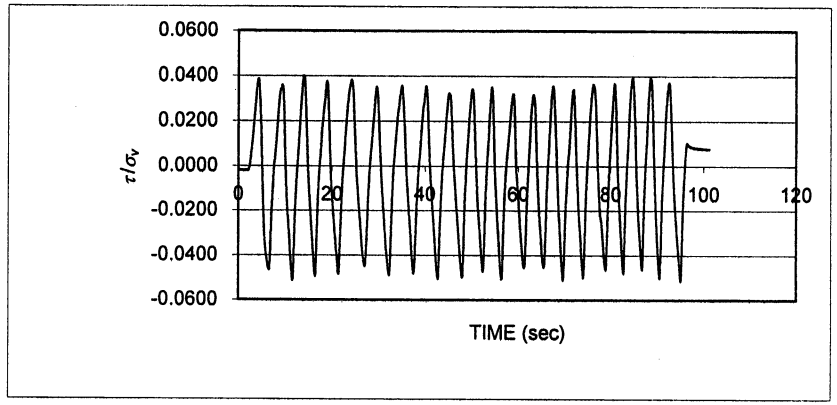

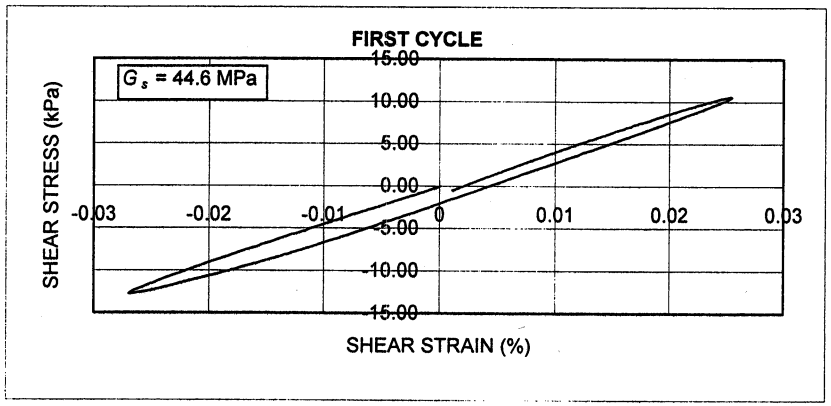

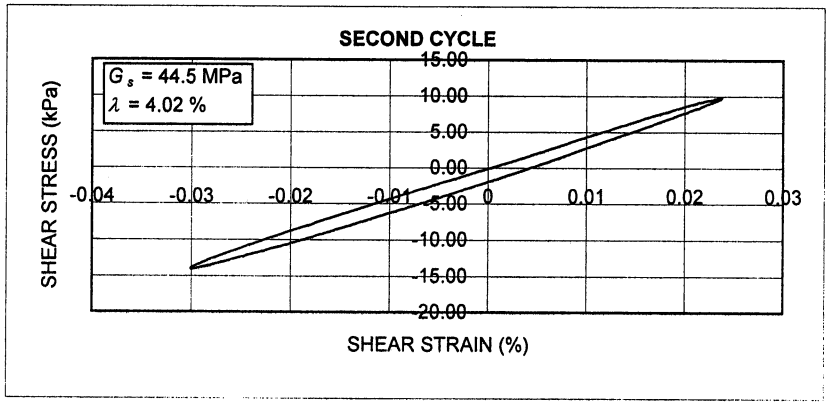

Halls Valley P-3					
DSDSS TEST - Step 7					
Type of soil: CH					
LL	84.7	PI	47.2	%Silt	32.5
e_0	1.08	S_0 (%)		%Clay	63.0
σ_v (kPa)	274	OCR	n/a	w (%)	38.1
γ_c (%)	~0.1	H_0 (mm)	18.82	Spec. Gr.	2.64

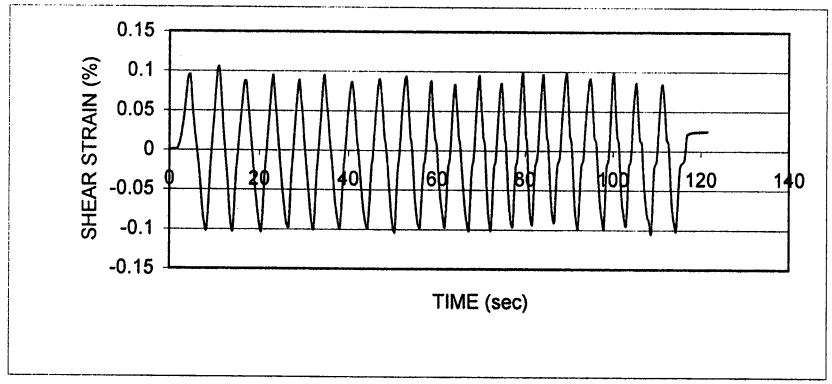

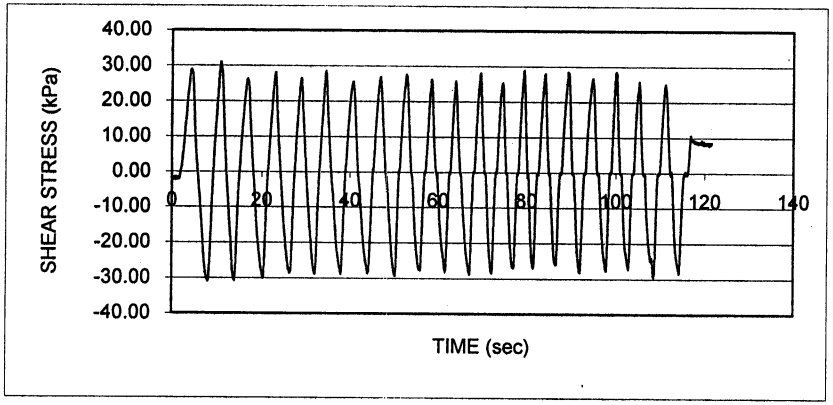

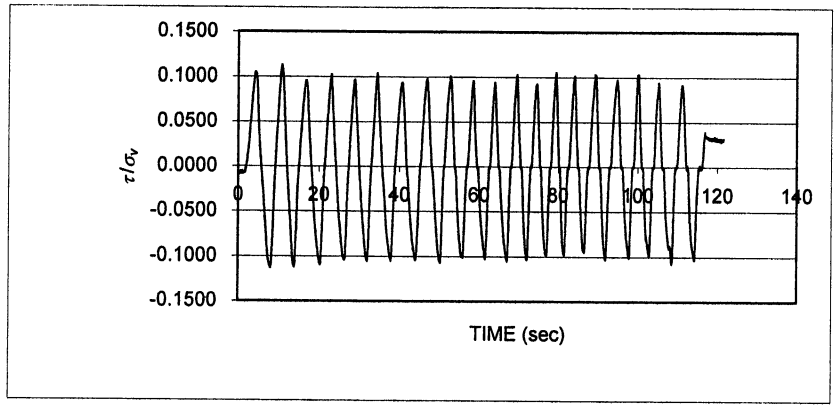

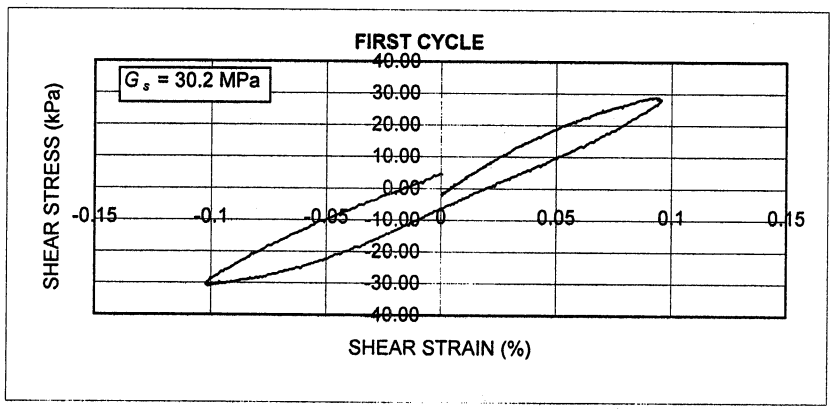

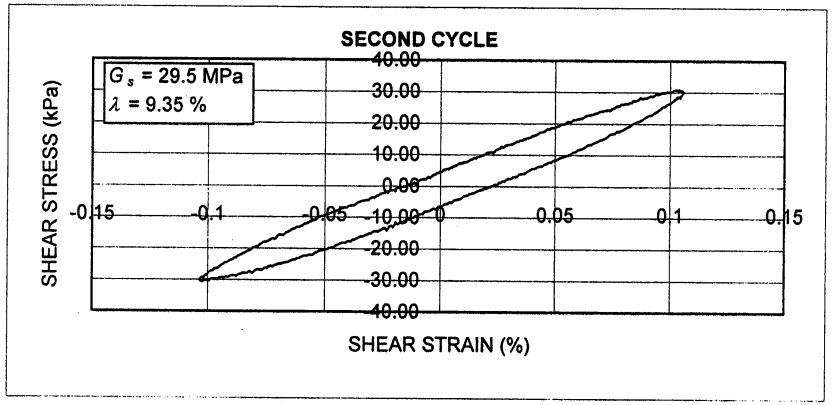

Halls Valley P-3					
DSDSS TEST - Step 8					
Type of soil: CH					
LL	84.7	PI	47.2	%Silt	32.5
e_0	1.08	S_0 (%)		%Clay	63.0
σ_v (kPa)	274	OCR	n/a	w (%)	38.1
γ_c (%)	~3.2	H_0 (mm)	18.82	Spec. Gr.	2.64

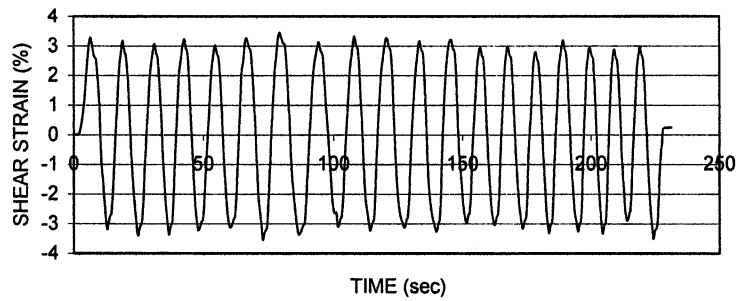

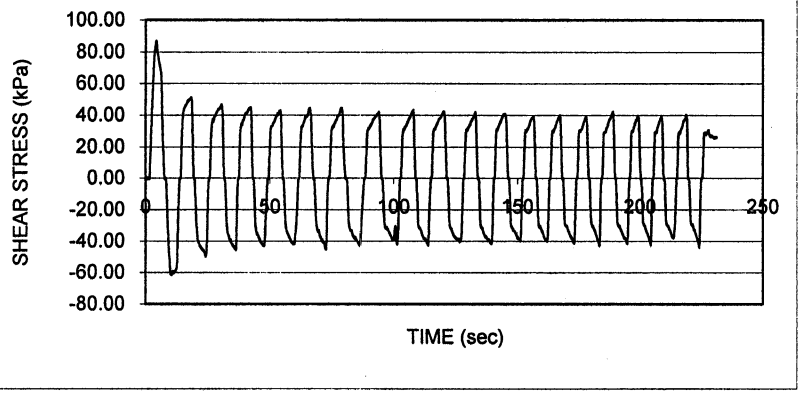

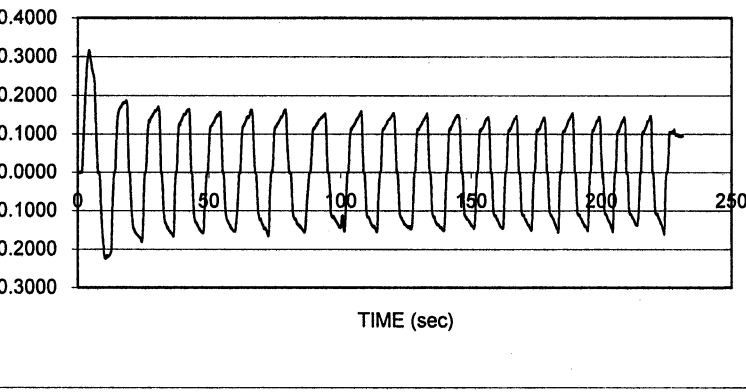

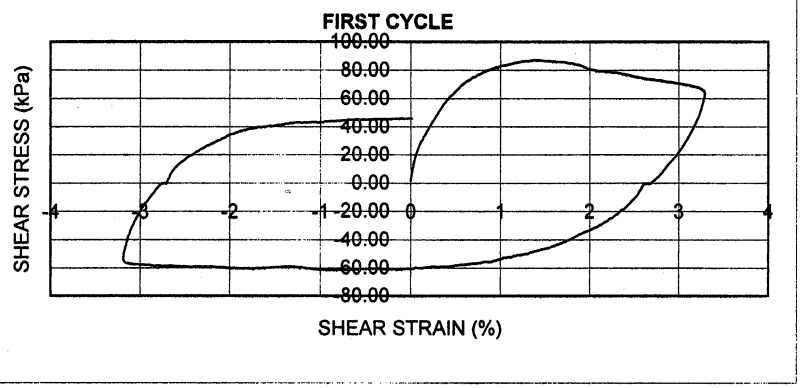

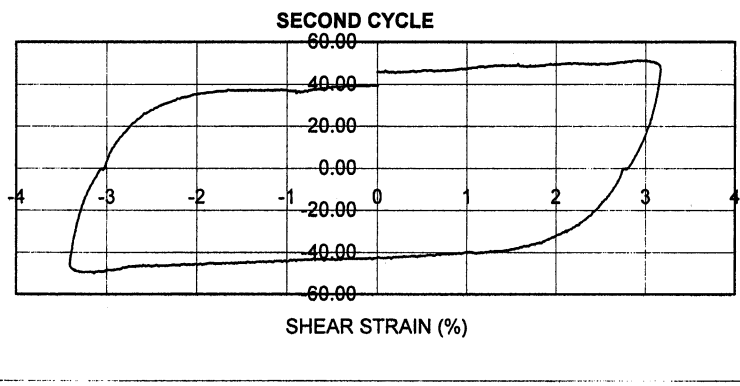

UCLA Soil Dynamics Laboratory

Double Specimen Direct Simple Shear (DSDSS) Test

Principal investigator: Mladen Vucetic, Professor

Test performed by Kentaro Tabata

Test no: 12

Project:	PEARL			Date:	2/21/2002
Sample name:	Halls Valley (P-3)			Depth (ft):	50.0
Symbol:	CH	LL (%):	84.7	Silt content (%):	32.5
Specific gravity:	2.64	PI:	47.2	Clay content (%):	63.0
Comments:	PEARL. Halls Valley P-3 (50-53 ft).				

Estimated G_{max} (MPa):	52.0

SHEAR MODULUS				DAMPING RATIO	
Step	γ_c (%)	G_s (MPa)	G_s/G_{max}	γ_c (%)	λ (%)
2b	0.000292	52.71	1.014		
2b	0.000337	50.76	0.976	0.000678	2.23
26x	0.000645	51.31	0.987	0.001085	2.49
26x	0.000678	50.60	0.973	0.002587	2.35
3x	0.000960	50.21	0.966	0.009845	2.54
3x	0.001085	51.18	0.984	0.026933	4.02
4x	0.002372	49.40	0.950	0.104745	9.35
4x	0.002587	49.80	0.958		
5x	0.009732	48.83	0.939		
5x	0.009845	49.22	0.946		
6x	0.026219	44.60	0.858		
6x	0.026933	44.46	0.855		
7x	0.099014	30.23	0.581		
7x	0.104745	29.47	0.567		
	γ (%)				
(Monotonic loading)	0.501652	13.00	0.250		
	1.003304	8.27	0.159		
	1.506818	5.74	0.110		
	2.004707	4.02	0.077		
	2.508221	3.01	0.058		
	2.508221	3.01	0.058		

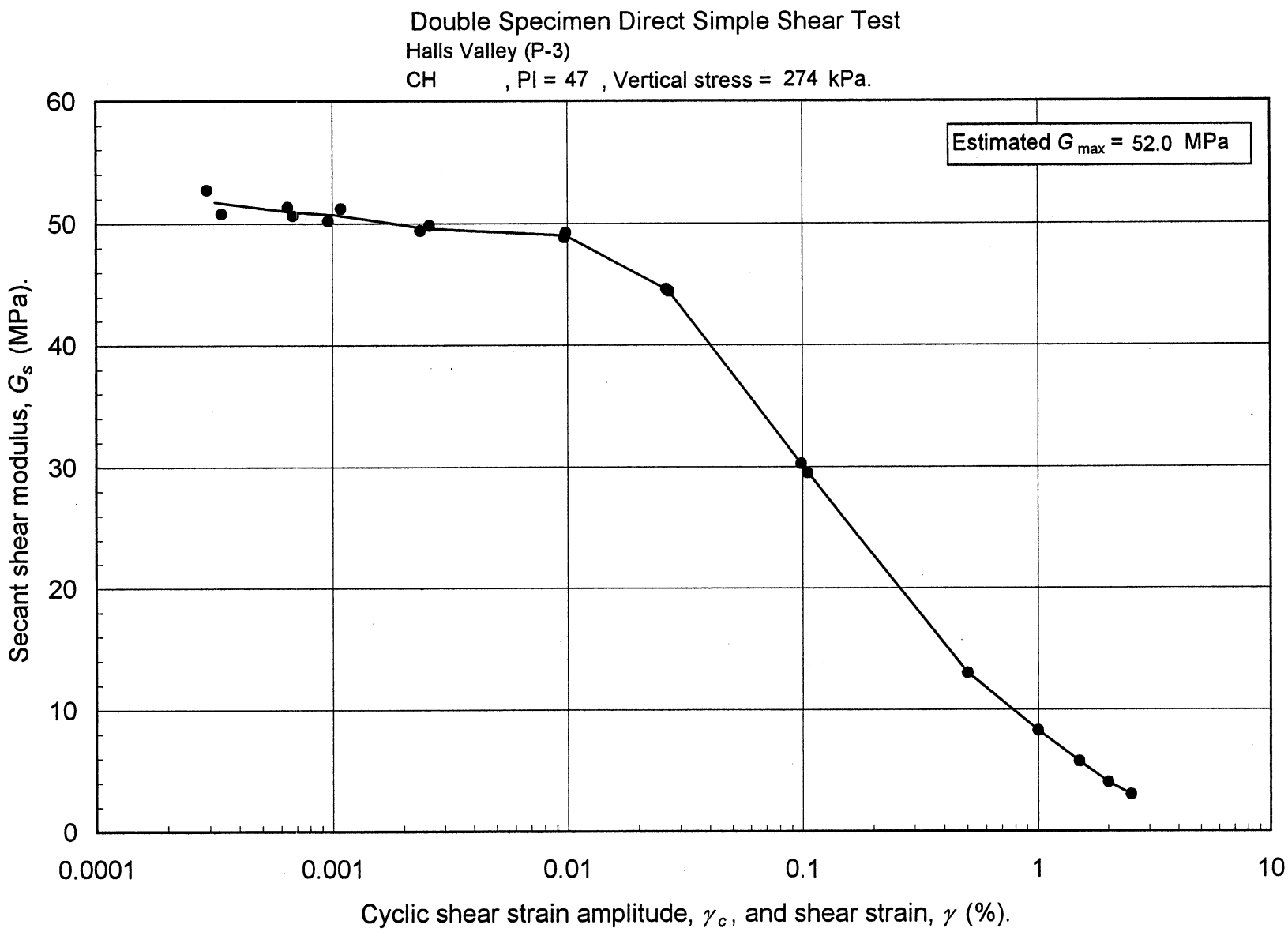
Double Specimen Direct Simple Shear Test
Halls Valley (P-3)
CH , PI = 47 , Vertical stress = 274 kPa.
Estimated G_{max} = 52.0 MPa
Secant shear modulus, G_s (MPa).
60
50
40
30
20
10
0
0.0001
0.001
0.01
0.1
1
10
Cyclic shear strain amplitude, γ_c, and shear strain, γ (%).

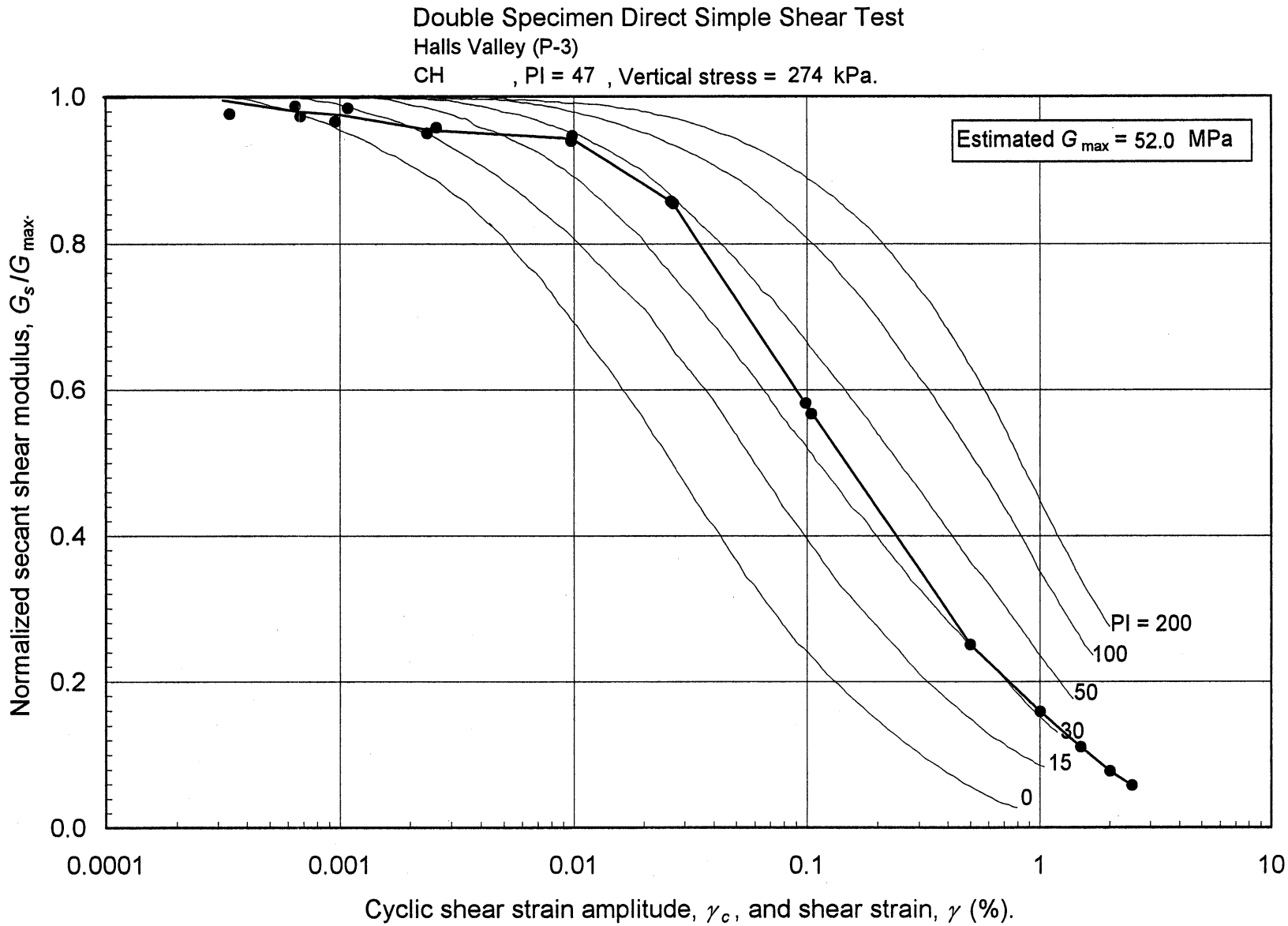
Double Specimen Direct Simple Shear Test
Halls Valley (P-3)
CH , PI = 47 , Vertical stress = 274 kPa.
Estimated G_{max} = 52.0 MPa
Normalized secant shear modulus, G_s/G_{max}.
1.0
0.8
0.6
0.4
0.2
0.0
0.0001
0.001
0.01
0.1
1
10
PI = 200
100
50
30
15
0
Cyclic shear strain amplitude, γ_c, and shear strain, γ (%).

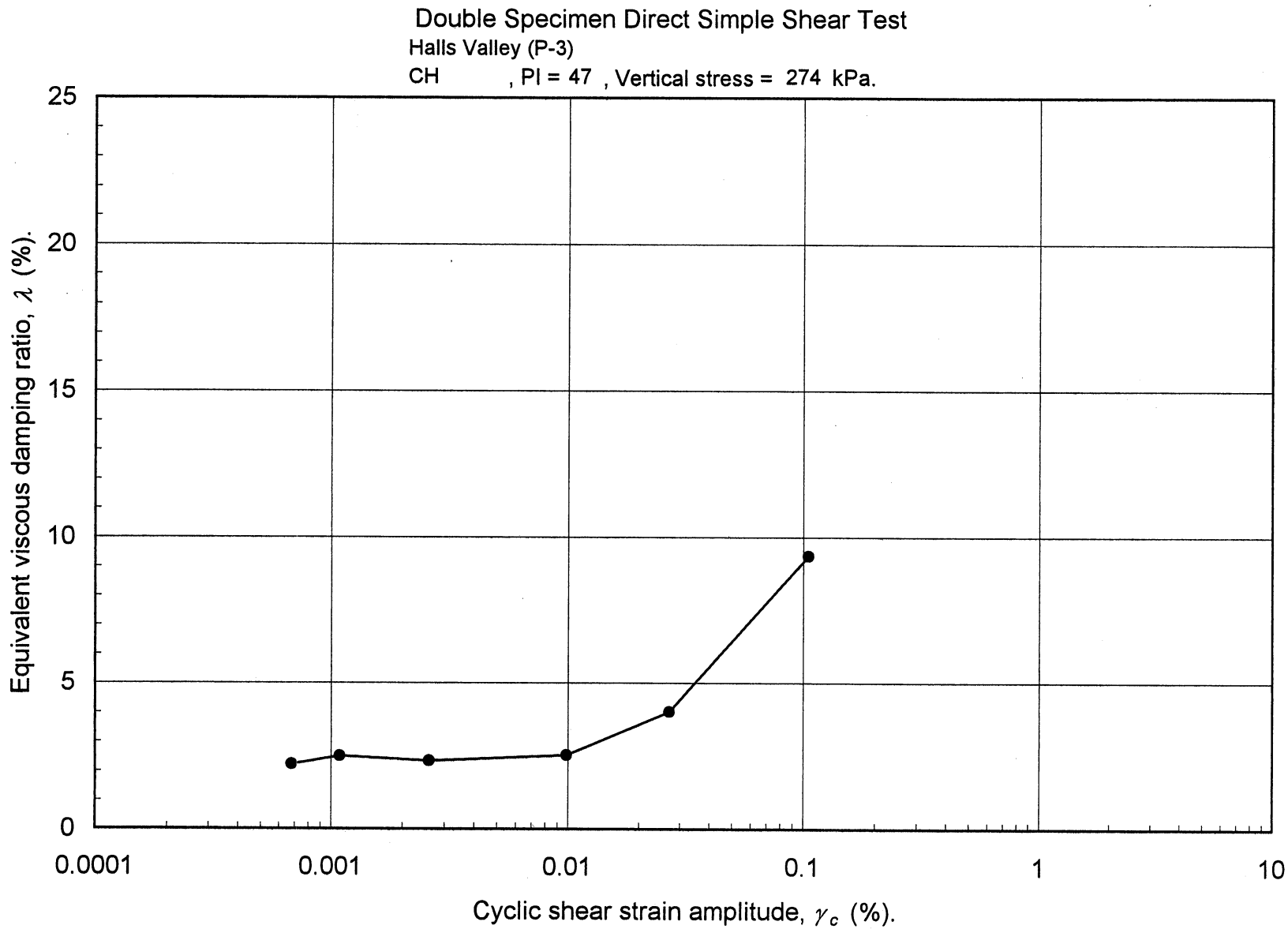
Double Specimen Direct Simple Shear Test
Halls Valley (P-3)
CH , PI = 47 , Vertical stress = 274 kPa.
Equivalent viscous damping ratio, λ (%).
25
20
15
10
5
0
0.0001
0.001
0.01
0.1
1
10
Cyclic shear strain amplitude, γc (%).

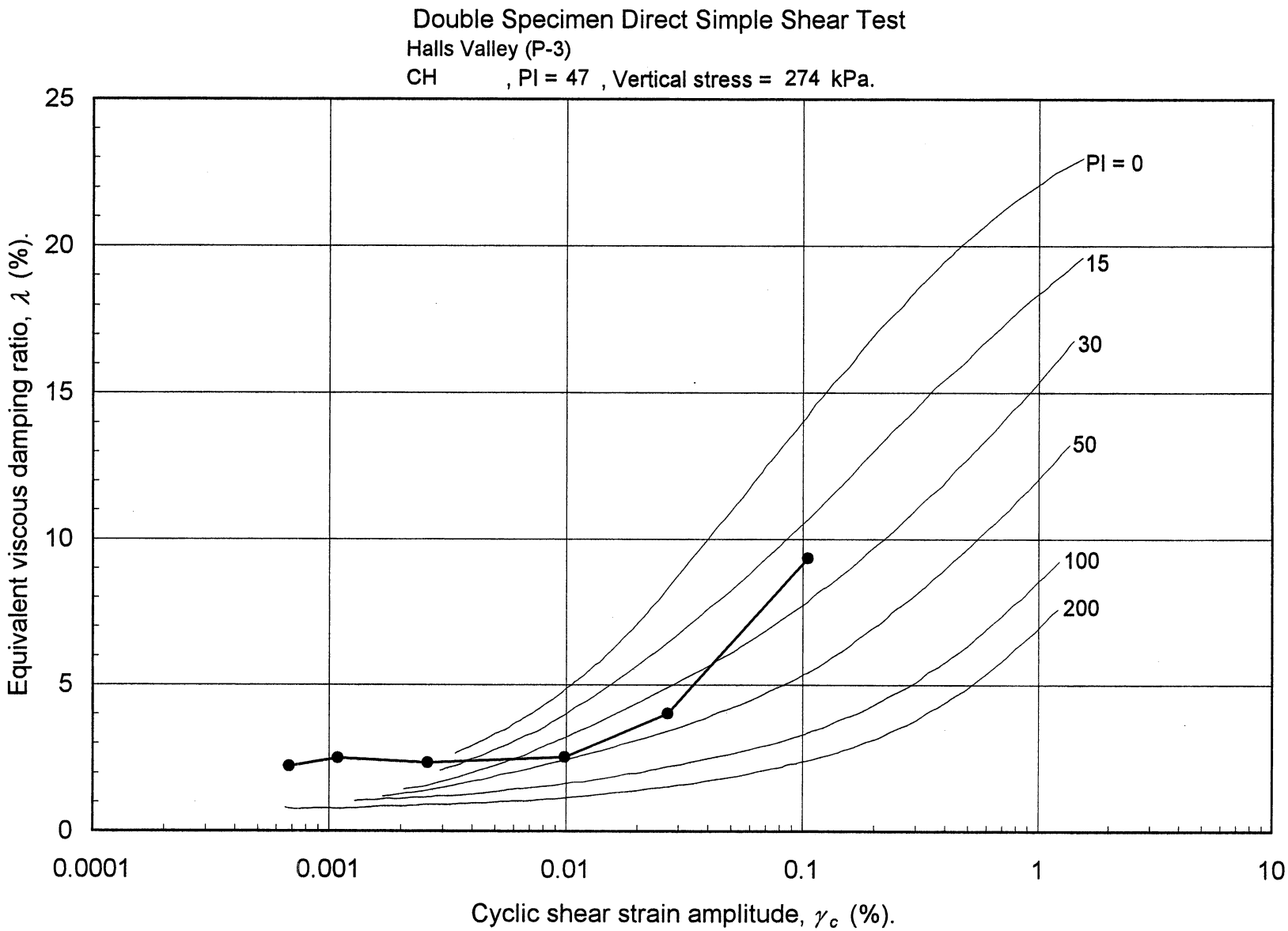
Double Specimen Direct Simple Shear Test
Halls Valley (P-3)
CH , PI = 47 , Vertical stress = 274 kPa.
Equivalent viscous damping ratio, λ (%).
Cyclic shear strain amplitude, γc (%).
0
5
10
15
20
25
0.0001
0.001
0.01
0.1
1
10
PI = 0
15
30
50
100
200

UCLA Soil Dynamics Laboratory

Specific Gravity Test

Principal investigator: Mladen Vucetic, Professor

Test performed by: Kentaro Tabata Test No.: 12

Project:	PEARL			Date:	2/26/2002
Boring:	Halls Valley				
Tube No.:	P-3	Depth (ft):	50.0 -53.0	GWT (ft):	65.0
Comments:	Dark greenish gray clay.				

SPECIFIC GRAVITY TEST

Test No.	1		
Bottle No.	3		
Wt. of bottle (g)	178.27		
Volume of bottle (cm^3)	500		
Wt. of bottle+water+soil (g)	689.72		
Temperature (°C)	22.0		
Wt. of bottle+water (g)	676.27		
Evaporating dish No.	B-5		
Weight of dish (g)	507.43		
Wt. of dish+dry soil (g)	529.08		
Wt. of dry soil (g)	21.65		
Specific gravity of water	0.9978		
Specific gravity of soil	**2.64**		

UCLA Soil Dynamics Laboratory

Grain Size Distribution

Principal investigator: Mladen Vucetic, Professor

Test performed by: Kentaro Tabata Test No.: 12

Project:	PEARL				
Boring:	Halls Valley				
Tube No.:	P-3	Depth (ft):	50.0 -53.0	GWT (ft):	65.0
Comments:	Dark greenish gray clay.				

GRAIN SIZE DISTRIBUTION

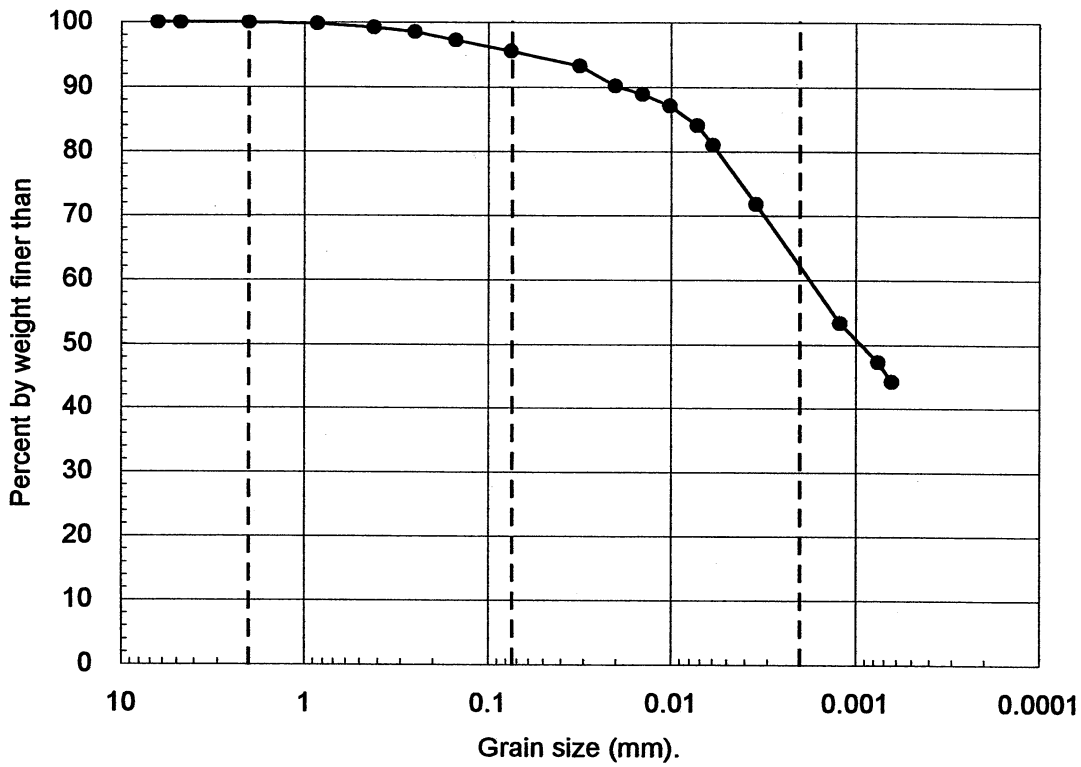

Clay (%)	Silt (%)	Sand (%)	Gravel (%)
63.0	32.5	4.5	0.0

UCLA Soil Dynamics Laboratory

Hydrometer Analysis

Principal investigator: Mladen Vucetic, Professor

Test performed by: Kentaro Tabata Test No.: 12

Project:	PEARL			Date:	3/1/2002
Boring:	Halls Valley				
Tube No.:	P-3	Depth (ft):	50.0 -53.0	GWT (ft):	65.0
Comments:	Dark greenish gray clay.				

HYDROMETER TEST

Time	Elapsed time t (sec)	Temp. T (°C)	Reading R'_T	Corr. reading $R_T=R'_T+c_m$	Depth H (cm)	Grain diameter D (mm)	Temp. corr. m_T	Corr. depth $R_T+m_T-c_d$	% by wt. finer than W_D (%)
12:40:46	0								
12:42:46	120	23.0	1018.5	1019.0	11.44	0.0317	0.700	1015.2	93.24
12:45:46	300	23.0	1018.0	1018.5	11.57	0.0202	0.700	1014.7	90.17
12:50:46	600	23.0	1017.8	1018.3	11.63	0.0143	0.700	1014.5	88.95
13:00:46	1200	23.0	1017.5	1018.0	11.71	0.0101	0.700	1014.2	87.11
13:20:46	2400	23.0	1017.0	1017.5	11.84	0.0072	0.700	1013.7	84.04
13:40:46	3600	23.0	1016.5	1017.0	11.97	0.0059	0.700	1013.2	80.97
15:40:46	10800	23.0	1015.0	1015.5	12.37	0.0035	0.700	1011.7	71.77
15:00:00	94754	23.0	1012.0	1012.5	13.18	0.0012	0.700	1008.7	53.37
9:46:00	248714	23.0	1011.0	1011.5	13.44	0.0008	0.700	1007.7	47.23
14:25:00	351854	23.0	1010.5	1011.0	13.58	0.0006	0.700	1007.2	44.17

APPARATUS

Hydrometer no.:	88-18587	a_0	284.03	a_1	-0.2675
Graduate no.:	1				

FACTORS

Meniscus corr., c_m:	0.5		
Disp. agent corr, c_d:	4.5		
Visc. of water, η.	23.0 °C	9.565E-06	g sec/cm^2
	°C		g sec/cm^3

WEIGHT

Dry soil (g)	25.09
Percent by wt (%)	95.51
Dry soil for sieve (g)	1.18
Total (g)	26.27

UNIT WEIGHT

Specific gravity:		2.64
T	γ_w	γ_s
(°C)	(g/cm^3)	(g/cm^3)
23.0	0.9976	2.6291

UCLA Soil Dynamics Laboratory

Sieve Analysis

Principal investigator: Mladen Vucetic, Professor

Test performed by: Kentaro Tabata Test No.: 12

Project:	PEARL			Date:	3/5/2002
Boring:	Halls Valley				
Tube No.:	P-3	Depth (ft):	50.0 -53.0	GWT (ft):	65.0
Comments:	Dark greenish gray clay.				

SIEVE ANALYSIS

Sieve No.	Diameter (mm)	Sieve (g)	S+wet (g)	S+dry (g)	Retained (g)	Retained (%)	Cumulated (g)	Cumulated (%)	Passing (%)
3	6.350	485.05		485.05	0.00	0.00	0.00	0.00	100.00
4	4.750	463.09		463.09	0.00	0.00	0.00	0.00	100.00
10	2.000	422.38		422.38	0.00	0.00	0.00	0.00	100.00
20	0.850	375.45		375.50	0.05	0.19	0.05	0.19	99.81
40	0.420	457.58		457.73	0.15	0.57	0.20	0.76	99.24
60	0.250	323.91		324.11	0.20	0.76	0.40	1.52	98.48
100	0.150	342.18		342.50	0.32	1.22	0.72	2.74	97.26
200	0.075	676.85		677.31	0.46	1.75	1.18	4.49	95.51
Total					1.18	4.49			

WEIGHT

Dry soil for sieve (g)	1.18
Dry soil for hydr. (g)	25.09
Total (g)	26.27
Percent coaser (%)	4.49

UCLA Soil Dynamics Laboratory

Atterberg Limit Determination

Principal investigator: Mladen Vucetic, Professor

Test performed by: Kentaro Tabata Test No.: 12

Project:	PEARL			Date:	3/25/2002
Boring:	Halls Valley				
Tube No.:	P-3	Depth (ft):	50.0 -53.0	GWT (ft):	65.0
Comments:	Dark greenish gray clay.				

LIQUID LIMIT TEST

Test No.	1	2	3	4	5			
Number of blows	49	42	34	24	18			
Container No.	ST-15	ST-23	ST-12	ST-2	ST-19			
Container (g)	30.26	30.57	30.28	30.26	29.99			
Cont+wet soil (g)	35.96	36.01	36.98	36.07	35.47			
Cont+dry soil (g)	33.46	33.59	33.95	33.42	32.90			
Water (g)	2.50	2.42	3.03	2.65	2.57			
Dry soil (g)	3.20	3.02	3.67	3.16	2.91			
Water content (%)	78.13	80.13	82.56	83.86	88.32			

PLASTIC LIMIT TEST

Test No.	1	2	3
Container No.	ST-10	ST-24	ST-14
Container (g)	30.32	29.98	30.45
Cont+wet soil (g)	33.11	32.20	33.45
Cont+dry soil (g)	32.36	31.58	32.64
Water (g)	0.75	0.62	0.81
Dry soil (g)	2.04	1.60	2.19
Water content (%)	36.76	38.75	36.99

ATTERBERG LIMITS

Liquid limit (%)	**84.7**
Plastic limit (%)	**37.5**
Plasticity index	**47.2**

CLASSIFICATION

CH

FLOW CHART

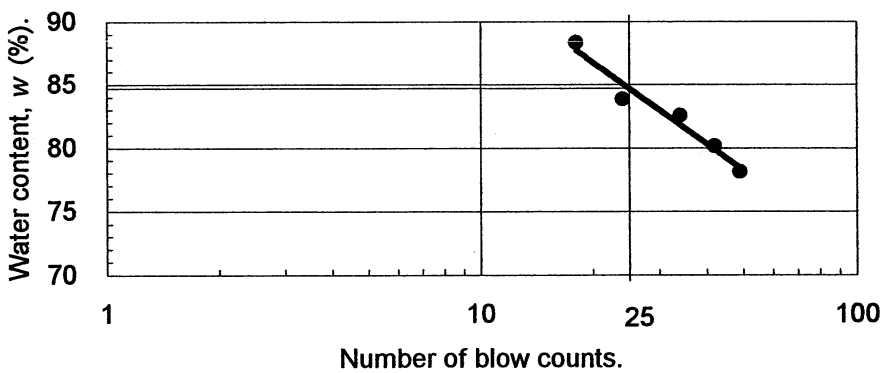

UCLA Soil Dynamics Laboratory

Atterberg Limit Determination

Principal investigator: Mladen Vucetic, Professor

Test performed by: Kentaro Tabata Test No.: 12

Project:	PEARL			Date:	3/25/2002
Boring:	Halls Valley				
Tube No.:	P-3	Depth (ft):	50.0 -53.0	GWT (ft):	65.0
Comments:	Dark greenish gray clay.				

PLASTICITY CHART

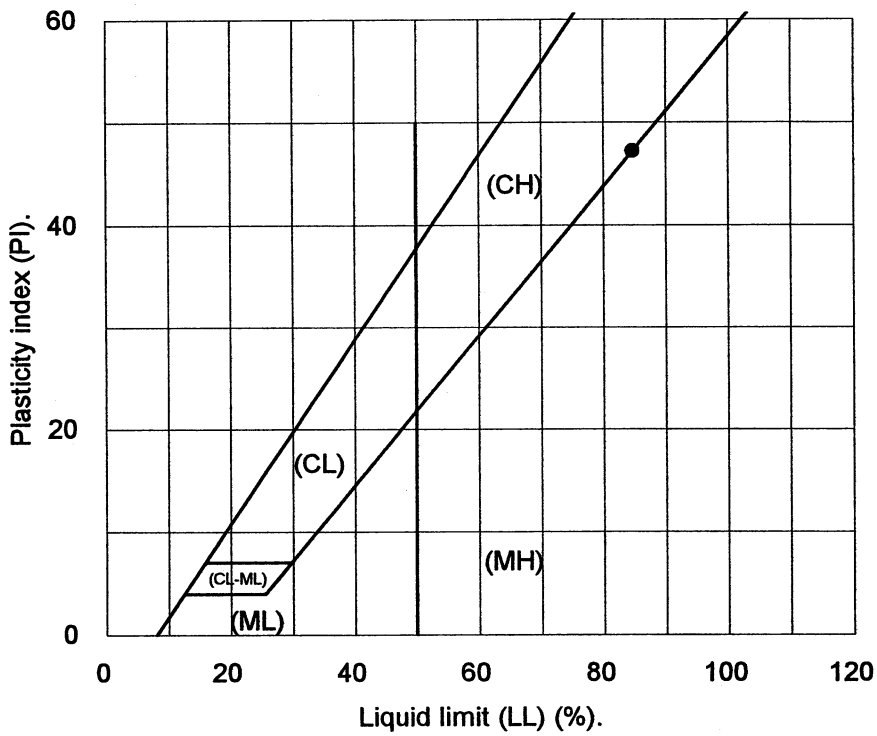

3.14 Test 13: YERMO P-4

UCLA Soil Dynamics Laboratory

Double Specimen Direct Simple Shear (DSDSS) Test

Principal investigator: Mladen Vucetic, Professor

Test performed by: Kentaro Tabata Test No.: 13

Project:	PEARL			Date:	2/7/2002
Boring:	Yermo				
Tube No.:	P-4	Depth (ft):	80.0 -83.0	GWT (ft):	135.0 (reported by others)
Comments:	Interlayerd sand and silt. Specimen obtained from the bottom of the tube (specimen depth ~ 82 ft).				

FORM 1: SPECIMEN PREPARATION

WATER CONTENT, SPECIFIC GRAVITY				UNIT WEIGHT, VOID RATIO, SATURATION			
	Before consol.	After shearing			Before consol.	Before shearing	After shearing
Container No.	ST-12	MT-13	MT-19	Average weight (g)	127.59	127.59	
Cont+wet soil (g)	51.48	173.40	180.10	Height (cm)	1.960	1.930	
Cont+dry soil (g)	49.12	159.91	166.14	Area (cm^2)	34.84	34.84	
Container (g)	30.29	49.57	50.15	Volume (cm^3)	68.28	67.22	
Water (g)	2.36	13.49	13.96	Unit weight (g/cm^3)	1.869	1.898	
Dry soil (g)	18.83	110.34	115.99	Unit weight (kN/m^3)	18.31	18.60	
Water content(%)	12.53	12.23	12.04	Void ratio	0.61	0.59	
Avg. water cont. (%)	12.53		12.13	Saturation (%)	54.7	55.2	
Spceific gravity			2.68				

HEIGHT OF SPECIMEN						
	Before consol.		Before shearing	After shearing		
	Top	Bottom	Average	Average		
Height (cm)	1.960	1.960	1.930	1.930		

AREA OF SPECIMEN						
Initial diameter (cm)			6.660	Initial area (cm^2)		34.837
Load (kg)	Stress (kg/cm^2)	Stress (kN/m^2)	Diameter (cm)	Membrane (cm)	Corrected diameter (cm)	Area (cm^2)

Yermo P-4					
DSDSS TEST - Step 2					
Type of soil: SM					
LL	NP	PI	NP	%Silt	5.9
e_0	0.58	S_0 (%)	56.3	%Clay	8.0
σ_v (kPa)	480	OCR	n/a	w (%)	12.1
γ_c (%)	~0.00035	H_0 (mm)	19.30	Spec. Gr.	2.68

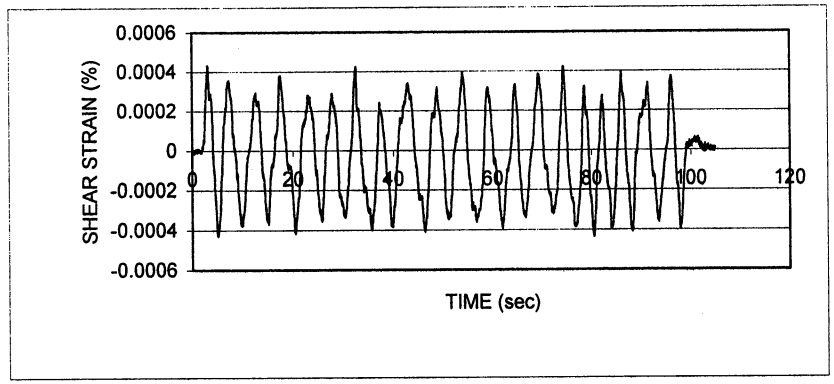

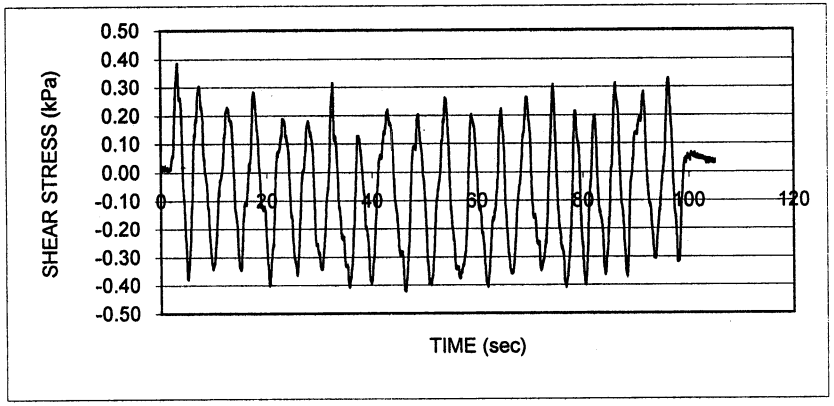

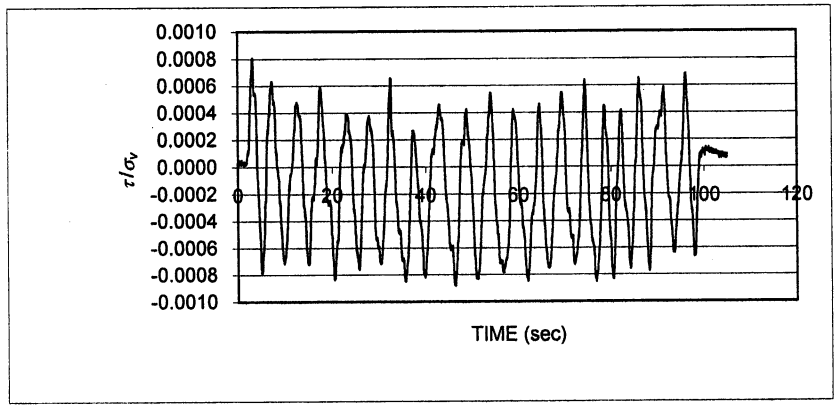

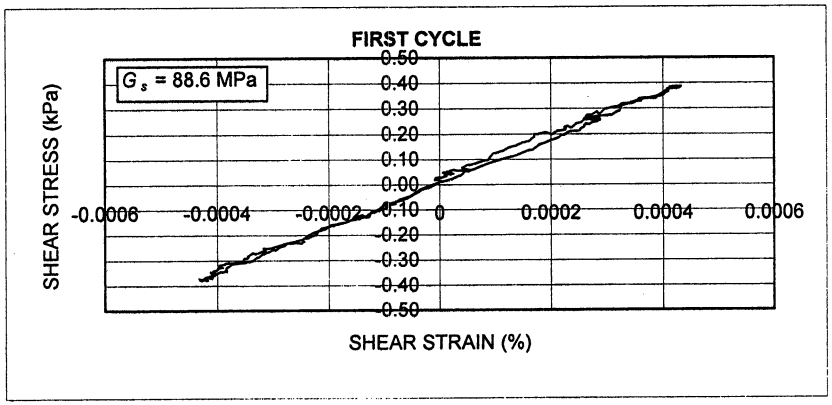

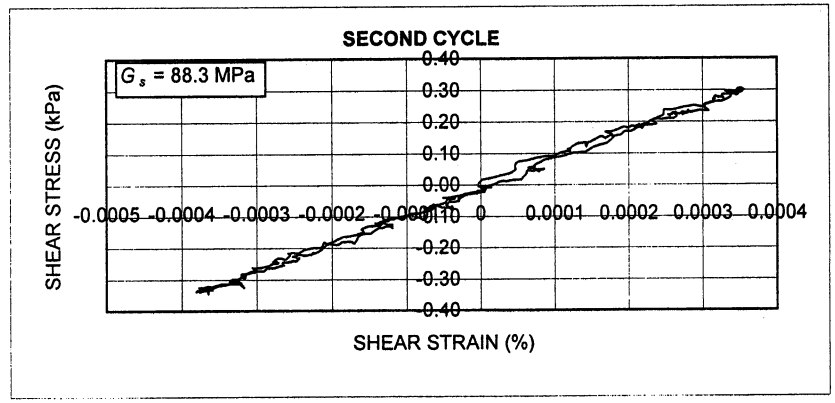

Yermo P-4					
DSDSS TEST - Step 26					
Type of soil: SM					
LL	NP	PI	NP	%Silt	5.9
e_0	0.58	S_0 (%)	56.3	%Clay	8.0
σ_v (kPa)	480	OCR	n/a	w (%)	12.1
γ_c (%)	~0.00075	H_0 (mm)	19.30	Spec. Gr.	2.68

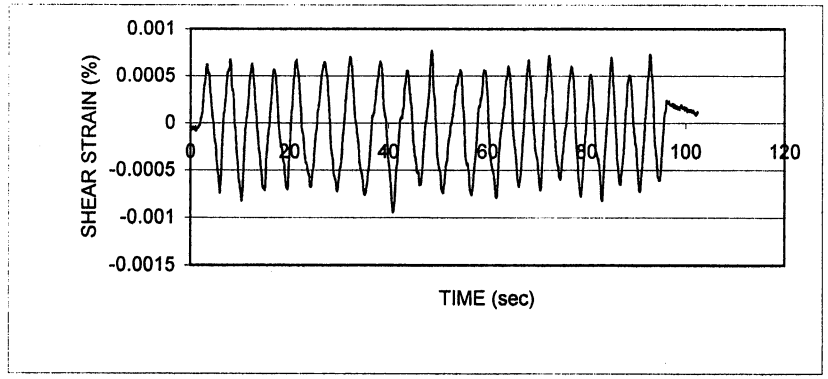

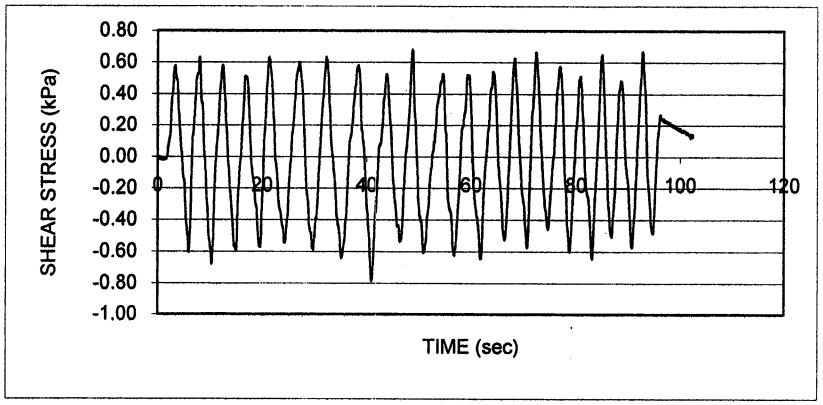

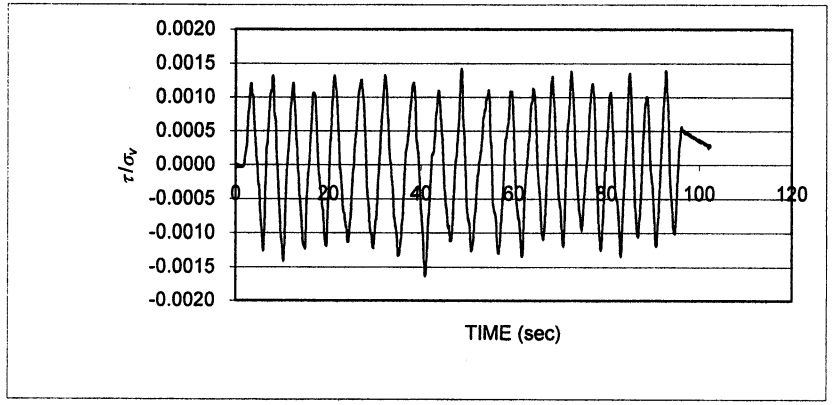

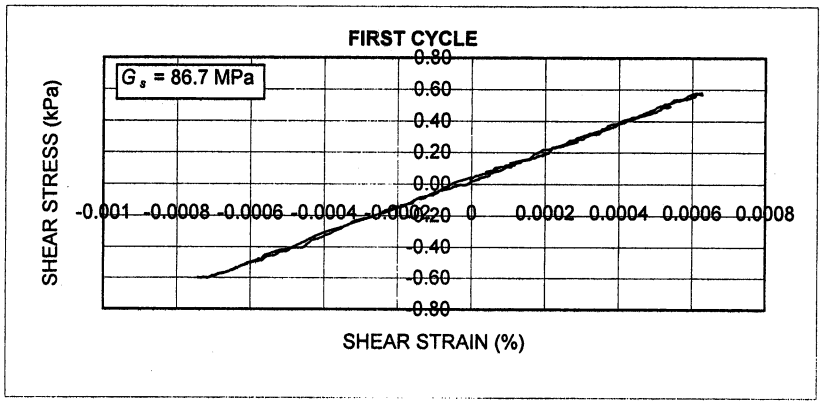

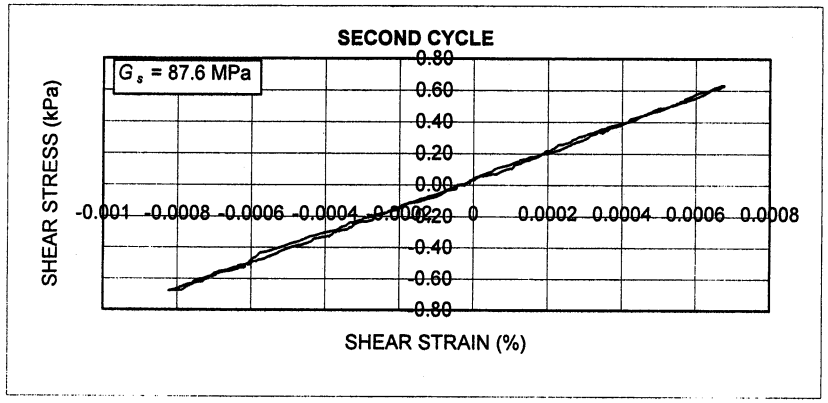

Yermo P-4					
DSDSS TEST - Step 3					
Type of soil: SM					
LL	NP	PI	NP	%Silt	5.9
e_0	0.58	S_0 (%)	56.3	%Clay	8.0
σ_v (kPa)	480	OCR	n/a	w (%)	12.1
γ_c (%)	~0.001	H_0 (mm)	19.30	Spec. Gr.	2.68

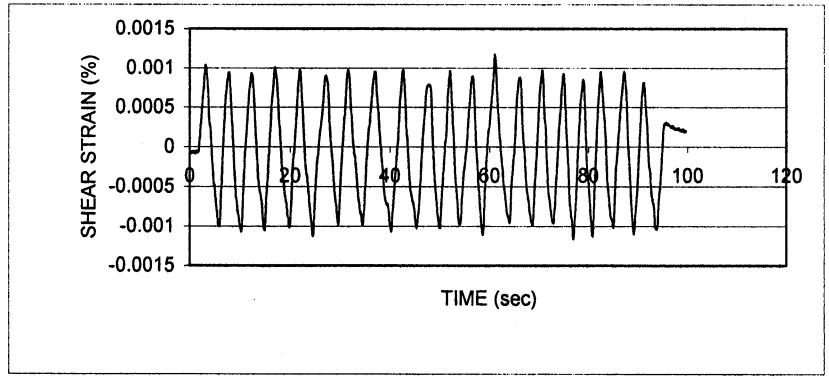

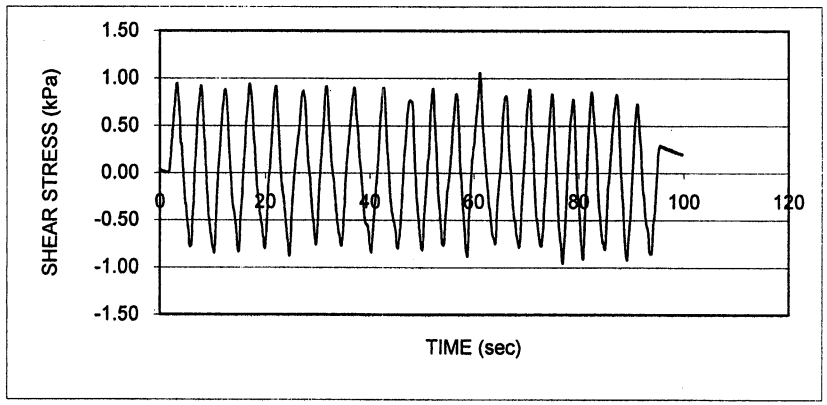

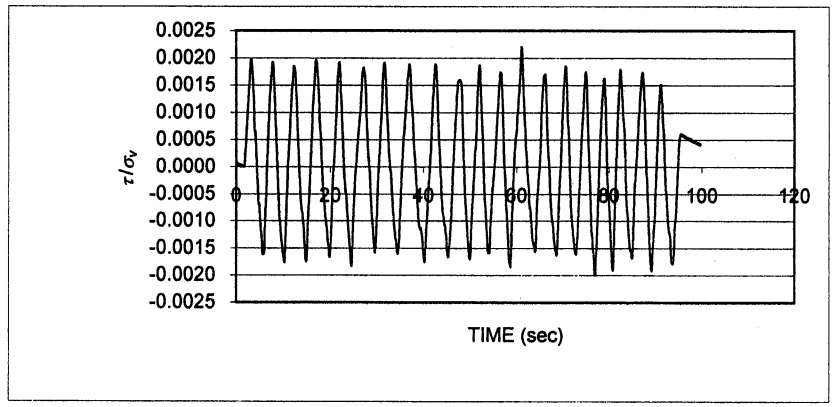

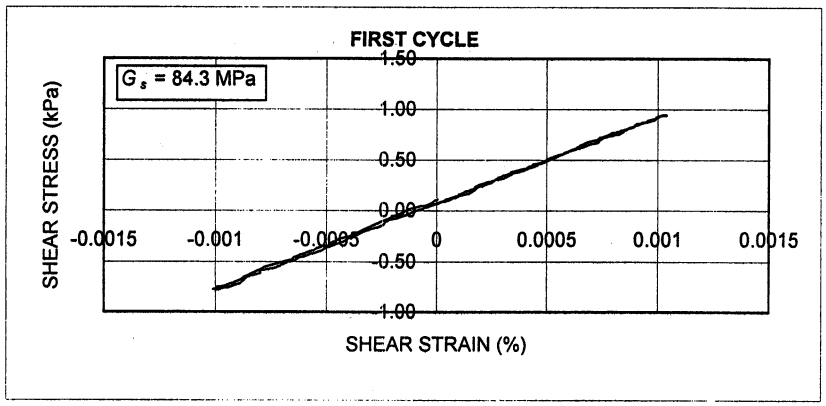

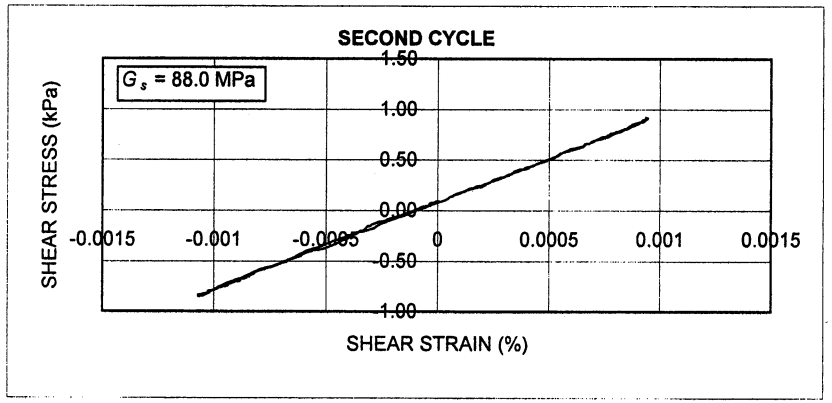

Yermo P-4					
DSDSS TEST - Step 4					
Type of soil: SM					
LL	NP	PI	NP	%Silt	5.9
e_0	0.58	S_0 (%)	56.3	%Clay	8.0
σ_v (kPa)	480	OCR	n/a	w (%)	12.1
γ_c (%)	~0.0024	H_0 (mm)	19.30	Spec. Gr.	2.68

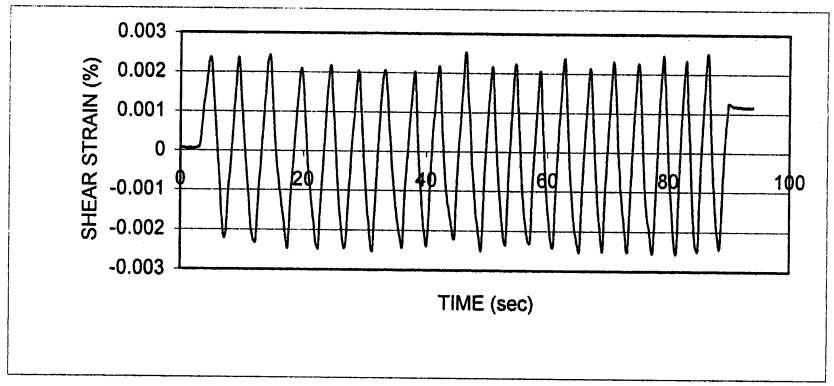

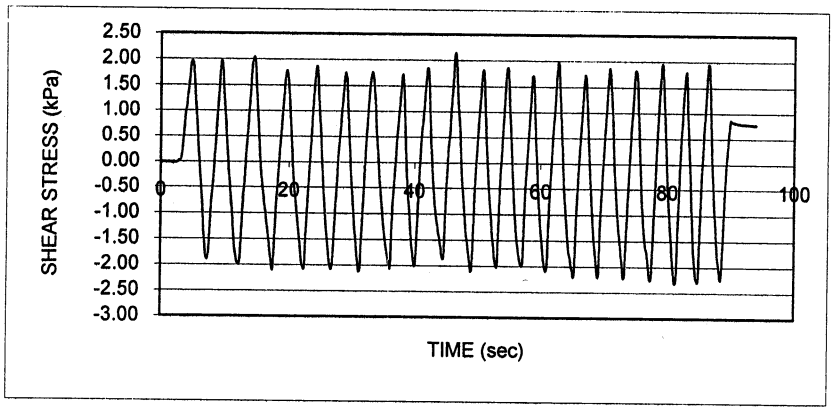

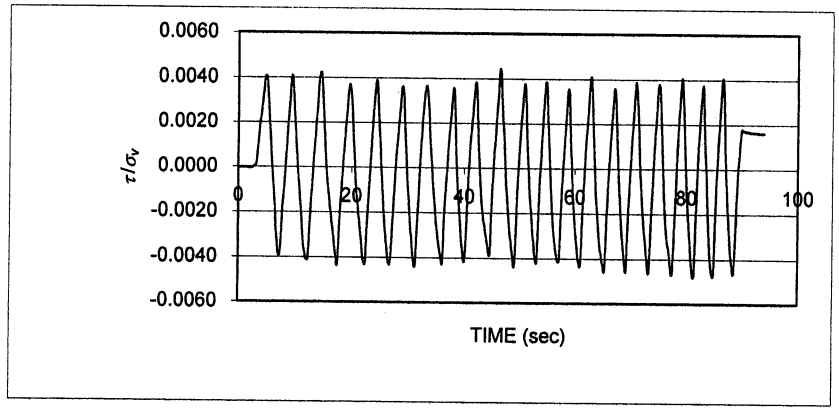

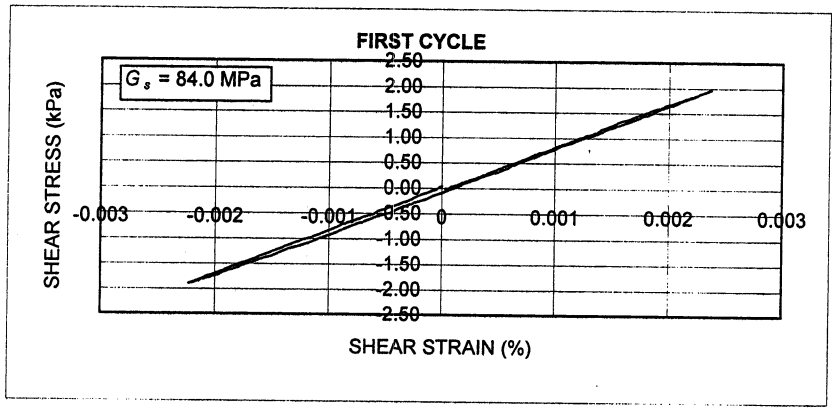

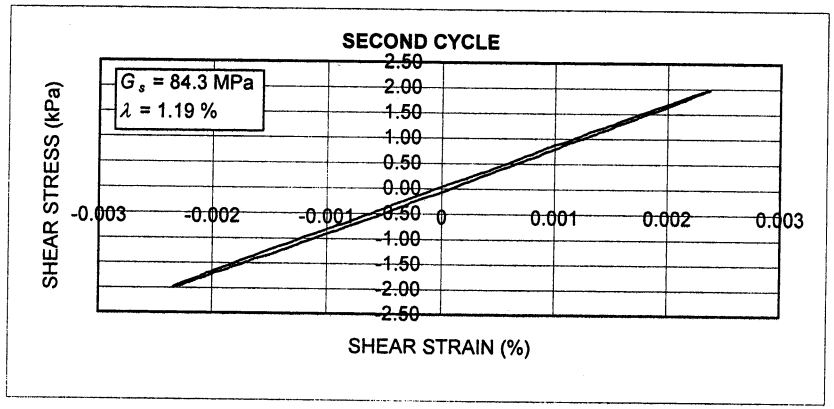

Yermo P-4					
DSDSS TEST - Step 5					
Type of soil: SM					
LL	NP	PI	NP	%Silt	5.9
e_0	0.58	S_0 (%)	56.3	%Clay	8.0
σ_v (kPa)	480	OCR	n/a	w (%)	12.1
γ_c (%)	~0.0098	H_0 (mm)	19.30	Spec. Gr.	2.68

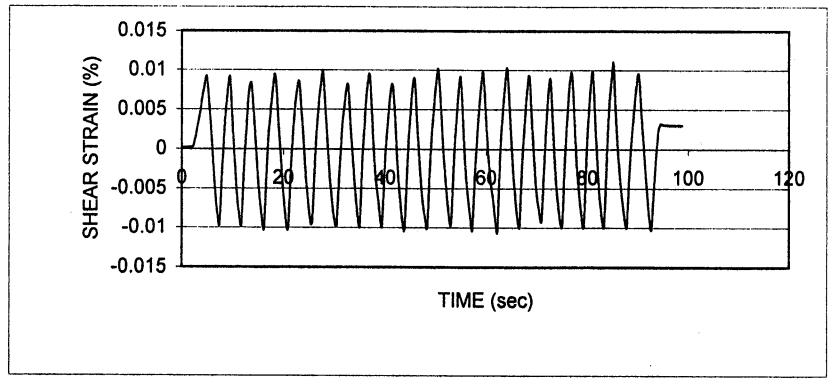

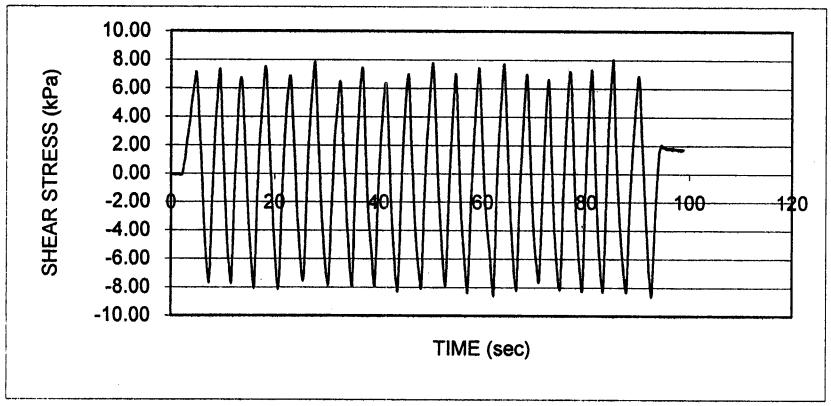

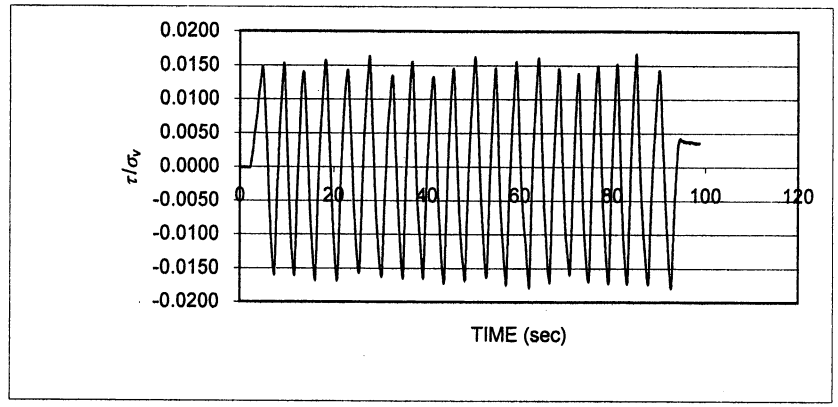

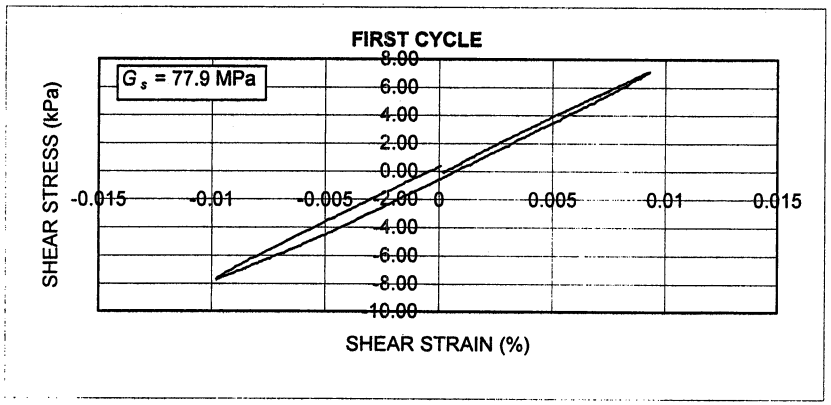

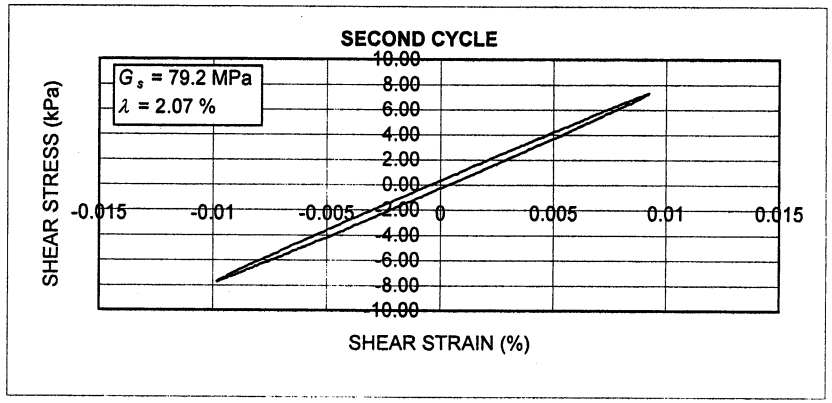

Yermo P-4					
DSDSS TEST - Step 6					
Type of soil: SM					
LL	NP	PI	NP	%Silt	5.9
e_0	0.58	S_0 (%)	56.3	%Clay	8.0
σ_v (kPa)	480	OCR	n/a	w (%)	12.1
γ_c (%)	~0.025	H_0 (mm)	19.30	Spec. Gr.	2.68

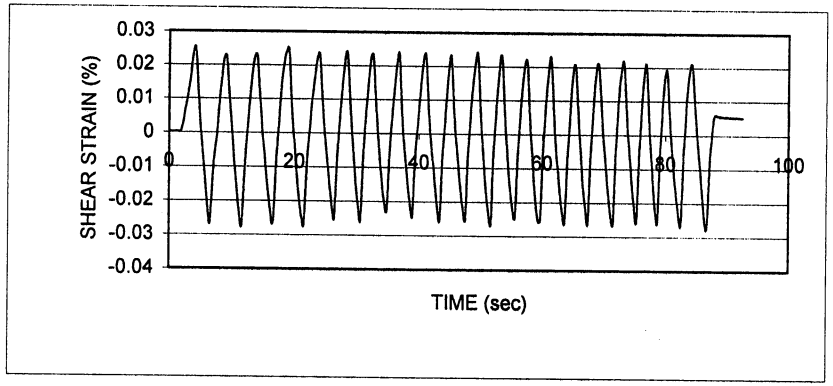

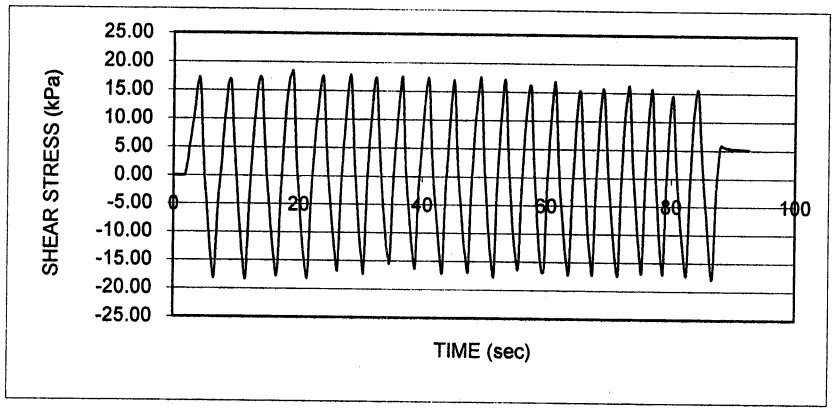

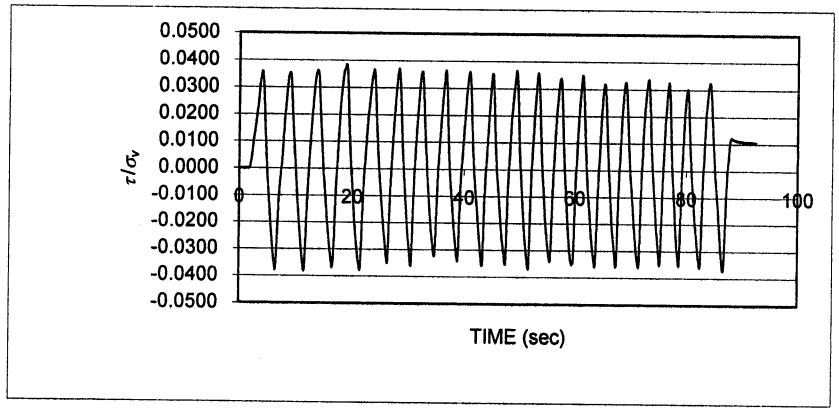

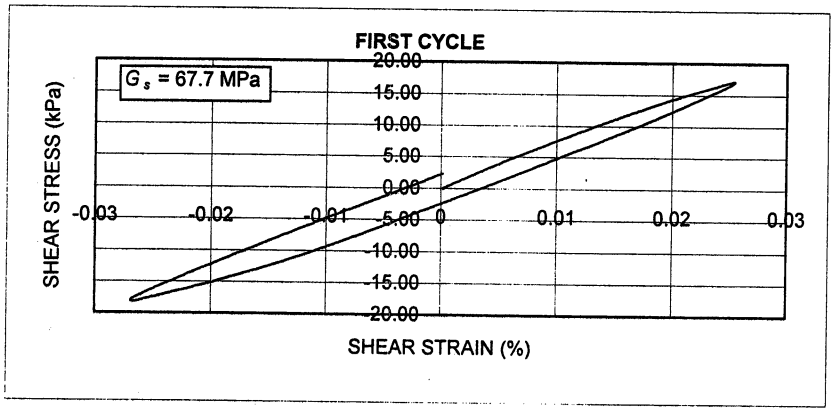

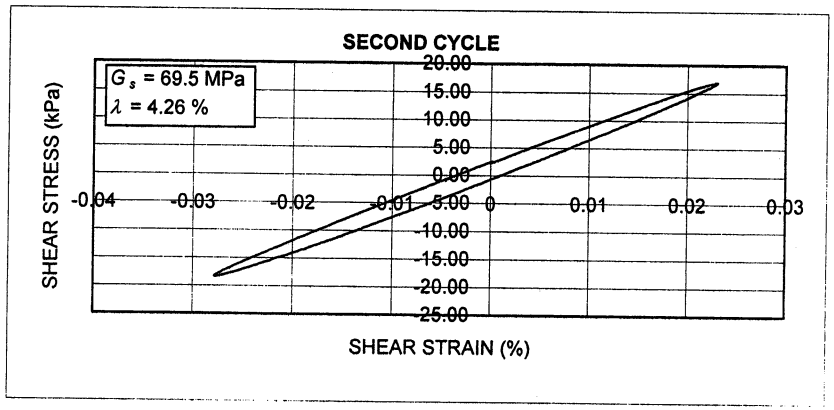

Yermo P-4					
DSDSS TEST - Step 7					
Type of soil: SM					
LL	NP	PI	NP	%Silt	5.9
e_0	0.58	S_0 (%)	56.3	%Clay	8.0
σ_v (kPa)	480	OCR	n/a	w (%)	12.1
γ_c (%)	~0.08	H_0 (mm)	19.30	Spec. Gr.	2.68

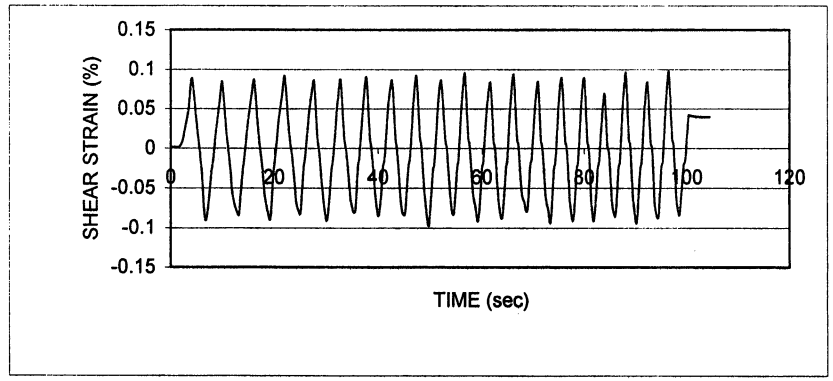

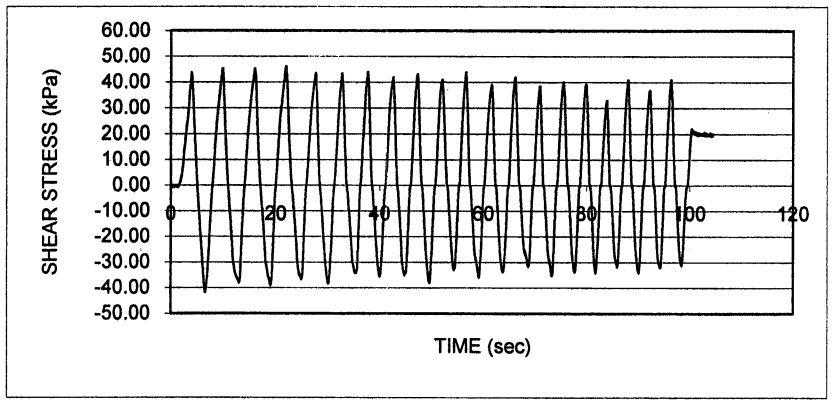

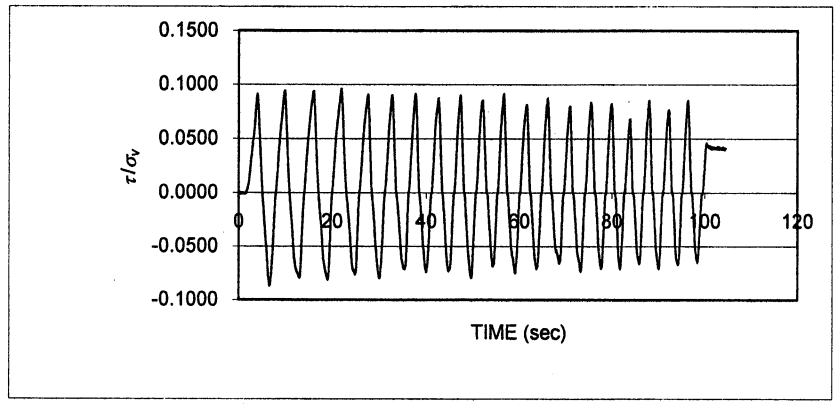

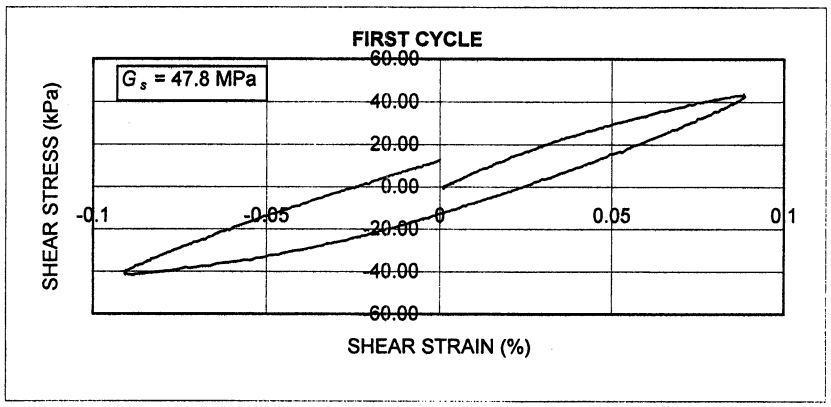

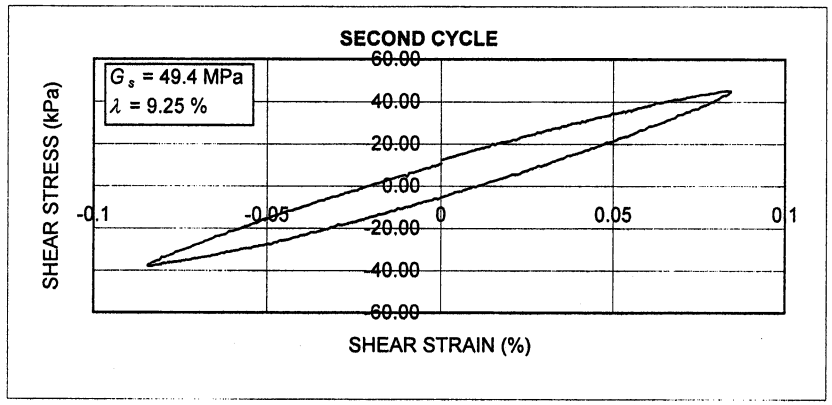

Yermo P-4					
DSDSS TEST - Step 8					
Type of soil: SM					
LL	NP	PI	NP	%Silt	5.9
e_0	0.58	S_0 (%)	56.3	%Clay	8.0
σ_v (kPa)	480	OCR	n/a	w (%)	12.1
γ_c (%)	~3.1	H_0 (mm)	19.30	Spec. Gr.	2.68

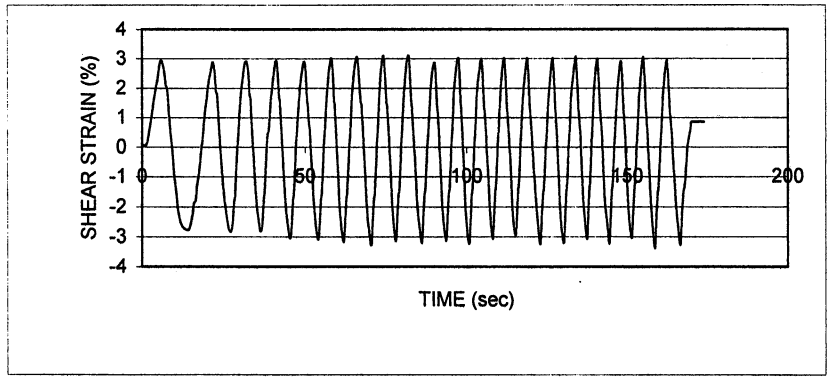

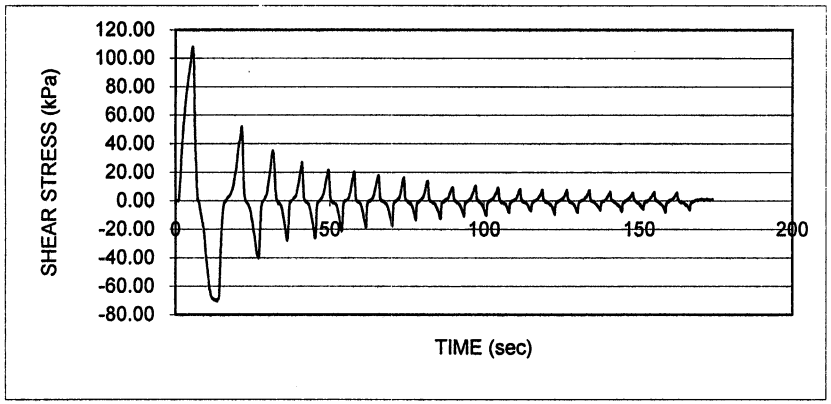

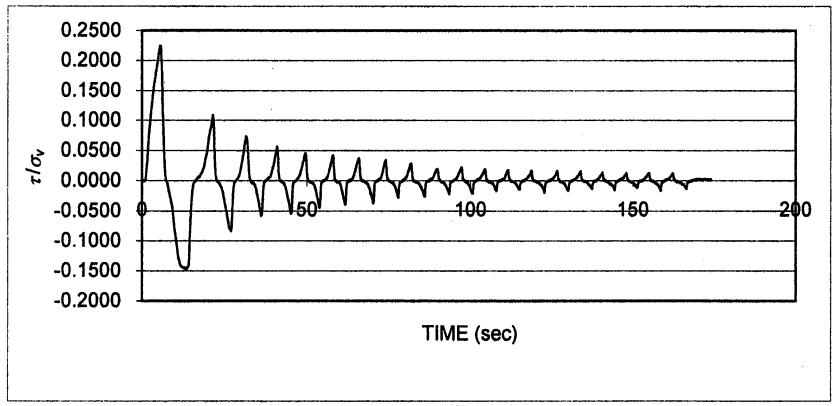

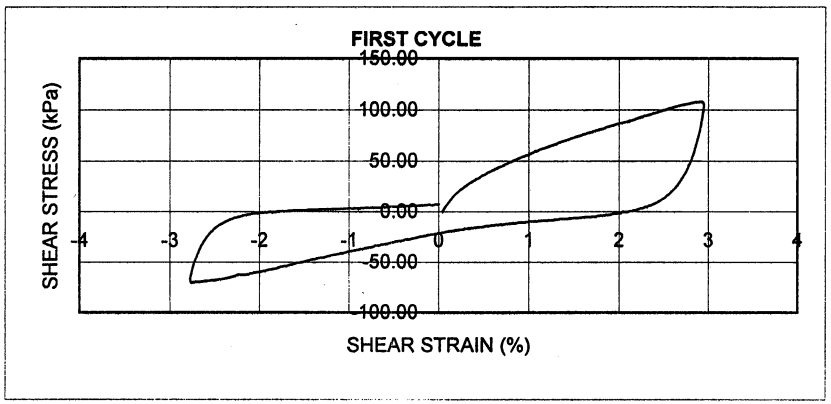

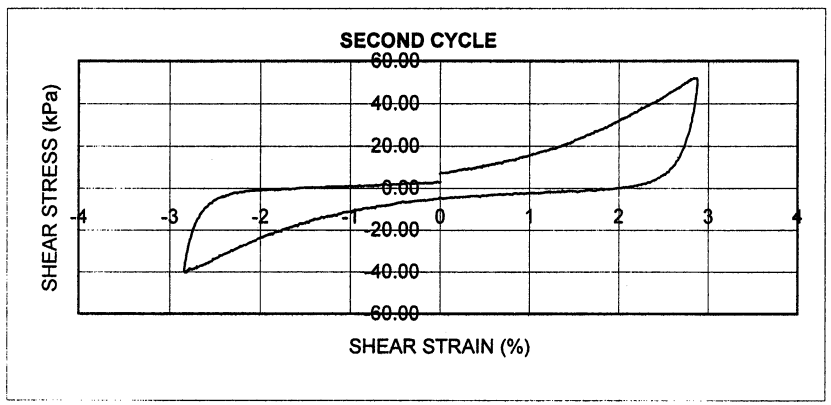

UCLA Soil Dynamics Laboratory
Double Specimen Direct Simple Shear (DSDSS) Test

Principal investigator: Mladen Vucetic, Professor
Test performed by Kentaro Tabata

Test no: 13

Project:	PEARL			Date:	2/7/2002
Sample name:	Yermo (P-4)			Depth (ft):	82.5
Symbol:	SM	LL (%):	0.0	Silt content (%):	5.9
Specific gravity:	2.68	PI:	0.0	Clay content (%):	8.0
Comments:					

Estimated G_{max} (MPa):	89.0

	SHEAR MODULUS			DAMPING RATIO	
Step	γ_c (%)	G_s (MPa)	G_s/G_{max}	γ_c (%)	λ (%)
2x	0.000432	88.62	0.996		
2x	0.000368	88.29	0.992		
26x	0.000684	86.66	0.974		
26x	0.000749	87.63	0.985	0.002357	1.19
3x	0.001025	84.31	0.947	0.009527	2.07
3x	0.001009	87.96	0.988	0.025420	4.26
4x	0.002301	83.98	0.944	0.084368	9.25
4x	0.002357	84.26	0.947		
5x	0.009536	77.93	0.876		
5x	0.009527	79.22	0.890		
6x	0.026181	67.67	0.760		
6x	0.025420	69.51	0.781		
7x	0.089773	47.75	0.536		
7x	0.084368	49.43	0.555		
	γ (%)				
(Monotonic loading)	1.000327	5.64	0.063		
	1.201852	5.27	0.059		
	1.507809	4.85	0.055		
	2.006138	4.34	0.049		
	2.500798	4.00	0.045		
	2.949654	3.59	0.040		

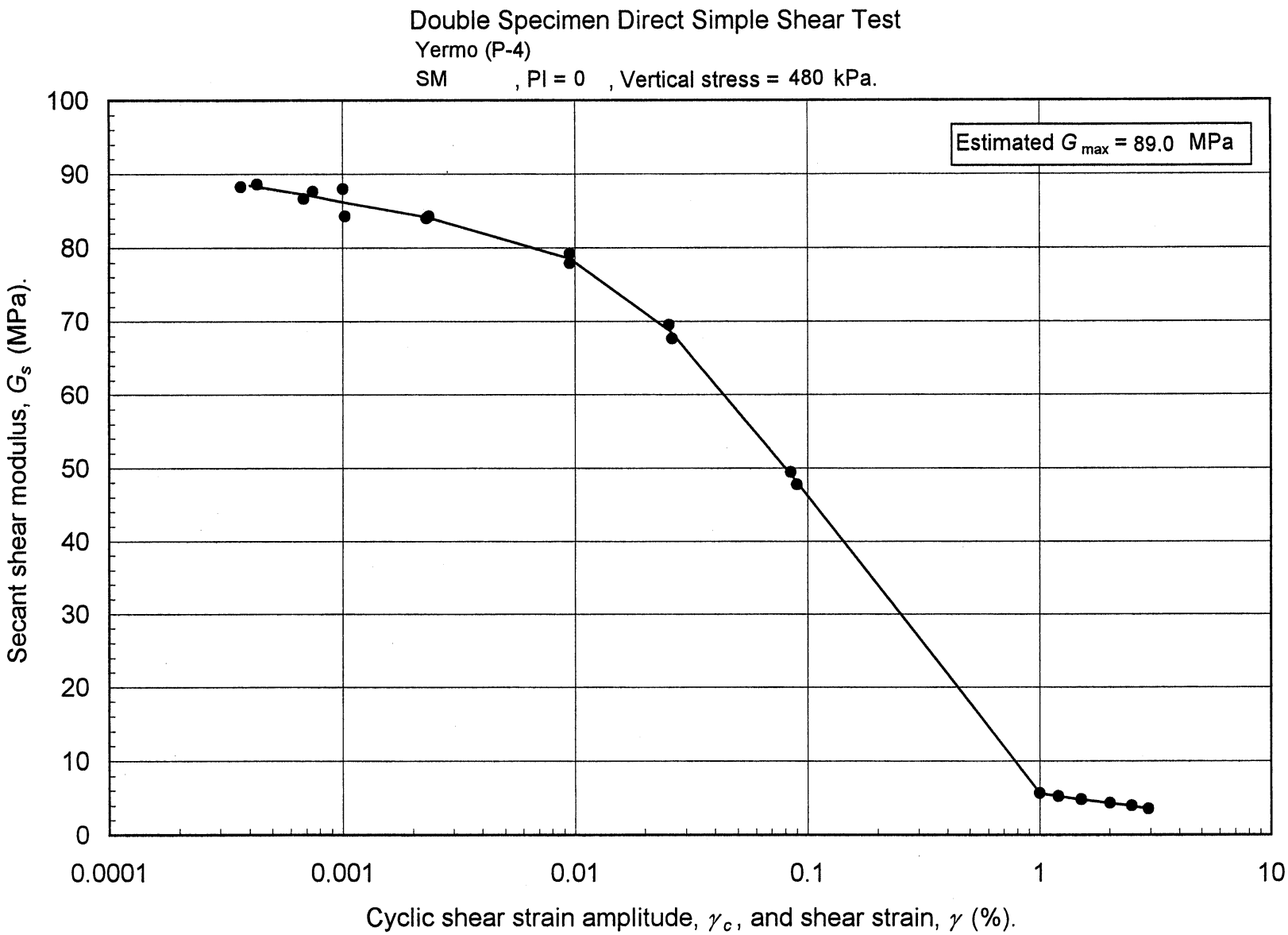
Double Specimen Direct Simple Shear Test
Yermo (P-4)
SM , PI = 0 , Vertical stress = 480 kPa.
Estimated G_{max} = 89.0 MPa
Secant shear modulus, G_s (MPa).
100
90
80
70
60
50
40
30
20
10
0
0.0001
0.001
0.01
0.1
1
10
Cyclic shear strain amplitude, γ_c, and shear strain, γ (%).

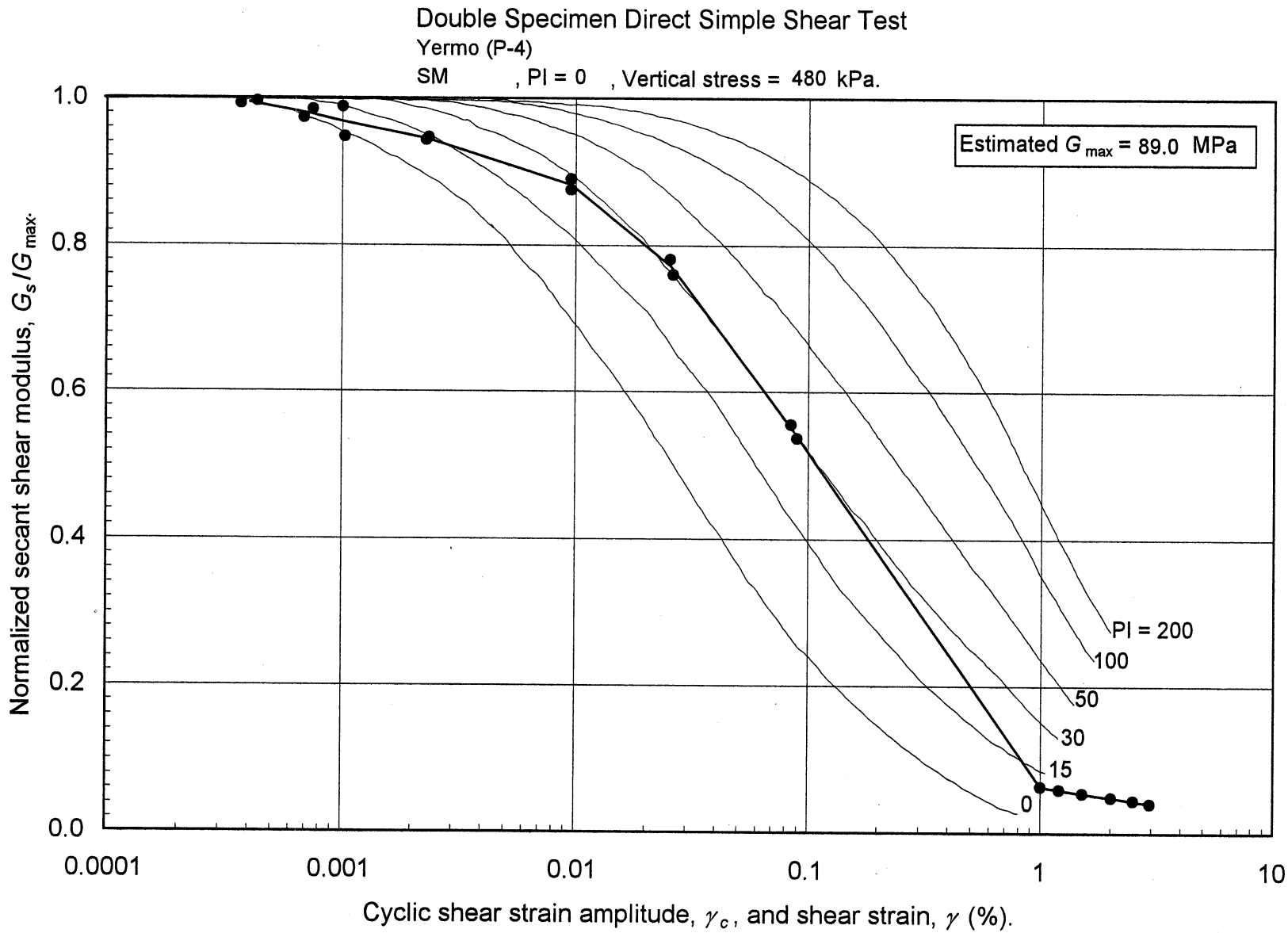
Double Specimen Direct Simple Shear Test
Yermo (P-4)
SM , PI = 0 , Vertical stress = 480 kPa.
Estimated G_{max} = 89.0 MPa
PI = 200
100
50
30
15
0
Normalized secant shear modulus, G_s/G_{max}
1.0
0.8
0.6
0.4
0.2
0.0
0.0001
0.001
0.01
0.1
1
10
Cyclic shear strain amplitude, γ_c, and shear strain, γ (%).

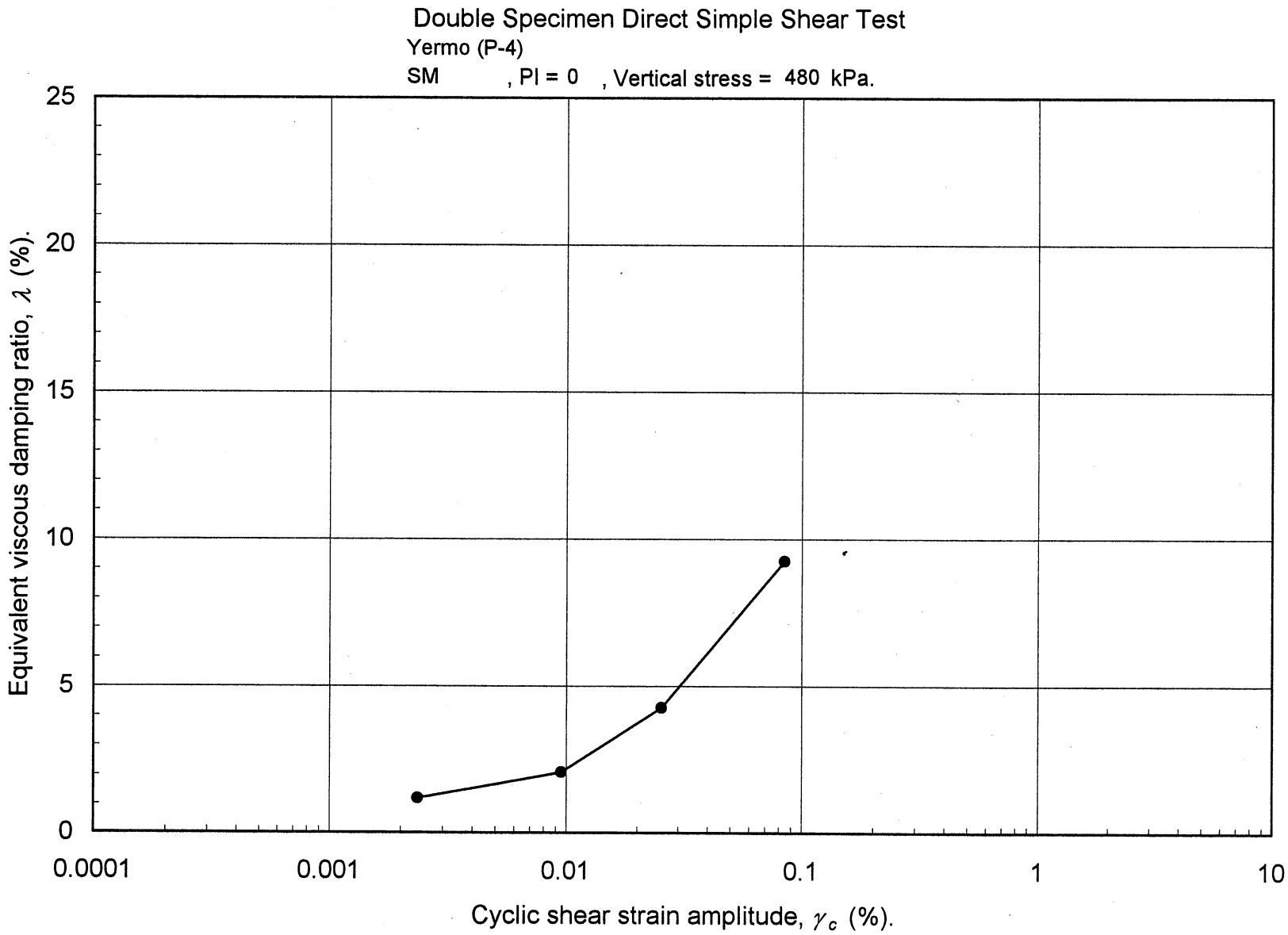
Double Specimen Direct Simple Shear Test
Yermo (P-4)
SM , PI = 0 , Vertical stress = 480 kPa.
Equivalent viscous damping ratio, λ (%).
25
20
15
10
5
0
0.0001
0.001
0.01
0.1
1
10
Cyclic shear strain amplitude, γc (%).

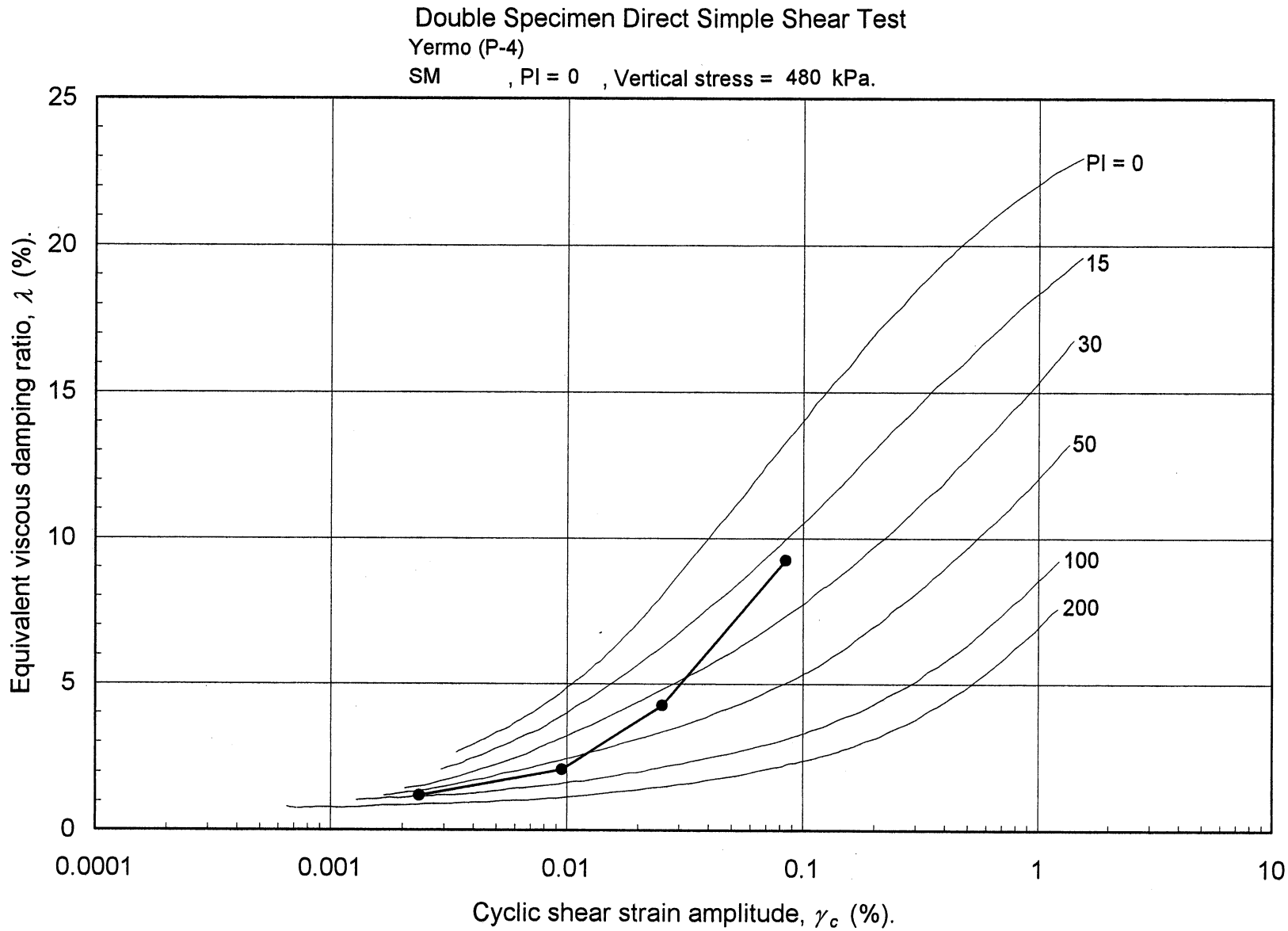
Double Specimen Direct Simple Shear Test
Yermo (P-4)
SM , PI = 0 , Vertical stress = 480 kPa.
Equivalent viscous damping ratio, λ (%).
Cyclic shear strain amplitude, γc (%).
0
5
10
15
20
25
0.0001
0.001
0.01
0.1
1
10
PI = 0
15
30
50
100
200

UCLA Soil Dynamics Laboratory

Specific Gravity Test

Principal investigator: Mladen Vucetic, Professor

Test performed by: Kentaro Tabata Test No.: 13

Project:	PEARL			Date:	2/14/2002
Boring:	Yermo				
Tube No.:	P-4	Depth (ft):	80.0 -83.0	GWT (ft):	125.0
Comments:	Interlayerd sand and silt.				

SPECIFIC GRAVITY TEST

Test No.	1		
Bottle No.	3		
Wt. of bottle (g)	178.27		
Volume of bottle (cm^3)	500		
Wt. of bottle+water+soil (g)	694.66		
Temperature (°C)	25.0		
Wt. of bottle+water (g)	675.86		
Evaporating dish No.	B-2		
Weight of dish (g)	537.21		
Wt. of dish+dry soil (g)	567.13		
Wt. of dry soil (g)	29.92		
Specific gravity of water	0.9971		
Specific gravity of soil	**2.68**		

UCLA Soil Dynamics Laboratory

Grain Size Distribution

Principal investigator: Mladen Vucetic, Professor

Test performed by: Kentaro Tabata Test No.: 13

Project:	PEARL				
Boring:	Yermo				
Tube No.:	P-4	Depth (ft):	80.0 -83.0	GWT (ft):	125.0
Comments:	Interlayerd sand and silt.				

GRAIN SIZE DISTRIBUTION

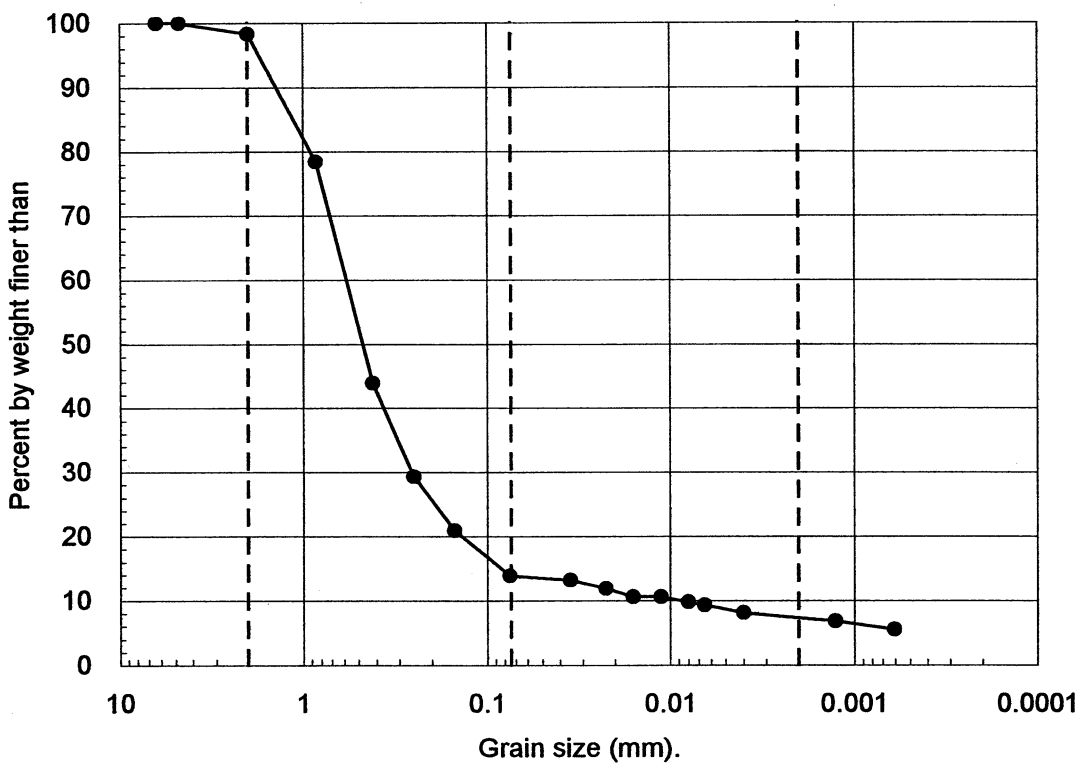

Clay (%)	Silt (%)	Sand (%)	Gravel (%)
8.0	5.9	84.4	1.7

UCLA Soil Dynamics Laboratory

Hydrometer Analysis

Principal investigator: Mladen Vucetic, Professor

Test performed by: Kentaro Tabata Test No.: 13

Project:	PEARL			Date:	2/13/2002
Boring:	Yermo				
Tube No.:	P-4	Depth (ft):	80.0 -83.0	GWT (ft):	125.0
Comments:	Interlayerd sand and silt.				

HYDROMETER TEST

Time	Elapsed time t (sec)	Temp. T (°C)	Reading R'_T	Corr. reading $R_T=R'_T+c_m$	Depth H (cm)	Grain diameter D (mm)	Temp. corr. m_T	Corr. depth $R_T+m_T-c_d$	% by wt. finer than W_D (%)
16:28:36	0								
16:30:36	120	23.0	1007.0	1007.5	14.51	0.0352	0.700	1005.2	13.15
16:33:36	300	23.0	1006.5	1007.0	14.65	0.0224	0.700	1004.7	11.88
16:38:36	600	23.0	1006.0	1006.5	14.78	0.0159	0.700	1004.2	10.62
16:48:36	1200	23.0	1006.0	1006.5	14.78	0.0112	0.700	1004.2	10.62
17:08:36	2400	23.0	1005.7	1006.2	14.86	0.0080	0.700	1003.9	9.86
17:28:36	3600	23.0	1005.5	1006.0	14.92	0.0065	0.700	1003.7	9.35
19:09:20	9644	23.0	1005.0	1005.5	15.05	0.0040	0.700	1003.2	8.09
19:25:00	96984	23.0	1004.5	1005.0	15.18	0.0013	0.700	1002.7	6.83
14:40:00	425484	23.0	1004.0	1004.5	15.32	0.0006	0.700	1002.2	5.56

APPARATUS

Hydrometer no.:	88-18587	a_0	284.03	a_1	-0.2675
Graduate no.:	1				

FACTORS

Meniscus corr., c_m:	0.5		
Disp. agent corr, c_d:	3.0		
Visc. of water, η.	23.0 °C	9.565E-06	g sec/cm^2
	°C		g sec/cm^3

WEIGHT

Dry soil (g)	8.75
Percent by wt (%)	13.87
Dry soil for sieve (g)	54.32
Total (g)	63.07

UNIT WEIGHT

Specific gravity:		2.68
T	γ_w	γ_s
(°C)	(g/cm^3)	(g/cm^3)
23.0	0.9976	2.6759

UCLA Soil Dynamics Laboratory

Sieve Analysis

Principal investigator: Mladen Vucetic, Professor

Test performed by: Kentaro Tabata Test No.: 13

Project:	PEARL			Date:	2/18/2002
Boring:	Yermo				
Tube No.:	P-4	Depth (ft):	80.0 -83.0	GWT (ft):	125.0
Comments:	Interlayerd sand and silt.				

SIEVE ANALYSIS

Sieve No.	Diameter (mm)	Sieve (g)	S+wet (g)	S+dry (g)	Retained (g)	Retained (%)	Cumulated (g)	Cumulated (%)	Passing (%)
3	6.350	485.05		485.05	0.00	0.00	0.00	0.00	100.00
4	4.750	463.11		463.11	0.00	0.00	0.00	0.00	100.00
10	2.000	422.42		423.48	1.06	1.68	1.06	1.68	98.32
20	0.850	375.41		387.98	12.57	19.93	13.63	21.61	78.39
40	0.420	457.57		479.35	21.78	34.53	35.41	56.14	43.86
60	0.250	323.87		333.01	9.14	14.49	44.55	70.64	29.36
100	0.150	342.18		347.53	5.35	8.48	49.90	79.12	20.88
200	0.075	676.88		681.30	4.42	7.01	54.32	86.13	13.87
Total					54.32	86.13			

WEIGHT

Dry soil for sieve (g)	54.32
Dry soil for hydr. (g)	8.75
Total (g)	63.07
Percent coaser (%)	86.13

3.15 Test 14: JOSHUA TREE P-3

UCLA Soil Dynamics Laboratory

Double Specimen Direct Simple Shear (DSDSS) Test

Principal investigator: Mladen Vucetic, Professor

Test performed by: Kentaro Tabata Test No.: 14

Project:	PEARL			Date:	12/19/2001
Boring:	Joshua Tree				
Tube No.:	P-3	Depth (ft):	40.0 -43	GWT (ft):	330.0 (reported by others)
Comments:	Sand. Specimen obtained from the bottom of the tube (specimen depth ~ 42.5 ft).				

FORM 1: SPECIMEN PREPARATION

WATER CONTENT, SPECIFIC GRAVITY				UNIT WEIGHT, VOID RATIO, SATURATION			
	Before consol.	After shearing			Before consol.	Before shearing	After shearing
Container No.	ST-20	MT-17	MT-23	Average weight (g)	144.39	144.39	
Cont+wet soil (g)	59.76	193.01	191.32	Height (cm)	1.960	1.937	
Cont+dry soil (g)	56.23	177.92	176.35	Area (cm^2)	34.84	34.84	
Container (g)	30.37	50.20	49.66	Volume (cm^3)	68.28	67.47	
Water (g)	3.53	15.09	14.97	Unit weight (g/cm^3)	2.115	2.140	
Dry soil (g)	25.86	127.72	126.69	Unit weight (kN/m^3)	20.72	20.97	
Water content(%)	13.65	11.81	11.82	Void ratio	0.46	0.44	
Avg. water cont. (%)	13.65		11.82	Saturation (%)	81.0	84.2	
Spceific gravity			2.71				

HEIGHT OF SPECIMEN						
	Before consol.		Before shearing	After shearing		
	Top	Bottom	Average	Average		
Height (cm)	1.960	1.960	1.937	1.937		

AREA OF SPECIMEN						
Initial diameter (cm)			6.660	Initial area (cm^2)		34.837
Load (kg)	Stress (kg/cm^2)	Stress (kN/m^2)	Diameter (cm)	Membrane (cm)	Corrected diameter (cm)	Area (cm^2)

Joshua Tree P-3					
DSDSS TEST - Step 2b					
Type of soil: SM-SC					
LL	15.5	PI	5.7	%Silt	18.7
e_0	0.44	S_0 (%)	84.2	%Clay	9.5
σ_v (kPa)	276	OCR	n/a	w (%)	13.7
γ_c (%)	~0.0004	H_0 (mm)	19.37	Spec. Gr.	2.71

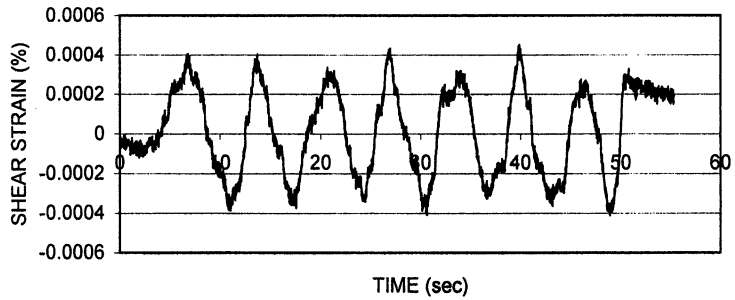

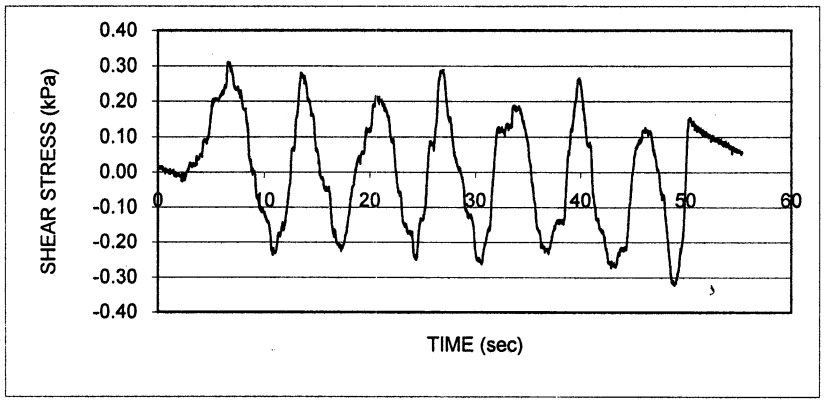

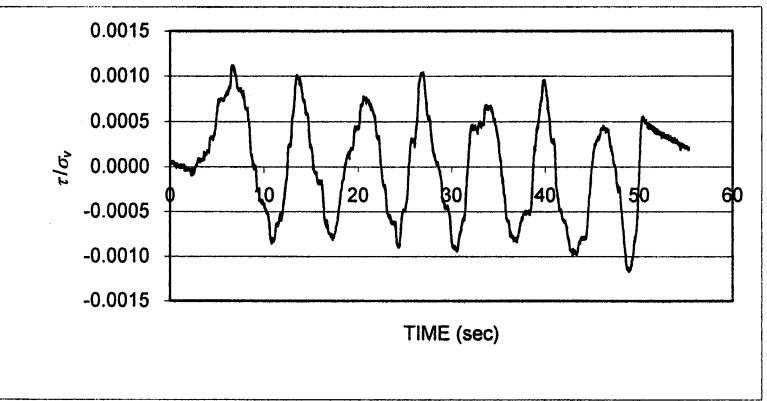

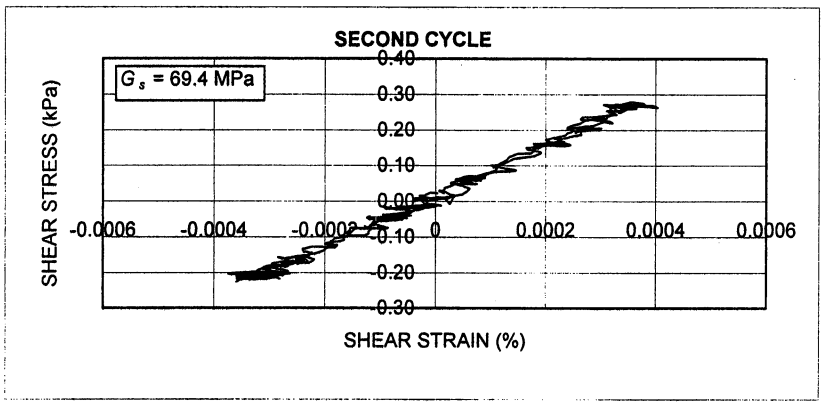

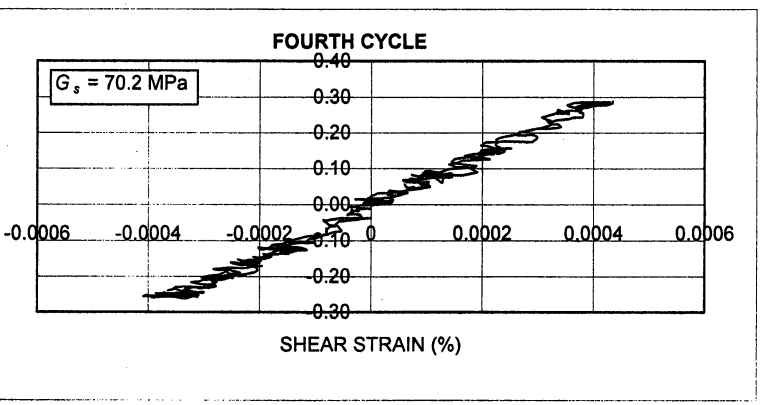

Joshua Tree P-3					
DSDSS TEST - Step 3					
Type of soil: SM-SC					
LL	15.5	PI	5.7	%Silt	18.7
e_0	0.44	S_0 (%)	84.2	%Clay	9.5
σ_v (kPa)	276	OCR	n/a	w (%)	13.7
γ_c (%)	~0.0009	H_0 (mm)	19.37	Spec. Gr.	2.71

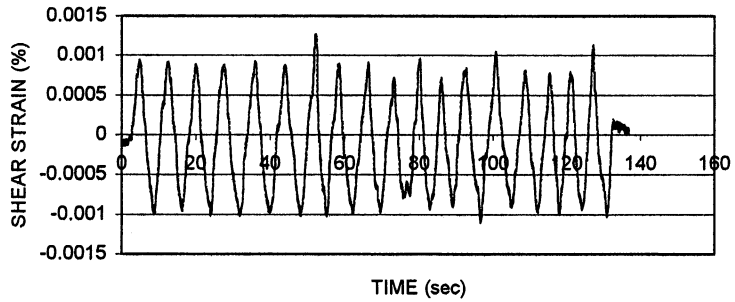

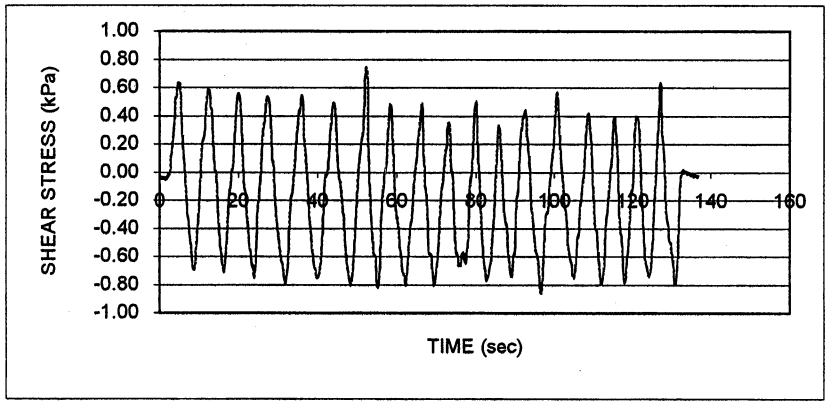

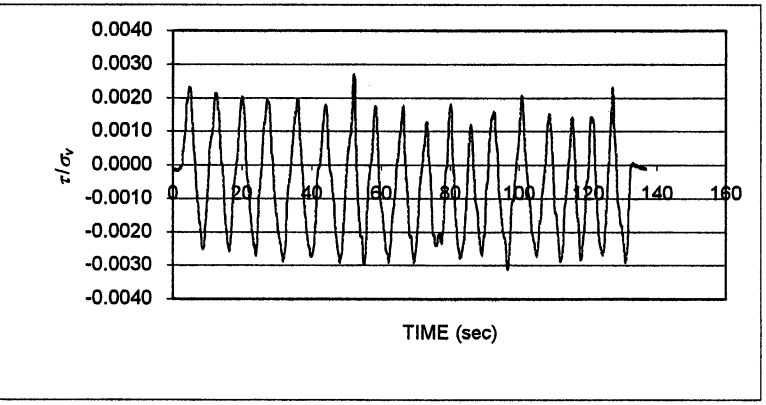

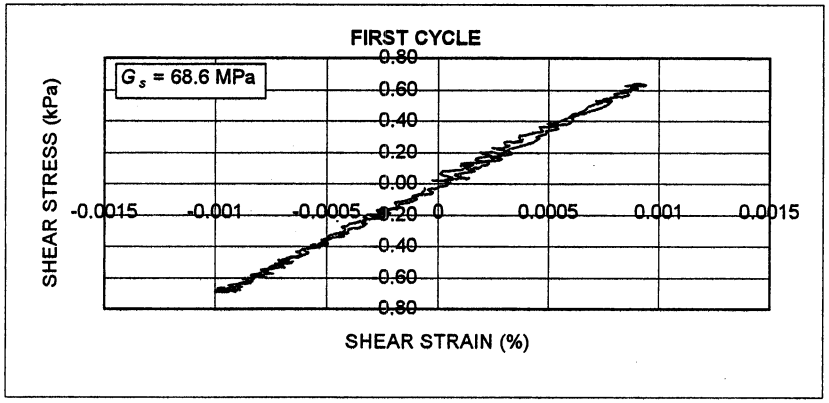

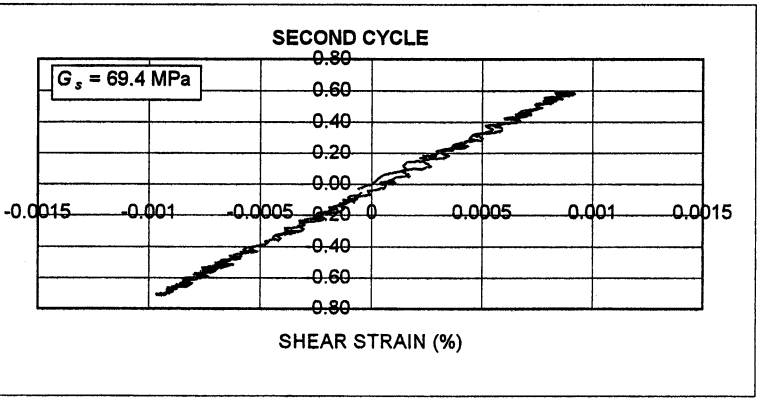

Joshua Tree P-3					
DSDSS TEST - Step 4					
Type of soil: SM-SC					
LL	15.5	PI	5.7	%Silt	18.7
e_0	0.44	S_0 (%)	84.2	%Clay	9.5
σ_v (kPa)	276	OCR	n/a	w (%)	13.7
γ_c (%)	~0.0028	H_0 (mm)	19.37	Spec. Gr.	2.71

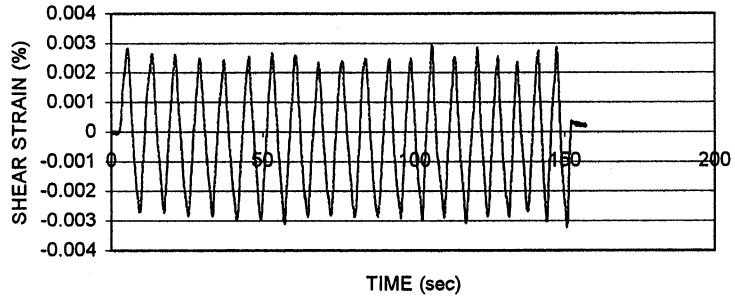

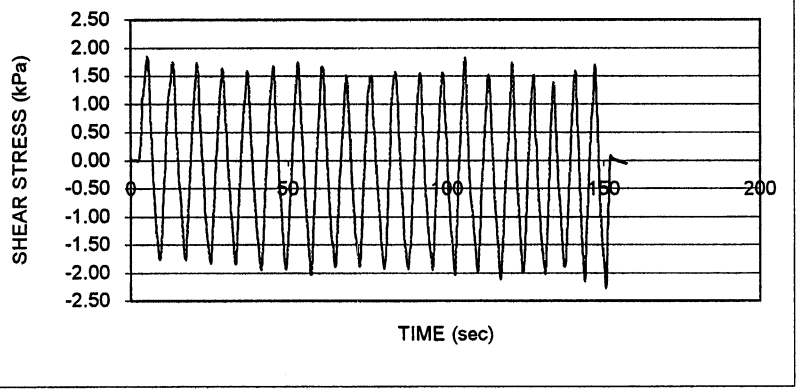

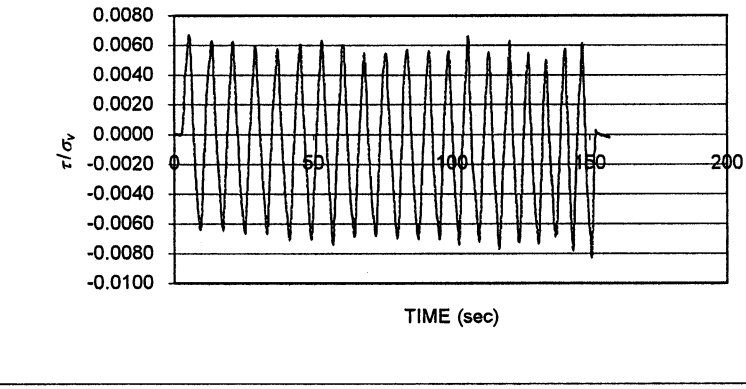

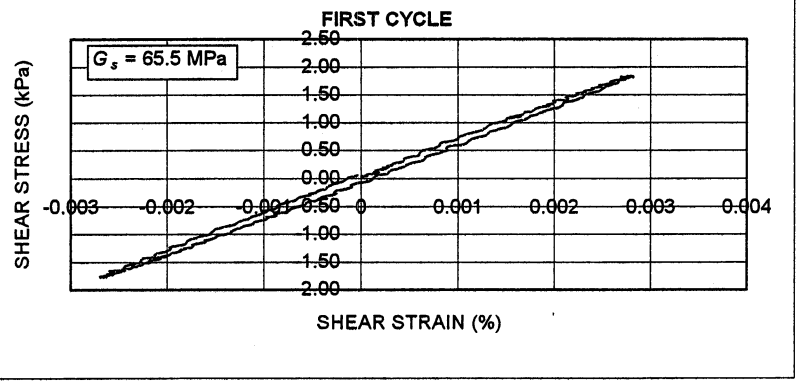

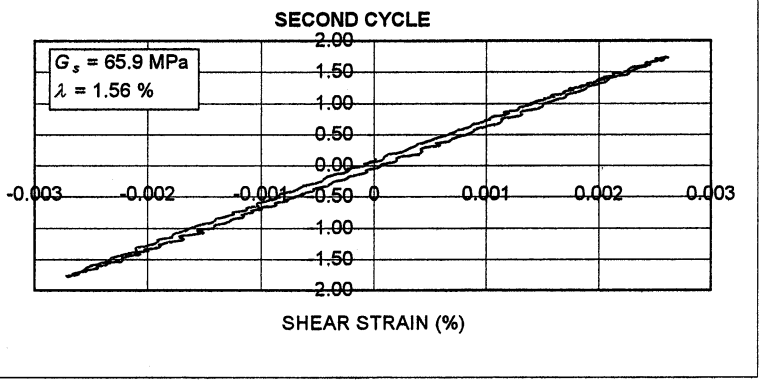

Joshua Tree P-3					
DSDSS TEST - Step 5					
Type of soil: SM-SC					
LL	15.5	PI	5.7	%Silt	18.7
e_0	0.44	S_0 (%)	84.2	%Clay	9.5
σ_v (kPa)	276	OCR	n/a	w (%)	13.7
γ_c (%)	~0.0095	H_0 (mm)	19.37	Spec. Gr.	2.71

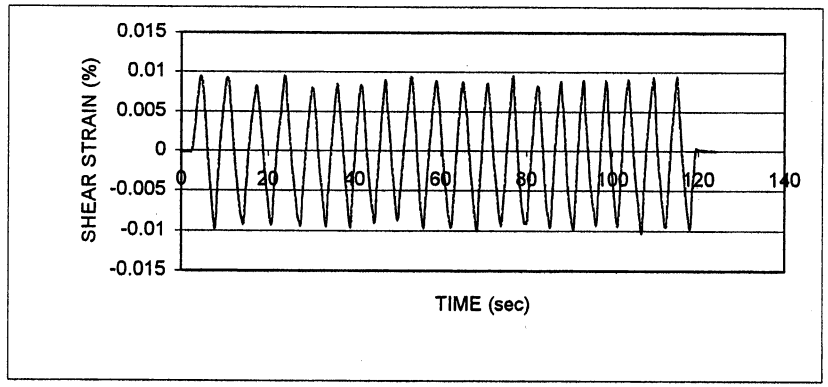

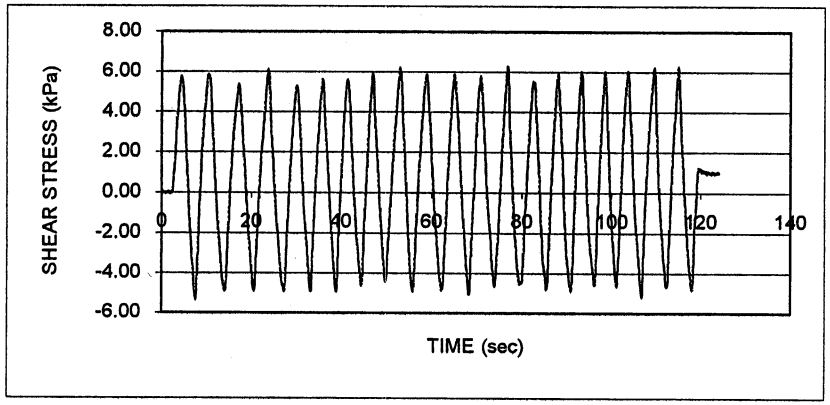

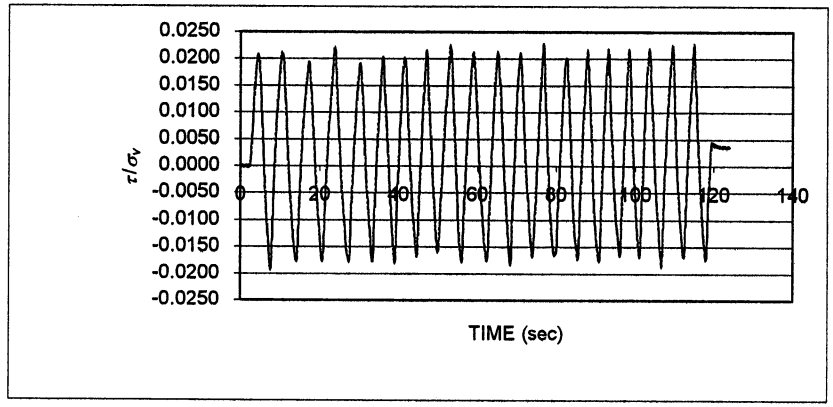

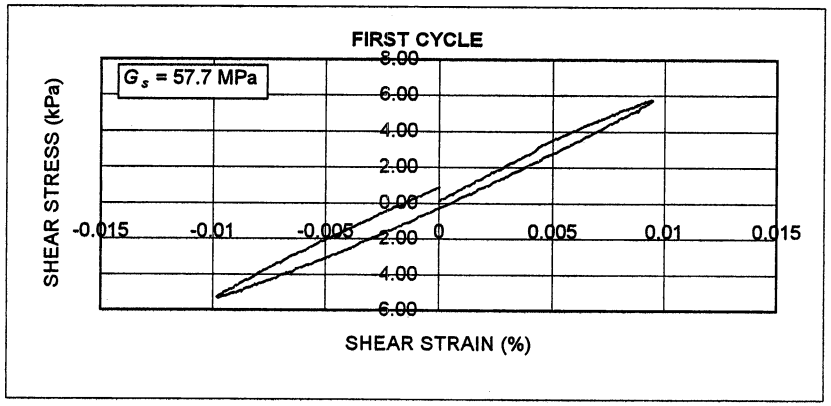

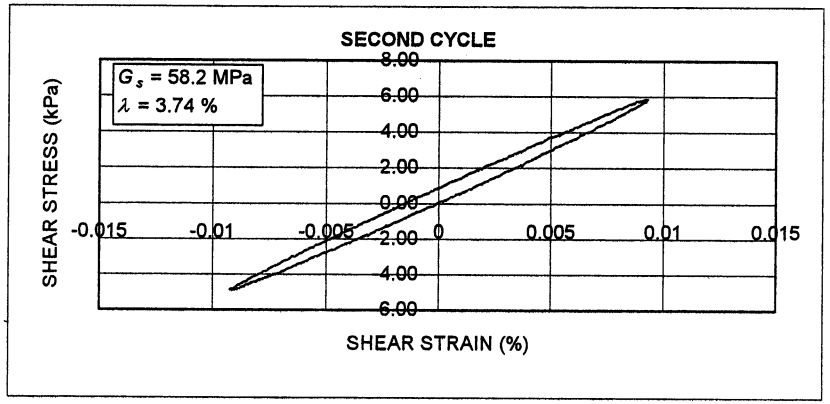

Joshua Tree P-3					
DSDSS TEST - Step 6					
Type of soil: SM-SC					
LL	15.5	PI	5.7	%Silt	18.7
e_0	0.44	S_0 (%)	84.2	%Clay	9.5
σ_v (kPa)	276	OCR	n/a	w (%)	13.7
γ_c (%)	~0.028	H_0 (mm)	19.37	Spec. Gr.	2.71

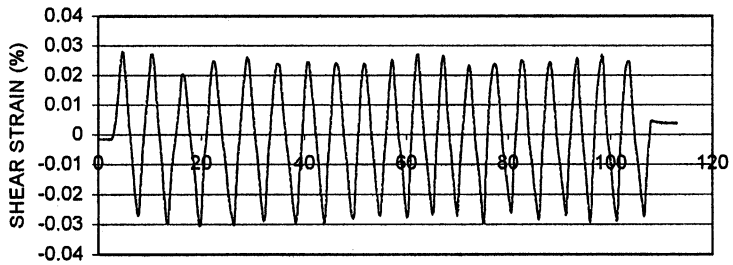

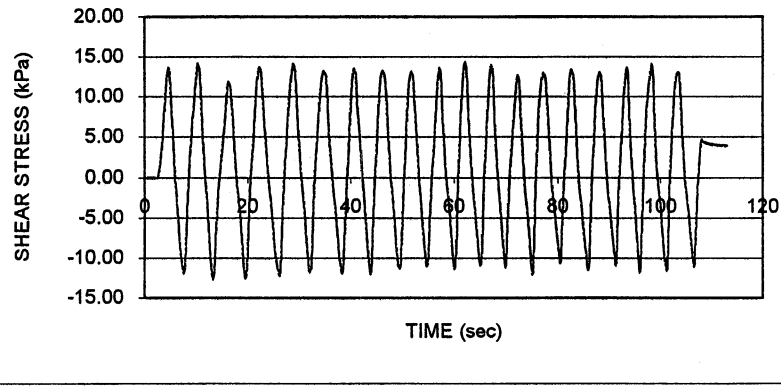

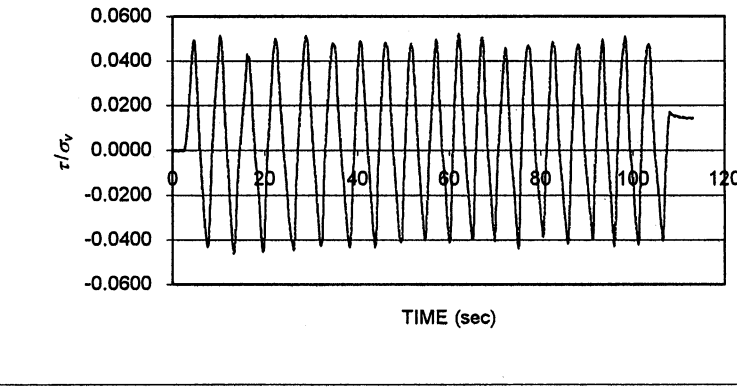

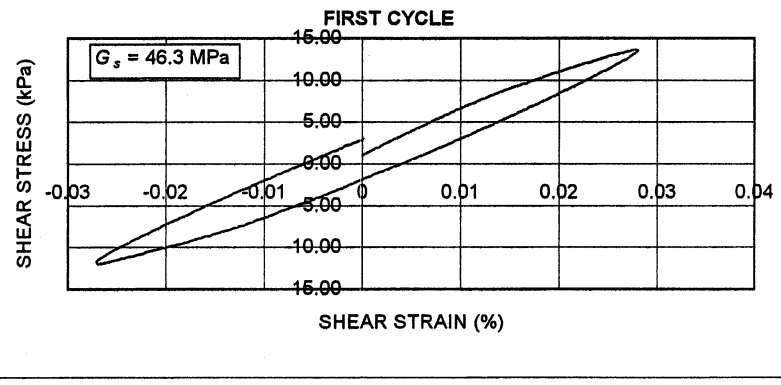

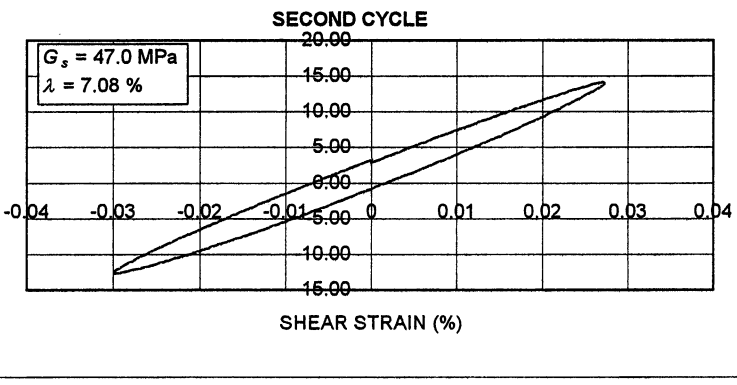

Joshua Tree P-3					
DSDSS TEST - Step 7					
Type of soil: SM-SC					
LL	15.5	PI	5.7	%Silt	18.7
e_0	0.44	S_0 (%)	84.2	%Clay	9.5
σ_v (kPa)	276	OCR	n/a	w (%)	13.7
γ_c (%)	~0.1	H_0 (mm)	19.37	Spec. Gr.	2.71

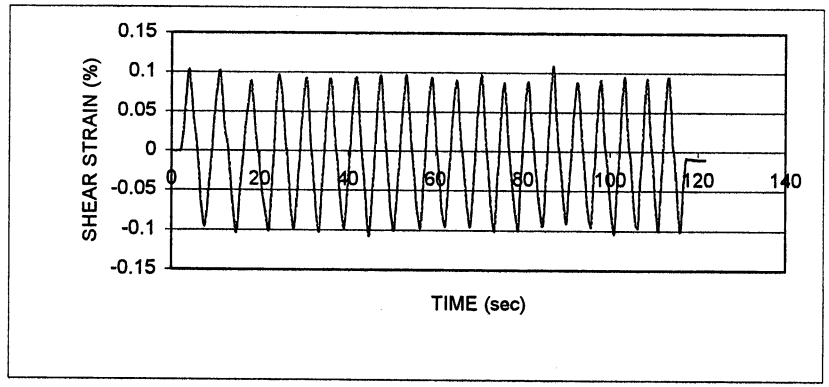

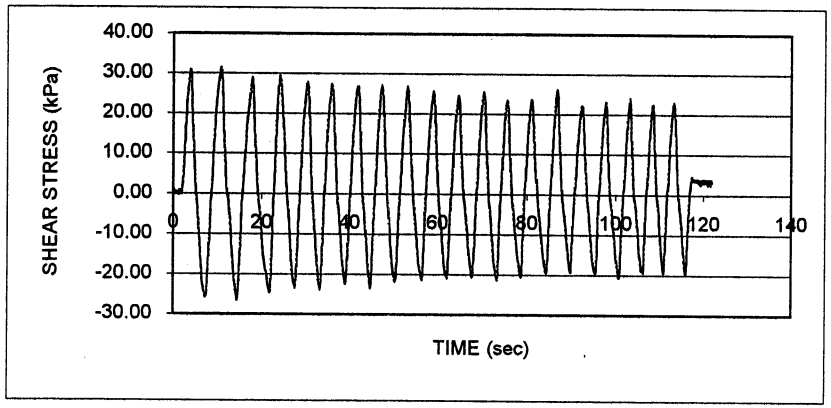

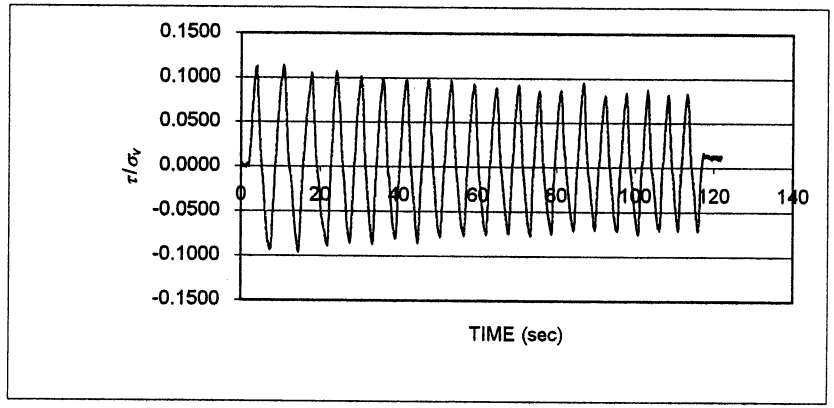

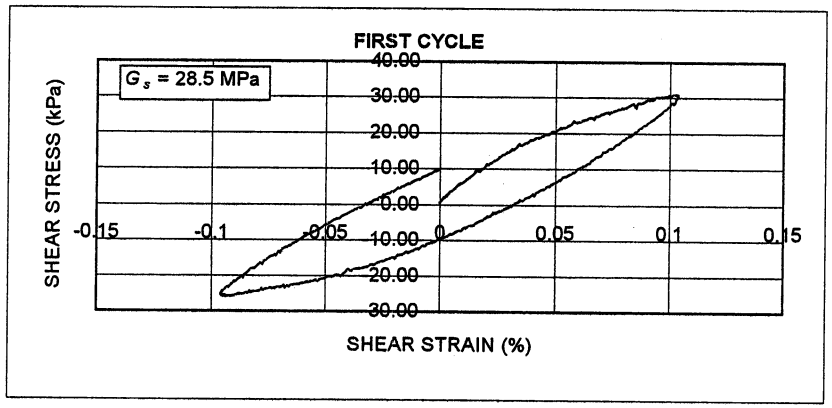

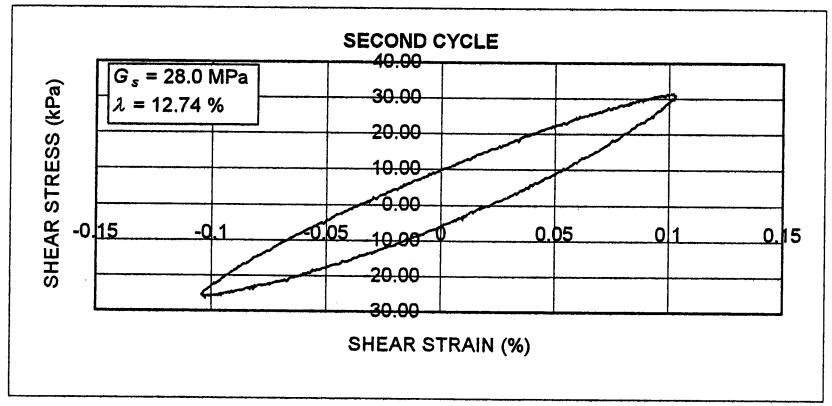

Joshua Tree P-3					
DSDSS TEST - Step 76					
Type of soil: SM-SC					
LL	15.5	PI	5.7	%Silt	18.7
e_0	0.44	S_0 (%)	84.2	%Clay	9.5
σ_v (kPa)	276	OCR	n/a	w (%)	13.7
γ_c (%)	~0.32	H_0 (mm)	19.37	Spec. Gr.	2.71

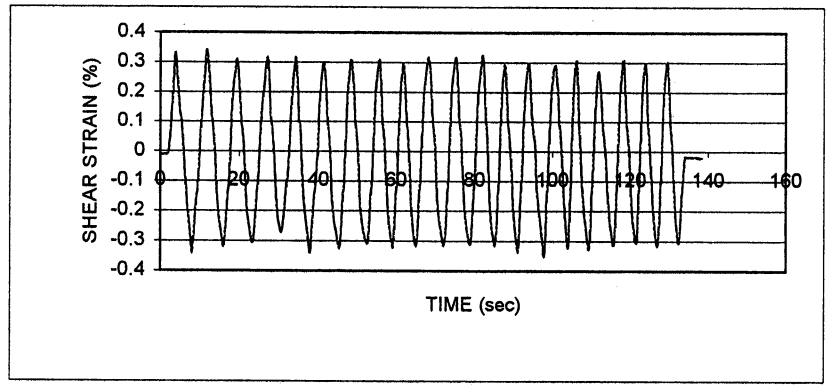

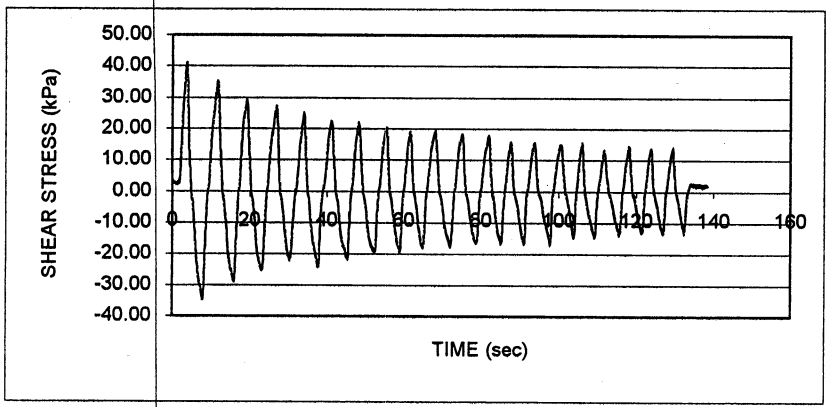

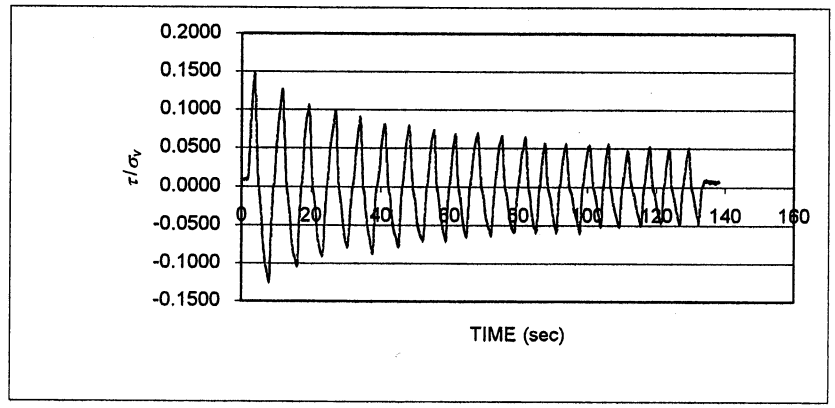

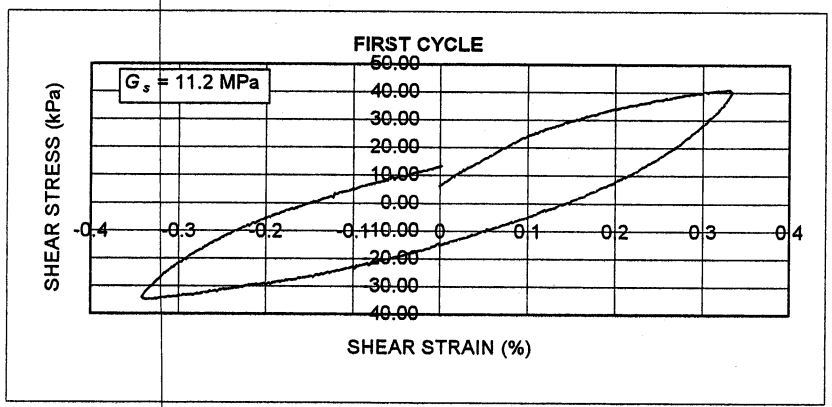

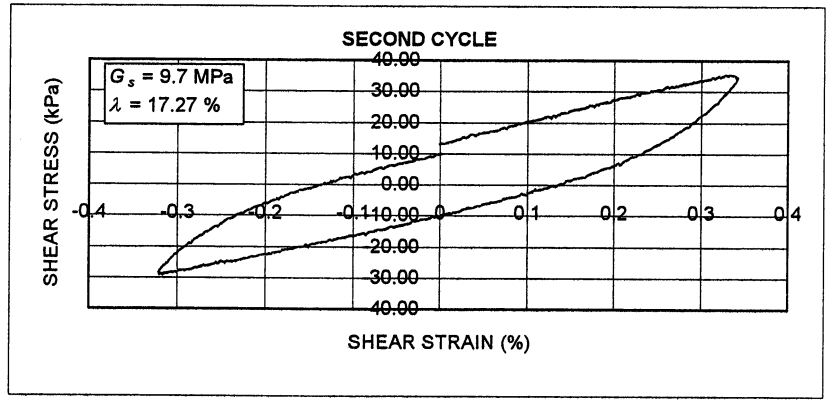

Joshua Tree P-3					
DSDSS TEST - Step 8					
Type of soil: SM-SC					
LL	15.5	PI	5.7	%Silt	18.7
e_0	0.44	S_0 (%)	84.2	%Clay	9.5
σ_v (kPa)	276	OCR	n/a	w (%)	13.7
γ_c (%)	~3.0	H_0 (mm)	19.37	Spec. Gr.	2.71

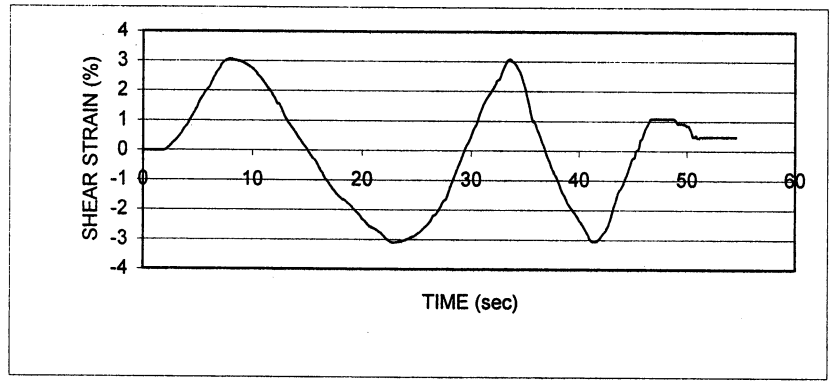

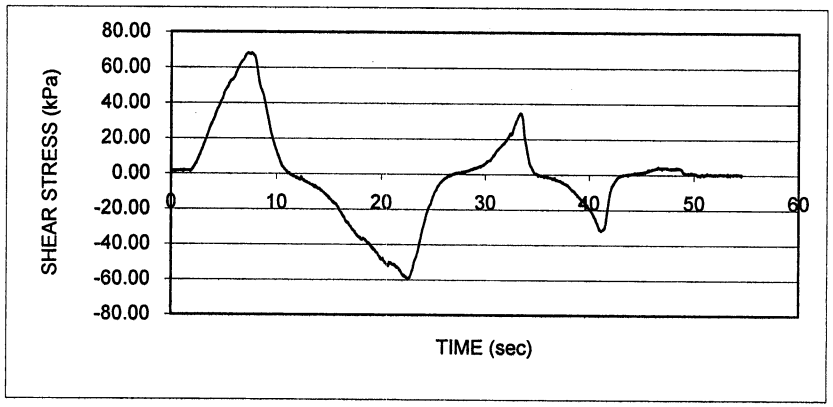

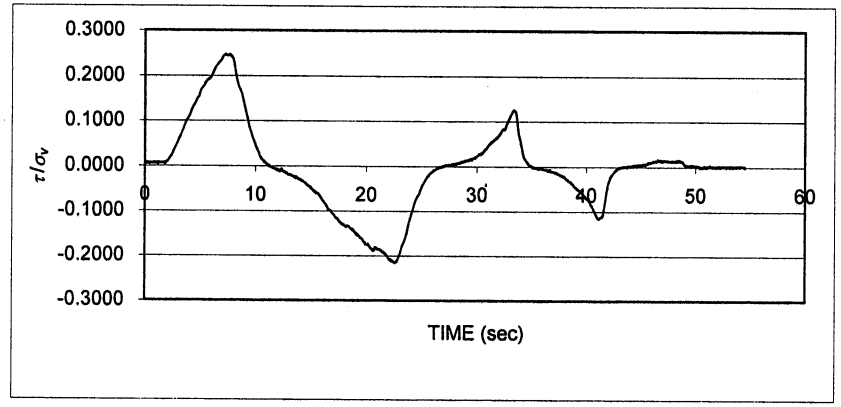

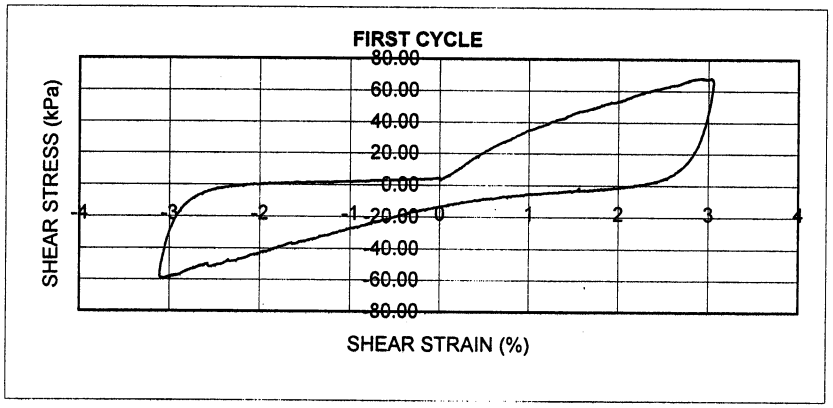

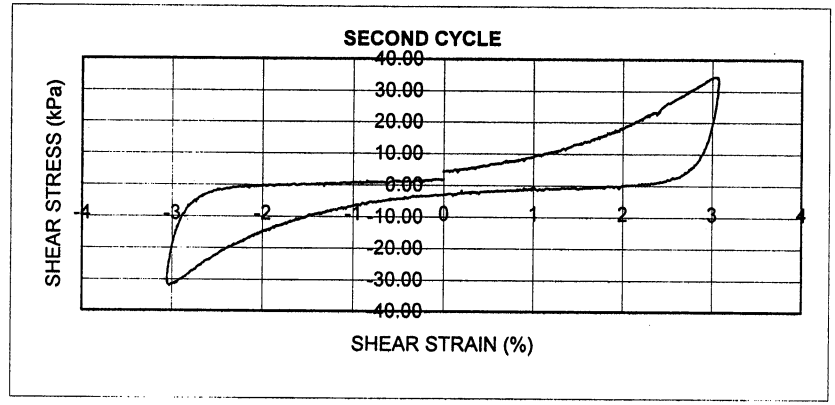

UCLA Soil Dynamics Laboratory
Double Specimen Direct Simple Shear (DSDSS) Test

Principal investigator: Mladen Vucetic, Professor
Test performed by Kentaro Tabata

Test no: 14

Project:	PEARL			Date:	12/19/2001
Sample name:	Joshua Tree (P-3)			Depth (ft):	42.5
Symbol:	SM-SC	LL (%):	15.5	Silt content (%):	18.7
Specific gravity:	2.71	PI:	5.7	Clay content (%):	9.5
Comments:	PEARL. Joshua Tree P-1 (42.5-43 ft).				

Estimated G_{max} (MPa):	70.5

SHEAR MODULUS				DAMPING RATIO	
Step	γ_c (%)	G_s (MPa)	G_s/G_{max}	γ_c (%)	λ (%)
2b	0.000389	69.43	0.985		
2b	0.000422	70.16	0.995		
3x	0.000971	68.61	0.973	0.002669	1.56
3x	0.000943	69.38	0.984	0.009273	3.74
4x	0.002758	65.47	0.929	0.028614	7.08
4x	0.002669	65.88	0.935	0.103412	12.74
5x	0.009648	57.71	0.819	0.331413	17.27
5x	0.009273	58.15	0.825		
6x	0.027601	46.34	0.657		
6x	0.028614	47.02	0.667		
7x	0.099762	28.49	0.404		
7x	0.103412	28.05	0.398		
76x	0.337620	11.25	0.160		
76x	0.331413	9.74	0.138		
	γ (%)				
(Monotonic loading)	1.002177	3.46	0.049		
	1.206629	3.24	0.046		
	1.504207	3.02	0.043		
	2.004353	2.66	0.038		
	2.500881	2.47	0.035		
	3.055824	2.17	0.031		

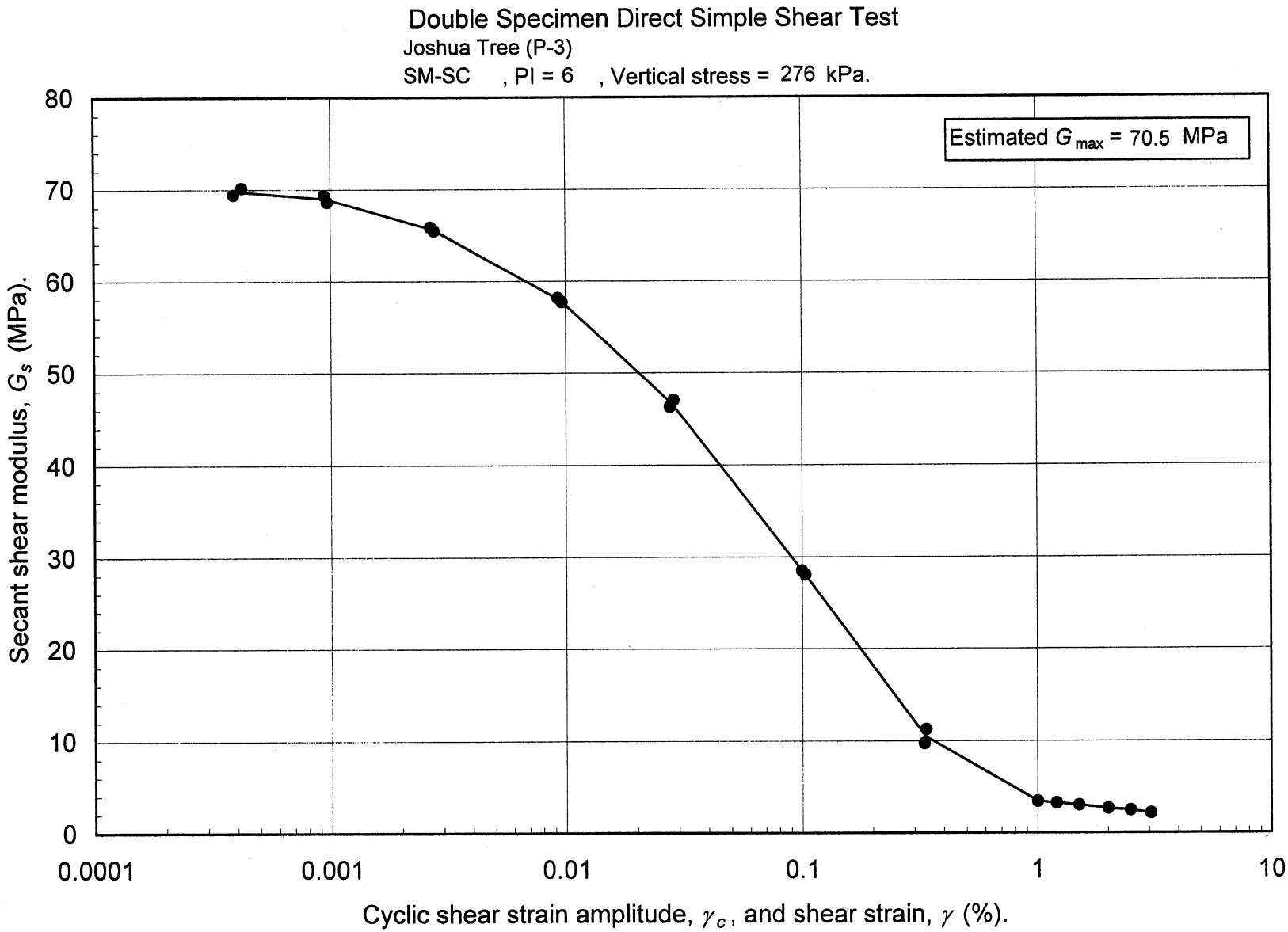
Double Specimen Direct Simple Shear Test
Joshua Tree (P-3)
SM-SC , PI = 6 , Vertical stress = 276 kPa.
Estimated G_{max} = 70.5 MPa
Secant shear modulus, G_s (MPa).
80
70
60
50
40
30
20
10
0
0.0001
0.001
0.01
0.1
1
10
Cyclic shear strain amplitude, γ_c, and shear strain, γ (%).

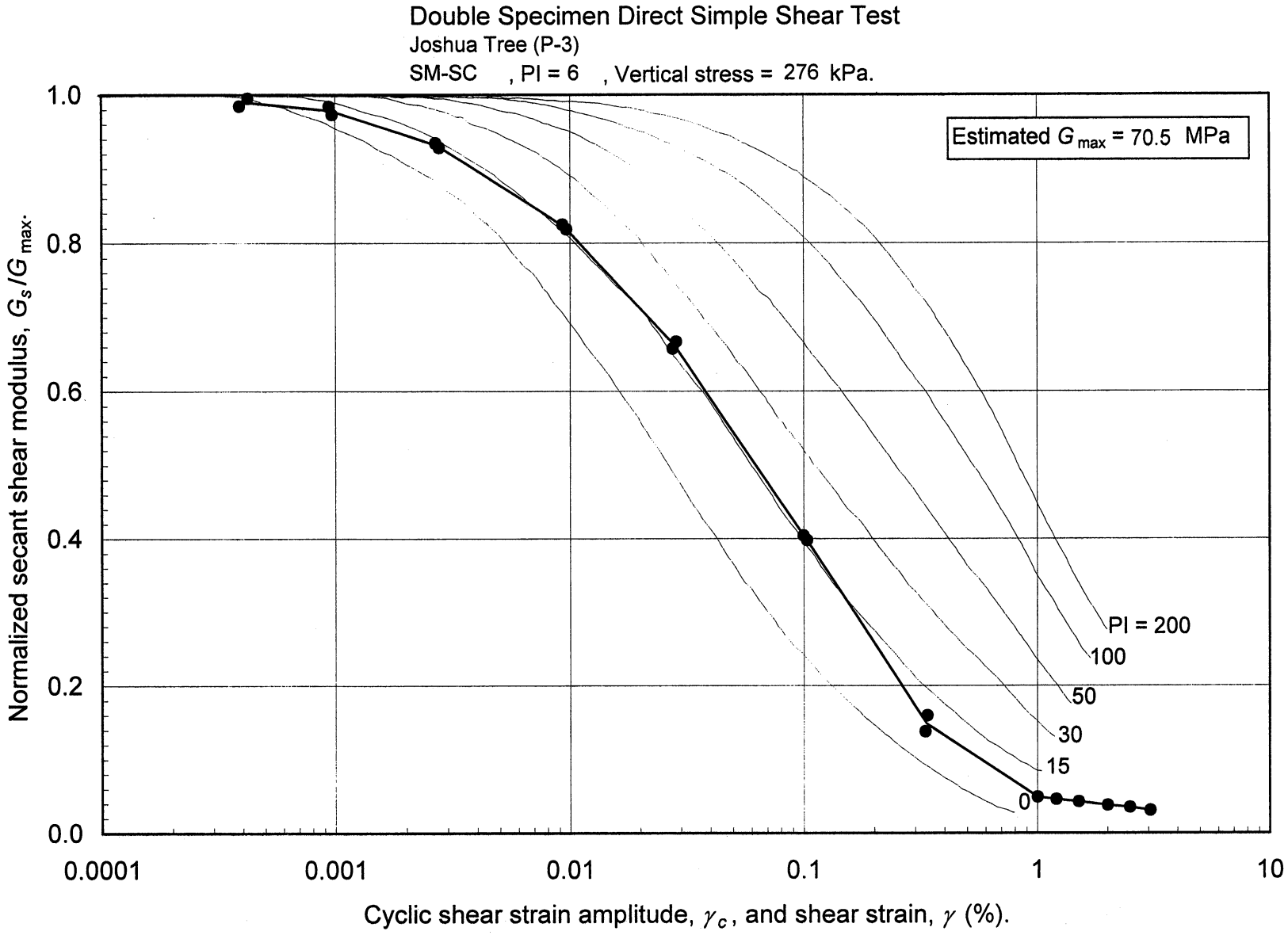
Double Specimen Direct Simple Shear Test
Joshua Tree (P-3)
SM-SC , PI = 6 , Vertical stress = 276 kPa.
Estimated G_{max} = 70.5 MPa
PI = 200
100
50
30
15
0
Normalized secant shear modulus, G_s/G_{max}.
1.0
0.8
0.6
0.4
0.2
0.0
0.0001
0.001
0.01
0.1
1
10
Cyclic shear strain amplitude, γ_c, and shear strain, γ (%).

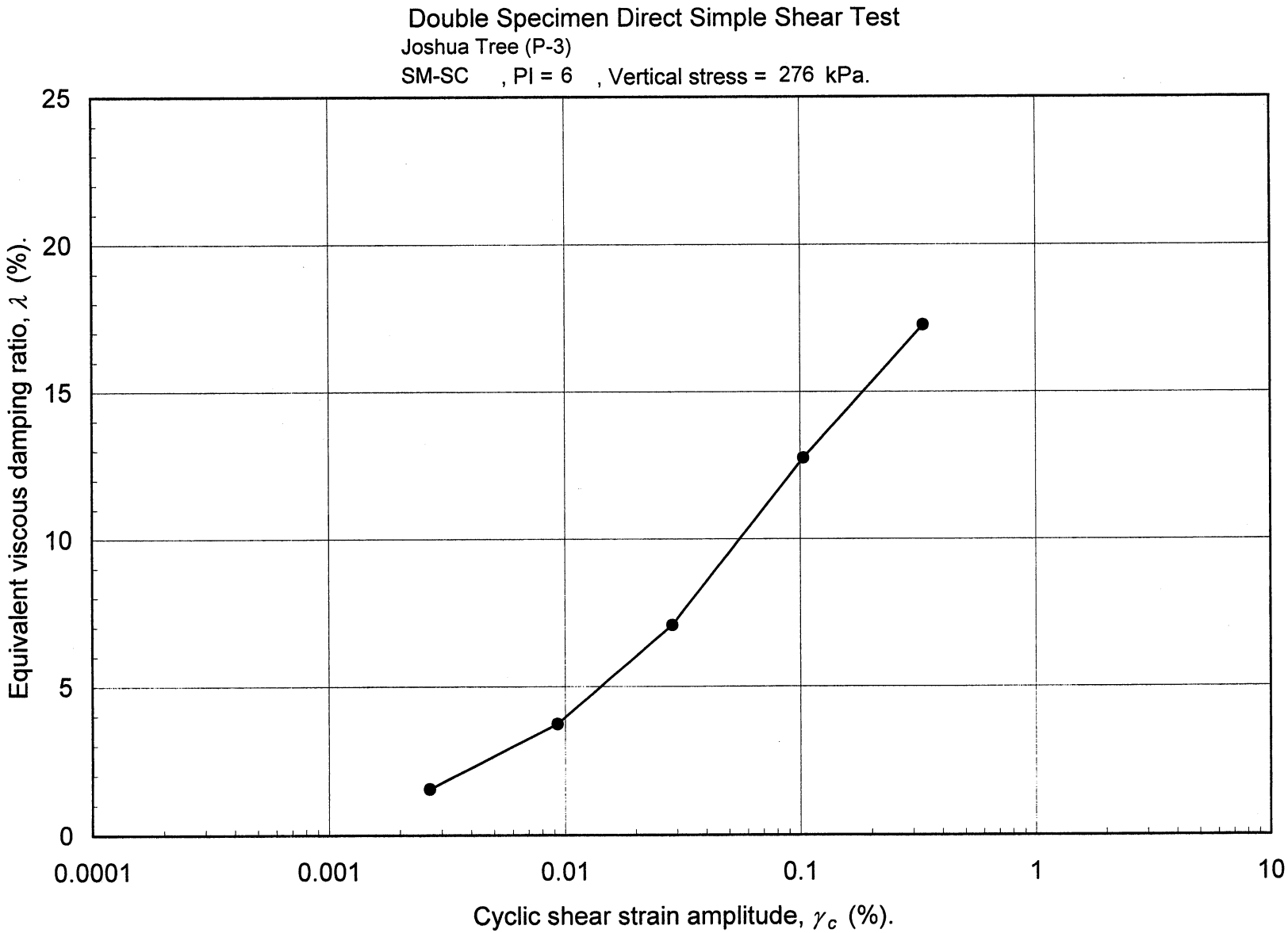
Double Specimen Direct Simple Shear Test
Joshua Tree (P-3)
SM-SC , PI = 6 , Vertical stress = 276 kPa.
Equivalent viscous damping ratio, λ (%).
25
20
15
10
5
0
0.0001
0.001
0.01
0.1
1
10
Cyclic shear strain amplitude, γc (%).

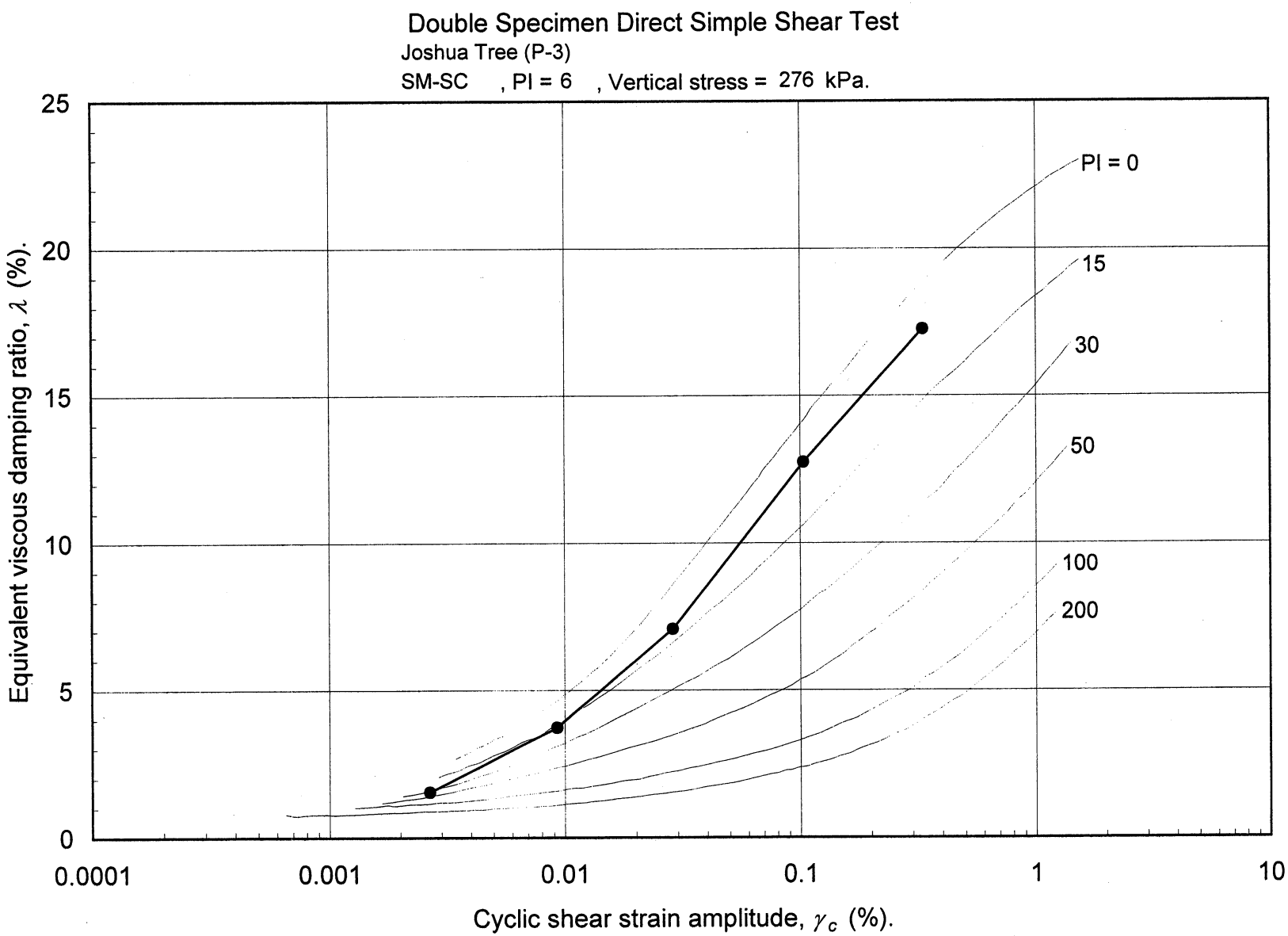
Double Specimen Direct Simple Shear Test
Joshua Tree (P-3)
SM-SC , PI = 6 , Vertical stress = 276 kPa.
Equivalent viscous damping ratio, λ (%).
Cyclic shear strain amplitude, γc (%).
0
5
10
15
20
25
0.0001
0.001
0.01
0.1
1
10
PI = 0
15
30
50
100
200

UCLA Soil Dynamics Laboratory

Specific Gravity Test

Principal investigator: Mladen Vucetic, Professor

Test performed by: Kentaro Tabata Test No.: 14

Project:	PEARL			Date:	12/25/2001
Boring:	Joshua Tree				
Tube No.:	P-3	Depth (ft):	40.0 -43.0	GWT (ft):	330.0
Comments:	Brown sand.				

SPECIFIC GRAVITY TEST

Test No.	1		
Bottle No.	3		
Wt. of bottle (g)	178.27		
Volume of bottle (cm^3)	500		
Wt. of bottle+water+soil (g)	703.68		
Temperature (°C)	23.0		
Wt. of bottle+water (g)	676.13		
Evaporating dish No.	B-2		
Weight of dish (g)	537.22		
Wt. of dish+dry soil (g)	580.80		
Wt. of dry soil (g)	43.58		
Specific gravity of water	0.9976		
Specific gravity of soil	**2.71**		

UCLA Soil Dynamics Laboratory

Grain Size Distribution

Principal investigator: Mladen Vucetic, Professor

Test performed by: Kentaro Tabata Test No.: 14

Project:	PEARL				
Boring:	Joshua Tree				
Tube No.:	P-3	Depth (ft):	40.0 -43.0	GWT (ft):	330.0
Comments:	Brown sand.				

GRAIN SIZE DISTRIBUTION

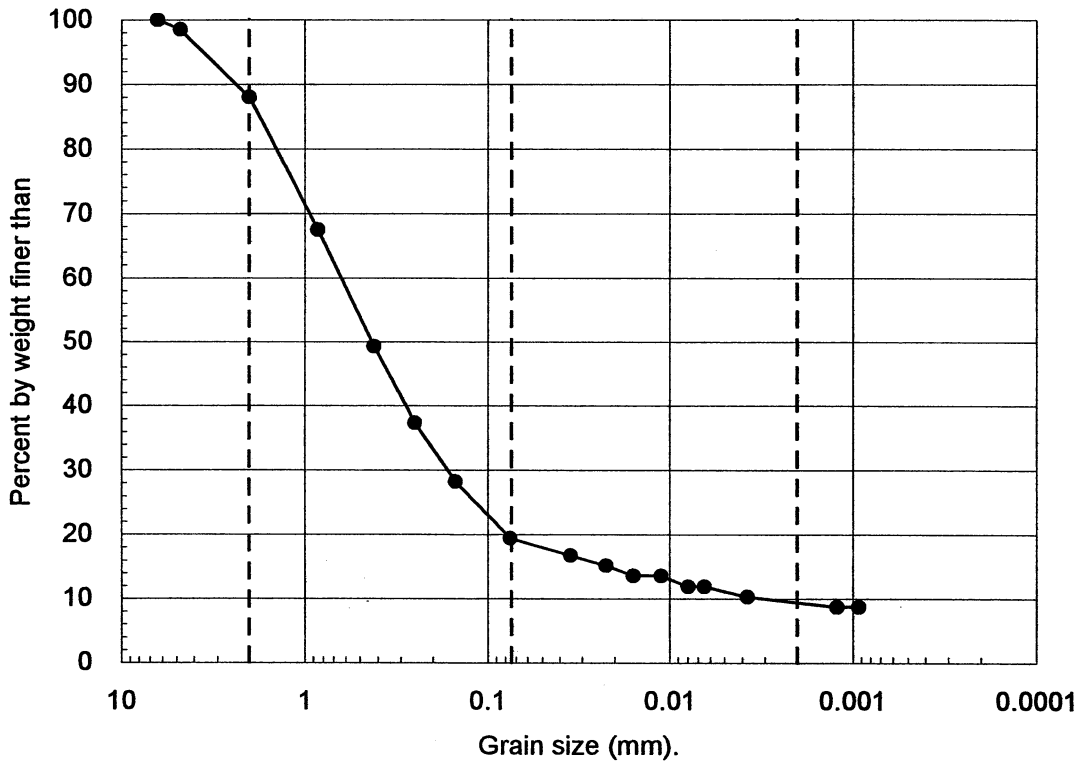

Clay (%)	Silt (%)	Sand (%)	Gravel (%)
9.5	18.7	59.8	12.0

UCLA Soil Dynamics Laboratory

Hydrometer Analysis

Principal investigator: Mladen Vucetic, Professor

Test performed by: Kentaro Tabata Test No.: 14

Project:	PEARL			Date:	12/8/2001
Boring:	Joshua Tree				
Tube No.:	P-3	Depth (ft):	40.0 -43.0	GWT (ft):	330.0
Comments:	Brown sand.				

HYDROMETER TEST

Time	Elapsed time t (sec)	Temp. T (°C)	Reading R'_T	Corr. reading $R_T=R'_T+c_m$	Depth H (cm)	Grain diameter D (mm)	Temp. corr. m_T	Corr. depth $R_T+m_T-c_d$	% by wt. finer than W_D (%)
12:56:01	0								
12:58:01	120	23.0	1007.0	1007.5	14.51	0.0349	0.700	1005.2	16.77
13:01:01	300	23.0	1006.5	1007.0	14.65	0.0222	0.700	1004.7	15.16
13:06:01	600	23.0	1006.0	1006.5	14.78	0.0158	0.700	1004.2	13.54
13:16:01	1200	23.0	1006.0	1006.5	14.78	0.0111	0.700	1004.2	13.54
13:36:01	2400	23.0	1005.5	1006.0	14.92	0.0079	0.700	1003.7	11.93
13:56:01	3600	23.0	1005.5	1006.0	14.92	0.0065	0.700	1003.7	11.93
15:56:01	10800	23.0	1005.0	1005.5	15.05	0.0037	0.700	1003.2	10.32
17:47:00	103859	23.0	1004.5	1005.0	15.18	0.0012	0.700	1002.7	8.71
14:30:00	178439	23.0	1004.5	1005.0	15.18	0.0009	0.700	1002.7	8.71

APPARATUS

Hydrometer no.:	88-18587	a_0	284.03	a_1	-0.2675
Graduate no.:	3				

FACTORS

Meniscus corr., c_m:	0.5		
Disp. agent corr, c_d:	3.0		
Visc. of water, η.	23.0 °C	9.565E-06	g sec/cm^2
	°C		g sec/cm^3

WEIGHT

Dry soil (g)	9.55
Percent by wt (%)	19.44
Dry soil for sieve (g)	39.58
Total (g)	49.13

UNIT WEIGHT

Specific gravity:		2.71
T	γ_w	γ_s
(°C)	(g/cm^3)	(g/cm^3)
23.0	0.9976	2.7053

UCLA Soil Dynamics Laboratory

Sieve Analysis

Principal investigator: Mladen Vucetic, Professor

Test performed by: Kentaro Tabata Test No.: 14

Project:	PEARL			Date:	1/10/2001
Boring:	Joshua Tree				
Tube No.:	P-3	Depth (ft):	40.0 -43.0	GWT (ft):	330.0
Comments:	Brown sand.				

SIEVE ANALYSIS

Sieve No.	Diameter (mm)	Sieve (g)	S+wet (g)	S+dry (g)	Retained (g)	Retained (%)	Cumulated (g)	Cumulated (%)	Passing (%)
3	6.350	485.05		485.05	0.00	0.00	0.00	0.00	100.00
4	4.750	463.14		463.86	0.72	1.47	0.72	1.47	98.53
10	2.000	422.43		427.60	5.17	10.52	5.89	11.99	88.01
20	0.850	375.44		385.50	10.06	20.48	15.95	32.46	67.54
40	0.420	457.58		466.54	8.96	18.24	24.91	50.70	49.30
60	0.250	324.08		329.93	5.85	11.91	30.76	62.61	37.39
100	0.150	342.17		346.68	4.51	9.18	35.27	71.79	28.21
200	0.075	338.71		343.02	4.31	8.77	39.58	80.56	19.44
Total					39.58	80.56			

WEIGHT

Dry soil for sieve (g)	39.58
Dry soil for hydr. (g)	9.55
Total (g)	49.13
Percent coaser (%)	80.56

UCLA Soil Dynamics Laboratory

Atterberg Limit Determination

Principal investigator: Mladen Vucetic, Professor

Test performed by: Kentaro Tabata Test No.: 14

Project:	PEARL			Date:	1/22/2002
Boring:	Joshua Tree				
Tube No.:	P-3	Depth (ft):	40.0 -43.0	GWT (ft):	330.0
Comments:	Brown sand.				

LIQUID LIMIT TEST

Test No.	1	2	3	4				
Number of blows	8	13	25	30				
Container No.	ST-23	ST-4	ST-6	ST-14				
Container (g)	30.59	30.17	30.10	30.46				
Cont+wet soil (g)	34.61	34.55	35.22	35.49				
Cont+dry soil (g)	33.95	33.88	34.54	34.84				
Water (g)	0.66	0.67	0.68	0.65				
Dry soil (g)	3.36	3.71	4.44	4.38				
Water content (%)	19.64	18.06	15.32	14.84				

PLASTIC LIMIT TEST

Test No.			
Container No.	ST-12	ST-3	ST-22
Container (g)	30.29	30.18	30.07
Cont+wet soil (g)	32.76	33.55	33.44
Cont+dry soil (g)	32.54	33.24	33.15
Water (g)	0.22	0.31	0.29
Dry soil (g)	2.25	3.06	3.08
Water content (%)	9.78	10.13	9.42

ATTERBERG LIMITS

Liquid limit (%)	**15.5**
Plastic limit (%)	**9.8**
Plasticity index	**5.7**

CLASSIFICATION

SM-SC

FLOW CHART

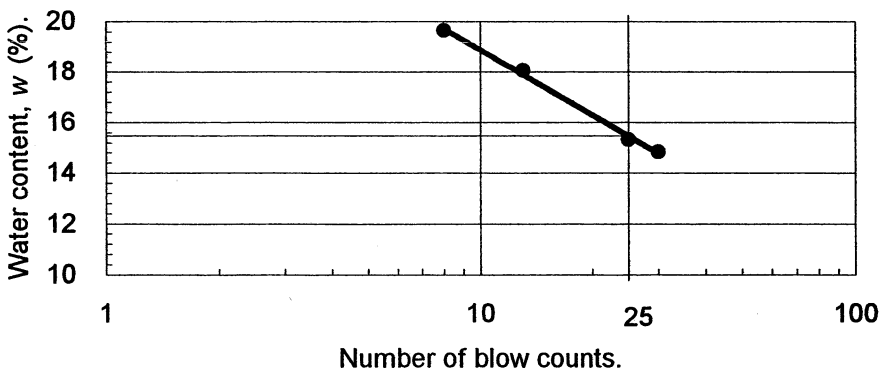

UCLA Soil Dynamics Laboratory

Atterberg Limit Determination

Principal investigator: Mladen Vucetic, Professor

Test performed by: Kentaro Tabata Test No.: 14

Project:	PEARL			Date:	1/22/2002
Boring:	Joshua Tree				
Tube No.:	P-3	Depth (ft):	40.0 -43.0	GWT (ft):	330.0
Comments:	Brown sand.				

PLASTICITY CHART

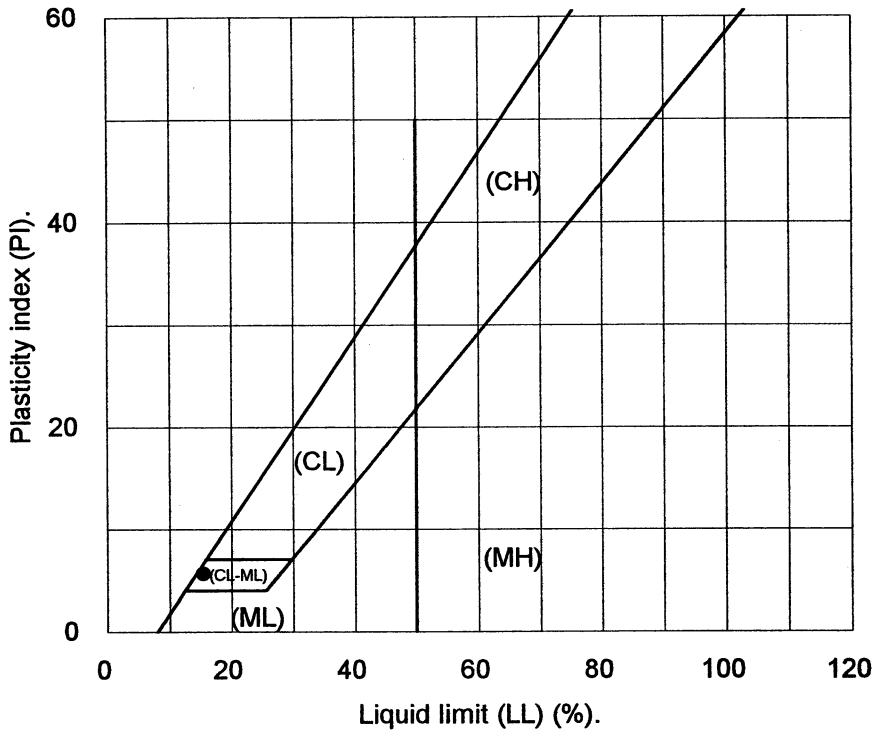

3.16 Test 15: GILROY #3 P-1

UCLA Soil Dynamics Laboratory

Double Specimen Direct Simple Shear (DSDSS) Test

Principal investigator: Mladen Vucetic, Professor

Test performed by: Kentaro Tabata Test No.: 15

Project:	PEARL			Date:	1/16/2002
Boring:	Gilroy #3				
Tube No.:	P-1	Depth (ft):	15.0 -18.0	GWT (ft):	35.0 (reported by others)
Comments:	Brown silt and sand. Specimen obtained from the bottom of the tube (specimen depth ~ 17.5 ft).				

FORM 1: SPECIMEN PREPARATION

WATER CONTENT, SPECIFIC GRAVITY				UNIT WEIGHT, VOID RATIO, SATURATION			
	Before consol.	After shearing			Before consol.	Before shearing	After shearing
Container No.	ST-1	MT-13	MT-19	Average weight (g)	136.69	136.69	
Cont+wet soil (g)	43.99	184.64	186.23	Height (cm)	1.960	1.911	
Cont+dry soil (g)	41.45	160.94	162.07	Area (cm^2)	34.84	34.84	
Container (g)	30.36	49.55	50.16	Volume (cm^3)	68.28	66.58	
Water (g)	2.54	23.70	24.16	Unit weight (g/cm^3)	2.002	2.053	
Dry soil (g)	11.09	111.39	111.91	Unit weight (kN/m^3)	19.62	20.12	
Water content(%)	22.90	21.28	21.59	Void ratio	0.61	0.57	
Avg. water cont. (%)	22.90		21.43	Saturation (%)	98.6	98.8	
Spceific gravity			2.62				

HEIGHT OF SPECIMEN					
	Before consol.		Before shearing	After shearing	
	Top	Bottom	Average	Average	
Height (cm)	1.960	1.960	1.911	1.911	

AREA OF SPECIMEN						
Initial diameter (cm)			6.660	Initial area (cm^2)		34.837
Load (kg)	Stress (kg/cm^2)	Stress (kN/m^2)	Diameter (cm)	Membrane (cm)	Corrected diameter (cm)	Area (cm^2)

Halls Valley P-2					
DSDSS TEST - Step 2					
Type of soil: CL					
LL	28.9	PI	14.6	%Silt	29.1
e_0	0.57	S_0 (%)	98.8	%Clay	28.5
σ_v (kPa)	108	OCR	n/a	w (%)	21.4
γ_c (%)	~0.0003	H_0 (mm)	19.11	Spec. Gr.	2.62

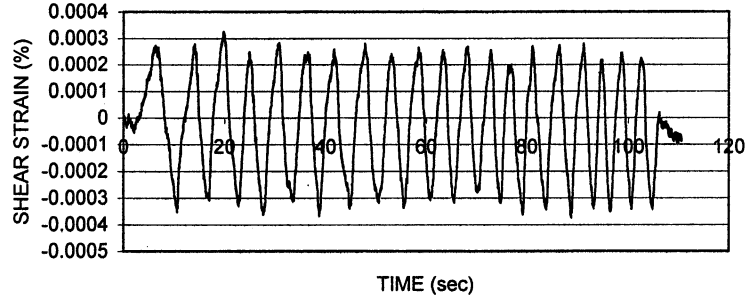

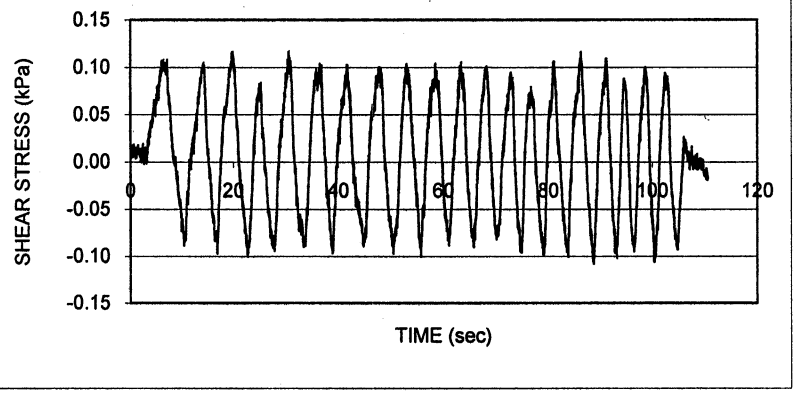

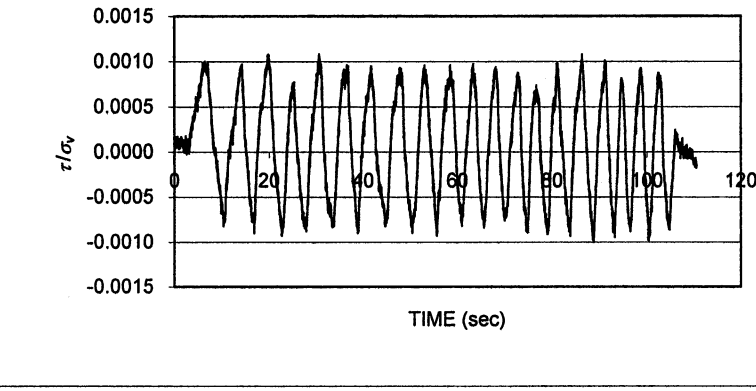

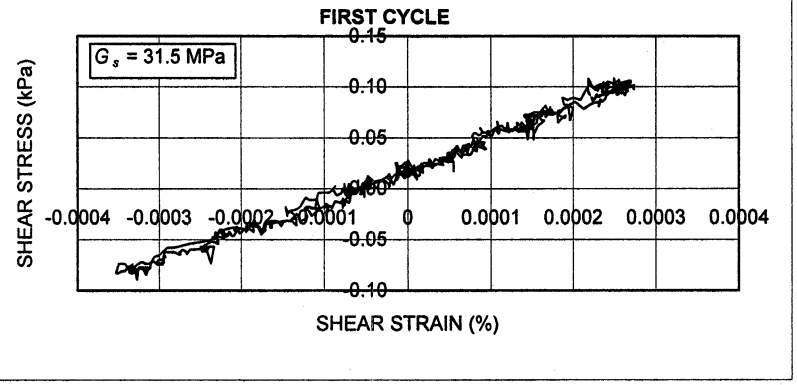

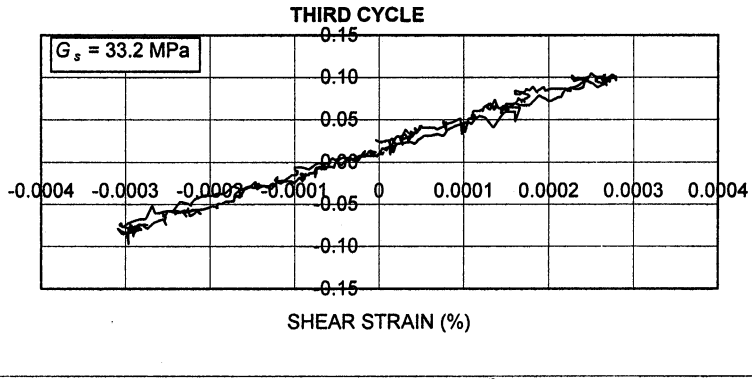

Halls Valley P-2					
DSDSS TEST - Step 3					
Type of soil: CL					
LL	28.9	PI	14.6	%Silt	29.1
e_0	0.57	S_0 (%)	98.8	%Clay	28.5
σ_v (kPa)	108	OCR	n/a	w (%)	21.4
γ_c (%)	~0.0009	H_0 (mm)	19.11	Spec. Gr.	2.62

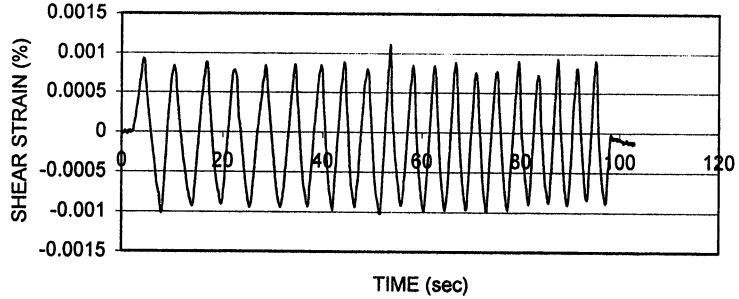

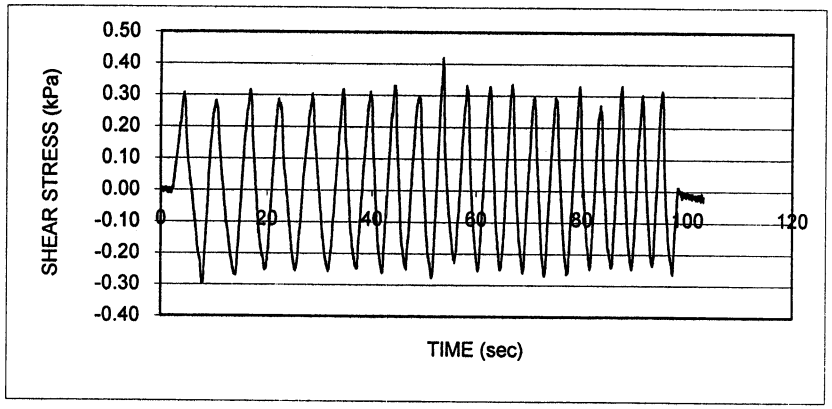

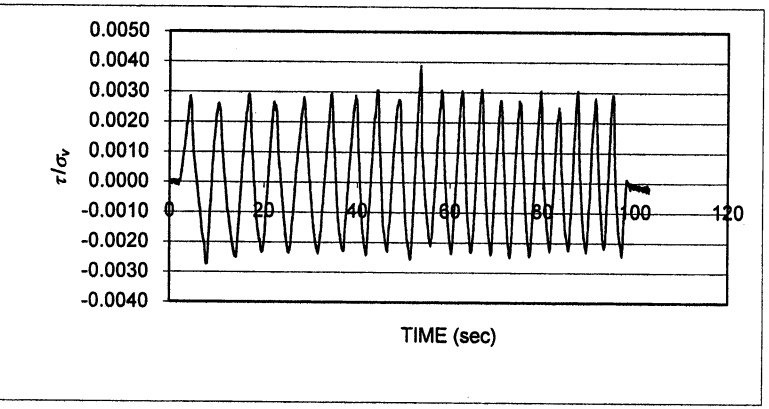

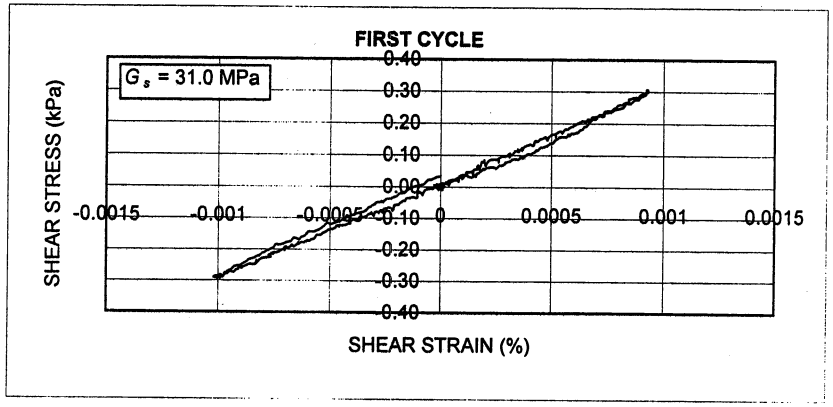

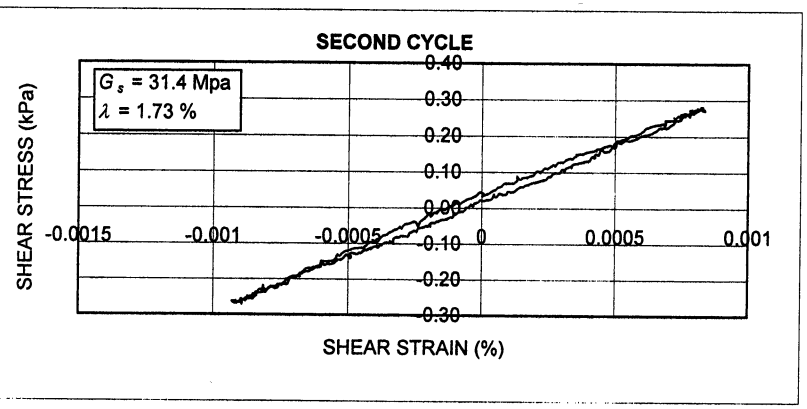

Halls Valley P-2					
DSDSS TEST - Step 4					
Type of soil: CL					
LL	28.9	PI	14.6	%Silt	29.1
e_0	0.57	S_0 (%)	98.8	%Clay	28.5
σ_v (kPa)	108	OCR	n/a	w (%)	21.4
γ_c (%)	~0.0028	H_0 (mm)	19.11	Spec. Gr.	2.62

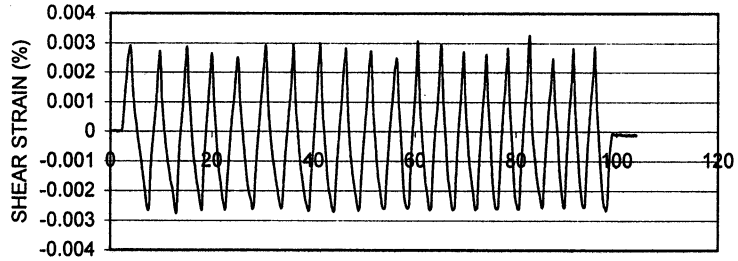

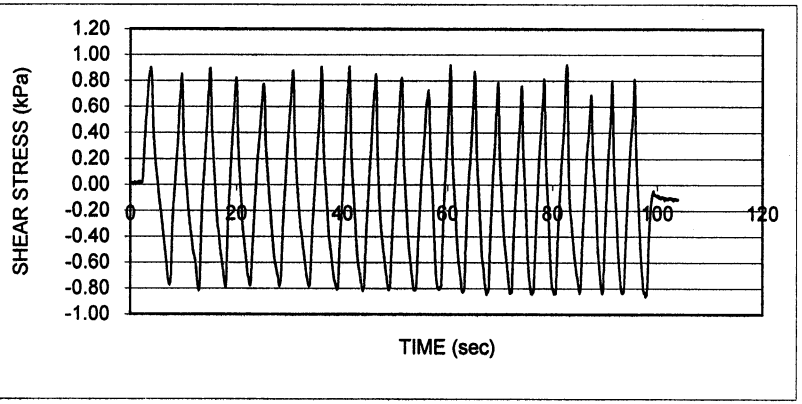

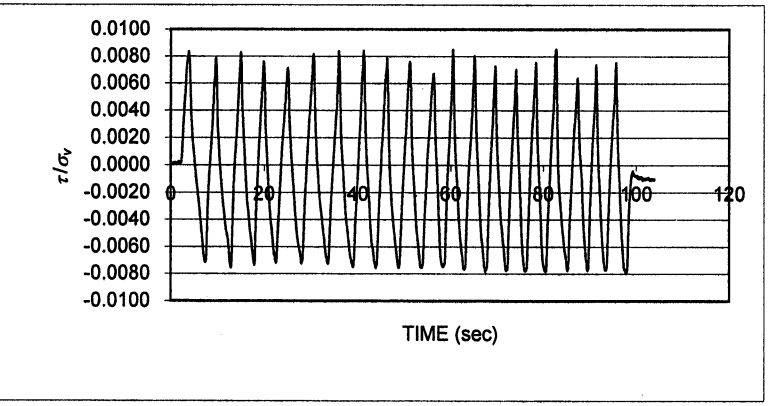

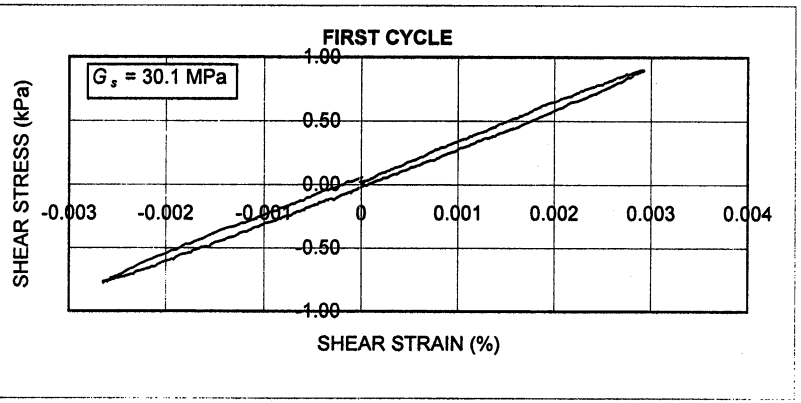

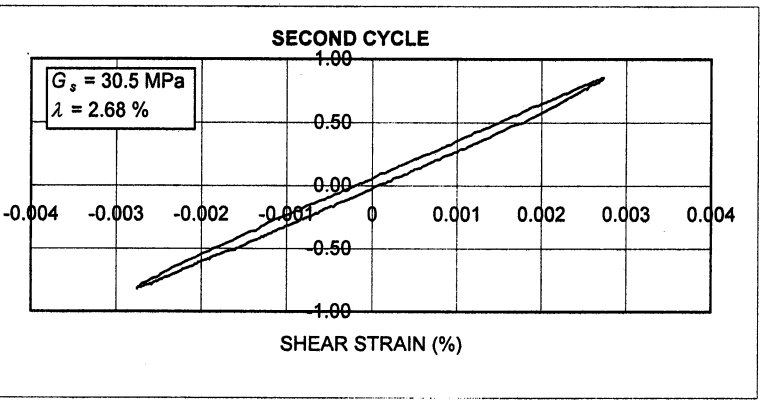

Halls Valley P-2					
DSDSS TEST - Step 5					
Type of soil: CL					
LL	28.9	PI	14.6	%Silt	29.1
e_0	0.57	S_0 (%)	98.8	%Clay	28.5
σ_v (kPa)	108	OCR	n/a	w (%)	21.4
γ_c (%)	~0.011	H_0 (mm)	19.11	Spec. Gr.	2.62

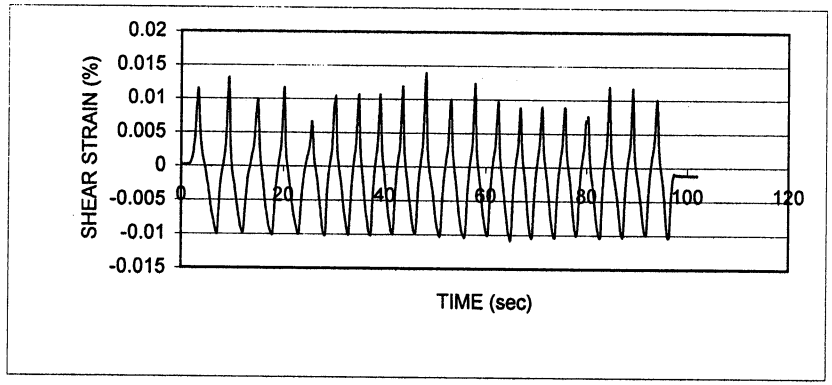

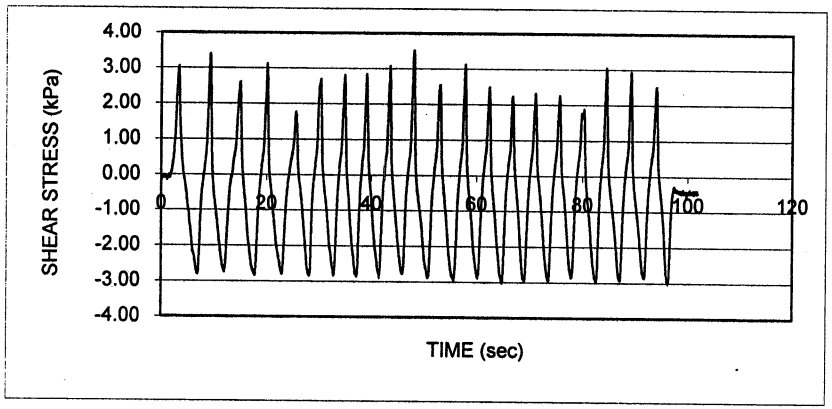

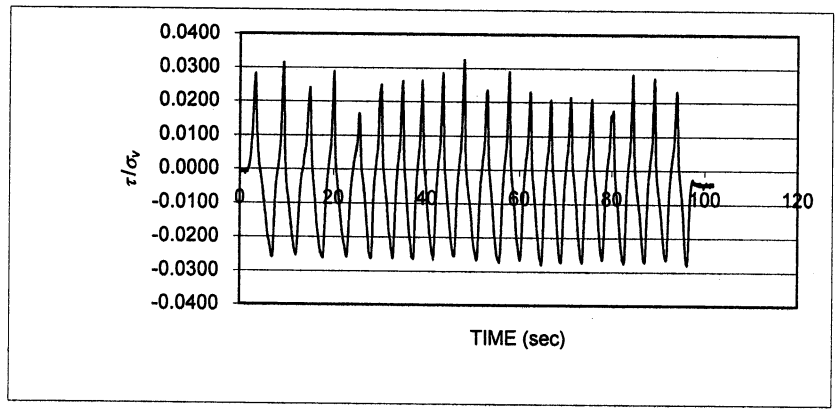

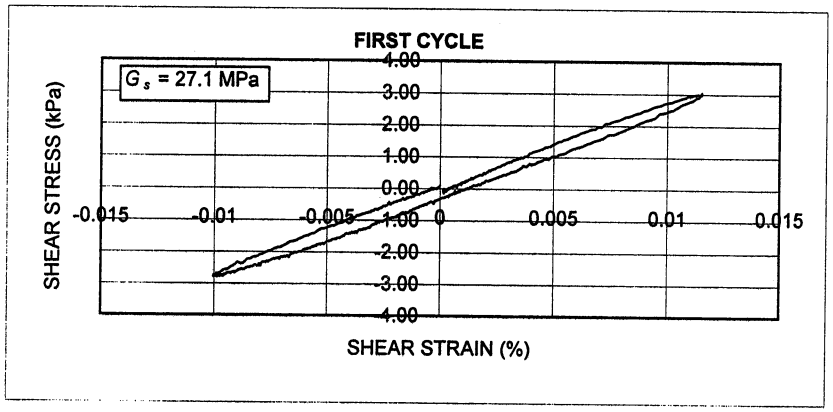

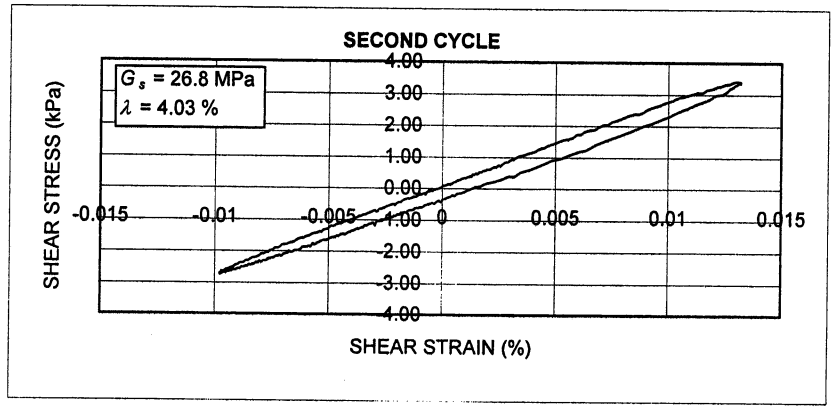

Halls Valley P-2					
DSDSS TEST - Step 6					
Type of soil: CL					
LL	28.9	PI	14.6	%Silt	29.1
e_0	0.57	S_0 (%)	98.8	%Clay	28.5
σ_v (kPa)	108	OCR	n/a	w (%)	21.4
γ_c(%)	~0.028	H_0 (mm)	19.11	Spec. Gr.	2.62

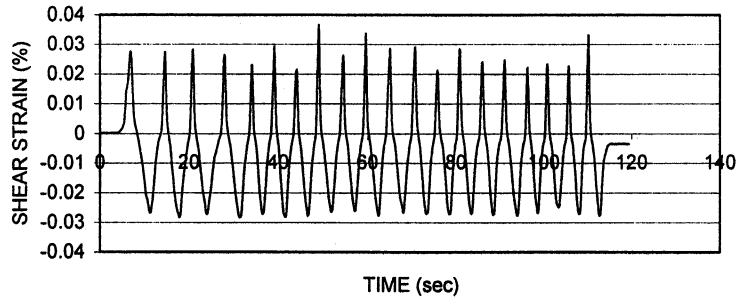

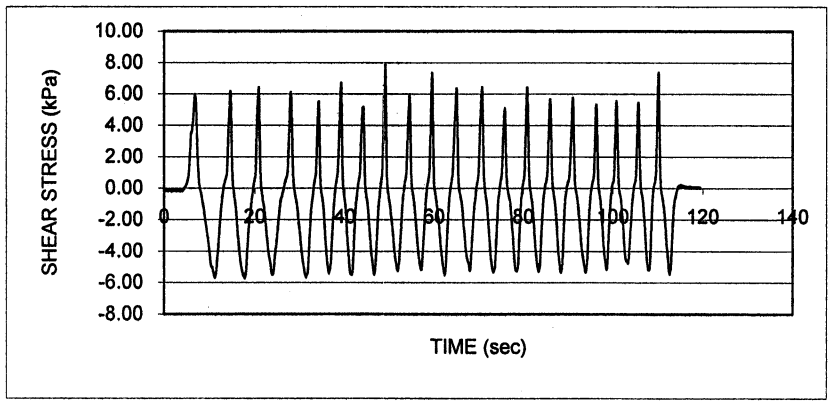

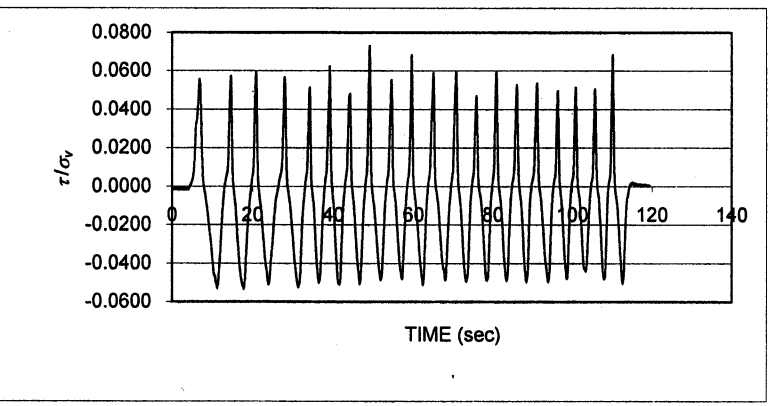

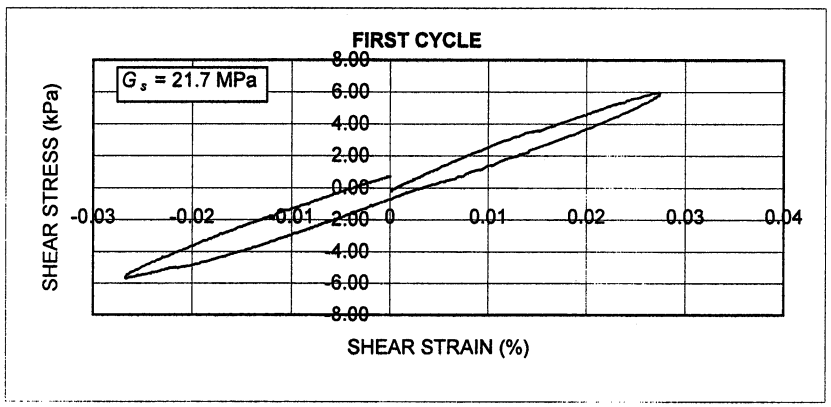

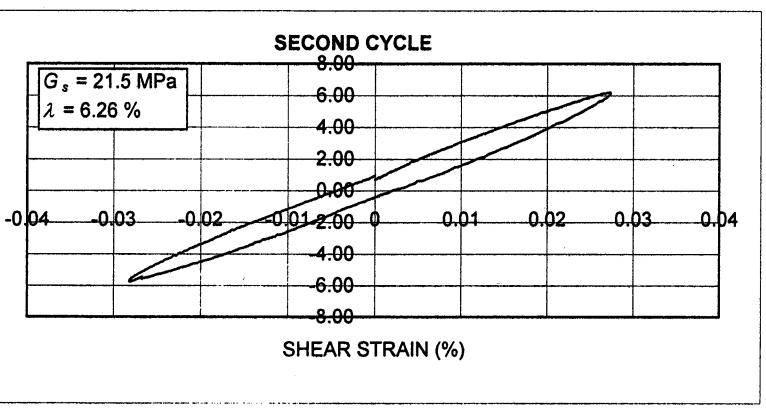

Halls Valley P-2					
DSDSS TEST - Step 7					
Type of soil: CL					
LL	28.9	PI	14.6	%Silt	29.1
e_0	0.57	S_0 (%)	98.8	%Clay	28.5
σ_v (kPa)	108	OCR	n/a	w (%)	21.4
γ_c (%)	~0.09	H_0 (mm)	19.11	Spec. Gr.	2.62

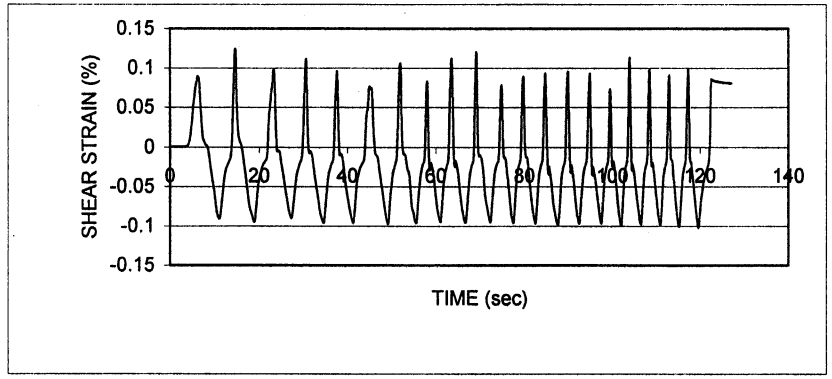

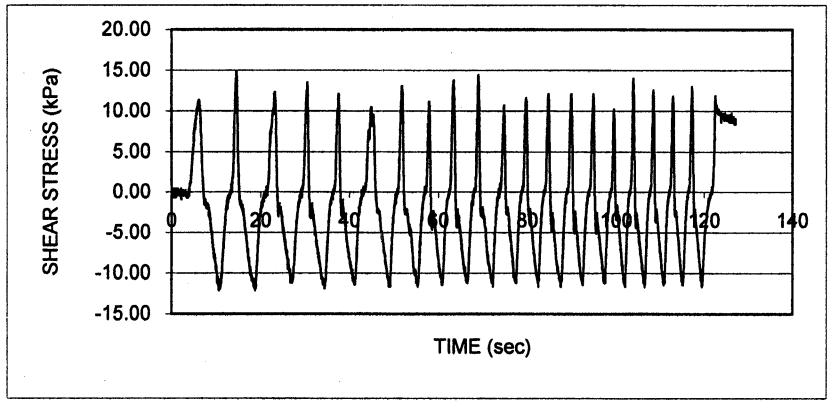

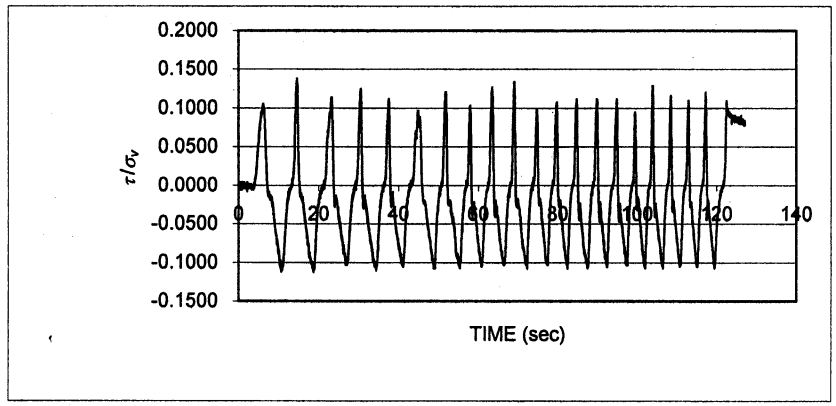

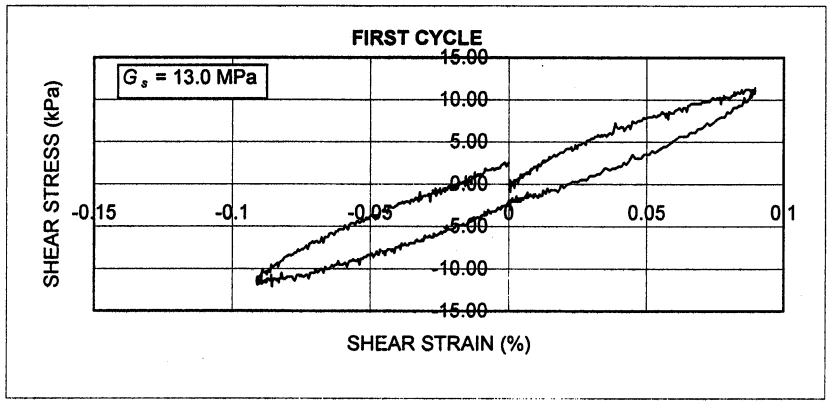

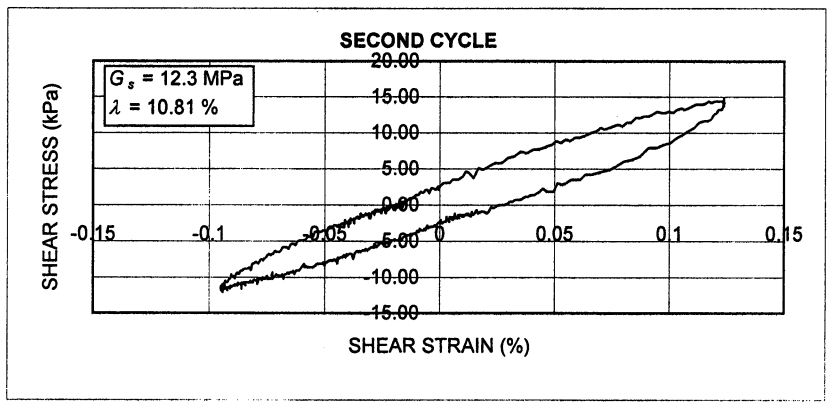

Halls Valley P-2					
DSDSS TEST - Step 76					
Type of soil: CL					
LL	28.9	PI	14.6	%Silt	29.1
e_0	0.57	S_0 (%)	98.8	%Clay	28.5
σ_v (kPa)	108	OCR	n/a	w (%)	21.4
γ_c (%)	~0.28	H_0 (mm)	19.11	Spec. Gr.	2.62

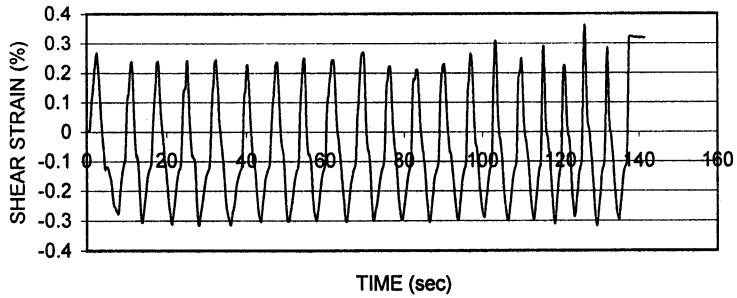

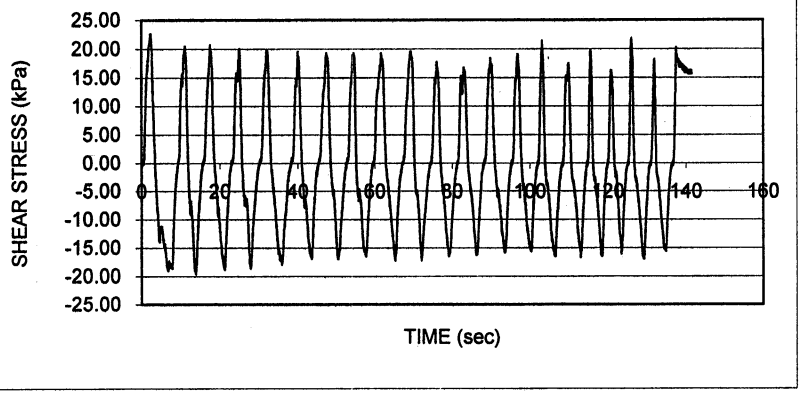

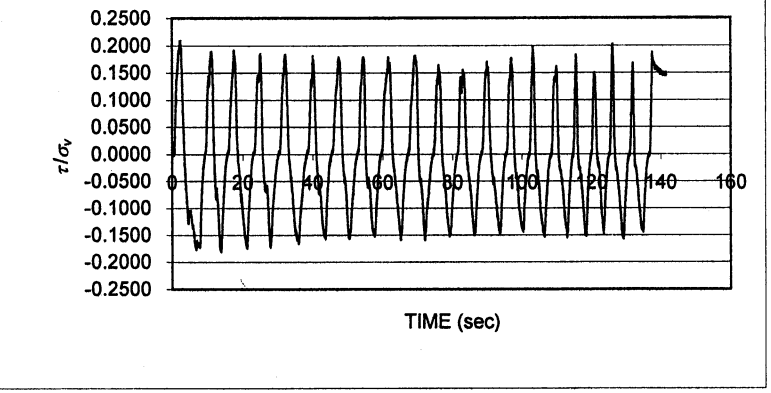

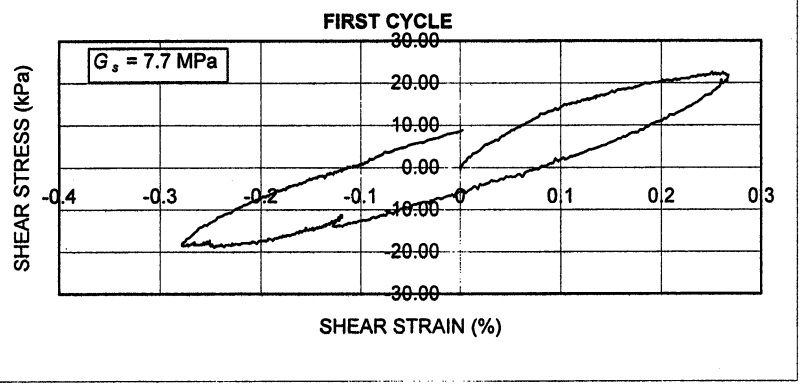

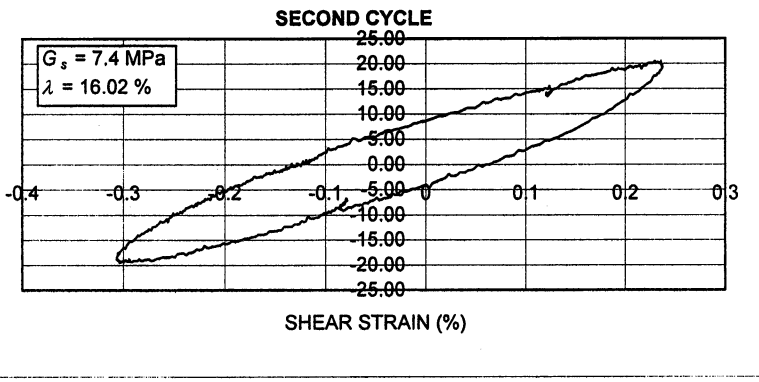

Halls Valley P-2					
DSDSS TEST - Step 8					
Type of soil: CL					
LL	28.9	PI	14.6	%Silt	29.1
e_0	0.57	S_0 (%)	98.8	%Clay	28.5
σ_v (kPa)	108	OCR	n/a	w (%)	21.4
γ_c (%)	~3.1	H_0 (mm)	19.11	Spec. Gr.	2.62

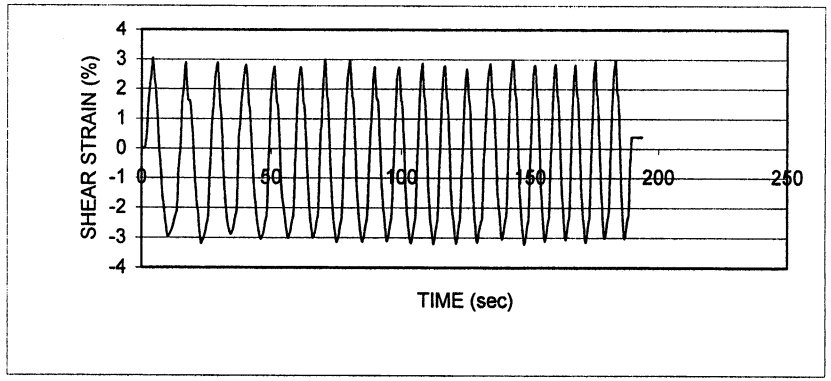

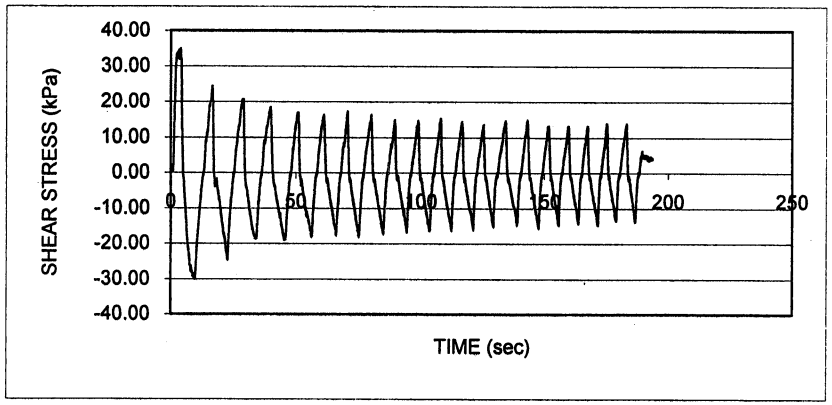

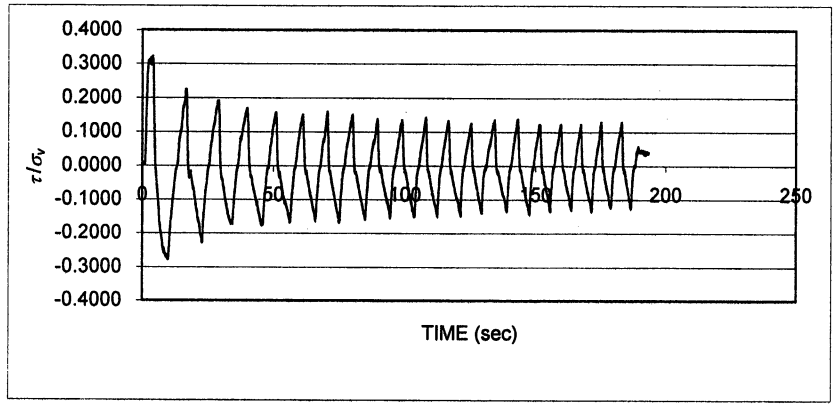

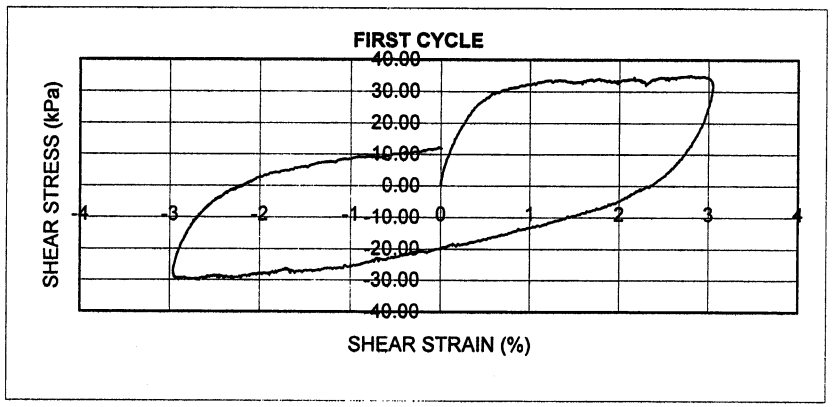

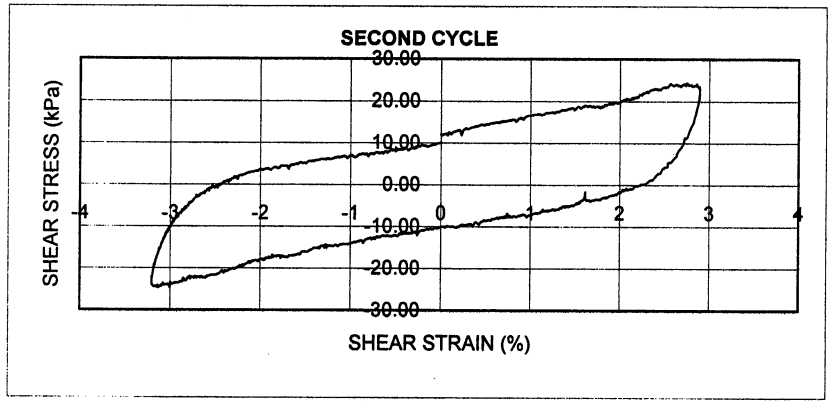

UCLA Soil Dynamics Laboratory
Double Specimen Direct Simple Shear (DSDSS) Test

Principal investigator: Mladen Vucetic, Professor
Test performed by Kentaro Tabata

Test no: 15

Project:	PEARL			Date:	1/16/2002
Sample name:	Gilroy #3 (P-1)			Depth (ft):	17.5
Symbol:	CL	LL (%):	28.9	Silt content (%):	29.1
Specific gravity:	2.62	PI:	14.6	Clay content (%):	28.5
Comments:					

Estimated G_{max} (MPa):	32.5

	SHEAR MODULUS			DAMPING RATIO	
Step	γ_c (%)	G_s (MPa)	G_s/G_{max}	γ_c (%)	λ (%)
2x	0.000314	31.48	0.969		
2x	0.000328	33.18	1.021	0.000883	1.73
3x	0.000976	30.95	0.952	0.002745	2.68
3x	0.000883	31.37	0.965	0.011481	4.03
4x	0.002789	30.11	0.926	0.027792	6.26
4x	0.002745	30.47	0.937	0.109538	10.81
5x	0.010778	27.13	0.835	0.271995	16.02
5x	0.011481	26.78	0.824		
6x	0.027107	21.66	0.666		
6x	0.027792	21.54	0.663		
7x	0.090295	13.03	0.401		
7x	0.109538	12.34	0.380		
76x	0.272642	7.65	0.235		
76x	0.271995	7.37	0.227		
	γ (%)				
(Monotonic loading)	0.503284	5.55	0.171		
	1.012106	3.18	0.098		
	1.502440	2.19	0.067		
	2.000185	1.65	0.051		
	2.503468	1.38	0.042		
	3.003047	1.13	0.035		

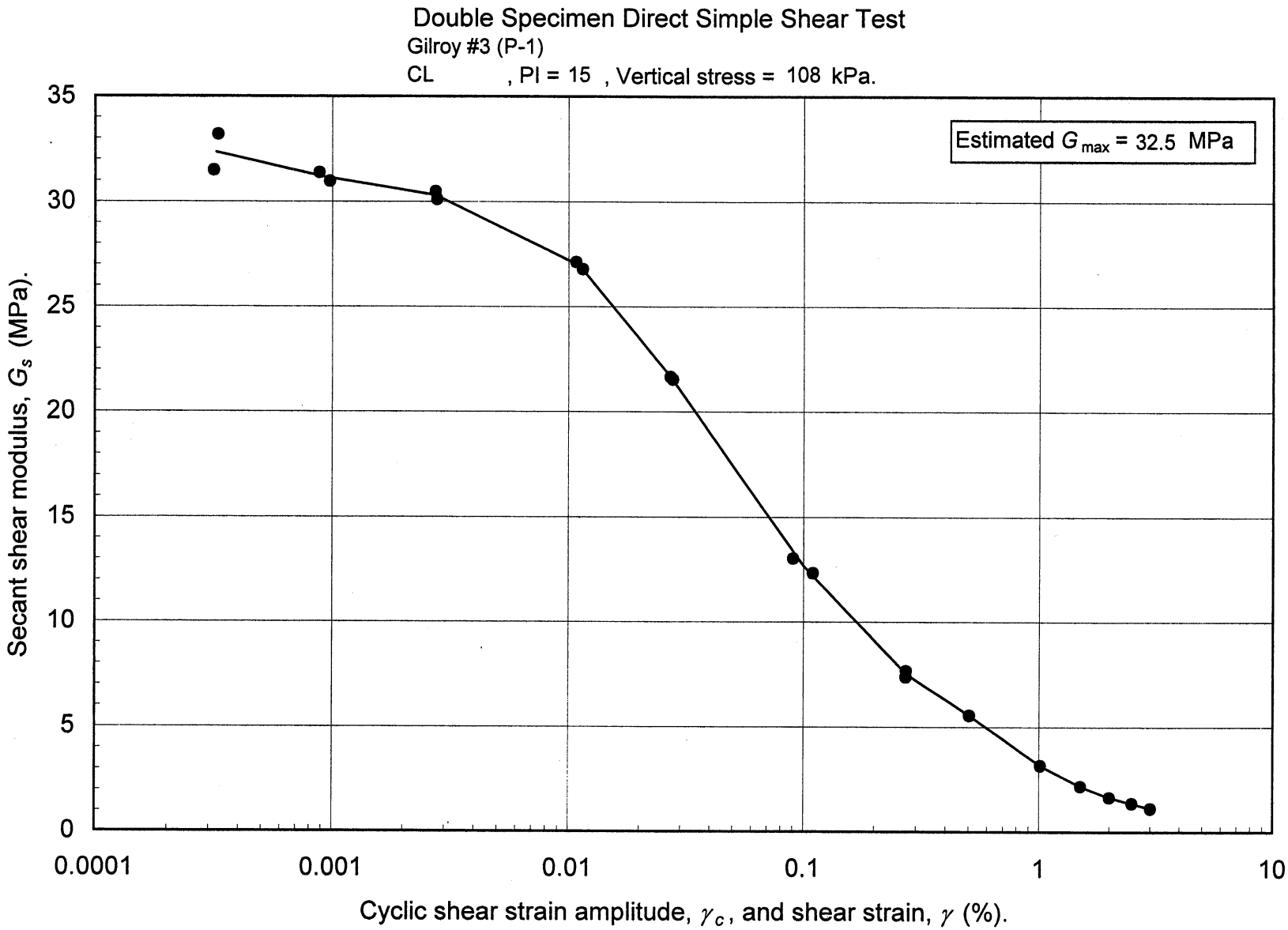
Double Specimen Direct Simple Shear Test
Gilroy #3 (P-1)
CL , PI = 15 , Vertical stress = 108 kPa.
Estimated G_{max} = 32.5 MPa
Secant shear modulus, G_s (MPa).
35
30
25
20
15
10
5
0
0.0001
0.001
0.01
0.1
1
10
Cyclic shear strain amplitude, γ_c, and shear strain, γ (%).

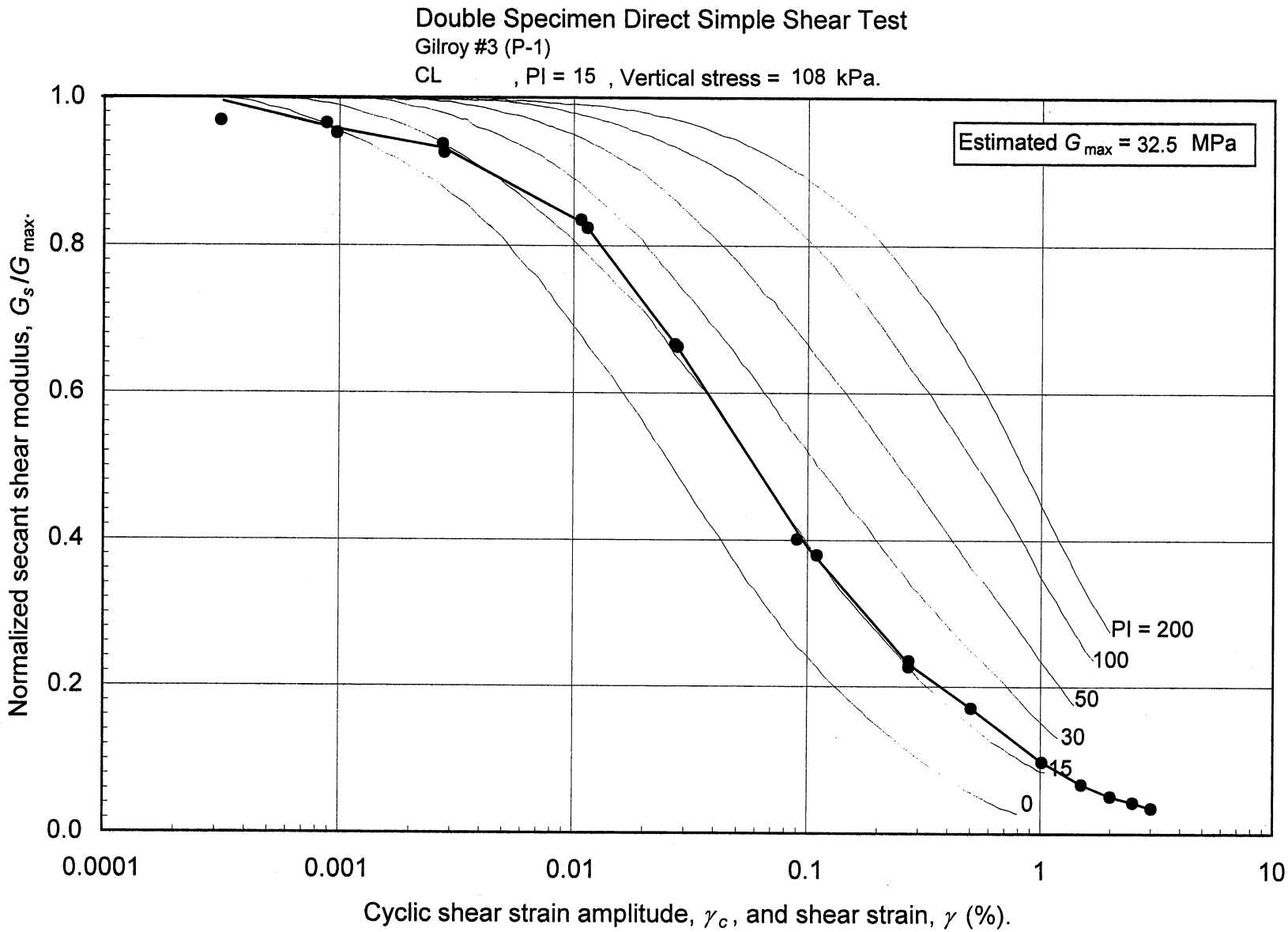
Double Specimen Direct Simple Shear Test
Gilroy #3 (P-1)
CL , PI = 15 , Vertical stress = 108 kPa.
Estimated G_{max} = 32.5 MPa
PI = 200
100
50
30
15
0
Normalized secant shear modulus, G_s/G_{max}
1.0
0.8
0.6
0.4
0.2
0.0
0.0001
0.001
0.01
0.1
1
10
Cyclic shear strain amplitude, γ_c, and shear strain, γ (%).

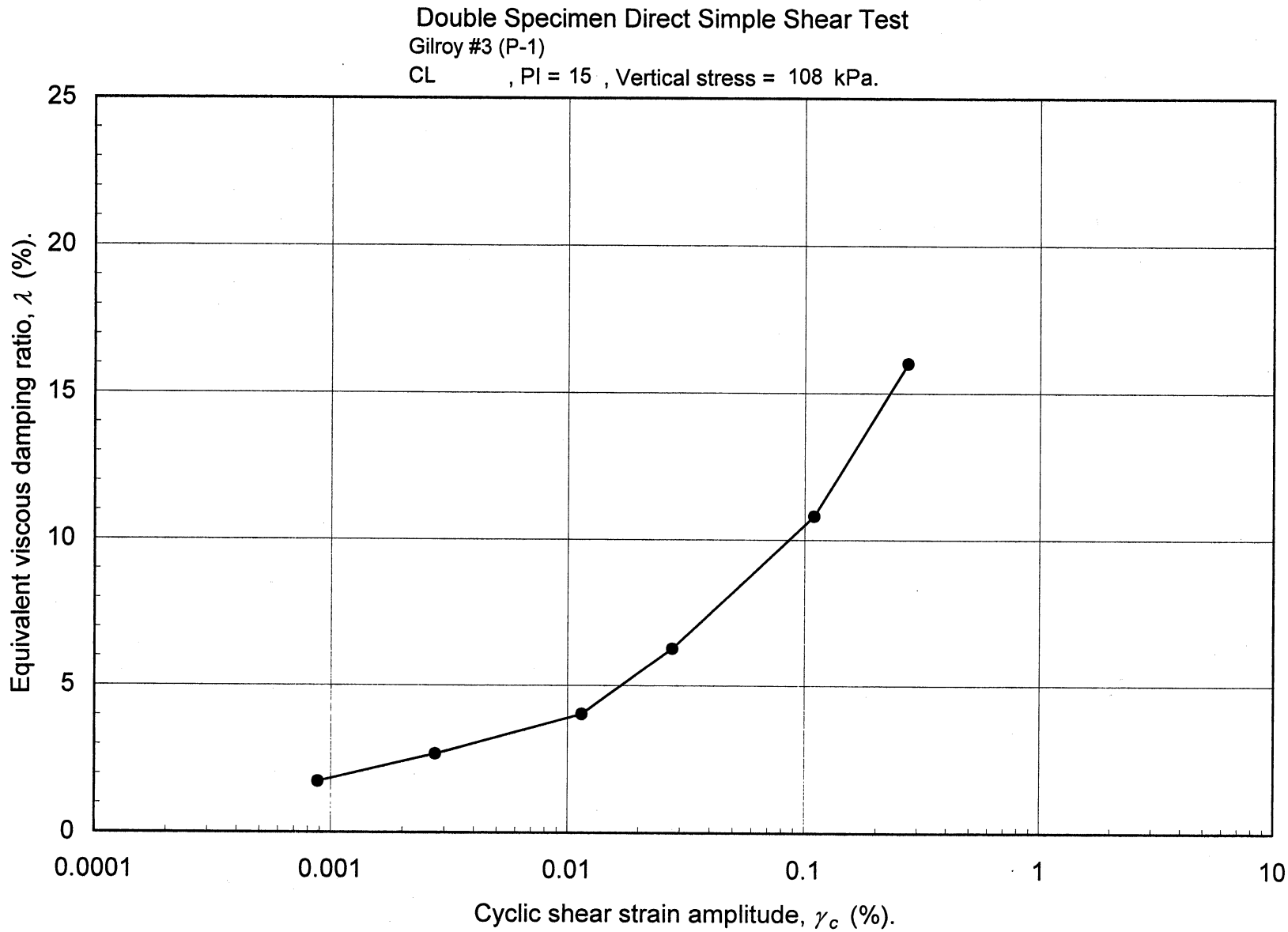
Double Specimen Direct Simple Shear Test
Gilroy #3 (P-1)
CL , PI = 15 , Vertical stress = 108 kPa.
Equivalent viscous damping ratio, λ (%).
25
20
15
10
5
0
0.0001
0.001
0.01
0.1
1
10
Cyclic shear strain amplitude, γc (%).

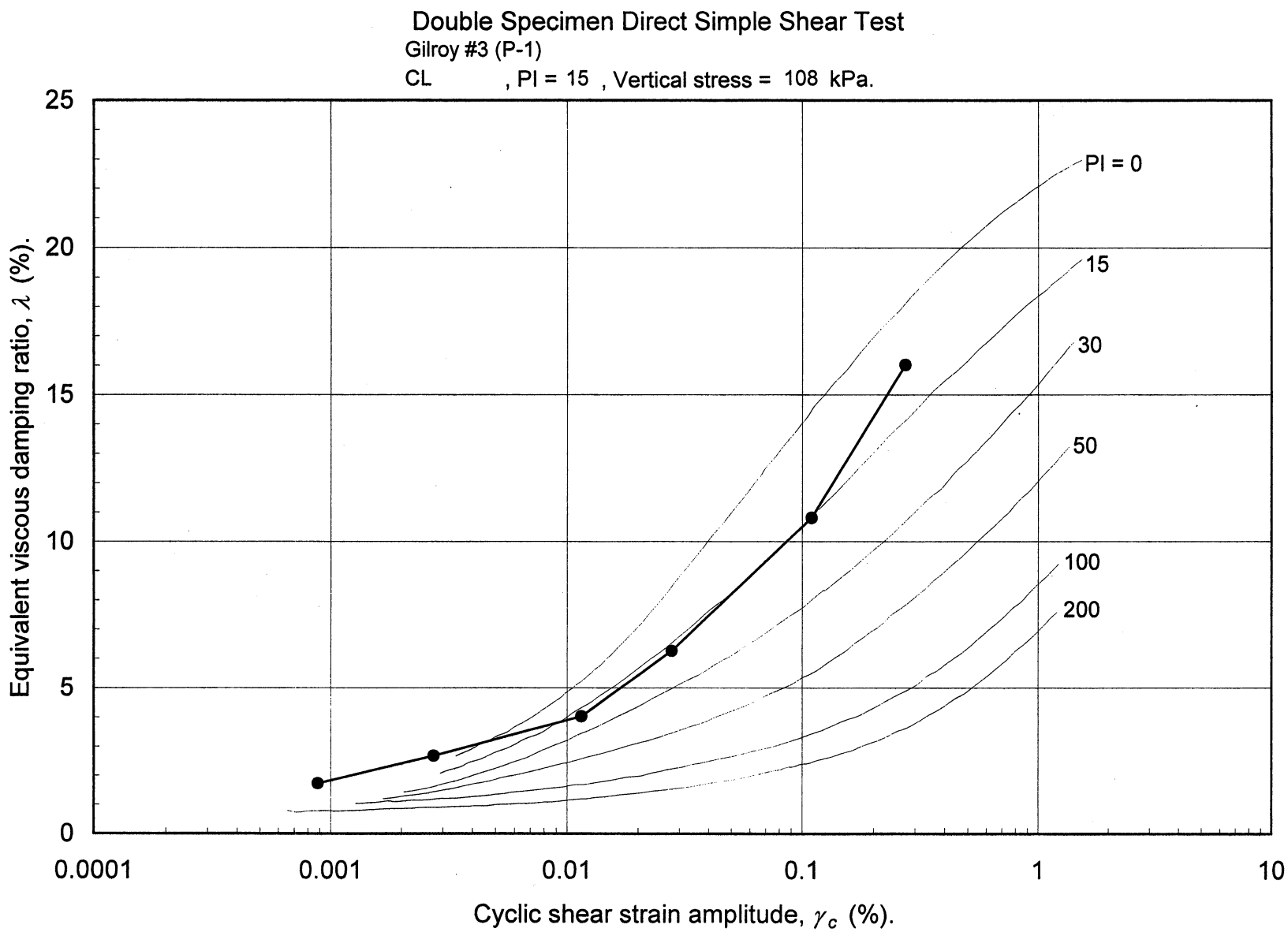
Double Specimen Direct Simple Shear Test
Gilroy #3 (P-1)
CL , PI = 15 , Vertical stress = 108 kPa.
Equivalent viscous damping ratio, λ (%).
Cyclic shear strain amplitude, γc (%).
0
5
10
15
20
25
0.0001
0.001
0.01
0.1
1
10
PI = 0
15
30
50
100
200

UCLA Soil Dynamics Laboratory

Specific Gravity Test

Principal investigator: Mladen Vucetic, Professor

Test performed by: Kentaro Tabata Test No.: 15

Project:	PEARL			Date:	1/17/2002
Boring:	Gilroy #3				
Tube No.:	P-1	Depth (ft):	15.0 -18.0	GWT (ft):	35.0
Comments:	Brown silt and sand.				

SPECIFIC GRAVITY TEST

Test No.	1		
Bottle No.	3		
Wt. of bottle (g)	178.27		
Volume of bottle (cm^3)	500		
Wt. of bottle+water+soil (g)	692.31		
Temperature (°C)	24.0		
Wt. of bottle+water (g)	676.00		
Evaporating dish No.	B-5		
Weight of dish (g)	507.42		
Wt. of dish+dry soil (g)	533.74		
Wt. of dry soil (g)	26.32		
Specific gravity of water	0.9973		
Specific gravity of soil	**2.62**		

UCLA Soil Dynamics Laboratory

Grain Size Distribution

Principal investigator: Mladen Vucetic, Professor

Test performed by: Kentaro Tabata Test No.: 15

Project:	PEARL				
Boring:	Gilroy #3				
Tube No.:	P-1	Depth (ft):	15.0 -18.0	GWT (ft):	35.0
Comments:	Brown silt and sand.				

GRAIN SIZE DISTRIBUTION

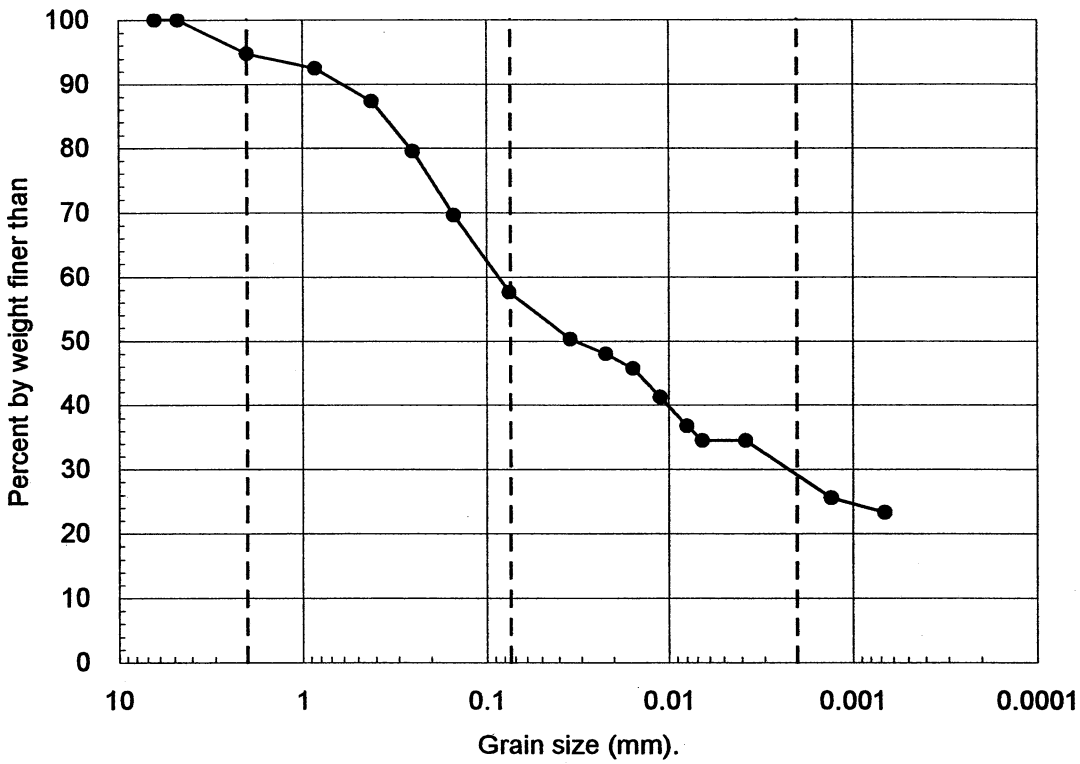

Clay (%)	Silt (%)	Sand (%)	Gravel (%)
28.5	29.1	37.2	5.3

UCLA Soil Dynamics Laboratory

Hydrometer Analysis

Principal investigator: Mladen Vucetic, Professor

Test performed by: Kentaro Tabata Test No.: 15

Project:	PEARL			Date:	1/24/2002
Boring:	Gilroy #3				
Tube No.:	P-1	Depth (ft):	15.0 -18.0	GWT (ft):	35.0
Comments:	Brown silt and sand.				

HYDROMETER TEST

Time	Elapsed time t (sec)	Temp. T (°C)	Reading R'_T	Corr. reading $R_T=R'_T+c_m$	Depth H (cm)	Grain diameter D (mm)	Temp. corr. m_T	Corr. depth $R_T+m_T-c_d$	% by wt. finer than W_D (%)
11:49:32	0								
11:51:32	120	21.0	1013.0	1013.5	12.91	0.0346	0.700	1011.2	50.21
11:54:32	300	21.0	1012.5	1013.0	13.04	0.0220	0.700	1010.7	47.97
11:59:32	600	21.0	1012.0	1012.5	13.18	0.0156	0.700	1010.2	45.73
12:09:32	1200	21.0	1011.0	1011.5	13.44	0.0112	0.700	1009.2	41.24
12:29:32	2400	21.0	1010.0	1010.5	13.71	0.0080	0.700	1008.2	36.76
12:49:32	3600	21.0	1009.5	1010.0	13.85	0.0065	0.700	1007.7	34.52
14:49:32	10800	21.0	1009.5	1010.0	13.85	0.0038	0.700	1007.7	34.52
14:04:30	94498	21.0	1007.5	1008.0	14.38	0.0013	0.700	1005.7	25.55
16:32:00	362548	21.0	1007.0	1007.5	14.51	0.0007	0.700	1005.2	23.31

APPARATUS

Hydrometer no.:	88-18587	a_0	284.03	a_1	-0.2675
Graduate no.:	1				

FACTORS

Meniscus corr., c_m:	0.5	
Disp. agent corr, c_d:	3.0	
Visc. of water, η.	21.0 °C	1.003E-05 g sec/cm^2
	°C	g sec/cm^3

WEIGHT

Dry soil (g)	20.75
Percent by wt (%)	57.56
Dry soil for sieve (g)	15.30
Total (g)	36.05

UNIT WEIGHT

Specific gravity:		2.62
T	γ_w	γ_s
(°C)	(g/cm^3)	(g/cm^3)
23.0	0.9980	2.6178

UCLA Soil Dynamics Laboratory

Sieve Analysis

Principal investigator: Mladen Vucetic, Professor

Test performed by: Kentaro Tabata Test No.: 15

Project:	PEARL			Date:	1/10/2001
Boring:	Gilroy #3				
Tube No.:	P-1	Depth (ft):	15.0 -18.0	GWT (ft):	35.0
Comments:	Brown silt and sand.				

SIEVE ANALYSIS

Sieve No.	Diameter (mm)	Sieve (g)	S+wet (g)	S+dry (g)	Retained (g)	Retained (%)	Cumulated (g)	Cumulated (%)	Passing (%)
3	6.350	485.05		485.05	0.00	0.00	0.00	0.00	100.00
4	4.750	463.12		463.12	0.00	0.00	0.00	0.00	100.00
10	2.000	422.40		424.30	1.90	5.27	1.90	5.27	94.73
20	0.850	375.65		376.48	0.83	2.30	2.73	7.57	92.43
40	0.420	457.57		459.42	1.85	5.13	4.58	12.70	87.30
60	0.250	323.87		326.70	2.83	7.85	7.41	20.55	79.45
100	0.150	342.17		345.74	3.57	9.90	10.98	30.46	69.54
200	0.075	676.88		681.20	4.32	11.98	15.30	42.44	57.56
Total					15.30	42.44			

WEIGHT

Dry soil for sieve (g)	15.30
Dry soil for hydr. (g)	20.75
Total (g)	36.05
Percent coaser (%)	42.44

UCLA Soil Dynamics Laboratory

Atterberg Limit Determination

Principal investigator: Mladen Vucetic, Professor

Test performed by: Kentaro Tabata Test No.: 15

Project:	PEARL			Date:	2/18/2002
Boring:	Gilroy #3				
Tube No.:	P-1	Depth (ft):	15.0 -18.0	GWT (ft):	35.0
Comments:	Brown silt and sand.				

LIQUID LIMIT TEST

Test No.	1	2	3	4				
Number of blows	31	18	15	9				
Container No.	ST-10	ST-8	ST-14	ST-4				
Container (g)	30.32	30.06	30.45	30.18				
Cont+wet soil (g)	38.77	38.73	39.31	40.10				
Cont+dry soil (g)	36.88	36.72	37.33	37.66				
Water (g)	1.89	2.01	1.98	2.44				
Dry soil (g)	6.56	6.66	6.88	7.48				
Water content (%)	28.81	30.18	28.78	32.62				

PLASTIC LIMIT TEST

Test No.	1	2	3
Container No.	ST-21	ST-15	ST-13
Container (g)	30.29	30.26	30.20
Cont+wet soil (g)	32.63	32.73	33.58
Cont+dry soil (g)	32.35	32.42	33.14
Water (g)	0.28	0.31	0.44
Dry soil (g)	2.06	2.16	2.94
Water content (%)	13.59	14.35	14.97

ATTERBERG LIMITS

Liquid limit (%)	**28.9**
Plastic limit (%)	**14.3**
Plasticity index	**14.6**

CLASSIFICATION

CL

FLOW CHART

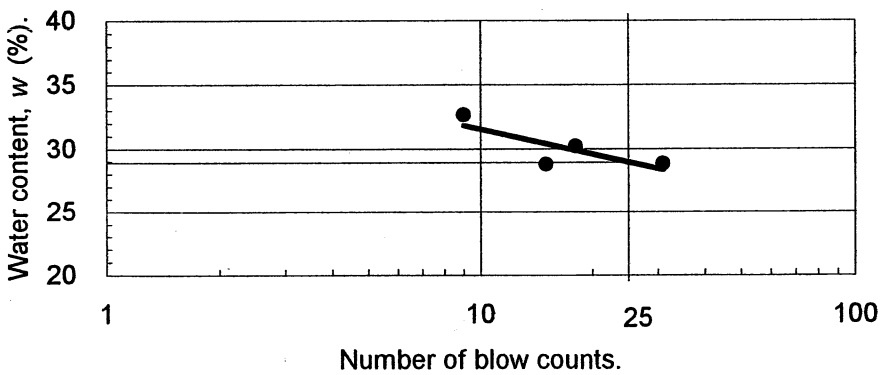

UCLA Soil Dynamics Laboratory

Atterberg Limit Determination

Principal investigator: Mladen Vucetic, Professor

Test performed by: Kentaro Tabata Test No.: 15

Project:	PEARL			Date:	2/18/2002
Boring:	Gilroy #3				
Tube No.:	P-1	Depth (ft):	15.0 -18.0	GWT (ft):	35.0
Comments:	Brown silt and sand.				

PLASTICITY CHART

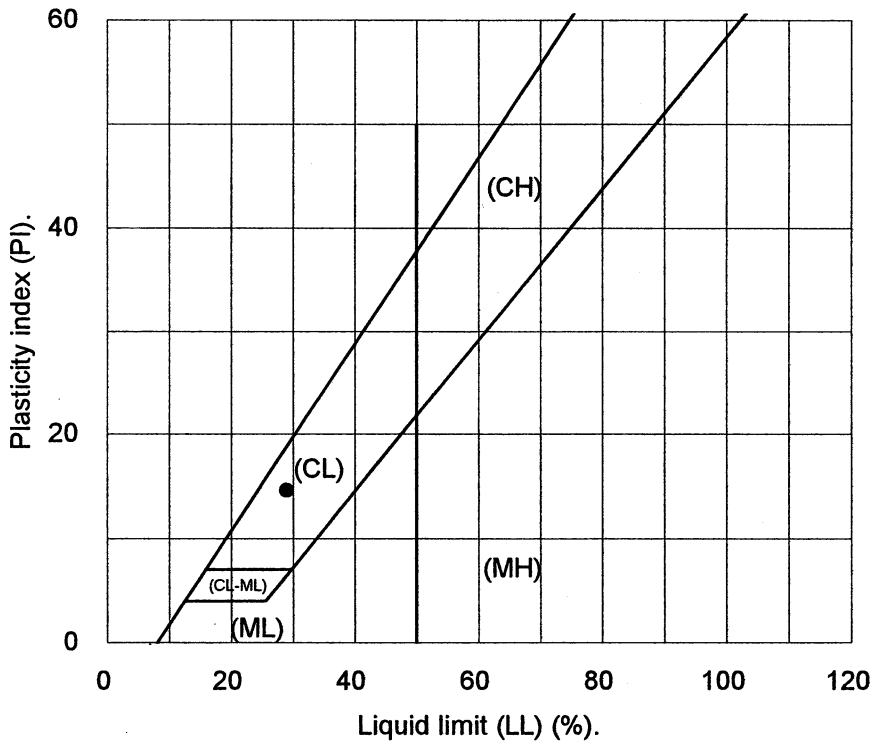

4 LIST OF SYMBOLS

The following symbols are used in this report:

e = void ratio during testing,

G_{max} = maximum shear modulus,

G_s = secant shear modulus corresponding to τ_c and γ_c; also specific gravity of soils,

LL = Atterberg liquid limit,

N = number of cycles,

OCR = overconsolidation ratio,

PI = LL – PL = plasticity index,

PL = Atterberg plastic limit,

S_r = degree of saturation,

u = pore water pressure buildup,

u_0 = hydrostatic pore water pressure,

w = water content,

β = critical damping ratio,

γ = shear strain,

γ_c = cyclic shear strain amplitude,

γ_{tv} = cyclic volumetric threshold shear strain,

ΔW = area of cyclic loop,

λ = equivalent viscous damping ratio,

σ'_h = effective horizontal stress,

σ'_{hc} = effective horizontal consolidation stress,

σ_v = total vertical stress,

σ'_v = effective vertical stress.

5 REFERENCES

ASTM D 421–85 (1992): Standard Practice for Dry Preparation of Soil Samples for Particle-Size Analysis and Determination of Soil Constants, *1992 Annual Book of ASTM Standards*, Vol. 04.08, pp. 92-93.

ASTM D 422–63 (1992): Standard Test method for Particle-Size Analysis of Soils, *1992 Annual Book of ASTM Standards*, Vol. 04.08, pp. 94-100.

ASTM D 2487–90 (1992): Standard Test Method for Classification of Soils for Engineering Purposes, *1992 Annual Book of ASTM Standards*, Vol. 04.08, pp. 326-336.

ASTM D 4318–90 (1992): Standard Test Method for Liquid Limit, Plastic Limit, and Plasticity Index of Soils, *1992 Annual Book of ASTM Standards*, Vol. 04.08, pp. 675-685.

Bjerrum, L. and Landva, A. (1966): Direct Simple-Shear Test on a Norwegian Quick Clay, *Géotechnique*, Vol. 16, No. 1, 1-20.

Dobry, R., Ladd, R.S., Yokel, F.Y., Chung, R.H., and Powell, D. (1982): Prediction of pore water pressure buildup and liquefaction of sand by the cyclic strain method, *Report*, National Bureau of Standards Building Science Series 138, Washington, D.C., 153 p.

Dobry, R. and Vucetic, M. (1987): Dynamic Properties and Seismic Response of Soft Clay Deposits, *Proceedings*, International Symposium on Geotechnical Engineering of Soft Soils, Mexico City, published by Sociedad Mexicana de Mecanica de Suelos, A.C., Vol. 2, pp. 49-85.

Doroudian, M. and Vucetic, M. (1995): A direct simple shear device for measuring small-strain behavior, *ASTM Geotechnical Testing Journal*, GTJODJ, Vol. 18, No. 1, pp. 69-85.

Doroudian, M. and Vucetic, M. (1998): Small-Strain Testing in an NGI-type Direct Simple Shear Device, *Proceedings*, The 11th Danube-European Conference on Soil Mechanics and Geotechnical Engineering, Porec, Croatia, published by A.A. Balkema, pp. 687-693.

Hsu, C.-C. and Vucetic, M. (1998): Results of classification tests for ROSRINE project, *UCLA Research Report*, No. ENG-98-199, Civil and Environmental Engineering Department, University of California, Los Angeles, 260 p.

Hsu, C.-C. and Vucetic, M. (1999): Results of cyclic and dynamic simple shear tests on soils from Tarzana and Rinaldi sites conducted for ROSRINE project and other research purposes, *UCLA Research Report*, No. ENG-99-205, Civil and Environmental Engineering Department, University of California, Los Angeles, 258 p.

Jacobsen, L.S. (1930): Steady Forced Vibrations as Influenced by Damping, *Transactions*, ASME, Vol. 52, No 15, pp. 169-181.

Kjellman, W. (1955): Testing the Shear Strength of Clay in Sweden, *Géotechnique*, Vol. 2, No. 3, pp. 225-232.

Lanzo, G., Vucetic, M., and Doroudian, M. (1997): Reduction of Shear Modulus at Small Strains in Simple Shear, *ASCE Journal of Geotechnical and Geoenvironmental Engineering*, Vol. 123, No. 11, pp.1035-1042.

Nigbor, R.L., Pyke, R., Roblee, C.J., Schneider, J.F., Silva, W.J., Steller, R., and Vucetic, M. (1997): Resolution of Site Response Issues from the Northridge Earthquake (ROSRINE), Progress Report, *Proceedings*, 1997 Seismological Society of America.

Roblee, C.J., Schneider, J.F., Pyke, R., Nigbor, R.L., Silva, W.J., Bardet, J.P., Ponti, D., Riemer, M., Steller, R., Stokoe, K., and Vucetic, M. (1998): Resolution of Site Response Issues from

the Northridge Earthquake (ROSRINE): Phase I Preliminary Findings, *Proceedings*, 5th Caltrans Seismic Research Workshop, Sacramento, California.

Roscoe, K.H. (1953): An Apparatus for the Application of Simple Shear to Soil Samples, *Proceedings*, International Conference on Soil Mechanics and Foundation Engineering, Vol., 1, Zurich, pp. 186-191.

Schneider, J.F., Roblee, C.J., Nigbor, R.L., Silva, W.J., and Pyke, R. (1997): Resolution of Site Response Issues from the Northridge Earthquake (ROSRINE), *Proceedings*, Northridge Earthquake Research Conference, California Universities for Research on Earthquake Engineering (CUREe), August 20-22, Los Angeles, CA, 8 p.

Seed, H.B. and Idriss, I.M. (1970): Soil Moduli and Damping Factors for Dynamic Response Analyses, *EERC Report*, No.70-10, University of California, Berkeley.

Tabata, K. and Vucetic, M. (2000): Results of cyclic simple shear tests on thirteen soils from Los Angeles basin conducted for ROSRINE project and other research purposes, *UCLA Research Report*, No. ENG-00-219, Civil and Environmental Engineering Department, University of California, Los Angles, 284 p.

Vucetic, M. (1994a): Cyclic Characterization for Seismic Regions Based on PI, *Proceedings*, 13th International Conference on Soil Mechanics and Foundation Engineering, New Delhi, India, Vol. 1, pp. 329-332.

Vucetic, M. (1994b): Cyclic Threshold Shear Strains in Soils, *ASCE Journal of Geotechnical Engineering*, Vol. 120, pp. 2208-2228.

Vucetic, M. and Dobry, R. (1991): Effect of Soil Plasticity on Cyclic Response, *Journal of the Geotechnical Engineering Division*, ASCE, Vol. 117, No. 1, pp. 89-107.

Vucetic, M., Hsu, C.-C., and Doroudian, M. (1998a): Results of cyclic and dynamic simple shear tests on soils from La Cienega site conducted for ROSRINE project and other research purposes, *UCLA Research Report*, No. ENG-98-200, Civil and Environmental Engineering Department, University of California, Los Angeles, 440 p.

Vucetic, M., Lanzo, G., and Doroudian, M. (1998b): Damping at Small Strains in Cyclic Simple Shear Test, *ASCE Journal of Geotechnical and Geoenvironmental Engineering*, Vol. 124, No. 7, pp.585-594.

Vucetic, M., Lanzo, G., and Doroudian, M. (1998c): Effect of the Shape of Cyclic Loading on Damping Ratio at Small Strains, *Soils and Foundations*, Vol. 38, No. 1, pp. 111-120.

Attachment C
University of Texas at Austin
Report for RC/TS Testing

Linear and Nonlinear Dynamic Properties Determined by Combined Resonant Column and Torsional Shear Tests; Phase II of the ROSRINE Project

Volume I – Test Results

by

Kenneth H. Stokoe, II
Won Kyoung Choi
Farn-Yuh Menq
CelestinoValle

March, 2003

Geotechnical Engineering Report GR03-1
Geotechnical Engineering Center
Civil Engineering Department
The University of Texas at Austin

TABLE OF CONTENTS – VOLUME 1 – TEST RESULTS

TABLE OF CONTENTS – VOLUME II–

LIST OF TABLES

LIST OF FIGURES

1. INTRODUCTION

The dynamic properties of 25 intact soil specimens that were recovered from boreholes at 10 sites in Southern California were evaluated in the Soil Dynamics Laboratory at the University of Texas at Austin (UTA). This work was conducted as part of the ROSRINE (Resolution Of Site Response Issues from the Northridge Earthquake) project. The purpose of the study was to evaluate the linear and nonlinear shear modulus and material damping characteristics of the intact specimens. The work was funded by the Pacific Earthquake Engineering Research Center (PEER) at the University of California at Berkeley under the PEER-Lifelines Program, Tasks 2B01 and 2B02. Dr. Michael Reimer was the program manager of the PEER-Lifelines Program. Dr. Clifford Roblee at Caltrans was the project liaison, and Dr. Donald Anderson of CH2MHill in Seattle, WA, was the project coordinator.

A total of 83 intact samples was delivered to the Soil Dynamic Laboratory at the University of Texas at Austin in mid July, 2001. Listings of the samples, site locations and associated information are given in Tables 1 through 3. Each sample was still in the thin-walled ("Shelby") steel tube used during field sampling. There were two different types of Shelby tubes, five steel tubes which had an outside diameter (OD) of 2 in. (5.1 cm), a wall thickness of 1/16 in. (0.16 cm), and a length of about 24 in. (61.0 cm) and seventy eight steel tubes which had an outside diameter (OD) of 3 in. (7.6 cm), a wall thickness of 1/16 in. (0.16 cm), and a length of about 36 in. (91.4 cm). The samples were transported from the University of California at Los Angeles (UCLA) to UTA in a minivan driven by Mr. Celestino Valle of UTA. The samples had been stored at UCLA, and initial index tests had been performed on many of them. The samples were carried to UTA in custom-made wooden boxes. Each wooden box was approximately 10 in. by 6 in. in plan dimensions and was about 3-ft tall. The top of each wooden box contained two holes, with diameters slightly greater than the steel tubes. The samples were secured in these holes during transportation and remained vertically

Table 1 Inventory of the ROSRINE Samples Transported to the University of Texas at Austin (UTA) and the UTA Inventory of Remaining Partial or Whole Sample Tubes at UTA

Site Name	Number of Samples		
	ROSRINE Sample Inventory (July 10, 2001)	UTA Inventory (Jan. 13, 2003) *	Samples Tested at UTA
Meloland	13	13	7
Tarzana	4	4	2
Lake Hughes #9	2	2	1
Obregon Park	3**	2	1
Saturn	2**	1	1
LA Bulk Mail	6**	8	5
Yermo	5	5	2
Joshua Tree	5	5	2
Gilroy #3	4	4	2
Halls Valley	3	3	2
Total	47	47	25

Note: * Some Shelby tubes are full or nearly full and other Shelby tubes are partial (or split) tubes because testing was performed on the other portion of the tube.
**ROSRINE Inventory list was incorrect about number of tubes transported to UTA.

Table 2 Inventory of the ROSRINE Sample Tubes at UTA from Sites Where No Samples were Tested

Site Name	Number of Samples		
	ROSRINE Sample Inventory (July 10, 2001)	UTA Inventory (Jan. 13, 2003) *	Samples Tested at UTA
Arleta	2	2	0
Kagel	11	11	0
La Cienega	6	6	0
Newhall	4	4	0
Pacoima	1**	0	0
Baldwin Hills	1	1	0
Dayton	4**	5	0
ESC #4	1	1	0
Potrero Canyon P-3	3	3	0
Rinaldi 2	3	3	0
Total	36	36	0

Note: * Some Shelby tubes are full or nearly full and other Shelby tubes are partial (or split) tubes because testing was performed on the other portion of the tube.
**ROSRINE Inventory list was incorrect about number of tubes transported to UTA.

Table 3. Complete List of UTA Inventory of 83 Remaining Partial or Whole Sample Tubes at UTA and Associated Sample Information Given to UTA

Site Name	Sample Label[1]	Sample Type	Cored Interval (ft)		Description[2]
			From	To	
Meloland	S-1	Shelby	8	10.5	Recovery: 18". Pale brown vf sand and silt in top of tube; lost bottom 7" of core and top 9"
Meloland	S-2	Shelby	18	20	Recovery: 14". Dark yellowish brown silt (ML) (from tip) UCS=0.7 tsf
Meloland	S-3	Shelby	28	30	Recovery: 20". Brown clay; sticky, plastic (CL). UCS=3.0 tsf
Meloland	S-4	Shelby	38	40	Recovery: 20". Yellowish brown fine sand w/ med sand size biotite. UCS=1.7 tsf. Pushed 20" to refusal; prob. slough in tube.
Meloland	S-6	Shelby	78	79.5	Recovery: 18". Yellowish brown, well-sorted vf running sand (SP) w/ tr silt; probably disturbed in core
Meloland	WS-1	Wireline Shelby	118	119.5	Recovery: 18". Grayish brown clay; stiff, mod. sticky and plastic (CL)
Meloland	WS-3	Wireline Shelby	198	200	Recovery: 20". Dark grayish brown silt loam (CL); sl. Sticky and plastic; tr. coal ?
Meloland	WS-4	Wireline Shelby	259	261	Recovery: 13". Grey clay w/ lighter grey silt partings; bedding may be inclined.
Meloland	WS-6	Wireline Shelby	378	380	Recovery: 13". Grayish brown clay; UCS > 4.8 tsf. Tube end crumpled.
Meloland	WS-7	Wireline Shelby	438	440	Recovery: 13". Dark grey clay; UCS > 4.8 tsf. Tube end crumpled.
Meloland	C-1	USGS Core Sample	555	560	Recovery: 33". Brown clay, v. sticky and plastic (CL-CH?), stiff; effervescent.
Meloland	C-2	USGS Core Sample	615	620	Recovery: 46". Dark grayish brown clay, sticky and plastic (CL); firm; viol. effervescence; salty taste
Meloland	C-3	USGS Core Sample	735	740	Recovery: 40". Dark yellowish brown f-vf sandy loam, non-sticky; v. sl. Plastic (ML); sl. effervescence

Notes: 1. Sample number used to designate the sample during the drilling and sampling operation
2. Soil type identified during the drilling and sampling operation

Table 3. Continued - Complete List of UTA Inventory of 83 Remaining Partial or Whole Sample Tubes at UTA and Associated Sample Information Given to UTA

Site Name	Sample Label[1]	Sample Type	Cored Interval (ft)		Description[2]
			From	To	
Arleta	P-1	Pitcher/2.8	20	22.5	Sample description was not given to UTA
Arleta	P-5	Pitcher/2.8	141	142.5	Sample description was not given to UTA
Kagel	T-1	Brass Tube/1.9	12.5	13.8	Sample description was not given to UTA
Kagel	T-2	Brass Tube/1.9	17.5	18.5	Sample description was not given to UTA
Kagel	T-3	Brass Tube/1.9	25	27.5	Sample description was not given to UTA
Kagel	T-4	Brass Tube/1.9	40	42.5	Sample description was not given to UTA
Kagel	T-4	Brass Tube/1.9	42.5	45	Sample description was not given to UTA
Kagel	T-5	Brass Tube/1.9	62.5	65	Sample description was not given to UTA
Kagel	T-6	Brass Tube/1.9	82.5	85	Sample description was not given to UTA
Kagel	T-8	Brass Tube/1.9	152.5	155	Sample description was not given to UTA
Kagel	T-9	Brass Tube/1.9	202.5	205	Sample description was not given to UTA
Kagel	T-10	Brass Tube/1.9	210	212.5	Sample description was not given to UTA
Kagel	T-11	Brass Tube/1.9	257.5	260	Sample description was not given to UTA

Notes: 1. Sample number used to designate the sample during the drilling and sampling operation
2. Soil type identified during the drilling and sampling operation

Table 3. Continued - Complete List of UTA Inventory of 83 Remaining Complete or Partial Samples at UTA and Sample Information Given to UTA

Site Name	Sample Label[1]	Sample Type	Cored Interval (ft)		Description[2]
			From	To	
La Cienega	S-2	Pitcher/2.8	10	12.5	Sample description was not given to UTA
La Cienega	S-6	Pitcher/2.8	30	32.5	Sample description was not given to UTA
La Cienega	S-7	Pitcher/2.8	35	37.5	Sample description was not given to UTA
La Cienega	S-8	Pitcher/2.8	45	47.5	Sample description was not given to UTA
La Cienega	S-9	Pitcher/2.8	55.5	58	Sample description was not given to UTA
Newhall	P-4	Pitcher/2.8	90	92.5	Sample description was not given to UTA
Newhall	P-6	Pitcher/2.8	255	257.5	Sample description was not given to UTA
Newhall	T-4	Pitcher/2.8	163.6	165	Sample description was not given to UTA
Newhall	T-5	Pitcher/2.8	122.5	125	Sample description was not given to UTA
Tarzana	P-1	Pitcher/2.8	10	12.5	Silty Clay
Tarzana	P-3	Pitcher/2.8	30	32	Silty Clay
Tarzana	P-4	Pitcher/2.8	40	42	Weathered Shale
Baldwin Hills	P-1	Pitcher/2.8	41	43	Sample description was not given to UTA

Notes: 1. Sample number used to designate the sample during the drilling and sampling operation
2. Soil type identified during the drilling and sampling operation

Table 3. Continued - Complete List of UTA Inventory of 83 Remaining Complete or Partial Samples at UTA and Sample Information Given to UTA

Site Name	Sample Label[1]	Sample Type	Cored Interval (ft)		Description[2]
			From	To	
Dayton	P-1	Pitcher/2.8	10	13	Sand
Dayton	P-2	Pitcher/2.8	25	28	Clay
Dayton	P-3	Pitcher/2.8	50	53	Clay
Dayton	P-4	Pitcher/2.8	70	73	Weathered Shale
Dayton	P-5	Pitcher/2.8	100	103	Weathered Shale
ESC #4	Tube -1	Pitcher/2.8	10	11.9	Sample description was not given to UTA
Lake Hughes #9	P-1	Pitcher/2.8	6	8	Silty Sand
Lake Hughes #9	P-2	Pitcher/2.8	70	70.8	Weathered Gneiss
Obregon Park	P-2	Pitcher/2.8	20	23	Silty Clay
Obregon Park	P-8	Pitcher/2.8	100	103	Clay
Potrero Canyon P-3	S1-1	Shelby/2.8	6	8.5	Sample description was not given to UTA
Potrero Canyon P-3	S2-5	Shelby/2.8	25	27.5	Sample description was not given to UTA
Potrero Canyon P-3	P1-10	Pitcher/2.8	115	117.5	Sample description was not given to UTA

Notes: 1. Sample number used to designate the sample during the drilling and sampling operation
2. Soil type identified during the drilling and sampling operation

Table 3. Continued - Complete List of UTA Inventory of 83 Remaining Complete or Partial Samples at UTA and Sample Information Given to UTA

Site Name	Sample Label[1]	Sample Type	Cored Interval (ft)		Description[2]
			From	To	
Rinaldi 2	P-7	Pitcher/2.8	32	33.3	Sands to Siltstone
Rinaldi 2	P-9	Pitcher/2.8	37.5	39	Sands to Siltstone
Rinaldi 2	P-11	Pitcher/2.8	60	61	Sands to Siltstone
Saturn	P-4	Pitcher/2.8	100	103	Silty Clay
LA Bulk Mail	P-1	Pitcher	15	18	Recovery: 25". Silt and clay
LA Bulk Mail	P-2	Pitcher	20	23	Recovery: 27.5". Silt and clay
LA Bulk Mail	P-3	Pitcher	50	53	Recovery: 27.5". Silt
LA Bulk Mail	P-4	Pitcher	100	103	Recovery: 36". Silt and clay
LA Bulk Mail	P-5	Pitcher	165	168	Recovery: 36". Silt
LA Bulk Mail	P-6	Pitcher	205	208	Recovery: 26". Sand and Silt
LA Bulk Mail	P-7	Pitcher	265	268	Recovery: 28". Sand and Silt
Yermo	P-3	Pitcher	40	43	Recovery: 30". Silt
Yermo	P-5	Pitcher	153	156	Recovery: 18". Sand

Notes: 1. Sample number used to designate the sample during the drilling and sampling operation
2. Soil type identified during the drilling and sampling operation

Table 3. Continued - Complete List of UTA Inventory of 83 Remaining Complete or Partial Samples at UTA and Sample Information Given to UTA

Site Name	Sample Label[1]	Sample Type	Cored Interval (ft)		Description[2]
			From	To	
Yermo	P-6	Pitcher	200	203	Recovery: 25". Fine sand and silt
Yermo	P-7	Pitcher	265	268	Recovery: 36". Fine sand
Yermo	P-8	Pitcher	325	328	Recovery: 15". Sand and gravel
Joshua Tree	P-2	Pitcher	20	23	Recovery: 20.5". Sand
Joshua Tree	P-4	Pitcher	75	78	Recovery: 21". Sand
Joshua Tree	P-5	Pitcher	160	163	Recovery: 12". Sand
Joshua Tree	P-7	Pitcher	235	238	Recovery: 32". Sand
Joshua Tree	P-8	Pitcher	327	330	Recovery: 18". Sand
Gilroy #3	P-2	Pitcher	50	53	Recovery: 16". Gravel
Gilroy #3	P-3	Pitcher	80	83	Recovery: 29". Silt and gravel
Gilroy #3	P-5	Pitcher	355	358	Recovery: 19". Silt and Sand, some gravel
Halls Valley	P-1	Pitcher	6	9	Recovery: 22". Silty clay
Halls Valley	P-3	Pitcher	50	53	Recovery: 36". Clay
Halls Valley	P-4	Pitcher	110	113	Recovery: 23". Clay and greenstone

Notes: 1. Sample number used to designate the sample during the drilling and sampling operation
2. Soil type identified during the drilling and sampling operation

upright in the boxes until testing. The soils in seven of the Shelby tubes were nonplastic sands, and the remaining soils were silts and clays.

The list of 83 samples in Table 3 also includes several intact samples that were delivered to UTA before July, 2001. Four Shelby tube samples recovered from Tarzana, CA, were sent by air freight to UTA in mid-March, 2001. These samples were in the larger Shelby tubes which had been cut to a length of about 18 in. (45.7 cm) and the ends re-waxed at UCLA before shipping.

The 25 intact specimens tested at UTA are listed in Table 4. Just before testing these specimens, each sample tube was cut to the desired length. The following sample lengths were used: approximately 5.6 in. (14.2 cm) if a 2.8-in. (7.1 cm) diameter specimen was to be tested; 4.0 in. (10.2 cm) if a 2.0-in. (5.1 cm) diameter specimen was to be tested; and 3.0 (7.6 cm) in. if a 1.5-in. (3.8 cm) diameter specimen was to be tested. For the nonplastic soils, after the tubes were cut to the proper length, they were removed by cutting each tube longitudinally into four pieces with a Dremel tool, rather than extruding the soils from the tubes as done with the plastic soils. The Dremel tool was operating at a very high frequency (about 30,000 rpm (500 Hz)), so any disturbance from the vibrations was minimized.

After each specimen was removed from the metal tube, it was set up in the combined resonant column and torsional shear (RCTS) equipment and tested as described in Section 2. The diameters of Specimens No. 5 through No. 9, No. 14, No. 17, No. 19 and No. 21 (see Table 3) were not trimmed so these specimens had the same diameter as the extruded sample. This diameter was either about 1.9 in. (4.8 cm) or 2.8 in. (7.1 cm), depending on the sampling tube. The steel tubes that contained these nine samples were not rusted on the inside. However, all specimens except for the above nine specimens were trimmed to a smaller size to remove the outer disturbed material (from the sampling process and from the rusted metal tube). All 25 specimens were tested as intact specimens. A summary of the initial properties of these specimens is presented in Table 5.

Table 4. Locations and Associated Information for the 25 ROSRINE Samples Dynamically Tested at the University of Texas at Austin

Location	Sample No.[1]	Sample Depth (ft)	Soil Type[2] (Initial Field Identification)	UTA[3] Specimen No.	Soil Type[4] Determined at UTA
Meloland	S-2	18-20	Silt	3	Clay (CH)
	S-3	28-30	Clay	4	Clay (CH)
	WS-1	118-120	Clay	5	Clay (CH)
	WS-3	198-200	Silt	6	Clay (CH)
	WS-4	259-261	Clay	7	Clay (CH)
	WS-6	378-380	Clay	8	Clay (CL)
	WS-7	438-440	Clay	9	Clay (CH)
Tarzana	P-3	30-33	Silty Clay	1	Silt (MH)
	P-4	40-43	Weathered Shale	2	Clay (CH)
Lake Hughes	P-1	6-8	Silty Sand	17	Silty Sand (SW-SM)
Obregon Park	P-8	100-103	Clay	25	Clay (CH)
Saturn	P-4	100-103	Silty Clay	24	Clay (CH)
LA Bulk Mail	P-1	15-18	Silt	10	Clay (CL)
	P-3	50-53	Silt	11	Clay (CL)
	P-5	165-168	Sand	12	Clay (CL)
	P-6	205-208	Silty Sand or Sandy Silt	13	Silty Sand (SM)
	P-7	265-268	Sand	14	Sand (SP)
Yermo	P-6	200-203	Interlayered Sand & Silt	20	Silty Sand (SM)
	P-7	265-268	Silty Sand with Gravels	21	Sand (SP)
Joshua Tree	P-7	235-238	Sand	18	Sand (SP)
	P-8	327-330	Sand	19	Sand (SW)
Gilroy #3	P-4	180-183	Silt, Sand, some Gravel	15	Clay (CL)
	P-5	355-358	Silt, Sand, some Gravel	16	Silt (ML)
Halls Valley	P-1	6-9	Silty Clay	22	Clay (CL)
	P-3	50-53	Clay	23	Clay (CH)

Notes: 1. Sample number used to designate the sample during the drilling and sampling operation
2. Soil type identified during the drilling and sampling operation
3. Specimen number used at UTA to designate the extruded and trimmed specimen
4. Soil type determined from index property testing at UTA

Table 5. Initial Properties of Soil Specimens from ROSRINE Sites: Combined Torsional Shear and Resonant Column Testing at the University of Texas

Spec. No.	UT Specimen ID	Soil Site Identification	Specimen Depth ft (m)	Soil Type (Unified Soil Classification)	Water Content %	Dry Density pcf (gr/cm^3)	% Passing Sieve #200	Liquid Limit %	Plasticity Index %	Void Ratio[1] e	Assumed Sp. Grav. G_s	Degree of Saturation Sr, (%)	Uniformity Coefficient[2] Cu	Coefficient of Curvature[3] Cc
1	UTA-25-B	Tarzana P-3	30 (9.1)	Silt (MH)	56	65.7 (1.05)	100 VO[4]	92	46	1.57	2.70	96	NA[5]	NA
2	UTA-25-A	Tarzana P-4	42 (12.8)	Clay (CH)	49	69.5 (1.11)	100 VO	77	42	1.42	2.70	94	NA	NA
3	UTA-27-F	Meloland S-2	20 (6.1)	Clay (CL)	20	100.5 (1.61)	100 VO	27	12	0.65	2.65	83	NA	NA
4	UTA-27-E	Meloland S-3	28 (8.5)	Clay (CH)	28	94.9 (1.52)	100 VO	59	36	0.74	2.65	100	NA	NA
5	UTA-27-B	Meloland WS-1	120 (36.6)	Clay (CH)	27	99.6 (1.60)	100 VO	71	43	0.66	2.65	100	NA	NA
6	UTA-27-A	Meloland WS-3	200 (61.0)	Clay (CH)	23	103.8 (1.66)	100 VO	65	42	0.62	2.70	98	NA	NA
7	UTA-27-C	Meloland WS-4	259 (78.9)	Clay (CH)	25	105.9 (1.70)	100 VO	62	40	0.56	2.65	100	NA	NA
8	UTA-27-D	Meloland WS-6	378 (115.2)	Clay (CL)	24	103.7 (1.66)	100 VO	31	12	0.60	2.65	100	NA	NA
9	UTA-27-G	Meloland WS-7	440 (134.1)	Clay (CH)	24	99.1 (1.59)	100 VO	58	35	0.70	2.70	93	NA	NA
10	UTA-27-S	LA Bulk Mail (P-1)	15 (4.6)	Clay (CL)	15	116.3 (1.86)	100 VO	24	8	0.45	2.70	91	NA	NA
11	UTA-27-T	LA Bulk Mail (P-3)	50 (15.2)	Clay (CL)	26	102.6 (1.64)	100 VO	45	22	0.64	2.70	100	NA	NA
12	UTA-27-I	LA Bulk Mail (P-5)	167.5 (51.1)	Clay (CL)	26	98.0 (1.57)	100 VO	46	25	0.72	2.70	96	NA	NA

Notes:

1. Void ratios were calculated based on the assumed value of G_s.
2. Uniformity Coefficient, $C_u = D_{60}/D_{10}$
3. Coefficient of Curvature, $C_c = (D_{30})^2/(D_{10}D_{60})$
4. VO = Based on Visual Observation
5. NA = Not Applicable
6. NP = Nonplastic

Table 5. Continued - Initial Properties of Soil Specimens from ROSRINE Sites: Combined Torsional Shear and Resonant Column Testing at the University of Texas

Spec. No.	UT Specimen ID	Soil Site Identification	Specimen Depth ft (m)	Soil Type (Unified Soil Classification)	Water Content %	Dry Density pcf (gr/cm3)	% Passing Sieve #200	Liquid Limit %	Plasticity Index %	Void Ratio[1] e	Assumed Sp. Grav. Gs	Degree of Saturation Sr,%	Uniformity Coefficient[2] Cu	Coefficient of Curvature[3] Cc
13	UTA-27-V	LA Bulk Mail (P-6)	205 (62.5)	Silty Sand (SM)	15	120.0 (1.92)	22.4	NP[6]	NP	0.41	2.70	100	NA[5]	NA
14	UTA-27-H	LA Bulk Mail (P-7)	267 (81.4)	Sand (SP)	22	103.3 (1.65)	1.6	NP	NP	0.60	2.65	97	3.43	0.79
15	UTA-27-J	Gilroy #3 P-4	182 (55.5)	Clay (CL)	18	106.6 (1.71)	100 VO[4]	26	10	0.58	2.70	85	NA	NA
16	UTA-27-K	Gilroy #3 P-5	357 (108.8)	Silt (ML)	21	105.5 (1.69)	100 VO	33	7	0.58	2.70	98	NA	NA
17	UTA-27-M	Lake Hughes P-1	6 (1.8)	Silty Sand (SW-SM)	17	100.2 (1.61)	10.4	NP	NP	0.68	2.70	69	11.80	1.02
18	UTA-27-N	Joshua Tree[7] P-7	236 (71.9)	Sand (SP)	12	116.0 (1.86)	2.5	NP	NP	0.45	2.70	69	5.00	0.90
19	UTA-27-O	Joshua Tree[7] P-8	328 (100.0)	Sand (SW)	10	118.2 (1.89)	2.3	NP	NP	0.43	2.70	65	7.33	1.51
20	UTA-27-P	Yermo P-6	201 (61.3)	Silty Sand (SM)	18	113.6 (1.82)	23.8	NP	NP	0.48	2.70	99	NA	NA
21	UTA-27-Q	Yermo P-7	266 (81.1)	Sand (SP)	19	106.3 (1.70)	0.5	NP	NP	0.59	2.70	87	1.64	1.06
22	UTA-27-L	Halls Valley (P-1)	7 (2.1)	Clay (CL)	23	99.8 (1.60)	100 VO	39	22	0.69	2.70	90	NA	NA
23	UTA-27-R	Halls Valley (P-3)	52 (15.8)	Clay (CH)	42	79.3 (1.27)	100 VO	75	45	1.12	2.70	100	NA	NA
24	UTA-27-U	Saturn P-4	100 (30.5)	Clay (CH)	33	85.2 (1.37)	100 VO	71	40	0.98	2.70	91	NA	NA
25	UTA-27-W	Obregon P-8	101 (30.8)	Clay (CH)	21	107.0 (1.71)	100 VO	52	37	0.57	2.70	97	NA	NA

Notes:

1. Void ratios were calculated based on the assumed value of G_s.
2. Uniformity Coefficient, $C_u = D_{60}/D_{10}$
3. Coefficient of Curvature, $C_c = (D_{30})^2/(D_{10}D_{60})$
4. VO = Based on Visual Observation
5. NA = Not Applicable
6. NP = Nonplastic
7. Bentonite slurry around the soil specimens

2. DYNAMIC LABORATORY TESTS

Combined resonant column and torsional shear (RCTS) equipment was used to investigate the dynamic characteristics of all 25 specimens. The RCTS equipment is described in detail in Appendix A. Verification of the equipment constants was performed under a companion project dealing with evaluating the dynamic material properties of specimens from Yacca Mountain, Nevada. However, it is worthwhile noting that the resonant column (RC) portion of this equipment had been calibrated to an NQA level in July 2000, and this level was reconfirmed in January, 2001 and March, 2002. The dynamic characteristics that were evaluated with the RCTS measurements are the shear modulus, G, and the material damping ratio in shear, D. The influence of the following variables on G and D were evaluated:

1. Magnitude of the isotropic state of stress, σ_o.

   Five isotropic pressures were typically used for each specimen which ranged from below to above the estimated in situ mean effective stress, σ'_m. When the samples were above the water table, the total effective stresses were assumed equal, because the samples were unsaturated and the values of (negative) pore water pressure were unknown.

2. Time of confinement at each isotropic state of stress, t

   Confinement times at each pressure were at least 1000 minutes for all specimens. Thus, all small-strain measurements of G and D at times of 1000 minutes were after primary consolidation for each specimen.

3. Shearing strain amplitude, γ.

Strains ranged from the small-strain range, less than about 0.0005% to rather large strain amplitudes, above about 0.1% for many specimens. Testing was performed over this strain range at σ_m and $4\sigma_m$ for many of the specimens.

4. Number of cycles of loading, N.

   Ten cycles of loading were used in the torsional shear (TS) test followed by about 1000 cycles in the resonant column (RC) test.

5. Excitation frequency, f.

   Frequencies ranging from 0.1 Hz to around 5 Hz were used in TS testing of the specimens. The frequency associated with resonance in the RC test varied with material stiffness and strain amplitude and ranged from about 25 Hz to slightly more than 250 Hz. Also, the maximum frequency in the TS test was $\leq$ 0.1 times the resonant frequency in the RC test.

6. Stress History.

   Small-strain values of G and D were evaluated at the estimated in-situ mean total stress, σ_m, and generally at two stress levels under and at two stress levels over the in-situ mean total stress.

2.1. Test Program

Dynamic testing of each soil specimen involved the evaluation of G and D over a range of isotropic confining pressures. As noted above, five isotropic confining pressures were generally used in a loading sequence, with the isotropic confining pressure, σ_o, doubled upon completion of the required tests at lower pressure. Low-amplitude resonant column testing was performed at each level of σ_o to determine the effects of magnitude of confinement and time of confinement on the small-strain shear modulus, G_{max}, and small-strain material damping ratio, D_{min}. Low-amplitude dynamic tests are defined as those

tests in which the resonant amplitude did not exceed 0.001% and was usually well below that level.

For each laboratory specimen, the range in confining pressures was based on the estimated in-situ mean effective stress, σ'_m. The estimated in-situ mean effective stress, σ'_m, was determined by assuming the following: (1) the depth of the water table (given in Table 6), (2) the total unit weights of all soils above the specimen, which were taken from the values in Table 6 combined with the value of total unit weight determined by measuring the volume and weight of the trimmed specimen before testing, (3) the initial estimate of the in-situ coefficient of lateral earth pressure at rest, K_o (assumed to be 0.5), and (4) the assumption that (negative) capillary stresses above the water could be ignored for specimens above the water table. Once this value of σ'_m was determined, the range in confining pressures over which G and D would be evaluated was determined.

Specimens were tested at small strains at the different confining pressures in an increasing confining pressure sequence. Each confining pressure sequence is listed in Table. 7. High-amplitude resonant column and torsional shear tests were performed during this loading path at the estimated in situ mean effective stress, σ'_m, (assuming K_o = 0.5) and, for 14 specimens, at four times the estimated in situ mean total stress. For the other 11 specimens, testing had to be stopped during the loading sequence due to sample tilting which caused the drive plate to touch the magnets and hence high amplitude testing was only performed at, σ'_m. High-amplitude testing was composed of two series of tests. The first involved cyclic torsional shear (TS) testing as illustrated in Figure 1. A complete set of torsional shear tests required about two hours to perform at each confining pressure. Torsional shear tests were conducted with the drainage line opened and involved shearing strains, γ, from less than 0.001% to above 0.02%. The majority of the measurements were performed at 0.5 Hz and are labeled as TS1 in Figure 1. However, two sets of TS tests at $\gamma \approx 0.001\%$ and $\gamma \approx 0.01\%$ were also conducted

Table 6. Ground Water and Total Unit Weight Information Given to UTA about the ROSRINE Sites

Location	Depth to Ground Water (ft)	Overburden Estimation		Comments
		Depth Interval (ft)	Total Unit Weight (pcf)	
Meloland	6.5	0-bottom of hole	125	Groundwater location based on P-wave velocity. Unit weight interpreted from UCLA tests. No boring log available
Tarzana	60	0-40	110	Groundwater location based on P-wave velocity. Unit weight interpreted from UCLA tests.
Lake Hughes	28	0-bottom of hole	115	Groundwater location based on P-wave velocity. Unit weight estimated from soil type.
Dayton	25	0-bottom of hole	120	Groundwater location based on P-wave velocity. Unit weight estimated from soil type and summary of index tests
Obregon Park	20	0-125	125	Groundwater location based on P-wave velocity. Unit weight interpreted from UCLA tests.
Saturn	30	0-50	135	Groundwater location based on P-wave velocity. Upper location may be perched on clay layer at 50ft. Unit weight interpreted from laboratory tests.
	85	50-bottom of hole	125	
LA Bulk Mail	135	0-bottom of hole	115	Groundwater location based on P-wave velocity, Unit weight estimated from soil type, water contents, and estimated saturation
Yermo	135	0-bottom of hole	125	Groundwater location based on P-wave velocity, Unit weight estimated from soil type, water contents, and estimated saturation
Joshua Tree	>330	0-bottom of hole	135	P-wave velocities < 1500 mps to bottom of hole. Unit weight estimated from soil type, water contents, and estimated saturation
Gilroy #3	35	0-80	120	Groundwater location based on P-wave velocity. Unit weight estimated from soil type and summary of index tests
		80-bottom of hole	135	
Halls Valley	65	0-150	120	Groundwater location based on P-wave velocity. Unit weight estimated from soil type and summary of index tests
		150-bottom of hole	135	

Table 7. Summary of Tests Perfomed on the Specimens from the ROSRINE Sites

Spec. No.	Soil Site Identification	Specimen Depth ft (m)	Depth to Groundwater ft (m)	In-Situ Effective Stess σ'_m, ksf	Initial Specimen Size		Isotropic Test Pressures		
					Height in. (cm)	Diameter in. (cm)	Low-Amplitude RC and TS Tests ksf (kPa)	High-Amplitude RC Tests ksf (kPa)	High-Amplitude TS Tests ksf (kPa)
1	Tarzana P-3	30 (9.1)	60 (18.3)	2.2	2.93 (7.44)	1.48 (3.75)	0.43, 0.86, 1.73, 3.46, 6.91 (21, 41, 83, 166, 331)	1.73*, 6.91 (82, 331)	1.73*, 6.91 (82, 331)
2	Tarzana P-4	42 (12.8)	60 (18.3)	3.08	3.88 (9.86)	2.04 (5.19)	0.86, 1.73, 3.46, 6.91, 13.82 (41, 83, 166, 331, 663)	3.46*, 13.82 (166, 663)	3.46*, 13.82 (166, 663)
3	Meloland S-2	20 (6.1)	6.5 (2.0)	1.11	3.79 (9.63)	1.98 (5.03)	0.22, 0.43, 0.86, 1.73, 3.46 (10, 21, 41, 83, 166)	0.86*, 3.46 (41, 166)	0.86*, 3.46 (41, 166)
4	Meloland S-3	28 (8.5)	6.5 (2.0)	1.44	4.18 (10.62)	2.00 (5.09)	0.36, 0.65, 1.30 (17, 31, 62)	1.30$^+$ (62*)	1.30$^+$ (62*)
5	Meloland WS-1	120 (36.6)	6.5 (2.0)	5.28	4.04 (10.27)	1.86 (4.72)	0.43, 1.08, 2.16, 4.32, 8.64, 17.28 (21, 52, 104, 207, 414, 828)	1.08, 4.32*, 17.28 (52, 207, 828)	1.08, 4.32*, 17.28 (52, 207, 828)
6	Meloland WS-3	200 (61.0)	6.5 (2.0)	8.62	3.94 (10.00)	1.88 (4.78)	0.86, 2.16, 4.32, 8.64, 17.28, 41.76 (41, 104, 207, 414, 828, 2002)	2.16, 8.64* (104, 414)	2.16, 8.64* (104, 414)
7	Meloland WS-4	259 (78.9)	6.5 (2.0)	11.08	3.88 (9.86)	1.86 (4.72)	2.59, 5.33, 10.80 (124, 255, 518)	10.80$^+$ (518*)	10.80$^+$ (518*)
8	Meloland WS-6	378 (115.2)	6.5 (2.0)	16.05	3.79 (9.62)	1.87 (4.75)	3.89, 7.92, 15.84, 31.68, 63.36 (186, 380, 759, 1519, 3037)	15.84*, 63.36 (759, 3037)	15.84*, 63.36 (759, 3037)
9	Meloland WS-7	440 (134.1)	6.5 (2.0)	18.63	3.78 (9.59)	1.91 (4.85)	4.61, 9.36, 18.72, 37.44, 64.80 (221, 449, 897, 1795, 3106)	18.72*, 64.80 (897, 3106)	18.72*, 64.80 (897, 3106)
10	LA Bulk Mail (P-1)	15 (4.6)	135 (41.1)	1.15	3.70 (9.40)	2.00 (5.08)	0.36, 0.58, 1.44, 2.88, 5.76 (17, 28, 69, 138, 276)	1.44*, 5.76 (69, 276)	1.44*, 5.76 (69, 276)
11	LA Bulk Mail (P-3)	50 (15.2)	135 (41.1)	3.83	3.80 (9.65)	2.01 (5.10)	1.15, 1.73, 3.60, 7.20, 14.40 (55, 83, 173, 345, 690)	3.60*, 14.40 (173, 690)	3.60*, 14.40 (173, 690)
12	LA Bulk Mail (P-5)	167.5 (51.1)	135 (41.1)	11.49	4.12 (10.46)	1.97 (5.01)	2.88, 5.76, 11.52, 23.04, 46.08 (138, 276, 552, 1105, 2209)	11.52$^+$ (552*)	11.52$^+$ (552*)

Notes: * Denotes test pressures used to represent estimated in-situ σ_o if K_o =0.5

$^+$ Test was stopped due to sample tilting

Table 7. Continued - Summary of Tests Perfomed on the Specimens from the ROSRINE Sites

Spec. No.	Soil Site Identification	Specimen Depth ft (m)	Depth to Groundwater ft (m)	In-Situ Effective Stess σ'_m, ksf	Initial Specimen Size		Isotropic Test Pressures		
					Height in. (cm)	Diameter in. (cm)	Low-Amplitude RC and TS Tests ksf (kPa)	High-Amplitude RC Tests ksf (kPa)	High-Amplitude TS Tests ksf (kPa)
13	LA Bulk Mail (P-6)	205 (62.5)	135 (41.1)	12.80	2.90 (7.37)	1.50 (3.81)	3.17, 6.48, 12.96 (152, 311, 621)	12.96^{+} (621*)	12.96^{+} (621*)
14	LA Bulk Mail (P-7)	267 (81.4)	135 (41.1)	14.98	4.99 (12.67)	2.69 (6.82)	3.60, 7.20, 14.40, 28.80, 57.60 (173, 345, 690, 1381, 2761)	14.40*, 57.60 (690, 2761)	14.40*, 57.60 (690, 2761)
15	Gilroy #3 P-4	182 (55.5)	35 (10.7)	10.26	2.44 (6.21)	1.48 (3.77)	3.02, 6.05, 12.10, 24.19, 48.38 (145, 290, 580, 1160, 2320)	12.10*, 48.38 (580, 2320)	12.10*, 48.38 (580, 2320)
16	Gilroy #3 P-5	357 (108.8)	35 (10.7)	18.73	3.61 (9.18)	2.08 (5.28)	5.90, 11.81, 23.76 (283, 566, 1139)	23.76^{+} (1139*)	23.76^{+} (1139*)
17	Lake Hughes P-1	6 (1.8)	28 (8.5)	0.46	5.61 (14.26)	2.86 (7.26)	0.12, 0.22, 0.43 (6, 10, 21)	0.43^{+} (21*)	0.43^{+} (21*)
18	Joshua Tree 5 P-7	236 (71.9)	> 330 (100.6)	21.24	3.61 (9.16)	1.95 (4.95)	4.75, 9.65, 19.44, 38.88 (228, 463, 932, 1864)	19.44^{+} (932*)	19.44^{+} (932*)
19	Joshua Tree 5 P-8	328 (100.0)	> 330 (100.6)	29.52	5.20 (13.22)	2.83 (7.20)	6.91, 13.68, 27.36, 54.72 (331, 656, 1312, 2623)	27.36^{++} (1312*)	27.36^{++} (1312*)
20	Yermo P-6	210 (64.0)	135 (41.1)	14.00	3.69 (9.38)	1.99 (5.06)	3.60, 7.20, 14.40, 28.80 (173, 345, 690, 1381)	14.40^{+} (690)	14.40^{+} (690)
21	Yermo P-7	266 (81.1)	135 (41.1)	16.72	5.33 (13.54)	2.78 (7.05)	4.32, 8.64, 17.28, 34.56, 69.12 (207, 414, 828, 1657, 3314)	17.28*, 69.12 (828, 3314)	17.28*, 69.12 (828, 3314)
22	Halls Valley (P-1)	7 (2.1)	65 (19.8)	0.56	4.18 (10.61)	2.03 (5.15)	0.14, 0.29, 0.58, 1.15, 2.30 (7, 14, 28, 55, 110)	0.58*, 2.30 (28, 110)	0.58*, 2.30 (28, 110)
23	Halls Valley (P-3)	52 (15.8)	65 (19.8)	4.16	3.81 (9.67)	2.02 (5.12)	1.08, 2.16, 4.32, 8.64, 17.28 (52, 104, 207, 414, 828)	4.32*, 17.28 (207, 828)	4.32*, 17.28 (207, 828)
24	Saturn P-4	100 (30.5)	85 (25.9)	7.71	3.60 (9.14)	2.10 (5.33)	1.44, 3.02, 6.05, 12.10 (69, 145, 290, 580)	6.05^{+} (290*)	6.05^{+} (290*)
25	Obregon P-8	101 (30.8)	20 (6.1)	5.05	3.60 (9.14)	2.05 (5.21)	1.15, 2.45, 5.04 (55, 117, 242)	5.04^{+} (242*)	5.04^{+} (242*)

Notes: * Denotes test pressures used to represent estimated in-situ σ_o if K_o =0.5

$^{+}$ Test was stopped due to sample tilting

$^{++}$ Test was stopped due to membrane rupture

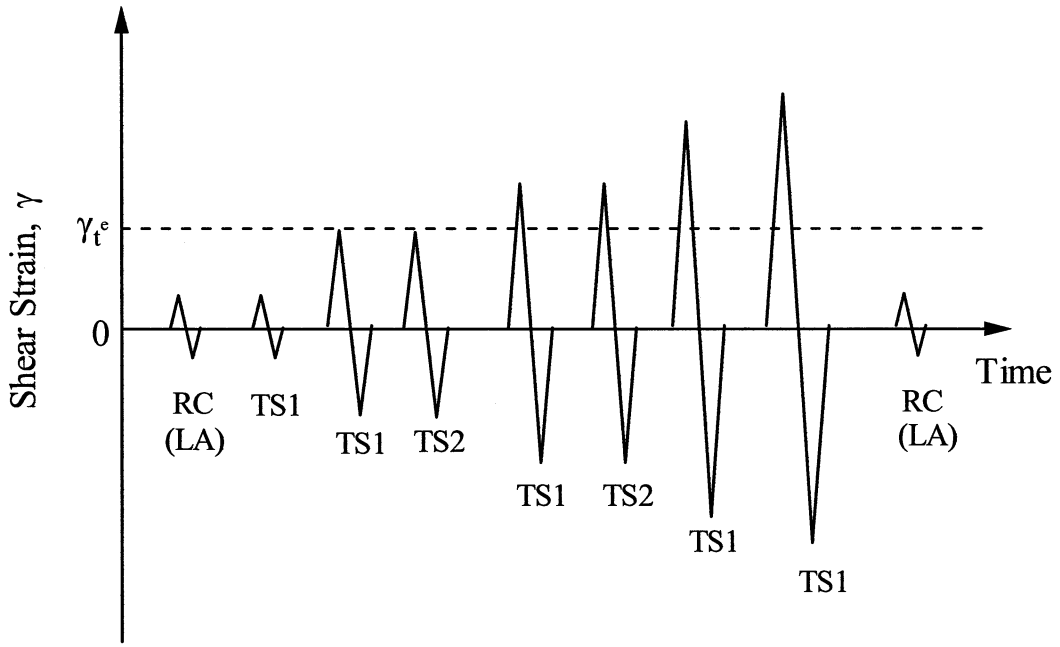

γ_t^e = elastic threshold strain; below γ_t^e, G is constant and equal to G_{max}

RC (LA) = resonant column test at low-amplitudes (strains < 0.001%)

TS1 = torsional shear test in which 10 cycles are applied at 0.5 Hz.

TS2 = torsional shear test in which 10 cycles are applied at each of four (or five) frequencies between 0.1 Hz to 5 (or 10) Hz (0.1, 0.5, 1, and 5 (and 10)) for the soil specimens.

Figure 1 Testing Procedure Used in the Torsional Shear (TS) Test to Investigate the Effects of Strain Amplitude, Number of Loading Cycles, and Excitation Frequency on G and D of the Test Specimens.

to evaluate the effect of excitation frequency on G and D at these strains. In these tests (denoted as TS2 in Figure 1), ten cycles of loading were applied at five different frequencies ranging from 0.1 Hz to 10 Hz (or 5Hz).

After the TS tests were completed, confinement of the specimen was continued at the given confining pressure, and specimens were allowed to re-gain any change in G_{max} for a period of one day. Then a series of high-amplitude resonant column (HARC) tests was performed. However, before high-amplitude RC testing commenced, small-strain RC tests were performed to determine any changes in the soil skeleton that might have occurred from the TS tests. No significant changes in G_{max} and D_{min} were measured after the 1-day rest period. Significant changes are defined herein as 5% in G_{max} and 10% in D_{min}.

High-amplitude resonant column testing was conducted to evaluate the influence of strain amplitude on G and D. This series of tests is illustrated in Figure 2. A complete set of resonant column tests took about two hours to perform and these tests were performed with the drainage line opened just as in the case of the TS tests. The HARC tests typically involved shearing strains from less than 0.0005% to above 0.05%, depending on the soil stiffness and material damping. In these tests, about 1000 cycles of loading were applied at each strain amplitude.

Upon completion of the high-amplitude RC tests, low-amplitude RC tests were again performed to determine if any changes in the soil skeleton had occurred from the high-amplitude tests. (No significant changes were measured in G_{max} and D_{min} after the 1-day rest period.) Then, the next stage of testing (low-amplitude tests at a higher confining pressure) was undertaken.

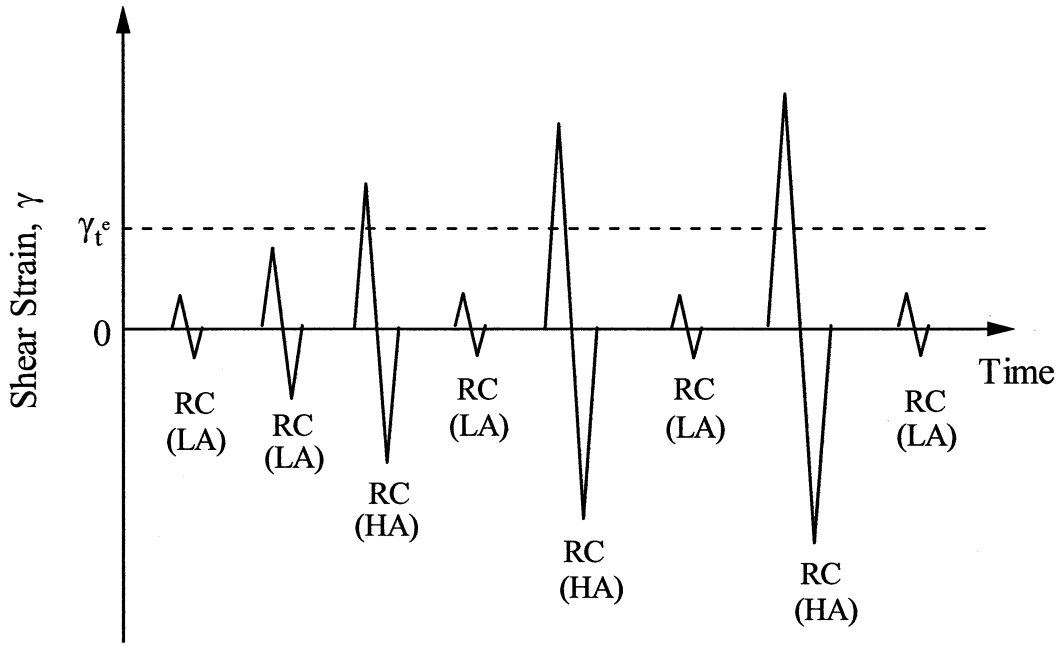

RC = resonant column test in which about 1000 cycles of loading are applied during each measurement

[ ] = elastic threshold strain; below [ ], G is constant and equal to G_{max}

RC (LA) = resonant column test at low-amplitudes (strains < 0.001%)

RC (HA) = resonant column test at amplitudes above [ ]

Figure 2 Testing Procedure Used in the Resonant Column (RC) Test to Investigate the Effect of Strain Amplitude on G and D of the Test Specimens.

2.2. Test Results

The results of the RC and TS tests are shown in Appendices B through Z for the 25 specimens. These 25 appendices are contained in Volume II. Each appendix presents all test results from one specimen. As an example, consider the general presentation of dynamic test results presented in Appendix B. The dynamic test results are presented as follows:

1. Figure B.1 shows the variation in low-amplitude shear modulus with magnitude and duration of isotropic confining pressure from resonant column tests.

2. Figure B.2 shows the variation in low-amplitude material damping ratio with magnitude and duration of isotropic confining pressure from resonant column tests.

3. Figure B.3 shows the variation in estimated void ratio with magnitude and duration of isotropic confining pressure from resonant column tests.

4. Figure B.4 shows the variation in low-amplitude shear wave velocity with isotropic confining pressure from resonant column tests.

5. Figure B.5 shows the variation in low-amplitude shear modulus with isotropic confining pressure from resonant column tests.

6. Figure B.6 shows the variation in low-amplitude material damping ratio with isotropic confining pressure from resonant column tests.

7. Figure B.7 shows the variation in estimated void ratio with isotropic confining pressure from resonant column tests.

8. Figure B.8 shows the variation in shear modulus with shearing strain and isotropic confining pressure.

9. Figure B.9 shows the variation in normalized shear modulus with shearing strain and isotropic confining pressure.

10. Figure B.10 shows the variation in material damping ratio with shearing strain and isotropic confining pressure.

11. Figure B.11 shows the variation in shear modulus with shearing strain at an isotropic confining pressure of 24 psi (= 3.46 ksf = 166 kPa) from RCTS tests.

12. Figure B.12 shows the variation in normalized shear modulus with shearing strain at an isotropic confining pressure of 24 psi(=3.46 ksf=166 kPa) from RCTS tests.

13. Figure B.13 shows the variation in material damping ratio with shearing strain at an isotropic confining pressure of 24 psi (= 3.46 ksf = 166 kPa) from RCTS tests.

14. Figure B.14 shows the variation in shear modulus with loading frequency at an isotropic confining pressure of 24 psi (= 3.46 ksf = 166 kPa) from RCTS tests.

15. Figure B.15 shows the variation in material damping ratio with loading frequency at an isotropic confining pressure of 24 psi (= 3.46 ksf = 166 kPa) from RCTS tests.

16. Figure B.16 shows the variation in shear modulus with shearing strain at an isotropic confining pressure of 96 psi (= 13.8 ksf = 663 kPa) from RCTS tests.

17. Figure B.17 shows the variation in normalized shear modulus with shearing strain at an isotropic confining pressure of 96 psi (= 13.8 ksf = 663 kPa) from RCTS tests.

18. Figure B.18 shows the variation in material damping ratio with shearing strain at an isotropic confining pressure of 96 psi (= 13.8 ksf = 663 kPa) from RCTS tests.

19. Figure B.19 shows the variation in shear modulus with loading frequency at an isotropic confining pressure of 96 psi (= 13.8 ksf = 663 kPa) from RCTS tests.

20. Figure B.20 shows the variation in material damping ratio with loading frequency at an isotropic confining pressure of 96 psi (= 13.8 ksf = 663 kPa) from RCTS tests.

21. Table B.1 presents the tabulated results of the variation in low-amplitude shear wave velocity, low-amplitude shear modulus, low-amplitude material damping ratio and estimated void ratio with isotropic confining pressure from RC tests.

22. Table B.2 presents the tabulated results of the variation in shear modulus, normalized shear modulus and material damping ratio with shearing strains from RC tests at an isotropic confining pressure of 24 psi (= 3.46 ksf = 166 kPa).

23. Table B.3 presents the tabulated results of the variation in shear modulus, normalized shear modulus and material damping ratio with shearing strain from TS tests at an isotropic confining pressure of 24 psi (= 3.46 ksf = 166 kPa).

24. Table B.4 presents the tabulated results of the variation in shear modulus, normalized shear modulus and material damping ratio with shearing strains from RC tests at an isotropic confining pressure of 96 psi (= 13.8 ksf = 663 kPa).

25. Table B.5 presents the tabulated results of the variation in shear modulus, normalized shear modulus and material damping ratio with shearing strain from TS tests at an isotropic confining pressure of 96 psi (= 13.8 ksf = 663 kPa).

3. DYNAMIC TEST RESULTS IN THE LINEAR RANGE

The discussion of the dynamic test results from the combined RCTS tests is divided into two main sections. The first section, Section 3, deals with the behavior of the specimens in the strain range where the dynamic properties are constant and independent of strain amplitude. This strain range is called the linear range, and measurements of dynamic properties in this range are often called small strain or low amplitude. The second section, Section 4, deals with the behavior of the specimens in the nonlinear range. In this strain range, the measurements and dynamic properties are often called nonlinear large strain or high amplitude. Both sections are subdivided into two parts, the first dealing with the nonplastic specimens and the second dealing with the plastic specimens. Furthermore, the results from the plastic specimens are subdivided into three groups based on the magnitude of the estimated in-situ confining pressure: low, medium and high.

3.1 Small-Strain Shear Wave Velocity, Shear Modulus, and Material Damping Ratio of the Seven Nonplastic Specimens

3.1.1 Log V_S – Log σ_0 Relationships – The variations of small-strain shear wave velocity, V_S, with isotropic confining pressure, σ_o, for the seven nonplastic specimens are shown in Figure 3. Total confining pressure and not the effective confining pressure is used because the samples were not saturated and the values of (negative) porewater pressure were unknown. It should also be noted that: (1) two specimens (Nos.13 and 17) were tested at only three different confining pressures, and (2) three other specimens (Nos. 18, 19, and 20) were tested at four different confining pressures. In all cases, the reason that testing had to be stopped was excessive specimen tilting.

As seen in Figure 3, each specimen exhibited V_S increasing with increasing isotropic confining pressure, as expected. Six of the specimens were recovered from depths ranging from 201 to 328 ft (61 to 100m). These are Specimen Nos. 13, 14, 18, 19, 20 and 21. The

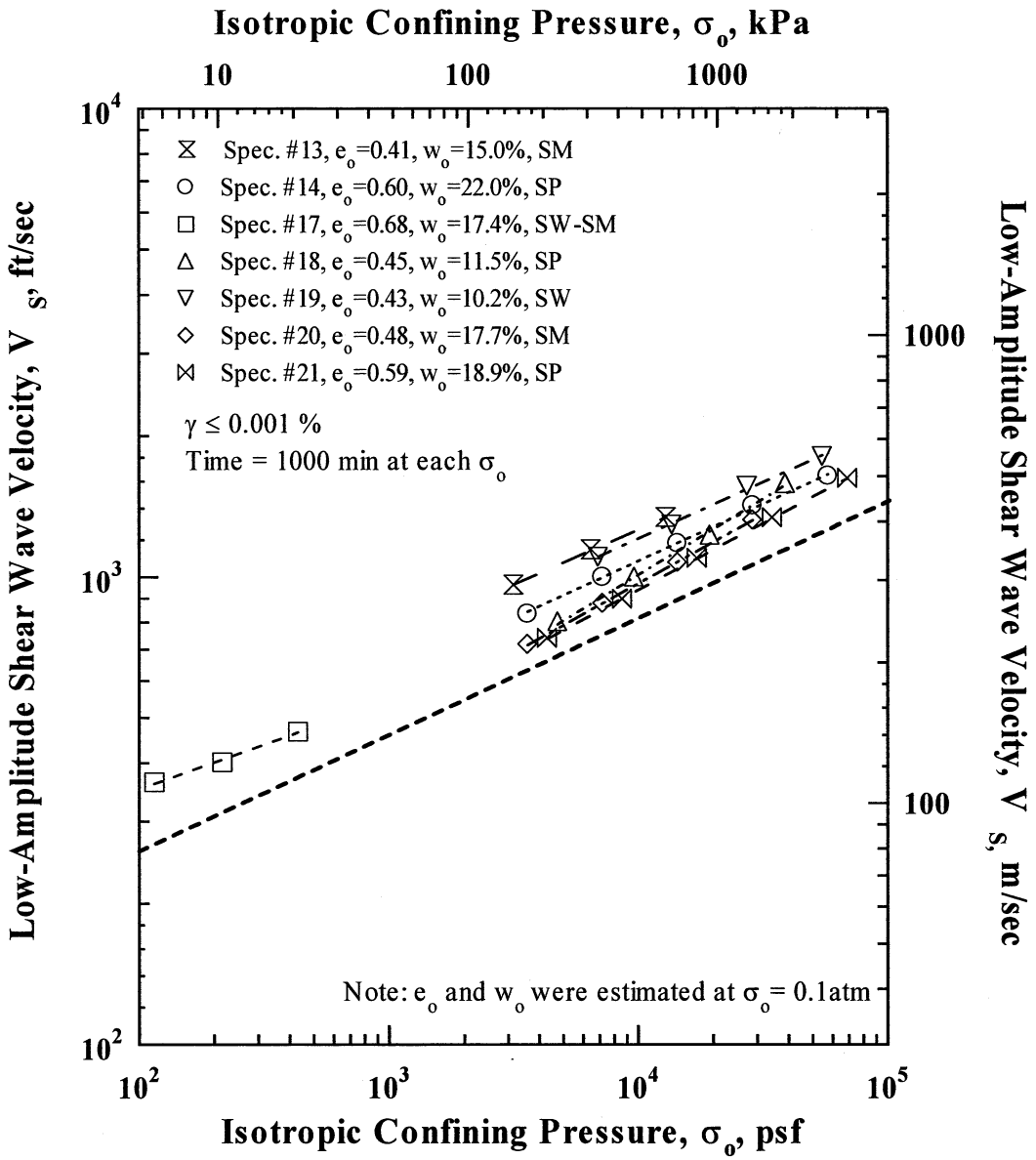

Figure 3 Variation in Low-Amplitude Shear Wave Velocity with Isotropic Confining Pressure of the Seven, Nonplastic Specimens as Determined from Resonant Column (RC) Tests

average depth of these specimens is 250 ft (76 m). The log V_S - log σ_o relationships for all the specimens are well represented by straight lines as seen in Figure 3. If a common confining pressure at which to compare the range in V_S values is selected, say 10,000 psf (= 69.4 psi = 497 kPa), the values range from about 937 to 1261 fps (285 to 384 m/s) and have an average value of 1077 fps (328 m/s). This range in values is rather small (-13% to 17% of the average), considering the specimens were recovered from three different sites. The one specimen that is somewhat different is Specimen No. 17 from a depth of 6 ft (1.8 m). This specimen shows a somewhat slower increase of V_S with σ_o, which indicates that this specimen behaves as a cemented and/or overconsolidated specimen over the entire confinement range. The somewhat larger increase in V_S with σ_o for Specimen No. 18 could possibly indicate that this specimen is somewhat disturbed. As discussed in Section 3.3, the change (decrease) in void ratio with increasing σ_o is also more than any of the other specimens which supports the evaluation of some disturbance.

Relationships between the small-strain shear wave velocity, confining pressure, and void ratio have been fit to the data shown in Figure 3. The equation relating confining pressure, void ratio, and V_s (patterned after Hardin's 1978 equation for small-strain shear modulus) is:

$$V_s = (A_V / \sqrt{F(e)}) \cdot (\sigma_o / P_a)^{n_V} \qquad (1)$$

where;

A_v= shear wave velocity at σ_o = 1 atm and e = 1.0,

$F(e) = 0.3 + 0.7e^2$,

e = void ratio,

σ_o = total isotropic confining pressure in the same units as P_a,

P_a = one atmosphere (2117 psf or 100 kPa), and

n_v is a dimensionless exponent (typically in the range of 0.21 to 0.30 for sands with C_u between 1.3 and 16 (Menq, 2003)

It should be noted again that total stress, σ_o, is used in place of effective stress, σ_o', in Equation 1. The best-fit lines from least-squares fitting of the loading results are presented in the Figure 3. The constants determined for Equation 1 from the best-fit lines are summarized in Table 8. The change in V_s with confining pressure is represented by the exponent n_V. This change, in terms of the relative trend, is shown by the heavy dashed line in Figure 3 for n_V = 0.25. As noted earlier, n_V of Specimen No. 17 shows the lowest value, 0.19, and Specimen No. 18 has the largest slope, 0.33.

3.1.2 Log G_{max} – Log σ_0 Relationships – The variations of the small-strain shear modulus, G_{max}, with isotropic confining pressure, σ_o, for the seven nonplastic specimens are presented in Figure 4. Relationships have been fit to the small-strain shear moduli data using the generalized relationship presented by Hardin (1978). The Hardin (1978) equation relating shear modulus, void ratio, and confining pressure (slightly modified) is:

$$G_{max} = (A_G / F(e)) \cdot (\sigma_o / P_a)^{n_G} \qquad (2)$$

where;

A_G = shear modulus at σ_o = 1 atm and e = 1.0,

$F(e) = 0.3 + 0.7e^2$,

e = void ratio,

σ_o = isotropic confining pressure in the same units as P_a,

P_a = one atmosphere (2117 psf or 100 kPa), and

n_G is a dimensionless exponent (typically in the range of 0.42 to 0.60 for sands with C_u between 1.3 and 16 (Menq, 2003).

Table 8 Constants and Exponents in Equations 1 through 3 from Least-Squares Fitting of the log V_s – log σ_o, log G_{max} – log σ_o, and log D_{min} – log σ_o Relationships for the Seven Nonplastic Specimens

Spec. No.	UT Specimen ID	Specimen Depth ft (m)	Soil Type (Unified Soil Classification	Initial Void Ratio[1] e_o	% Passing Sieve #200	D_{10}[2] mm	D_{30}[2] mm	D_{60}[2] mm	Uniformity Coefficient[3] C_u	Coefficient of Gradation[4] C_c	Shear Wave Velocity		Shear Modulus		Damping Ratio	
											A_v, fps (m/sec)	n_V	A_G, ksf (MPa)	n_G	A_D (%)	n_D
13	UTA-27-V	205 (62.5)	Silty Sand (SM)	0.41	22.4	NA[5]	0.10	0.21	NA[5]	NA[5]	565 (172)	0.24	1375 (66)	0.47	2.16	-0.20
14	UTA-27-H	267 (81.4)	Sand (SP)	0.60	1.6	0.14	0.23	0.48	3.43	0.79	550 (168)	0.24	1200 (58)	0.49	1.35	-0.08
17	UTA-27-M	6 (1.8)	Silty Sand (SW-SM)	0.68	10.4	0.07	0.25	0.85	11.81	1.02	498 (152)	0.19	897 (43)	0.39	2.24	-0.17
18	UTA-27-N[6]	236 (71.9)	Sand (SP)	0.45	2.5	0.20	0.43	1.00	5.00	0.90	404 (123)	0.33[6]	629 (30)	0.68[6]	2.53	-0.12
19	UTA-27-O	328 (100.0)	Sand (SW)	0.43	2.3	0.30	1.00	2.20	7.33	1.51	544 (166)	0.24	1204 (58)	0.48	1.65	-0.18
20	UTA-27-P	201 (61.3)	Silty Sand (SM)	0.48	23.8	NA[5]	0.09	0.23	NA[5]	NA[5]	415 (127)	0.30	715 (34)	0.60	2.05	-0.07
21	UTA-27-Q	266 (81.1)	Sand (SP)	0.59	0.5	0.22	0.29	0.36	1.64	1.06	444 (135)	0.28	771 (37)	0.57	1.08	-0.02

Notes:

1. Void ratios were calculated based on the assumed value of G_s.
2. D_{10}, D_{10}, and D_{60} = the particle-size diameters corresponding to 10, 30, and 60 %, respectively, passing on the cumulative particle-size distribution
3. Uniformity Coefficient, Cu = D60/D10
4. Coefficient of Curvature, Cc = (D30)2/(D10D60)
5. NA = Not Applicable
6. Specimen seems to be quite disturbed based on the steepness of the log G_{max} - log σ_o relationship

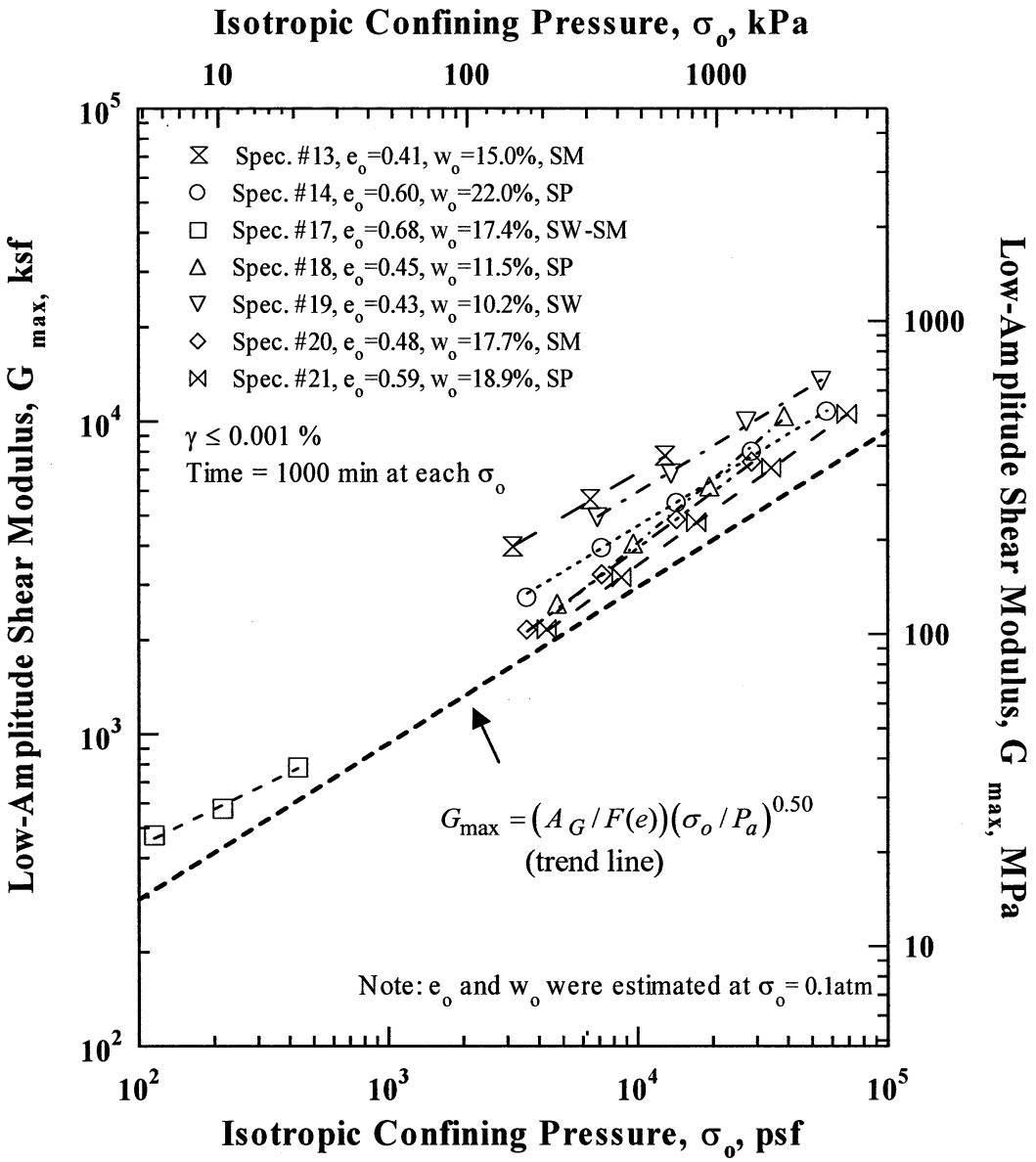

Figure 4 Variation in Low-Amplitude Shear Modulus with Isotropic Confining Pressure of the Seven, Nonplastic Specimens as Determined from Resonant Column (RC) Tests

As in Equation 1, total stress, σ_o, is used in place of effective stress, σ_o', in Equation 2. The best-fit lines determined by least-squares fitting of the loading results are presented in the Figure 4. The constants determined for Equation 2 from the best-fit lines are summarized in Table 8.

As cited in the comparison of shear wave velocities, the steepness of the best-fit lines determined for Specimen No. 18 in Figure 4 is the highest value, 0.68, while Specimen No. 17 shows the smallest increase of modulus with increasing confining pressure. Specimen Nos. 13, 14, 19, 20, and 21 have values of n_G that range from 0.47 and 0.60. This range in values is indicative of granular specimens that are either normally consolidated specimens and exhibit limited disturbance or have been disturbed enough to eliminate any history of overconsolidation. The change in G_{max} with σ_o predicted by Equation 2 (in terms of the trend line with $n_G = 0.50$) is shown by the heavy dashed line in Figure 4. If the specimens were overconsolidated and retained this stress history, the log G_{max} – log σ_o relationship would be composed of two linear segments, with the initial segment in the overconsolidated range having a flatter slope (smaller values of n_G). This behavior is shown by many of the plastic soil specimens discussed in Section 3.2.2, but it is not shown by any of the granular specimens (possibly because they are so deep and hence are likely normally consolidated) except Specimens No. 17, the specimen from a depth of 6 ft (1.8 m).

3.1.3 ***Log D_{min} – Log σ_0 Relationships*** – The relationship between the small-strain material damping ratio, D_{min}, measured from resonant column tests and isotropic confining pressure, σ_o, can be written as:

$$D_{\min} = A_D \cdot (\sigma_o / P_a)^{n_D} \qquad (3)$$

where;

A_D = small-strain material damping ratio at σ_o = 1atm,

σ_o = isotropic confining pressure in the same units as P_a,

P_a = one atmosphere (2117 psf or 100 kPa), and

n_D = a dimensionless exponent.

As in Equations 1 and 2, total stress, σ_o, is used in place of effective stress, σ_o', in Equation 3. The best-fit lines calculated by least-squares fitting of the loading results are presented in the Figure 5 and are summarized in Table 8.

All seven nonplastic specimens exhibited the trend of material damping ratio decreasing as confining pressure increased (as expected). For Specimen No. 21, the last two measurements exhibited a sudden increase in the values of D_{min} with increasing confining pressure. For this specimen, the confining chamber had to be opened at the fourth and fifth confining pressure levels due to sample tilting. It is felt that this release and re-application of the pressure caused the damping values to increase and these two data points were not used in fitting Equation 3 to the data.

3.2 Small-Strain Shear Wave Velocity, Shear Modulus, and Material Damping Ratio of the Plastic Specimens

The plastic soil group (eighteen specimens) is divided into three groups according to the magnitude of the estimated in-situ confining pressure. The lowest confining pressure group consists of eight specimens (Nos. 1, 2, 3, 4, 10, 11, 22, and 23) having an estimated in-situ confining pressure (if K_0 = 0.5) ranging from 0.56 ksf (27 kPa) through 4.16 ksf (199 kPa). This confining pressure range corresponds to a depth range of 7 to 52 ft (2.1 to 15.8 m). The middle confining pressure group consists of seven specimens (Nos. 5, 6, 7, 12, 15, 24, and 25) with an estimated in-situ confining pressure (if K_0 = 0.5) ranging from 5.05 ksf (242 kPa) to 11.49 ksf (551 kPa). This confining pressure range corresponds to a depth range of 100 to 259 ft (30.5 to 78.9 m). Specimen Nos. 8, 9, and 16 have been tested under confining

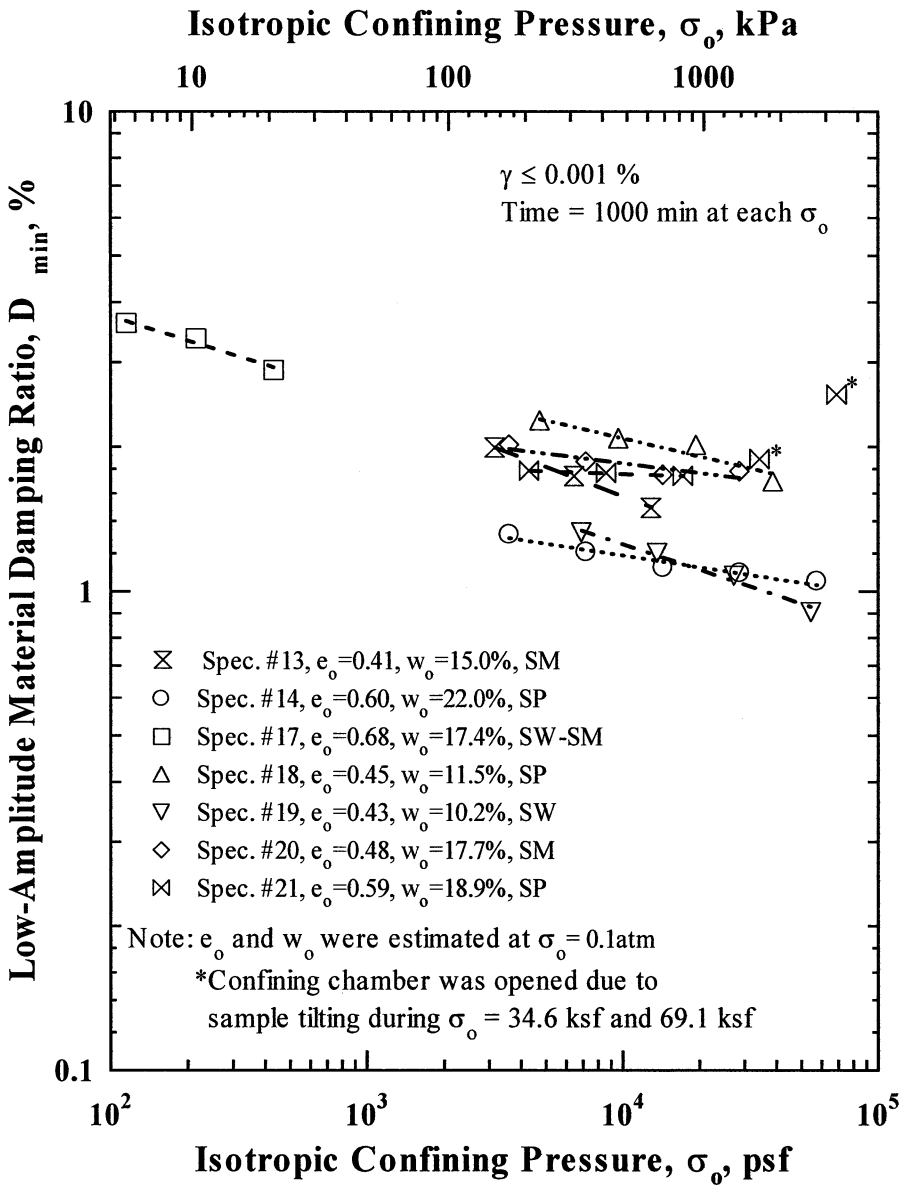

Figure 5 Variation in Low-Amplitude Material Damping Ratio, D_{min}, with Isotropic Confining Pressure of the Seven, Nonplastic Specimens as Determined from Resonant Column (RC) Tests

pressures between 16.05 ksf (769 kPa) and 18.73 ksf (898 kPa), and they are grouped into group three. The reasons that the plastic soils are divided into three groups are: (1) to look for trends with depth and (2) to keep the amount of data in each figure within manageable limits.

3.2.1 Log V_S – Log σ_0 Relationships –The variations of small-strain shear wave velocity, V_s, with isotropic confining pressure, σ_o, are shown in Figures 6 through 8. The log V_S – log σ_o relationships for the eight specimens in the low confining pressure group are shown in Figure 6. The same relationships for the seven specimens in the middle confining pressure group and the three specimens in the high confining pressure group are shown in Figures 7 and 8, respectively. The shear wave velocity for each specimen increased with the increasing confining pressure as observed above for the nonplastic specimens. However, the specimens exhibited two different slopes in these relationships, showing their degree of overconsolidation. Some specimens, such as Specimen No. 22 exhibited an abrupt increase after testing at the fourth confining pressure while other specimens like, Specimen No. 2 show two clear straight lines which have different slopes with the break in the relationship around the estimated in-situ confining pressure of 3.08 ksf (148 kPa) as shown in Figure 6.

Relationships between V_S, σ_o, and e have been fit to the data shown in Figures 6, 7 and 8 using Equation 1. In the case of these plastic soils, two relationships have been fit, one in the overconsolidated region (determined from the loading response at the first few pressures) and the second in the normally consolidated region (determined by the steeper slope in the normally consolidated range if it existed). The best-fit lines from least-squares fitting are presented in Figures 6 through 8. The constants determined for Equation 1 in the overconsolidated and normally consolidated regions are summarized in Tables 9 through 11.

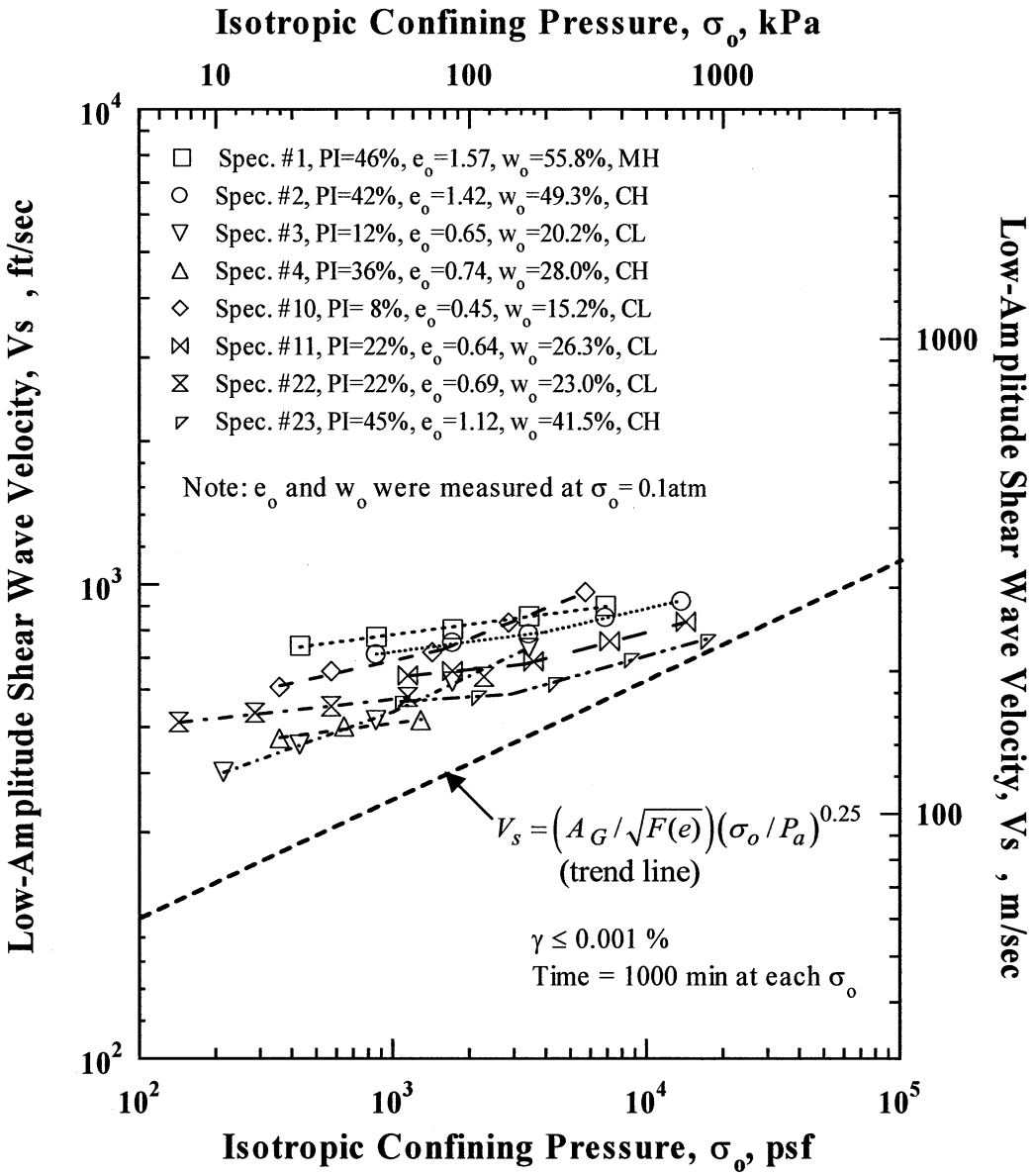

Figure 6 Variation in Low-Amplitude Shear Wave Velocity with Isotropic Confining Pressure of the Eight, Plastic Specimens in the Low In-Situ Confining Pressure Group as Determined from Resonant Column (RC) Tests

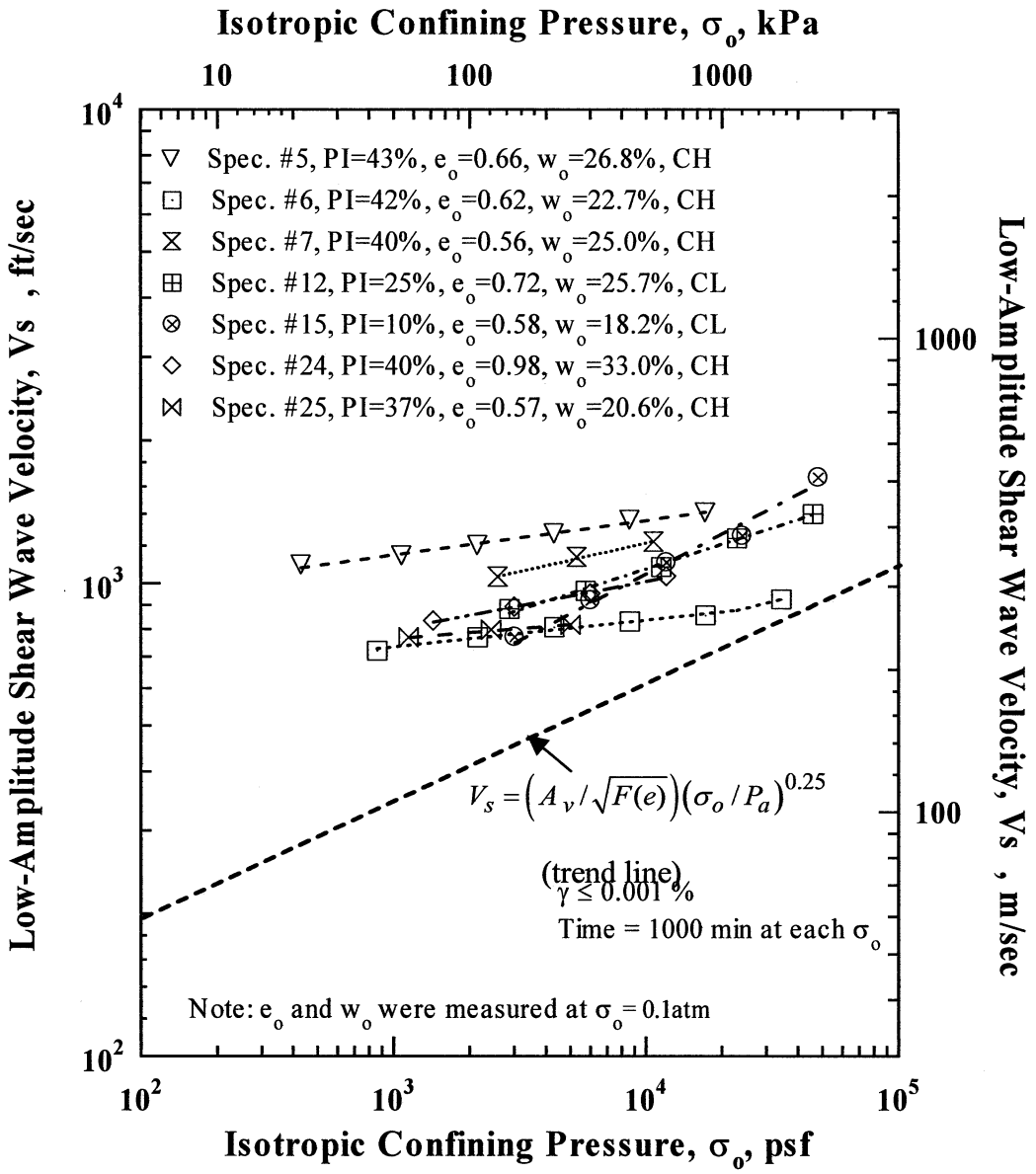

Figure 7 Variation in Low-Amplitude Shear Wave Velocity with Isotropic Confining Pressure of the Seven, Plastic Specimens in the Medium In-Situ Confining Pressure Group as Determined from Resonant Column (RC) Tests

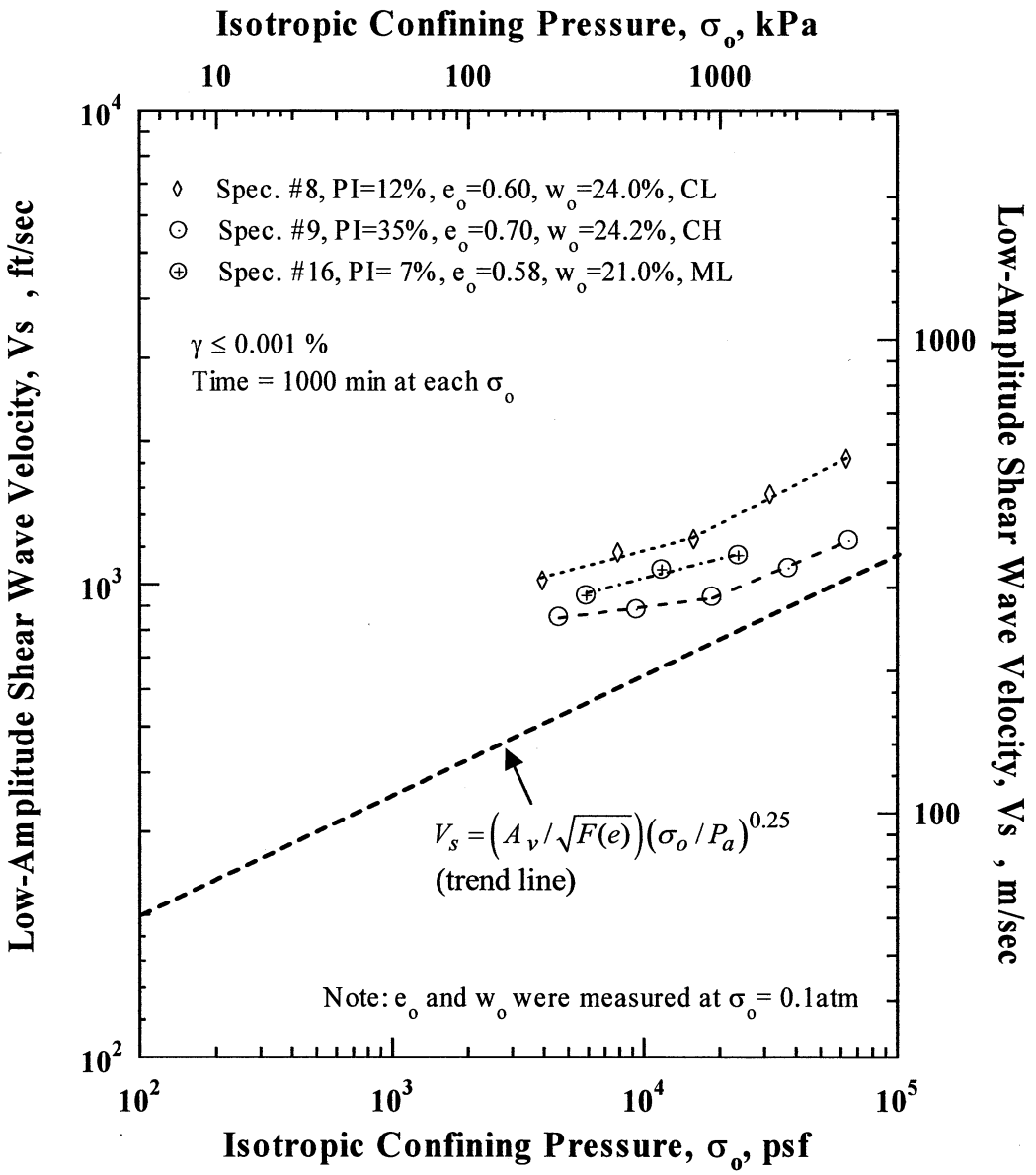

Figure 8 Variation in Low-Amplitude Shear Wave Velocity with Isotropic Confining Pressure of the Three, Plastic Specimens in the High In-Situ Confining Pressure Group as Determined from Resonant Column (RC) Tests

Table 9 Constants and Exponents in Equations 1 through 3 from Least-Squares Fitting of log V_s – log σ_o, log G_{max} – log σ_o, and log D_{min} – log σ_o, Relationships for the Eight Plastic Specimens in the Low In-Situ Confining Pressure Group as Determined from Resonant Column (RC) Tests

Spec. No.	UT Specimen ID	Specimen Depth ft (m)	Soil Type (Unified Soil Classification)	Initial Void Ratio e_o[1]	Plasticity Index %	Shear Wave Velocity				Shear Modulus				Material Damping Ratio				Estimated OCR[4]
						O.C.[2]		N.C.[3]		O.C.[2]		N.C.[3]		O.C.[2]		N.C.[3]		
						A_v, fps (m / sec)	n_V	A_v, fps (m / sec)	n_V	A_G, ksf (MPa)	n_G	A_G, ksf (MPa)	n_G	A_D (%)	n_D	A_D (%)	n_D	
1	UTA-25-B	30 (9.1)	Silt (MH)	1.57	46	684 (208)	0.07	–[5]	–[5]	1449 (69.5)	0.14	–[5]	–[5]	4.17	-0.14	–[5]	–[5]	≥4 H - O.C.
2	UTA-25-A	42 (12.8)	Clay (CH)	1.42	42	578 (176)	0.07	376 (115)	0.12	1063 (50.9)	0.14	446 (21.4)	0.25	4.14	-0.12	6.77	-0.18	1 ~ 2 S - O.C.
3	UTA-27-F	20 (6.1)	Clay (CL)	0.65	12	110 (34)	0.19	73 (22)	0.25	44 (2.1)	0.39	19 (0.9)	0.51	11.33	-0.27	15.82	-0.32	1 ~ 2 S - O.C.
4	UTA-27-E	28 (8.5)	Clay (CH)	0.74	36	263 (80)	0.07	–[5]	–[5]	144 (6.9)	0.23	–[5]	–[5]	3.69	-0.06	–[5]	–[5]	1 N.C.
10	UTA-27-S	15 (4.6)	Clay (CL)	0.45	8	202 (62)	0.12	101 (31)	0.21	184 (8.8)	0.23	40 (1.9)	0.43	6.87	-0.11	7.02	-0.11	1 ~ 2 S - O.C.
11	UTA-27-T	50 (15.2)	Clay (CL)	0.64	22	337 (103)	0.05	169 (52)	0.14	453 (21.7)	0.11	104 (5.0)	0.29	4.44	-0.04	4.21	-0.03	1 N.C.
22	UTA-27-L	7 (2.1)	Clay (CL)	0.69	22	306 (93)	0.06	–[5]	–[5]	355 (17.0)	0.12	–[5]	–[5]	5.46	-0.01	–[5]	–[5]	2 ~ 4 M - O.C.
23	UTA-27-R	52 (15.8)	Clay (CH)	1.12	45	480 (146)	0.04	191 (58)	0.15	771 (37.0)	0.08	111 (5.3)	0.32	7.02	-0.12	3.22	-0.03	1 N.C.

Notes:
1. Void ratios were calculated based on the assumed value of G_s.
2. O.C .= Overconsolidated state
3. N.C. = Normally consolidated state
4. Estimated OCR
   N.C. = Normally consolidated (OCR=1.0)
   S-O.C. = Slightly overconsolidated
   M-O.C. = Moderately overconsolidated
   H-O.C. = Heavily overconsolidated
5. Insufficient data to determine parameter

Table 10 Constants and Exponents in Equations 1 through 3 from Least-Squares Fitting of log V_s – log σ_o, log G_{max} – log σ_o, and log D_{min} – log σ_o, Relationships for the Seven Plastic Specimens in the Middle In-Situ Confining Pressure Group as Determined from Resonant Column (RC) Tests

Spec. No.	UT Specimen ID	Specimen Depth ft (m)	Soil Type (Unified Soil Classification)	Initial Void Ratio e_o[1]	Plasticity Index %	Shear Wave Velocity				Shear Modulus				Material Damping Ratio				Estimated OCR[4]
						O.C.[2]		N.C.[3]		O.C.[2]		N.C.[3]		O.C.[2]		N.C.[3]		
						A_v, fps (m / sec)	n_V	A_v, fps (m / sec)	n_V	A_G, ksf (MPa)	n_G	A_G, ksf (MPa)	n_G	A_D (%)	n_D	A_D (%)	n_D	
5	UTA-27-B	120 (36.6)	Clay (CH)	0.66	43	538 (164)	0.07	–[5]	–[5]	1104 (52.9)	0.15	–[5]	–[5]	7.02	-0.19	–[5]	–[5]	≥4 H - O.C.
6	UTA-27-A	200 (61.0)	Clay (CH)	0.62	42	374 (114)	0.06	–[5]	–[5]	549 (26.3)	0.11	–[5]	–[5]	2.57	-0.03	–[5]	–[5]	2 ~ 4 M - O.C.
7	UTA-27-C	259 (78.9)	Clay (CH)	0.56	40	292 (89)	0.12	–[5]	–[5]	349 (16.7)	0.24	–[5]	–[5]	11.06	-0.21	–[5]	–[5]	–[5] O.C.
12	UTA-27-I	167.5 (51.1)	Clay (CL)	0.72	25	178[6] (54)	0.17[6]	–[5]	–[5]	100[6] (4.8)	0.37[6]	–[5]	–[5]	4.49[6]	-0.09[6]	–[5]	–[5]	–[6]
15	UTA-27-J	182 (55.5)	Clay (CL)	0.58	10	–[6]	–[6]	58.22 (18)	0.28	–[6]	–[6]	0.84 (0.04)	0.61	–[6]	–[6]	14.87	-0.14	–[6]
24	UTA-27-U	100 (30.5)	Clay (CH)	0.98	40	388 (118)	0.10	–[5]	–[5]	503 (24.1)	0.21	–[5]	–[5]	9.57	-0.13	–[5]	–[5]	≥2 O.C.
25	UTA-27-W	101 (30.8)	Clay (CH)	0.57	37	415 (126)	0.04	–[5]	–[5]	684 (32.8)	0.09	–[5]	–[5]	7.18	-0.04	–[5]	–[5]	–[5] O.C.

Notes:
1. Void ratios were calculated based on the assumed value of G_s.
2. O.C .= Overconsolidated state
3. N.C. = Normally consolidated state
4. Estimated OCR
   N.C. = Normally consolidated (OCR=1.0)
   S-O.C. = Slightly overconsolidated
   M-O.C. = Moderately overconsolidated
   H-O.C. = Heavily overconsolidated
5. Insufficient data to determine parameter
6. Spemimen appears to be disturbed

Table 11 Constants and Exponents in Equations 1 through 3 from Least-Squares Fitting of log V_s – log σ_o, log G_{max} – log σ_o, and log D_{min} – log σ_o, Relationships for the Three Plastic Specimens in the High In-Situ Confining Pressure Group as Determined from Resonant Column (RC) Tests

Spec. No.	UT Specimen ID	Specimen Depth ft (m)	Soil Type (Unified Soil Classification)	Initial Void Ratio e_o[1]	Plasticity Index %	Shear Wave Velocity				Shear Modulus				Material Damping Ratio				Estimated OCR[4]
						O.C.[2]		N.C.[3]		O.C.[2]		N.C.[3]		O.C.[2]		N.C.[3]		
						A_v, fps (m / sec)	n_V	A_v, fps (m / sec)	n_V	A_G, ksf (MPa)	n_G	A_G, ksf (MPa)	n_G	A_D (%)	n_D	A_D (%)	n_D	
8	UTA-27-D	378 (115.2)	Clay (CL)	0.60	12	242 (74)	0.14	64 (20)	0.28	238 (11.4)	0.28	16 (0.8)	0.56	3.40	-0.10	1.97	-0.04	1 N.C.
9	UTA-27-G	440 (134.1)	Clay (CH)	0.70	35	379 (115)	0.07	82 (25)	0.22	521 (25.0)	0.15	21 (1.0)	0.47	1.83	-0.03	1.48	-0.01	1 N.C.
16	UTA-27-K	357 (108.8)	Silt (ML)	0.58	7	215[6] (65)	0.14[6]	–[5]	–[5]	187[6] (9.0)	0.27[6]	–[5]	–[5]	4.41[6]	-0.03[6]	–[5]	–[5]	–[6]

Notes:

1. Void ratios were calculated based on the assumed value of G_s.
2. O.C .= Overconsolidated state
3. N.C. = Normally consolidated state
4. Estimated OCR
   N.C. = Normally consolidated (OCR=1.0)
   S-O.C. = Slightly overconsolidated
   M-O.C. = Moderately overconsolidated
   H-O.C. = Heavily overconsolidated
5. Insufficient data to determine parameter
6. Specimen appears to be disturbed based on $G_{max,lab}/G_{max,field}$ =0.2

3.2.2 Log G_{max} – Log σ_0 Relationships – The variations of small-strain shear modulus with confining pressure, log G_{max} – log σ_o relationships, are shown in Figures 9 through 11 for the low, medium and high in-situ confining pressure groups, respectively. Best-fit lines from least-squares fitting of Equation 2 to each data set are shown in the figures. The constants determined from the fitting are presented in Tables 9 through 11. As with the log V_S- log σ_o relationship for the soils with plasticity, best fits have been performed in both the overconsolidated and normally consolidated regions when both were presented.

The log G_{max} – log σ_o relationships differentiate the overconsolidated and normally consolidated regions more dramatically than the log V_S – log σ_o relationships (because the vertical scale is expanded when G_{max} (= ρV_S^2) is used). Consider, for instance, Specimen No. 2 in Figure 9. A bi-linear relationship described by a flatter slope (overconsolidated region) followed by a steeper slope (normally consolidated region) clearly exists. Furthermore, the confining pressure at which there is a change in slope occurs at the third confining pressure. The third confining pressure is the one estimated before testing commenced to be the in-situ mean stress if the specimen is normally consolidated at K_o which is approximately 0.5. Therefore, Specimen No. 2 is estimated to be normally consolidated as listed in Table 9. On the other hand, Specimen Nos. 5 and 6 in Figure 10 are clearly heavily overconsolidated.

Each log G_{max} – log σ_o relationship has a rather flat slope (n_G well below 0.5) meaning that each specimen remains overconsolidated throughout the complete set of pressures used, with the highest pressure equal to four times the mean confining pressure estimated for the specimens if they were normally consolidated.

The log G_{max} – log σ_o relationships in Figures 9 through 11 were all analyzed to estimate the qualitative state of overconsolidation of the specimens using the confining pressure at which there was a change in the relationship as described above. The finings are listed in Tables 9 through 11. Four specimens are felt to be essentially normally consolidated (Specimens Nos. 2, 8, 11 and 23), three specimens are slightly overconsolidated (Specimen Nos. 2, 3, and 10), two specimens are moderately overconsolidated (Specimen Nos. 6 and 22) and two specimens are

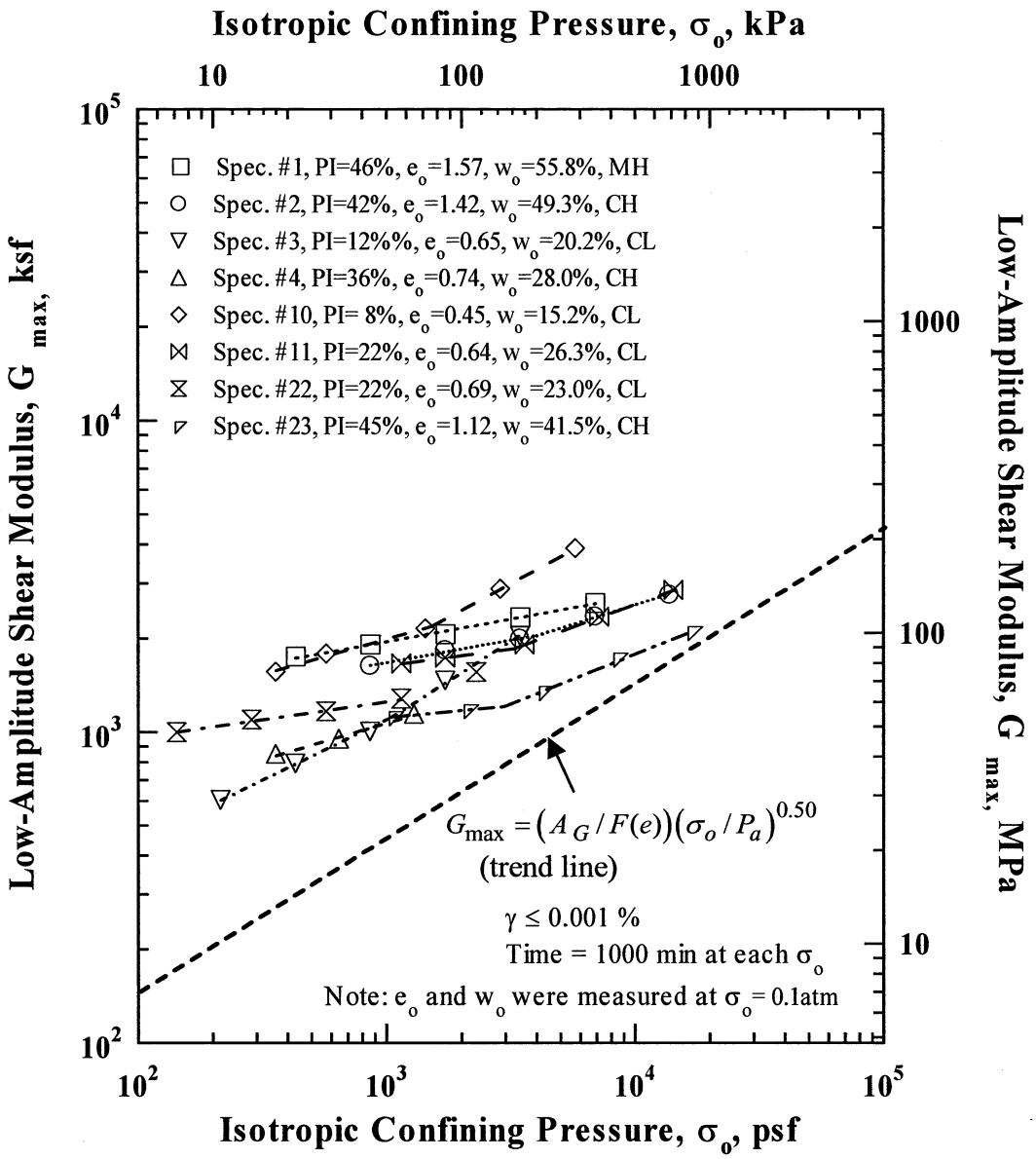

Figure 9 Variation in Low-Amplitude Shear Modulus with Isotropic Confining Pressure of the Eight Plastic Specimens in the Low In-Situ Confining Pressure Group as Determined from Resonant Column (RC) Tests

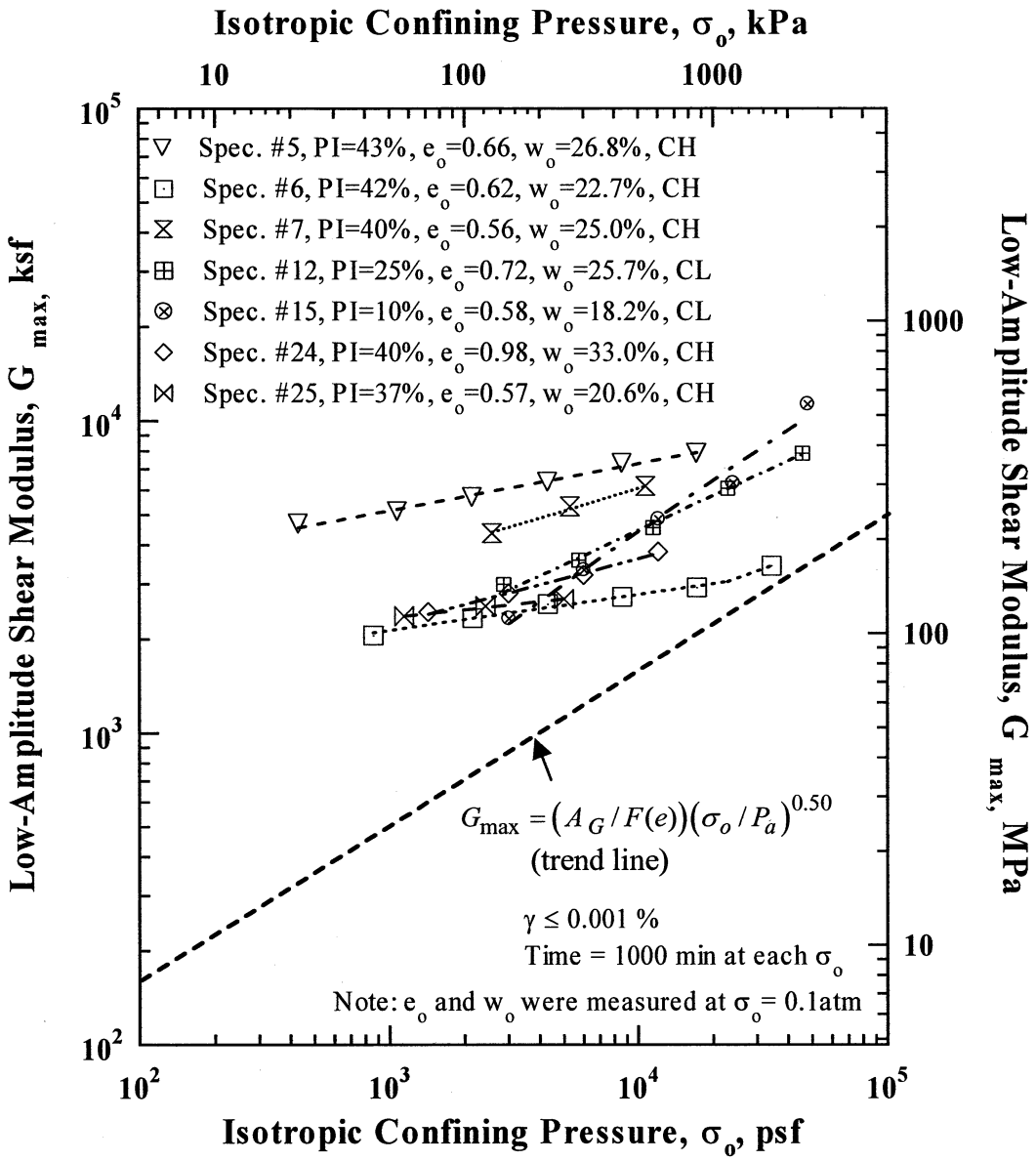

Figure 10 Variation in Low-Amplitude Shear Modulus with Isotropic Confining Pressure of the Seven, Plastic Specimens in the Medium In-Situ Confining Pressure Group as Determined from Resonant Column (RC) Tests

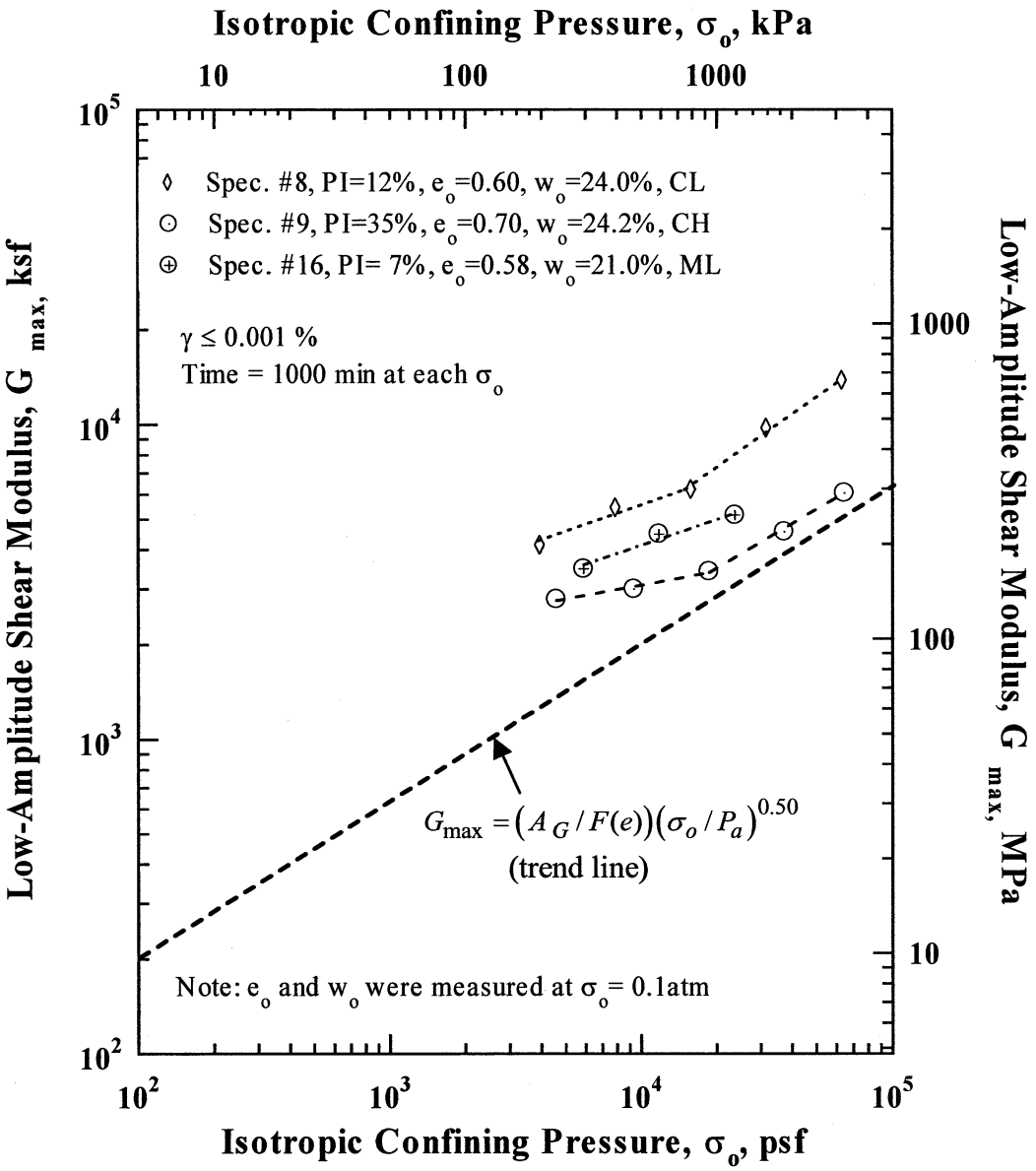

Figure 11 Variation in Low-Amplitude Shear Modulus with Isotropic Confining Pressure of the Three Plastic Specimens in the High In-Situ Confining Pressure Group as Determined from Resonant Column (RC) Tests

heavily overconsolidated (Specimen Nos. 1 and 5). The heavily overconsolidated specimens had mean confining pressures above those used. Due to excessive tilting of five specimens, testing above the estimated in-situ σ_m for the normally consolidated state could not be performed so no estimate of OCR could be made (Specimen Nos. 4, 7, 16, 24 and 25). Additionally, the steepness of the log G_{max} – log σ_o relationship (as if it were normally consolidated) combined with the lack of a change in the slope seems to reveal that Specimen Nos. 12 and 15 are disturbed (Figure 10). Specimen No. 16 also seems to be disturbed based on the ratio of shear modulus measured in the laboratory to shear modulus measured in the field by the suspension logging method. The value of the moduli ratio is 0.2. (This point is discussed further in Section 5 and the moduli ratio is shown in Table 14.)

3.2.3 Log D_{min} – Log σ_0 Relationships – The variations of material damping ratio with confining pressure, log D_{min} – log σ_o relationships, are shown in Figures 12, 13 and 14 for the low, medium and high confining pressure groups, respectively. As confining pressure increases, damping values for most specimens decrease. For some specimens, such as Specimen No. 15 in Figure 13, the specimens began to tilt excessively so that one of the drive magnets touched one of the drive coils. In this case, the confining chamber had to be opened in an attempt to continue the test. In the experience of the researchers, this process can lead to large changes in material damping, although it may not affect shear wave velocity and shear modulus very much.

The constants determined for Equation 3 from the best-fit lines by least-squares fitting of the loading results shown in Figures 9 through 11 are summarized in Tables 9 through 11. Reasonable values of the constants could be obtained when one tended to discount damping values which turned out to be outliers based on the trends found in the V_s and G_{max} relationships. In general, the heavily or moderately overconsolidated specimens exhibited a constant decrease in damping values. Constants for slightly overconsolidated and normally consolidated specimens were found in both the overcosolidated and normally consolidated regions. For Specimen No. 15, which is possibly quite disturbed, the first three damping values were weighted very lightly in an attempt to avoid misleading results.

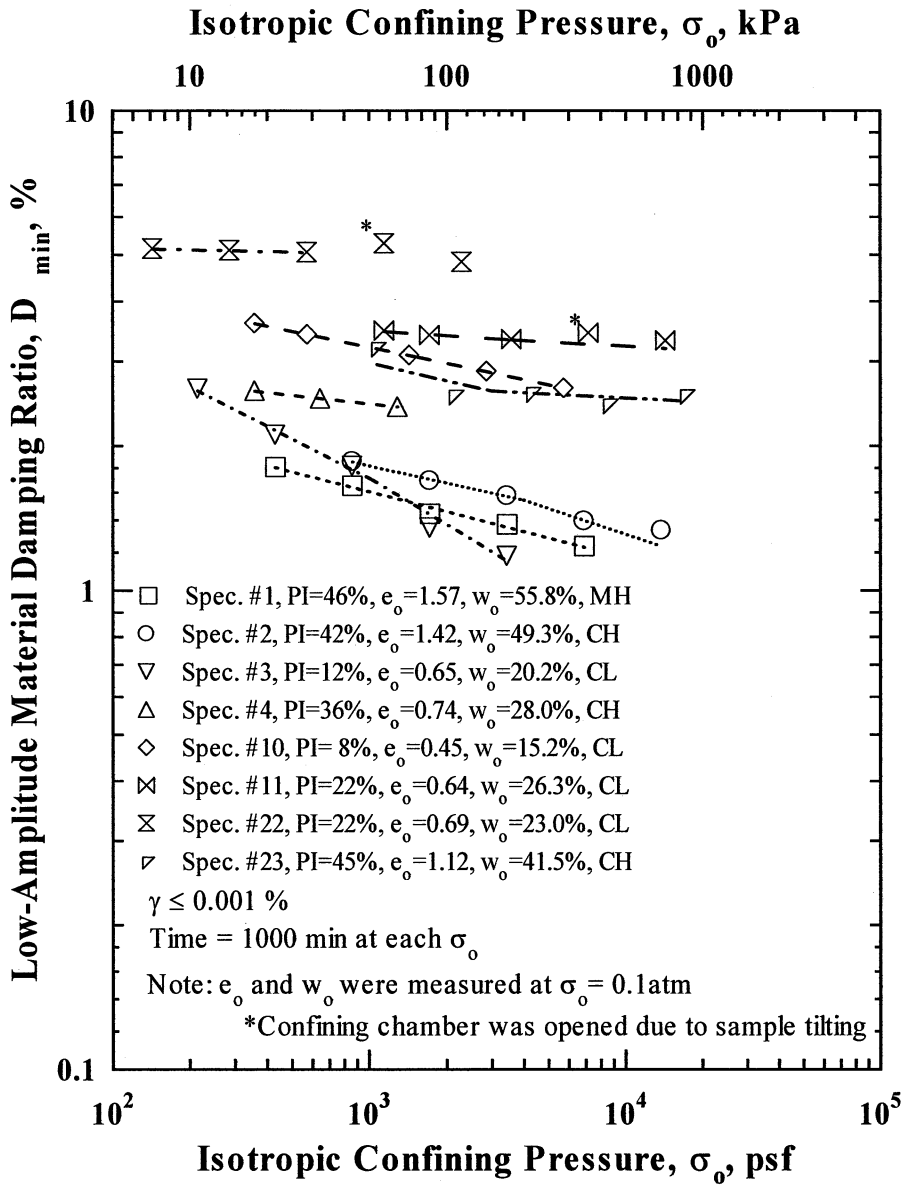

Figure 12 Variation in Material Damping Ratio with Isotropic Confining Pressure of the Eight, Plastic Specimens in the Low In-Situ Confining Pressure Group as Determined from Resonant Column (RC) Tests

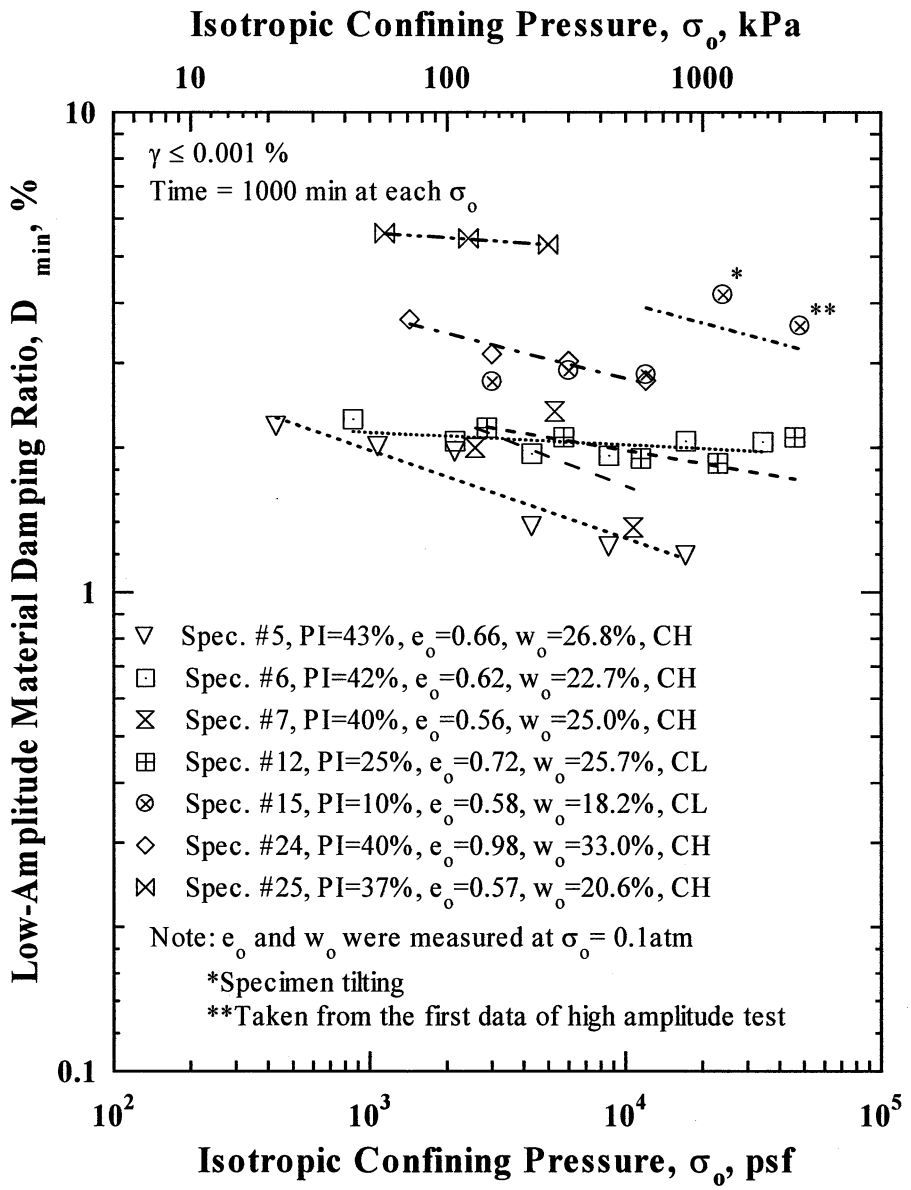

Figure 13 Variation in Material Damping Ratio with Isotropic Confining Pressure of the Seven, Plastic Specimens in the Medium In-Situ Confining Pressure Group as Determined from Resonant Column (RC) Tests

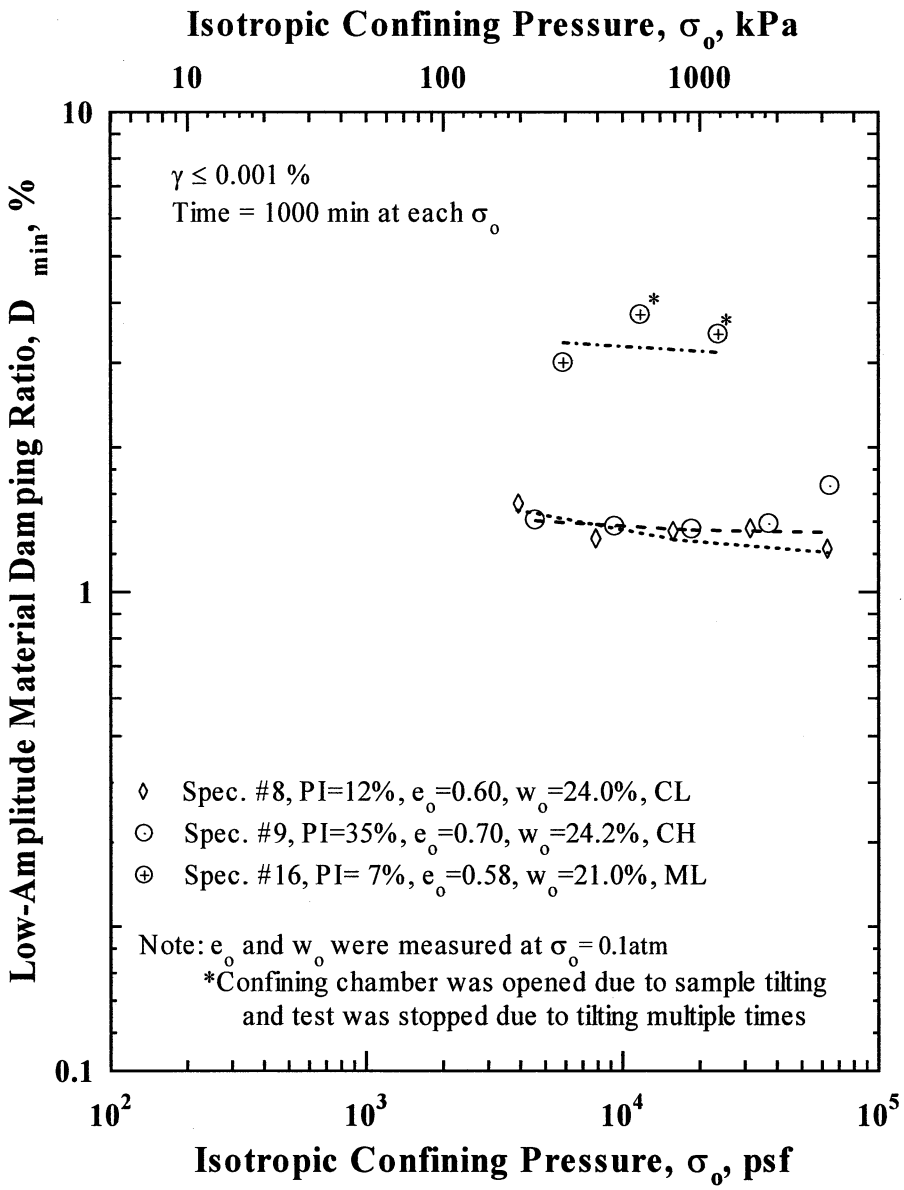

Figure 14 Variation in Material Damping Ratio with Isotropic Confining Pressure of the Three, Plastic Specimens in the High In-Situ Confining Pressure Group as Determined from Resonant Column (RC) Tests

3.3 Variations of Void Ratio with Confining Pressure

3.3.1 Nonplastic Specimens - The variations of void ratio, e, with isotropic confining pressure, σ_o, for the seven sand specimens are presented in Figure 15. As discussed previously, Specimen No. 17 exhibited the smallest void ratio change over all three confining pressure levels because this specimen is thought to be cemented and/or overconsolidated. The largest change (decrease) in void ratio with increasing σ_o was exhibited by Specimen No. 18, which likely results from disturbance. Specimen No. 13 exhibited a relatively small change in void ratio with pressure, compared with the other specimens having similar values of n_G and n_V. This small change resulted, at least in part, from the initially low void ratio of Specimen No. 13.

3.3.2 Plastic Specimens - For the plastic specimens, the variations of void ratio with increasing isotropic confining pressure are shown in Figures 16 through 18 for the low, medium and high in-situ confining pressure groups, respectively. The shapes of the e-log σ_o curves support, in general terms, the estimation of overconsolidation state discussed earlier and presented in Tables 9, 10 and 11.

3.4 Changes in G_{max} and D_{min} with Excitation Frequency

3.4.1 Nonplasic Specimens - The effect of loading frequency on the small-strain shear modulus, G_{max}, at γ = 0.001 % of the seven, nonplastic specimens is shown in Figure 19. The effect of loading frequency on the small-strain material damping ratio, D_{min} (γ = 0.001 %), for these specimens is shown in Figure 20. Both the shear modulus, G_{max}, and the material damping ratio, D_{min}, have been normalized by the values measured in the torsional shear tests at 1Hz. All measurements were performed at only one σ_o, the estimated in-situ σ_o if K_o = 0.5.
As shown in Figure 19, loading frequency has little effect on G_{max}. The shear moduli measured at frequencies around 100 Hz in the RC tests are, on average, about 5 to 10 % greater

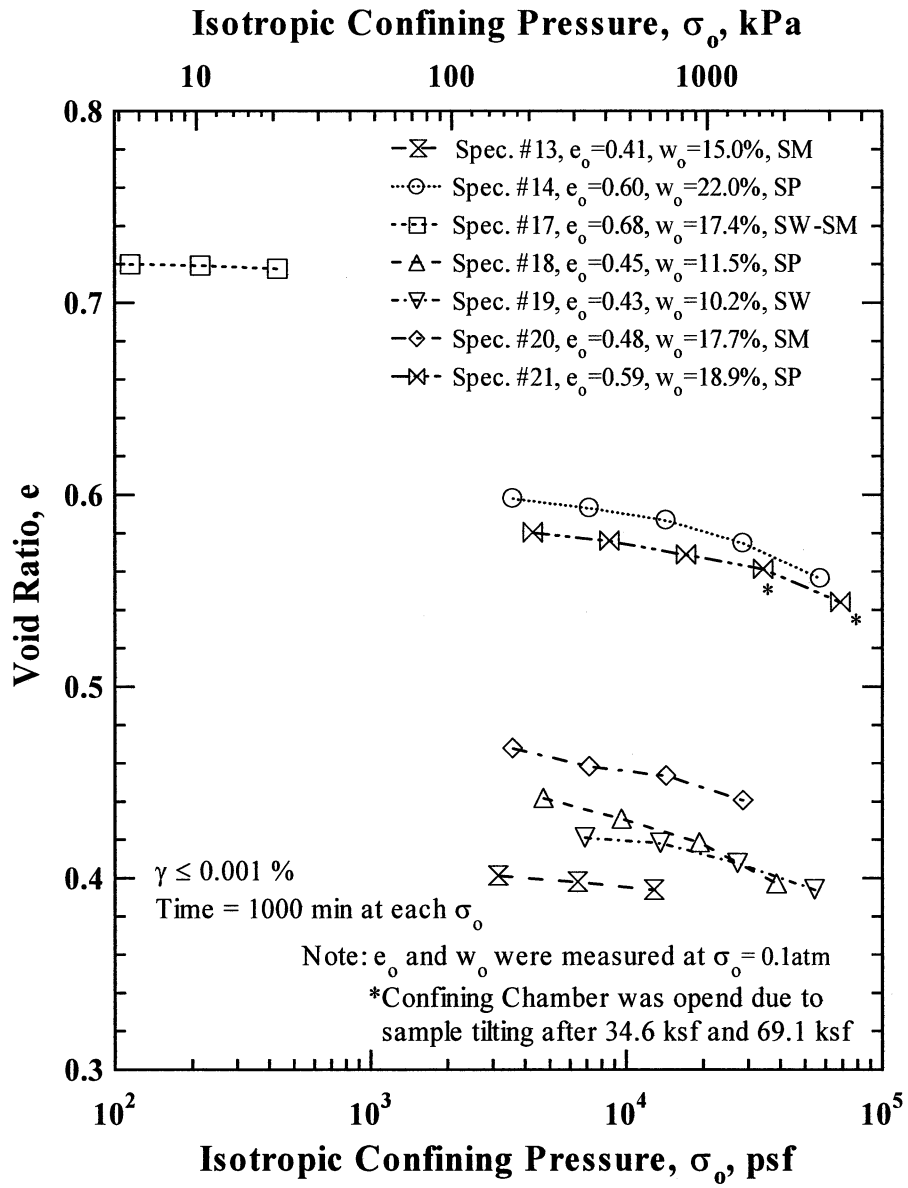

Figure 15 Variation in Void Ratio with Isotropic Confining Pressure of the Seven, Nonplastic Specimens as Determined from Resonant Column (RC) Test

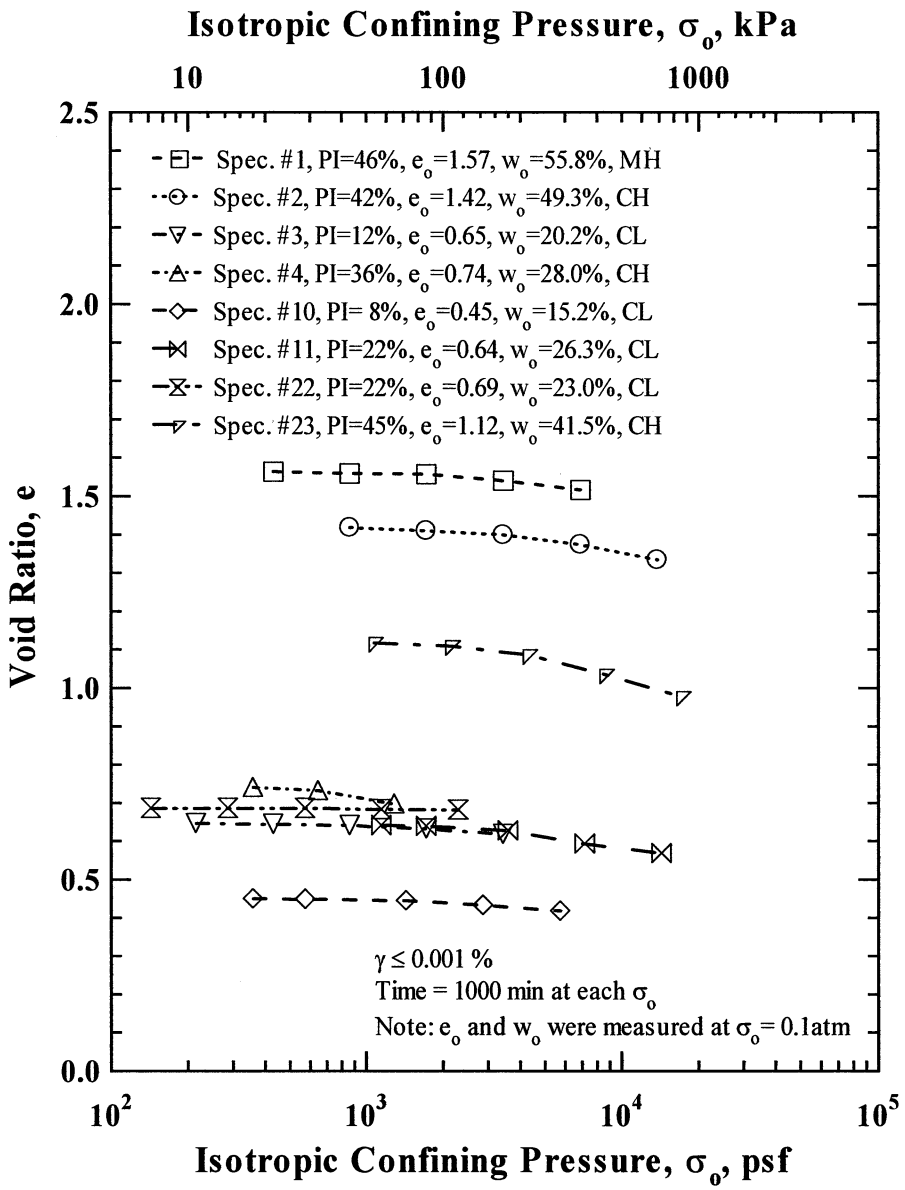

Figure 16 Variation in Void Ratio with Isotropic Confining Pressure of the Eight, Plastic Specimens in the Low In-Situ Confining Pressure Group as Determined from Resonant Column (RC) Tests

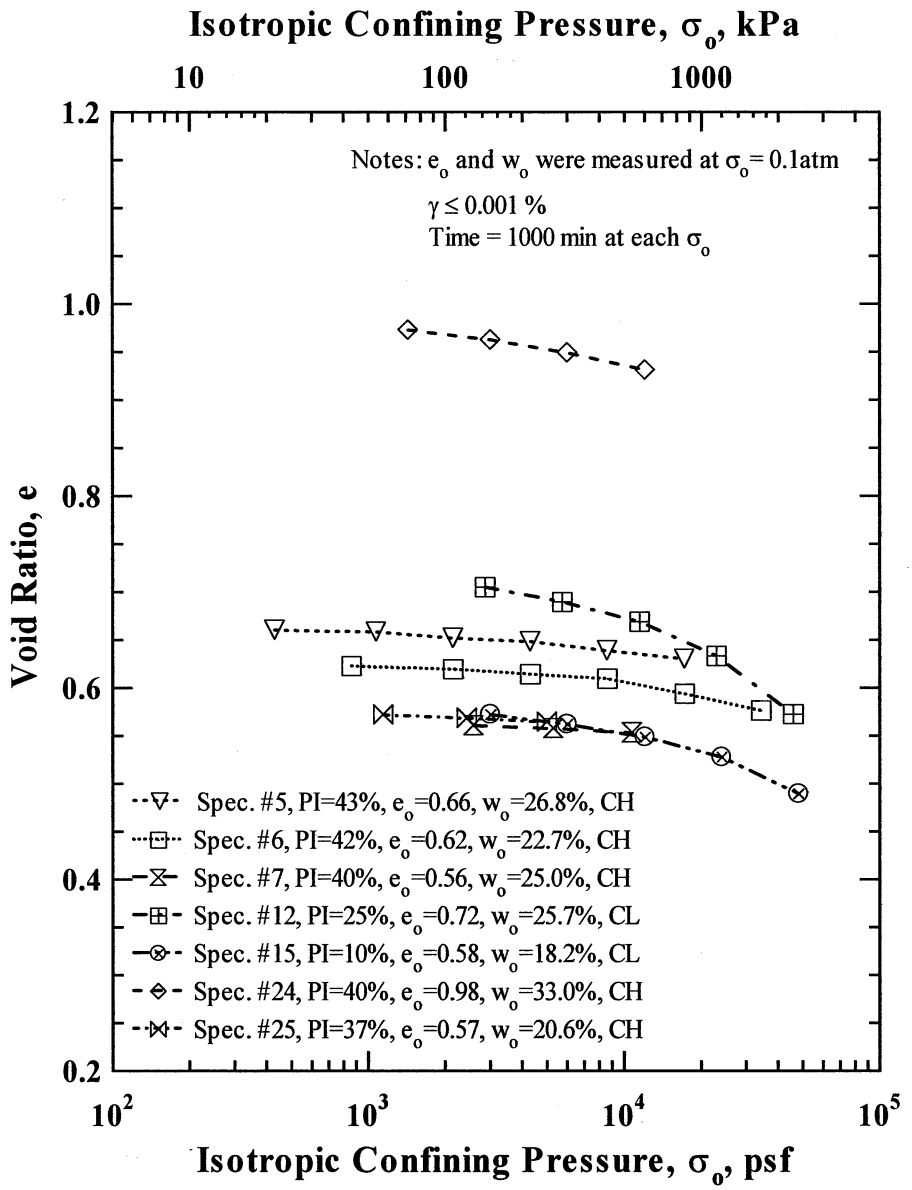

Figure 17 Variation in Void Ratio with Isotropic Confining Pressure of the Seven, Plastic Specimens in the Medium In-Situ Confining Pressure Group as Determined from Resonant Column (RC) Tests

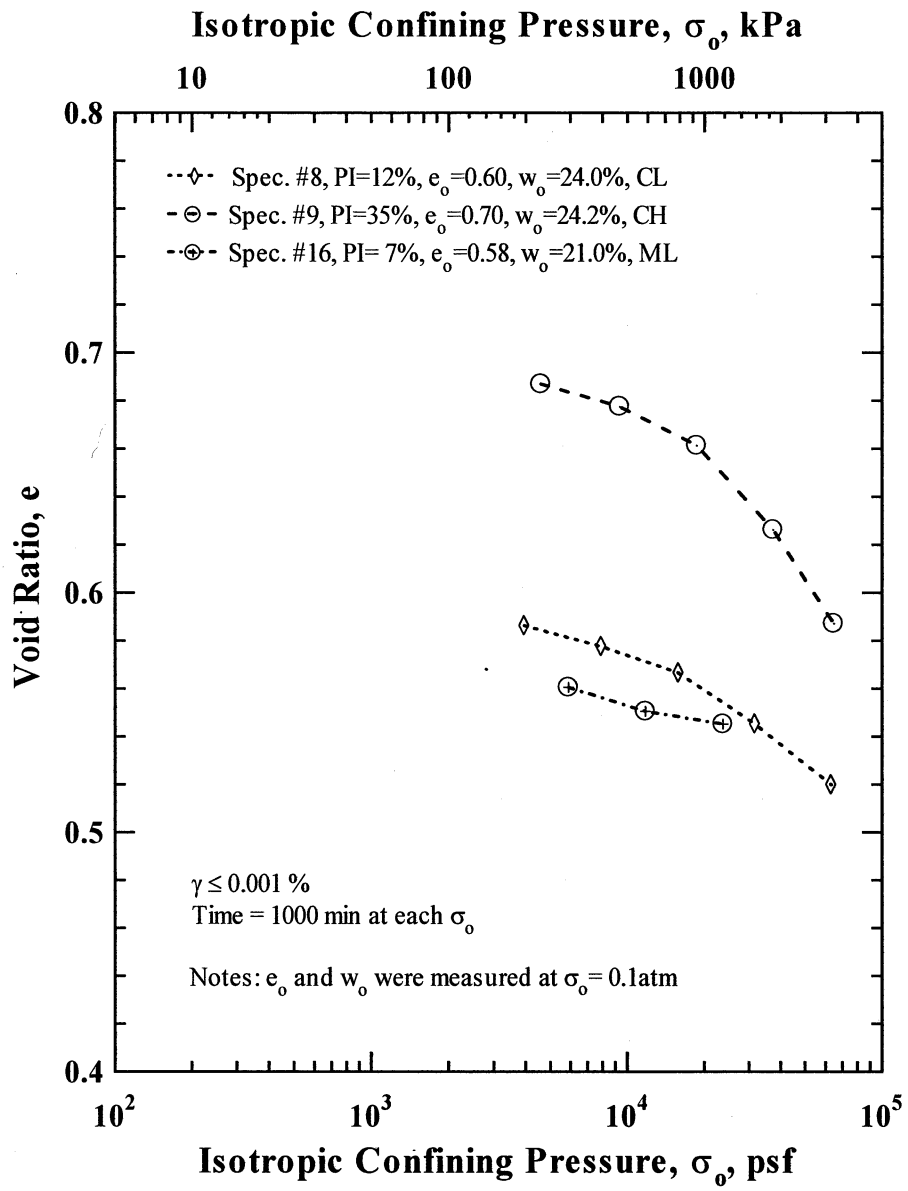

Figure 18 Variation in Void Ratio with Isotropic Confining Pressure of the Three, Plastic Specimens in the High In-Situ Confining Pressure Group as Determined from Resonant Column (RC) Tests

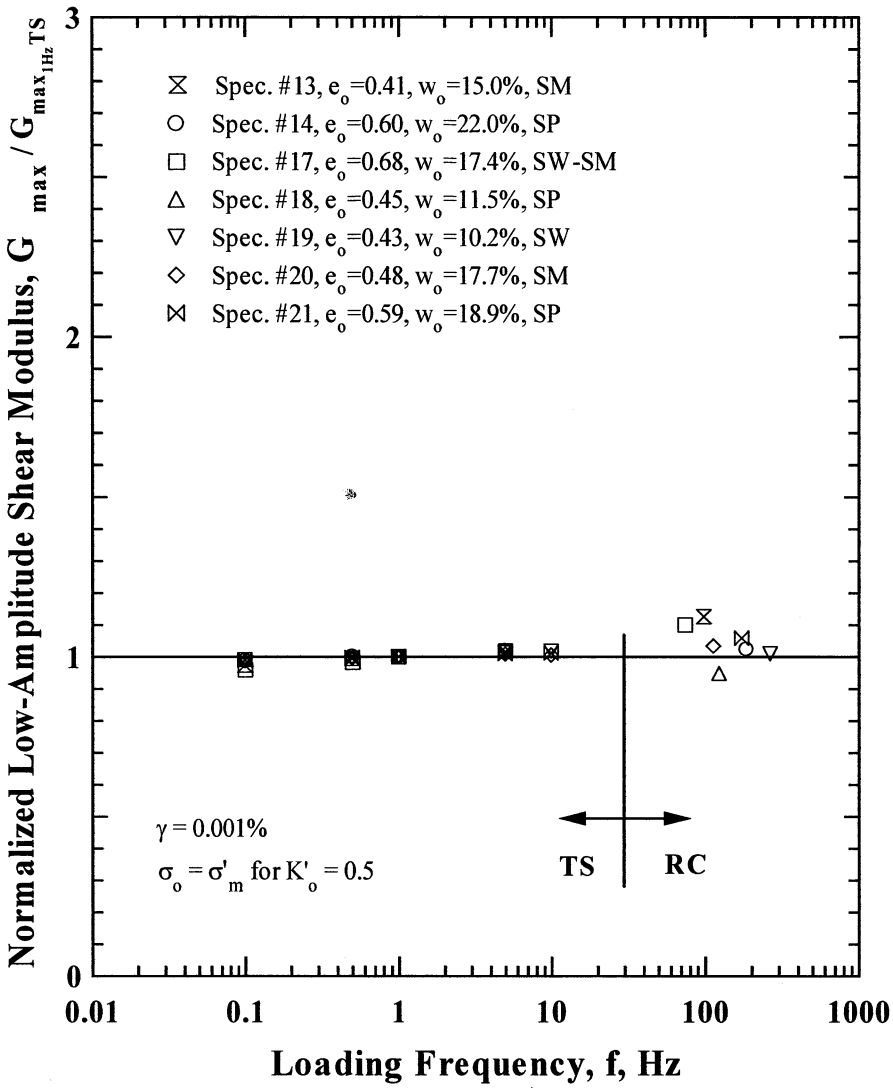

Figure 19 Variation in Normalized Low-Amplitude Shear Modulus with Loading Frequency of the Seven, Nonplastic Specimens as Determined from Resonant Column (RC) and Torsional Shear (TS) Tests at Estimated In-Situ Confining Pressures

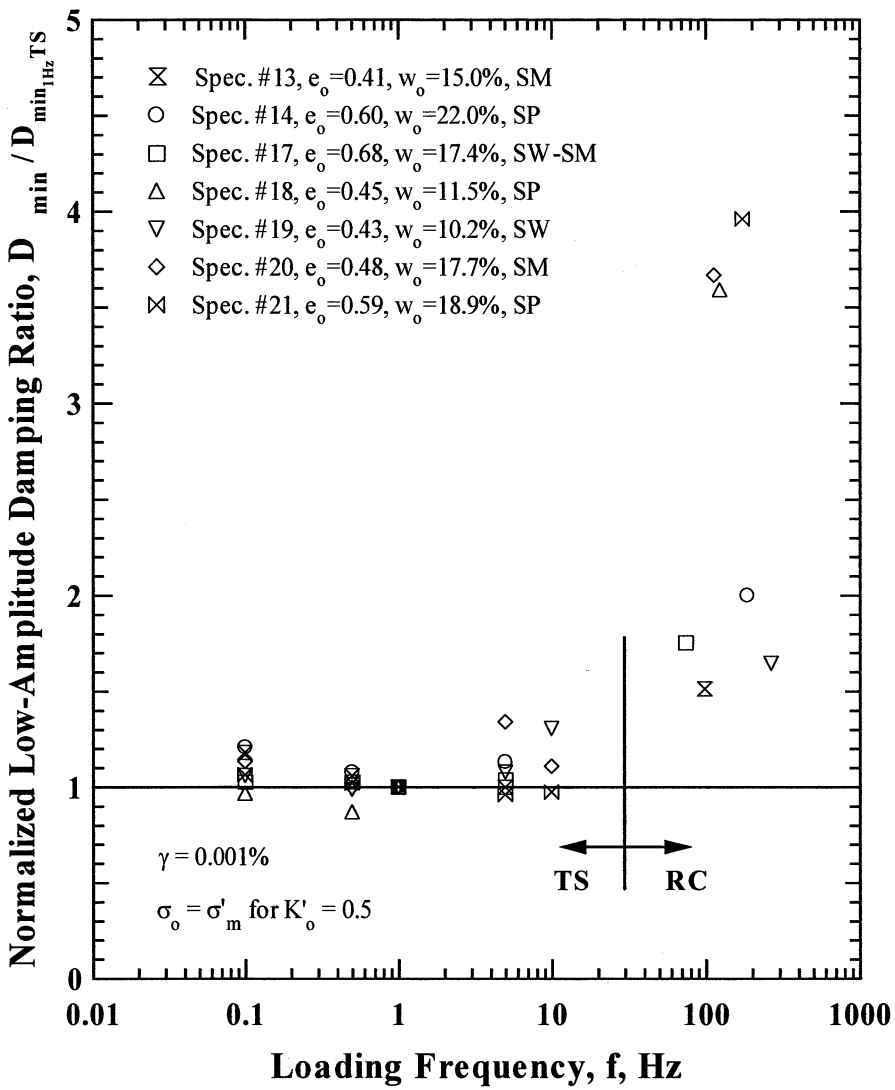

Figure 20 Variation in Normalized Low-Amplitude Material Damping Ratio with Loading Frequency of the Seven, Nonplastic Specimens as Determined from Resonant Column (RC) and Torsional Shear (TS) Tests

than the values measured at 1 Hz. The largest change is about 15% which is exhibited by Specimen No. 13.

A much larger effect of loading frequency occurs on D_{min} than on G_{max}. This effect occurs over the range of frequencies between 5 and 265 Hz as shown in Figure 20. Since the RC tests involve measurements at the resonant frequency of the specimen (74 to 265 Hz in these particular tests) and the TS tests involve measurements at considerably lower frequencies (0.1 to 10 Hz), the frequency dependency of D_{min} is readily evaluated by combined RC and TS testing. It is also interesting to note that Specimen Nos. 18, 20, and 21, which exhibit the steepest slopes in the confining pressure domain, also show the largest frequency dependency. However, there is no clear trend between frequency dependency and void ratio, water content or material classification.. Material damping ratios measured in the resonant column tests are about 1.5 to 4 times higher than those measured in the torsional shear tests at 1 Hz.

3.4.2 Plastic Specimens - The effect of loading frequency on the small-strain shear modulus, G_{max}, at $\gamma = 0.001$ % of the 18 plastic specimens is shown in Figures 21 through 23, dividing the three groups into the confining pressure ranges previously used. The effect of loading frequency on the material damping ratio, D_{min}, at small strains ($\gamma = 0.001$ %) for these specimens is shown in Figures 24 through 26.

As measured with the nonplastic specimens, the frequency dependency of G_{max} of the plastic specimens is quite similar, but just slightly greater.

A similar frequency dependency of D_{min} with the previous comparison with the sand specimens is observed in Figures 24 through 26, with difference of frequency effects shown at 0.1Hz, 0.5Hz, and 5Hz in the torsional shear tests. In comparison with nonplastic soil, relatively larger frequency effects at 0.1 Hz, especially, occurred in the plastic soils.

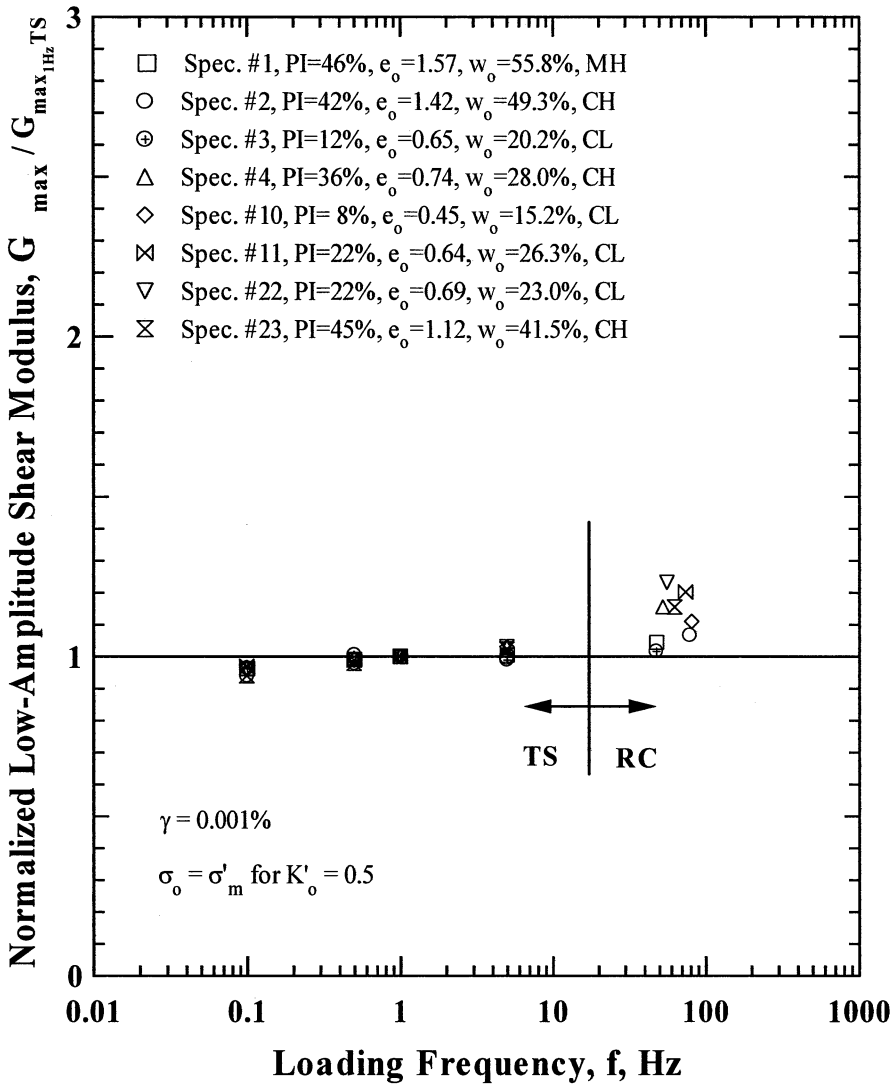

Figure 21 Variation in Normalized Low-Amplitude Shear Modulus with Isotropic Confining Pressure of the Eight, Plastic Specimens in the Low In-Situ Confining Pressure Group as Determined from Resonant Column (RC) and Torsional Shear (TS) Tests

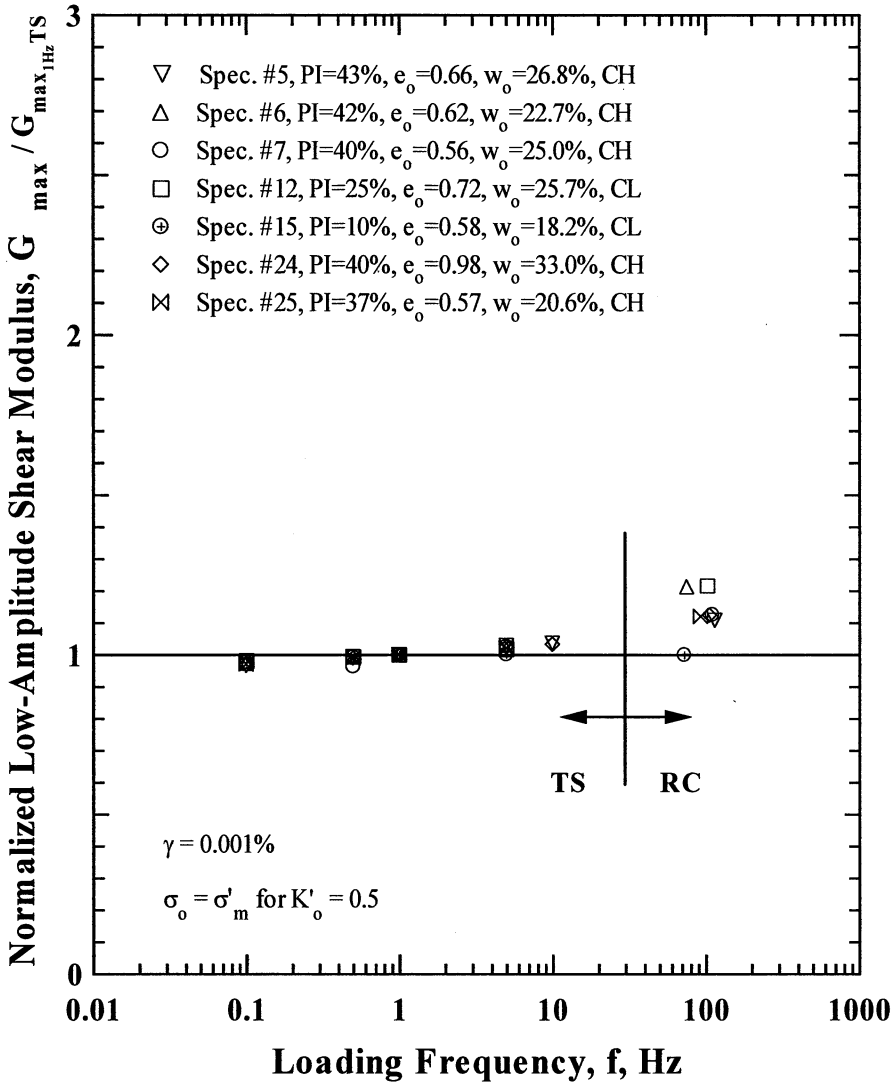

Figure 22 Variation in Normalized Low-Amplitude Shear Modulus with Isotropic Confining Pressure of the Seven, Plastic Specimens in the Medium In-Situ Confining Pressure Group as Determined from Resonant Column (RC) and Torsional Shear (TS) Tests

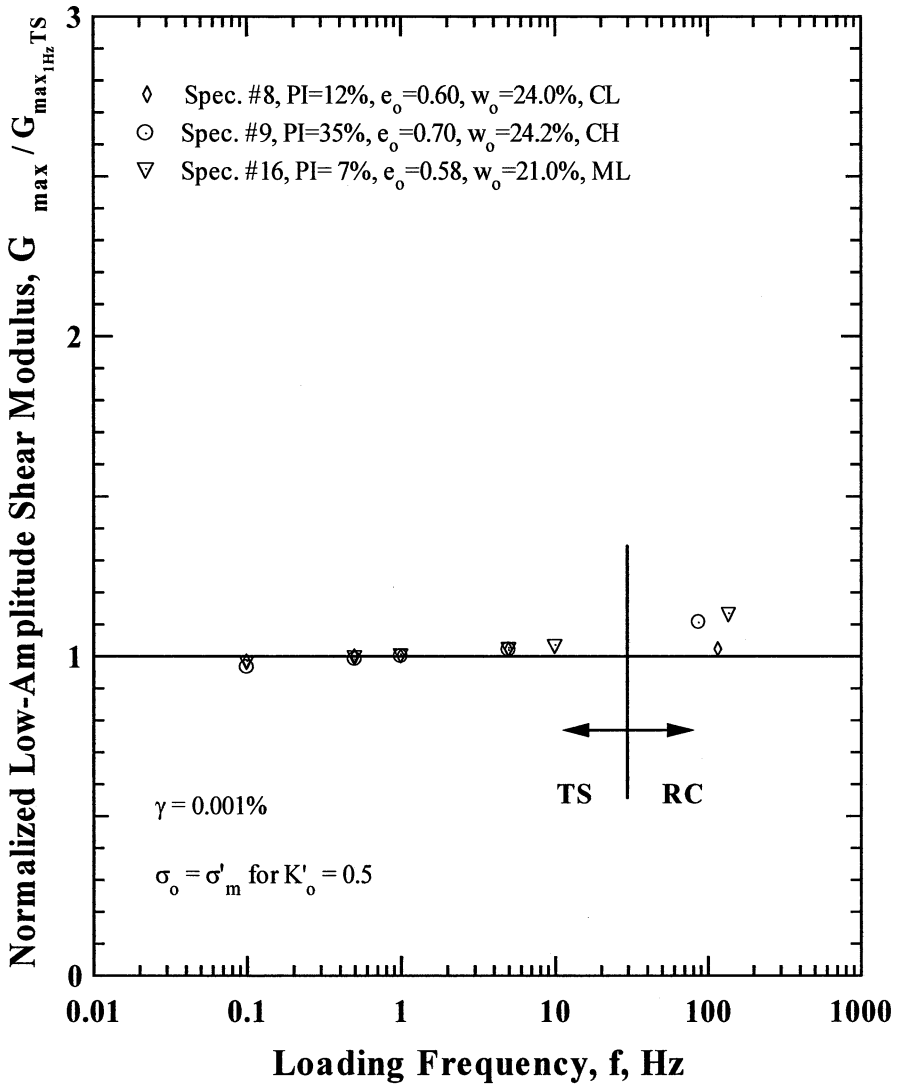

Figure 23 Variation in Normalized Low-Amplitude Shear Modulus with Isotropic Confining Pressure of the Three, Plastic Specimens in the High In-Situ Confining Pressure Group as Determined from Resonant Column (RC) and Torsional Shear (TS) Tests

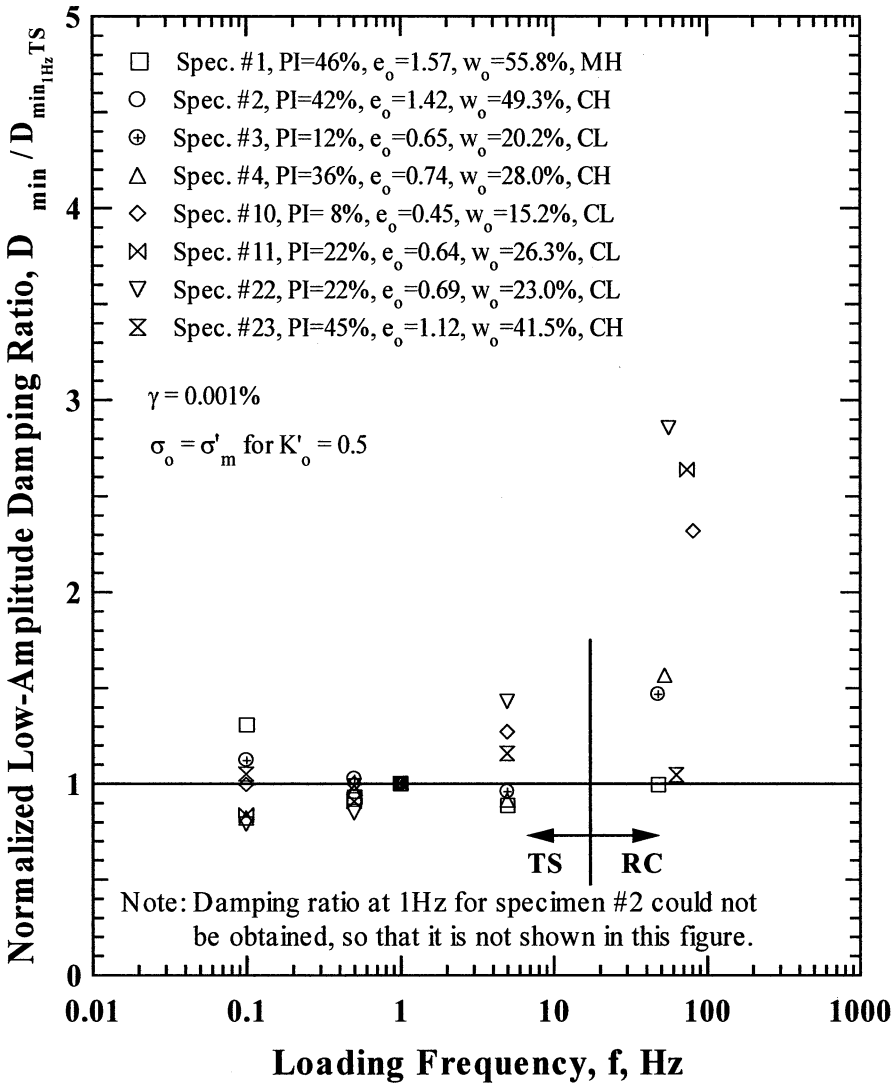

Figure 24 Variation in Normalized Low-Amplitude Material Damping Ratio with Isotropic Confining Pressure of the Eight, Plastic Specimens in the Low In-Situ Confining Pressure Group Specimens as Determined from Resonant Column (RC) and Torsional Shear (TS) Tests

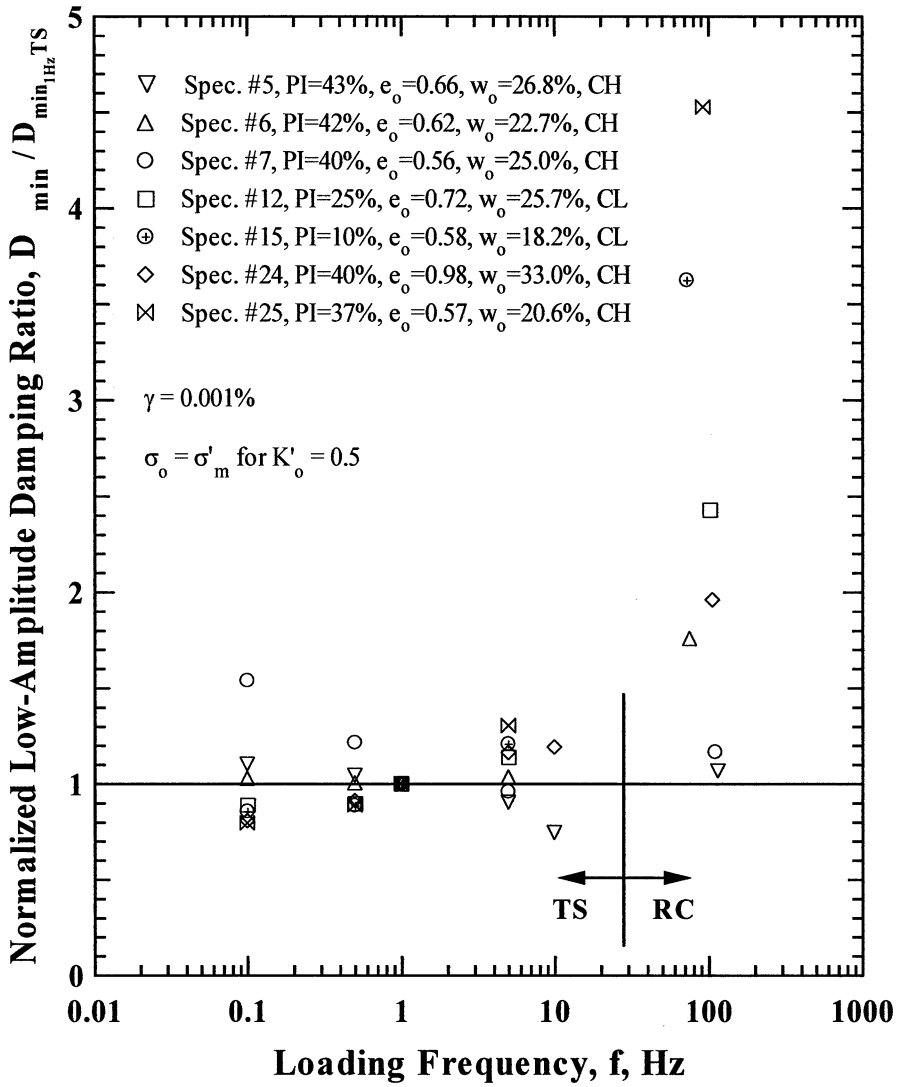

Figure 25 Variation in Normalized Low-Amplitude Material Damping Ratio with Isotropic Confining Pressure of the Seven, Plastic Specimens in the Medium In-Situ Confining Pressure Group Specimens as Determined from Resonant Column (RC) and Torsional Shear (TS) Tests

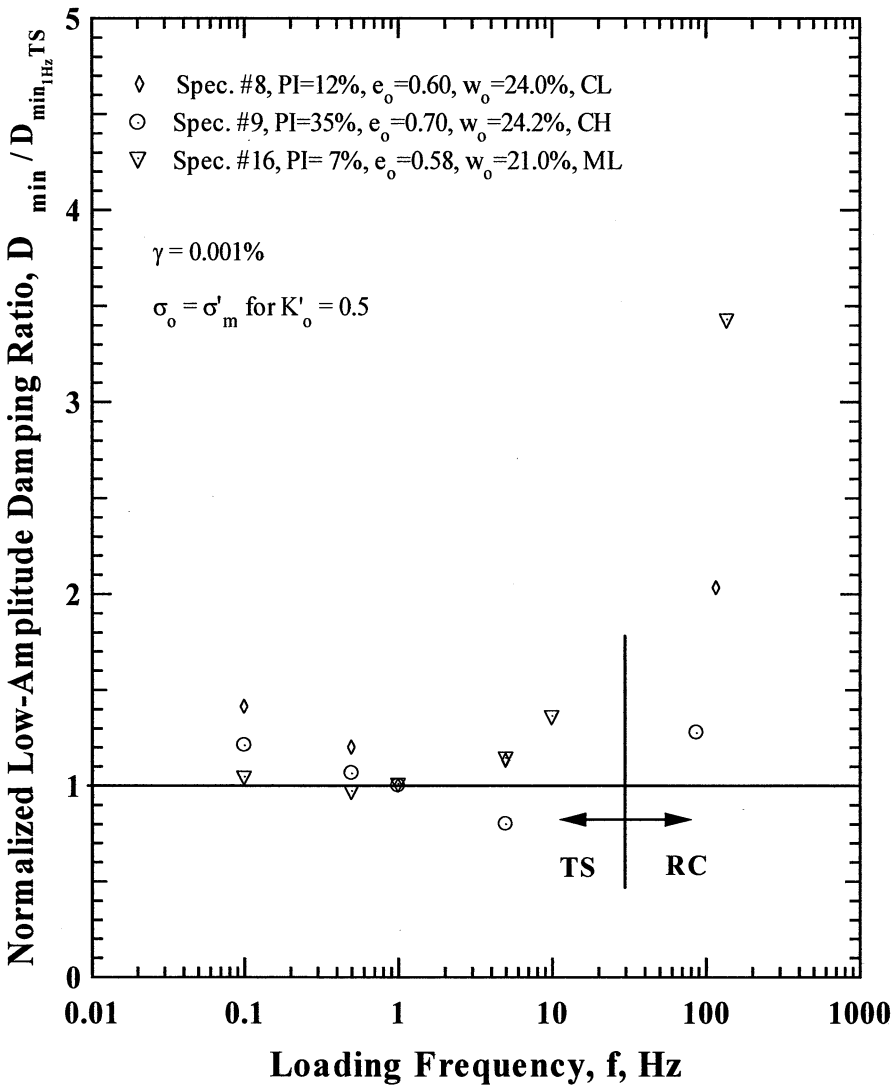

Figure 26 Variation in Normalized Low-Amplitude Material Damping Ratio with Isotropic Confining Pressure of the Three, Plastic Specimens in the High In-Situ Confining Pressure Group Specimens as Determined from Resonant Column (RC) and Torsional Shear (TS) Tests

4 DYNAMIC TEST RESULTS IN THE NONLINEAR RANGE

The discussion of the RCTS measurements in the nonlinear range, the strain range where G and D are dependent on strain amplitude, are presented in this section. The section is divided into two sub-sections, the first dealing with the G – log γ and G/Gmax – log γ relationships and the second dealing with the D - log γ relationships. Further, each sub-section is divided into the following four parts: (1) the first one dealing with the seven nonplastic specimens, (2) the second one dealing with the eighteen plastic specimens, (3) the third part dealing with comparisons between the dynamic properties measured in this study and dynamic properties predicted with nonlinear models proposed by Seed et al. 1986, and Vucetic and Dobry, 1991, and (4) the fourth part comparing the measured values with those predicted with the nonlinear model proposed by Darendeli, 2001.

4.1 Nonlinear G – Log γ and G/G_{max} – Log γ Relationships

***4.1.1 Nonlinear G - Log γ* and G/G_{max} – Log γ *Relationships of the Nonplastic Specimens* -** Results of the G - log γ measurements of the seven nonplastic specimens determined by the RC tests are presented in Figure 27 for measurements at the estimated in-situ confining pressures which ranged from of 0.43 ksf (21 kPa) to 27.36 ksf (1312 kPa). As expected, the shear moduli of all specimens exhibit a linear range (where G is constant and equal to G_{max}) followed by a nonlinear range where G decreases with increasing shearing strain.

Comparisons of the G - log γ relationships measured in the RC and TS tests are shown in Figure 28 for Specimen Nos. 14 and 20. Comparisons for the other specimens are shown in the appendices. Two points are clearly shown in these figures. First, similar G – log γ curves are measured in both tests, with the main difference related to the effect of excitation frequency. Second, the RC test can excite the specimens to larger strains because of dynamic amplification which enters the RC test but does not enter the "slow cyclic" TS tests which were conducted at 0.5 Hz.

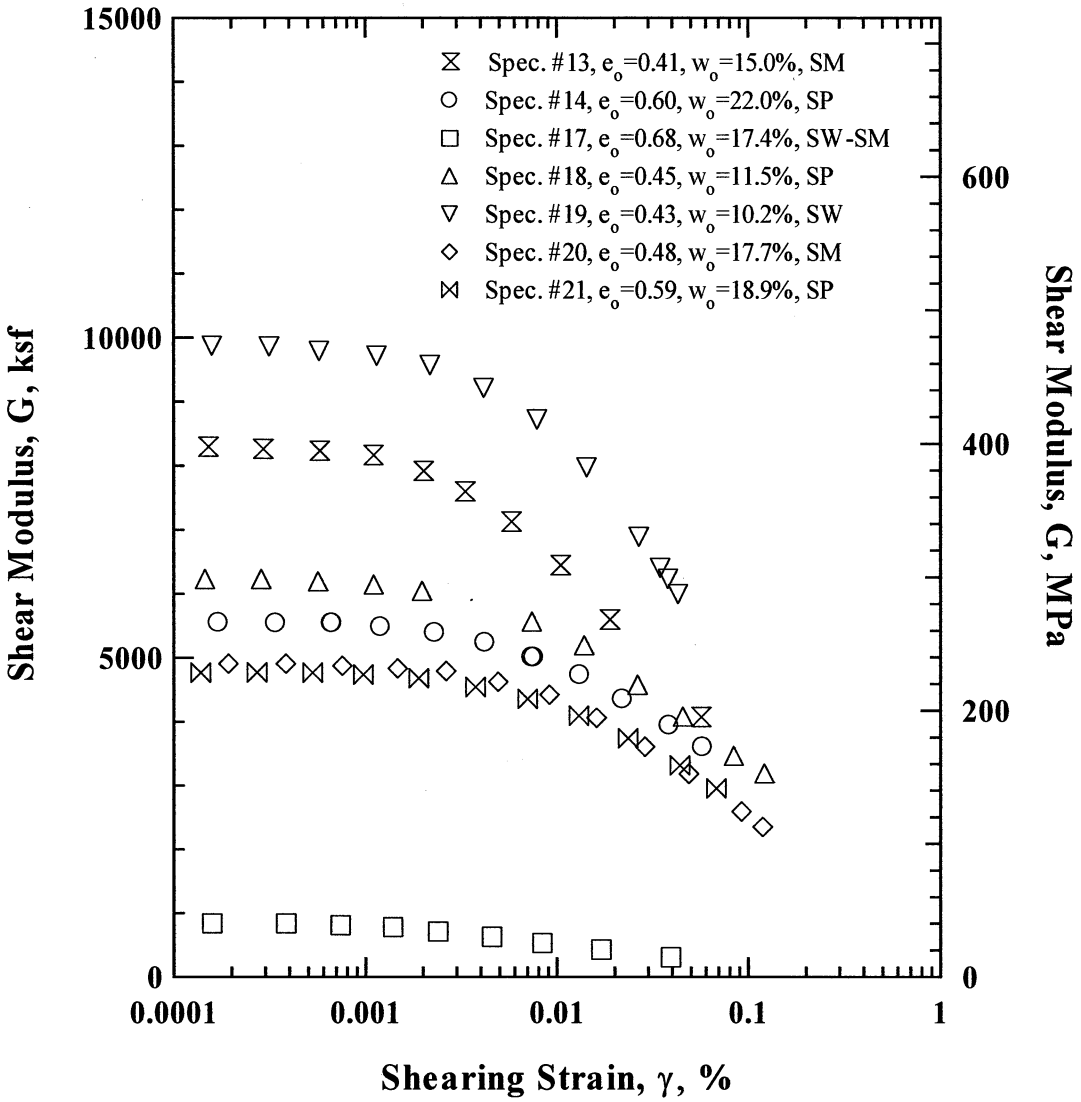

Figure 27 Variation in Shear Modulus with Shearing Strain from Resonant Column (RC) Tests of the Seven, Nonplastic Specimens Tested at Their Estimated In-Situ Confining Pressures

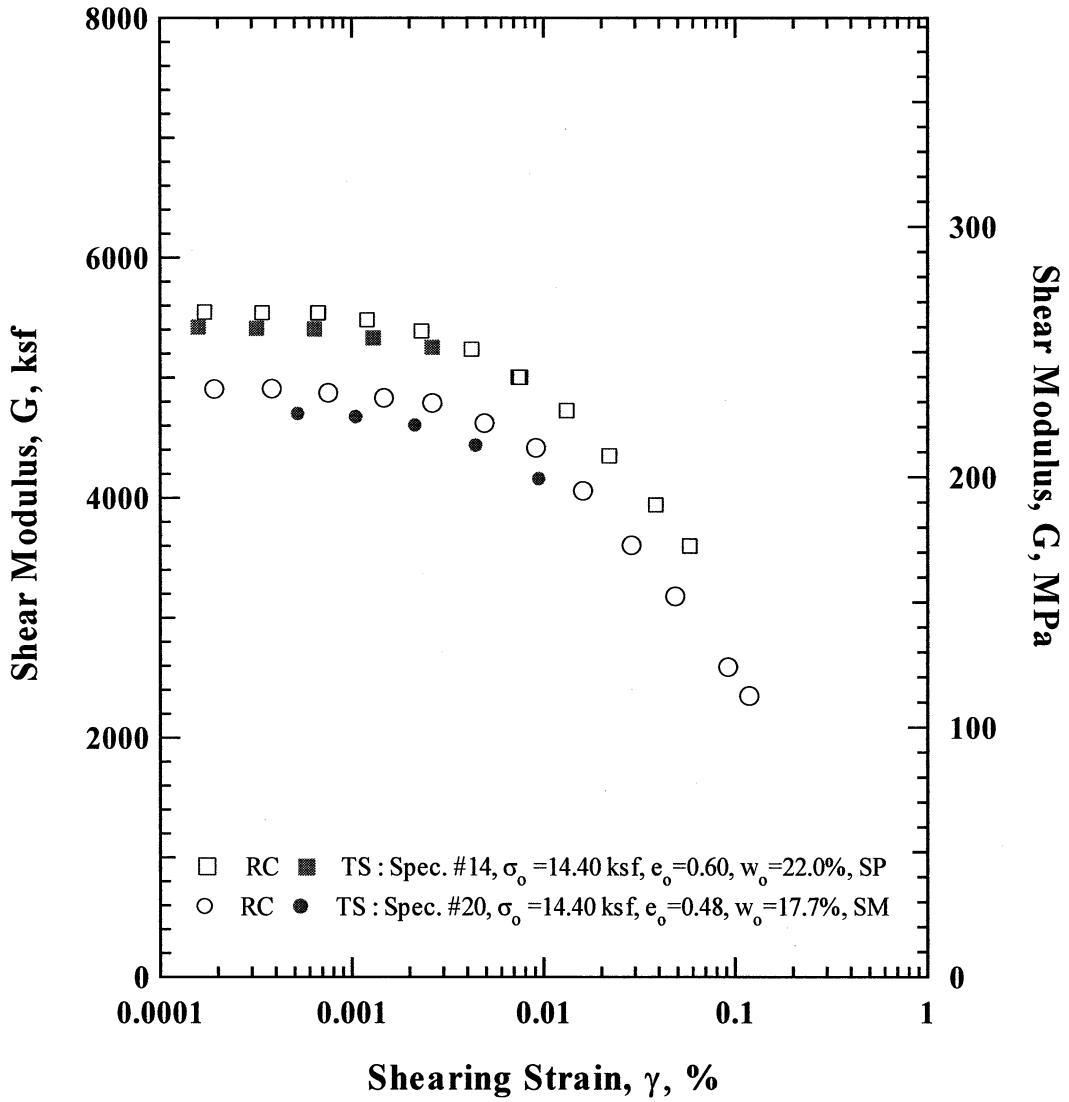

Figure 28 Variation in Shear Modulus with Shearing Strain from Resonant Column (RC) and Torsional Shear (TS) Tests of Nonplastic Specimen Nos. 14 and 20 Tested at Their Estimated In-Situ Confining Pressures

The normalized shear modulus relationships (G/G_{max} - log γ) of all nonplastic specimens measured in the RC tests are shown in Figure 29. The same RC and TS comparisons cited above are presented in terms of G/G_{max} – log γ in Figure 30. Similar relationships were found with both testing techniques, with the difference being the lack of higher strain measurements in the TS tests. All normalized modulus degradation curves are compared with the relationship suggested by Seed et al. (1986) in Figure 29. All specimens, except Specimen No. 17, behave more linearly than the mean Seed et al. relationship; that is, the normalized modulus reduction curves are above the mean curve of Seed et al. (1986). Specimen No. 17 exhibits less linear behavior because it is confined at a very low pressure ($\sigma_o \sim 0.2$ atm), relatively speaking. (This point is discussed further in Section 4.1.3.) The overconsolidation and/or possible cementation of the specimen may also contribute to the nonlinearity measured in Specimen No. 17. The other specimens were tested at much higher confining pressures (σ_o ranging from about 6.1 to 12.9 atm, and averaging 8.3 atm).

It is interesting to replot the data in Figure 29 in the following sub-sets: (1) without Specimen No.17 as shown in Figure 31, (2) with only Specimen Nos. 13 and 20 (Figure 32), and (3) with only Specimen Nos. 14, 18 and 21 as shown in Figure 33. The results in Figure 31 show the impact of confining pressure; that is, all measured nonlinear relationships plot above the mean sand curve from Seed et al. (1986) because this curve was generally developed (implicitly) for $\sigma_o \sim 1$ atm. The results in Figure 32 are for silty sands (SM). In this case, each specimen has about the same parameters and is tested at nearly the same pressure (within about 10%). Therefore, the results seem to be indicative of the variation that may be found in the general behavior of "similar" soils. (This point is discussed further in Section 4.1.4 and shown in Figure 52.) However, they may also be influenced by parameters that have not been measured (such as mineral content of the fines). Figure 33 shows only the SP specimens. In this case, a close comparison between the G/G_{max} – log γ curves is found. Also, the maximum difference in confining pressures for the three SP specimens is about 30 %, so this change in pressure is insignificant in this comparison.

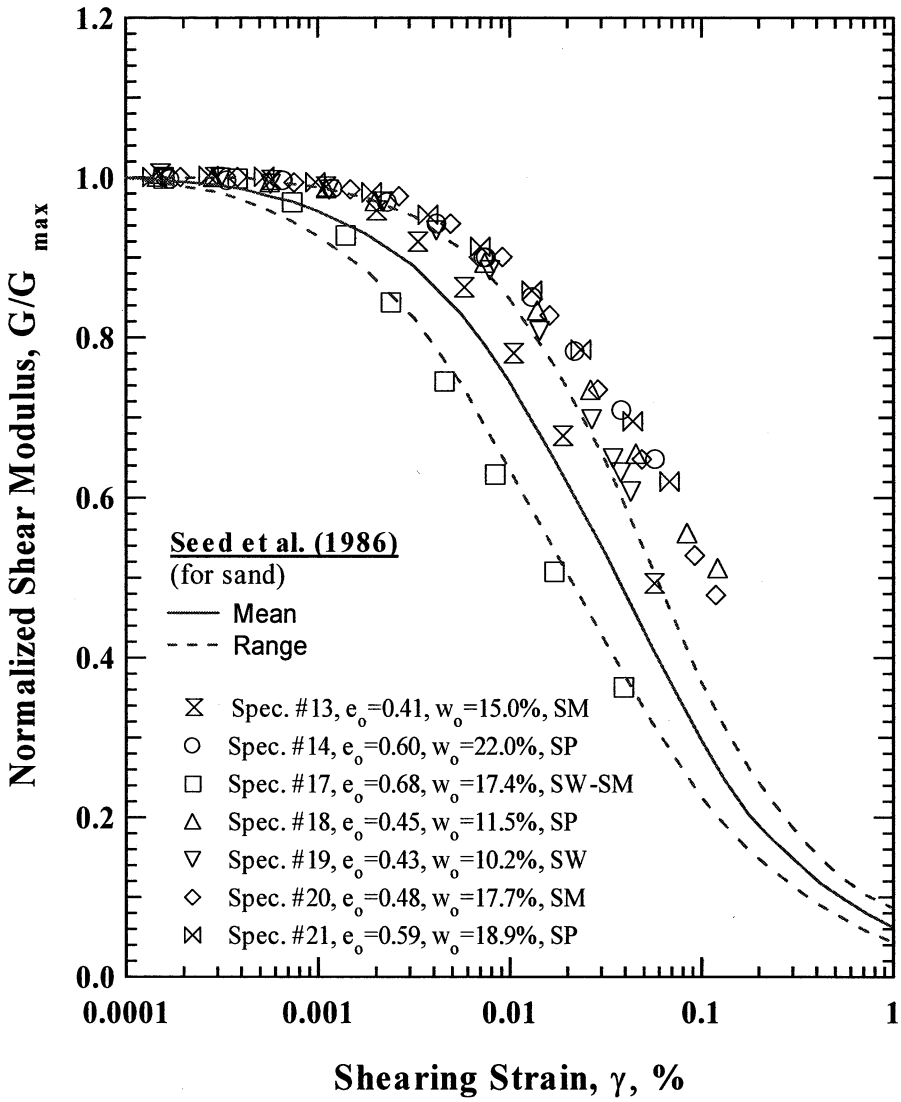

Figure 29 Variation in Normalized Shear Modulus with Shearing Strain from Resonant Column (RC) Tests of the Seven, Nonplastic Specimens Tested at Their Estimated In-Situ Confining Pressures

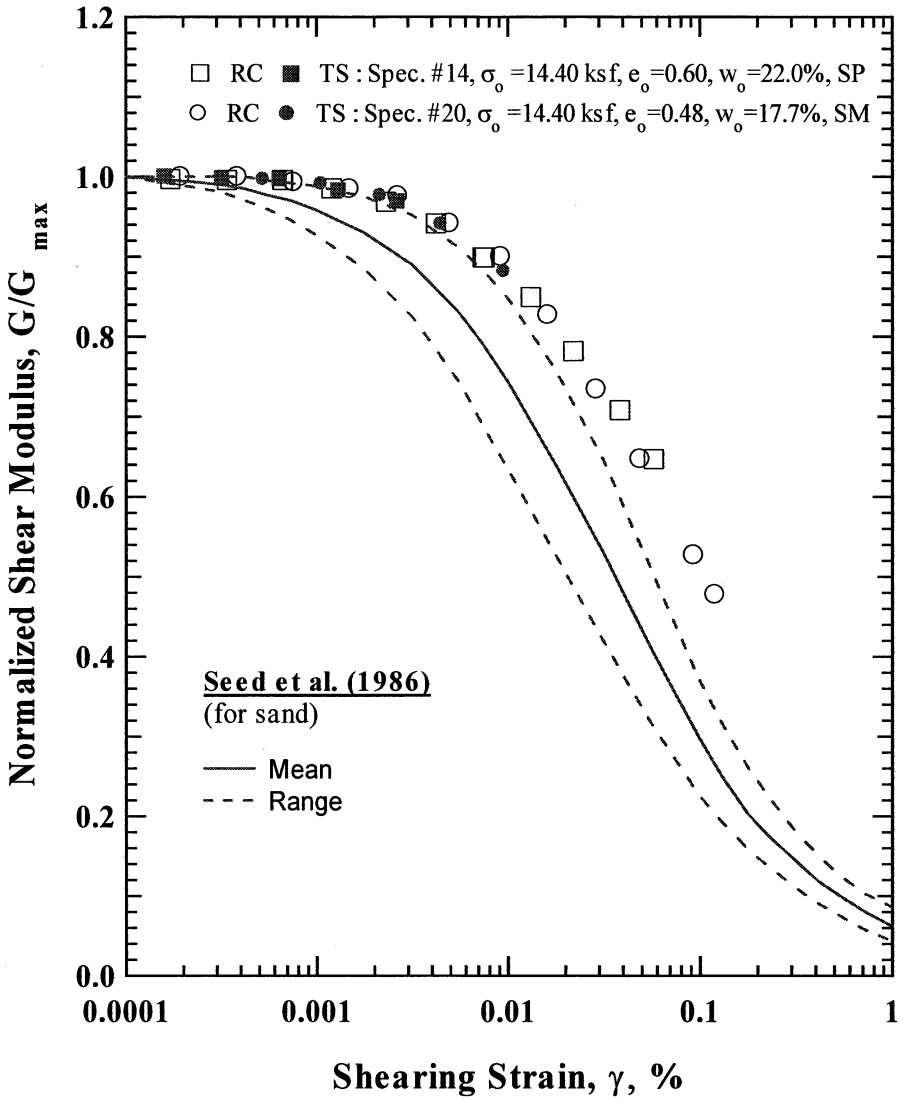

Figure 30 Variation in Normalized Shear Modulus with Shearing Strain from Resonant Column (RC) and Torsional Shear (TS) Tests of Nonplastic Specimen Nos. 14 and 20 Tested at Their Estimated In-Situ Confining Pressures

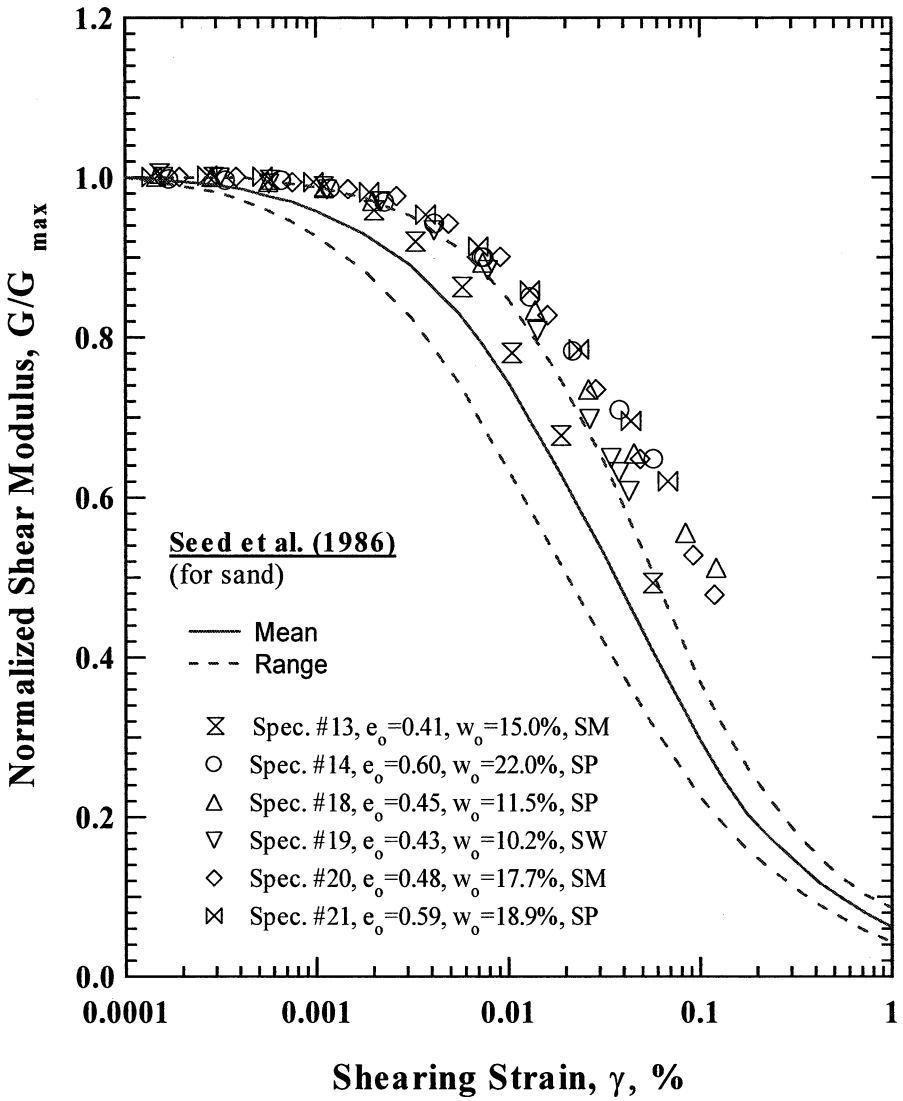

Figure 31 Variation in Normalized Shear Modulus with Shearing Strain from Resonant Column (RC) Tests of the Nonplastic Specimens, excluding Specimen No. 17, Tested at Their Estimated In-Situ Confining Pressures

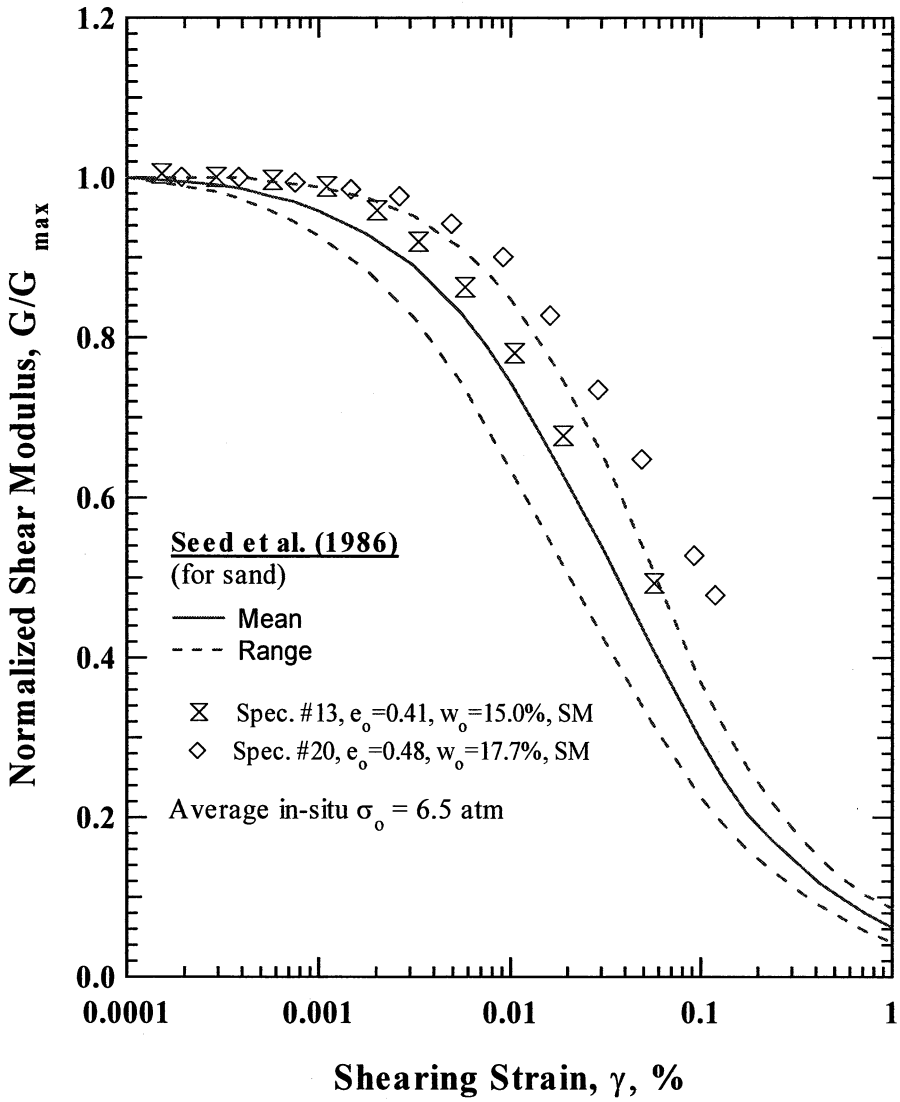

Figure 32 Variation in Normalized Shear Modulus with Shearing Strain from Resonant Column (RC) Tests of the Two, Silty Sand (SM) Specimens Tested at Their Estimated In-Situ Confining Pressures

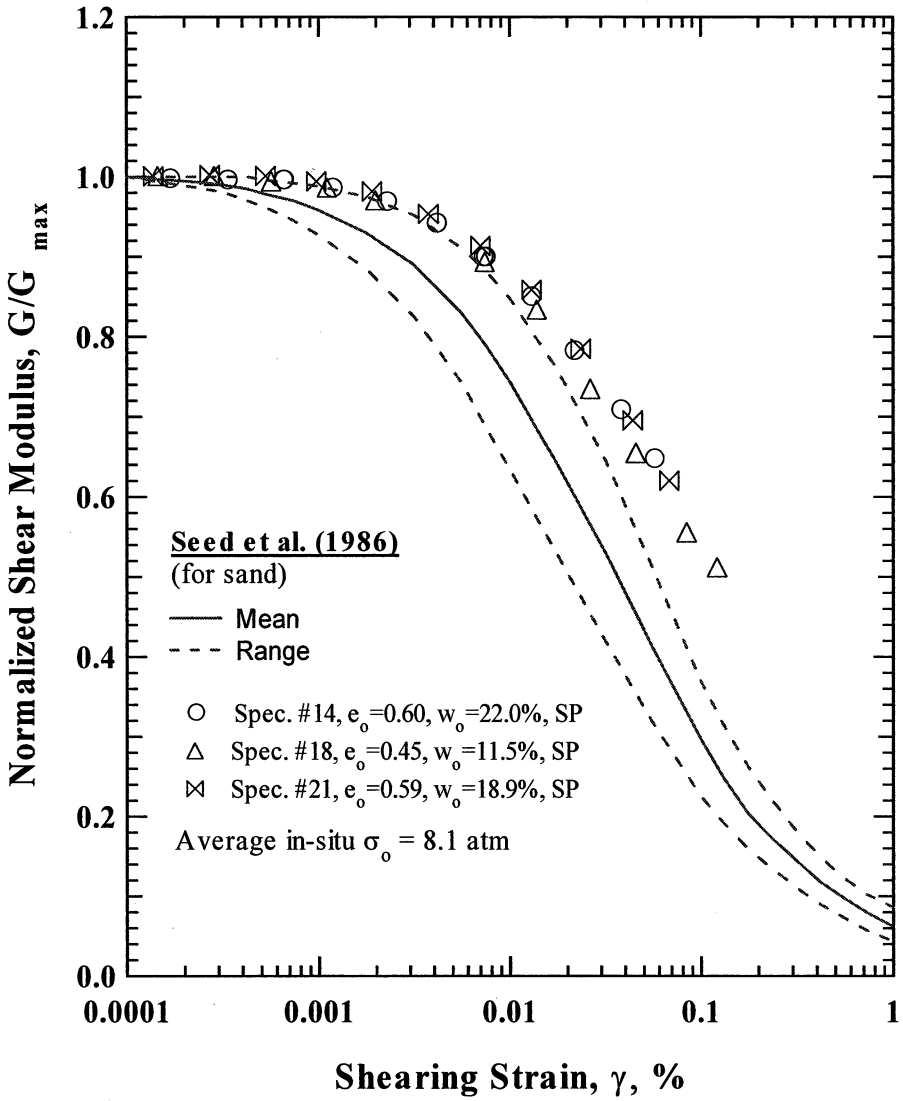

Figure 33 Variation in Normalized Shear Modulus with Shearing Strain from Resonant Column (RC) Tests of the Three, Poorly Graded Sand (SP) Specimens Tested at Their Estimated In-Situ Confining Pressures

4.1.2 Nonlinear G - Log γ and G/G_{max} – Log γ Relationships of the Plastic Specimens - Results of the G - log γ measurements of the eighteen plastic specimens determined by the RC tests are shown in Figures 34 through 36. The results are divided into three groups according to the confining pressure at which high-amplitude testing was performed; low, medium, and high in Figures 34, 35 and 36, respectively. These three groups are the same groups used in the discussion of the log G_{max} – log σ_o relationships in Section 3. Also, for reference purposes, average values of the estimated in-situ σ_o are about 1, 4, and 9 atm for the low, medium, and high pressure groups, respectively.

Comparisons of the G - log γ relationships measured in the RC and TS tests are shown in Figure 37 for Specimen Nos. 10 and 22. Comparisons for the other specimens are shown in the appendices.

The normalized shear modulus relationships (G/G_{max} - log γ) of all plastic specimens measured in the RC tests are shown in Figures 38 through 40 for the low, medium, and high confining pressure groups, respectively. Comparisons of the RC and TS results, presented in the form of G/G_{max} – log γ, are shown in Figure 41 for Specimen Nos. 10 and 22. The same relative comparison between the RC and TS test results as found for the nonplastic specimens is shown in Figure 41; that is, similar normalized degradation curves are found in both types of tests and the RC tests involve measurements to higher strains, although the strains are much closer in this case because the plastic specimens were much softer than the nonplastic specimens. It is worth noting that the main difference between the G – log γ curves measured in the RC and TS tests shown in Figure 37 is attributed to measurement frequency. The measurement frequency in the RC test ranged from 54.6 to 82.0 Hz for Specimen No. 10 and 19.5 to 66.3 Hz for Specimen No 22, while the TS tests were performed at 0.5 Hz.

4.1.3 Comparisons of Measured and Empirical G/G_{max} - Log γ Relationships –

4.1.3.1 Sand Curve of Seed et al. (1986) – The measured G/Gmax – log γ relationships of the nonplastic soils are compared in Figures 29 through 33 with the empirical sand curve proposed

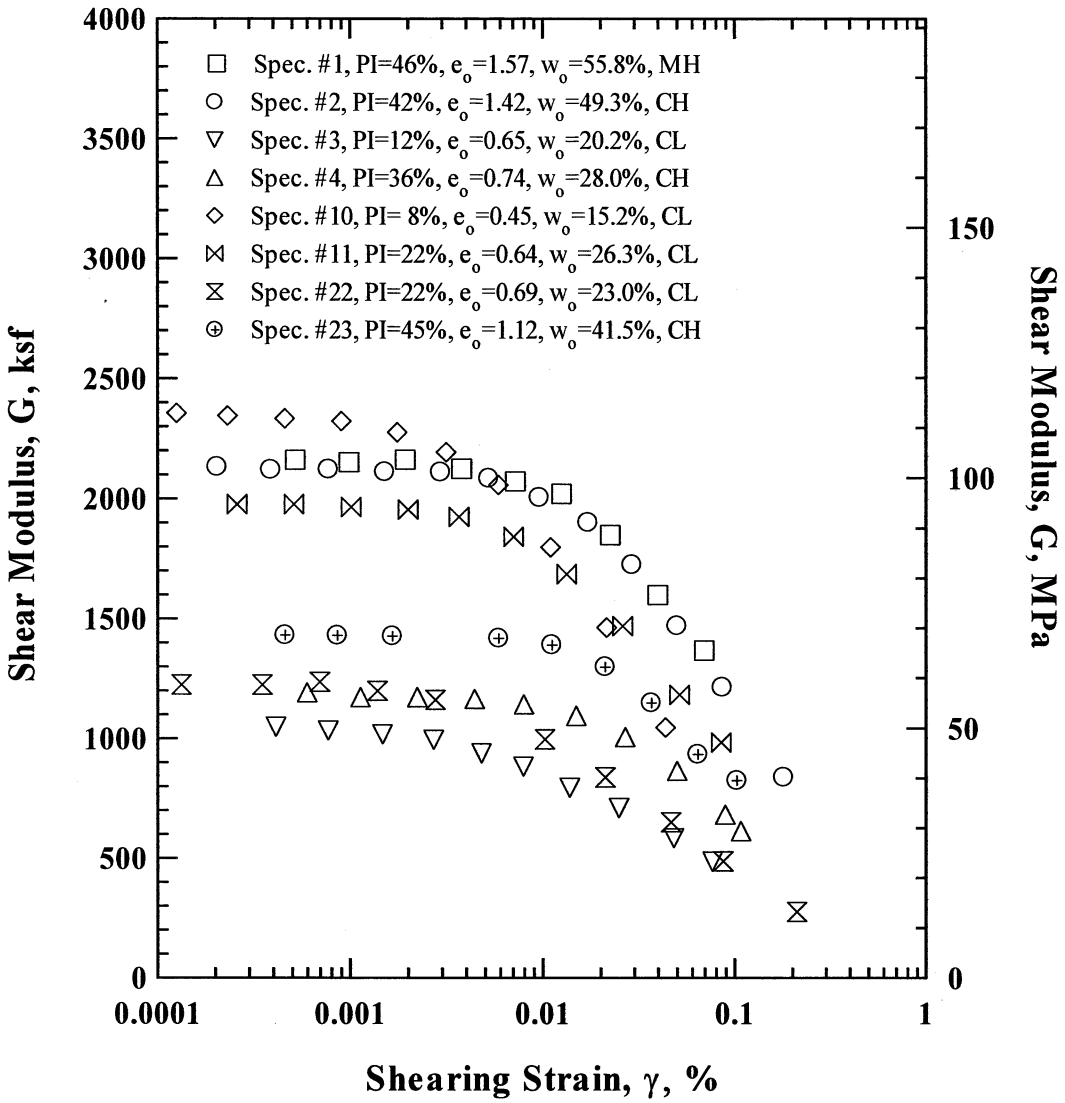

Figure 34 Variation in Shear Modulus with Shearing Strain from Resonant Column (RC) Tests of the Eight, Plastic Specimens in the Low In-Situ Confining Pressure Group Tested at Their Estimated In-Situ Confining Pressures

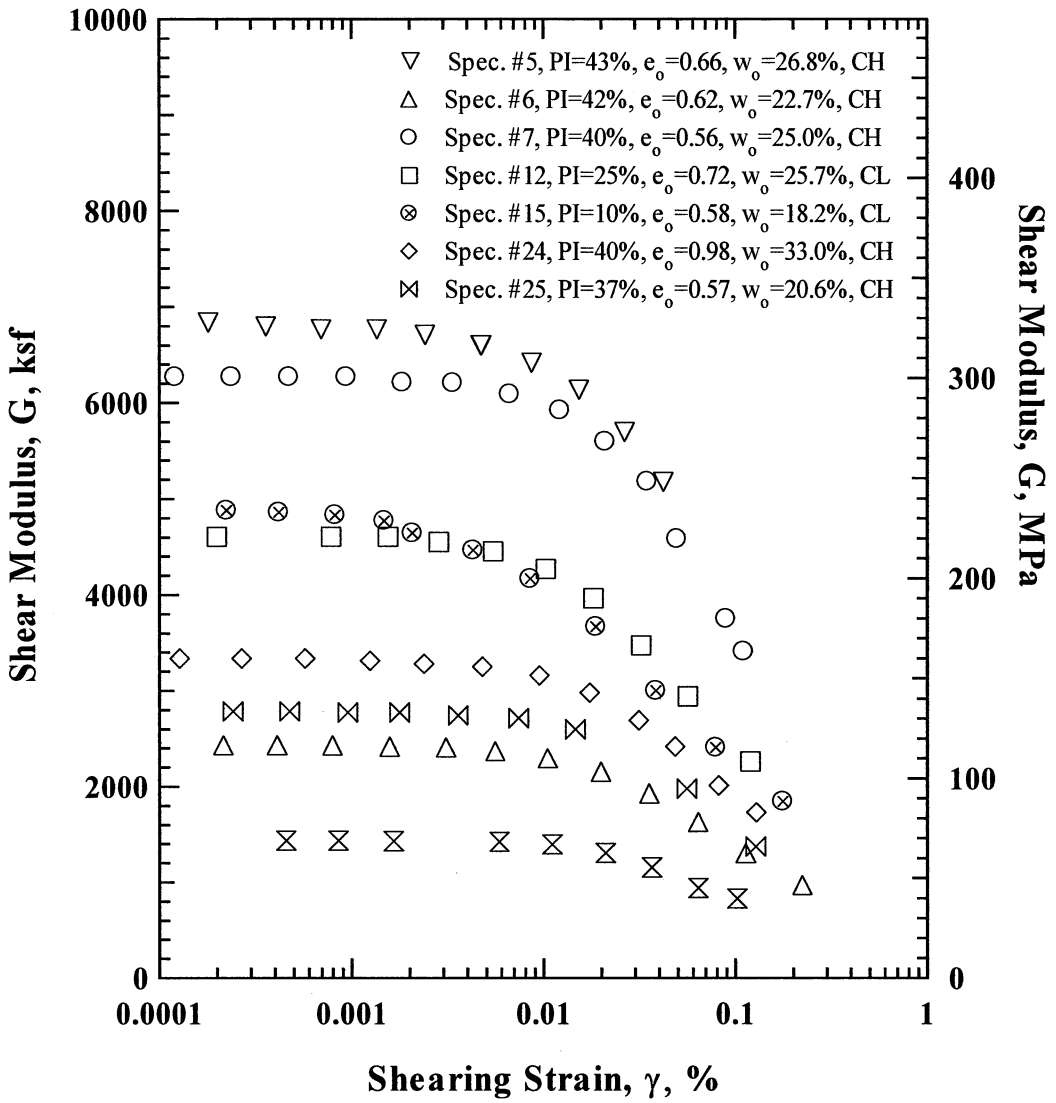

Figure 35 Variation in Shear Modulus with Shearing Strain from Resonant Column (RC) Tests of the Seven, Plastic Specimens in the Medium In-Situ Confining Pressure Group Tested at Their Estimated In-Situ Confining Pressures

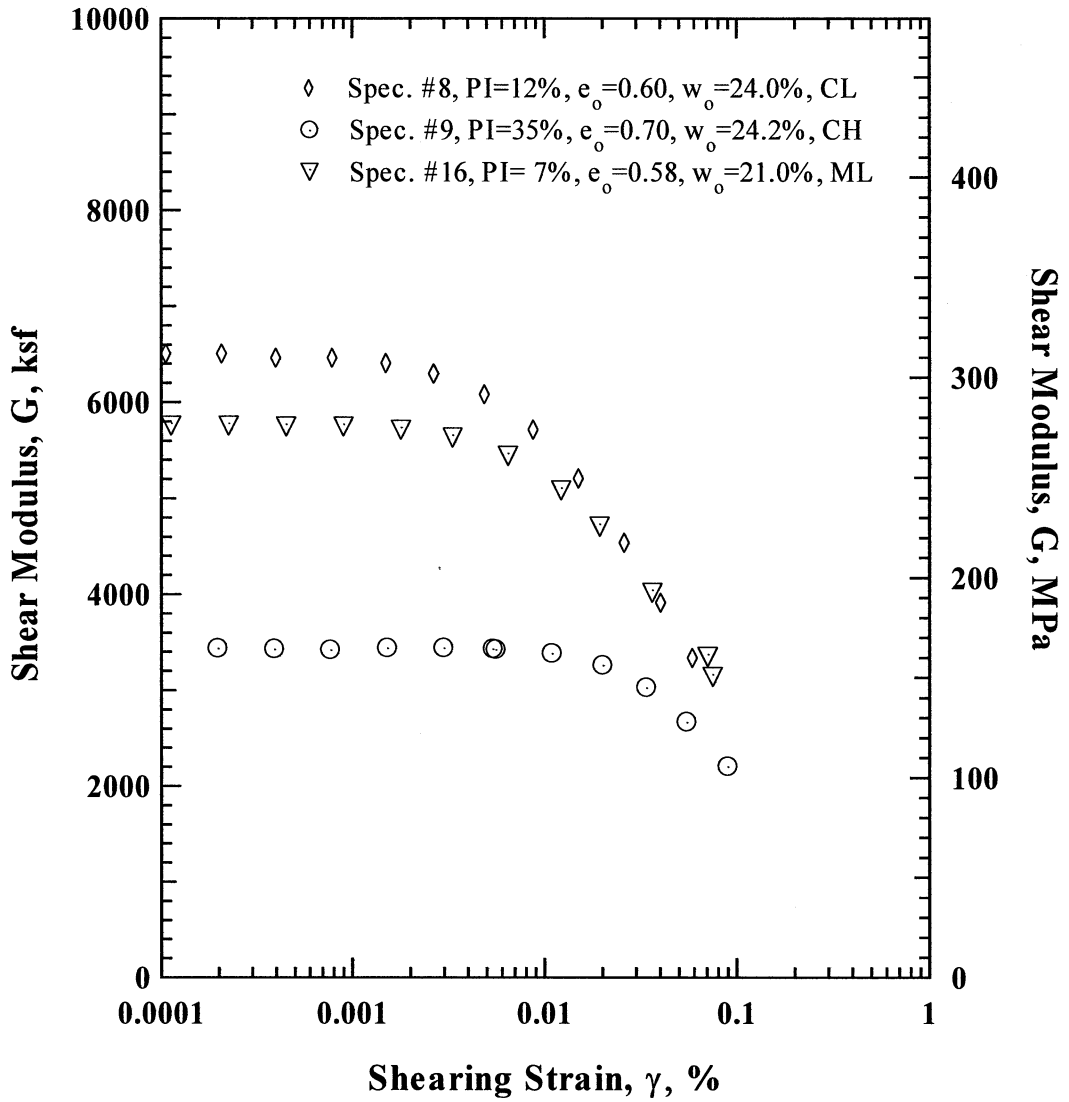

Figure 36 Variation in Shear Modulus with Shearing Strain from Resonant Column (RC) Tests of the Three, Plastic Specimens in the High In-Situ Confining Pressure Group Tested at Their Estimated In-Situ Confining Pressures

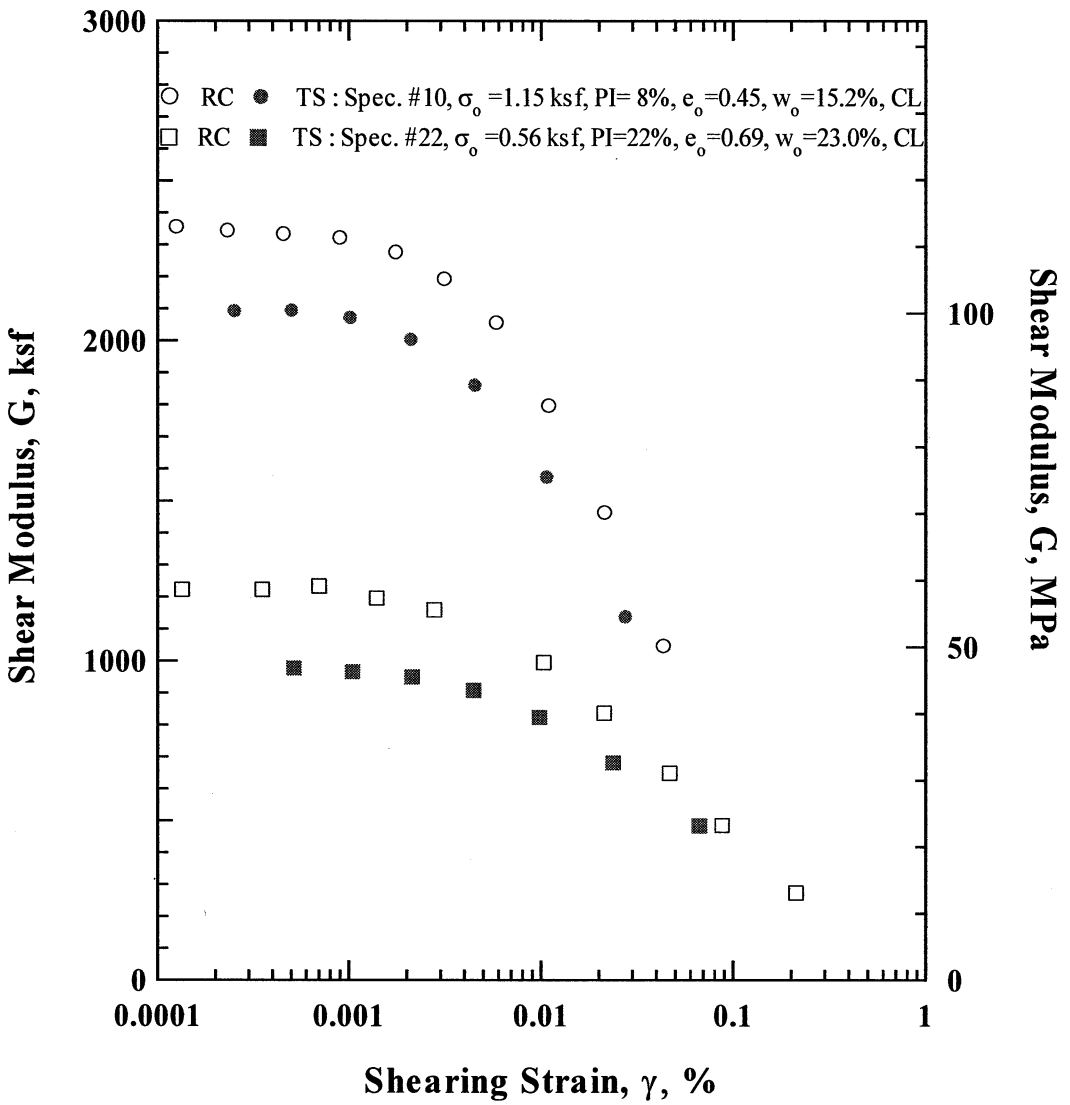

Figure 37 Variation in Shear Modulus with Shearing Strain from Resonant Column (RC) and Torsional Shear (TS) Tests of Plastic Specimen Nos. 10 and 22 Tested at Their Estimated In-Situ Confining Pressures

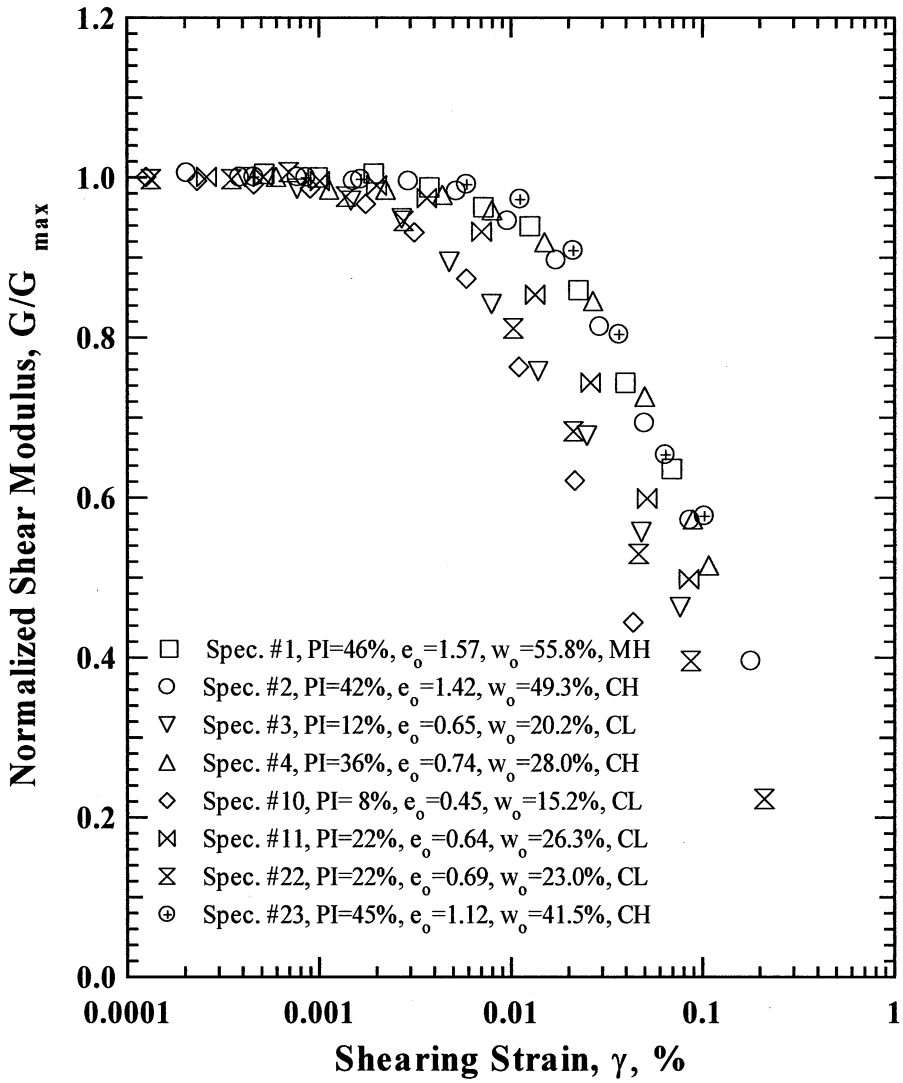

Figure 38 Variation in Normalized Shear Modulus with Shearing Strain from Resonant Column (RC) Tests of the Eight, Plastic Specimens in the Low In-Situ Confining Pressure Group Tested at Their Estimated In-Situ Confining Pressures.

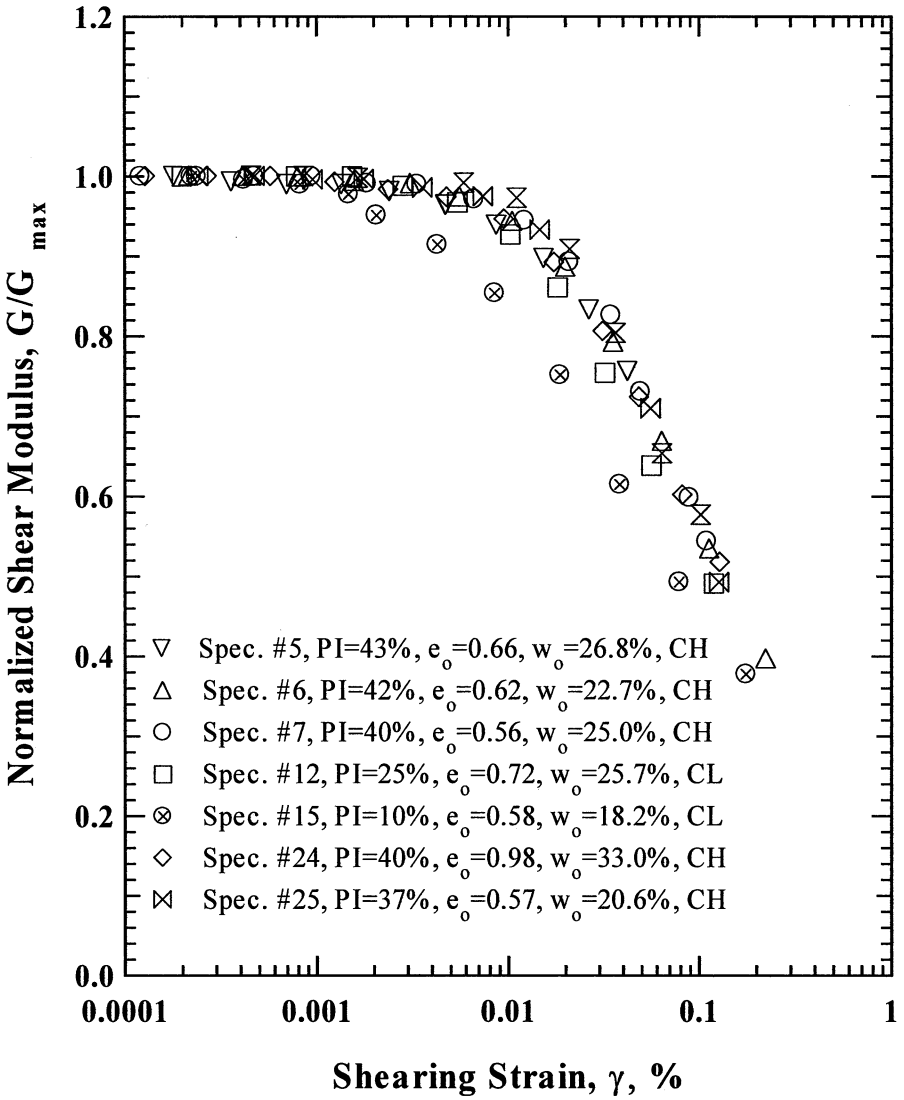

Figure 39 Variation in Normalized Shear Modulus with Shearing Strain from Resonant Column (RC) Tests of the Seven, Plastic Specimens in the Medium In-Situ Confining Pressure Group Tested at Their Estimated In-Situ Confining Pressures.

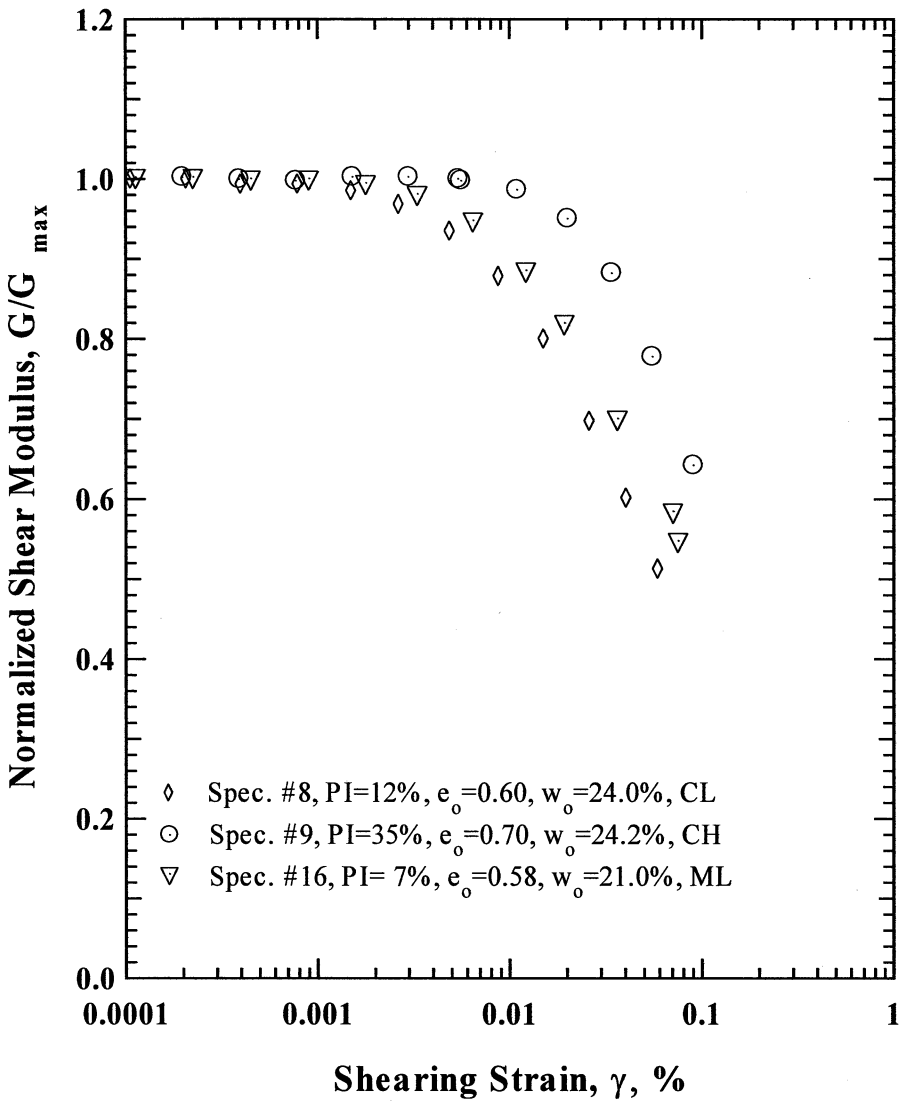

Figure 40 Variation in Normalized Shear Modulus with Shearing Strain from Resonant Column (RC) Tests of the Three, Plastic Specimens in the High In-Situ Confining Pressure Group Tested at Their Estimated In-Situ Confining Pressures

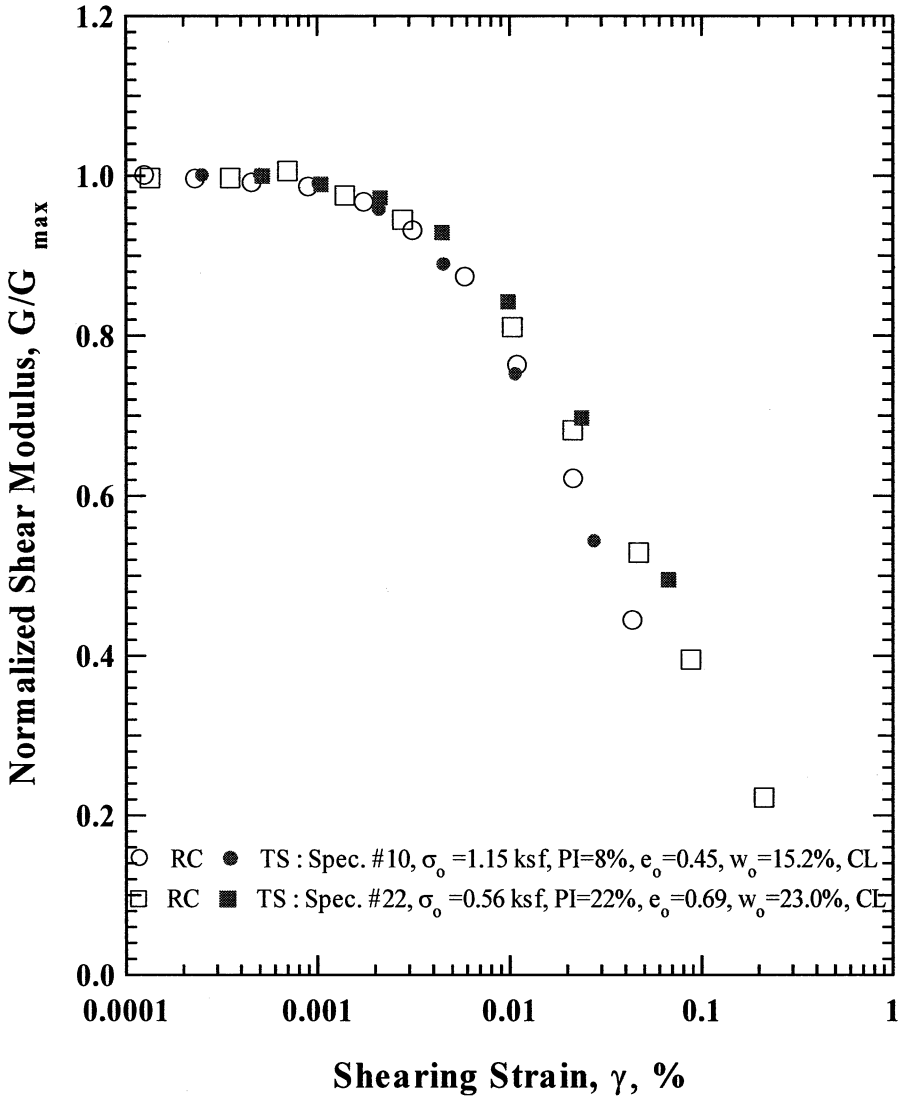

Figure 41 Variation in Normalized Shear Modulus with Shearing Strain from Resonant Column (RC) and Torsional Shear Tests (TS) of Plastic Specimens Nos. 10 and 22 at Their Estimated In-Situ Confining Pressures.

by Seed et al. (1986). As discussed earlier, six of the seven specimens show a more linear response than the "sand curve" that has been in use for more than 30 years because it originated with Seed and Idriss (1970). This difference in response results mainly from the higher confining pressures at which the specimens were tested (average of σ_0 = 8.3 atm). The seventh specimen was tested at a low pressure (about 0.2 atm) and this specimen shows a more nonlinear response than the empirical sand curve (see Figure 29); once again because of the difference in test pressure and the implicit pressure of 1 atm represented by the empirical curve.

4.1.3.2 Curves for Plastic Soils of Vucetic and Dobry (1991) -The measured normalized modulus degradation curves are compared in Figures 42 through 47 with the degradation curves recommended by Vucetic and Dobry (1991) for soils with plasticity indices (PI) of 0, 15, 30, 50, and 100 %. For the specimens in the low confining pressure group, these specimens can be further grouped according to their average PI values. The average values of PI are 10, 22, and 42 % and the comparisons with the Vucetic and Dobry curves are shown in Figures 42 through 44, respectively. There is good agreement between the measured G/G_{max} – log γ relationships and the curves proposed by Vecitic and Dobry (1991). A good comparison was also found for the plastic specimens tested in the medium pressure range (an average in-situ σ_o of about 4 atm) as shown in Figures 45 and 46. The only small difference in the measured and predicted trends occurs for the highest PI materials (Figure 44 for soil with an average PI = 42 % and Figure 46 for soil with an average PI = 40%). In this case, the measured relationships exhibit slightly more linearity than the predicted curves followed by a slightly more rapid decrease in G with γ. The somewhat different pattern between the measured G/G_{max} – log γ relationships and the predicted curves from Vucetic and Dobry is most clearly seen in the tests at the high confining pressures (average in-situ $\sigma_o \sim 9$ atm). These results are shown in Figure 47 where all three specimens clearly exhibited a larger elastic range and a more rapid strain degradation than the predicted curves for the respective plasticities of the test specimens.

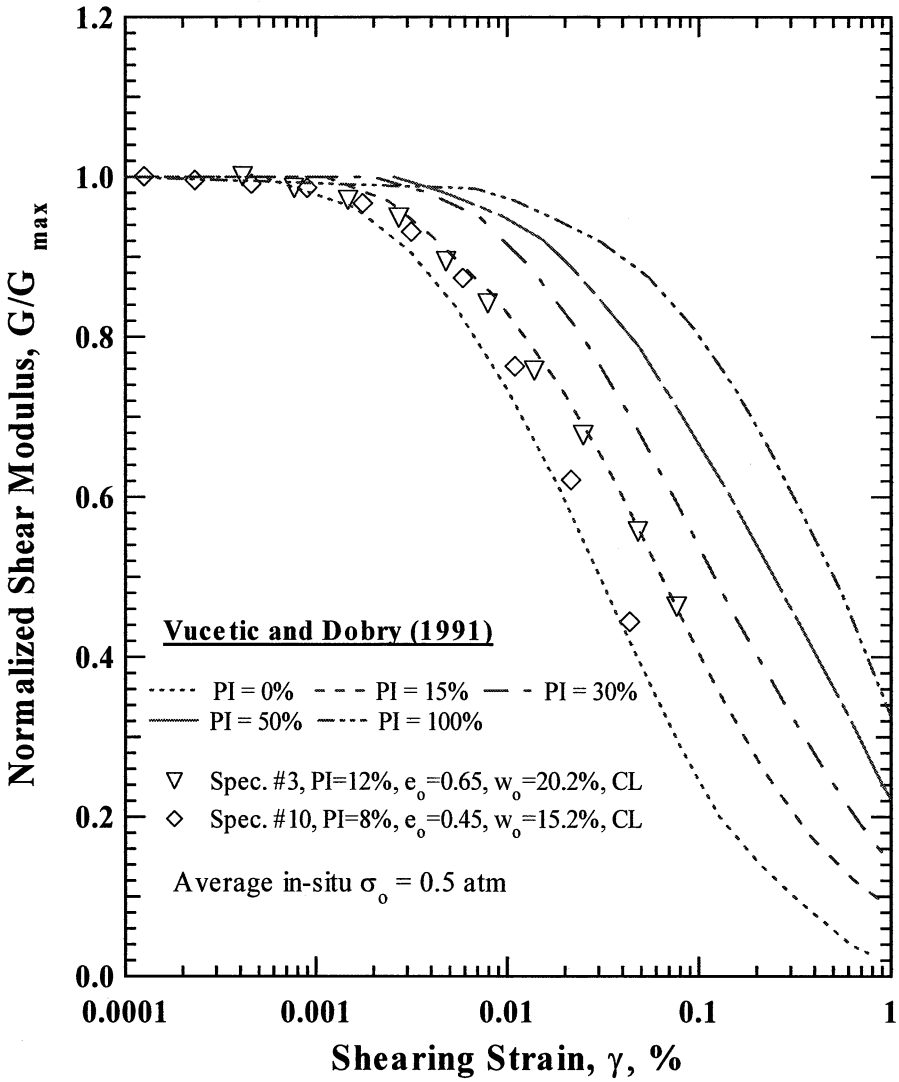

Figure 42 Comparison between the Trends Predicted by Vucetic and Dobry (1991) and the Variation in Normalized Shear Modulus with Shearing Strain from Resonant Column (RC) Tests of Two Specimens with an Average PI = 10 % in the Low In-Situ Confining Pressure Group Tested at Their Estimated In-Situ Confining Pressures

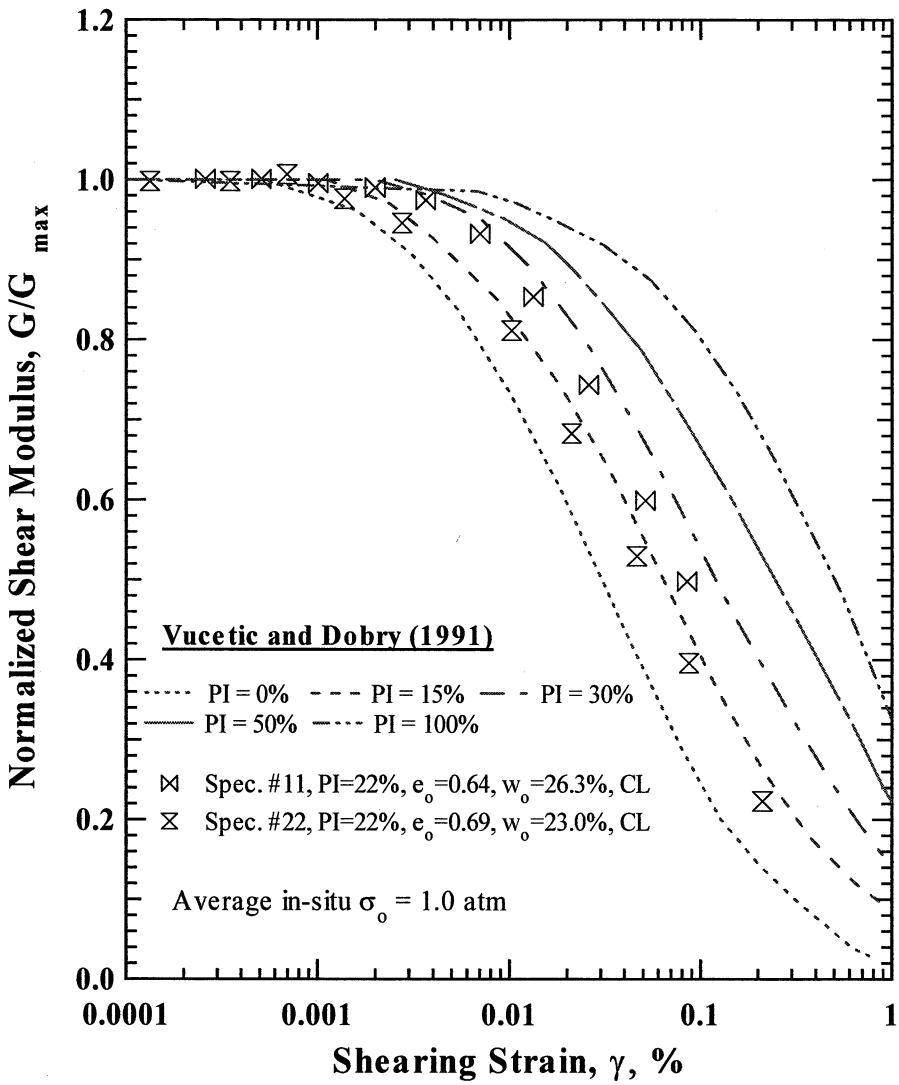

Figure 43 Comparison between the Trends Predicted by Vucetic and Dobry (1991) and the Variation in Normalized Shear Modulus with Shearing Strain from Resonant Column (RC) Tests of Two Specimens with PI = 22 % in the Low In-Situ Confining Pressure Group Tested at Their Estimated In-Situ Confining Pressures

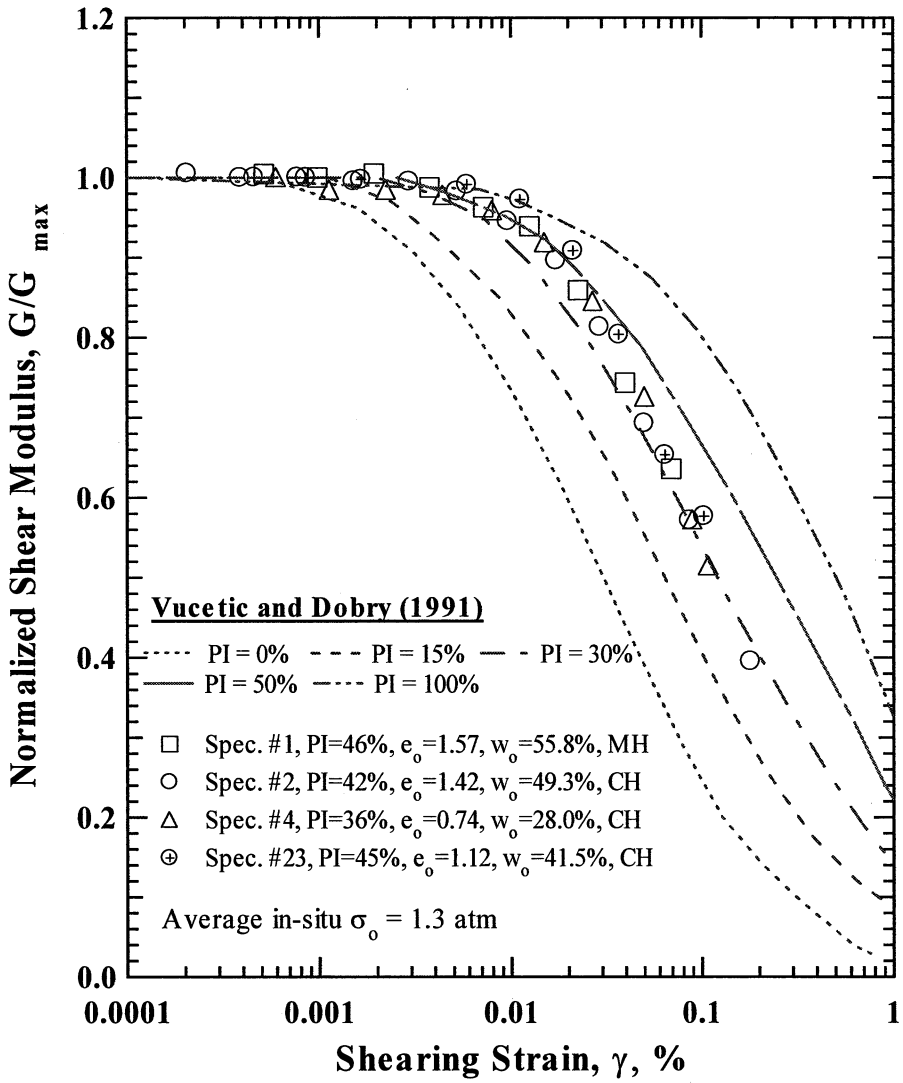

Figure 44 Comparison between the Trends Predicted by Vucetic and Dobry (1991) and the Variation in Normalized Shear Modulus with Shearing Strain from Resonant Column (RC) Tests of Four Specimens with an Average PI = 42 % in the Low In-Situ Confining Pressure Group Tested at Their Estimated In-Situ Confining Pressures

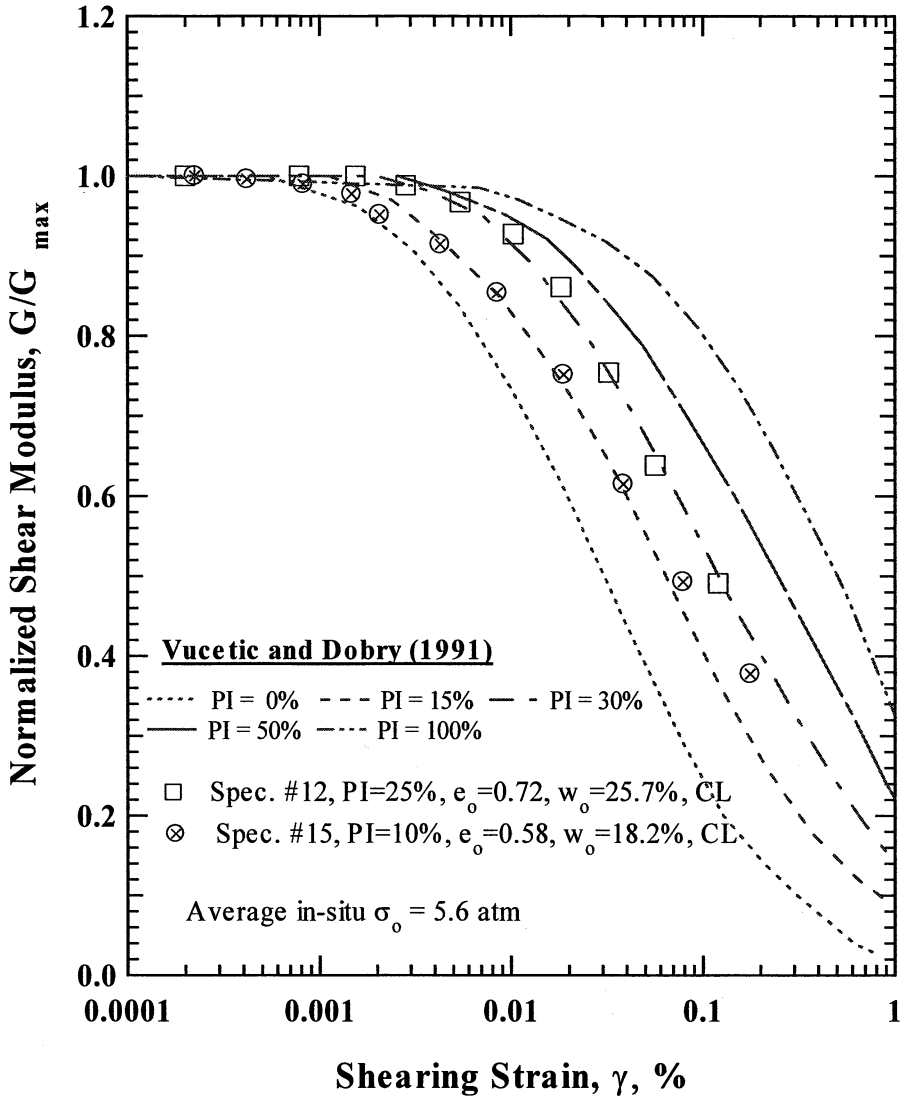

Figure 45 Comparison between the Trends Predicted by Vucetic and Dobry (1991) and the Variation in Normalized Shear Modulus with Shearing Strain from Resonant Column (RC) Tests of Two Specimens with Lower Plasticity in the Medium In-Situ Confining Pressure Group Tested at Their Estimated In-Situ Confining Pressures

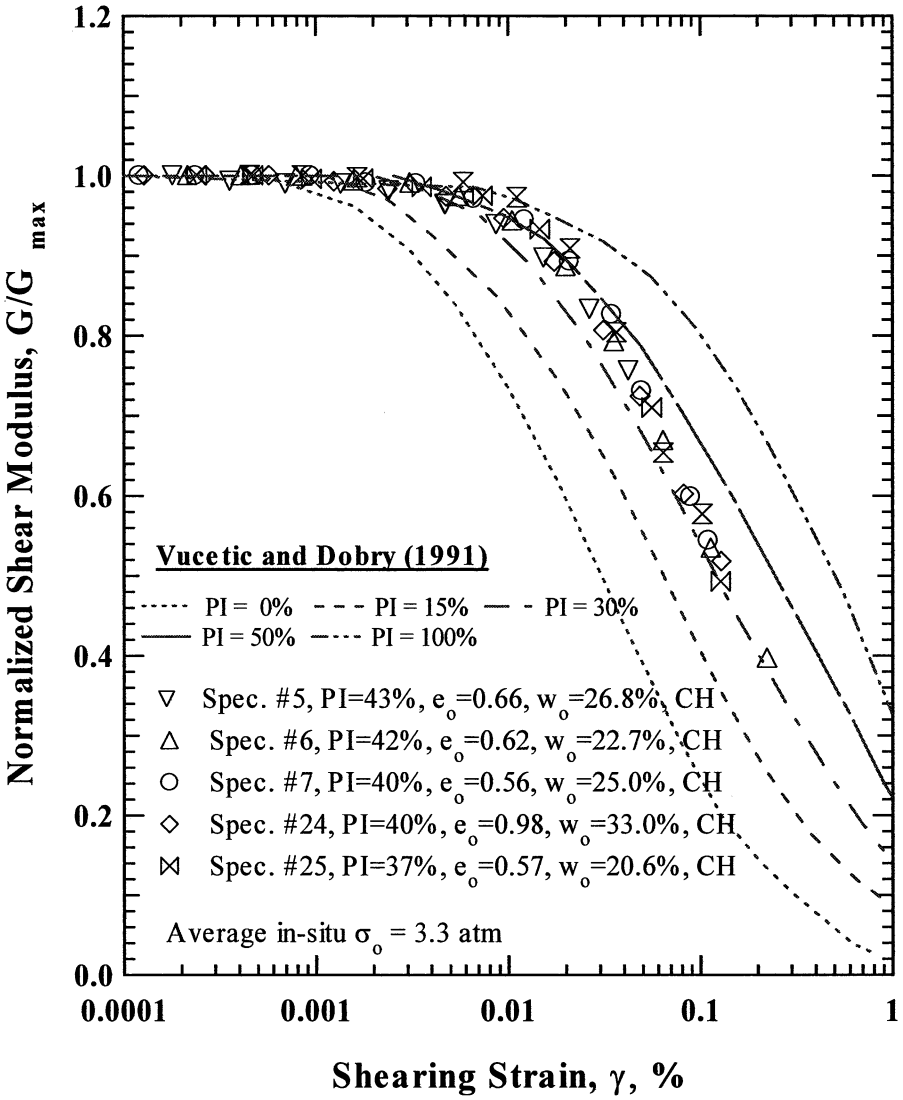

Figure 46 Comparison between the Trends Predicted by Vucetic and Dobry (1991) and the Variation in Normalized Shear Modulus with Shearing Strain from Resonant Column (RC) Tests of Five Specimens with an Average PI = 40% in the Medium In-Situ Confining Pressure Group Tested at Their Estimated In-Situ Confining Pressures

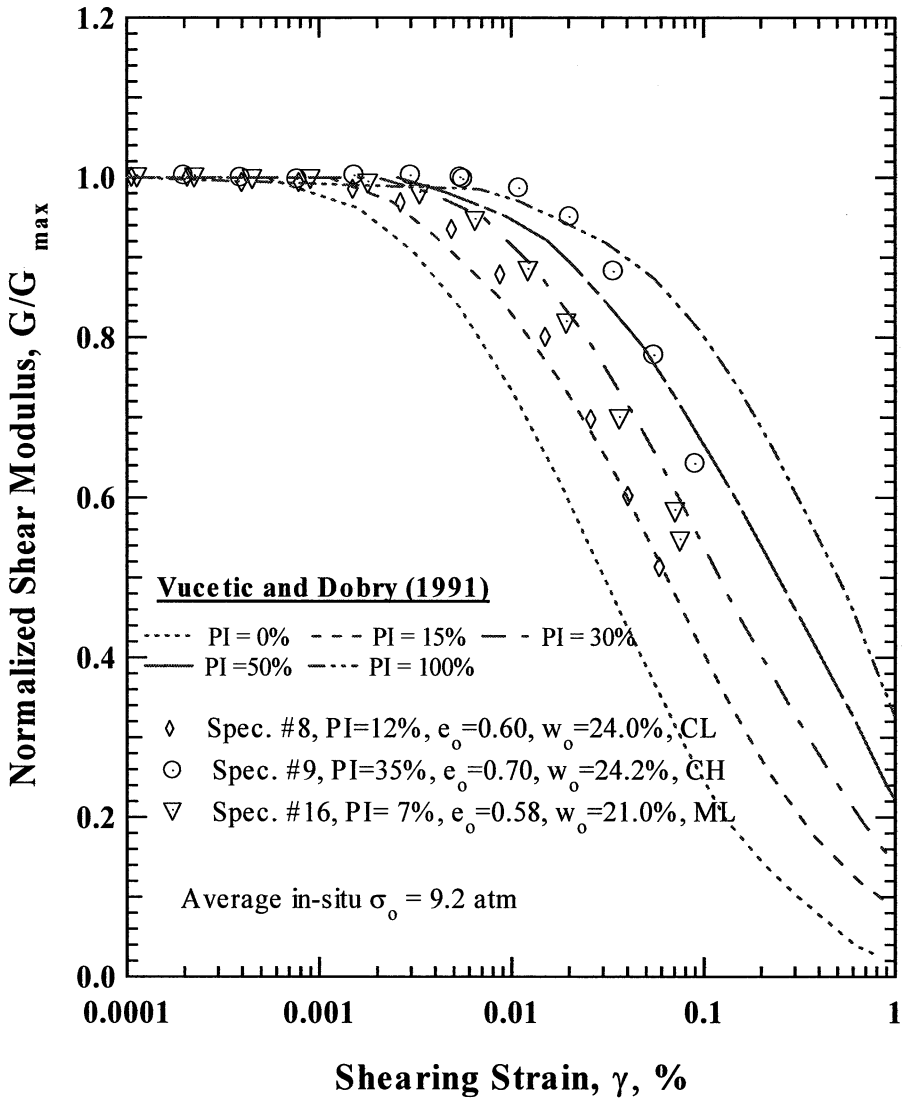

Figure 47 Comparison between the Trends Predicted by Vucetic and Dobry (1991) and the Variation in Normalized Shear Modulus with Shearing Strain from Resonant Column (RC) Tests of the Three Specimens in the High In-Situ Confining Pressure Group Tested at Their Estimated In-Situ Confining Pressures

4.1.4 Comparison with the Nonlinear Model for G/G_{max} – Log γ Proposed by Darendeli (2001)

In 2001, Mehmet Darendeli proposed a modified version of the hyperbolic equation originally recommended by Hardin and Drnevich (1972) to model the G/ G_{max} – log γ relationship of soils. Darendeli's equation can be expressed as:

$$\frac{G}{G_{max}} = \frac{1}{1+\left(\frac{\gamma}{\gamma_r}\right)^a} \tag{4}$$

in which γ = any given shearing strain,

γ_r = the reference shearing strain, and

a = dimensionless exponent.

The reference strain, γ_r, is used simply for curve fitting purposes in Darendeli's model and is defined as the value of γ equal to the shearing strain at which G/G_{max} equals 0.5. (This definition of γ_r is different from the one proposed by Hardin and Drnevich, 1972.) The reference strain is denoted as $\gamma_{r,G}$ hereafter. As an example, the best-fit lines determined by least-squares fitting of the nonlinear results for Specimen Nos. 14 and 20 are presented in the Figure 48. In this case, a value of a = 0.92 was used as recommended by Darendeli. Clearly, the modified hyperbolic model fits the data very well.

The constants determined for Equation 4 from the best-fit lines are summarized in Table 12 for the nonplastic specimens and in Table 13 for the plastic specimens. A constant value of a = 0.92 was assumed to fit the data.

In his nonlinear model, Darendeli also developed empirical equations to estimate the values of $\gamma_{r,G}$ and a. His equations are:

$$\gamma_{r,G} = (\phi_1 + \phi_2 * PI * OCR^{\phi 3}) + \sigma_0'^{\,\phi 4} \tag{5}$$

$$a = \phi_5 \tag{6}$$

in which

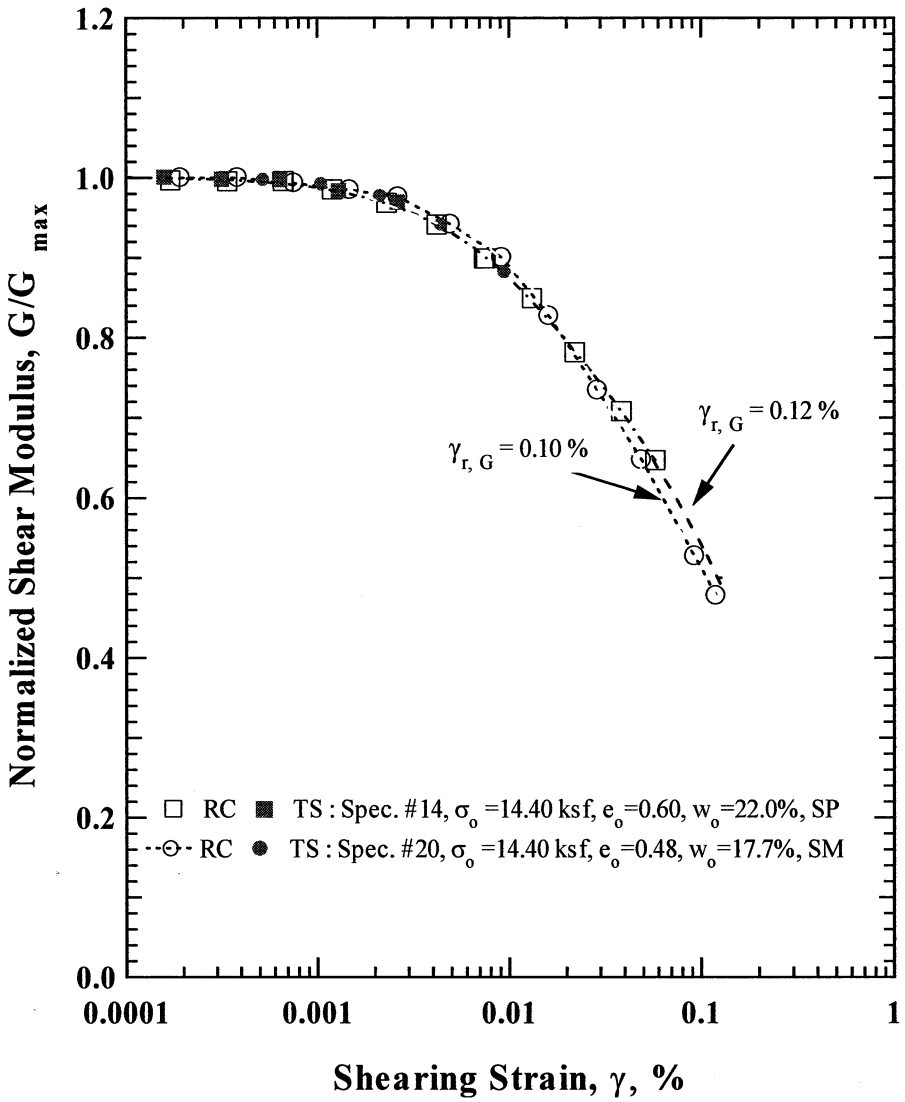

Figure 48 Best-Fit Curves of the Variation in Normalized Shear Moduli with Shearing Strain from Resonant Column (RC) Tests of Nonplastic Specimens No. 14 and No. 20 at Estimated In-Situ Confining Pressures

Table 12 Values of Reference Strain ($\gamma_{r,G}$) from the G/G_{max}-log γ Curves of the Seven Nonplastic Specimens Using the Darendeli (2001) Model

Specimen No.	UT Specimen ID	Soil Site Identification	Specimen Depth, ft (m)	Confining Pressure, σ_o, ksf (kPa)	Reference Strain Values, $\gamma_{r,G}$ (%)
13	UTA-27-V	LA Bulk Mail (P-6)	205 (62.5)	12.96 (621)	0.06
14	UTA-27-H	LA Bulk Mail (P-7)	267 (81.4)	14.40, 57.60 (690, 2761)	0.12, 0.18
17	UTA-27-M	Lake Hughes P-1	6 (1.8)	0.43 (21)	0.02
18	UTA-27-N	Joshua Tree 5 P-7	236 (71.9)	19.44 (932)	0.11
19	UTA-27-O	Joshua Tree 5 P-8	328 (100.0)	27.36 (1312)	0.08
20	UTA-27-P	Yermo P-6	201 (61.3)	14.40 (690)	0.10
21	UTA-27-Q	Yermo P-7	266 (81.1)	17.28, 69.12 (828, 3314)	0.11, 0.15

Table 13 Values of Reference Strain ($\gamma_{r,G}$) from the G/G_{max}-log γ Curves of the Eighteen Plastic Specimens Using the Darendeli (2001) Model

Specimen No.	UT Specimen ID	Soil Site Identification	Specimen Depth, ft (m)	Confining Pressure, σ_o, ksf (kPa)	Reference Strain Values, $\gamma_{r,G}$ (%)
1	UTA-25-B	Tarzana P-3	30 (9.1)	1.73, 6.91 (82, 331)	0.10, 0.14
2	UTA-25-A	Tarzana P-4	42 (12.8)	3.46, 13.82 (166, 663)	0.11, 0.15
3	UTA-27-F	Meloland S-2	20 (6.1)	0.86, 3.46 (41, 166)	0.06, 0.08
4	UTA-27-E	Meloland S-3	28 (8.5)	1.30 (62)	0.10
5	UTA-27-B	Meloland WS-1	120 (36.6)	1.08, 4.32, 17.28 (52, 207, 828)	0.03, 0.11, 0.14
6	UTA-27-A	Meloland WS-3	200 (61.0)	2.16, 8.64 (104, 414)	0.13
7	UTA-27-C	Meloland WS-4	259 (78.9)	10.80 (518)	0.13
8	UTA-27-D	Meloland WS-6	378 (115.2)	15.84, 63.36 (759, 3037)	0.06, 0.13
9	UTA-27-G	Meloland WS-7	440 (134.1)	18.72, 64.80 (897, 3106)	0.14, 0.18
10	UTA-27-S	LA Bulk Mail (P-1)	15 (4.6)	1.44, 5.76 (69, 276)	0.04, 0.04
11	UTA-27-T	LA Bulk Mail (P-3)	50 (15.2)	3.60, 14.40 (173, 690)	0.08, 0.11
12	UTA-27-I	LA Bulk Mail (P-5)	167.5 (51.1)	11.52 (552)	0.12
15	UTA-27-J	Gilroy P-4	182 (55.5)	12.10, 48.38 (580, 2320)	0.08, 0.13
16	UTA-27-K	Gilroy P-5	357 (108.8)	23.76 (1139)	0.10
22	UTA-27-L	Halls Valley (P-1)	7 (2.1)	0.58, 2.30 (28, 110)	0.05, 0.06
23	UTA-27-R	Halls Valley (P-3)	52 (15.8)	4.32, 17.28 (207, 828)	0.12
24	UTA-27-U	Saturn P-5	100 (30.5)	6.05 (290)	0.13
25	UTA-27-W	Obregon P-8	101 (30.8)	5.04 (242)	0.12

σ_o' = mean effective confining pressure (atm),

PI = soil plasticity (%),

OCR = overconsolidation ratio,

ϕ_1 = 0.0352,

ϕ_2 = 0.0010,

ϕ_3 = 0.3246,

ϕ_4 = 0.3483, and

ϕ_5 = 0.9190.

As shown above, the input parameters required in Equations 5 and 6 are σ_0', PI and OCR. The values for these parameters are listed in Table 14 (using σ_0 for σ_0'). The resulting predicted values of $\gamma_{r,G}$ are given in Table 15. These comparisons are shown for all 25 specimens in Figures 49 and 50. As seen in the two figures, Darendeli's (2001) model predicted the measured G/G_{max} – log γ curves very well, with the mean predicted value of $\gamma_{r,G}$ with 2 % of the mean of the measured values and the mean predicted value of G/G_{max} at the measured $\gamma_{r,G}$ of 0.49 (compared with the measured value of 0.50). To investigate if there is any trend with soil type and confining pressure, the results in Figures 49 and 50 have been replotted in Figure 51 as follows: the nonplastic specimens in Figure 51a and the three groups of plastic soils that were divided according to low, medium and high confining pressures in Figures 51b, 51c and 51d, respectively. No clear pattern emerges.

Additional comparisons between the measured G/G_{max} – log γ curves and the curves predicted by Darendeli's model are presented in Figures 52 through 59. The results in Figure 52 show the generally good agreement between the measured and predicted effect of confining pressure on the nonplastic specimens. Darendeli's model also included the variation to be expected in the normalized modulus degradation curves in terms of plus or minus one standard deviation, +/– σ. Two comparisons for the nonplastic soils are shown in Figures 53 and 54 which show the measured results fall within these ranges.

Finally, specific comparisons for the plastic soils between the measured normalized modulus degradation curves and the ones predicted by Vucetic and Dobry (1991) and by Darendeli's (2001) models are presented in Figures 55 through 59. The +/– σ range around the

Table 14 Input Parameters Used in Equations (5) and (6) to Predict Nonlinear Behavior of the 25 ROSRINE Specimens Using Darendeli's (2001) Model

Spec. No.	UT Specimen ID	Soil Site Identification	Specimen Depth ft (m)	Soil Type (Unified Soil Classification)	Plasticity Index %	Estimated OCR	Estimated In-Situ Pressure atm
1	UTA-25-B	Tarzana	30	MH	46	≥ 4*	0.82
2	UTA-25-A	Tarzana	42	CH	42	1 2**	1.63
3	UTA-27-F	Meloland	20	CL	12	1 2**	0.41
4	UTA-27-E	Meloland	28	CH	36	1	0.61
5	UTA-27-B	Meloland	120	CH	43	≥ 4*	2.04
6	UTA-27-A	Meloland	200	CH	42	2 4+	4.08
7	UTA-27-C	Meloland	259	CH	40	NA**	5.10
8	UTA-27-D	Meloland	378	CL	12	1	7.49
9	UTA-27-G	Meloland	440	CH	35	1	8.85
10	UTA-27-S	LA Bulk	15	CL	8	1 2**	0.68
11	UTA-27-T	LA Bulk	50	CL	22	1	1.70
12	UTA-27-I	LA Bulk	167.5	CL	25	NA**	5.44
13	UTA-27-V	LA Bulk	205	SM	NP	NA	6.12
14	UTA-27-H	LA Bulk	267	SP	NP	NA	6.80
15	UTA-27-J	Gilroy #3	182	CL	10	NA**	5.72
16	UTA-27-K	Gilroy #3	357	ML	7	NA**	11.23
17	UTA-27-M	Lake Hughes	6	SW-SM	NP	NA	0.20
18	UTA-27-N	Joshua Tree	236	SP	NP	NA	9.19
19	UTA-27-O	Joshua Tree	328	SW	NP	NA	12.93
20	UTA-27-P	Yermo	201	SM	NP	NA	6.80
21	UTA-27-Q	Yermo	266	SP	NP	NA	8.17
22	UTA-27-L	Halls	7	CL	22	2 4+	0.27
23	UTA-27-R	Halls	52	CH	45	1	2.04
24	UTA-27-U	Saturn	100	CH	40	≥ 2+	2.86
25	UTA-27-W	Obregon	101	CH	37	NA**	2.38

Notes: * OCR of 4 was used.
** OCR of 1 was used.
+ OCR of 2 was used.

Table 15 Comparison between Measured Reference Strain from RC Tests and Predicted Reference Strain from Darendeli's (2001) Four-Parameter Model for the 25 ROSRINE Specimens

Specimen No.	UT Specimen ID	Plastic Index %	Confining Pressure, psi	Measured γ_r	Predicted γ_r	Predicted γ_r / Measured γ_r
1	UTA-25-B	46	12	0.10	0.10	1.00
1	UTA-25-B*	46	48	0.14	0.16	1.16
2	UTA-25-A	42	24	0.11	0.09	0.84
2	UTA-25-A*	42	96	0.15	0.15	0.99
3	UTA-27-F	12	6	0.06	0.04	0.58
3	UTA-27-F*	12	24	0.08	0.06	0.70
4	UTA-27-E	36	9	0.10	0.06	0.60
5	UTA-27-B	43	30	0.11	0.13	1.20
5	UTA-27-B*	43	120	0.14	0.21	1.52
6	UTA-27-A	42	60	0.13	0.14	0.10
7	UTA-27-C	40	75	0.13	0.13	1.02
8	UTA-27-D	12	110	0.06	0.10	1.58
8	UTA-27-D*	12	440	0.13	0.15	1.18
9	UTA-27-G	35	130	0.14	0.15	1.07
9	UTA-27-G*	35	450	0.18	0.23	1.28
10	UTA-27-S	8	10	0.04	0.04	0.95
10	UTA-27-S*	8	40	0.04	0.06	1.53
11	UTA-27-T	22	25	0.08	0.07	0.86
11	UTA-27-T*	22	100	0.11	0.11	1.02
12	UTA-27-I	25	80	0.12	0.11	0.91
13	UTA-27-V	NP	90	0.06	0.07	1.10
14	UTA-27-H	NP	100	0.12	0.07	0.58
14	UTA-27-H*	NP	400	0.18	0.11	0.62
15	UTA-27-J	10	84	0.08	0.08	1.04
15	UTA-27-J2	10	336	0.13	0.13	1.03
16	UTA-27-K	7	165	0.10	0.10	0.98
17	UTA-27-M	NP	3	0.02	0.02	1.00
18	UTA-27-N	NP	135	0.11	0.08	0.69
19	UTA-27-O	NP	190	0.08	0.09	1.08
20	UTA-27-P	NP	100	0.10	0.07	0.69
21	UTA-27-Q	NP	120	0.11	0.07	0.66
21	UTA-27-Q*	NP	480	0.15	0.12	0.79
22	UTA-27-L	22	4	0.05	0.04	0.80
22	UTA-27-L*	22	16	0.06	0.07	1.08
23	UTA-27-R	45	30	0.12	0.10	0.86
24	UTA-27-U	40	42	0.13	0.12	0.95
25	UTA-27-W	37	35	0.12	0.10	0.82

Note: * Test was performed at about 4 times greater than the estimated in-situ confining pressure

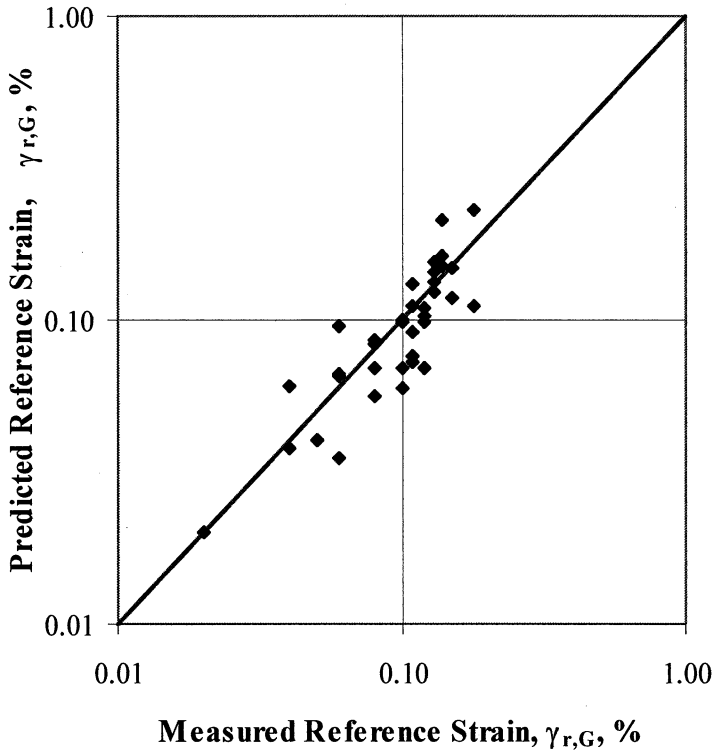

a. Predicted versus Measured Values of $\gamma_{r,G}$

Statistical Summary of the Ratio of Predicted γ_r to Measured γ_r	
Mean	0.97
Standard Deviation	0.25
Minimum	0.58
Maximum	1.58
Count	37

b. Statistical Summary of Results

Figure 49 Comparison Between Reference Strains Determined from the Measured G/G_{max} – log γ Relationships and $\gamma_{r,G}$ Predicted by Darendeli's (2001) Four-Parameter Model for all 25 ROSRINE Specimens

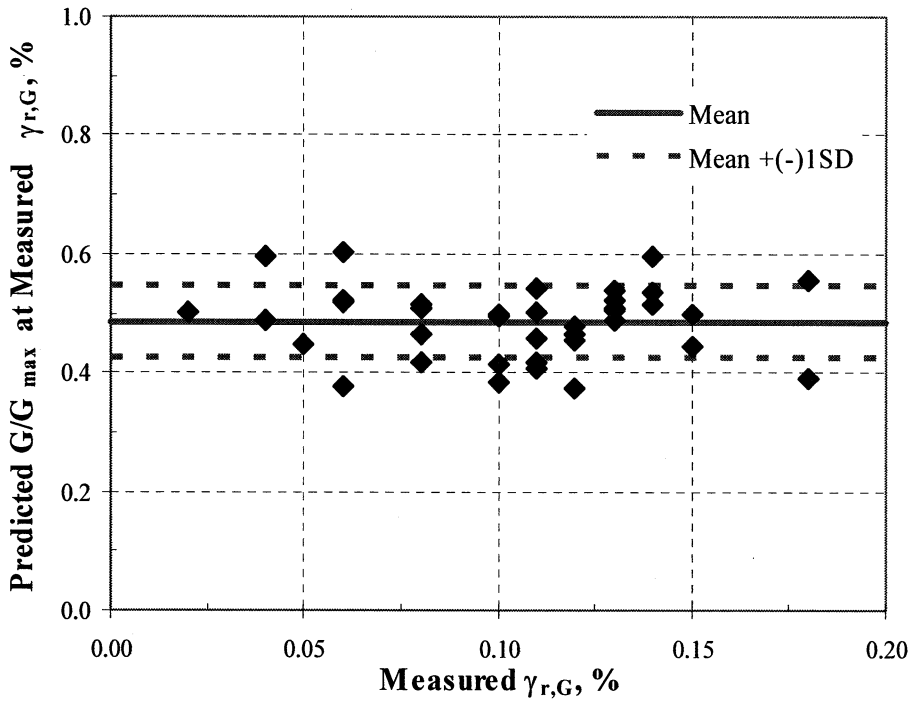

a. Values of Predicted G/G_{max} at Measured $\gamma_{r,G}$

Statistical Summary of Predicted G/G_{max} at Measured γ_r	
Mean	0.49
Standard Deviation	0.06
Minimum	0.37
Maximum	0.60
Count	37

b. Statistical Summary of Results

Figure 50 Values of Normalized Shear Modulus Predicted by Darendeli's (2001) Four-Parameter Model at the Reference Strains Determined from the RC Test Results for all 25 ROSRINE Specimens

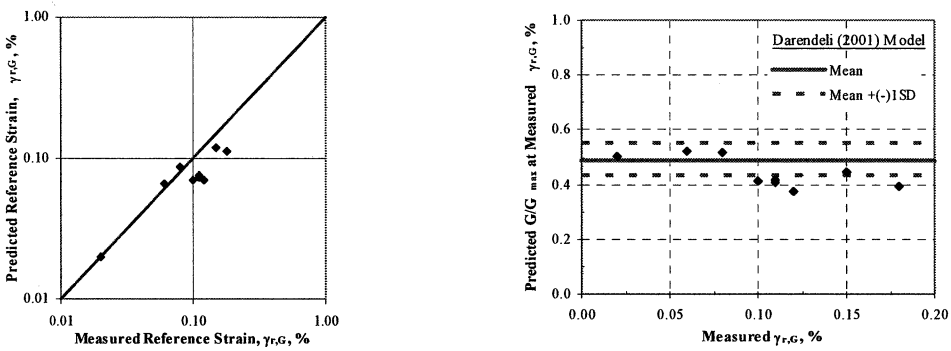

a. Seven Nonplastic Specimens

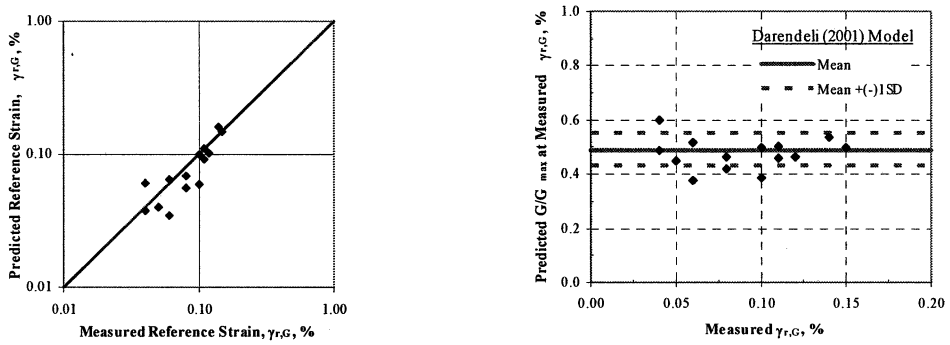

b. Eight Plastic Specimens in the Low Confining Pressure Group

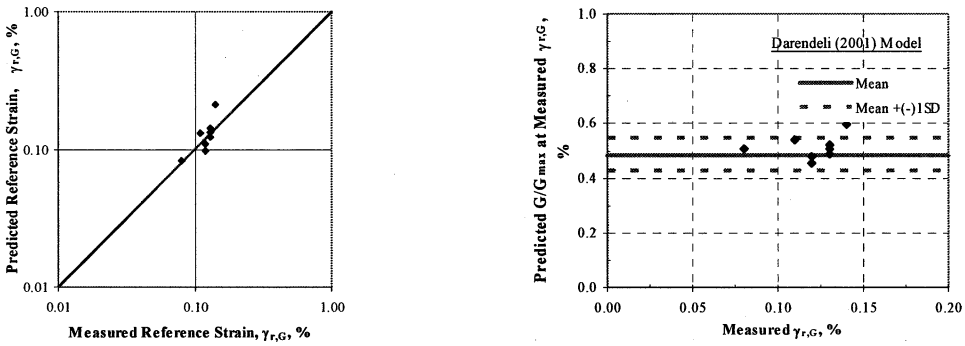

c. Seven Plastic Specimens in the Medium Confining Pressure Group

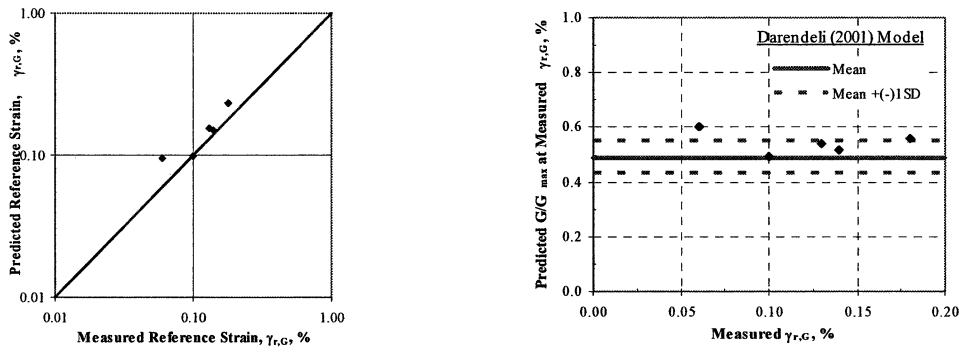

d. Three Plastic Specimens in the High Confining Pressure Group

Figure 51 Comparison Between Reference Strains Determined from the Measured G/G_{max}-log γ Relationships and $\gamma_{r,G}$ Predicted by Darendeli's (2001) Four–Parameter Model Subdivided According to Soil Groupings

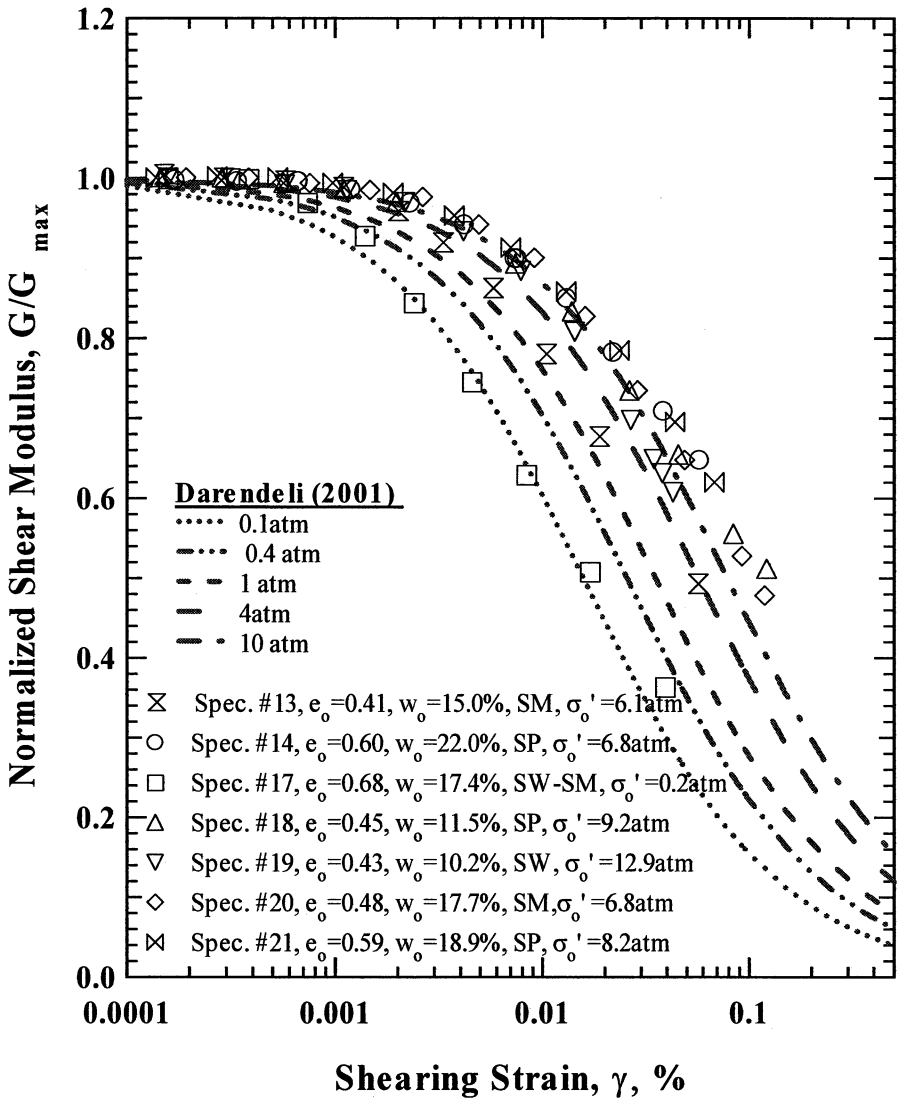

Figure 52 Comparison between the Trends Predicted by Darendeli (2001) and the Variation in Normalized Shear Modulus with Shearing Strain from Resonant Column (RC) Tests of the Seven, Nonplastic Specimens Tested at Their Estimated In-Situ Confining Pressures

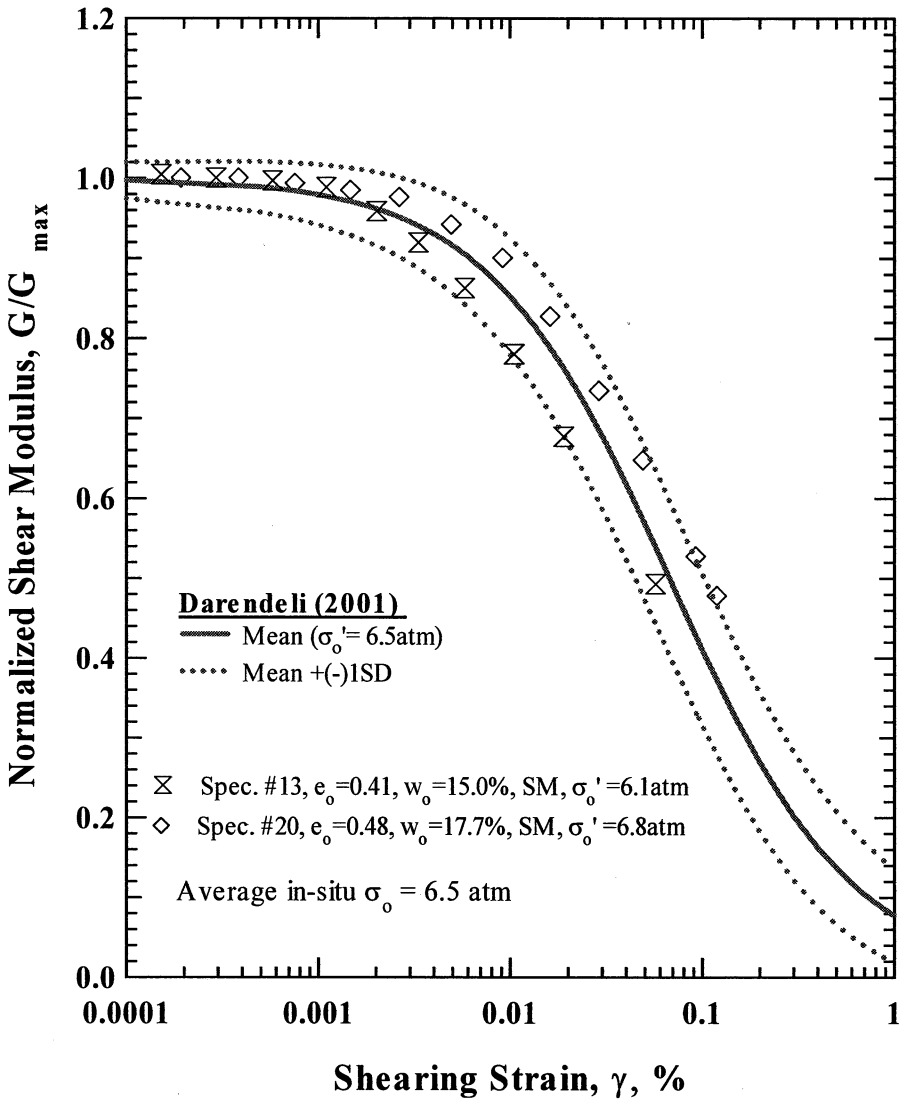

Figure 53 Comparison between the Trends Predicted by Darendeli (2001) and the Variation in Normalized Shear Modulus with Shearing Strain from Resonant Column (RC) Tests of the Two, Silty Sand (SM) Specimens Tested at Their Estimated In-Situ Confining Pressures

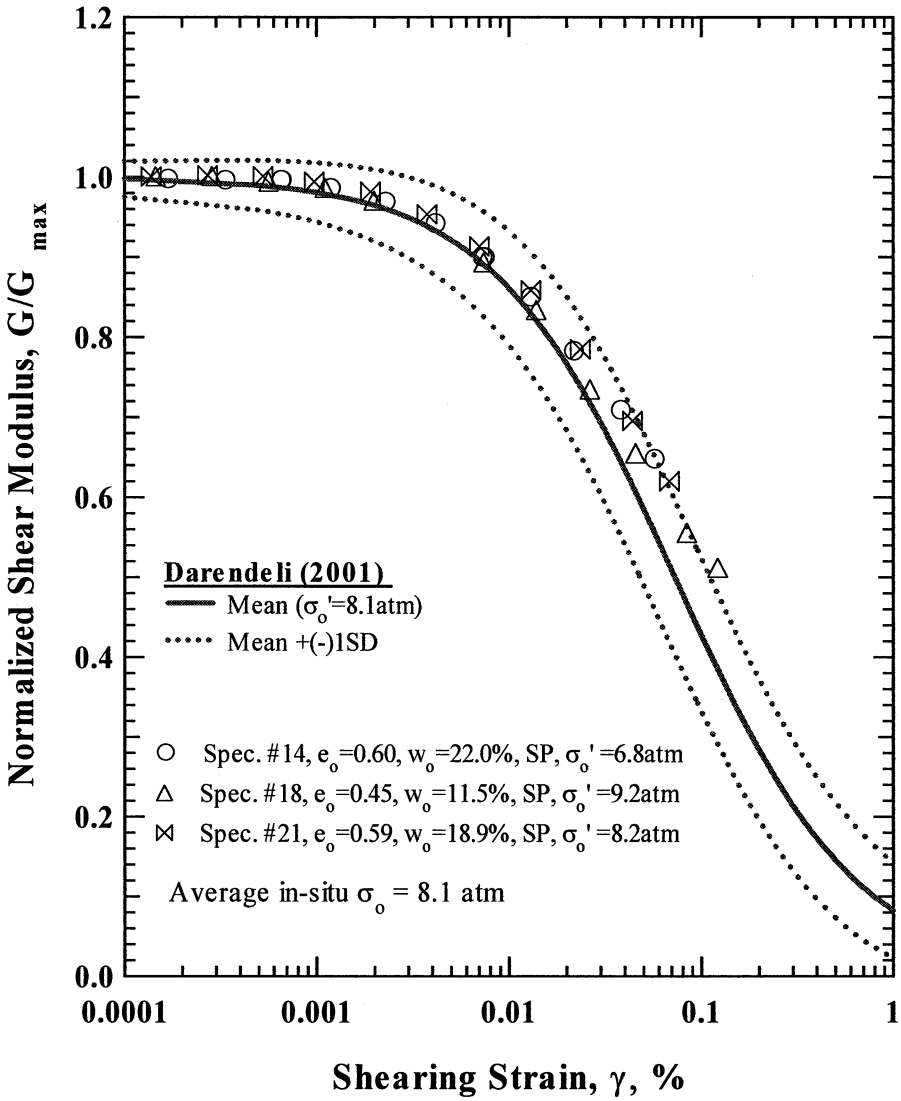

Figure 54 Comparison between the Trends Predicted by Darendeli (2001) and the Variation in Normalized Shear Modulus with Shearing Strain from Resonant Column (RC) Tests of the Three, Poorly Graded Sand (SP) Specimens Tested at Their Estimated In-Situ Confining Pressures

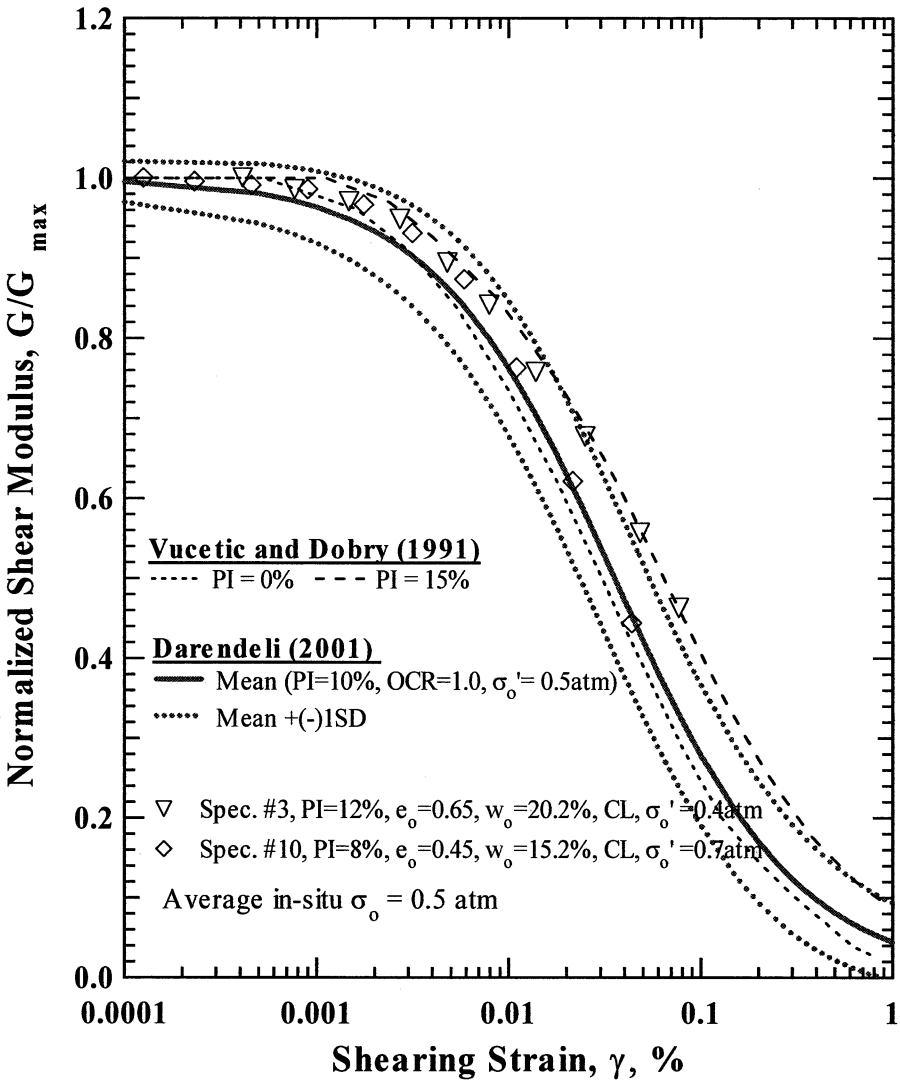

Figure 55 Comparison between the Trends Predicted by Derendeli (2001) and Vucetic and Dobry (1991), and the Variation in Normalized Shear Modulus with Shearing Strain from Resonant Column (RC) Tests of Two Specimens with an Average PI = 10 % in the Low In-Situ Confining Pressure Group Tested at Their Estimated In-Situ Confining Pressures

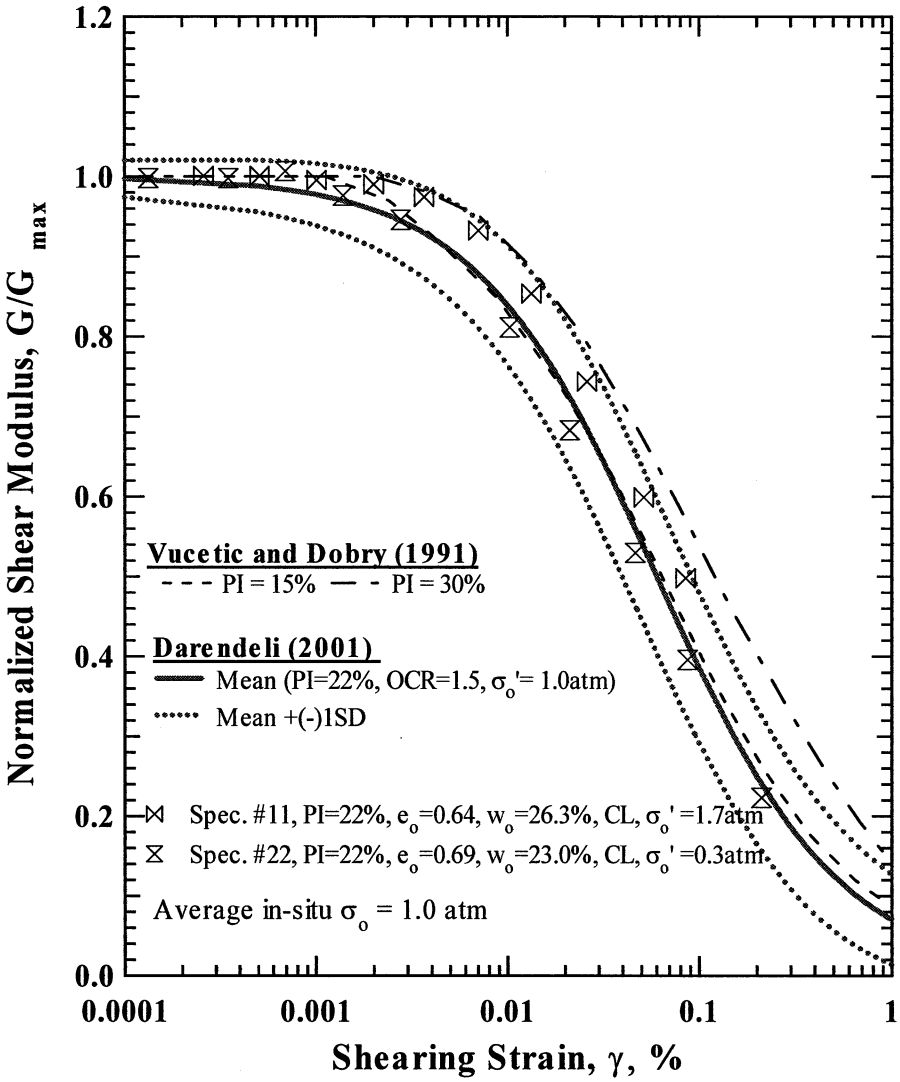

Figure 56 Comparison between the Trends Predicted by Darendeli (2001) and Vucetic and Dobry (1991), and the Variation in Normalized Shear Modulus with Shearing Strain from Resonant Column (RC) Tests of Two Specimens with PI = 22 % in the Low In-Situ Confining Pressure Group Tested at Their Estimated In-Situ Confining Pressures

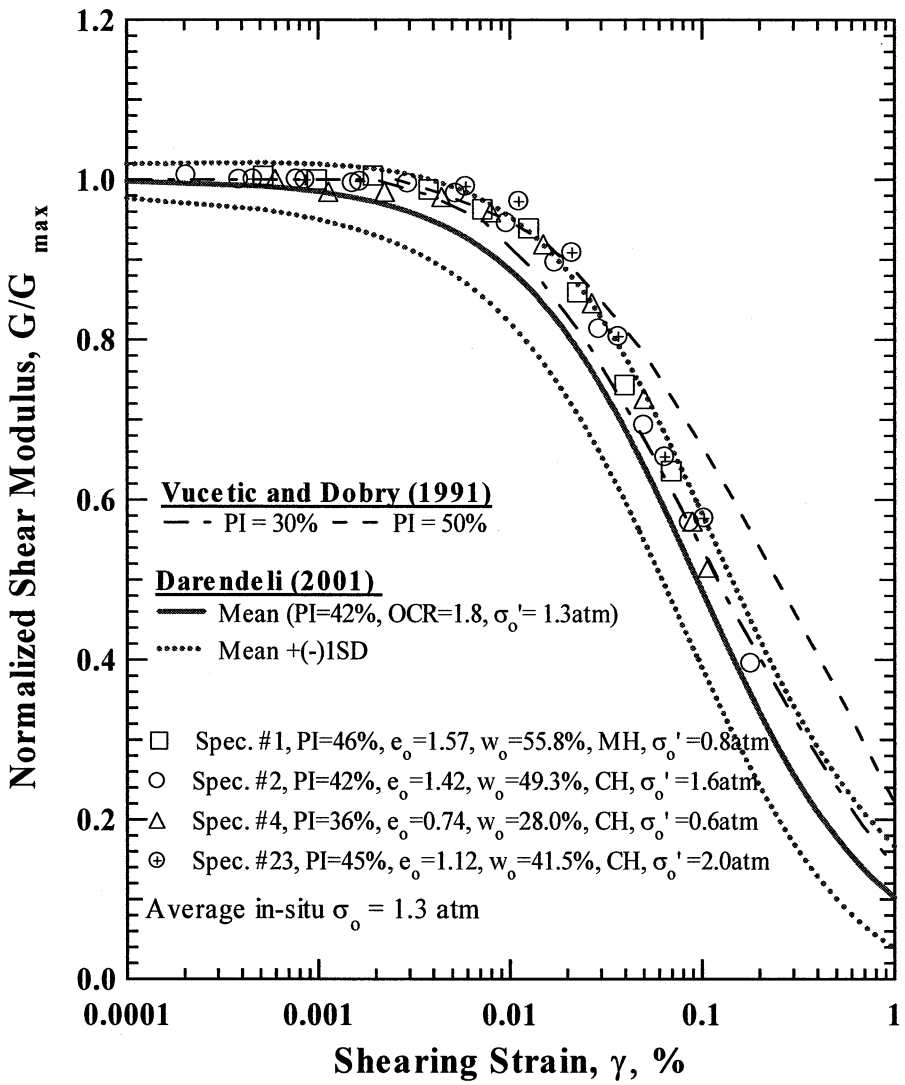

Figure 57 Comparison between the Trends Predicted by Darendeli (2001) and Vucetic and Dobry (1991) and the Variation in Normalized Shear Modulus with Shearing Strain from Resonant Column (RC) Tests of Four Specimens with an Average PI = 42 % in the Low In-Situ Confining Pressure Group Tested at Their Estimated In-Situ Confining Pressures

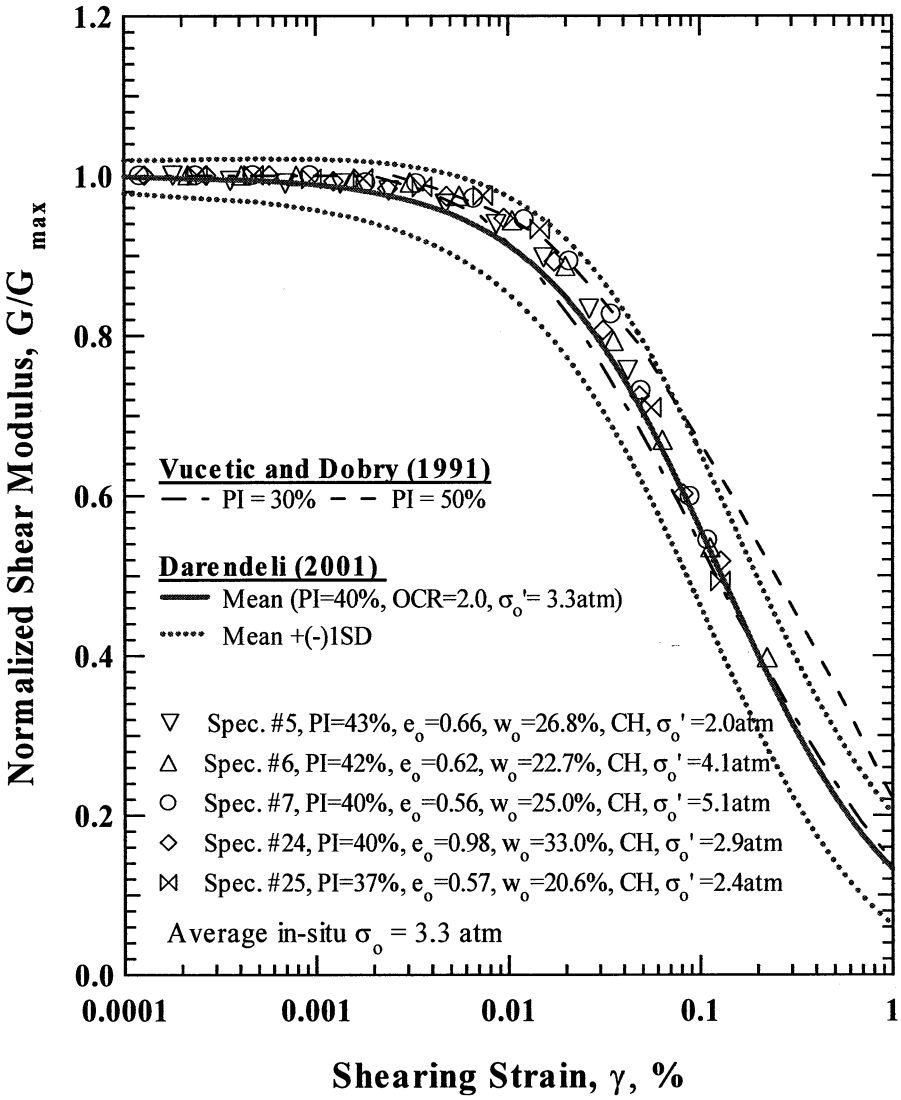

Figure 58 Comparison between the Trends Predicted by Darendeli (2001) and Vucetic and Dobry (1991) and the Variation in Normalized Shear Modulus with Shearing Strain from Resonant Column (RC) Tests of Five Specimens with an Average PI = 40% in the Medium In-Situ Confining Pressure Group Tested at Their Estimated In-Situ Confining Pressures

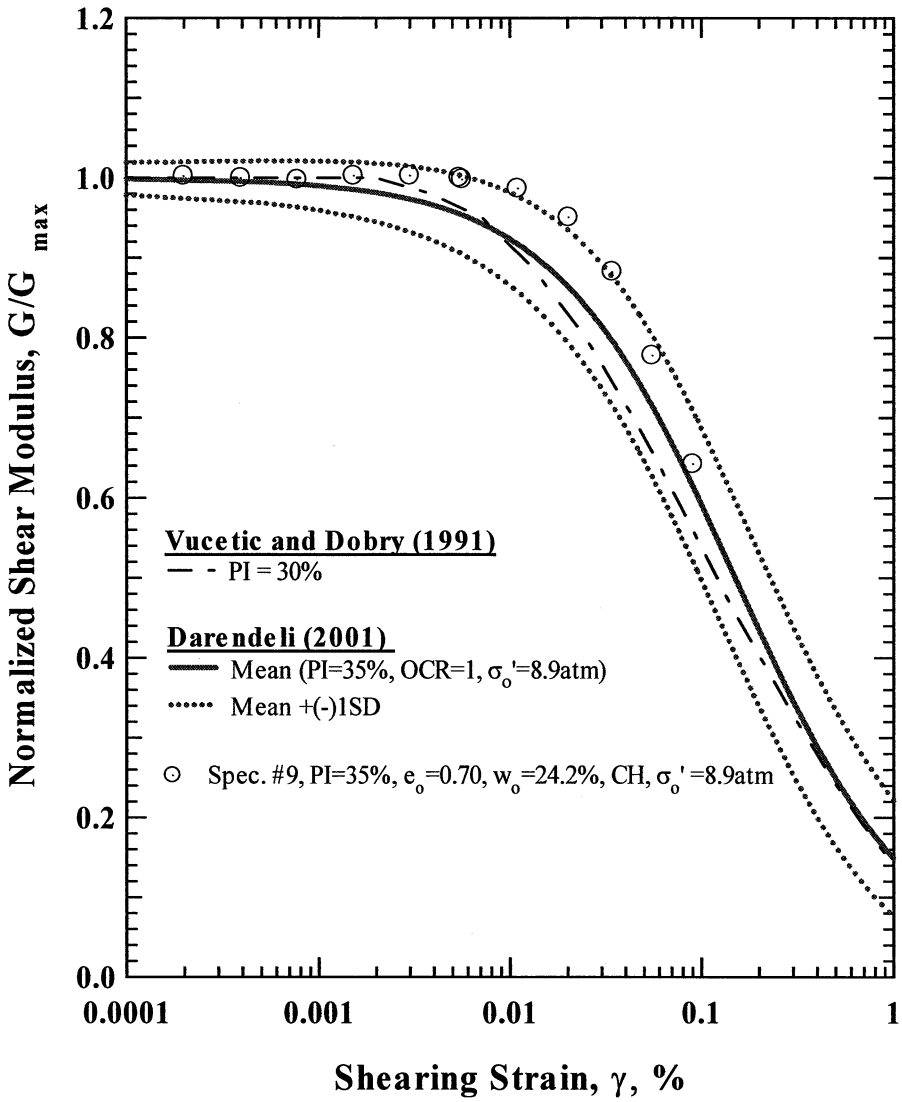

Figure 59 Comparison between the Trends Predicted by Darendeli (2001) and Vucetic and Dobry (1991) and the Variation in Normalized Shear Modulus with Shearing Strain from Resonant Column (RC) Tests of the Three Specimens in the High In-Situ Confining Pressure Group Tested at Their Estimated In-Situ Confining Pressures

mean Darendeli curves have also been added to the figures. In general, all results compare quite well at confining pressures from 0.5 to 3.3 atm (see Figures 55 through 58). The main difference occurs at the highest confining pressure (8.9 atm) with Specimen No. 9 (PI = 35%) which exhibits more linear behavior in the strain range of about 0.005 to 0.05% than the Vucetic and Dobry curve for PI = 30% and the mean Darendeli curve (see Figure 59). It is interesting to note that this more linear behavior could be taken into account in Darendeli's model simply by increasing the value of "a".

4.2 Nonlinear D – Log γ Relationships

4.2.1 Nonlinear D – Log γ Relationships of Nonplastic Specimens - Results of the D - log γ measurements of the seven nonplastic specimens determined by the RC tests are presented in Figure 60 for measurements at the estimated in-situ confining pressure which ranged from 0.43 ksf (21 kPa) to 27.36 ksf (1312 kPa). As expected, the values of the material damping ratio of all specimens exhibit a linear range (where D is constant and equal to D_{min}) followed by a nonlinear range where D increases with increasing shearing strain.

Comparisons of the D - log γ relationships measured in the RC and TS tests are shown in Figure 61 for Specimen Nos. 14 and 20. Comparisons for the other specimens are shown in the appendices. Two points are clearly shown in these figures. First, similar D – log γ curves are measured in both tests, with the main differences related to the effect of excitation frequency at small strains and the combined effects of frequency and number of cycles at larger strains. Second, the RC test can excite the specimens to larger strains because of dynamic amplification which enters the RC test but does not enter the "slow cyclic" TS tests which were conducted at 0.5 Hz. Finally, the RC results represent measurements after about 1000 cycles while the TS results were determined from the tenth cycle of loading.

For comparison of purposes, all material damping ratio curves determined from the TS tests are plotted in Figure 62. The D – log γ relationship suggested by Seed et al. (1986) is also included in Figure 62. As shown in the previous discussion about the modulus reduction curves,

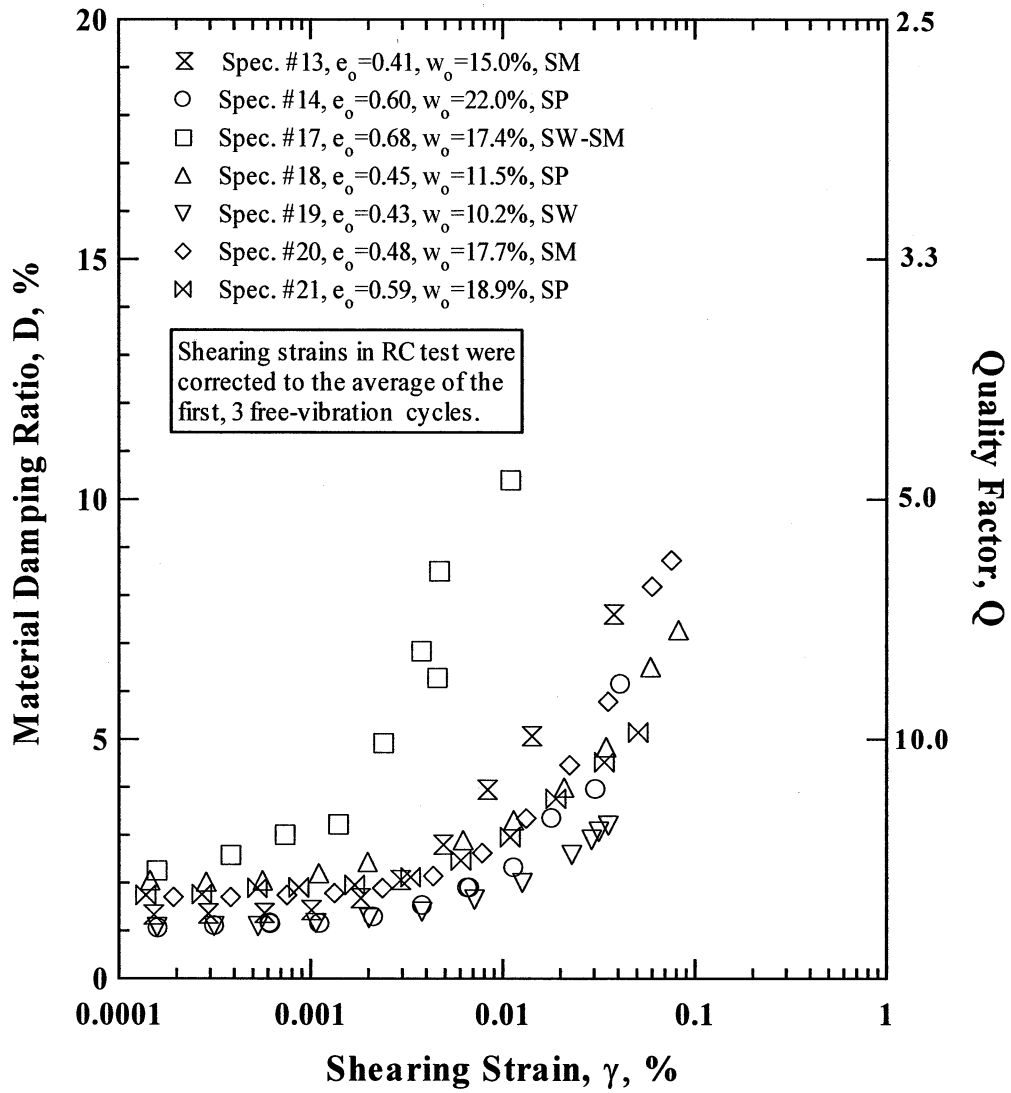

Figure 60 Variation in Material Damping Ratio with Shearing Strain from Resonant Column (RC) Tests of the Seven, Nonplastic Specimens Tested at Their Estimated In-Situ Confining Pressures

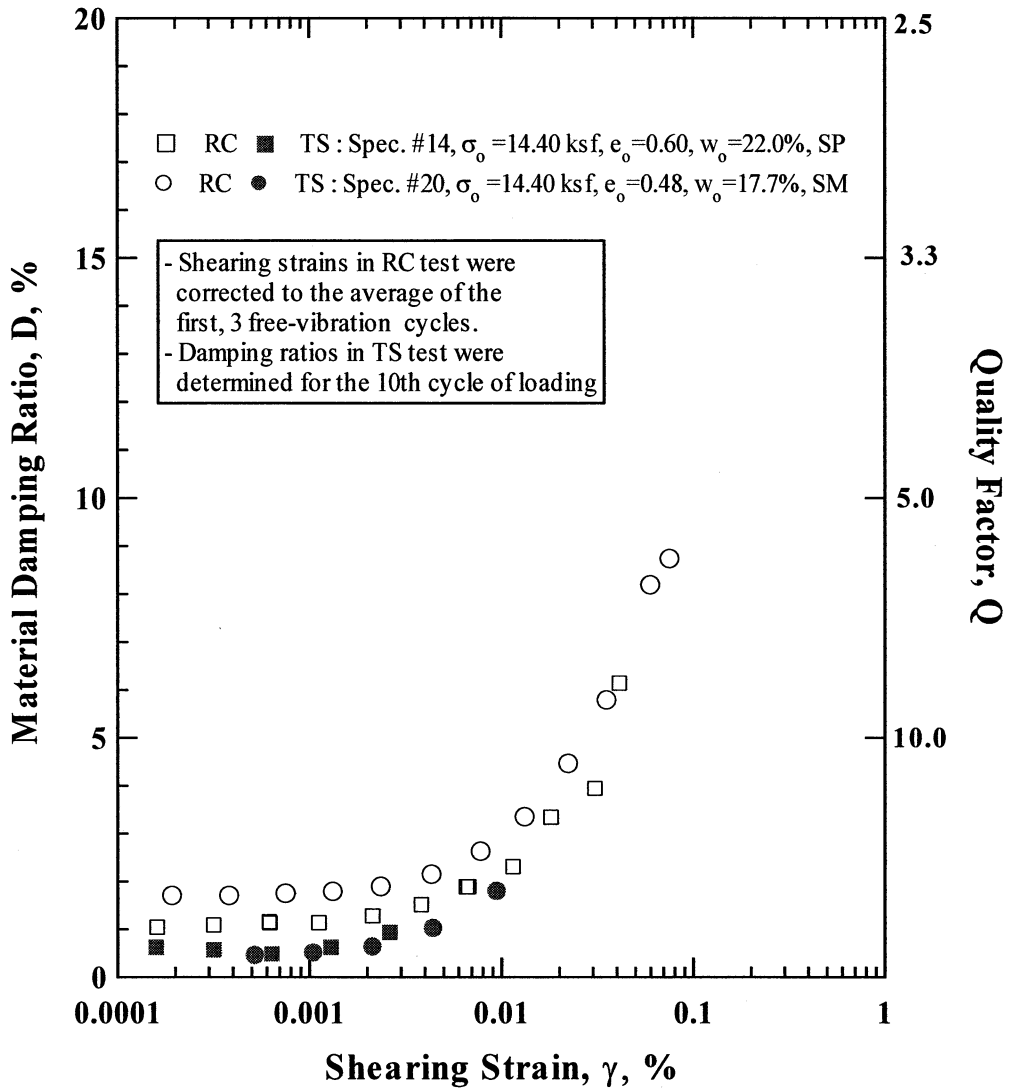

Figure 61 Variation in Material Damping Ratio with Shearing Strain from Resonant Column (RC) and Torsional Shear (TS) Tests of Nonplastic Specimen Nos. 14 and 20 Tested at Their Estimated In-Situ Confining Pressures

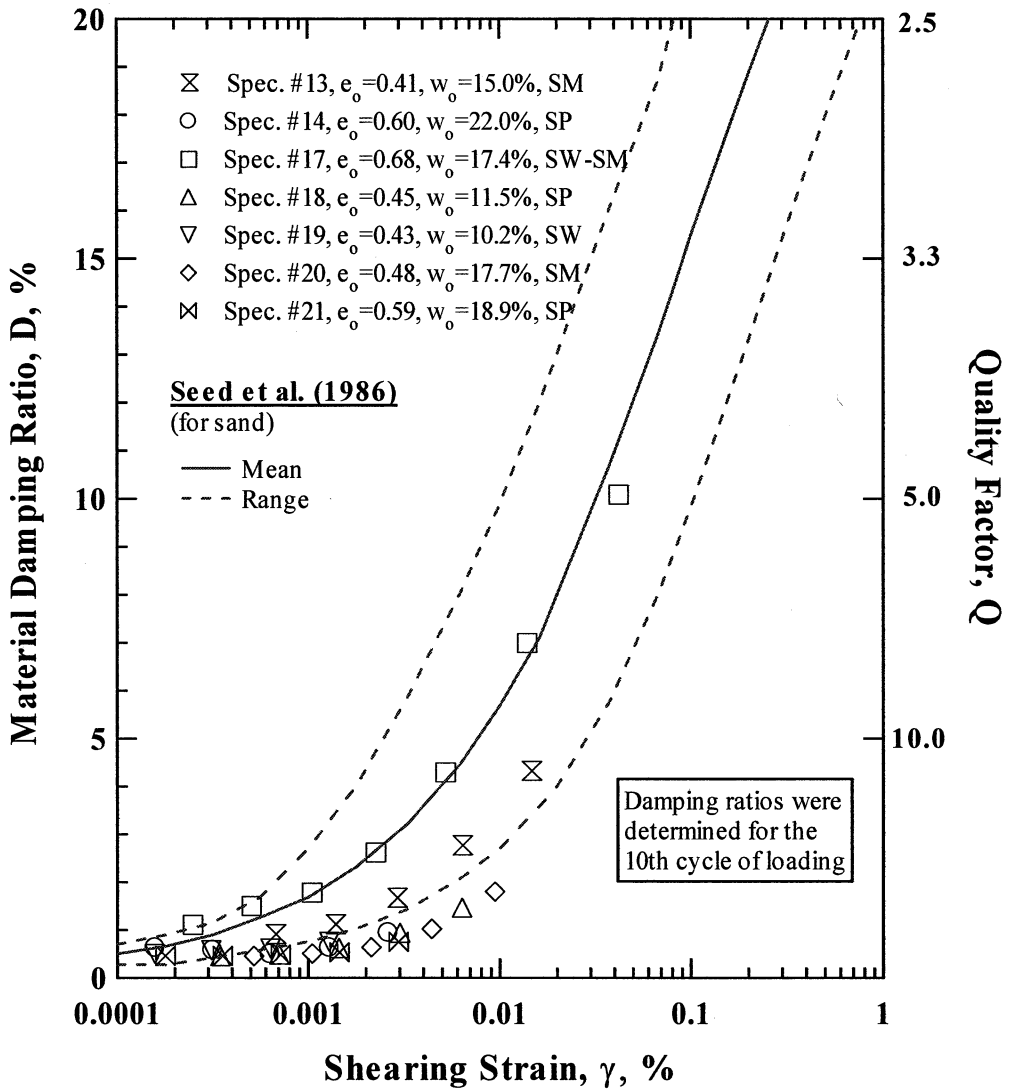

Figure 62 Variation in Material Damping Ratio with Shearing Strain from Torsional Shear (TS) Tests of the Seven, Nonplastic Specimens Tested at Their Estimated In-Situ Confining Pressures

all specimens except Specimen No. 17 behave more linearly than the mean Seed et al. relationship; that is, the material damping curves are below the mean sand curve proposed by Seed et al. (1986). Specimen No. 17 exhibits less linear behavior and higher material damping values over the entire strain range because it is confined at a very low pressure ($\sigma_o \sim 0.2$ atm). The overconsolidation and/or possible cementation of this specimen may also contribute to the nonlinearity and higher damping values. The other specimens were tested at much higher confining pressures, with σ_o ranging from about 6.1 to 12.9 atm and averaging 8.3 atm.

Following the discussion of the nonlinear shear modulus in Section 4.1.1, the D-log γ data in Figure 62 are repotted in the following sub-sets: (1) without Specimen No.17 as shown in Figure 63, (2) with only Specimen Nos. 13 and 20 (Figure 64), and (3) with only Specimen Nos. 14, 18 and 21 as shown in Figure 65. The results in Figure 63 show the impact of confining pressure; that is, all D-log γ curves are below the mean sand curve from Seed et al. (1986) because this curve was generally developed (implicitly) for $\sigma_o \sim 1$ atm (unfortunately, the maximum strain was about 0.02%. However, the curves are extended to higher strains in Section 4.2.4 using Darendeli's (2001) model.). The results in Figure 64 are for the two silty sand (SM) specimens. In this case, each specimen has about the same parameters and is tested at nearly the same pressure (within about 10%). Therefore, as with the G/G_{max}- log γ curves, the results seem to be indicative of the variation that may be found in the general behavior of "similar" soils. (This point is discussed further in Section 4.2.4 and shown in Figure 80.) However, they may also be influenced by parameters that have not been measured (such as mineral content of the fines). Figure 65 shows only the three SP specimens. In this case, a close comparison between the D – log γ curves is found. Also, the maximum difference in confining pressures for the three SP specimens is about 30 %, so this change in pressure is insignificant in this comparison.

4.2.2 D - Log γ Relationships of Plastic Specimens - Results of the D - log γ measurements of the eighteen plastic specimens determined by the RC tests are shown in Figures 66 through 68. The results are divided into three groups according to the confining pressure at which high-amplitude testing was performed; low, medium, and high in Figures 66, 67 and 68, respectively.

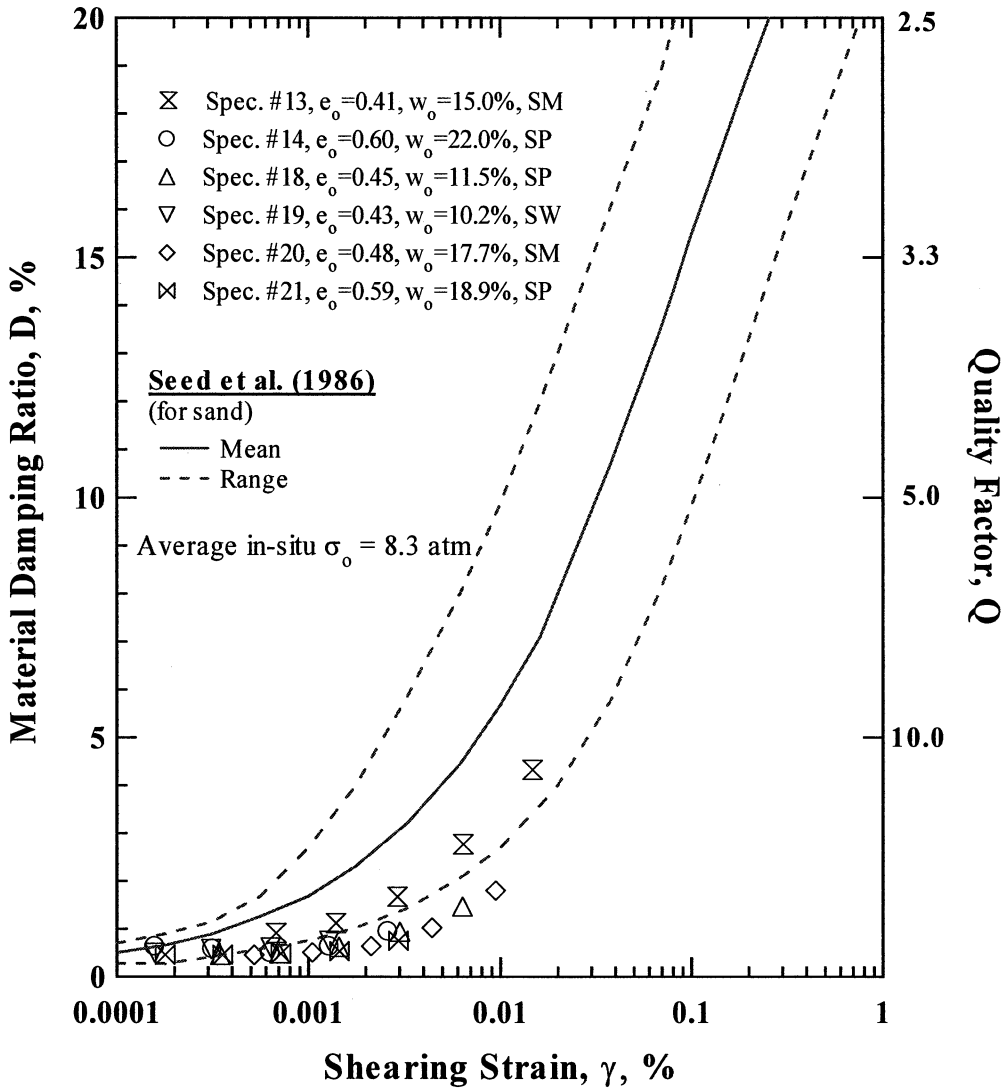

Figure 63 Variation in Material Damping Ratio with Shearing Strain from Torsional Shear (TS) Tests of the Nonplastic Specimens, excluding Specimen No. 17, Tested at Their Estimated In-Situ Confining Pressures

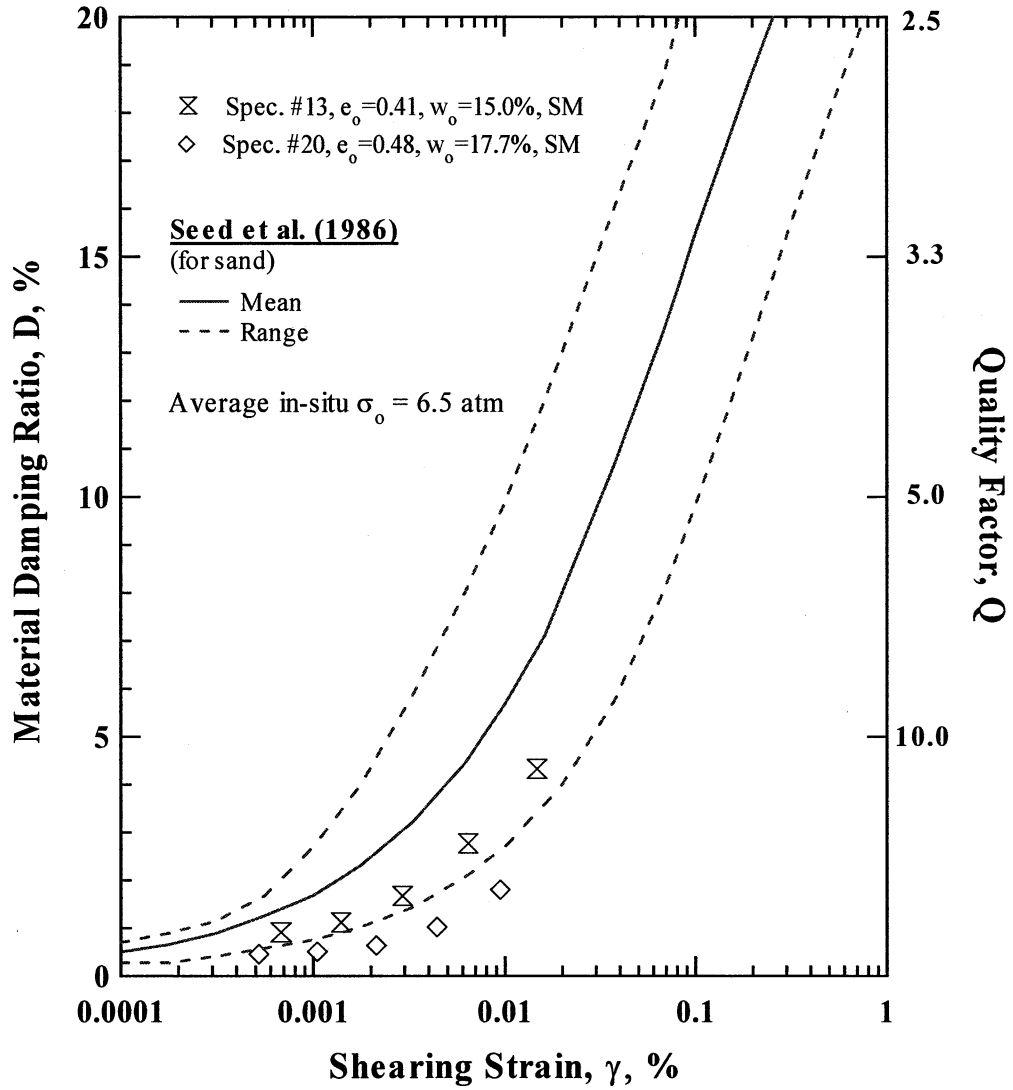

Figure 64 Variation in Material Damping Ratio with Shearing Strain from Torsional Shear (TS) Tests of the Two, Silty Sand (SM) Specimens Tested at Their Estimated In-Situ Confining Pressures

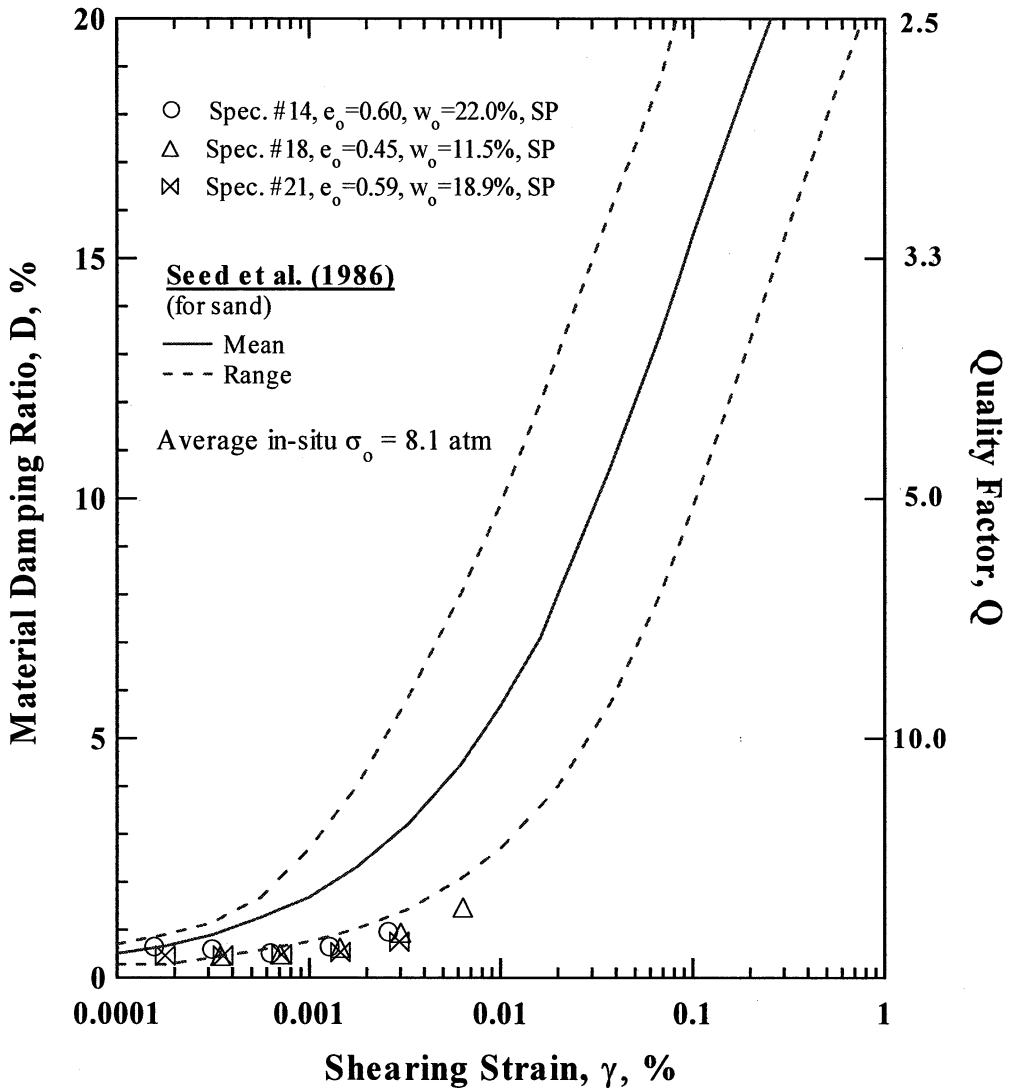

Figure 65 Variation in Material Damping Ratio with Shearing Strain from Torsional Shear (TS) Tests of the Three, Poorly Graded Sand (SP) Specimens Tested at Their Estimated In-Situ Confining Pressures

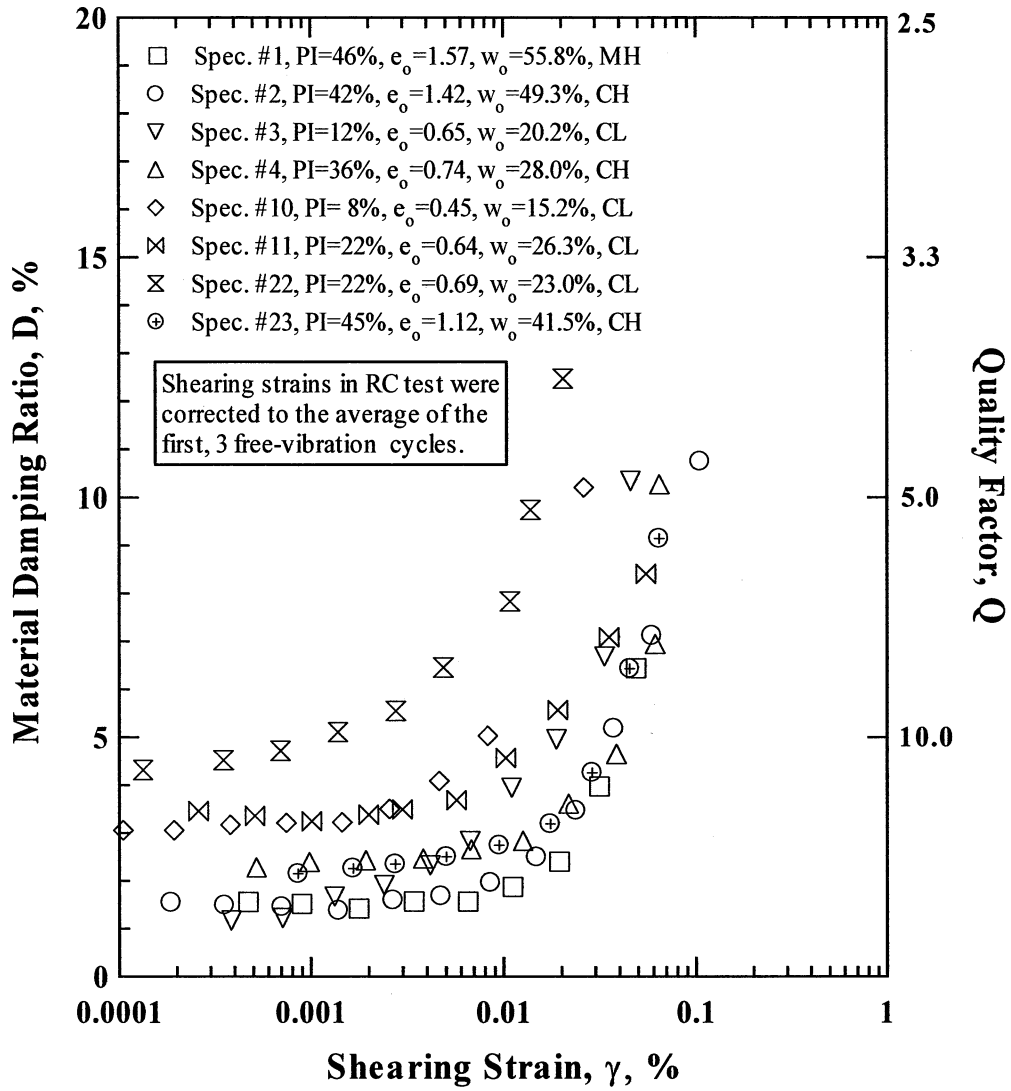

Figure 66 Variation in Material Damping Ratio with Shearing Strain from Resonant Column (RC) Tests of the Eight, Plastic Specimens in the Low In-Situ Confining Pressure Group Tested at Their Estimated In-Situ Confining Pressures

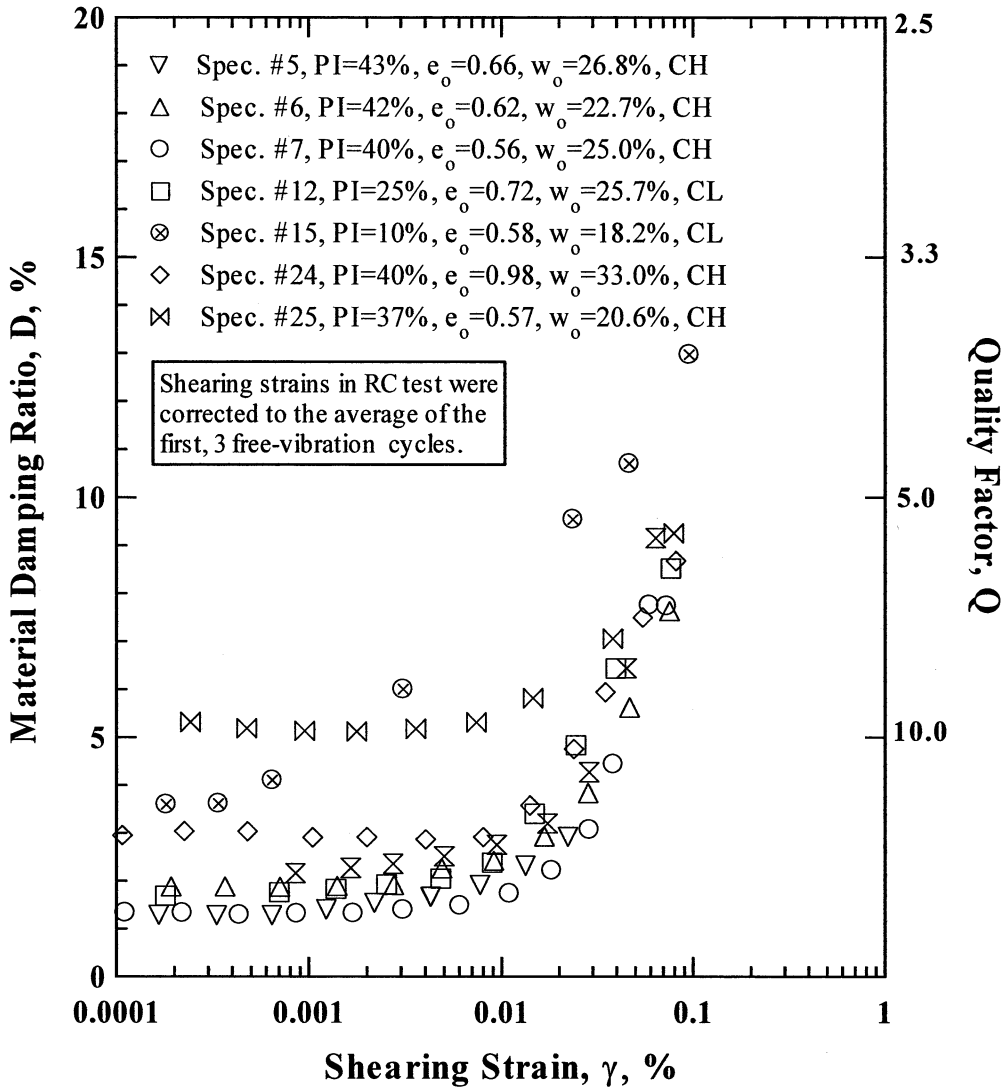

Figure 67 Variation in Material Damping Ratio with Shearing Strain from Resonant Column (RC) Tests of the Seven, Plastic Specimens in the Medium In-Situ Confining Pressure Group Tested at Their Estimated In-Situ Confining Pressures

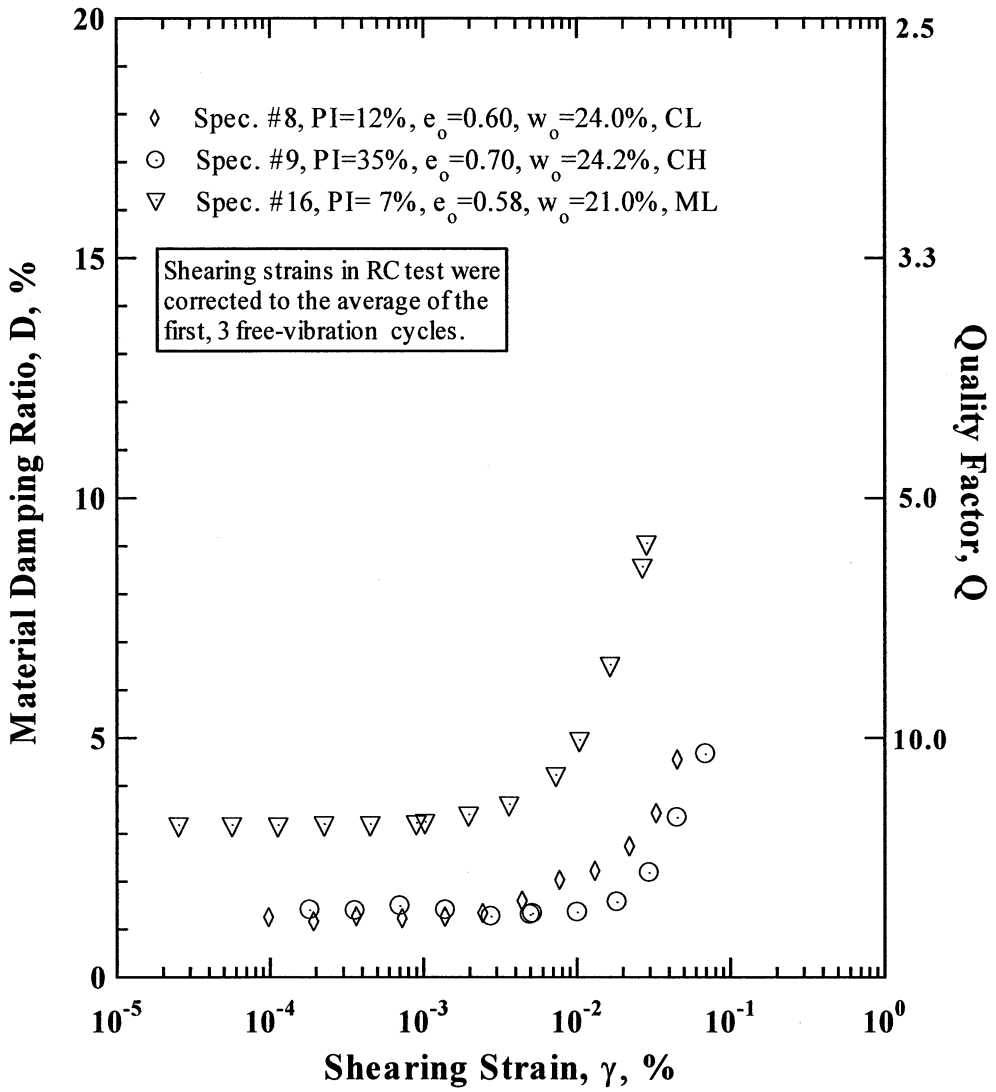

Figure 68 Variation in Material Damping Ratio with Shearing Strain from Resonant Column (RC) Tests of the Three, Plastic Specimens in the High In-Situ Confining Pressure Group Tested at Their Estimated In-Situ Confining Pressures

These three groups are the same groups used in the discussion of the G – log γ and G/G_{max} – log γ relationships in Section 4.1. Also, for reference purposes, the average values of the estimated in-situ σ_o are about 1, 4, and 9 atm for the low, medium, and high pressure groups, respectively.

Comparisons of the D - log γ relationships measured in the RC and TS tests are shown in Figure 69 for Specimen Nos. 10 and 22. As seen in the figure, similar shapes in the D – log γ curves are measured with each testing technique; that is, the RC and TS curves nearly parallel each other. The main difference in the D – log γ curve is the higher value of D measured at each γ in the RC test due primary to the higher test frequencies. Therefore, since frequencies associated with earthquake shaking are generally in the range of 0.1 to 10 Hz, material damping ratios measured in TS testing represent the nonlinear D – log γ relationships for use in geotechnical earthquake engineering problems.

Comparisons of the D - log γ relationships determined from the TS tests for the three confining pressure groups are shown in Figures 70 through 72 for the low, medium and high confining pressure groups, respectively. As confining pressure increases, the D – log γ relationships move down and to the right; that is, lower D_{min} and lower D at higher strains (average values of D_{min} of 1.20, 1.13, and 1.01, average D at γ = 0.001% of 1.27, 1.08, 0.93, and average D at γ = 0.01% of 2.57, 1.69, 1.51 for low, medium, and high in-situ confining pressure groups, respectively).

4.2.3 Comparisons of Measured and Empirical D- Log γ Relationships

4.2.3.1 Sand Curve of Seed et al. (1986) – The D – log γ relationships measured in the TS tests for the nonplastic soils are compared in Figures 62 through 65 with the empirical sand curve proposed by Seed et al. As discussed earlier, six of the specimens exhibit a more linear response than predicted by the sand curve (see Figure 63), due mainly to the higher confining pressures used in these tests. Unfortunately, the maximum strain in any of these six tests did not exceed 0.02%. Therefore, the shape of the D – log γ relationships can not be compared at higher strains. However, theses laboratory results are extrapolated to larger strains using Darendeli's (2001) model in Section 4.2.4.

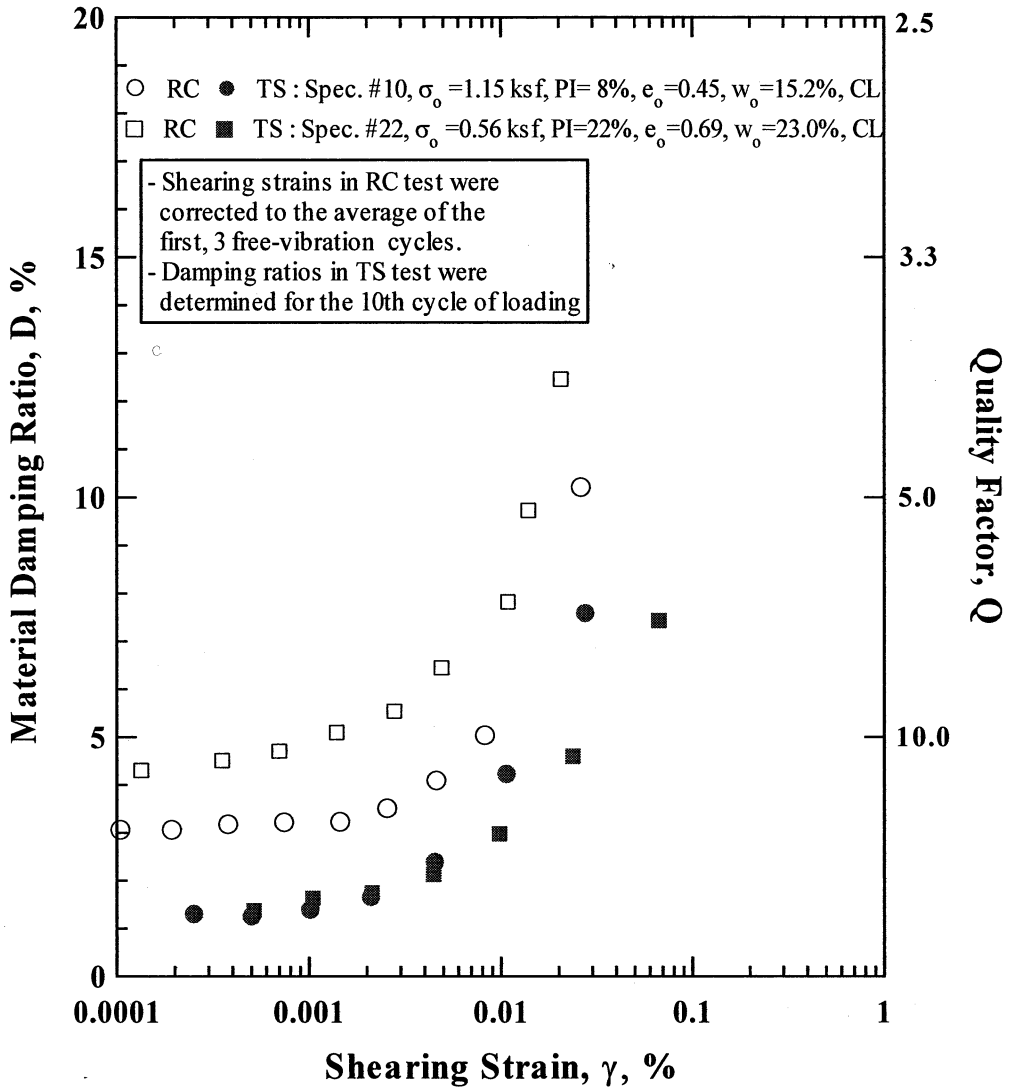

Figure 69 Variation in Material Damping Ratio with Shearing Strain from Resonant Column (RC) and Torsional Shear (TS) Tests of Specimen Nos. 10 and 22 Tested at Their Estimated In-situ Confining Pressures

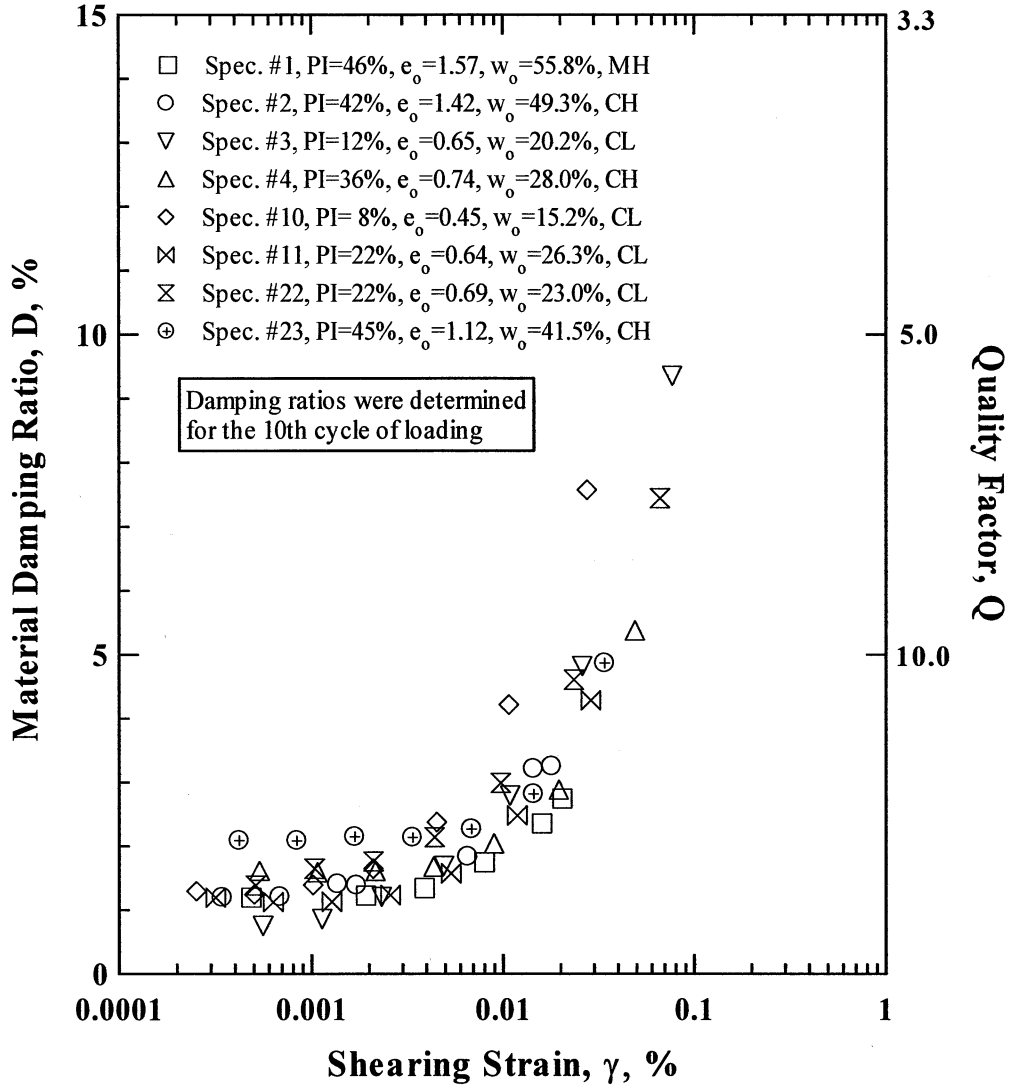

Figure 70 Variation in Material Damping Ratio with Shearing Strain from Torsional Shear (TS) Tests of the Eight, Plastic Specimens in the Low In-Situ Confining Pressure Group Tested at Their Estimated In-Situ Confining Pressures

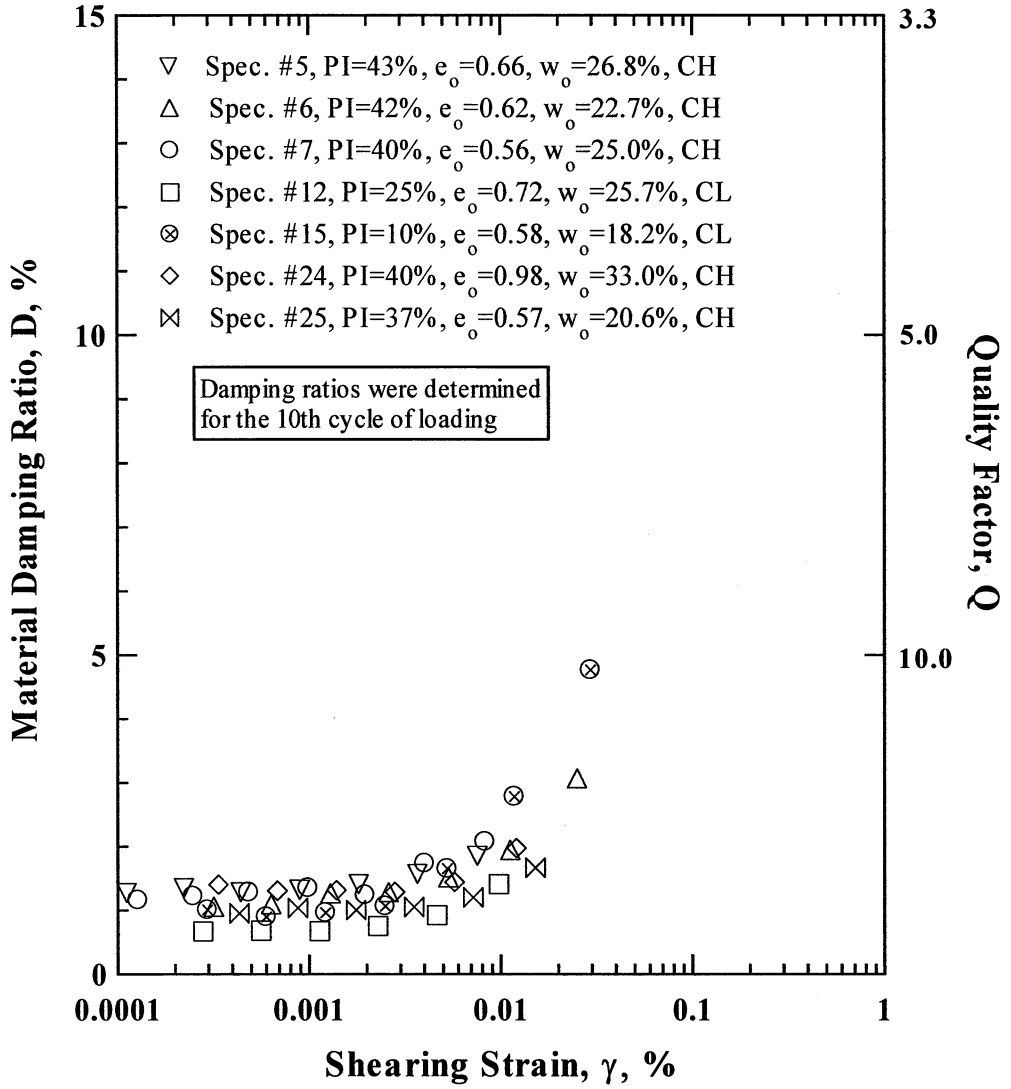

Figure 71 Variation in Material Damping Ratio with Shearing Strain from Torsional Shear (TS) Tests of the Seven, Plastic Specimens in the Medium In-Situ Confining Pressure Group Tested at Their Estimated In-Situ Confining Pressures

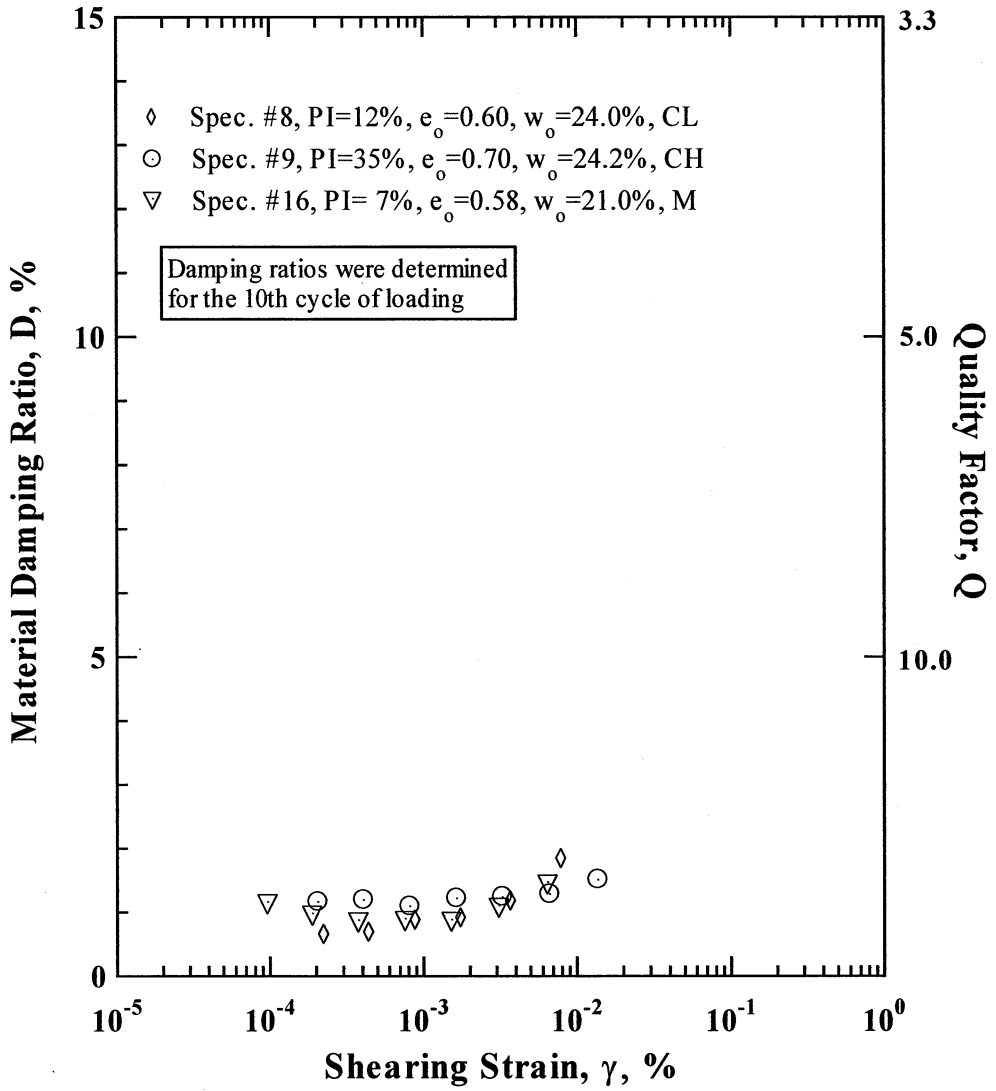

Figure 72 Variation in Material Damping Ratio with Shearing Strain from Torsional Shear (TS) Tests of the Three, Plastic Specimens in the High In-Situ Confining Pressure Group Tested at Their Estimated In-Situ Confining Pressures

4.2.3.2 Curves for Plastic Soils of Vucetic and Dobry (1991) – The D – log γ relationships measured in the TS tests at 0.5 Hz are compared in Figures 73 through 78 with the D – log γ curves recommended by Vucetic and Dobry for soils with plasticity indices (PI) of 0, 15, 30, 50 and 100%. The specimens that were tested in low confining group are further sub-divided according to their average values of PI of 10, 22, and 42 % in Figures 73, 74 and 75, respectively. There are two important observations worth pointing out in these figures: 1) the measured damping values in the small-strain range, D_{min}, are below the strain range covered by the Vucetic and Dobry curves, and (2) as observed in comparison of the G/G_{max} – log γ relationships in Section 4.1.3, the measured relationships exhibit slightly more linearity than the predicted curves (the second point is most obvious in Figure 75). Also, a somewhat different pattern between the measured D – log γ relationships and the predicted Vucetic and Dobry curves is most clearly seen in the tests at the high confining pressures. These results are shown in the medium confining pressure group, Figures 76 and 77, and in the high confining pressure group in Figure 78. In these cases, all specimens clearly exhibited a larger linear range than the predicted curves for the respective plasticities of the test specimens. Also, at higher strains, the linearity is followed by a slightly more rapid increase in D with γ. The specimens tested at the lowest confining pressure also show this generalized trend of a rapid increase in D with γ in Figures 73 through 75.

4.2.4 Comparison with the Nonlinear Model for D-Log γ Proposed by Darendeli (2001)

Mehmet Darendeli (2001) derived an equation for a damping curve based on a modified hyperbolic stress-strain curve and Masing behavior as:

$$D_{\text{Masing}} = c_1 D_{\text{Masing, a=1.0}} + c_2 D_{\text{Masing, a=1.0}}^{\ 2} + c_3 D_{\text{Masing, a=1.0}}^{\ 3} \qquad (7)$$

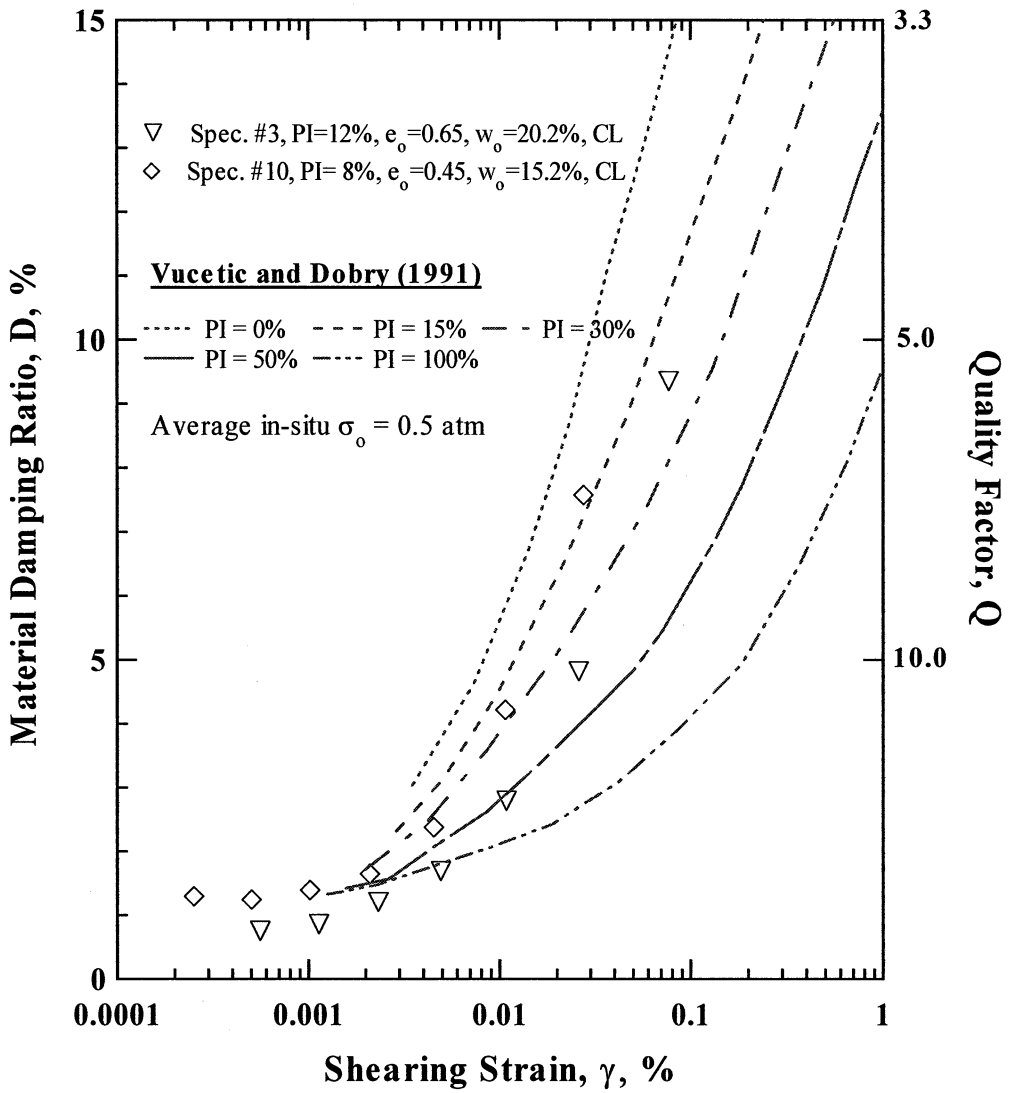

Figure 73 Comparison between the Trends Predicted by Vucetic and Dobry (1991) and the Variation in Material Damping Ratio with Shearing Strain from Torsional Shear (TS) Tests of Two Specimens with an Average PI = 10 % in the Low In-Situ Confining Pressure Group Tested at Their Estimated In-Situ Confining Pressures

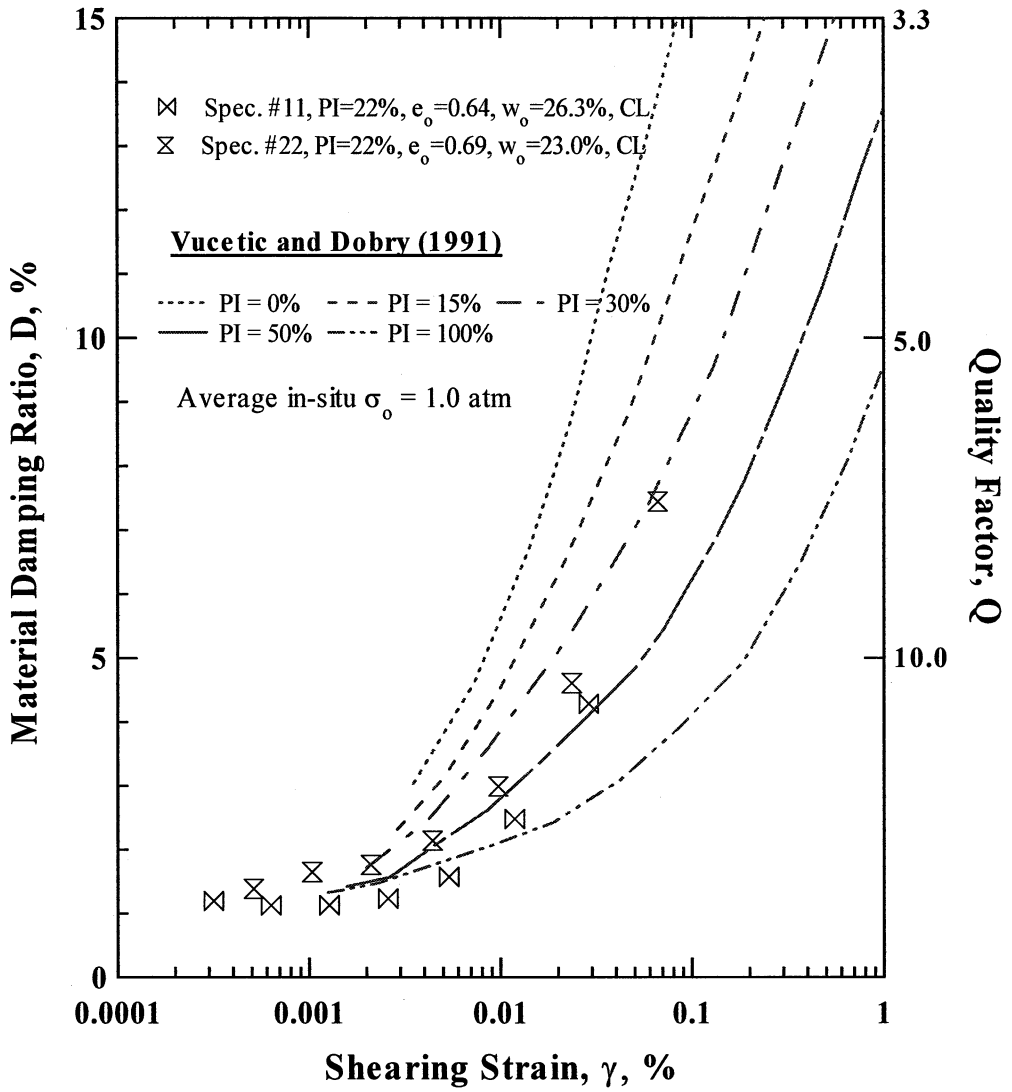

Figure 74 Comparison between the Trends Predicted by Vucetic and Dobry (1991) and the Variation in Material Damping Ratio with Shearing Strain from Torsional Shear (TS) Tests of Two Specimens with PI = 22 % in the Low In-Situ Confining Pressure Group Tested at Their Estimated In-Situ Confining Pressures

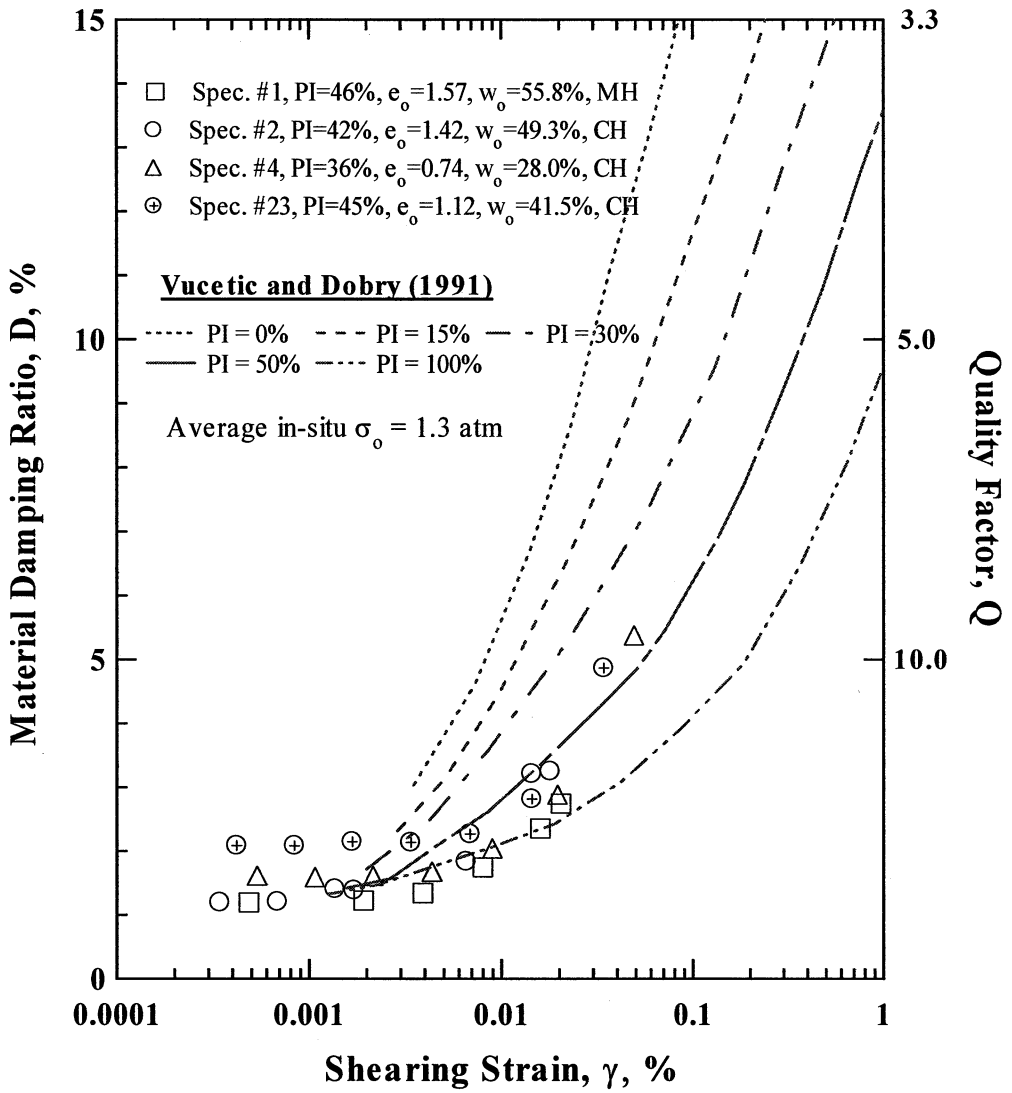

Figure 75 Comparison between the Trends Predicted by Vucetic and Dobry (1991) and the Variation in Material Damping Ratio with Shearing Strain from Torsional Shear (TS) Tests of Four Specimens with an Average PI = 42 % in the Low In-Situ Confining Pressure Group Tested at Their Estimated In-Situ Confining Pressures

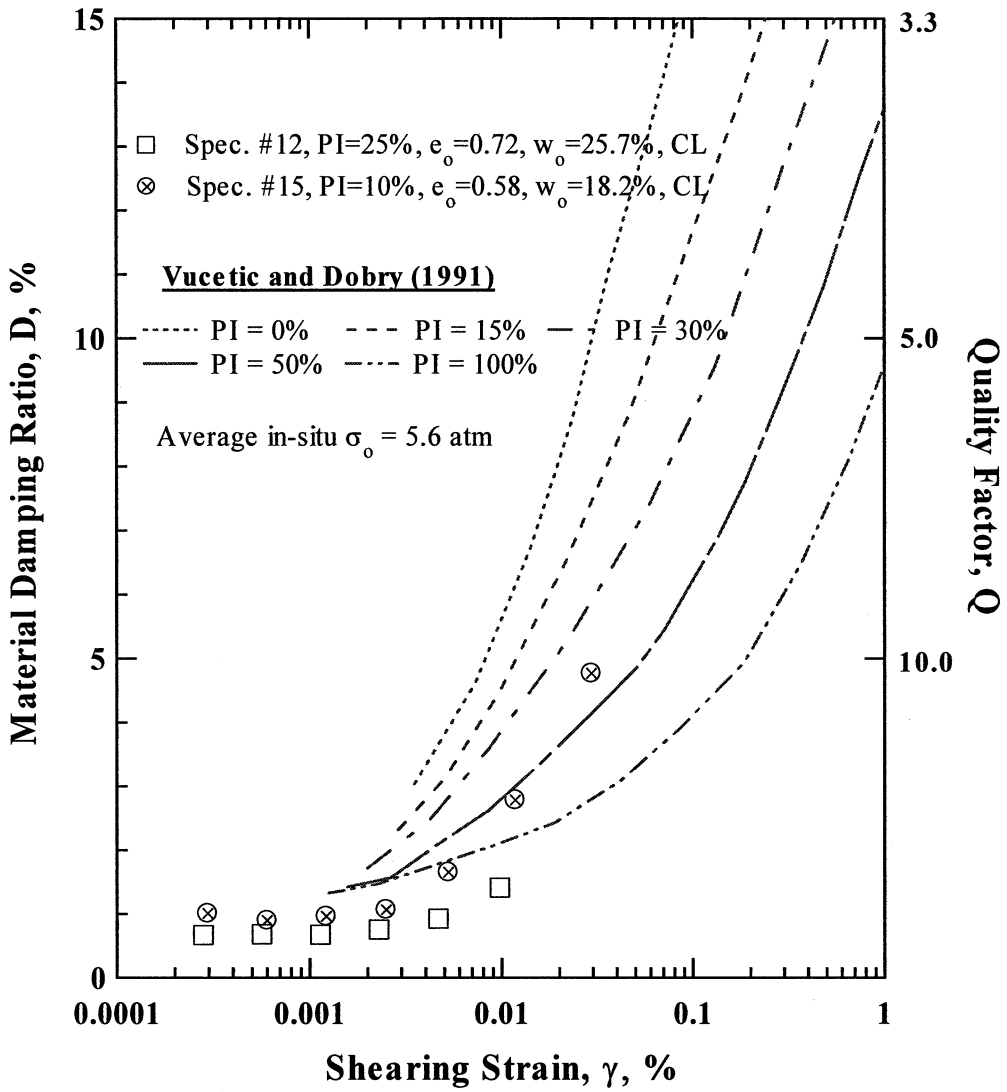

Figure 76 Comparison between the Trends Predicted by Vucetic and Dobry (1991) and the Variation in Material Damping Ratio with Shearing Strain from Torsional Shear (TS) Tests of Two Specimens with Lower Plasticity in the Medium In-Situ Confining Pressure Group Tested at Their Estimated In-Situ Confining Pressures

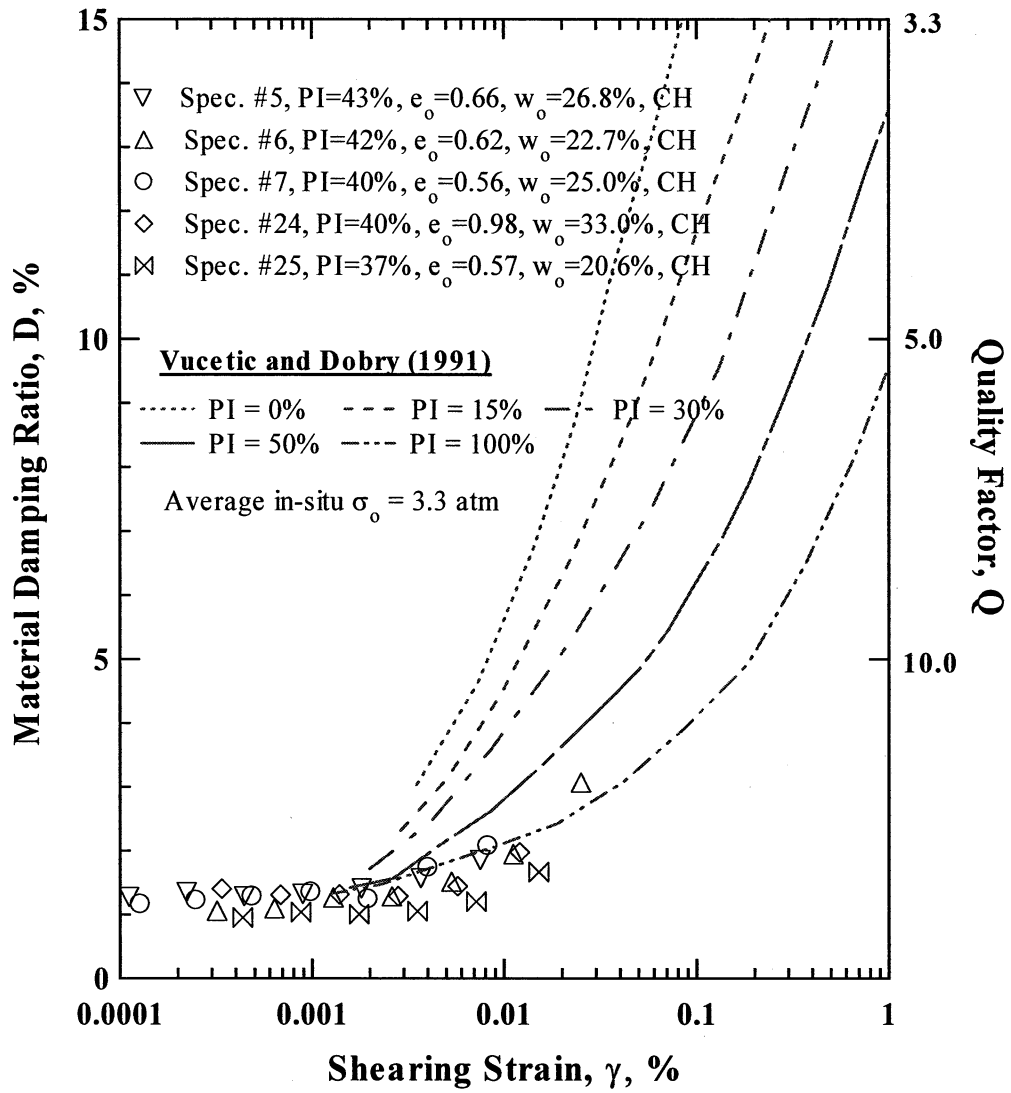

Figure 77 Comparison between the Trends Predicted by Vucetic and Dobry (1991) and the Variation in Material Damping Ratio with Shearing Strain from Torsional Shear (TS) Tests of Five Specimens with an Average PI = 40% in the Medium In-Situ Confining Pressure Group Tested at Their Estimated In-Situ Confining Pressures

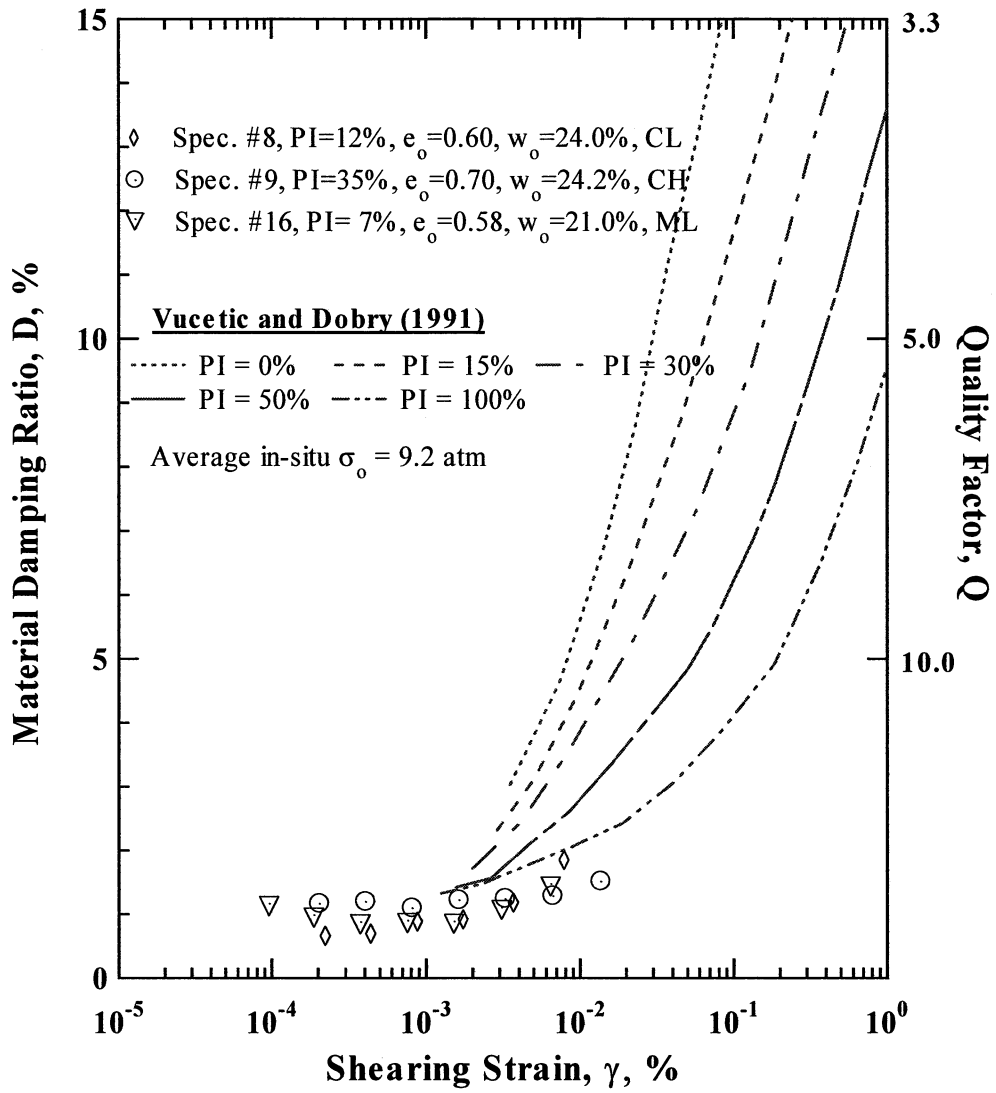

Figure 78 Comparison between the Trends Predicted by Vucetic and Dobry (1991) and the Variation in Material Damping Ratio with Shearing Strain from Torsional Shear (TS) Tests of the Three Specimens in the High In-Situ Confining Pressure Group Tested at Their Estimated In-Situ Confining Pressures

$$D_{\text{Masing, a=1.0}} = \frac{100}{\Pi}\left[4\frac{\gamma - \gamma_r \ln\left(\frac{\gamma+\gamma_r}{\gamma_r}\right)}{\frac{\gamma^2}{\gamma+\gamma_r}} - 2\right](\%) \tag{8}$$

and

$\Pi = 3.1416$,

$\gamma_r = \gamma_{r,G}$,

$c_1 = -1.1143a^2 + 1.8618a + 0.2523$,

$c_2 = 0.0805a^2 - 0.0710a + 0.0095$.

$c_3 = -0.0005a^2 + 0.0002a + 0.0003$

This estimation based on Masing behavior yields higher damping ratios at higher strains than values reported in the literature (e.g., Seed et al., 1986 and Vucetic and Dobry, 1991). Also, Masing damping ratios lack the small-strain material damping ratio, D_{min}, because D_{Masing} goes to zero in the linear range. Therefore, the equation above was modified to take into account the experimental observations as follows:

$$D = F * D_{\text{Masing}} + D_{\text{min}} \tag{9}$$

$$F = b * \left(\frac{G}{G_{\text{max}}}\right)^{0.1} \tag{10}$$

$$b = \phi_{11} + \phi_{12} * \ln(N) \tag{11}$$

and

$$D_{\text{min}} = \left(\phi_6 + \phi_7 * PI * OCR^{\phi_8}\right) * \sigma_o'^{\phi_9} * \left[1 + \phi_{10} * \ln(freq)\right] \tag{12}$$

in which

σ_o' = mean effective confining pressure (atm),

PI = soil plasticity (%),

OCR = overconsolidation ratio,

freq = loading frequency,

$\phi_6 = 0.8005$,

$\phi_7 = 0.0129$,

$\phi_8 = -0.1069$,

$\phi_9 = -0.2889$,

$\phi_{10} = 0.2919$,

$\phi_{11} = 0.6329$, and

$\phi_{12} = -0.0057$.

As in the model equations for the G/G_{max} – log γ relationship (Equations 4 and 5), σ_o', PI and OCR are input parameters. In addition, loading frequency is now an input parameter.

Comparisons between the measured D-log γ curves and the curves predicted by Darendeli's model are presented in Figures 79 through 86. The results in Figure 79 show the generally good agreement between the measured and predicted effect of confining pressure on the nonplastic specimens. Darendeli's model also includes the variation to be expected in the damping curves in terms of plus or minus one standard deviation, +/- σ. Two comparisons for the nonplastic soils are shown in Figures 80 and 81 which show that the measured results fall within these ranges. As discussed previously, strain amplitude in the TS tests did not exceed about 0.02% (with one exception) and Darendeli's model was used to extend these curves.

Finally, specific comparisons for the plastic soils between the measured damping ratio curves and the ones predicted by Darendeli's model and Vucetic and Dobry (1991) are presented in Figures 82 through 86. The +/- σ range around the mean Darendeli curves have also been added to the figures. All observed damping curves fall within these ranges as was found for the nonplastic soils. As discussed previously, damping curves measured in the torsional shear tests exhibited more linearity and then increased more rapidly than predicted by the Vucetic and Dobry (1991) curves. The differences become more evident as the PI of the soil increases and as confining pressure increase. Figures 82 and 83 show all measured and proposed trends are matching well, while more sensitive changes in damping to PI are predicted in the Vucetic and Dobry curves than measured or predicted by the Darendeli curves as shown in Figures 84 though 86.

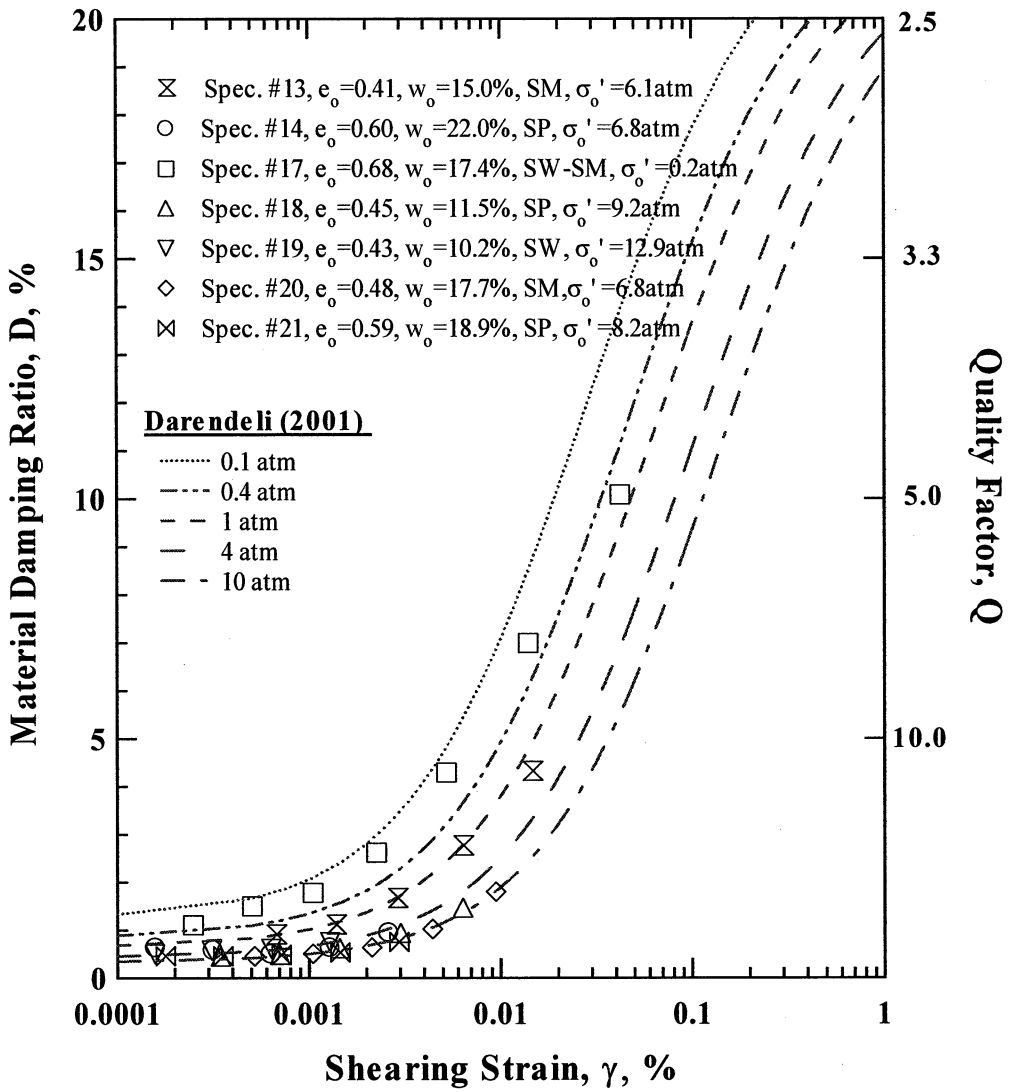

Figure 79 Comparison between the Trends Predicted by Darendeli (2001) and the Variation in Material Damping Ratio with Shearing Strain from Torsional Shear (TS) Tests of the Seven, Nonplastic Specimens Tested at Their Estimated In-Situ Confining Pressures

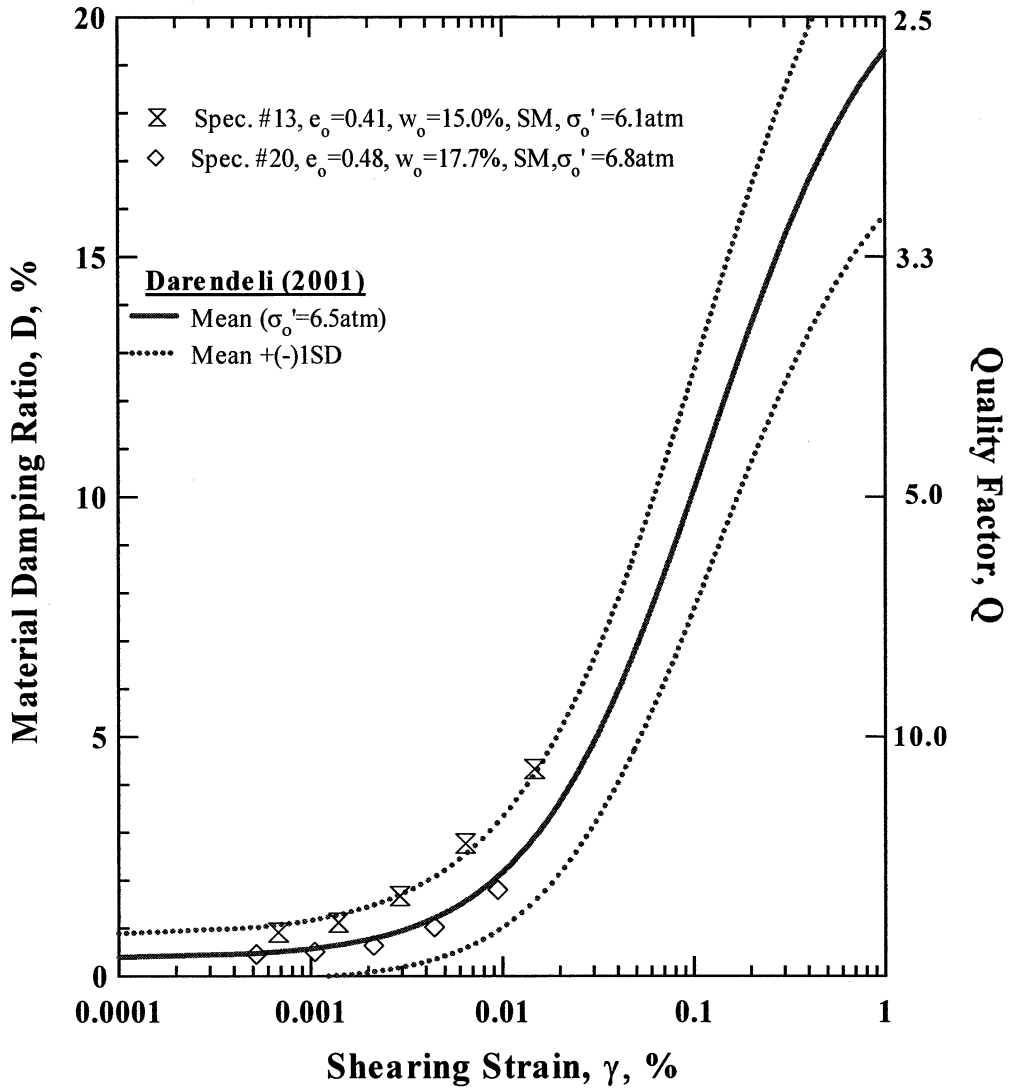

Figure 80 Comparison between the Trends Predicted by Darendeli (2001) and the Variation in Material Damping Ratio with Shearing Strain from Torsional Shear (TS) Tests of the Two, Silty Sand (SM) Specimens Tested at Their Estimated In-Situ Confining Pressures

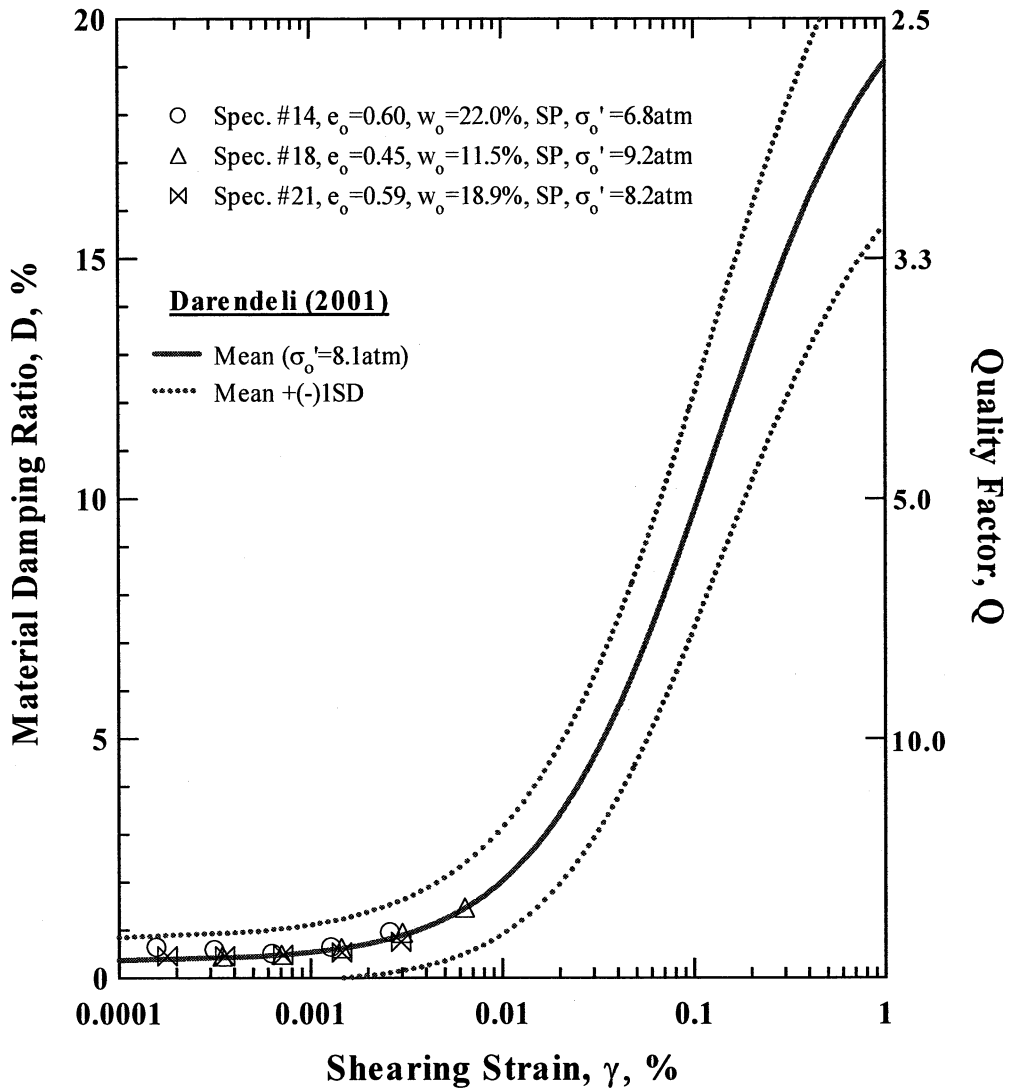

Figure 81 Comparison between the Trends Predicted by Darendeli (2001) and the Variation in Material Damping Ratio with Shearing Strain from Torsional Shear (TS) Tests of the Three, Poorly Graded Sand (SP) Specimens Tested at Their Estimated In-Situ Confining Pressures

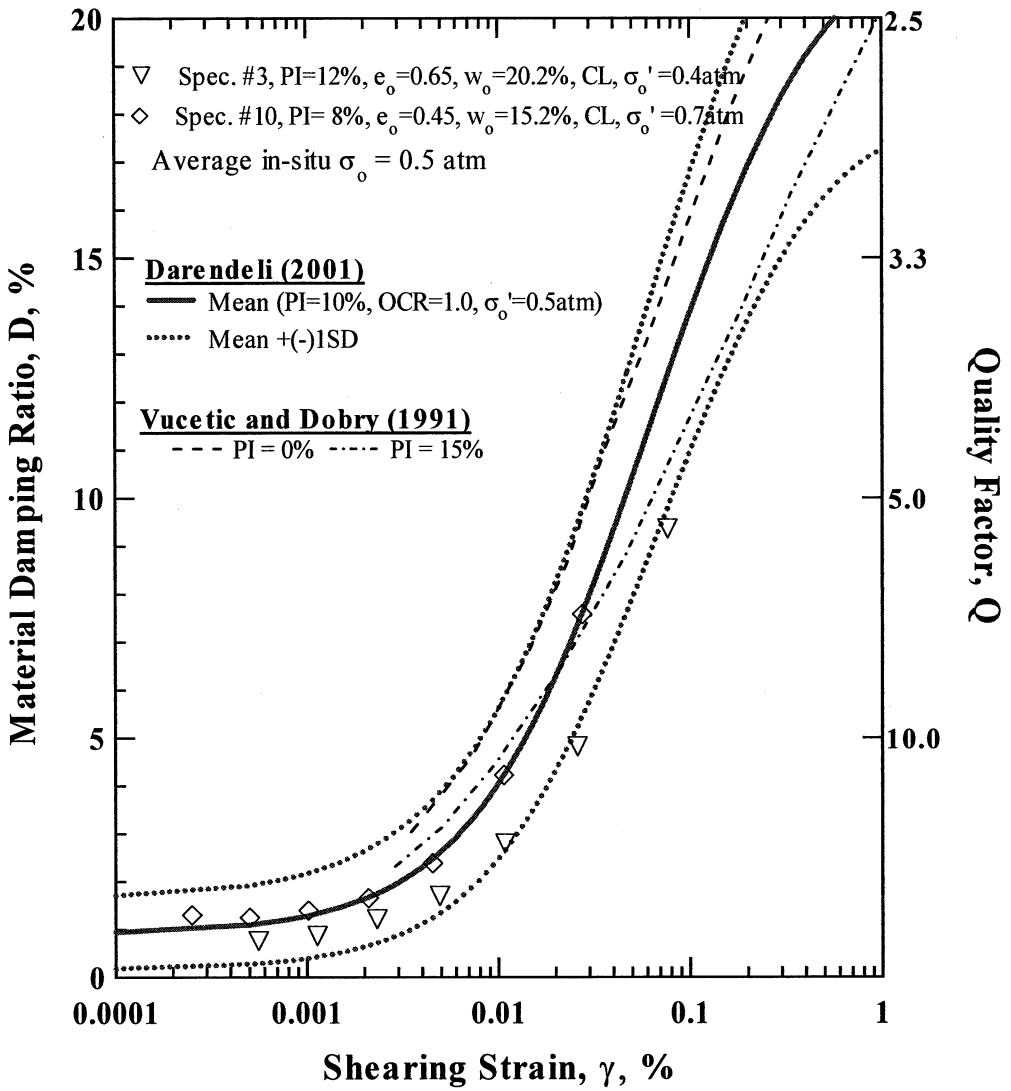

Figure 82 Comparison between the Trends Predicted by Derendeli (2001) and Vucetic and Dobry (1991), and the Variation in Material Damping Ratio with Shearing Strain from Torsional Shear (TS) Tests of Two Specimens with an Average PI = 10 % in the Low In-Situ Confining Pressure Group Tested at Their Estimated In-Situ Confining Pressures

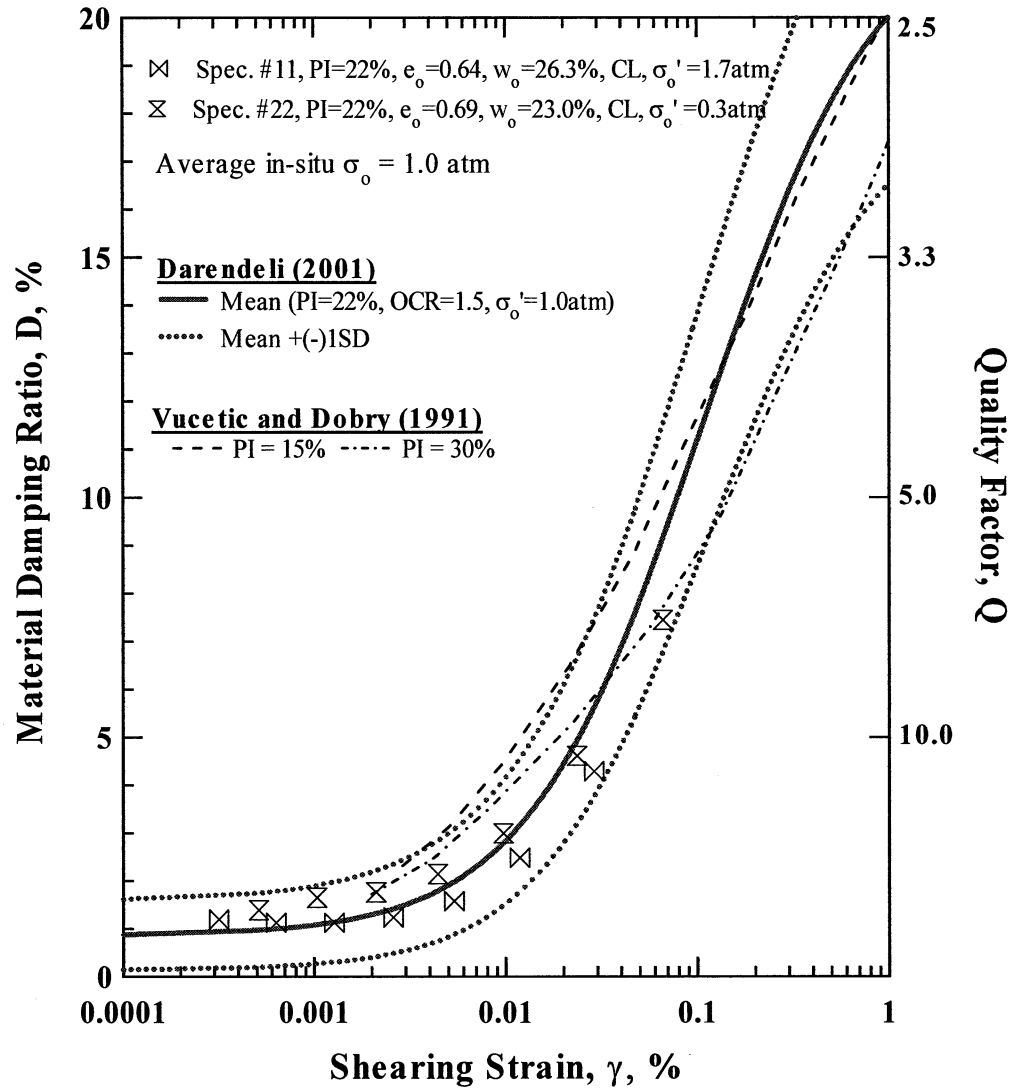

Figure 83 Comparison between the Trends Predicted by Darendeli (2001) and Vucetic and Dobry (1991), and the Variation in Material Damping Ratio with Shearing Strain from Torsional Shear (TS) Tests of Two Specimens with PI = 22 % in the Low In-Situ Confining Pressure Group Tested at Their Estimated In-Situ Confining Pressures

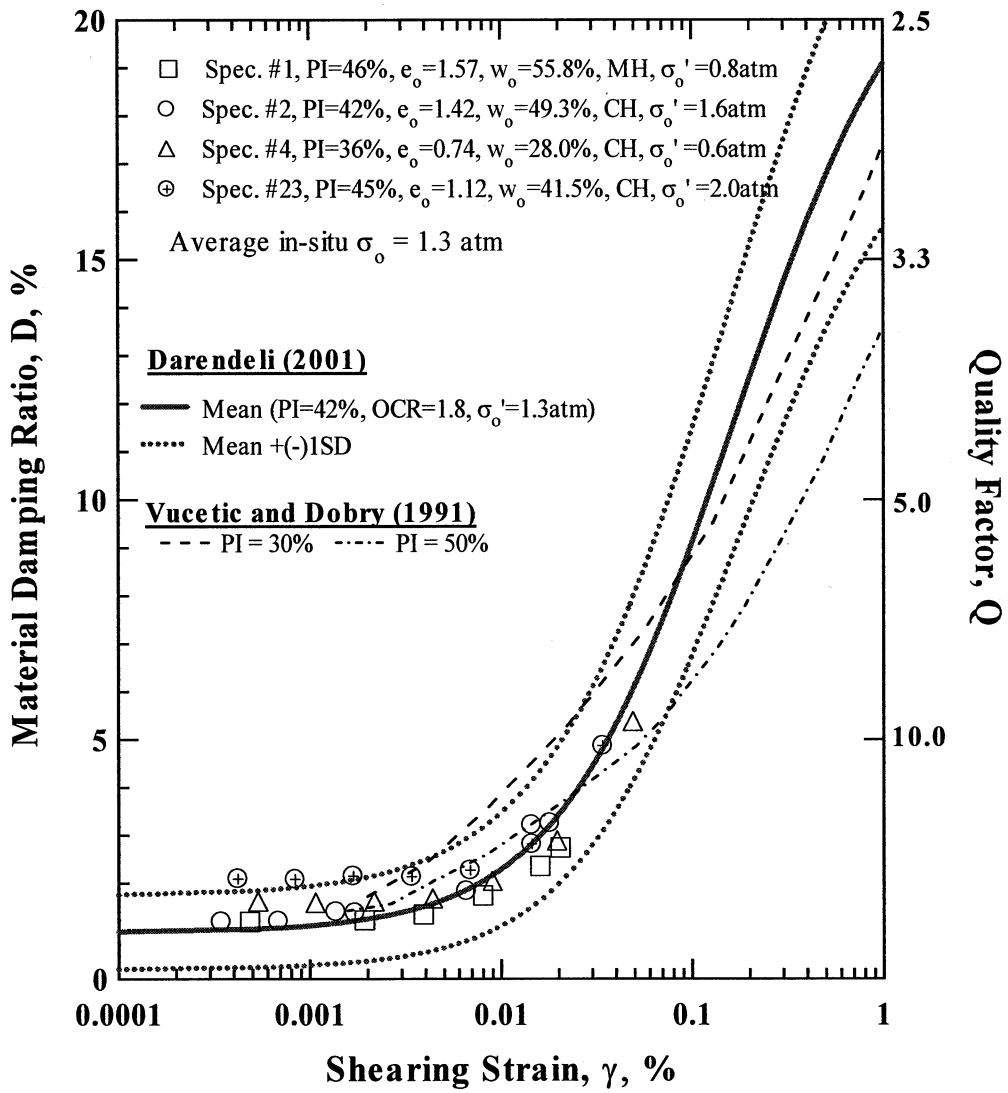

Figure 84 Comparison between the Trends Predicted by Darendeli (2001) and Vucetic and Dobry (1991) and the Variation in Material Damping Ratio with Shearing Strain from Torsional Shear (TS) Tests of Four Specimens with an Average PI = 42 % in the Low In-Situ Confining Pressure Group Tested at Their Estimated In-Situ Confining Pressures

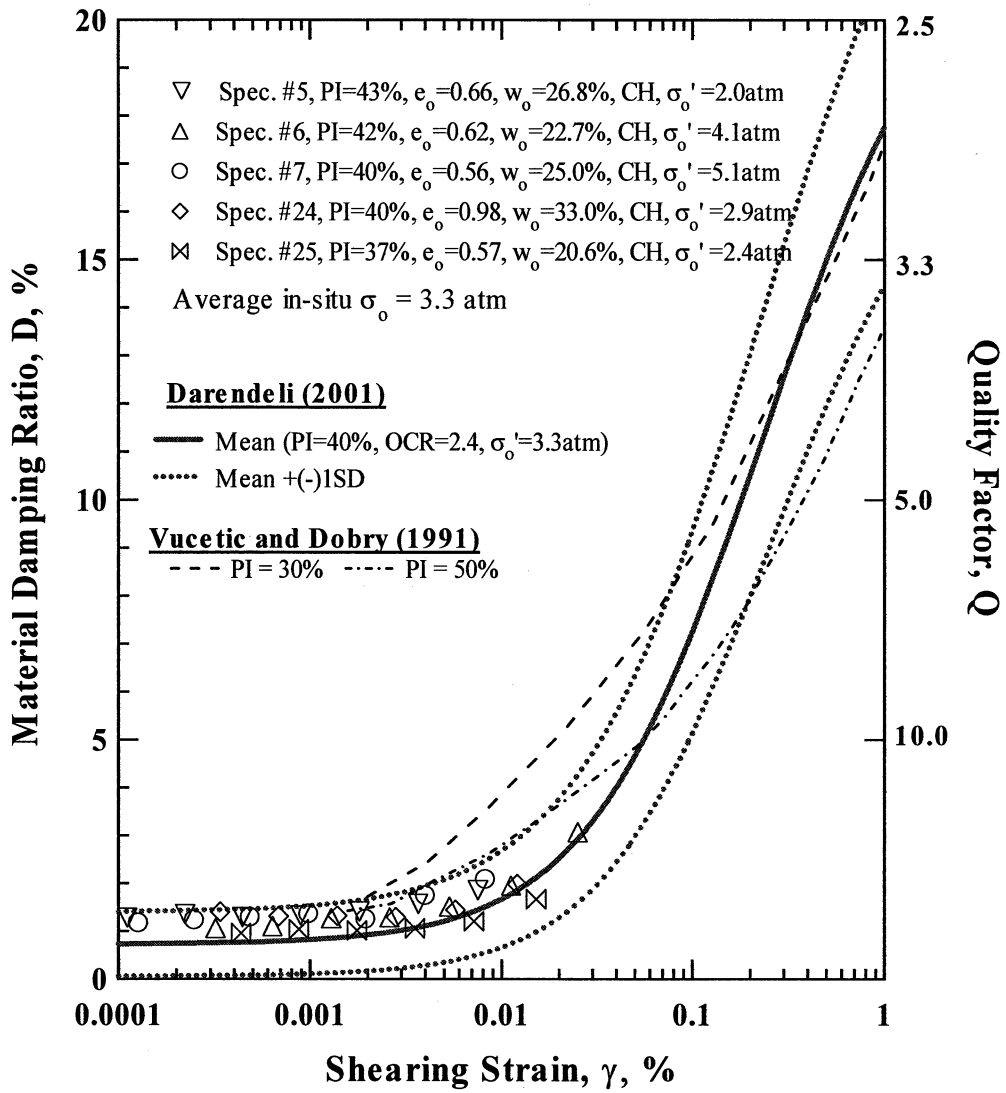

Figure 85 Comparison between the Trends Predicted by Darendeli (2001) and Vucetic and Dobry (1991) and the Variation in Material Damping Ratio with Shearing Strain from Torsional Shear (TS) Tests of Five Specimens with an Average PI = 40% in the Medium In-Situ Confining Pressure Group Tested at Their Estimated In-Situ Confining Pressures

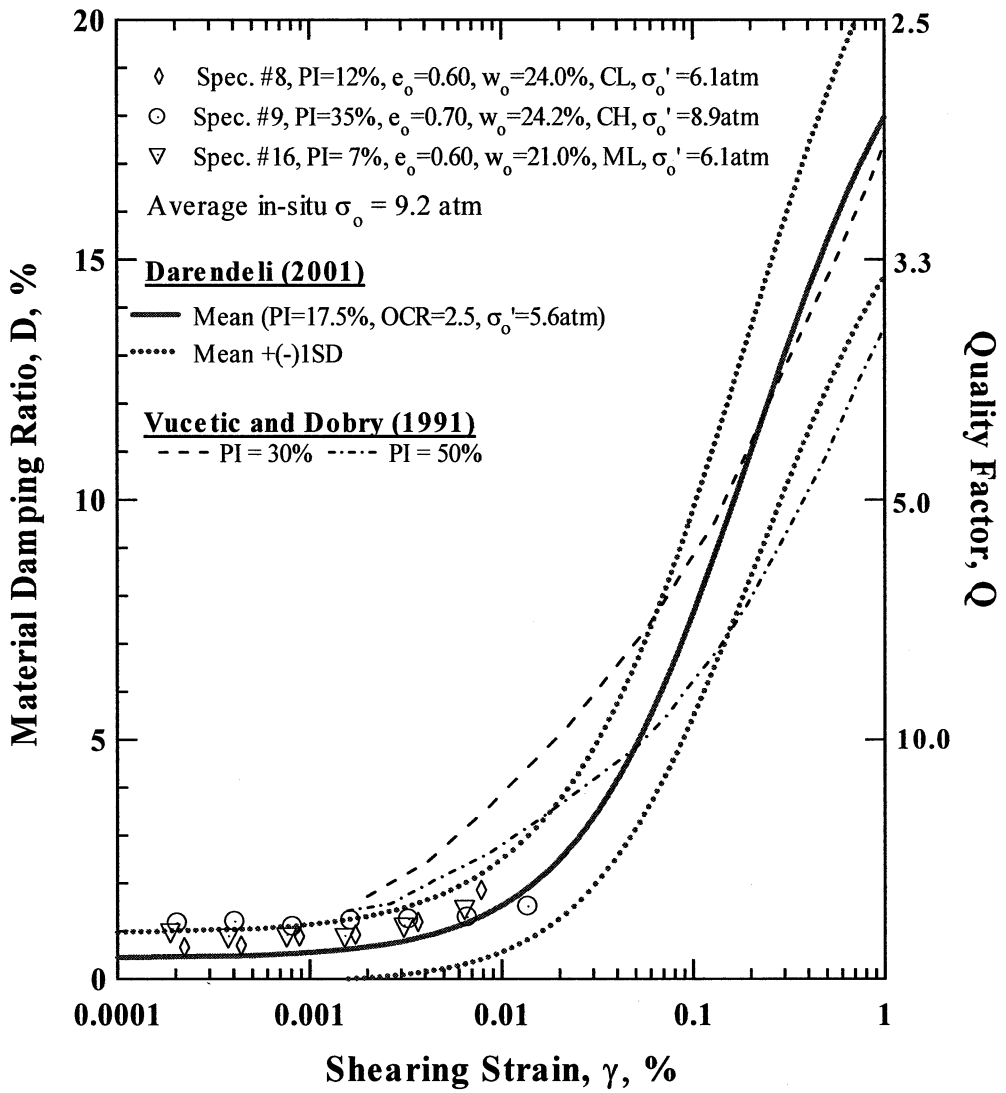

Figure 86 Comparison between the Trends Predicted by Darendeli (2001) and Vucetic and Dobry (1991) and the Variation in Material Damping Ratio with Shearing Strain from Torsional Shear (TS) Tests of the Three Specimens in the High In-Situ Confining Pressure Group Tested at Their Estimated In-Situ Confining Pressures

5. COMPARISON BETWEEN FIELD AND LABORATORY VALUES OF G_{max} and V_S

Shear moduli measured in the laboratory by the resonant column test were compared with shear moduli determined from the field V_s values measured in the suspension logging test. The suspension logging data were obtained from the Internet web site http://geoinfo.usc.edu/rosrine, a ROSRINE homepage. Shear moduli were calculated by:

$$G_{max} = \rho V_s^2 \tag{13}$$

where:

ρ = unit mass density of the specimen, and

V_S = field shear wave velocity from suspension logging tests.

The comparison between shear moduli measured in the laboratory, $G_{max, lab}$, and shear moduli measured in the field, $G_{max, field}$, from the suspension logging measurements is shown in Figure 87. Theses results are presented quantitatively in Table 16, with the ratio of $G_{max, lab}$ to $G_{max, field}$ shown in the last column. A total of 23 comparisons is presented in Table 16. Comparions for two specimens, Specimen Nos. 17 and 22 (UTA-27-M and UTA27-L), could not be made because these specimens were recovered from depths less than 10 ft (3 m) and suspension logging tests could not be performed at these shallow depths. Also, the comparison for Specimen No. 5 (UTA-27-B) is not included in Figure 87 because this specimen is considered not to be representative of the conditions measured in the field. The ratio of $G_{max, lab}$ to $G_{max, field}$ is 3.28 which is abnormally high. The comparisons for the remaining 22 specimens in Figure 87 show the ratio of $G_{max, lab}$ to $G_{max, field}$ ranges from 0.19 to 1.24 and averages 0.62.

Comparisons of the shear wave velocities obtained in the field and laboratory are also tabulated in Table 16. These results are plotted in Figure 88. As noted above, comparisons for only 22 of the 25 specimens tested in the laboratory are shown in Figure 88. The ratio of $V_{s, lab}$ to $V_{s, field}$ ranges from 0.42 to 1.10 and averages 0.75.

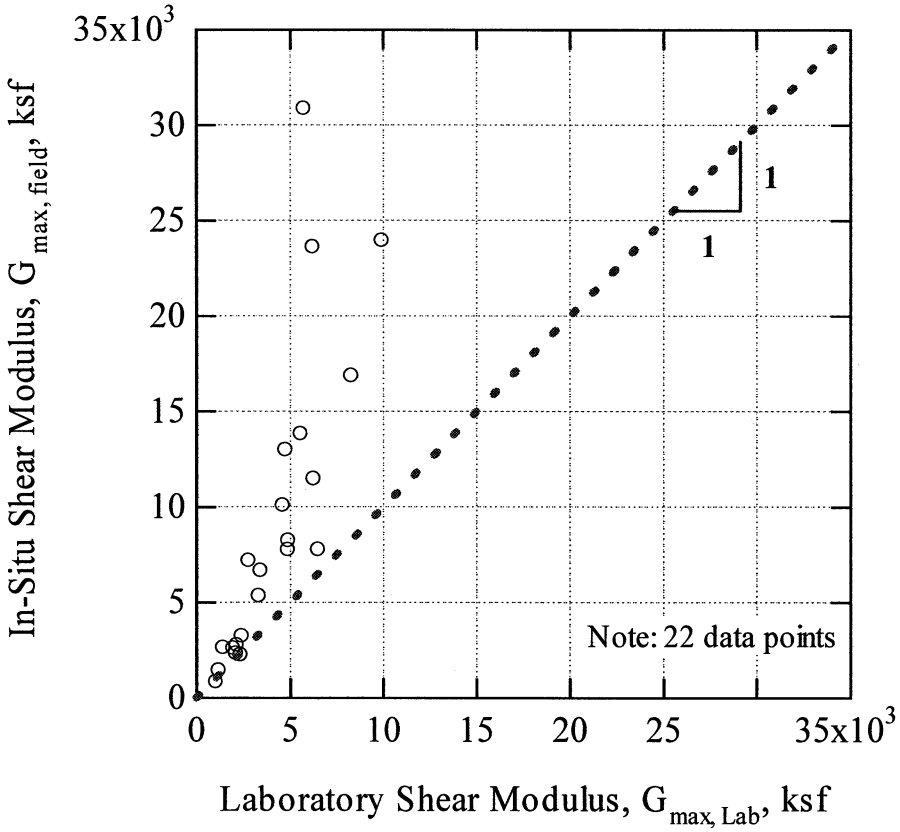

Figure 87 Comparison of Shear Moduli Measured in the Laboratory, $G_{max,\ lab}$, and in the Field, $G_{max,\ field}$ (Note: $G_{max,\ field}$ calculated from shear wave velocity measured in the field by the Suspension Logging Method)

Table 16 Comparison of In-Situ and Laboratory Measurements, in terms of Shear Wave Velocity, V_s, and Shear Modulus, G_{max}

Spec. No.	Specimen ID	Soil Layer Identification	Specimen Depth, ft	Estimated Confining Pressure*, ksf	Laboratory Shear Wave Velocity, fps	Suspension Log Shear Wave Velocity, fps	Vs, lab / Vs, field	Laboratory Shear Modulus, ksf	In-Situ G_{max}, ksf	$G_{max, lab}$ / $G_{max, field}$
1	UTA-25-B	Tarzana P-3	30	1.73	804	900	0.89	2151	2767	0.80
2	UTA-25-A	Tarzana P-4	42	3.46	783	827	0.95	2120	2336	0.90
3	UTA-27-F	Meloland S-2	20	0.86	516	468	1.10	1049	840	1.21
4	UTA-27-E	Meloland S-3	28	1.30	516	609	0.85	1189	1440	0.72
5	UTA-27-B	Meloland WS-1	120	4.32	1269	703	1.81++	6830	1917	3.28++
6	UTA-27-A	Meloland WS-3	200	8.64	829	912	0.91	2426	3229	0.83
7	UTA-27-C	Meloland WS-4	259	10.80	1221	1719	0.71	6269	11471	0.50
8	UTA-27-D	Meloland WS-6	378	15.84	1241	1414	0.88	6499	7765	0.77
9	UTA-27-G	Meloland WS-7	440	18.72	938	1310	0.72	3425	6665	0.51
10	UTA-27-S	LA Bulk Mail P-1	15	1.44	717	794	0.90	2354	2249	0.82
11	UTA-27-T	LA Bulk Mail P-3	50	3.60	686	852	0.81	1974	2589	0.65
12	UTA-27-I	LA Bulk Mail P-5	167.5	11.52	1081	1680	0.64	4603	10076	0.41
13	UTA-27-V	LA Bulk Mail P-6	205	12.96	1339	2173	0.62	8289	16864	0.38
14	UTA-27-H	LA Bulk Mail P-7	267	14.40	1178	1967	0.60	5563	13823	0.36
15	UTA-27-J	Gilroy P-4	182	12.10	1105	1359	0.81	4880	7747	0.66
16	UTA-27-K	Gilroy P-5	357	23.76	1149	2713	0.42	5738	30866	0.18
17	UTA-27-M	Lake Hughes P-1	6	0.43	467	–+	–+	838	–+	–+
18	UTA-27-N	Joshua Tree P-7	236	19.44	1227	2373	0.52	6223	23614	0.27
19	UTA-27-O**	Joshua Tree P-8	328	27.36	1560	2390	0.65	9927	23948	0.43
20	UTA-27-P	Yermo P-6	201	14.40	1073	1457	0.74	4899	8235	0.54
21	UTA-27-Q	Yermo P-7	266	17.28	1095	1829	0.60	4756	12983	0.36
22	UTA-27-L	Halls Valley P-1	7	0.56	551	–+	–+	1222	–+	–+
23	UTA-27-R	Halls Valley P-3	52	4.32	619	841	0.74	1430	2633	0.54
24	UTA-27-U	Saturn P-5	100	6.05	949	1173	0.81	3332	5337	0.66
25	UTA-27-W	Obregon P-10	101	5.04	815	1361	0.60	2779	7191	0.36

Notes: * Estimated confining pressures are based on $K_o = 0.5$

** Suspension log shear wave velocity at depth of 328 ft was extrapolated from the one at 318 ft

+ No V_s values were taken from Suspension Log Profiles at depths less than 10 ft (3m)

++ The laboratory specimen was abnormally stiff compared with field measurements and was assumed to represent a thin layer of soil that was not tested by the suspension logger in the field

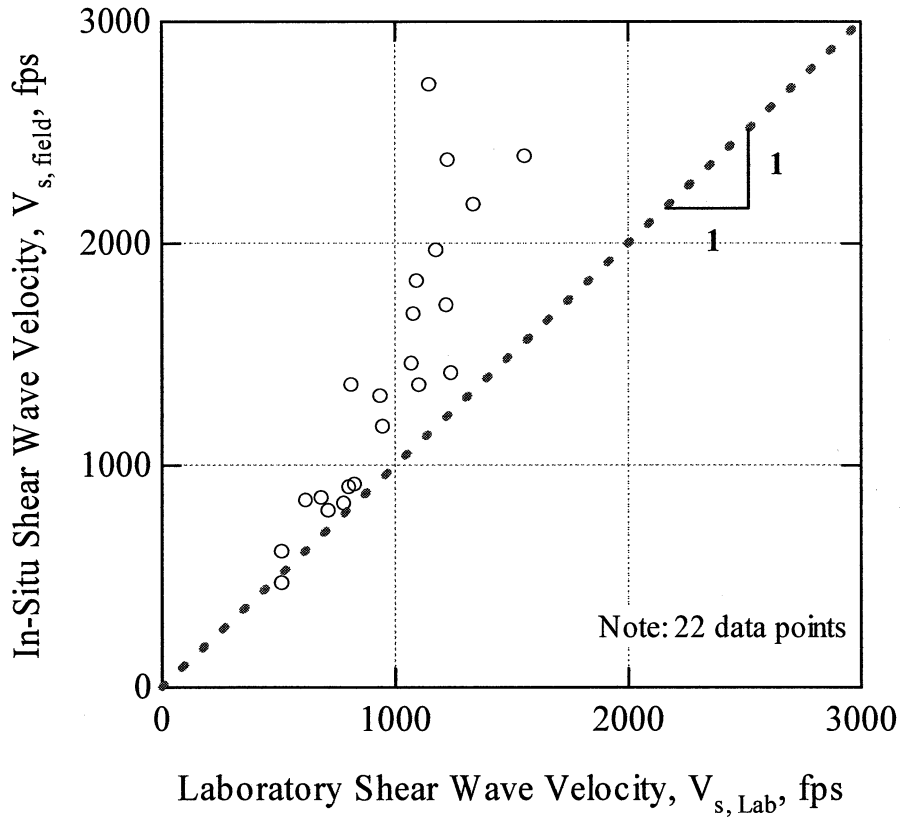

Figure 88 Comparison of Shear Wave Velocities Measured in the Laboratory, $V_{s, lab}$, and Shear Wave Velocities Measured by the Suspension Logging Method in the Field, $V_{s, field}$

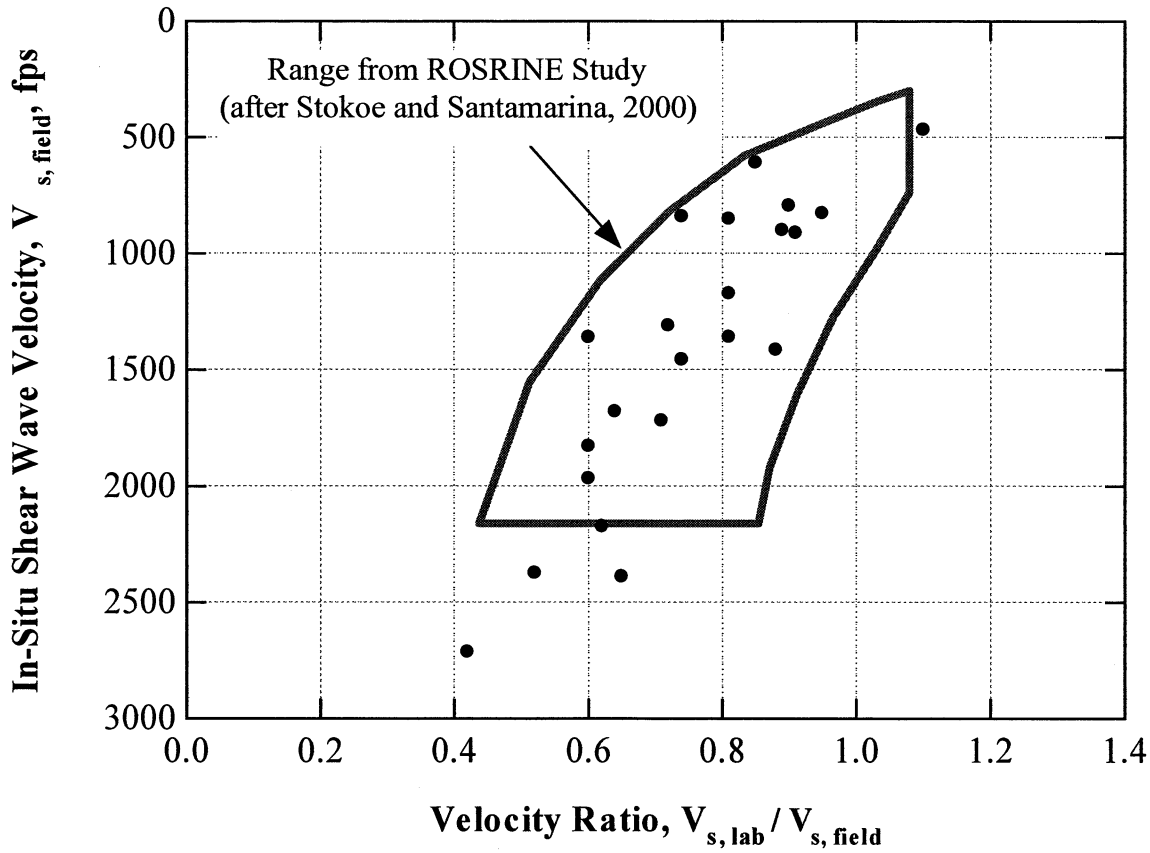

Figure 89 Variation in the Ratio of Laboratory-to-Field Shear Wave Velocities ($V_{s,\,lab}$/ $V_{s,\,field}$) with the In-Situ Value of $V_{s,\,field}$; Comparison of the ROSRINE Specimens Tested in this Study with the Range from the Earlier ROSRINE Study (Stokoe and Santamarina (2000))

The ratios of $V_{s,\,lab}$ to $V_{s,\,field}$ found in this study for the 22 specimens are compared with results found in an earlier ROSRINE study in Figure 89. The earlier ROSRINE study was conducted by Darendeli (2001). As seen in Figure 89, the differences between field and laboratory measurements for the 22 specimens in this study follow the trend of the other ROSRINE data as presented by Stokoe and Santamarina (2000).

One other comparison between field and laboratory values of V_s is made. This comparison is with the study performed by Chiara (2001). He investigated the database at the University of Texas of 90 comparisons involving sands and clays. In-situ V_s measurements were performed by the crosshole, downhole and suspension logging methods. Chiara performed a regression analysis and found the best-fit relationship is:

$$V_{s,field} = 0.56V_{s,lab}^{1.16} \tag{14}$$

This relationship had R^2 = 80 %. He also found the mean ± 1σ and mean ± 2σ boundary equations given in Table 17. The results from his study are shown in Figure 90. The results from the 22 specimens in this study are compared with Chiara's predictive equations in Figure 91. As seen in the figure, the differences between field and laboratory measurements for the 22 specimens in this study follow the mean regression line found by Chiara (2001). The comparisons for 19 out of the 22 specimens fall within ± 1σ of the mean regression line.

Table 17 Regression analysis boundaries (After Chiara, 2001)

Boundary	Regression Equation
Mean	$V_{s,field} = 0.56 * V_{s,lab}^{1.16}$
Mean +1stdv	$V_{s,field} = 0.68 * V_{s,lab}^{1.16}$
Mean -1stdv	$V_{s,field} = 0.44 * V_{s,lab}^{1.16}$
Mean +2stdv	$V_{s,field} = 0.86 * V_{s,lab}^{1.16}$
Mean -2stdv	$V_{s,field} = 0.26 * V_{s,lab}^{1.16}$

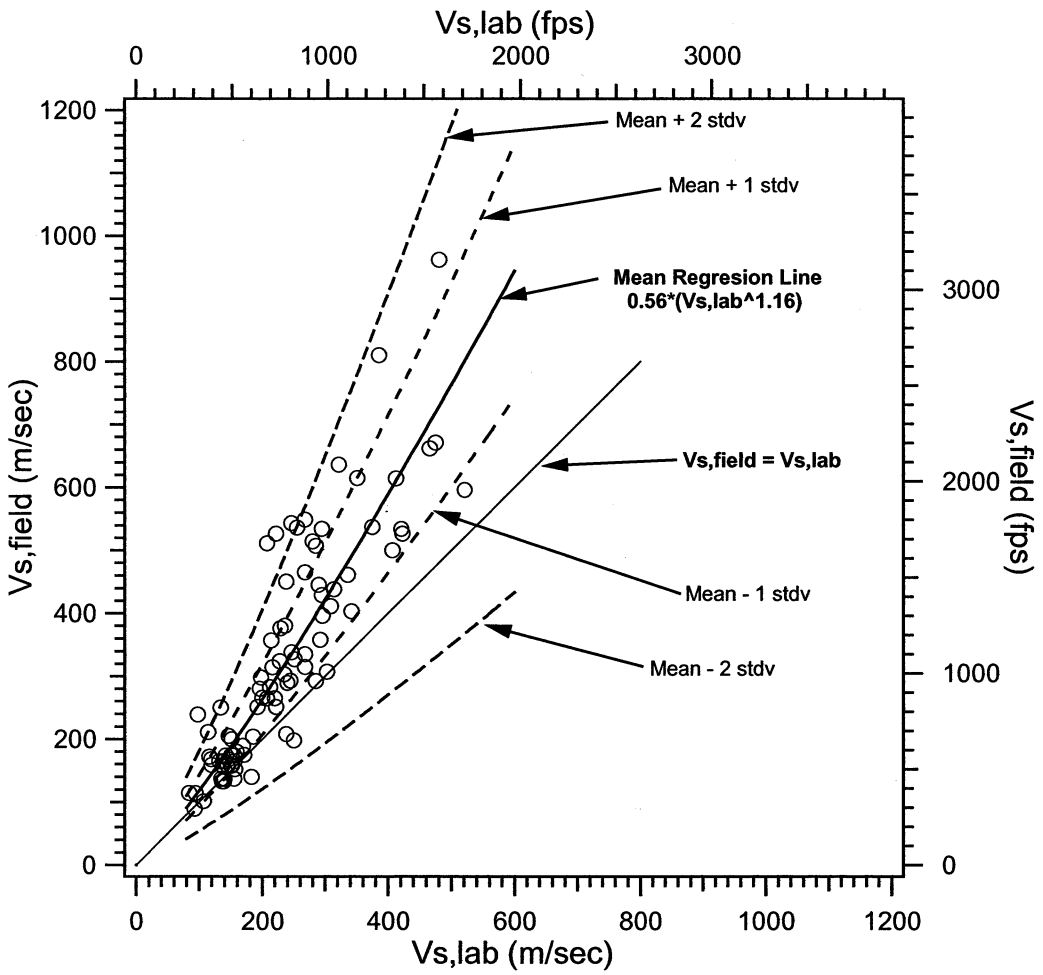

Figure 90 Regression analysis plot: UT database (90 data) (After Chiara, 2001)

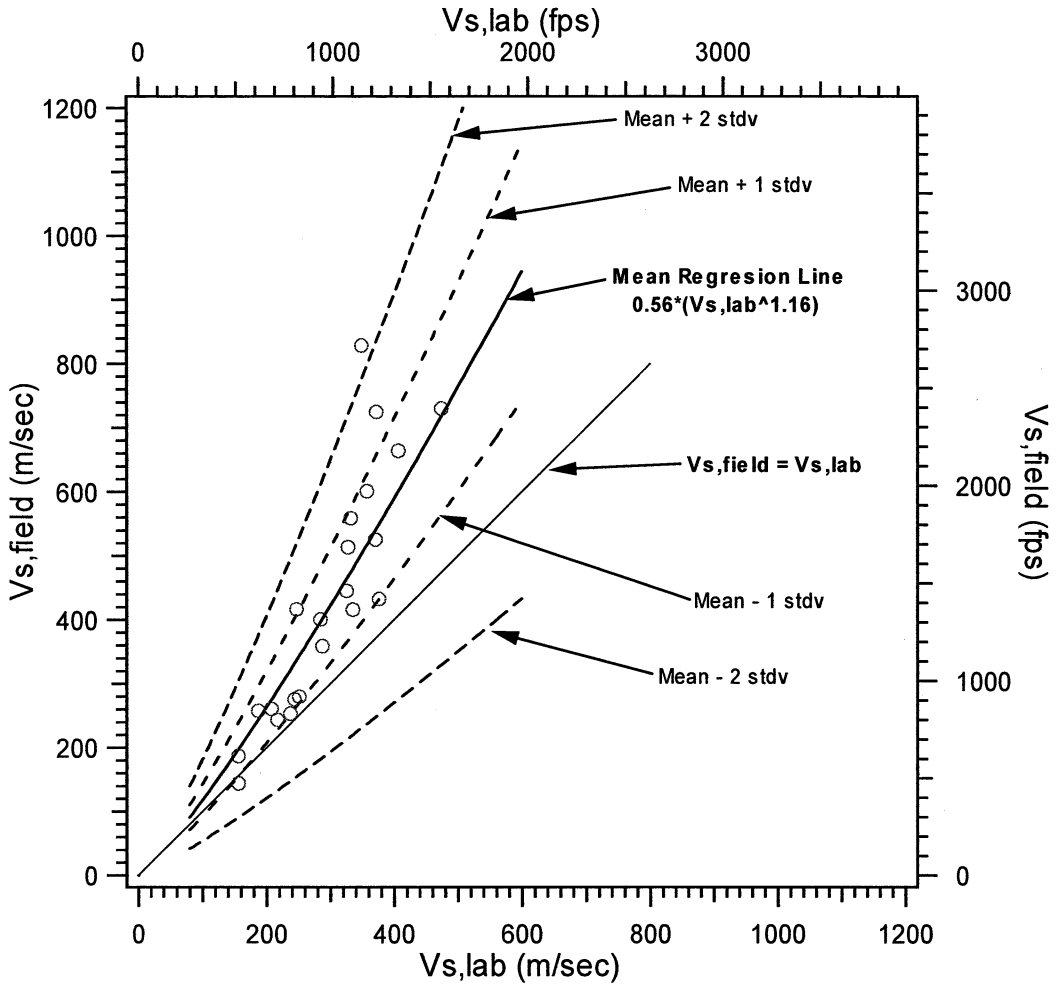

Figure 91 Variation in Shear Wave Velocities Measured in the Laboratory, $V_{s,\,lab}$, and Shear Wave Velocities Measured by the Suspension Logging Method in the Field, $V_{s,\,field}$; Comparison of the ROSRINE Specimens Tested in this Study with the Predicted Ranges from the Regression Analysis with the University of Texas Database (Chiara, (2001))

6. SUMMARY AND CONCLUSIONS

6.1 Summary

The linear and nonlinear dynamic properties of 25 intact specimens from the Phase II Portion of the ROSRINE Project were evaluated in this study. All related information on the specimens and sample preparation are described in Section 1. Dynamic tests were performed with the combined resonant column and torsional shear (RCTS) device in a fixed-free boundary condition, as described in Section 2 and Appendix A. Initial properties of all specimens are summarized in Table 5.

In the linear range, where shearing strain (γ) is normally lower than 0.001%, small-strain shear modulus (G_{max}) and small-strain material damping ratio (D_{min}) are constant and independent of shearing strain amplitude. As confining pressure (σ_o) increases, these constant material properties change (G_{max} increases and D_{min} decreases), as shown and discussed in Section 3. The shape of this trend (especially the change of log G_{max} with log σ_o) provides a type of evaluation of the degree of overconsolidation, the presence of any cementation, and potential disturbance of the specimens. For nonplastic specimens, a flat log G_{max} - log σ_o relationship (n_G roughly in the range of 0.05 to 0.15) indicates that the materials are heavily overconsolidated and/or cemented. For plastic specimens, such a flat slope for the log G_{max} - log σ_o relationship generally indicates overconsolidation. If the slope of the log G_{max} - log σ_o relationship changes at a confining pressure larger than the estimated in-situ confining pressure for a plastic soil (based on calculating the estimated in-situ σ_o with $K_o = 0.5$), this difference also indicates that the soil is overconsolidated. The OCR can also be estimated qualitatively by observing the void ratio change with confining pressure as discussed by Choi (2003). Additionally, the degree of disturbance can be qualitatively evaluated based on values and changes of normalized void ratios before the in-situ pressure (Choi, 2003).

The effect of loading frequency on the small-strain shear modulus and small-strain material damping ratio of the 7 nonplastic specimens and the 18 plastic specimens is discussed in Section 3.4. A much larger effect of loading frequency occurs on D_{min} than G_{max} for both nonplastic and plastic specimens.

The dynamic soil properties, shear modulus (G) and material damping ratio (D) in the nonlinear range where these values change with shear strain (γ), are presented in Section 4. Six of the seven nonplastic specimens exhibit a more linear response in both the G/G_{max} – log γ and D – log γ relationships than the empirical sand curve proposed by Seed et al. (1986). However, the Seed et al. (1986) sand curve was determined at a confining pressure of about 1 atm. The difference in response results mainly from testing at confining pressures much higher than 1 atm. One nonplastic specimen that was tested at a pressure lower than 1 atm shows a more nonlinear response than the empirical sand curve from Seed et al. (1986), as expected.

For the eighteen plastic specimens, the normalized modulus reduction and damping curves (G/G_{max} – log γ and D – log γ) are divided into three different groups according to the confining pressure at which high-amplitude testing was performed. The results from theses tests are compared with the curves for plastic soils proposed by Vucetic and Dobry (1991). There is generally good agreement between the measured and proposed curves in the two lower confining pressure groups, especially for the lower PI materials (PI in the range of 8 to 25 %). As the plasticity index and confining pressure for a specimen become larger, a larger linear range and a more rapid reduction in normalized shear modulus curve and a more rapid increase in material damping ratio curve are observed compared with the trends from Vucetic and Dobry (1991).

The G/G_{max} – log γ and D – log γ curves using the four-parameter model (Darandeli, 2001) are estimated and compared with the measured curves. Darendeli's equation for the normalized modulus reduction curve is expressed with the reference strain ($\gamma_{r,G}$) and the curvature coefficient (a) as shown in the Equation 4. The values of $\gamma_{r,G}$ and "a" for all 7

nonplastic specimens and 18 plastic specimens were evaluated by least-squares fitting Equation 4 to the measured curves. In this study, the plasticity index turned out to be the most dominant parameter in determining both values of $\gamma_{r,G}$ and "a", while confining pressure was less dominant. As the plasticity index and confining pressure increase, the values of $\gamma_{r,G}$ and "a" increase. The same phenomenon is observed in the D – log γ relationships.

6.2 Conclusions

6.2.1 Small-Strain Dynamic Properties – Since the small-strain dynamic properties (V_s, G_{max}, and D_{min}) are constant values below a certain shearing strain amplitude, changes in these values with confining pressure at a given time after primary consolidation can represent stress history and the current state of stress of the specimen. Overconsolidation ratio can be estimated from the log G_{max} – log σ_o relationship (assuming the values of (negative) pore water pressure are small compared with σ_o so that $\sigma_o \approx \sigma_o'$). This estimate of OCR was supported by the studies of the normalized e – log σ_o relationships (Choi, 2003).

6.2.2 Dynamic Properties in the Nonlinear Range – All nonplastic specimens tested at confining pressures larger than 1 atm exhibit larger linear ranges in the measured G/G_{max} – log γ curves and D – log γ curves compared with curves proposed (for σ_o of 1 atm) by Seed et al. (1986). For plastic specimens, the trends of normalized modulus reduction and damping relationships predicted by Vucetic and Dobry (1991) are compared with the measured trends. The measured curves match well the proposed curves at low to medium confining pressures (0.4 to 5.4 atm) for low to medium plasticity (8 to 25 %) specimens. As confining pressure increases for specimens with higher PI's, a more rapid change in the normalized modulus reduction and damping increase curves occurs, and the curves exhibit larger reference strains. Especially for the normalized modulus reduction curve, the modified hyperbolic equation suggested by

Darendeli (2001) can be used to evaluate quantitatively the effects of PI and confining pressure. The reference strain ($\gamma_{r,G}$) and the curvature coefficient (a) can be determined by least-squares fitting to the equation. Figure 92 illustrates the effect of a and $\gamma_{r,G}$ As confining pressure increases, larger $\gamma_{r,G}$ and a values were found in this study, as discussed in Section 4.1.4. The mean curvature coefficient for the 7 nonplastic specimens is 0.86, which is nearly equal to the value of 0.92 recommended by Darendeli (2001). When a standard deviation of 0.06 for the nonplastic specimens is added to the mean value, it becomes close to the recommended value. On the other hand, a mean curvature coefficient of 1.09 was determined to fit the measured modulus reduction curves for the 18 plastic specimens. The value of 1.09 is larger than the curvature coefficient of 0.92 recommended by Darendeli (2001). The curvature coefficients of 15 out of 18 specimens exceed Darendeli's recommended value.

The trends in the normalized modulus reduction curves with plasticity index (PI) that have been suggested by Vucetic and Dobry (1991) are shown in Figure 93. The values of reference strain ($\gamma_{r,G}$) and curvature coefficient (a) that fit these curves are determined using Equation 4 and are listed in Figure 93. The reference strains ($\gamma_{r,G}$) for these curves increase as PI increases, but the curvature coefficient remains about constant except for the value of the nonplastic soils. The effect of confining pressure on the curvature coefficient should be considered in modifying the trends predicted by the Vucetic and Dobry (1991) curves. The four-parameter model from Darendeli (2001) accounts for the effect of confining pressure as well as the effects of frequency and overconslidation ratio on the reference strain ($\gamma_{r,G}$). However, the single value of curvature coefficient value (0.92) as suggested by Darendeli (2001) causes the prediction of normalized modulus reduction curves to begin to become less precise for high plastic soils (PI > 36%) at higher confining pressures (σ_o > 7.5 atm).

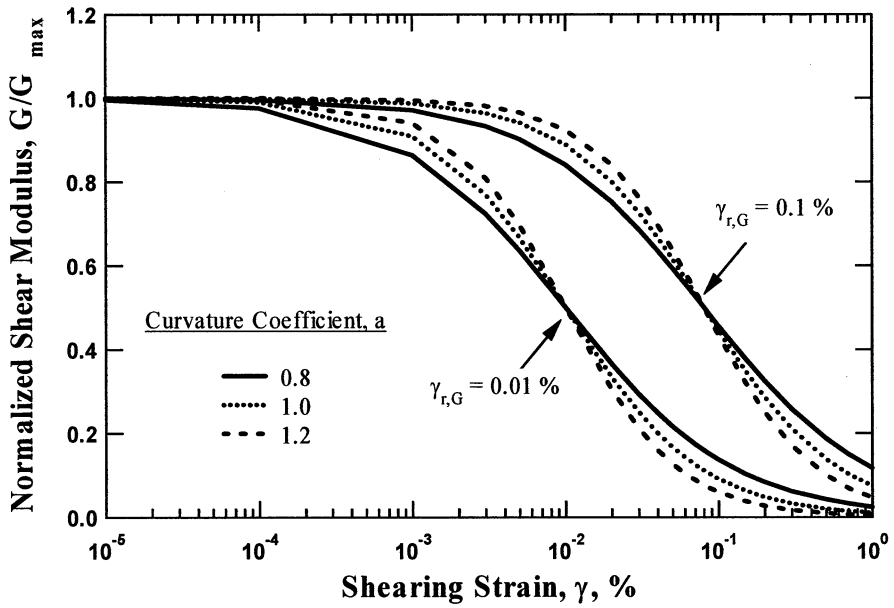

Figure 92 Effect of the Curvature Coefficient (a) and Reference Strain ($\gamma_{r,G}$) on the Normalized Modulus Reduction Curve

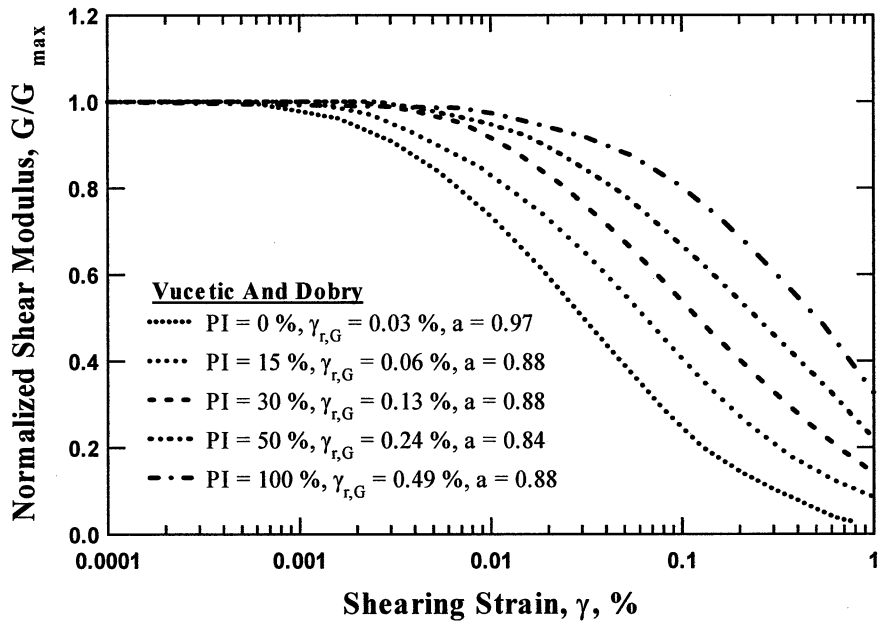

Figure 93 Values of Curvature Coefficient (a) and Reference Strain ($\gamma_{r,G}$) of the Normalized Modulus Reduction Curves Proposed by Vucetic and Dobry (1991) though Least-Squares Fitting

7. REFERENCES

Chiara, N. (2001), "Investigation of Small-Strain Shear Stiffness Measured in Field and Laboratory Geotechnical Studies," M.S. Thesis, University of Texas at Austin, 95 pp.

Choi, W.K. (2003), "Linear and Nonlinear Dynamic Properties from Combined Resonant Column and Torsional Shear Tests of ROSRINE Phase – II Specimens," M.S. Thesis, University of Texas at Austin, pp 59.

Darendeli, B. M. (2001) "Develop of a New Family of Normalize Modulus Reduction and Material Damping Curves" Ph.D. Dissertation, University of Texas at Austin, 362 p.

Hardin, B.O. and V.P. Drnevich (1972), "Shear Modulus and Damping in Soils: Design Equations and Curves," Journal of the Soil Mechanics and Foundations Division, ASCE, Vol. 98, No. SM6, Proc. Paper 9006, July.

Hardin, B.O. (1978), "The Nature of Stress-Strain Behavior of Soils," Proceedings, Ceotech. Eng. Div. Specialty Conference on Earthquake Eng. And Soil Dynamics, Vol. 1 ASCE, Psadena, June, pp. 3-90.

Menq, F.-Y. (2003), "Dynamic Properties of Sandy and Gravelly Soils," Ph.D.Dissertation, University of Texas at Austin, 192 pp.

Seed, H.B., R.T. Wong, I.M. Idriss, and K. Tokimatsu (1986), "Moduli and Damping Factors For Dynamic Analyses of Cohesionless Soils," Journal of the Soil Mechanics and Foundations Division, Vol. 112, No. SM11, pp. 1016-1032.

Vucetic, Mladen and Dobry, Ricardo (1991), "Effect of Soil Plasticity on Cyclic Response," Journal of Geotechnical Engineering, Vol.117, No. 1, Jan. pp. 89-107

APPENDIX A

Brief Background on Combined RCTS Equipment

Background on Combined RCTS Equipment

The effects of various parameters on G and D are conveniently evaluated in the laboratory with combined RCTS equipment as discussed by Stokoe et al., 1994a. This equipment is of the fixed-free type, with the bottom of the specimen fixed and torsional excitation applied to the top as illustrated in Fig. A.1. The equipment has two important attributes. First, both resonant column (RC) and torsional shear (TS) tests can be performed with the same piece of equipment. Switching from one type of test to the other is simply done outside the confining chamber by changing: 1. the input excitation frequency used to drive the specimen and 2. the motion monitoring devices used to record the specimen response. As a result, variability due to testing different specimens is eliminated so that results from both tests can be compared effectively. Second, the loading frequency in the torsional shear test can be easily changed from 0.01 to about 10 Hz. Therefore, the effect of frequency and number of loading cycles on the deformational characteristics of intact specimens can be conveniently investigated.

The basic operational principle in the RC test is to vibrate the cylindrical specimen in first-mode torsional resonance. At the University of Texas (UT), this process is completely automated so that first-mode resonance can be quickly and accurately established as illustrated in Fig. A.2a (Ni, 1987). Determinations of resonant frequency and amplitude of vibration are made from the response curve. These values are then combined with equipment characteristics and specimen size to calculate shear wave velocity, V_S, shear modulus, G, and shearing strain amplitude, γ.

Material damping in the RC test is evaluated from the dynamic soil response using either the free-vibration decay curve or the half-power bandwidth method. The free-vibration decay curve is recorded by shutting off the driving force after the specimen is vibrating in steady-state motion at the resonant frequency. Figure A.3 shows an example of this process. The logarithmic decrement, δ, is defined from the decay curve as:

$$\delta = \ln(z_1/z_2) \tag{A.1}$$

where z_1 and z_2 are the amplitudes of two successive cycles. Material damping ratio, D, can then be determined from δ by:

$$D = [\delta^2/(4\pi^2+\delta^2)]^{1/2} \tag{A.2}$$

The half-power bandwidth method is based on measurement of the width of the dynamic response curve around the resonance peak. For small values of material damping, one can approximate damping as:

$$D \cong (f_2 - f_1)/2f_r \tag{A.3}$$

where f_1 and f_2 are the two frequencies at which the amplitude is 0.707 times the amplitude at the resonant frequency , f_r, as illustrated in Fig. A.4.

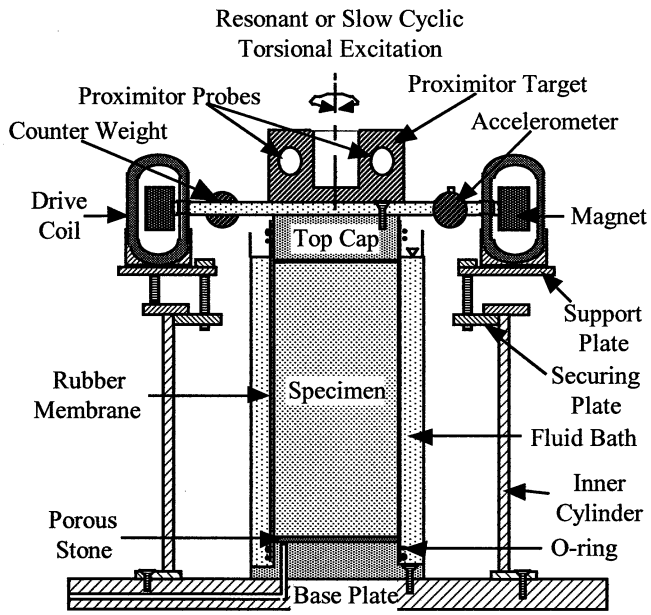

Figure A.1 Simplified Diagram of a Combined Resonant Column (RC) and Torsional Shear (TS) Device (Confining Chamber not Shown)

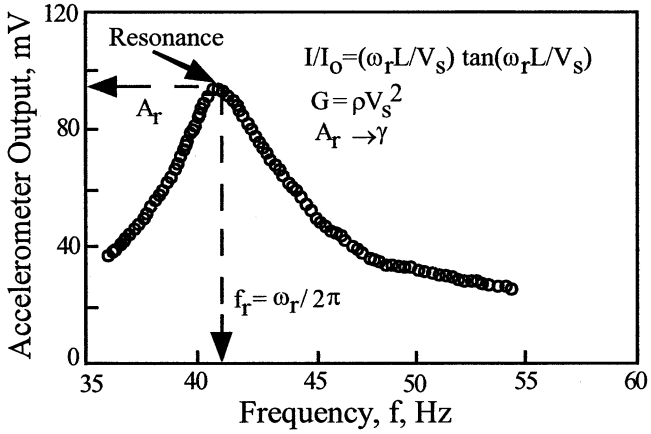

a) Dynamic Response Curve Measured in the RC Test

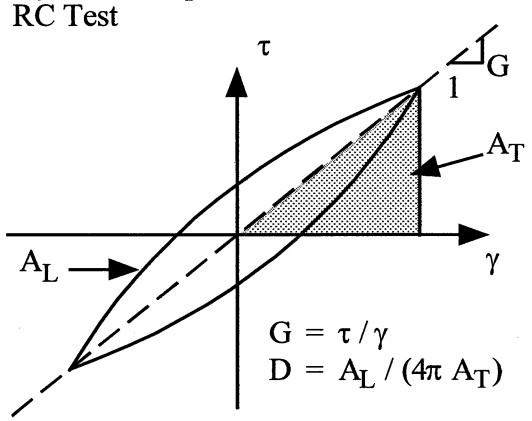

b) Hysteresis Loop Measured in the TS Test

Figure A.2 Examples of Measurements Performed in the RC and TS Tests

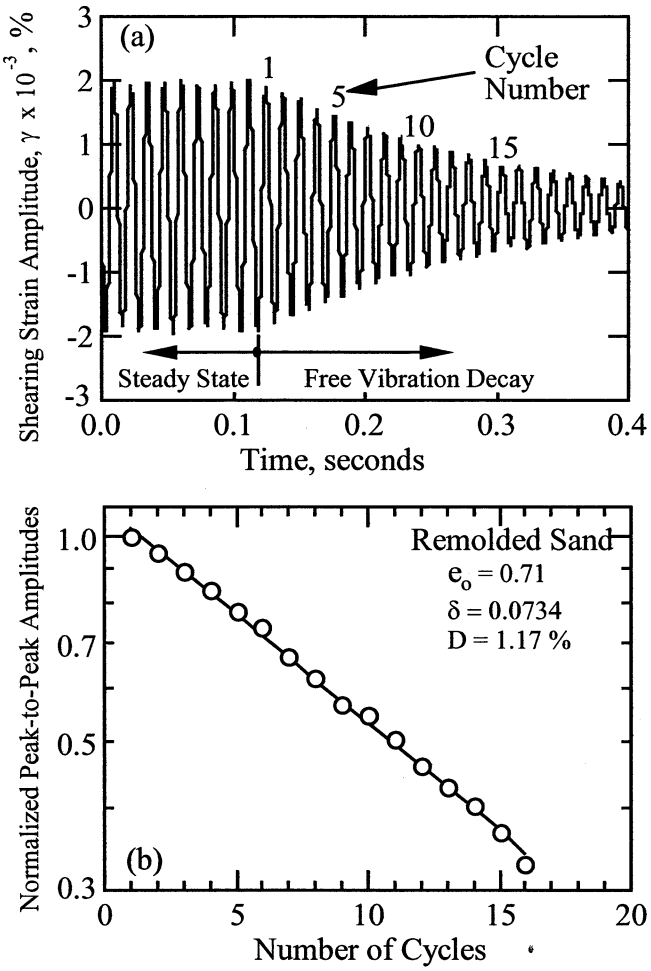

Figure A.3 Material Damping Measurement in the RC Test Using the Free-Vibration Decay Curve

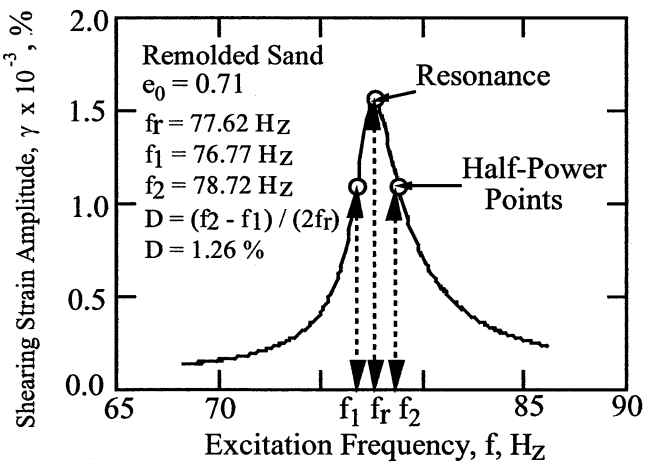

Figure A.4 Material Damping Measurement in the RC Test Using the Half-Power Bandwidth (Same Specimen as Shown in Fig. A.3)

For measurements at small strains ($\gamma<10^{-3}$ %), background noise can have a more adverse effect on the free-vibration decay curve than on the frequency response curve. On the other hand, at large strains, the assumptions implied in the derivation of Equation A.3 are no longer valid, and serious errors can be introduced into values of D determined by the half-power bandwidth method (Ni, 1987). In this study, both methods were used at shearing strains less than about 0.002 %, but only the free-vibration decay method was applied at larger strains. In addition, the strain at which the damping measurement was assumed to occur was taken as the average of the first three cycles of free vibration. This procedure is not conventionally employed at $\gamma > 0.002$ % but more correctly represents the strain associated with damping measurements from the free vibration decay curve.

In the TS test, shear modulus and material damping are measured using the same RCTS equipment, but the equipment is operated in slow cyclic torsional loading at a given frequency. Instead of determining the resonant frequency, the stress-strain hysteresis loop is determined from measuring the torque-twist response of the specimen as shown in Fig. A.2b. Proximitors are used to measure the angle of twist while the voltage applied to the coil is calibrated to yield torque. Shear modulus is calculated from the slope of a line through the end points of the hysteresis loop. Material damping is determined from the hysteresis loop as the ratio of the energy dissipated in one cycle of loading (A_L) to the peak strain energy stored during the cycle (A_T) times a factor of 4π as shown in Fig. A.2b.

As discussed by Stokoe et al., (1994a), the RCTS equipment at UT is calibrated so that equipment-generated damping can be subtracted from the measurements. Equipment-generated damping, D_{eq}, is measured along with material damping of the specimen when the damping measurements are performed following the procedures outlined in Figs. A.2 through A.4. Equipment-generated damping results from the back-electromagnetic force generated by the magnets moving through the drive coils. It is important to calibrate the drive system of each RCTS device over the entire range of frequencies used in testing so that equipment-generated damping can be determined before testing any specimens. Typical results for D_{eq} in

RC testing are shown in Fig. A.5 (Hwang, 1997). This damping is then subtracted from the combined measurement to yield material damping of the specimen. In all results where material damping ratios of soil specimens are presented, these values have been corrected by subtracting D_{eq} from the combined measurement of D.

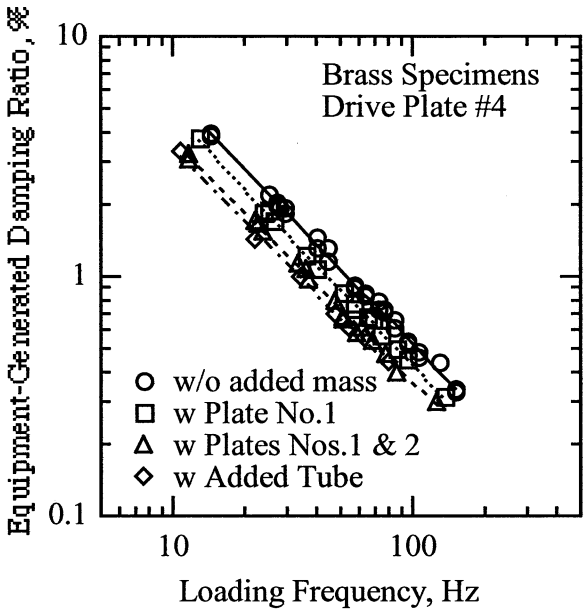

Figure A.5 Example of Equipment-Generated Damping Measured in the Resonant Column Device Using Metal Specimens (from Hwang, 1997)

Linear and Nonlinear Dynamic Properties Determined by Combined Resonant Column and Torsional Shear Tests: Phase II of the ROSRINE Project

Volume II

by

Kenneth H. Stokoe, II
Won Kyoung Choi
Farn-Yuh Menq
CelestinoValle

March 2003

Geotechnical Engineering Report GR03-1
Geotechnical Engineering Center
Civil Engineering Department
The University of Texas at Austin

TABLE OF CONTENTS – VOLUME II

Overview of Contents in Appendices B through Z

List of Soil Specimens from ROSRINE Sites in Appendices B through M

Appendix No.	Spec. No.	UT Specimen ID	Specimen Depth ft (m)	Soil Type (Unified Soil Classification)	Soil Type (Unified Soil Classification)
B	1	UTA-25-B	Tarzana P-3	30 (9.1)	Silt (MH)
C	2	UTA-25-A	Tarzana P-4	42 (12.8)	Clay (CH)
D	3	UTA-27-F	Meloland S-2	20 (6.1)	Clay (CL)
E	4	UTA-27-E	Meloland S-3	28 (8.5)	Clay (CH)
F	5	UTA-27-B	Meloland WS-1	120 (36.6)	Clay (CH)
G	6	UTA-27-A	Meloland WS-3	200 (61.0)	Clay (CH)
H	7	UTA-27-C	Meloland WS-4	259 (78.9)	Clay (CH)
I	8	UTA-27-D	Meloland WS-6	378 (115.2)	Clay (CL)
J	9	UTA-27-G	Meloland WS-7	440 (134.1)	Clay (CH)
K	10	UTA-27-S	LA Bulk Mail (P-1)	15 (4.6)	Clay (CL)
L	11	UTA-27-T	LA Bulk Mail (P-3)	50 (15.2)	Clay (CL)
M	12	UTA-27-I	LA Bulk Mail (P-5)	167.5 (51.1)	Clay (CL)

List of Soil Specimens from ROSRINE Sites in Appendices N through Z

Appendix No.	Spec. No.	UT Specimen ID	Soil Site Identification	Specimen Depth ft (m)	Soil Type (Unified Soil Classification)
N	12	UTA-27-V	LA Bulk Mail (P-6)	205 (62.5)	Silty Sand (SM)
O	13	UTA-27-H	LA Bulk Mail (P-7)	267 (81.4)	Sand (SP)
P	14	UTA-27-J	Gilroy P-4	182 (55.5)	Clay (CL)
Q	15	UTA-27-K	Gilroy P-5	357 (108.8)	Silt (ML)
R	17	UTA-27-M	Lake Hughes P-1	6 (1.8)	Silty Sand (SW-SM)
S	18	UTA-27-N	Joshua Tree 7 P-7	236 (71.9)	Sand (SP)
T	19	UTA-27-O	Joshua Tree 7 P-8	328 (100.0)	Sand (SW)
U	20	UTA-27-P	Yermo P-6	201 (61.3)	Silty Sand (SM)
V	21	UTA-27-Q	Yermo P-7	266 (81.1)	Sand (SP)
W	22	UTA-27-L	Halls Valley (P-1)	7 (2.1)	Clay (CL)
X	23	UTA-27-R	Halls Valley (P-3)	52 (15.8)	Clay (CH)
Y	24	UTA-27-U	Saturn P-4	100 (30.5)	Clay (CH)
Z	25	UTA-27-W	Obregon P-10	101 (30.8)	Clay (CH)

APPENDIX B

Specimen No. 1
UT Specimen ID: UTA-25-B

Tarzana P-3
Depth = 30 ft (=9.14m)
Soil Type: Silt (MH)

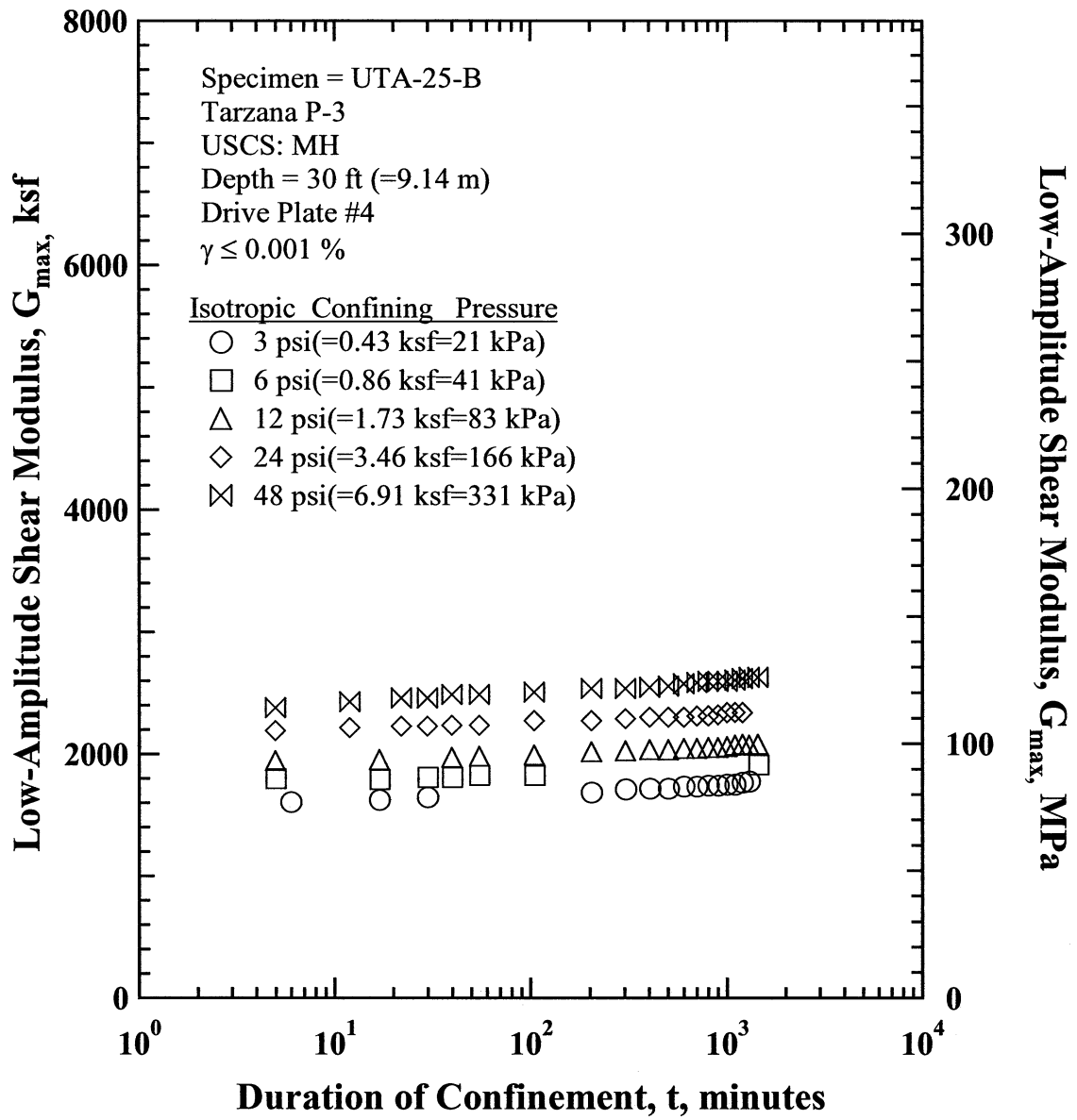

Figure B.1 Variation in Low-Amplitude Shear Modulus with Magnitude and Duration of Isotropic Confining Pressure from Resonant Column Tests of Specimen UTA-25-B.

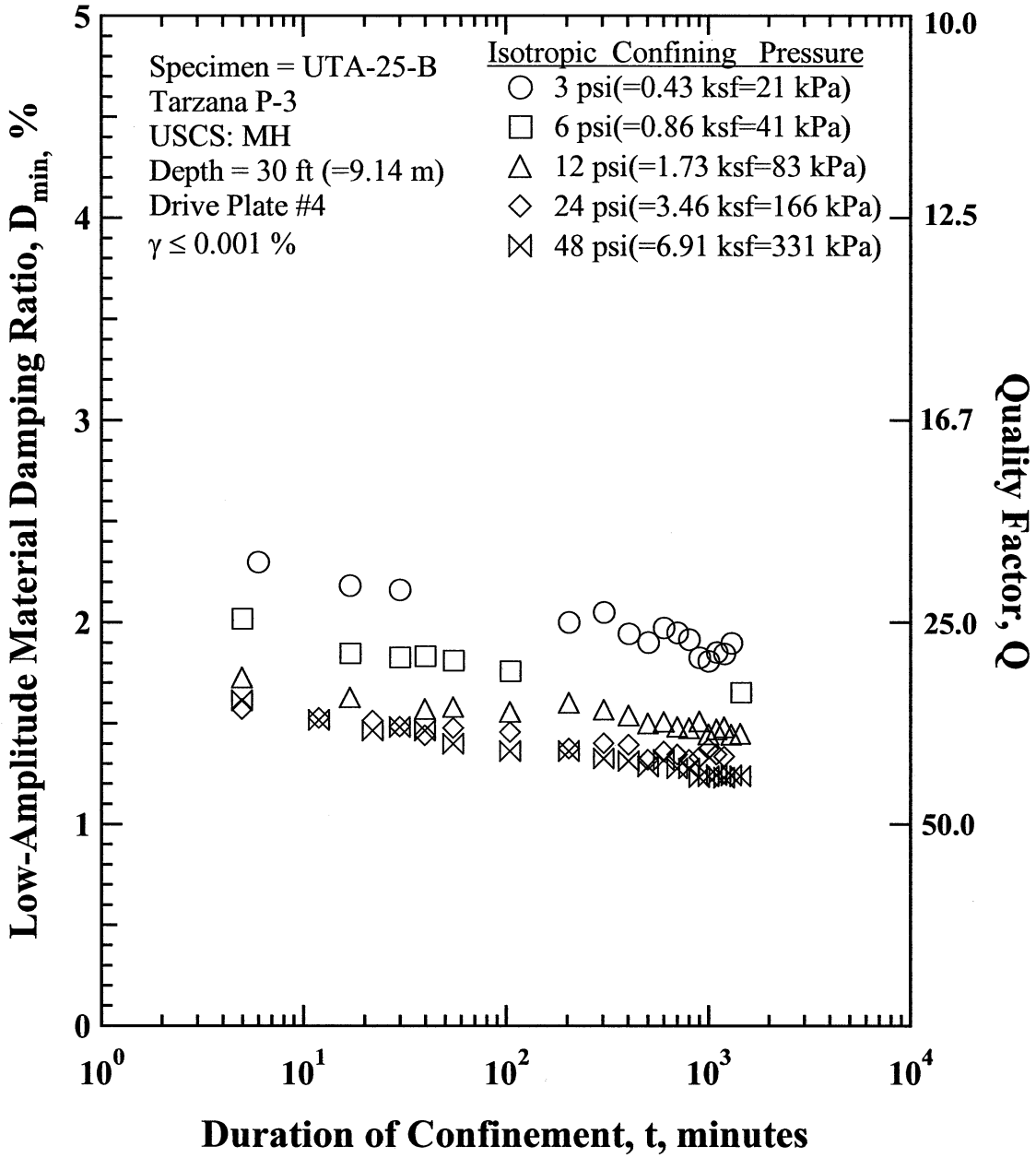

Figure B.2 Variation in Low-Amplitude Material Damping Ratio with Magnitude and Duration of Isotropic Confining Pressure from Resonant Column Tests of Specimen UTA-25-B

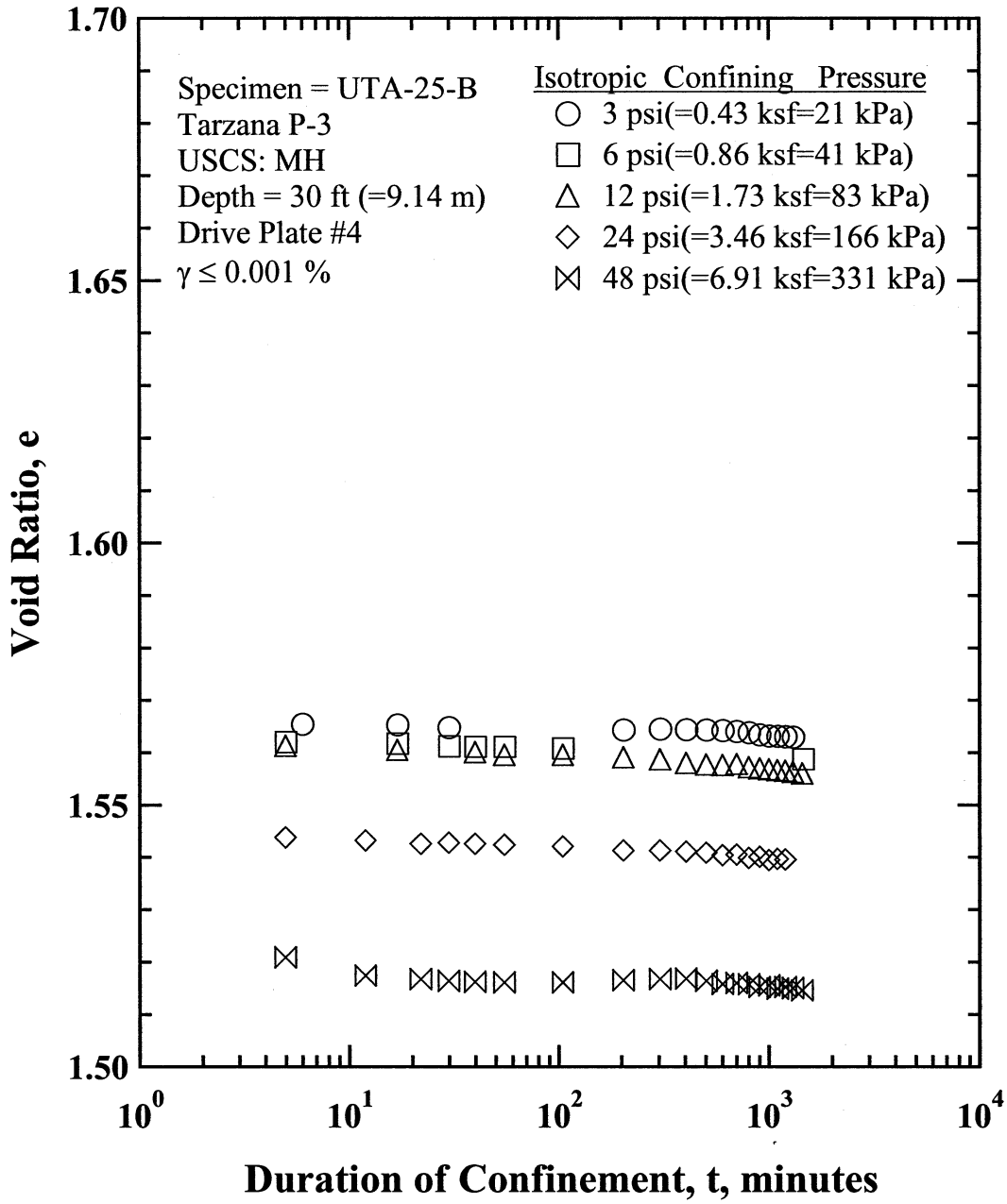

Figure B.3 Variation in Estimated Void Ratio with Magnitude and Duration of Isotropic Confining Pressure from Resonant Column Tests of Specimen UTA-25-B

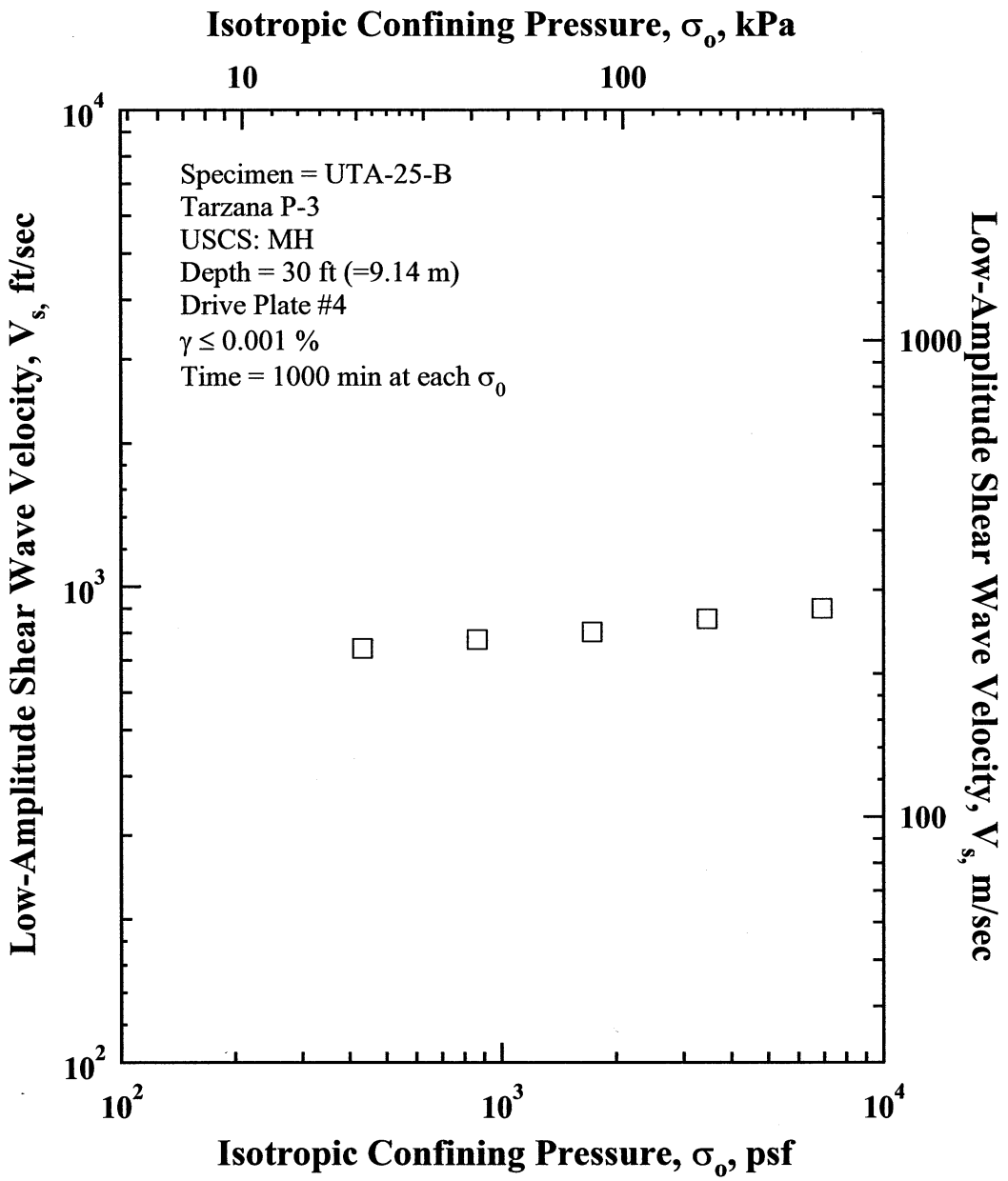

Figure B.4 Variation in Low-Amplitude Shear Wave Velocity with Isotropic Confining Pressure from Resonant Column Tests of Specimen UTA-25-B.

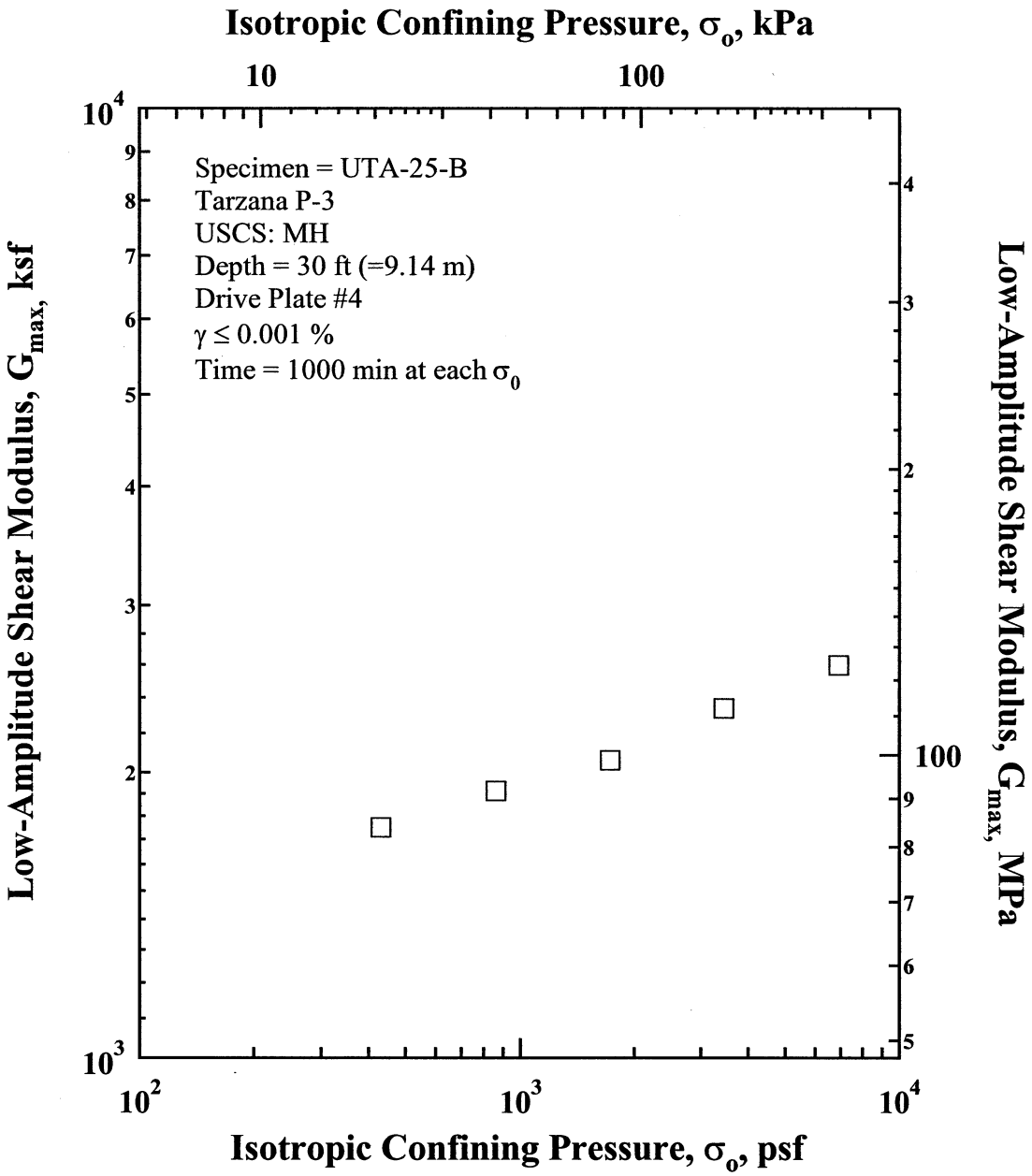

Figure B.5 Variation in Low-Amplitude Shear Modulus with Isotropic Confining Pressure from Resonant Column Tests of Specimen UTA-25-B.

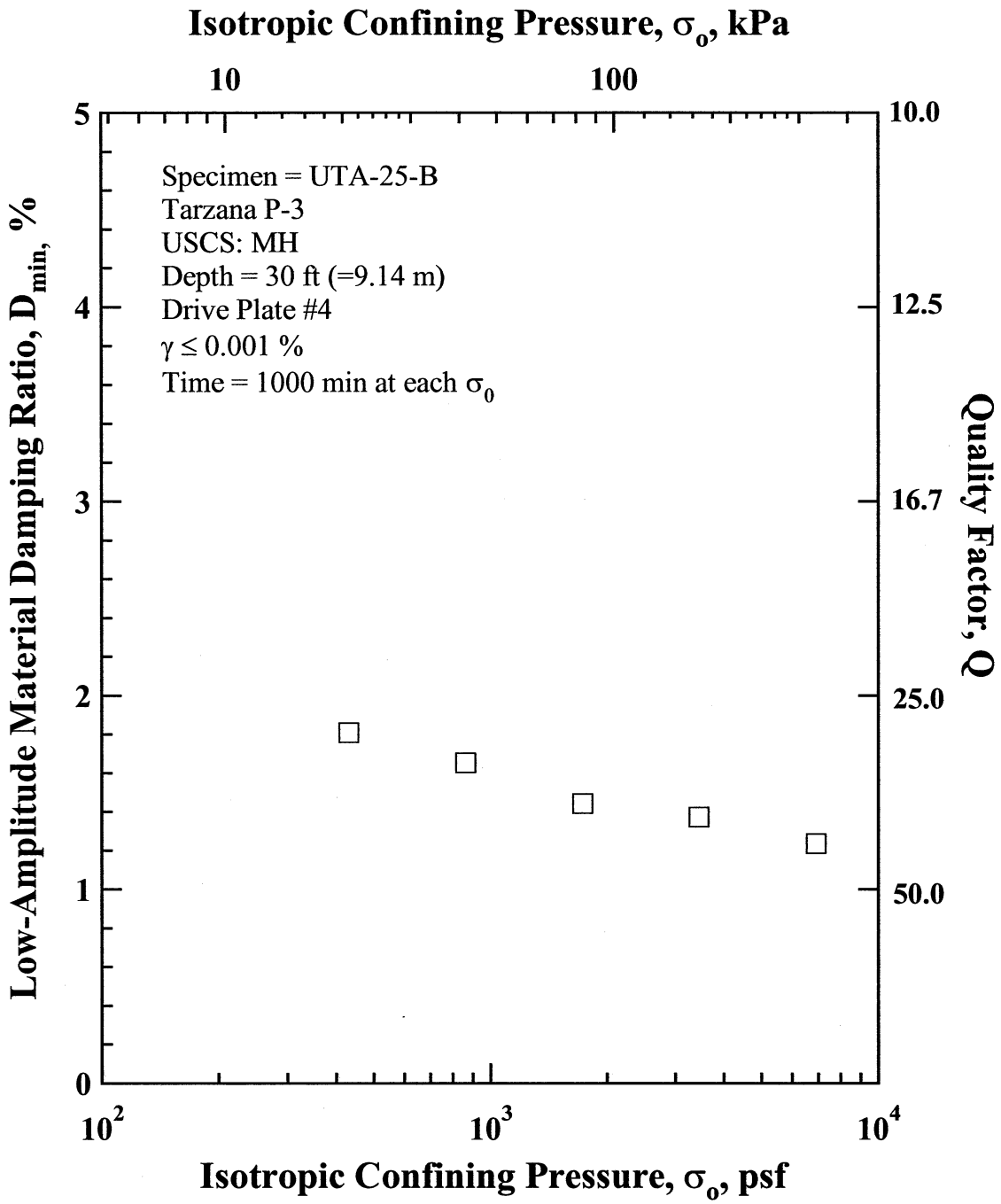

Figure B.6 Variation in Low-Amplitude Material Damping Ratio with Isotropic Confining Pressure from Resonant Column Tests of Specimen UTA-25-B.

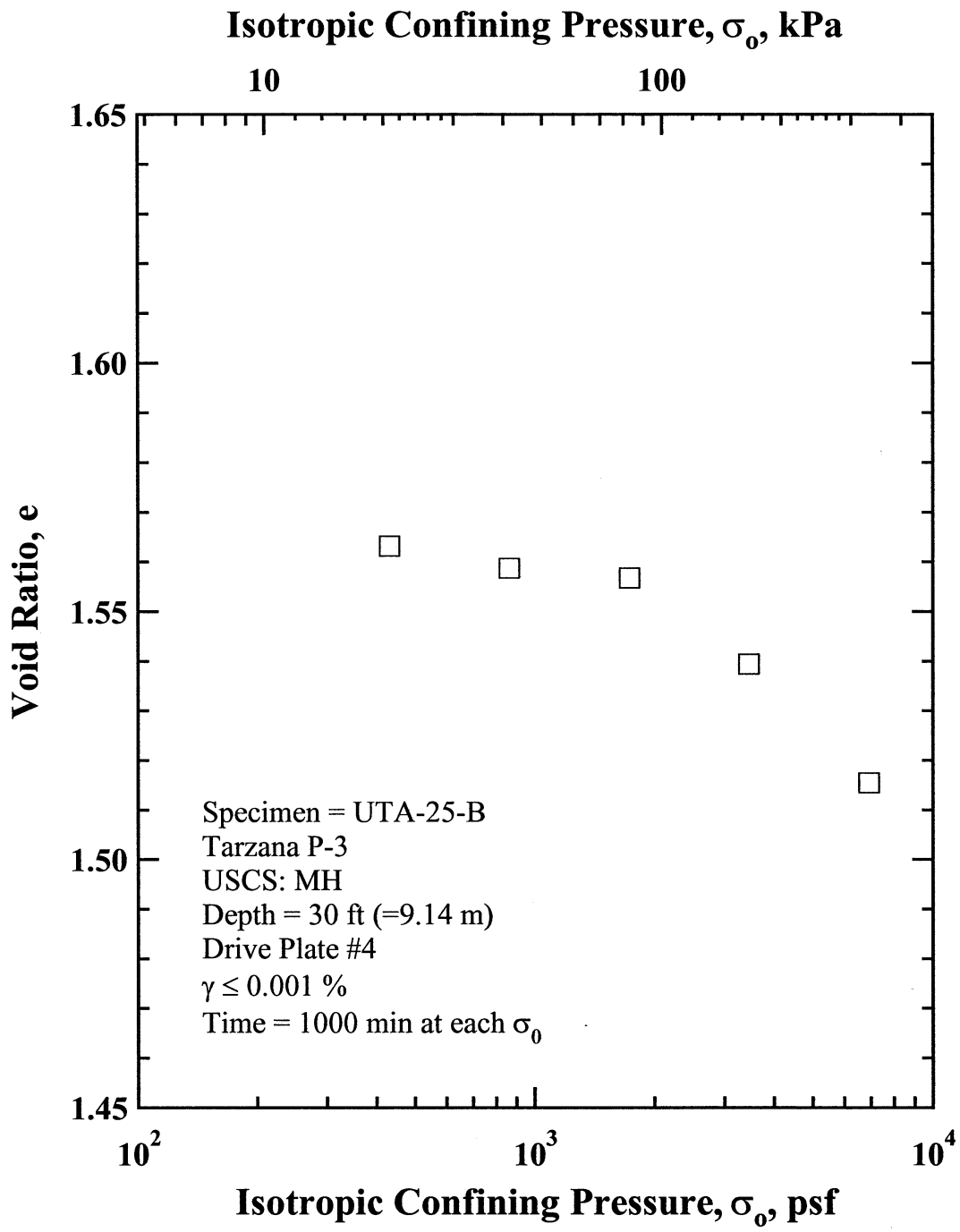

Figure B.7 Variation in Estimated Void Ratio with Isotropic Confining Pressure from Resonant Column Tests of Specimen UTA-25-B.

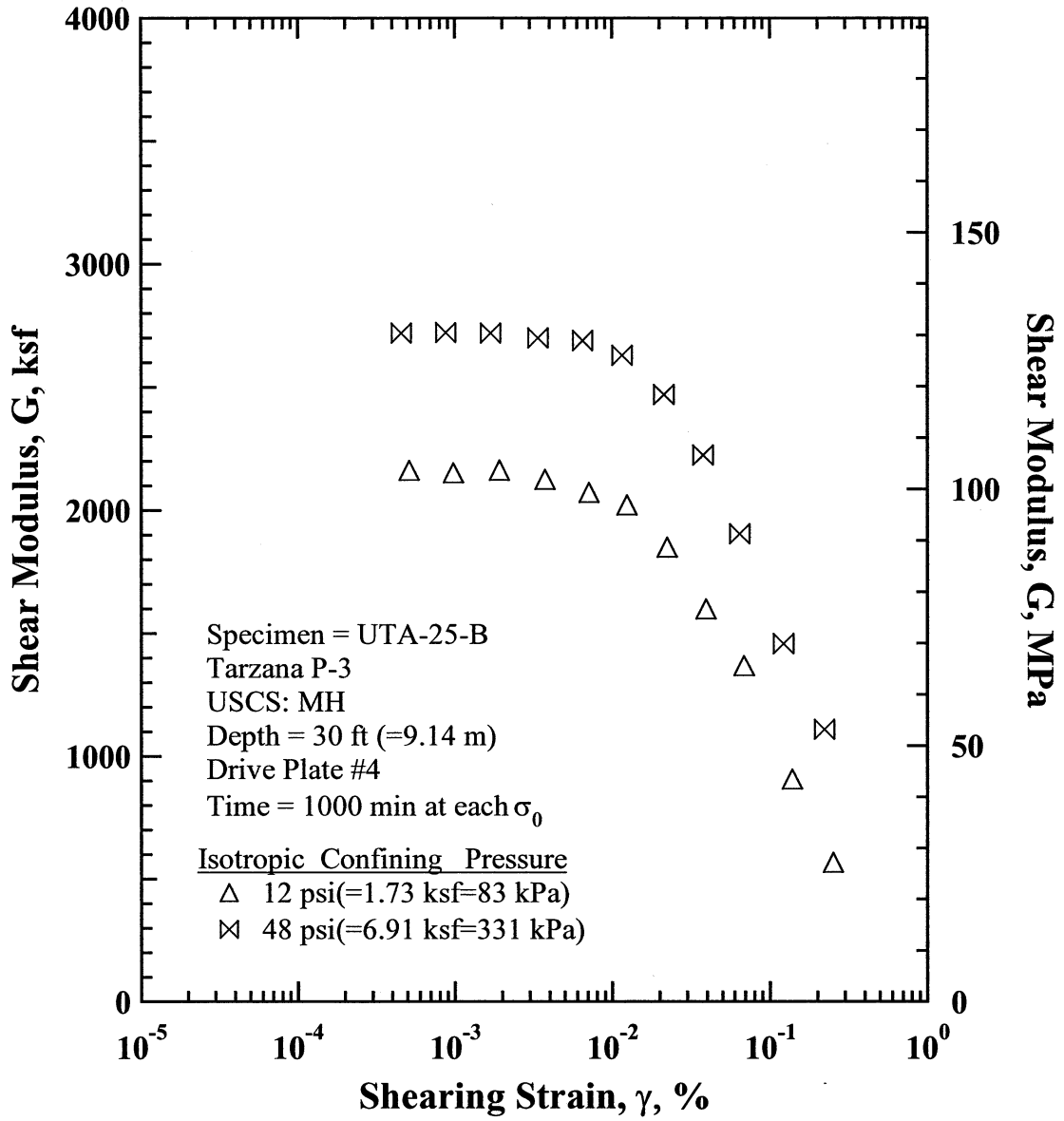

Figure B.8 Comparison of the Variation in Shear Modulus with Shearing Strain and Isotropic Confining Pressure from the Resonant Column Tests of Specimen UTA-25-B.

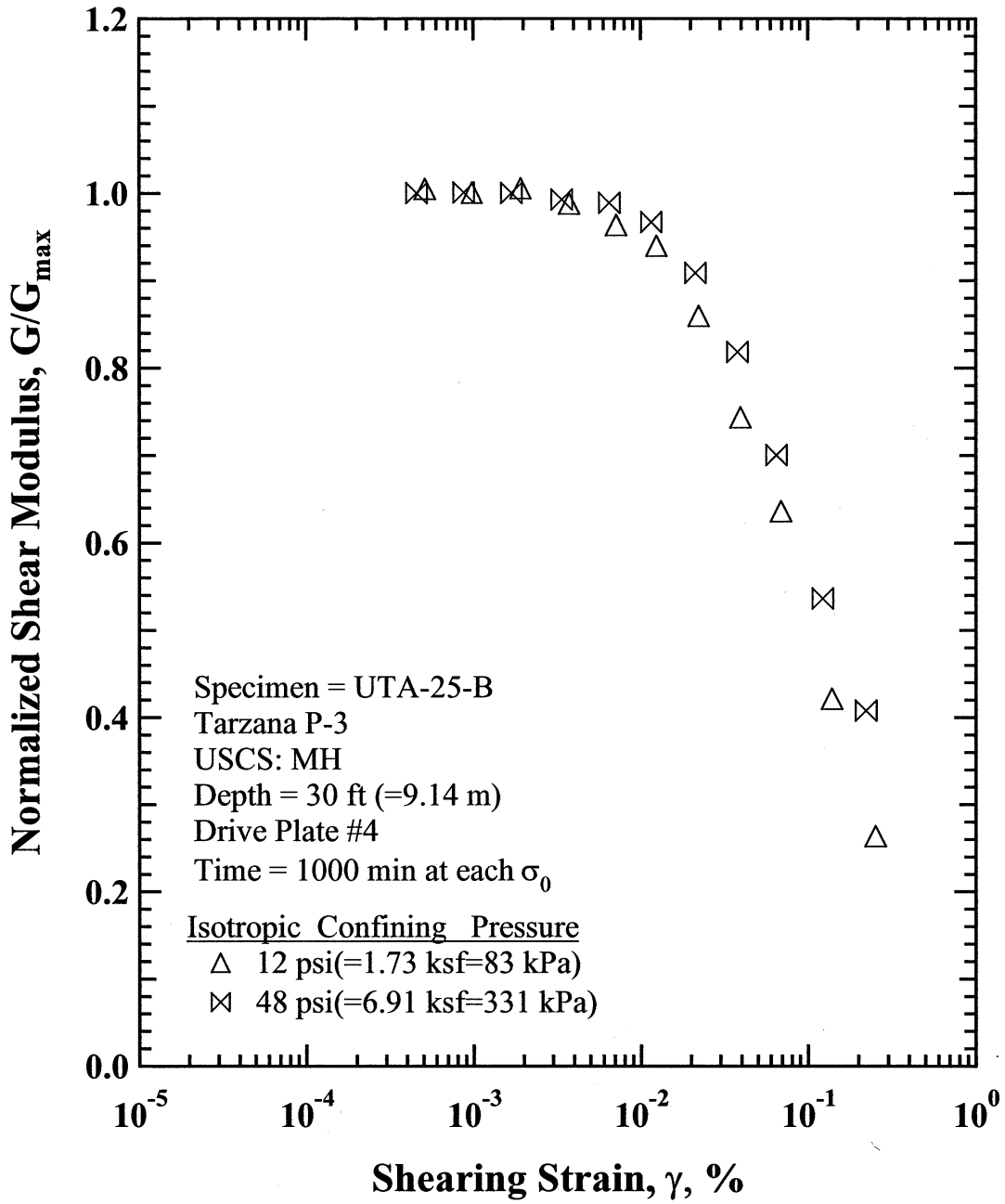

Figure B.9 Comparison of the Variation in Normalized Shear Modulus with Shearing Strain and Isotropic Confining Pressure from the Resonant Column Tests of Specimen UTA-25-B.

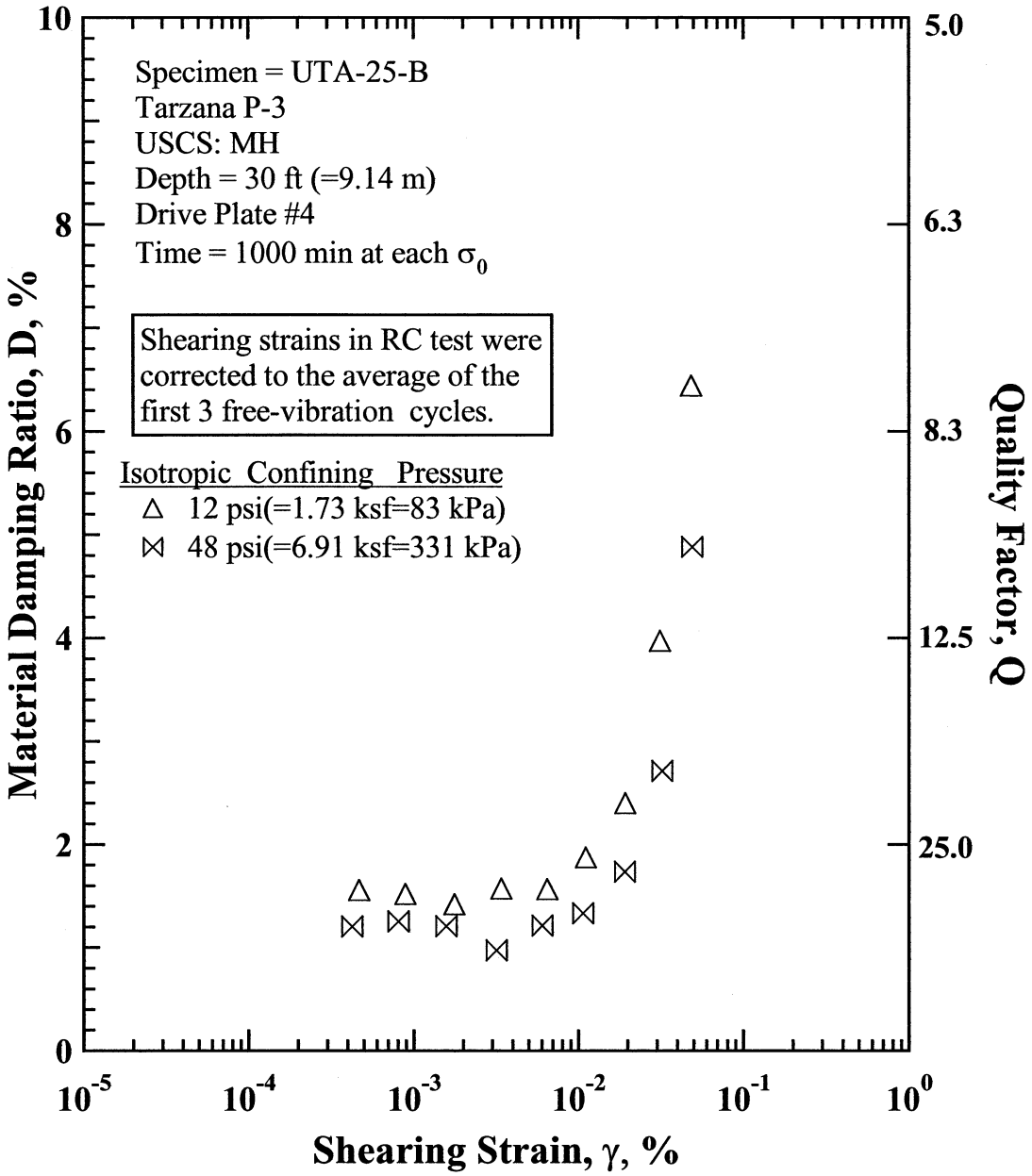

Figure B.10 Comparison of the Variation in Material Damping Ratio with Shearing Strain and Isotropic Confining Pressure from the Resonant Column Tests of Specimen UTA-25-B.

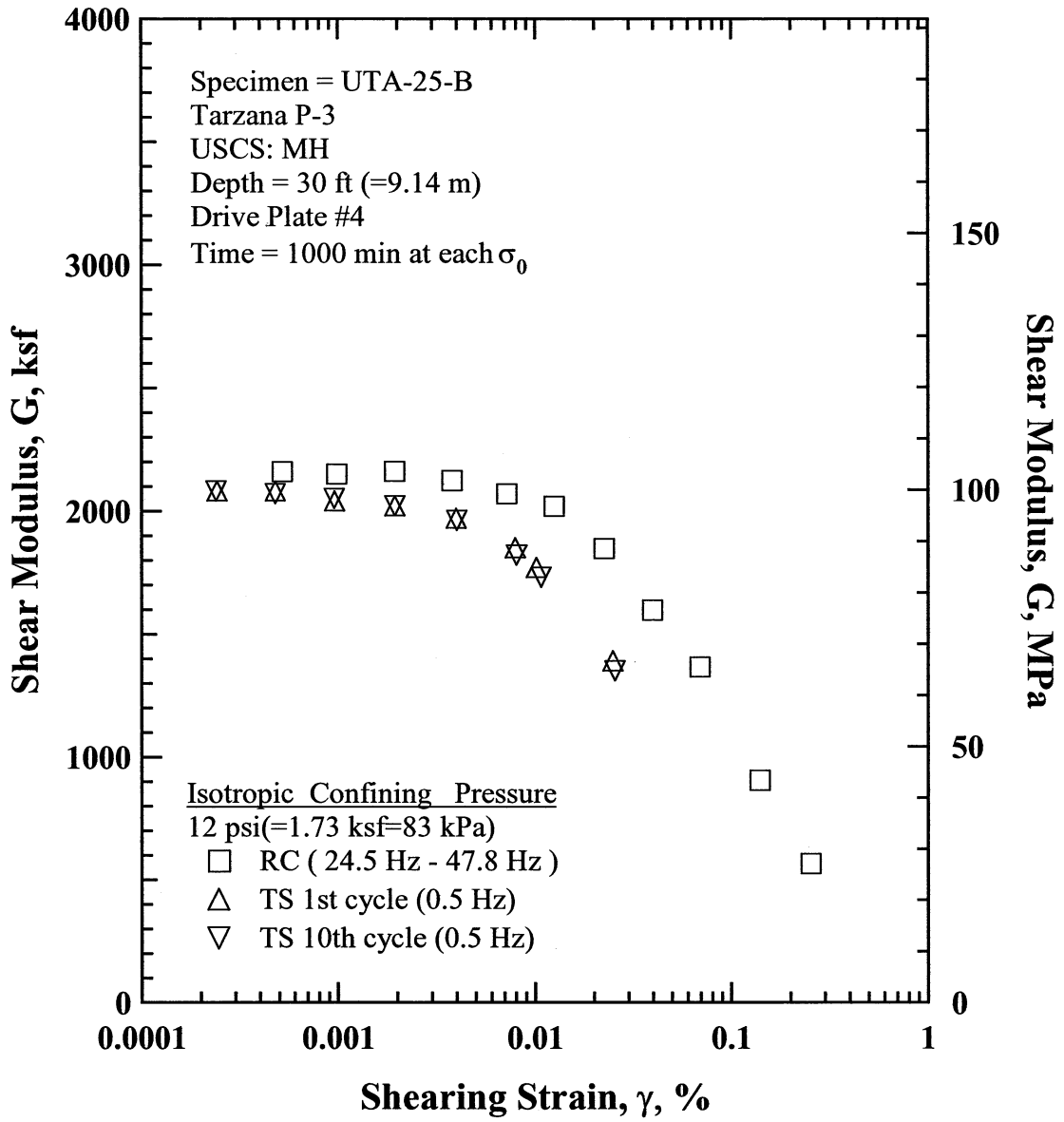

Figure B.11 Comparison of the Variation in Shear Modulus with Shearing Strain at an Isotropic Confining Pressure of 12 psi(=1.73 ksf=83 kPa) from the Combined RCTS Tests of Specimen UTA-25-B.

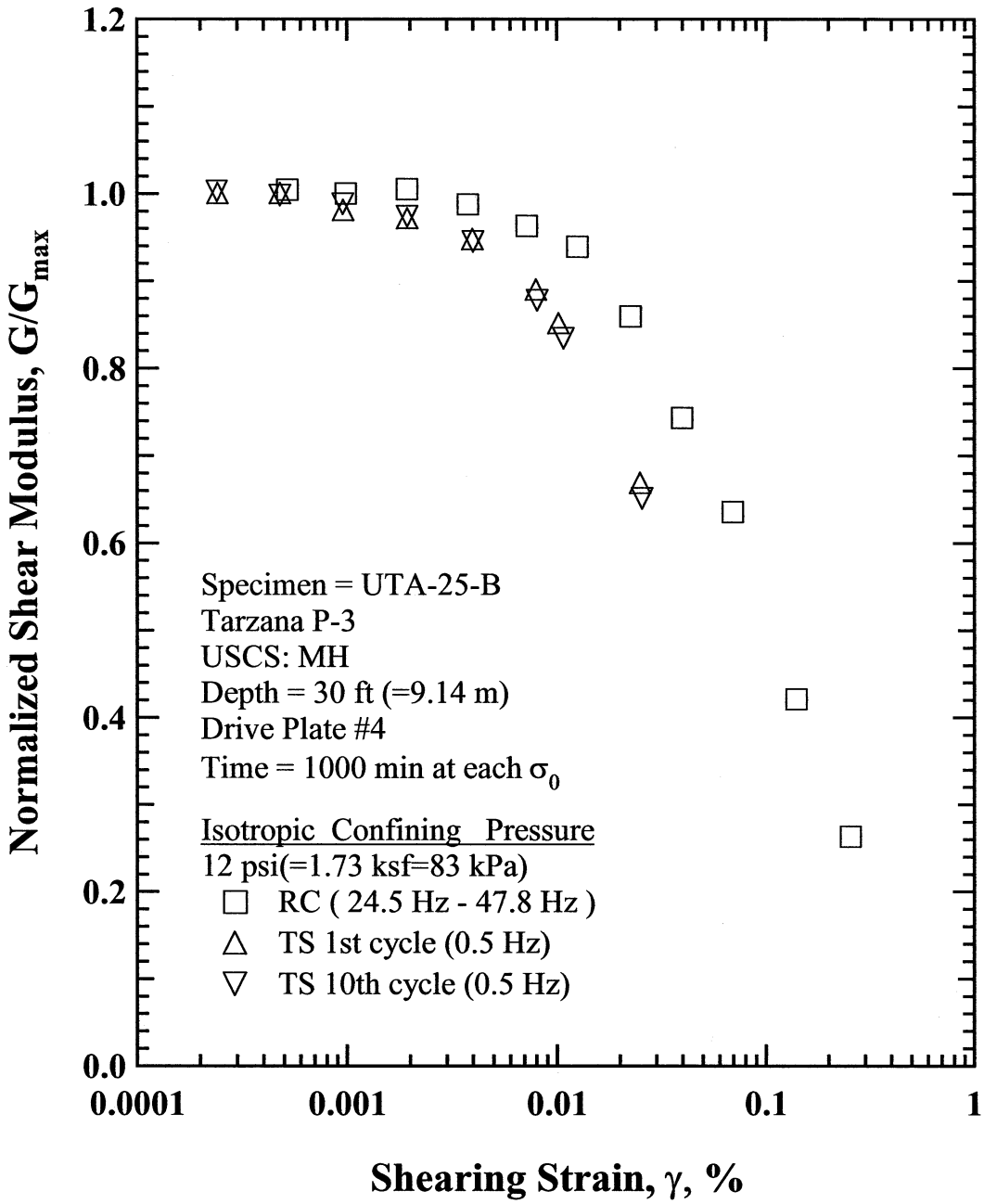

Figure B.12 Comparison of the Variation in Normalized Shear Modulus with Shearing Strain at an Isotropic Confining Pressure of 12 psi(=1.73 ksf=83 kPa) from the Combined RCTS Tests of Specimen UTA-25-B.

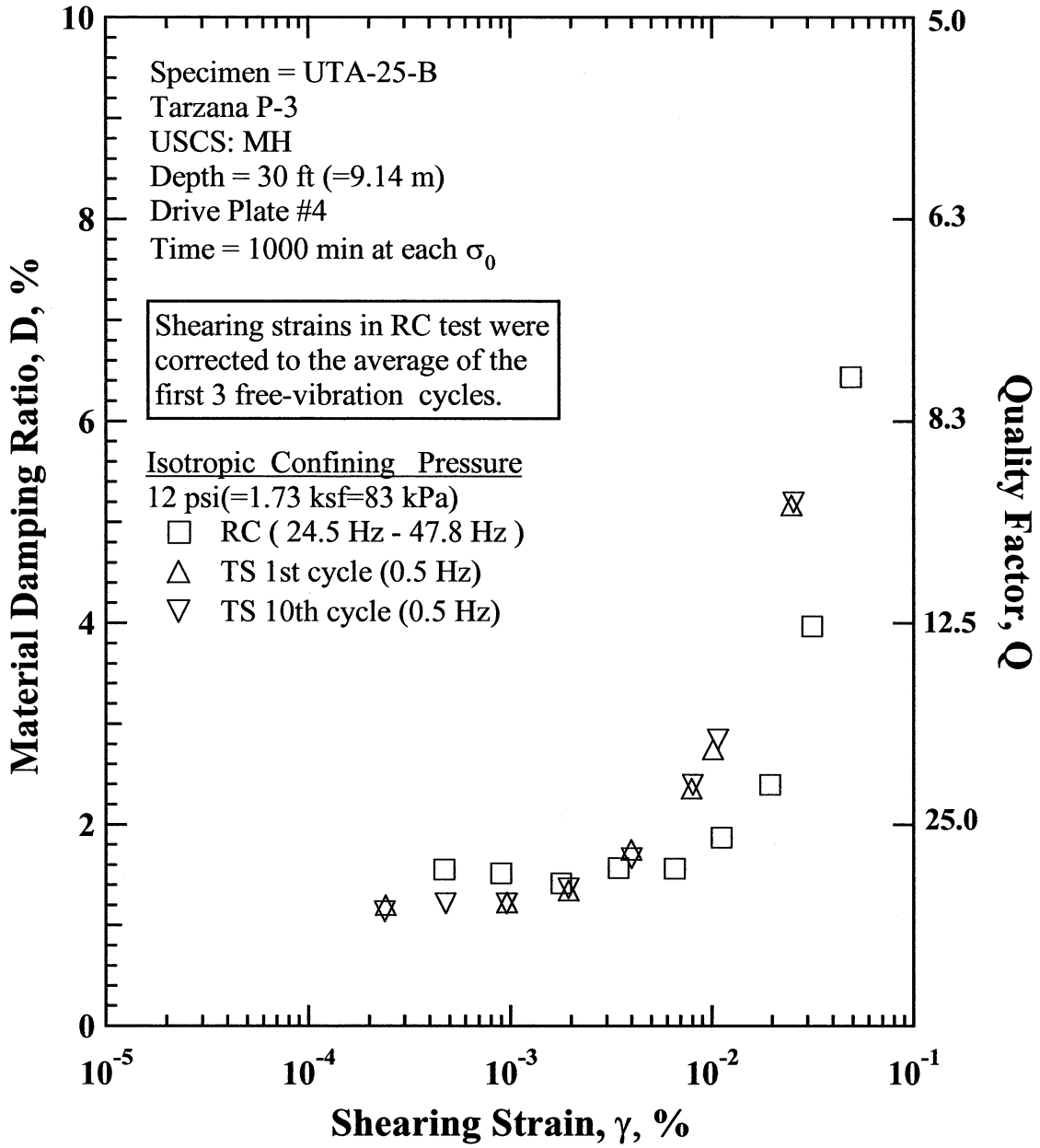

Figure B.13 Comparison of the Variation in Material Damping Ratio with Shearing Strain at an Isotropic Confining Pressure of 12 psi(=1.73 ksf=83 kPa) from the Combined RCTS Tests of Specimen UTA-25-B.

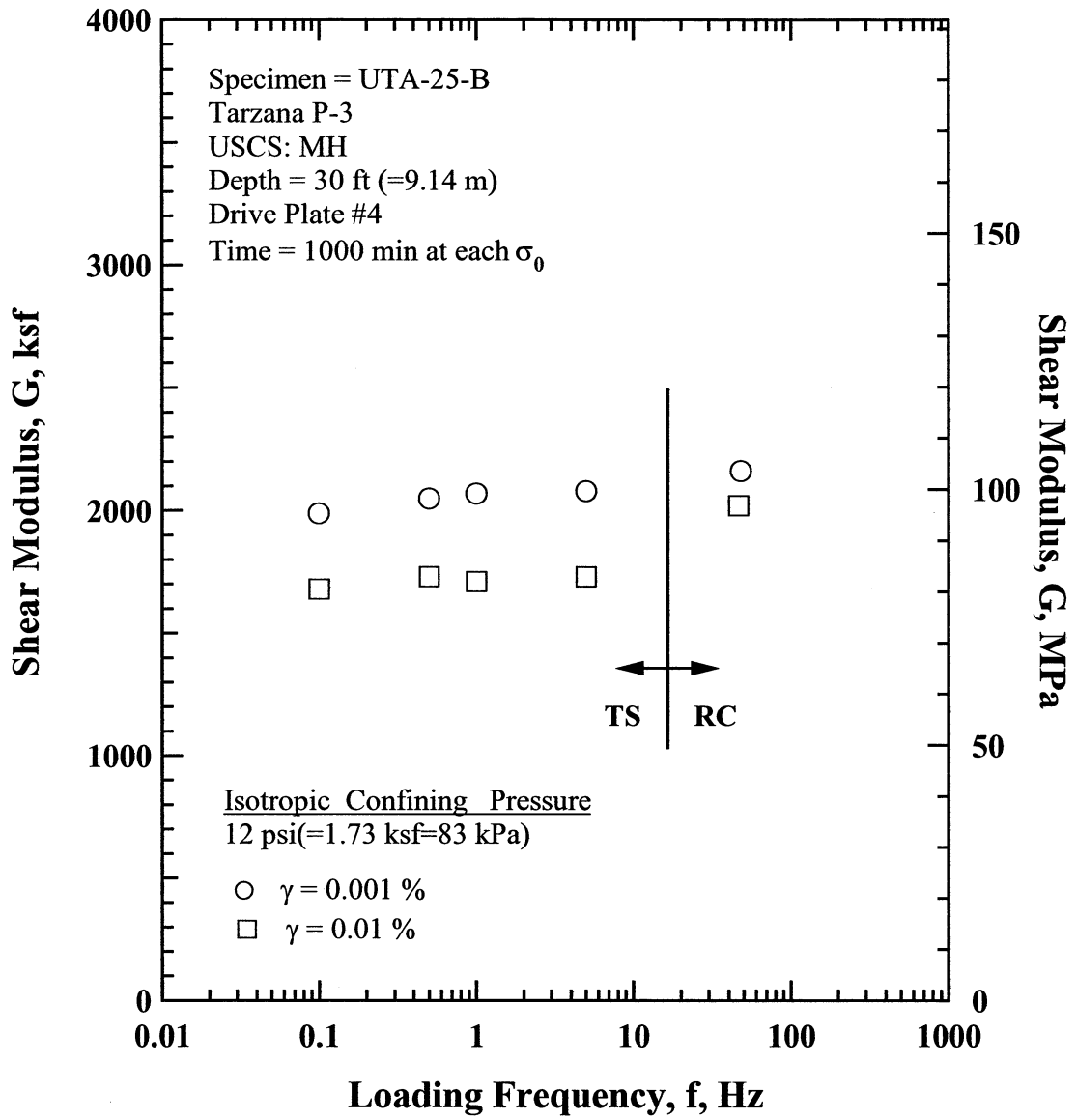

Figure B.14 Comparison of the Variation in Shear Modulus with Loading Frequency at an Isotropic Confining Pressure of 12 psi(=1.73 ksf=83 kPa) from the Combined RCTS Tests of Specimen UTA-25-B.

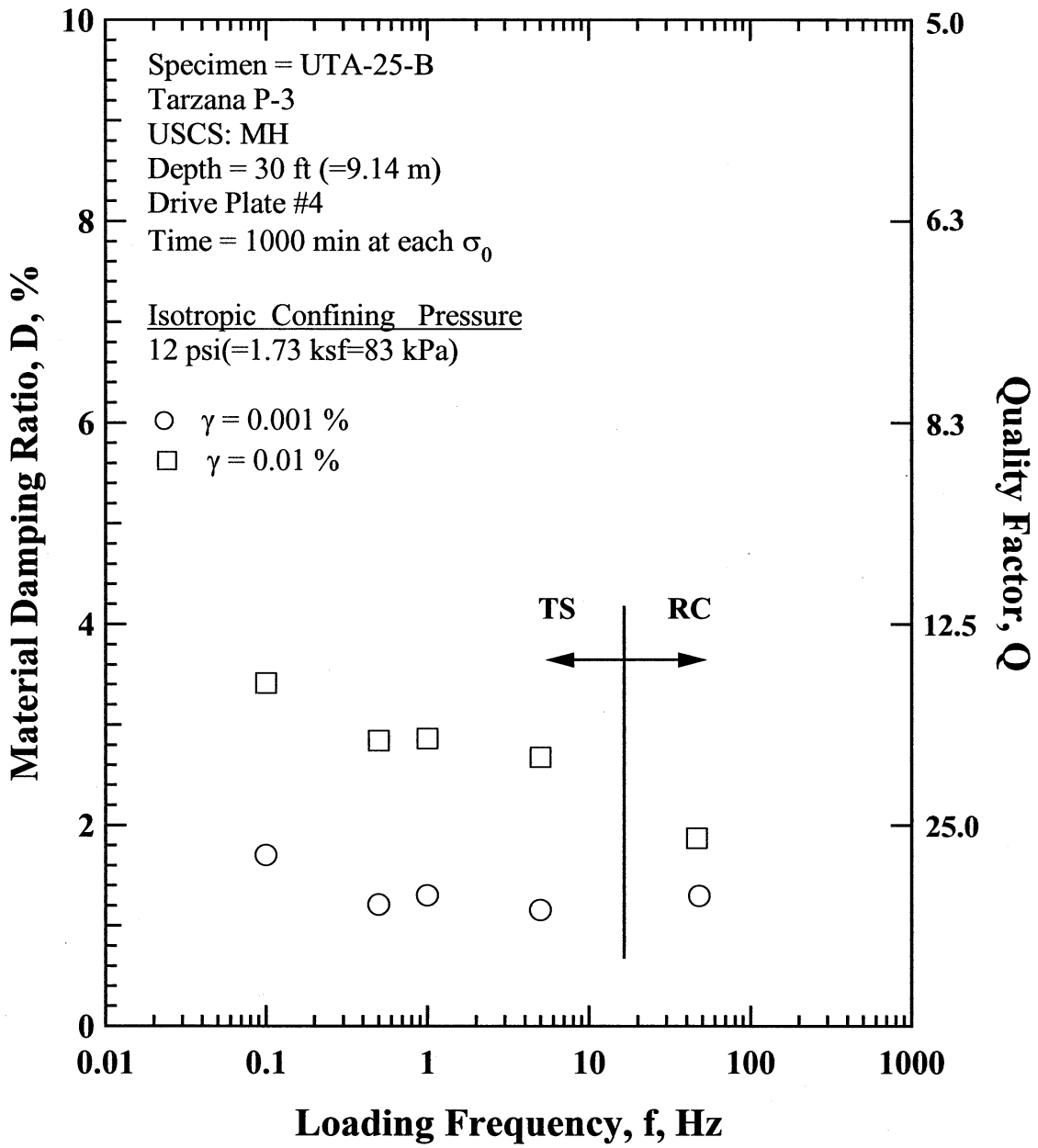

Figure B.15 Comparison of the Variation in Material Damping Ratio with Loading Frequency at an Isotropic Confining Pressure 12 psi(=1.73 ksf=83 kPa) from the Combined RCTS Tests of Specimen UTA-25-B.

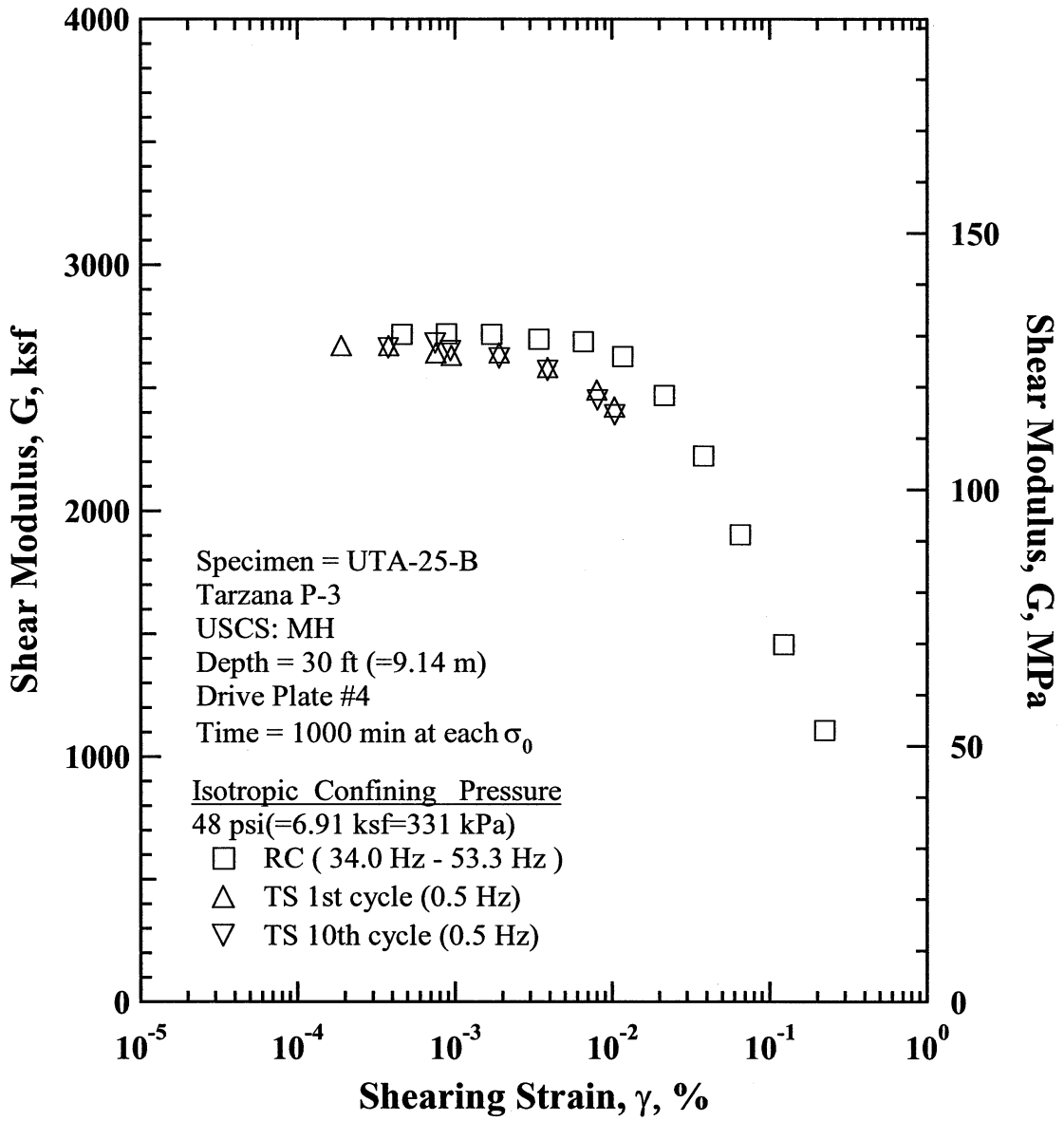

Figure B.16 Comparison of the Variation in Shear Modulus with Shearing Strain at an Isotropic Confining Pressure of 48 psi(=6.91 ksf=331 kPa) from the Combined RCTS Tests of Specimen UTA-25-B.

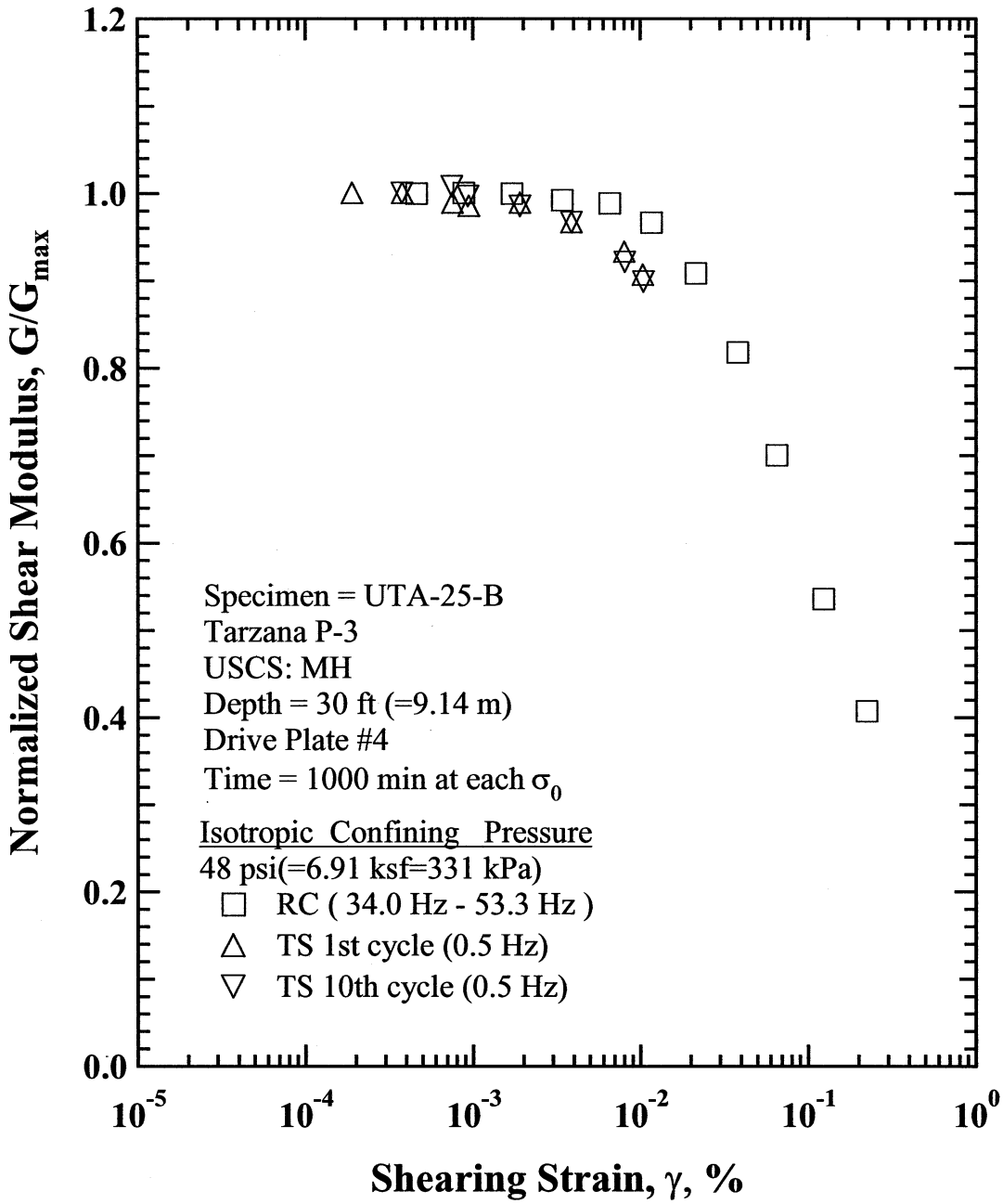

Figure B.17 Comparison of the Variation in Normalized Shear Modulus with Shearing Strain at an Isotropic Confining Pressure of 48 psi(=6.91 ksf=331 kPa) from the Combined RCTS Tests of Specimen UTA-25-B.

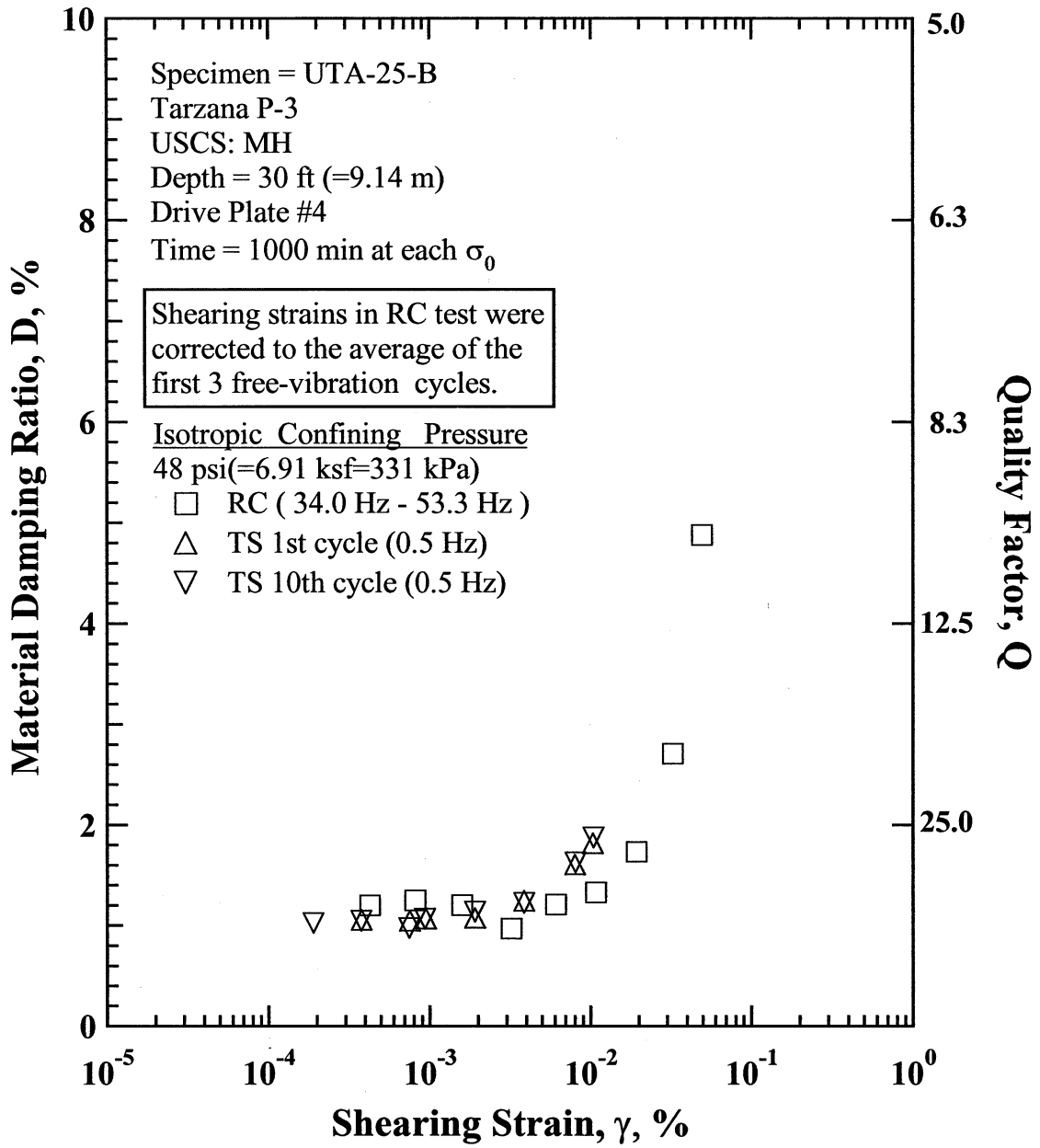

Figure B.18 Comparison of the Variation in Material Damping Ratio with Shearing Strain at an Isotropic Confining Pressure of 48 psi(=6.91 ksf=331 kPa) from the Combined RCTS Tests of Specimen UTA-25-B.

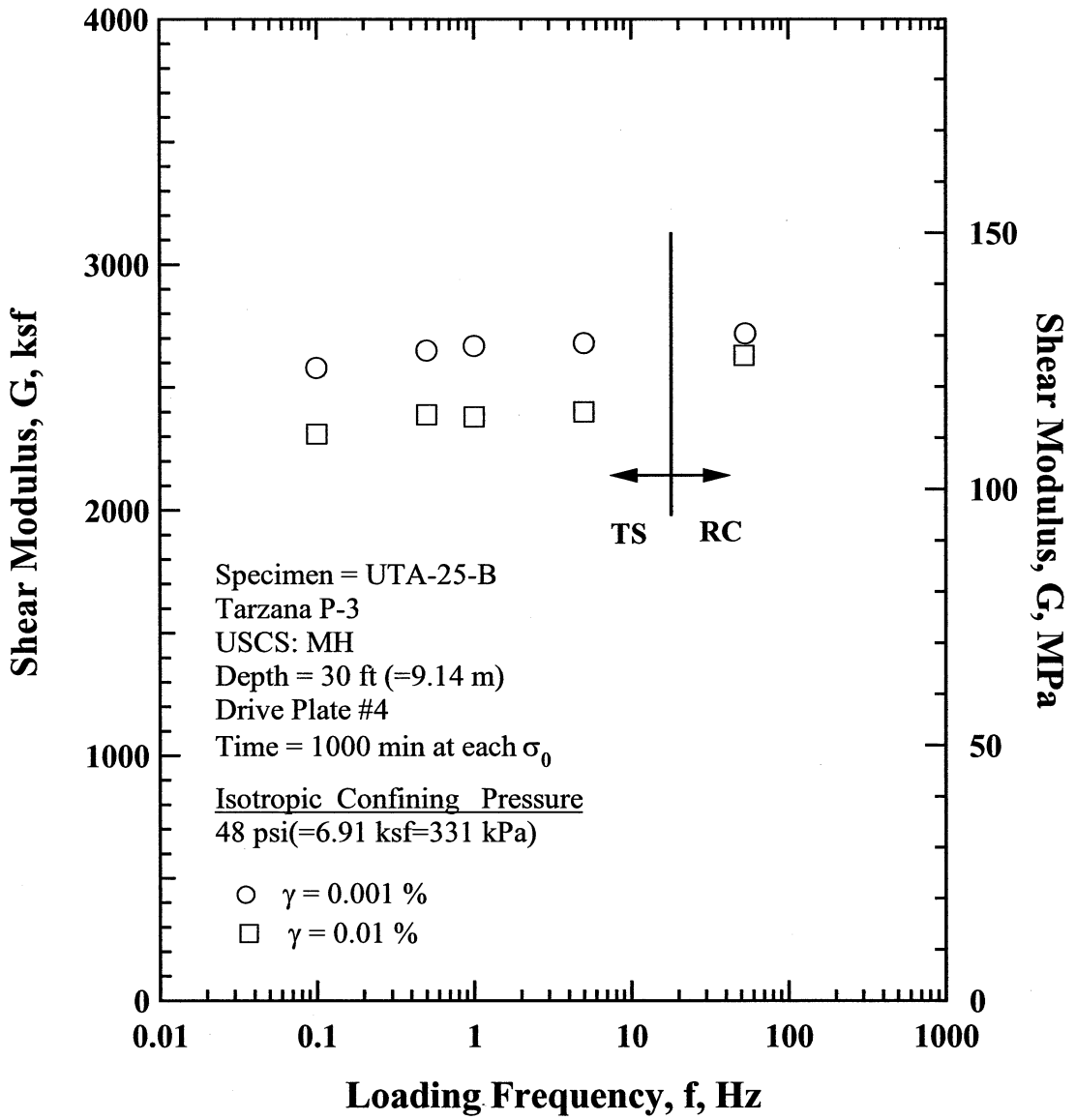

Figure B.19 Comparison of the Variation in Shear Modulus with Loading Frequency at an Isotropic Confining Pressure of 48 psi(=6.91 ksf=331 kPa) from the Combined RCTS Tests of Specimen UTA-25-B.

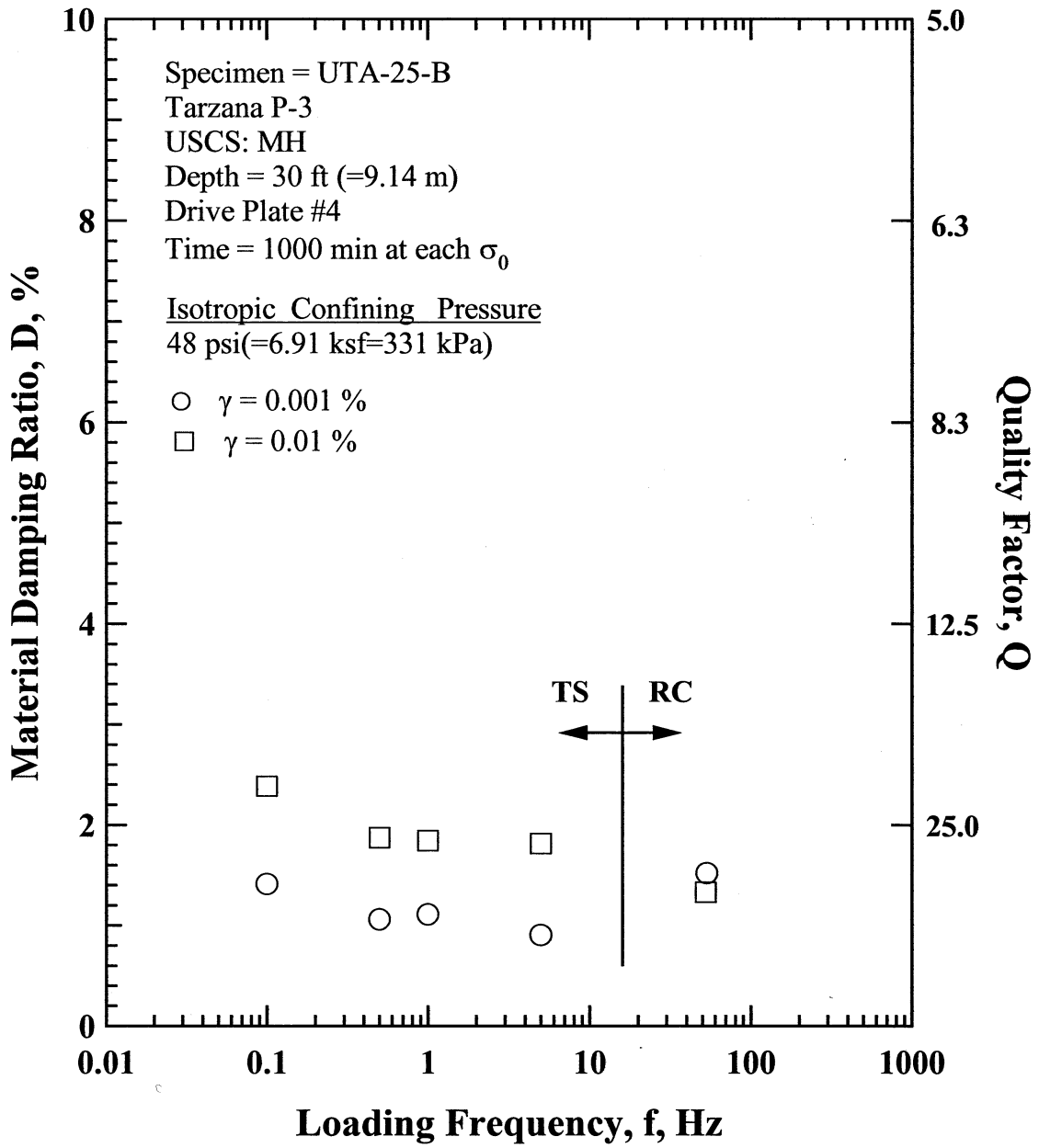

Figure B.20 Comparison of the Variation in Material Damping Ratio with Loading Frequency at an Isotropic Confining Pressure 48 psi(=6.91 ksf=331 kPa) from the Combined RCTS Tests of Specimen UTA-25-B.

Table B.1 Variation in Low-Amplitude Shear Wave Velocity, Low-Amplitude Shear Modulus, Low-Amplitude Material Damping Ratio and Estimated Void Ratio with Isotropic Confining Pressure from RC Tests of Specimen UTA-25-B.

Effective Isotropic Confining Pressure, σ_o'			Low-Amplitude Shear Modulus, G_{max}		Low-Amplitude Shear Wave Velocity, Vs	Low-Amplitude Material Damping Ratio,	Estimated Void Ratio, e
(psi)	(psf)	(kPa)	(ksf)	(MPa)	(fps)	D_{min}, %	
3	432	20.7	1750	83.9	742	1.81	1.563
6	864	41.4	1911	91.6	775	1.65	1.559
12	1728	82.8	2059	98.7	804	1.44	1.557
24	3456	165.7	2338	112.1	856	1.37	1.539
48	6912	331.4	2594	124.3	900	1.24	1.515

Table B.2 Variation in Shear Modulus, Normalized Shear Modulus and Material Damping Ratio with Shearing Strain from RC Tests of Specimen UTA-25-B; Confining Pressure, σ_o' = 12 psi(=1.73 ksf=83 kPa).

Peak Shearing Strain, %	Shear Modulus, G, ksf	Normalized Shear Modulus, G/G_{max}	Average[+] Shearing Strain, %	Material Damping Ratio[x], D, %
9.85E-04	2151	1.00	8.99E-04	1.52
5.18E-04	2160	1.00	4.71E-04	1.55
1.94E-03	2162	1.01	1.78E-03	1.42
3.77E-03	2124	0.99	3.43E-03	1.57
7.18E-03	2070	0.96	6.53E-03	1.56
1.25E-02	2020	0.94	1.12E-02	1.87
2.25E-02	1848	0.86	1.95E-02	2.39
3.97E-02	1598	0.74	3.16E-02	3.97
6.94E-02	1367	0.64	4.88E-02	6.44
1.40E-01	905	0.42		
2.54E-01	566	0.26		

[+] Average Shearing Strain from the First Three Cycles of the Free Vibration Decay Curve

[x] Average Damping Ratio from the First Three Cycles of the Free Vibration Decay Curve

Table B.3 Variation in Shear Modulus, Normalized Shear Modulus and Material Damping Ratio with Shearing Strain from TS Tests of Specimen UTA-25-B; Confining Pressure, σ_o' = 12 psi(=1.73 ksf=83 kPa).

First Cycle				Tenth Cycle			
Peak Shearing Strain, %	Shear Modulus, G, ksf	Normalized Shear Modulus, G/G_{max}	Material Damping Ratio, D, %	Peak Shearing Strain, %	Shear Modulus, G, ksf	Normalized Shear Modulus, G/G_{max}	Material Damping Ratio, D, %
4.86E-04	2080	1.00	1.19	4.82E-04	2080	1.00	1.13
9.62E-04	2080	1.00		9.62E-04	2070	1.00	1.21
1.93E-03	2040	0.98	1.22	1.92E-03	2050	0.99	1.21
3.90E-03	2020	0.97	1.34	3.90E-03	2020	0.97	1.36
8.00E-03	1970	0.95	1.74	8.04E-03	1960	0.94	1.66
1.60E-02	1850	0.89	2.35	1.62E-02	1820	0.88	2.39
2.04E-02	1770	0.85	2.74	2.16E-02	1730	0.83	2.84
5.02E-02	1390	0.67	5.16	5.14E-02	1350	0.65	5.19

Table B.4 Variation in Shear Modulus, Normalized Shear Modulus and Material Damping Ratio with Shearing Strain from RC Tests of Specimen UTA-25-B; Confining Pressure, σ_o' = 48 psi(=6.91 ksf=331 kPa).

Peak Shearing Strain, %	Shear Modulus, G, ksf	Normalized Shear Modulus, G/G_{max}	Average[+] Shearing Strain, %	Material Damping Ratio[x], D, %
8.81E-04	2720	1.00	8.16E-04	1.25
4.61E-04	2717	1.00	4.28E-04	1.20
1.71E-03	2718	1.00	1.59E-03	1.20
3.40E-03	2698	0.99	3.21E-03	0.97
6.55E-03	2687	0.99	6.08E-03	1.21
1.17E-02	2627	0.97	1.08E-02	1.33
2.14E-02	2469	0.91	1.93E-02	1.73
3.81E-02	2223	0.82	3.25E-02	2.71
6.52E-02	1903	0.70	4.94E-02	4.88
1.23E-01	1456	0.54		
2.23E-01	1107	0.41		

[+] Average Shearing Strain from the First Three Cycles of the Free Vibration Decay Curve

[x] Average Damping Ratio from the First Three Cycles of the Free Vibration Decay Curve

Table B.5 Variation in Shear Modulus, Normalized Shear Modulus and Material Damping Ratio with Shearing Strain from TS Tests of Specimen UTA-25-B; Confining Pressure, σ_o' = 48 psi(=6.91 ksf=331 kPa).

First Cycle				Tenth Cycle			
Peak Shearing Strain, %	Shear Modulus, G, ksf	Normalized Shear Modulus, G/G_{max}	Material Damping Ratio, D, %	Peak Shearing Strain, %	Shear Modulus, G, ksf	Normalized Shear Modulus, G/G_{max}	Material Damping Ratio, D, %
3.82E-04	2670	1.00		3.82E-04		1.02	1.02
7.64E-04	2670	1.00	1.05	7.60E-04	2660	1.00	1.04
1.52E-03	2640	0.99	1.04	1.51E-03	2680	1.01	0.97
1.90E-03	2630	0.99	1.06	1.88E-03	2650	1.00	1.06
3.84E-03	2640	0.99	1.07	3.84E-03	2620	0.98	1.13
7.80E-03	2580	0.97	1.24	7.80E-03	2570	0.97	1.22
1.61E-02	2490	0.93	1.60	1.63E-02	2450	0.92	1.62
2.08E-02	2420	0.91	1.81	2.10E-02	2390	0.90	1.87

APPENDIX C

Specimen No. 2
UT Specimen ID: UTA-25-A

Tarzana P-4
Depth = 42 ft (12.8m)
Soil Type: Clay (CH)

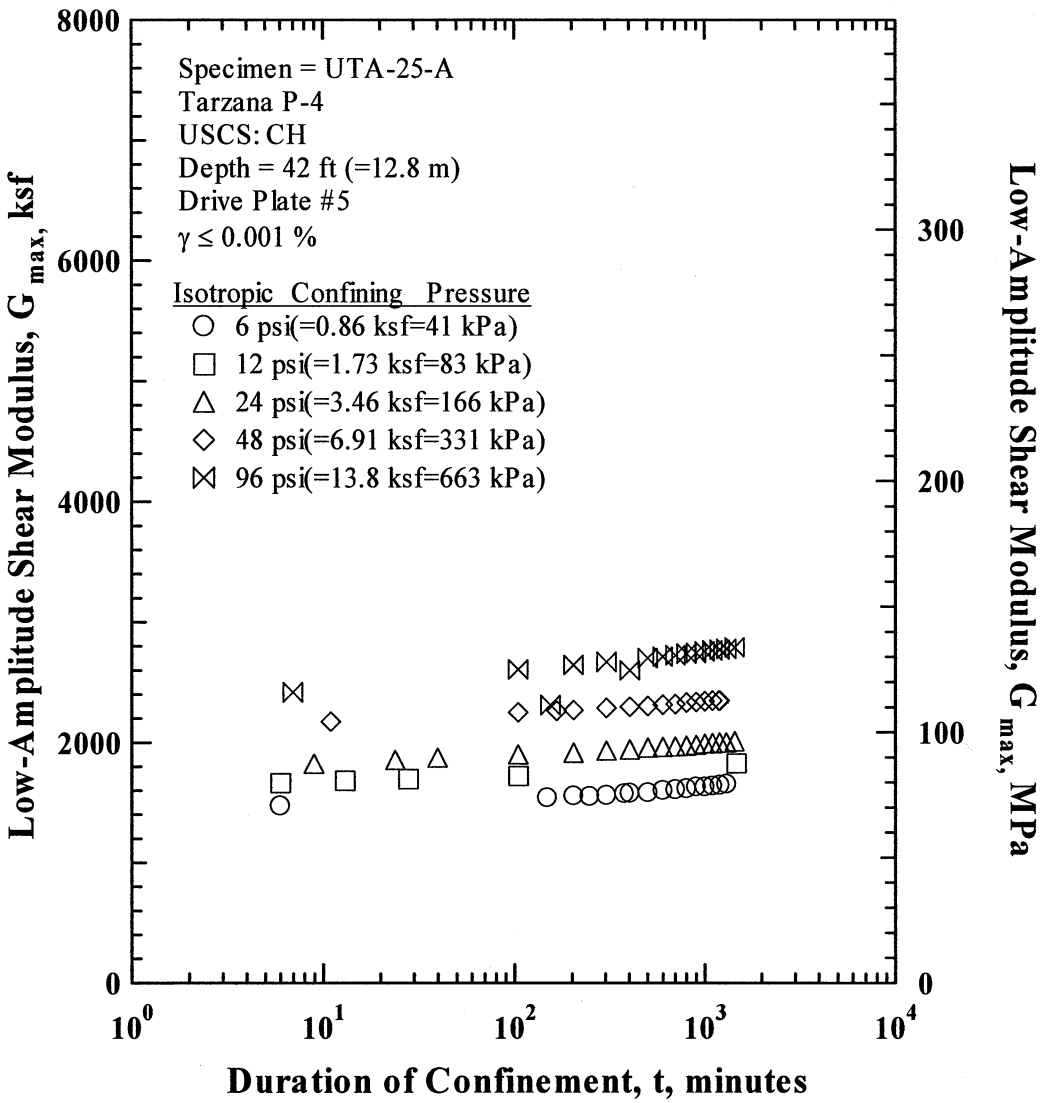

Figure C.1 Variation in Low-Amplitude Shear Modulus with Magnitude and Duration of Isotropic Confining Pressure from Resonant Column Tests of Specimen UTA-25-A.

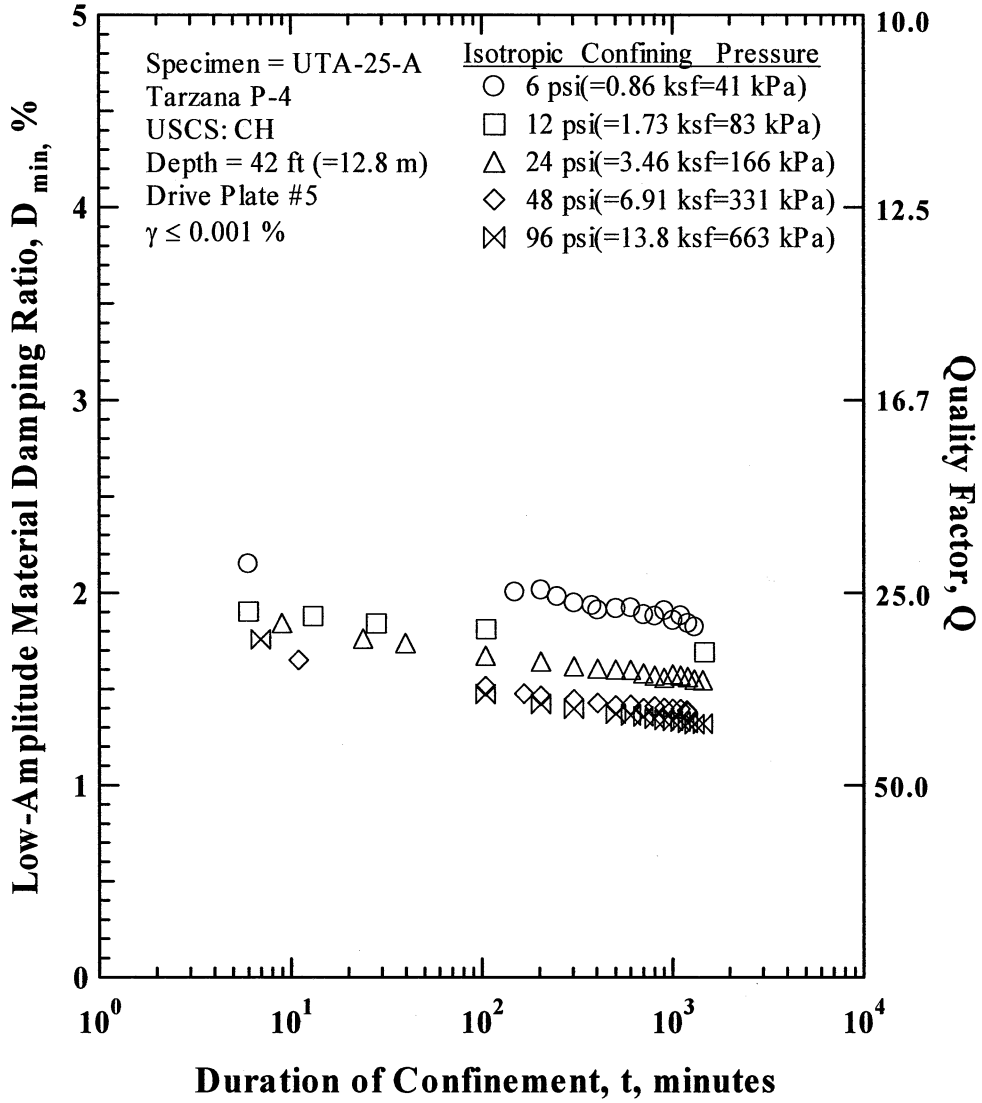

Figure C.2 Variation in Low-Amplitude Material Damping Ratio with Magnitude and Duration of Isotropic Confining Pressure from Resonant Column Tests of Specimen UTA-25-A

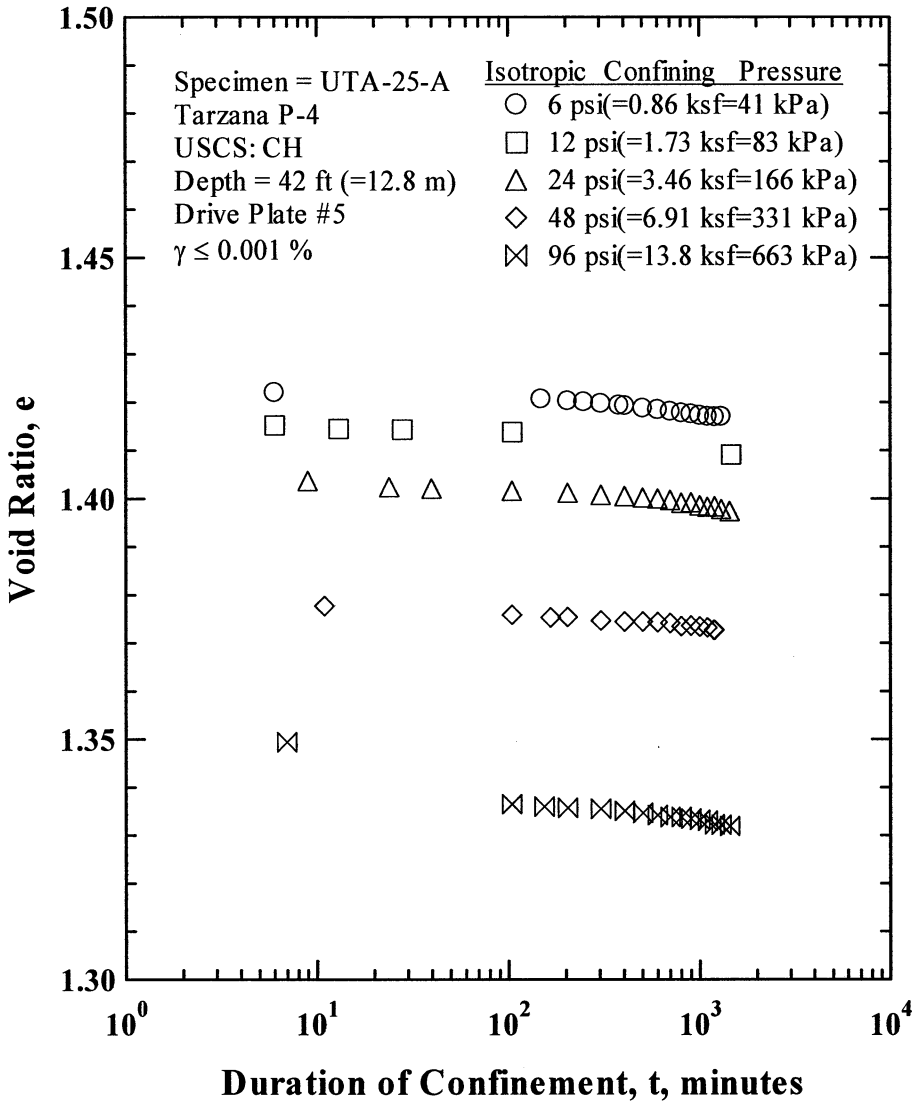

Figure C.3 Variation in Estimated Void Ratio with Magnitude and Duration of Isotropic Confining Pressure from Resonant Column Tests of Specimen UTA-25-A

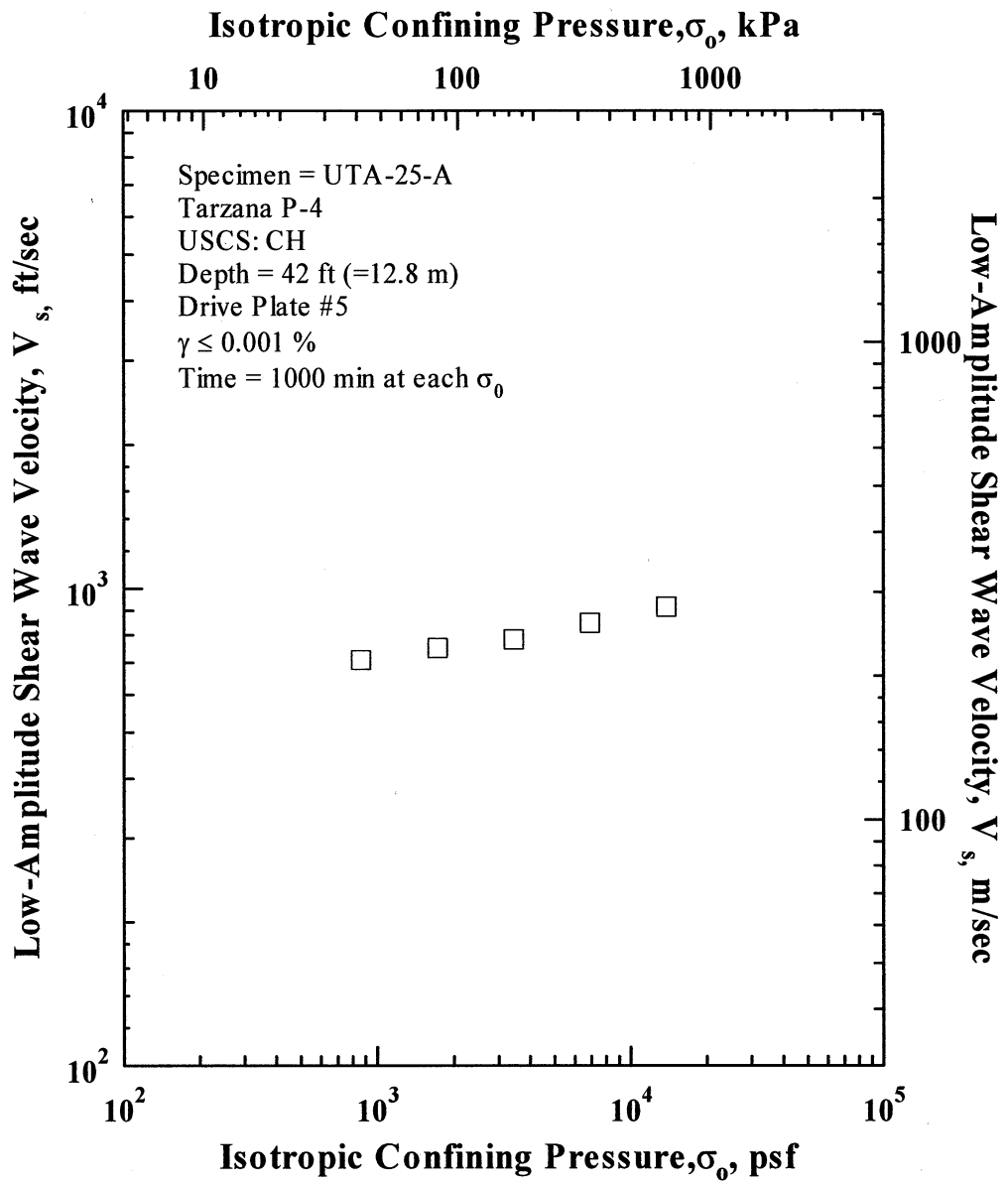

Figure C.4 Variation in Low-Amplitude Shear Wave Velocity with Isotropic Confining Pressure from Resonant Column Tests of Specimen UTA-25-A.

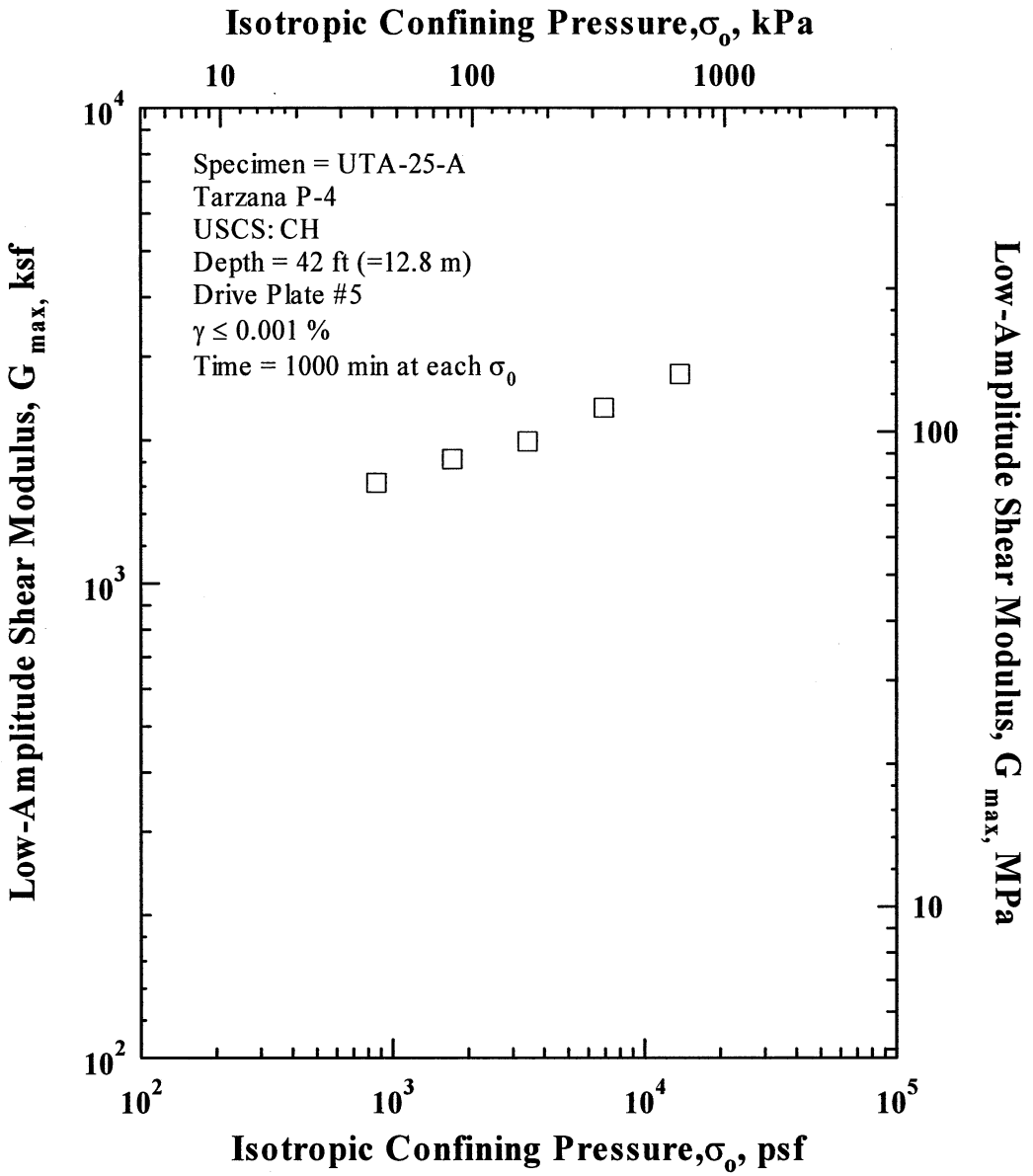

Figure C.5 Variation in Low-Amplitude Shear Modulus with Isotropic Confining Pressure from Resonant Column Tests of Specimen UTA-25-A.

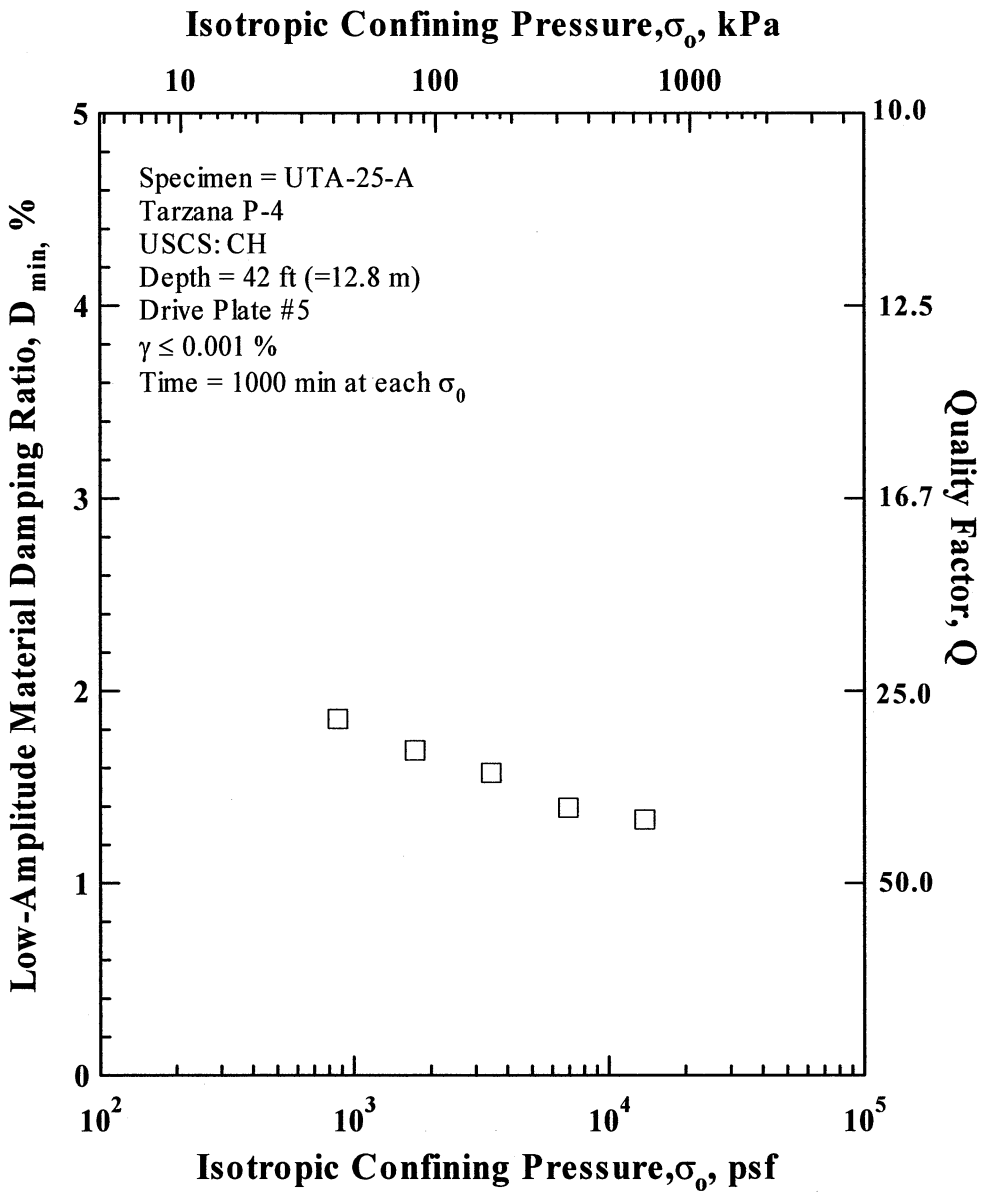

Figure C.6 Variation in Low-Amplitude Material Damping Ratio with Isotropic Confining Pressure from Resonant Column Tests of Specimen UTA-25-A.

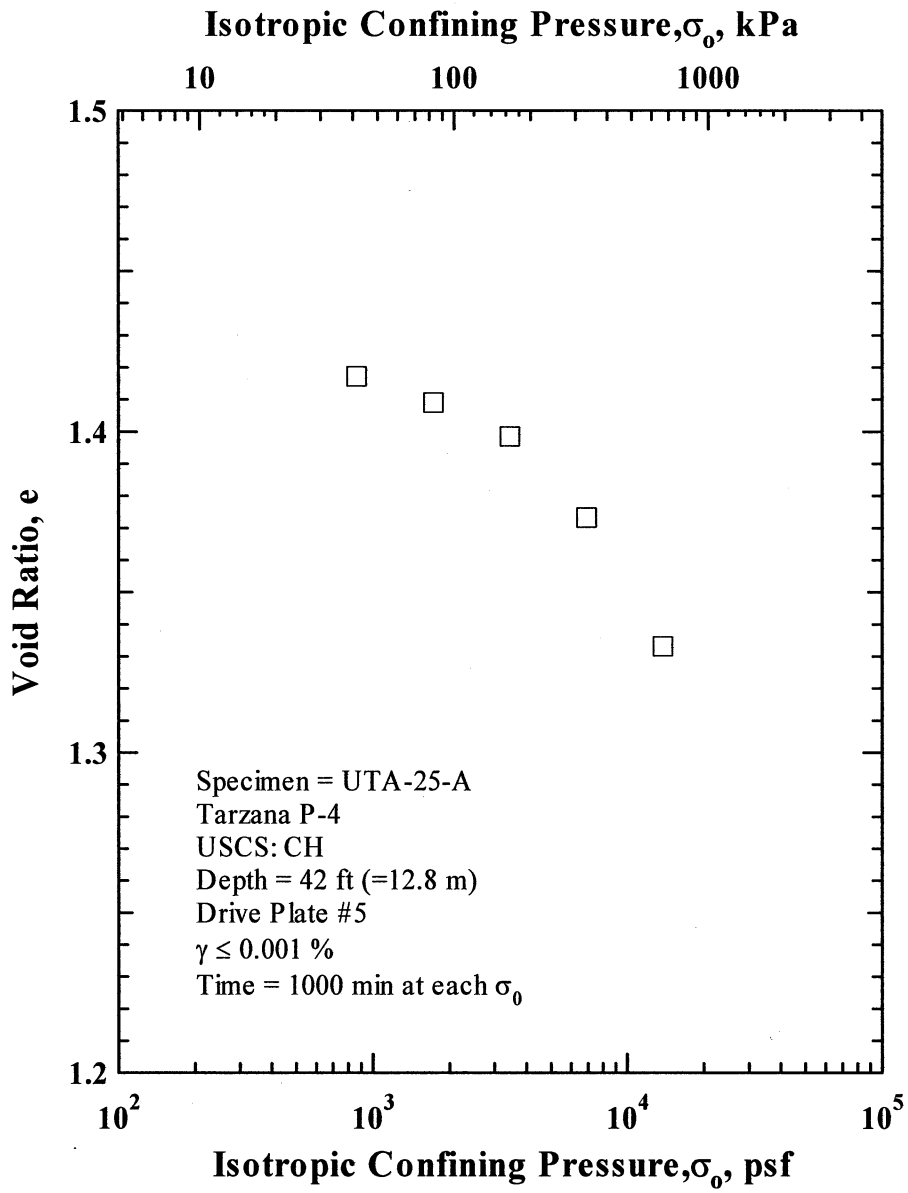

Figure C.7 Variation in Estimated Void Ratio with Isotropic Confining Pressure from Resonant Column Tests of Specimen UTA-25-A.

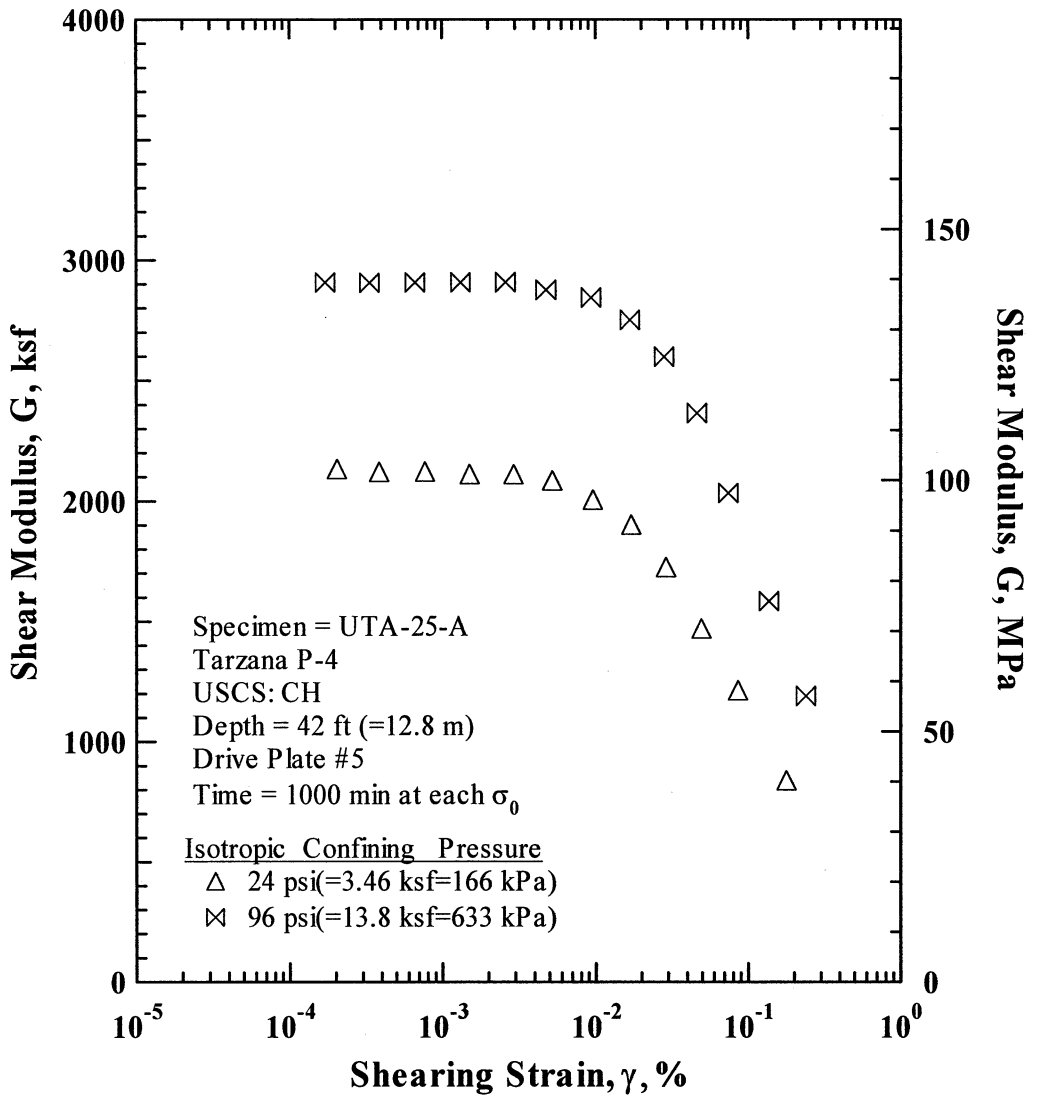

Figure C.8 Comparison of the Variation in Shear Modulus with Shearing Strain and Isotropic Confining Pressure from the Resonant Column Tests of Specimen UTA-25-A.

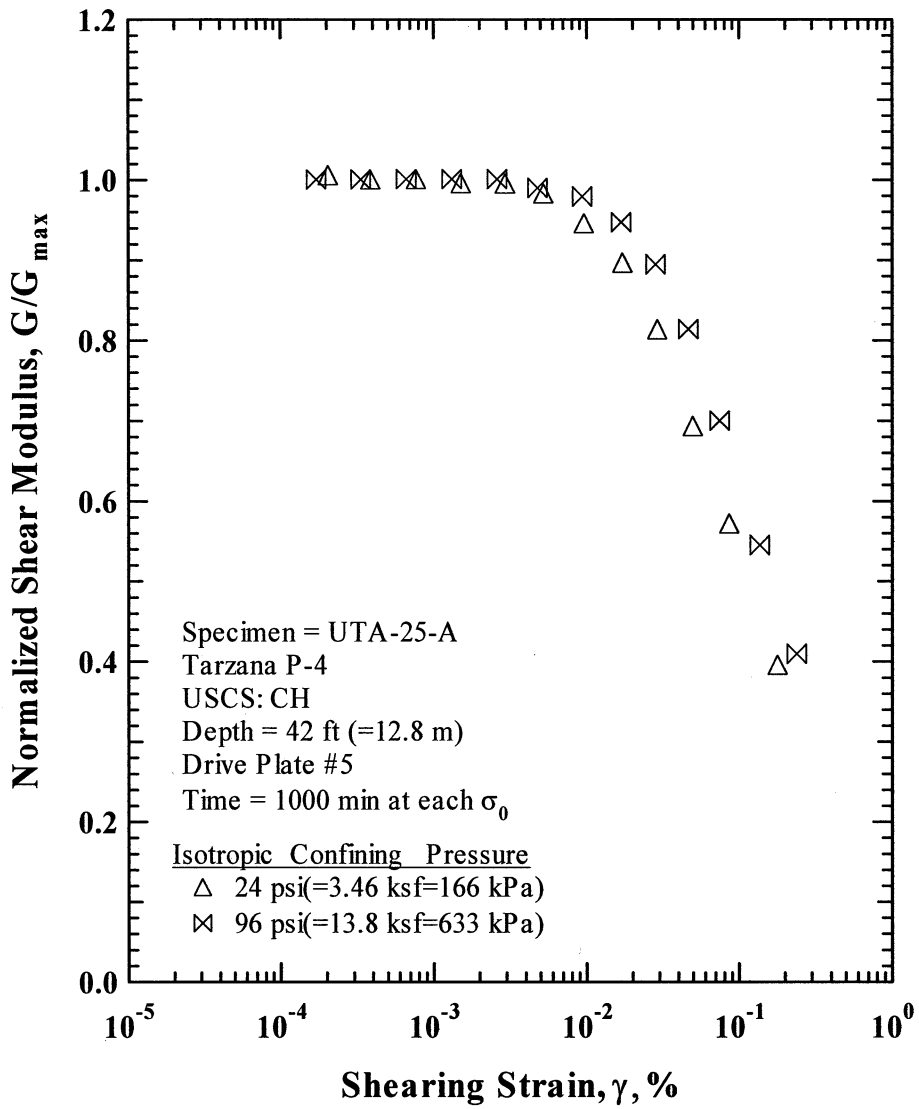

Figure C.9 Comparison of the Variation in Normalized Shear Modulus with Shearing Strain and Isotropic Confining Pressure from the Resonant Column Tests of Specimen UTA-25-A.

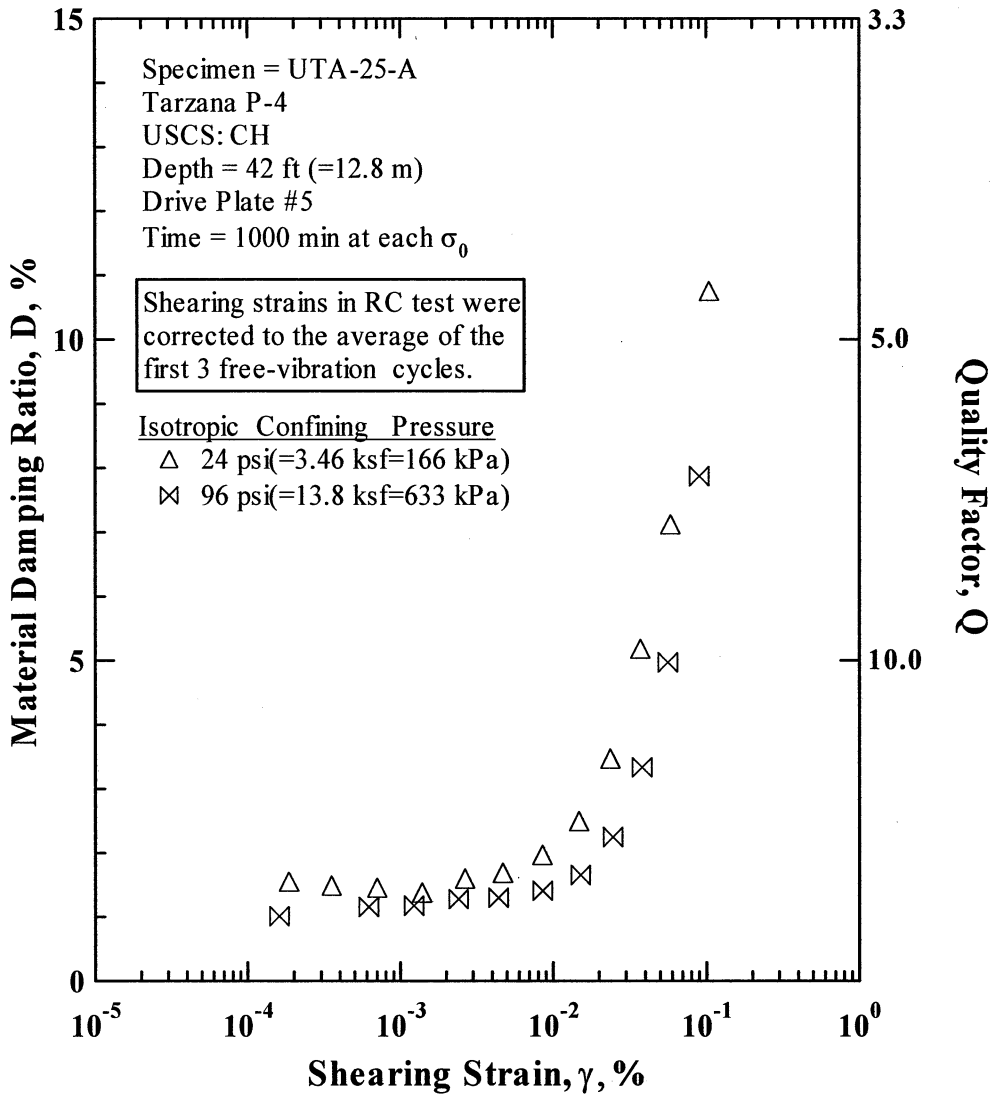

Figure C.10 Comparison of the Variation in Material Damping Ratio with Shearing Strain and Isotropic Confining Pressure from the Resonant Column Tests of Specimen UTA-25-A.

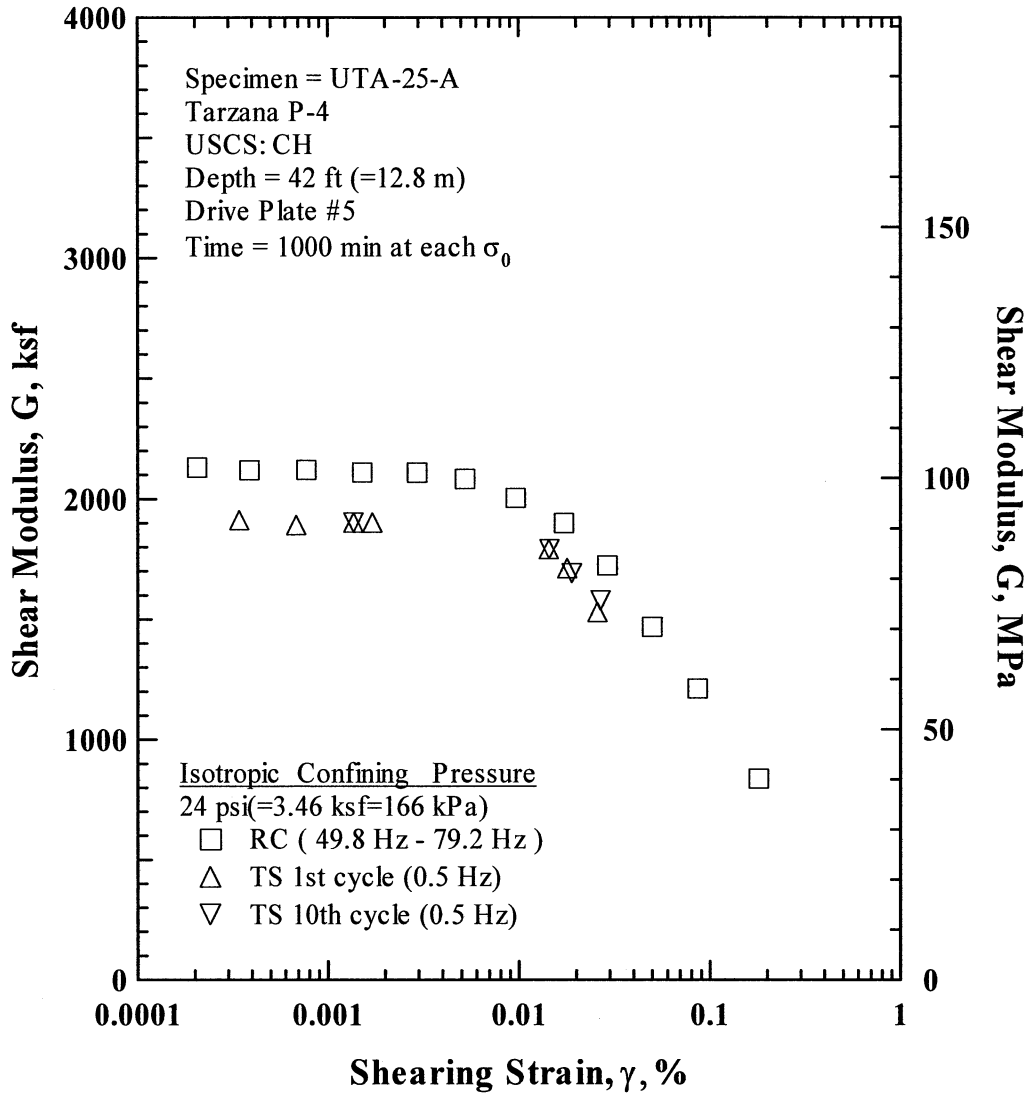

Figure C.11 Comparison of the Variation in Shear Modulus with Shearing Strain at an Isotropic Confining Pressure of 24 psi (=3.46 ksf=166 kPa) from the Combined RCTS Tests of Specimen UTA-25-A.

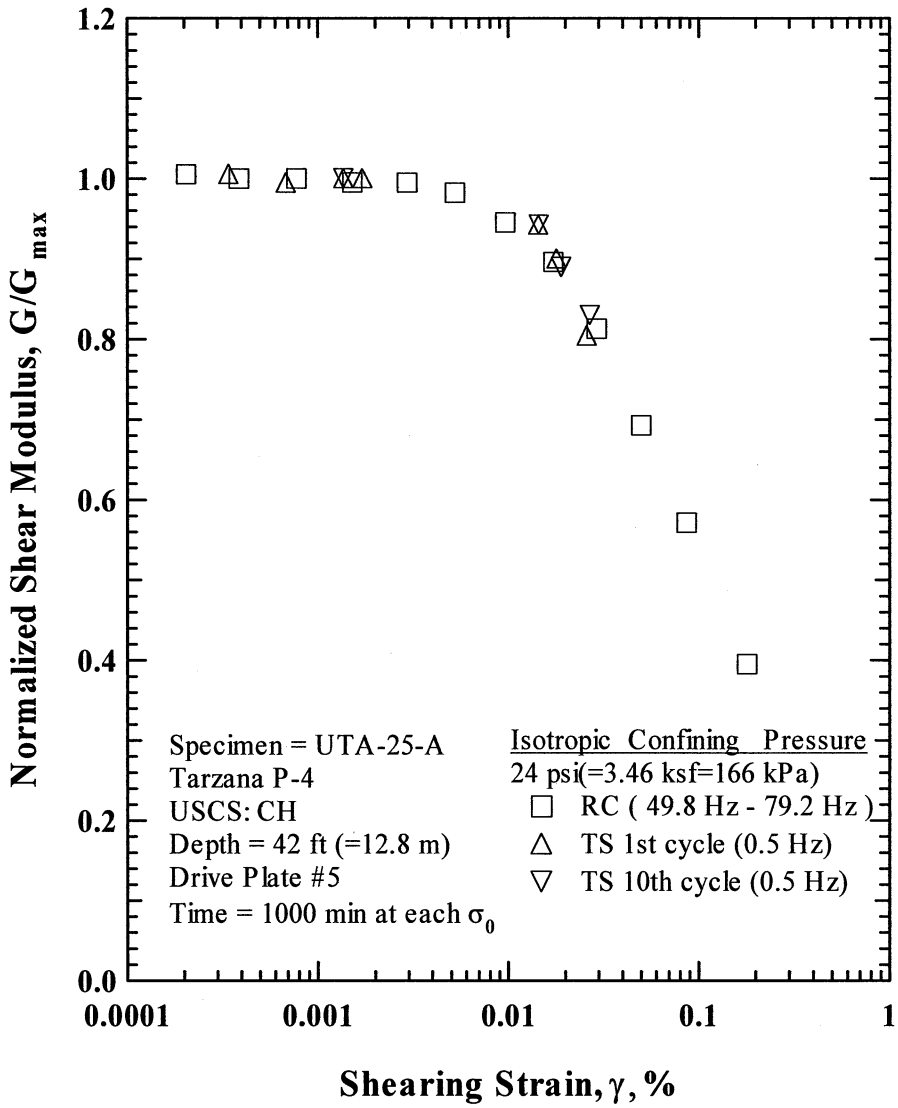

Figure C.12 Comparison of the Variation in Normalized Shear Modulus with Shearing Strain at an Isotropic Confining Pressure of 24 psi (=3.46 ksf=166 kPa) from the Combined RCTS Tests of Specimen UTA-25-A.

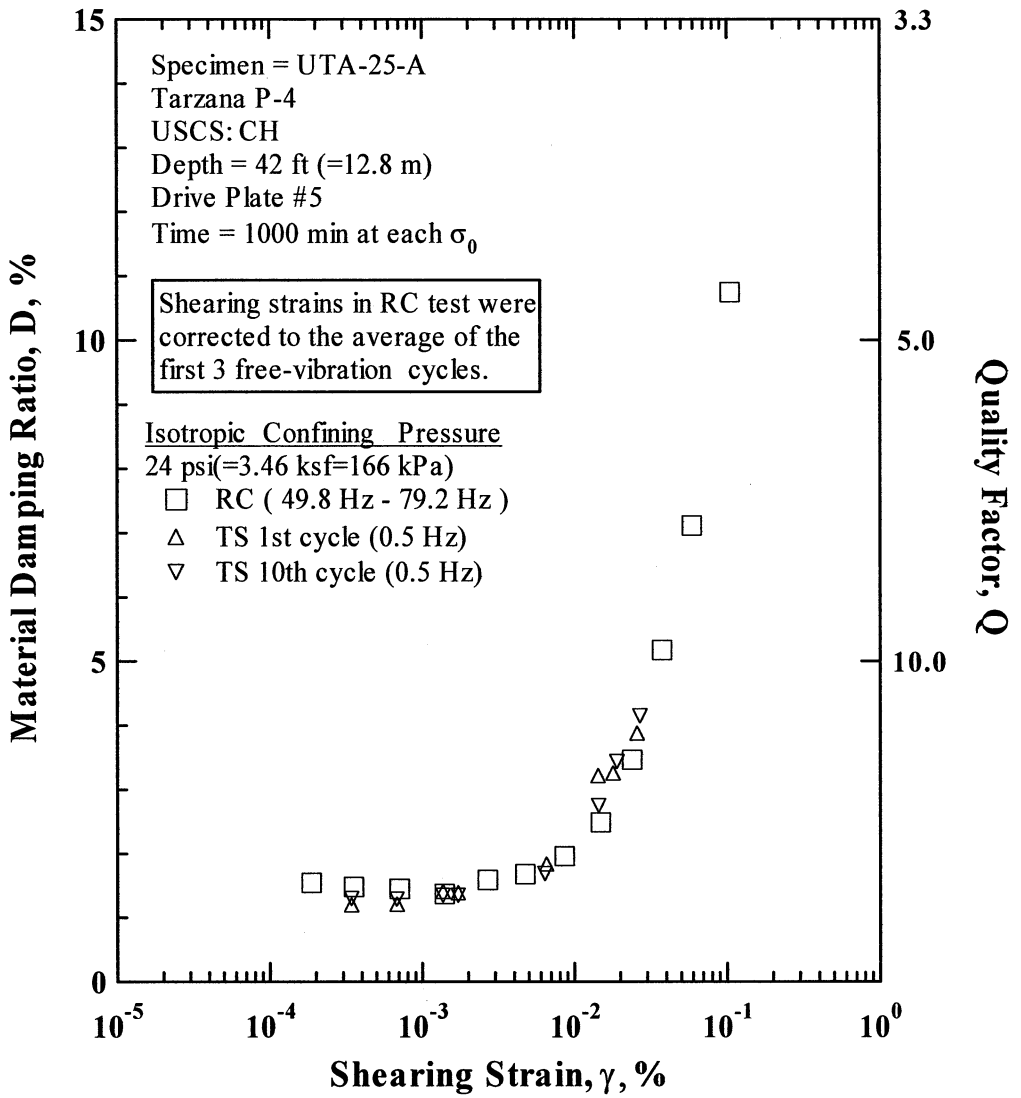

Figure C.13 Comparison of the Variation in Material Damping Ratio with Shearing Strain at an Isotropic Confining Pressure of 24 psi (=3.46 ksf=166 kPa) from the Combined RCTS Tests of Specimen UTA-25-A.

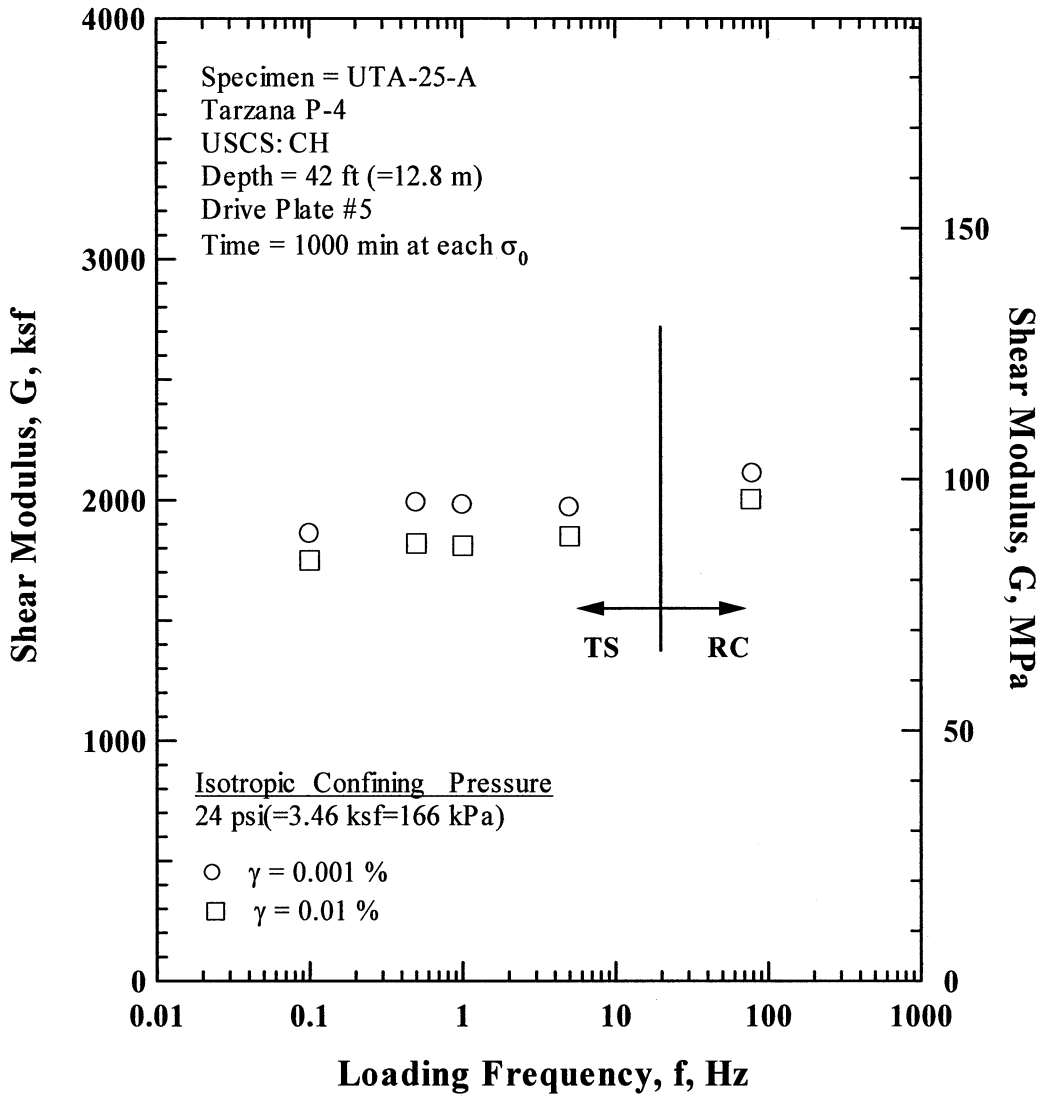

Figure C.14 Comparison of the Variation in Shear Modulus with Loading Frequency at an Isotropic Confining Pressure of 24 psi (=3.46 ksf=166 kPa) from the Combined RCTS Tests of Specimen UTA-25-A.

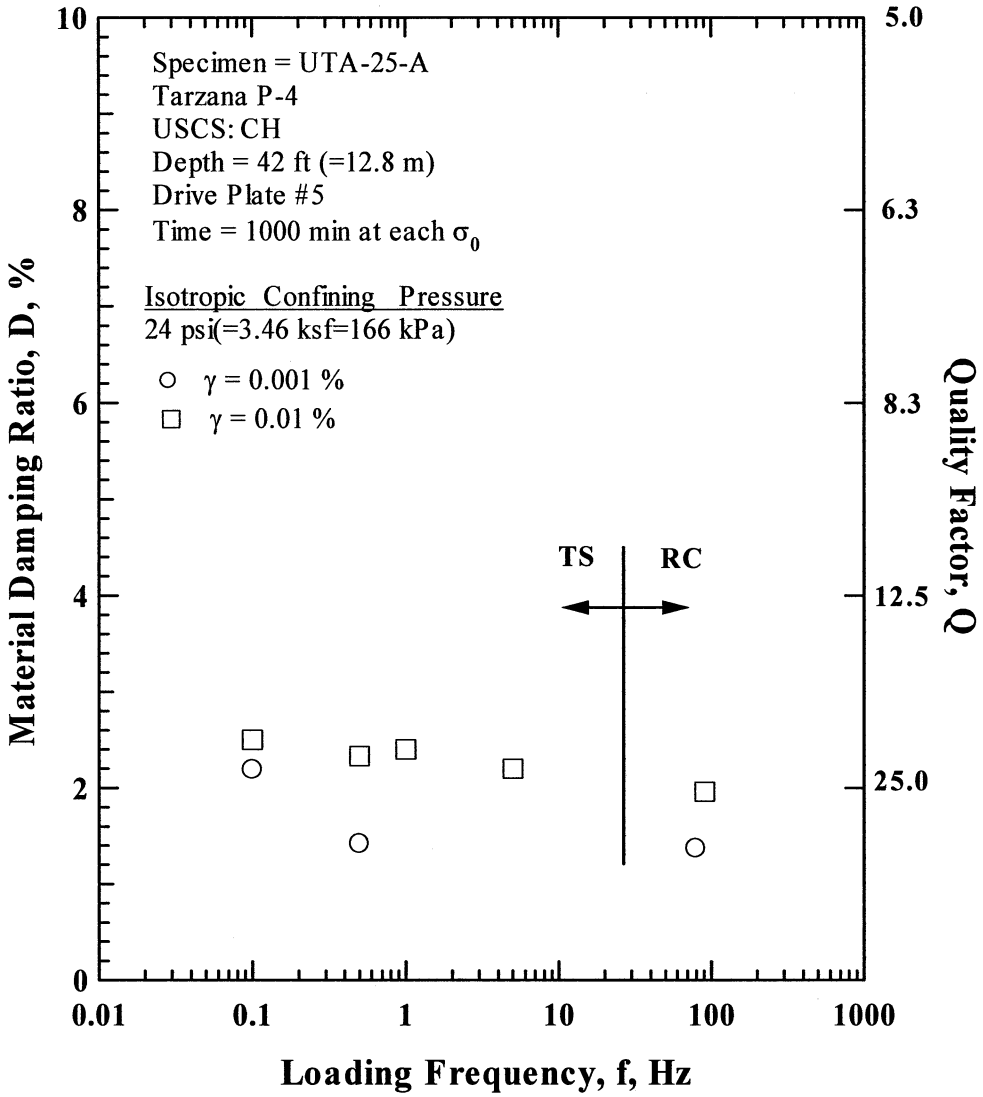

Figure C.15 Comparison of the Variation in Material Damping Ratio with Loading Frequency at an Isotropic Confining Pressure 24 psi (=3.46 ksf=166 kPa) from the Combined RCTS Tests of Specimen UTA-25-A.

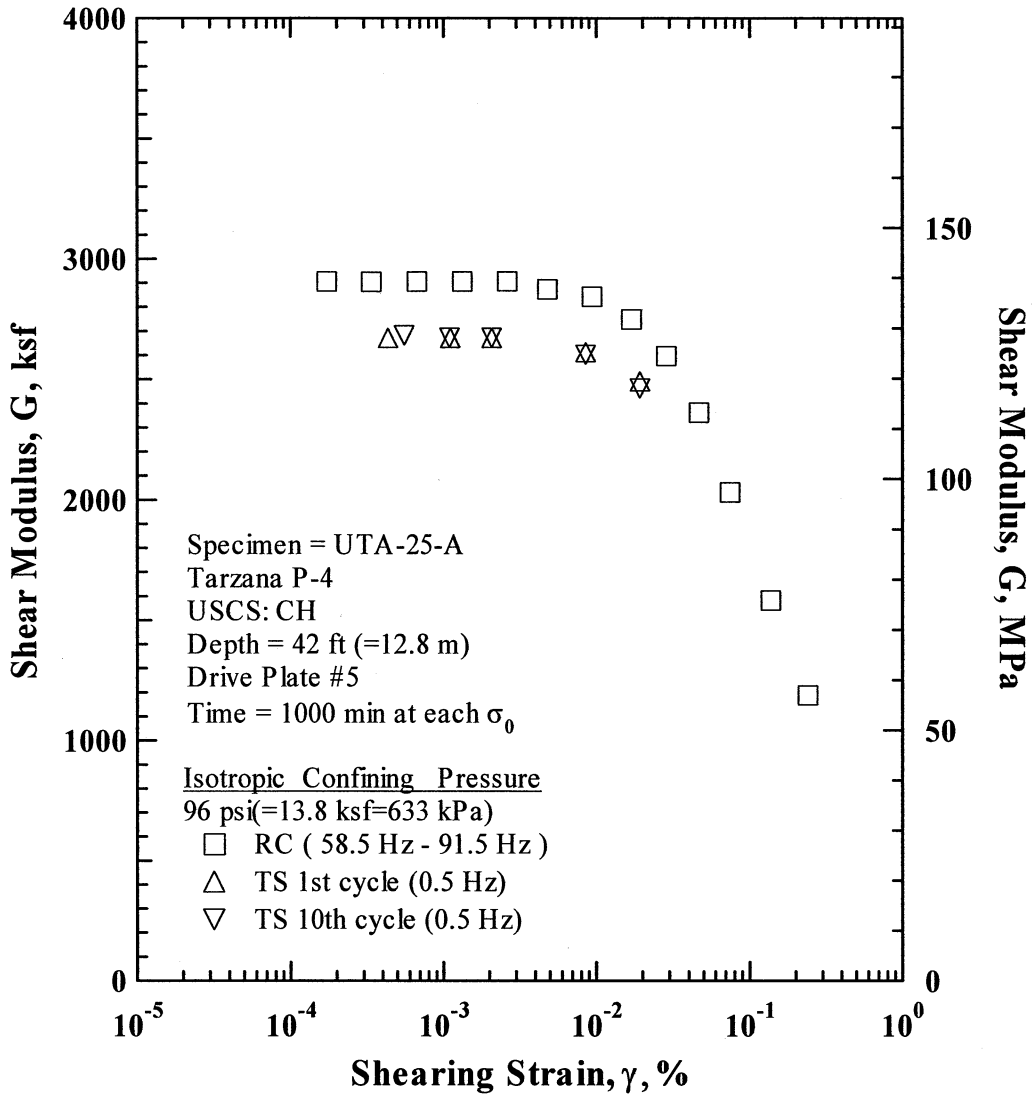

Figure C.16 Comparison of the Variation in Shear Modulus with Shearing Strain at an Isotropic Confining Pressure of 96 psi (=13.8 ksf=663 kPa) from the Combined RCTS Tests of Specimen UTA-25-A.

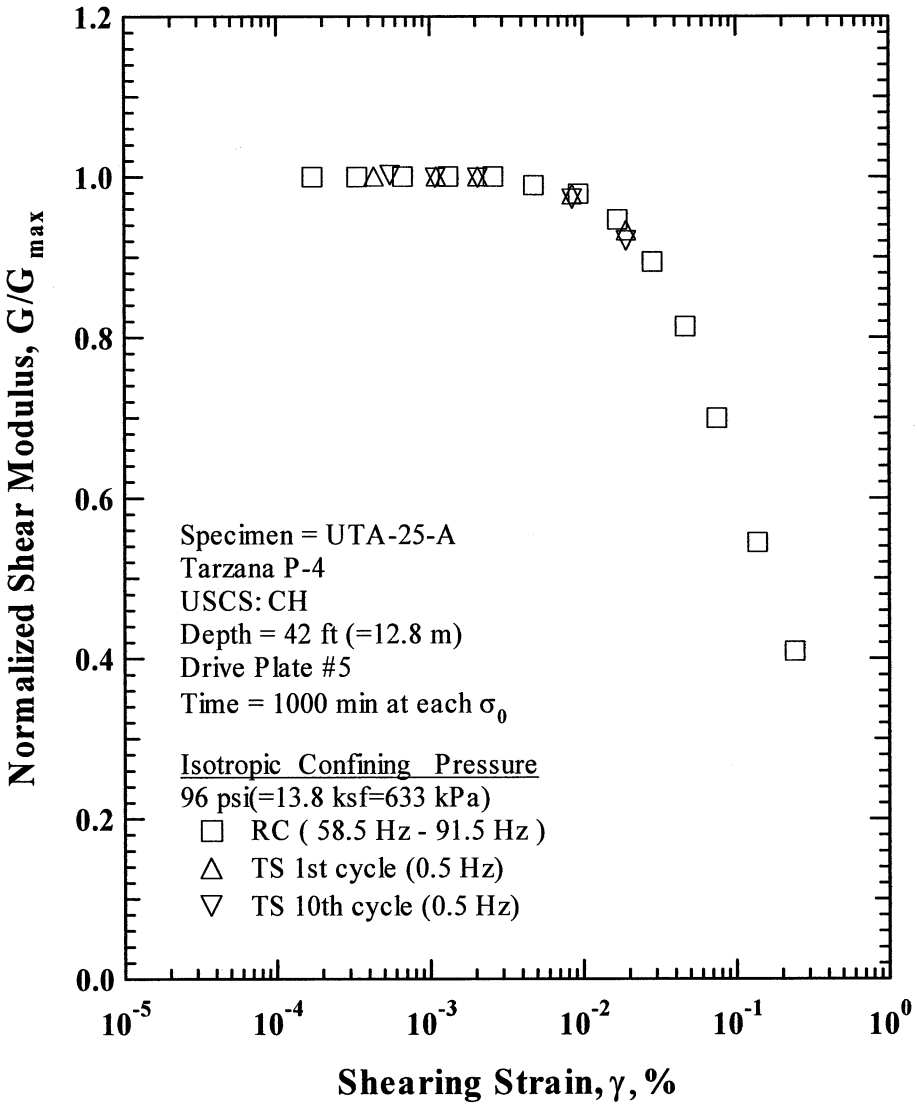

Figure C.17 Comparison of the Variation in Normalized Shear Modulus with Shearing Strain at an Isotropic Confining Pressure of 96 psi (=13.8 ksf=663 kPa) from the Combined RCTS Tests of Specimen UTA-25-A.

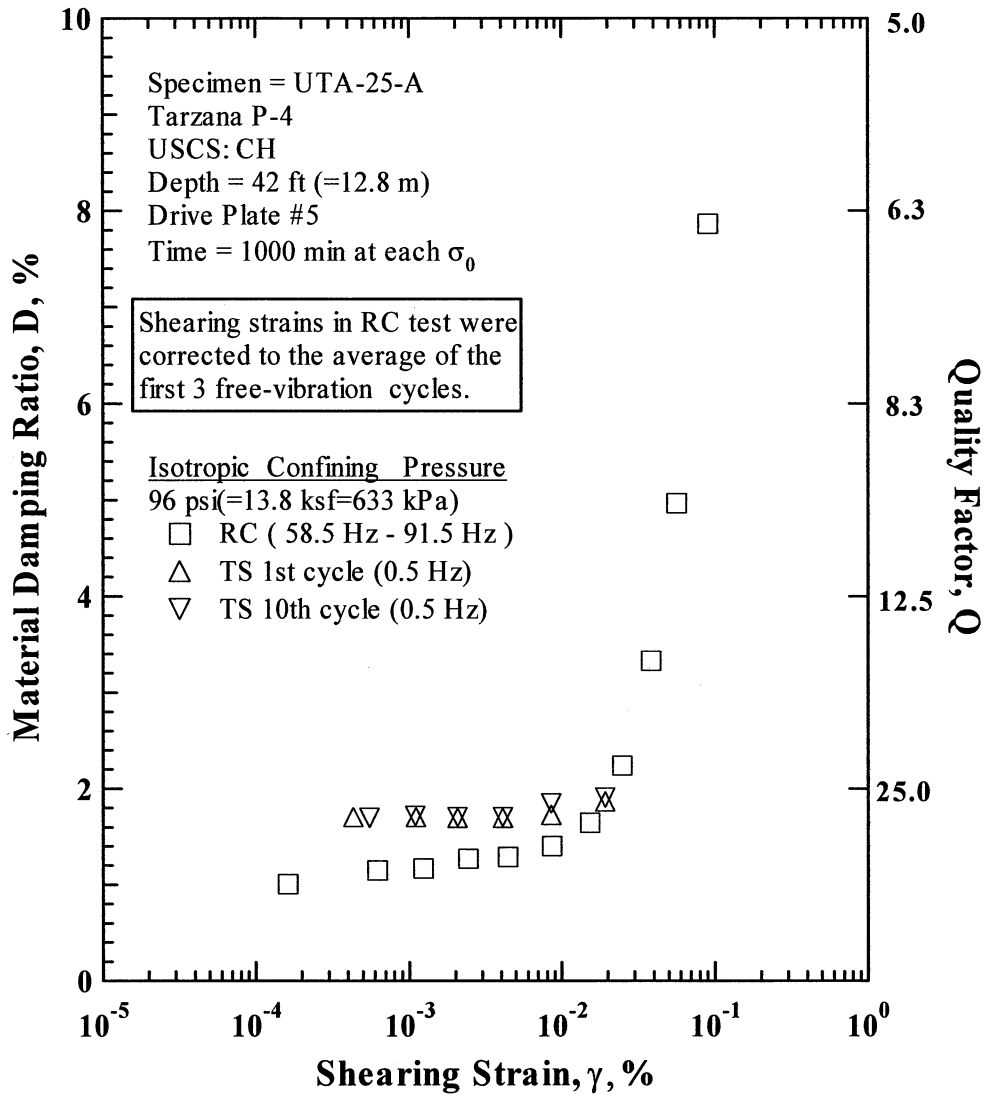

Figure C.18 Comparison of the Variation in Material Damping Ratio with Shearing Strain at an Isotropic Confining Pressure of 96 psi (=13.8 ksf=663 kPa) from the Combined RCTS Tests of Specimen UTA-25-A.

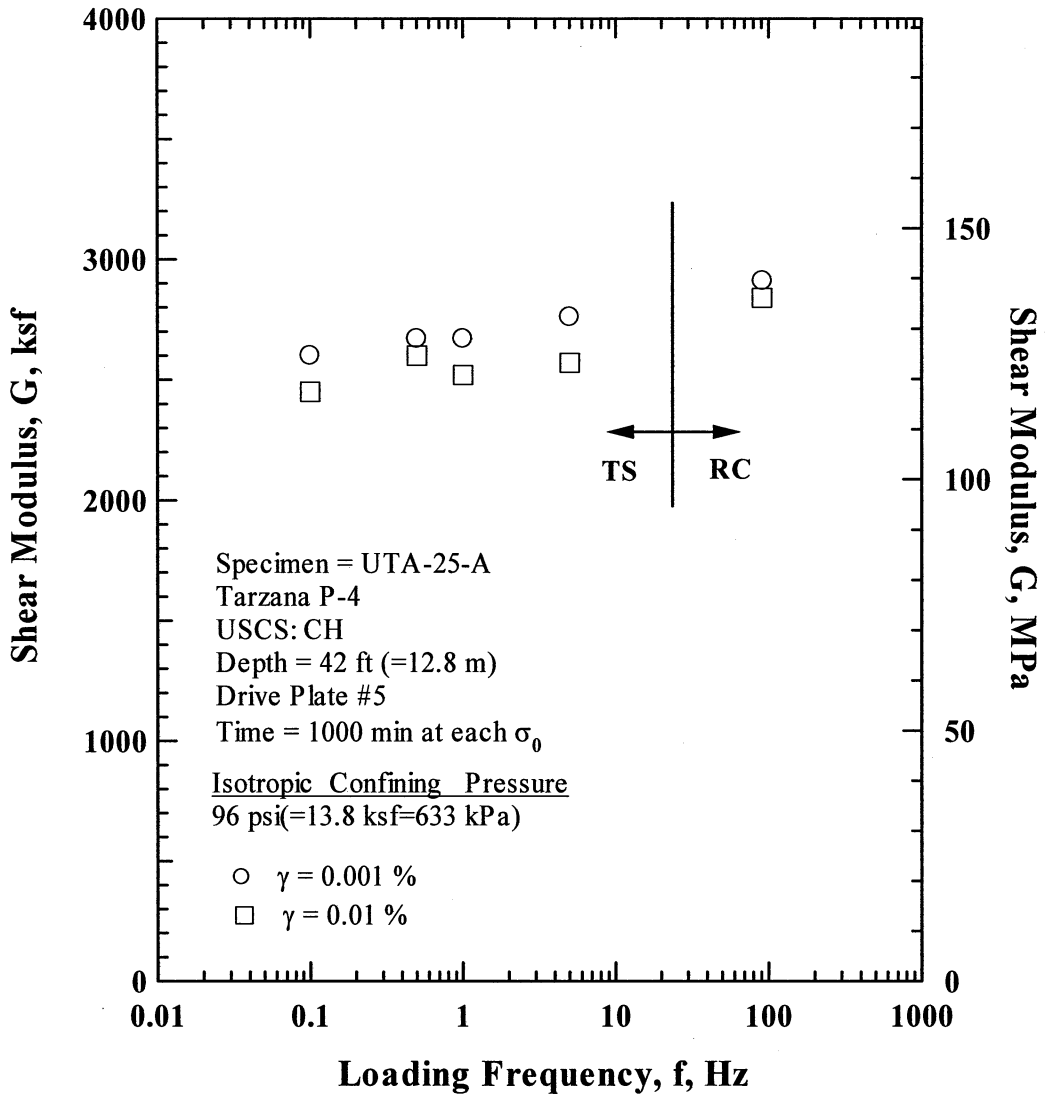

Figure C.19 Comparison of the Variation in Shear Modulus with Loading Frequency at an Isotropic Confining Pressure of 96 psi (=13.8 ksf=663 kPa) from the Combined RCTS Tests of Specimen UTA-25-A.

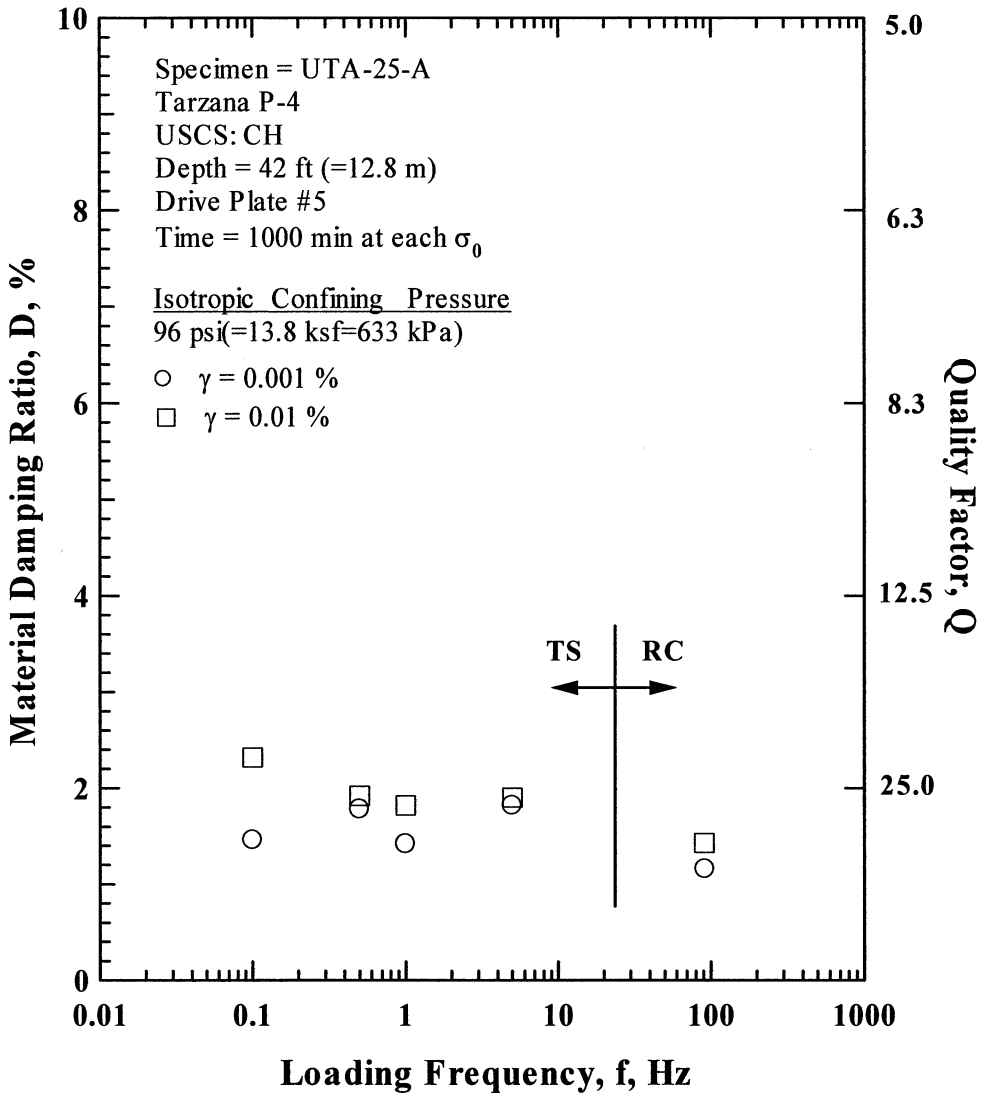

Figure C.20 Comparison of the Variation in Material Damping Ratio with Loading Frequency at an Isotropic Confining Pressure 96 psi (=13.8 ksf=663 kPa) from the Combined RCTS Tests of Specimen UTA-25-A.

Table C.1 Variation in Low-Amplitude Shear Wave Velocity, Low-Amplitude Shear Modulus, Low-Amplitude Material Damping Ratio and Estimated Void Ratio with Isotropic Confining Pressure from RC Tests of Specimen UTA-25-A.

Isotropic Confining Pressure, σ_o			Low-Amplitude Shear Modulus, G_{max}		Low-Amplitude Shear Wave Velocity, Vs	Low-Amplitude Material Damping Ratio,	Estimated Void Ratio, e
(psi)	(psf)	(kPa)	(ksf)	(MPa)	(fps)	D_{min}, %	
6	864	41.4	1629	78.1	710	1.86	1.417
12	1728	82.8	1827	87.6	752	1.69	1.409
24	3456	165.7	1987	95.3	783	1.57	1.399
48	6912	331.4	2340	112.2	848	1.39	1.373
96	13824	662.7	2755	132.1	917	1.33	1.333

Table C.2 Variation in Shear Modulus, Normalized Shear Modulus and Material Damping Ratio with Shearing Strain from RC Tests of Specimen UTA-25-A; Confining Pressure, σ_o = 24 psi (=3.46 ksf=166 kPa).

Peak Shearing Strain, %	Shear Modulus, G, ksf	Normalized Shear Modulus, G/G_{max}	Average[+] Shearing Strain, %	Material Damping Ratio[x], D, %
3.88E-04	2120	1.00	3.54E-04	1.48
2.05E-04	2131	1.01	1.87E-04	1.54
7.72E-04	2121	1.00	7.07E-04	1.45
1.52E-03	2110	1.00	1.39E-03	1.37
2.94E-03	2110	1.00	2.67E-03	1.59
5.24E-03	2083	0.98	4.73E-03	1.68
9.63E-03	2004	0.95	8.56E-03	1.96
1.72E-02	1900	0.90	1.48E-02	2.49
2.91E-02	1724	0.81	2.38E-02	3.46
5.00E-02	1469	0.69	3.74E-02	5.18
8.64E-02	1212	0.57	5.89E-02	7.11
1.80E-01	838	0.40	1.05E-01	10.75

[+] Average Shearing Strain from the First Three Cycles of the Free Vibration Decay Curve

[x] Average Damping Ratio from the First Three Cycles of the Free Vibration Decay Curve

Table C.3 Variation in Shear Modulus, Normalized Shear Modulus and Material Damping Ratio with Shearing Strain from TS Tests of Specimen UTA-25-A; Confining Pressure, σ_o = 24 psi (=3.46 ksf=166 kPa).

First Cycle				Tenth Cycle			
Peak Shearing Strain, %	Shear Modulus, G, ksf	Normalized Shear Modulus, G/G_{max}	Material Damping Ratio, D, %	Peak Shearing Strain, %	Shear Modulus, G, ksf	Normalized Shear Modulus, G/G_{max}	Material Damping Ratio, D, %
3.44E-04	1910	1.01	1.19	3.44E-04			1.29
6.86E-04	1890	0.99	1.20	6.84E-04			1.28
1.37E-03	1900	1.00	1.40	1.37E-03	1900	1.00	1.34
1.72E-03	1900	1.00	1.38	1.72E-03			1.34
6.57E-03			1.83	6.39E-03			1.68
1.44E-02	1790	0.94	3.21	1.45E-02	1790	0.94	2.74
1.80E-02	1710	0.90	3.25	1.91E-02	1690	0.89	3.43
2.59E-02	1528	0.80	3.87	2.70E-02	1576	0.83	4.14

Table C.4 Variation in Shear Modulus, Normalized Shear Modulus and Material Damping Ratio with Shearing Strain from RC Tests of Specimen UTA-25-A; Confining Pressure, σ_o = 96 psi (=13.8 ksf=633 kPa).

Peak Shearing Strain, %	Shear Modulus, G, ksf	Normalized Shear Modulus, G/G_{max}	Average[+] Shearing Strain, %	Material Damping Ratio[x], D, %
3.36E-04	2905	1.00		
1.72E-04	2905	1.00	1.62E-04	1.00
6.67E-04	2906	1.00	6.21E-04	1.15
1.33E-03	2906	1.00	1.24E-03	1.17
2.62E-03	2906	1.00	2.42E-03	1.27
4.80E-03	2874	0.99	4.44E-03	1.29
9.37E-03	2843	0.98	8.61E-03	1.40
1.69E-02	2749	0.95	1.53E-02	1.64
2.84E-02	2597	0.89	2.49E-02	2.24
4.66E-02	2363	0.81	3.84E-02	3.33
7.47E-02	2032	0.70	5.64E-02	4.97
1.38E-01	1582	0.54	9.06E-02	7.86
2.41E-01	1189	0.41		

[+] Average Shearing Strain from the First Three Cycles of the Free Vibration Decay Curve

[x] Average Damping Ratio from the First Three Cycles of the Free Vibration Decay Curve

Table C.5 Variation in Shear Modulus, Normalized Shear Modulus and Material Damping Ratio with Shearing Strain from TS Tests of Specimen UTA-25-A; Confining Pressure, σ_o = 96 psi (=13.8 ksf=633 kPa).

First Cycle				Tenth Cycle			
Peak Shearing Strain, %	Shear Modulus, G, ksf	Normalized Shear Modulus, G/G_{max}	Material Damping Ratio, D, %	Peak Shearing Strain, %	Shear Modulus, G, ksf	Normalized Shear Modulus, G/G_{max}	Material Damping Ratio, D, %
2.18E-04	2670	1.00	1.70	5.56E-04	2680	1.00	1.69
1.11E-03	2670	1.00	1.70	1.10E-03	2670	1.00	1.71
2.08E-03	2670	1.00	1.69	2.08E-03	2670	1.00	1.70
4.12E-03			1.69	4.12E-03			1.70
8.56E-03	2610	0.98	1.72	8.58E-03	2600	0.97	1.84
1.93E-02	2490	0.93	1.86	1.93E-02	2460	0.92	1.90

APPENDIX D

Specimen No. 3
UT Specimen ID: UTA-27-F

Meloland S-2
Depth= 20 ft (6.1 m)
Soil Type: Clay (CL)

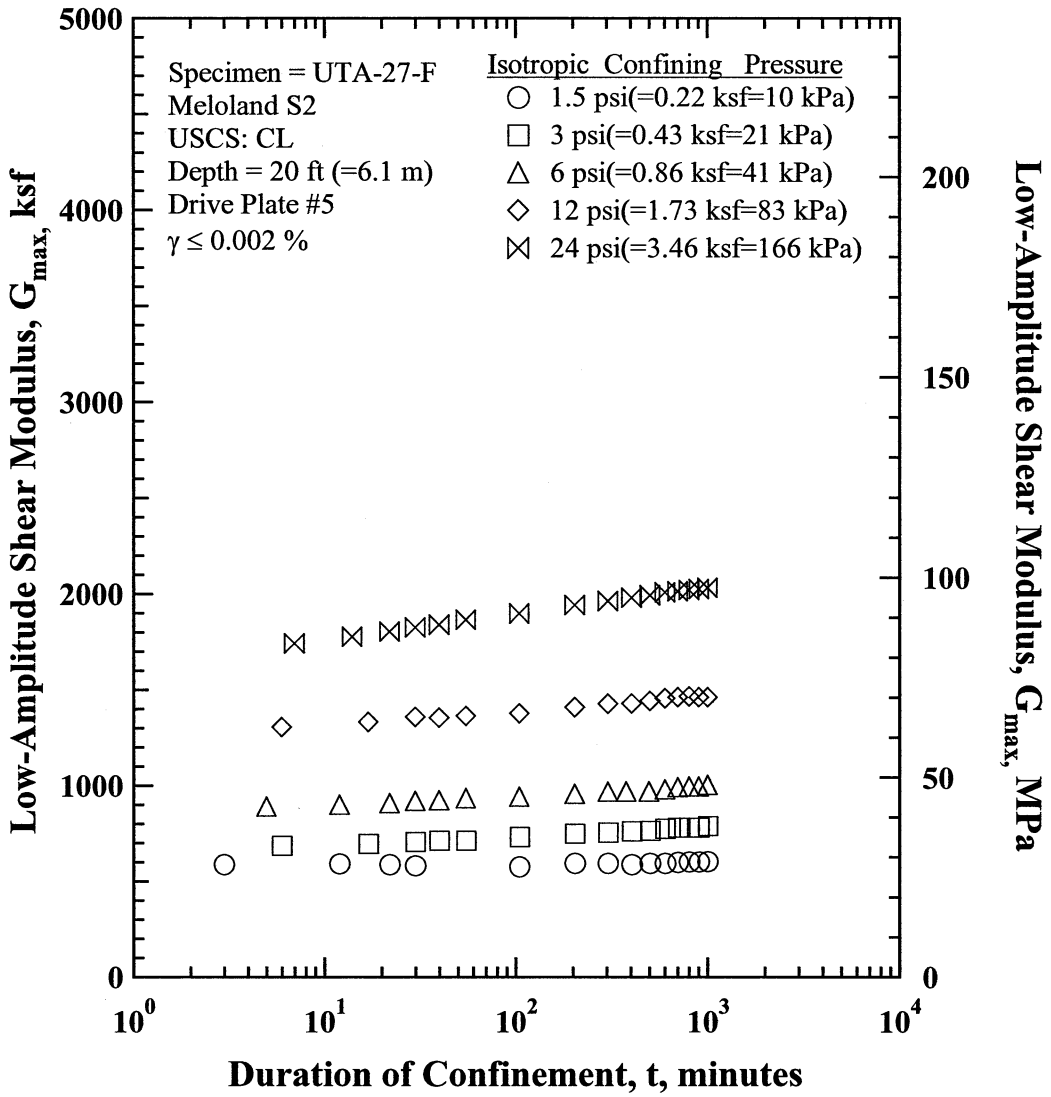

Figure D.1 Variation in Low-Amplitude Shear Modulus with Magnitude and Duration of Isotropic Confining Pressure from Resonant Column Tests of Specimen UTA-27-F.

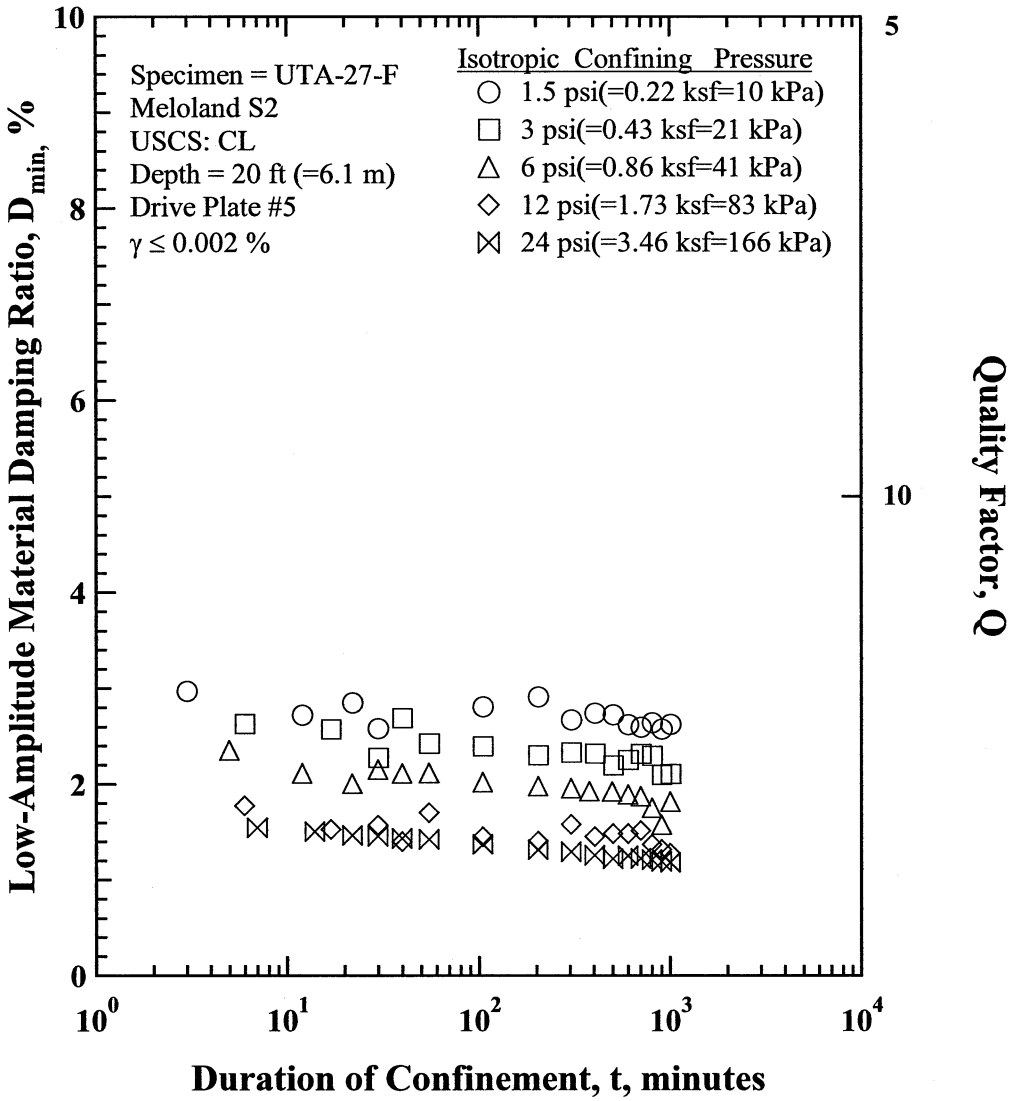

Figure D.2 Variation in Low-Amplitude Material Damping Ratio and Duration of Isotropic Confining Pressure from Resonant Column Tests of Specimen UTA-27-F

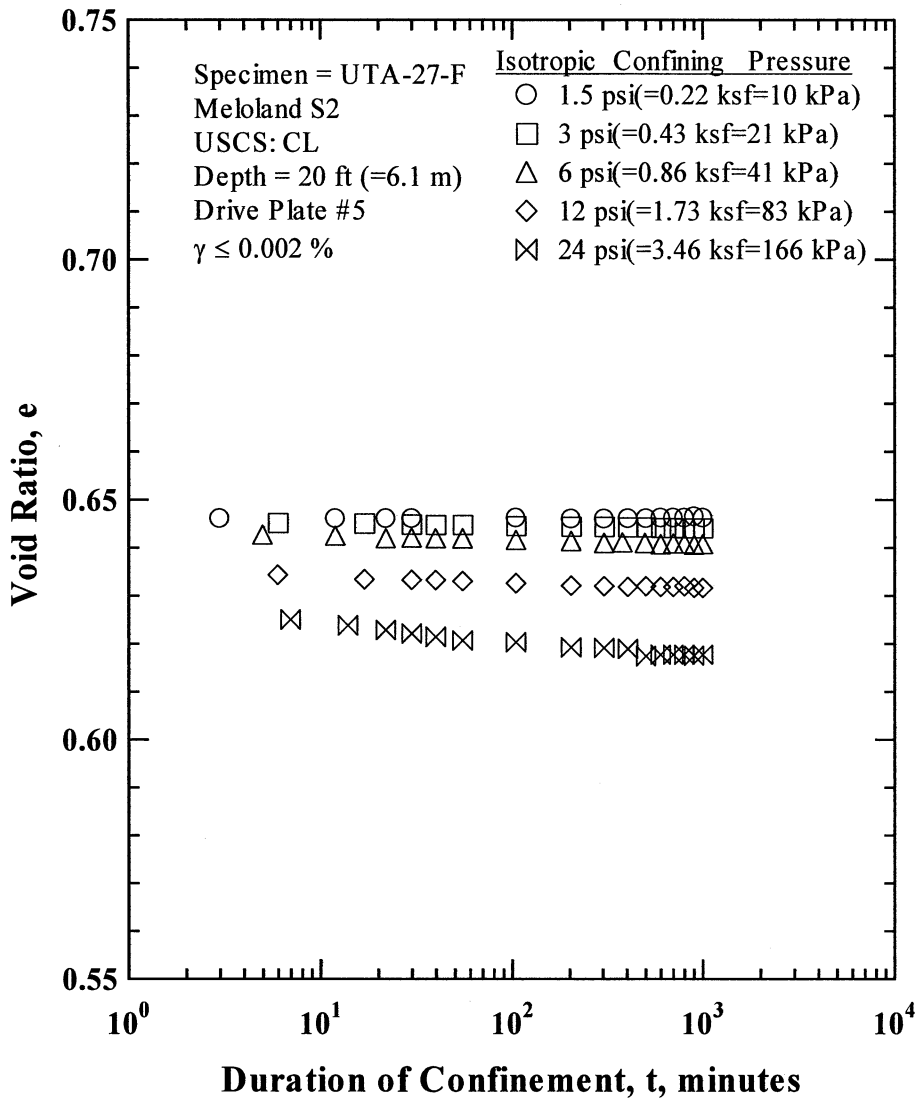

Figure D.3 Variation in Estimated Void Ratio with Magnitude and Duration of Isotropic Confining Pressure from Resonant Column Tests of Specimen UTA-27-F

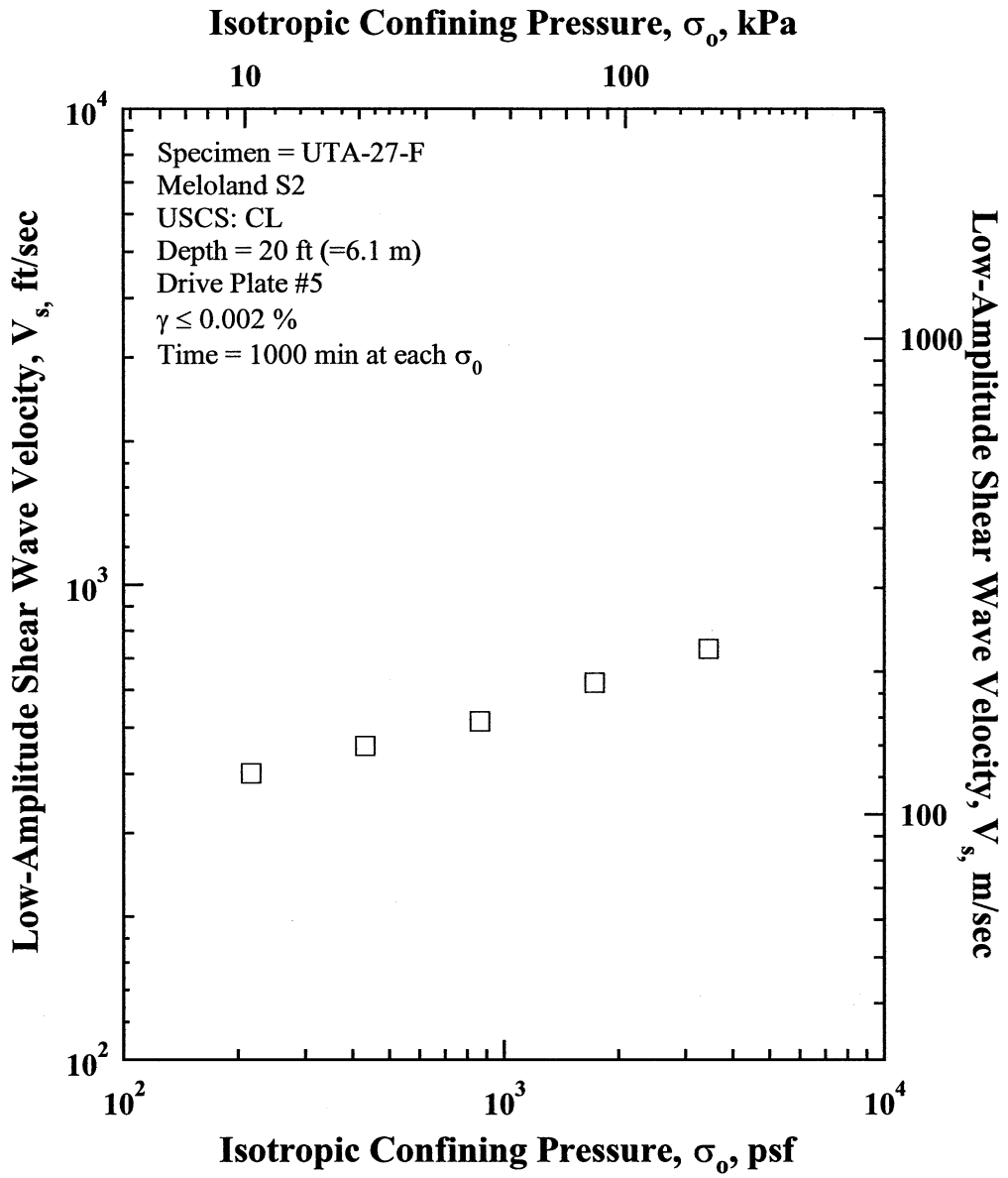

Figure D.4 Variation in Low-Amplitude Shear Wave Velocity with Isotropic Confining Pressure from Resonant Column Tests of Specimen UTA-27-F.

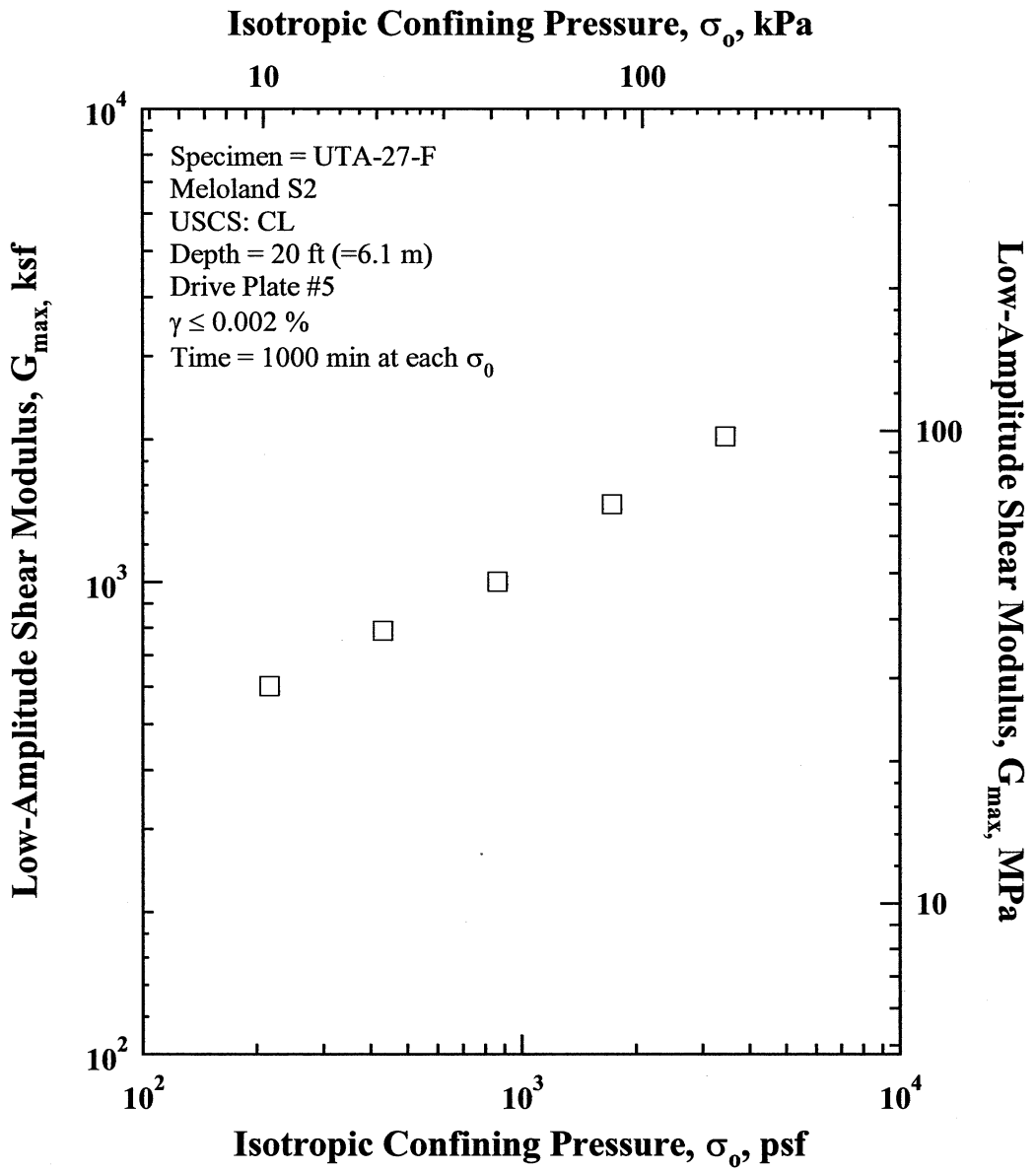

Figure D.5 Variation in Low-Amplitude Shear Modulus with Isotropic Confining Pressure from Resonant Column Tests of Specimen UTA-27-F.

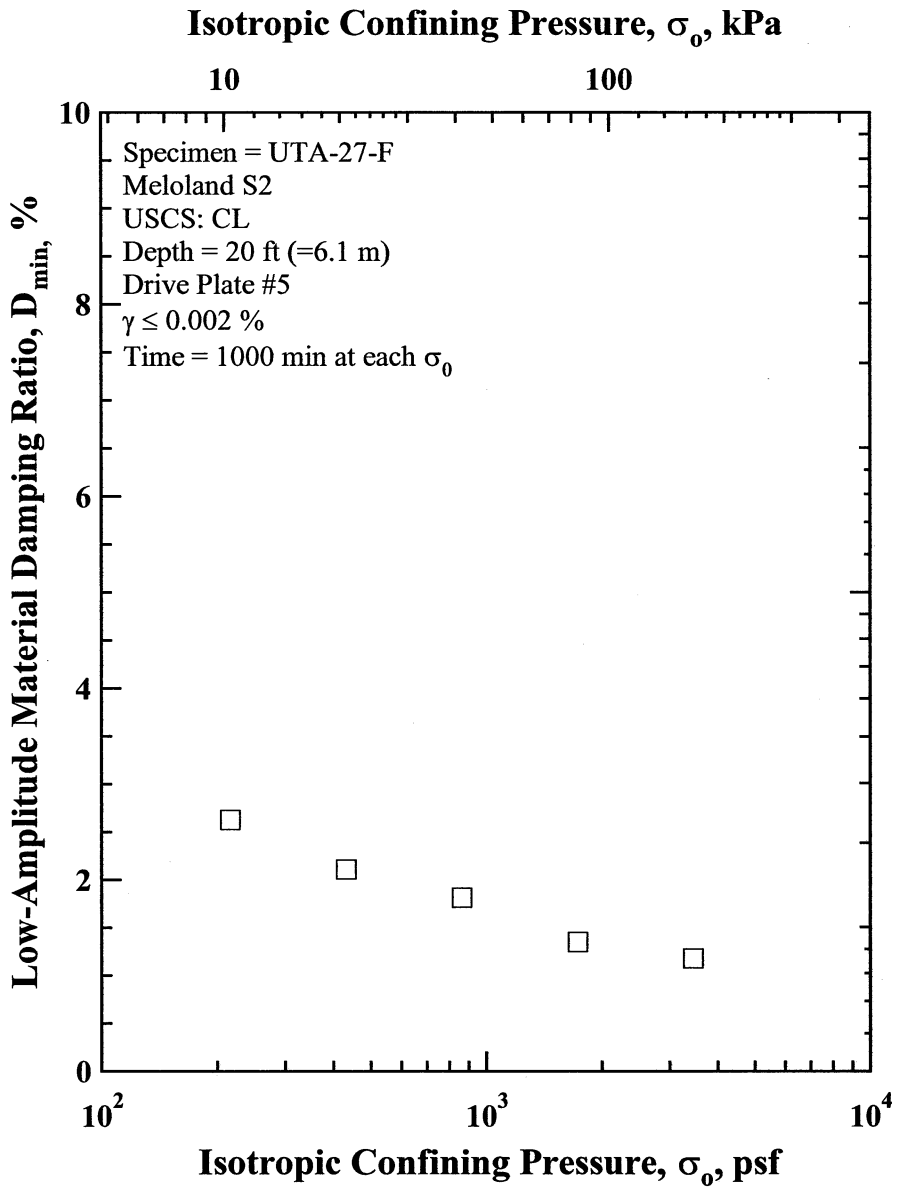

Figure D.6 Variation in Material Damping Ratio with Isotropic Confining Pressure from Resonant Column Tests of Specimen UTA-27-F.

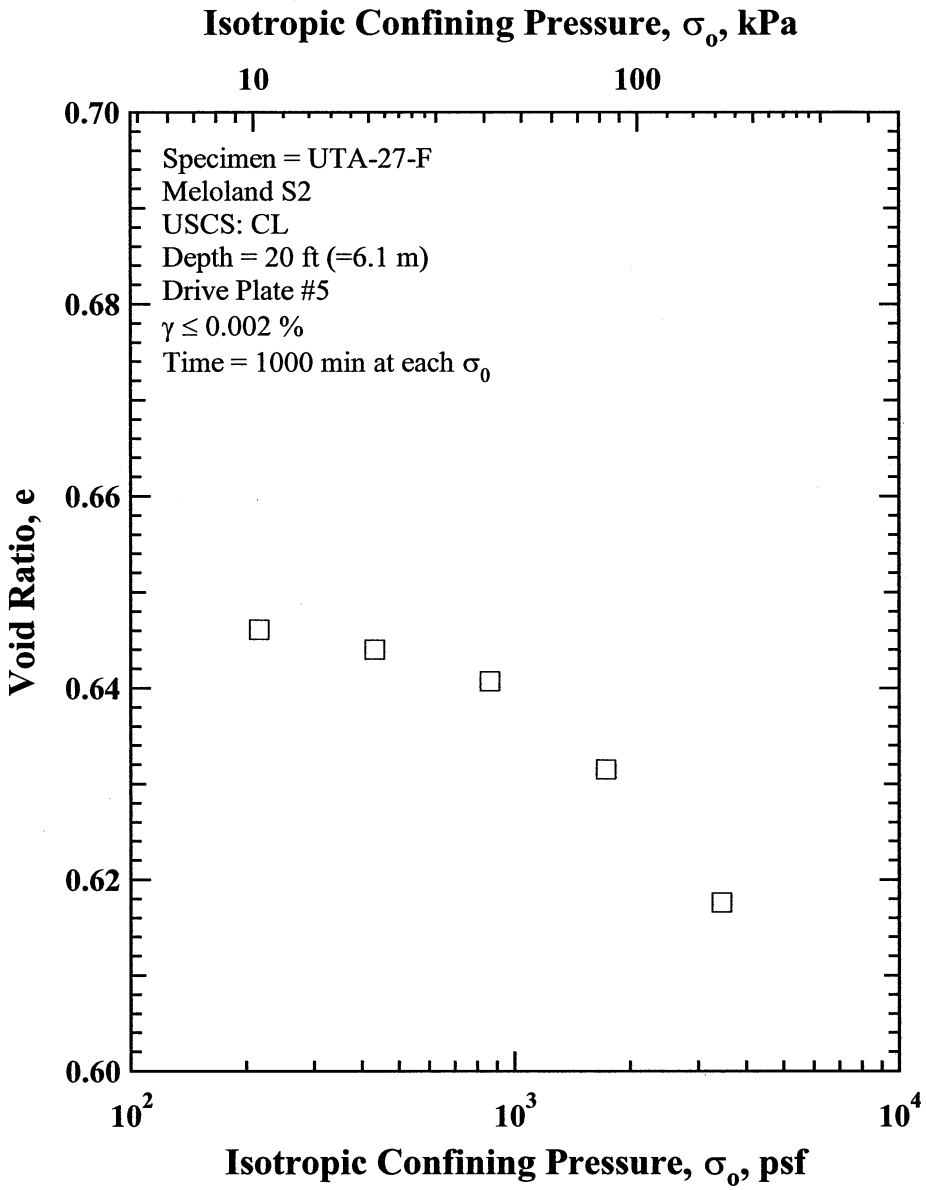

Figure D.7 Variation in Estimated Void Ratio with Isotropic Confining Pressure from Resonant Column Tests of Specimen UTA-27-F.

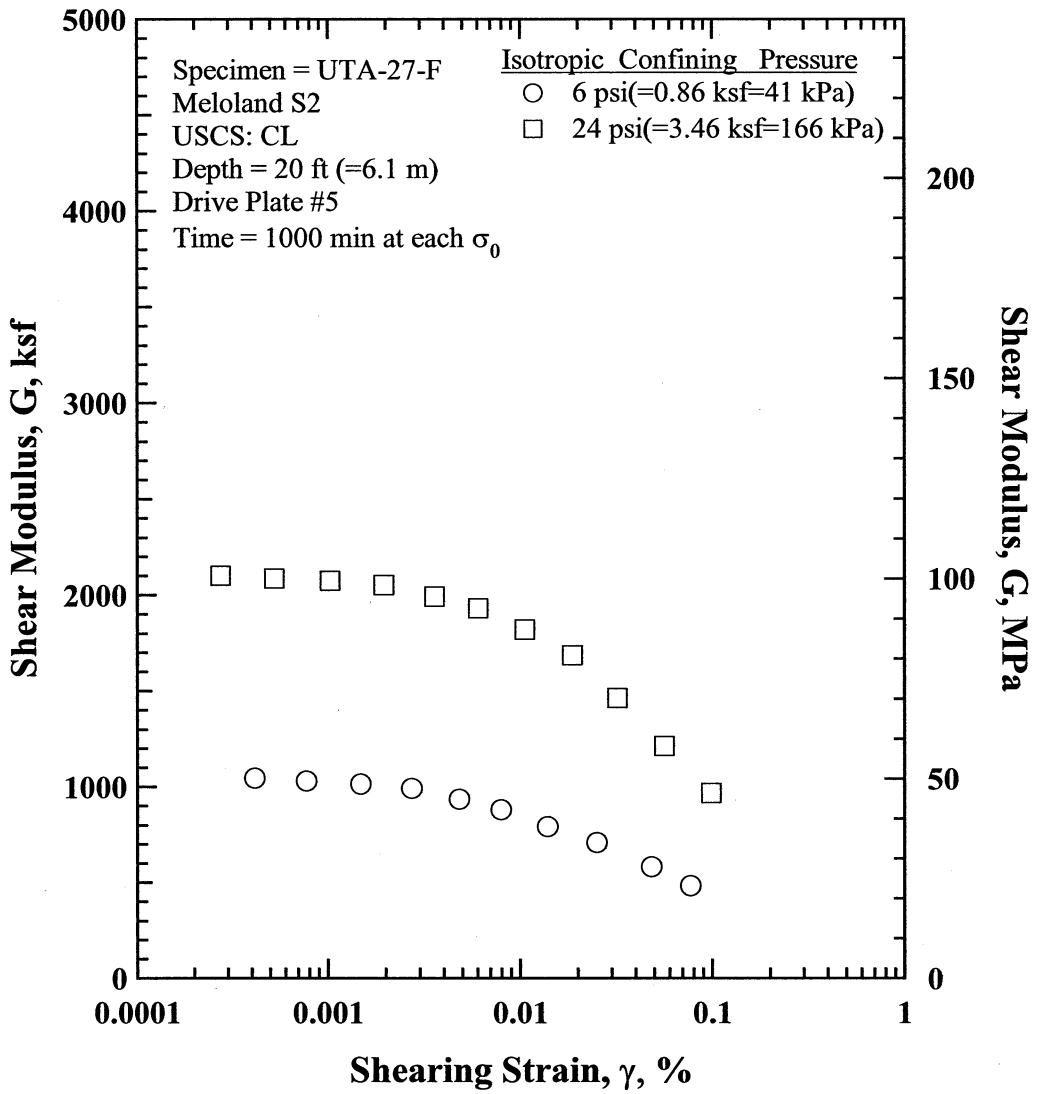

Figure D.8 Comparison of the Variation in Shear Modulus with Shearing Strain and Isotropic Confining Pressure from the Resonant Column Tests of Specimen UTA-27-F.

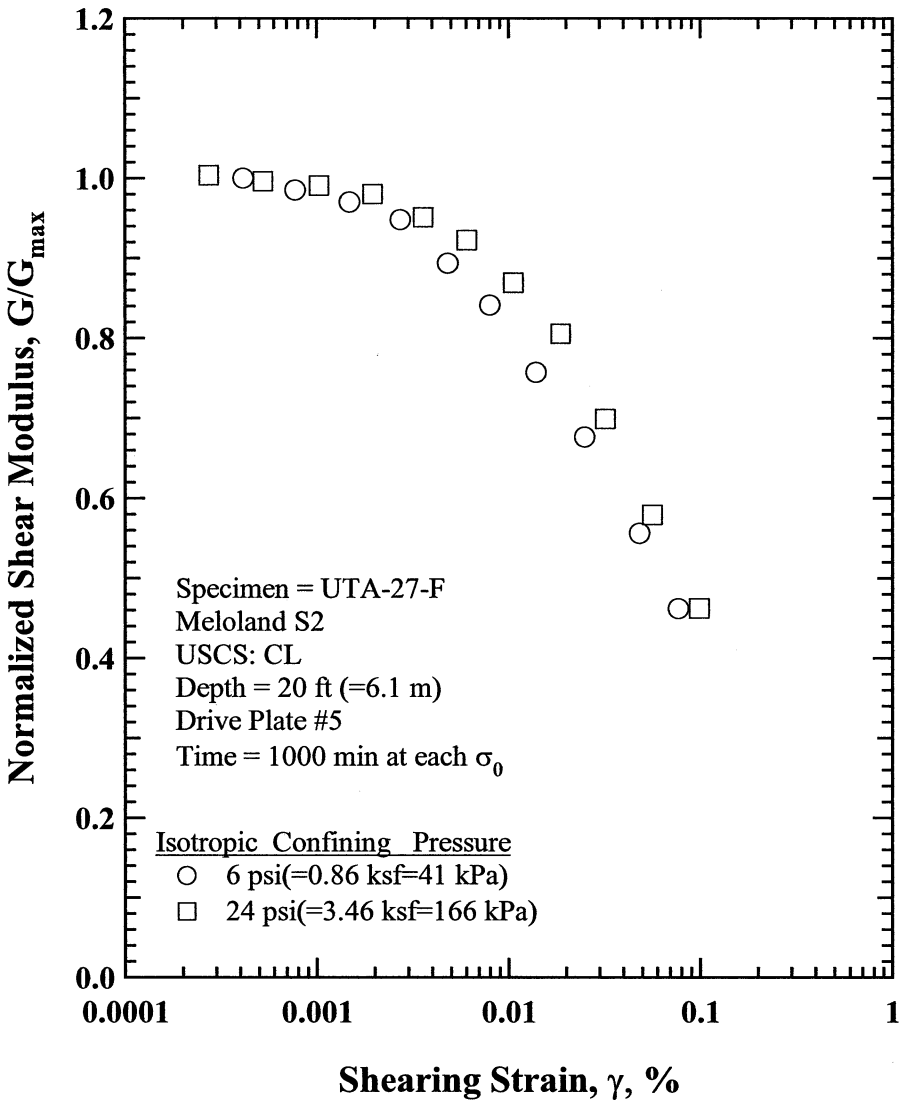

Figure D.9 Comparison of the Variation in Normalized Shear Modulus with Shearing Strain and Isotropic Confining Pressure from the Resonant Column Tests of Specimen UTA-27-F.

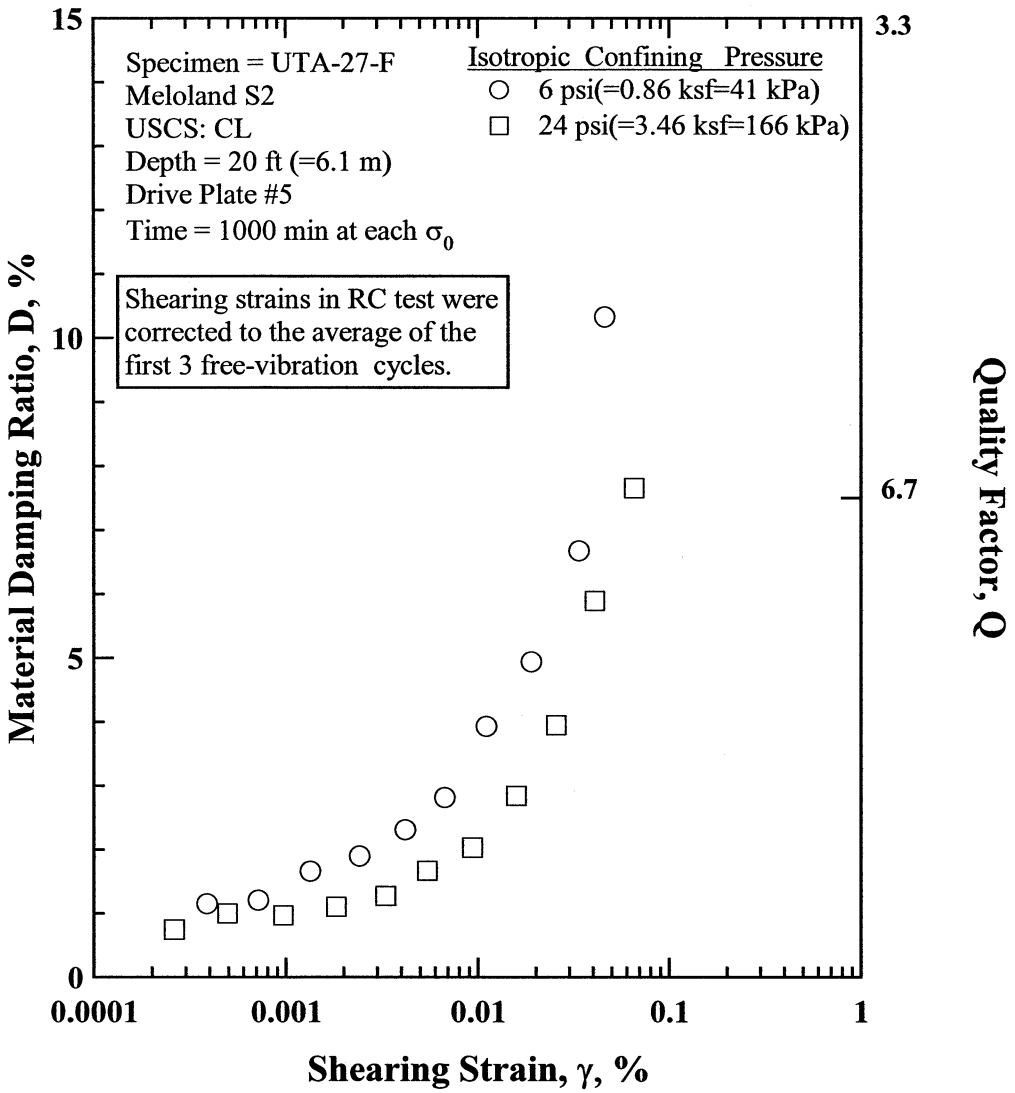

Figure D.10 Comparison of the Variation in Material Damping Ratio with Shearing Strain and Isotropic Confining Pressure from the Resonant Column Tests of Specimen UTA-27-F.

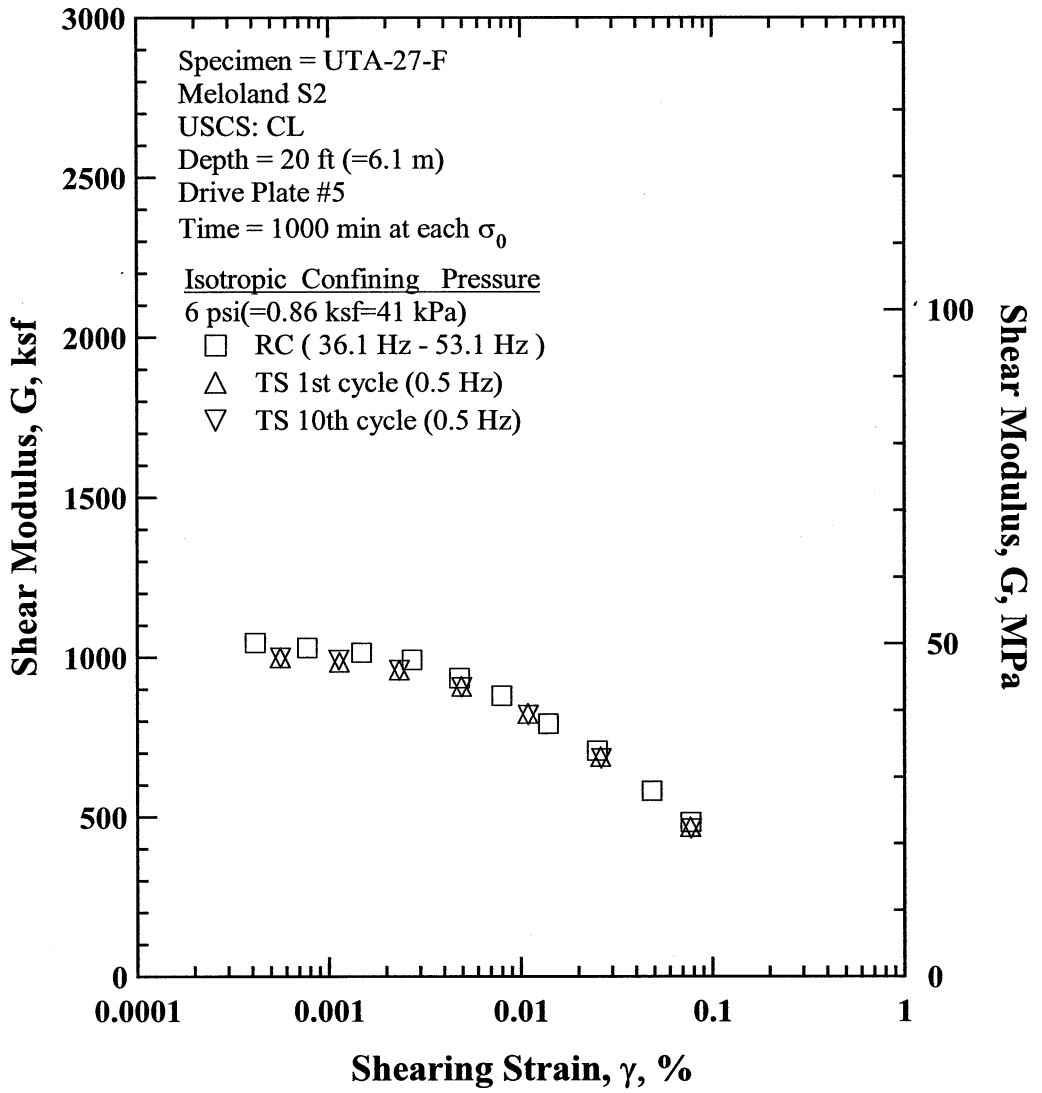

Figure D.11 Comparison of the Variation in Shear Modulus with Shearing Strain at an Isotropic Confining Pressure of 6 psi(=0.86 ksf=41 kPa) from the Combined RCTS Tests of Specimen UTA-27-F.

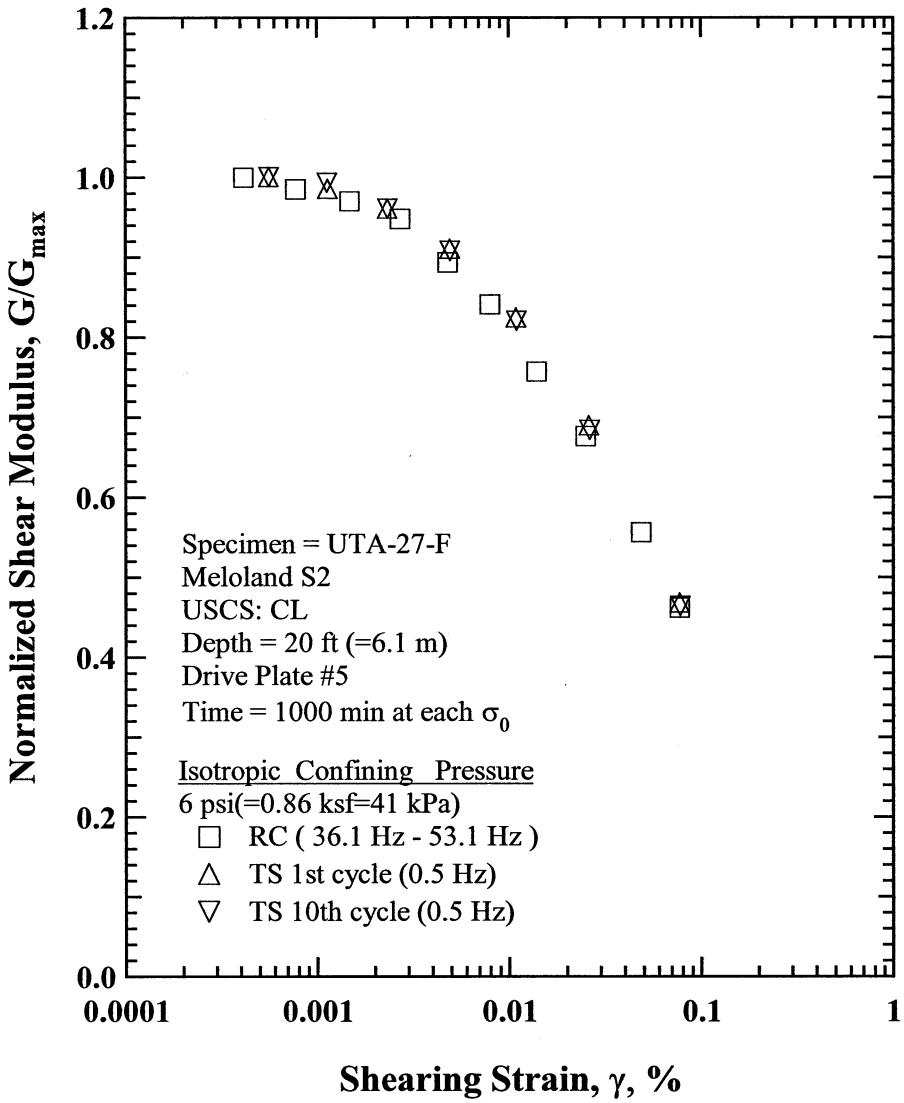

Figure D.12 Comparison of the Variation in Normalized Shear Modulus with Shearing Strain at an Isotropic Confining Pressure of 6 psi(=0.86 ksf=41 kPa) from the Combined RCTS Tests of Specimen UTA-27-F.

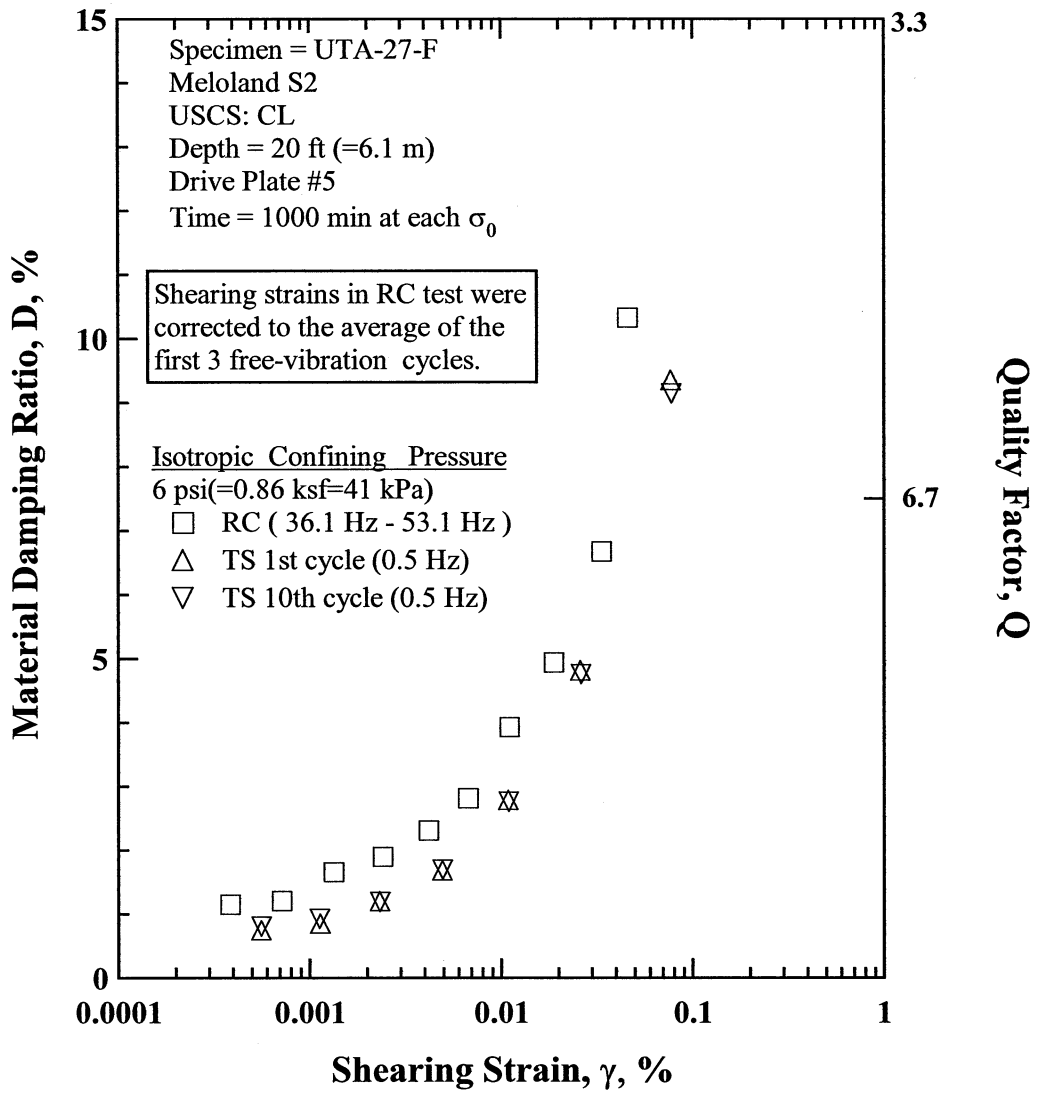

Figure D.13 Comparison of the Variation in Material Damping Ratio with Shearing Strain at an Isotropic Confining Pressure of 6 psi(=0.86 ksf=41 kPa) from the Combined RCTS Tests of Specimen UTA-27-F.

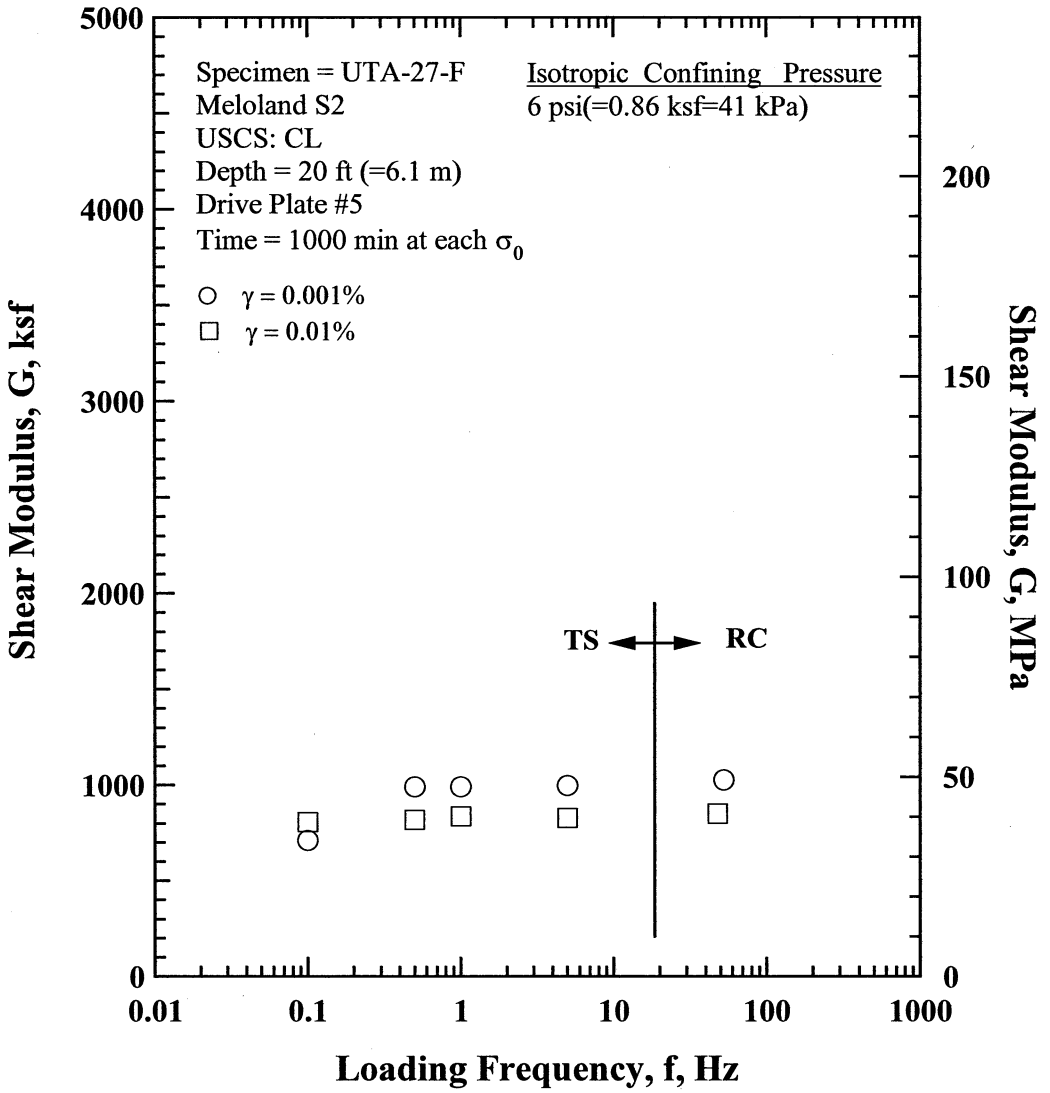

Figure D.14 Comparison of the Variation in Shear Modulus with Loading Frequency at an Isotropic Confining Pressure of 6 psi(=0.86 ksf=41 kPa) from the Combined RCTS Tests of Specimen UTA-27-F.

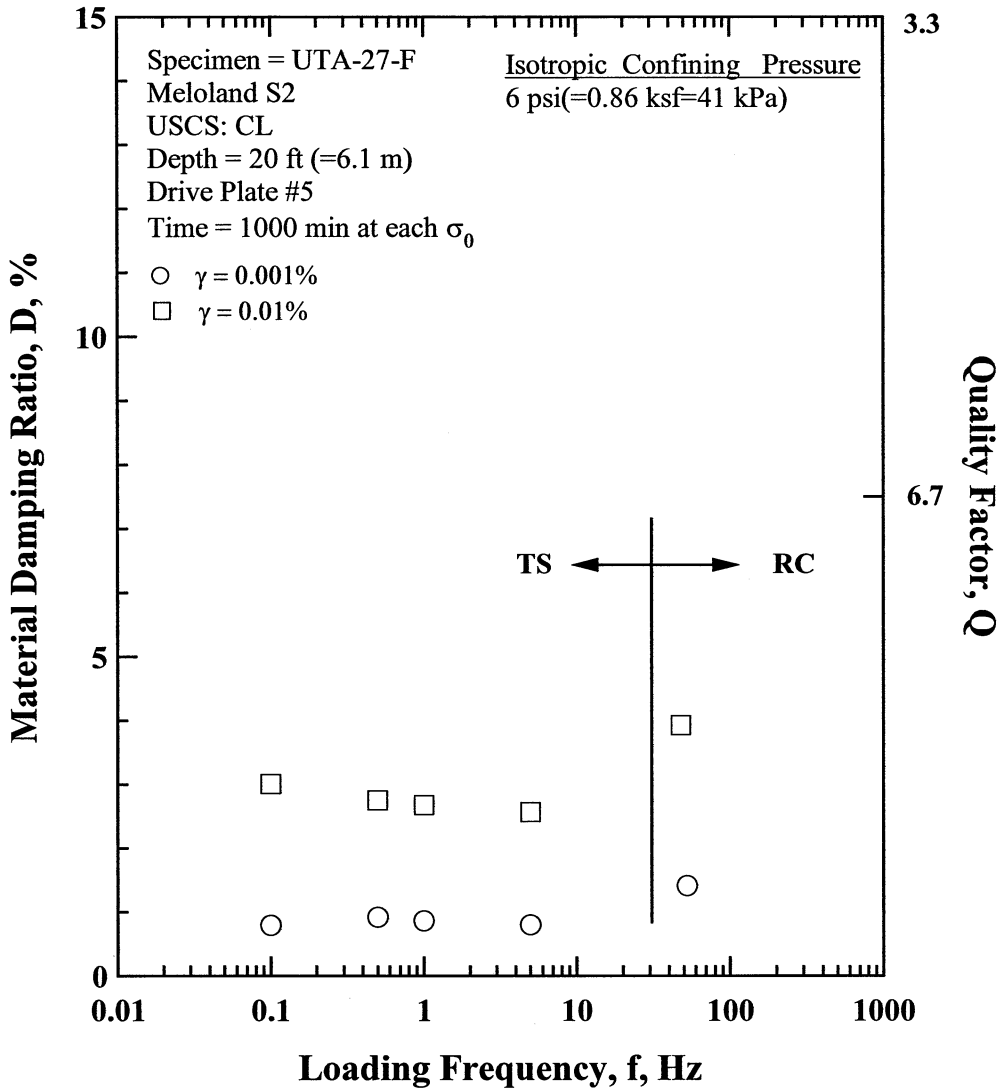

Figure D.15 Comparison of the Variation in Material Damping Ratio with Loading Frequency at an Isotropic Confining Pressure 6 psi(=0.86 ksf=41 kPa) from the Combined RCTS Tests of Specimen UTA-27-F.

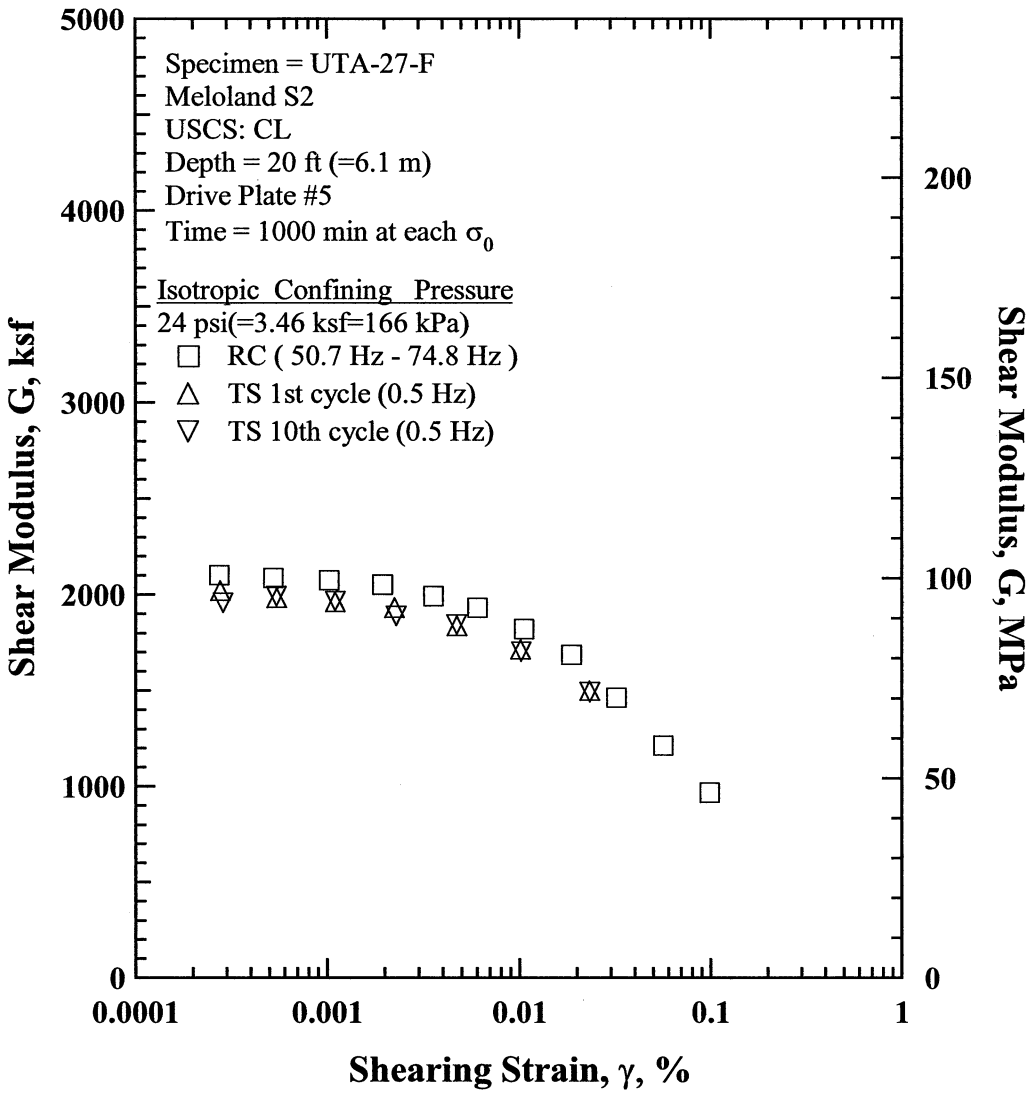

Figure D.16 Comparison of the Variation in Shear Modulus with Shearing Strain at an Isotropic Confining Pressure of 24 psi(=3.46 ksf=166 kPa) from the Combined RCTS Tests of Specimen UTA-27-F.

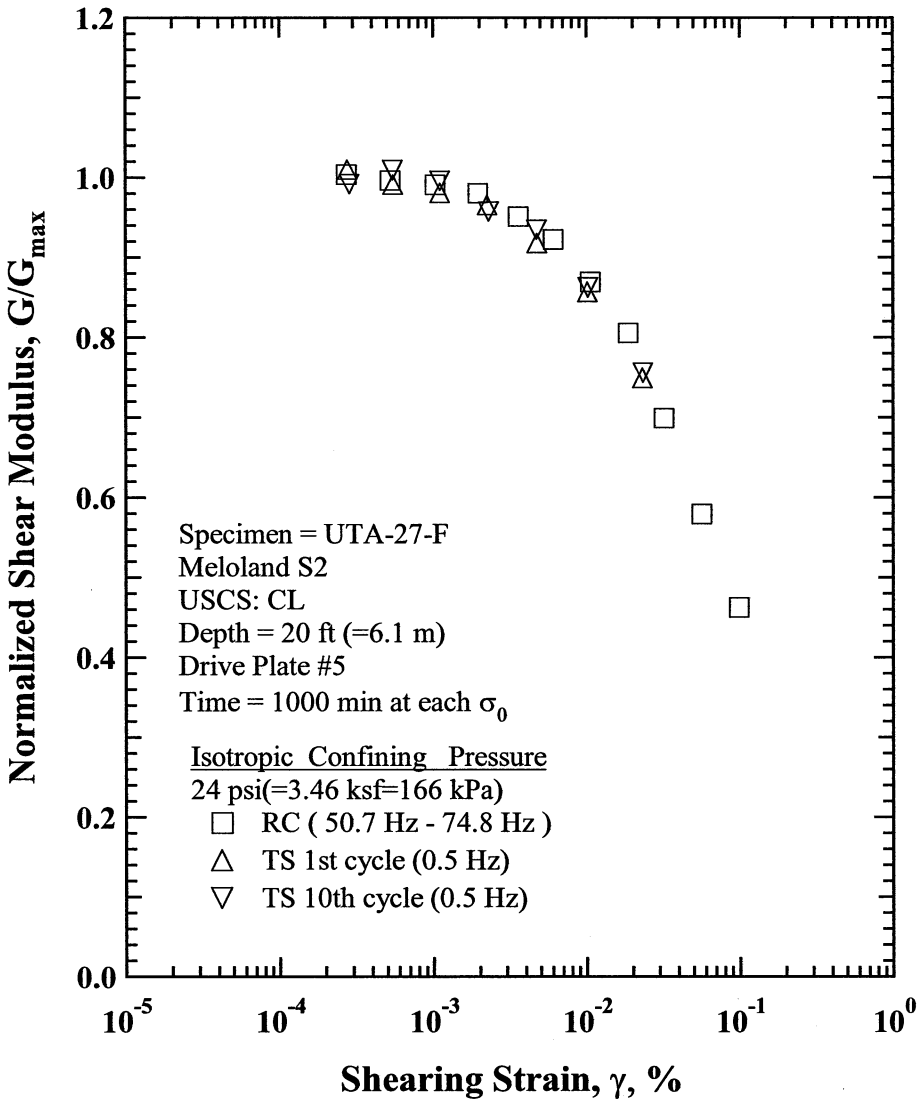

Figure D.17 Comparison of the Variation in Normalized Shear Modulus with Shearing Strain at an Isotropic Confining Pressure of 24 psi(=3.46 ksf=166 kPa) from the Combined RCTS Tests of Specimen UTA-27-F.

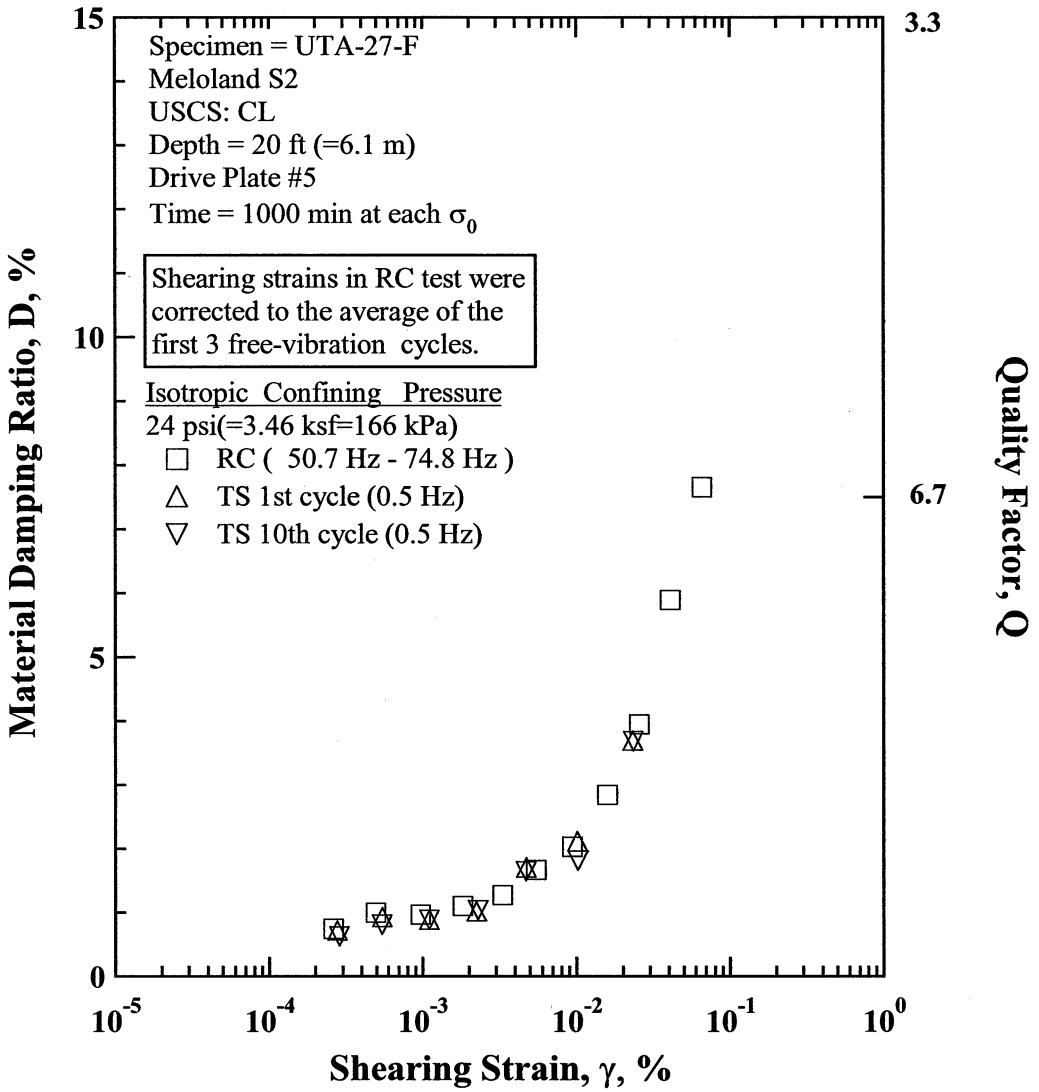

Figure D.18 Comparison of the Variation in Material Damping Ratio with Shearing Strain at an Isotropic Confining Pressure of 24 psi(=3.46 ksf=166 kPa) from the Combined RCTS Tests of Specimen UTA-27-F.

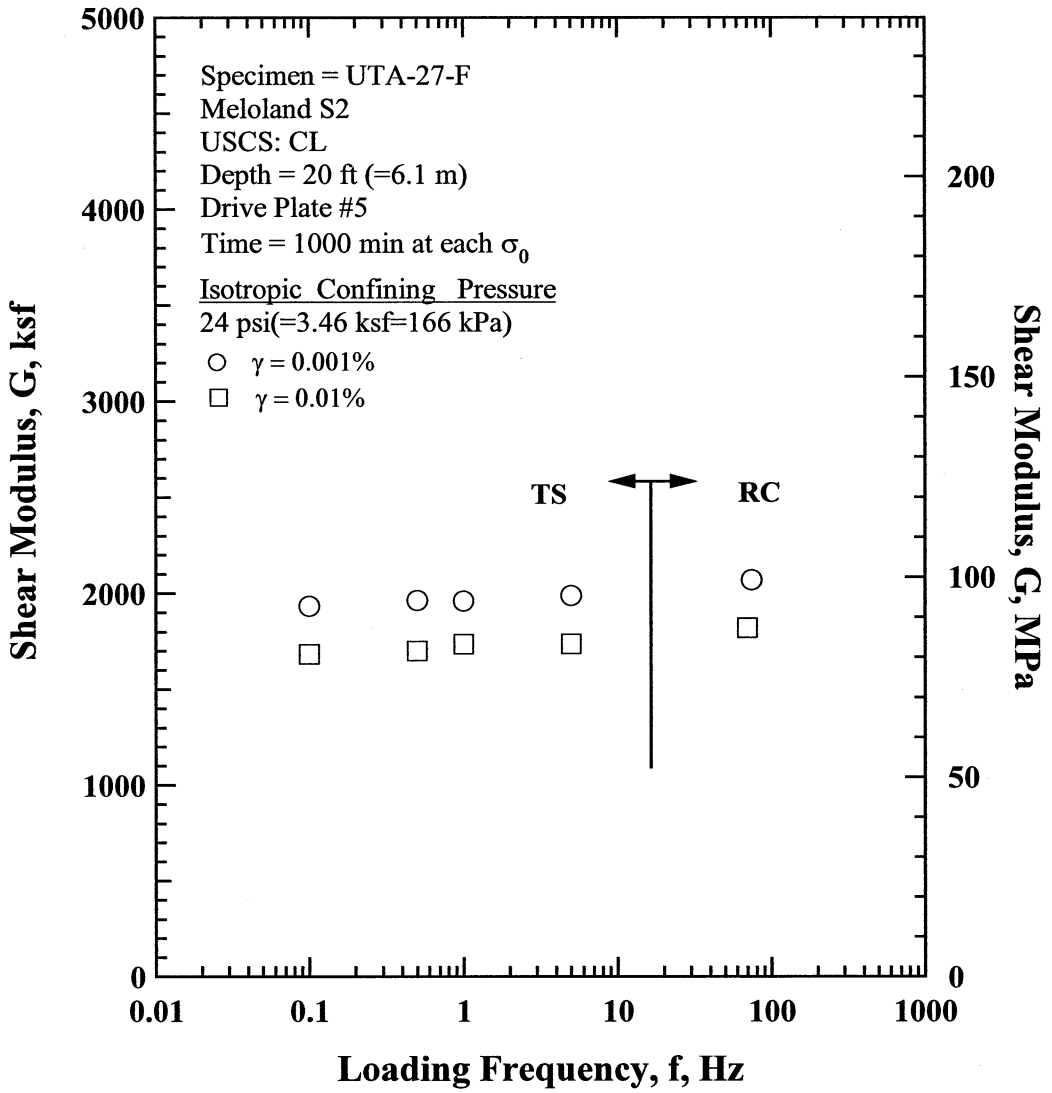

Figure D.19 Comparison of the Variation in Shear Modulus with Loading Frequency at an Isotropic Confining Pressure of 24 psi(=3.46 ksf=166 kPa) from the Combined RCTS Tests of Specimen UTA-27-F.

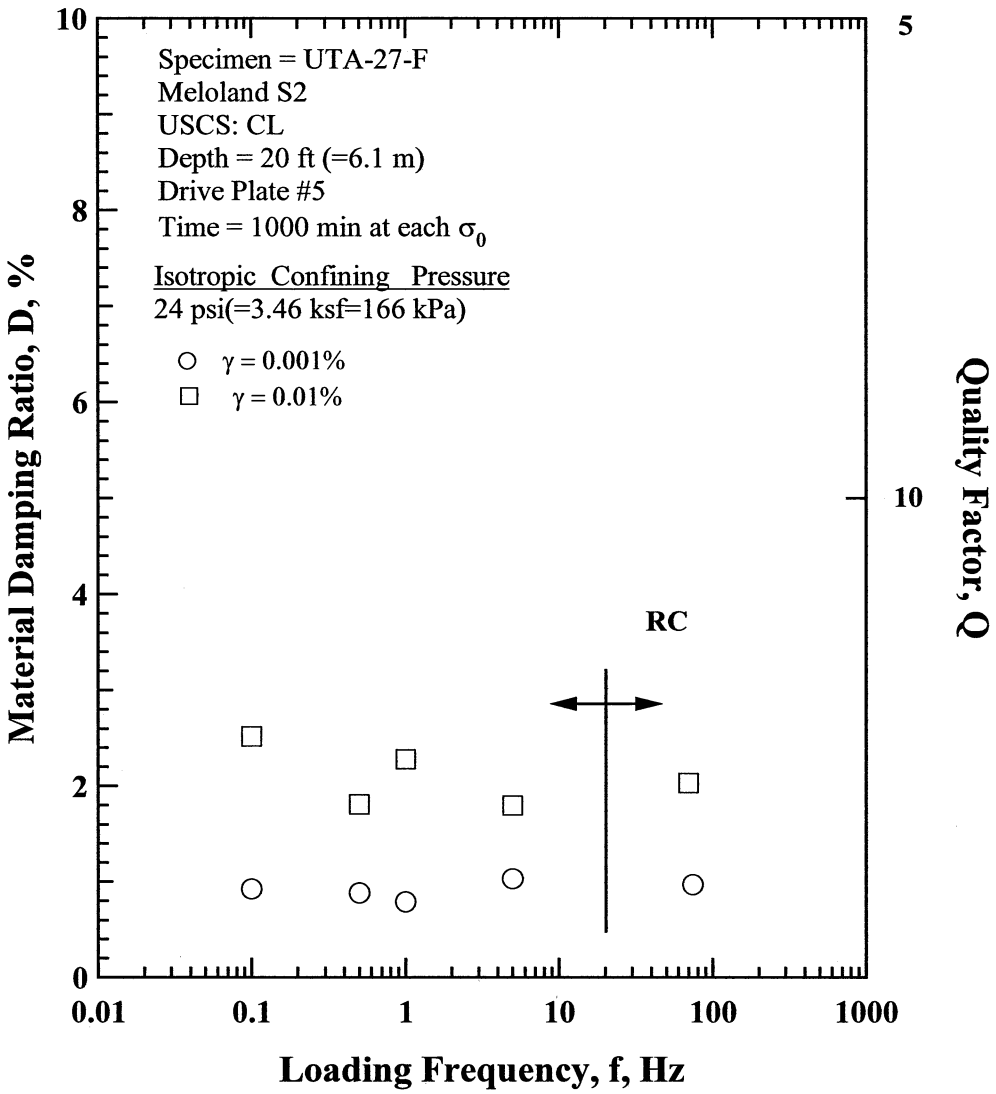

Figure D.20 Comparison of the Variation in Material Damping Ratio with Loading Frequency at an Isotropic Confining Pressure 24 psi(=3.46 ksf=166 kPa) from the Combined RCTS Tests of Specimen UTA-27-F.

Table D.1 Variation in Low-Amplitude Shear Wave Velocity, Low-Amplitude Shear Modulus, Low-Amplitude Material Damping Ratio and Estimated Void Ratio with Isotropic Confining Pressure from RC Tests of Specimen UTA-27-F.

Effective Isotropic Confining Pressure, σ_o'			Low-Amplitude Shear Modulus, G_{max}		Low-Amplitude Shear Wave Velocity, Vs	Low-Amplitude Material Damping Ratio, D_{min}, %	Estimated Void Ratio, e
(psi)	(psf)	(kPa)	(ksf)	(MPa)	(fps)		
2	216	10.4	602	28.9	401	2.62	0.646
3	432	20.7	789	37.8	458	2.11	0.644
6	864	41.4	1001	48.0	516	1.81	0.641
12	1728	82.8	1460	70.0	622	1.35	0.632
24	3456	165.7	2029	97.3	732	1.18	0.618

Table D.2 Variation in Shear Modulus, Normalized Shear Modulus and Material Damping Ratio with Shearing Strain from RC Tests of Specimen UTA-27-F; Confining Pressure, σ_o' = 6 psi(=0.86 ksf=41 kPa).

Peak Shearing Strain, %	Shear Modulus, G, ksf	Normalized Shear Modulus, G/G_{max}	Average[+] Shearing Strain, %	Material Damping Ratio[x], D, %
4.15E-04	1046	1.00	3.86E-04	1.15
7.72E-04	1031	0.99	7.17E-04	1.21
1.48E-03	1015	0.97	1.34E-03	1.66
2.72E-03	992	0.95	2.43E-03	1.90
4.82E-03	935	0.89	4.19E-03	2.31
7.96E-03	880	0.84	6.74E-03	2.82
1.39E-02	792	0.76	1.11E-02	3.93
2.50E-02	708	0.68	1.89E-02	4.94
4.84E-02	582	0.56	3.37E-02	6.67
7.71E-02	484	0.46	4.61E-02	10.33

[+] Average Shearing Strain from the First Three Cycles of the Free Vibration Decay Curve

[x] Average Damping Ratio from the First Three Cycles of the Free Vibration Decay Curve

Table D.3 Variation in Shear Modulus, Normalized Shear Modulus and Material Damping Ratio with Shearing Strain from TS Tests of Specimen UTA-27-F; Confining Pressure, σ_o' = 6 psi(=0.86 ksf=41 kPa).

First Cycle				Tenth Cycle			
Peak Shearing Strain, %	Shear Modulus, G, ksf	Normalized Shear Modulus, G/G_{max}	Material Damping Ratio, D, %	Peak Shearing Strain, %	Shear Modulus, G, ksf	Normalized Shear Modulus, G/G_{max}	Material Damping Ratio, D, %
5.63E-04	998	1.00	0.74	5.63E-04	998	1.00	0.80
1.14E-03	983	0.99	0.85	1.13E-03	991	0.99	0.92
2.35E-03	959	0.96	1.20	2.35E-03	958	0.96	1.18
4.96E-03	908	0.91	1.68	4.97E-03	905	0.91	1.69
1.09E-02	822	0.82	2.78	1.10E-02	818	0.82	2.75
2.62E-02	688	0.69	4.81	2.64E-02	682	0.68	4.75
7.73E-02	467	0.47	9.34	7.80E-02	462	0.46	9.14

Table D.4 Variation in Shear Modulus, Normalized Shear Modulus and Material Damping Ratio with Shearing Strain from RC Tests of Specimen UTA-27-F; Confining Pressure, σ_o' = 24 psi(=3.46 ksf=166 kPa).

Peak Shearing Strain, %	Shear Modulus, G, ksf	Normalized Shear Modulus, G/G_{max}	Average[+] Shearing Strain, %	Material Damping Ratio[x], D, %
2.74E-04	2102	1.00	2.61E-04	0.75
5.25E-04	2086	1.00	4.94E-04	1.00
1.03E-03	2074	0.99	9.68E-04	0.97
1.95E-03	2052	0.98	1.82E-03	1.11
3.57E-03	1992	0.95	3.30E-03	1.27
6.04E-03	1931	0.92	5.46E-03	1.67
1.06E-02	1820	0.87	9.37E-03	2.03
1.87E-02	1687	0.81	1.58E-02	2.84
3.21E-02	1463	0.70	2.55E-02	3.95
5.65E-02	1213	0.58	4.08E-02	5.89
9.87E-02	968	0.46	6.57E-02	7.66

[+] Average Shearing Strain from the First Three Cycles of the Free Vibration Decay Curve

[x] Average Damping Ratio from the First Three Cycles of the Free Vibration Decay Curve

Table D.5 Variation in Shear Modulus, Normalized Shear Modulus and Material Damping Ratio with Shearing Strain from TS Tests of Specimen UTA-27-F; Confining Pressure, σ_o' = 24 psi(=3.46 ksf=166 kPa).

First Cycle				Tenth Cycle			
Peak Shearing Strain, %	Shear Modulus, G, ksf	Normalized Shear Modulus, G/G_{max}	Material Damping Ratio, D, %	Peak Shearing Strain, %	Shear Modulus, G, ksf	Normalized Shear Modulus, G/G_{max}	Material Damping Ratio, D, %
2.79E-04	2019	1.01	0.71	2.88E-04	1955	0.99	0.62
5.50E-04	1981	0.99	0.92	5.47E-04	1989	1.01	0.80
1.11E-03	1960	0.98	0.88	1.11E-03	1963	1.00	0.88
2.26E-03	1930	0.96	1.01	2.31E-03	1887	0.96	1.03
4.75E-03	1834	0.92	1.70	4.73E-03	1842	0.93	1.64
1.02E-02	1712	0.86	2.11	1.03E-02	1700	0.86	1.81
2.33E-02	1497	0.75	3.69	2.35E-02	1490	0.76	3.68

APPENDIX E

Specimen No. 4
UT Specimen ID: UTA-27-E

Meloland S-3
Depth= 28 ft (= 8.5 m)
Soil Type: Clay (CH)

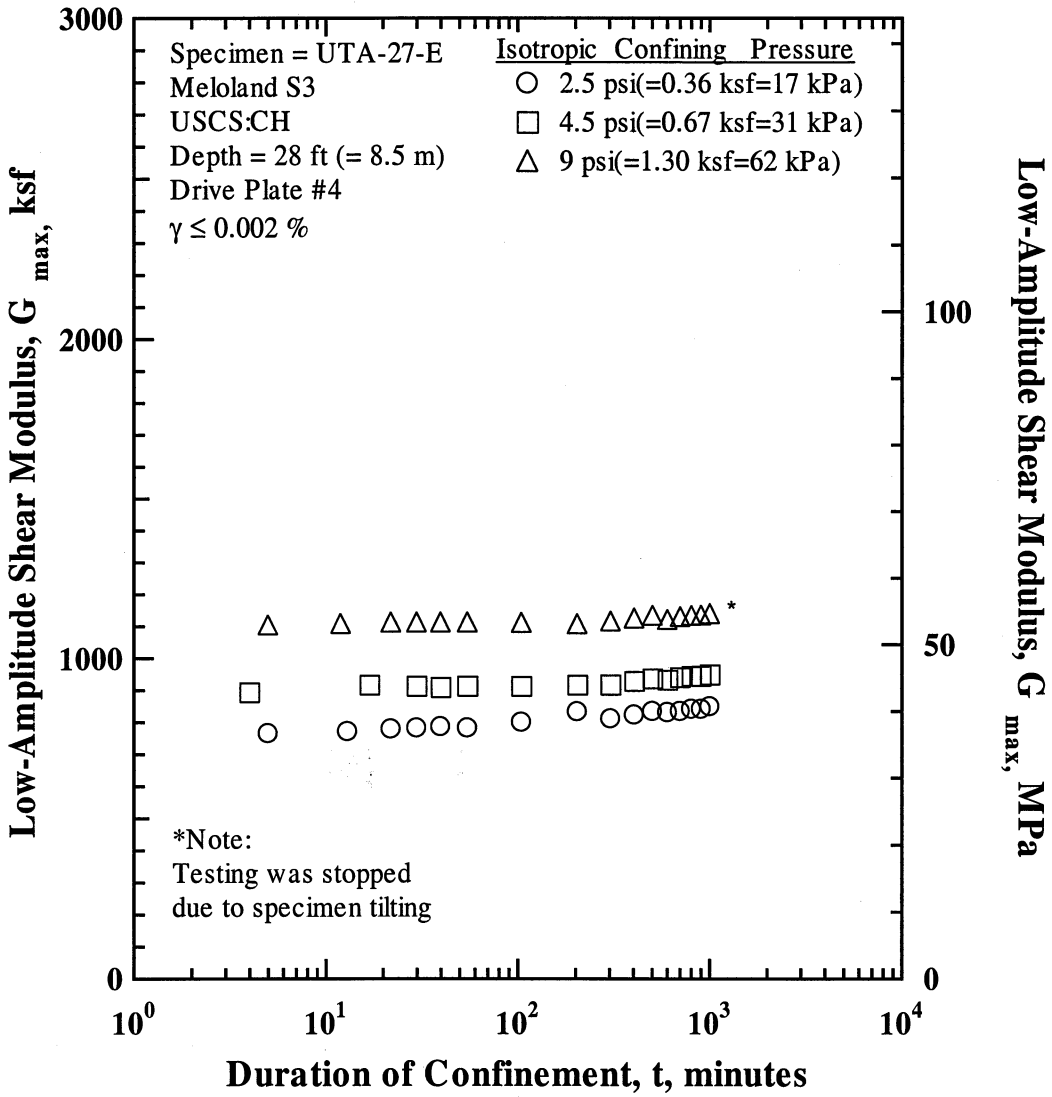

Figure E.1 Variation in Low-Amplitude Shear Modulus with Magnitude and Duration of Isotropic Confining Pressure from Resonant Column Tests of Specimen UTA-27-E.

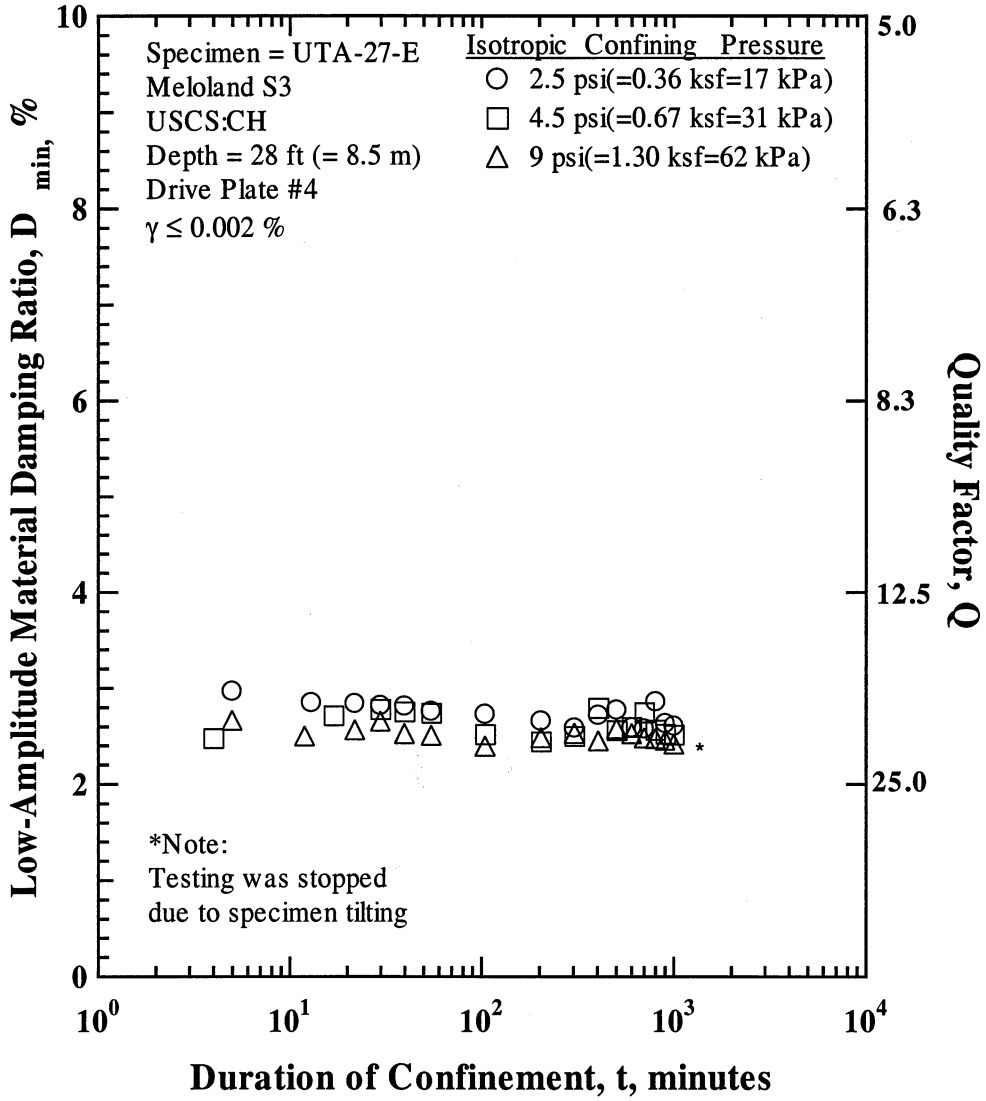

Figure E.2 Variation in Low-Amplitude Material Damping Ratio and Duration of Isotropic Confining Pressure from Resonant Column Tests of Specimen UTA-27-E

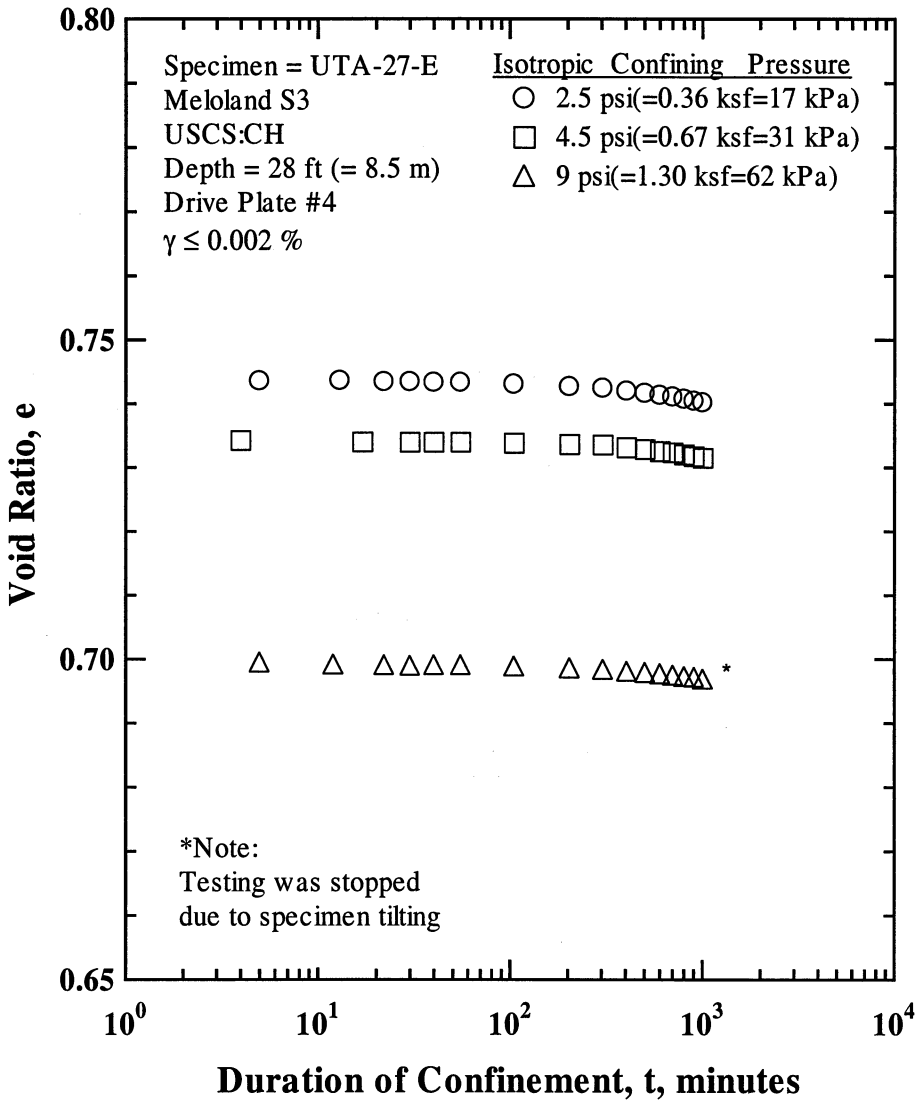

Figure E.3 Variation in Estimated Void Ratio with Magnitude and Duration of Isotropic Confining Pressure from Resonant Column Tests of Specimen UTA-27-E

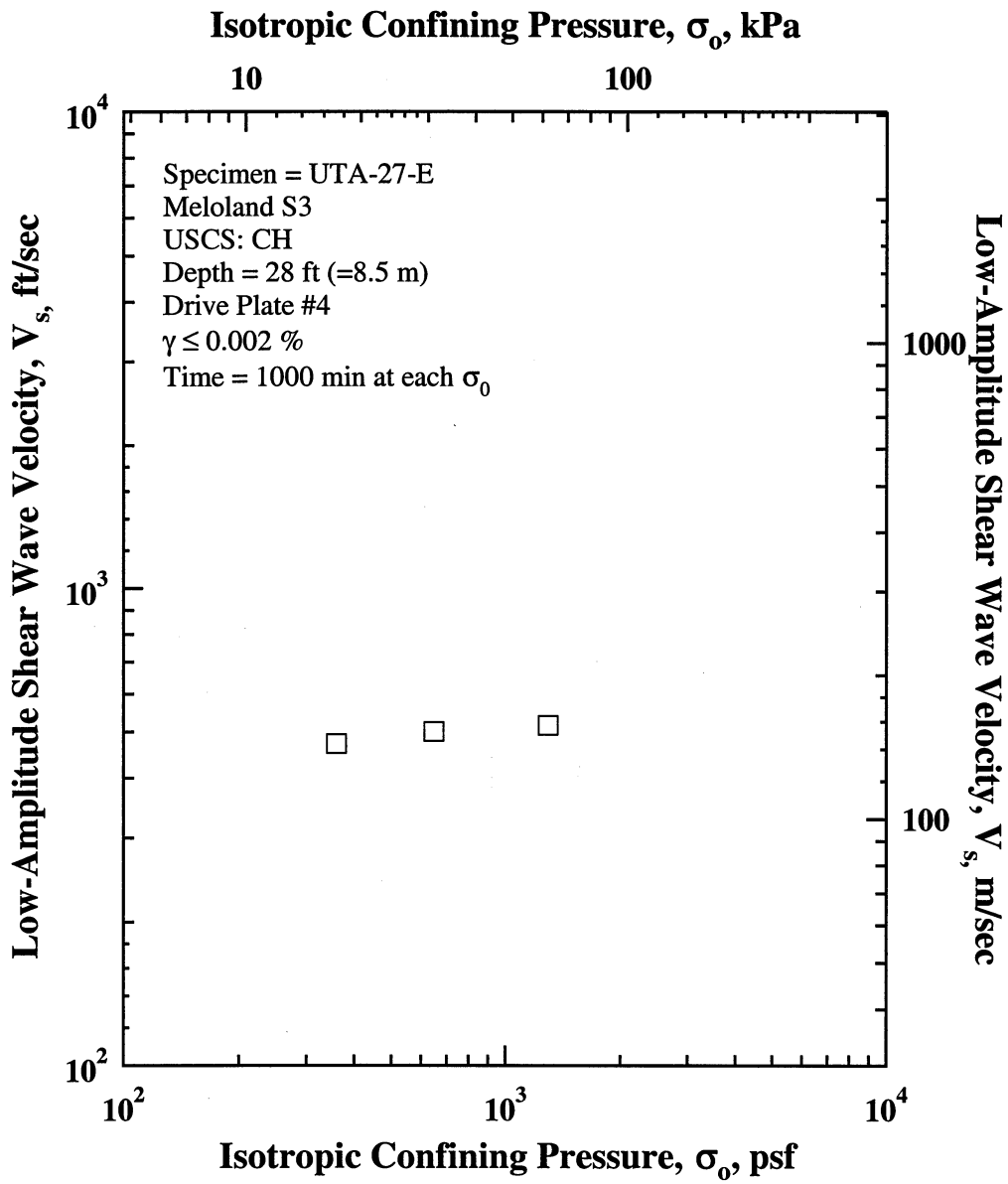

Figure E.4 Variation in Low-Amplitude Shear Wave Velocity with Isotropic Confining Pressure from Resonant Column Tests of Specimen UTA-27-E.

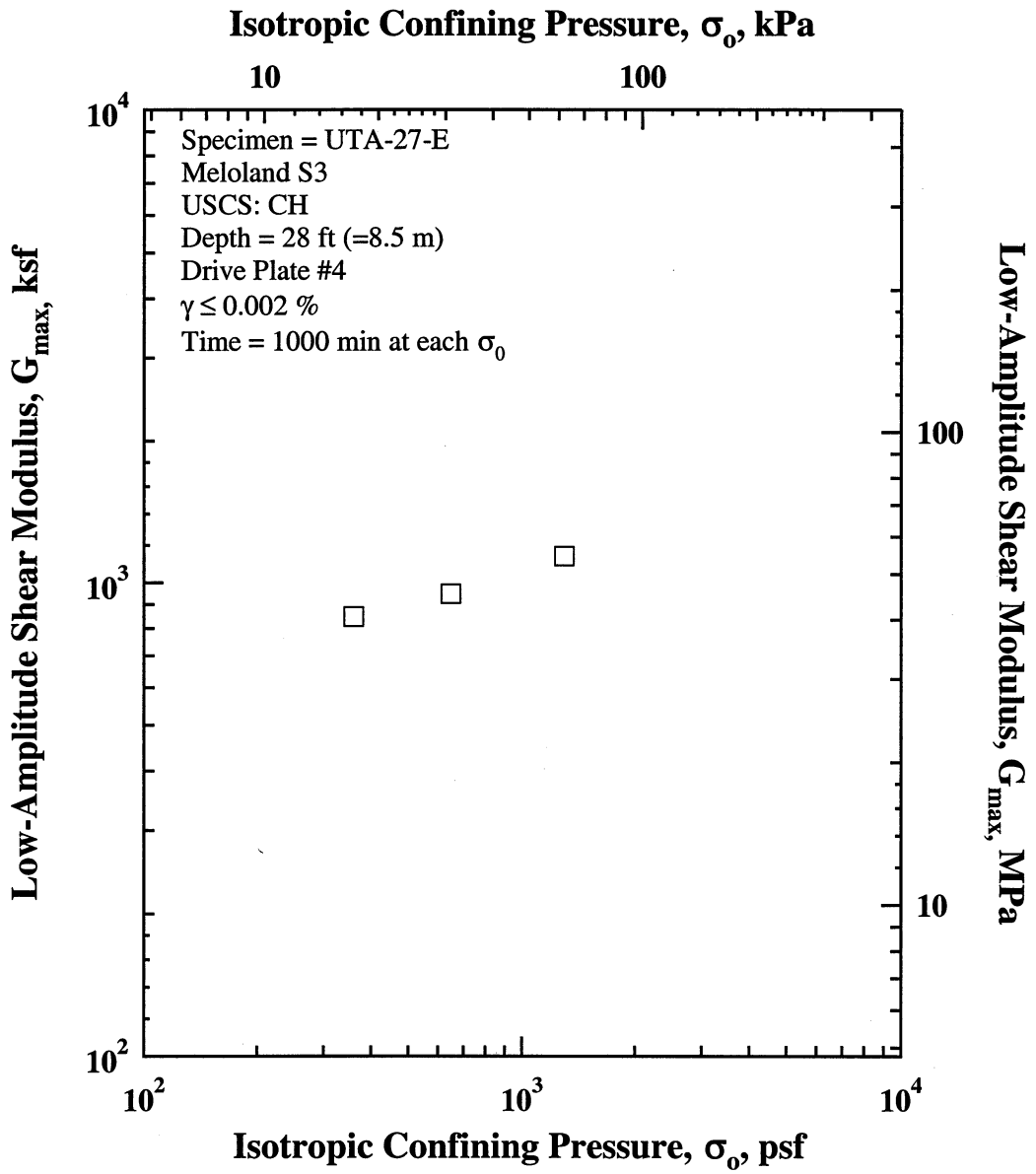

Figure E.5 Variation in Low-Amplitude Shear Modulus with Isotropic Confining Pressure from Resonant Column Tests of Specimen UTA-27-E.

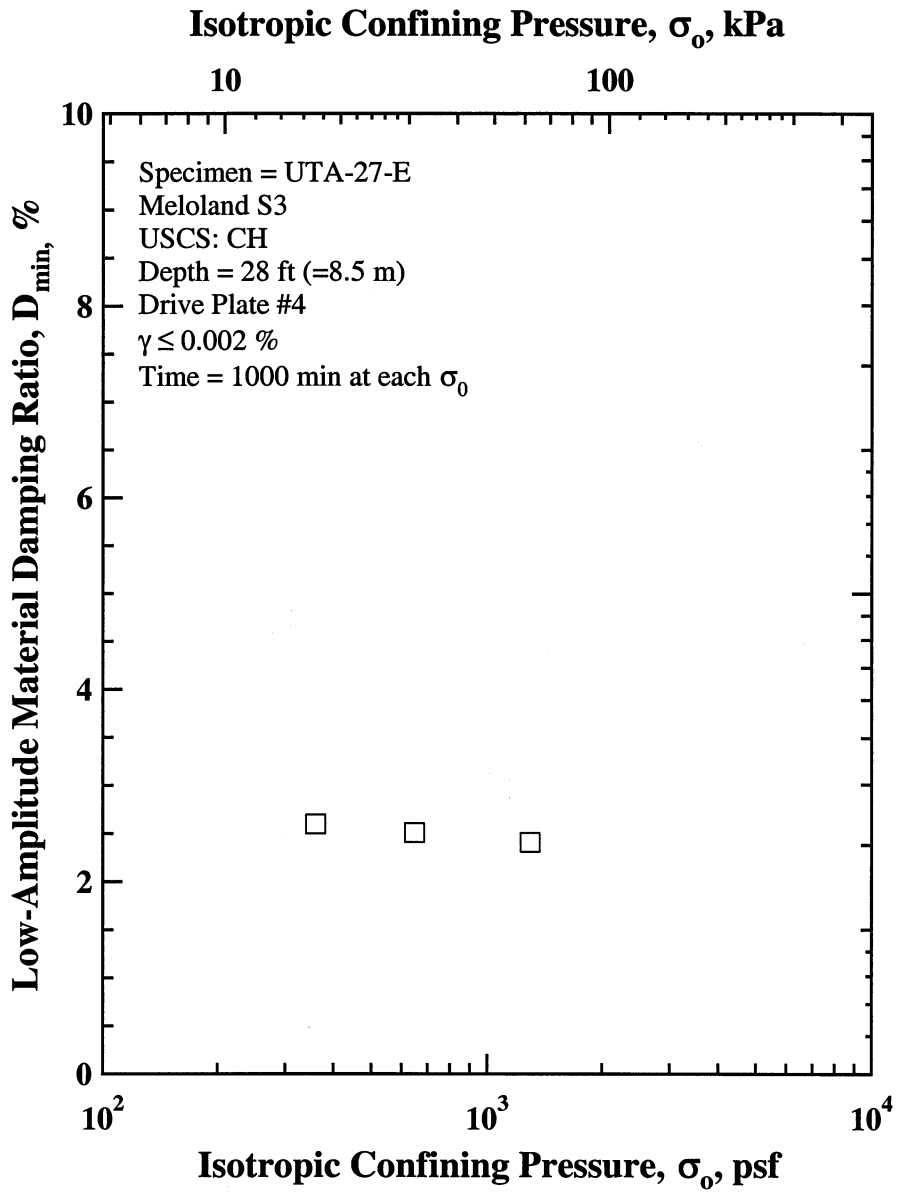

Figure E.6 Variation in Low-Amplitude Material Damping Ratio with Isotropic Confining Pressure from Resonant Column Tests of Specimen UTA-27-E.

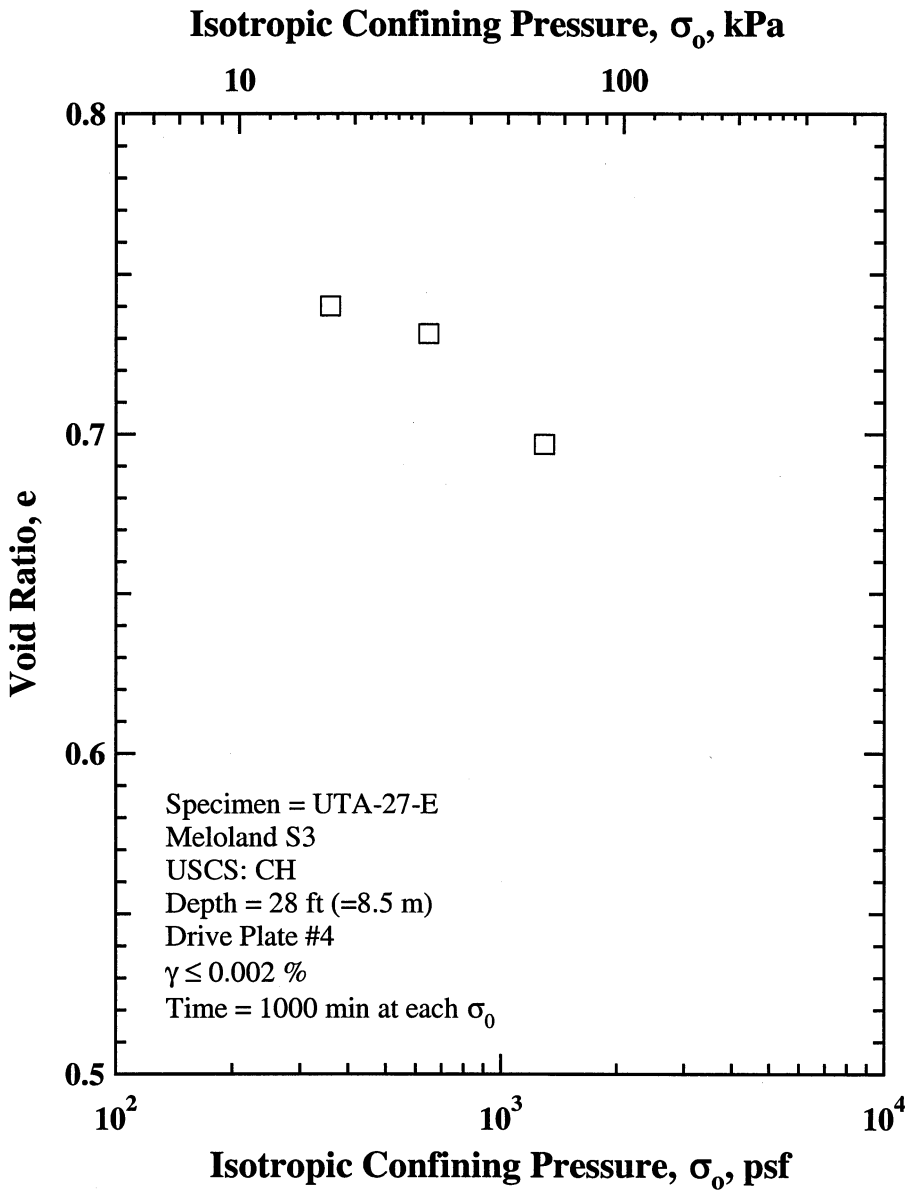

Figure E.7 Variation in Estimated Void Ratio with Isotropic Confining Pressure from Resonant Column Tests of Specimen UTA-27-E.

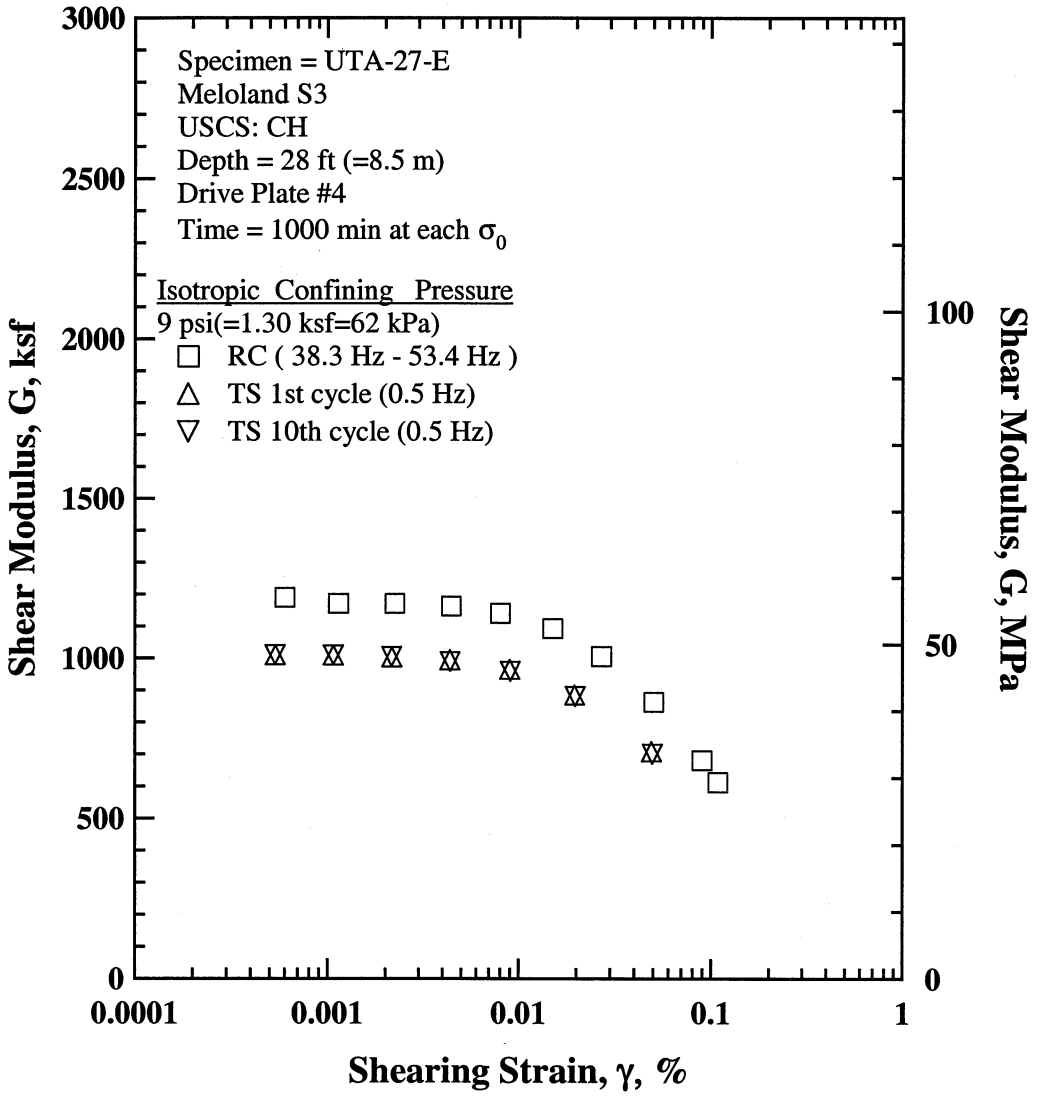

Figure E.8 Comparison of the Variation in Shear Modulus with Shearing Strain at an Isotropic Confining Pressure of 9 psi(=1.30 ksf=62 kPa) from the Combined RCTS Tests of Specimen UTA-27-E.

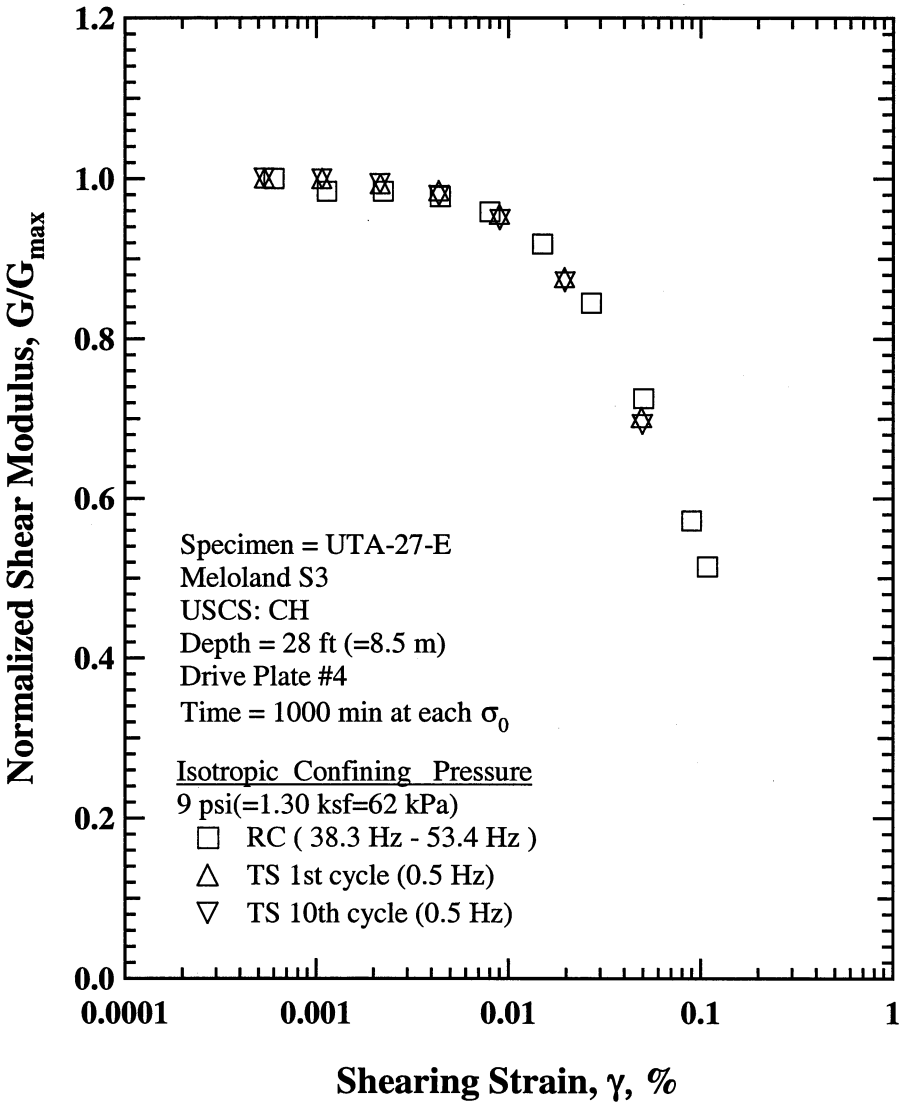

Figure E.9 Comparison of the Variation in Normalized Shear Modulus with Shearing Strain at an Isotropic Confining Pressure of 9 psi(=1.30 ksf=62 kPa) from the Combined RCTS Tests of Specimen UTA-27-E.

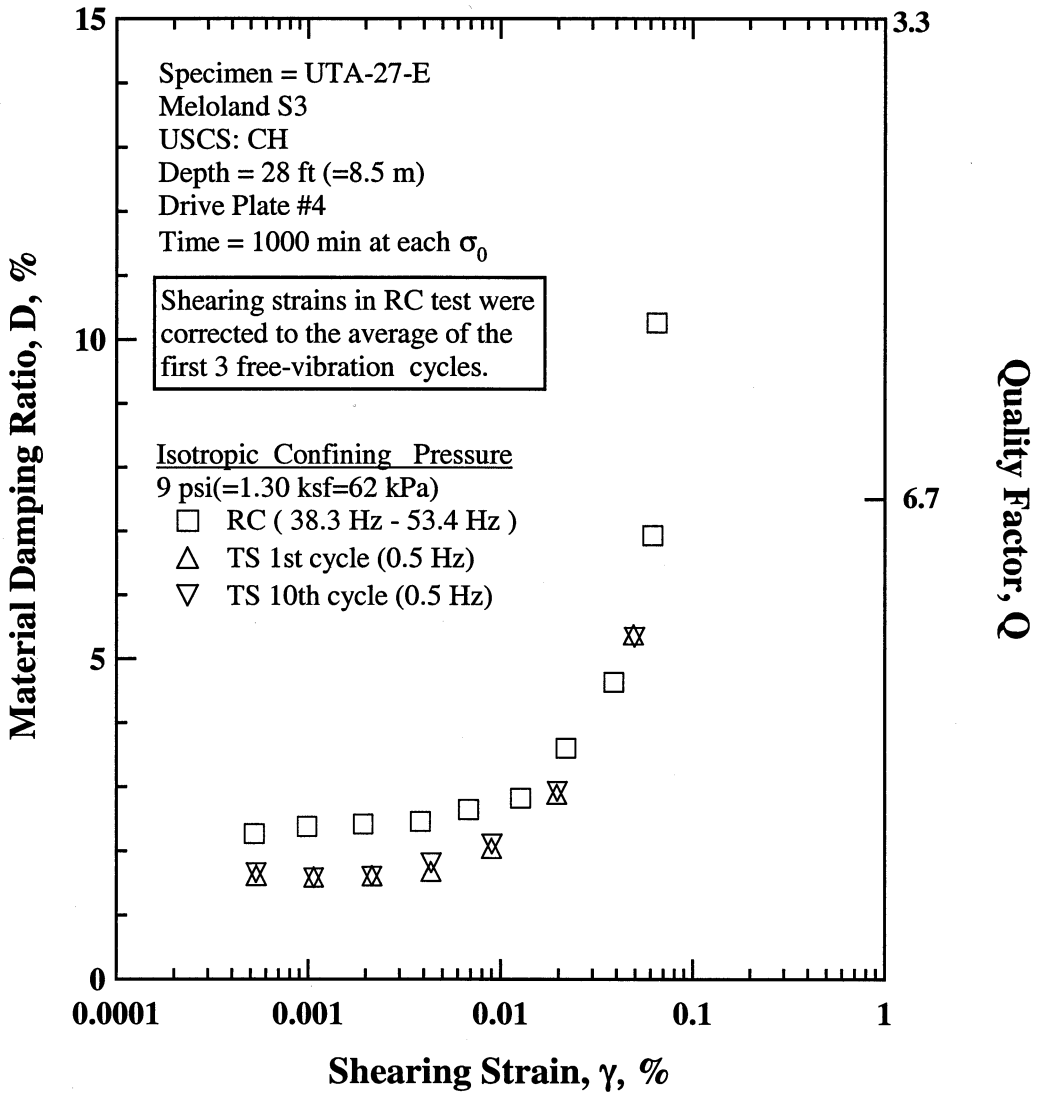

Figure E.10 Comparison of the Variation in Material Damping Ratio with Shearing Strain at an Isotropic Confining Pressure of 9 psi(=1.30 ksf=62 kPa) from the Combined RCTS Tests of Specimen UTA-27-E.

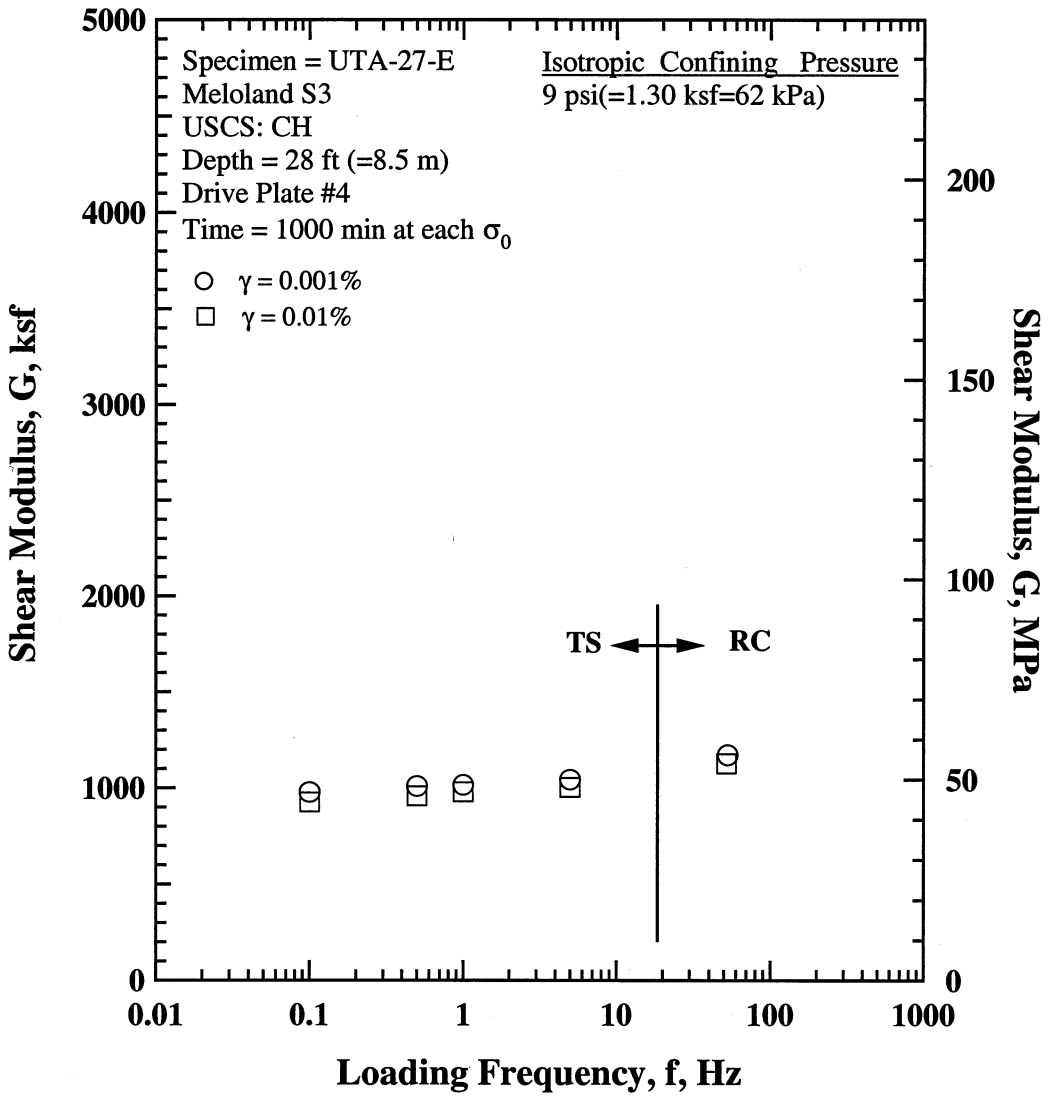

Figure E.11 Comparison of the Variation in Shear Modulus with Loading Frequency at an Isotropic Confining Pressure of 9 psi(=1.30 ksf=62 kPa) from the Combined RCTS Tests of Specimen UTA-27-E.

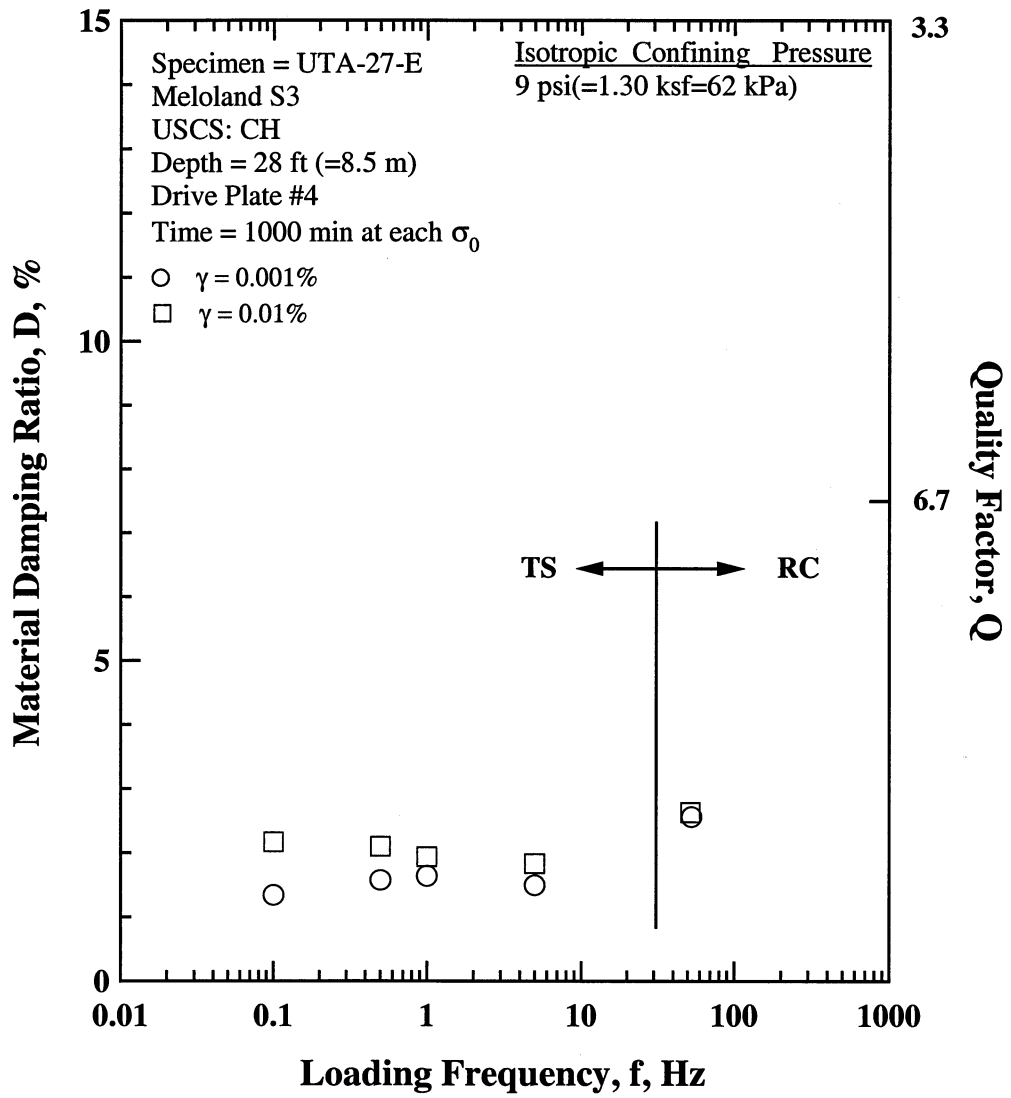

Figure E.12 Comparison of the Variation in Material Damping Ratio with Loading Frequency at an Isotropic Confining Pressure 9 psi(=1.30 ksf=62 kPa) from the Combined RCTS Tests of Specimen UTA-27-E.

Table E.1 Variation in Low-Amplitude Shear Wave Velocity, Low-Amplitude Shear Modulus, Low-Amplitude Material Damping Ratio and Estimated Void Ratio with Isotropic Confining Pressure from RC Tests of Specimen UTA-27-E.

Effective Isotropic Confining Pressure, σ_o'			Low-Amplitude Shear Modulus, G_{max}		Low-Amplitude Shear Wave Velocity, Vs	Low-Amplitude Material Damping Ratio, D_{min}, %	Estimated Void Ratio, e
(psi)	(psf)	(kPa)	(ksf)	(MPa)	(fps)		
3	360	17.3	602	28.9	401	2.62	0.646
5	648	31.1	789	37.8	458	2.11	0.644
9	1296	62.1	1001	48.0	516	1.81	0.641

Table E.2 Variation in Shear Modulus, Normalized Shear Modulus and Material Damping Ratio with Shearing Strain from RC Tests of Specimen UTA-27-E; Confining Pressure, σ_o' = 9 psi(=1.3 ksf=62 kPa).

Peak Shearing Strain, %	Shear Modulus, G, ksf	Normalized Shear Modulus, G/G_{max}	Average[+] Shearing Strain, %	Material Damping Ratio[x], D, %
6.00E-04	1189	1.00	5.24E-04	2.27
1.14E-03	1170	0.98	9.88E-04	2.38
2.24E-03	1170	0.98	1.94E-03	2.42
4.44E-03	1163	0.98	3.84E-03	2.46
8.00E-03	1140	0.96	6.84E-03	2.65
1.50E-02	1092	0.92	1.27E-02	2.82
2.70E-02	1005	0.84	2.19E-02	3.60
5.04E-02	863	0.73	3.87E-02	4.63
8.98E-02	680	0.57	6.18E-02	6.93
1.09E-01	612	0.51	6.50E-02	10.26

[+] Average Shearing Strain from the First Three Cycles of the Free Vibration Decay Curve

[x] Average Damping Ratio from the First Three Cycles of the Free Vibration Decay Curve

Table E.3 Variation in Shear Modulus, Normalized Shear Modulus and Material Damping Ratio with Shearing Strain from TS Tests of Specimen UTA-27-E; Confining Pressure, σ_o' =9 psi(=1.3 ksf=62 kPa).

First Cycle				Tenth Cycle			
Peak Shearing Strain, %	Shear Modulus, G, ksf	Normalized Shear Modulus, G/G_{max}	Material Damping Ratio, D, %	Peak Shearing Strain, %	Shear Modulus, G, ksf	Normalized Shear Modulus, G/G_{max}	Material Damping Ratio, D, %
5.39E-04	1008	1.00	1.61	5.38E-04	1009	1.00	1.65
1.08E-03	1007	1.00	1.58	1.08E-03	1008	1.00	1.57
2.17E-03	1001	0.99	1.60	2.17E-03	1002	0.99	1.59
4.38E-03	992	0.98	1.67	4.40E-03	987	0.98	1.81
9.03E-03	962	0.95	2.03	9.09E-03	957	0.95	2.10
1.97E-02	883	0.88	2.88	1.98E-02	878	0.87	2.92
4.93E-02	706	0.70	5.37	4.99E-02	698	0.69	5.33

APPENDIX F

Specimen No. 5
UT Specimen ID: UTA-27-B

Meloland WS-1
Depth = 120 ft (= 36.6m)
Soil Type: Clay (CH)

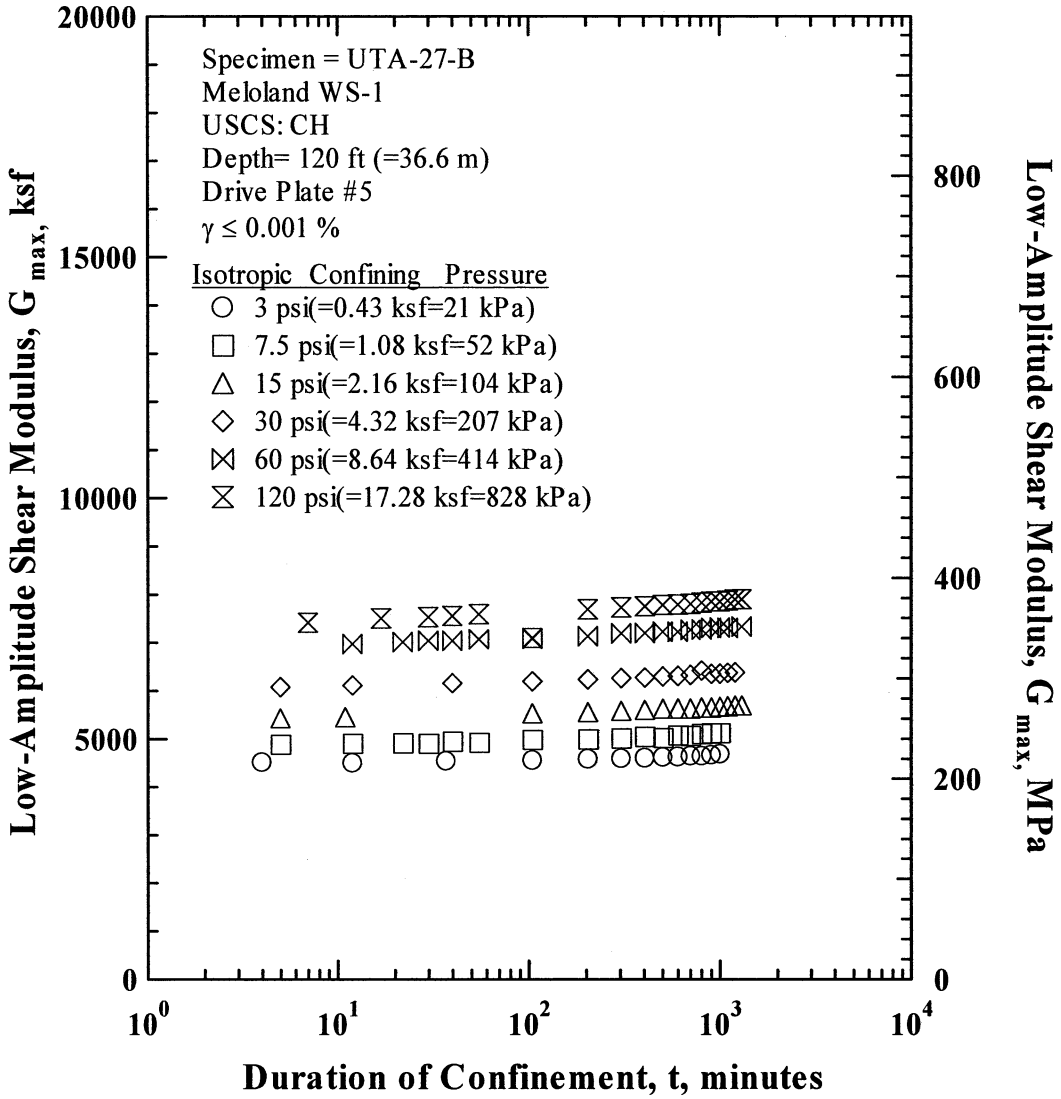

Figure F.1 Variation in Low-Amplitude Shear Modulus with Magnitude and Duration of Isotropic Confining Pressure from Resonant Column Tests of Specimen UTA-27-B.

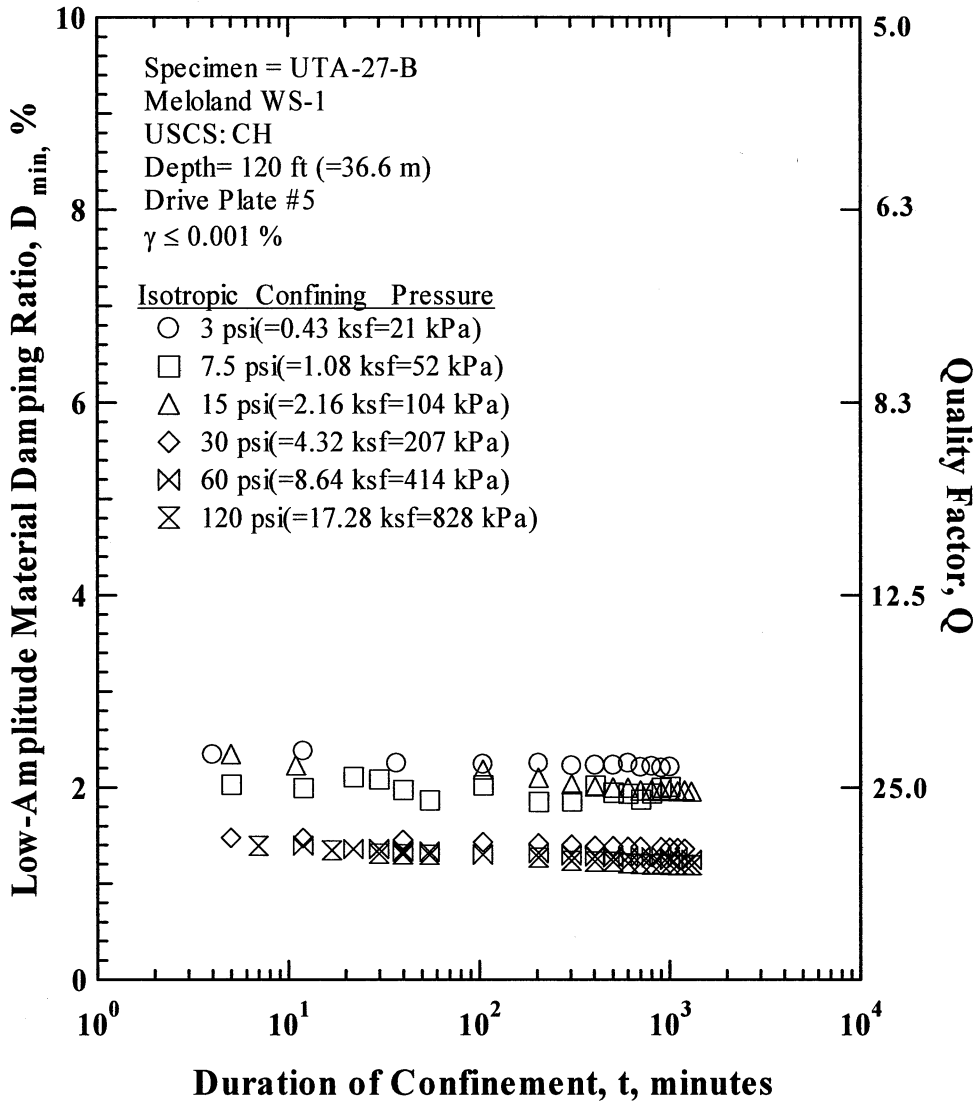

Figure F.2 Variation in Low-Amplitude Material Damping Ratio with Magnitude and Duration of Isotropic Confining Pressure from Resonant Column Tests of Specimen UTA-27-B

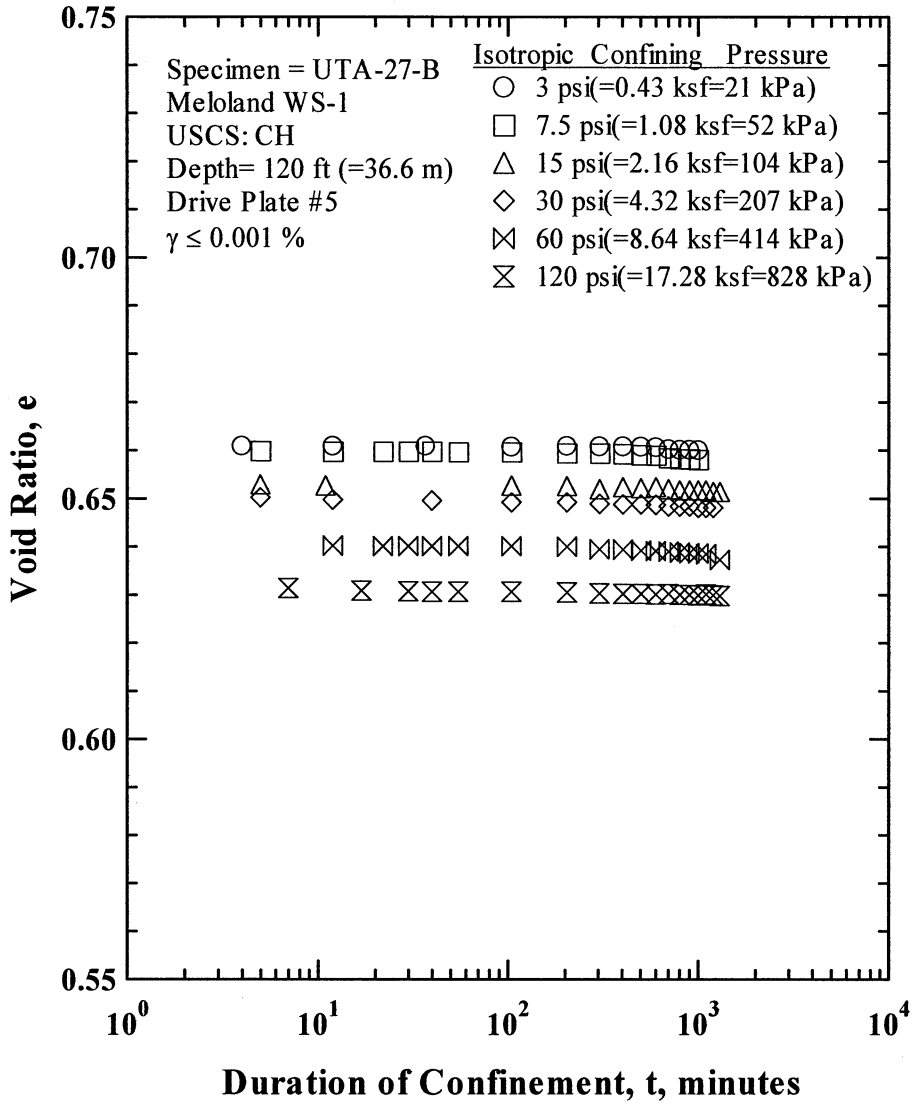

Figure F.3 Variation in Estimated Void Ratio with Magnitude and Duration of Isotropic Confining Pressure from Resonant Column Tests of Specimen UTA-27-B

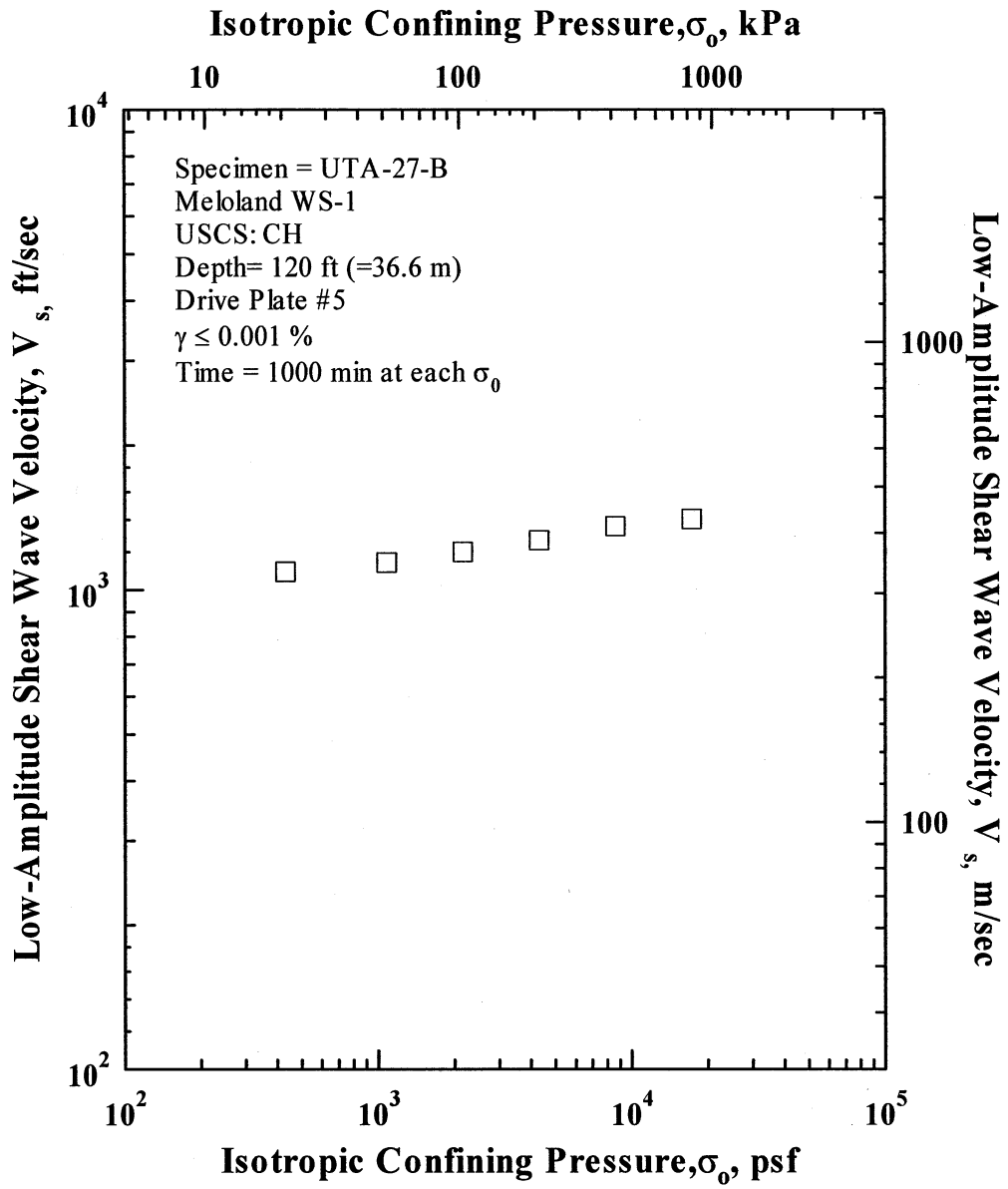

Figure F.4 Variation in Low-Amplitude Shear Wave Velocity with Isotropic Confining Pressure from Resonant Column Tests of Specimen UTA-27-B.

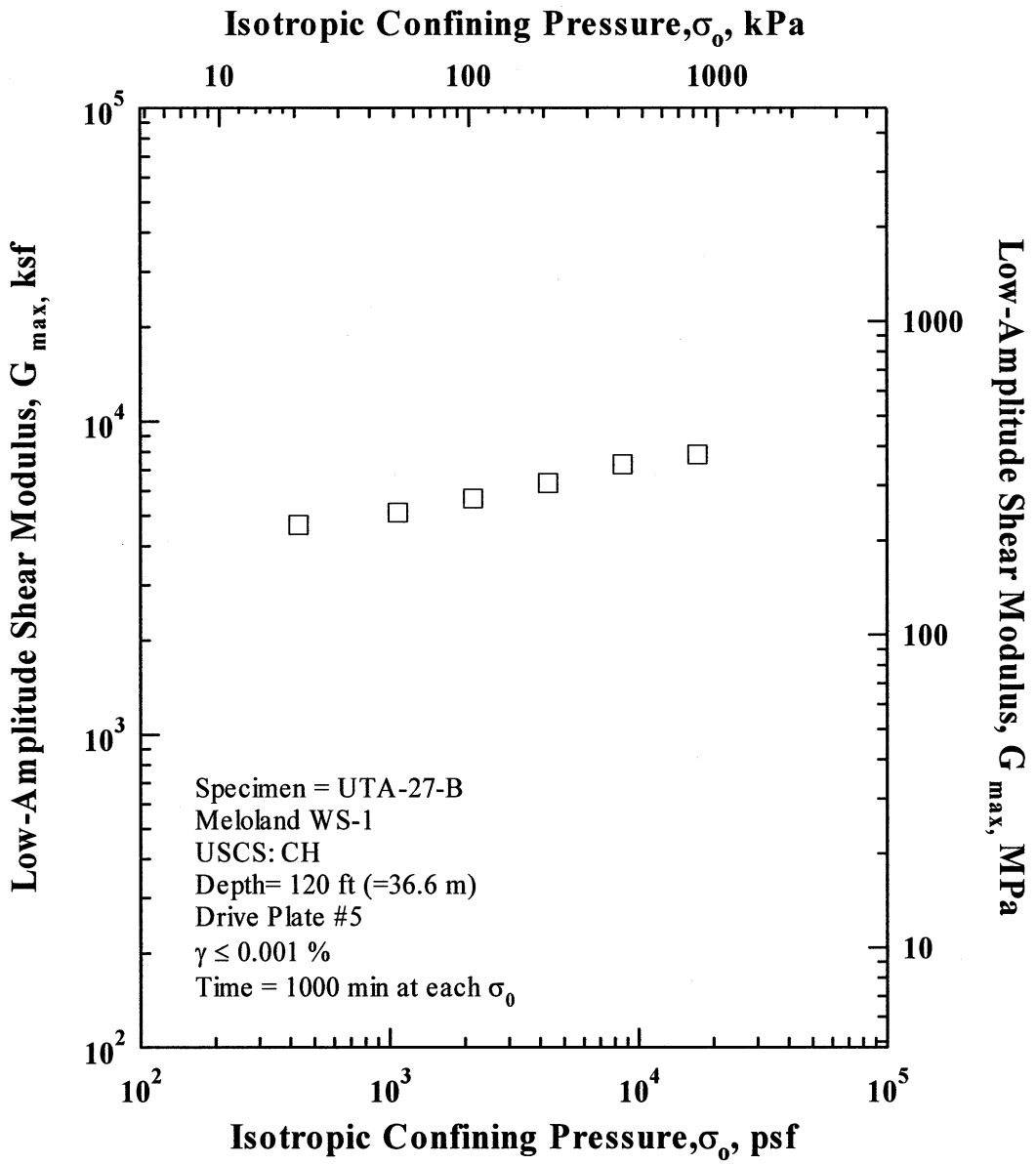

Figure F.5 Variation in Low-Amplitude Shear Modulus with Isotropic Confining Pressure from Resonant Column Tests of Specimen UTA-27-B.

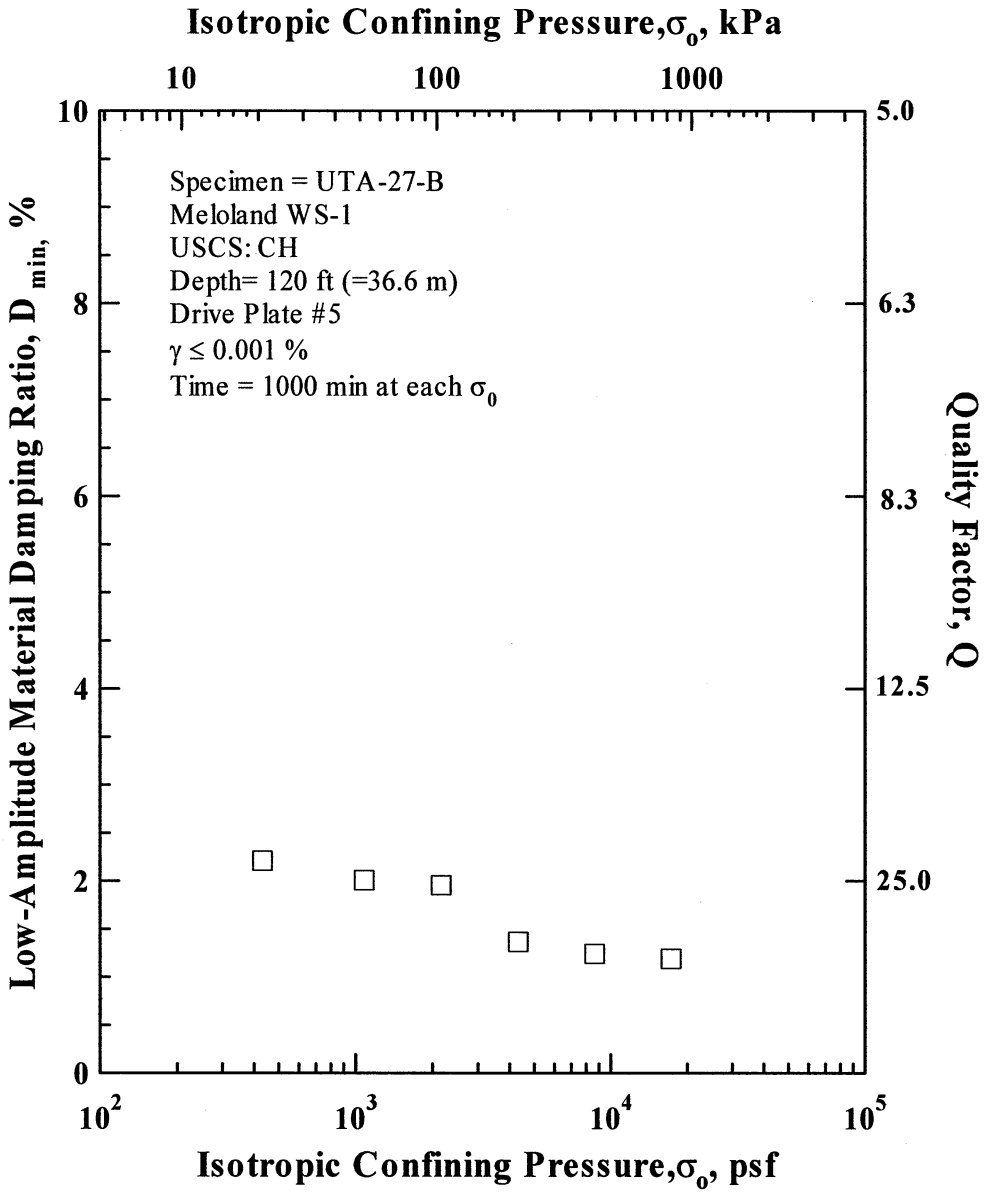

Figure F.6 Variation in Low-Amplitude Material Damping Ratio with Isotropic Confining Pressure from Resonant Column Tests of Specimen UTA-27-B.

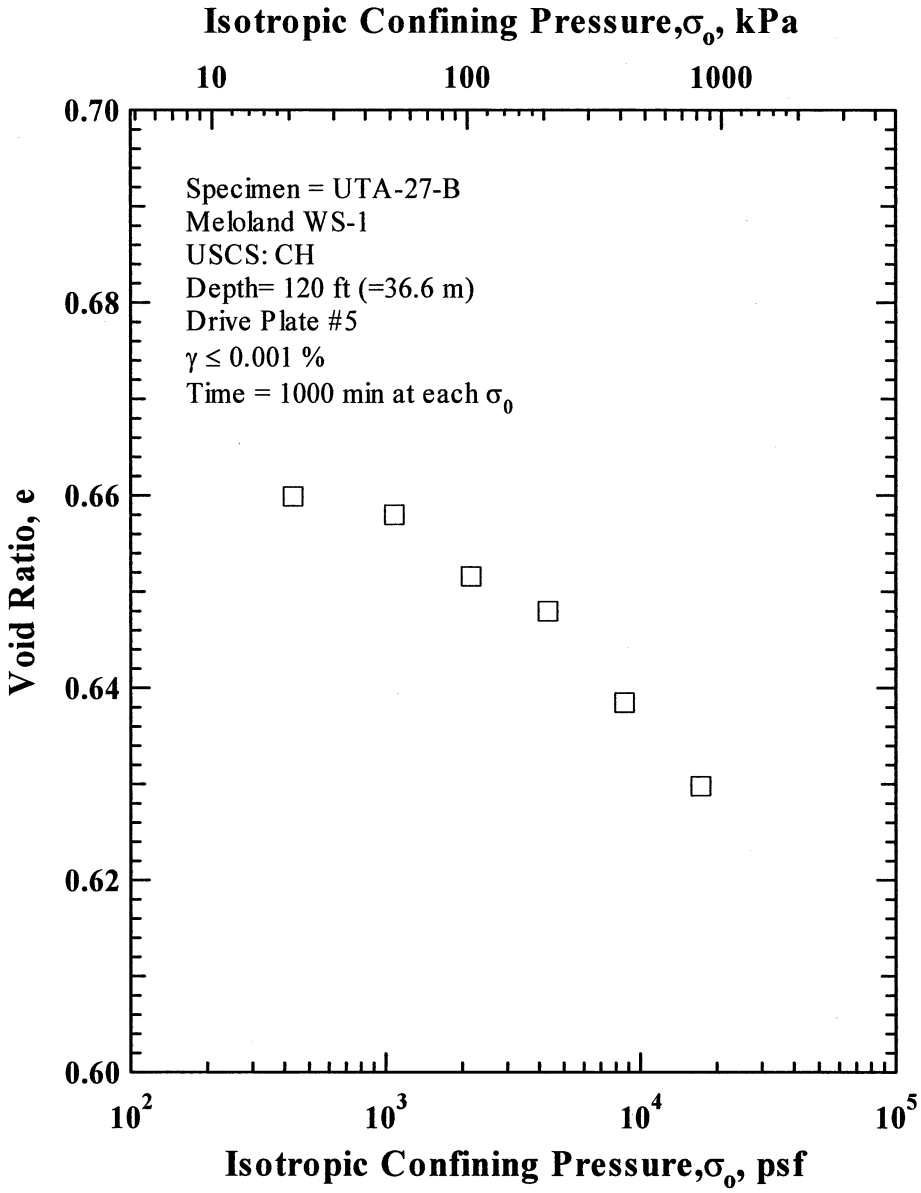

Figure F.7 Variation in Estimated Void Ratio with Isotropic Confining Pressure from Resonant Column Tests of Specimen UTA-27-B.

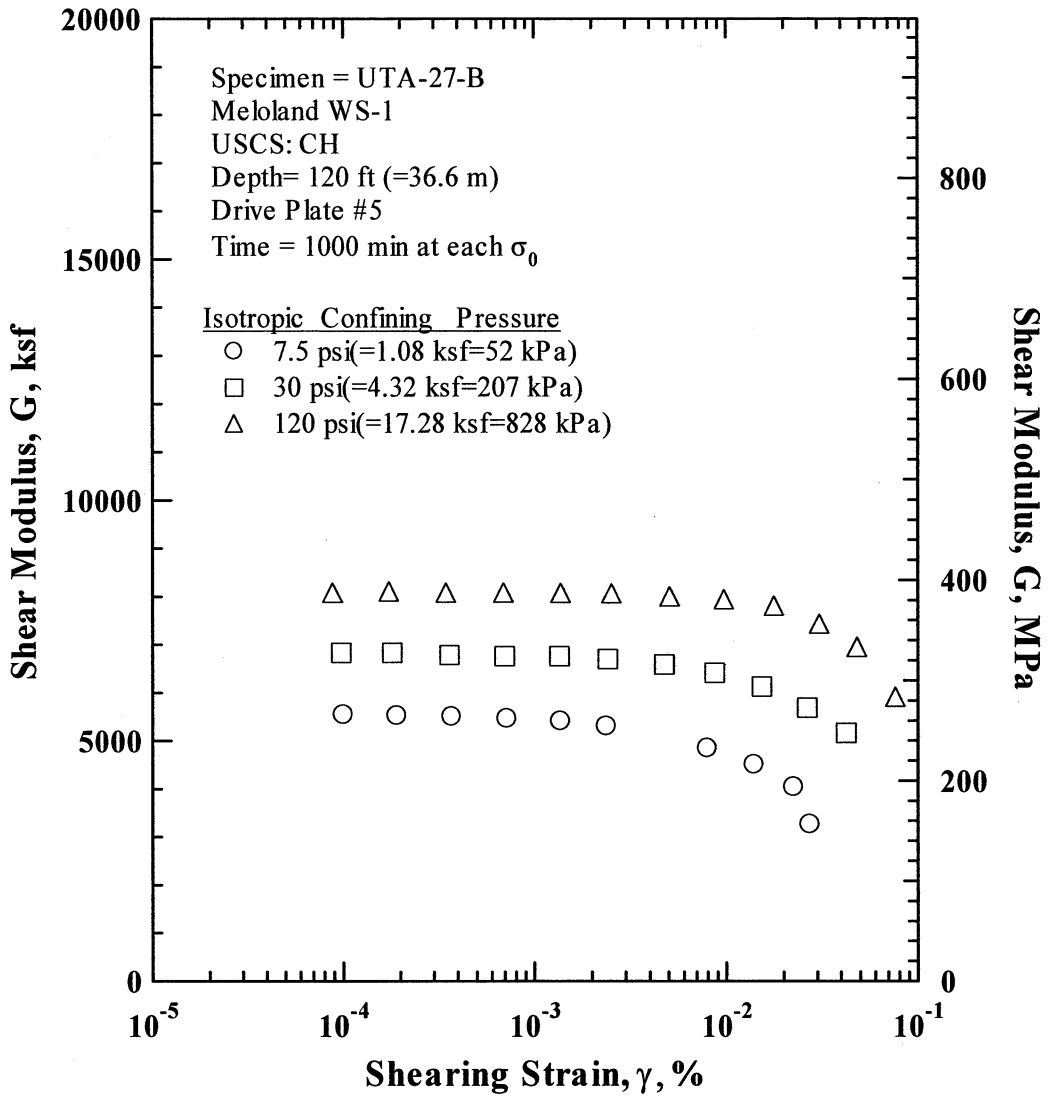

Figure F.8 Comparison of the Variation in Shear Modulus with Shearing Strain and Isotropic Confining Pressure from the Resonant Column Tests of Specimen UTA-27-B.

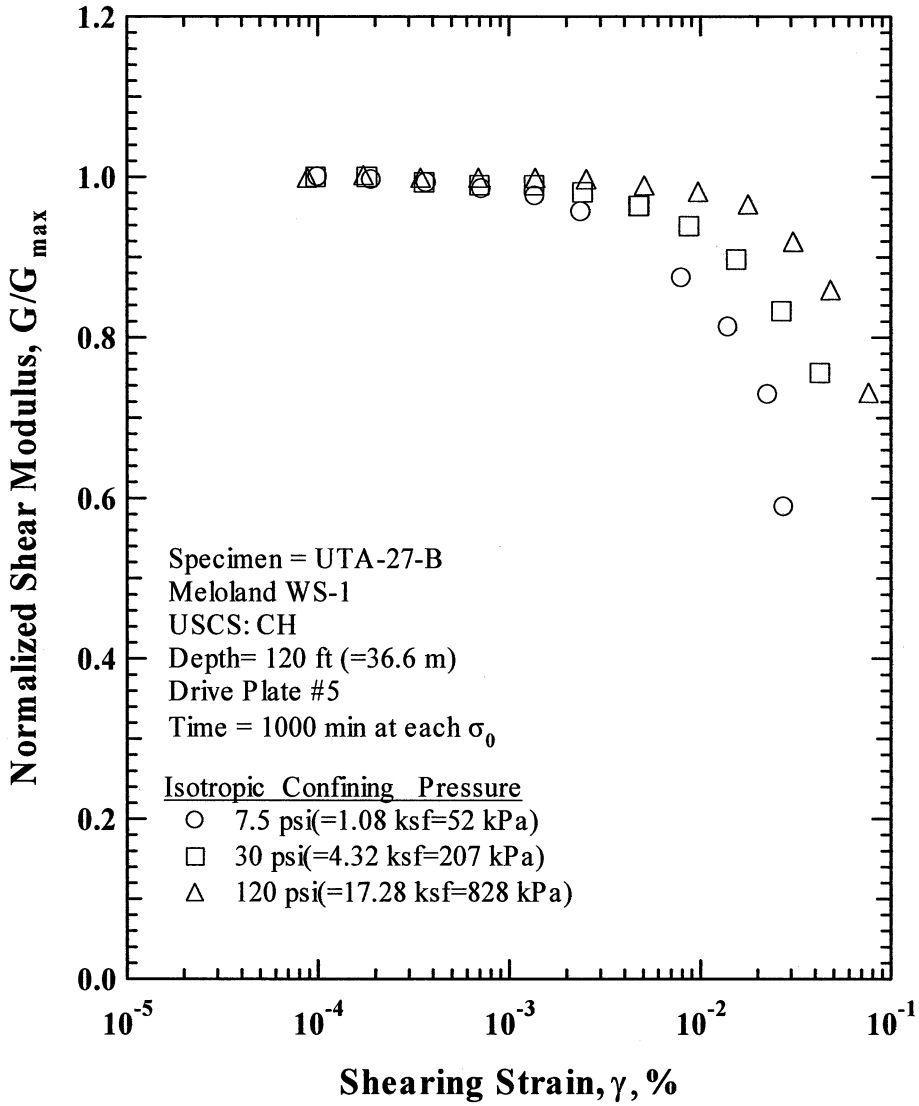

Figure F.9 Comparison of the Variation in Normalized Shear Modulus with Shearing Strain and Isotropic Confining Pressure from the Resonant Column Tests of Specimen UTA-27-B.

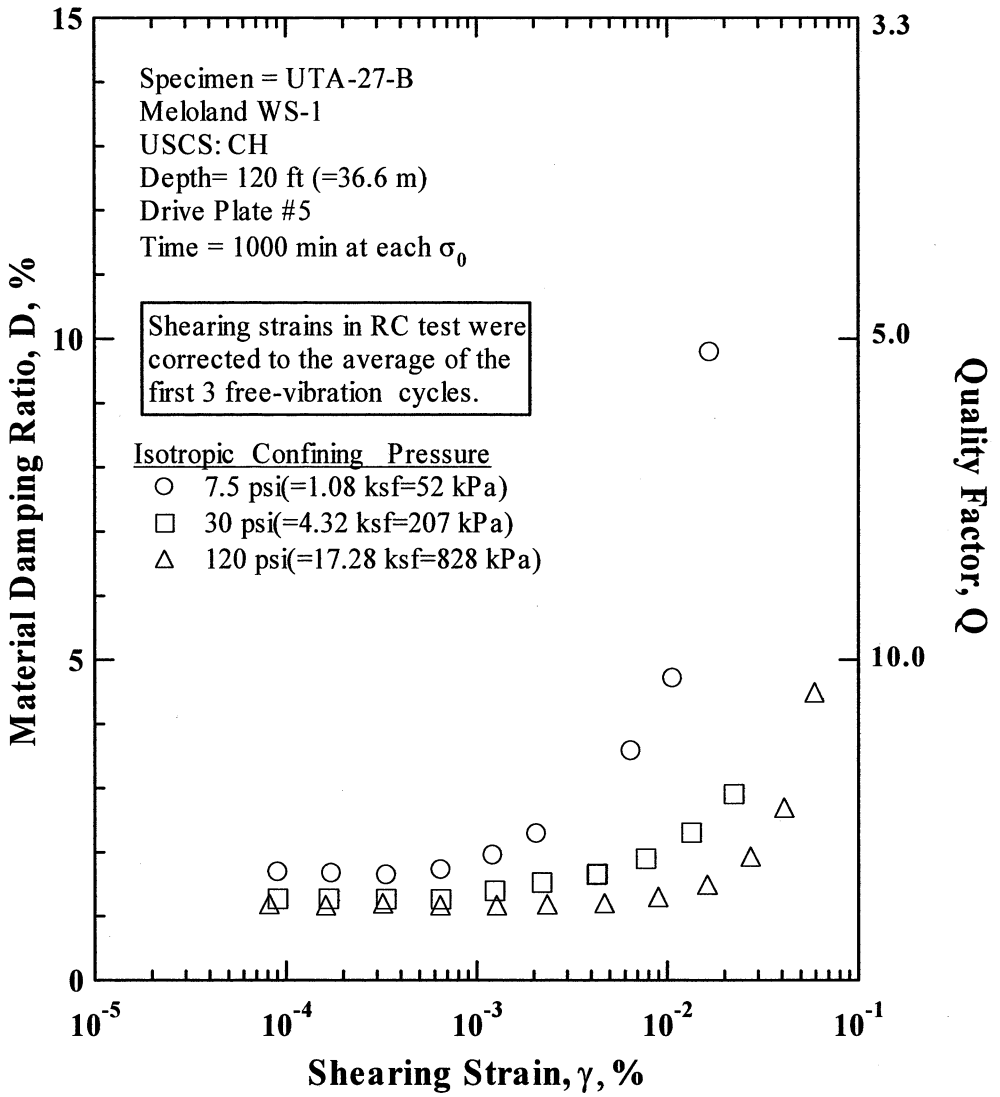

Figure F.10 Comparison of the Variation in Material Damping Ratio with Shearing Strain and Isotropic Confining Pressure from the Resonant Column Tests of Specimen UTA-27-B.

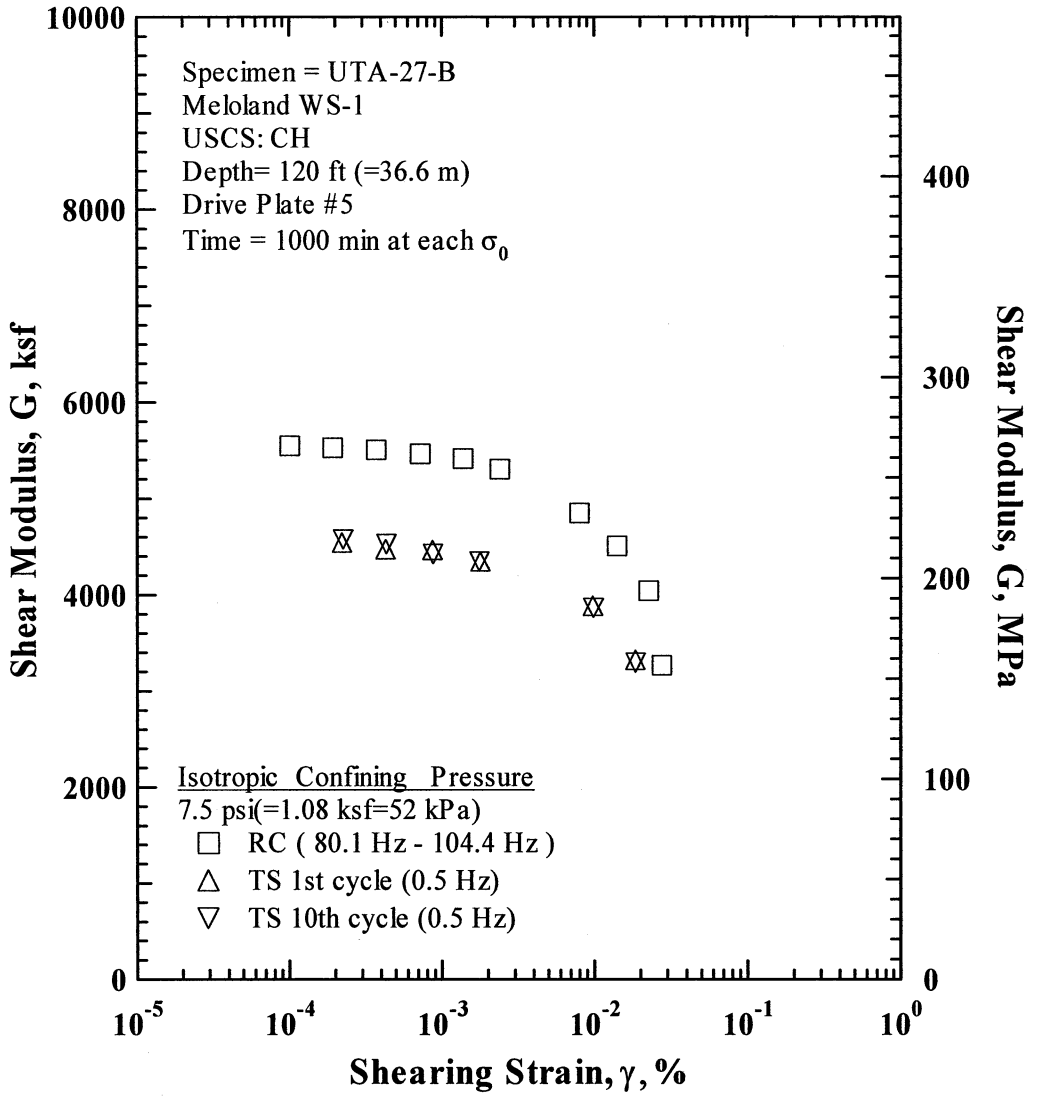

Figure F.11 Comparison of the Variation in Shear Modulus with Shearing Strain at an Isotropic Confining Pressure of 7.5 psi(=1.08 ksf=52 kPa) from the Combined RCTS Tests of Specimen UTA-27-B.

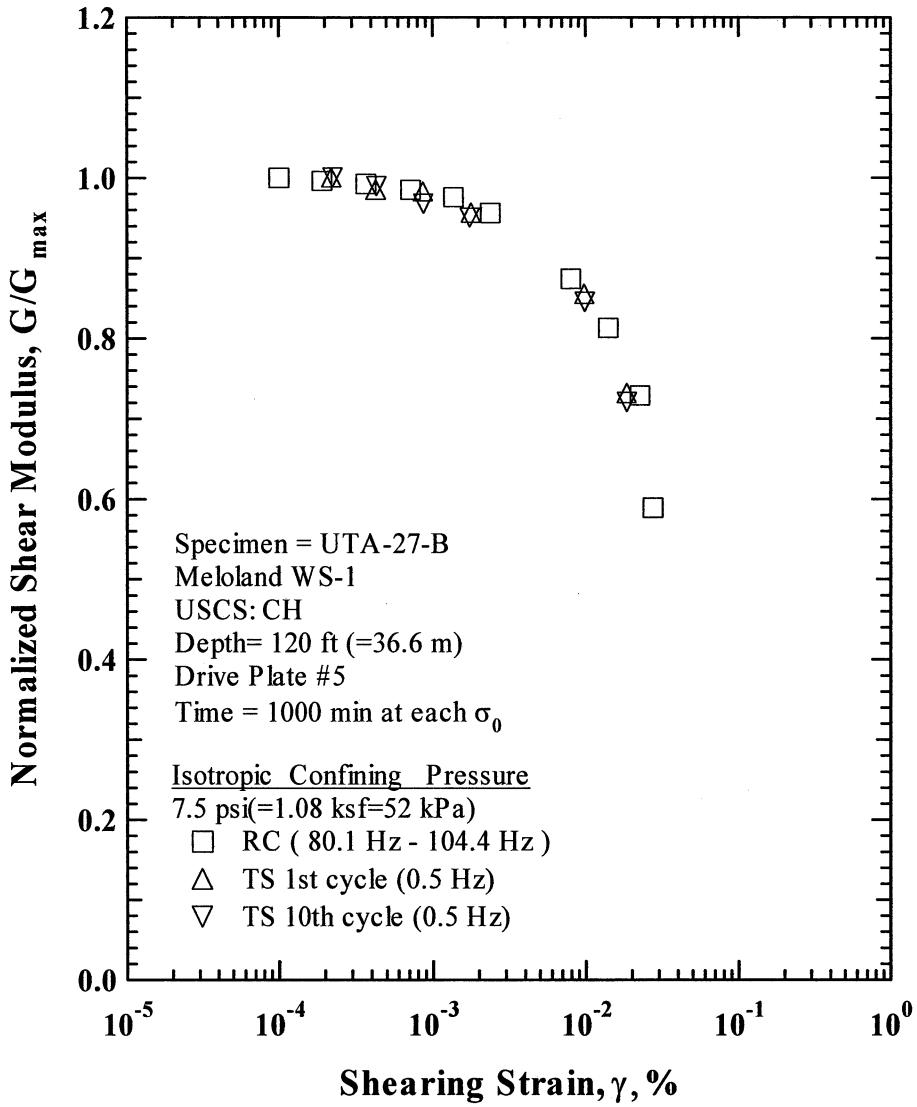

Figure F.12 Comparison of the Variation in Normalized Shear Modulus with Shearing Strain at an Isotropic Confining Pressure of 7.5 psi(=1.08 ksf=52 kPa) from the Combined RCTS Tests of Specimen UTA-27-B.

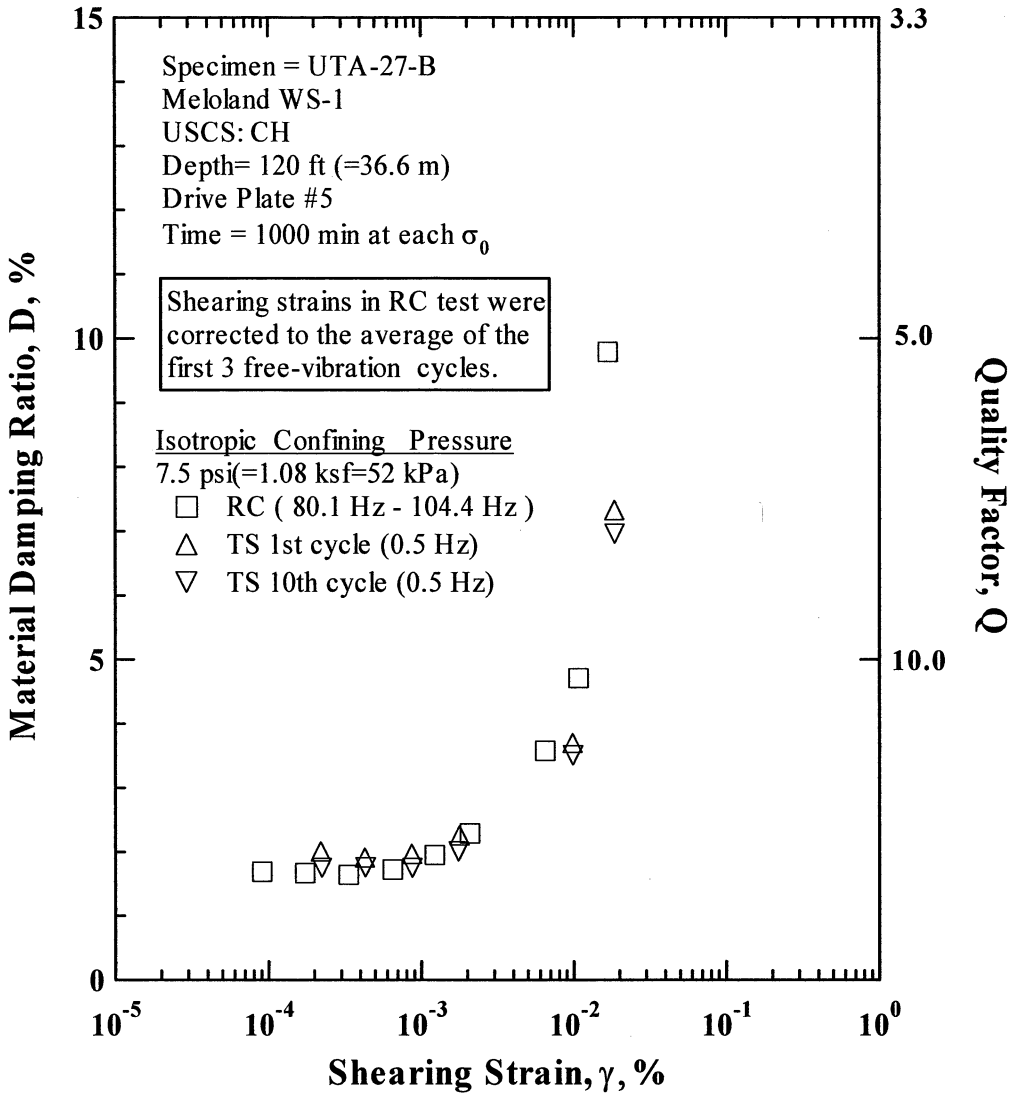

Figure F.13 Comparison of the Variation in Material Damping Ratio with Shearing Strain at an Isotropic Confining Pressure of 7.5 psi(=1.08 ksf=52 kPa) from the Combined RCTS Tests of Specimen UTA-27-B.

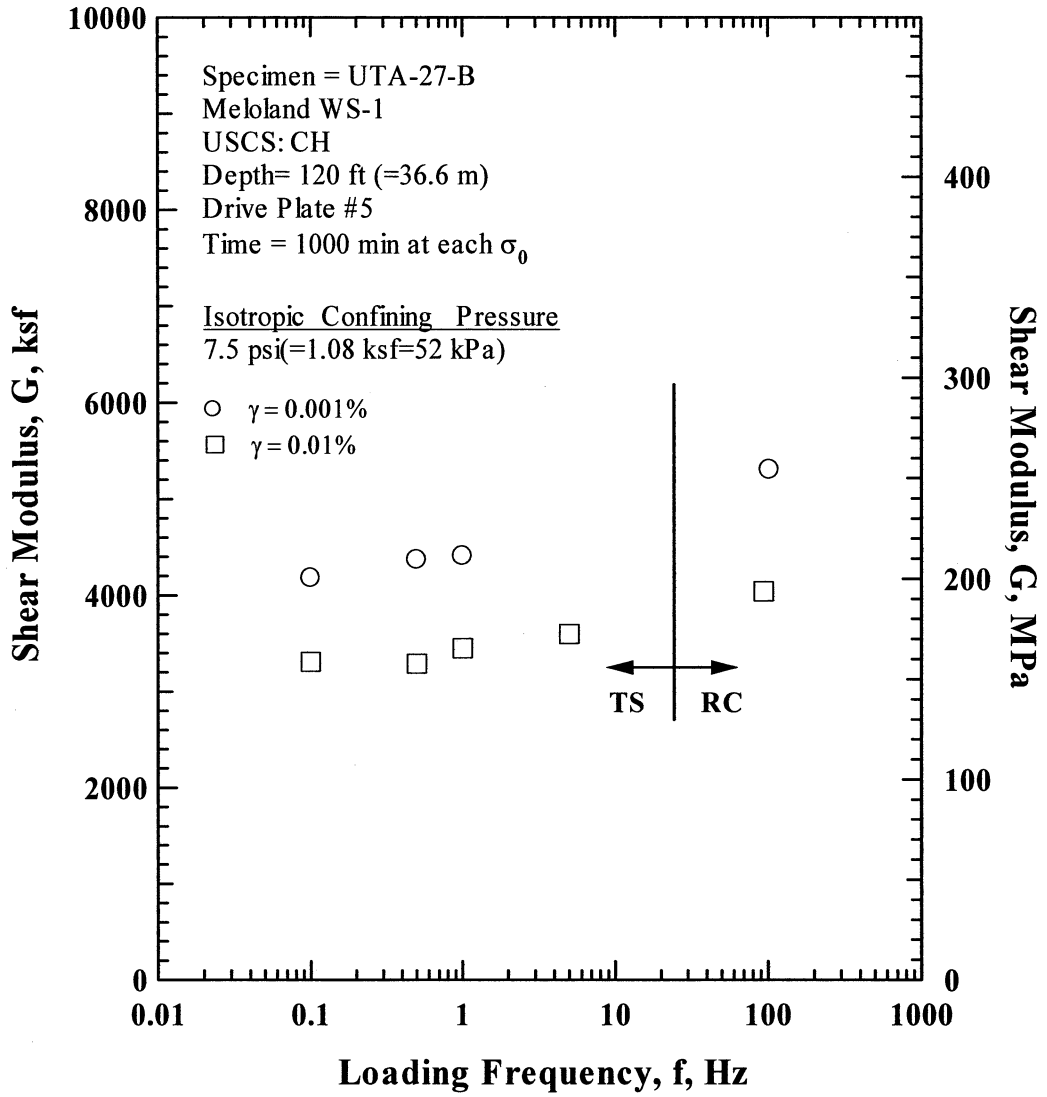

Figure F.14 Comparison of the Variation in Shear Modulus with Loading Frequency at an Isotropic Confining Pressure of 7.5 psi(=1.08 ksf=52 kPa) from the Combined RCTS Tests of Specimen UTA-27-B.

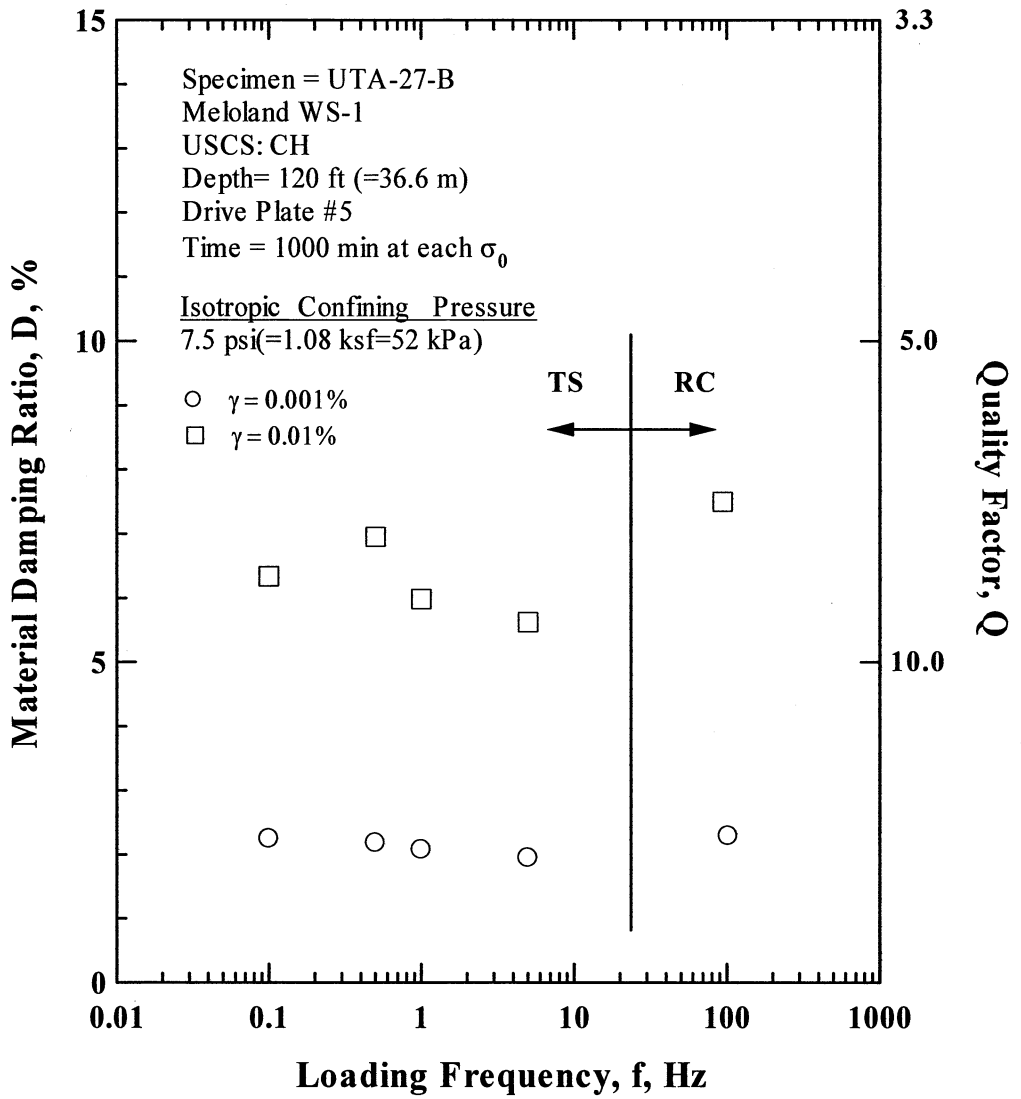

Figure F.15 Comparison of the Variation in Material Damping Ratio with Loading Frequency at an Isotropic Confining Pressure 7.5 psi(=1.08 ksf=52 kPa) from the Combined RCTS Tests of Specimen UTA-27-B.

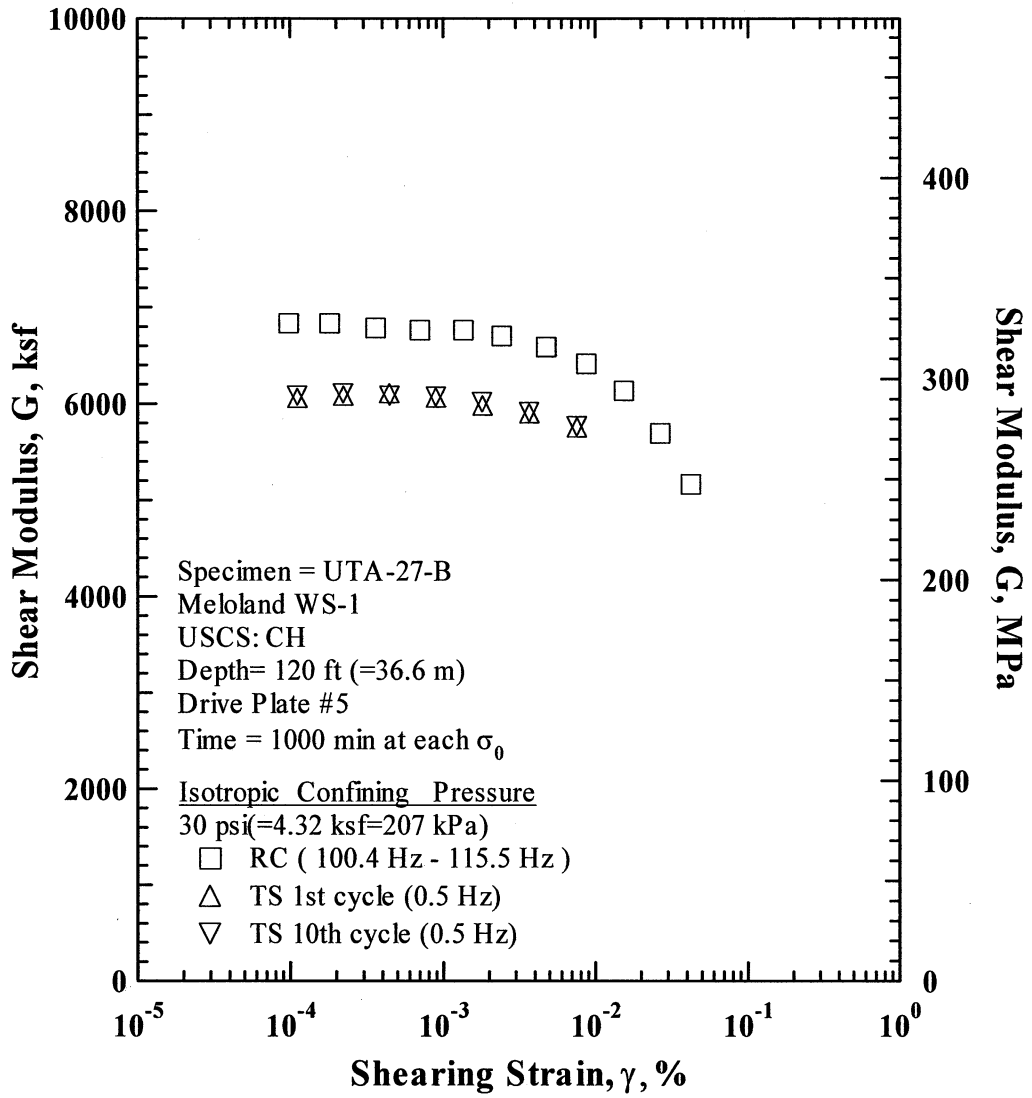

Figure F.16 Comparison of the Variation in Shear Modulus with Shearing Strain at an Isotropic Confining Pressure of 30 psi(=4.32 ksf=207 kPa) from the Combined RCTS Tests of Specimen UTA-27-B.

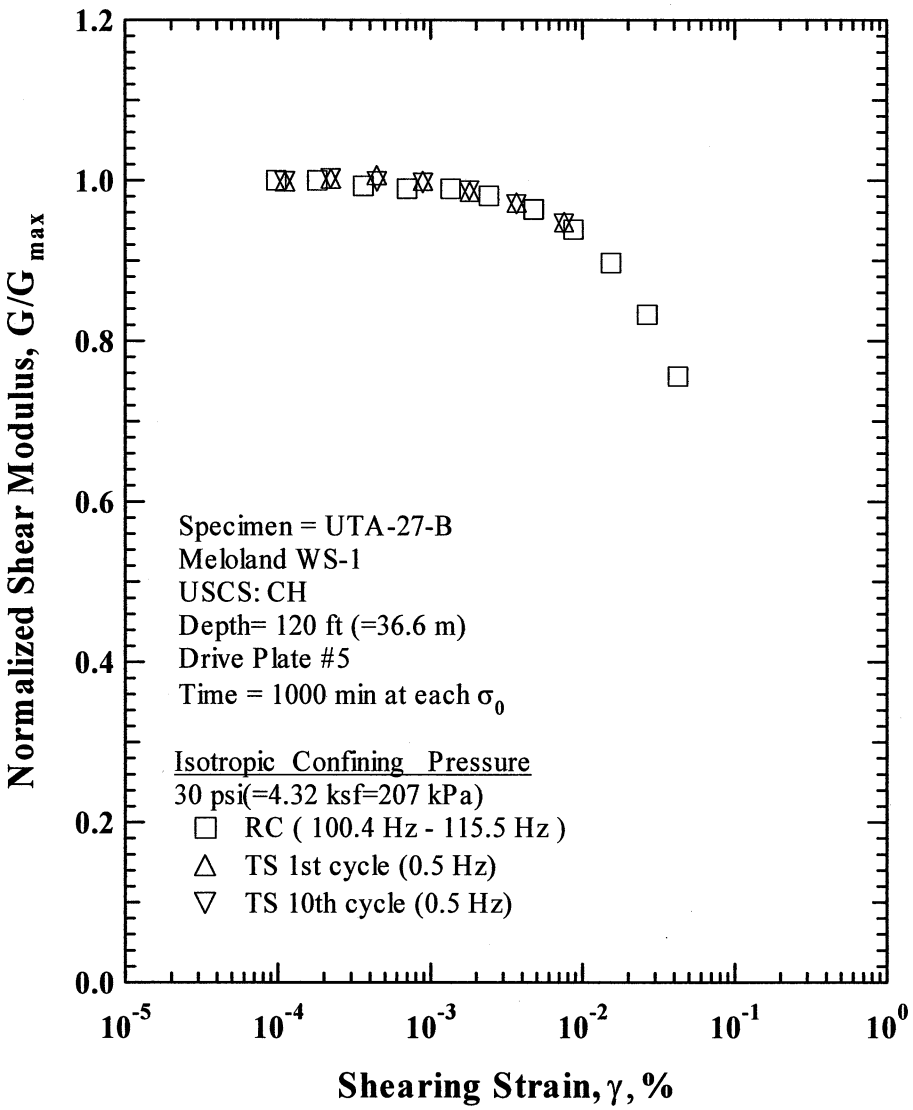

Figure F.17 Comparison of the Variation in Normalized Shear Modulus with Shearing Strain at an Isotropic Confining Pressure of 30 psi(=4.32 ksf=207 kPa) from the Combined RCTS Tests of Specimen UTA-27-B.

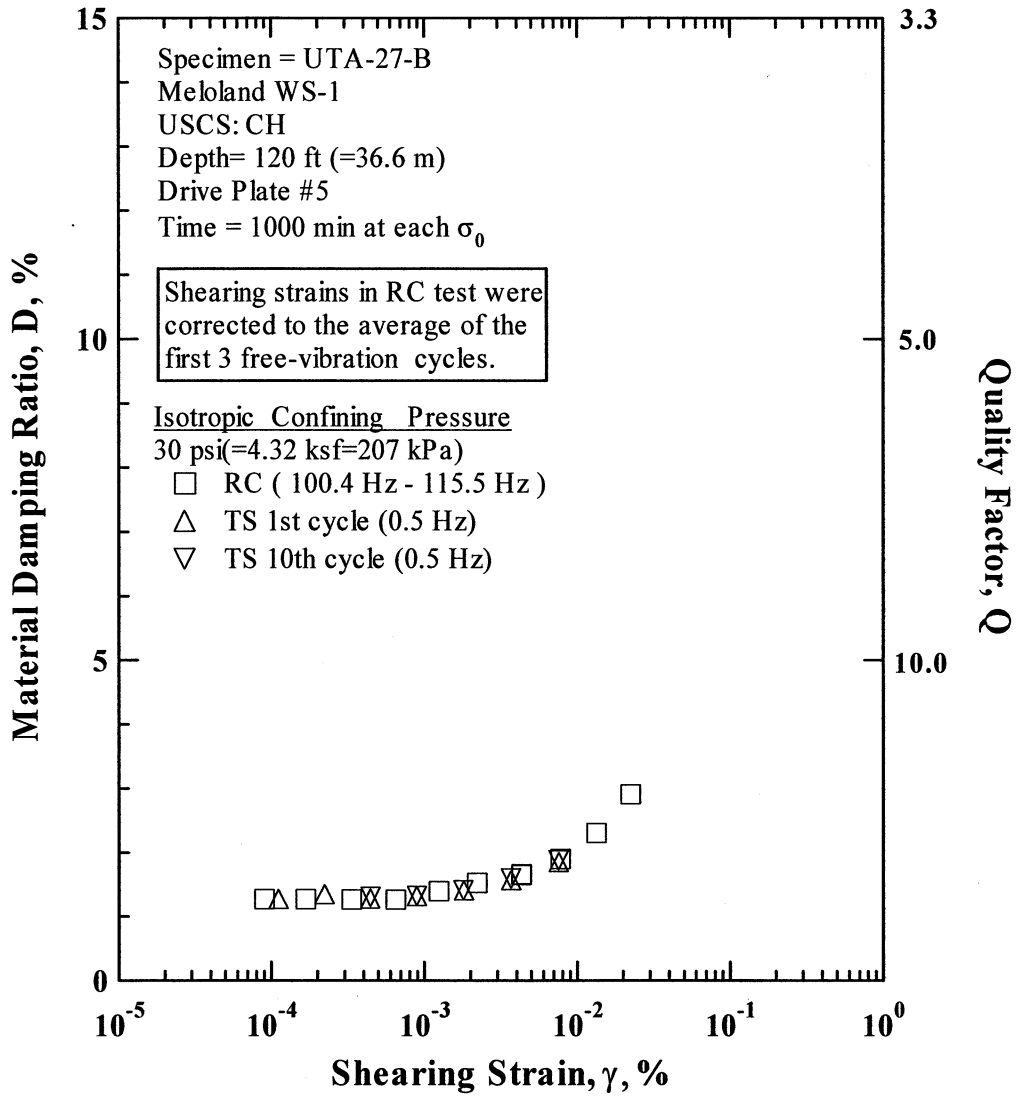

Figure F.18 Comparison of the Variation in Material Damping Ratio with Shearing Strain at an Isotropic Confining Pressure of 30 psi(=4.32 ksf=207 kPa) from the Combined RCTS Tests of Specimen UTA-27-B.

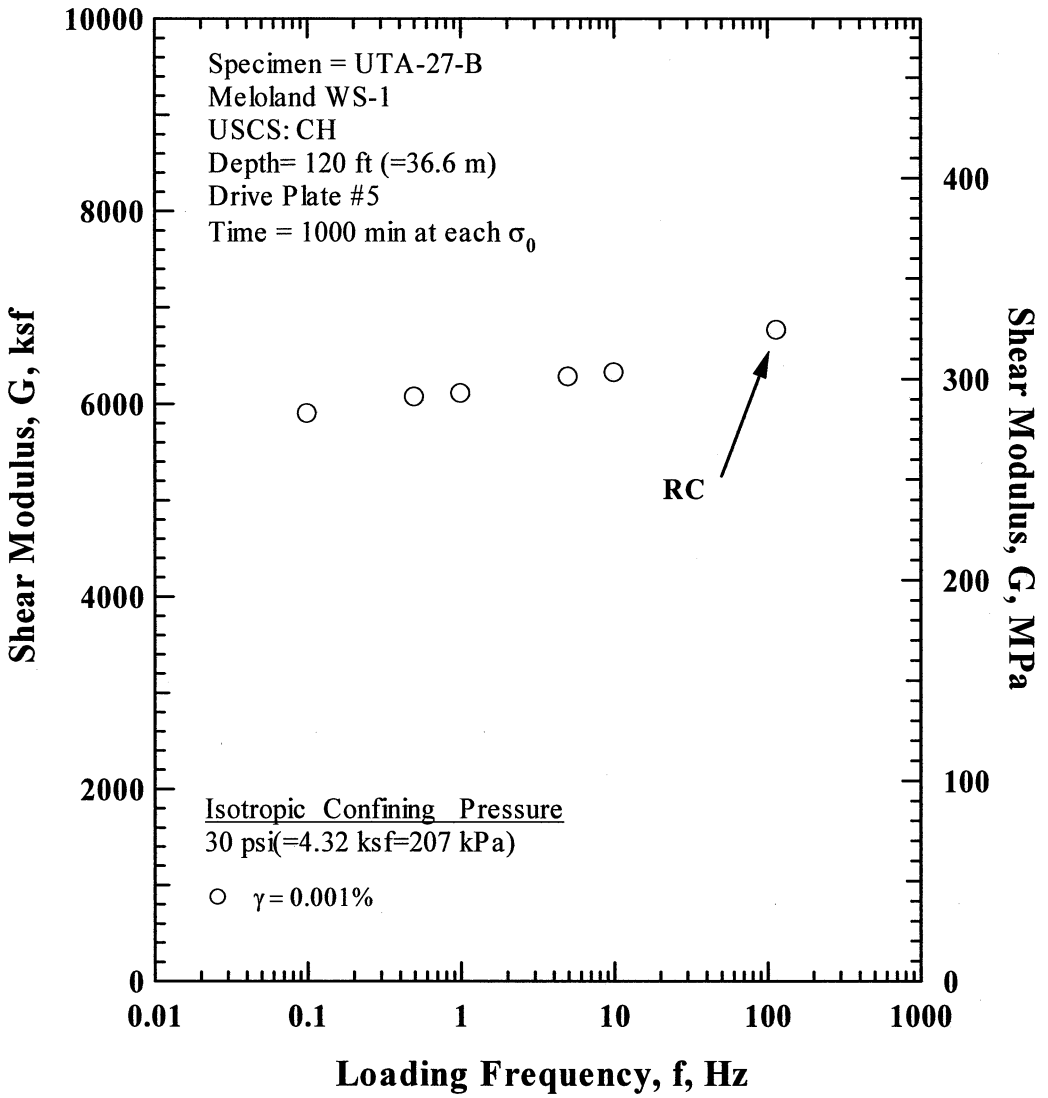

Figure F.19 Comparison of the Variation in Shear Modulus with Loading Frequency at an Isotropic Confining Pressure of 30 psi(=4.32 ksf=207 kPa) from the Combined RCTS Tests of Specimen UTA-27-B.

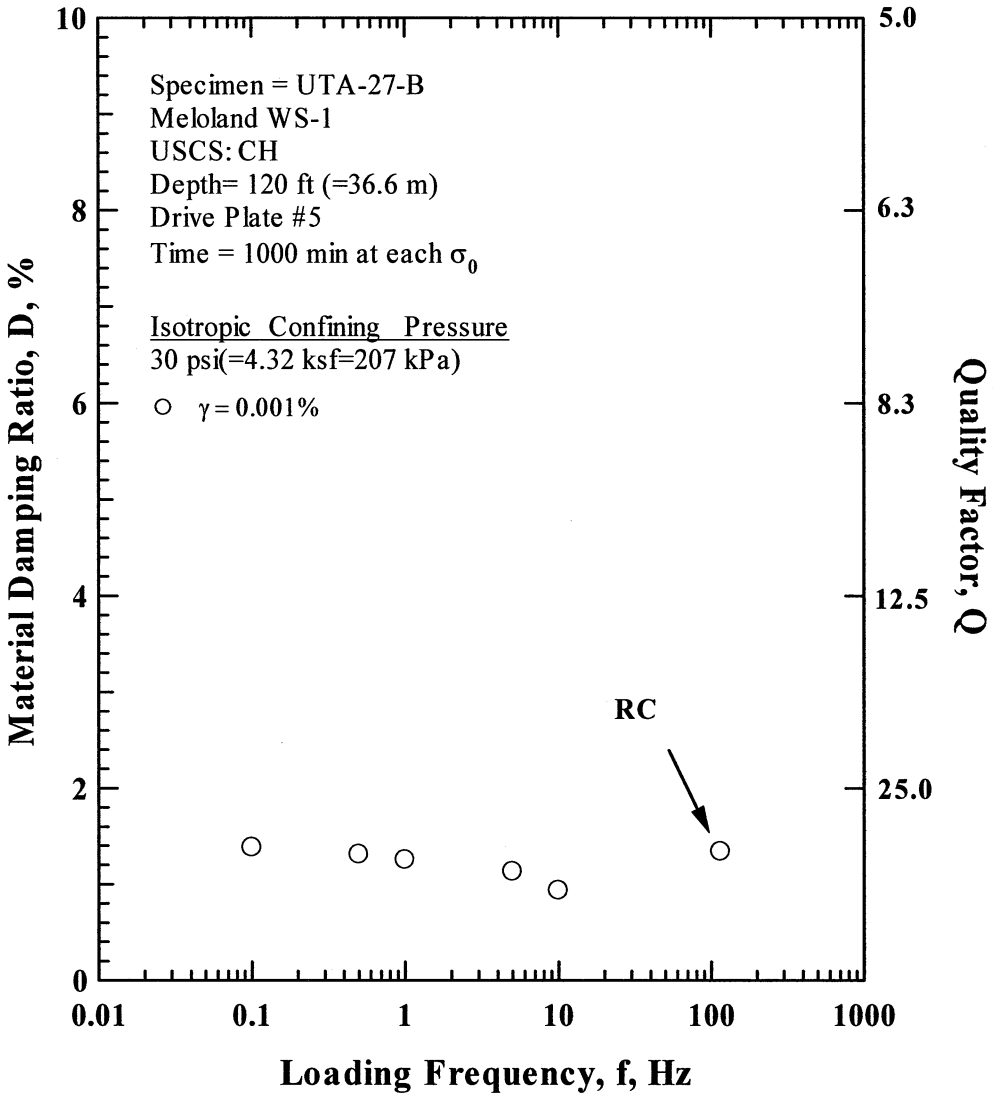

Figure F.20 Comparison of the Variation in Material Damping Ratio with Loading Frequency at an Isotropic Confining Pressure 30 psi(=4.32 ksf=207 kPa) from the Combined RCTS Tests of Specimen UTA-27-B.

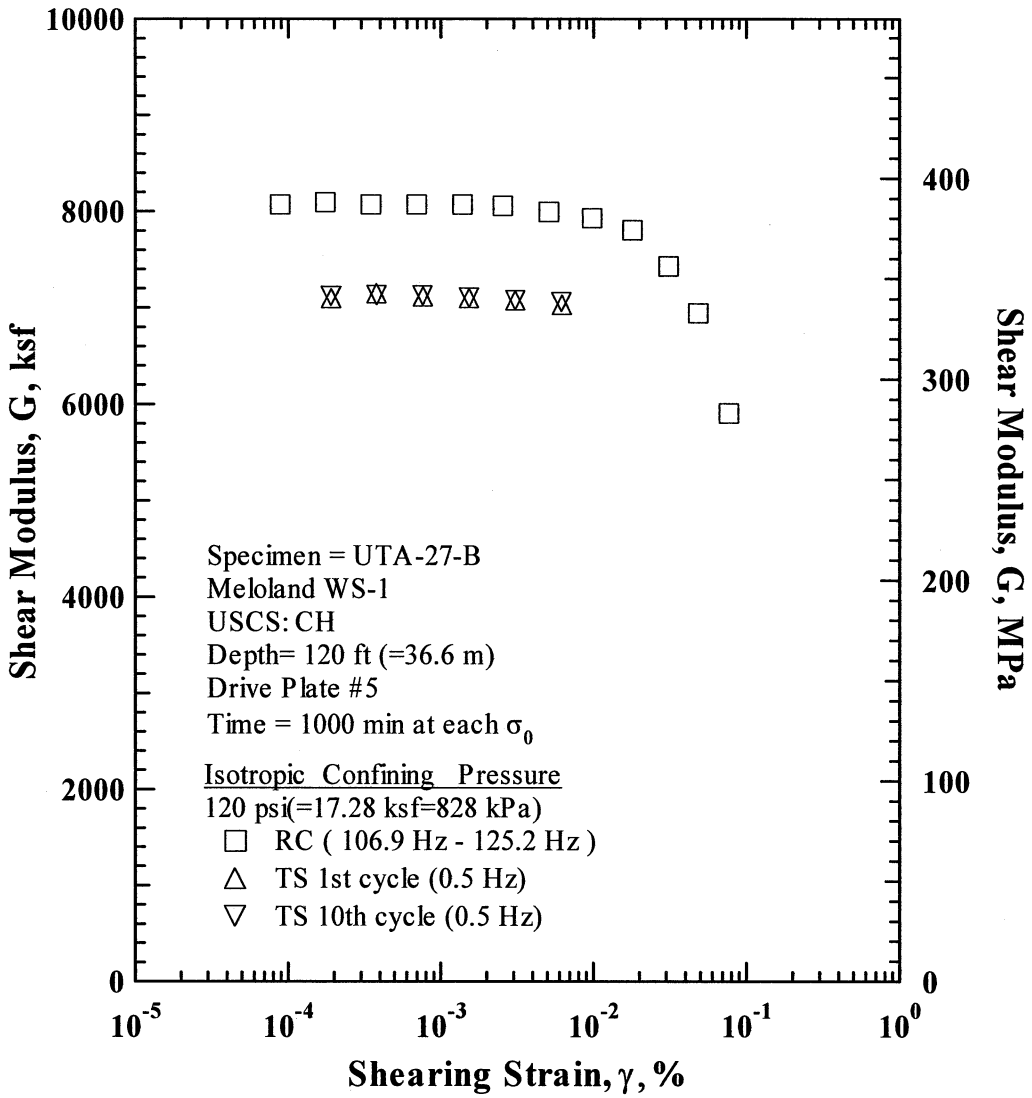

Figure F.21 Comparison of the Variation in Shear Modulus with Shearing Strain at an Isotropic Confining Pressure of 120 psi(=17.28 ksf=828 kPa) from the Combined RCTS Tests of Specimen UTA-27-B.

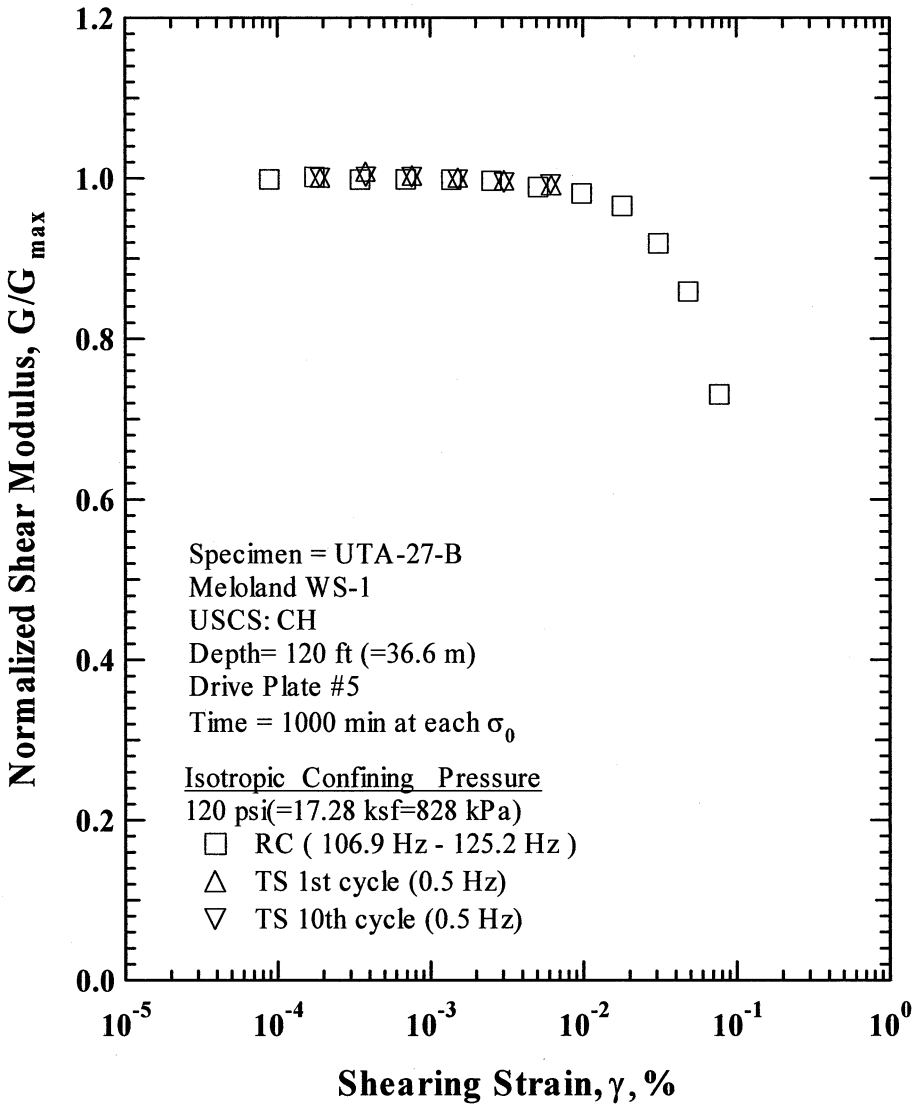

Figure F.22 Comparison of the Variation in Normalized Shear Modulus with Shearing Strain at an Isotropic Confining Pressure of 120 psi(=17.28 ksf=828 kPa) from the Combined RCTS Tests of Specimen UTA-27-B.

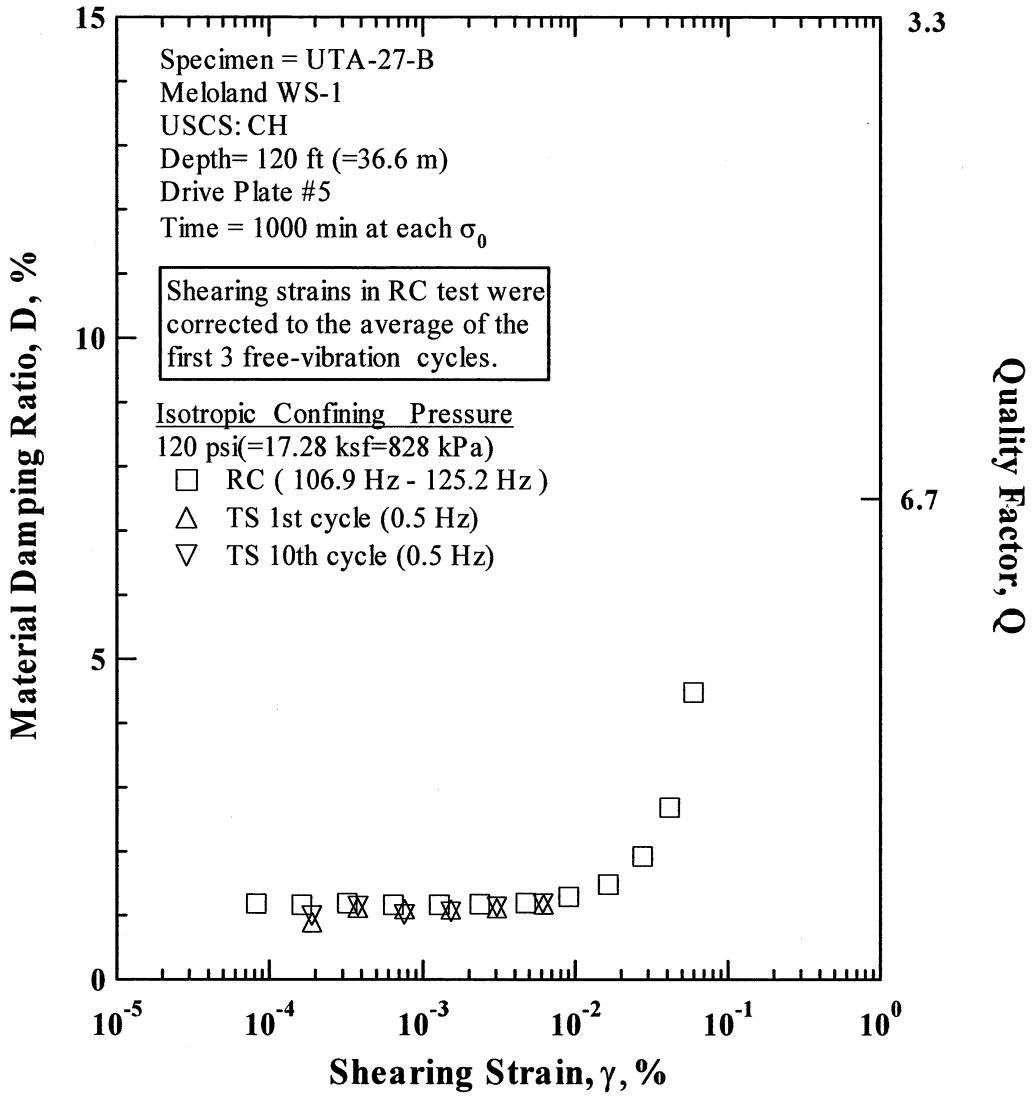

Figure F.23 Comparison of the Variation in Material Damping Ratio with Shearing Strain at an Isotropic Confining Pressure of 120 psi(=17.28 ksf=828 kPa) from the Combined RCTS Tests of Specimen UTA-27-B.

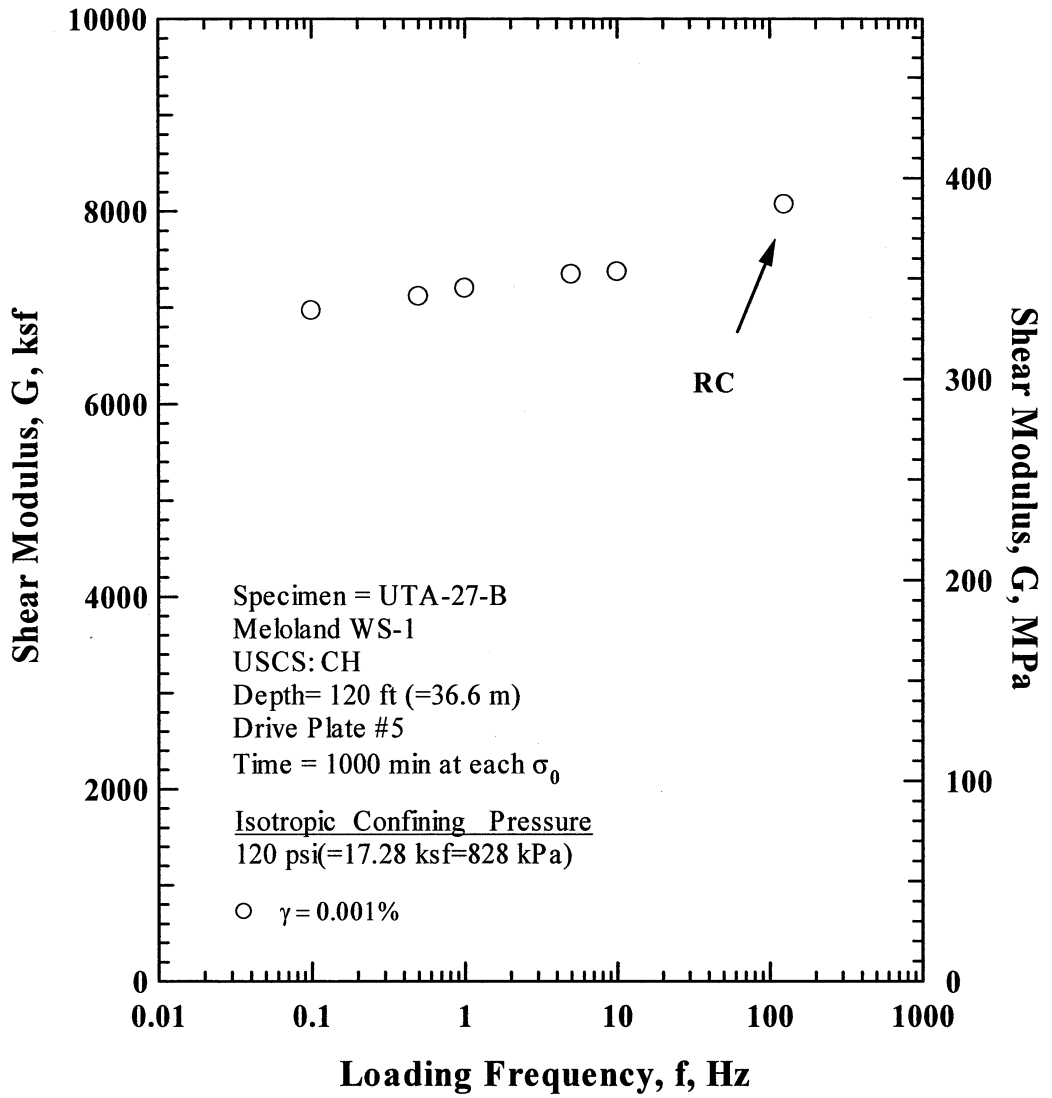

Figure F.24 Comparison of the Variation in Shear Modulus with Loading Frequency at an Isotropic Confining Pressure of 120 psi(=17.28 ksf=828 kPa) from the Combined RCTS Tests of Specimen UTA-27-B.

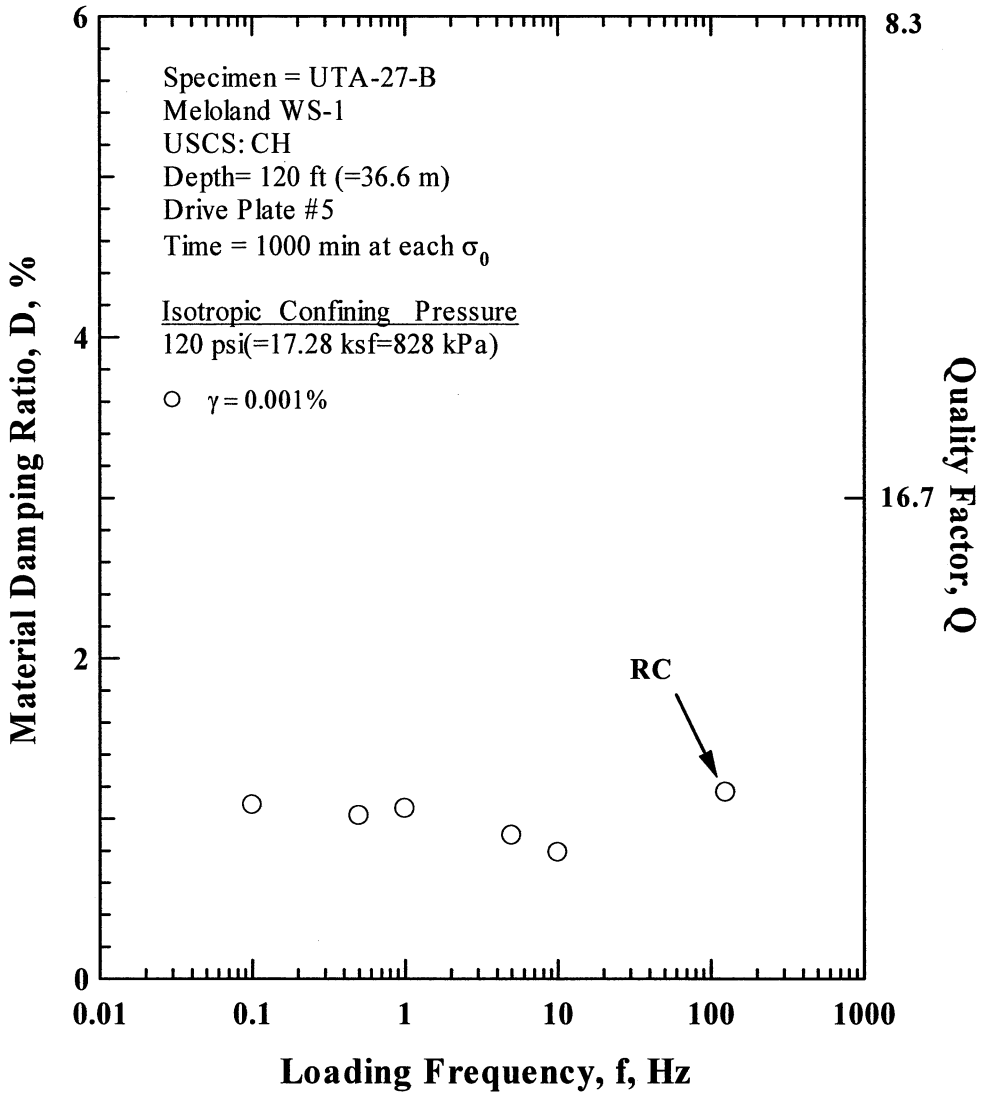

Figure F.25 Comparison of the Variation in Material Damping Ratio with Loading Frequency at an Isotropic Confining Pressure 120 psi(=17.28 ksf=828 kPa) from the Combined RCTS Tests of Specimen UTA-27-B.

Table F.1 Variation in Low-Amplitude Shear Wave Velocity, Low-Amplitude Shear Modulus, Low-Amplitude Material Damping Ratio and Estimated Void Ratio with Isotropic Confining Pressure from RC Tests of Specimen UTA-27-B.

Effective Isotropic Confining Pressure, σ_o'			Low-Amplitude Shear Modulus, G_{max}		Low-Amplitude Shear Wave Velocity, Vs	Low-Amplitude Material Damping Ratio, D_{min}, %	Estimated Void Ratio, e
(psi)	(psf)	(kPa)	(ksf)	(MPa)	(fps)		
3	432	20.7	4675	224.1	1091	2.21	0.660
7.5	1080	51.8	5119	245.4	1141	2.01	0.658
15	2160	103.5	5673	272.0	1200	1.96	0.652
30	4320	207.1	6351	304.5	1269	1.37	0.648
60	8640	414.2	7300	350.0	1358	1.24	0.639
120	17280	828.4	7846	376.1	1406	1.19	0.630

Table F.2 Variation in Shear Modulus, Normalized Shear Modulus and Material Damping Ratio with Shearing Strain from RC Tests of Specimen UTA-27-B; Confining Pressure, σ_o' = 7.5 psi(=1.08 ksf=52 kPa).

Peak Shearing Strain, %	Shear Modulus, G, ksf	Normalized Shear Modulus, G/G_{max}	Average[+] Shearing Strain, %	Material Damping Ratio[x], D, %
1.00E-04	5547	1.00	9.05E-05	1.69
1.92E-04	5526	1.00	1.73E-04	1.67
3.71E-04	5506	0.99	3.36E-04	1.64
7.20E-04	5464	0.98	6.49E-04	1.72
1.37E-03	5413	0.98	1.22E-03	1.95
2.38E-03	5305	0.96	2.07E-03	2.29
7.97E-03	4849	0.87	6.47E-03	3.58
1.40E-02	4508	0.81	1.07E-02	4.71
2.26E-02	4042	0.73	2.26E-02	
2.75E-02	3267	0.59	1.68E-02	9.79

[+] Average Shearing Strain from the First Three Cycles of the Free Vibration Decay Curve

[x] Average Damping Ratio from the First Three Cycles of the Free Vibration Decay Curve

Table F.3 Variation in Shear Modulus, Normalized Shear Modulus and Material Damping Ratio with Shearing Strain from TS Tests of Specimen UTA-25-A; Confining Pressure, σ_o' = 7.5 psi(=1.08 ksf=52 kPa).

First Cycle				Tenth Cycle			
Peak Shearing Strain, %	Shear Modulus, G, ksf	Normalized Shear Modulus, G/G_{max}	Material Damping Ratio, D, %	Peak Shearing Strain, %	Shear Modulus, G, ksf	Normalized Shear Modulus, G/G_{max}	Material Damping Ratio, D, %
2.22E-04	4540	1.00	2.00	2.26E-04	4570	1.00	1.74
4.30E-04	4470	0.98	1.90	4.36E-04	4520	0.99	1.75
8.72E-04	4460	0.98	1.96	8.78E-04	4420	0.97	1.74
1.79E-03	4340	0.96	2.25	1.76E-03	4340	0.95	2.00
9.86E-03	3880	0.85	3.69	9.90E-03	3860	0.84	3.50
1.86E-02	3320	0.73	7.32	1.87E-02	3290	0.72	6.95

Table F.4 Variation in Shear Modulus, Normalized Shear Modulus and Material Damping Ratio with Shearing Strain from RC Tests of Specimen UTA-27-B; Confining Pressure, σ_o' = 30 psi(=4.32 ksf=207 kPa).

Peak Shearing Strain, %	Shear Modulus, G, ksf	Normalized Shear Modulus, G/G_{max}	Average[+] Shearing Strain, %	Material Damping Ratio[x], D, %
1.81E-04	6833	1.00	1.67E-04	1.27
9.75E-05	6834	1.00	9.02E-05	1.27
3.61E-04	6787	0.99	3.34E-04	1.27
7.00E-04	6763	0.99	6.48E-04	1.26
1.36E-03	6763	0.99	1.24E-03	1.39
2.42E-03	6704	0.98	2.20E-03	1.52
4.73E-03	6587	0.96	4.28E-03	1.65
4.76E-03	6588	0.96	4.31E-03	1.66
8.70E-03	6414	0.94	7.76E-03	1.90
1.54E-02	6132	0.90	1.34E-02	2.30
2.66E-02	5692	0.83	2.24E-02	2.91
4.23E-02	5165	0.76		

[+] Average Shearing Strain from the First Three Cycles of the Free Vibration Decay Curve

[x] Average Damping Ratio from the First Three Cycles of the Free Vibration Decay Curve

Table F.5 Variation in Shear Modulus, Normalized Shear Modulus and Material Damping Ratio with Shearing Strain from TS Tests of Specimen UTA-27-B; Confining Pressure, σ_o' = 30 psi(=4.32 ksf=207 kPa).

First Cycle				Tenth Cycle			
Peak Shearing Strain, %	Shear Modulus, G, ksf	Normalized Shear Modulus, G/G_{max}	Material Damping Ratio, D, %	Peak Shearing Strain, %	Shear Modulus, G, ksf	Normalized Shear Modulus, G/G_{max}	Material Damping Ratio, D, %
1.12E-04	6056	1.00	1.27	1.12E-04	6078	1.00	
2.23E-04	6079	1.00	1.34	2.23E-04	6101	1.00	
4.45E-04	6104	1.01	1.27	4.47E-04	6078	1.00	1.30
8.98E-04	6060	1.00	1.31	8.97E-04	6066	1.00	1.31
1.82E-03	5978	0.99	1.40	1.81E-03	6011	0.99	1.40
3.69E-03	5897	0.97	1.56	3.69E-03	5905	0.97	1.59
7.59E-03	5749	0.95	1.84	7.58E-03	5759	0.95	1.87

Table F.6 Variation in Shear Modulus, Normalized Shear Modulus and Material Damping Ratio with Shearing Strain from RC Tests of Specimen UTA-27-B; Confining Pressure, σ_o' = 120 psi(=17.3 ksf=828 kPa).

Peak Shearing Strain, %	Shear Modulus, G, ksf	Normalized Shear Modulus, G/G_{max}	Average[+] Shearing Strain, %	Material Damping Ratio[x], D, %
1.75E-04	8097	1.00	1.63E-04	1.17
8.83E-05	8073	1.00	8.21E-05	1.19
3.47E-04	8072	1.00	3.23E-04	1.19
6.93E-04	8073	1.00	6.45E-04	1.16
1.38E-03	8070	1.00	1.28E-03	1.16
2.54E-03	8058	1.00	2.36E-03	1.18
5.09E-03	7995	0.99	4.73E-03	1.19
9.77E-03	7931	0.98	9.03E-03	1.29
1.79E-02	7804	0.97	1.64E-02	1.48
3.09E-02	7429	0.92	2.75E-02	1.92
4.85E-02	6942	0.86	4.13E-02	2.69
7.66E-02	5907	0.73	5.93E-02	4.48

[+] Average Shearing Strain from the First Three Cycles of the Free Vibration Decay Curve

[x] Average Damping Ratio from the First Three Cycles of the Free Vibration Decay Curve

Table F.7 Variation in Shear Modulus, Normalized Shear Modulus and Material Damping Ratio with Shearing Strain from TS Tests of Specimen UTA-27-B; Confining Pressure, σ_o' = 120 psi(=17.3 ksf=828 kPa).

First Cycle				Tenth Cycle			
Peak Shearing Strain, %	Shear Modulus, G, ksf	Normalized Shear Modulus, G/G_{max}	Material Damping Ratio, D, %	Peak Shearing Strain, %	Shear Modulus, G, ksf	Normalized Shear Modulus, G/G_{max}	Material Damping Ratio, D, %
1.92E-04	7094	1.00	0.88	1.91E-04	7116	1.00	0.99
3.81E-04	7147	1.01	1.11	3.82E-04	7125	1.00	1.14
7.67E-04	7112	1.00	1.09	7.65E-04	7121	1.00	1.01
1.54E-03	7094	1.00	1.09	1.54E-03	7100	1.00	1.05
3.09E-03	7070	1.00	1.11	3.08E-03	7073	0.99	1.13
6.22E-03	7027	0.99	1.17	6.19E-03	7056	0.99	1.18

APPENDIX G

Specimen No. 6
UT Specimen ID: UTA-27-A

Meloland WS-3
Depth = 200 ft (=61.0m)
Soil Type: Clay (CH)

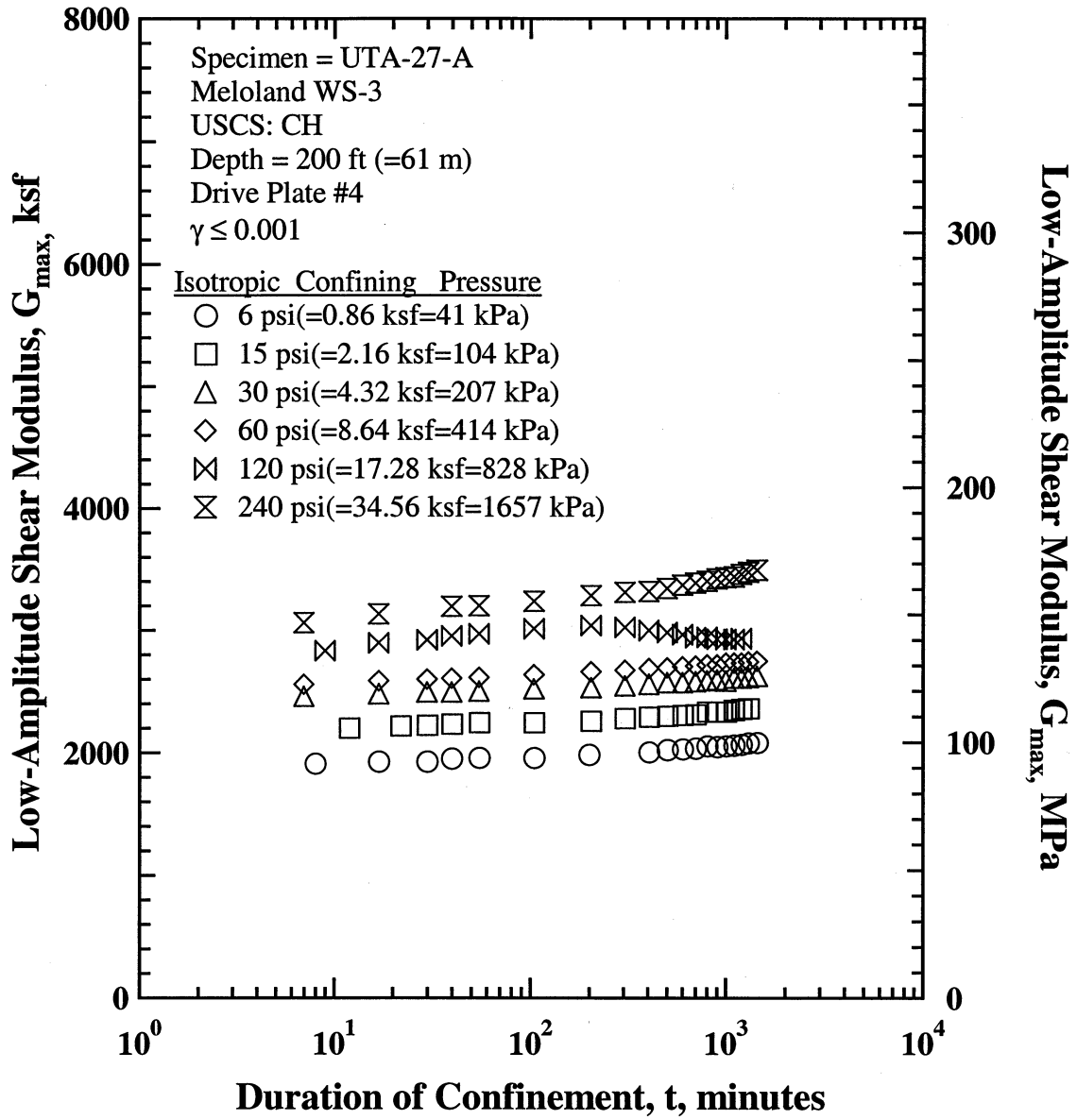

Figure G.1 Variation in Low-Amplitude Shear Modulus with Magnitude and Duration of Isotropic Confining Pressure from Resonant Column Tests of Specimen UTA-27-A.

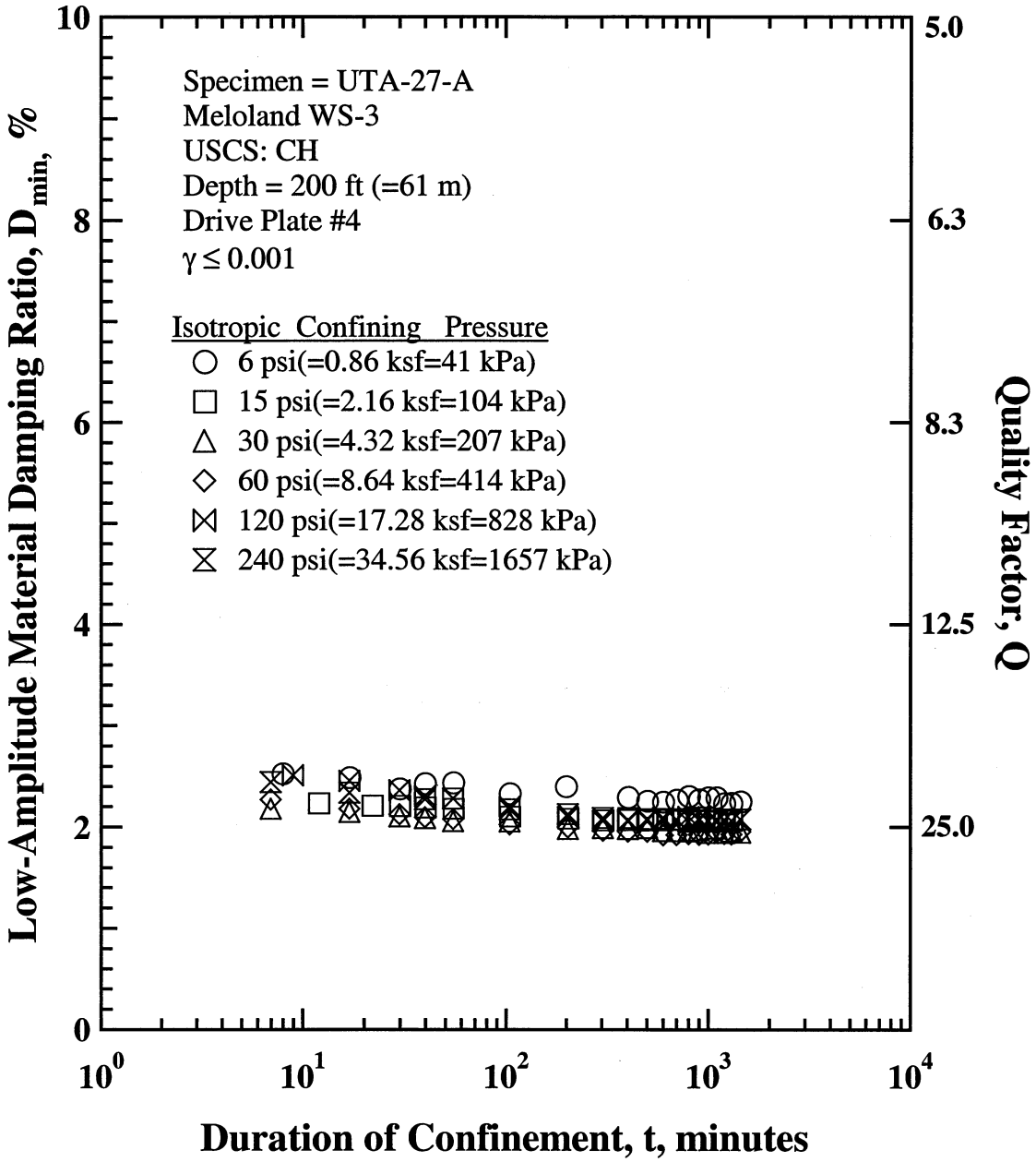

Figure G.2 Variation in Low-Amplitude Material Damping Ratio with Magnitude and Duration of Isotropic Confining Pressure from Resonant Column Tests of Specimen UTA-27-A

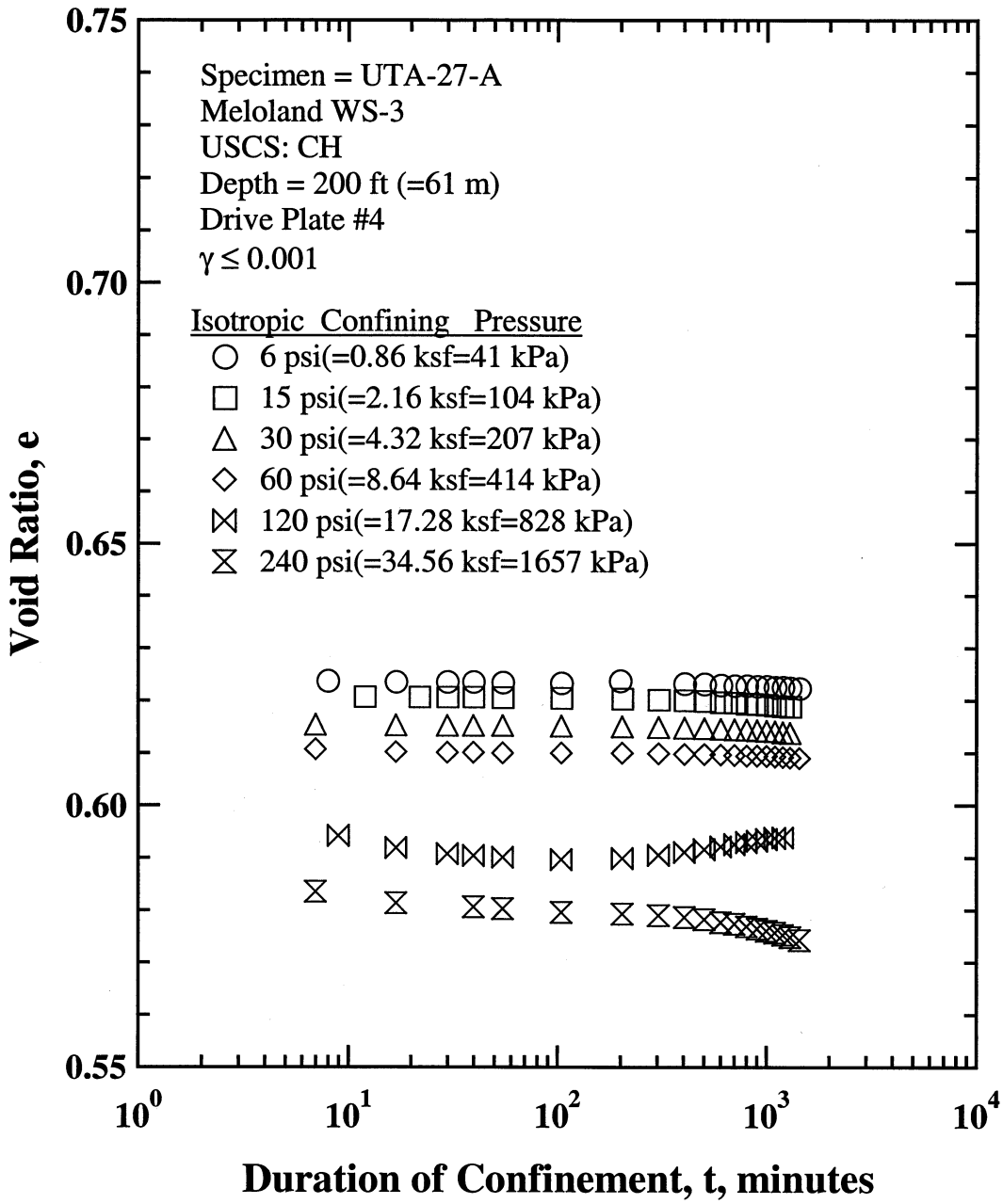

Figure G.3 Variation in Estimated Void Ratio with Magnitude and Duration of Isotropic Confining Pressure from Resonant Column Tests of Specimen UTA-27-A.

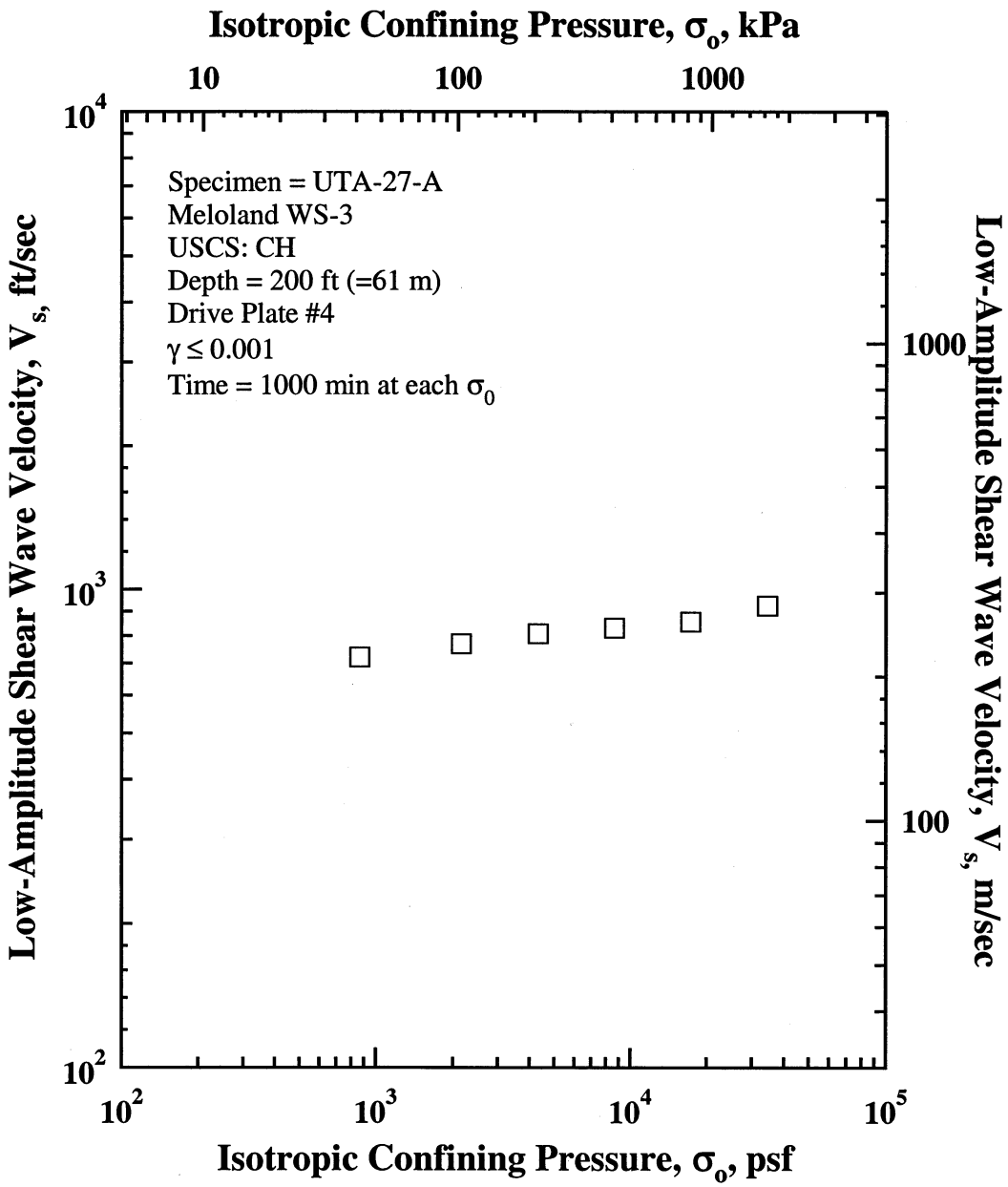

Figure G.4 Variation in Low-Amplitude Shear Wave Velocity with Isotropic Confining Pressure from Resonant Column Tests of Specimen UTA-27-A.

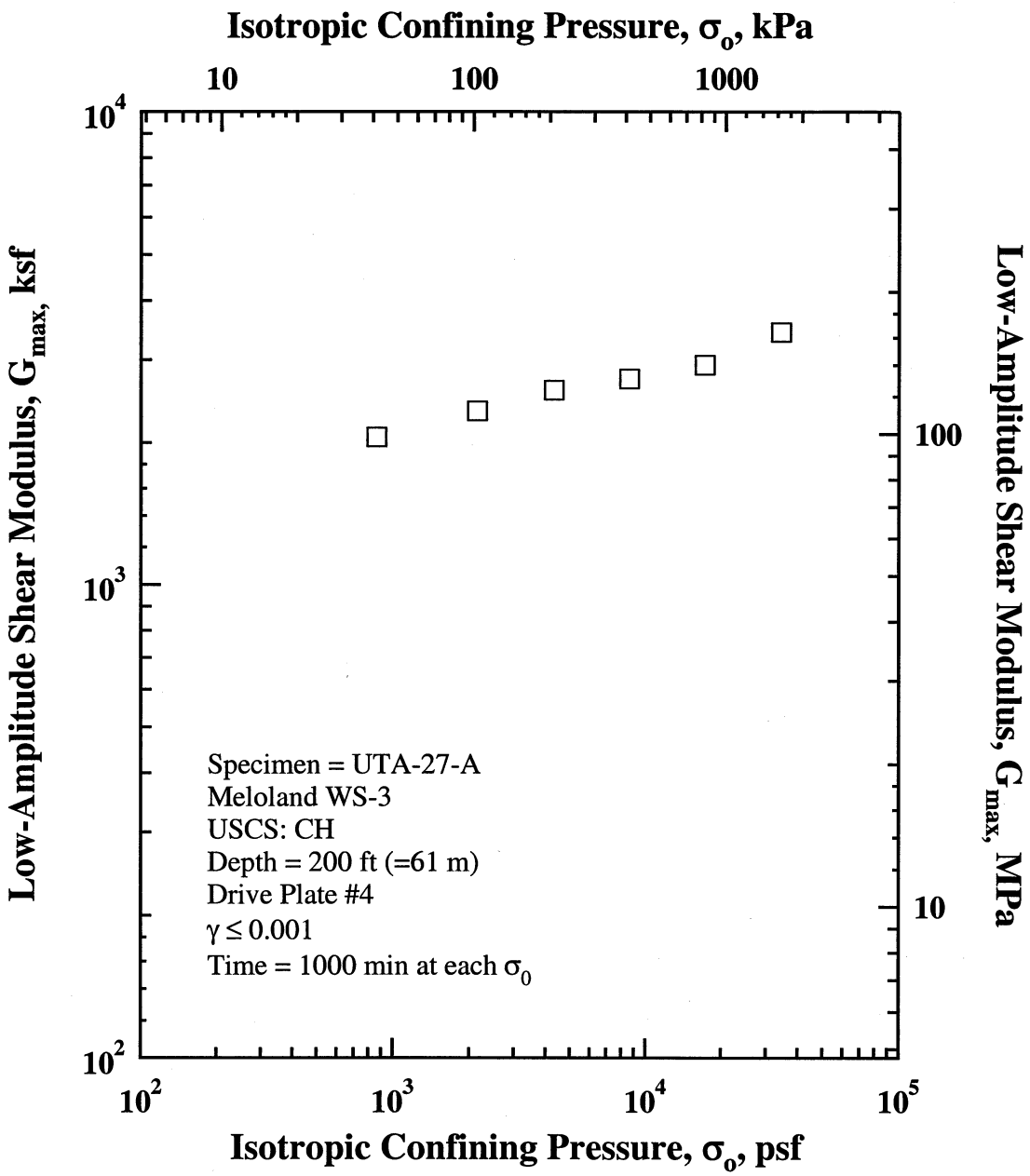

Figure G.5 Variation in Low-Amplitude Shear Modulus with Isotropic Confining Pressure from Resonant Column Tests of Specimen UTA-27-A.

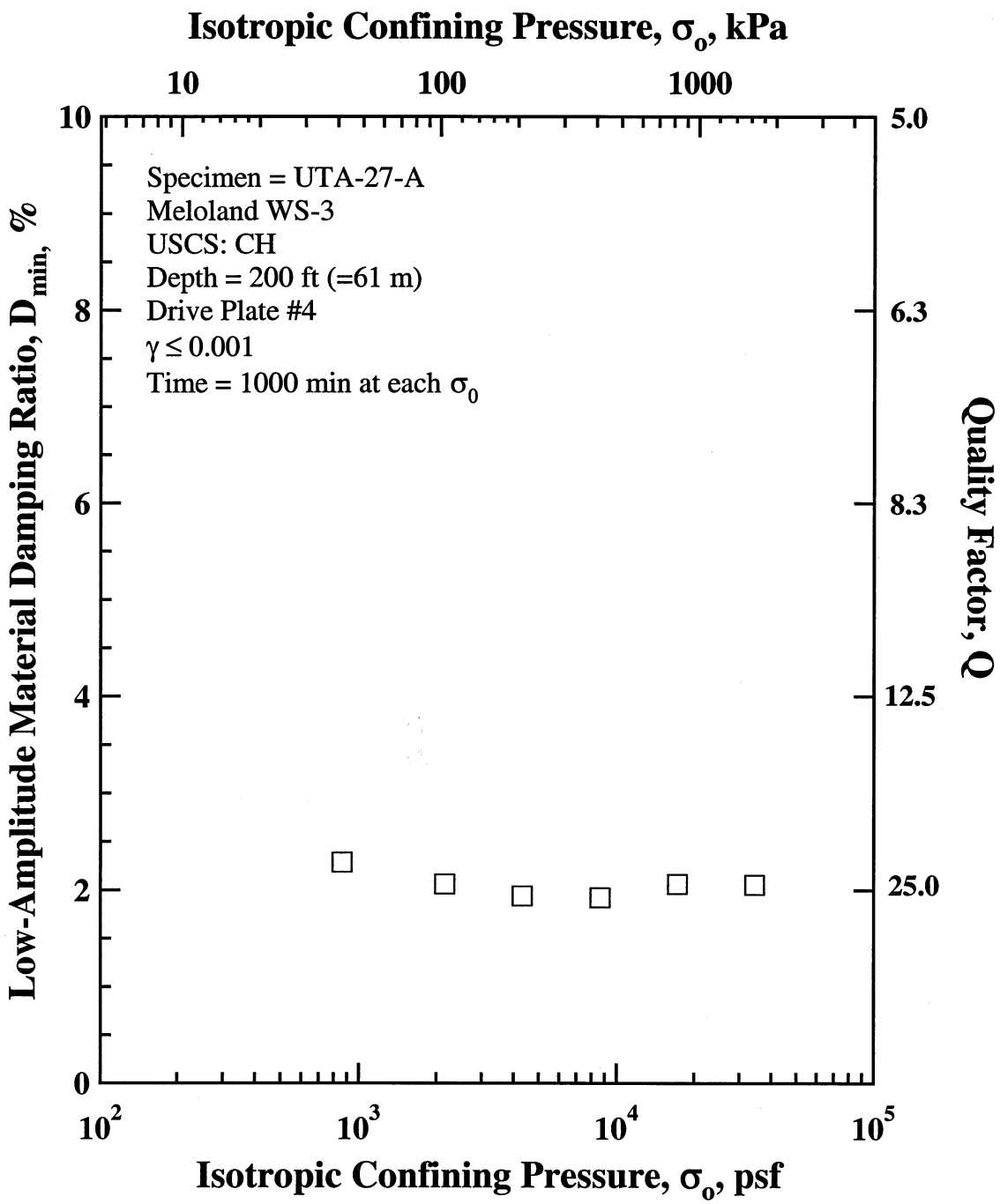

Figure G.6 Variation in Material Damping Ratio with Isotropic Confining Pressure from Resonant Column Tests of Specimen UTA-27-A.

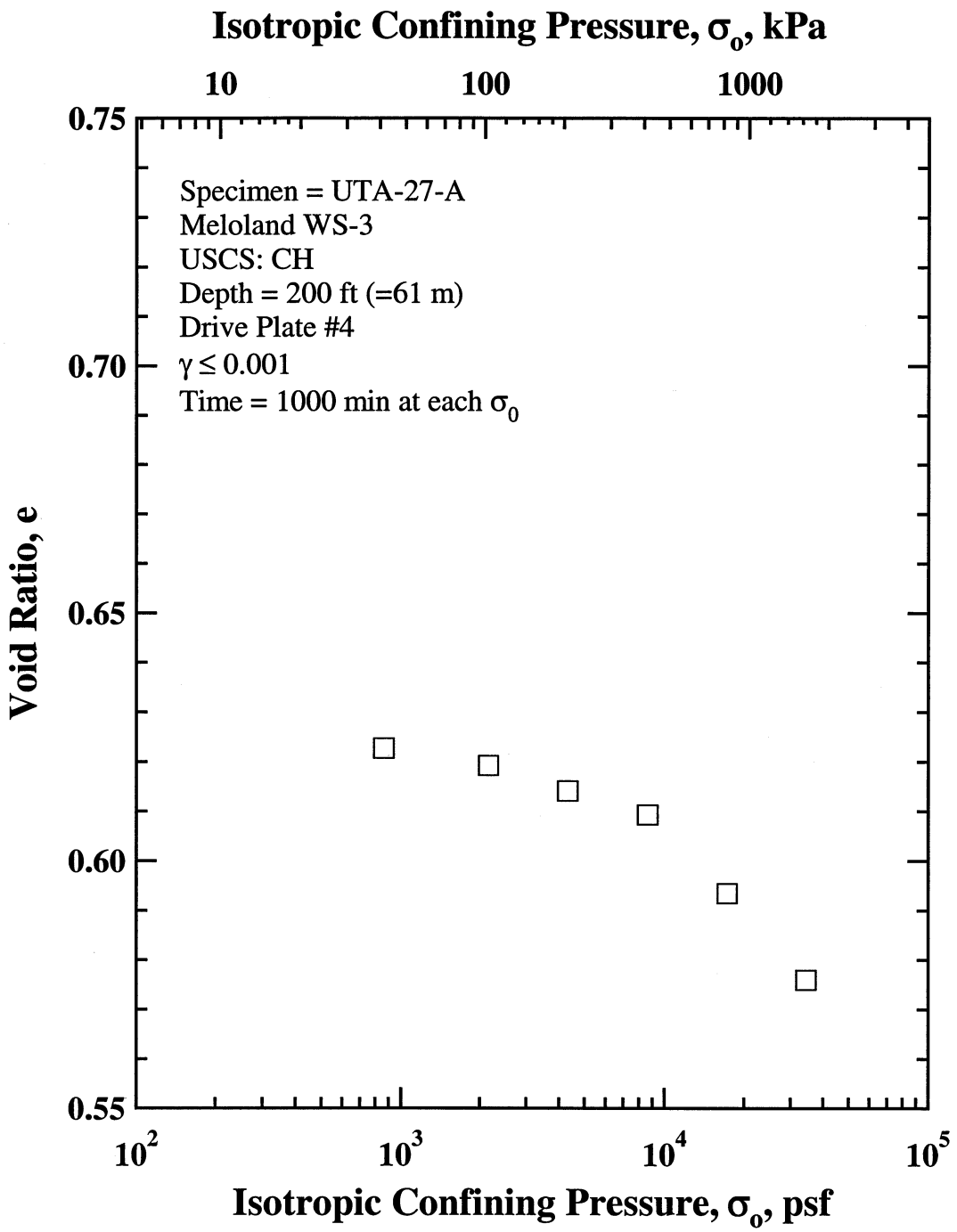

Figure G.7 Variation in Estimated Void Ratio with Isotropic Confining Pressure from Resonant Column Tests of Specimen UTA-27-A.

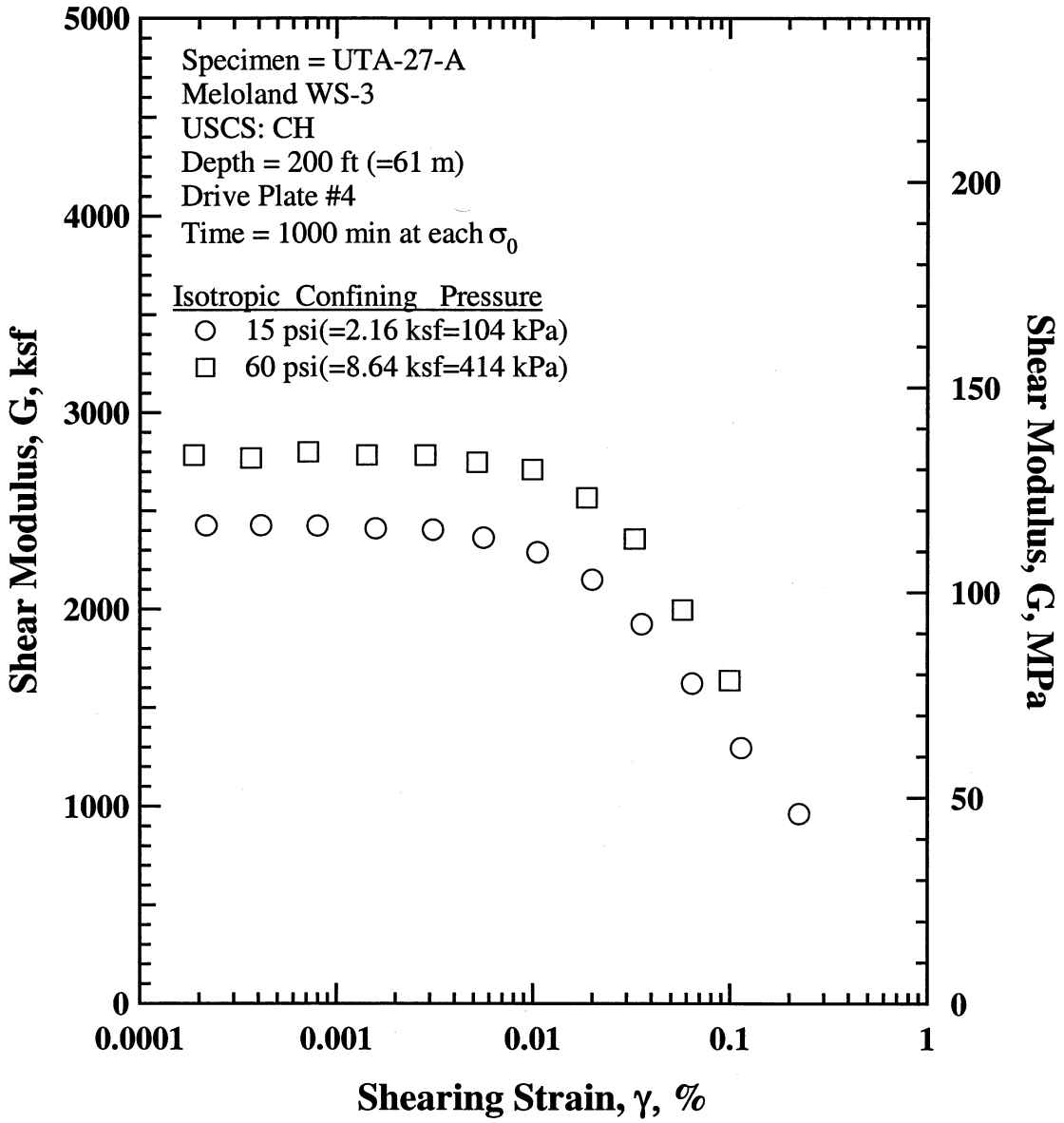

Figure G.8 Comparison of the Variation in Shear Modulus with Shearing Strain and Isotropic Confining Pressure from the Resonant Column Tests of Specimen UTA-27-A.

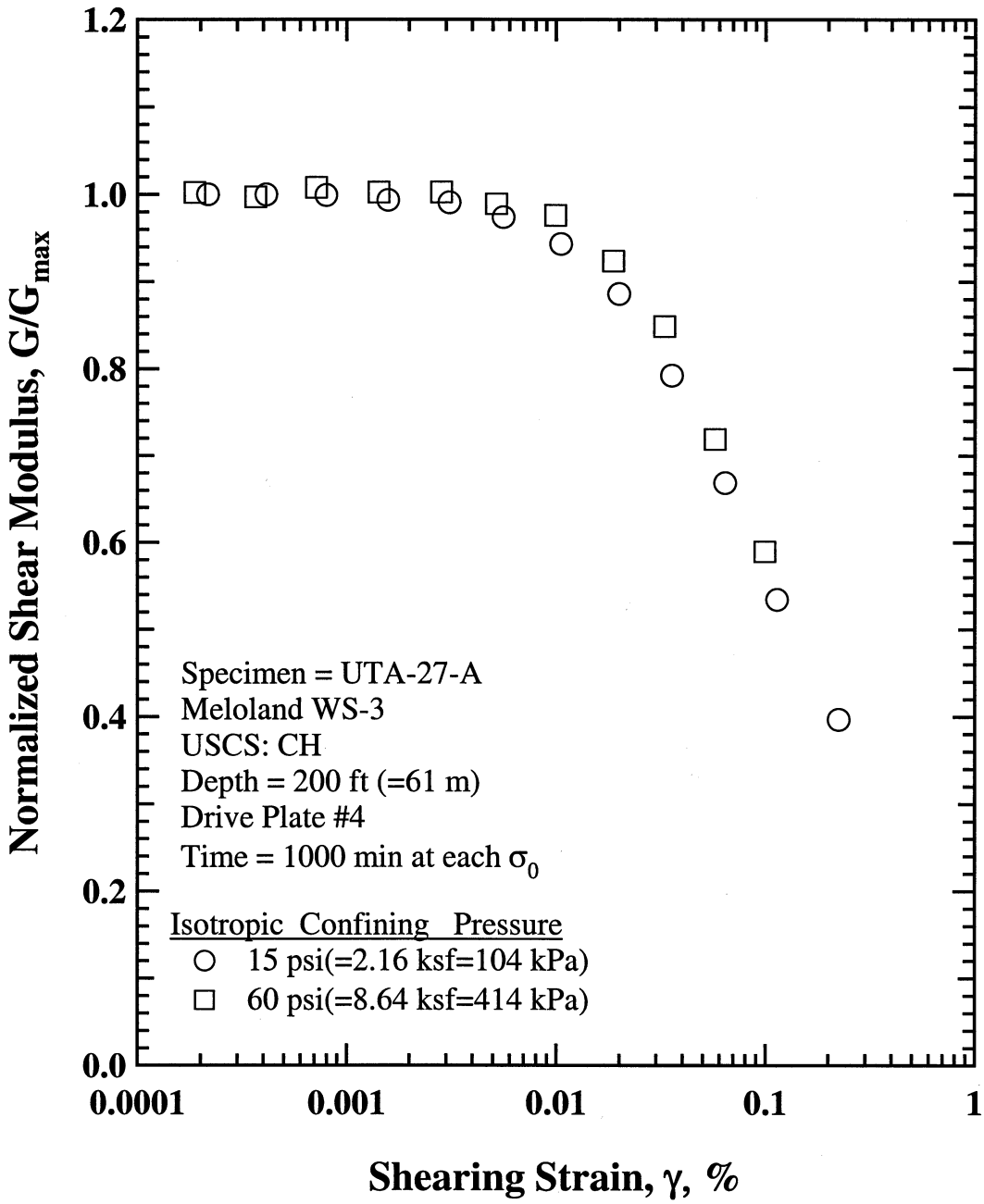

Figure G.9 Comparison of the Variation in Normalized Shear Modulus with Shearing Strain and Isotropic Confining Pressure from the Resonant Column Tests of Specimen UTA-27-A.

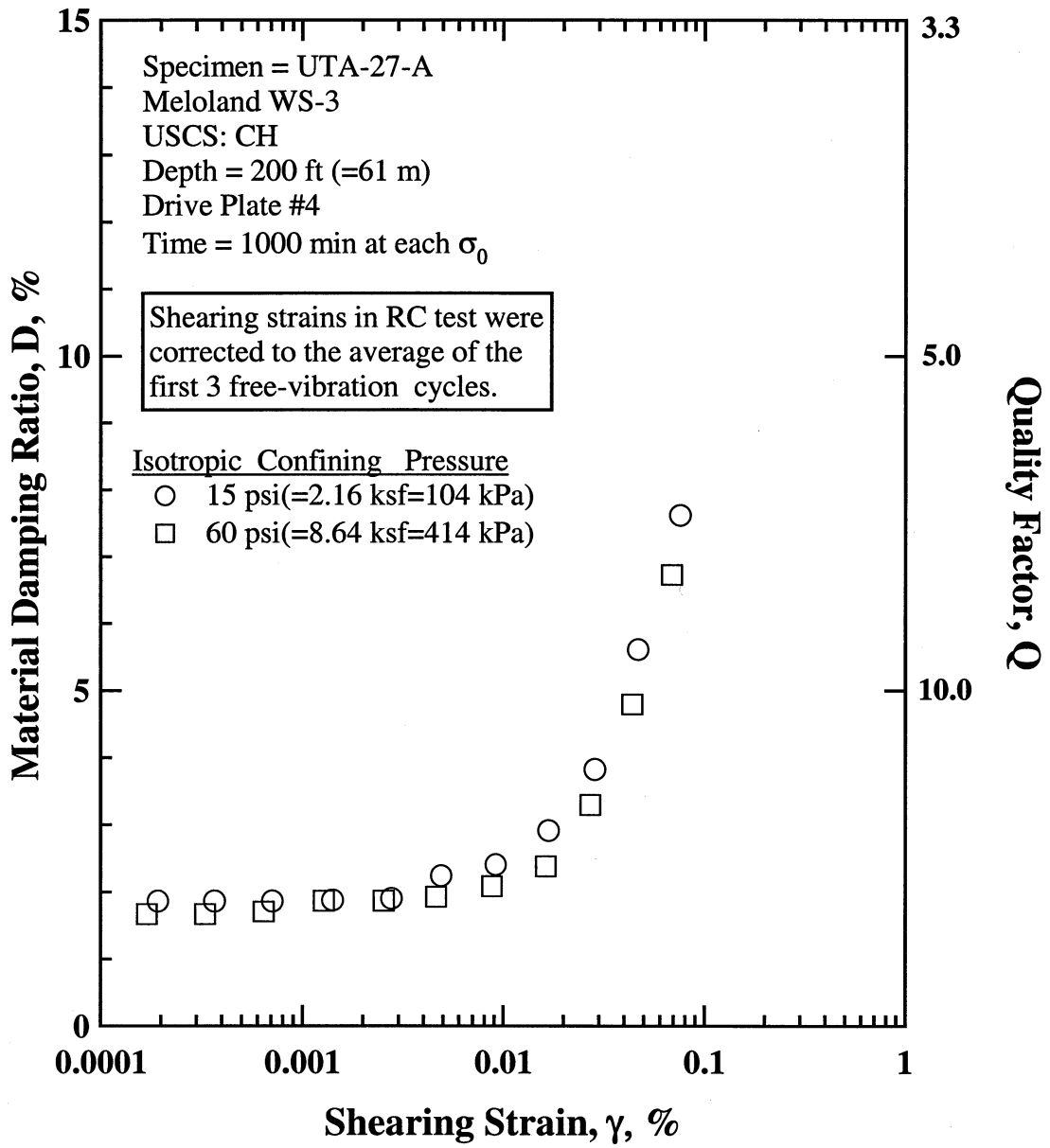

Figure G.10 Comparison of the Variation in Material Damping Ratio with Shearing Strain and Isotropic Confining Pressure from the Resonant Column Tests of Specimen UTA-27-A.

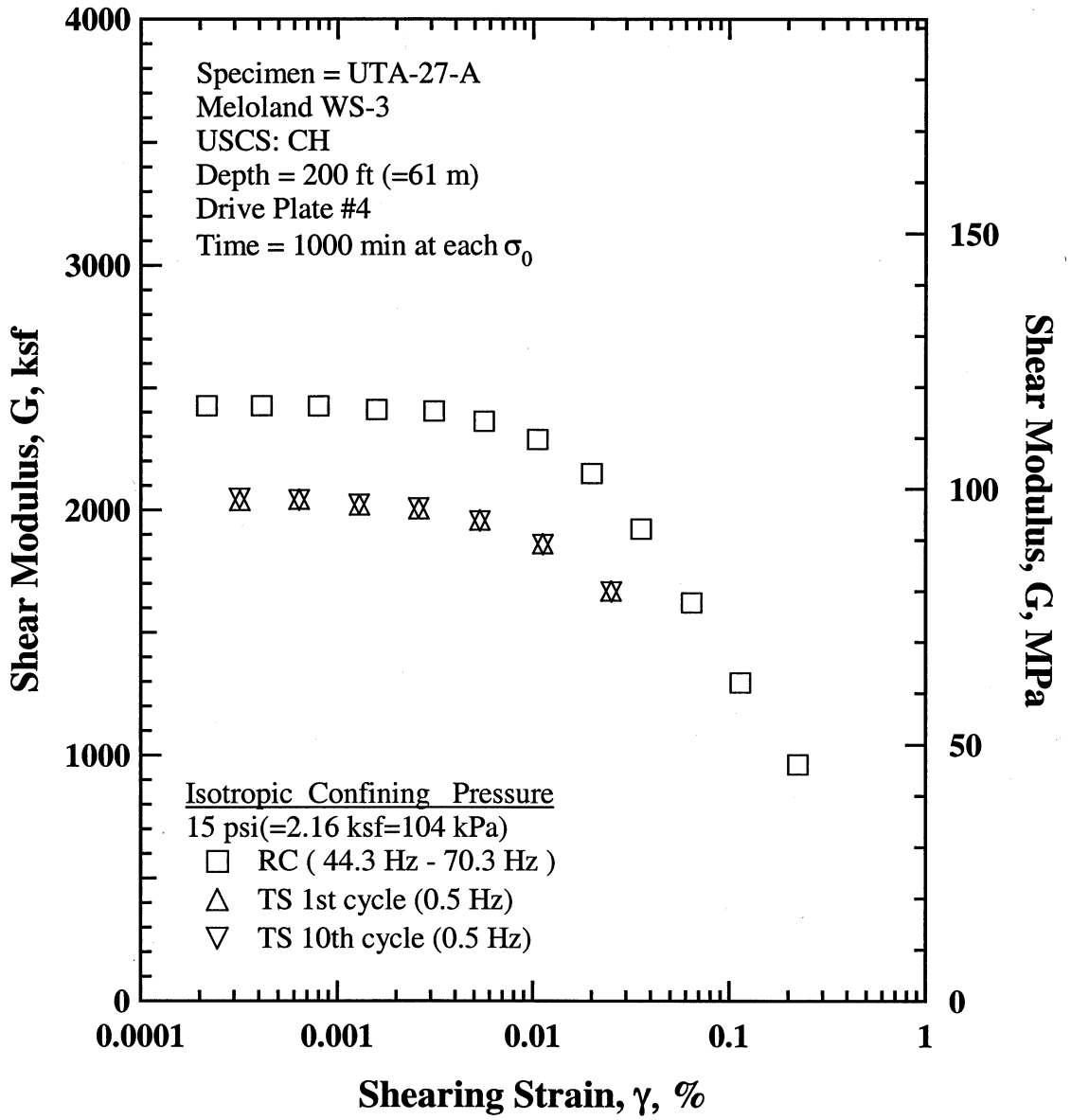

Figure G.11 Comparison of the Variation in Shear Modulus with Shearing Strain at an Isotropic Confining Pressure of 15 psi(=2.16 ksf=104 kPa) from the Combined RCTS Tests of Specimen UTA-27-A.

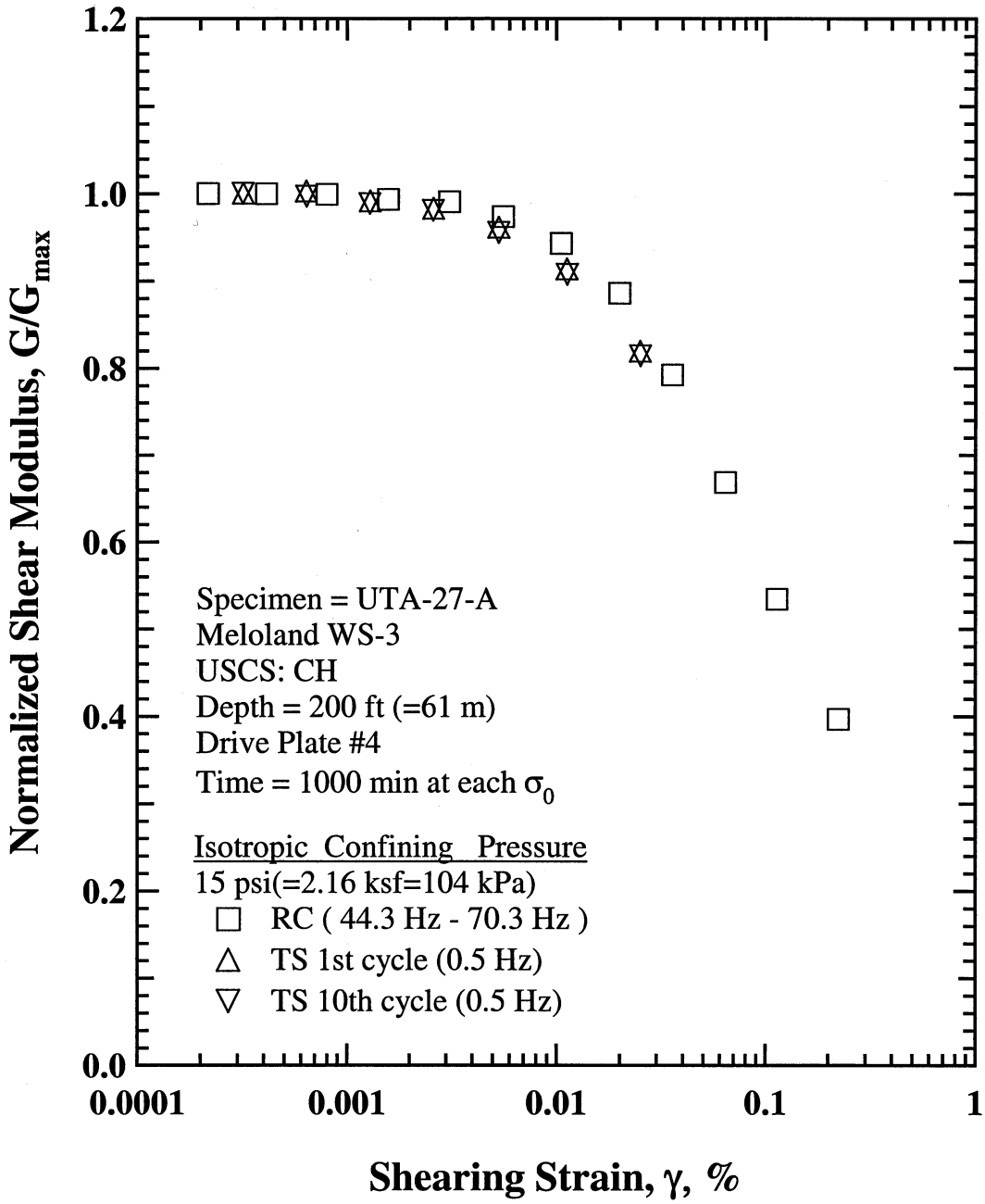

Figure G.12 Comparison of the Variation in Normalized Shear Modulus with Shearing Strain at an Isotropic Confining Pressure of 15 psi(=2.16 ksf=104 kPa) from the Combined RCTS Tests of Specimen UTA-27-A.

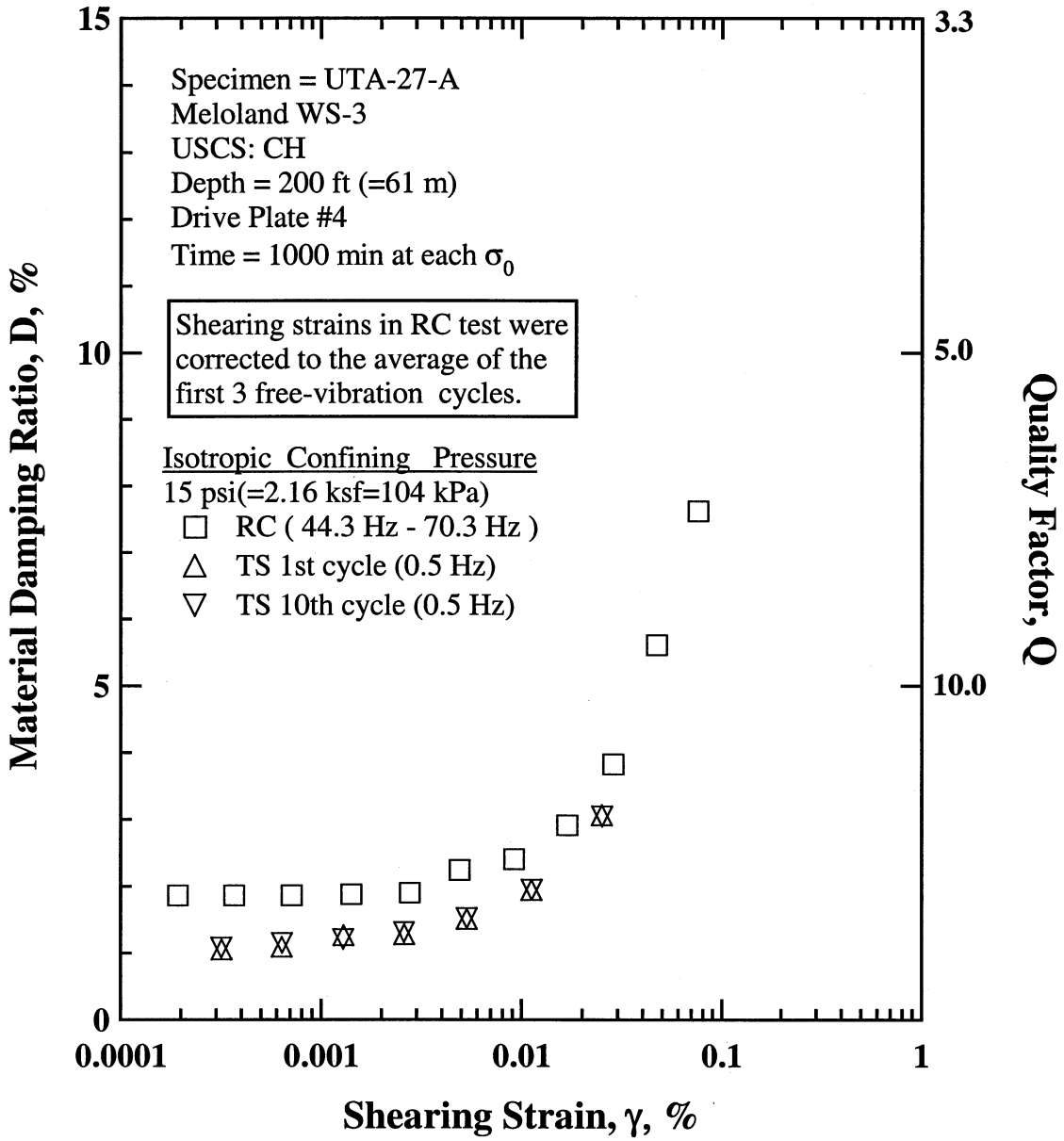

Figure G.13 Comparison of the Variation in Material Damping Ratio with Shearing Strain at an Isotropic Confining Pressure of 15 psi(=2.16 ksf=104 kPa) from the Combined RCTS Tests of Specimen UTA-27-A.

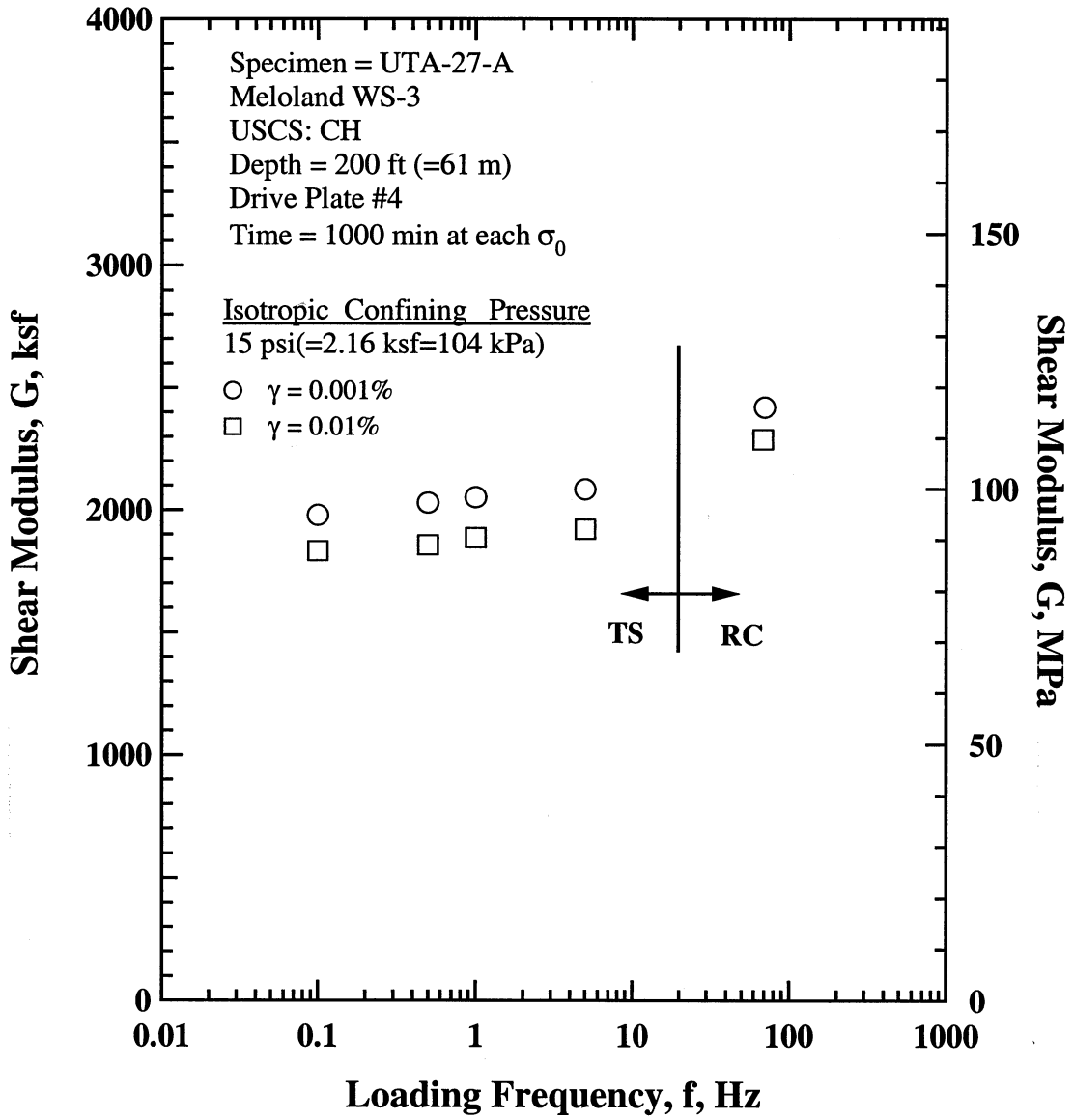

Figure G.14 Comparison of the Variation in Shear Modulus with Loading Frequency at an Isotropic Confining Pressure of 15 psi(=2.16 ksf=104 kPa) from the Combined RCTS Tests of Specimen UTA-27-A.

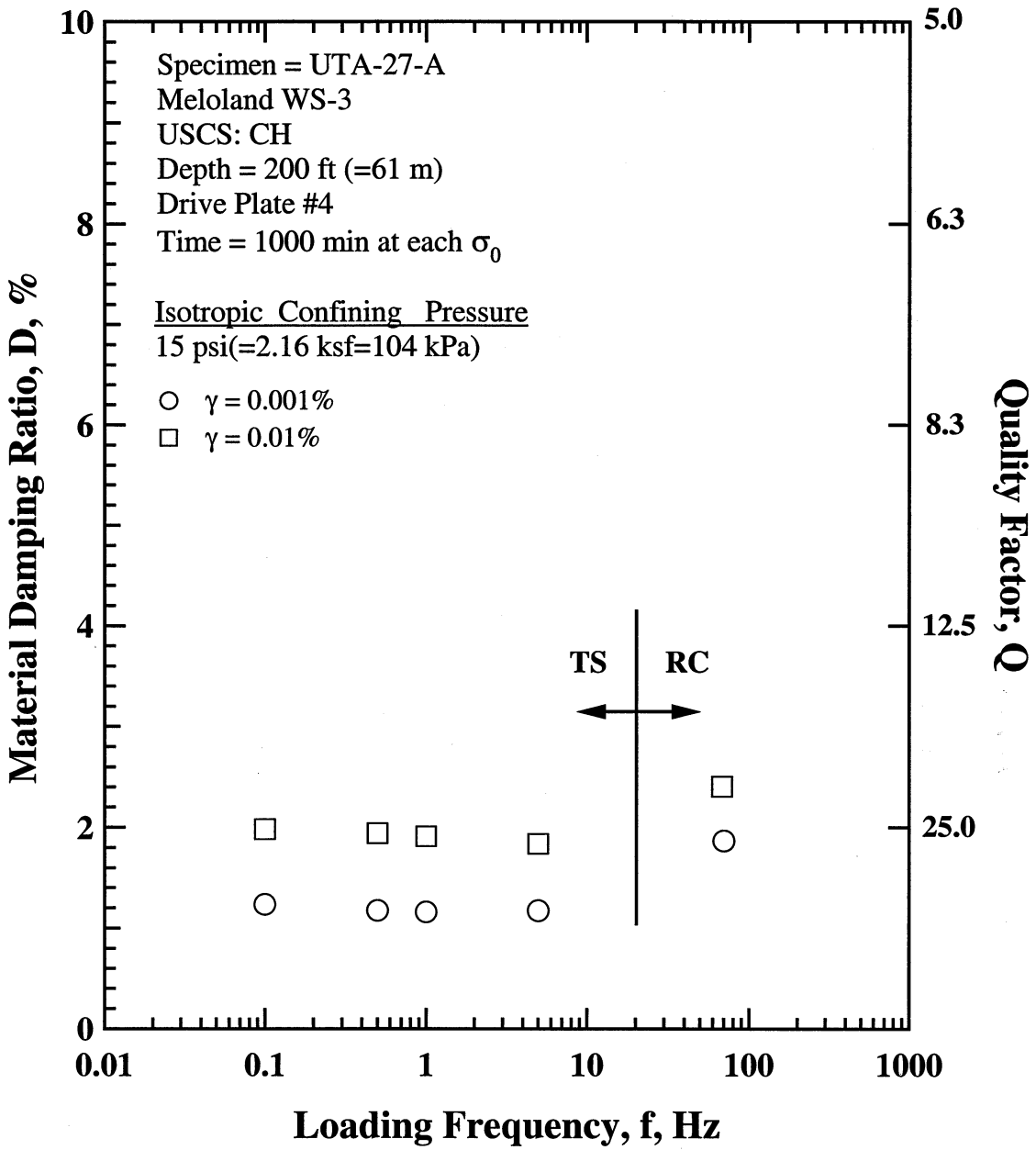

Figure G.15 Comparison of the Variation in Material Damping Ratio with Loading Frequency at an Isotropic Confining Pressure 15 psi(=2.16 ksf=104 kPa) from the Combined RCTS Tests of Specimen UTA-27-A.

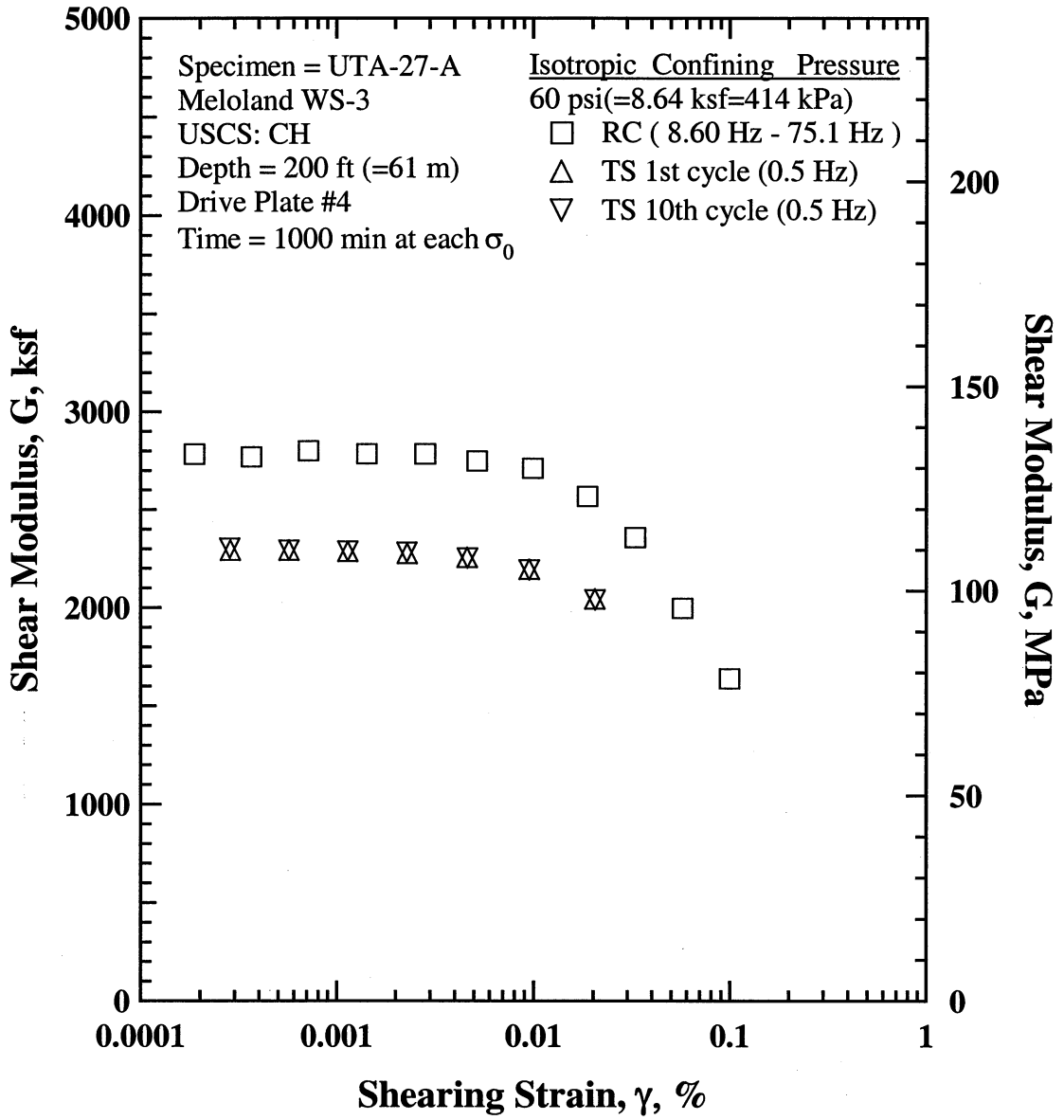

Figure G.16 Comparison of the Variation in Shear Modulus with Shearing Strain at an Isotropic Confining Pressure of 60 psi(=8.64 ksf=414 kPa) from the Combined RCTS Tests of Specimen UTA-27-A.

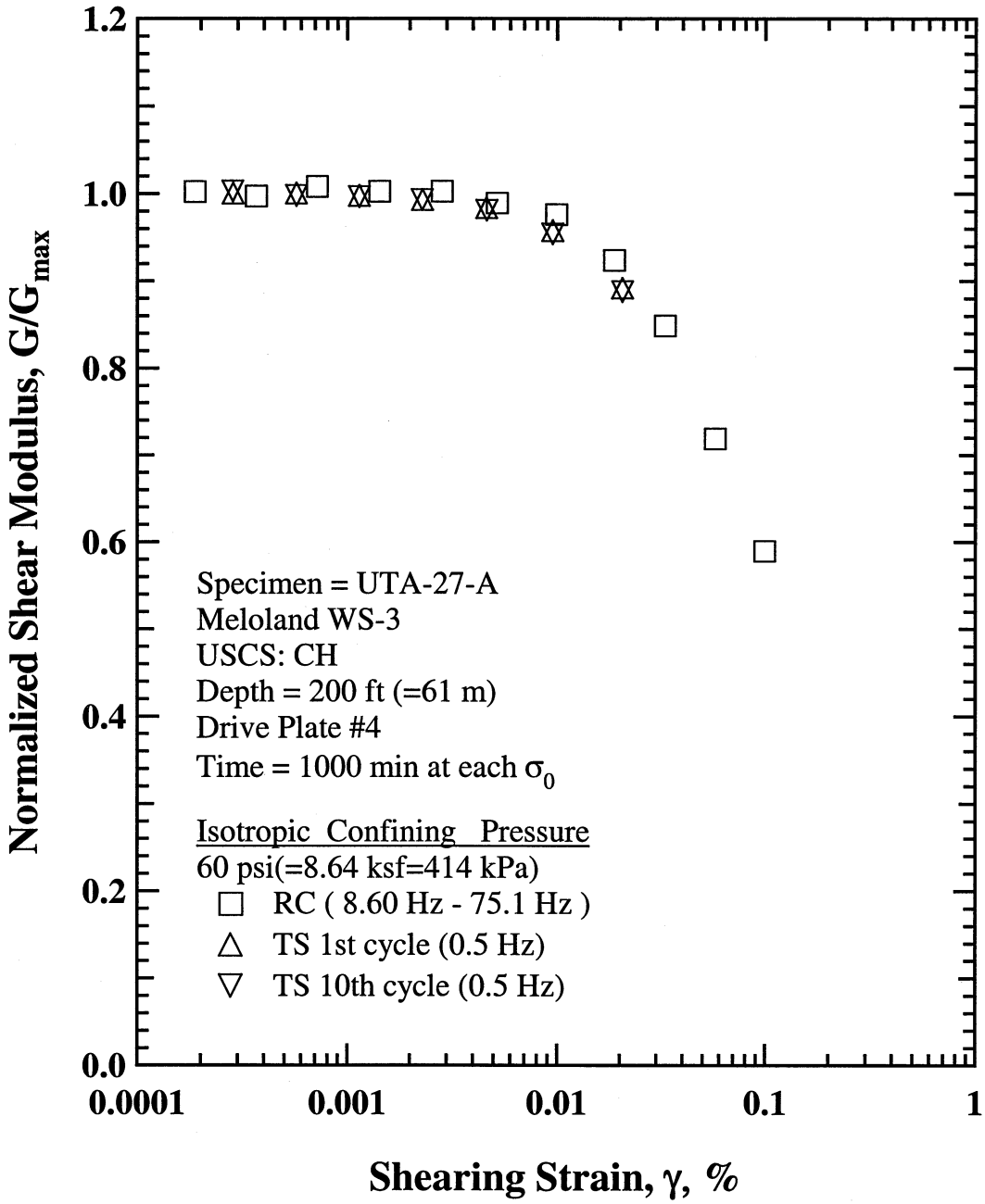

Figure G.17 Comparison of the Variation in Normalized Shear Modulus with Shearing Strain at an Isotropic Confining Pressure of 60 psi(=8.64 ksf=414 kPa) from the Combined RCTS Tests of Specimen UTA-27-A.

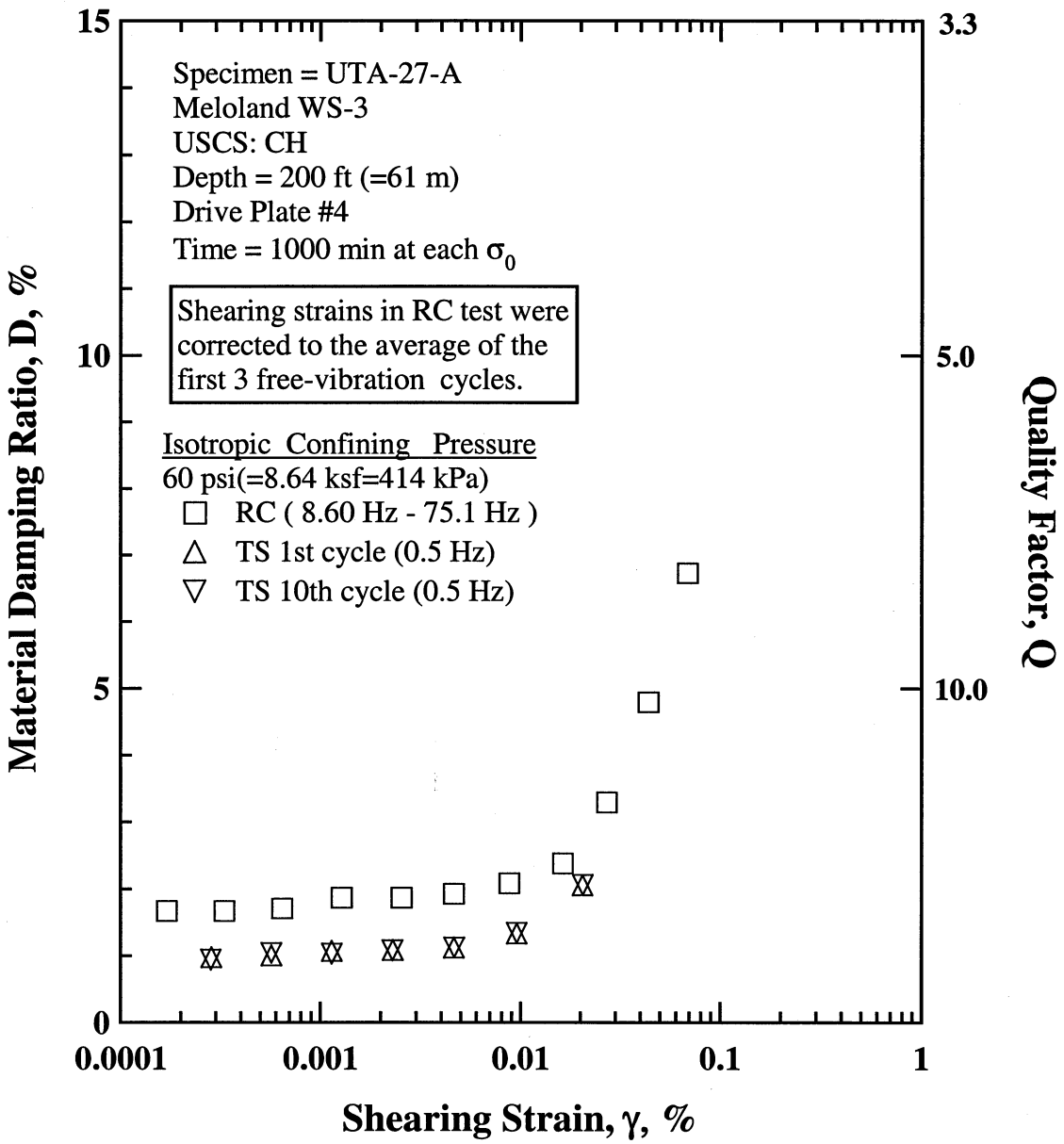

Figure G.18 Comparison of the Variation in Material Damping Ratio with Shearing Strain at an Isotropic Confining Pressure of 60 psi(=8.64 ksf=414 kPa) from the Combined RCTS Tests of Specimen UTA-27-A.

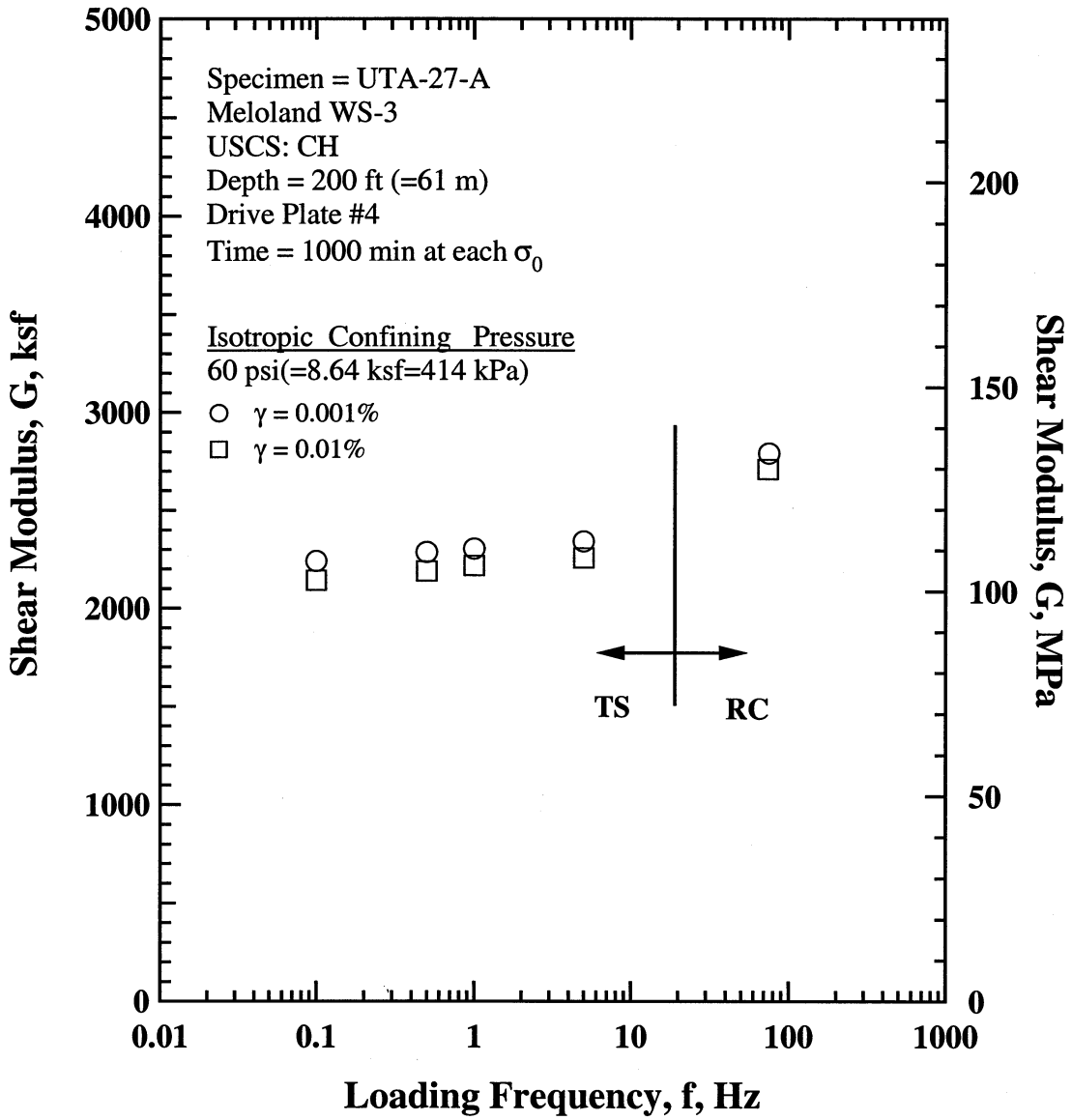

Figure G.19 Comparison of the Variation in Shear Modulus with Loading Frequency at an Isotropic Confining Pressure of 60 psi(=8.64 ksf=414 kPa) from the Combined RCTS Tests of Specimen UTA-27-A.

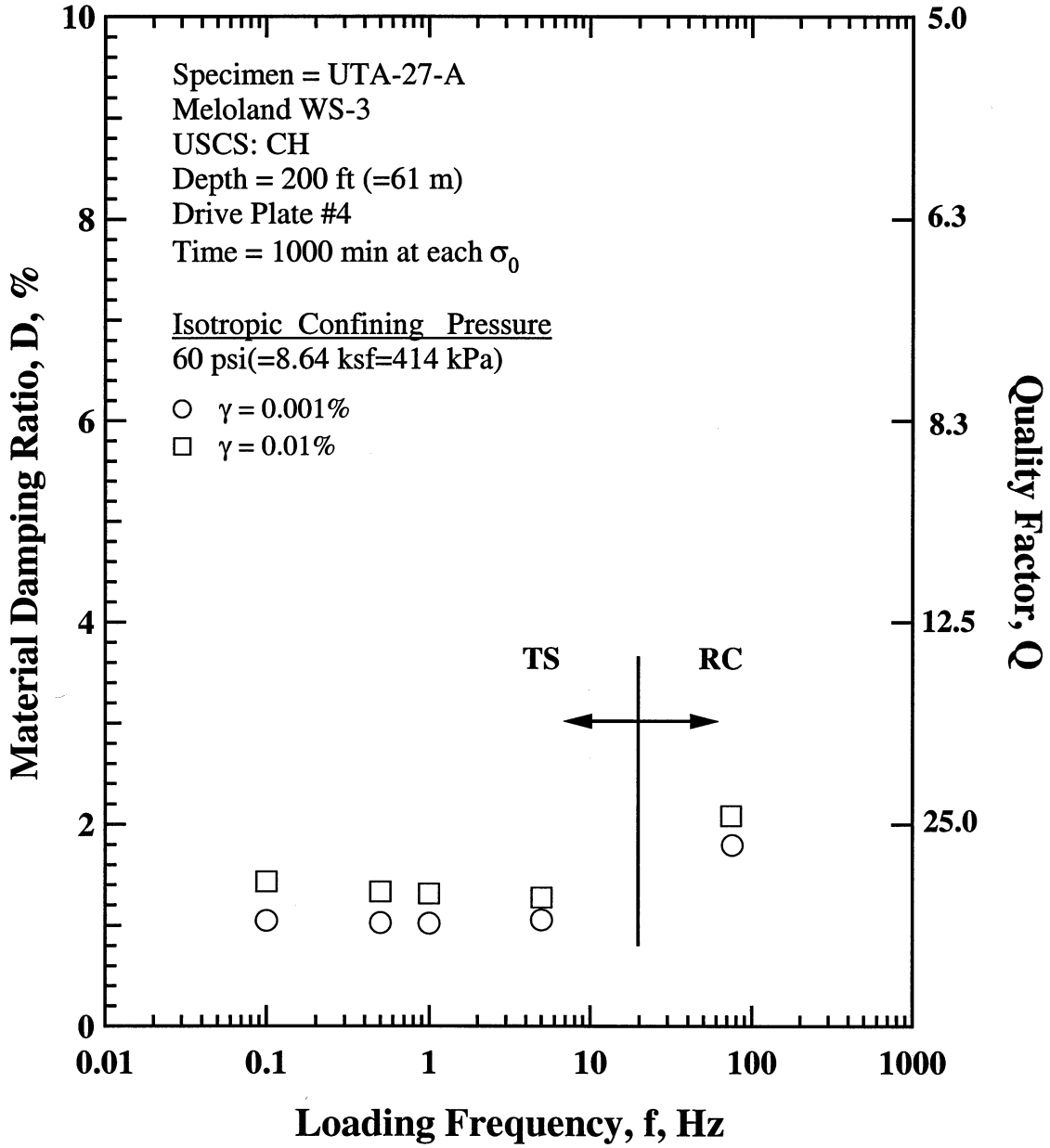

Figure G.20 Comparison of the Variation in Material Damping Ratio with Loading Frequency at an Isotropic Confining Pressure 60 psi(=8.64 ksf=414 kPa) from the Combined RCTS Tests of Specimen UTA-27-A.

Table G.1 Variation in Low-Amplitude Shear Wave Velocity, Low-Amplitude Shear Modulus, Low-Amplitude Material Damping Ratio and Estimated Void Ratio with Isotropic Confining Pressure from RC Tests of Specimen UTA-27-A.

Effective Isotropic Confining Pressure, σ_o'			Low-Amplitude Shear Modulus, G_{max}		Low-Amplitude Shear Wave Velocity, Vs	Low-Amplitude Material Damping Ratio,	Estimated Void Ratio, e
(psi)	(psf)	(kPa)	(ksf)	(MPa)	(fps)	D_{min}, %	
6	864	41.4	2054	98.5	720	2.29	0.623
15	2160	103.5	2335	111.9	768	2.06	0.619
30	4320	207.1	2584	123.9	807	1.94	0.614
60	8640	414.2	2729	130.8	829	1.92	0.609
120	17280	828.4	2923	140.1	855	2.06	0.594
240	34560	1656.8	3429	164.4	924	2.05	0.576

Table G.2 Variation in Shear Modulus, Normalized Shear Modulus and Material Damping Ratio with Shearing Strain from RC Tests of Specimen UTA-27-A; Confining Pressure, σ_o' = 15 psi(=2.16 ksf=104 kPa).

Peak Shearing Strain, %	Shear Modulus, G, ksf	Normalized Shear Modulus, G/G_{max}	Average[+] Shearing Strain, %	Material Damping Ratio[x], D, %
4.12E-04	2426	1.00	3.68E-04	1.86
2.17E-04	2426	1.01	1.94E-04	1.86
7.97E-04	2425	1.00	7.13E-04	1.86
1.58E-03	2411	1.00	1.41E-03	1.88
3.11E-03	2404	1.00	2.77E-03	1.90
5.61E-03	2363	0.98	4.91E-03	2.24
1.06E-02	2289	0.95	9.15E-03	2.41
2.00E-02	2150	0.90	1.68E-02	2.92
3.57E-02	1923	0.81	2.86E-02	3.82
6.41E-02	1622	0.69	4.70E-02	5.61
1.14E-01	1296	0.57	7.59E-02	7.62
2.24E-01	963	0.40		

[+] Average Shearing Strain from the First Three Cycles of the Free Vibration Decay Curve

[x] Average Damping Ratio from the First Three Cycles of the Free Vibration Decay Curve

Table G.3 Variation in Shear Modulus, Normalized Shear Modulus and Material Damping Ratio with Shearing Strain from TS Tests of Specimen UTA-27-A; Confining Pressure, σ_o' = 15 psi(=2.16 ksf=104 kPa).

First Cycle				Tenth Cycle			
Peak Shearing Strain, %	Shear Modulus, G, ksf	Normalized Shear Modulus, G/G_{max}	Material Damping Ratio, D, %	Peak Shearing Strain, %	Shear Modulus, G, ksf	Normalized Shear Modulus, G/G_{max}	Material Damping Ratio, D, %
3.21E-04	2036	1.00	1.19	3.20E-04	2045	1.00	1.08
6.40E-04	2041	1.00	1.20	6.41E-04	2039	1.00	1.14
1.30E-03	2018	0.99	1.40	1.30E-03	2021	0.99	1.20
2.62E-03	2002	0.98	1.38	2.61E-03	2005	0.98	1.30
5.36E-03	1957	0.96	1.83	5.36E-03	1953	0.96	1.51
1.13E-02	1860	0.91	3.21	1.13E-02	1856	0.91	1.94
2.52E-02	1668	0.82	3.25	2.52E-02	1664	0.81	3.04

Table G.4 Variation in Shear Modulus, Normalized Shear Modulus and Material Damping Ratio with Shearing Strain from RC Tests of Specimen UTA-27-A; Confining Pressure, σ_o' = 60 psi(=8.64 ksf=414 kPa).

Peak Shearing Strain, %	Shear Modulus, G, ksf	Normalized Shear Modulus, G/G_{max}	Average[+] Shearing Strain, %	Material Damping Ratio[x], D, %
1.88E-04	2784	1.00	1.70E-04	1.67
3.66E-04	2770	1.00	3.31E-04	1.67
7.16E-04	2799	1.01	6.46E-04	1.71
1.43E-03	2785	1.00	1.28E-03	1.87
2.84E-03	2784	1.00	2.54E-03	1.87
5.20E-03	2748	0.99	4.63E-03	1.93
9.94E-03	2711	0.98	8.77E-03	2.09
1.88E-02	2566	0.92	1.63E-02	2.38
3.29E-02	2357	0.85	2.71E-02	3.30
5.75E-02	1997	0.72	4.38E-02	4.79
9.93E-02	1638	0.59	6.89E-02	6.73

[+] Average Shearing Strain from the First Three Cycles of the Free Vibration Decay Curve

[x] Average Damping Ratio from the First Three Cycles of the Free Vibration Decay Curve

Table G.5 Variation in Shear Modulus, Normalized Shear Modulus and Material Damping Ratio with Shearing Strain from TS Tests of Specimen UTA-27-A; Confining Pressure, σ_o' = 60 psi(=8.64 ksf=414 kPa).

First Cycle				Tenth Cycle			
Peak Shearing Strain, %	Shear Modulus, G, ksf	Normalized Shear Modulus, G/G_{max}	Material Damping Ratio, D, %	Peak Shearing Strain, %	Shear Modulus, G, ksf	Normalized Shear Modulus, G/G_{max}	Material Damping Ratio, D, %
2.86E-04	2290	1.00	0.97	2.85E-04	2301	1.00	0.93
5.72E-04	2290	1.00	1.00	5.72E-04	2289	1.00	1.03
1.15E-03	2284	1.00	1.07	1.15E-03	2285	1.00	1.02
2.31E-03	2274	0.99	1.08	2.30E-03	2278	0.99	1.07
4.66E-03	2252	0.98	1.11	4.66E-03	2250	0.98	1.12
9.58E-03	2192	0.96	1.33	9.59E-03	2189	0.95	1.34
2.06E-02	2042	0.89	2.05	2.06E-02	2037	0.89	2.05

APPENDIX H

Specimen No. 7
UT Specimen ID: UTA-27-C

Meloland WS-4
Depth = 259 ft (=78.9m)
Soil Type: Clay (CH)

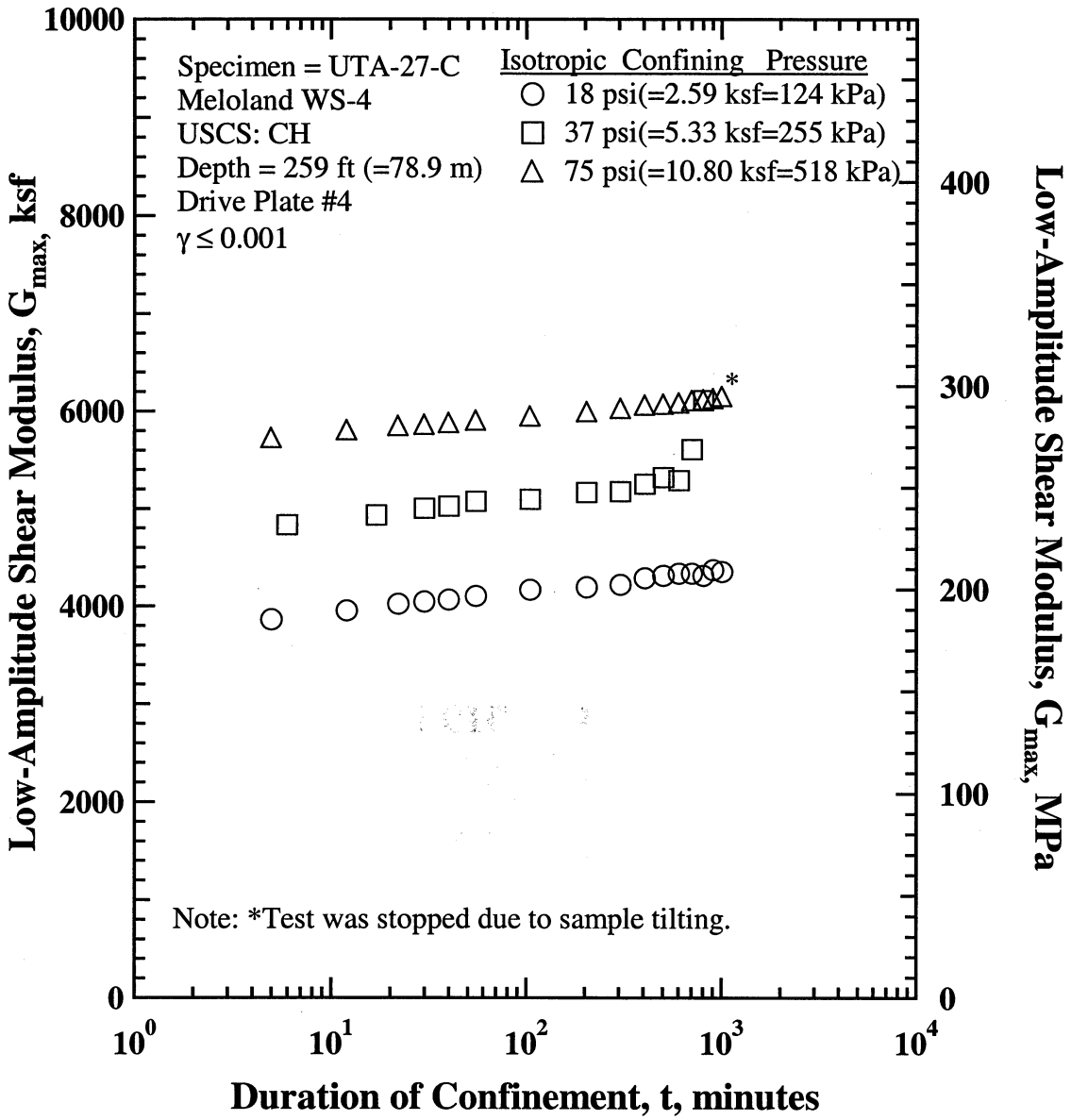

Figure H.1 Variation in Low-Amplitude Shear Modulus with Magnitude and Duration of Isotropic Confining Pressure from Resonant Column Tests of Specimen UTA-27-C.

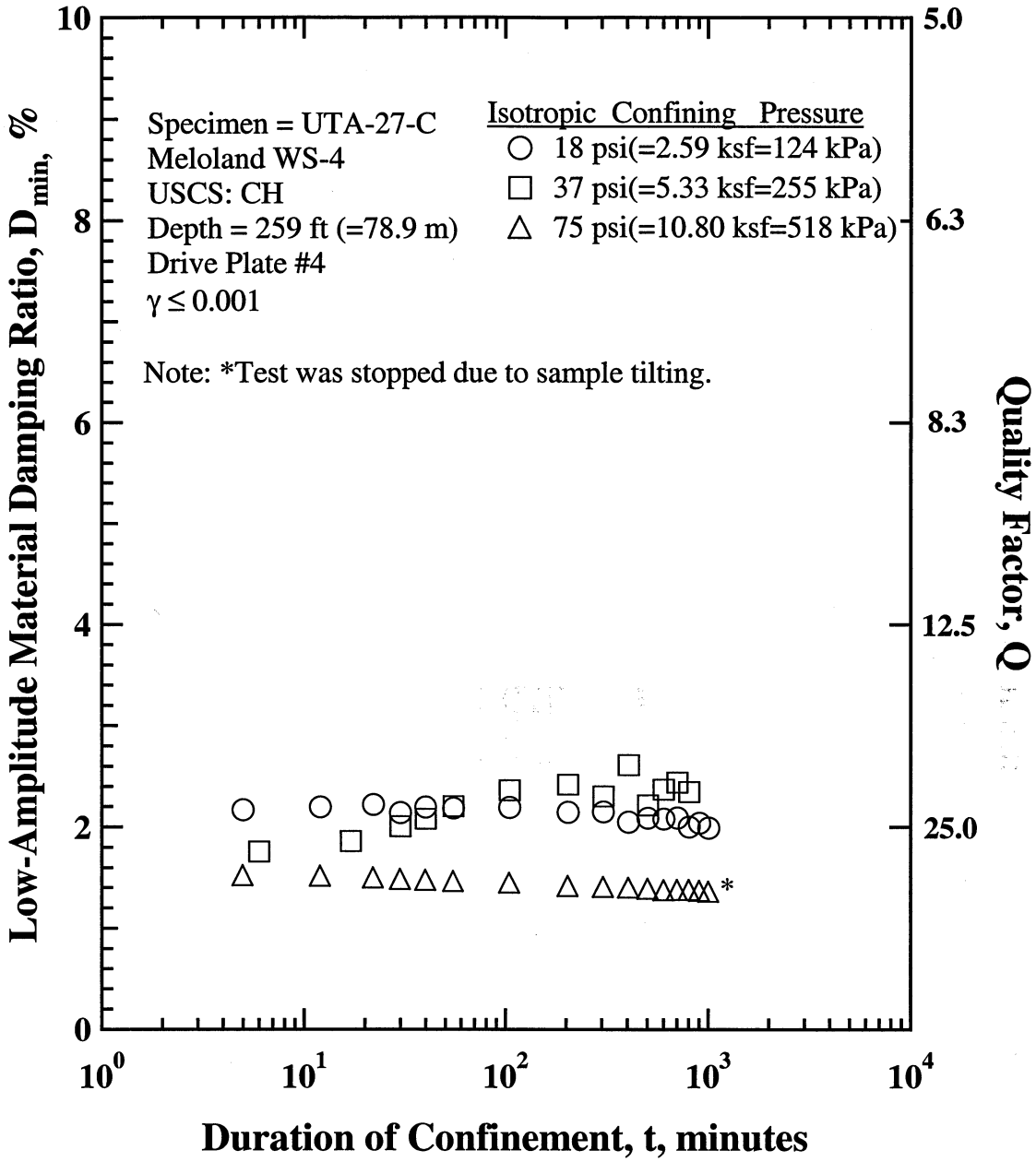

Figure H.2 Variation in Low-Amplitude Material Damping Ratio with Magnitude and Duration of Isotropic Confining Pressure from Resonant Column Tests of Specimen UTA-27-C

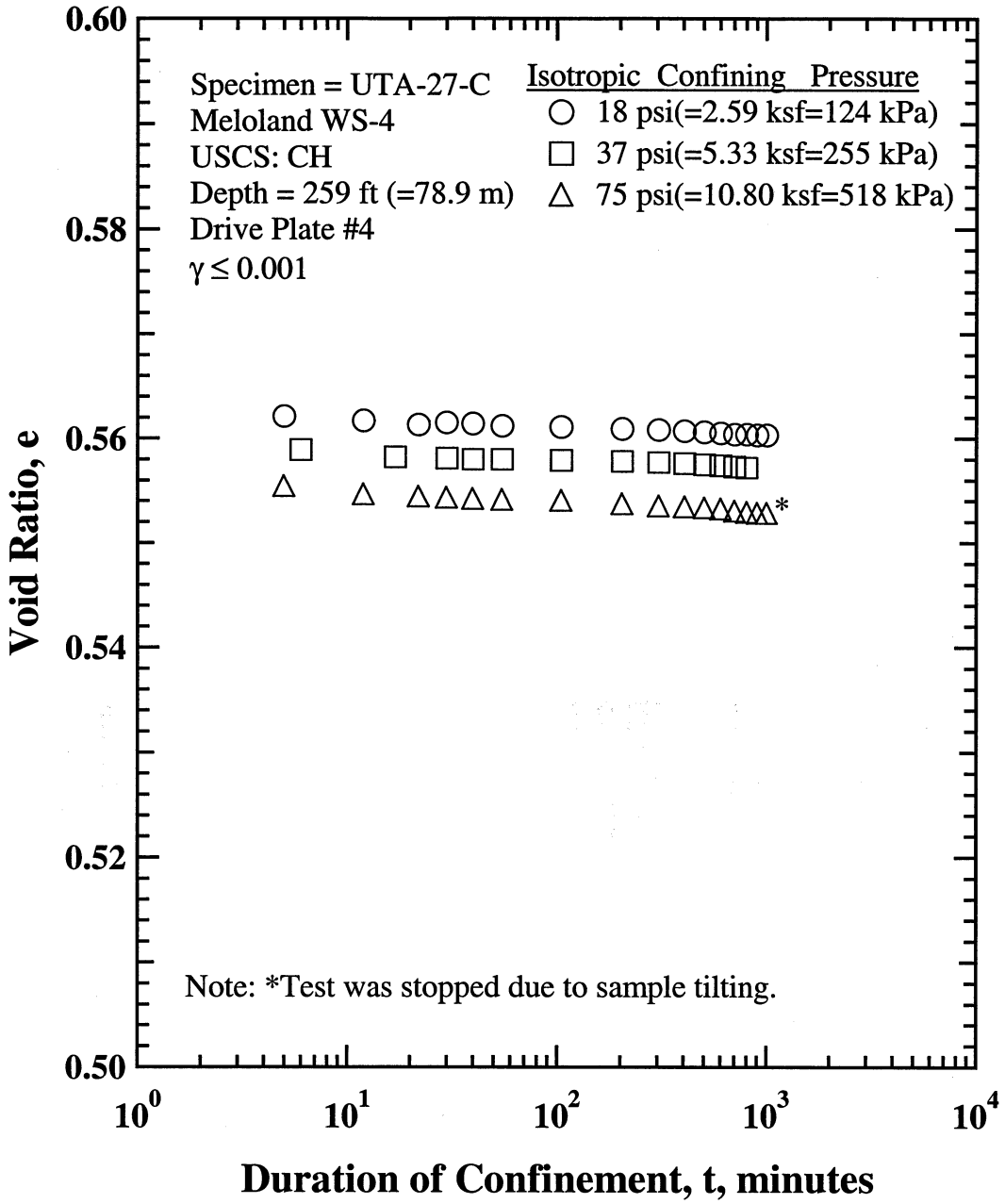

Figure H.3 Variation in Estimated Void Ratio with Magnitude and Duration of Isotropic Confining Pressure from Resonant Column Tests of Specimen UTA-27-C

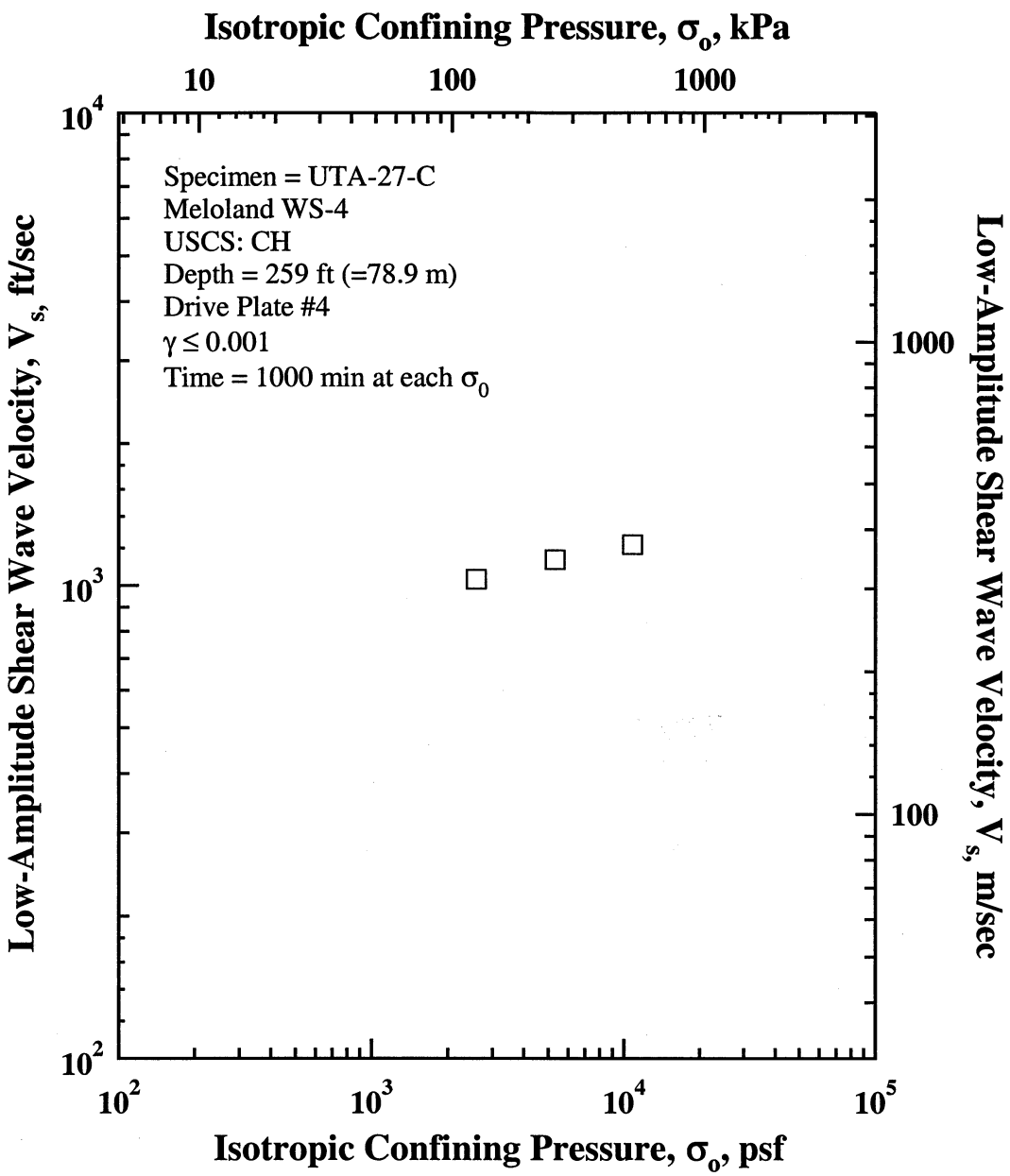

Figure H.4 Variation in Low-Amplitude Shear Wave Velocity with Isotropic Confining Pressure from Resonant Column Tests of Specimen UTA-27-C.

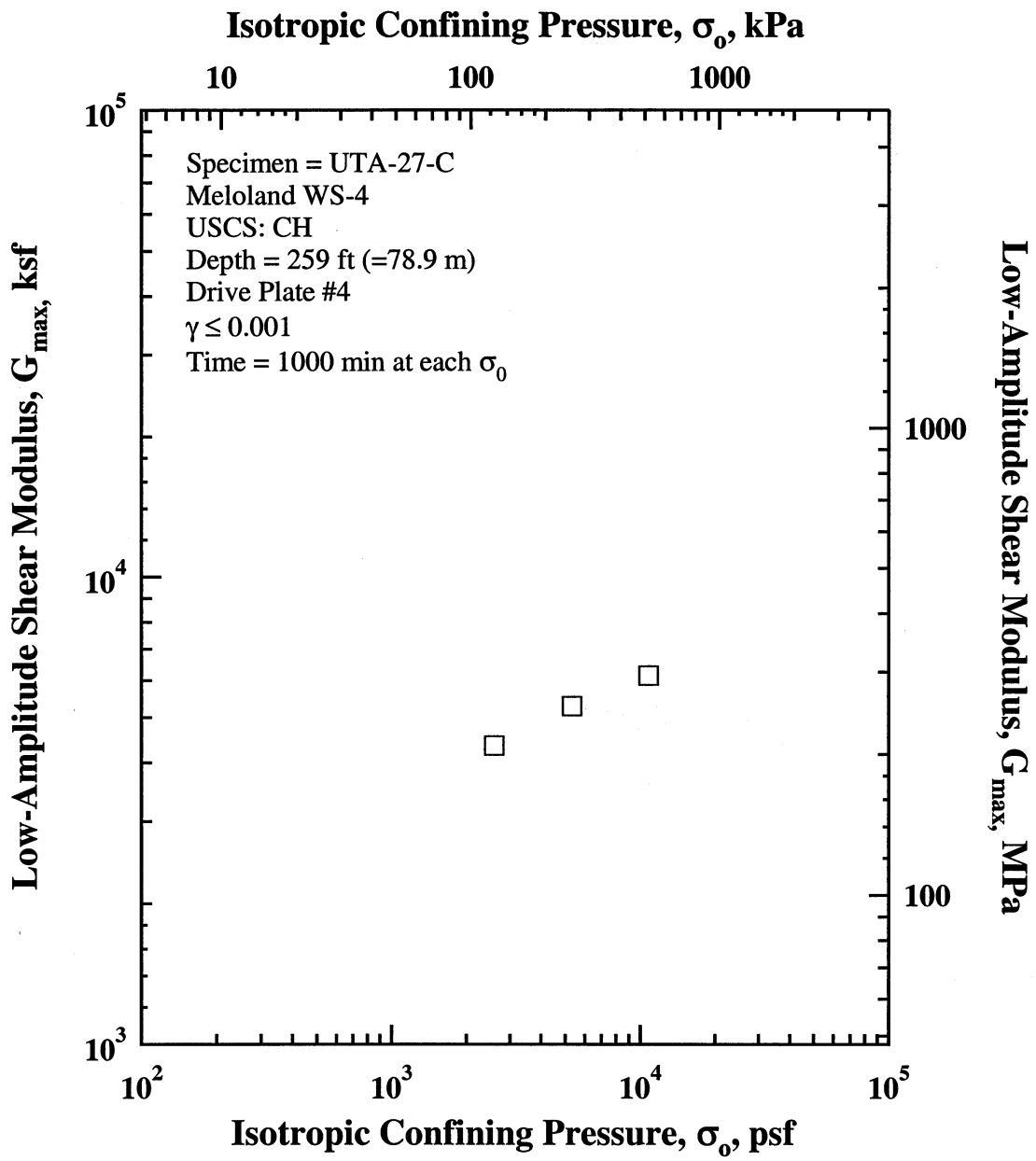

Figure H.5 Variation in Low-Amplitude Shear Modulus with Isotropic Confining Pressure from Resonant Column Tests of Specimen UTA-27-C.

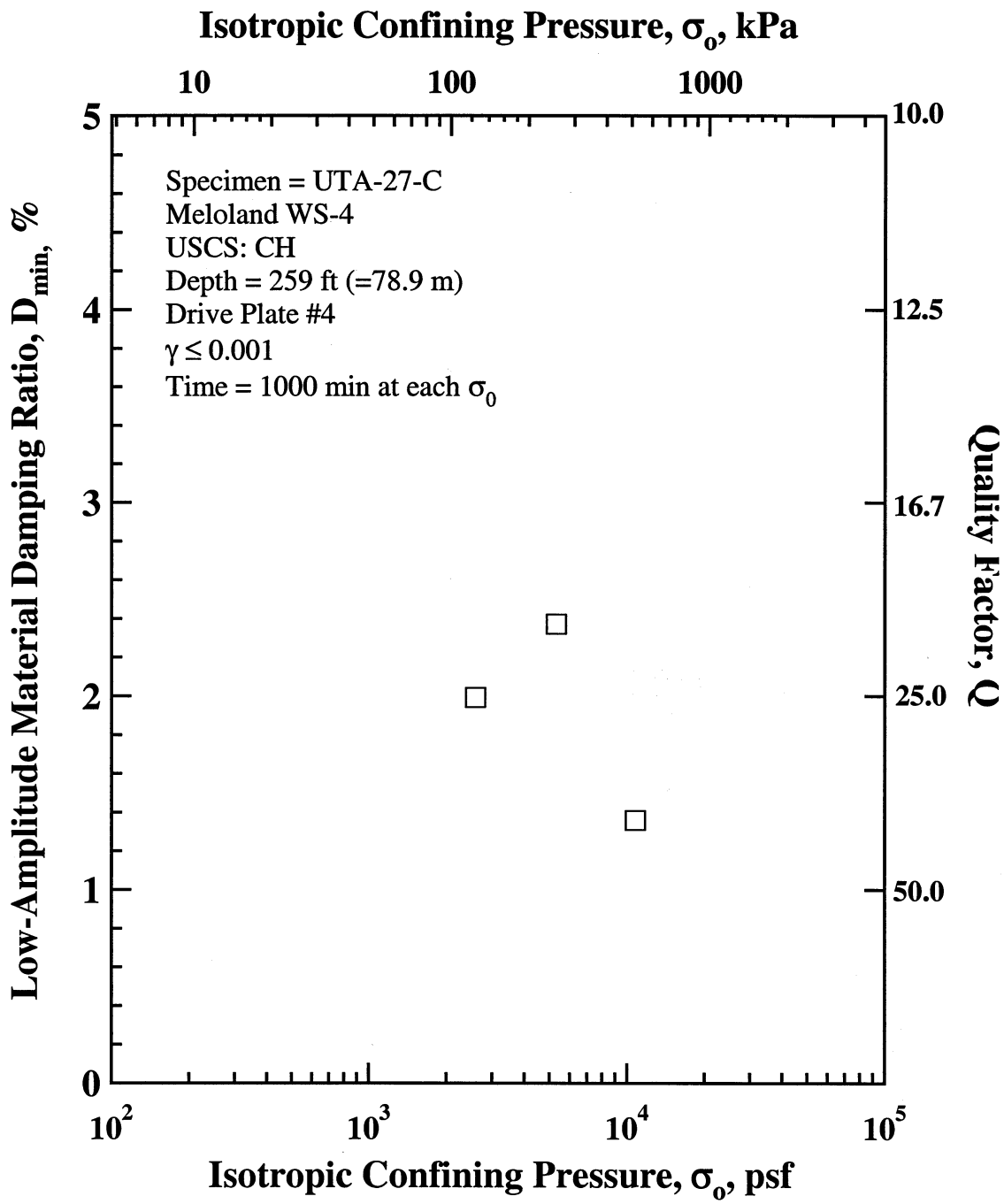

Figure H.6 Variation in Material Damping Ratio with Isotropic Confining Pressure from Resonant Column Tests of Specimen UTA-27-C.

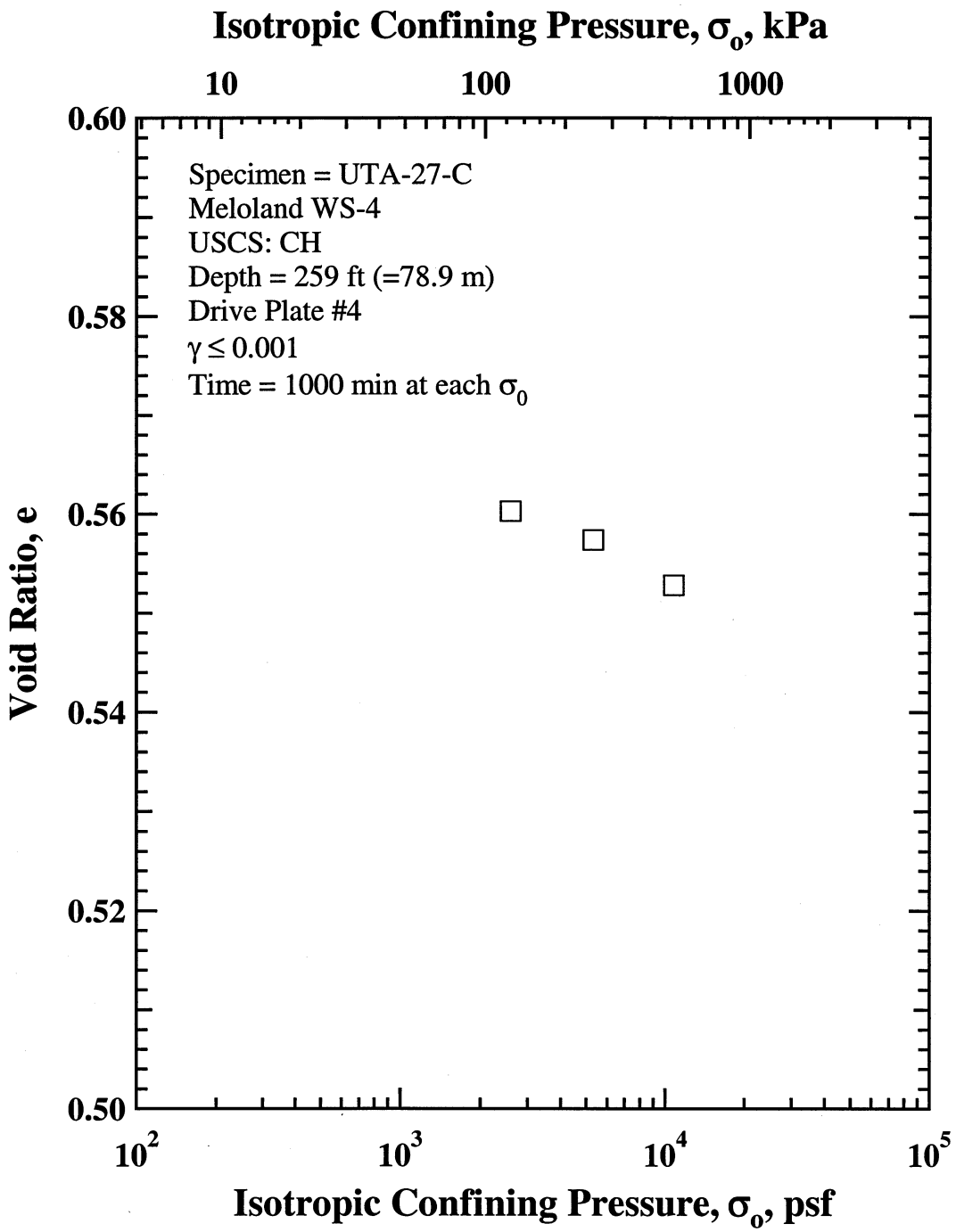

Figure H.7 Variation in Estimated Void Ratio with Isotropic Confining Pressure from Resonant Column Tests of Specimen UTA-27-C.

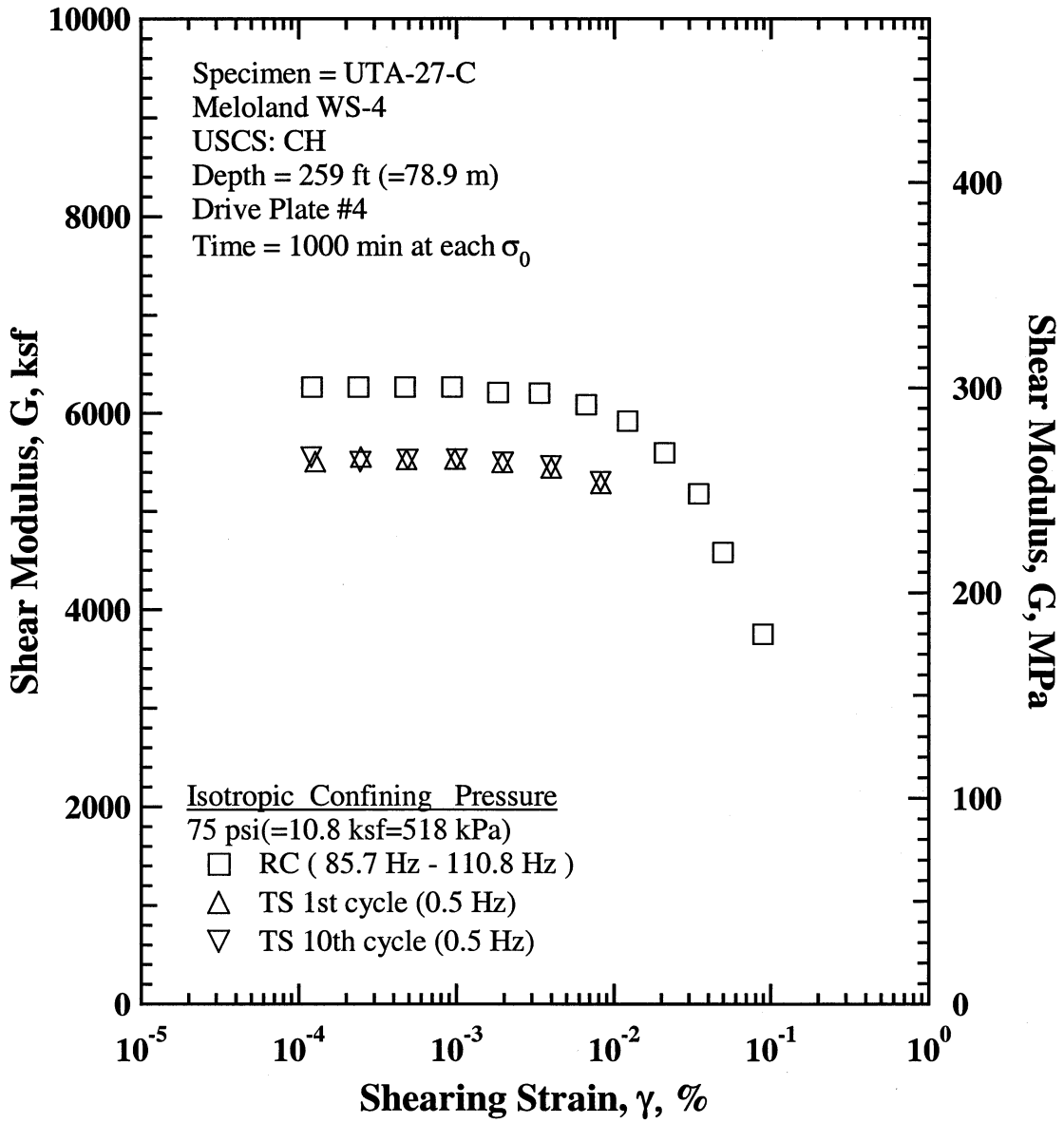

Figure H.8 Comparison of the Variation in Shear Modulus with Shearing Strain at an Isotropic Confining Pressure of 75 psi(=10.8 ksf=518 kPa) from the Combined RCTS Tests of Specimen UTA-27-C.

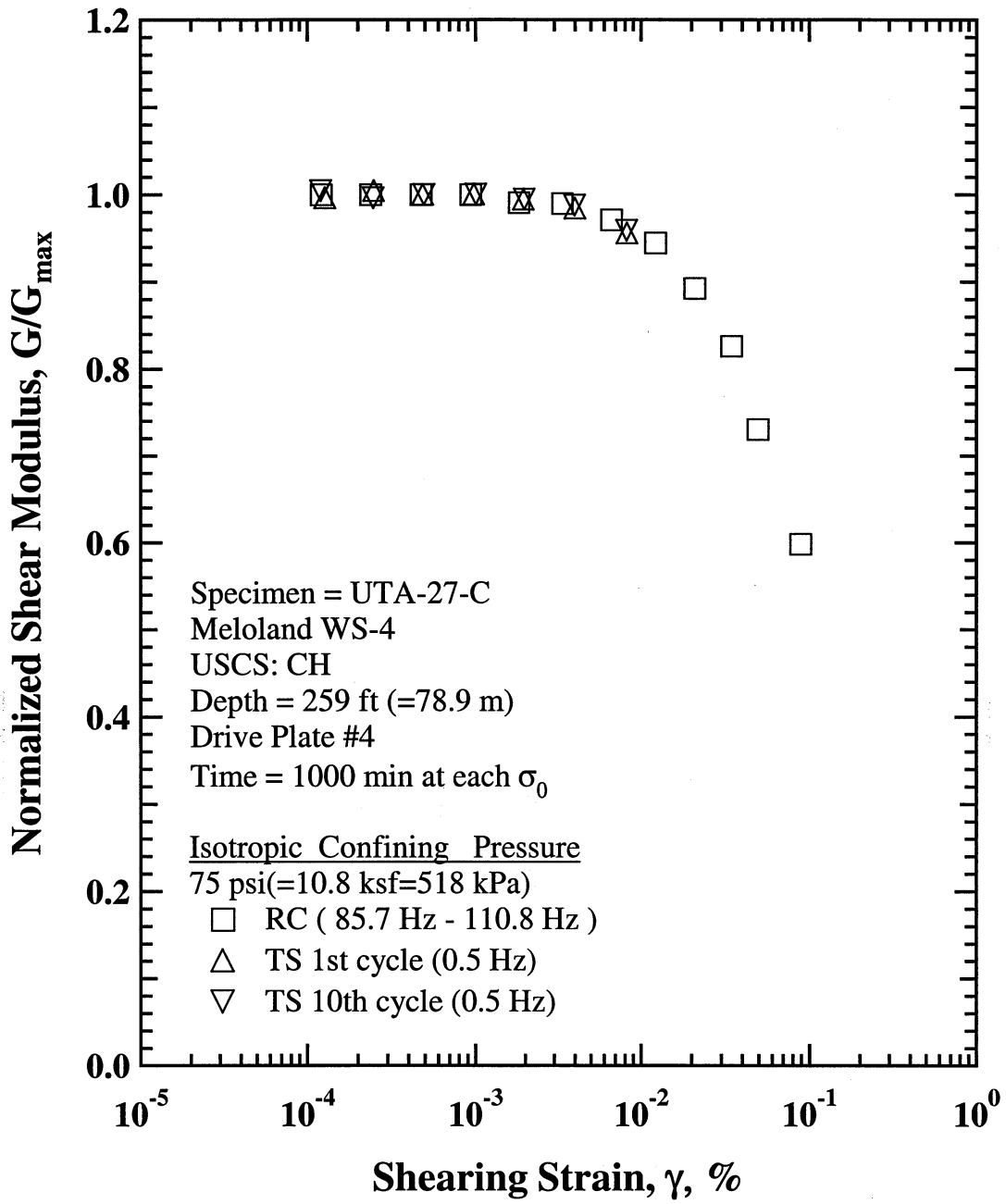

Figure H.9 Comparison of the Variation in Normalized Shear Modulus with Shearing Strain at an Isotropic Confining Pressure of 75 psi(=10.8 ksf=518 kPa) from the Combined RCTS Tests of Specimen UTA-27-C.

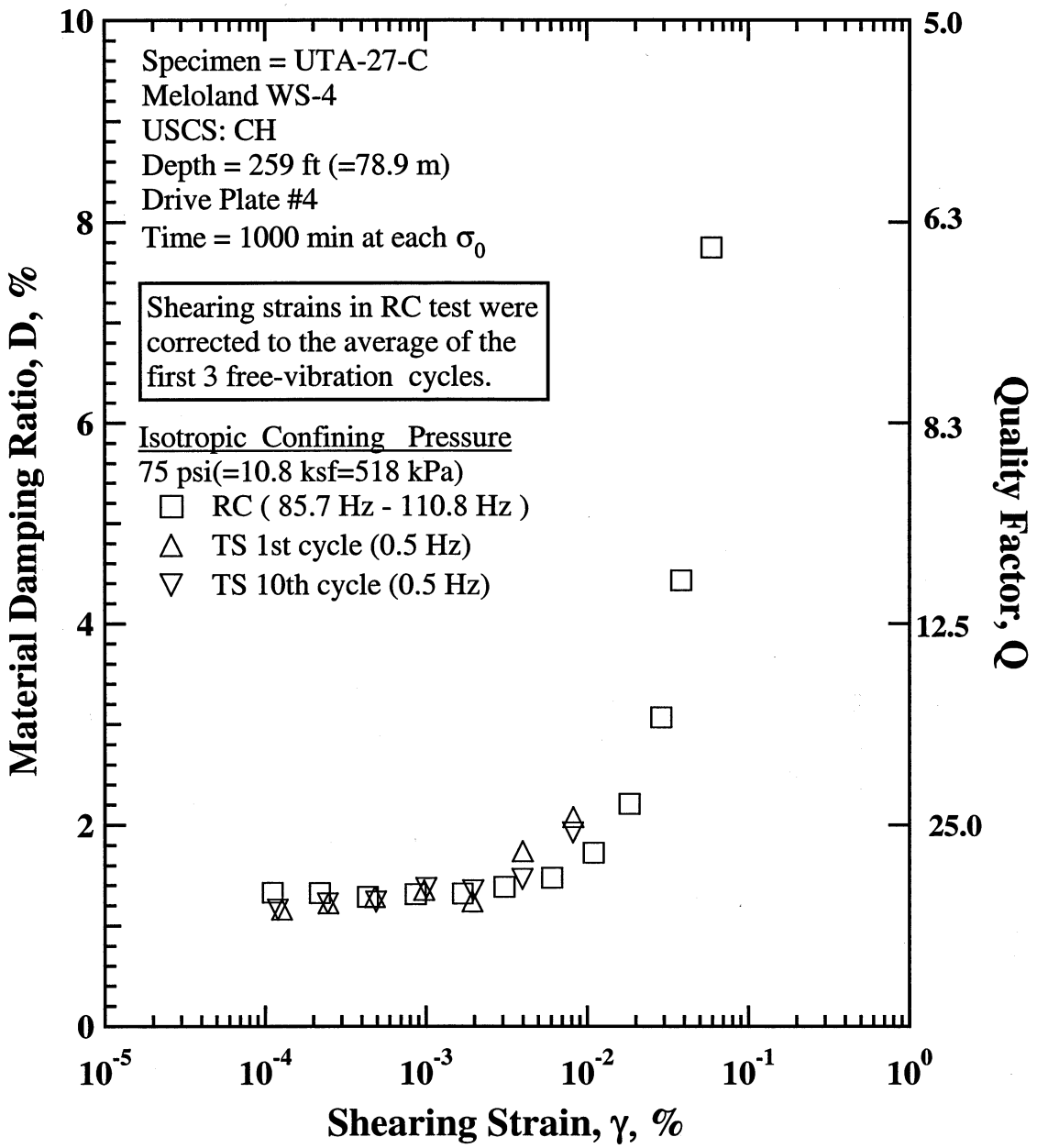

Figure H.10 Comparison of the Variation in Material Damping Ratio with Shearing Strain at an Isotropic Confining Pressure of 75 psi(=10.8 ksf=518 kPa) from the Combined RCTS Tests of Specimen UTA-27-C.

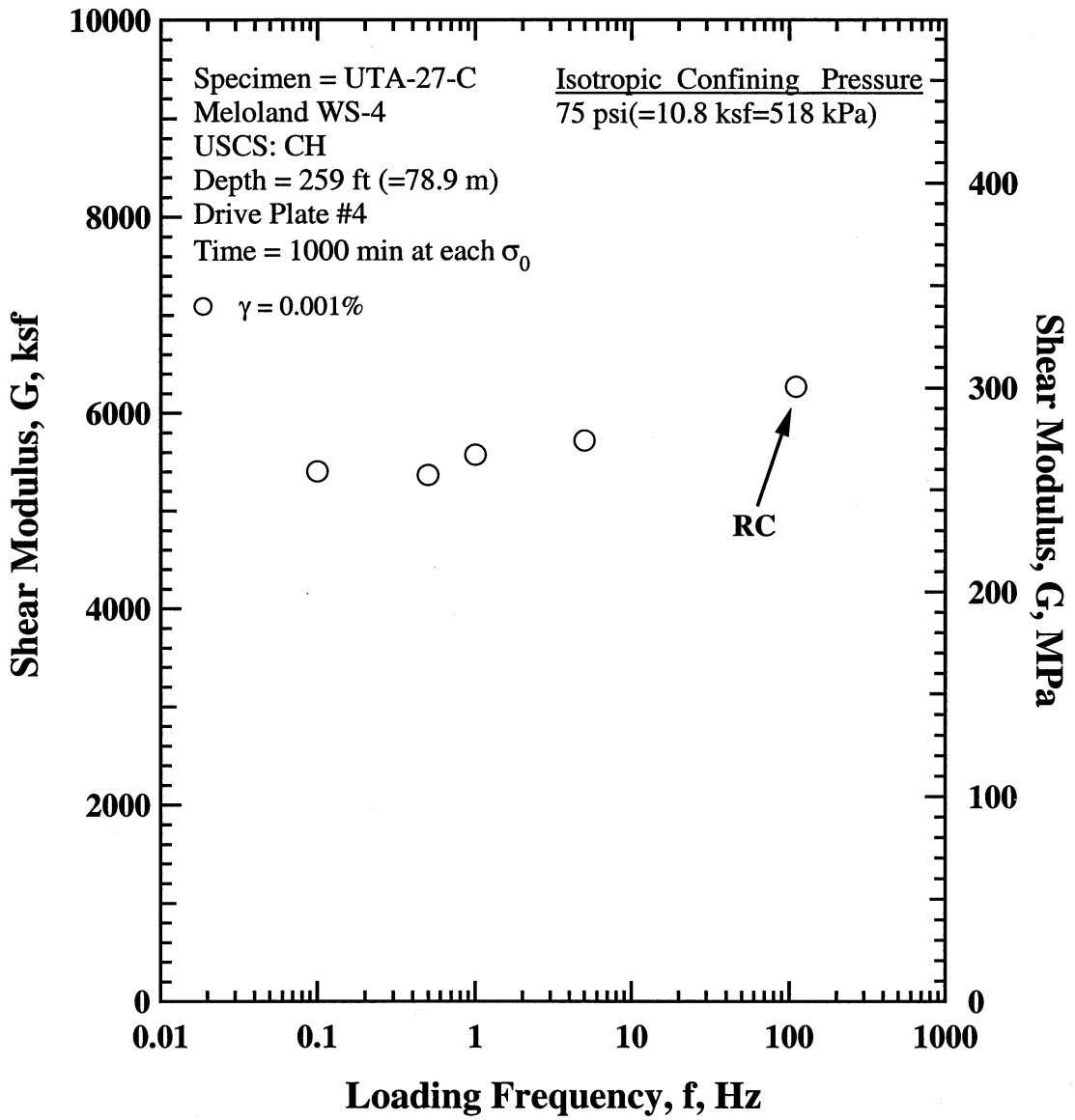

Figure H.11 Comparison of the Variation in Shear Modulus with Loading Frequency at an Isotropic Confining Pressure of 75 psi(=10.8 ksf=518 kPa) from the Combined RCTS Tests of Specimen UTA-27-C.

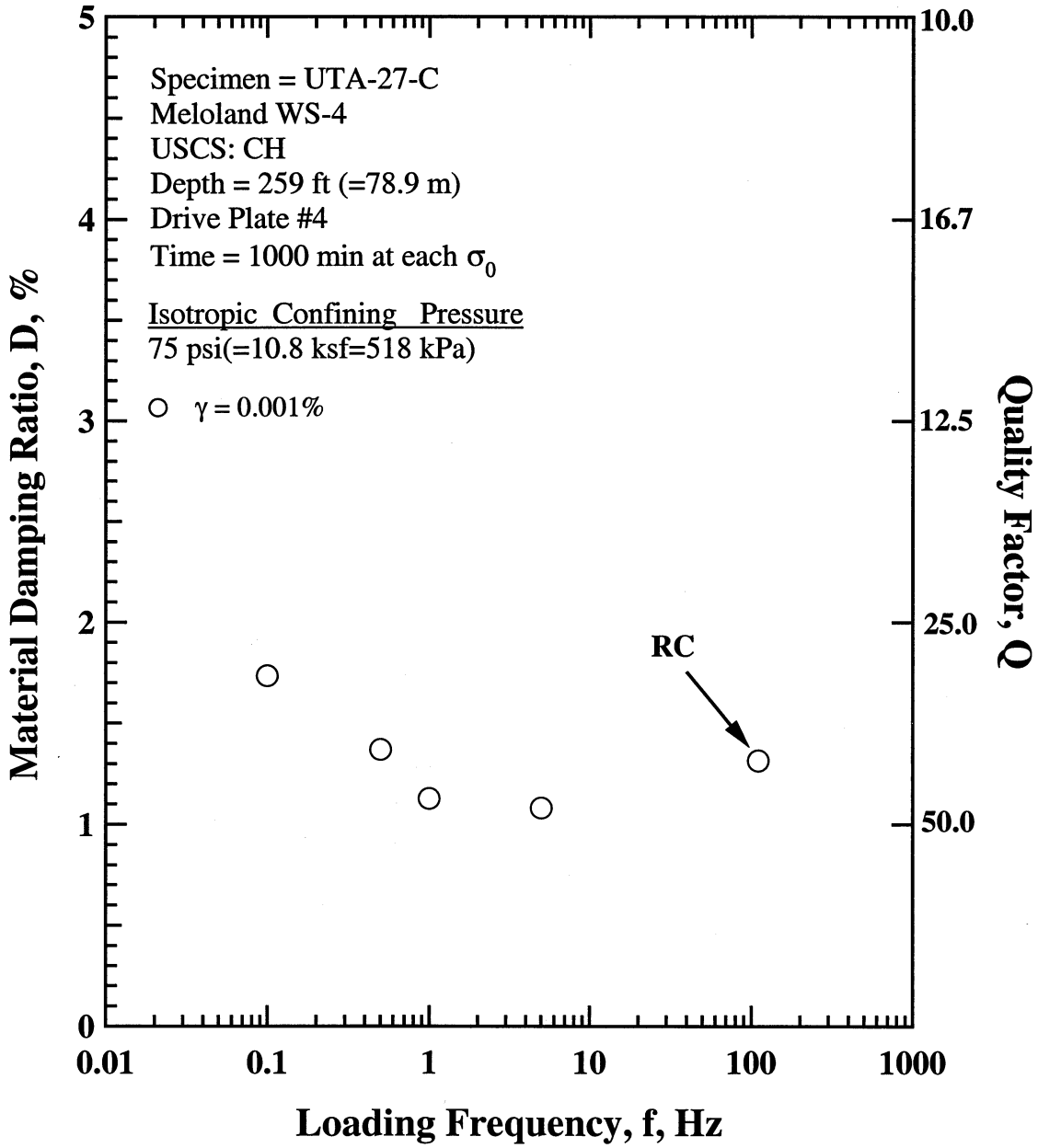

Figure H.12 Comparison of the Variation in Material Damping Ratio with Loading Frequency at an Isotropic Confining Pressure 75 psi(=10.8 ksf=518 kPa) from the Combined RCTS Tests of Specimen UTA-27-C.

Table H.1 Variation in Low-Amplitude Shear Wave Velocity, Low-Amplitude Shear Modulus, Low-Amplitude Material Damping Ratio and Estimated Void Ratio with Isotropic Confining Pressure from RC Tests of Specimen UTA-27-C.

Effective Isotropic Confining Pressure, σ_o'			Low-Amplitude Shear Modulus, G_{max}		Low-Amplitude Shear Wave Velocity, Vs	Low-Amplitude Material Damping Ratio, D_{min}, %	Estimated Void Ratio, e
(psi)	(psf)	(kPa)	(ksf)	(MPa)	(fps)		
18	2592	124.3	4351	208.6	1029	1.81	1.993
37	5328	255.4	5290	253.6	1133	1.65	2.371
75	10800	517.7	6148	294.7	1221	1.44	1.359

Table H.2 Variation in Shear Modulus, Normalized Shear Modulus and Material Damping Ratio with Shearing Strain from RC Tests of Specimen UTA-27-C; Confining Pressure, σ_o' = 75 psi(=10.8 ksf=518 kPa).

Peak Shearing Strain, %	Shear Modulus, G, ksf	Normalized Shear Modulus, G/G_{max}	Average[+] Shearing Strain, %	Material Damping Ratio[x], D, %
1.21E-04	6269	1.00	1.11E-04	1.33
2.38E-04	6269	1.00	2.20E-04	1.33
4.72E-04	6268	1.00	4.36E-04	1.29
9.38E-04	6269	1.00	8.65E-04	1.31
1.84E-03	6212	0.99	1.70E-03	1.32
3.36E-03	6206	0.99	3.08E-03	1.39
6.65E-03	6089	0.97	6.07E-03	1.48
1.22E-02	5922	0.94	1.10E-02	1.73
2.09E-02	5597	0.89	1.83E-02	2.21
3.46E-02	5179	0.83	2.88E-02	3.07
4.95E-02	4580	0.73	3.84E-02	4.43
8.91E-02	3751	0.60	5.91E-02	7.75

[+] Average Shearing Strain from the First Three Cycles of the Free Vibration Decay Curve

[x] Average Damping Ratio from the First Three Cycles of the Free Vibration Decay Curve

Table H.3 Variation in Shear Modulus, Normalized Shear Modulus and Material Damping Ratio with Shearing Strain from TS Tests of Specimen UTA-27-C; Effective Confining Pressure, σ_o' = 75 psi(=10.8 ksf=518 kPa).

First Cycle				Tenth Cycle			
Peak Shearing Strain, %	Shear Modulus, G, ksf	Normalized Shear Modulus, G/G_{max}	Material Damping Ratio, D, %	Peak Shearing Strain, %	Shear Modulus, G, ksf	Normalized Shear Modulus, G/G_{max}	Material Damping Ratio, D, %
1.28E-04	5504	1.00	1.16	1.21E-04	5550	1.00	1.16
2.49E-04	5550	1.00	1.22	2.48E-04	5504	1.00	1.22
4.87E-04	5525	1.00	1.28	4.94E-04	5525	1.00	1.24
9.88E-04	5526	1.00	1.35	1.02E-03	5526	1.00	1.37
1.96E-03	5496	0.99	1.24	1.99E-03	5496	0.99	1.35
4.02E-03	5437	0.98	1.73	4.00E-03	5457	0.99	1.46
8.28E-03	5281	0.96	2.07	8.26E-03	5298	0.96	1.92

APPENDIX I

Specimen No. 8
UT Specimen ID: UTA-27-D

Meloland WS-6
Depth = 378 ft (=115.2m)
Soil Type: Clay (CL)

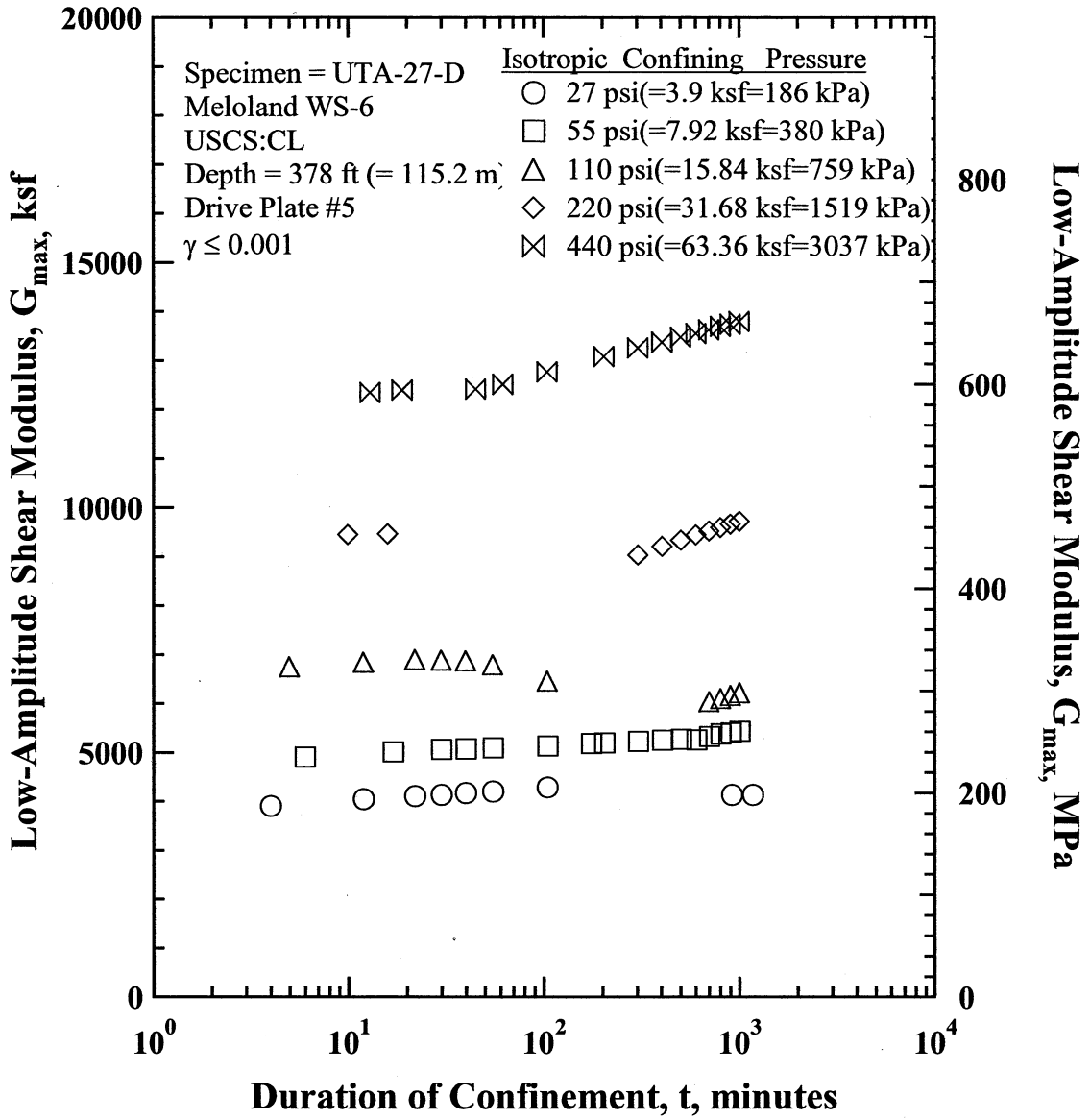

Figure I.1 Variation in Low-Amplitude Shear Modulus with Magnitude and Duration of Isotropic Confining Pressure from Resonant Column Tests of Specimen UTA-27-D.

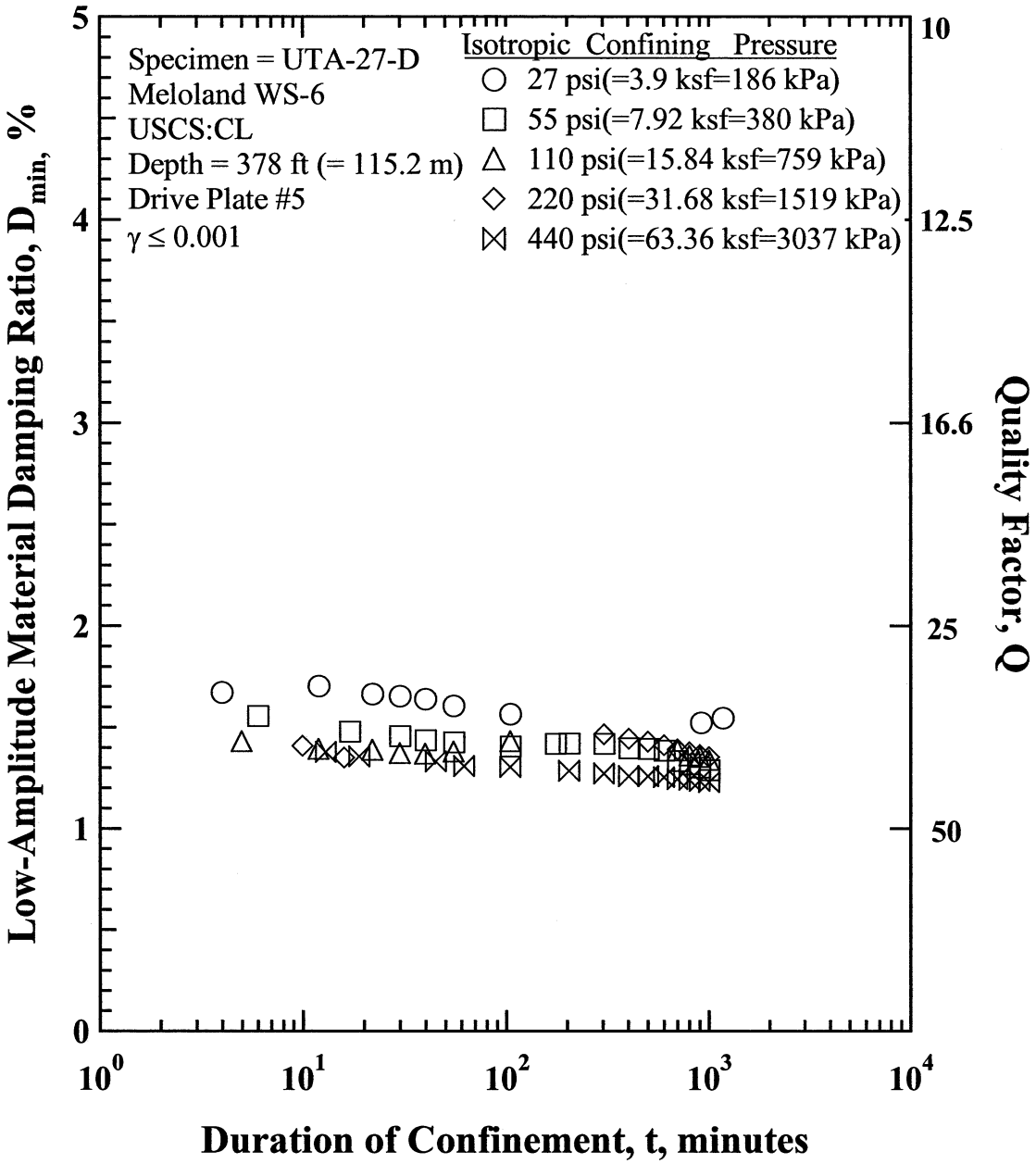

Figure I.2 Variation in Low-Amplitude Material Damping Ratio with Magnitude and Duration of Isotropic Confining Pressure from Resonant Column Tests of Specimen UTA-27-D

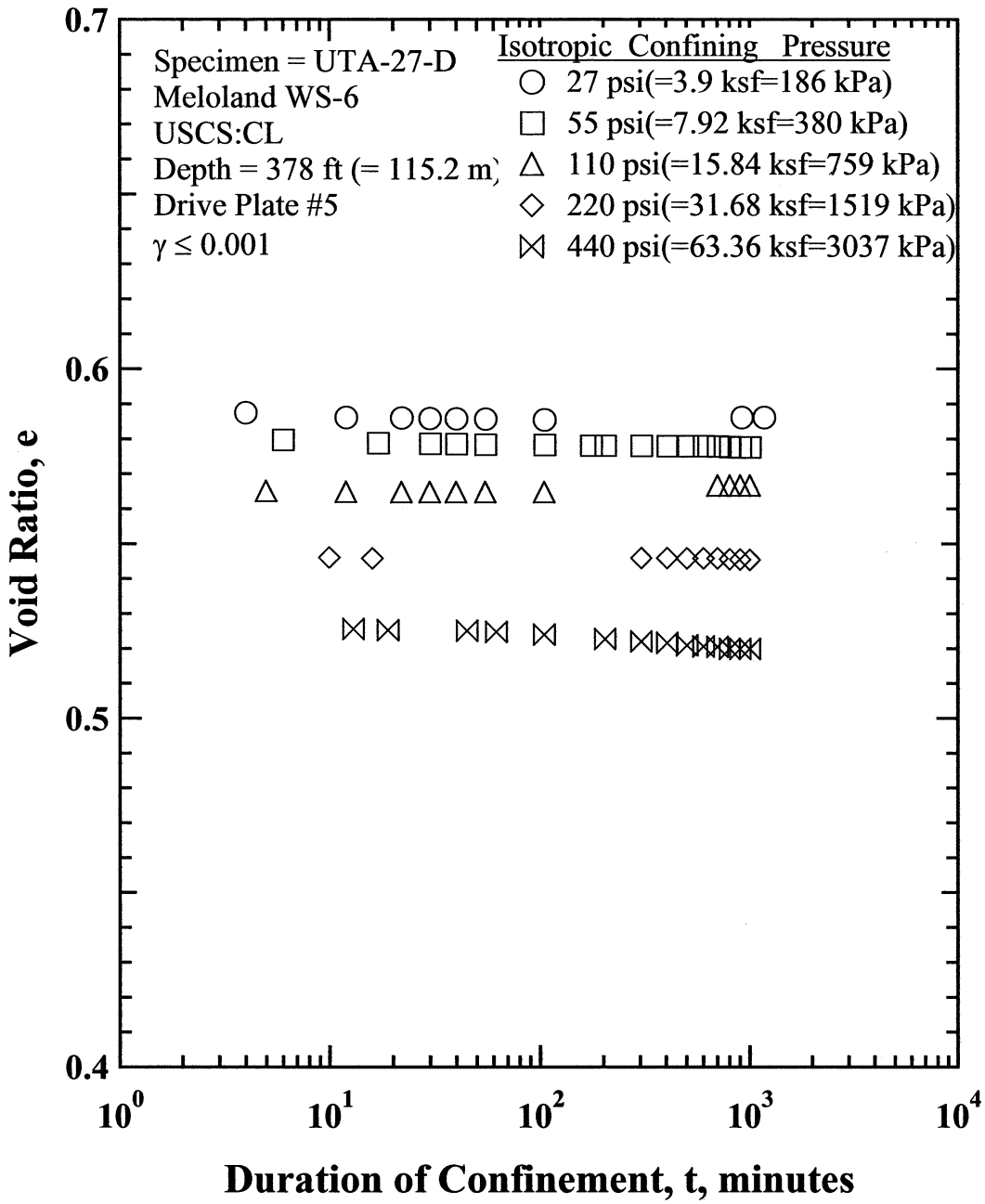

Figure I.3 Variation in Estimated Void Ratio with Magnitude and Duration of Isotropic Confining Pressure from Resonant Column Tests of Specimen UTA-27-D

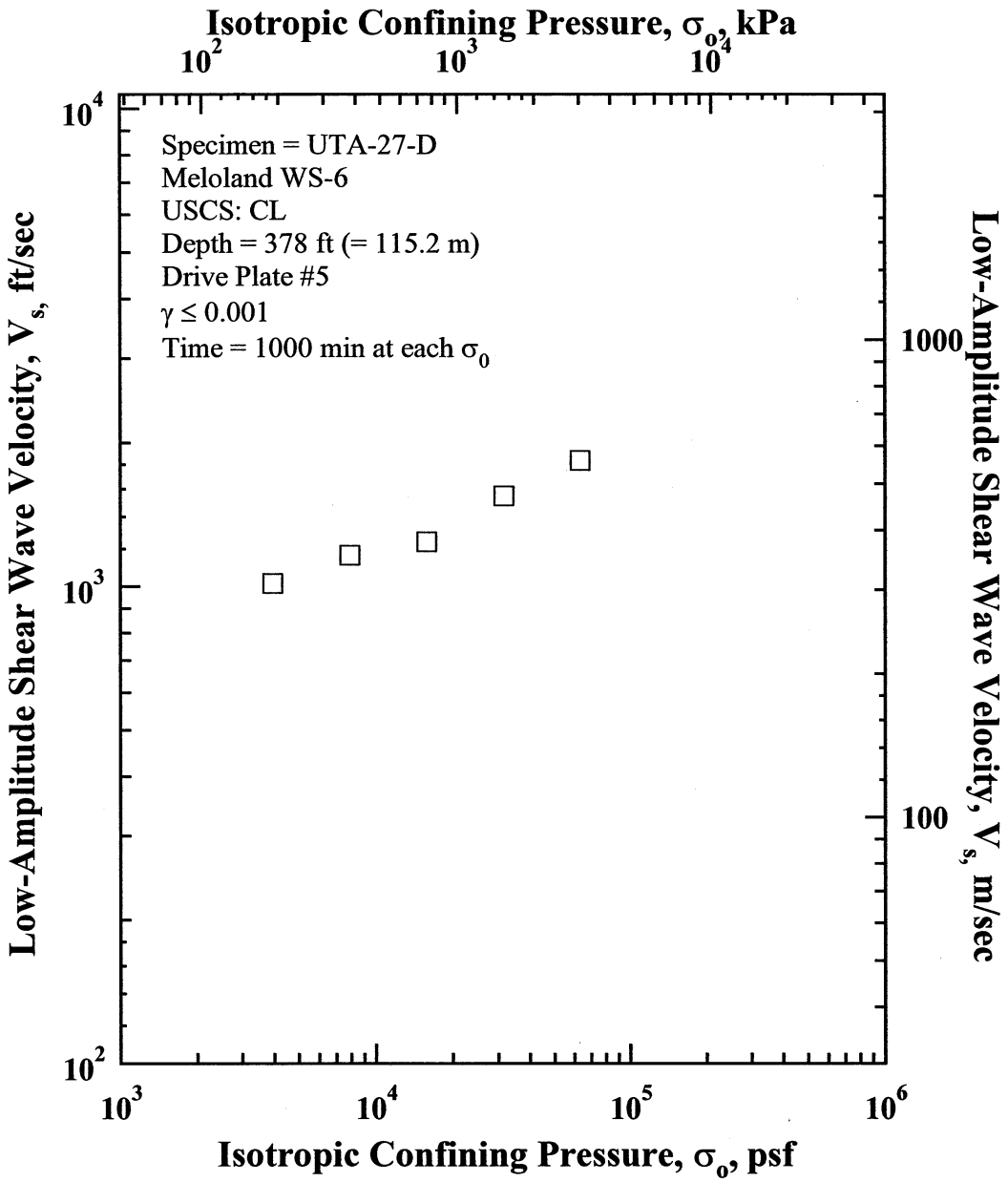

Figure I.4 Variation in Low-Amplitude Shear Wave Velocity with Isotropic Confining Pressure from Resonant Column Tests of Specimen UTA-27-D.

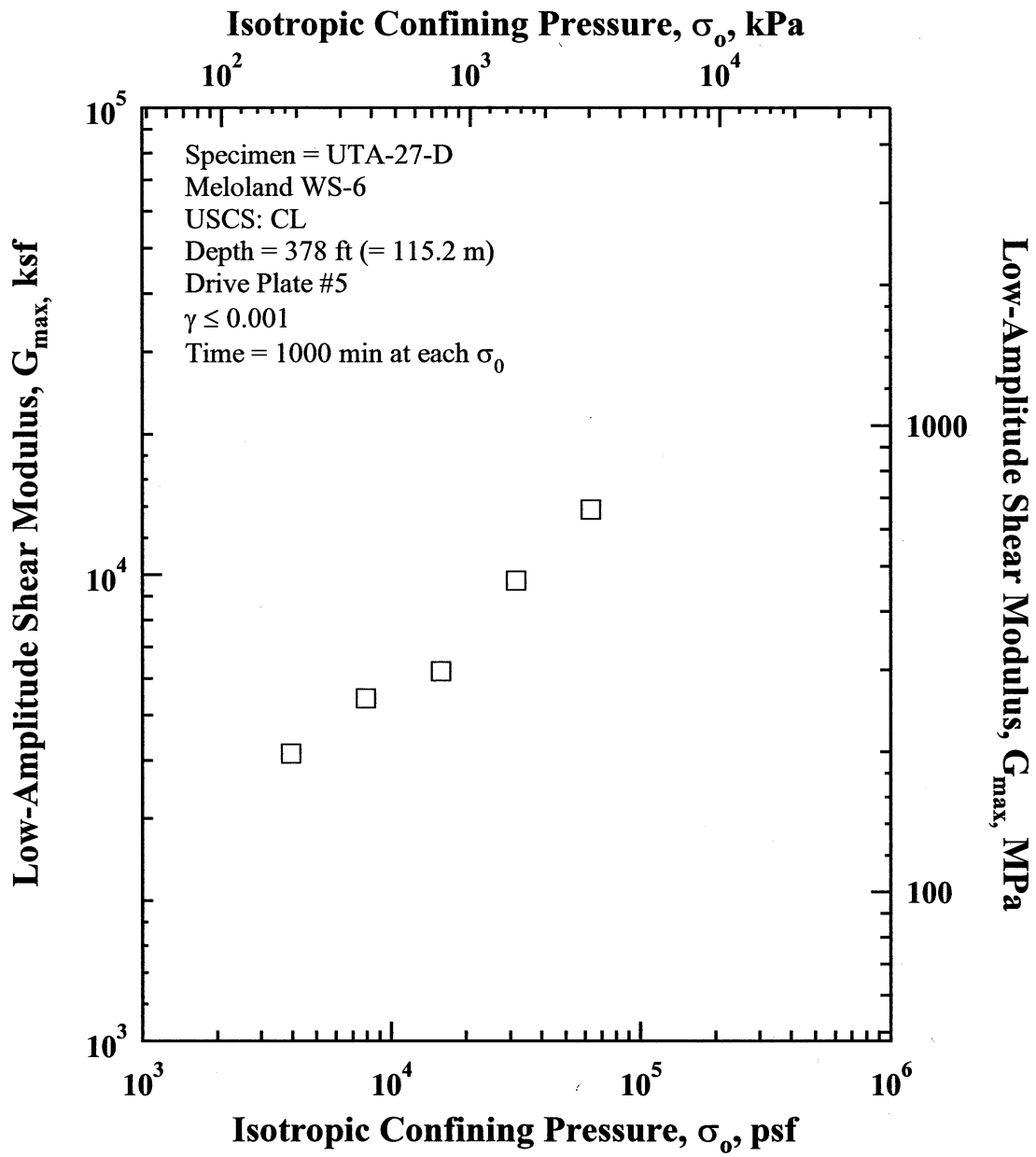

Figure I.5 Variation in Low-Amplitude Shear Modulus with Isotropic Confining Pressure from Resonant Column Tests of Specimen UTA-27-D.

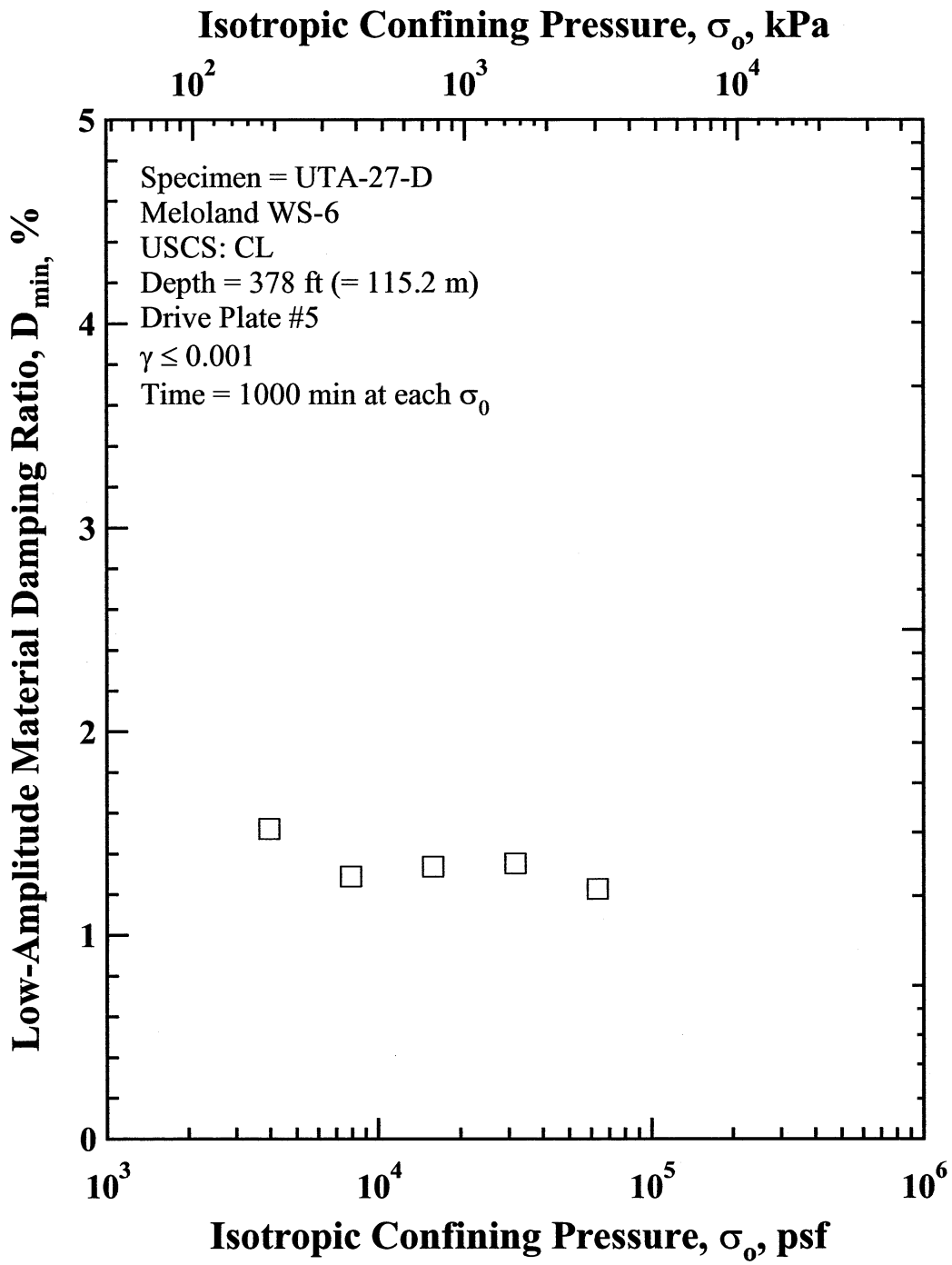

Figure I.6 Variation in Material Damping Ratio with Isotropic Confining Pressure from Resonant Column Tests of Specimen UTA-27-D.

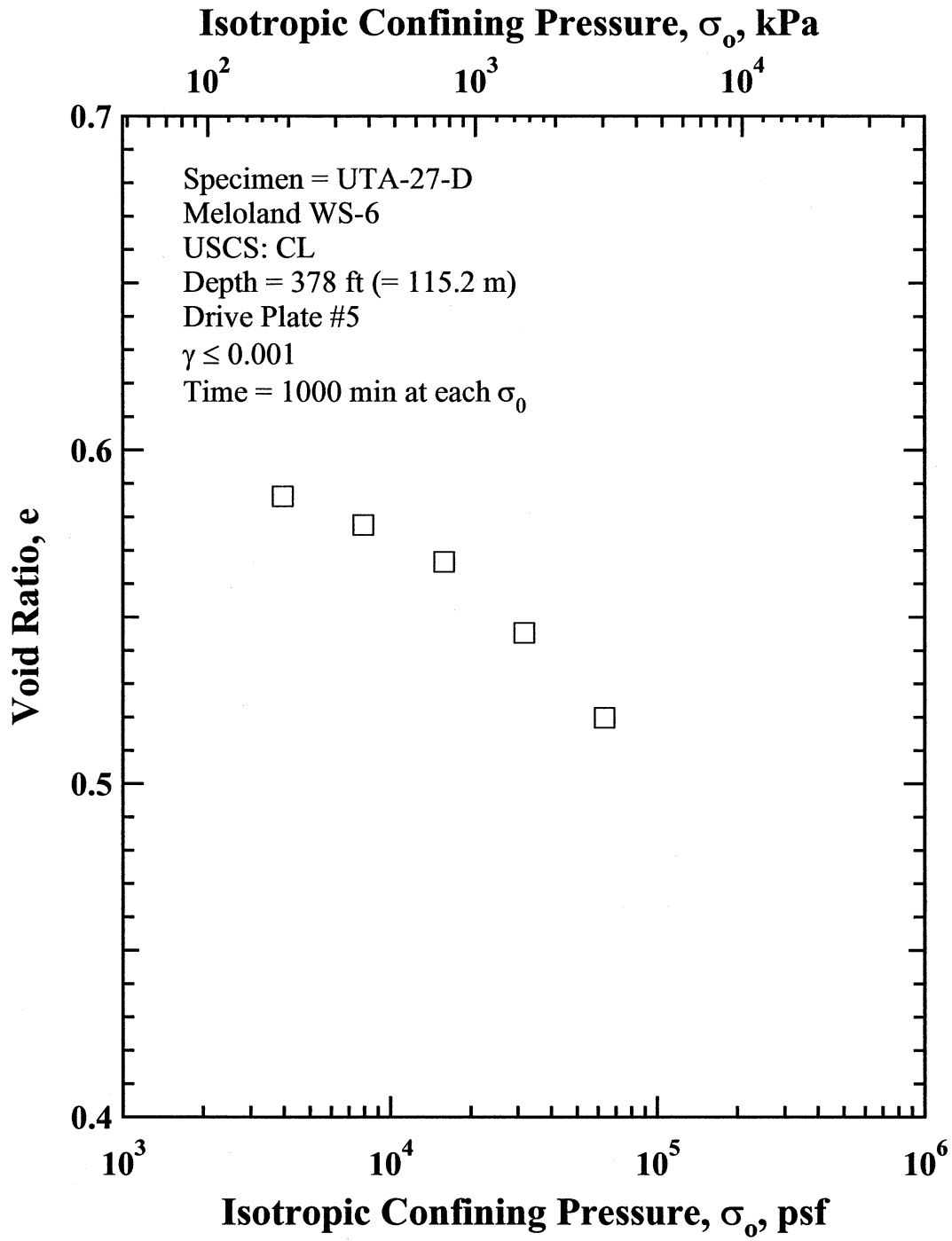

Figure I.7 Variation in Estimated Void Ratio with Isotropic Confining Pressure from Resonant Column Tests of Specimen UTA-27-D.

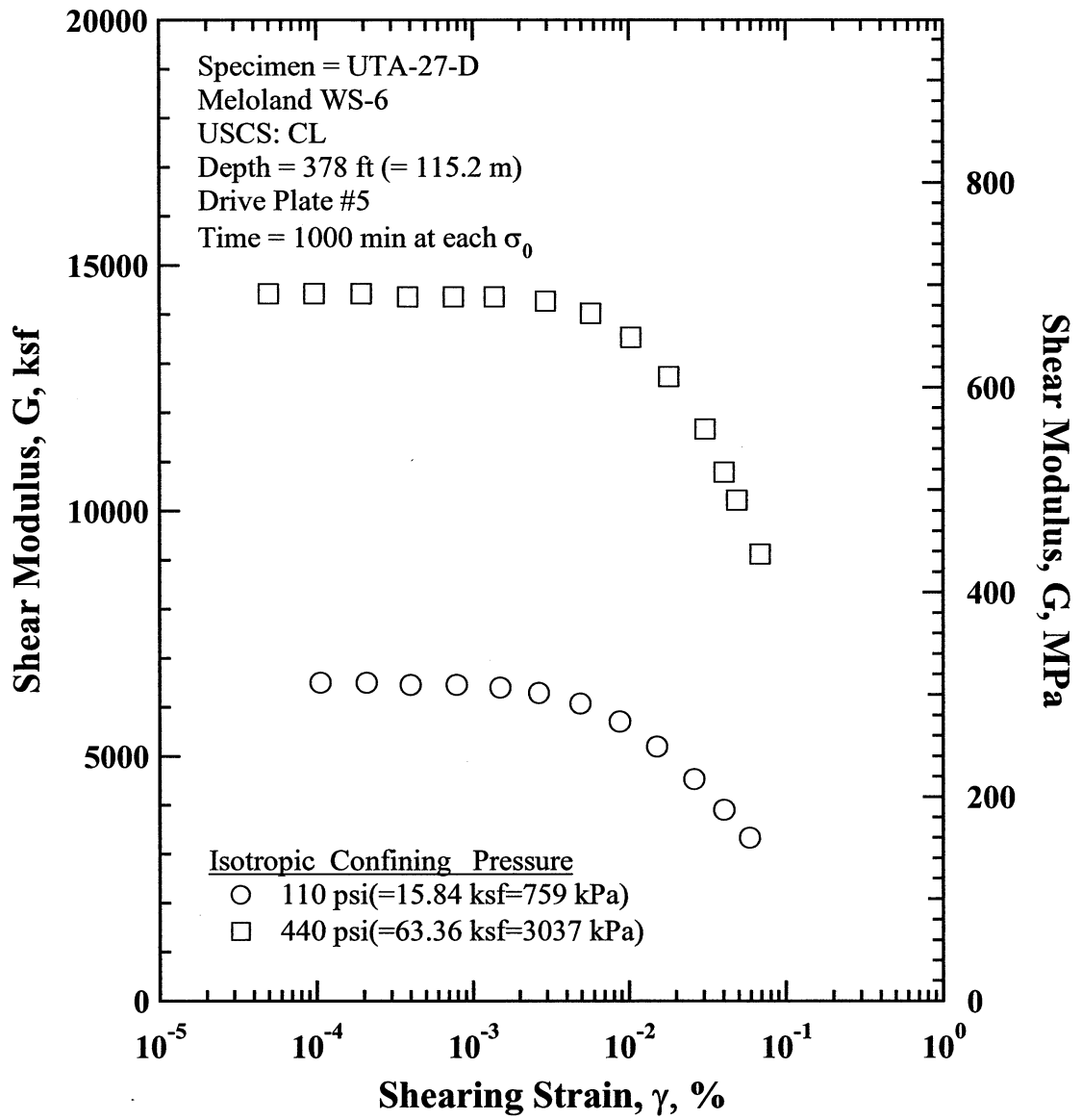

Figure I.8 Comparison of the Variation in Shear Modulus with Shearing Strain and Isotropic Confining Pressure from the Resonant Column Tests of Specimen UTA-27-D.

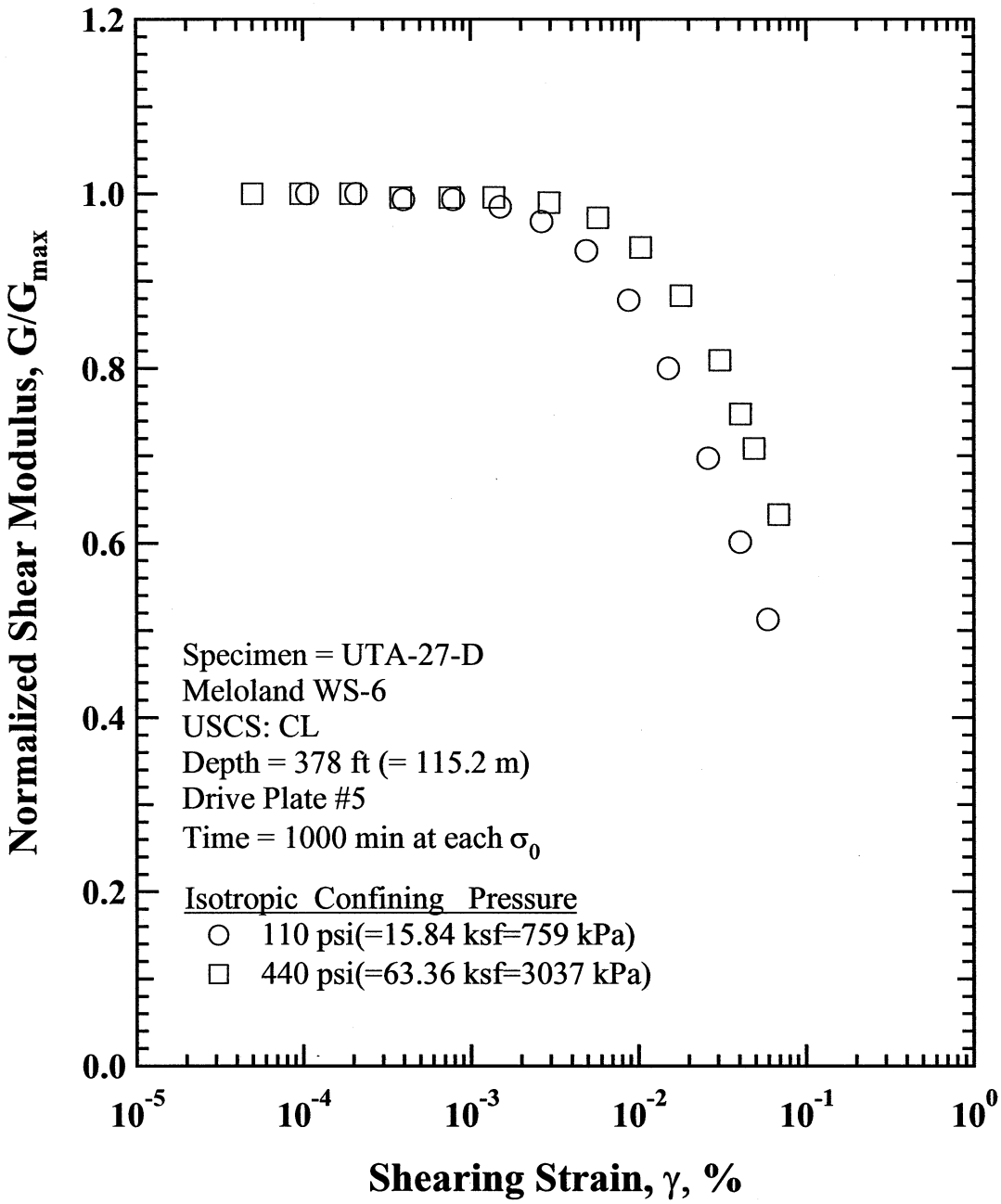

Figure I.9 Comparison of the Variation in Normalized Shear Modulus with Shearing Strain and Isotropic Confining Pressure from the Resonant Column Tests of Specimen UTA-27-D.

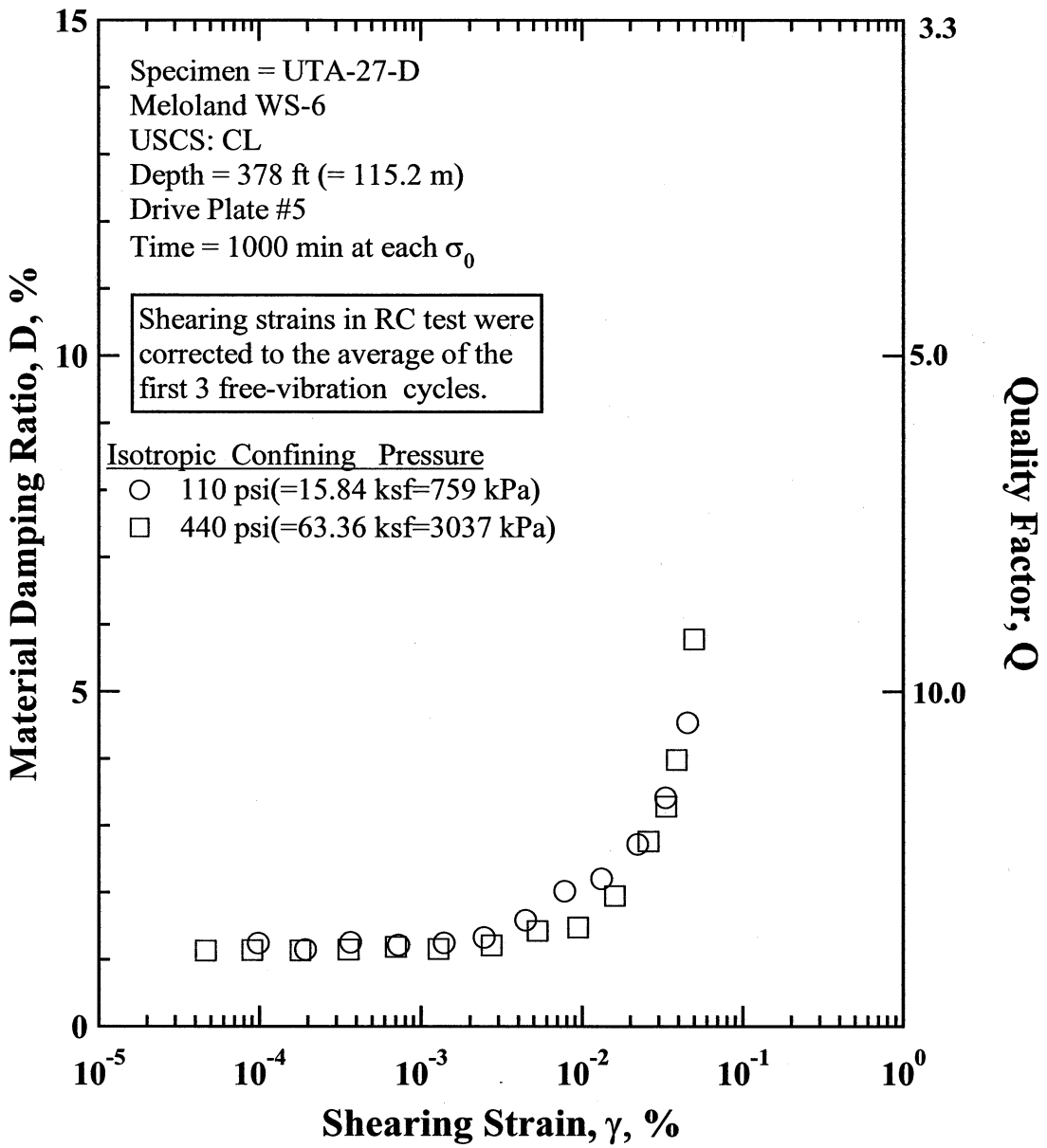

Figure I.10 Comparison of the Variation in Material Damping Ratio with Shearing Strain and Isotropic Confining Pressure from the Resonant Column Tests of Specimen UTA-27-D.

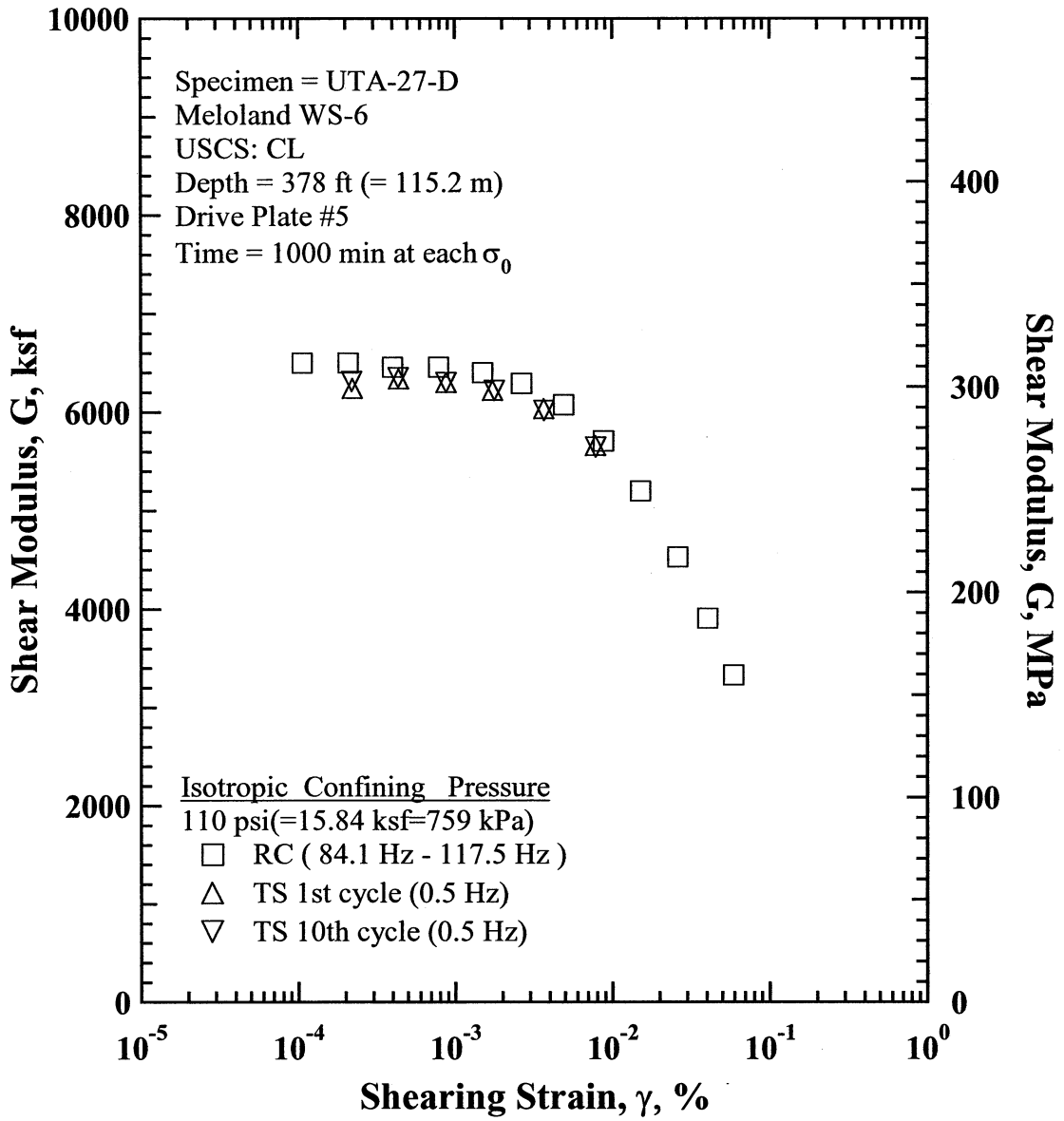

Figure I.11 Comparison of the Variation in Shear Modulus with Shearing Strain at an Isotropic Confining Pressure of 110 psi(=15.84 ksf=759 kPa) from the Combined RCTS Tests of Specimen UTA-27-D.

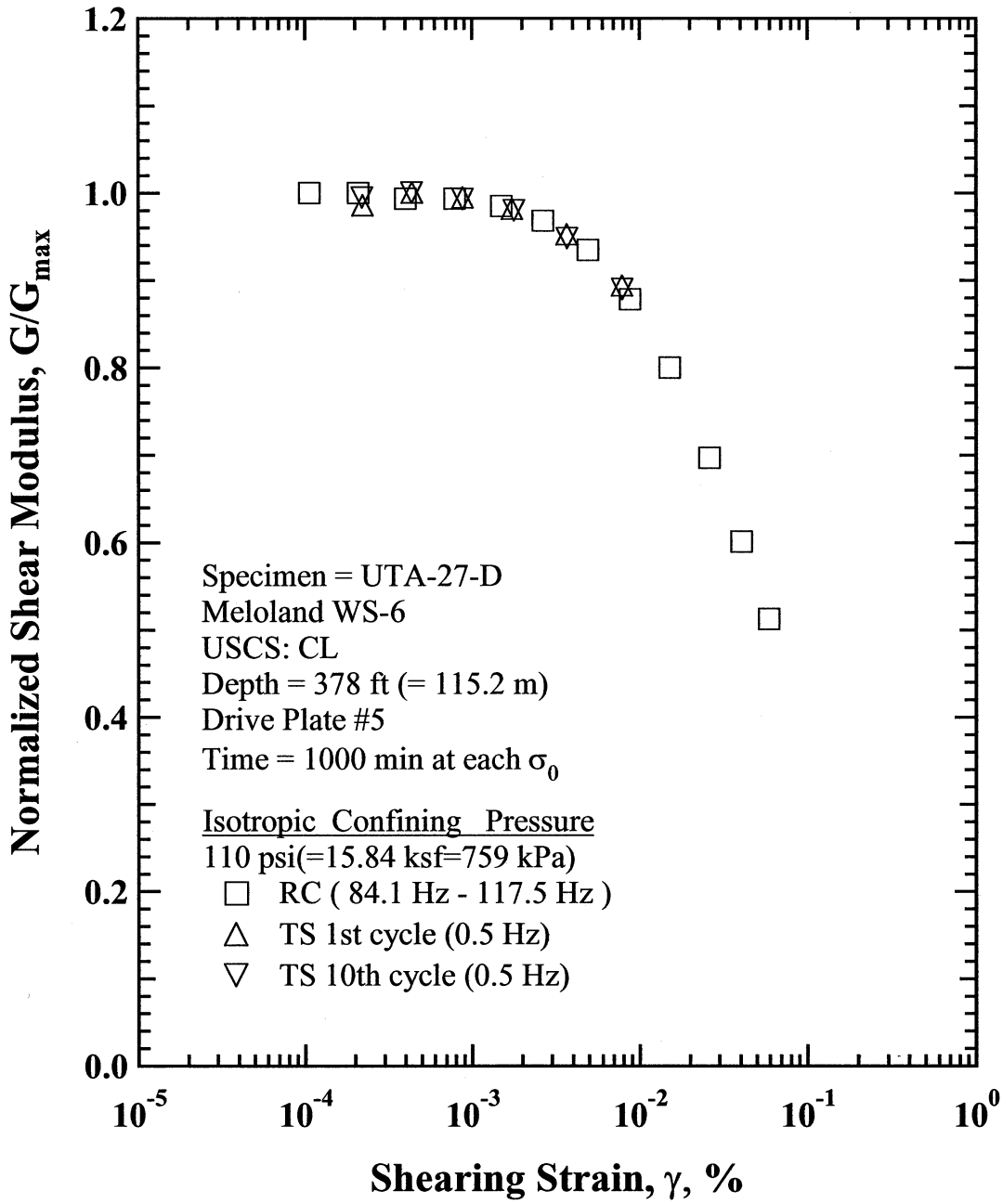

Figure I.12 Comparison of the Variation in Normalized Shear Modulus with Shearing Strain at an Isotropic Confining Pressure of 110 psi(=15.84 ksf=759 kPa) from the Combined RCTS Tests of Specimen UTA-27-D.

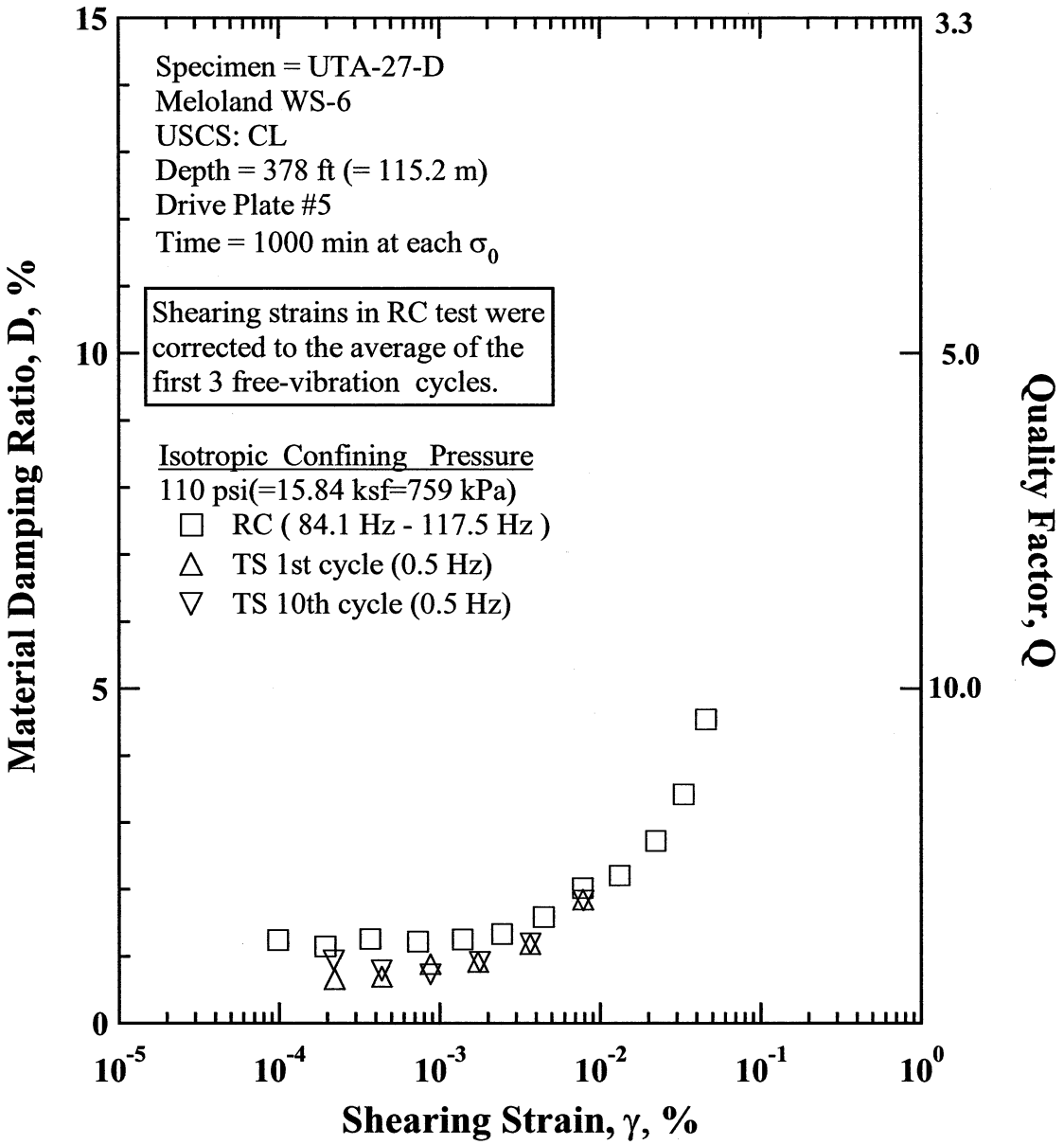

Figure I.13 Comparison of the Variation in Material Damping Ratio with Shearing Strain at an Isotropic Confining Pressure of 110 psi(=15.84 ksf=759 kPa) from the Combined RCTS Tests of Specimen UTA-27-D.

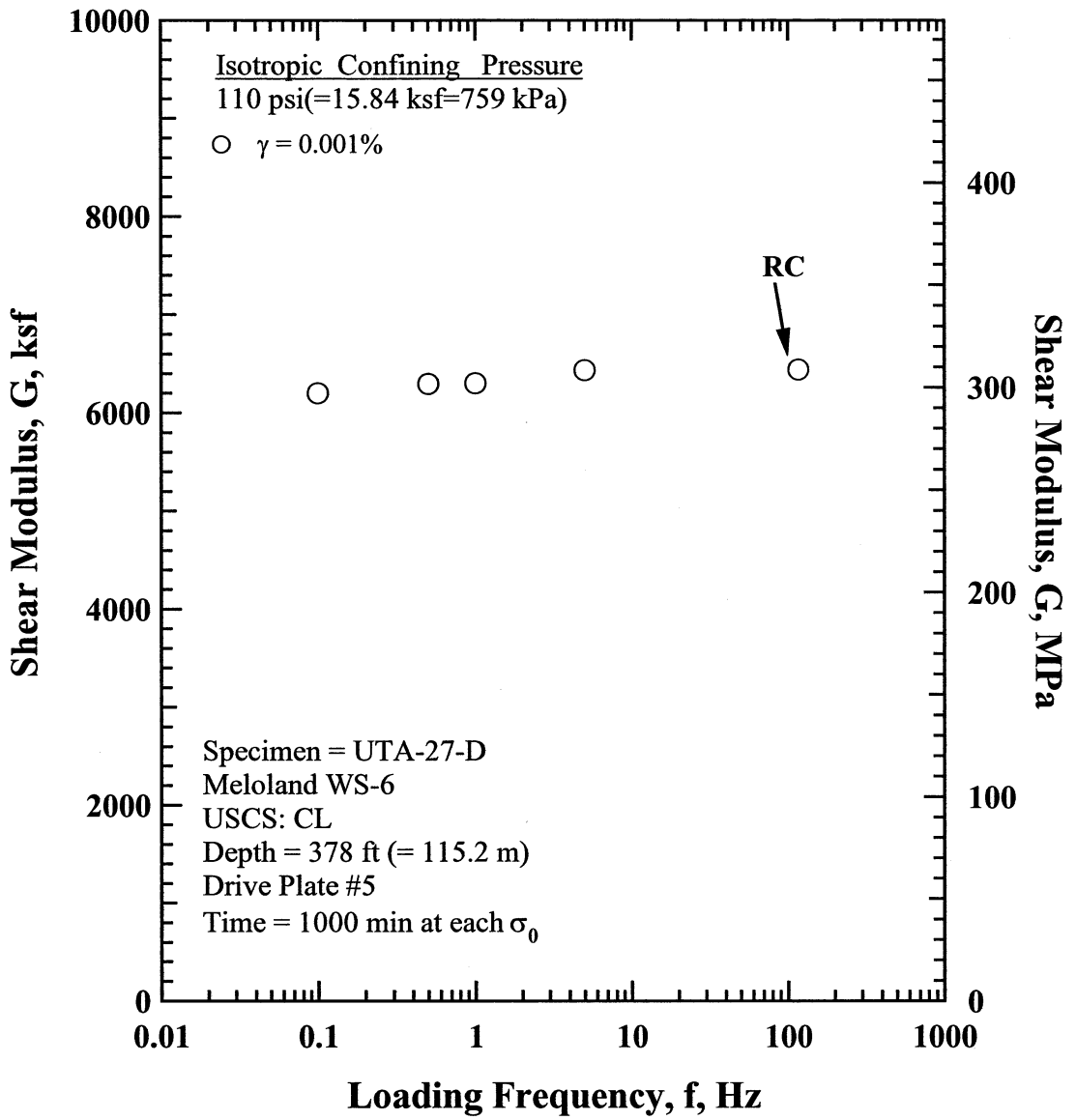

Figure I.14 Comparison of the Variation in Shear Modulus with Loading Frequency at an Isotropic Confining Pressure of 110 psi(=15.84 ksf=759 kPa) from the Combined RCTS Tests of Specimen UTA-27-D.

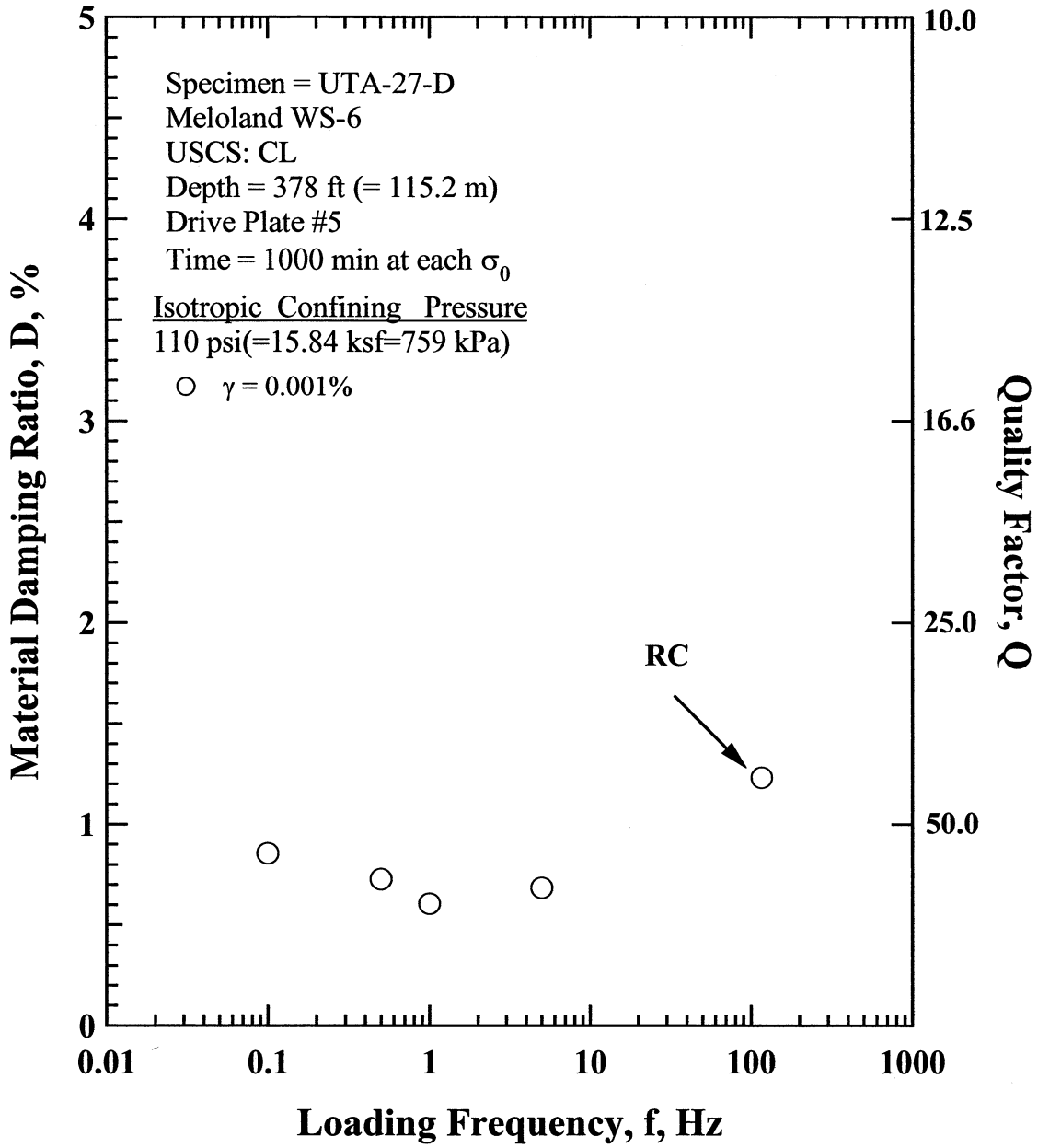

Figure I.15 Comparison of the Variation in Material Damping Ratio with Loading Frequency at an Isotropic Confining Pressure 110 psi(=15.84 ksf=759 kPa) from the Combined RCTS Tests of Specimen UTA-27-D.

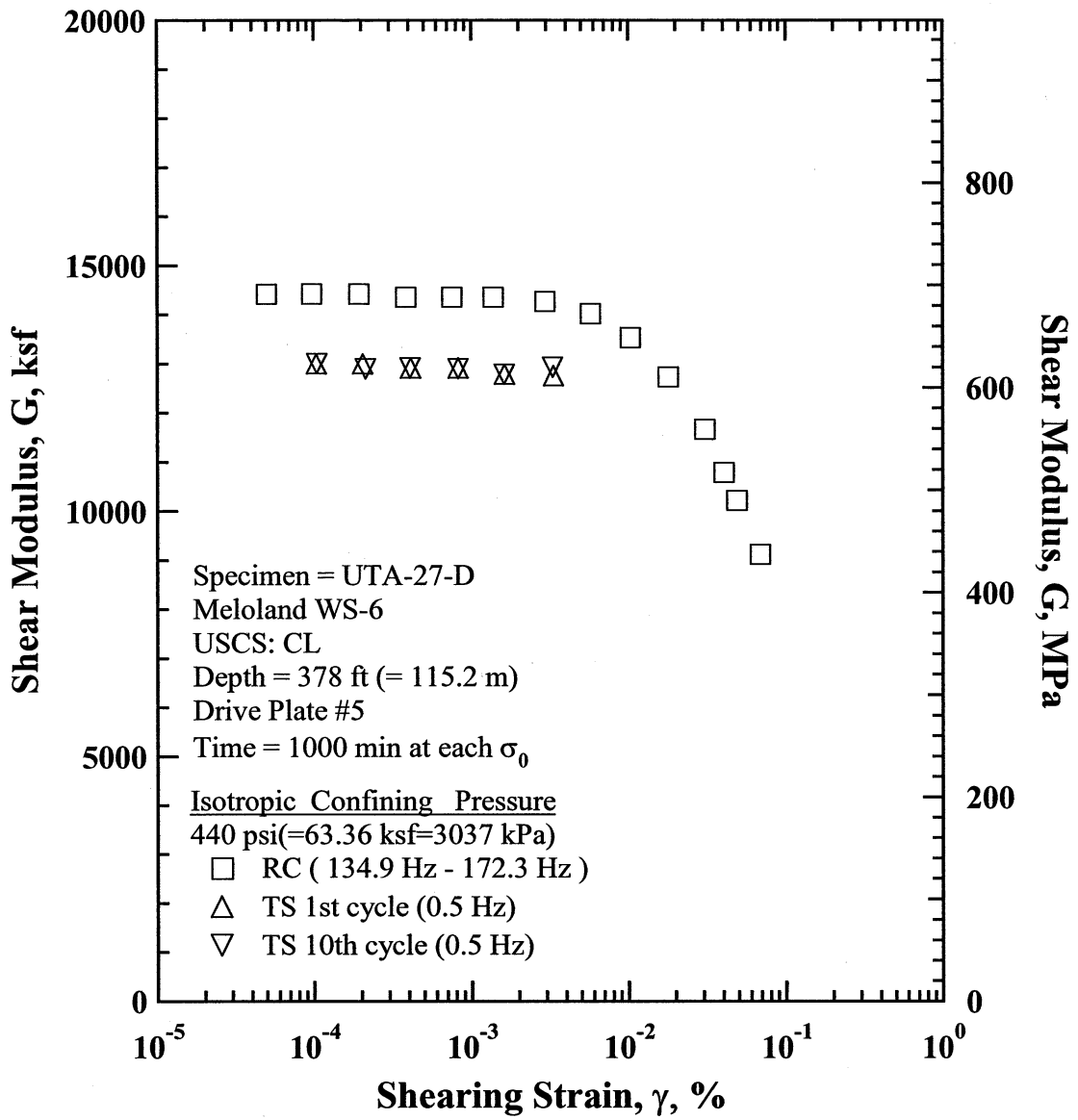

Figure I.16 Comparison of the Variation in Shear Modulus with Shearing Strain at an Isotropic Confining Pressure of 440 psi(=63.36 ksf=3037 kPa) from the Combined RCTS Tests of Specimen UTA-27-D.

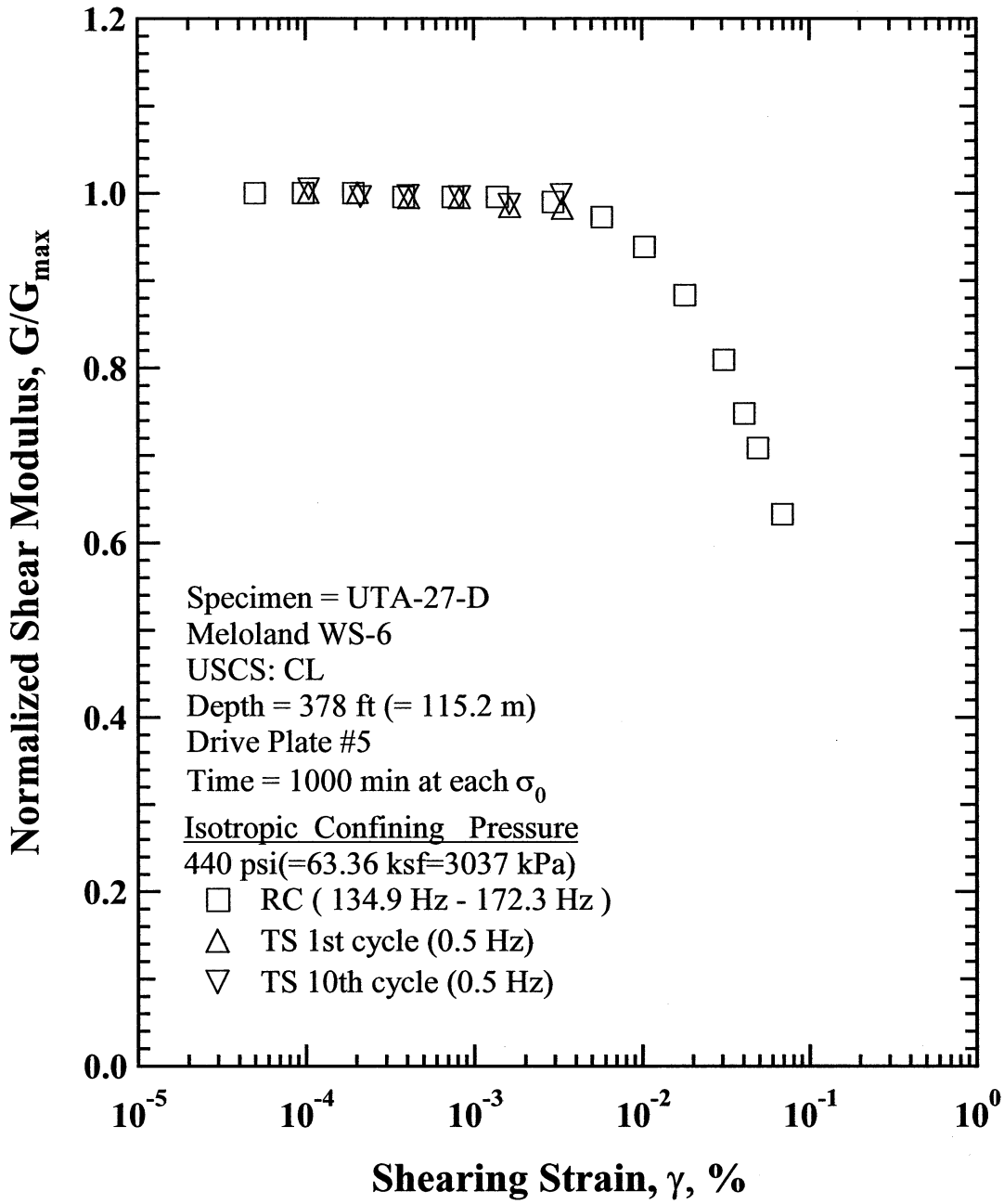

Figure I.17 Comparison of the Variation in Normalized Shear Modulus with Shearing Strain at an Isotropic Confining Pressure of 440 psi(=63.36 ksf=3037 kPa) from the Combined RCTS Tests of Specimen UTA-27-D.

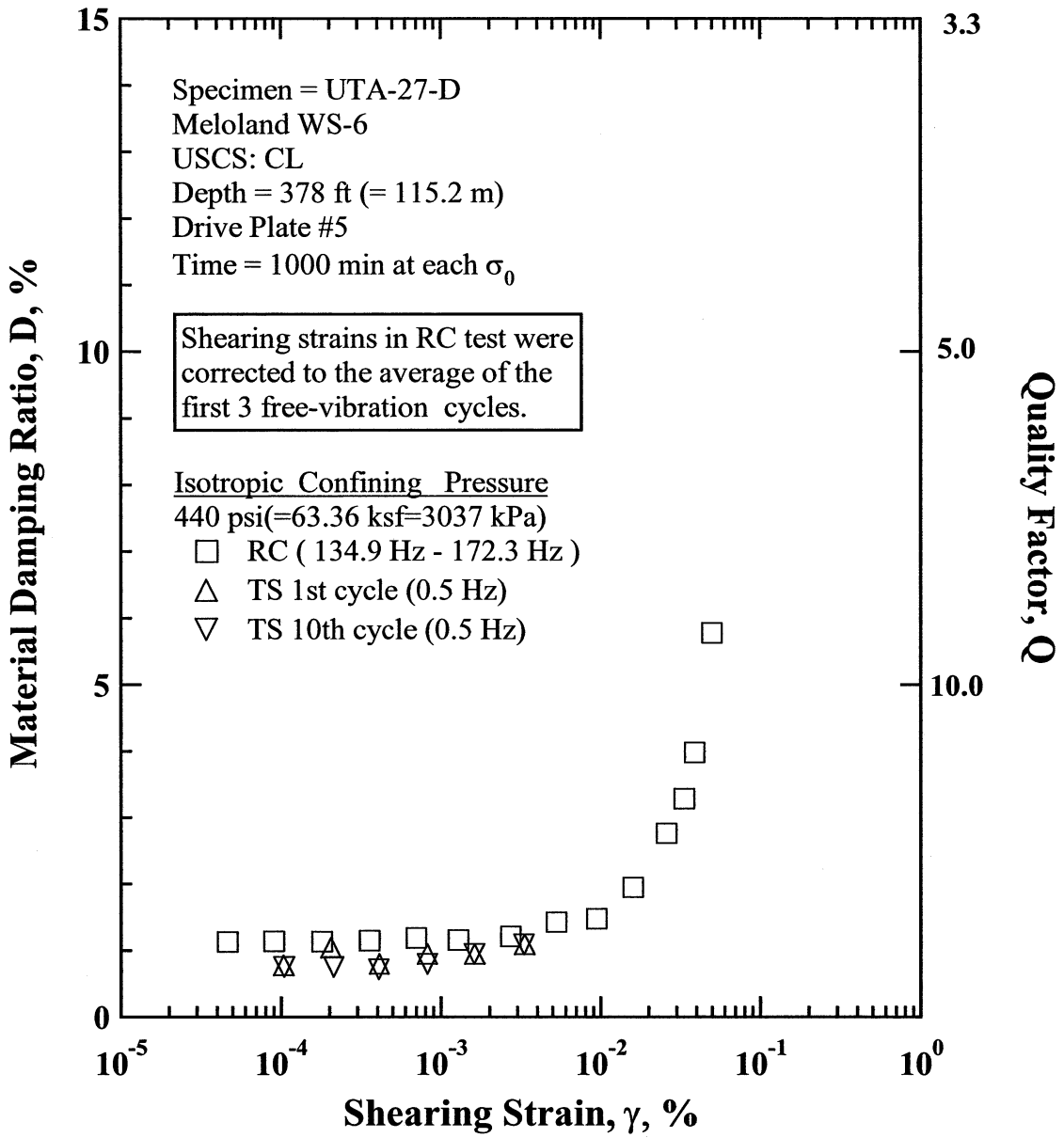

Figure I.18 Comparison of the Variation in Material Damping Ratio with Shearing Strain at an Isotropic Confining Pressure of 440 psi(=63.36 ksf=3037 kPa) from the Combined RCTS Tests of Specimen UTA-27-D.

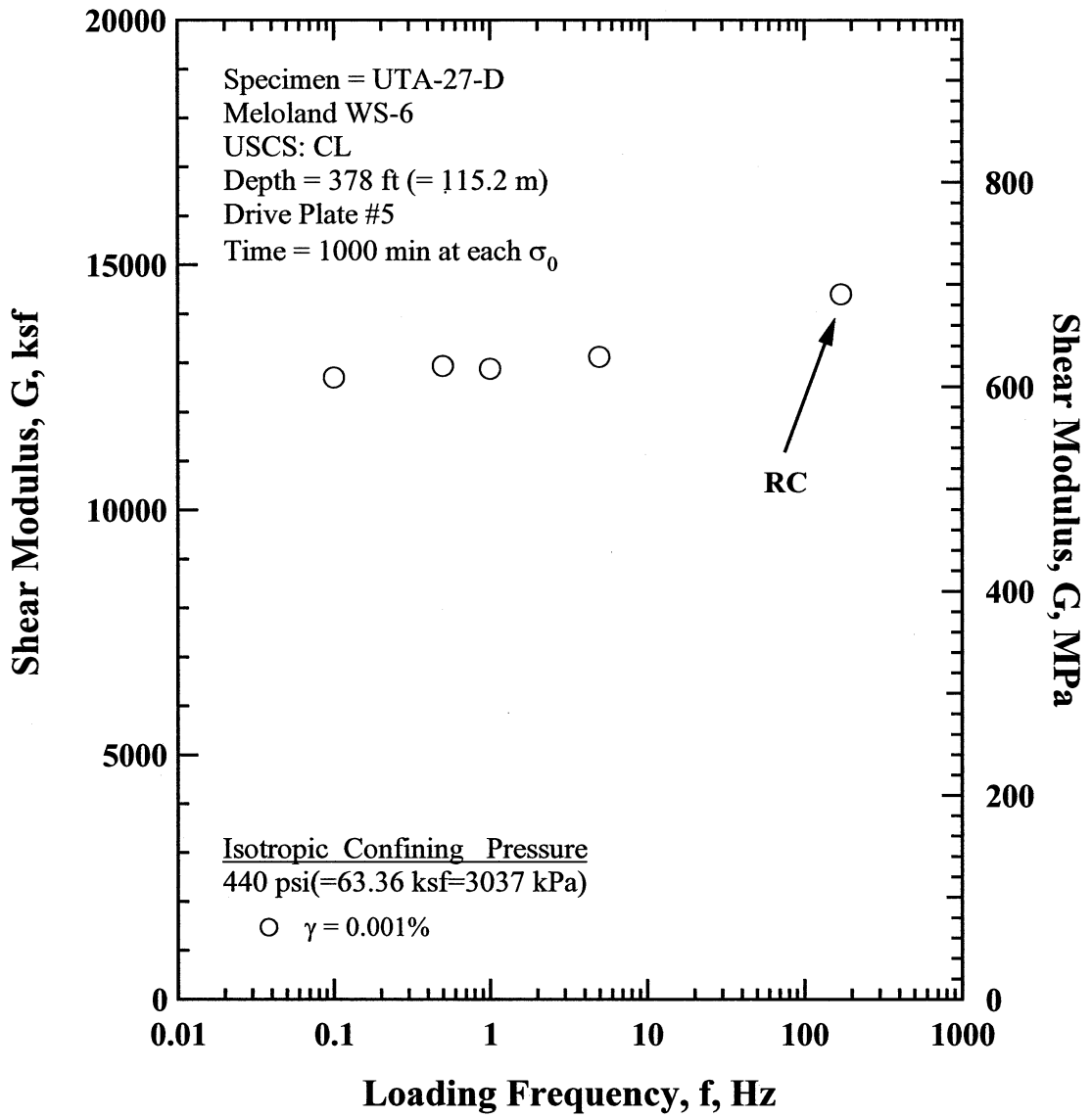

Figure I.19 Comparison of the Variation in Shear Modulus with Loading Frequency at an Isotropic Confining Pressure of 440 psi(=63.36 ksf=3037 kPa) from the Combined RCTS Tests of Specimen UTA-27-D.

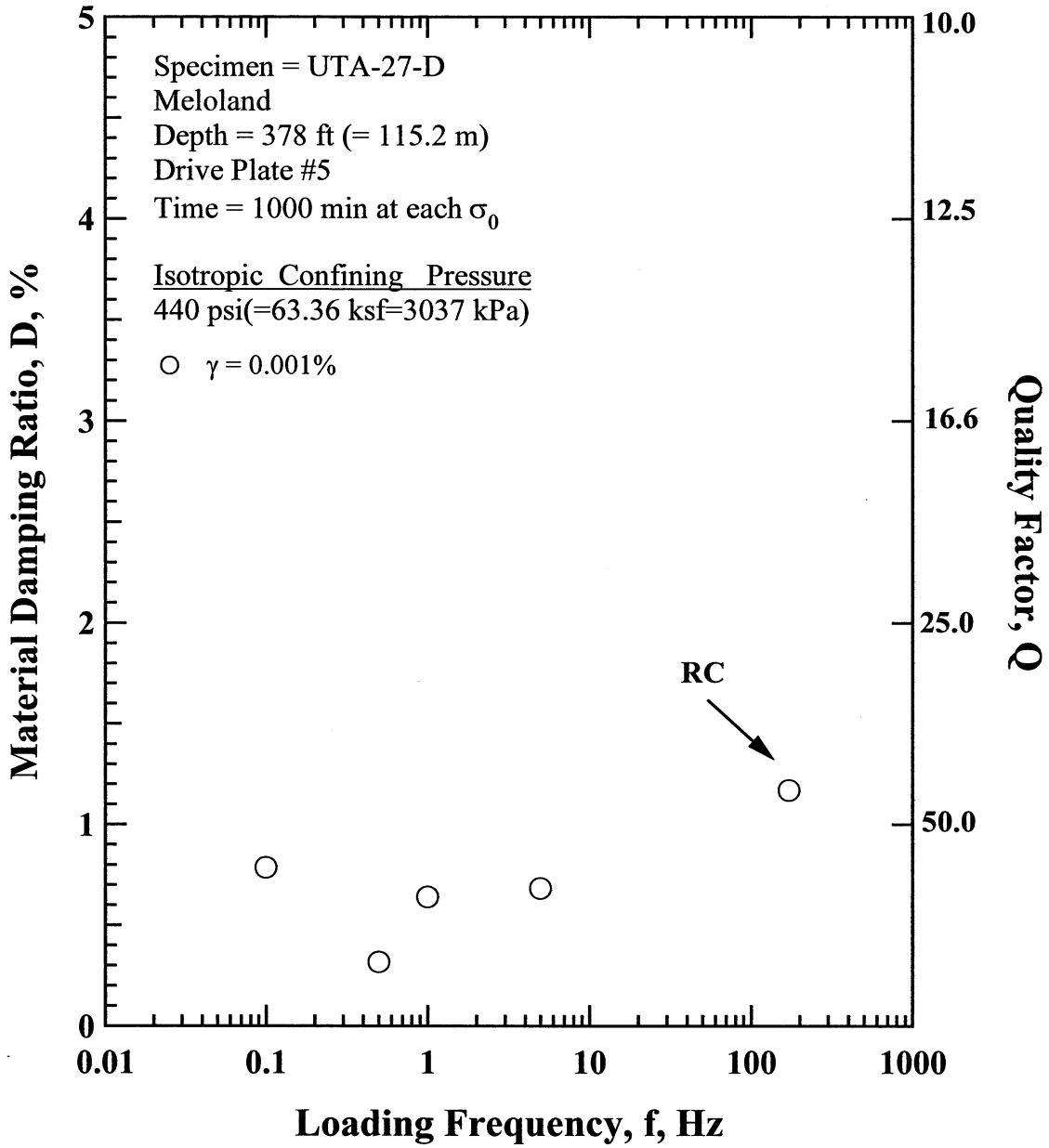

Figure I.20 Comparison of the Variation in Material Damping Ratio with Loading Frequency at an Isotropic Confining Pressure 440 psi(=63.36 ksf=3037 kPa) from the Combined RCTS Tests of Specimen UTA-27-D.

Table I.1 Variation in Low-Amplitude Shear Wave Velocity, Low-Amplitude Shear Modulus, Low-Amplitude Material Damping Ratio and Estimated Void Ratio with Isotropic Confining Pressure from RC Tests of Specimen UTA-27-D.

Effective Isotropic Confining Pressure, σ_o'			Low-Amplitude Shear Modulus, G_{max}		Low-Amplitude Shear Wave Velocity, Vs	Low-Amplitude Material Damping Ratio, D_{min}, %	Estimated Void Ratio, e
(psi)	(psf)	(kPa)	(ksf)	(MPa)	(fps)		
28	3960	189.8	4134	198.2	1016	1.52	0.586
55	7920	379.7	5432	260.4	1163	1.29	0.578
110	15840	759.4	6213	297.8	1241	1.34	0.567
220	31680	1518.7	9714	465.7	1547	1.35	0.545
440	63360	3037.5	13786	660.9	1834	1.23	0.520

Table I.2 Variation in Shear Modulus, Normalized Shear Modulus and Material Damping Ratio with Shearing Strain from RC Tests of Specimen UTA-27-D; Confining Pressure, σ_o' = 110 psi(=15.84 ksf=759 kPa).

Peak Shearing Strain, %	Shear Modulus, G, ksf	Normalized Shear Modulus, G/G_{max}	Average[+] Shearing Strain, %	Material Damping Ratio[x], D, %
1.06E-04	6499	1.00	9.84E-05	1.24
2.08E-04	6499	1.00	1.94E-04	1.15
3.99E-04	6456	0.99	3.70E-04	1.26
7.88E-04	6456	0.99	7.32E-04	1.22
1.50E-03	6401	0.98	1.39E-03	1.25
2.66E-03	6292	0.97	2.45E-03	1.33
4.90E-03	6076	0.93	4.45E-03	1.59
8.77E-03	5707	0.88	7.77E-03	2.02
1.51E-02	5200	0.80	1.32E-02	2.21
2.61E-02	4531	0.70	2.22E-02	2.72
4.04E-02	3907	0.60	3.31E-02	3.42
5.90E-02	3331	0.51	4.56E-02	4.54

[+] Average Shearing Strain from the First Three Cycles of the Free Vibration Decay Curve

[x] Average Damping Ratio from the First Three Cycles of the Free Vibration Decay Curve

Table I.3 Variation in Shear Modulus, Normalized Shear Modulus and Material Damping Ratio with Shearing Strain from TS Tests of Specimen UTA-27-D; Confining Pressure, σ_o' = 110 psi(=15.84 ksf=759 kPa).

First Cycle				Tenth Cycle			
Peak Shearing Strain, %	Shear Modulus, G, ksf	Normalized Shear Modulus, G/G_{max}	Material Damping Ratio, D, %	Peak Shearing Strain, %	Shear Modulus, G, ksf	Normalized Shear Modulus, G/G_{max}	Material Damping Ratio, D, %
2.23E-04	6240	0.99	0.65	2.21E-04	6310	0.99	0.93
4.40E-04	6334	1.00	0.69	4.39E-04	6345	1.00	0.78
8.86E-04	6296	0.99	0.88	8.85E-04	6298	0.99	0.73
1.75E-03	6216	0.98	0.91	1.79E-03	6216	0.98	0.91
3.70E-03	6031	0.95	1.18	3.71E-03	6014	0.95	1.18
7.89E-03	5659	0.89	1.84	7.91E-03	5644	0.89	1.83

Table I.4 Variation in Shear Modulus, Normalized Shear Modulus and Material Damping Ratio with Shearing Strain from RC Tests of Specimen UTA-27-D; Confining Pressure, σ_o' = 440 psi(=63.36ksf=3038 kPa).

Peak Shearing Strain, %	Shear Modulus, G, ksf	Normalized Shear Modulus, G/G_{max}	Average[+] Shearing Strain, %	Material Damping Ratio[x], D, %
4.97E-05	14419	1.00	4.64E-05	1.13
9.69E-05	14420	1.00	9.04E-05	1.14
1.93E-04	14421	1.00	1.80E-04	1.13
3.83E-04	14355	1.00	3.57E-04	1.15
7.53E-04	14355	1.00	7.00E-04	1.19
1.37E-03	14355	1.00	1.28E-03	1.16
2.93E-03	14269	0.99	2.72E-03	1.21
5.74E-03	14022	0.97	5.26E-03	1.43
1.03E-02	13533	0.94	9.41E-03	1.48
1.79E-02	12732	0.88	1.60E-02	1.95
3.05E-02	11665	0.81	2.59E-02	2.76
4.05E-02	10784	0.75	3.34E-02	3.28
4.88E-02	10217	0.71	3.88E-02	3.98
6.01E-02	9524	0.66	4.34E-02	5.88
6.86E-02	9121	0.63	4.98E-02	5.78

[+] Average Shearing Strain from the First Three Cycles of the Free Vibration Decay Curve

[x] Average Damping Ratio from the First Three Cycles of the Free Vibration Decay Curve

Table I.5 Variation in Shear Modulus, Normalized Shear Modulus and Material Damping Ratio with Shearing Strain from TS Tests of Specimen UTA-27-D; Confining Pressure, σ_o' = 440 psi(=63.36ksf=3038 kPa).

First Cycle				Tenth Cycle			
Peak Shearing Strain, %	Shear Modulus, G, ksf	Normalized Shear Modulus, G/G_{max}	Material Damping Ratio, D, %	Peak Shearing Strain, %	Shear Modulus, G, ksf	Normalized Shear Modulus, G/G_{max}	Material Damping Ratio, D, %
1.05E-04	12988	1.00	0.77	1.05E-04	13002	1.00	0.75
2.06E-04	12988	1.00	1.03	2.15E-04	12891	1.00	0.75
4.15E-04	12907	0.99	0.79	4.11E-04	12907	1.00	0.71
8.29E-04	12907	0.99	0.94	8.30E-04	12891	1.00	0.79
1.63E-03	12777	0.98	0.94	1.63E-03	12777	0.99	0.94
3.36E-03	12749	0.98	1.08	3.32E-03	12924	1.00	1.08

APPENDIX J

Specimen No. 9
UT Specimen ID: UTA-27-G

Meloland WS-7
Depth = 440 ft (=134.1 m)
Soil Type: Clay (CH)

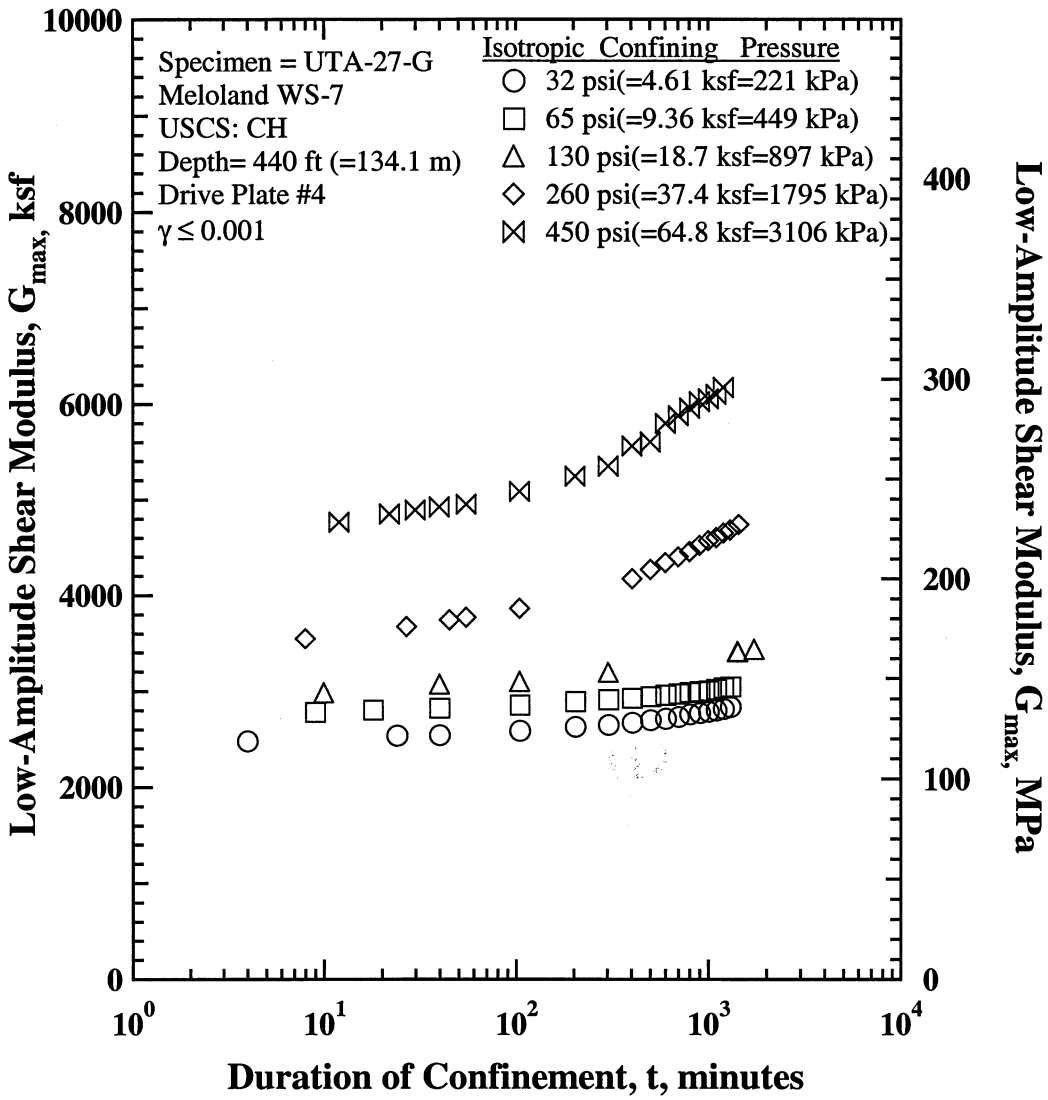

Figure J.1 Variation in Low-Amplitude Shear Modulus with Magnitude and Duration of Isotropic Confining Pressure from Resonant Column Tests of Specimen UTA-27-G.

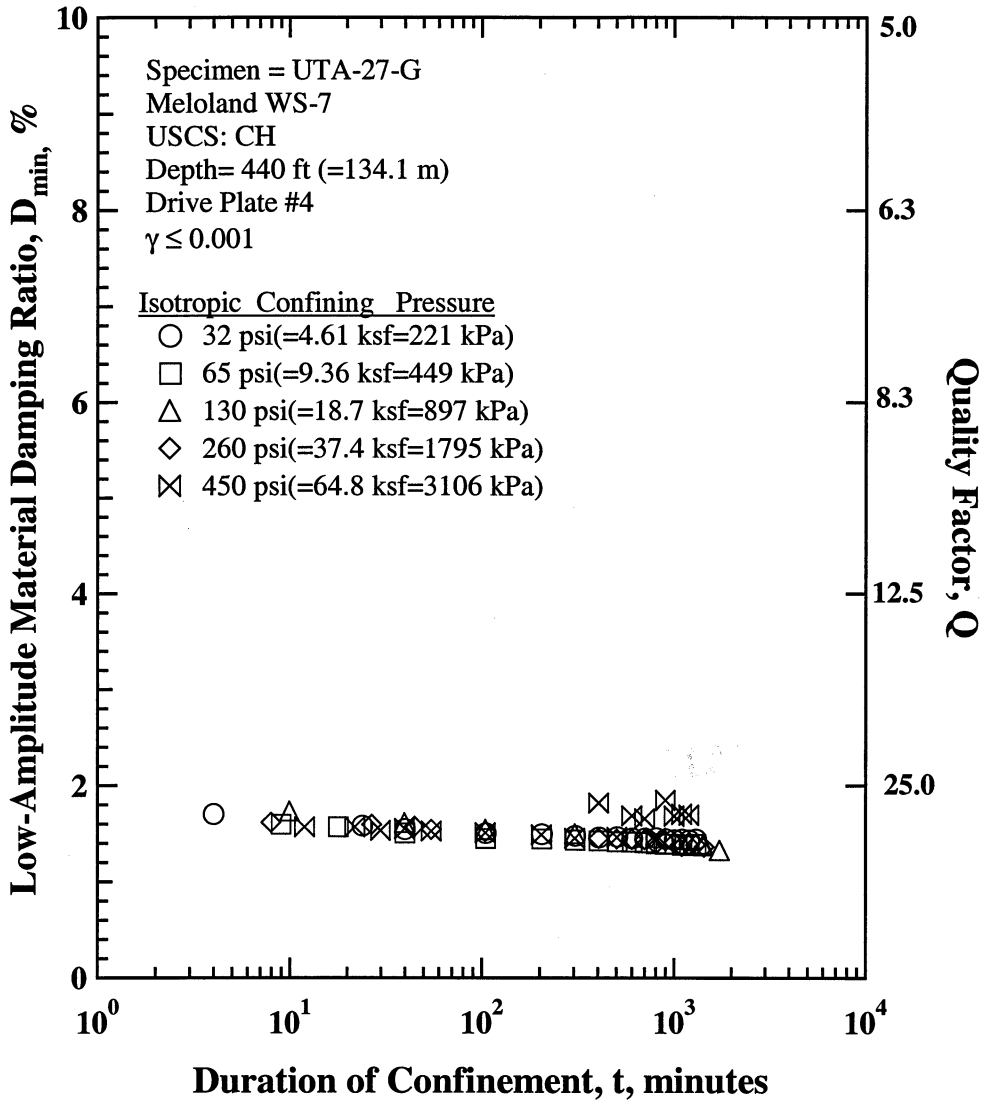

Figure J.2 Variation in Low-Amplitude Material Damping Ratio with Magnitude and Duration of Isotropic Confining Pressure from Resonant Column Tests of Specimen UTA-27-G

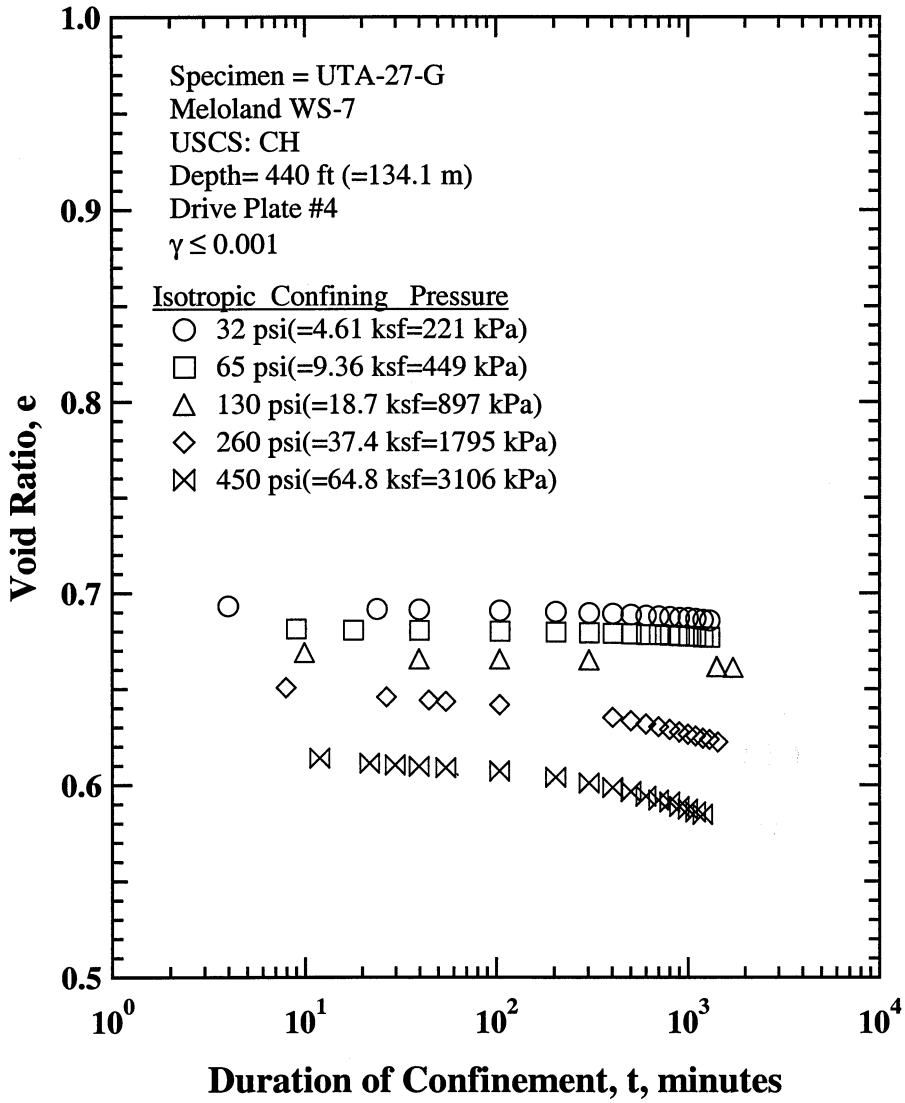

Figure J.3 Variation in Estimated Void Ratio with Magnitude and Duration of Isotropic Confining Pressure from Resonant Column Tests of Specimen UTA-27-G

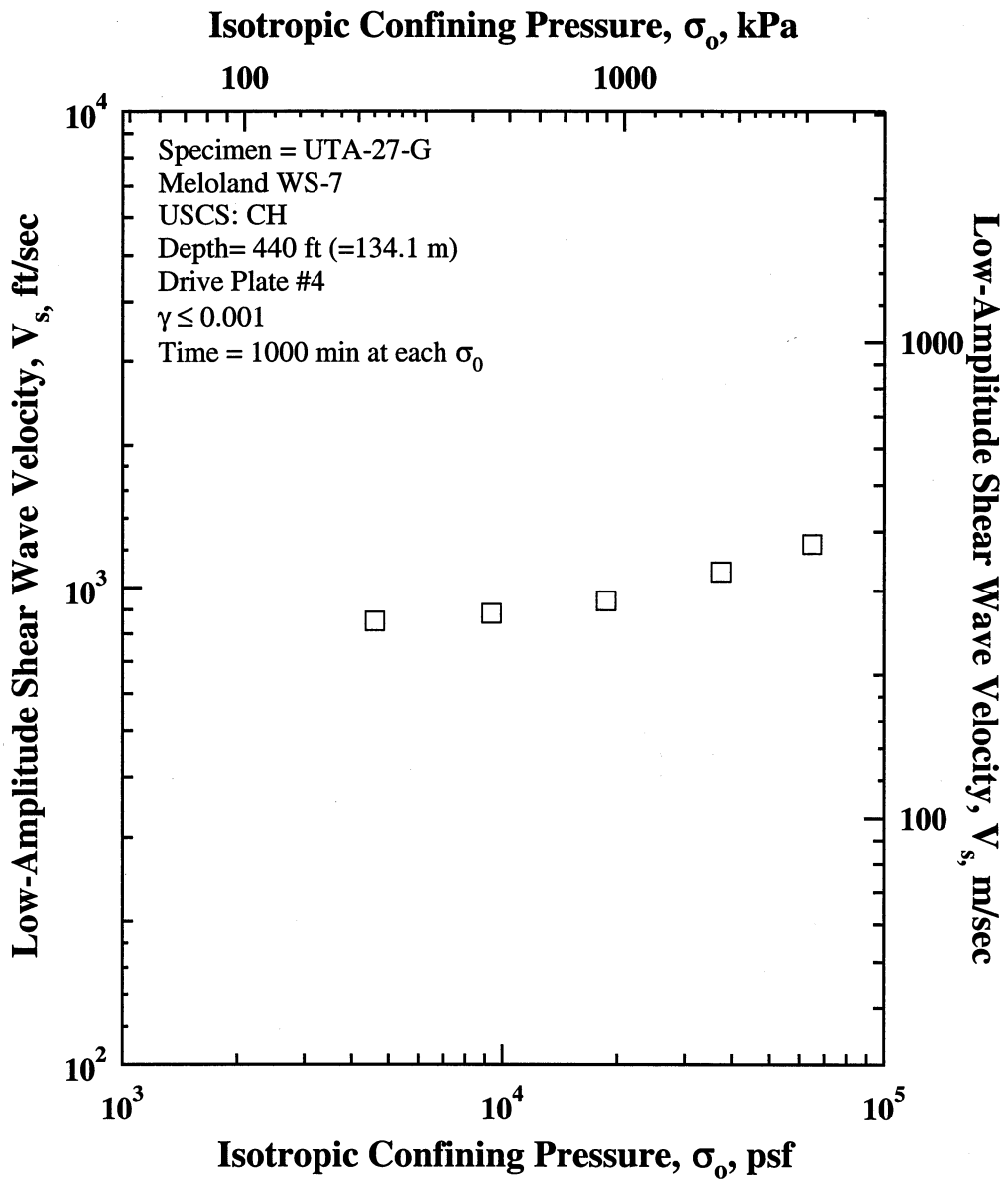

Figure J.4 Variation in Low-Amplitude Shear Wave Velocity with Isotropic Confining Pressure from Resonant Column Tests of Specimen UTA-27-G.

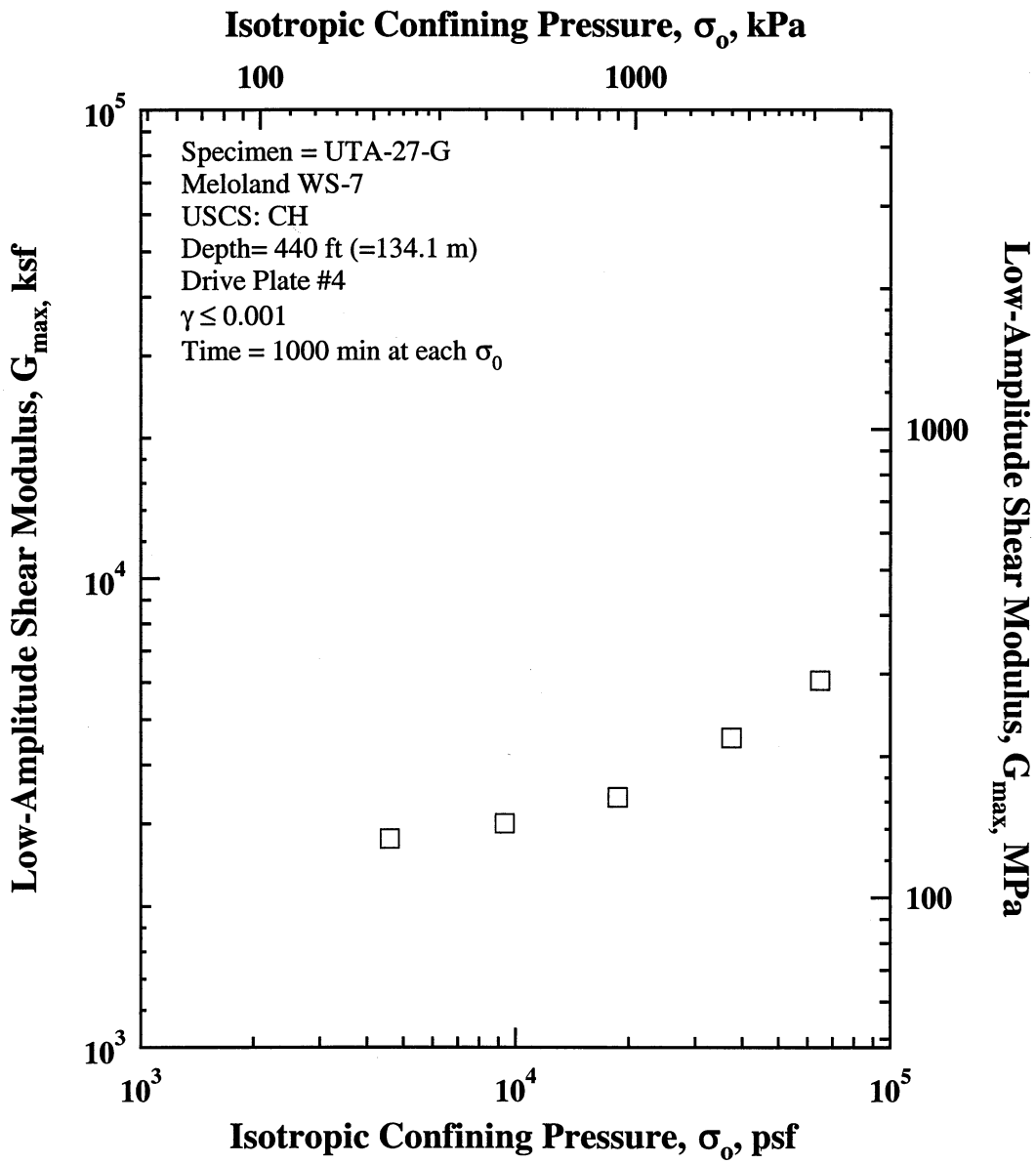

Figure J.5 Variation in Low-Amplitude Shear Modulus with Isotropic Confining Pressure from Resonant Column Tests of Specimen UTA-27-G.

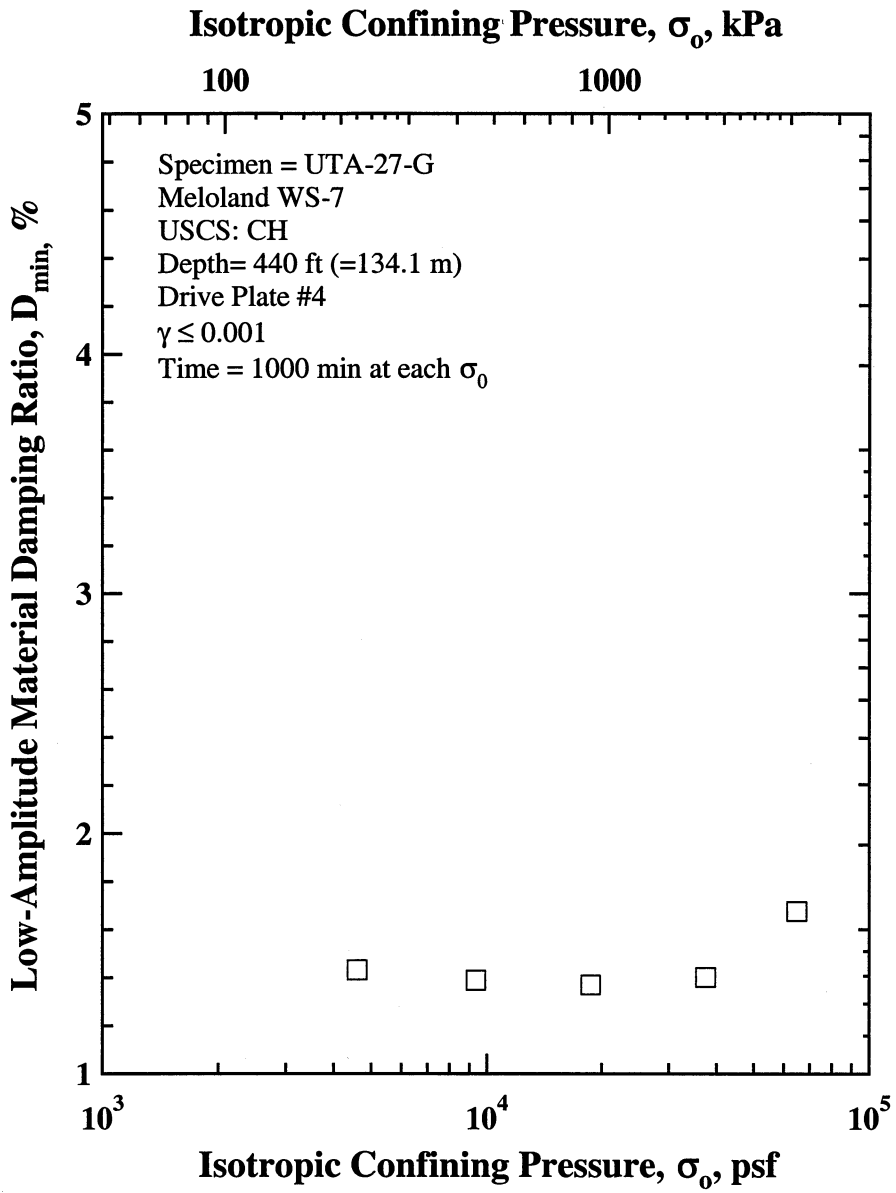

Figure J.6 Variation in Low-Amplitude Material Damping Ratio with Isotropic Confining Pressure from Resonant Column Tests of Specimen UTA-27-G.

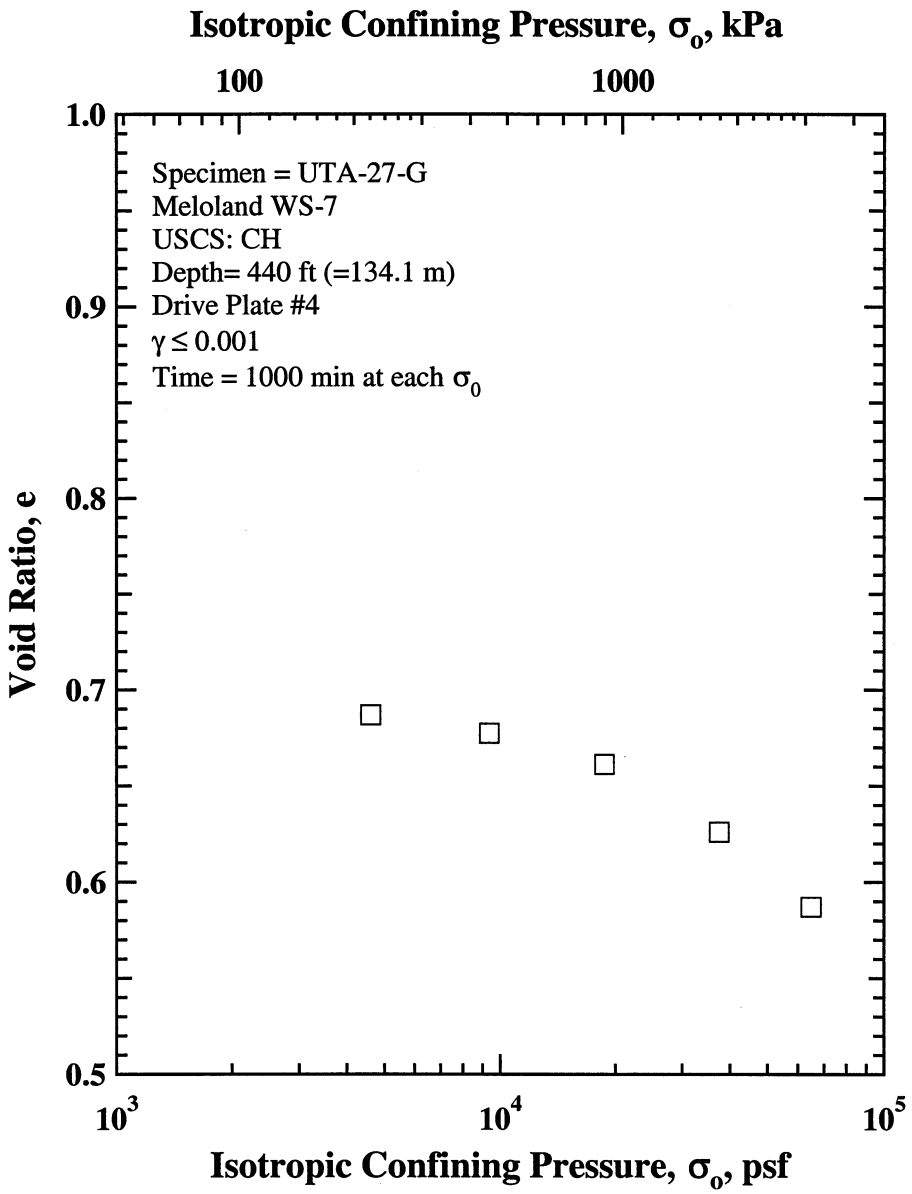

Figure J.7 Variation in Estimated Void Ratio with Isotropic Confining Pressure from Resonant Column Tests of Specimen UTA-27-G.

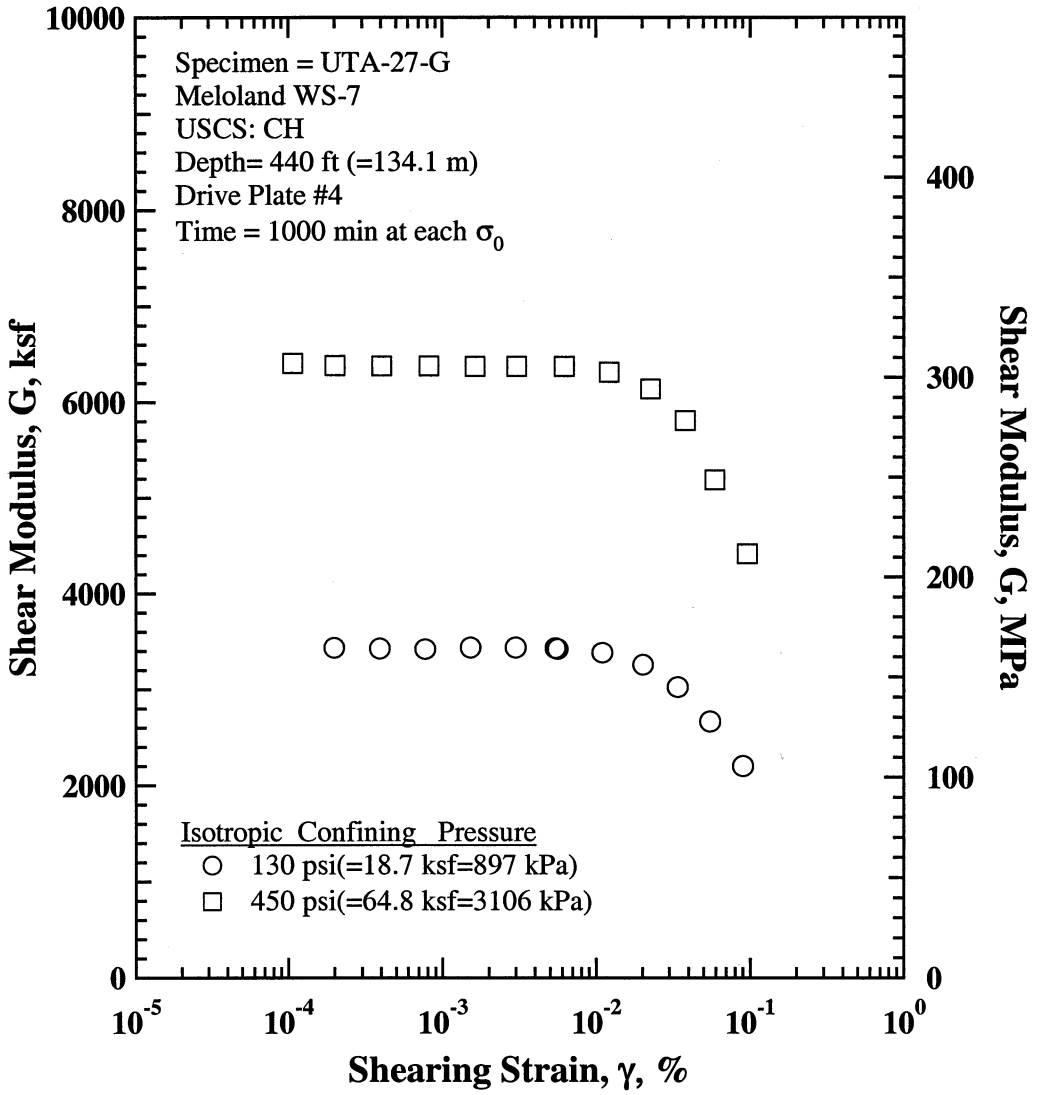

Figure J.8 Comparison of the Variation in Shear Modulus with Shearing Strain and Isotropic Confining Pressure from the Resonant Column Tests of Specimen UTA-27-G.

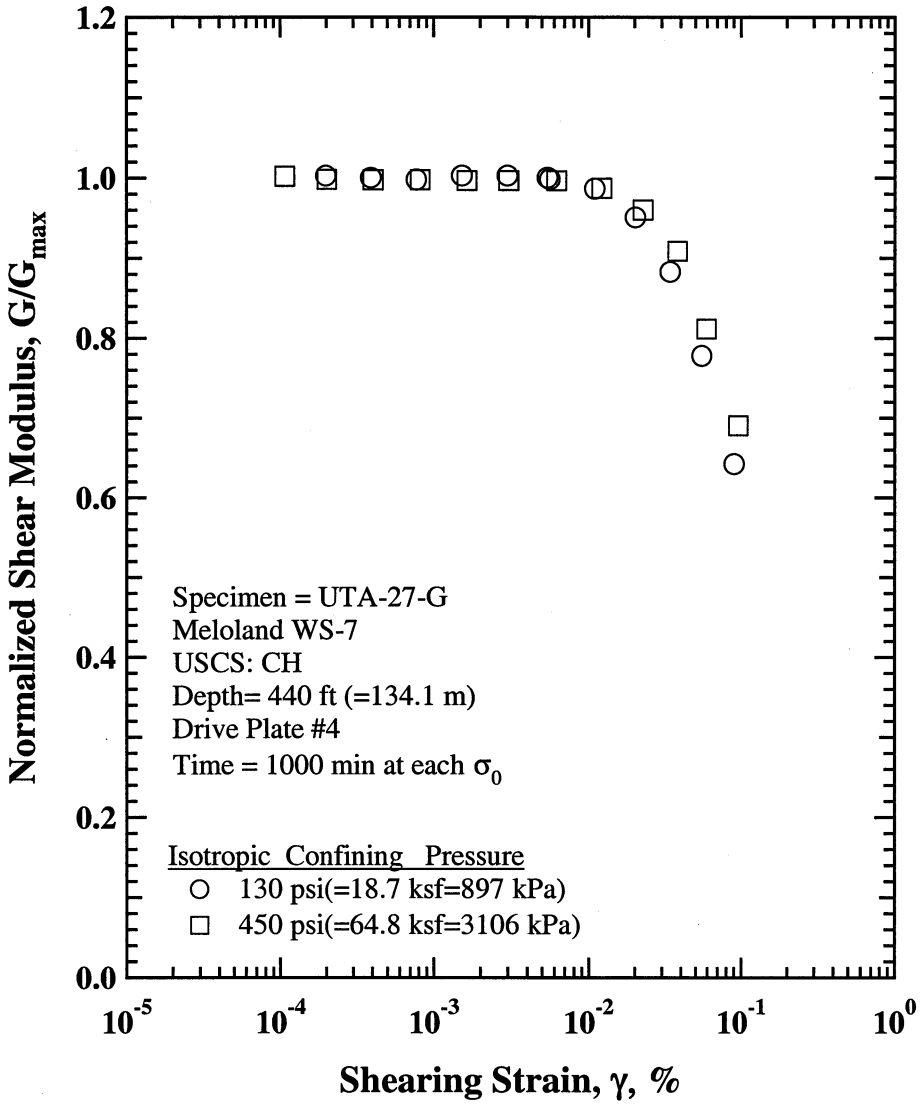

Figure J.9 Comparison of the Variation in Normalized Shear Modulus with Shearing Strain and Isotropic Confining Pressure from the Resonant Column Tests of Specimen UTA-27-G.

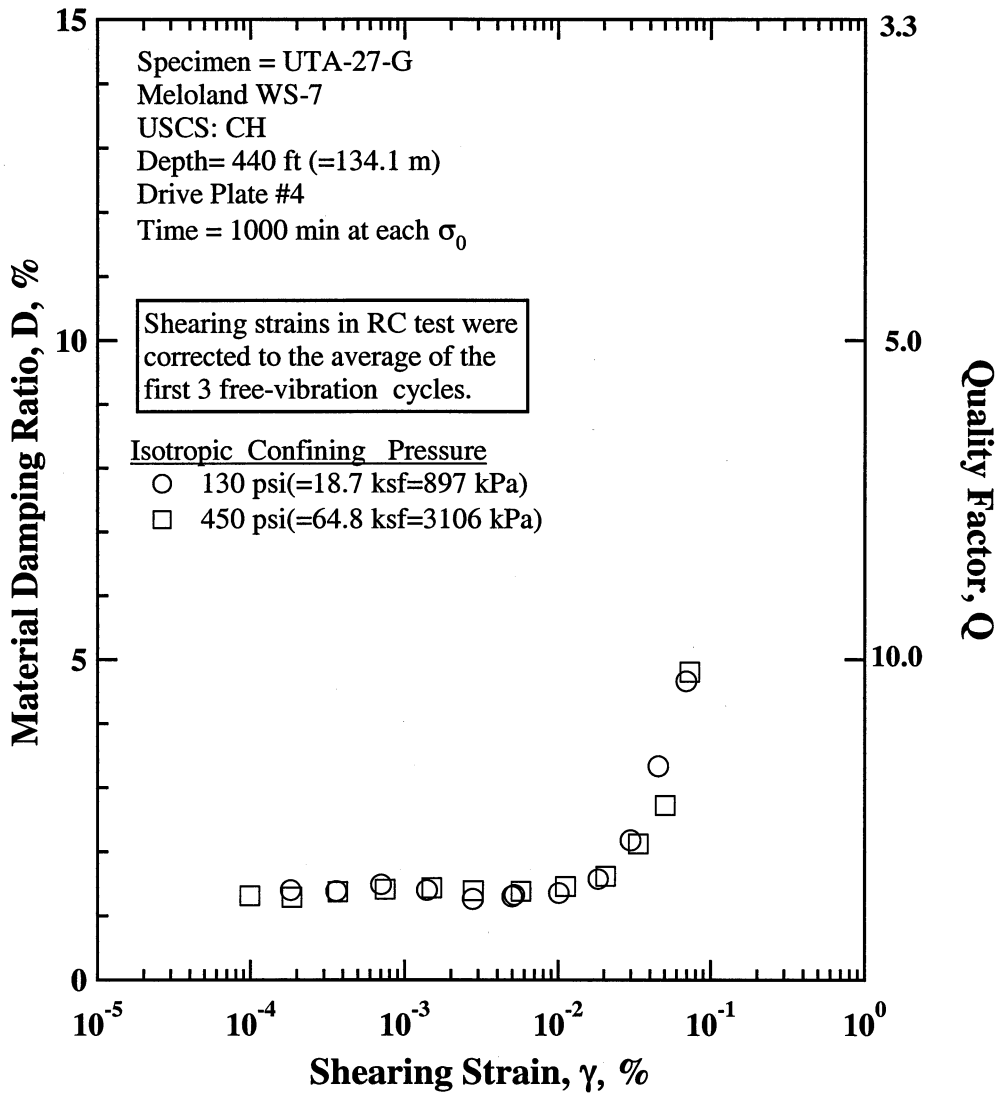

Figure J.10 Comparison of the Variation in Material Damping Ratio with Shearing Strain and Isotropic Confining Pressure from the Resonant Column Tests of Specimen UTA-27-G.

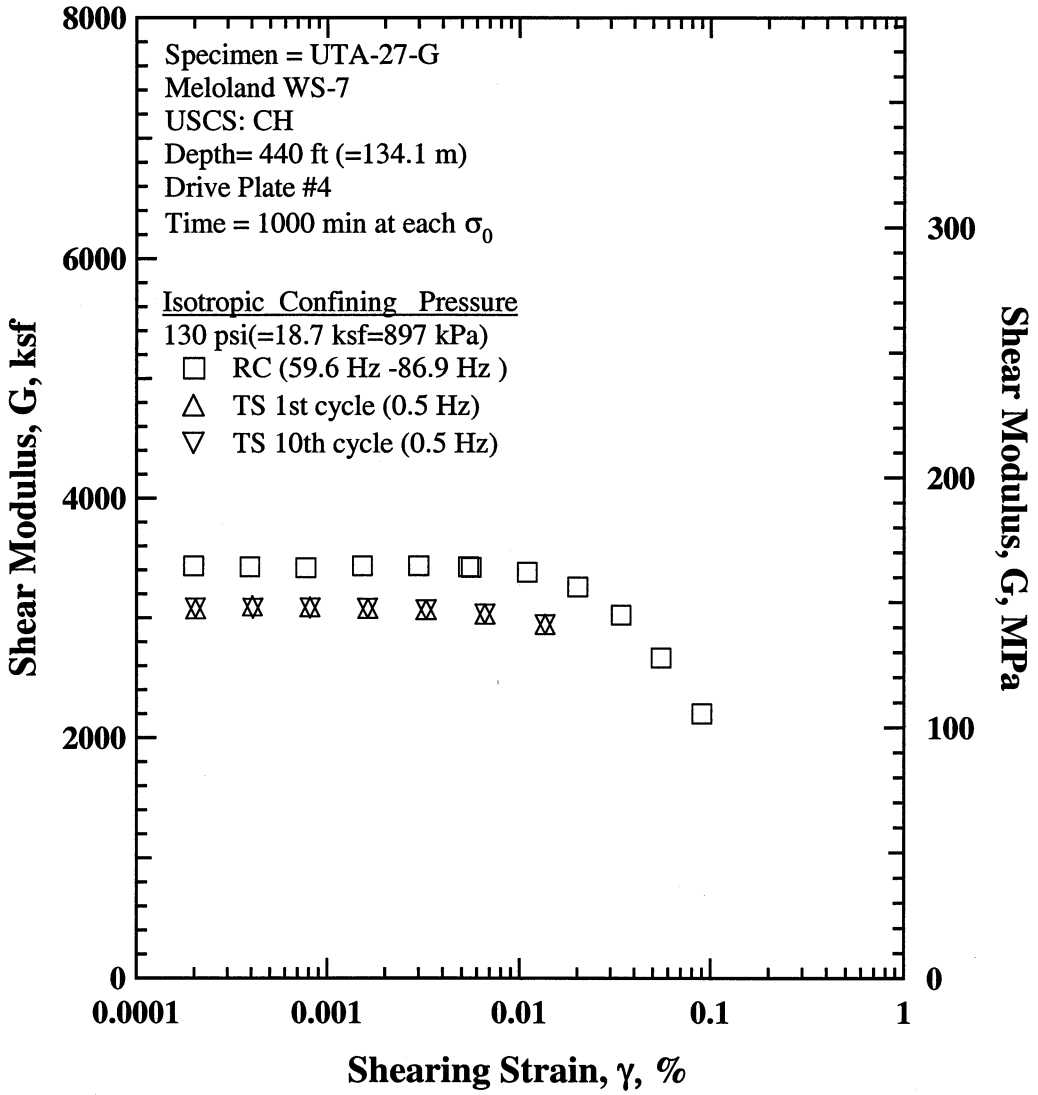

Figure J.11 Comparison of the Variation in Shear Modulus with Shearing Strain at an Isotropic Confining Pressure of 130 psi(=18.7 ksf=897 kPa) from the Combined RCTS Tests of Specimen UTA-27-G.

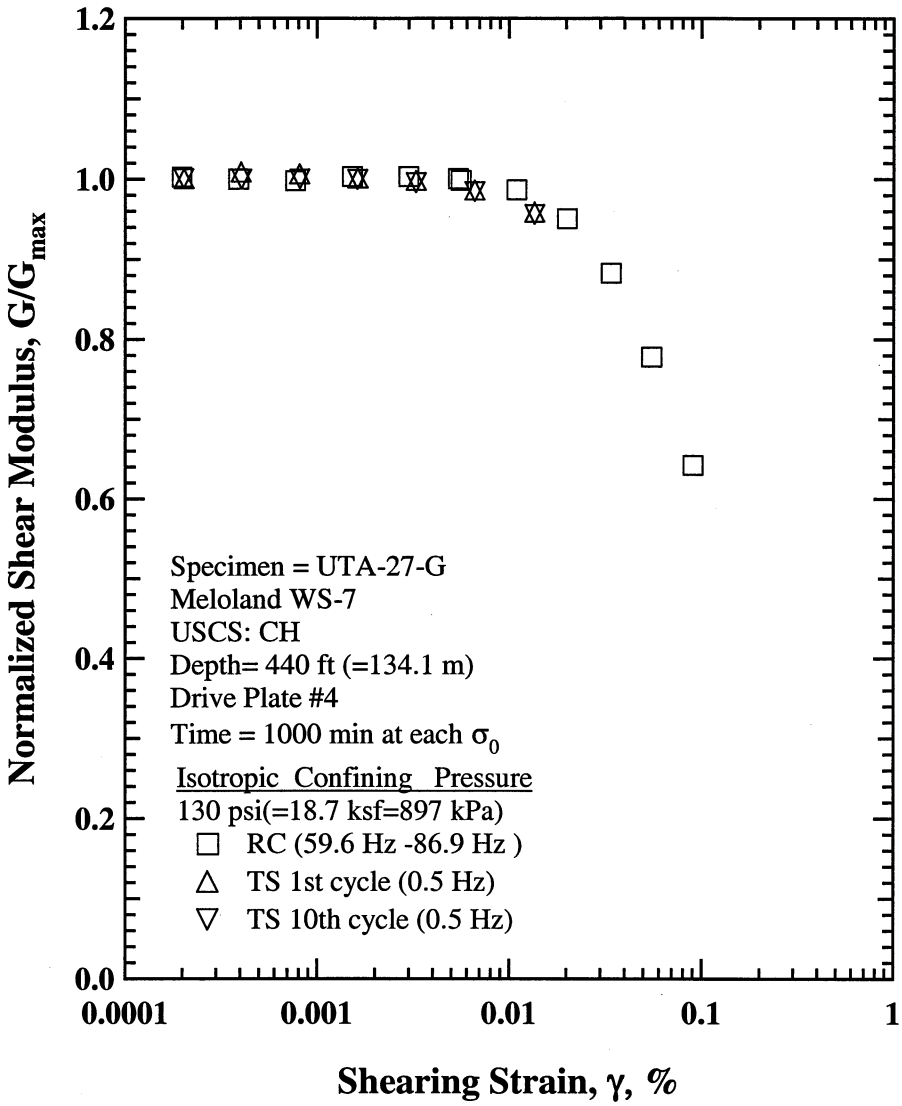

Figure J.12 Comparison of the Variation in Normalized Shear Modulus with Shearing Strain at an Isotropic Confining Pressure of 130 psi(=18.7 ksf=897 kPa) from the Combined RCTS Tests of Specimen UTA-27-G.

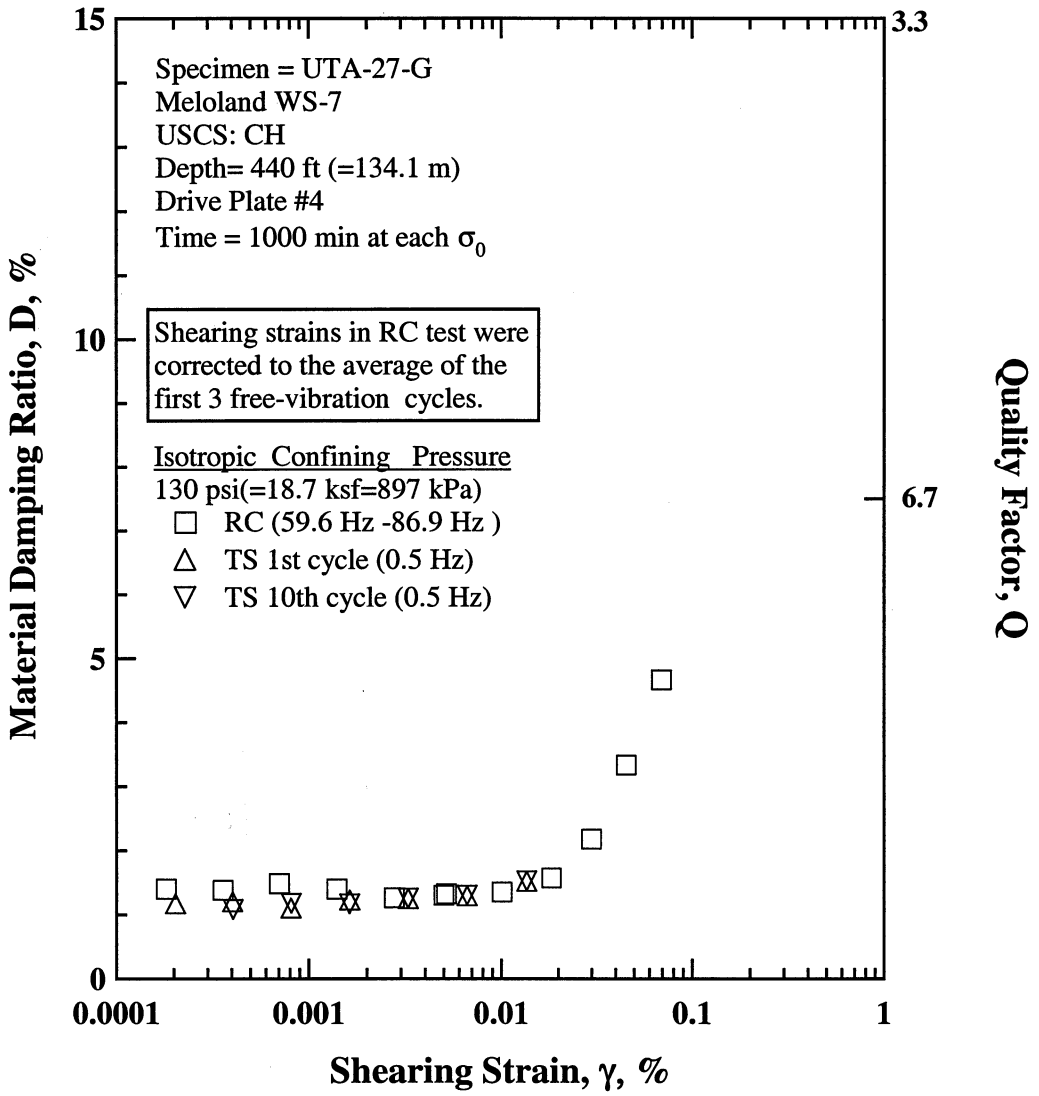

Figure J.13 Comparison of the Variation in Material Damping Ratio with Shearing Strain at an Isotropic Confining Pressure of 130 psi(=18.7 ksf=897 kPa) from the Combined RCTS Tests of Specimen UTA-27-G.

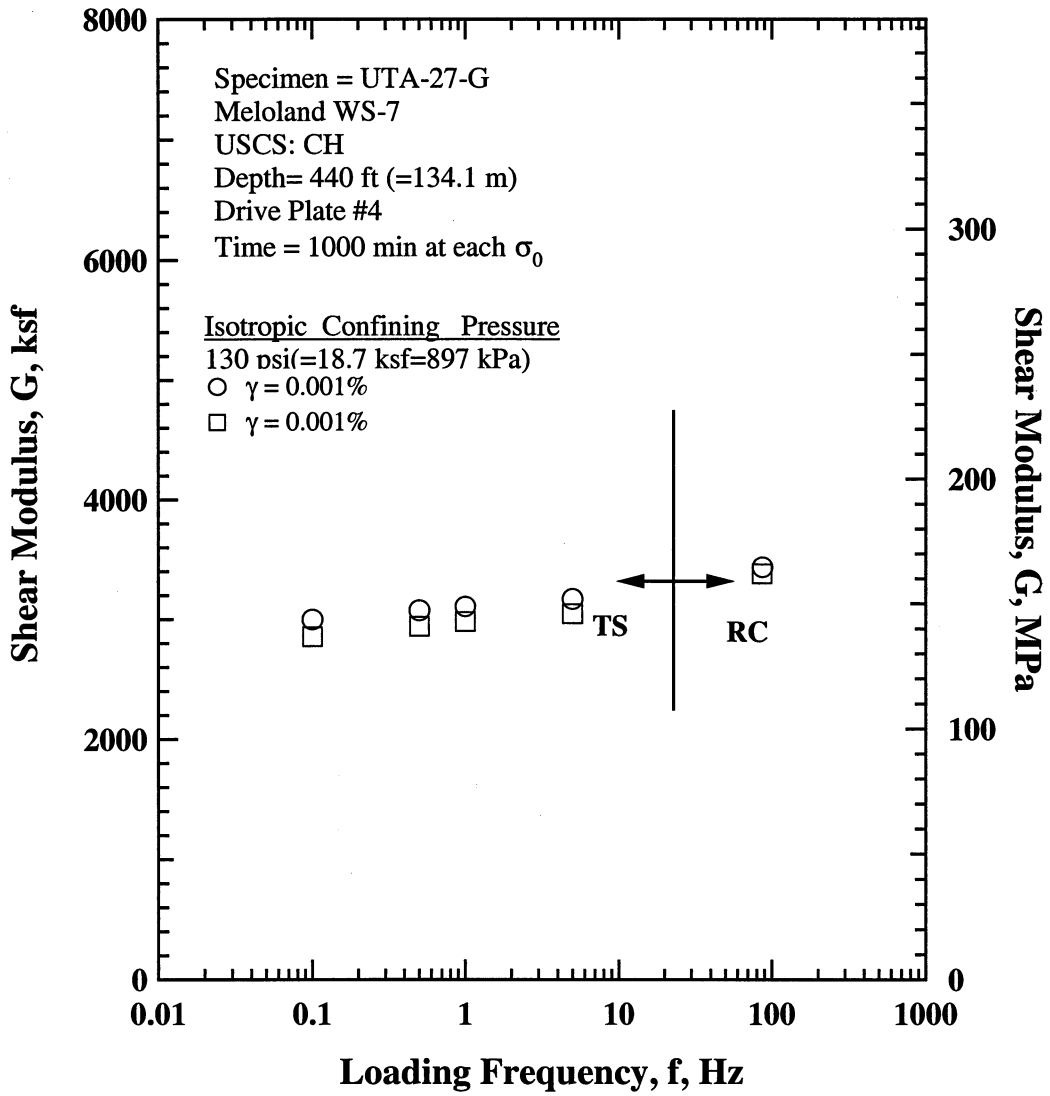

Figure J.14 Comparison of the Variation in Shear Modulus with Loading Frequency at an Isotropic Confining Pressure of 130 psi(=18.7 ksf=897 kPa) from the Combined RCTS Tests of Specimen UTA-27-G.

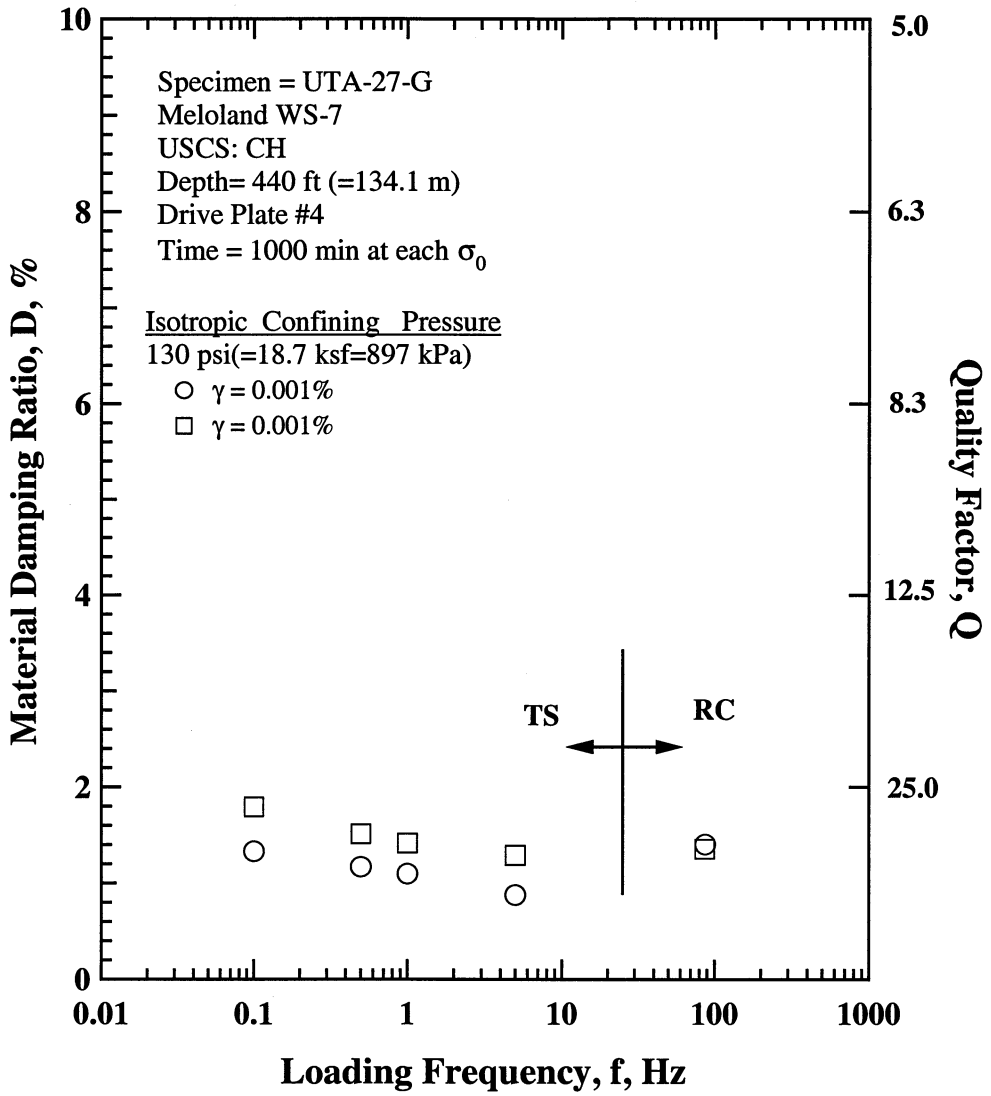

Figure J.15 Comparison of the Variation in Material Damping Ratio with Loading Frequency at an Isotropic Confining Pressure 130 psi(=18.7 ksf=897 kPa) from the Combined RCTS Tests of Specimen UTA-27-G.

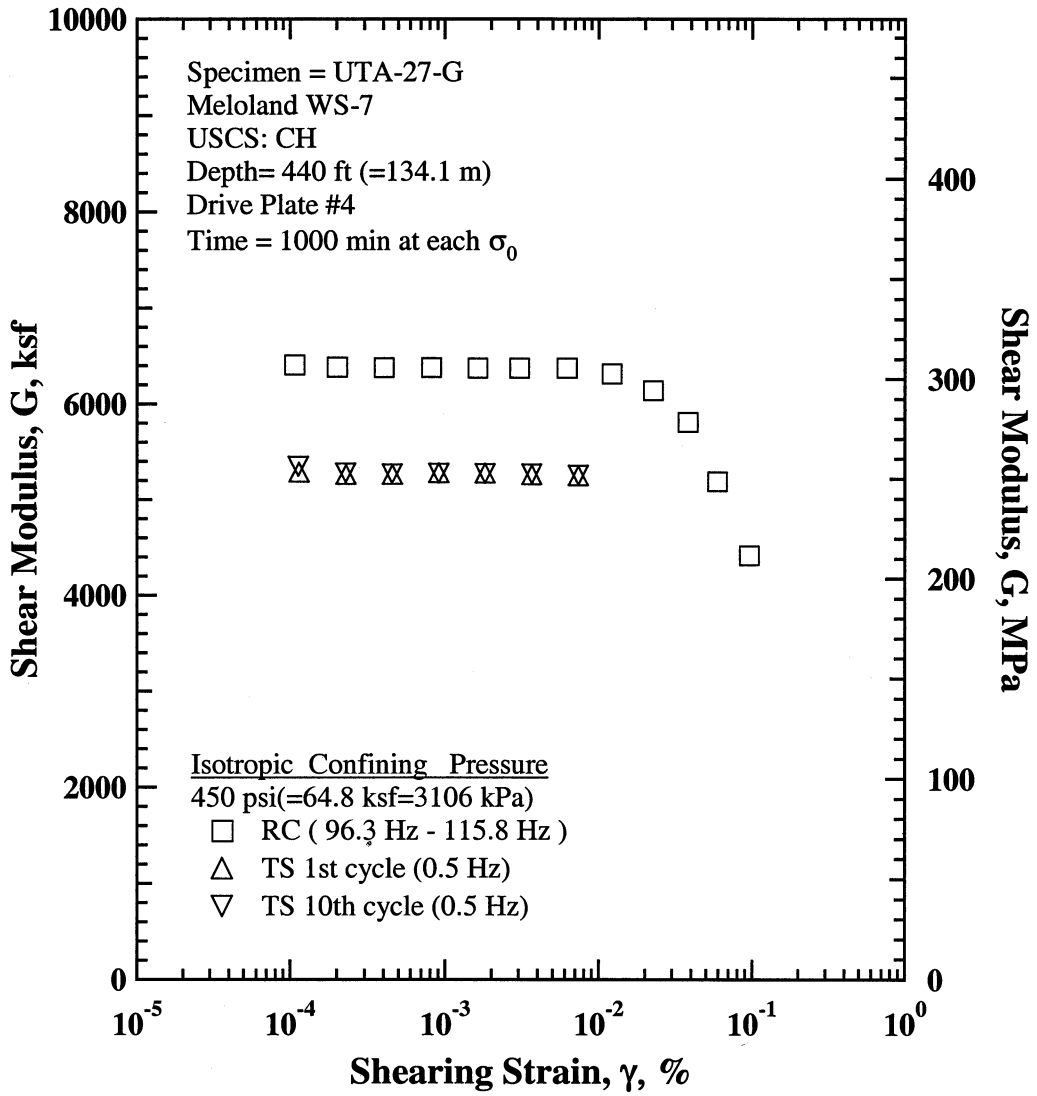

Figure J.16 Comparison of the Variation in Shear Modulus with Shearing Strain at an Isotropic Confining Pressure of 450 psi(=64.8 ksf=3106 kPa) from the Combined RCTS Tests of Specimen UTA-27-G.

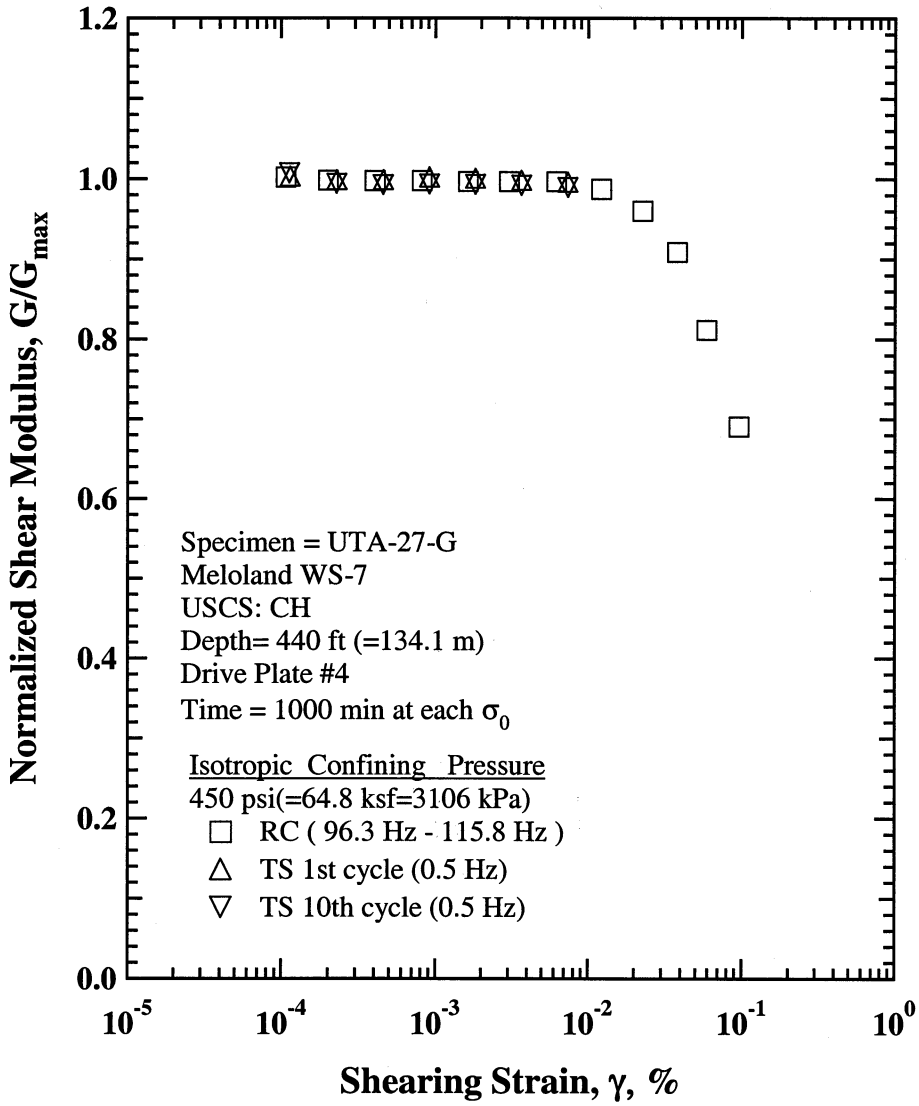

Figure J.17 Comparison of the Variation in Normalized Shear Modulus with Shearing Strain at an Isotropic Confining Pressure of 450 psi(=64.8 ksf=3106 kPa) from the Combined RCTS Tests of Specimen UTA-27-G.

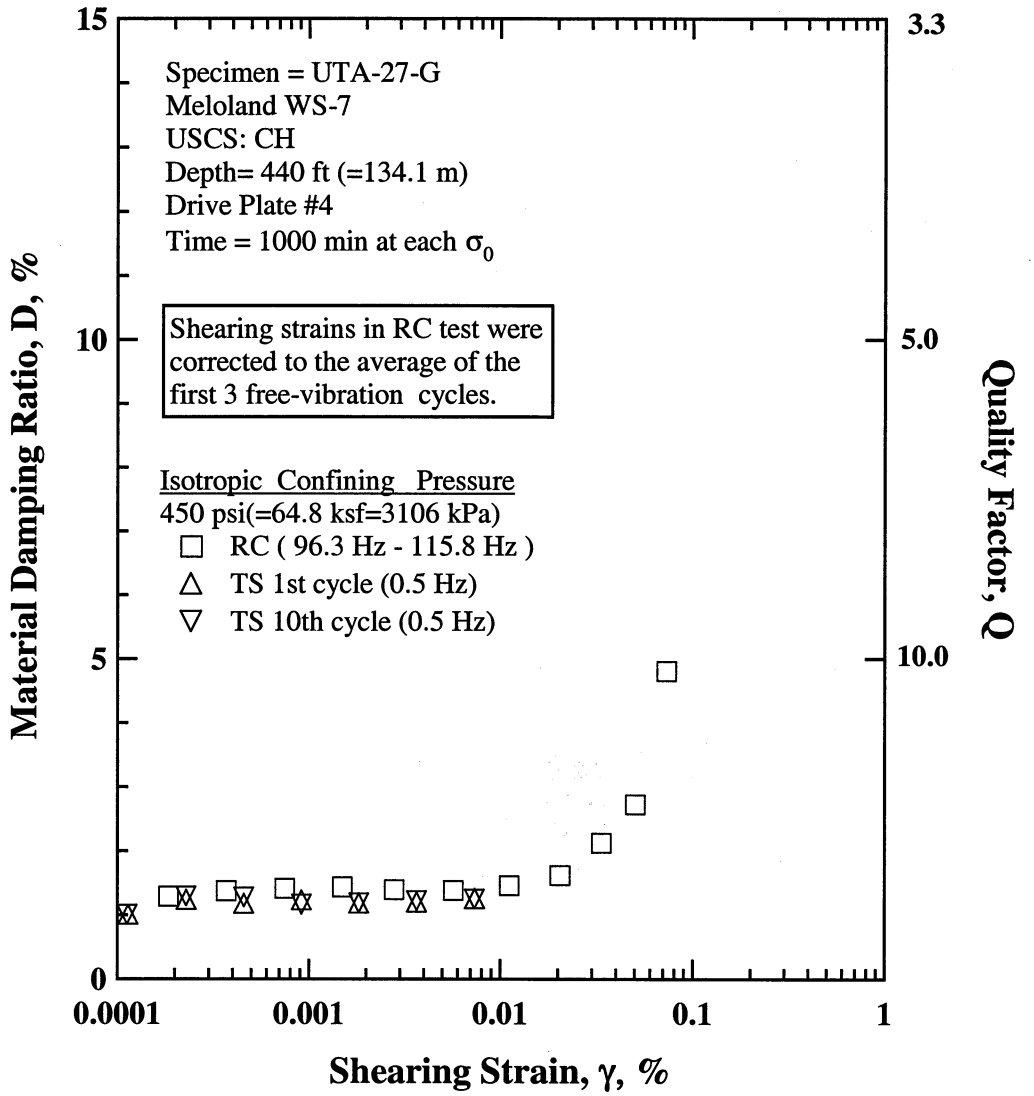

Figure J.18 Comparison of the Variation in Material Damping Ratio with Shearing Strain at an Isotropic Confining Pressure of 450 psi(=64.8 ksf=3106 kPa) from the Combined RCTS Tests of Specimen UTA-27-G.

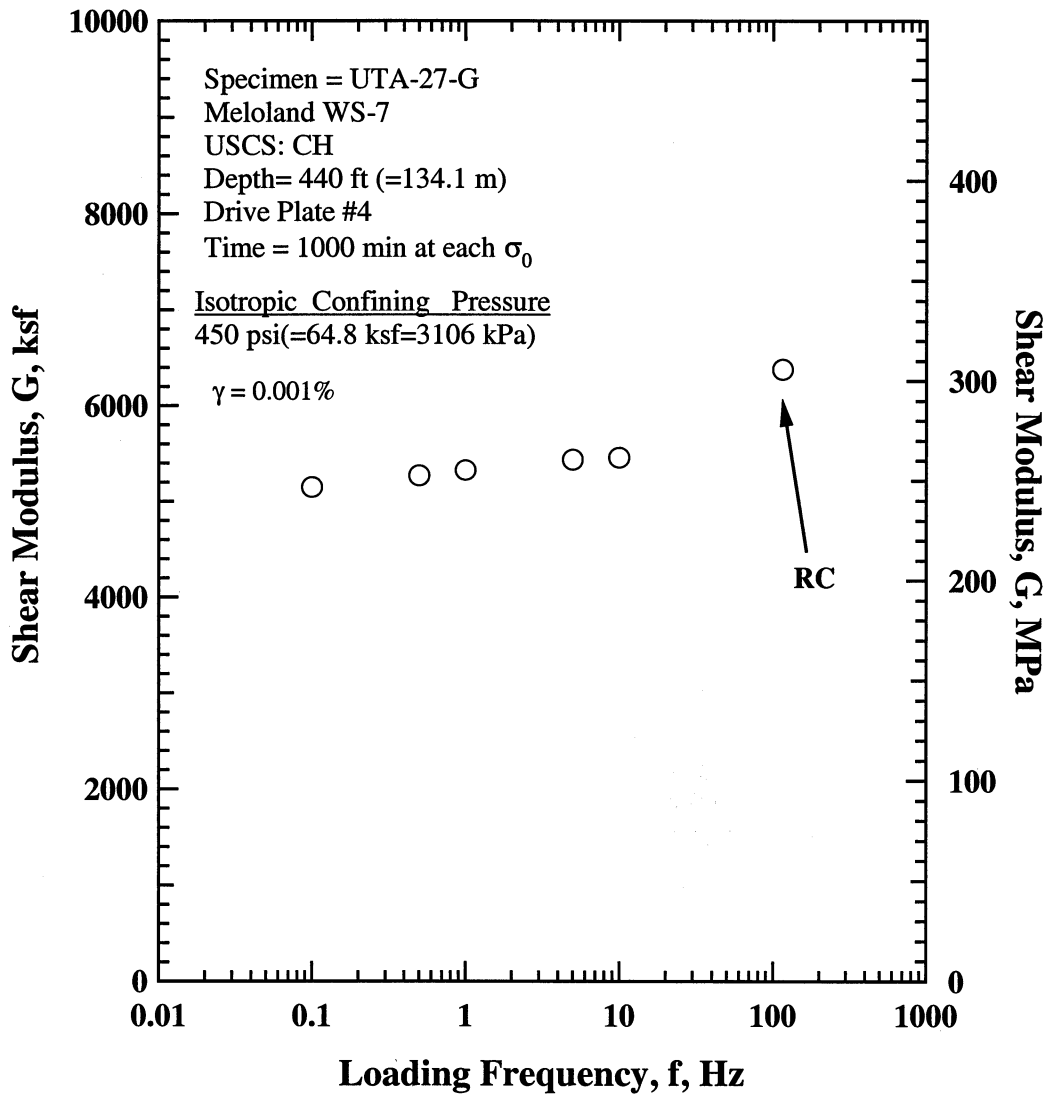

Figure J.19 Comparison of the Variation in Shear Modulus with Loading Frequency at an Isotropic Confining Pressure of 450 psi(=64.8 ksf=3106 kPa) from the Combined RCTS Tests of Specimen UTA-27-G.

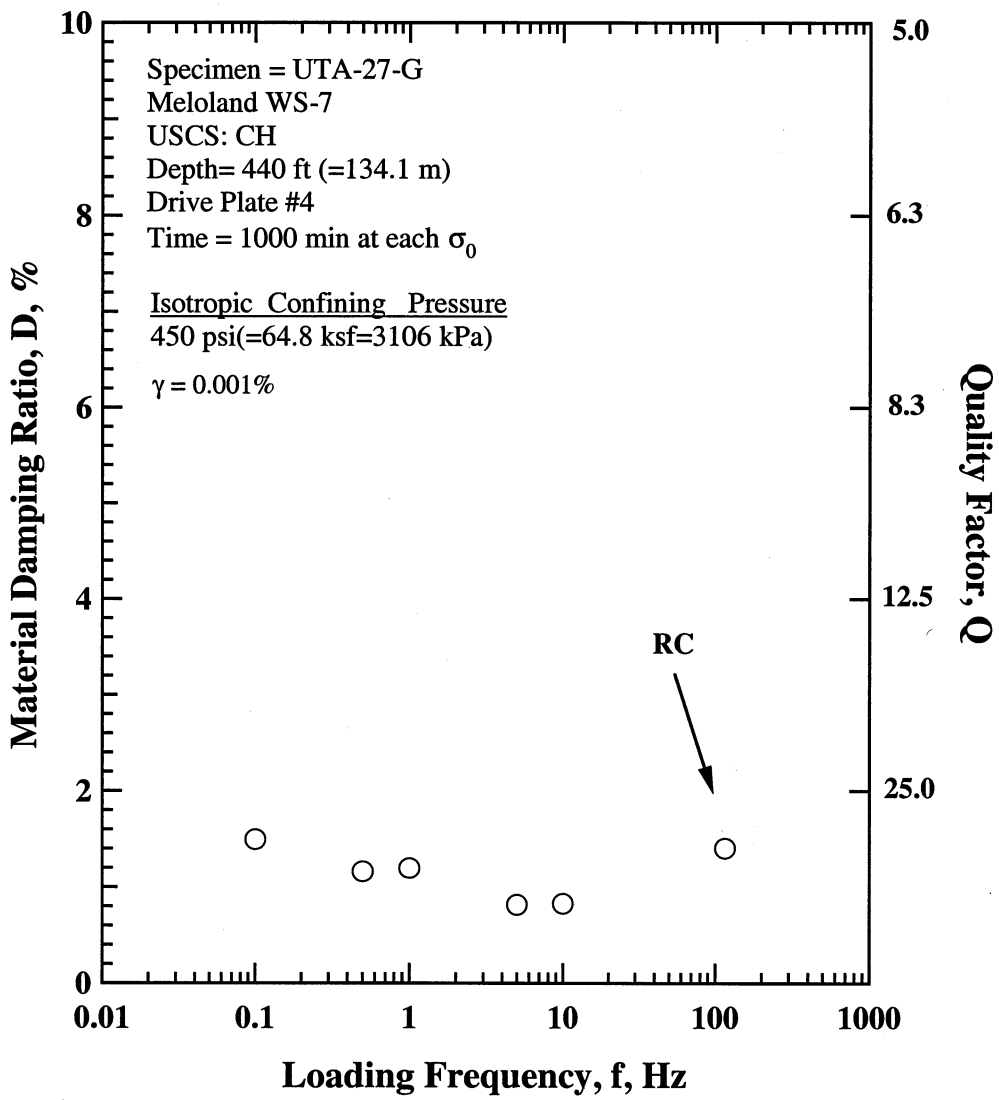

Figure J.20 Comparison of the Variation in Material Damping Ratio with Loading Frequency at an Isotropic Confining Pressure 450 psi(=64.8 ksf=3106 kPa) from the Combined RCTS Tests of Specimen UTA-27-G.

Table J.1 Variation in Low-Amplitude Shear Wave Velocity, Low-Amplitude Shear Modulus, Low-Amplitude Material Damping Ratio and Estimated Void Ratio with Isotropic Confining Pressure from RC Tests of Specimen UTA-27-G.

Effective Isotropic Confining Pressure, σ_o'			Low-Amplitude Shear Modulus, G_{max}		Low-Amplitude Shear Wave Velocity, Vs	Low-Amplitude Material Damping Ratio, D_{min}, %	Estimated Void Ratio, e
(psi)	(psf)	(kPa)	(ksf)	(MPa)	(fps)		
32	4608	220.9	2781	133.3	851	1.41	0.687
65	9360	448.7	3001	143.8	883	1.37	0.677
130	18720	897.4	3409	163.4	938	1.35	0.661
260	37440	1794.9	4566	218.9	1080	1.38	0.626
450	64800	3106.5	6050	290.0	1235	1.66	0.587

Table J.2 Variation in Shear Modulus, Normalized Shear Modulus and Material Damping Ratio with Shearing Strain from RC Tests of Specimen UTA-27-G; Confining Pressure, σ_o' = 130 psi(=18.72 ksf=897 kPa).

Peak Shearing Strain, %	Shear Modulus, G, ksf	Normalized Shear Modulus, G/G_{max}	Average[+] Shearing Strain, %	Material Damping Ratio[x], D, %
3.92E-04	3425	1.00	3.61E-04	1.36
1.99E-04	3433	1.00	1.99E-04	
7.72E-04	3418	1.00	7.06E-04	1.46
1.52E-03	3434	1.00	1.40E-03	1.38
2.99E-03	3434	1.00	2.77E-03	1.24
5.42E-03	3426	1.00	5.01E-03	1.28
5.61E-03	3419	1.00	5.18E-03	1.30
1.10E-02	3379	0.99	1.01E-02	1.33
2.02E-02	3255	0.95	1.84E-02	1.55
3.41E-02	3022	0.88	2.99E-02	2.15
5.52E-02	2664	0.78	4.55E-02	3.31
9.03E-02	2200	0.64	6.94E-02	4.63
1.69E-01	1609	0.47	1.69E-01	

[+] Average Shearing Strain from the First Three Cycles of the Free Vibration Decay Curve

[x] Average Damping Ratio from the First Three Cycles of the Free Vibration Decay Curve

Table J.4 Variation in Shear Modulus, Normalized Shear Modulus and Material Damping Ratio with Shearing Strain from TS Tests of Specimen UTA-27-G; Confining Pressure, σ_o' =130 psi(=18.72 ksf=897 kPa).

First Cycle				Tenth Cycle			
Peak Shearing Strain, %	Shear Modulus, G, ksf	Normalized Shear Modulus, G/G_{max}	Material Damping Ratio, D, %	Peak Shearing Strain, %	Shear Modulus, G, ksf	Normalized Shear Modulus, G/G_{max}	Material Damping Ratio, D, %
2.05E-04	3069	1.00	1.16	2.04E-04	3076	1.00	
4.06E-04	3093	1.01	1.20	4.09E-04	3074	1.00	1.08
8.15E-04	3085	1.01	1.09	8.18E-04	3074	1.00	1.17
1.64E-03	3070	1.00	1.22	1.64E-03	3072	1.00	1.16
3.29E-03	3061	1.00	1.24	3.29E-03	3060	0.99	1.25
6.66E-03	3025	0.99	1.28	6.65E-03	3026	0.98	1.29
1.37E-02	2940	0.96	1.51	1.37E-02	2938	0.96	1.51

Table J.4 Variation in Shear Modulus, Normalized Shear Modulus and Material Damping Ratio with Shearing Strain from RC Tests of Specimen UTA-27-G; Confining Pressure, σ_o' = 450 psi(=64.8 ksf=3107 kPa).

Peak Shearing Strain, %	Shear Modulus, G, ksf	Normalized Shear Modulus, G/G_{max}	Average[+] Shearing Strain, %	Material Damping Ratio[x], D, %
2.01E-04	6382	1.00	2.01E-04	
1.07E-04	6406	1.00	9.87E-05	1.30
4.03E-04	6378	1.00	3.71E-04	1.36
8.16E-04	6378	1.00	7.50E-04	1.39
1.64E-03	6371	1.00	1.50E-03	1.42
3.04E-03	6372	1.00	2.80E-03	1.37
6.20E-03	6373	1.00	5.71E-03	1.37
1.22E-02	6312	0.99	1.12E-02	1.44
2.27E-02	6139	0.96	2.06E-02	1.60
3.82E-02	5808	0.91	3.36E-02	2.10
5.93E-02	5187	0.81	5.05E-02	2.70
9.61E-02	4414	0.69	7.32E-02	4.78

[+] Average Shearing Strain from the First Three Cycles of the Free Vibration Decay Curve

[x] Average Damping Ratio from the First Three Cycles of the Free Vibration Decay Curve

Table J.5 Variation in Shear Modulus, Normalized Shear Modulus and Material Damping Ratio with Shearing Strain from TS Tests of Specimen UTA-27-G; Confining Pressure, σ_o' = 450 psi(=64.8 ksf=3107 kPa).

First Cycle				Tenth Cycle			
Peak Shearing Strain, %	Shear Modulus, G, ksf	Normalized Shear Modulus, G/G_{max}	Material Damping Ratio, D, %	Peak Shearing Strain, %	Shear Modulus, G, ksf	Normalized Shear Modulus, G/G_{max}	Material Damping Ratio, D, %
1.15E-04	5279	1.00		1.13E-04	5341	1.01	
2.30E-04	5255	1.00	1.23	2.29E-04	5273	0.99	1.28
4.60E-04	5256	1.00	1.17	4.60E-04	5263	0.99	1.27
9.18E-04	5273	1.00	1.22	9.19E-04	5269	0.99	1.16
1.84E-03	5268	1.00	1.18	1.84E-03	5265	0.99	1.18
3.69E-03	5254	1.00	1.19	3.68E-03	5260	0.99	1.21
7.40E-03	5241	1.00	1.25	7.39E-03	5246	0.99	1.24

APPENDIX K

Specimen No. 10
UT Specimen ID: UTA-27-S

LA Bulk Mail P-1
Depth = 15 ft (= 4.60m)
Soil Type: Clay (CL)

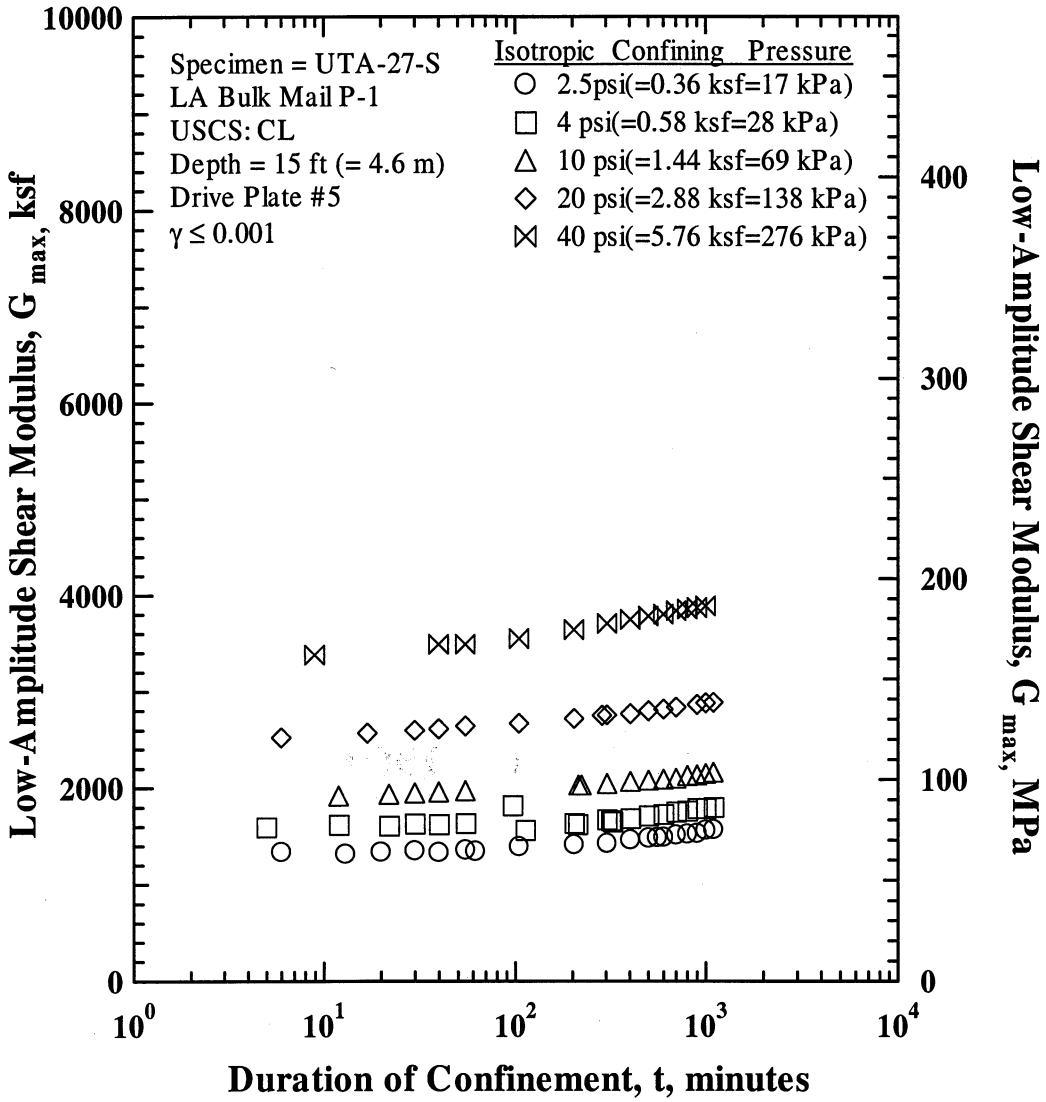

Figure K.1 Variation in Low-Amplitude Shear Modulus with Magnitude and Duration of Isotropic Confining Pressure from Resonant Column Tests of Specimen UTA-27-S.

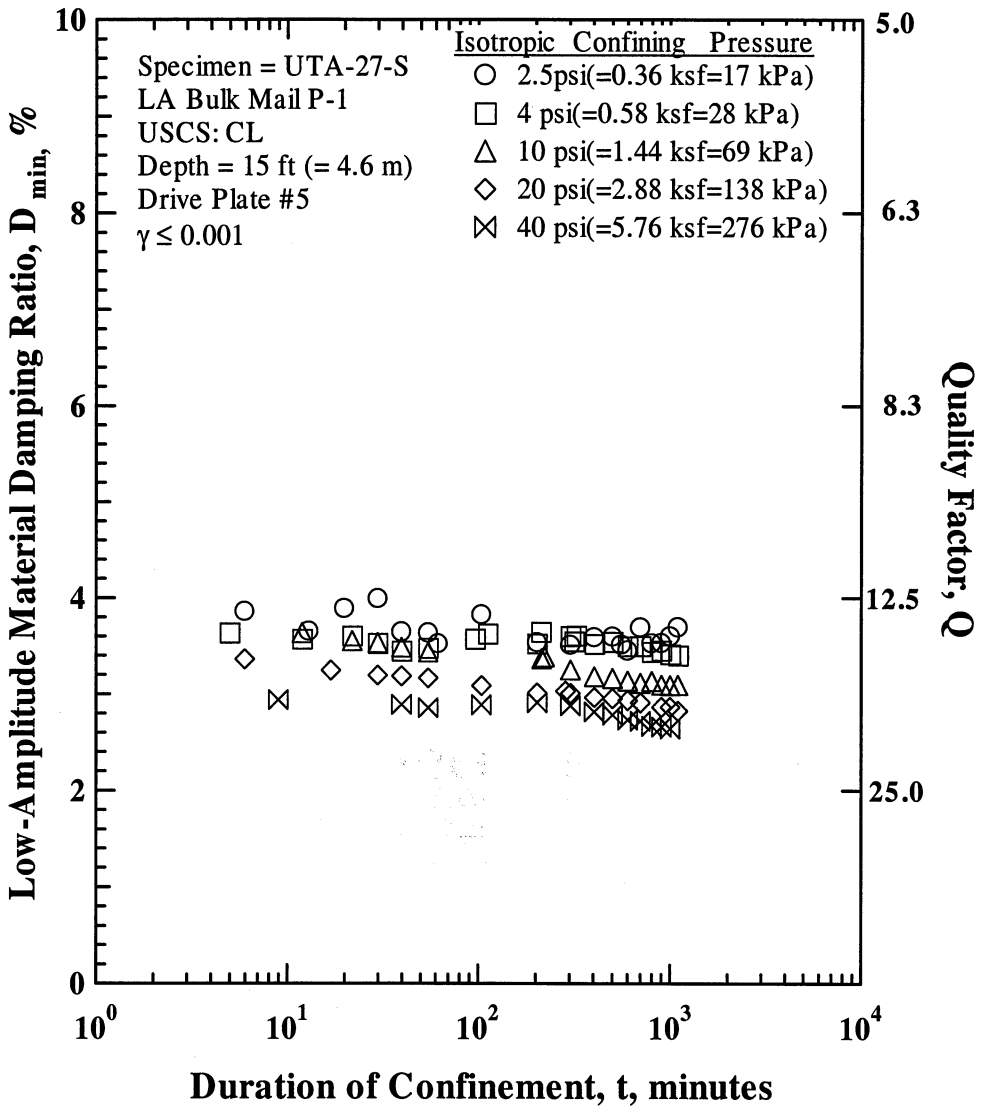

Figure K.2 Variation in Low-Amplitude Material Damping Ratio with Magnitude and Duration of Isotropic Confining Pressure from Resonant Column Tests of Specimen UTA-27-S

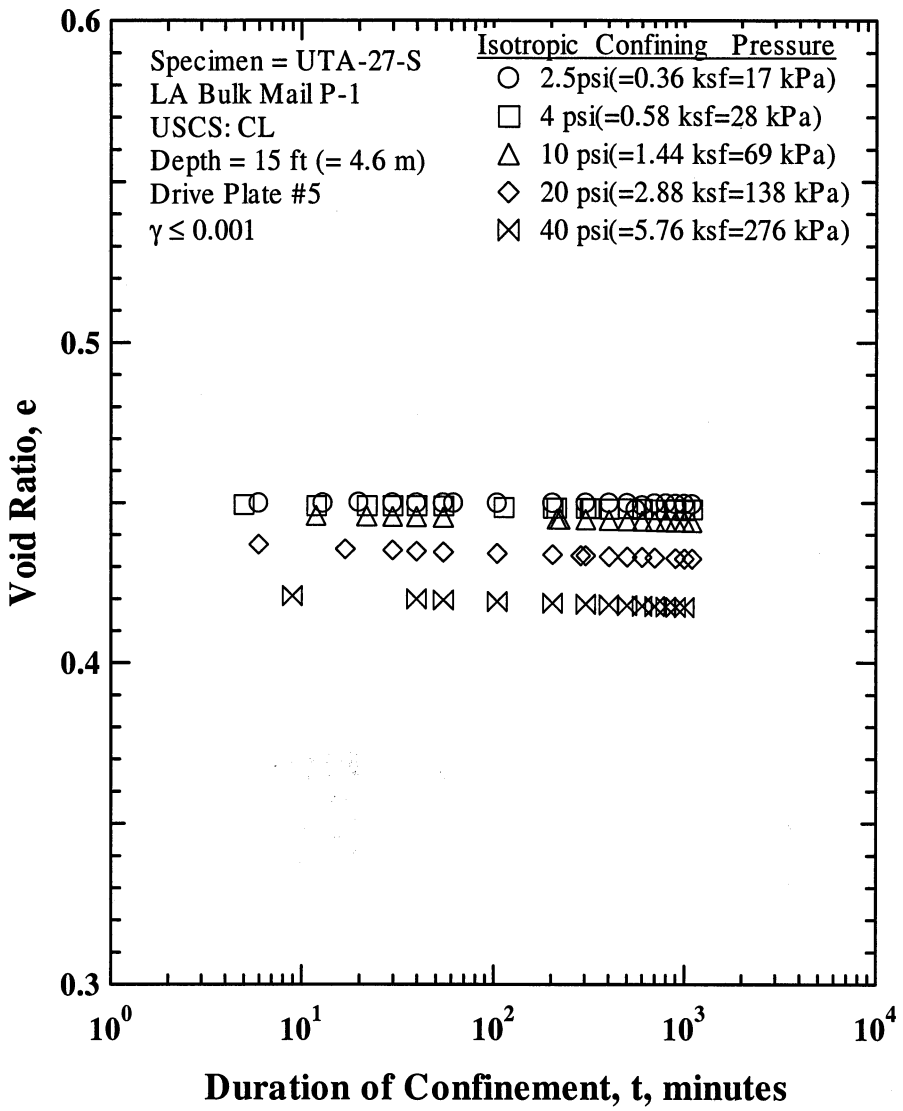

Figure K.3 Variation in Estimated Void Ratio with Magnitude and Duration of Isotropic Confining Pressure from Resonant Column Tests of Specimen UTA-27-S.

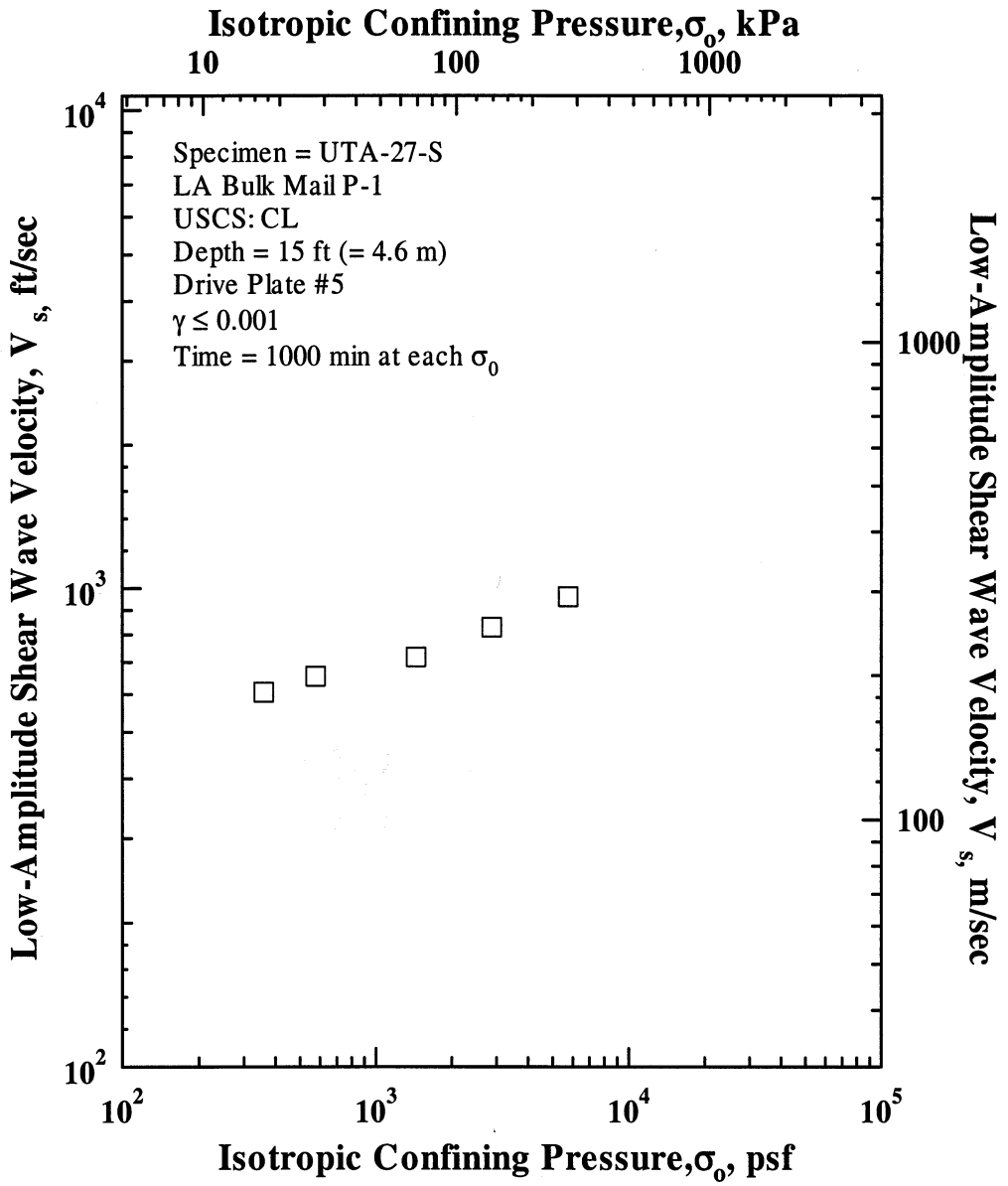

Figure K.4 Variation in Low-Amplitude Shear Wave Velocity with Isotropic Confining Pressure from Resonant Column Tests of Specimen UTA-27-S.

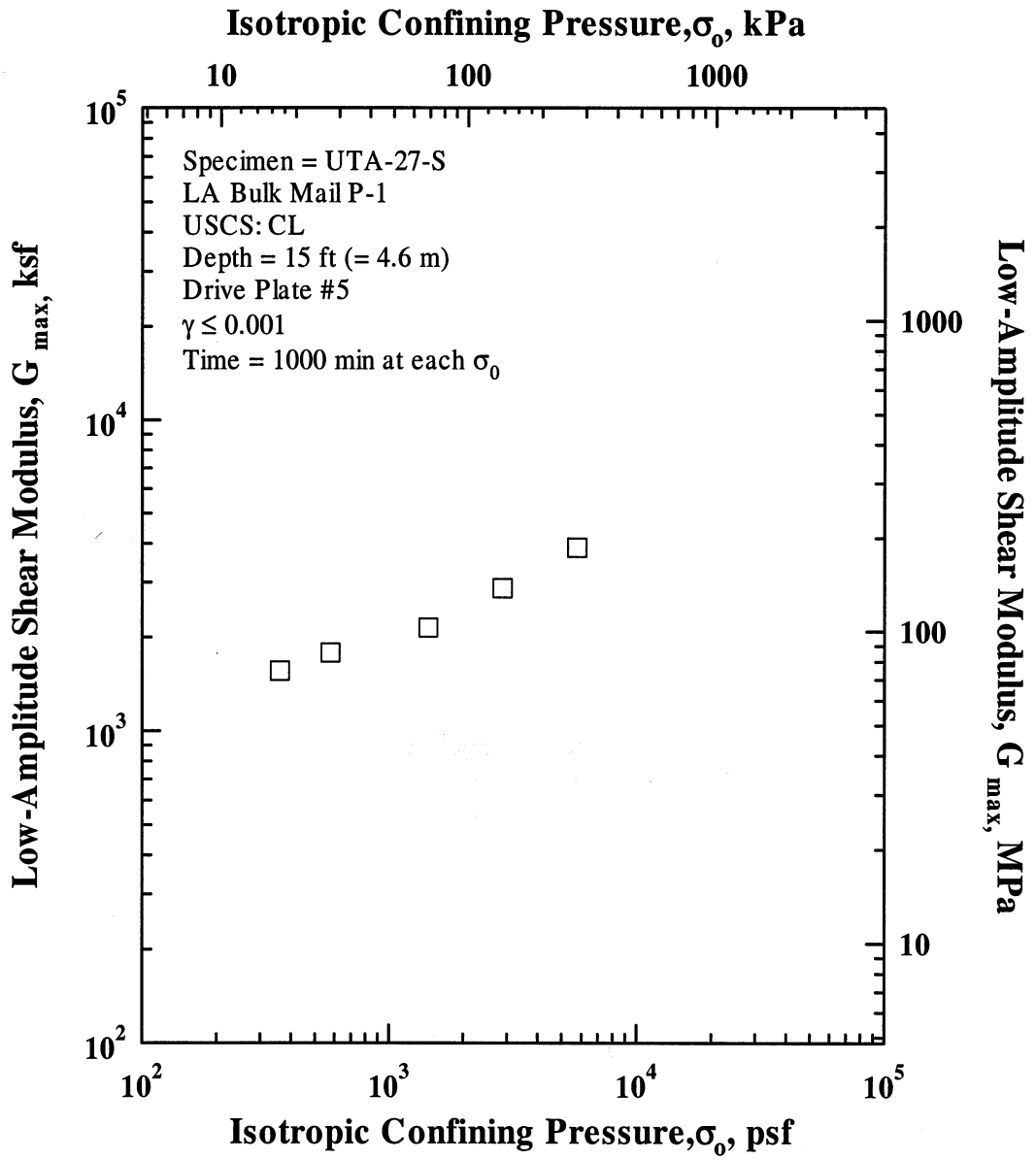

Figure K.5 Variation in Low-Amplitude Shear Modulus with Isotropic Confining Pressure from Resonant Column Tests of Specimen UTA-27-S.

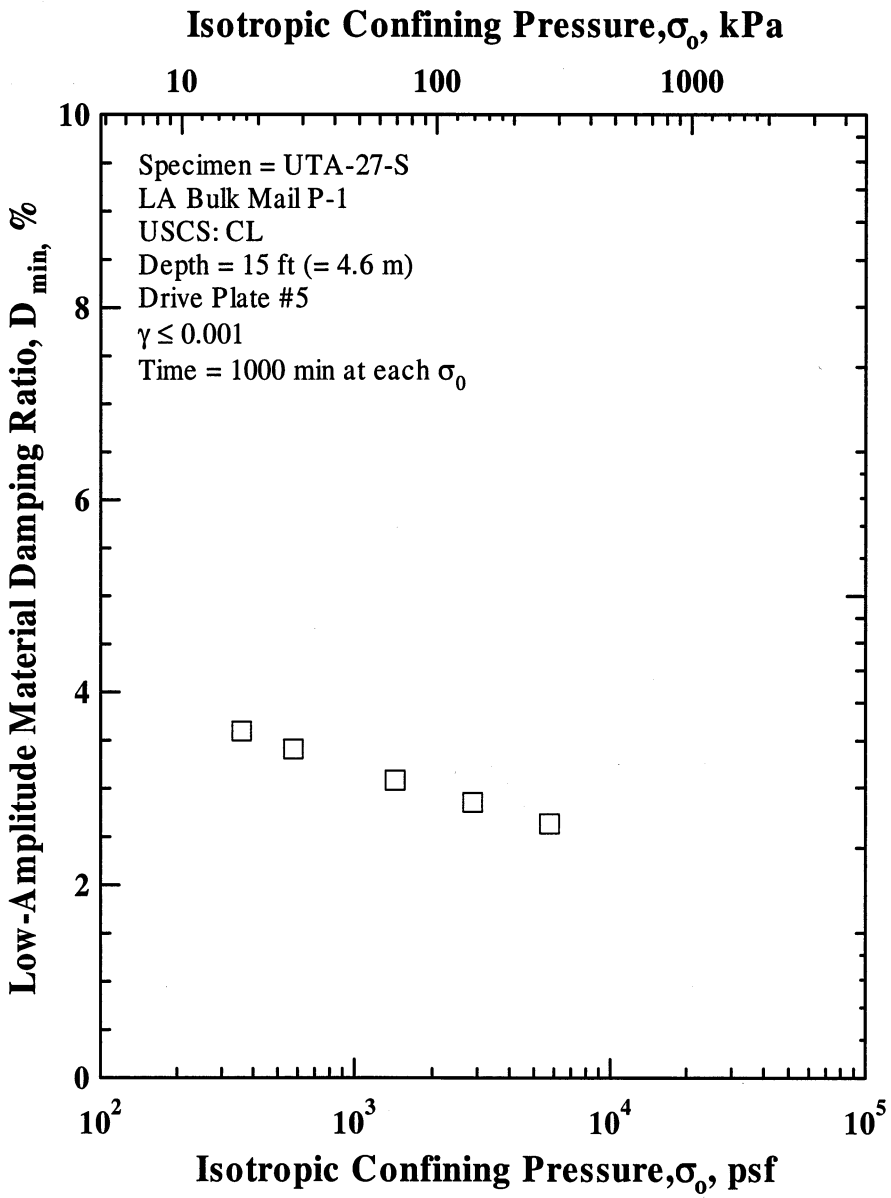

Figure K.6 Variation in Low-Amplitude Material Damping Ratio with Isotropic Confining Pressure from Resonant Column Tests of Specimen UTA-27-S.

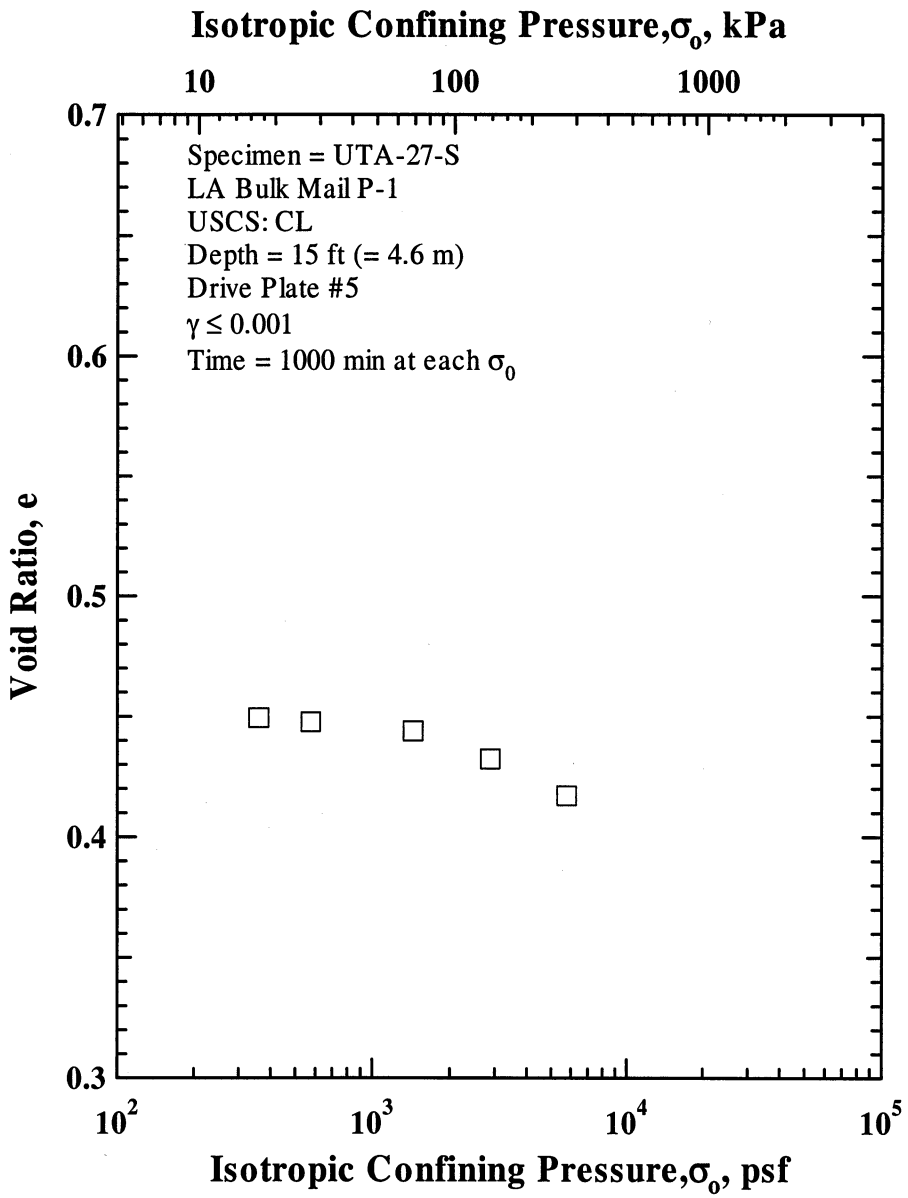

Figure K.7 Variation in Estimated Void Ratio with Isotropic Confining Pressure from Resonant Column Tests of Specimen UTA-27-S.

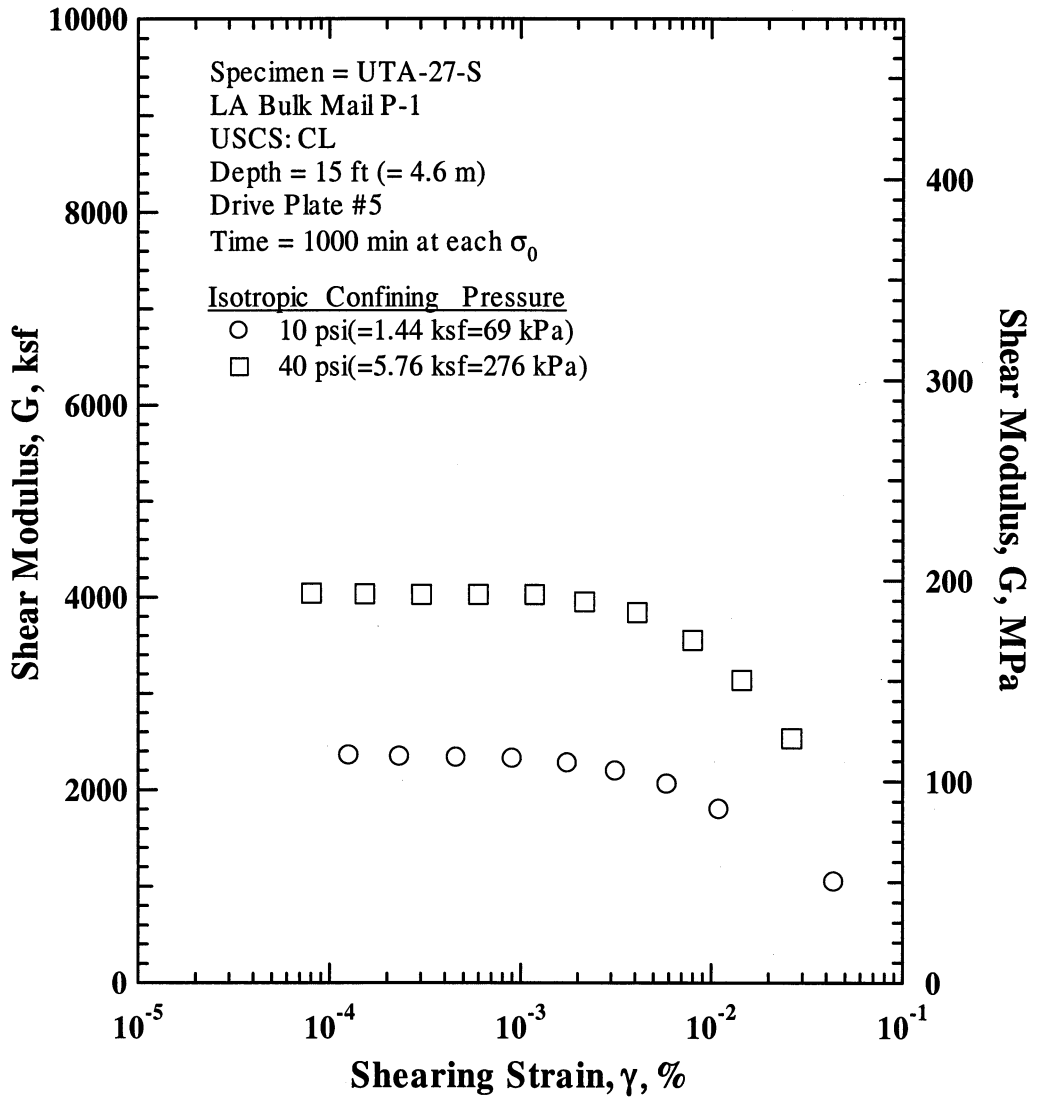

Figure K.8 Comparison of the Variation in Shear Modulus with Shearing Strain and Isotropic Confining Pressure from the Resonant Column Tests of Specimen UTA-27-S.

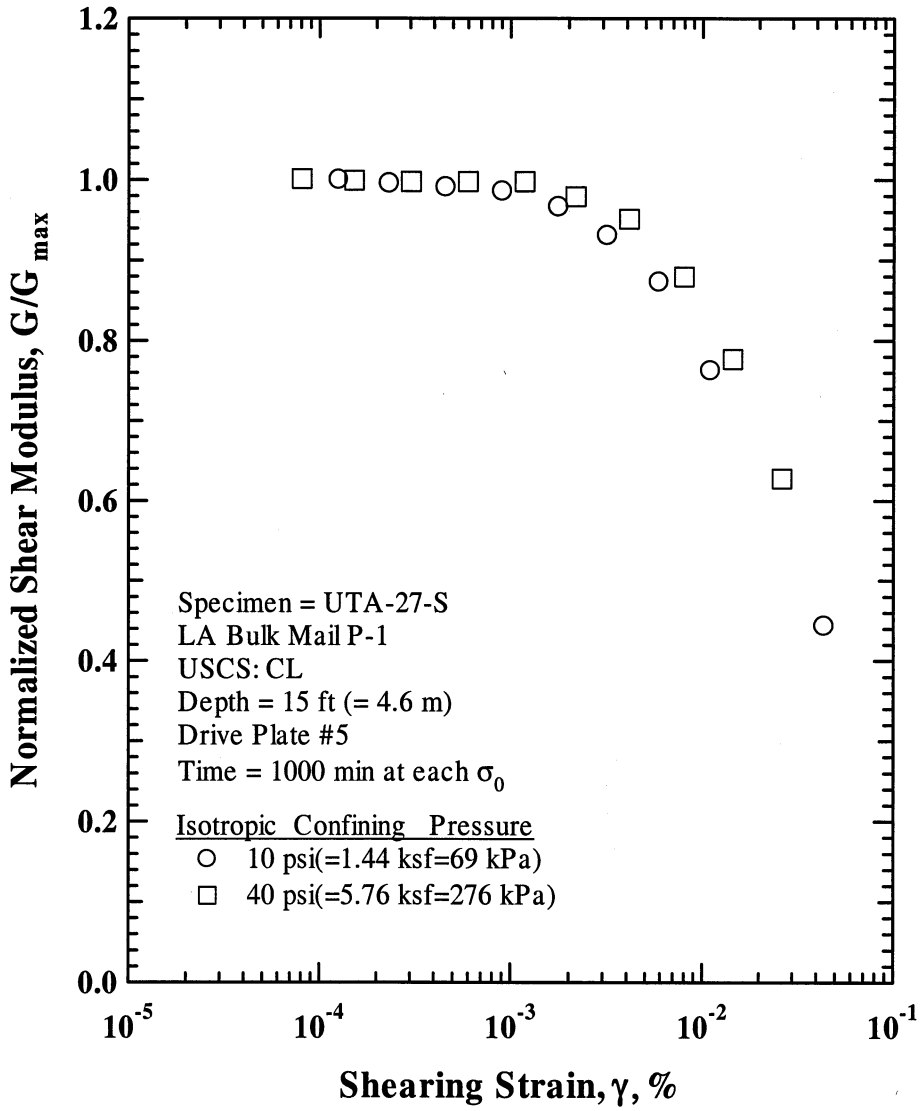

Figure K.9 Comparison of the Variation in Normalized Shear Modulus with Shearing Strain and Isotropic Confining Pressure from the Resonant Column Tests of Specimen UTA-27-S.

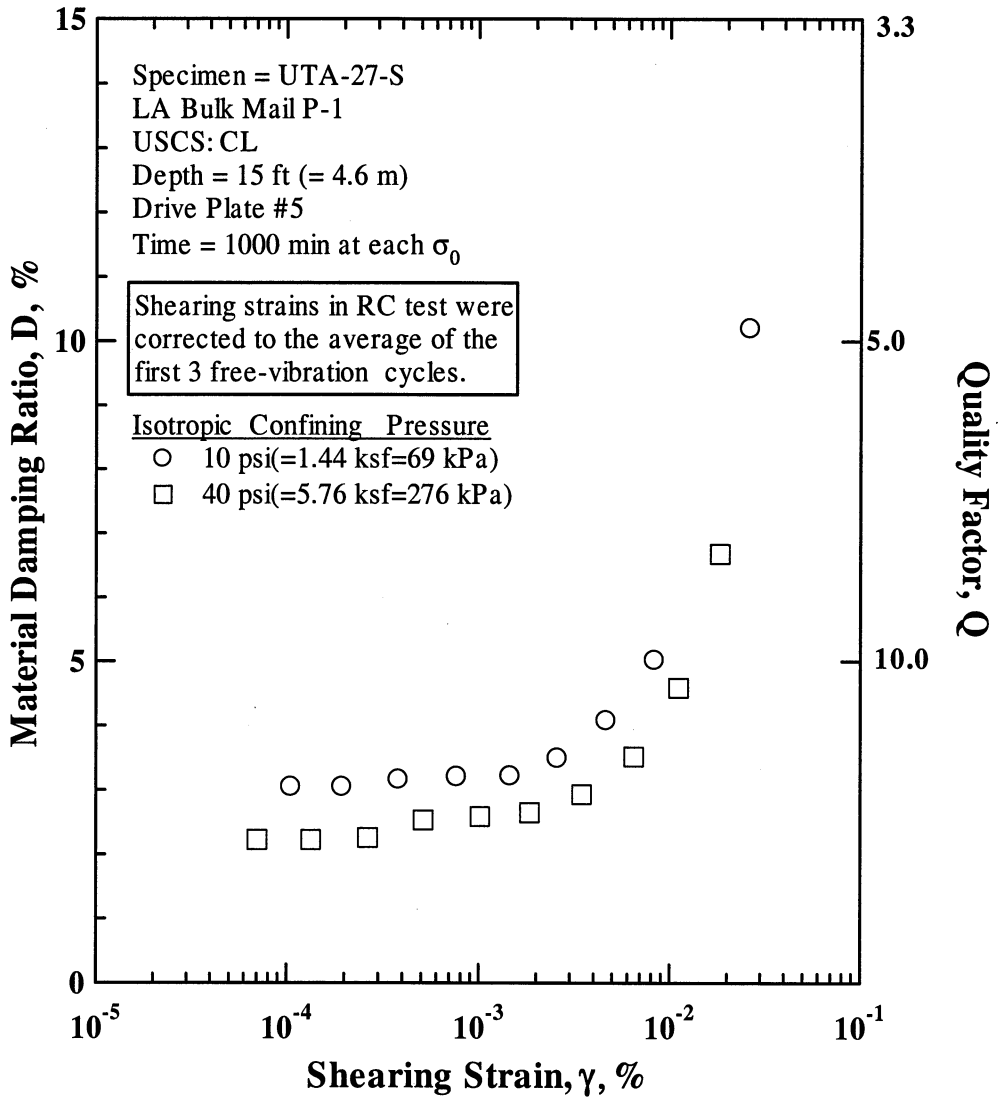

Figure K.10 Comparison of the Variation in Material Damping Ratio with Shearing Strain and Isotropic Confining Pressure from the Resonant Column Tests of Specimen UTA-27-S.

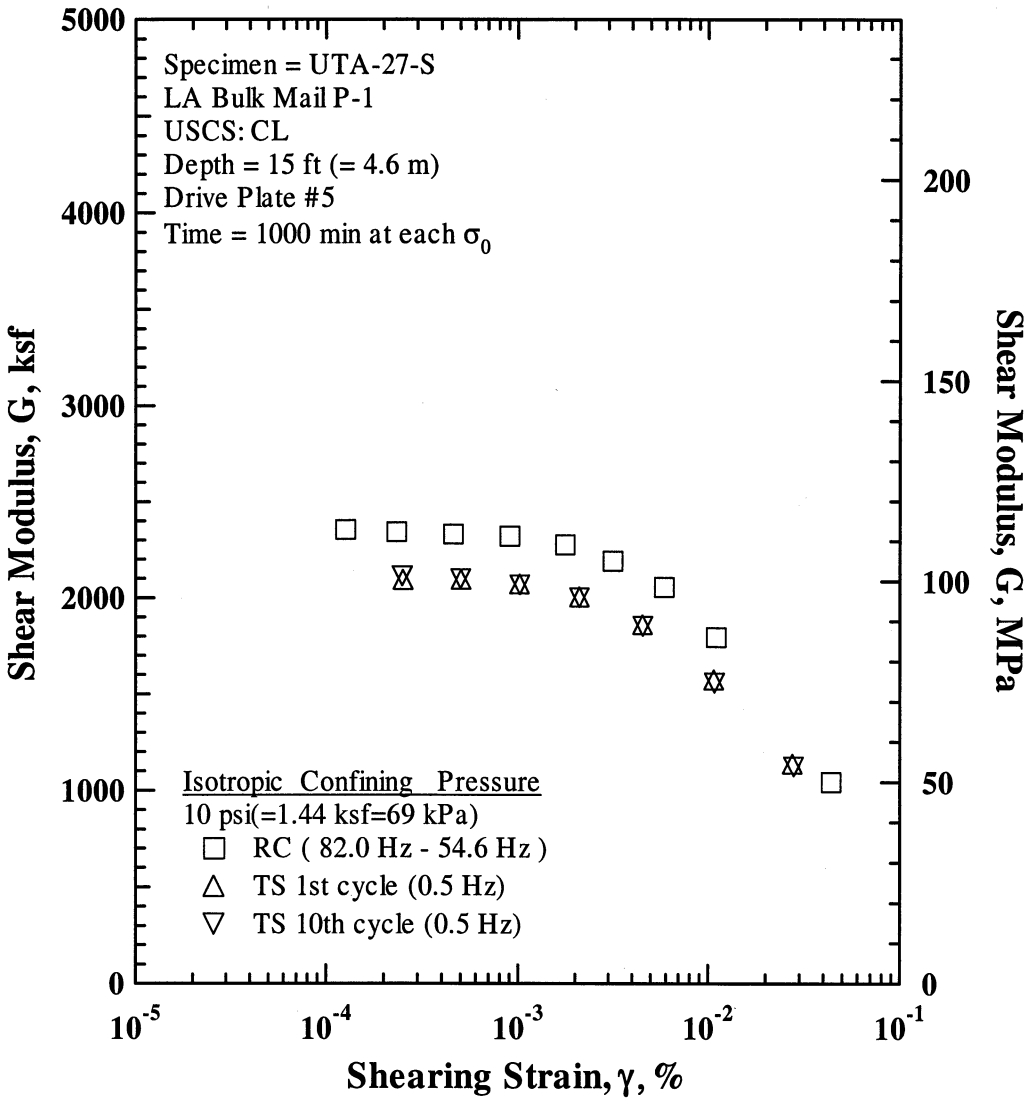

Figure K.11 Comparison of the Variation in Shear Modulus with Shearing Strain at an Isotropic Confining Pressure of 10 psi (=1.44 ksf=69 kPa) from the Combined RCTS Tests of Specimen UTA-27-S.

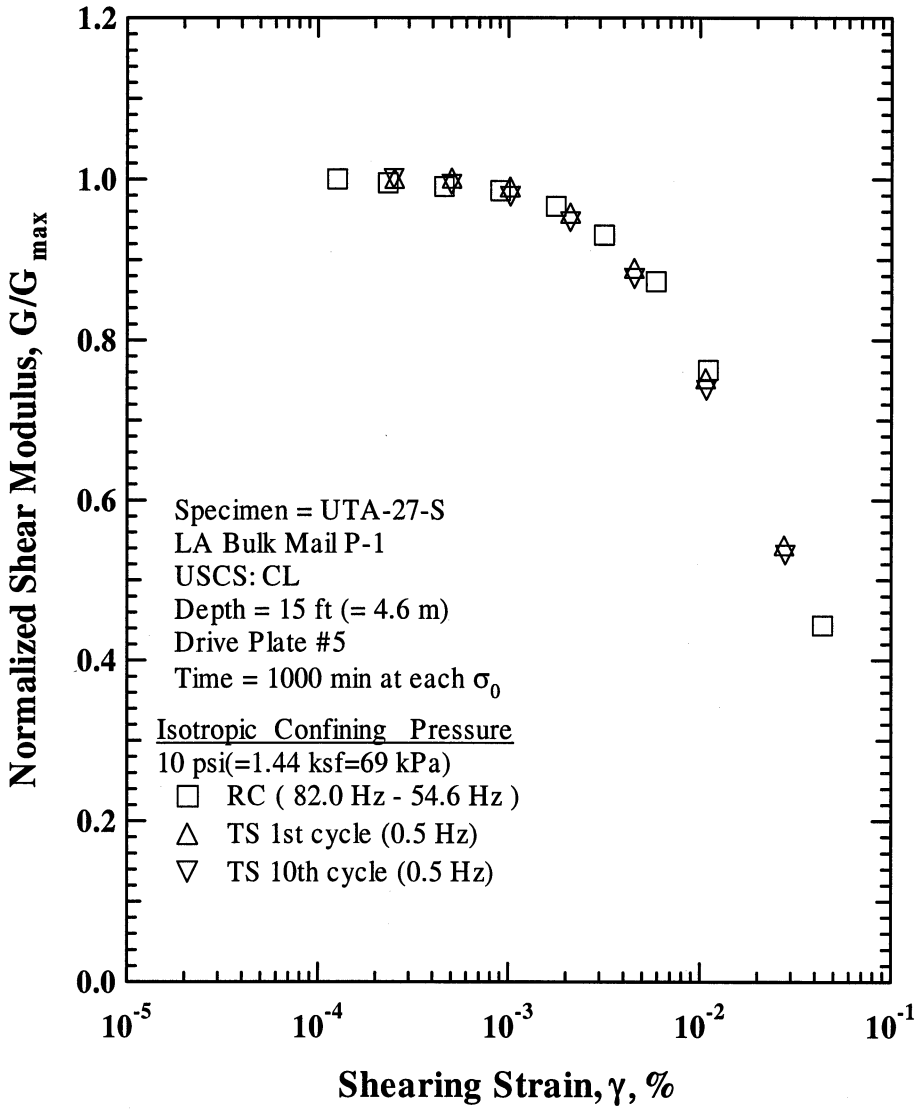

Figure K.12 Comparison of the Variation in Normalized Shear Modulus with Shearing Strain at an Isotropic Confining Pressure of 10 psi (=1.44 ksf=69 kPa) from the Combined RCTS Tests of Specimen UTA-27-S.

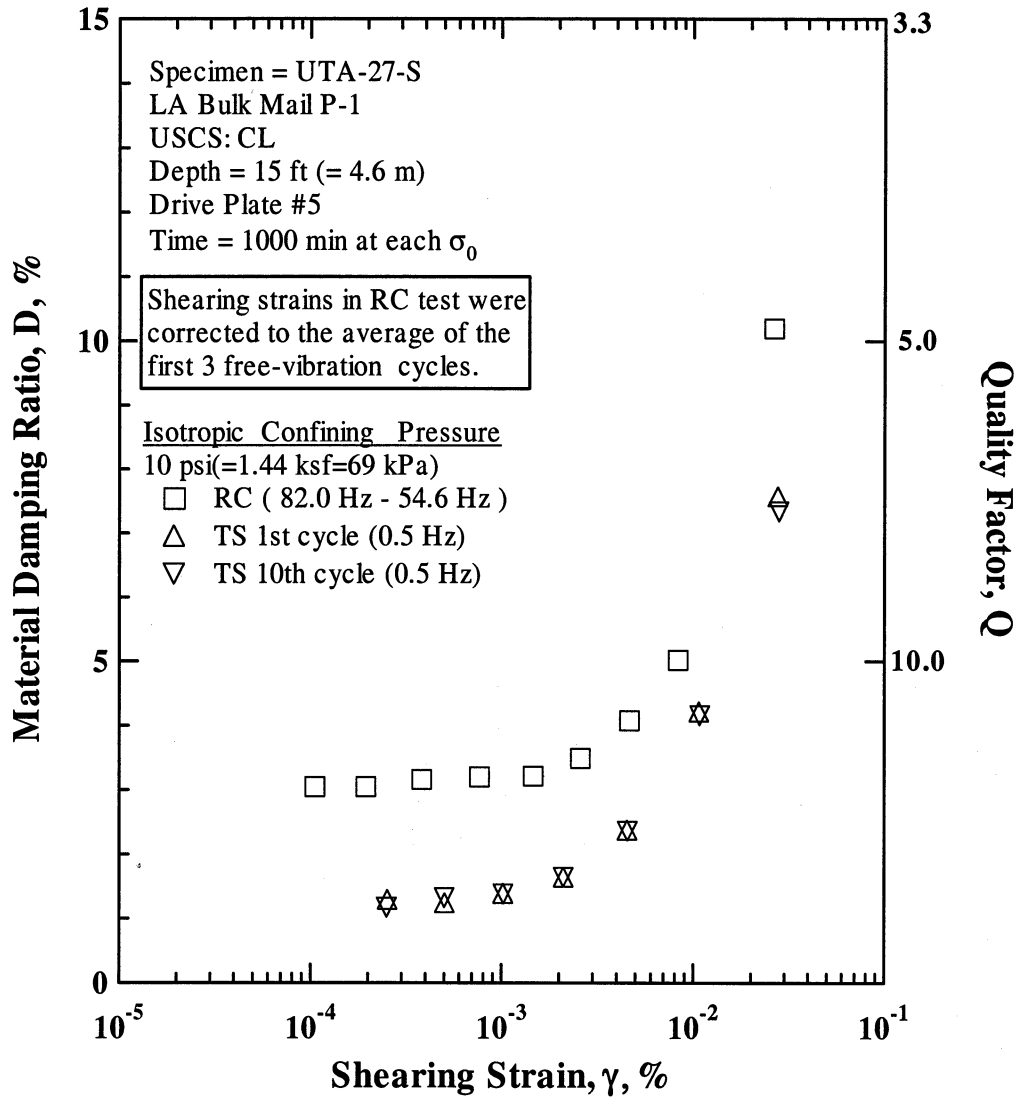

Figure K.13 Comparison of the Variation in Material Damping Ratio with Shearing Strain at an Isotropic Confining Pressure of 10 psi (=1.44 ksf=69 kPa) from the Combined RCTS Tests of Specimen UTA-27-S.

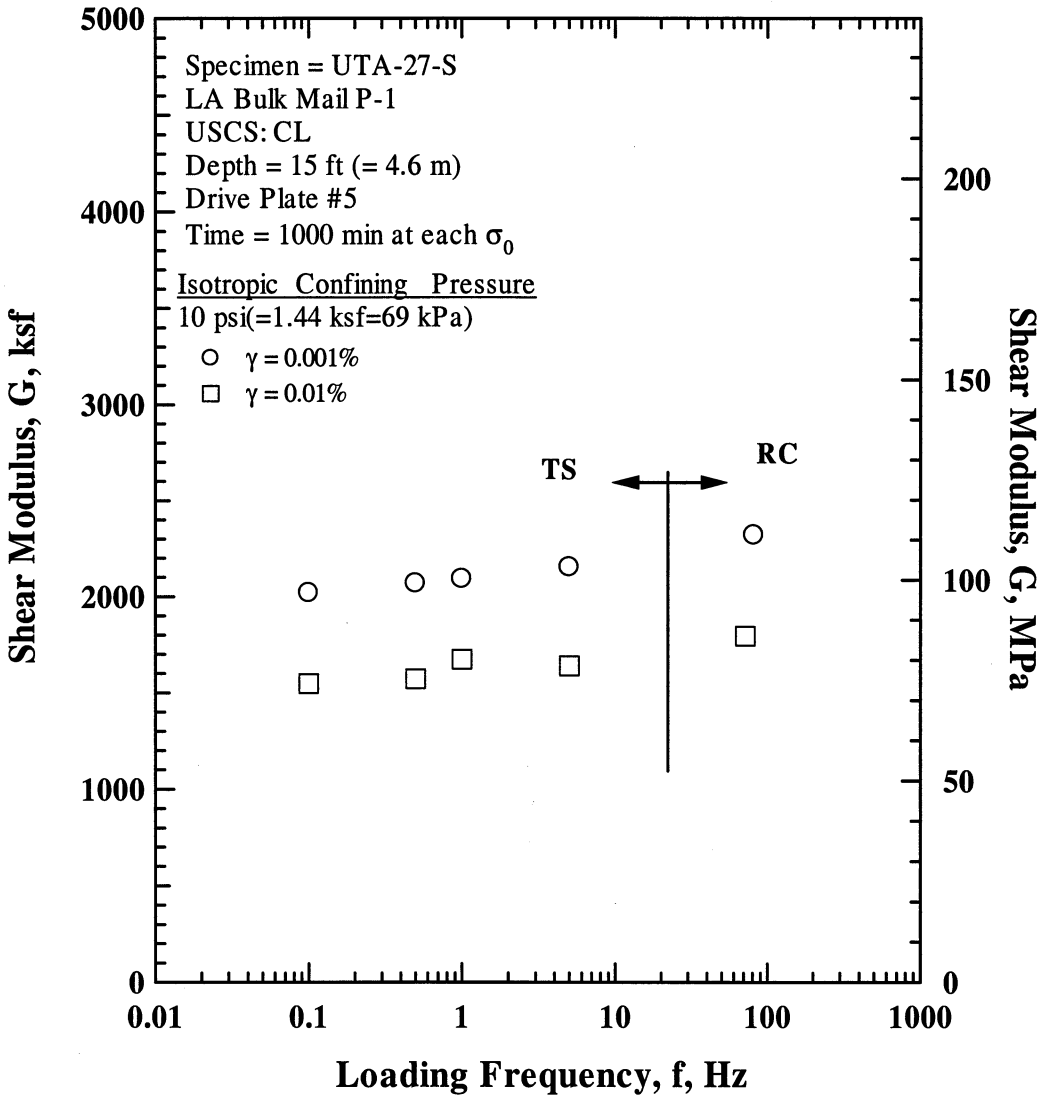

Figure K.14 Comparison of the Variation in Shear Modulus with Loading Frequency at an Isotropic Confining Pressure of 10 psi (=1.44 ksf=69 kPa) from the Combined RCTS Tests of Specimen UTA-27-S.

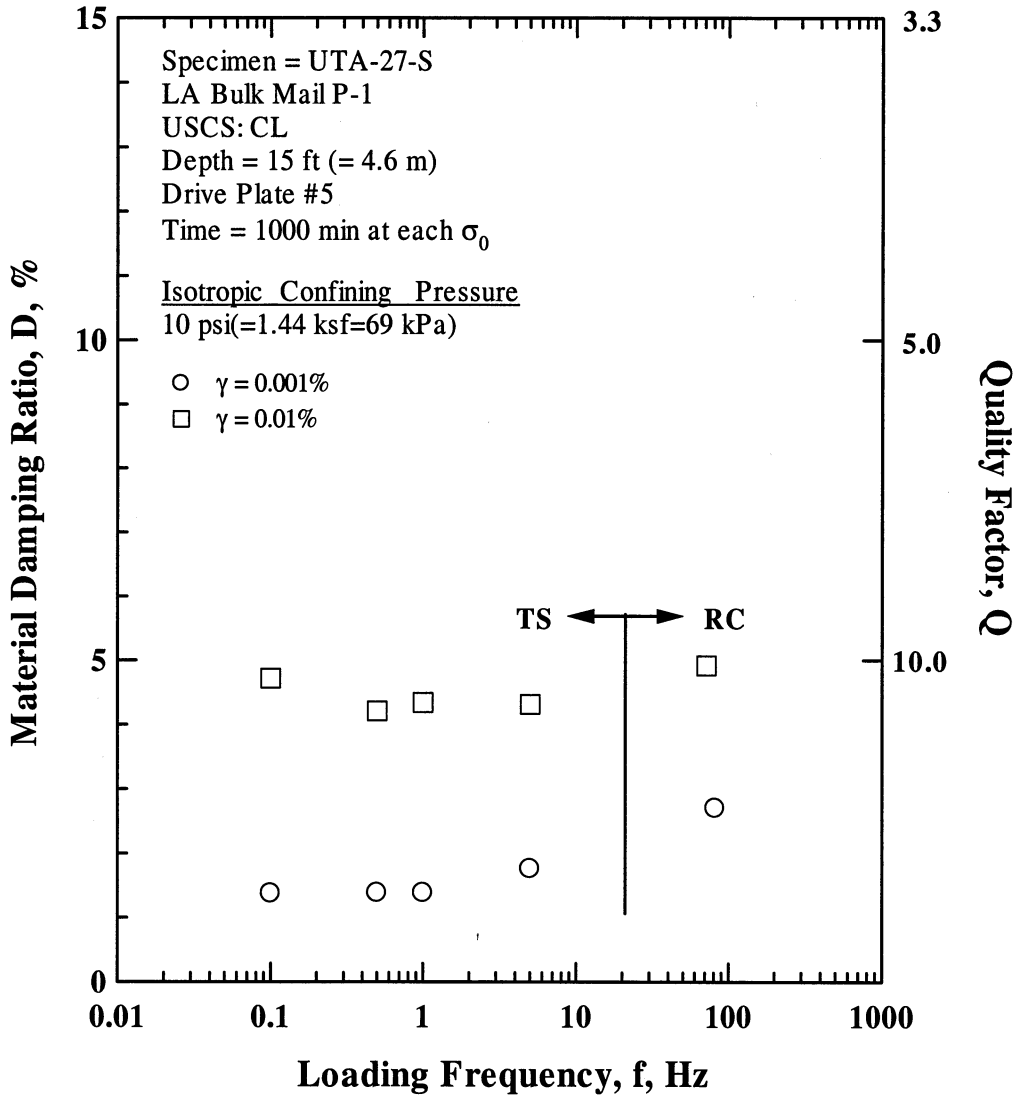

Figure K.15 Comparison of the Variation in Material Damping Ratio with Loading Frequency at an Isotropic Confining Pressure 10 psi (=1.44 ksf=69 kPa) from the Combined RCTS Tests of Specimen UTA-27-S.

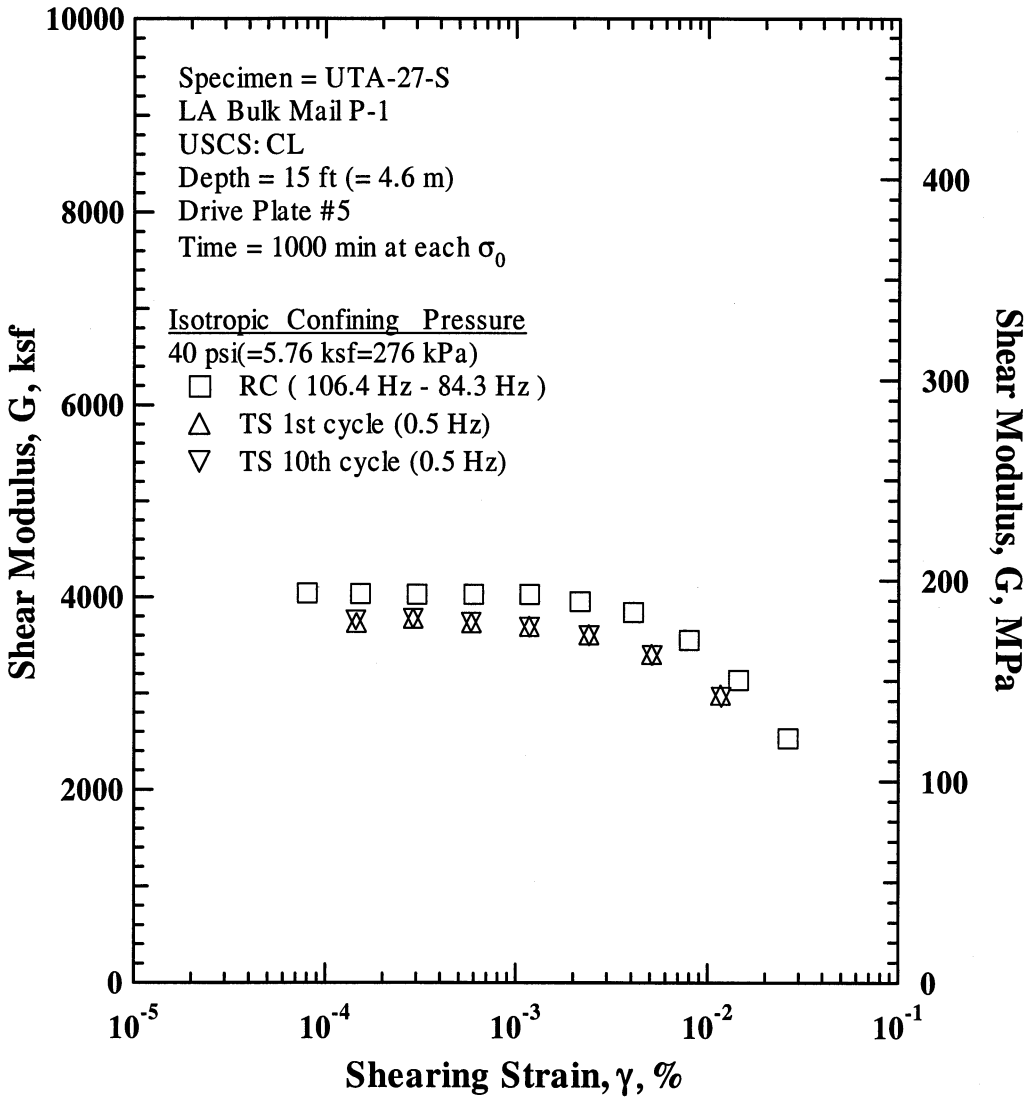

Figure K.16 Comparison of the Variation in Shear Modulus with Shearing Strain at an Isotropic Confining Pressure of 40 psi (=5.76 ksf=276 kPa) from the Combined RCTS Tests of Specimen UTA-27-S.

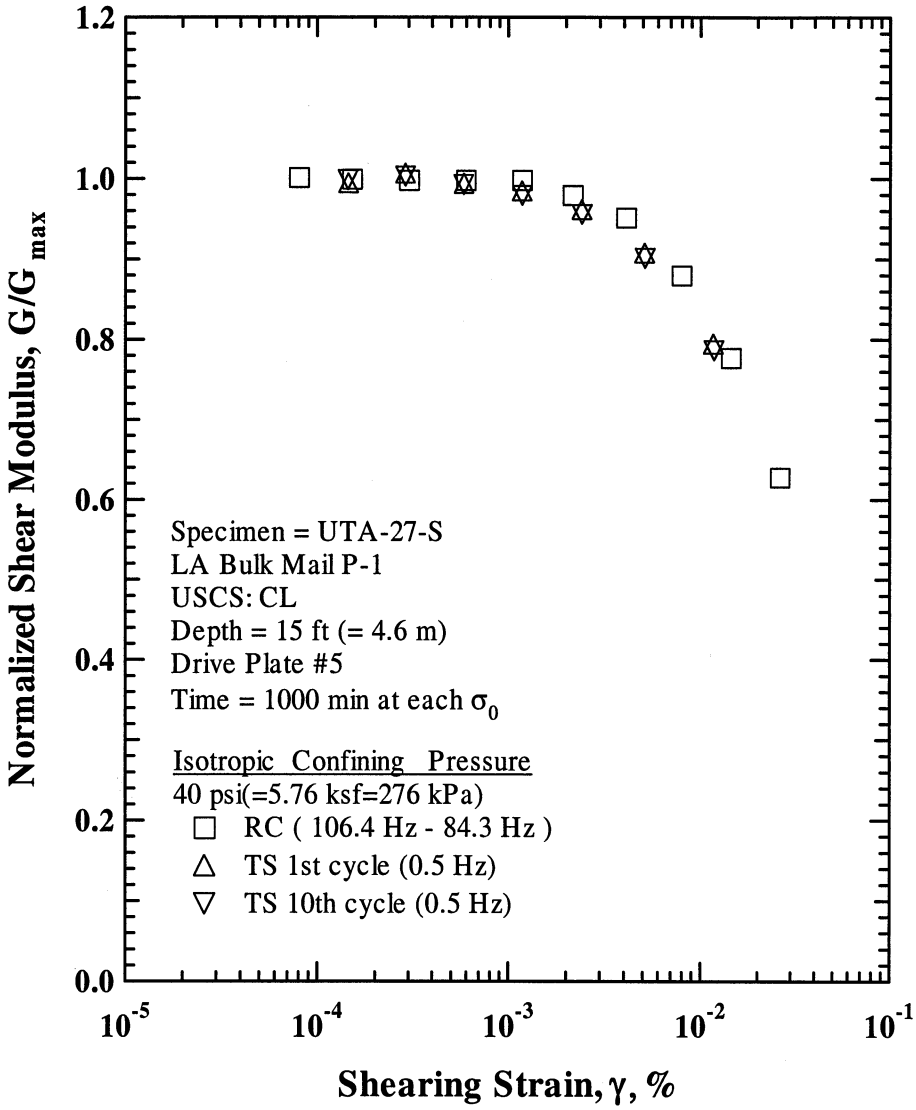

Figure K.17 Comparison of the Variation in Normalized Shear Modulus with Shearing Strain at an Isotropic Confining Pressure of 40 psi (=5.76 ksf=276 kPa) from the Combined RCTS Tests of Specimen UTA-27-S.

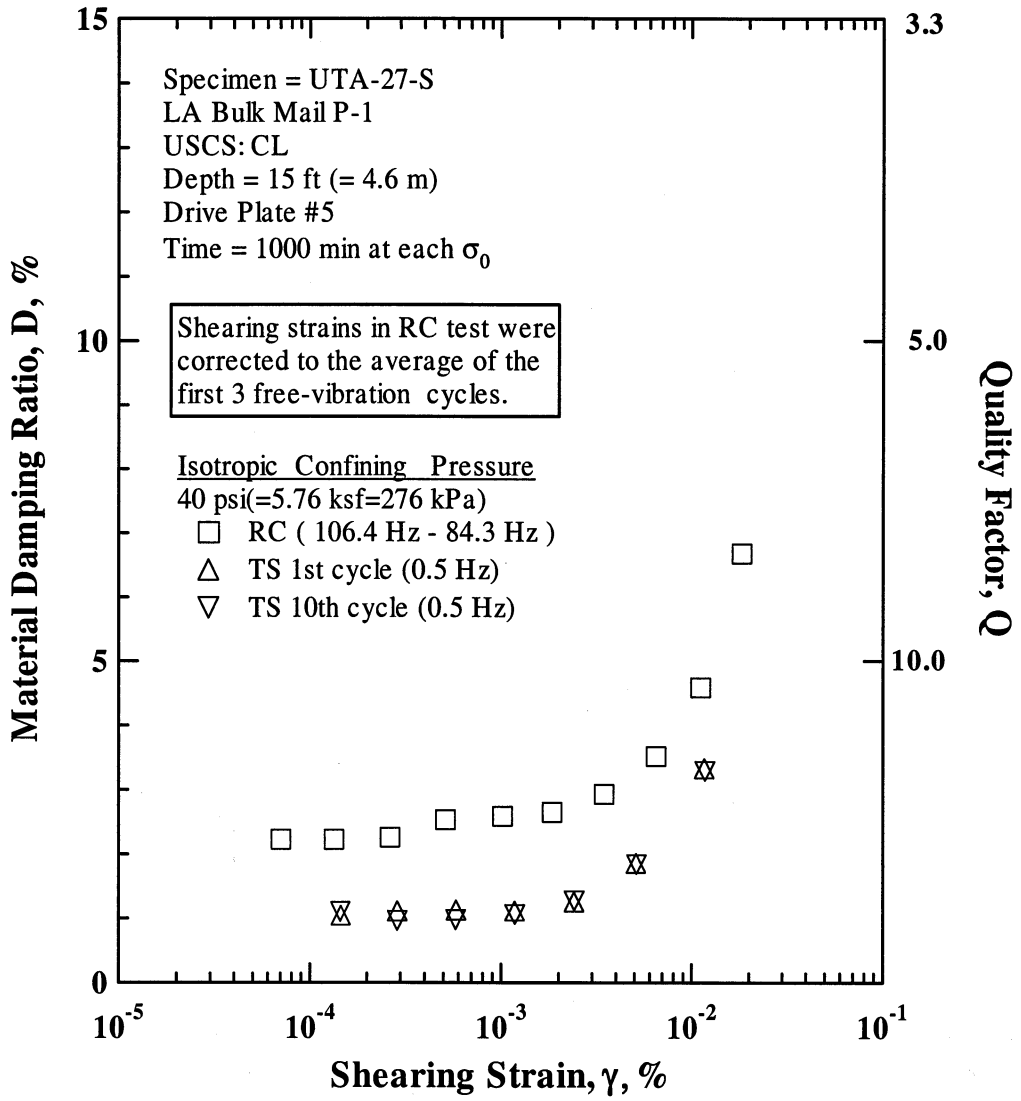

Figure K.18 Comparison of the Variation in Material Damping Ratio with Shearing Strain at an Isotropic Confining Pressure of 40 psi (=5.76 ksf=276 kPa) from the Combined RCTS Tests of Specimen UTA-27-S.

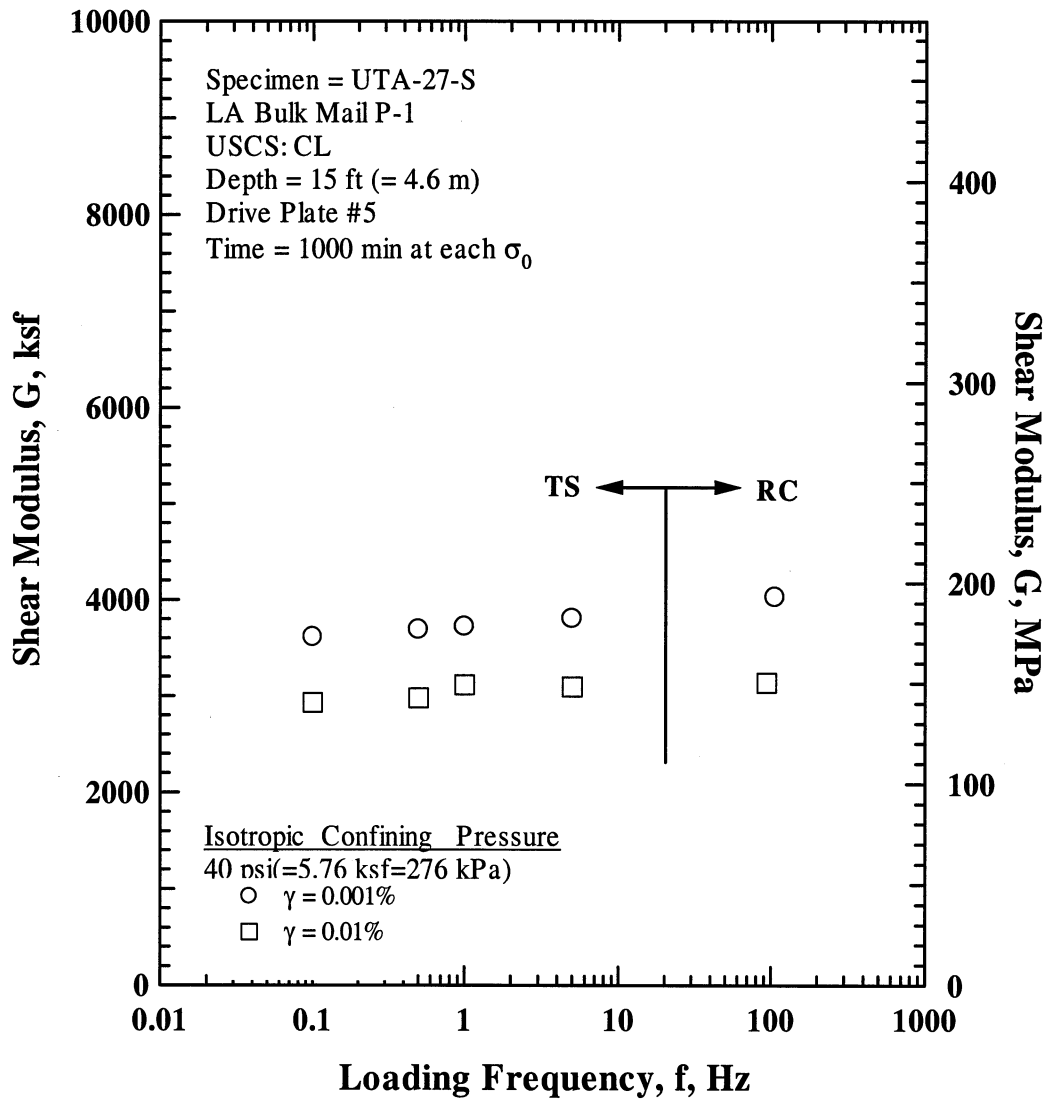

Figure K.19 Comparison of the Variation in Shear Modulus with Loading Frequency at an Isotropic Confining Pressure of 40 psi (=5.76 ksf=276 kPa) from the Combined RCTS Tests of Specimen UTA-27-S.

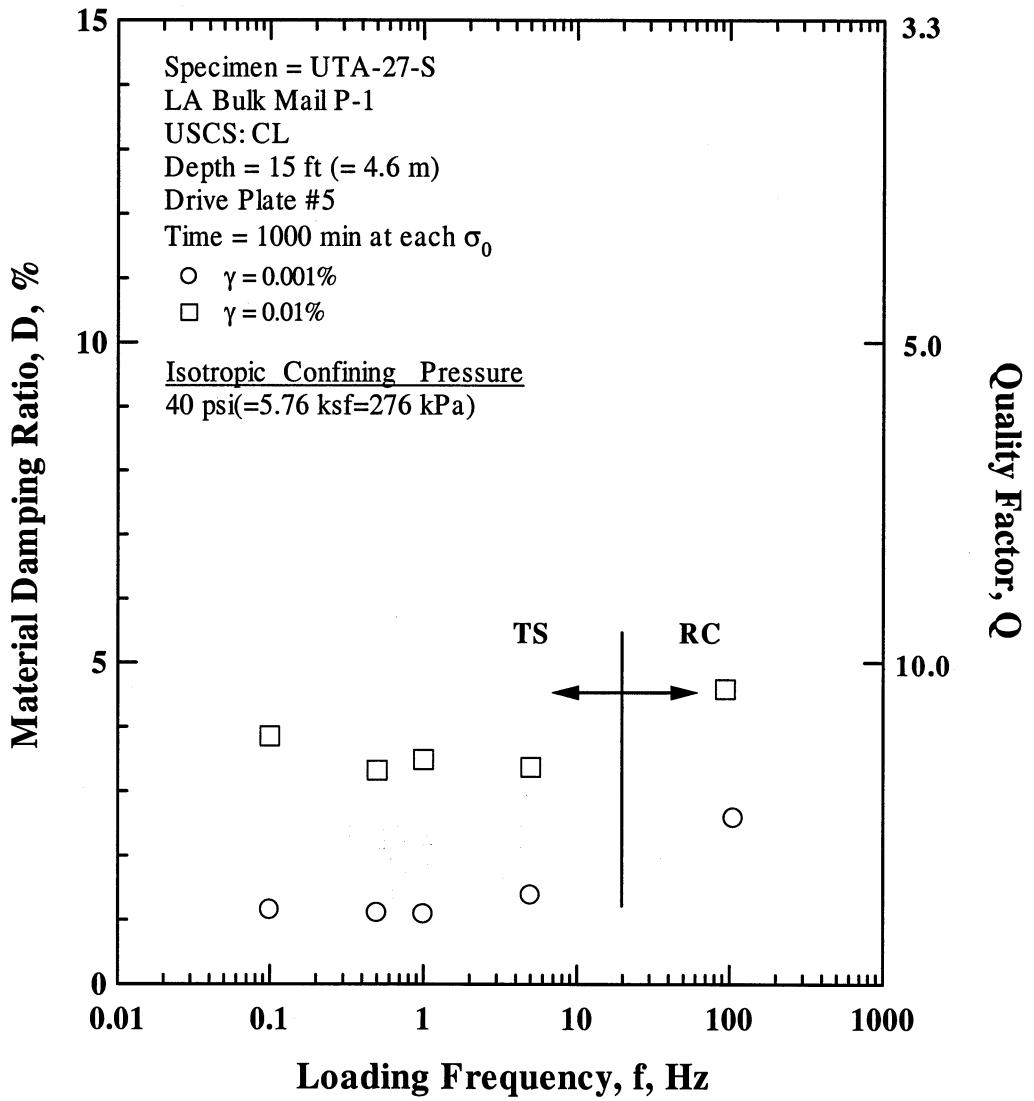

Figure K.20 Comparison of the Variation in Material Damping Ratio with Loading Frequency at an Isotropic Confining Pressure 40 psi (=5.76 ksf=276 kPa) from the Combined RCTS Tests of Specimen UTA-27-S.

Table K.1 Variation in Low-Amplitude Shear Wave Velocity, Low-Amplitude Shear Modulus, Low-Amplitude Material Damping Ratio and Estimated Void Ratio with Isotropic Confining Pressure from RC Tests of Specimen UTA-27-S.

Effective Isotropic Confining Pressure, σ_o'			Low-Amplitude Shear Modulus, G_{max}		Low-Amplitude Shear Wave Velocity, Vs	Low-Amplitude Material Damping Ratio, Dmin	Estimated Void Ratio, e
(psi)	(psf)	(kPa)	(ksf)	(MPa)	(fps)	(%)	
3	360	17	1558	74.7	606	3.59	0.449
4	576	28	1783	85.5	654	3.41	0.448
10	1440	69	2144	102.8	717	3.08	0.444
20	2880	138	2875	137.8	828	2.86	0.432
40	5760	276	3883	186.2	960	2.64	0.417

Table K.2 Variation in Shear Modulus, Normalized Shear Modulus and Material Damping Ratio with Shearing Strain from RC Tests of Specimen UTA-27-S; Confining Pressure, σ_o' = 10 psi (=1.44 ksf=69 kPa).

Peak Shearing Strain, %	Shear Modulus, G, ksf	Normalized Shear Modulus, G/G_{max}	Average[+] Shearing Strain, %	Material Damping Ratio[x], D, %
1.26E-04	2354	1.00	1.06E-04	3.04
2.33E-04	2342	1.00	1.94E-04	3.04
4.59E-04	2331	0.99	3.82E-04	3.16
9.05E-04	2320	0.99	7.50E-04	3.20
1.77E-03	2274	0.97	1.46E-03	3.21
3.16E-03	2190	0.93	2.58E-03	3.49
5.89E-03	2054	0.87	4.66E-03	4.07
1.10E-02	1795	0.76	8.32E-03	5.02
4.38E-02	1044	0.44	2.63E-02	10.20

[+] Average Shearing Strain from the First Three Cycles of the Free Vibration Decay Curve

[x] Average Damping Ratio from the First Three Cycles of the Free Vibration Decay Curve

Table K.3 Variation in Shear Modulus, Normalized Shear Modulus and Material Damping Ratio with Shearing Strain from TS Tests of Specimen UTA-27-S; Confining Pressure, σ_o' = 10 psi (=1.44 ksf=69 kPa).

First Cycle				Tenth Cycle			
Peak Shearing Strain, %	Shear Modulus, G, ksf	Normalized Shear Modulus, G/G_{max}	Material Damping Ratio, D, %	Peak Shearing Strain, %	Shear Modulus, G, ksf	Normalized Shear Modulus, G/G_{max}	Material Damping Ratio, D, %
2.53E-04	2091	1.00	1.28	2.51E-04	2110	1.00	1.16
5.06E-04	2092	1.00	1.23	5.05E-04	2094	0.99	1.31
1.02E-03	2069	0.99	1.38	1.03E-03	2063	0.98	1.37
2.11E-03	2001	0.96	1.64	2.12E-03	1997	0.95	1.63
4.55E-03	1858	0.89	2.37	4.58E-03	1849	0.88	2.35
1.08E-02	1572	0.75	4.21	1.09E-02	1555	0.74	4.15
2.77E-02	1135	0.54	7.57	2.81E-02	1120	0.53	7.33

Table K.4 Variation in Shear Modulus, Normalized Shear Modulus and Material Damping Ratio with Shearing Strain from RC Tests of Specimen UTA-27-S; Confining Pressure, σ_o' = 40 psi (=5.76 ksf=276 kPa).

Peak Shearing Strain, %	Shear Modulus, G, ksf	Normalized Shear Modulus, G/G_{max}	Average[+] Shearing Strain, %	Material Damping Ratio[x], D, %
1.53E-04	4032	1.00	1.34E-04	2.22
8.05E-05	4040	1.00	7.05E-05	2.22
3.02E-04	4026	1.00	2.64E-04	2.25
5.98E-04	4026	1.00	5.15E-04	2.53
1.18E-03	4026	1.00	1.02E-03	2.58
2.16E-03	3951	0.98	1.85E-03	2.64
4.11E-03	3839	0.95	3.46E-03	2.93
7.98E-03	3549	0.88	6.50E-03	3.51
1.44E-02	3135	0.78	1.11E-02	4.59
2.64E-02	2532	0.63	1.84E-02	6.68

[+] Average Shearing Strain from the First Three Cycles of the Free Vibration Decay Curve

[x] Average Damping Ratio from the First Three Cycles of the Free Vibration Decay Curve

Table K.5 Variation in Shear Modulus, Normalized Shear Modulus and Material Damping Ratio with Shearing Strain from TS Tests of Specimen UTA-27-S; Confining Pressure, σ_o' = 40 psi (=5.76 ksf=276 kPa).

First Cycle				Tenth Cycle			
Peak Shearing Strain, %	Shear Modulus, G, ksf	Normalized Shear Modulus, G/G_{max}	Material Damping Ratio, D, %	Peak Shearing Strain, %	Shear Modulus, G, ksf	Normalized Shear Modulus, G/G_{max}	Material Damping Ratio, D, %
1.46E-04	3725	0.99	1.03	1.45E-04	3752	1.00	1.09
2.90E-04	3770	1.01	1.10	2.90E-04	3769	1.00	0.95
5.87E-04	3723	0.99	1.12	5.85E-04	3730	0.99	0.97
1.18E-03	3688	0.98	1.10	1.18E-03	3680	0.98	1.05
2.42E-03	3601	0.96	1.24	2.43E-03	3592	0.96	1.26
5.13E-03	3399	0.91	1.85	5.15E-03	3387	0.90	1.83
1.17E-02	2976	0.79	3.32	1.18E-02	2954	0.79	3.28

APPENDIX L

Specimen No. 11
UT Specimen ID: UTA-27-T

LA Bulk Mail P-3
Depth = 50ft (=15.2m)
Soil Type: Clay (CL)

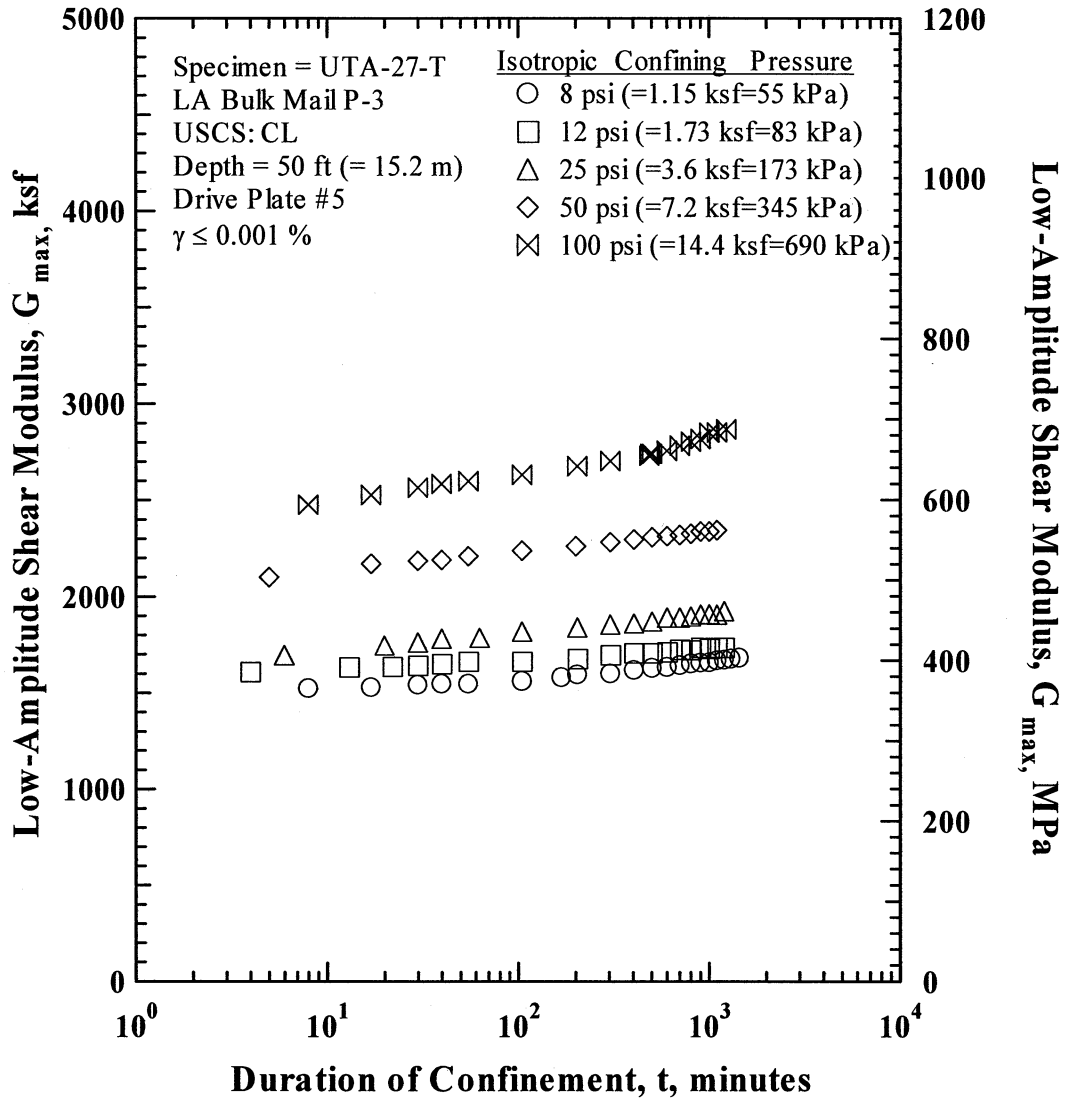

Figure L.1 Variation in Low-Amplitude Shear Modulus with Magnitude and Duration of Isotropic Confining Pressure from Resonant Column Tests of Specimen UTA-27-T.

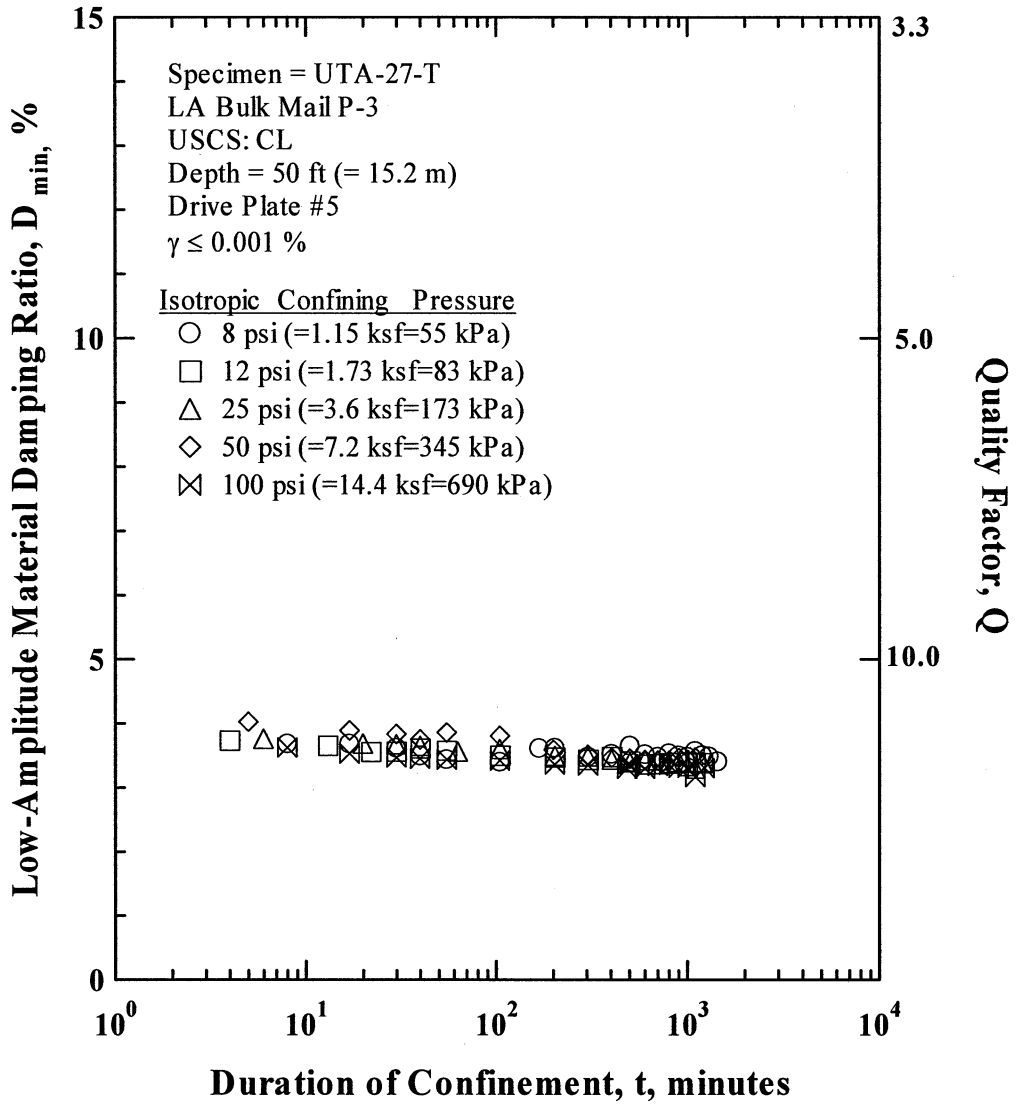

Figure L.2 Variation in Low-Amplitude Material Damping Ratio with Magnitude and Duration of Isotropic Confining Pressure from Resonant Column Tests of Specimen UTA-27-T

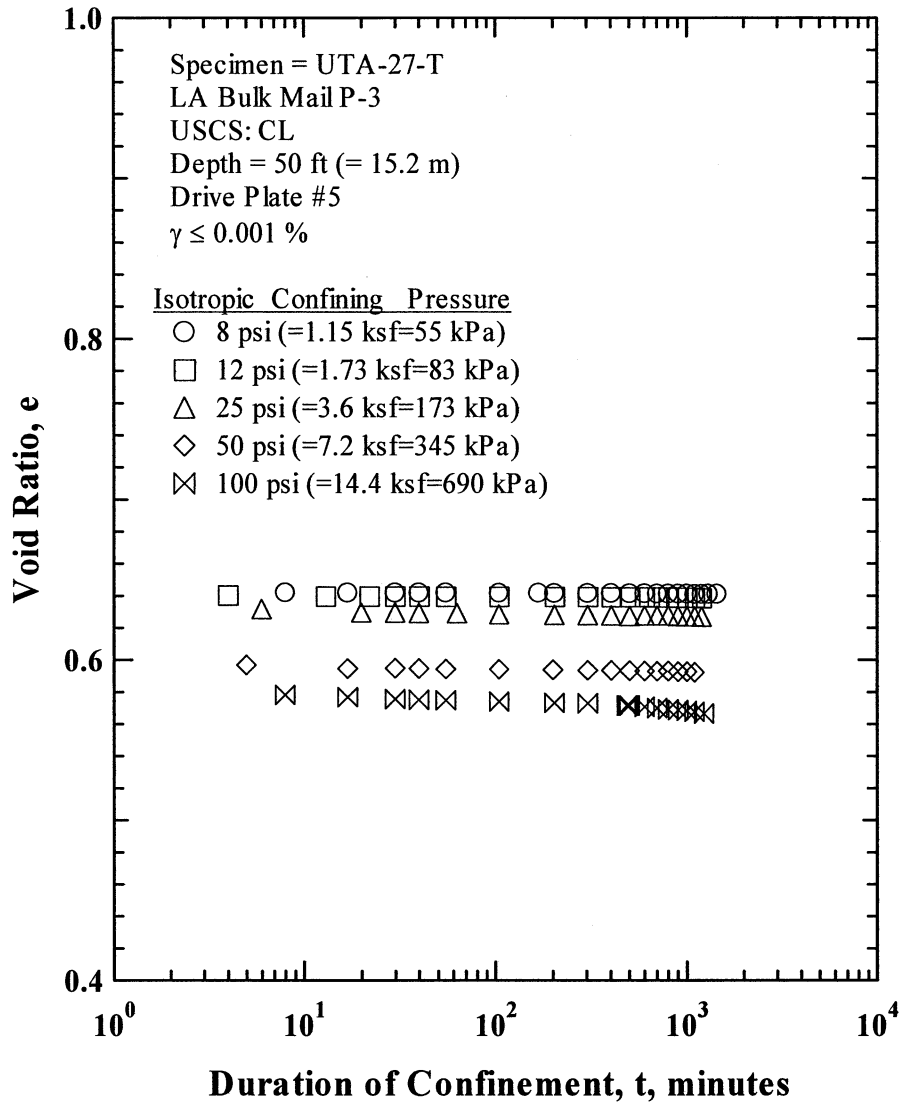

Figure L.3 Variation in Estimated Void Ratio with Magnitude and Duration of Isotropic Confining Pressure from Resonant Column Tests of Specimen UTA-27-T.

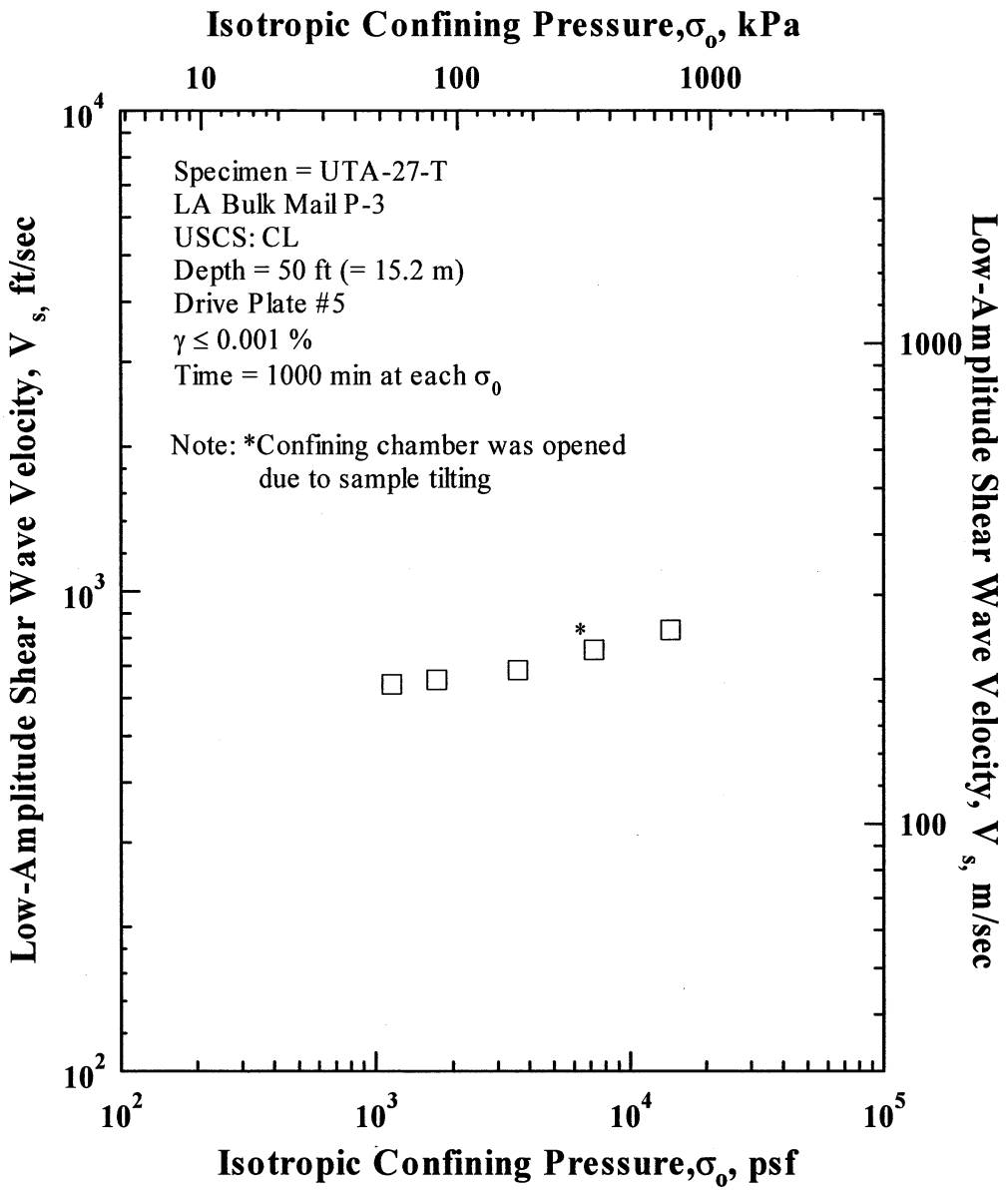

Figure L.4 Variation in Low-Amplitude Shear Wave Velocity with Isotropic Confining Pressure from Resonant Column Tests of Specimen UTA-27-T.

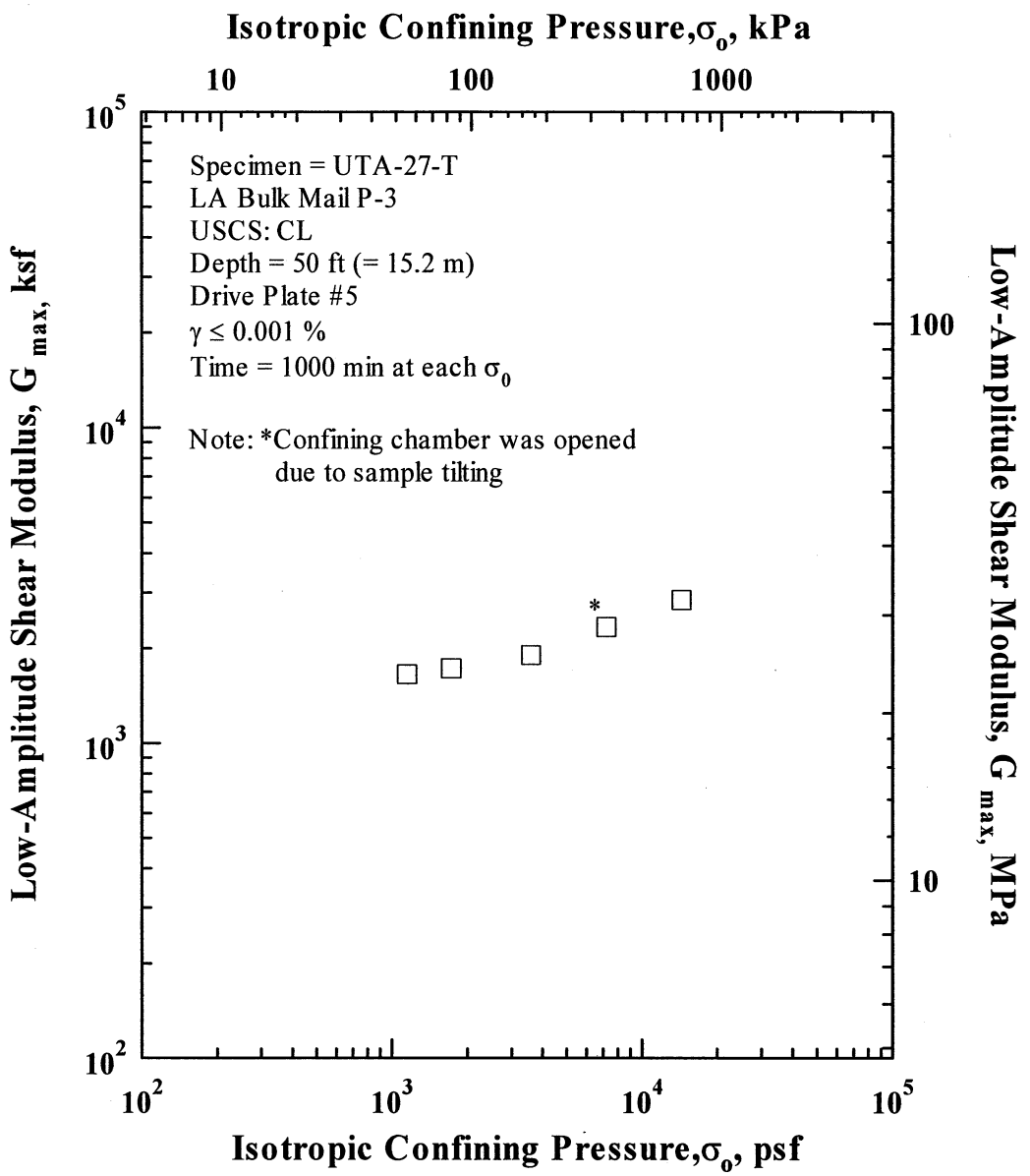

Figure L.5 Variation in Low-Amplitude Shear Modulus with Isotropic Confining Pressure from Resonant Column Tests of Specimen UTA-27-T.

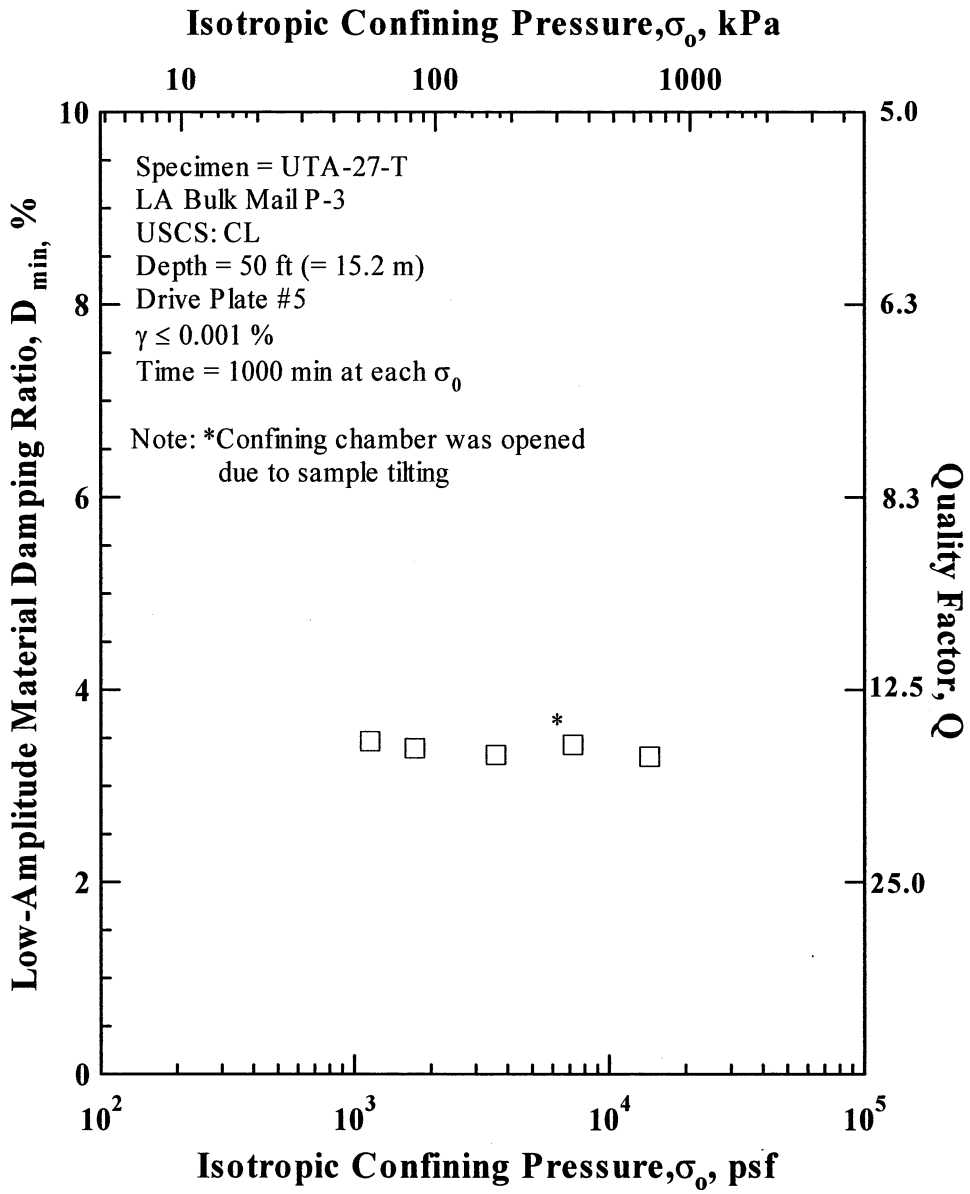

Figure L.6 Variation in Low-Amplitude Material Damping Ratio with Isotropic Confining Pressure from Resonant Column Tests of Specimen UTA-27-T.

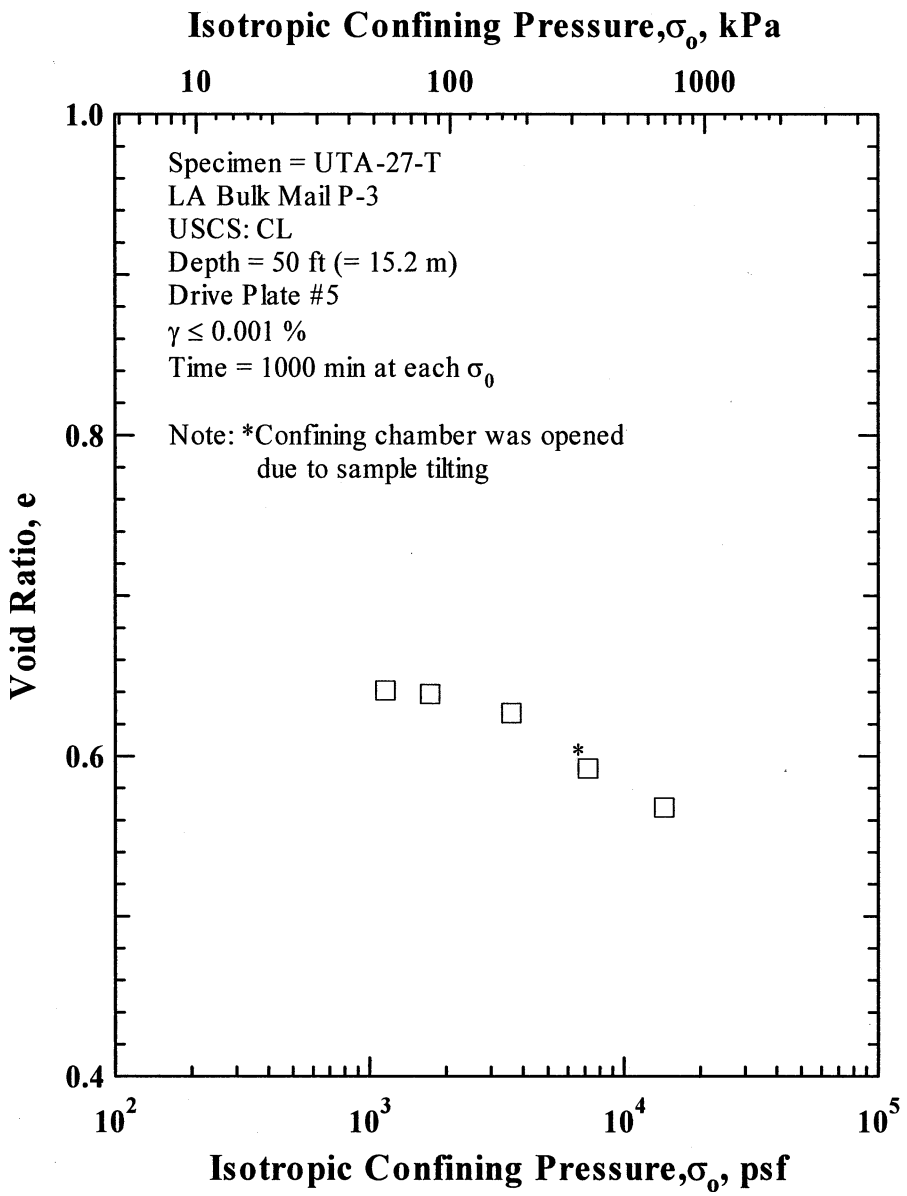

Figure L.7 Variation in Estimated Void Ratio with Isotropic Confining Pressure from Resonant Column Tests of Specimen UTA-27-T.

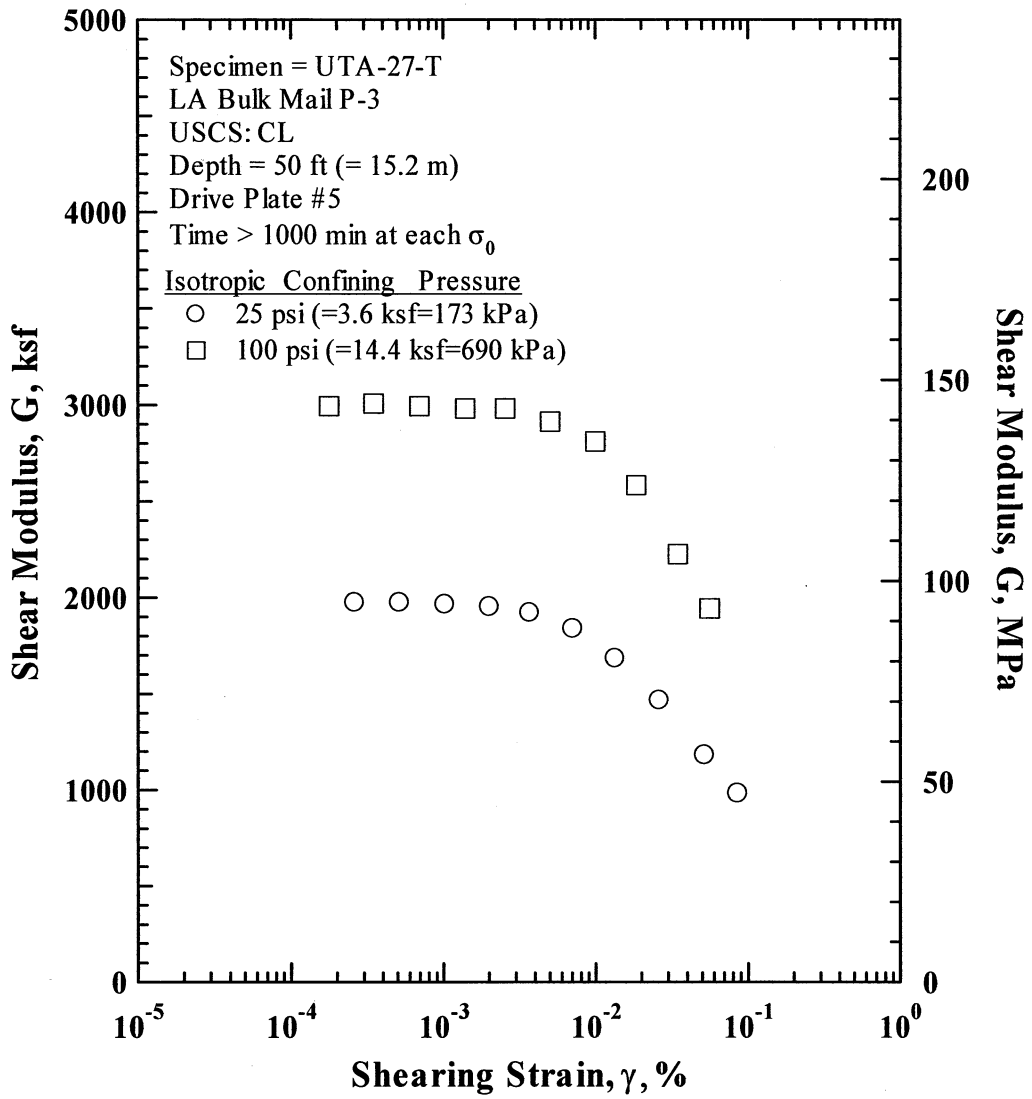

Figure L.8 Comparison of the Variation in Shear Modulus with Shearing Strain and Isotropic Confining Pressure from the Resonant Column Tests of Specimen UTA-27-T.

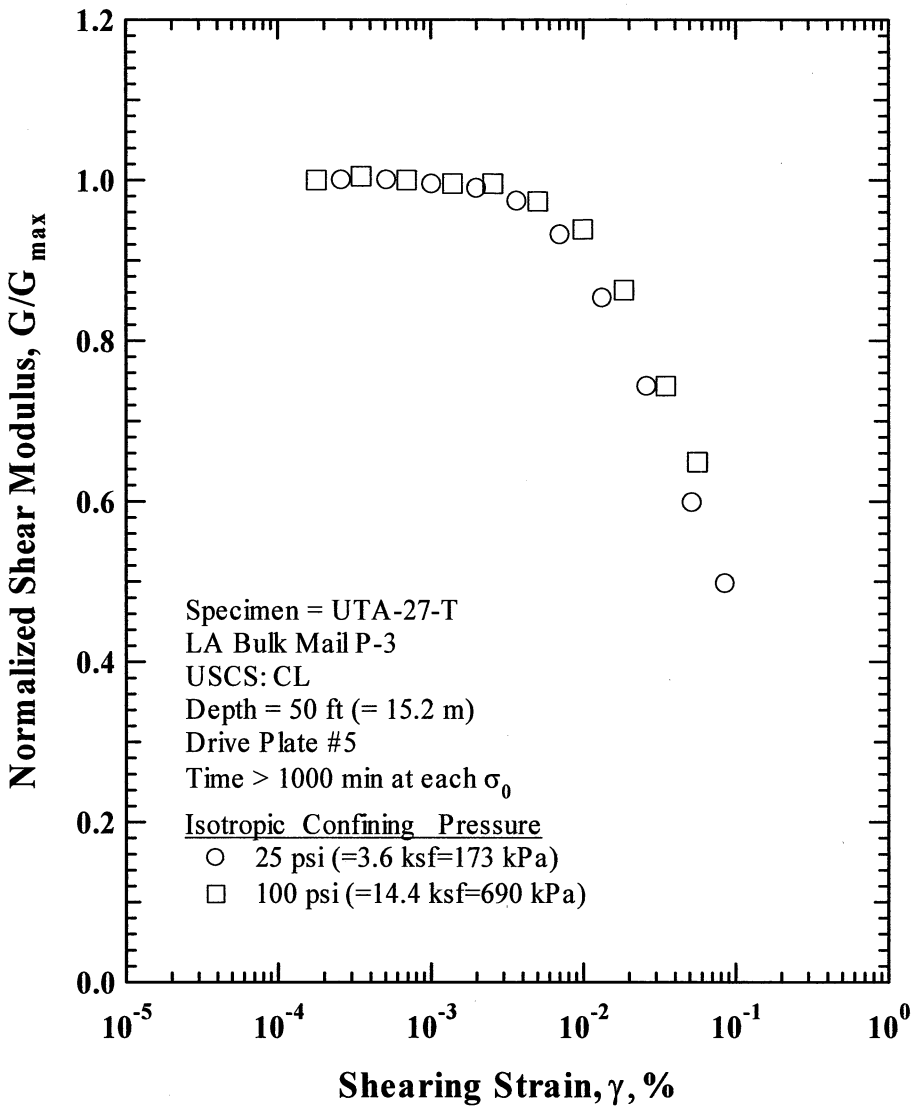

Figure L.9 Comparison of the Variation in Normalized Shear Modulus with Shearing Strain and Isotropic Confining Pressure from the Resonant Column Tests of Specimen UTA-27-T.

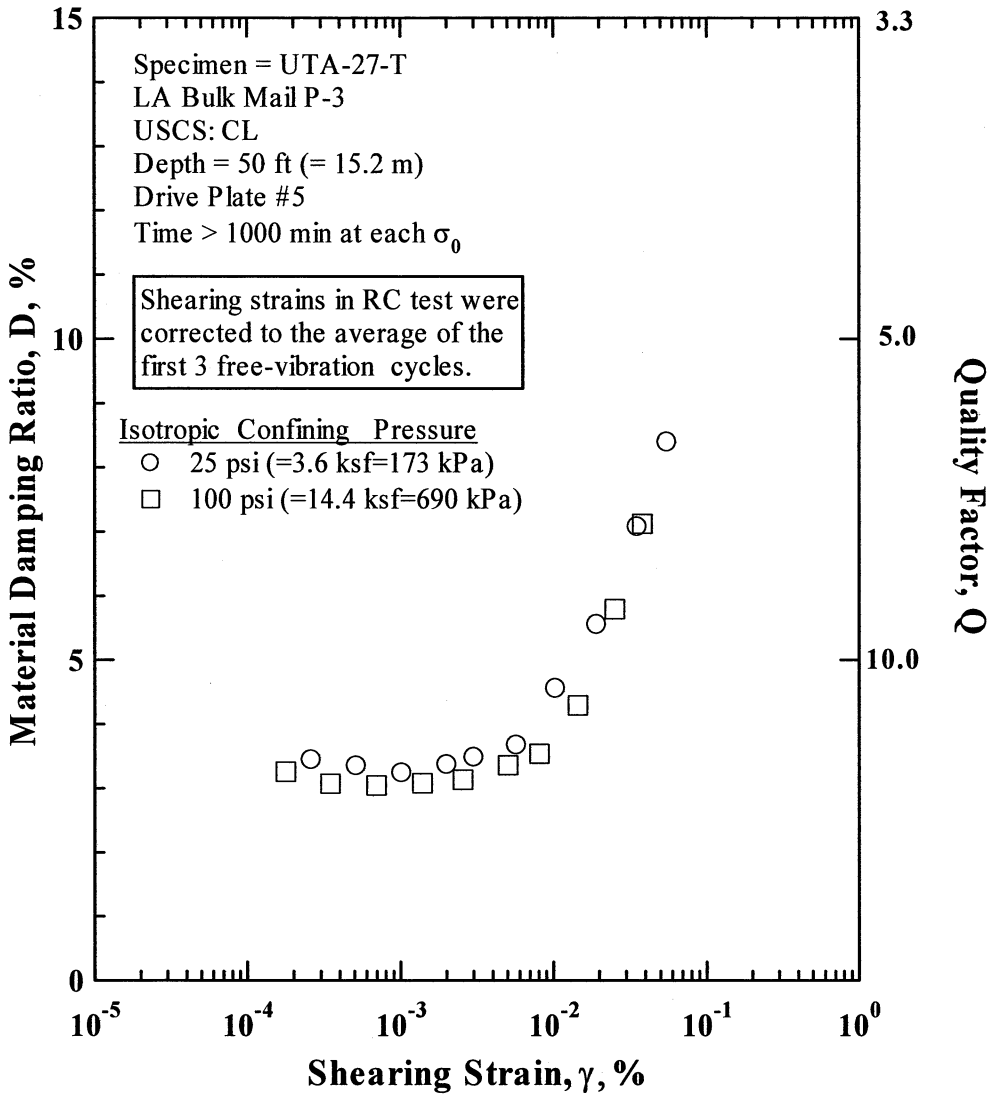

Figure L.10 Comparison of the Variation in Material Damping Ratio with Shearing Strain and Isotropic Confining Pressure from the Resonant Column Tests of Specimen UTA-27-T.

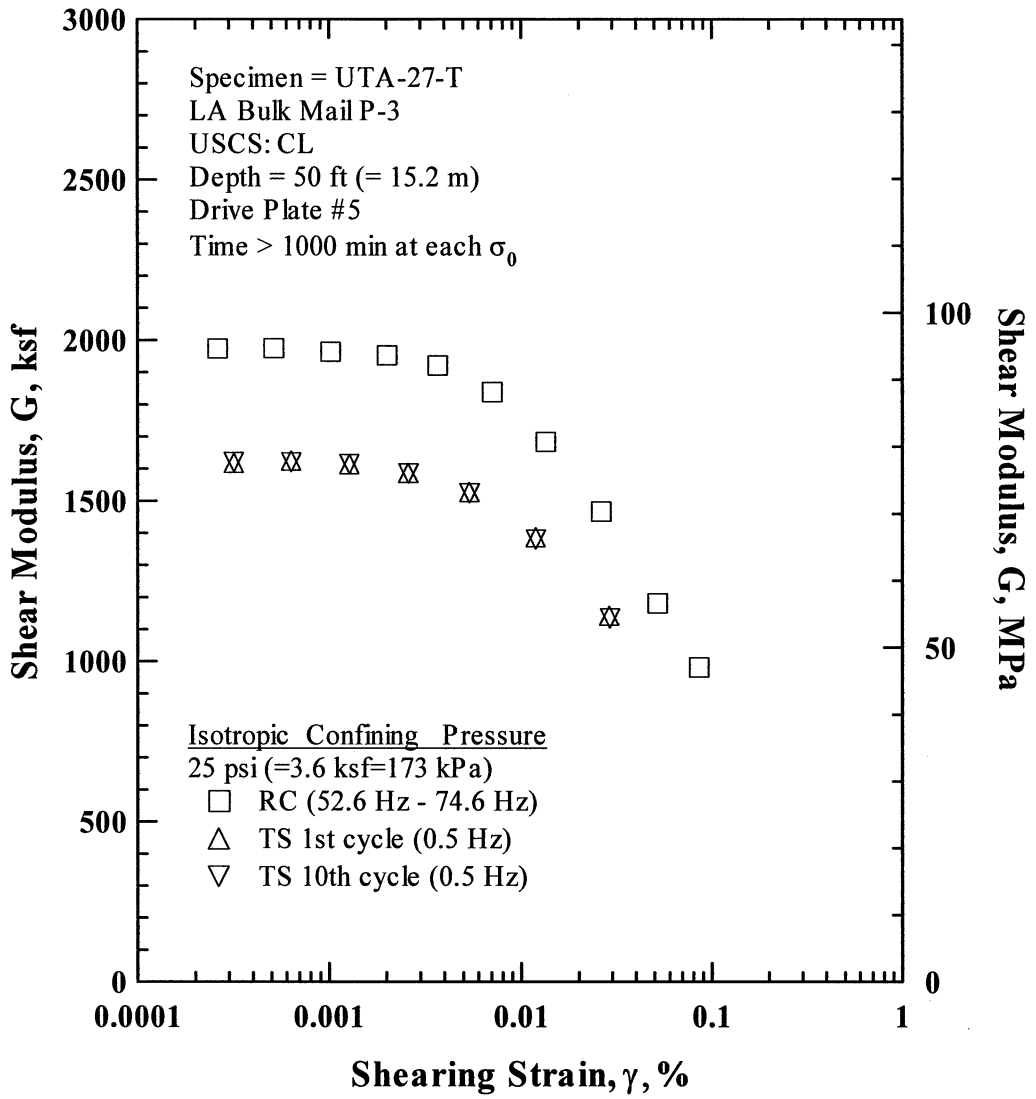

Figure L.11 Comparison of the Variation in Shear Modulus with Shearing Strain at an Isotropic Confining Pressure of 25 psi (=3.6 ksf=173 kPa) from the Combined RCTS Tests of Specimen UTA-27-T.

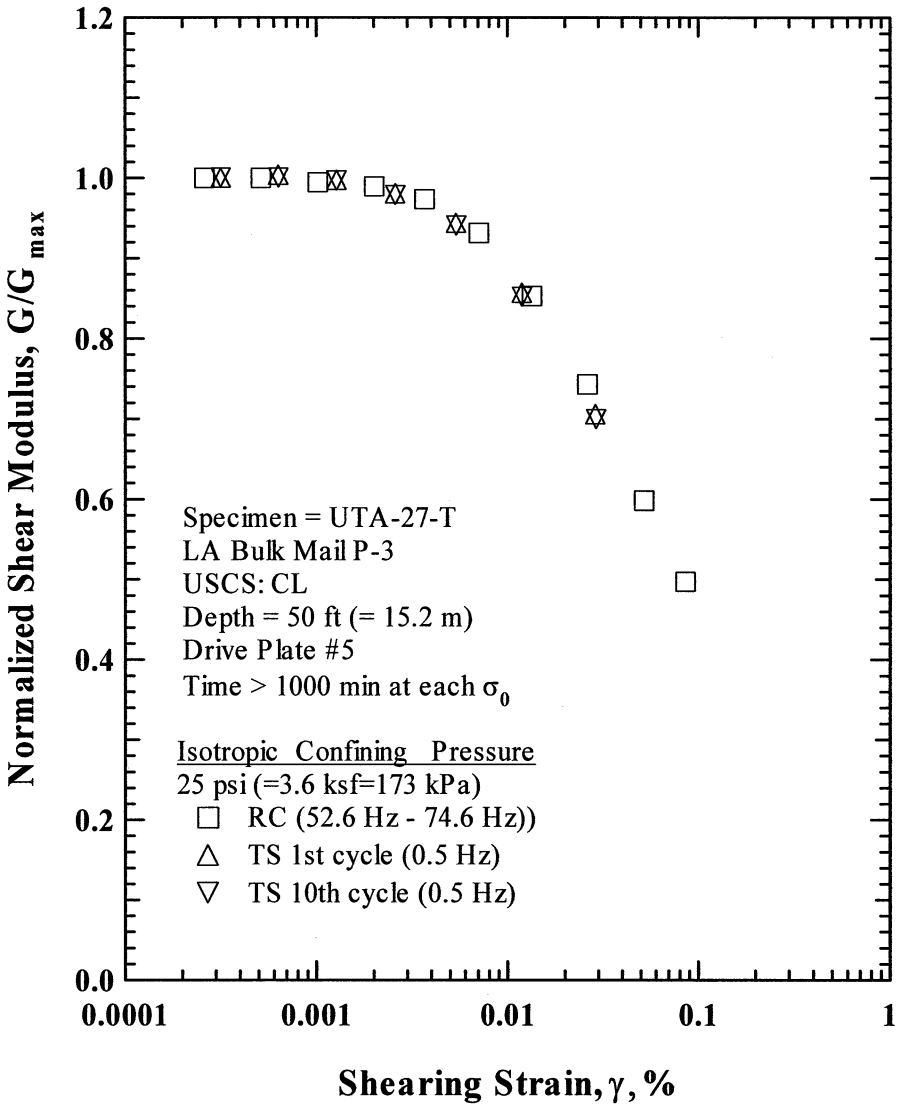

Figure L.12 Comparison of the Variation in Normalized Shear Modulus with Shearing Strain at an Isotropic Confining Pressure of 25 psi (=3.6 ksf=173 kPa) from the Combined RCTS Tests of Specimen UTA-27-T.

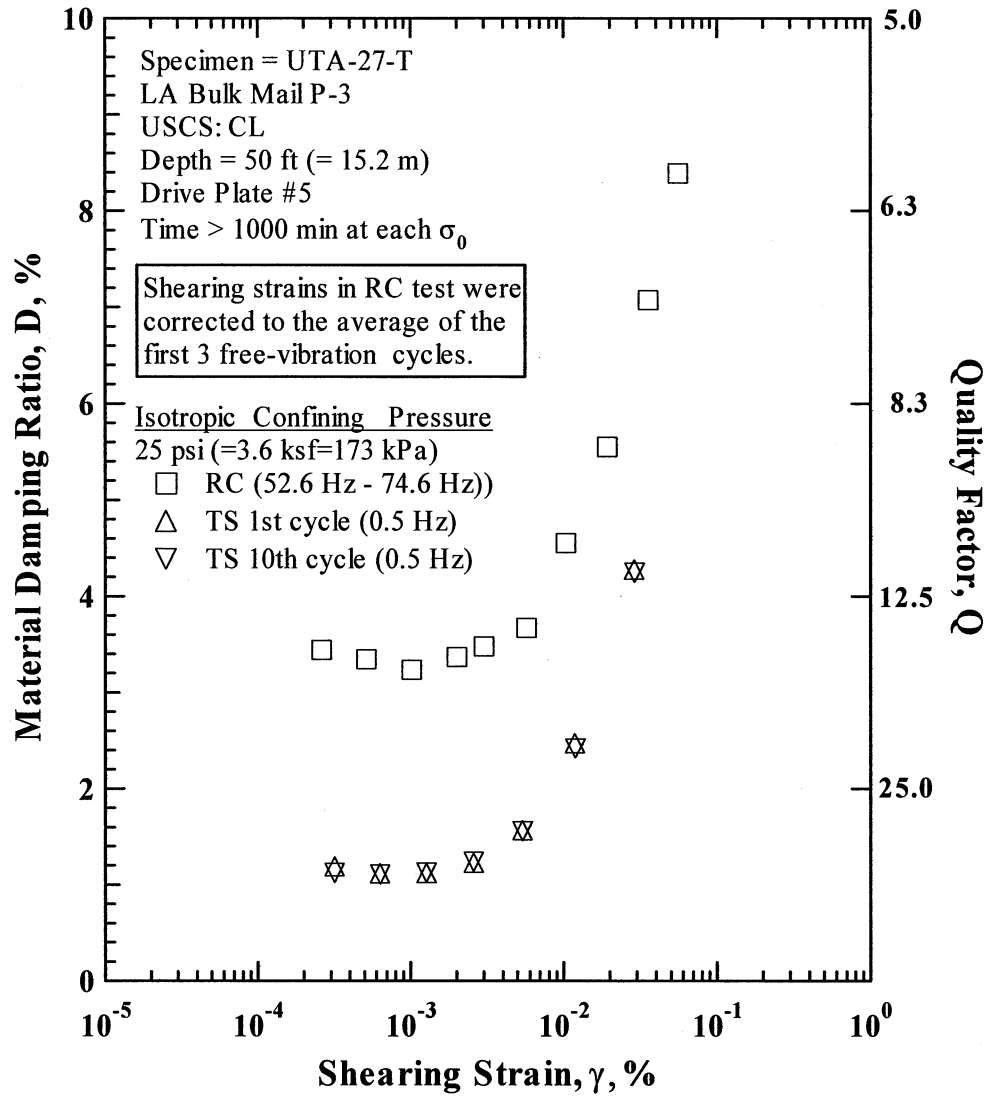

Figure L.13 Comparison of the Variation in Material Damping Ratio with Shearing Strain at an Isotropic Confining Pressure of 25 psi (=3.6 ksf=173 kPa) from the Combined RCTS Tests of Specimen UTA-27-T.

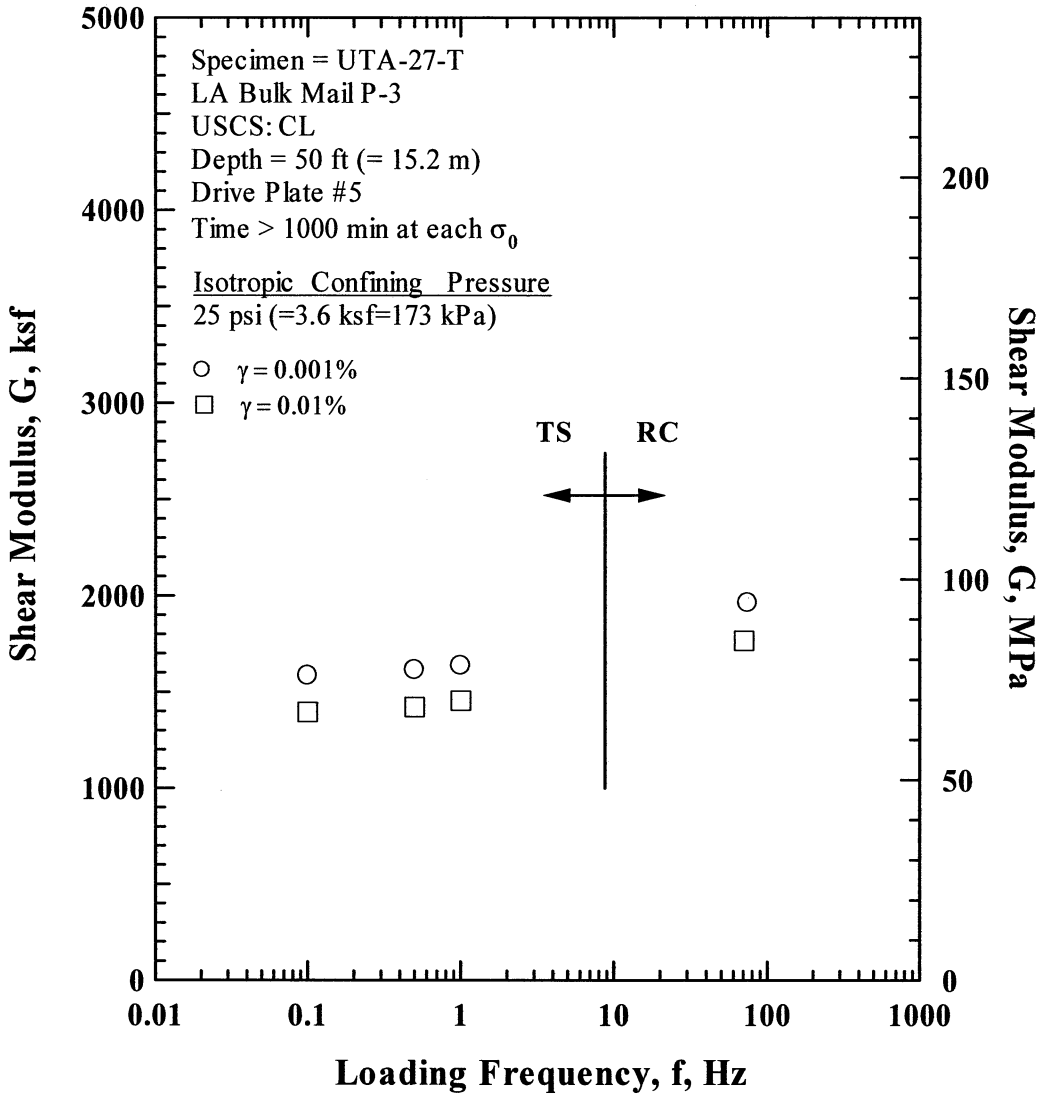

Figure L.14 Comparison of the Variation in Shear Modulus with Loading Frequency at an Isotropic Confining Pressure of 25 psi (=3.6 ksf=173 kPa) from the Combined RCTS Tests of Specimen UTA-27-T.

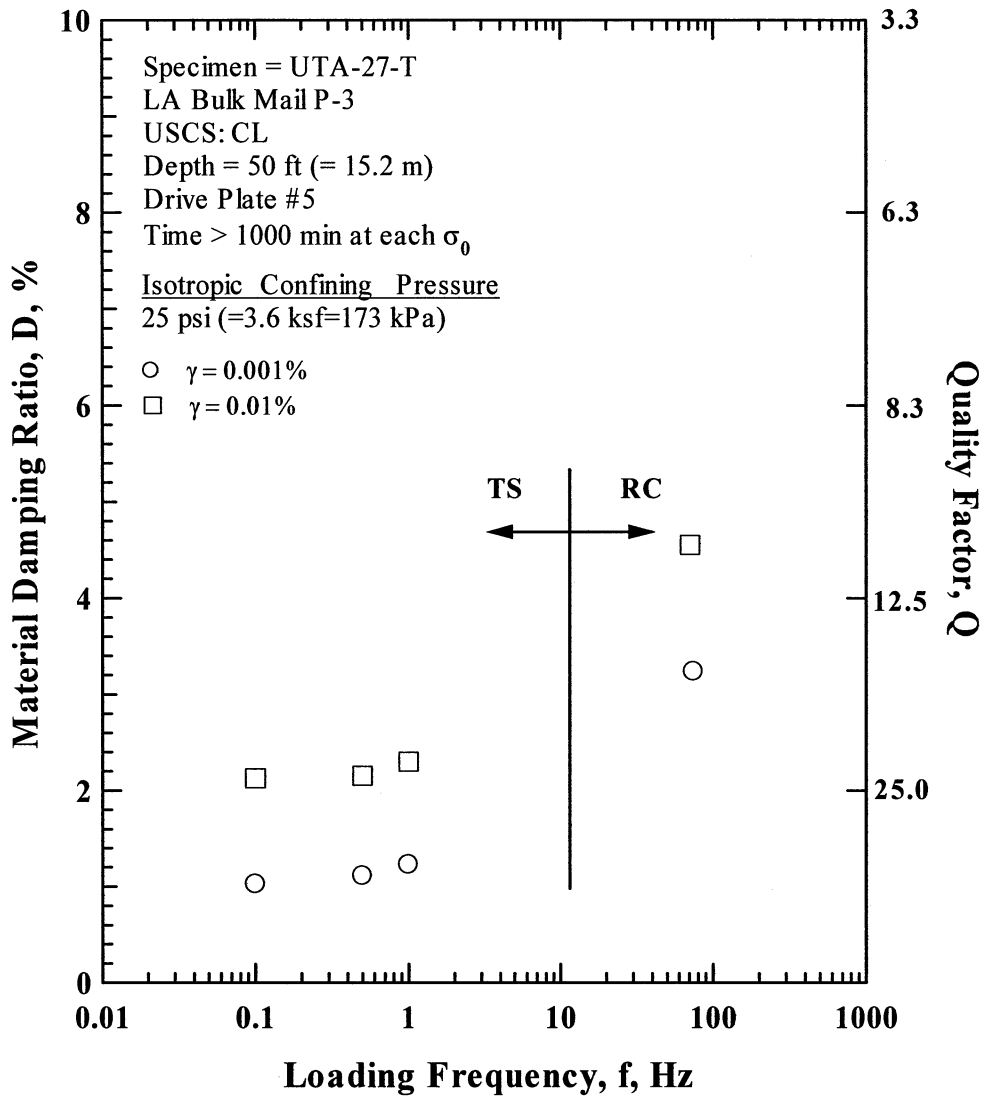

Figure L.15 Comparison of the Variation in Material Damping Ratio with Loading Frequency at an Isotropic Confining Pressure 25 psi (=3.6 ksf=173 kPa) from the Combined RCTS Tests of Specimen UTA-27-T.

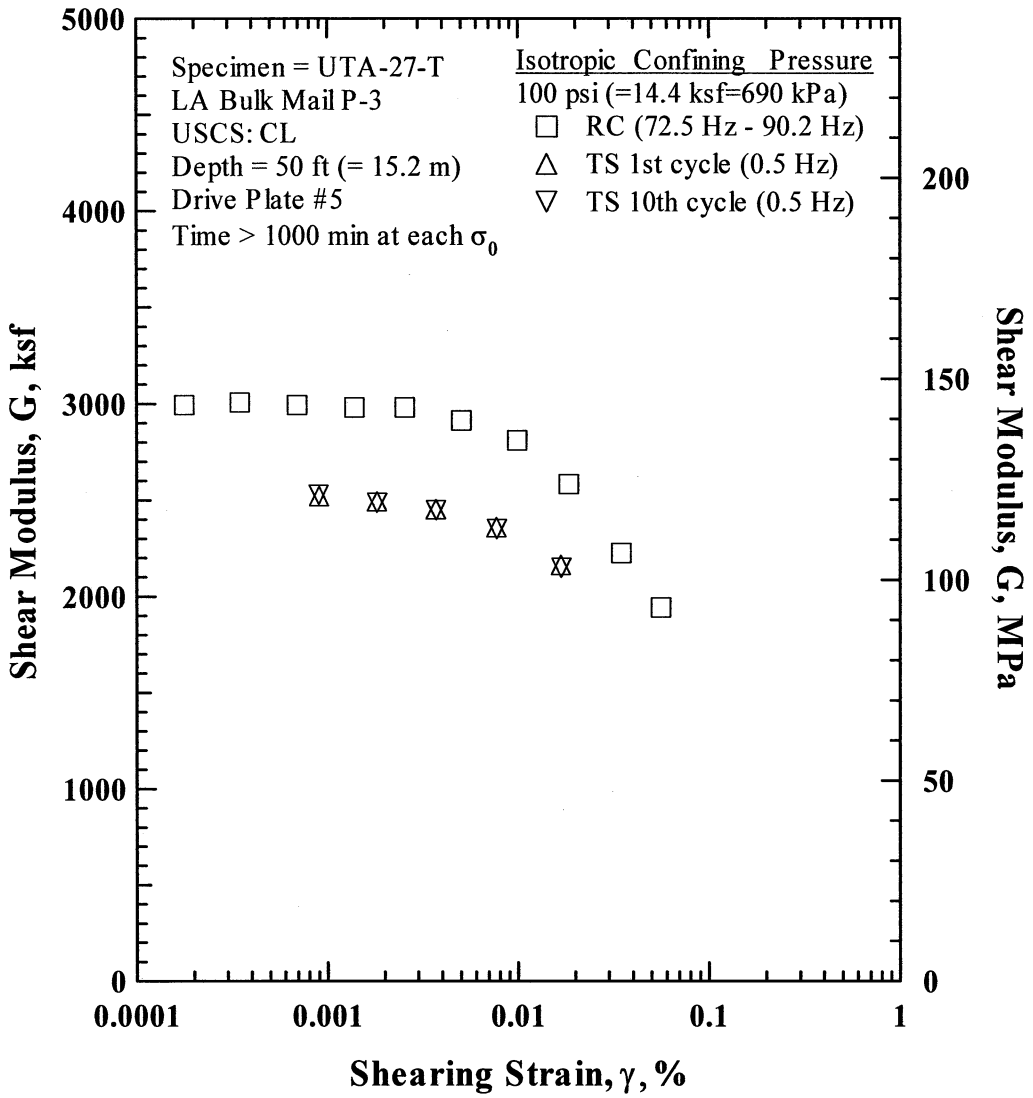

Figure L.16 Comparison of the Variation in Shear Modulus with Shearing Strain at an Isotropic Confining Pressure of 100 psi (=14.4 ksf=690 kPa) from the Combined RCTS Tests of Specimen UTA-27-T.

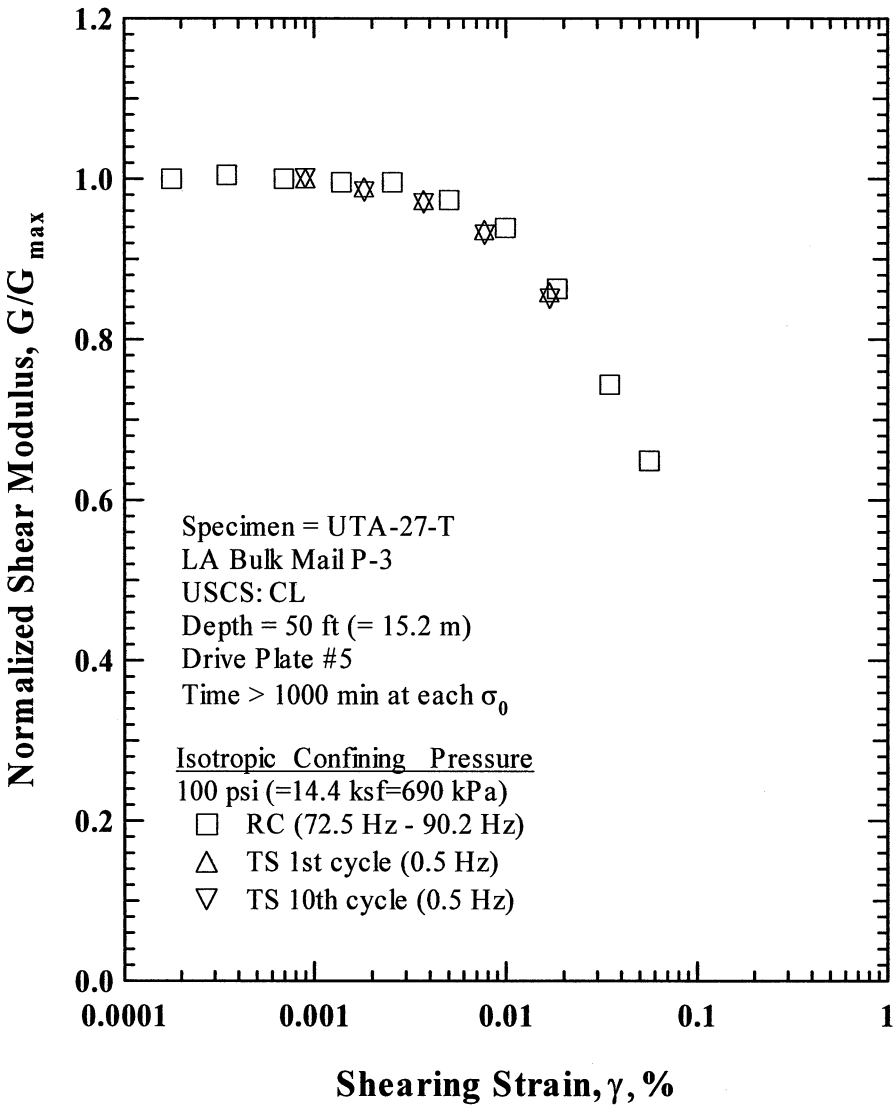

Figure L.17 Comparison of the Variation in Normalized Shear Modulus with Shearing Strain at an Isotropic Confining Pressure of 100 psi (=14.4 ksf=690 kPa) from the Combined RCTS Tests of Specimen UTA-27-T.

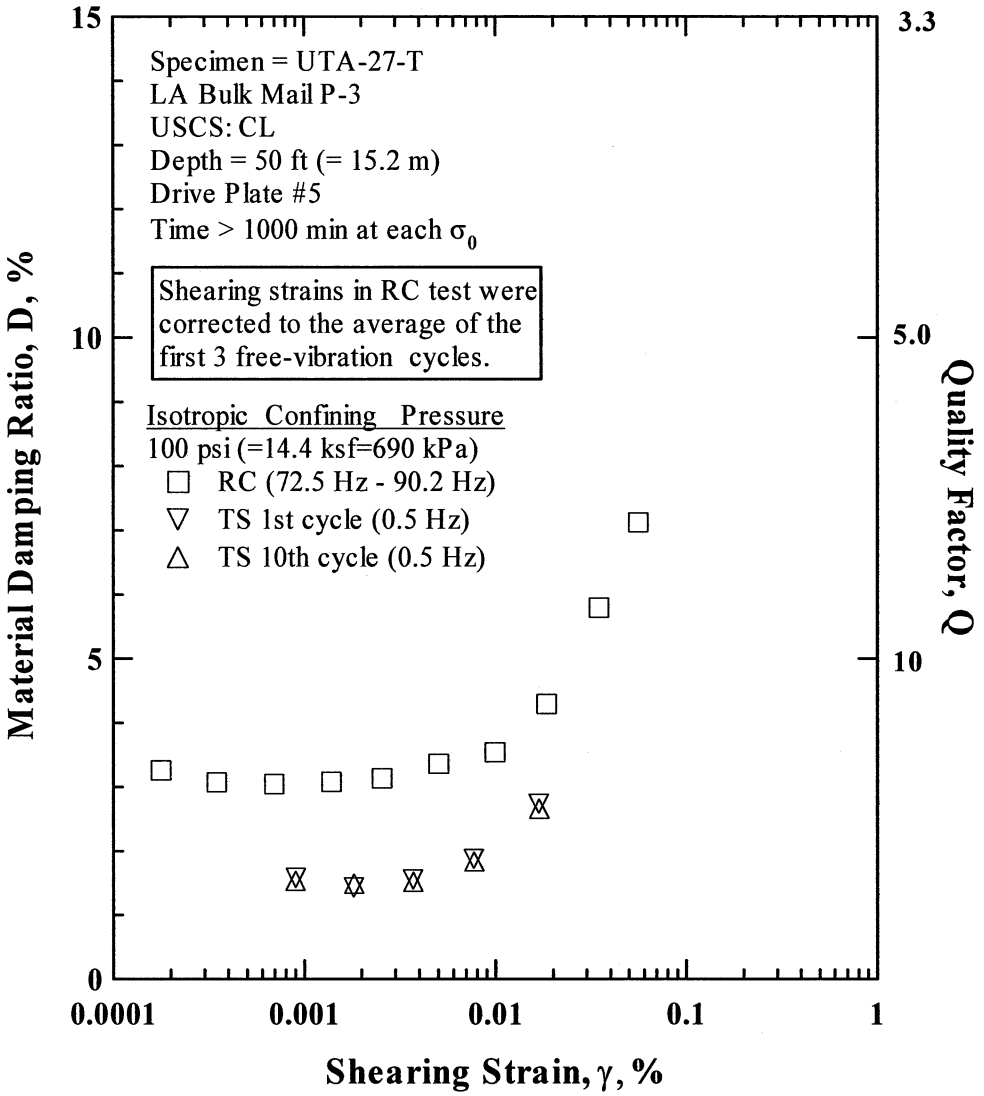

Figure L.18 Comparison of the Variation in Material Damping Ratio with Shearing Strain at an Isotropic Confining Pressure of 100 psi (=14.4 ksf=690 kPa) from the Combined RCTS Tests of Specimen UTA-27-T.

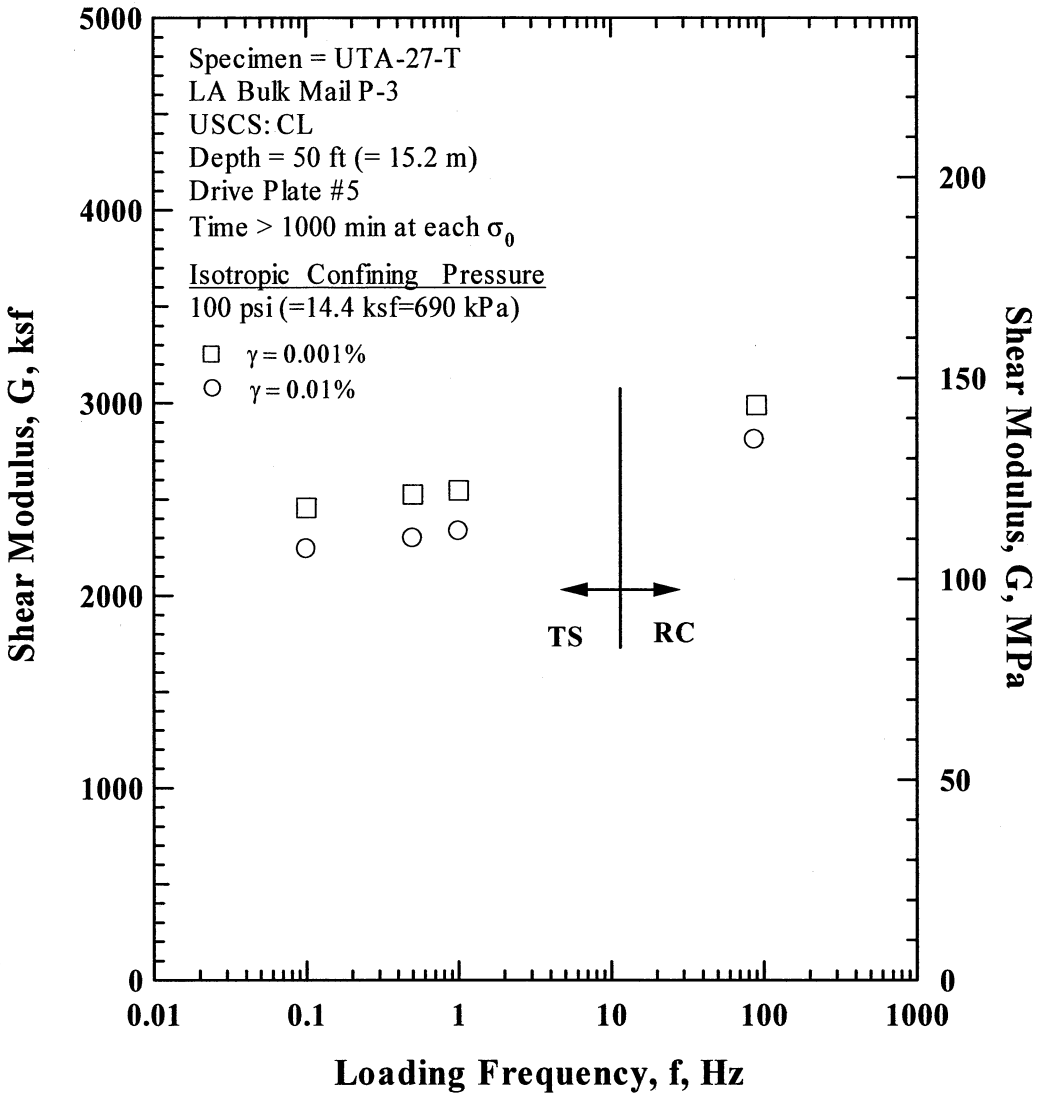

Figure L.19 Comparison of the Variation in Shear Modulus with Loading Frequency at an Isotropic Confining Pressure of 100 psi (=14.4 ksf=690 kPa) from the Combined RCTS Tests of Specimen UTA-27-T.

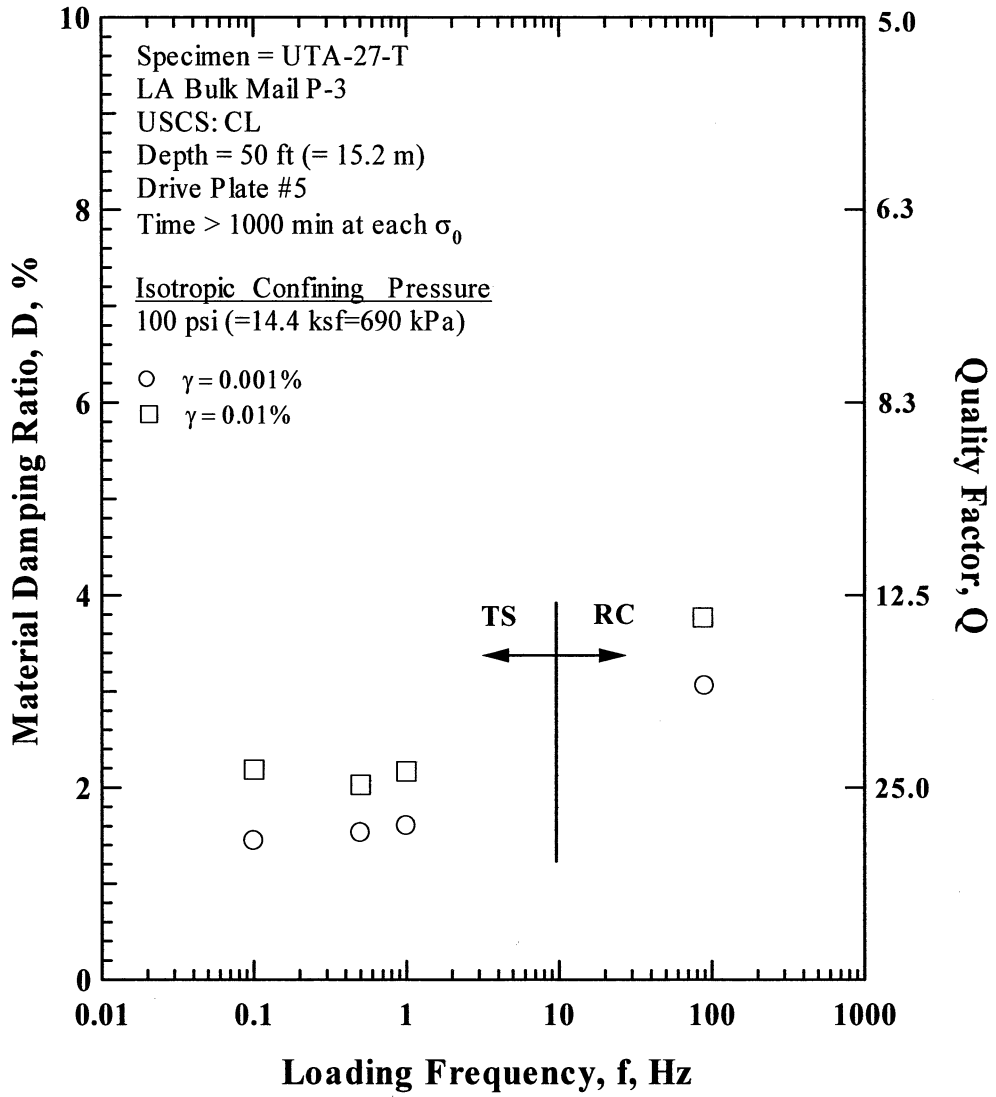

Figure L.20 Comparison of the Variation in Material Damping Ratio with Loading Frequency at an Isotropic Confining Pressure 100 psi (=14.4 ksf=690 kPa) from the Combined RCTS Tests of Specimen UTA-27-T.

Table L.1 Variation in Low-Amplitude Shear Wave Velocity, Low-Amplitude Shear Modulus, Low-Amplitude Material Damping Ratio and Estimated Void Ratio with Isotropic Confining Pressure from RC Tests of Specimen UTA-27-T.

Effective Isotropic Confining Pressure, σ_o'			Low-Amplitude Shear Modulus, G_{max}		Low-Amplitude Shear Wave Velocity, Vs	Low-Amplitude Material Damping Ratio, Dmin	Estimated Void Ratio, e
(psi)	(psf)	(kPa)	(ksf)	(MPa)	(fps)	(%)	H
8	1152	55	1655	79.3	641	3.47	0.641
12	1728	83	1729	82.9	655	3.39	0.639
25	3600	173	1906	91.4	686	3.33	0.627
50	7200	345	2336	112.0	756	3.43	0.592
100	14400	690	2848	136.5	831	3.31	0.568

Table L.2 Variation in Shear Modulus, Normalized Shear Modulus and Material Damping Ratio with Shearing Strain from RC Tests of Specimen UTA-27-T; Confining Pressure, σ_o' =25 psi (=3.6 ksf=173 kPa).

Peak Shearing Strain, %	Shear Modulus, G, ksf	Normalized Shear Modulus, G/G_{max}	Average[+] Shearing Strain, %	Material Damping Ratio[x], D, %
2.61E-04	1974	1.00	2.61E-04	3.44
5.13E-04	1974	1.00	5.13E-04	3.35
1.02E-03	1963	0.99	1.02E-03	3.24
2.01E-03	1952	0.99	2.01E-03	3.37
3.68E-03	1921	0.97	3.01E-03	3.48
7.08E-03	1838	0.93	5.72E-03	3.67
1.34E-02	1683	0.85	1.03E-02	4.55
2.62E-02	1466	0.74	1.92E-02	5.55
5.19E-02	1181	0.60	3.55E-02	7.07
8.57E-02	981	0.50	5.53E-02	8.39

[+] Average Shearing Strain from the First Three Cycles of the Free Vibration Decay Curve

[x] Average Damping Ratio from the First Three Cycles of the Free Vibration Decay Curve

Table L.3 Variation in Shear Modulus, Normalized Shear Modulus and Material Damping Ratio with Shearing Strain from TS Tests of Specimen UTA-27-T; Confining Pressure, σ_o' = 25 psi (=3.6 ksf=173 kPa).

First Cycle				Tenth Cycle			
Peak Shearing Strain, %	Shear Modulus, G, ksf	Normalized Shear Modulus, G/G_{max}	Material Damping Ratio, D, %	Peak Shearing Strain, %	Shear Modulus, G, ksf	Normalized Shear Modulus, G/G_{max}	Material Damping Ratio, D, %
3.20E-04	1617	1.00	1.18	3.19E-04	1619	1.00	1.12
6.37E-04	1623	1.00	1.11	6.39E-04	1618	1.00	1.10
1.28E-03	1612	1.00	1.12	1.28E-03	1613	1.00	1.12
2.60E-03	1586	0.98	1.22	2.61E-03	1583	0.98	1.23
5.41E-03	1526	0.94	1.56	5.43E-03	1522	0.94	1.55
1.19E-02	1385	0.86	2.47	1.20E-02	1378	0.85	2.41
2.90E-02	1141	0.71	4.27	2.92E-02	1132	0.70	4.24

Table L.4 Variation in Shear Modulus, Normalized Shear Modulus and Material Damping Ratio with Shearing Strain from RC Tests of Specimen UTA-27-T; Confining Pressure, σ_o' = 100 psi (=14.4 ksf=690 kPa).

Peak Shearing Strain, %	Shear Modulus, G, ksf	Normalized Shear Modulus, G/G_{max}	Average[+] Shearing Strain, %	Material Damping Ratio[x], D, %
1.78E-04	2993	1.00	1.78E-04	3.26
3.48E-04	3007	1.00	3.48E-04	3.07
6.93E-04	2993	1.00	6.93E-04	3.04
1.38E-03	2980	1.00	1.38E-03	3.08
2.55E-03	2980	1.00	2.55E-03	3.13
5.03E-03	2913	0.97	5.03E-03	3.36
9.92E-03	2810	0.94	8.07E-03	3.54
1.85E-02	2583	0.86	1.44E-02	4.29
3.47E-02	2225	0.74	2.52E-02	5.79
5.60E-02	1942	0.65	3.82E-02	7.12

[+] Average Shearing Strain from the First Three Cycles of the Free Vibration Decay Curve

[x] Average Damping Ratio from the First Three Cycles of the Free Vibration Decay Curve

Table L.5 Variation in Shear Modulus, Normalized Shear Modulus and Material Damping Ratio with Shearing Strain from TS Tests of Specimen UTA-27-T; Confining Pressure, σ_o' = 100 psi (=14.4 ksf=690 kPa).

First Cycle				Tenth Cycle			
Peak Shearing Strain, %	Shear Modulus, G, ksf	Normalized Shear Modulus, G/G_{max}	Material Damping Ratio, D, %	Peak Shearing Strain, %	Shear Modulus, G, ksf	Normalized Shear Modulus, G/G_{max}	Material Damping Ratio, D, %
9.06E-04	2519	1.00	1.57	9.04E-04	2525	1.00	1.53
1.83E-03	2490	0.99	1.42	1.83E-03	2483	0.98	1.48
3.72E-03	2451	0.97	1.55	3.73E-03	2446	0.97	1.51
7.73E-03	2357	0.94	1.87	7.77E-03	2347	0.93	1.83
1.69E-02	2161	0.86	2.73	1.70E-02	2146	0.85	2.65

APPENDIX M

Specimen No. 12
UT Specimen ID: UTA-27-I

LA Bulk Mail P-5
Depth = 167.5 ft (= 51.1m)
Soil Type: Clay (CL)

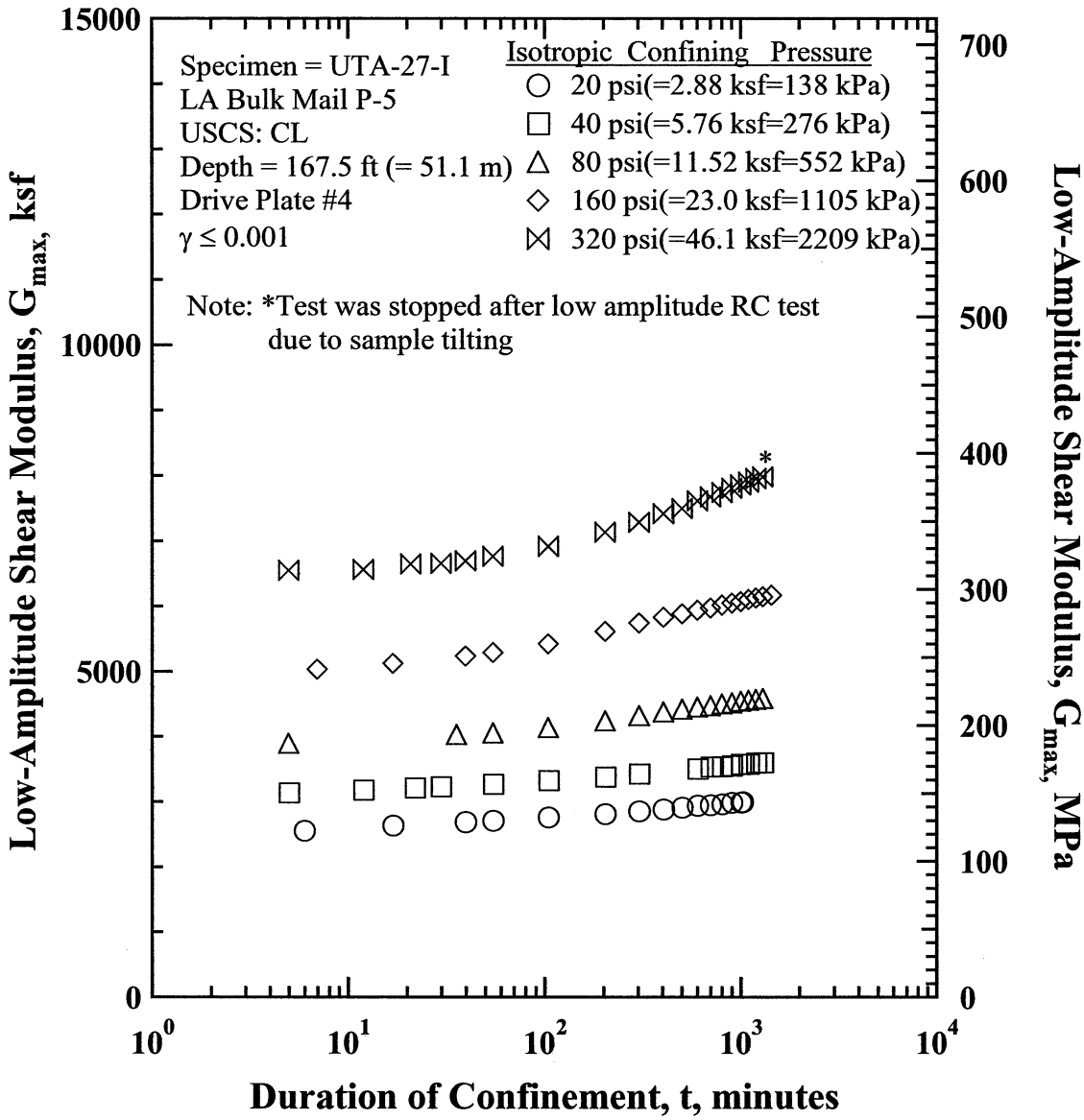

Figure M.1 Variation in Low-Amplitude Shear Modulus with Magnitude and Duration of Isotropic Confining Pressure from Resonant Column Tests of Specimen UTA-27-I.

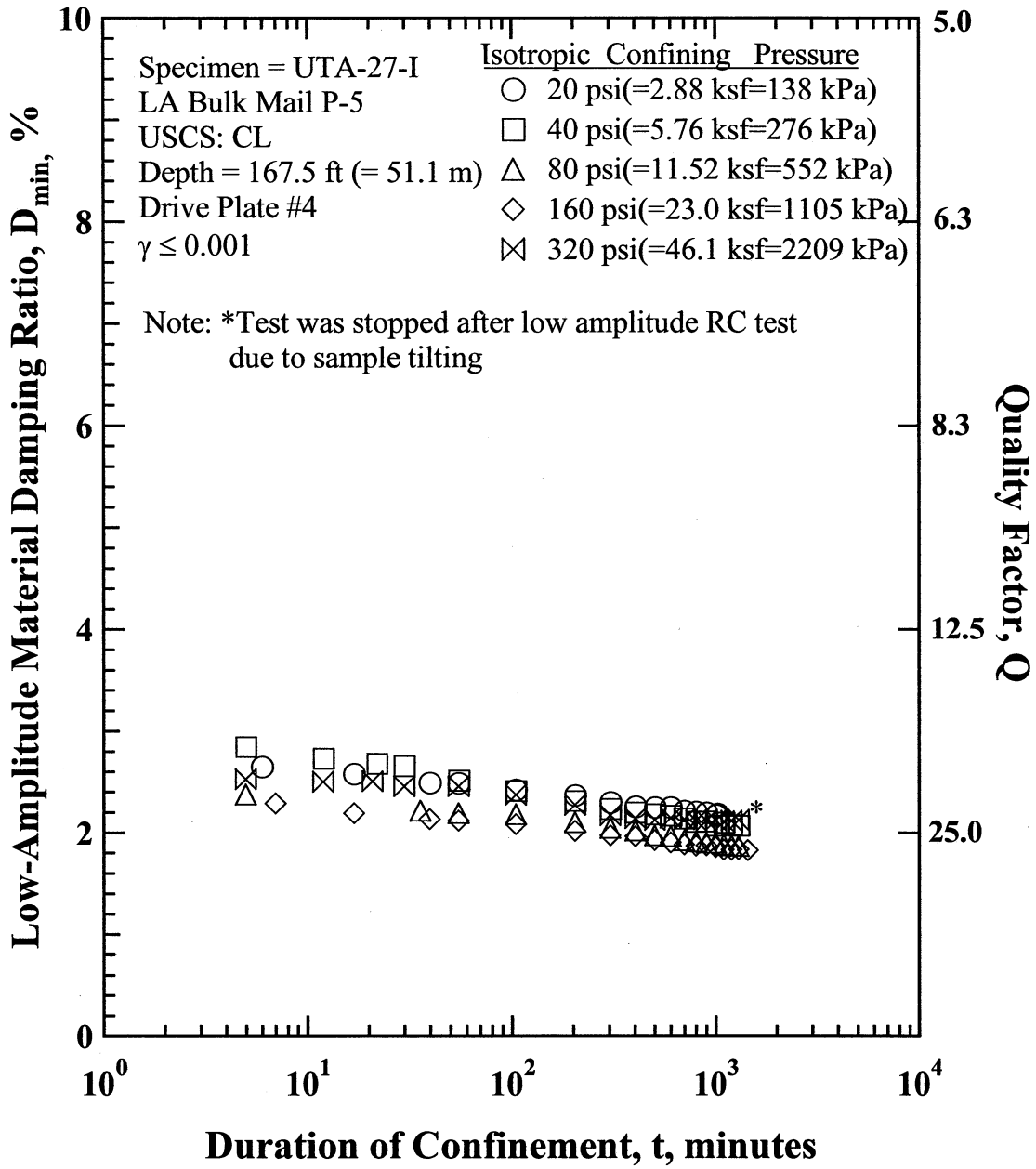

Figure M.2 Variation in Low-Amplitude Material Damping Ratio with Magnitude and Duration of Isotropic Confining Pressure from Resonant Column Tests of Specimen UTA-27-I

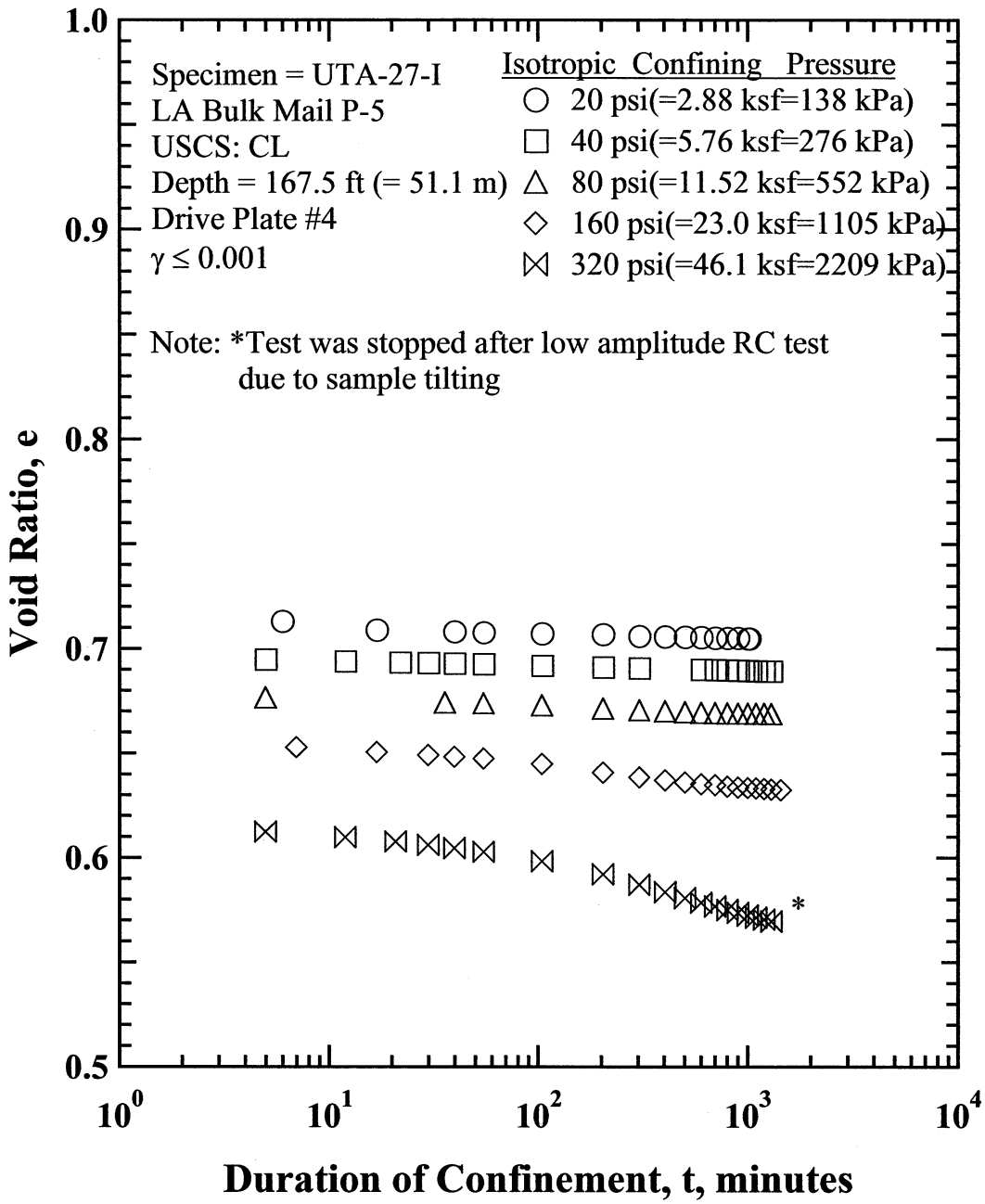

Figure M.3 Variation in Estimated Void Ratio with Magnitude and Duration of Isotropic Confining Pressure from Resonant Column Tests of Specimen UTA-27-I.

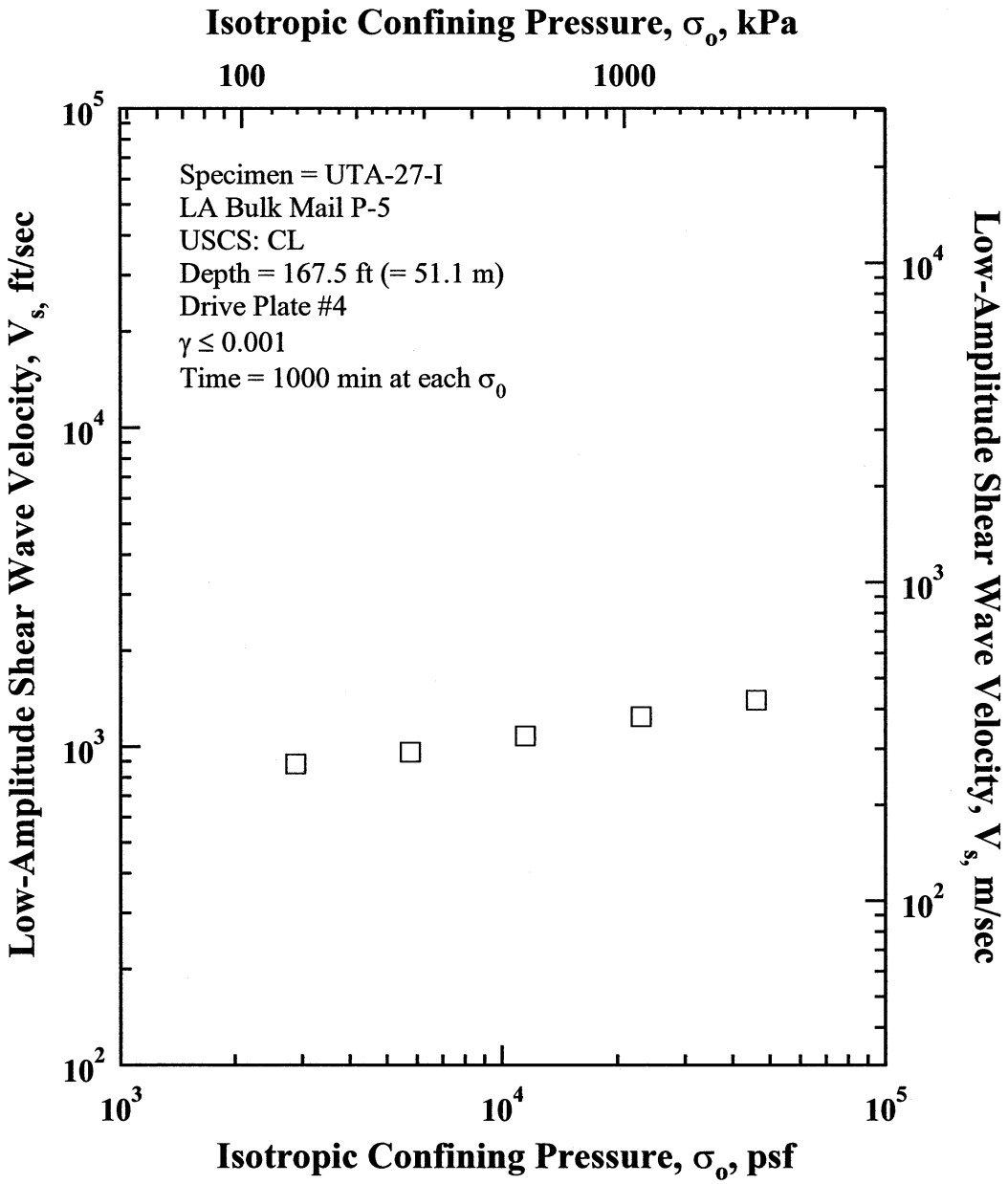

Figure M.4 Variation in Low-Amplitude Shear Wave Velocity with Isotropic Confining Pressure from Resonant Column Tests of Specimen UTA-27-I.

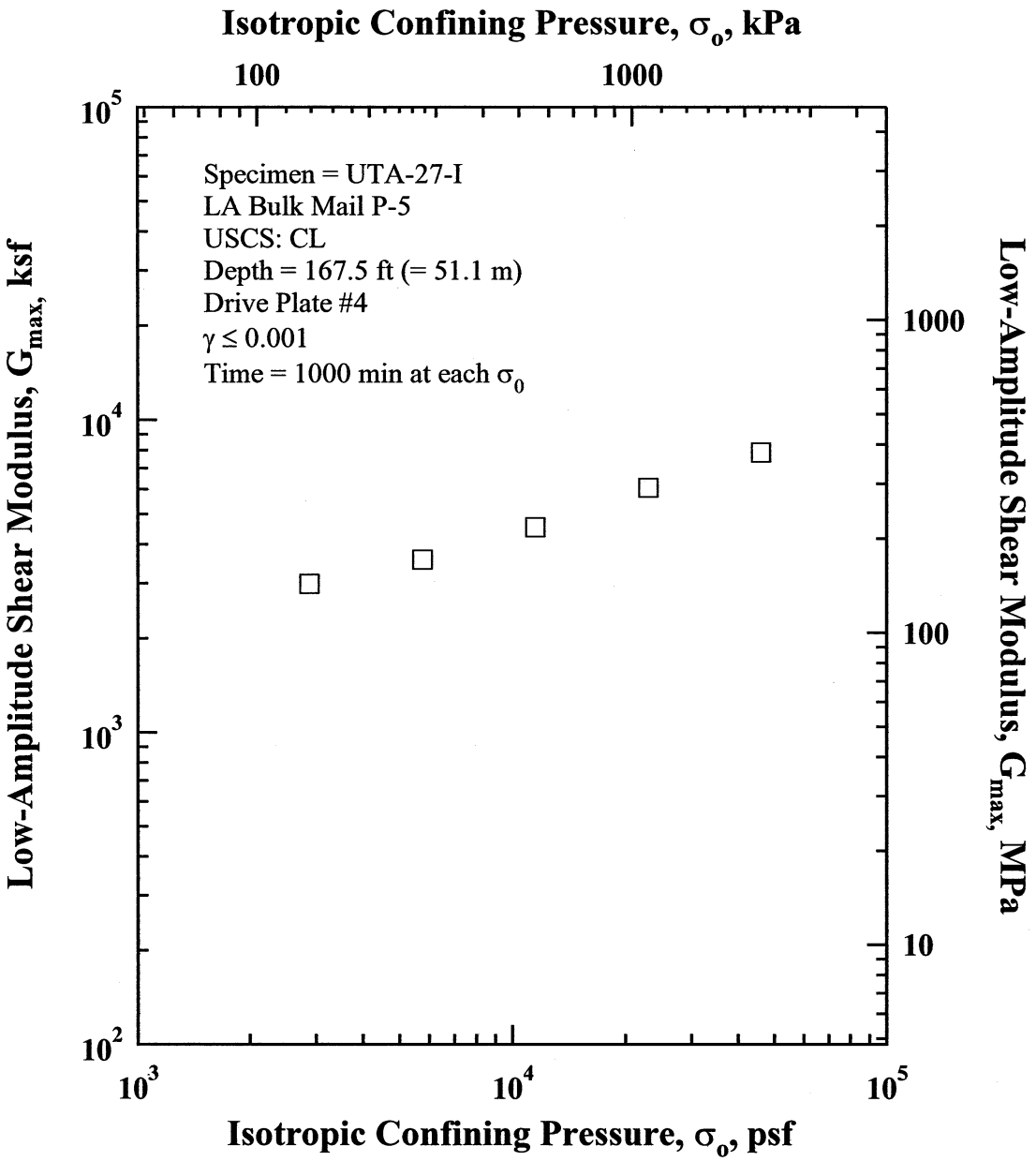

Figure M.5 Variation in Low-Amplitude Shear Modulus with Isotropic Confining Pressure from Resonant Column Tests of Specimen UTA-27-I.

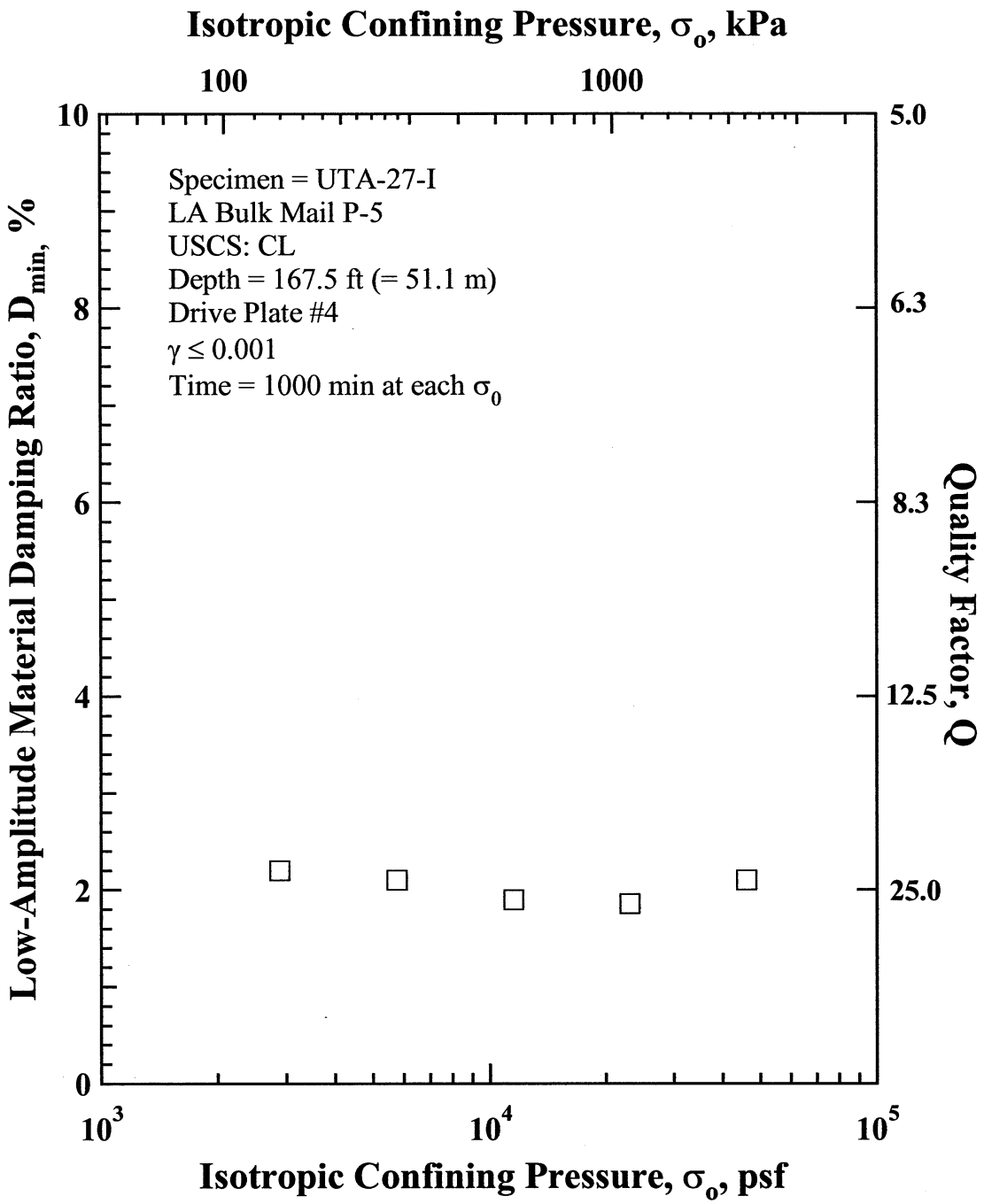

Figure M.6 Variation in Low-Amplitude Material Damping Ratio with Isotropic Confining Pressure from Resonant Column Tests of Specimen UTA-27-I.

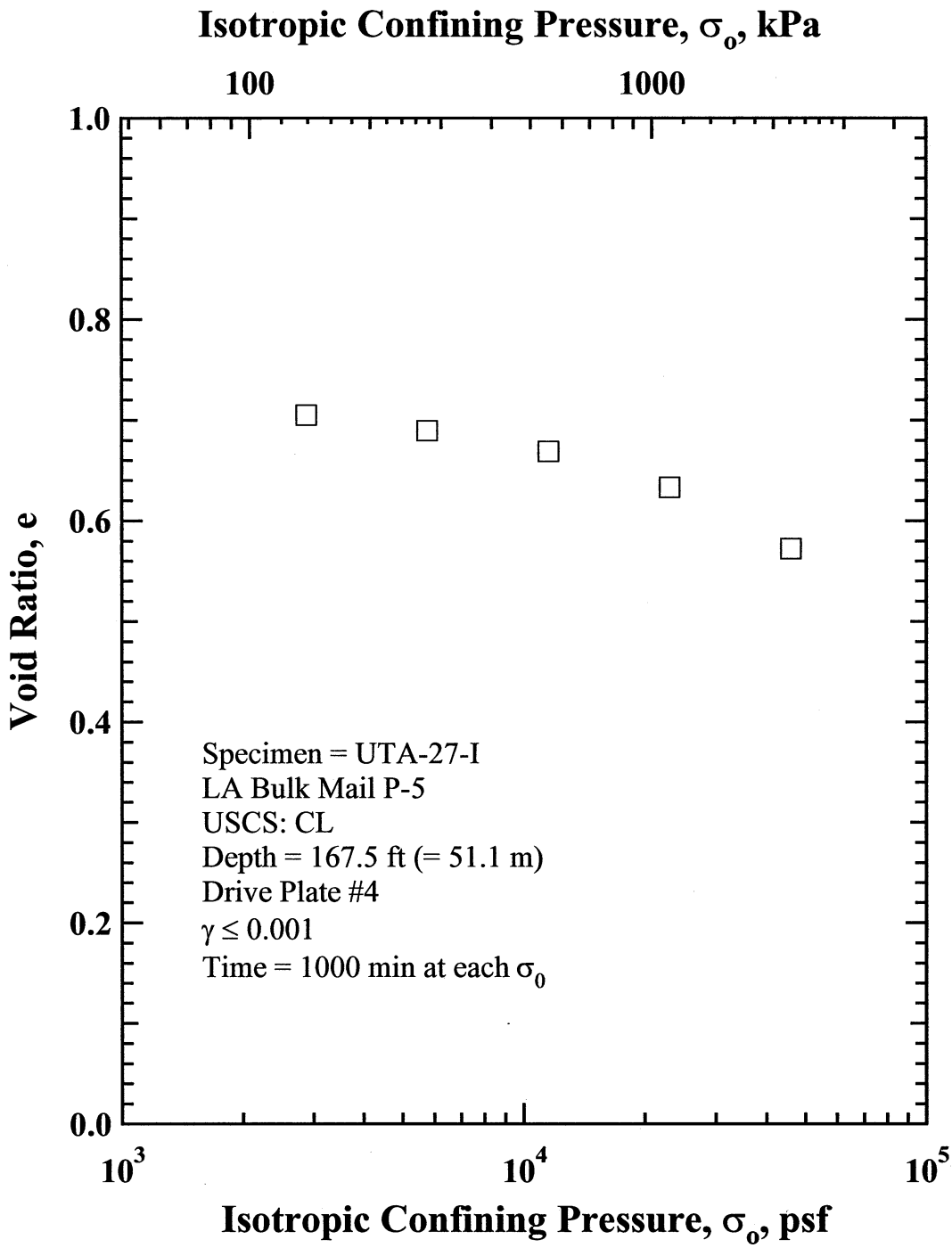

Figure M.7 Variation in Estimated Void Ratio with Isotropic Confining Pressure from Resonant Column Tests of Specimen UTA-27-I.

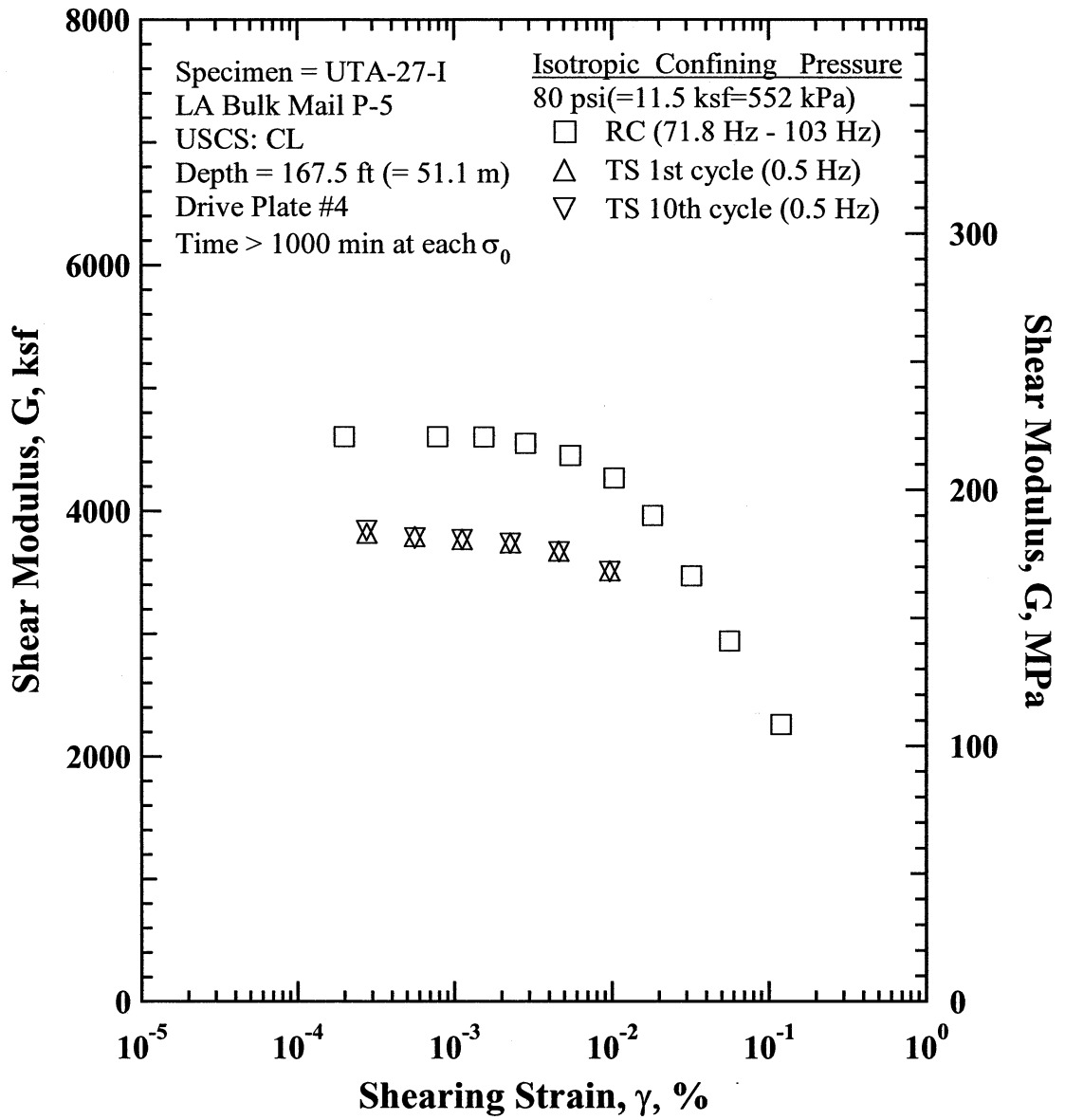

Figure M.8 Comparison of the Variation in Shear Modulus with Shearing Strain at an Isotropic Confining Pressure of 80 psi (=11.5 ksf=552 kPa) from the Combined RCTS Tests of Specimen UTA-27-I.

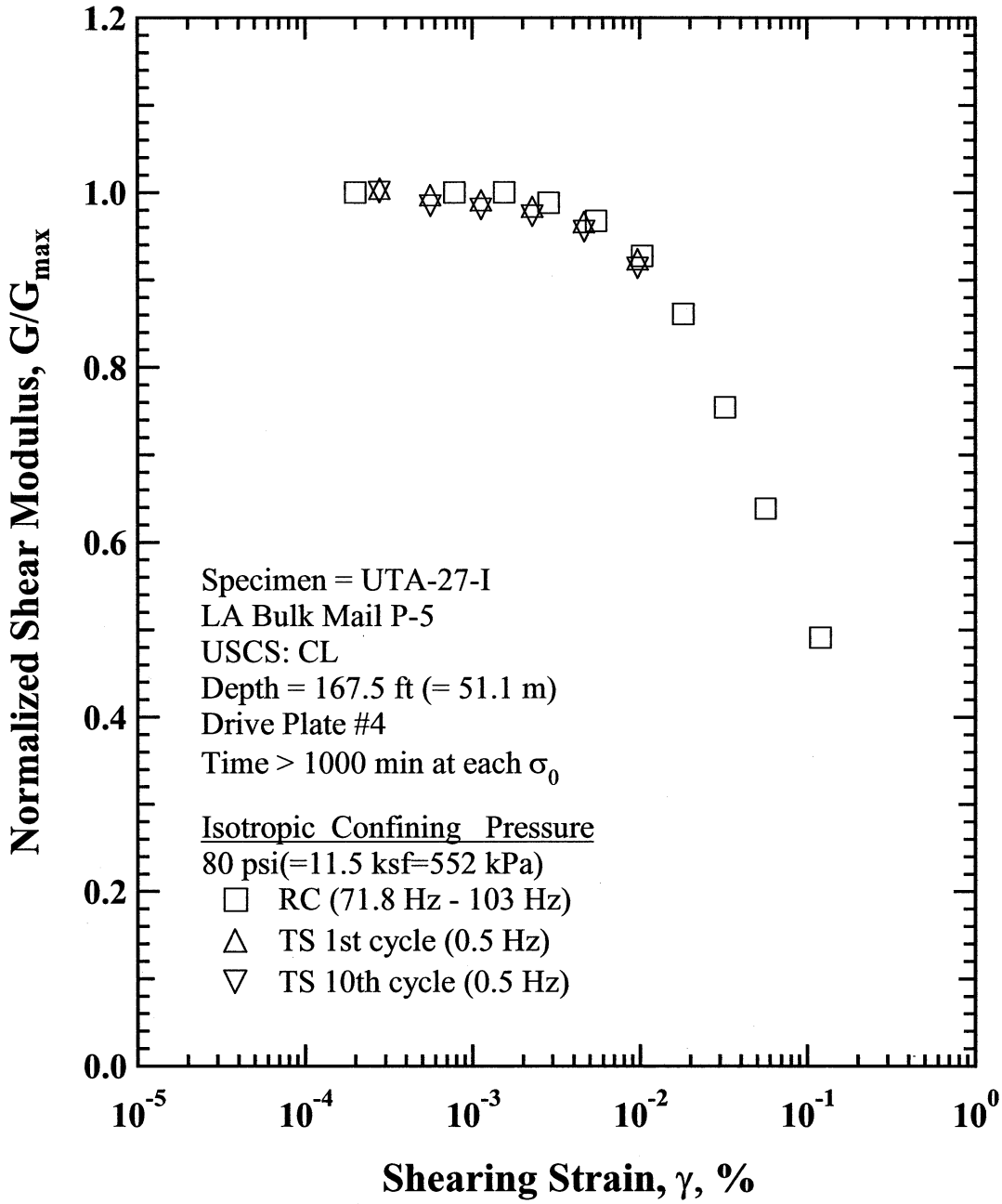

Figure M.9 Comparison of the Variation in Normalized Shear Modulus with Shearing Strain at an Isotropic Confining Pressure of 80 psi (=11.5 ksf=552 kPa) from the Combined RCTS Tests of Specimen UTA-27-I.

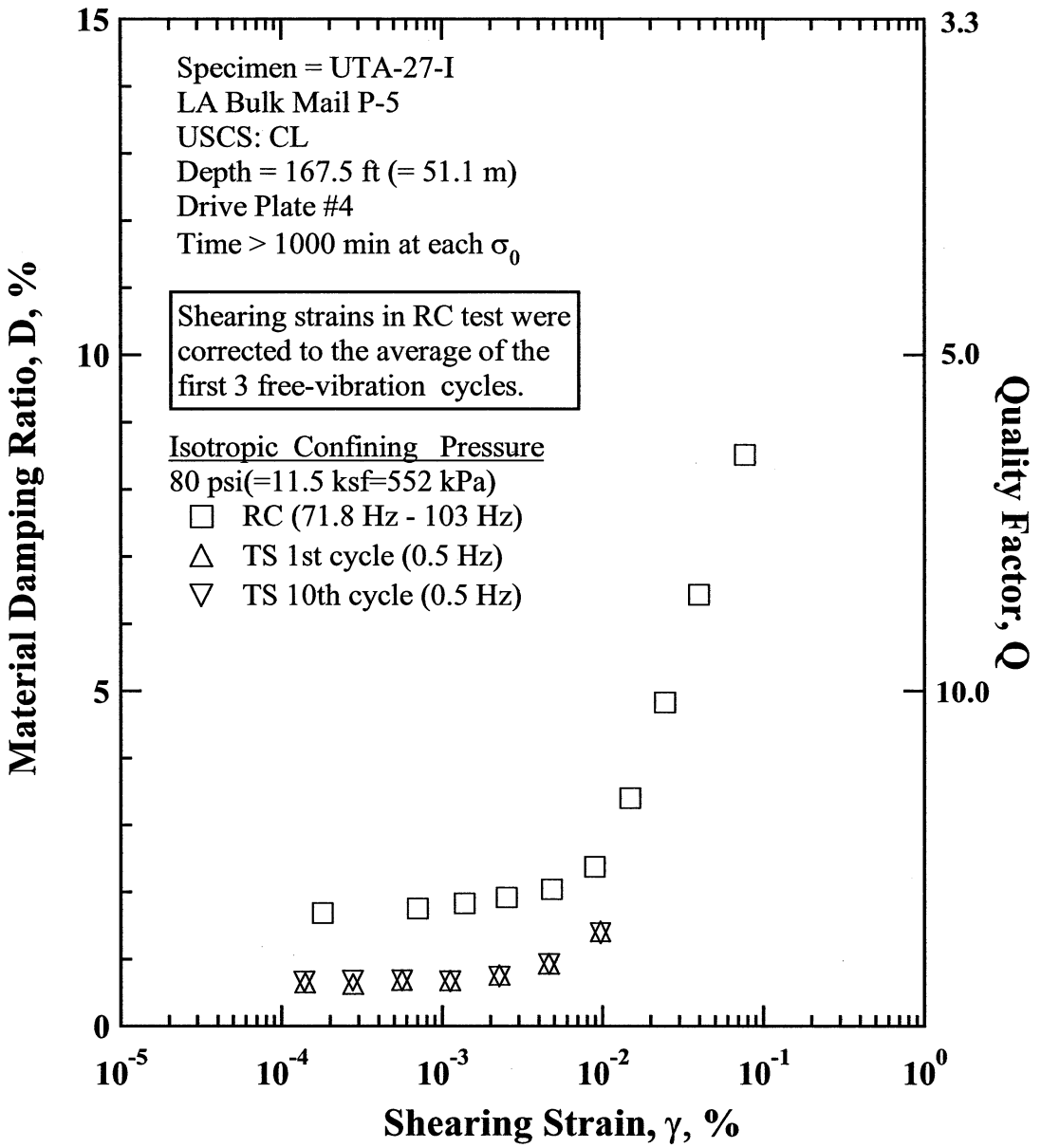

Figure M.10 Comparison of the Variation in Material Damping Ratio with Shearing Strain at an Isotropic Confining Pressure of 80 psi (=11.5 ksf=552 kPa) from the Combined RCTS Tests of Specimen UTA-27-I.

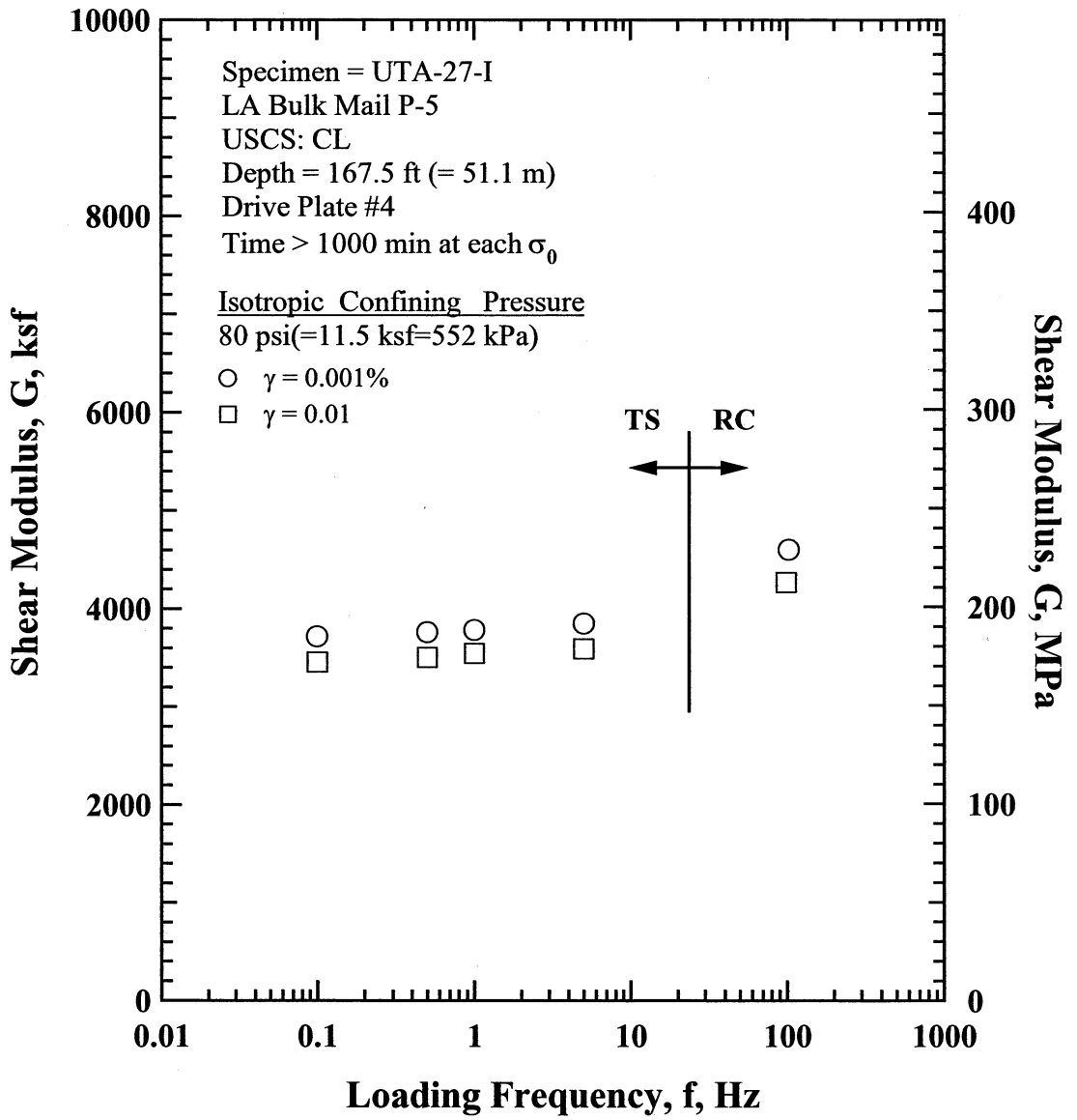

Figure M.11 Comparison of the Variation in Shear Modulus with Loading Frequency at an Isotropic Confining Pressure of 80 psi (=11.5 ksf=552 kPa) from the Combined RCTS Tests of Specimen UTA-27-I.

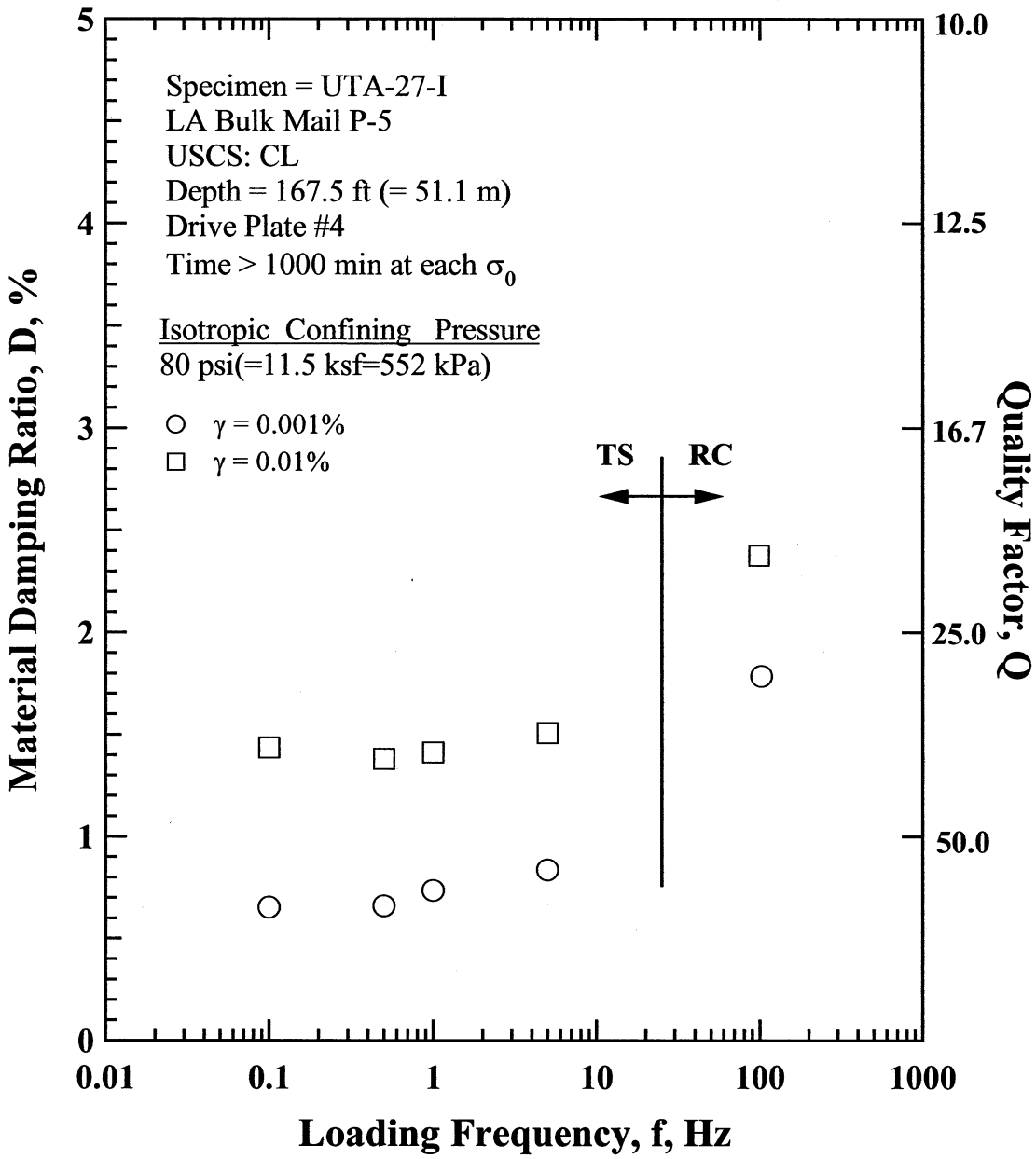

Figure M.12 Comparison of the Variation in Material Damping Ratio with Loading Frequency at an Isotropic Confining Pressure 80 psi (=11.5 ksf=552 kPa) from the Combined RCTS Tests of Specimen UTA-27-I.

Table M.1 Variation in Low-Amplitude Shear Wave Velocity, Low-Amplitude Shear Modulus, Low-Amplitude Material Damping Ratio and Estimated Void Ratio with Isotropic Confining Pressure from RC Tests of Specimen UTA-27-I.

Effective Isotropic Confining Pressure, σ_o'			Low-Amplitude Shear Modulus, G_{max}		Low-Amplitude Shear Wave Velocity, Vs	Low-Amplitude Material Damping Ratio,	Estimated Void Ratio, e
(psi)	(psf)	(kPa)	(ksf)	(MPa)	(fps)	D_{min}, %	
20	2880	138.1	2992	143.4	882	2.20	0.705
40	5760	276.1	3576	171.4	962	2.10	0.689
80	11520	552.3	4540	217.6	1081	1.90	0.669
160	23040	1104.5	6065	290.8	1242	1.85	0.633
320	46080	2209.1	7853	376.5	1399	2.10	0.572

Table M.2 Variation in Shear Modulus, Normalized Shear Modulus and Material Damping Ratio with Shearing Strain from RC Tests of Specimen UTA-27-I; Confining Pressure, σ_o' = 80 psi(=11.5 ksf=552 kPa).

Peak Shearing Strain, %	Shear Modulus, G, ksf	Normalized Shear Modulus, G/G_{max}	Average[+] Shearing Strain, %	Material Damping Ratio[x], D, %
1.99E-04	4880	1.00	1.80E-04	1.68
1.04E-04	4860	1.00	0.00E+00	
3.91E-04	4830	1.00	3.91E-04	
7.81E-04	4770	1.00	7.03E-04	1.75
1.54E-03	4642	1.00	1.38E-03	1.83
2.83E-03	4463	0.99	2.52E-03	1.92
5.44E-03	4167	0.97	4.81E-03	2.04
1.03E-02	3668	0.93	8.92E-03	2.38
1.82E-02		0.86	1.49E-02	3.40
3.22E-02	2999	0.75	2.45E-02	4.83
5.63E-02	2405	0.64	3.97E-02	6.43
1.20E-01	1843	0.49	7.67E-02	8.52

[+] Average Shearing Strain from the First Three Cycles of the Free Vibration Decay Curve

[x] Average Damping Ratio from the First Three Cycles of the Free Vibration Decay Curve

Table M.3 Variation in Shear Modulus, Normalized Shear Modulus and Material Damping Ratio with Shearing Strain from TS Tests of Specimen UTA-27-I; Confining Pressure, σ_o' = 80 psi(=11.5 ksf=552 kPa).

First Cycle				Tenth Cycle			
Peak Shearing Strain, %	Shear Modulus, G, ksf	Normalized Shear Modulus, G/G_{max}	Material Damping Ratio, D, %	Peak Shearing Strain, %	Shear Modulus, G, ksf	Normalized Shear Modulus, G/G_{max}	Material Damping Ratio, D, %
1.41E-04			0.64	1.40E-04			0.66
2.80E-04	3814	1.00	0.62	2.78E-04	3837	1.00	0.67
5.65E-04	3786	1.00	0.68	5.66E-04	3777	0.98	0.67
1.13E-03	3764	0.99	0.67	1.13E-03	3763	0.98	0.66
2.29E-03	3735	0.98	0.75	2.29E-03	3733	0.97	0.73
4.66E-03	3668	0.97	0.92	4.66E-03	3664	0.95	0.92
9.76E-03	3507	0.92	1.40	9.77E-03	3504	0.91	1.38

APPENDIX N

Specimen No. 13
UT Specimen ID: UTA-27-V

LA Bulk Mail P-6
Depth = 205 ft (=62.5m)
Soil Type: Silty Sand (SM)

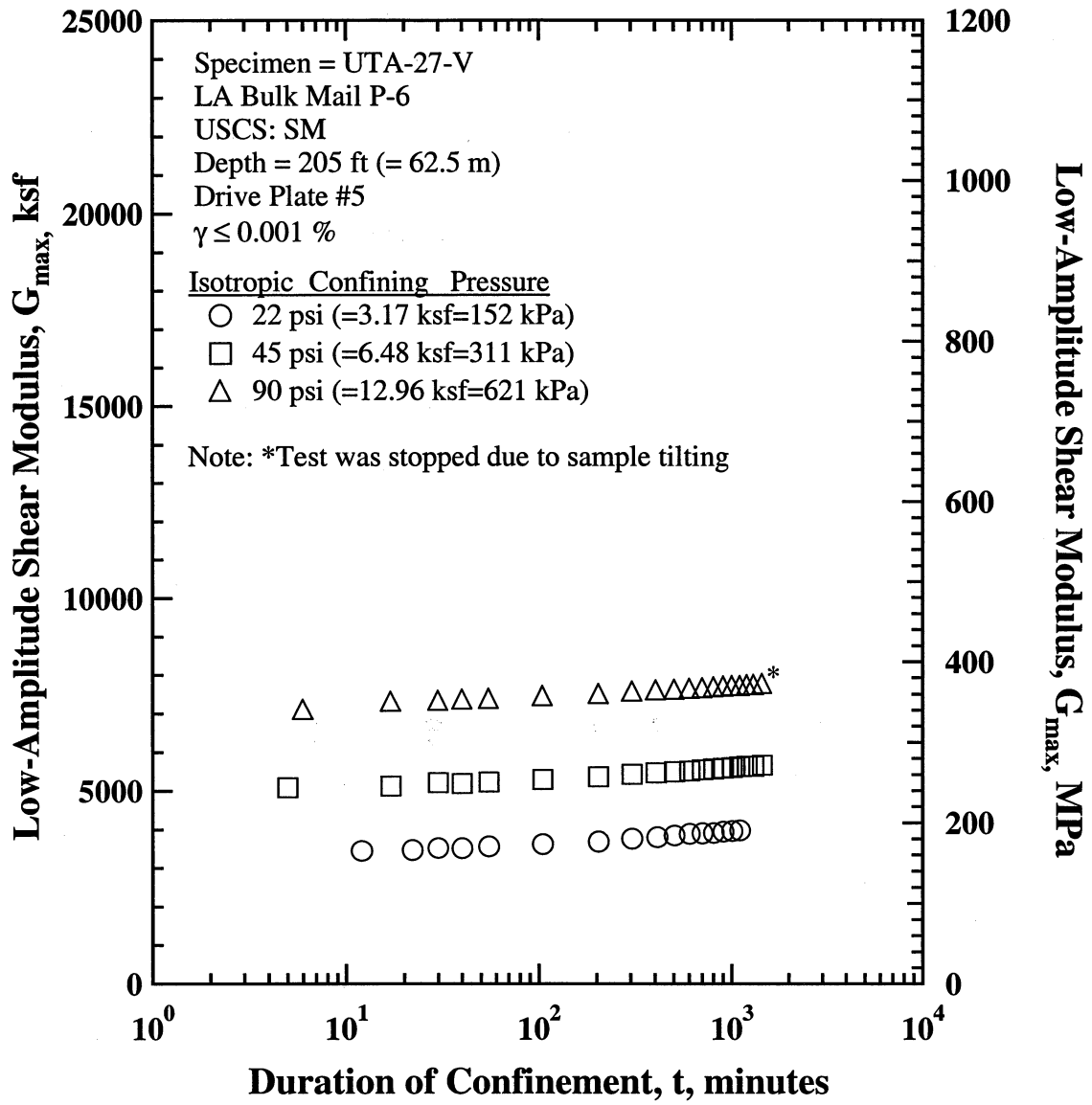

Figure N.1 Variation in Low-Amplitude Shear Modulus with Magnitude and Duration of Isotropic Confining Pressure from Resonant Column Tests of Specimen UTA-27-V.

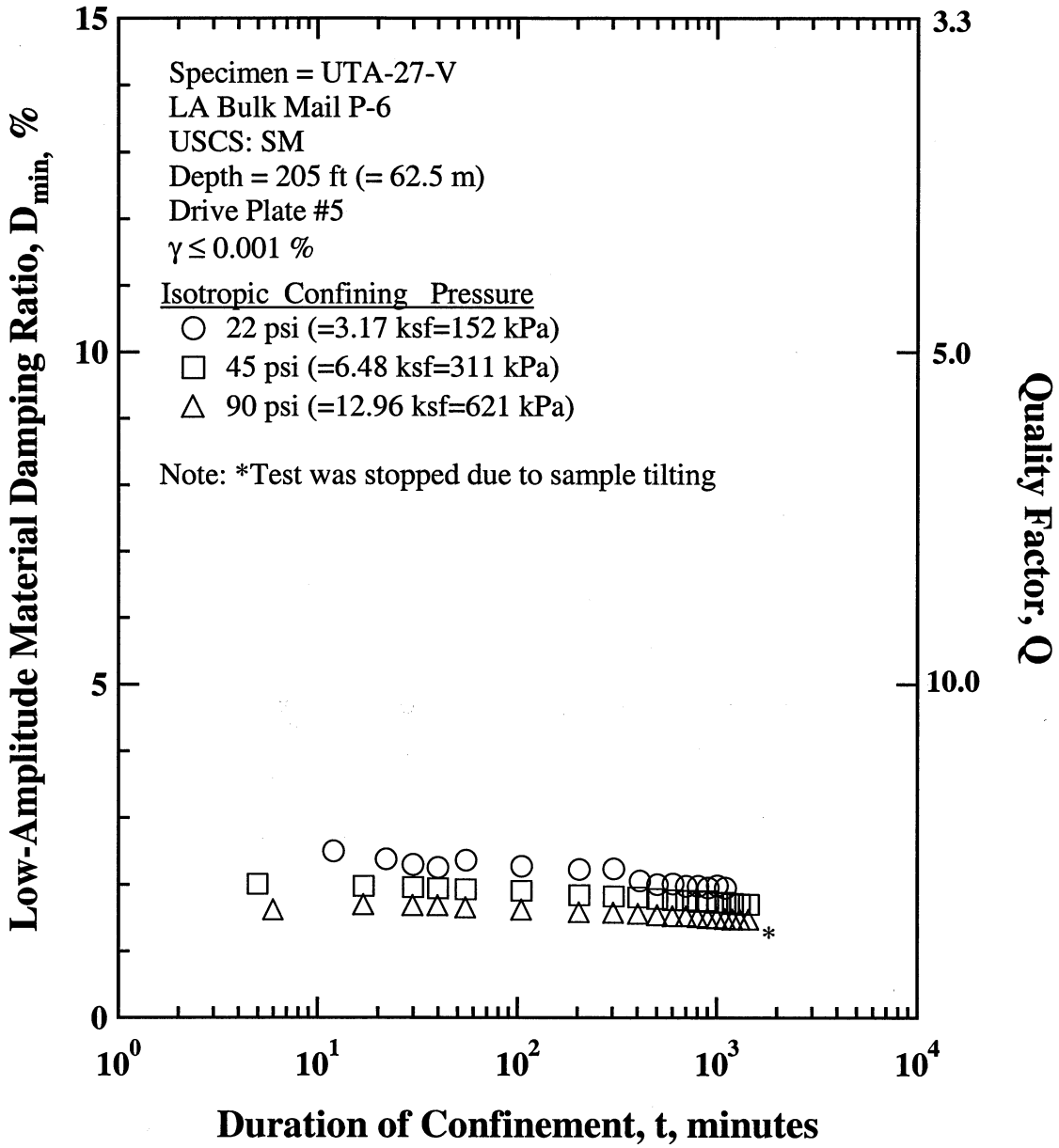

Figure N.2 Variation in Low-Amplitude Material Damping Ratio with Magnitude and Duration of Isotropic Confining Pressure from Resonant Column Tests of Specimen UTA-27-V

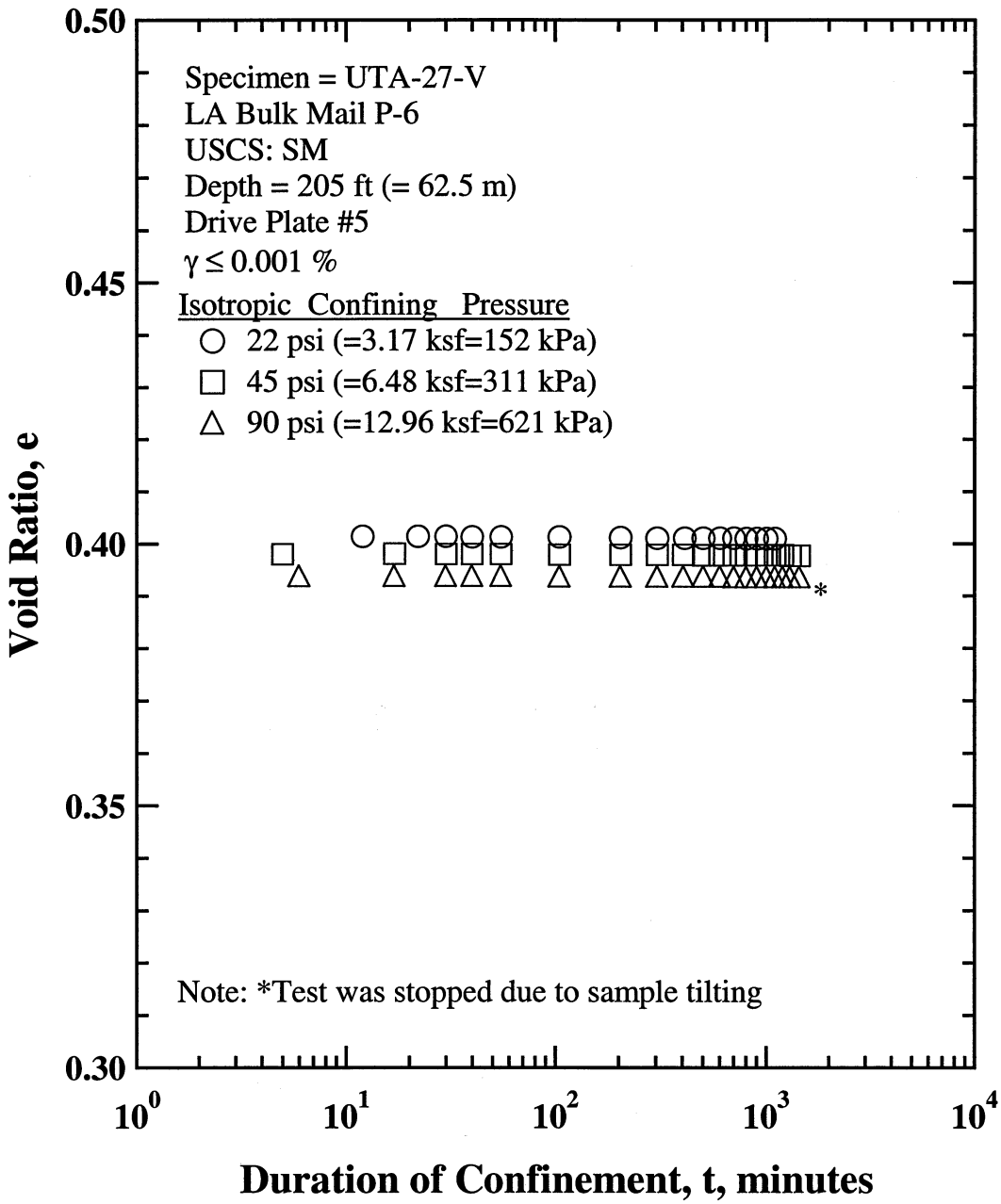

Figure N.3 Variation in Estimated Void Ratio with Magnitude and Duration of Isotropic Confining Pressure from Resonant Column Tests of Specimen UTA-27-V.

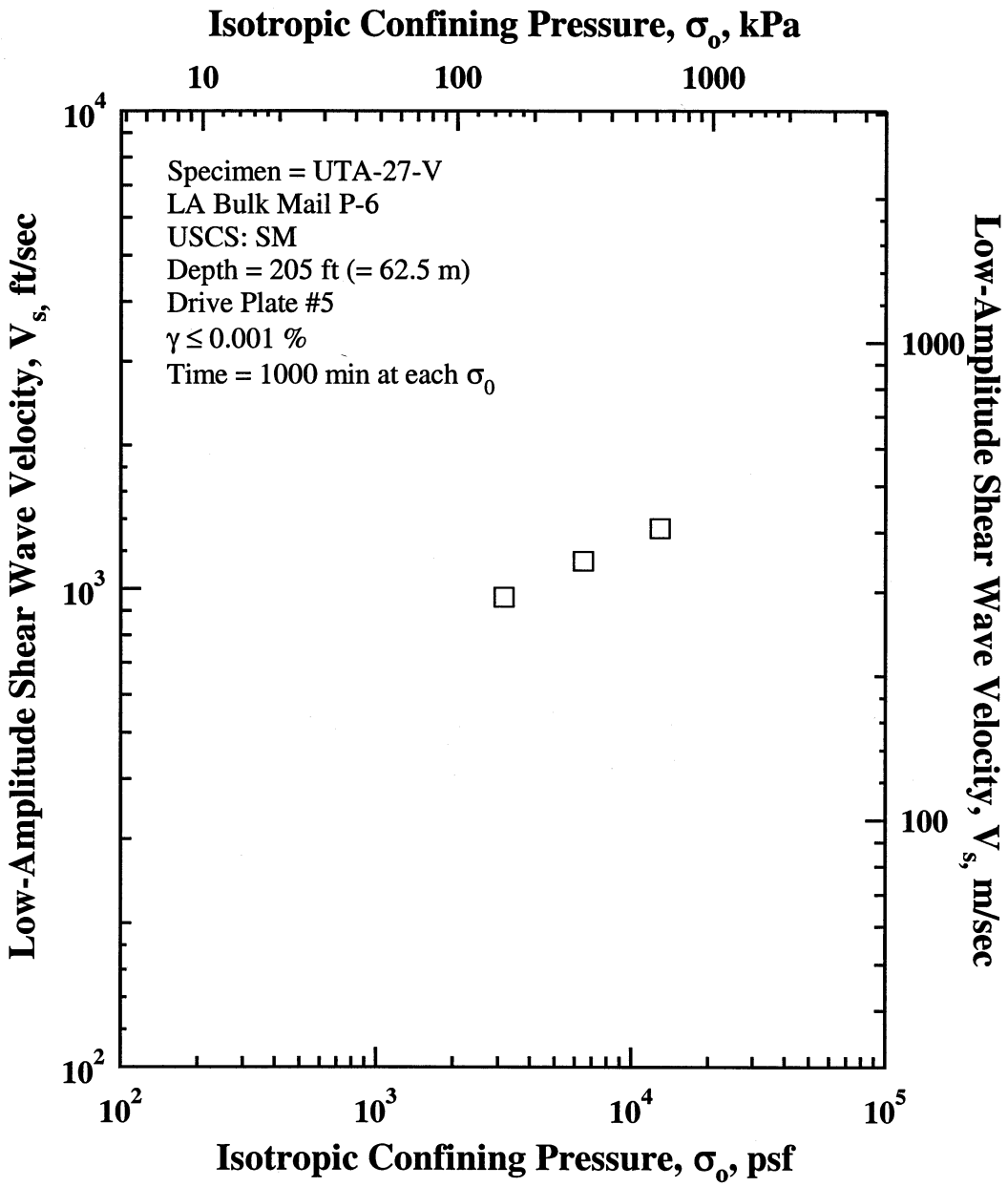

Figure N.4 Variation in Low-Amplitude Shear Wave Velocity with Isotropic Confining Pressure from Resonant Column Tests of Specimen UTA-27-V.

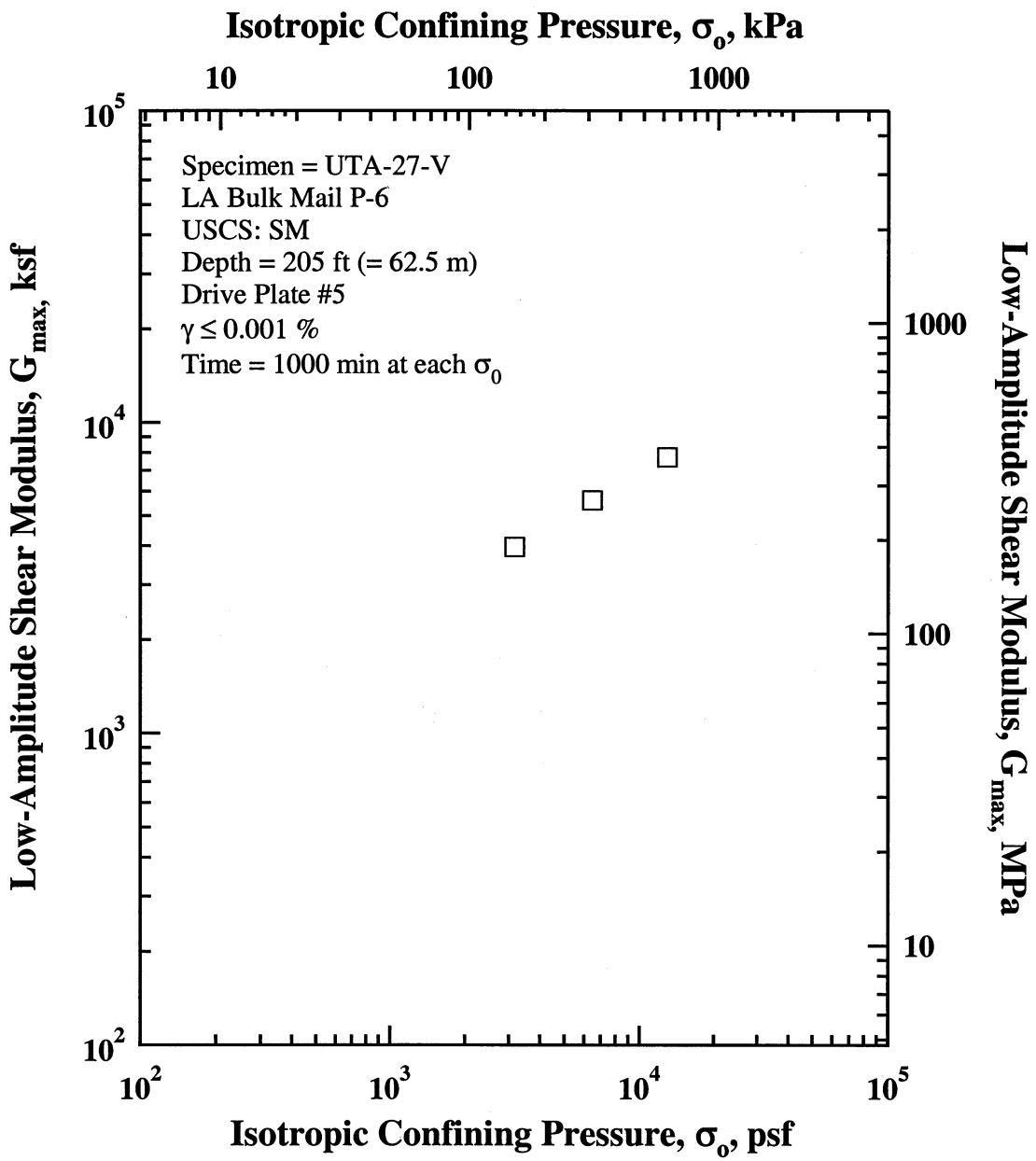

Figure N.5 Variation in Low-Amplitude Shear Modulus with Isotropic Confining Pressure from Resonant Column Tests of Specimen UTA-27-V.

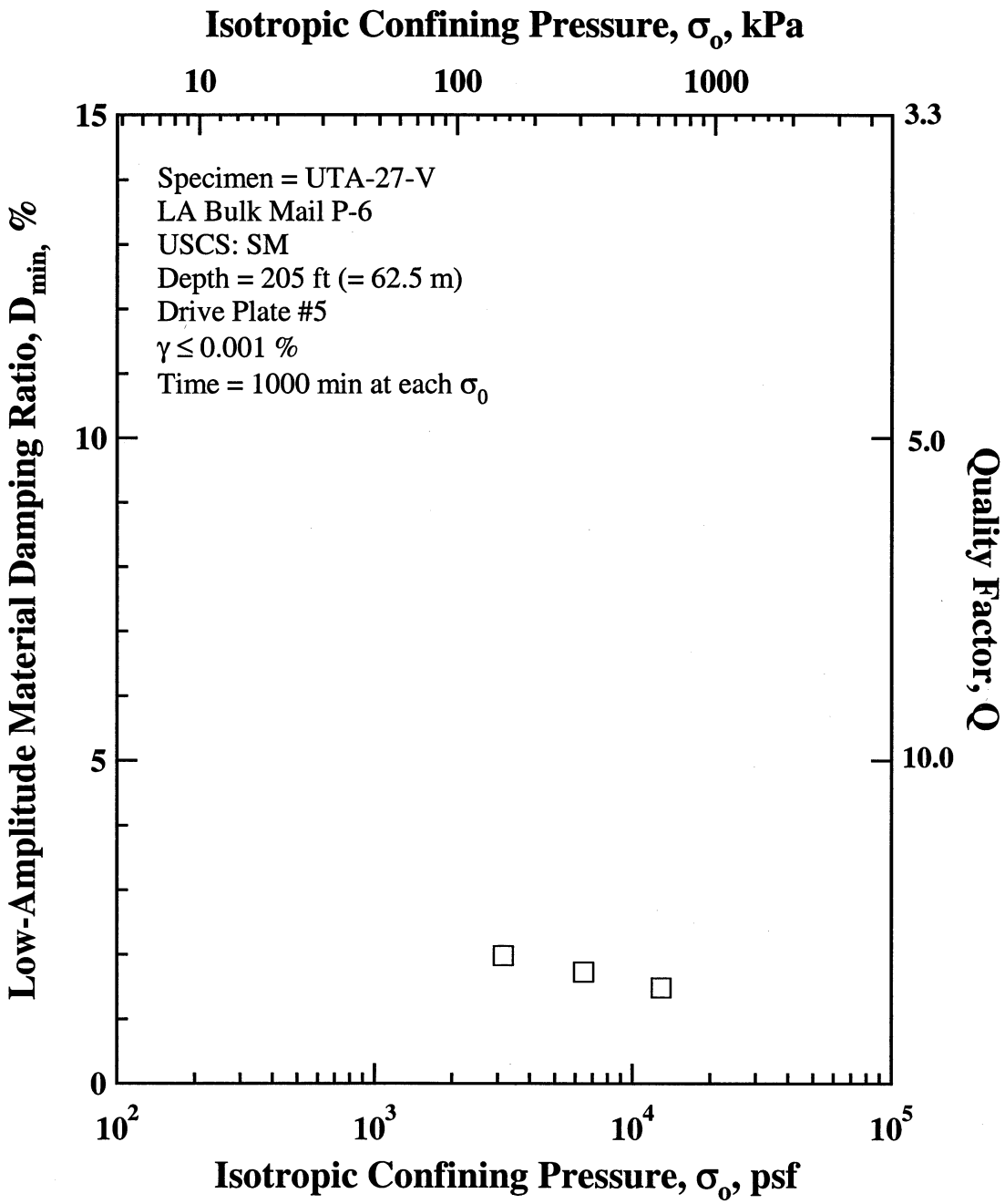

Figure N.6 Variation in Low-Amplitude Material Damping Ratio with Isotropic Confining Pressure from Resonant Column Tests of Specimen UTA-27-V.

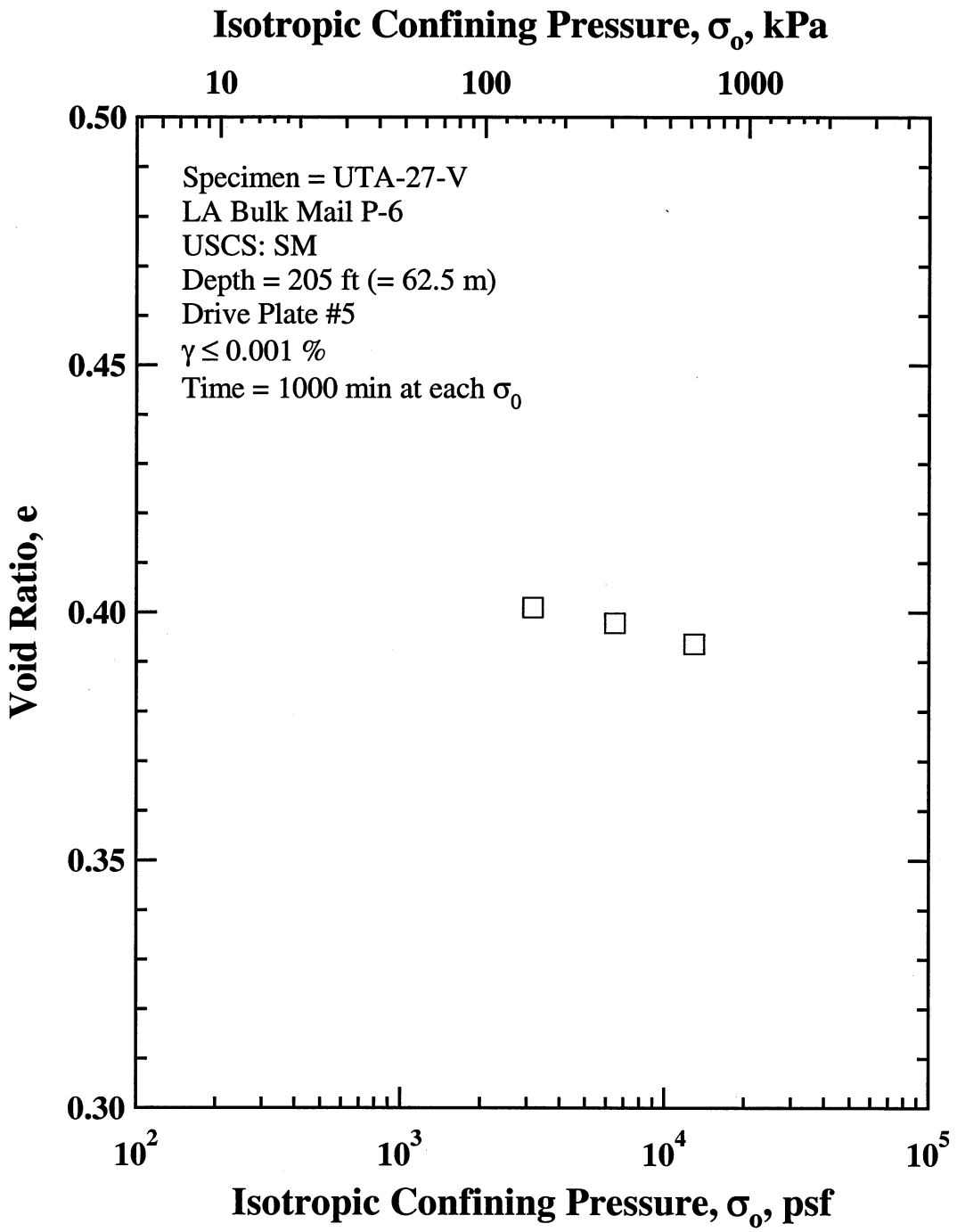

Figure N.7 Variation in Estimated Void Ratio with Isotropic Confining Pressure from Resonant Column Tests of Specimen UTA-27-V.

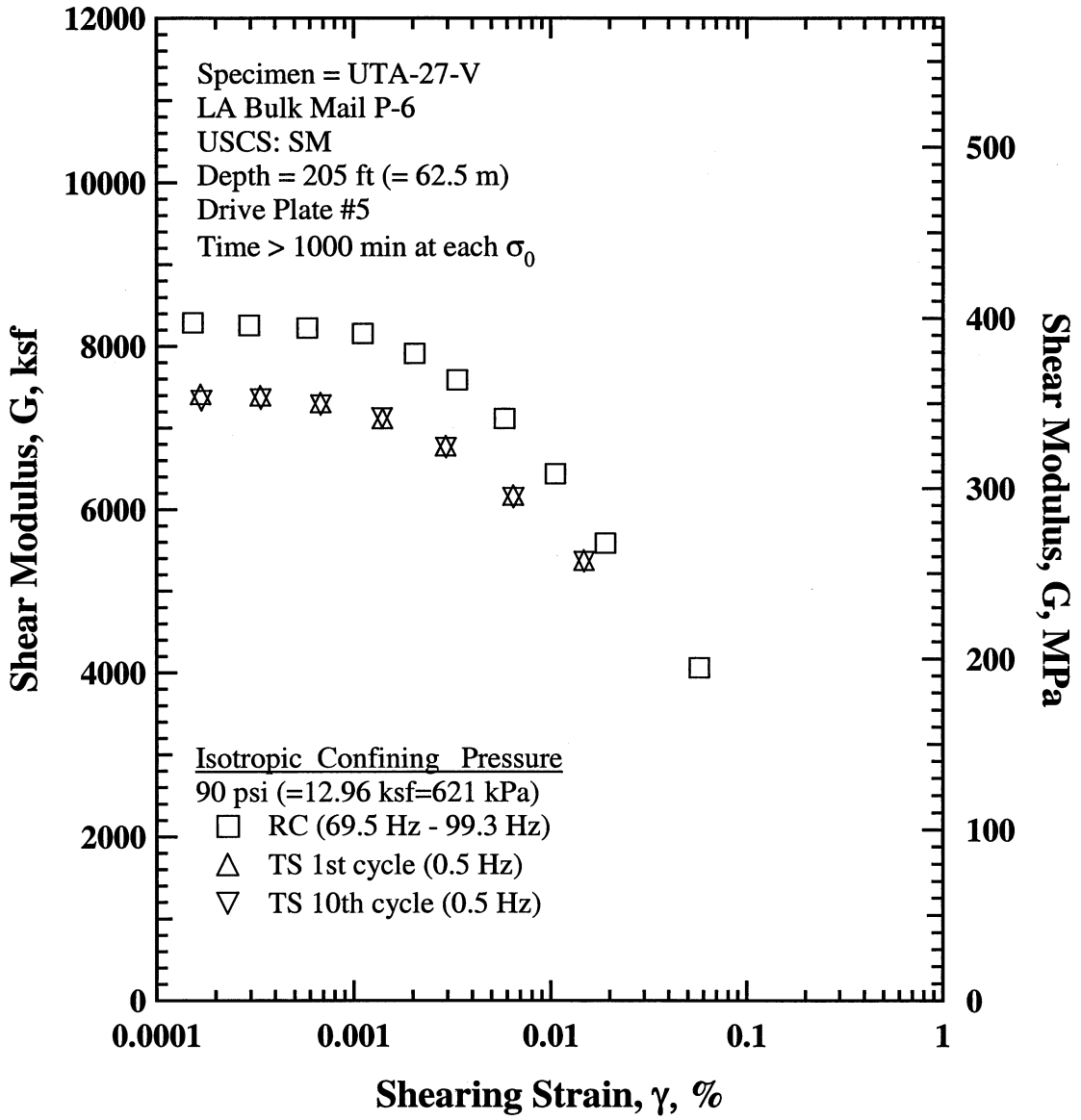

Figure N.8 Comparison of the Variation in Shear Modulus with Shearing Strain at an Isotropic Confining Pressure of 90 psi (=12.96 ksf=621 kPa) from the Combined RCTS Tests of Specimen UTA-27-V.

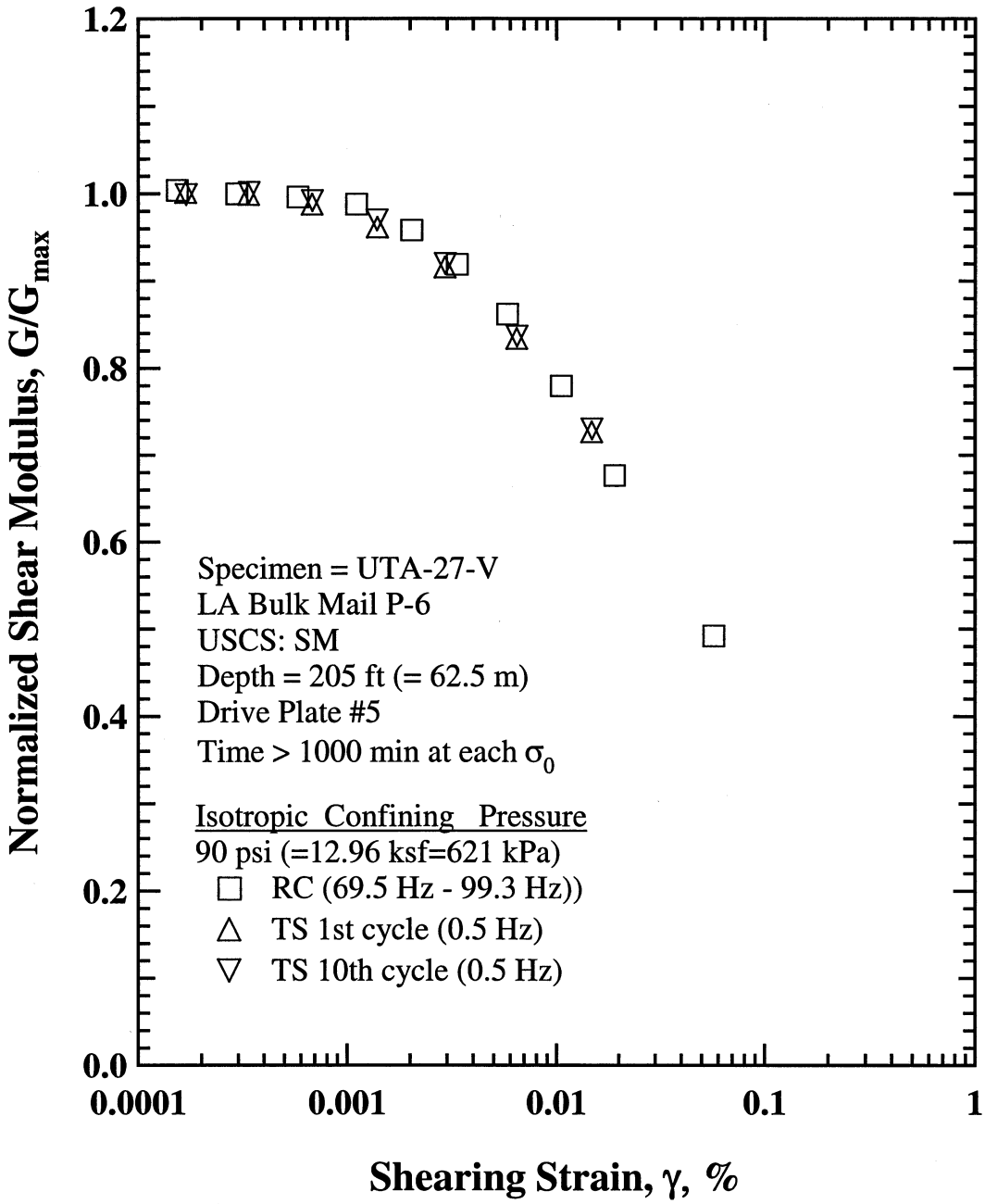

Figure N.9 Comparison of the Variation in Normalized Shear Modulus with Shearing Strain at an Isotropic Confining Pressure of 90 psi (=12.96 ksf=621 kPa) from the Combined RCTS Tests of Specimen UTA-27-V.

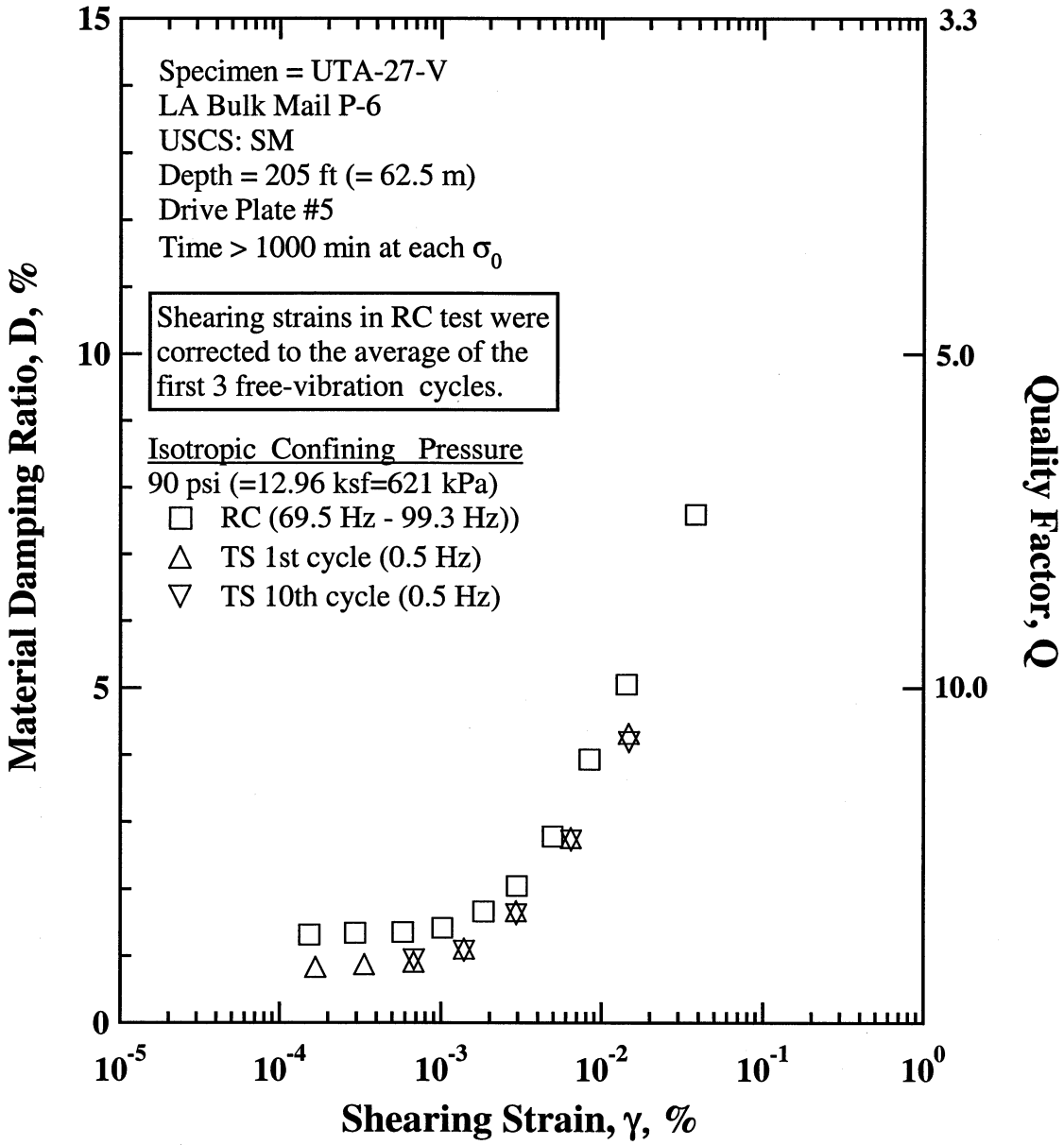

Figure N.10 Comparison of the Variation in Material Damping Ratio with Shearing Strain at an Isotropic Confining Pressure of 90 psi (=12.96 ksf=621 kPa) from the Combined RCTS Tests of Specimen UTA-27-V.

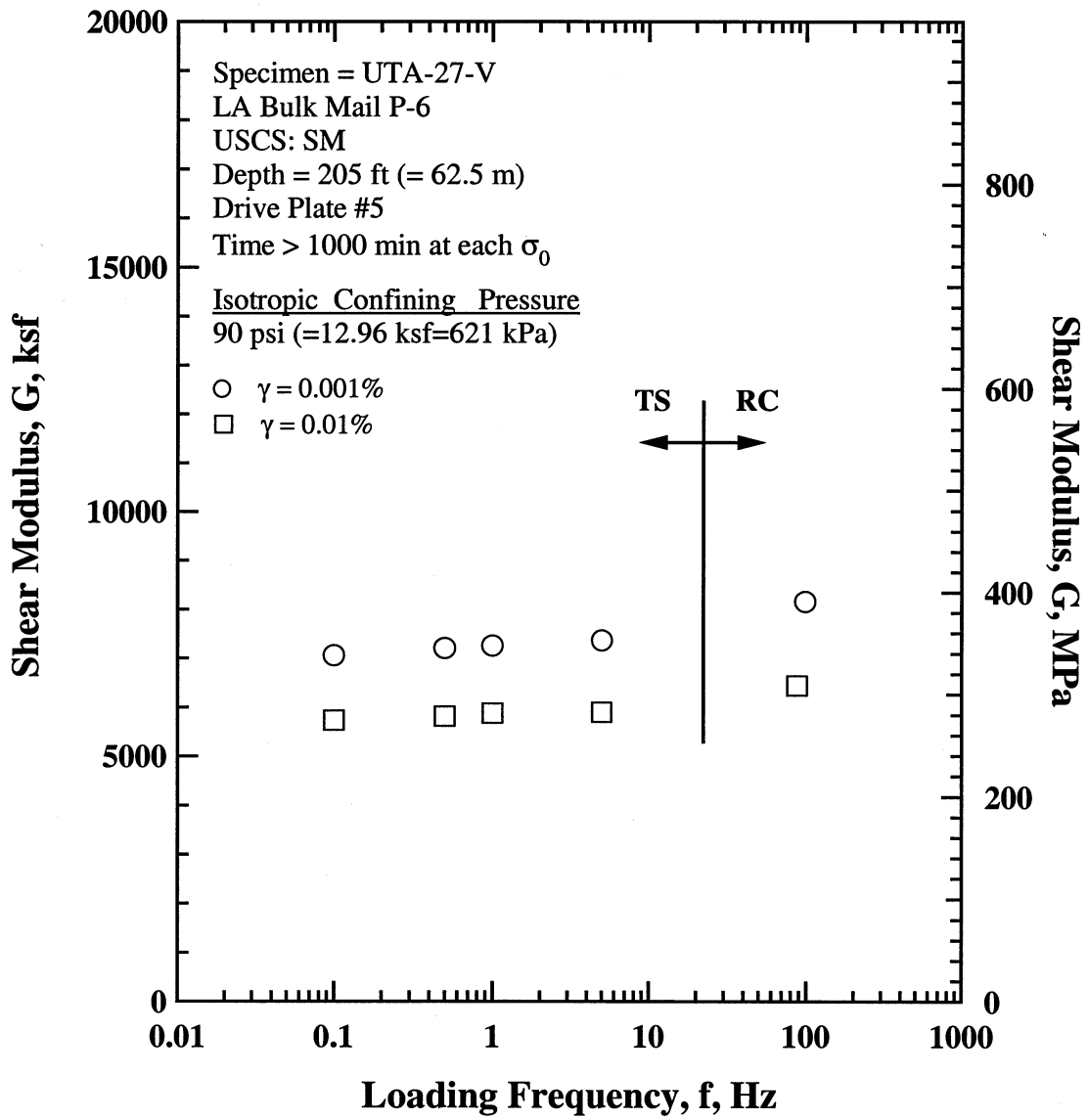

Figure N.11 Comparison of the Variation in Shear Modulus with Loading Frequency at an Isotropic Confining Pressure of 90 psi (=12.96 ksf=621 kPa) from the Combined RCTS Tests of Specimen UTA-27-V.

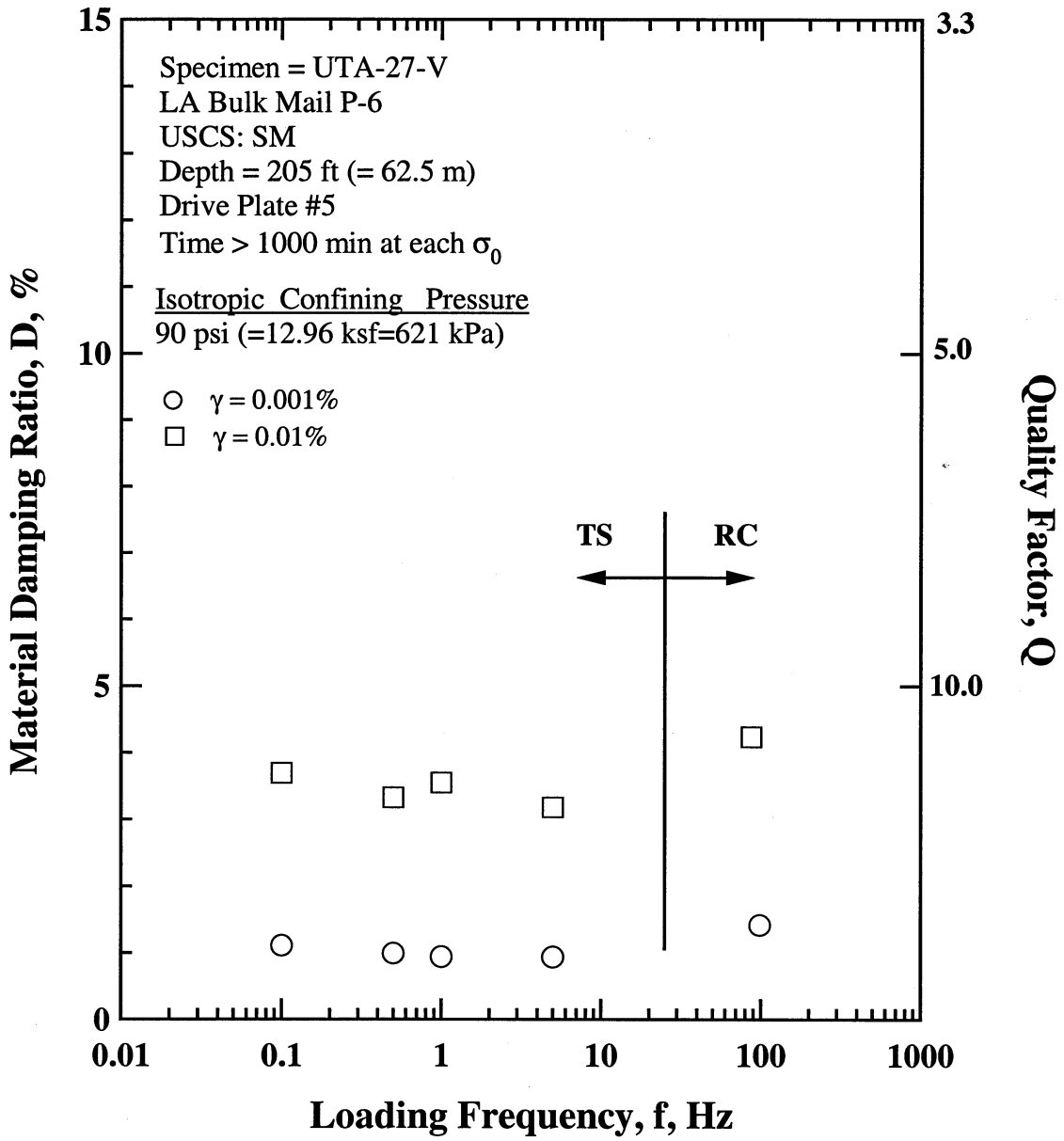

Figure N.12 Comparison of the Variation in Material Damping Ratio with Loading Frequency at an Isotropic Confining Pressure 90 psi (=12.96 ksf=621 kPa) from the Combined RCTS Tests of Specimen UTA-27-V.

Table N.1 Variation in Low-Amplitude Shear Wave Velocity, Low-Amplitude Shear Modulus, Low-Amplitude Material Damping Ratio and Estimated Void Ratio with Isotropic Confining Pressure from RC Tests of Specimen UTA-27-V.

Effective Isotropic Confining Pressure, σ_o'			Low-Amplitude Shear Modulus, G_{max}		Low-Amplitude Shear Wave Velocity, Vs	Low-Amplitude Material Damping Ratio, Dmin	Estimated Void Ratio, e
(psi)	(psf)	(kPa)	(ksf)	(MPa)	(fps)	(%)	
22	3168	152	3958	189.8	960	1.99	0.401
45	6480	311	5607	268.8	1142	1.73	0.398
90	12960	621	7716	369.9	1339	1.49	0.394

Table N.2 Variation in Shear Modulus, Normalized Shear Modulus and Material Damping Ratio with Shearing Strain from RC Tests of Specimen UTA-27-V; Confining Pressure, σ_o' =90 psi (=12.96 ksf=621 kPa).

Peak Shearing Strain, %	Shear Modulus, G, ksf	Normalized Shear Modulus, G/G_{max}	Average[+] Shearing Strain, %	Material Damping Ratio[x], D, %
1.53E-04	8289	1.00	1.53E-04	1.32
2.95E-04	8255	1.00	2.95E-04	1.34
5.82E-04	8224	1.00	5.82E-04	1.36
1.11E-03	8157	0.99	1.02E-03	1.42
2.03E-03	7911	0.96	1.84E-03	1.67
3.35E-03	7588	0.92	2.96E-03	2.05
5.83E-03	7117	0.86	4.95E-03	2.78
1.05E-02	6438	0.78	8.40E-03	3.93
1.90E-02	5586	0.68	1.43E-02	5.05
5.72E-02	4062	0.49	3.82E-02	7.59

[+] Average Shearing Strain from the First Three Cycles of the Free Vibration Decay Curve

[x] Average Damping Ratio from the First Three Cycles of the Free Vibration Decay Curve

Table N.3 Variation in Shear Modulus, Normalized Shear Modulus and Material Damping Ratio with Shearing Strain from TS Tests of Specimen UTA-27-V; Confining Pressure, σ_o' =90 psi (=12.96 ksf=621 kPa).

First Cycle				Tenth Cycle			
Peak Shearing Strain, %	Shear Modulus, G, ksf	Normalized Shear Modulus, G/G_{max}	Material Damping Ratio, D, %	Peak Shearing Strain, %	Shear Modulus, G, ksf	Normalized Shear Modulus, G/G_{max}	Material Damping Ratio, D, %
1.68E-04	7407	1.00	0.82	1.70E-04	7328	1.00	
3.38E-04	7386	1.00	0.87	3.40E-04	7348	1.00	
6.84E-04	7303	0.99	0.90	6.86E-04	7276	0.99	0.94
1.40E-03	7110	0.96	1.10	1.40E-03	7116	0.97	1.07
2.94E-03	6772	0.92	1.66	2.95E-03	6750	0.92	1.62
6.47E-03	6167	0.83	2.75	6.50E-03	6136	0.84	2.72
1.49E-02	5371	0.73	4.31	1.49E-02	5355	0.73	4.19

APPENDIX O

Specimen No. 14
UT Specimen ID: UTA-27-H

LA Bulk Mail P-7
Depth = 267 ft (=81.4m)
Soil Type: Sand (SP)

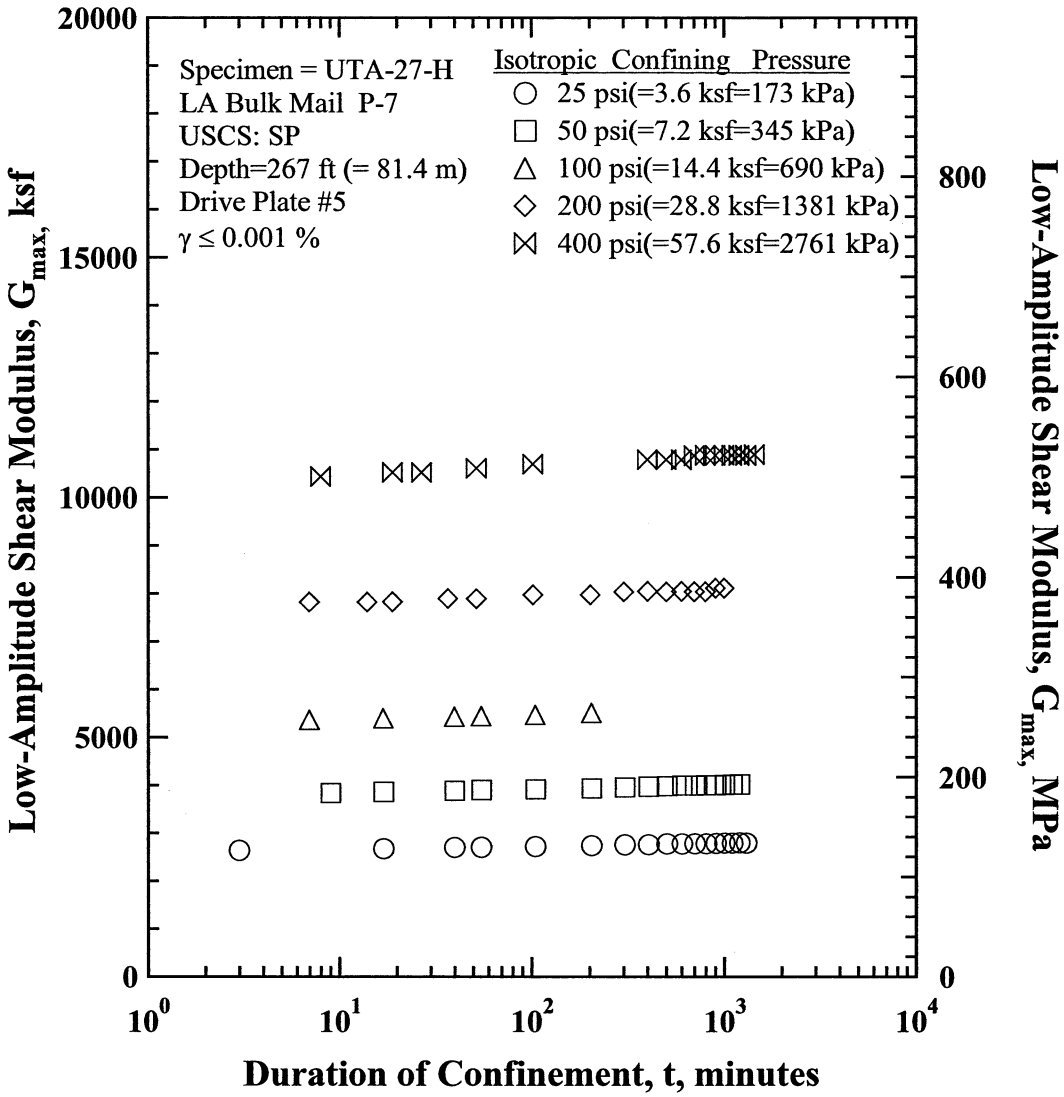

Figure O.1 Variation in Low-Amplitude Shear Modulus with Magnitude and Duration of Isotropic Confining Pressure from Resonant Column Tests of Specimen UTA-27-H.

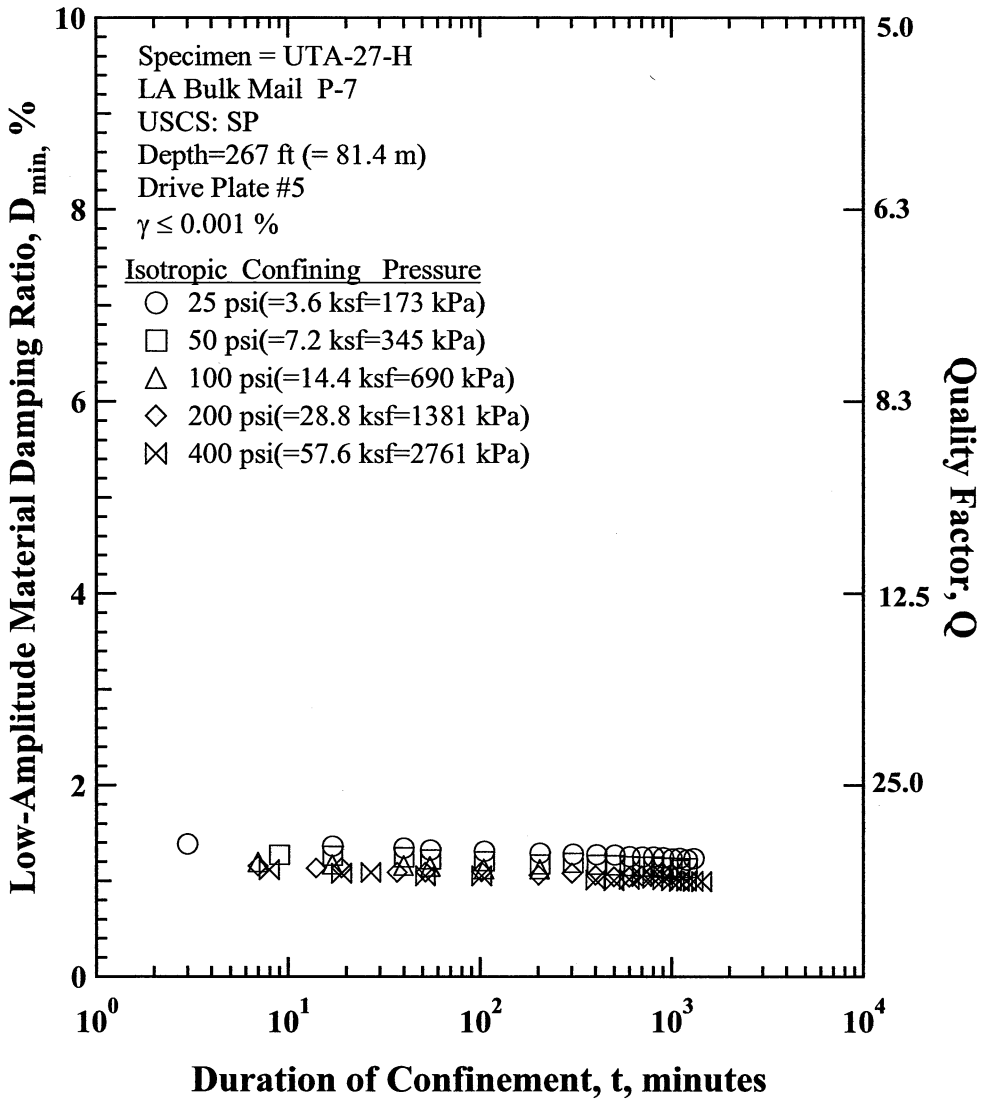

Figure O.2 Variation in Low-Amplitude Material Damping Ratio with Magnitude and Duration of Isotropic Confining Pressure from Resonant Column Tests of Specimen UTA-27-H

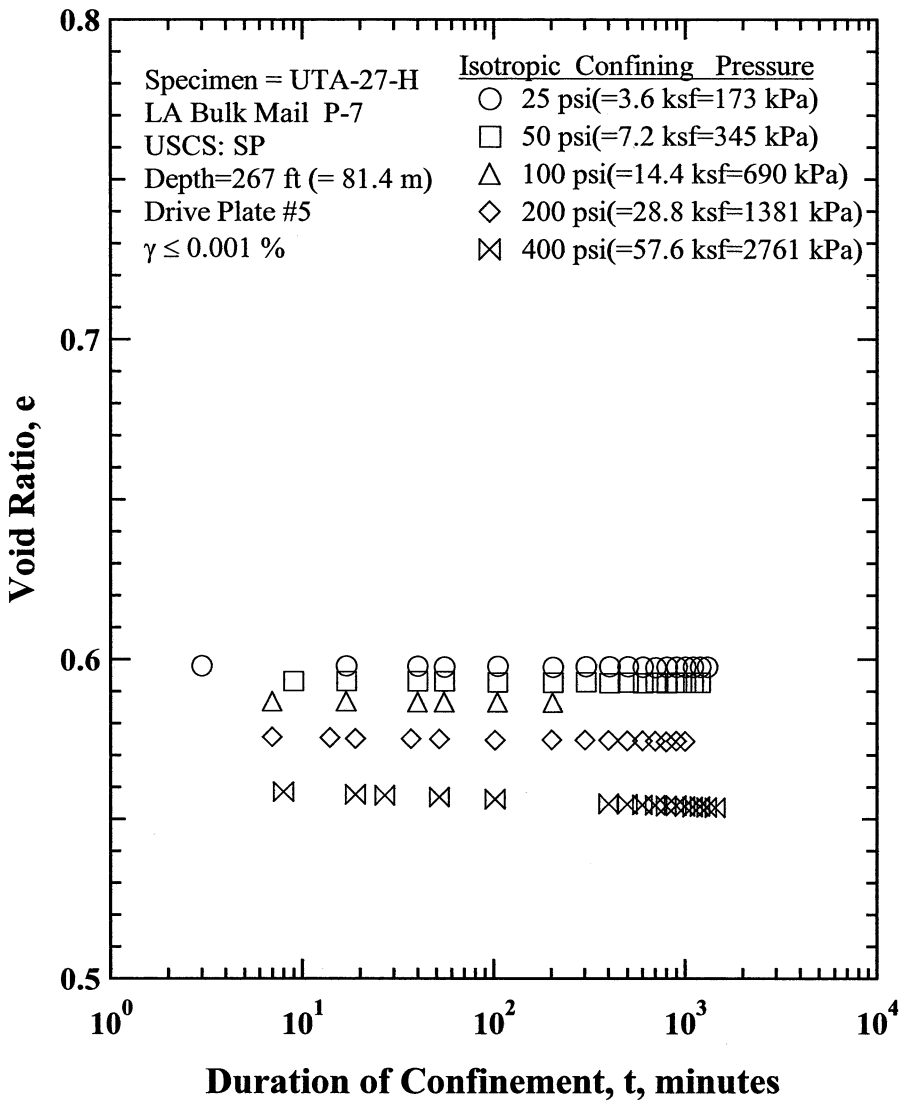

Figure O.3 Variation in Estimated Void Ratio with Magnitude and Duration of Isotropic Confining Pressure from Resonant Column Tests of Specimen UTA-27-H

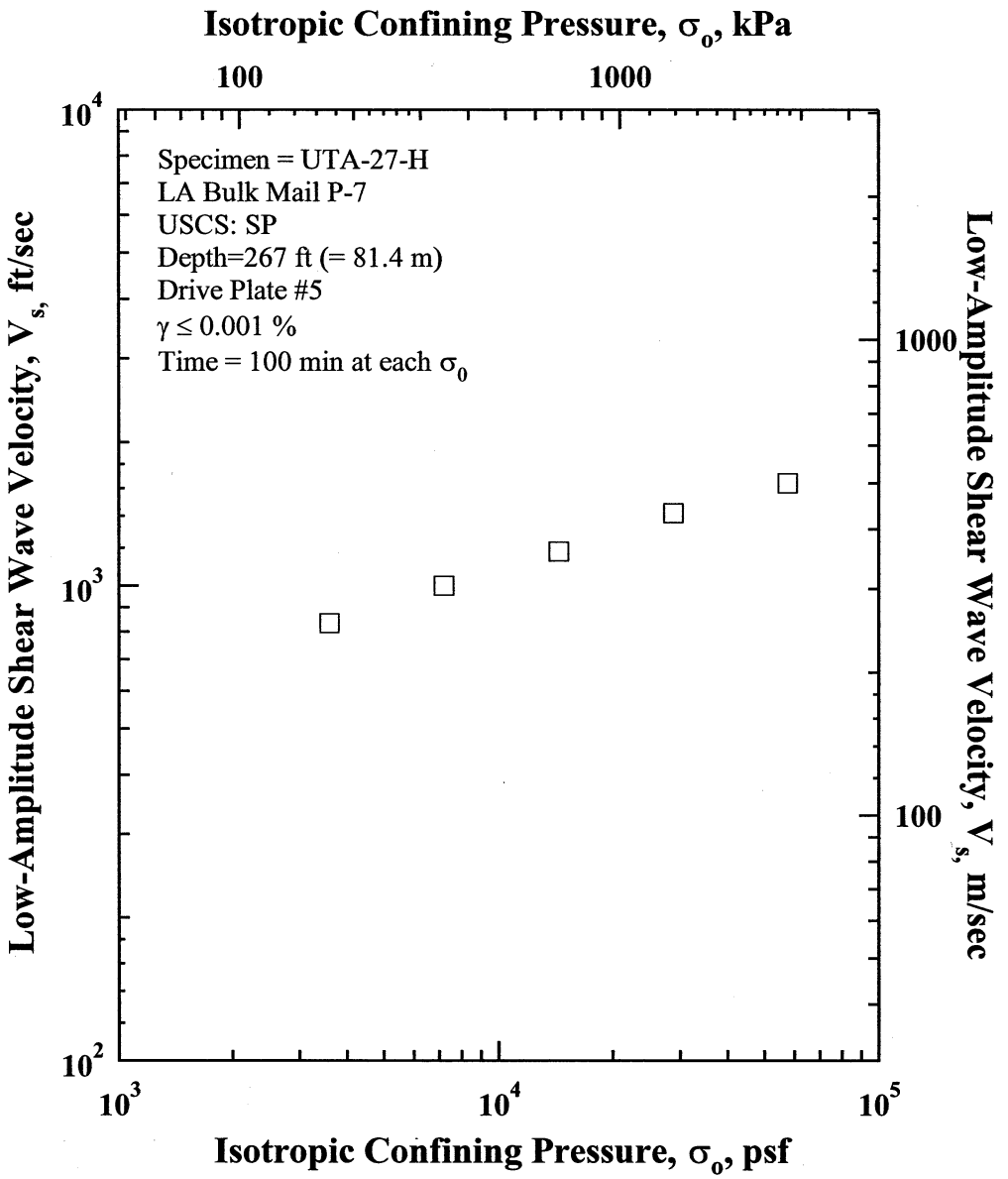

Figure O.4 Variation in Low-Amplitude Shear Wave Velocity with Isotropic Confining Pressure from Resonant Column Tests of Specimen UTA-27-H.

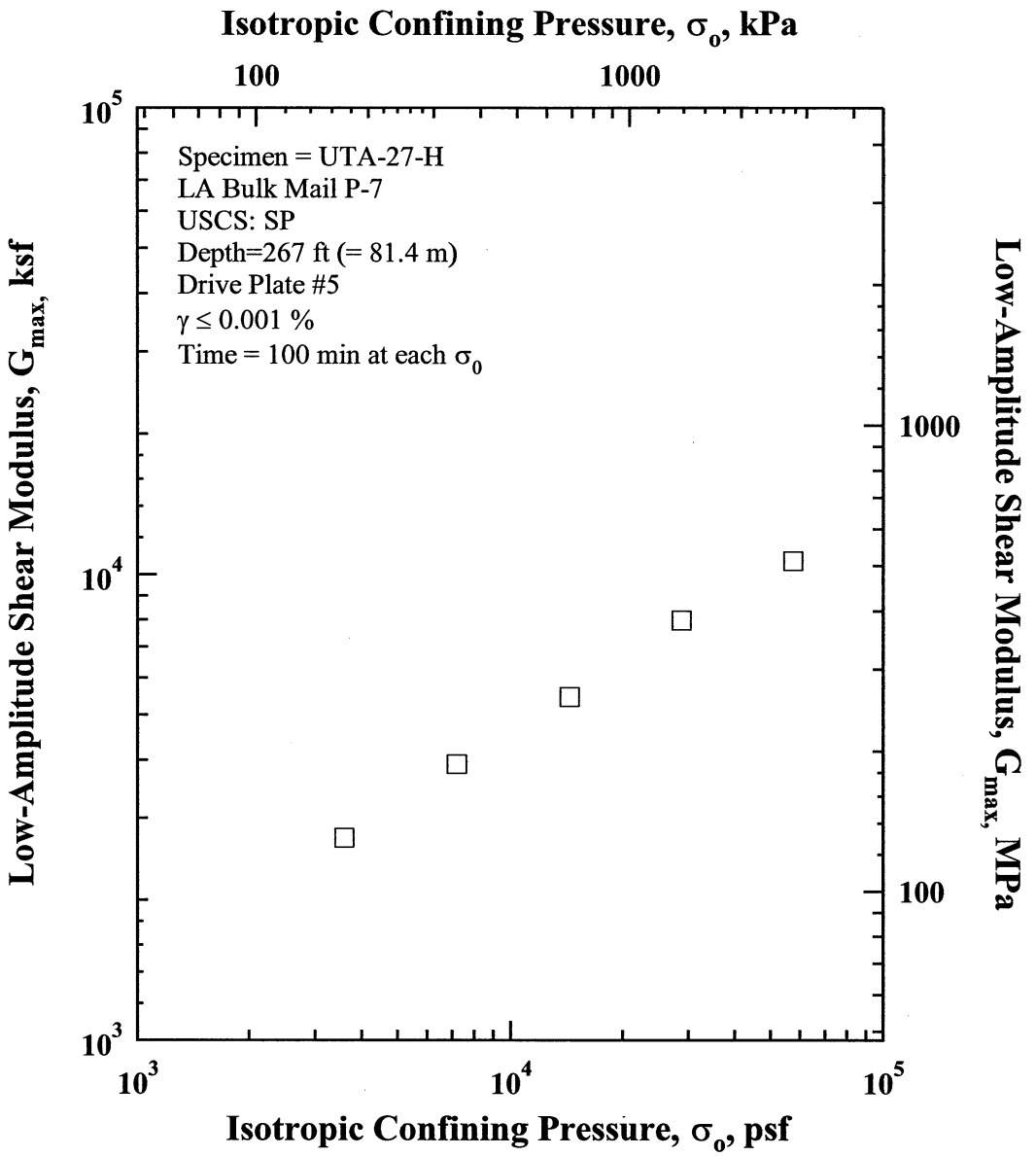

Figure O.5 Variation in Low-Amplitude Shear Modulus with Isotropic Confining Pressure from Resonant Column Tests of Specimen UTA-27-H.

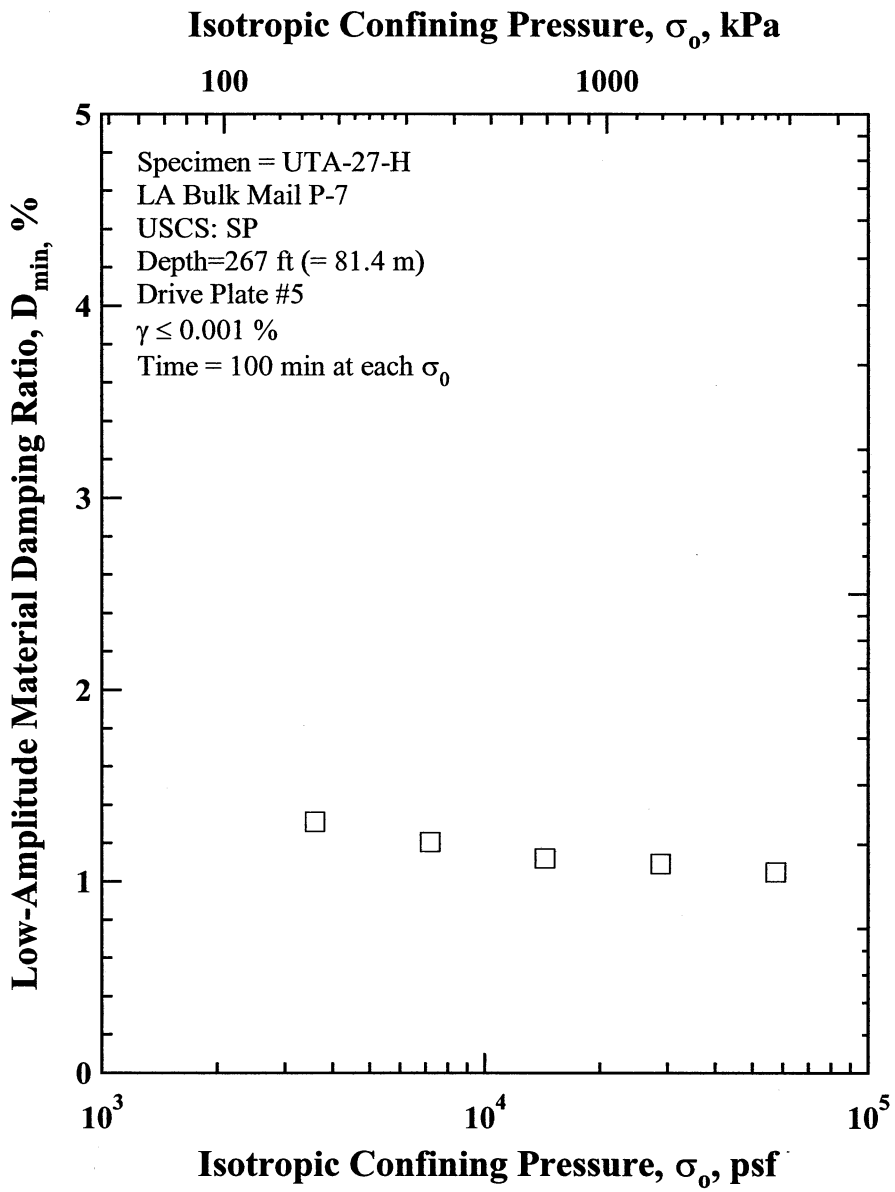

Figure O.6 Variation in Low-Amplitude Material Damping Ratio with Isotropic Confining Pressure from Resonant Column Tests of Specimen UTA-27-H.

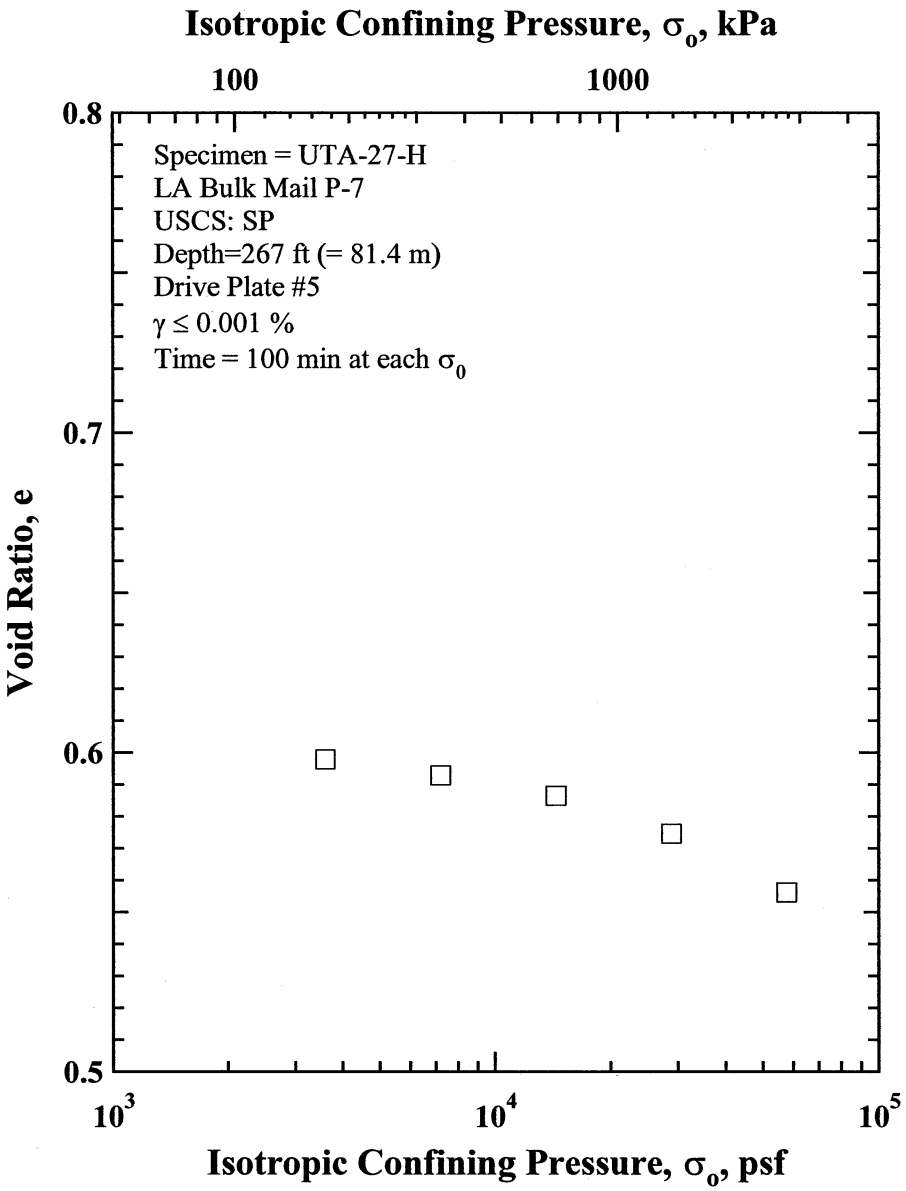

Figure O.7 Variation in Estimated Void Ratio with Isotropic Confining Pressure from Resonant Column Tests of Specimen UTA-27-H.

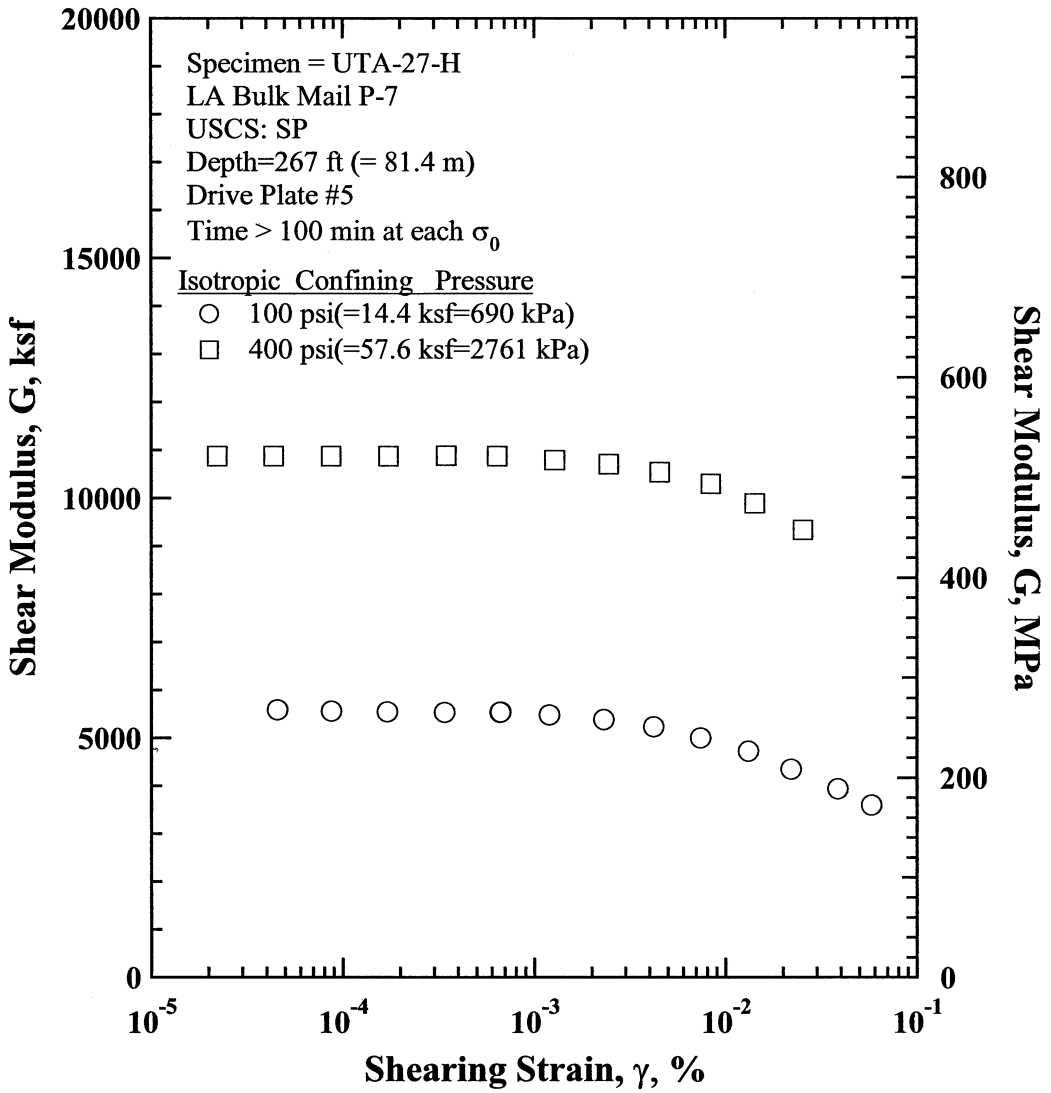

Figure O.8 Comparison of the Variation in Shear Modulus with Shearing Strain and Isotropic Confining Pressure from the Resonant Column Tests of Specimen UTA-27-H.

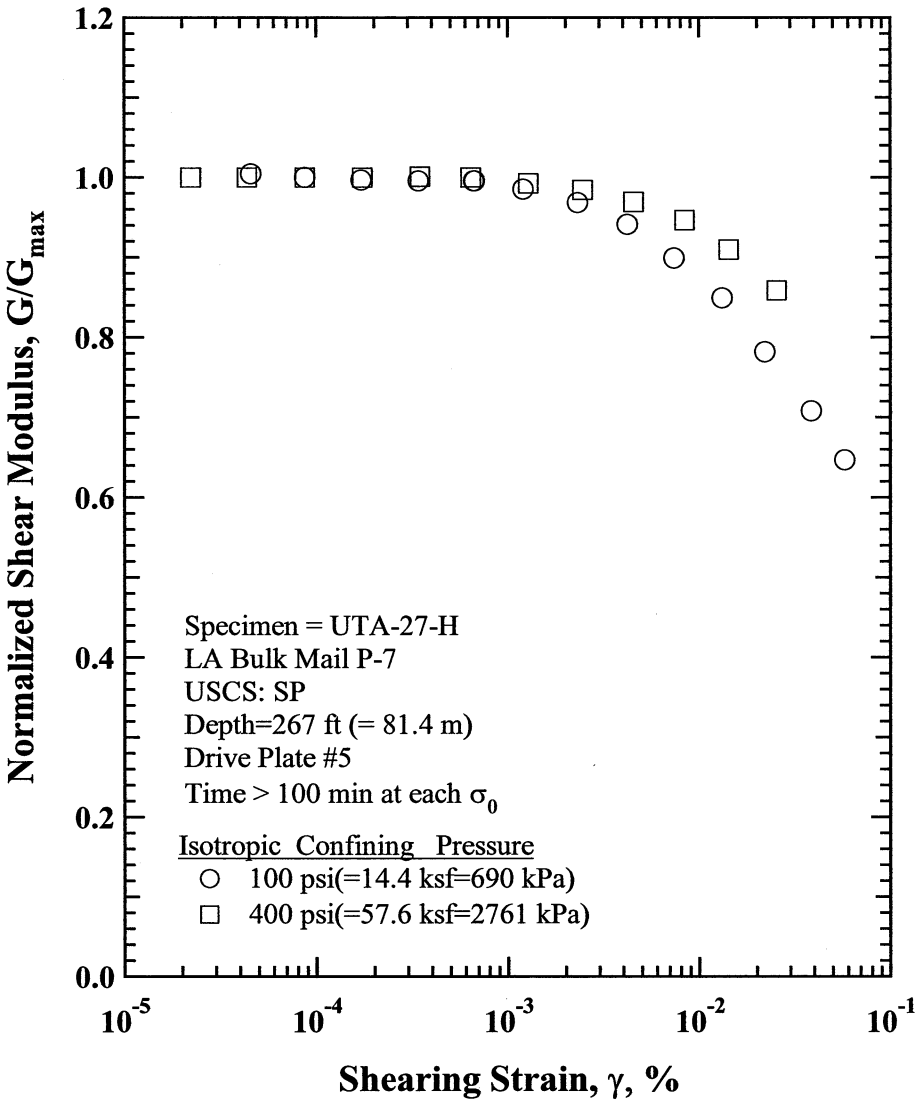

Figure O.9 Comparison of the Variation in Normalized Shear Modulus with Shearing Strain and Isotropic Confining Pressure from the Resonant Column Tests of Specimen UTA-27-H.

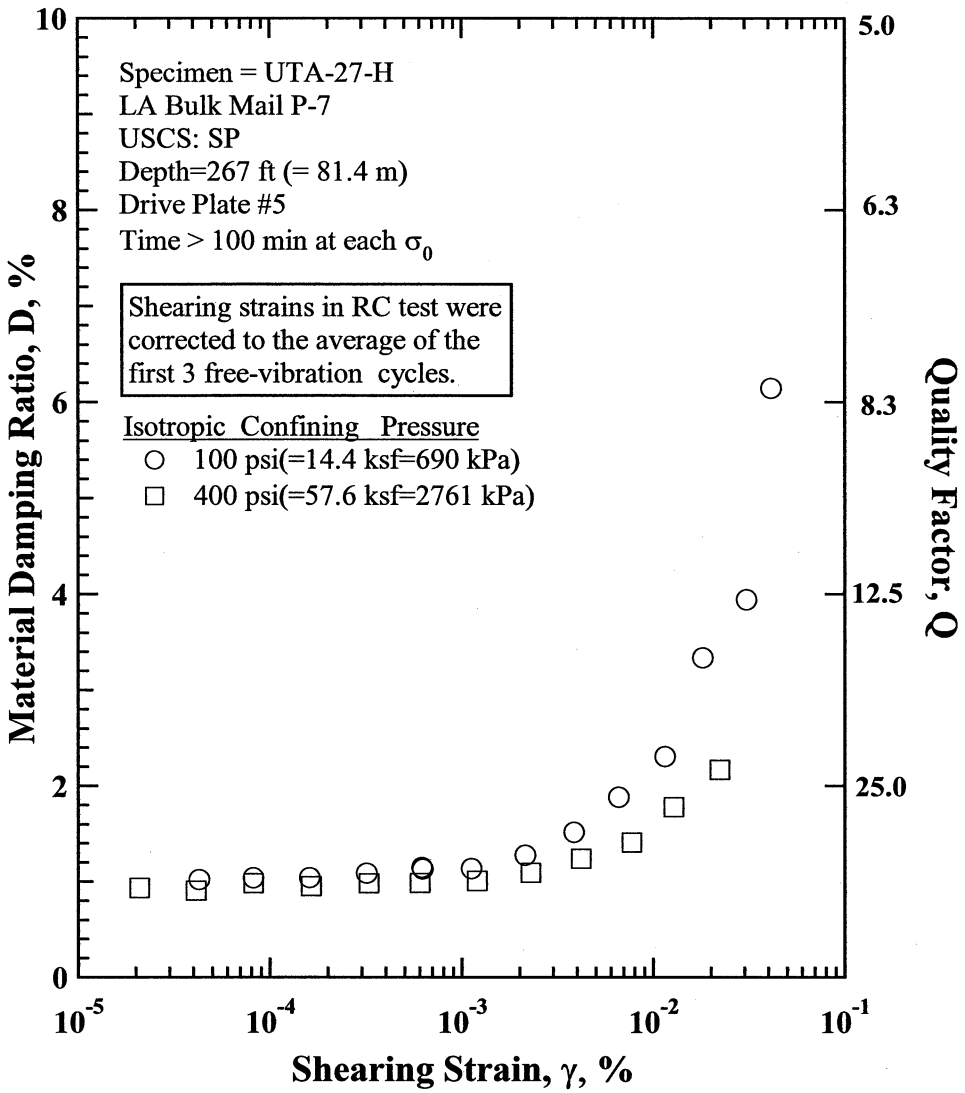

Figure O.10 Comparison of the Variation in Material Damping Ratio with Shearing Strain and Isotropic Confining Pressure from the Resonant Column Tests of Specimen UTA-27-H.

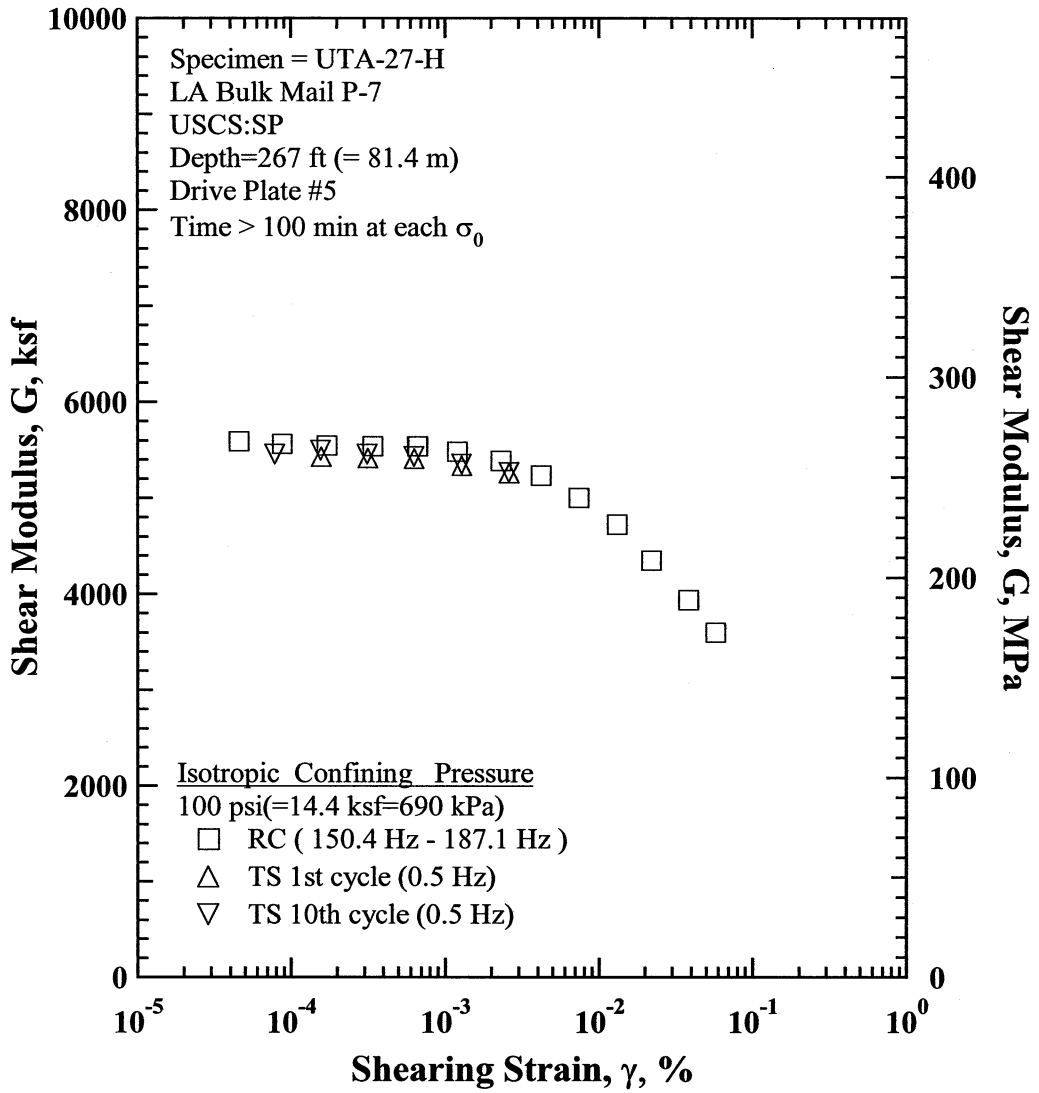

Figure O.11 Comparison of the Variation in Shear Modulus with Shearing Strain at an Isotropic Confining Pressure of 100 psi(=14.4 ksf=690 kPa) from the Combined RCTS Tests of Specimen UTA-27-H.

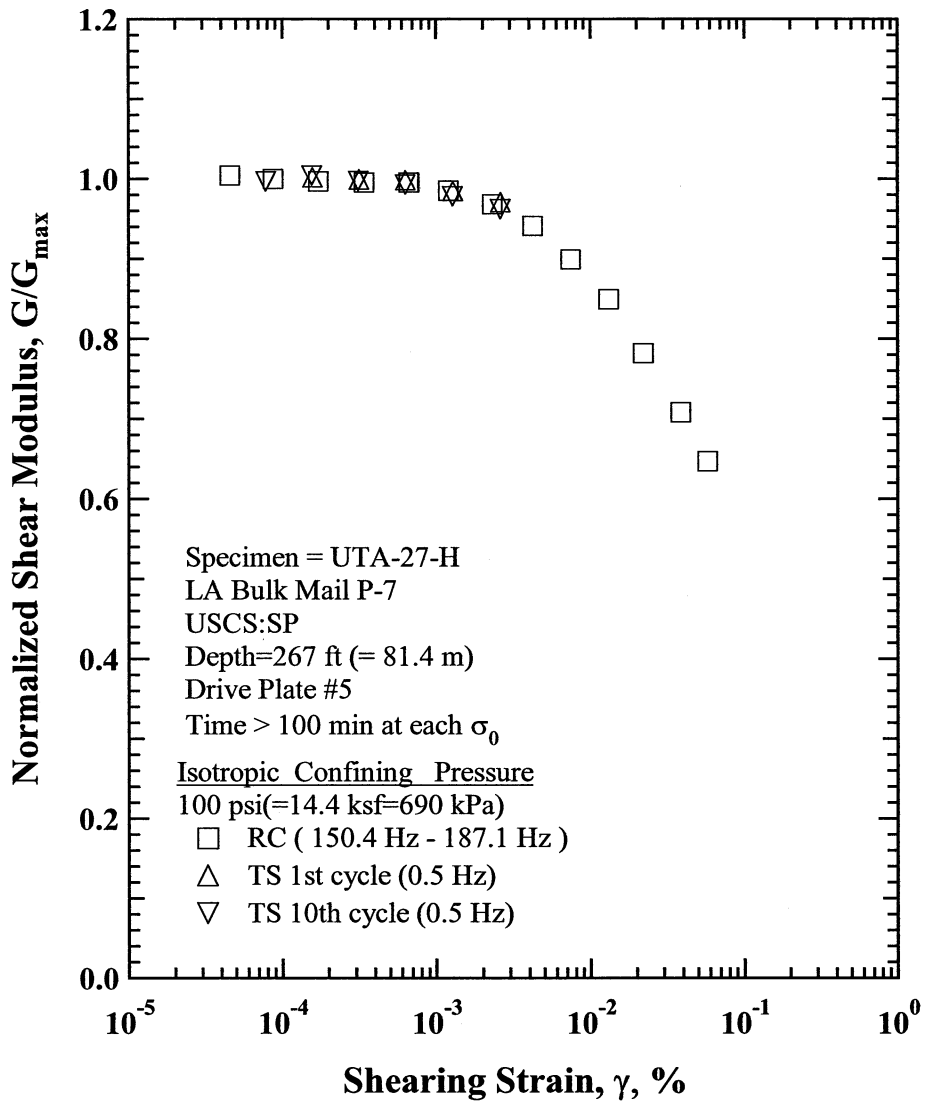

Figure O.12 Comparison of the Variation in Normalized Shear Modulus with Shearing Strain at an Isotropic Confining Pressure of 100 psi(=14.4 ksf=690 kPa) from the Combined RCTS Tests of Specimen UTA-27-H.

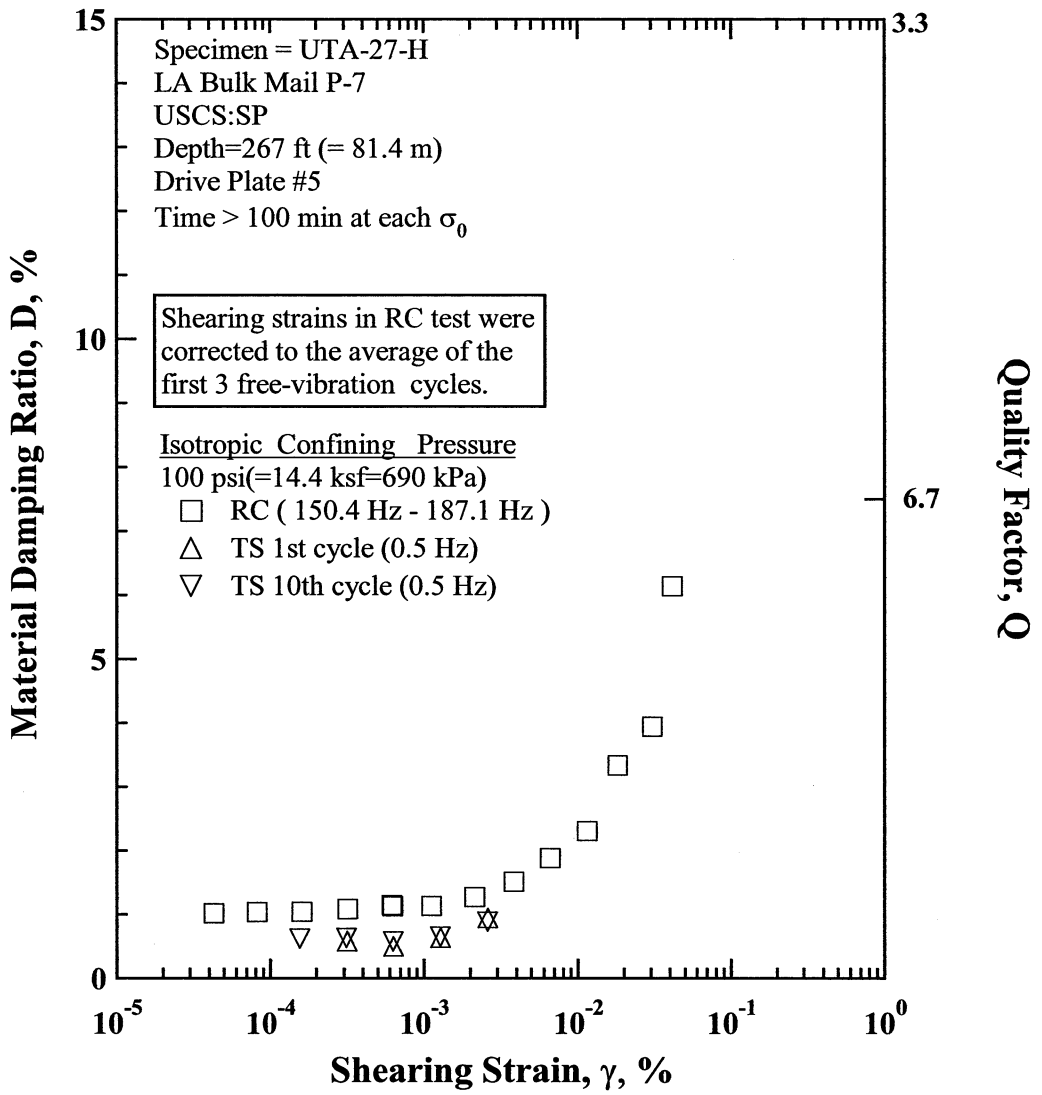

Figure O.13 Comparison of the Variation in Material Damping Ratio with Shearing Strain at an Isotropic Confining Pressure of 100 psi(=14.4 ksf=690 kPa) from the Combined RCTS Tests of Specimen UTA-27-H.

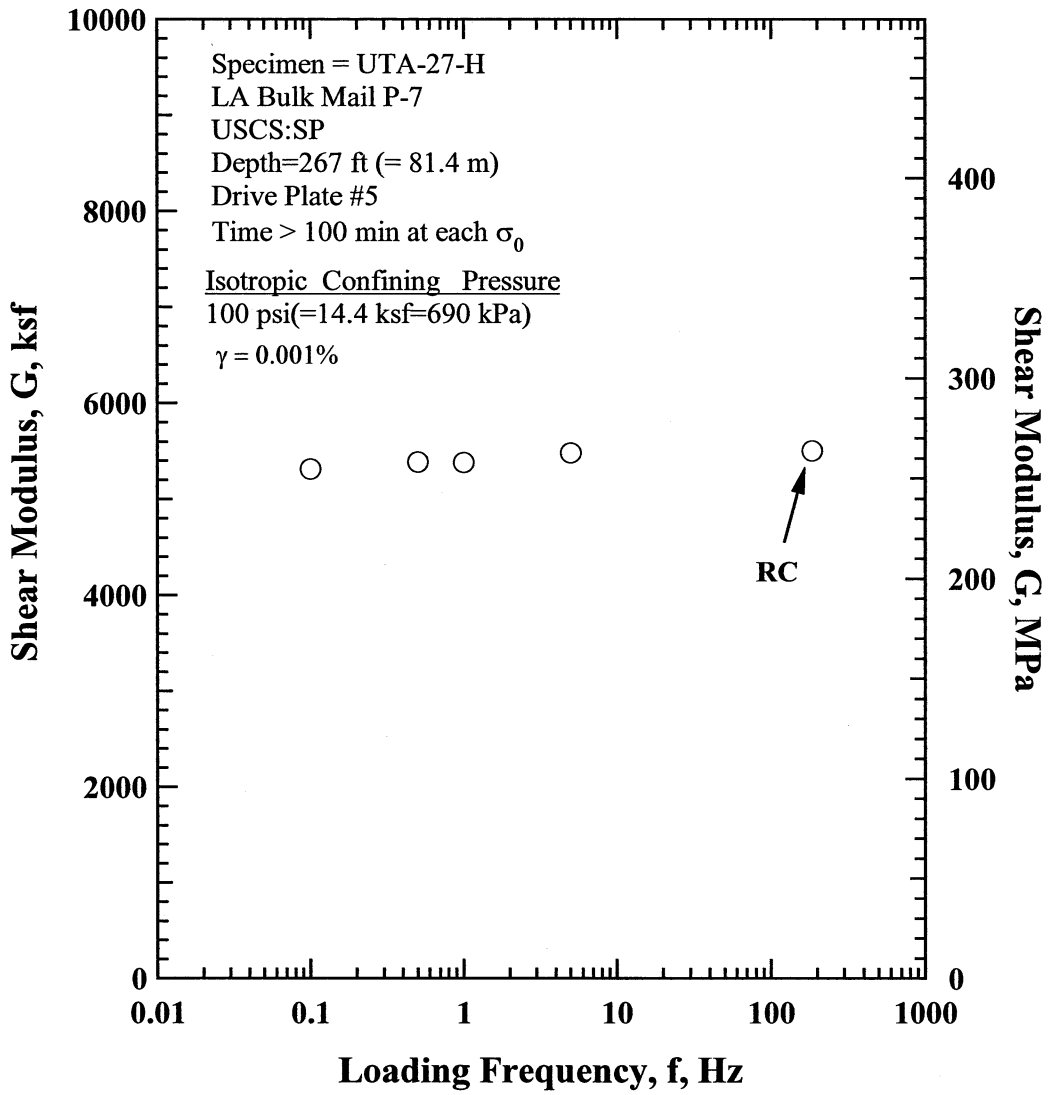

Figure O.14 Comparison of the Variation in Shear Modulus with Loading Frequency at an Isotropic Confining Pressure of 100 psi(=14.4 ksf=690 kPa) from the Combined RCTS Tests of Specimen UTA-27-H.

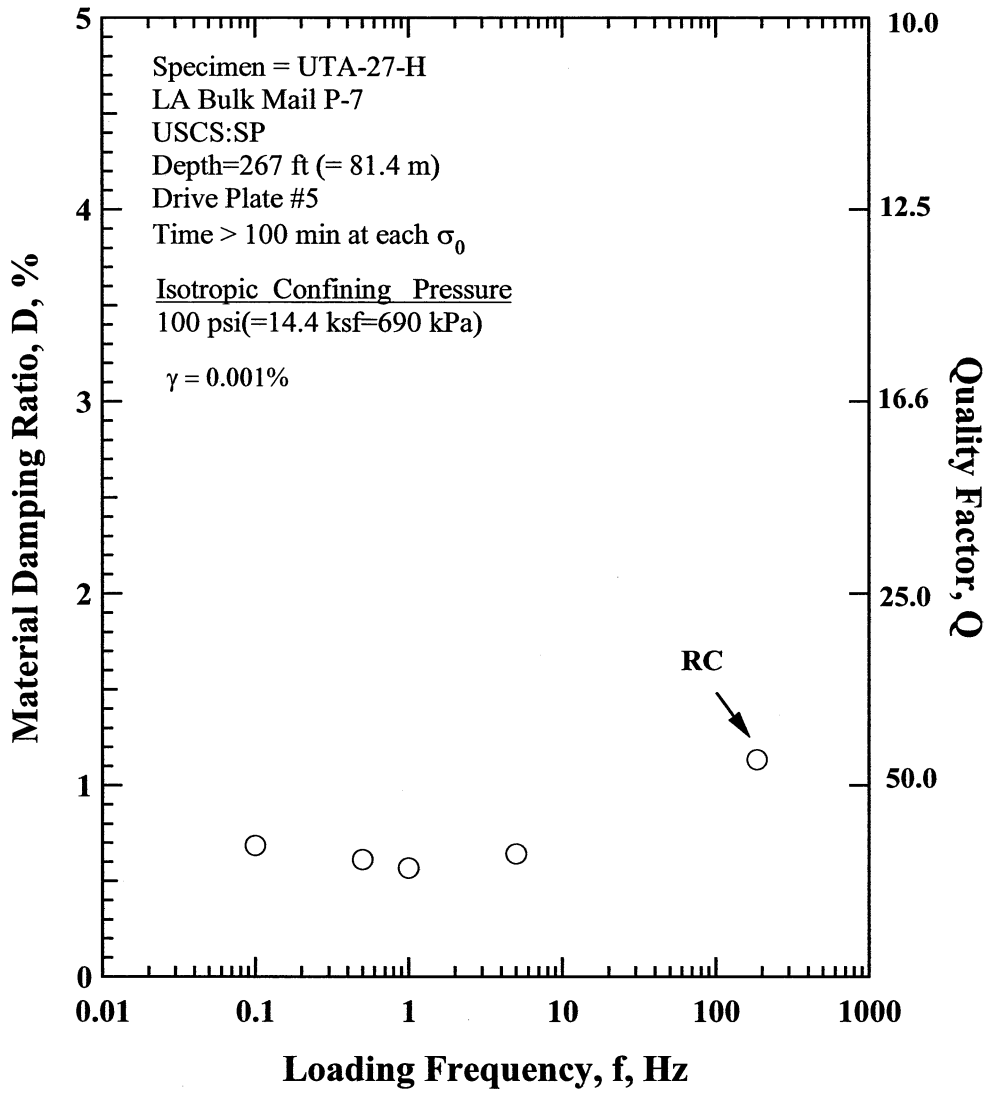

Figure O.15 Comparison of the Variation in Material Damping Ratio with Loading Frequency at an Isotropic Confining Pressure 100 psi(=14.4 ksf=690 kPa) from the Combined RCTS Tests of Specimen UTA-27-H.

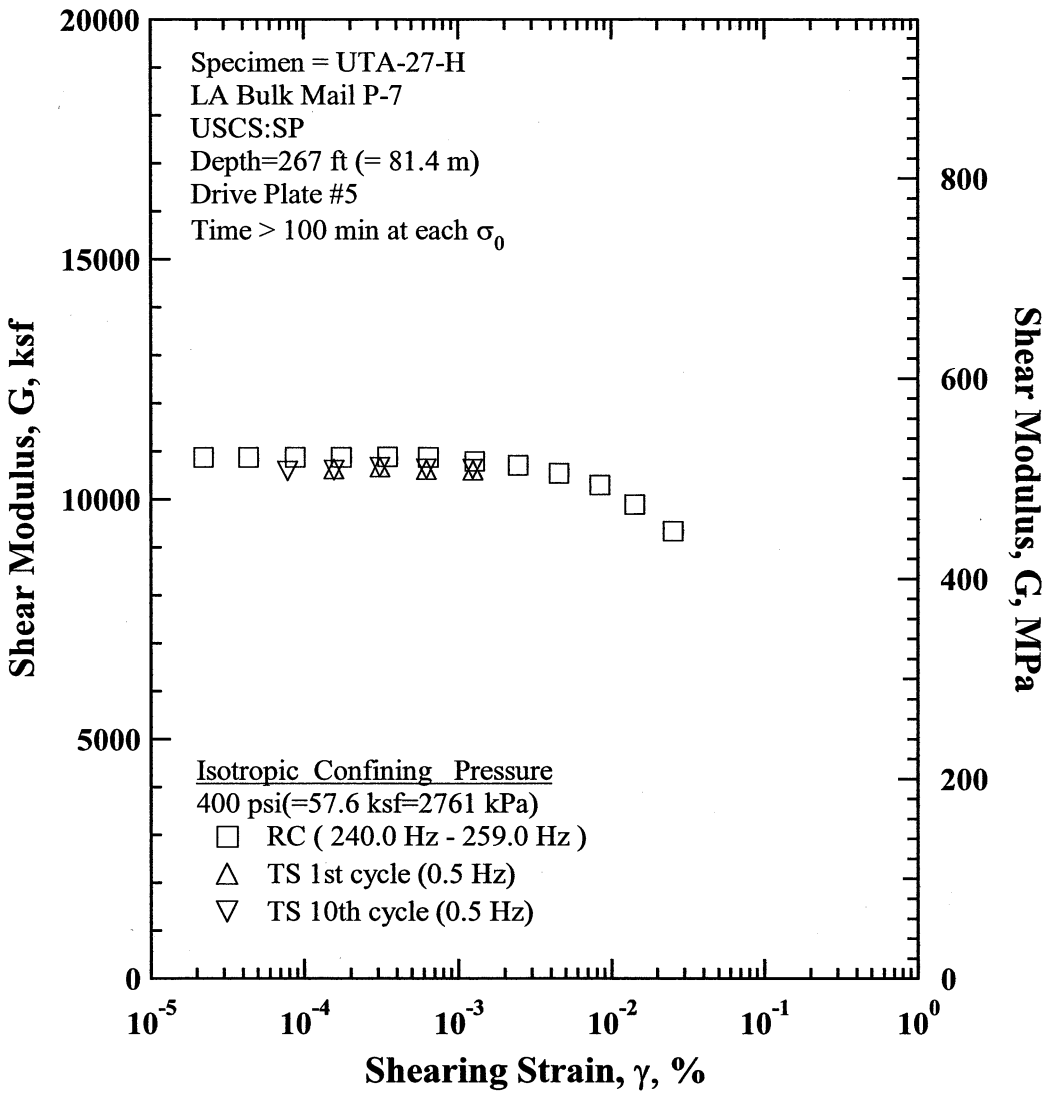

Figure O.16 Comparison of the Variation in Shear Modulus with Shearing Strain at an Isotropic Confining Pressure of 400 psi(=57.6 ksf=2761 kPa) from the Combined RCTS Tests of Specimen UTA-27-H.

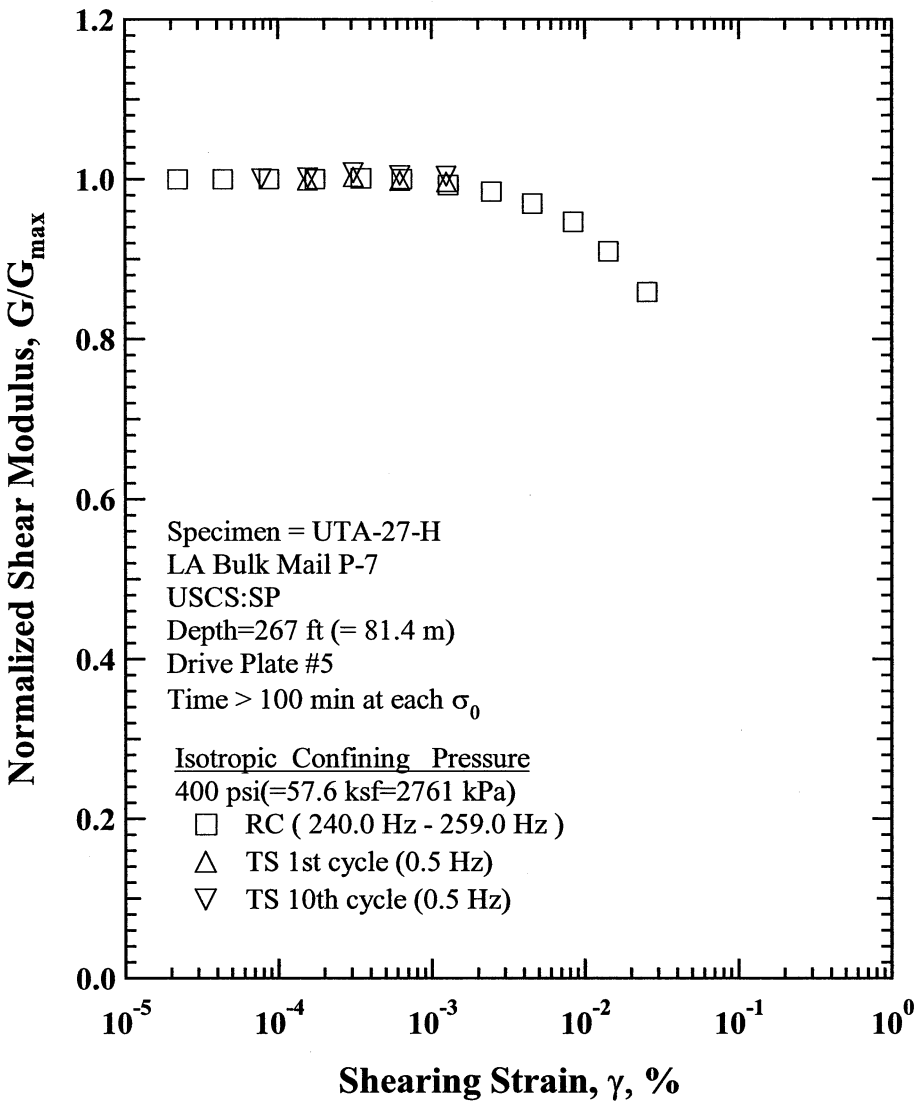

Figure O.17 Comparison of the Variation in Normalized Shear Modulus with Shearing Strain at an Isotropic Confining Pressure of 400 psi(=57.6 ksf=2761 kPa) from the Combined RCTS Tests of Specimen UTA-27-H.

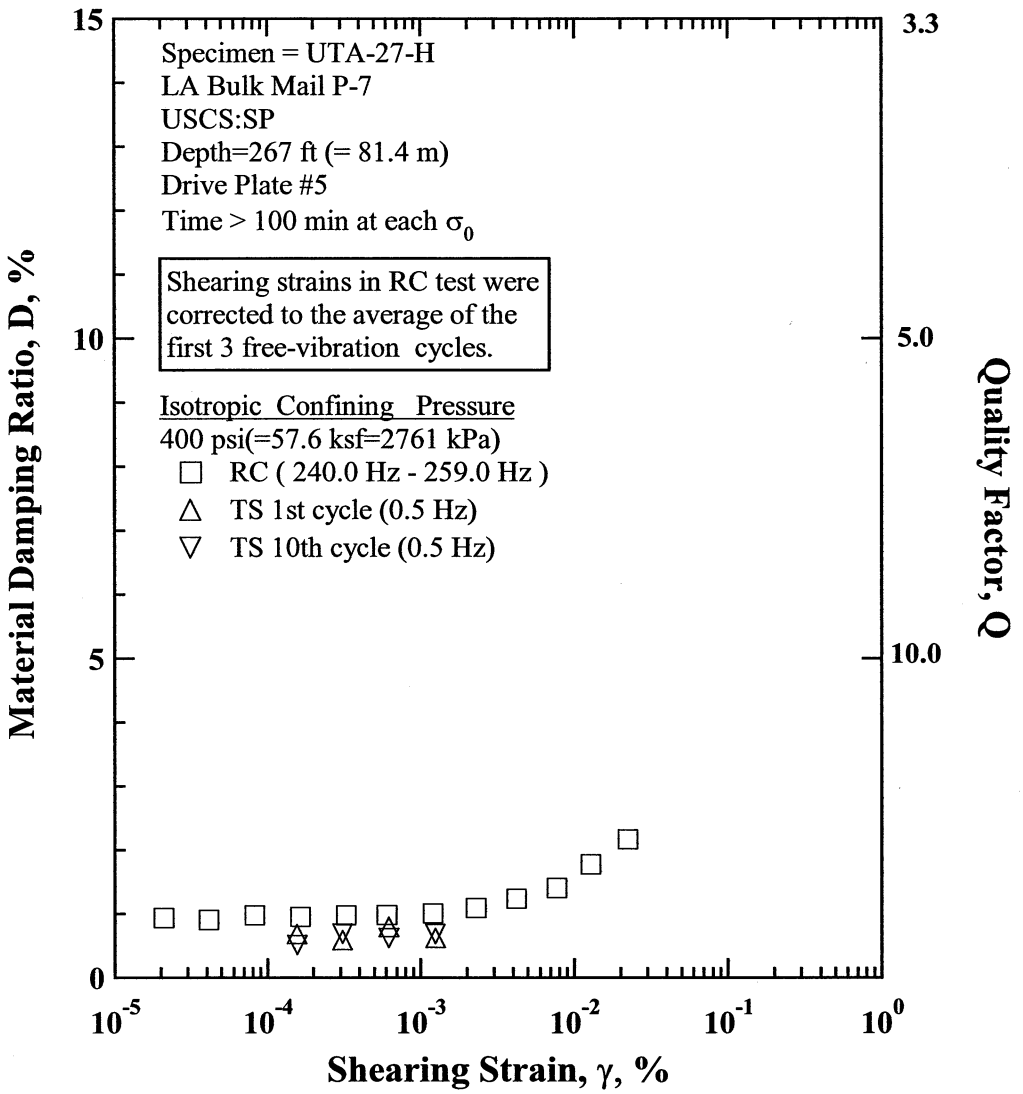

Figure O.18 Comparison of the Variation in Material Damping Ratio with Shearing Strain at an Isotropic Confining Pressure of 400 psi(=57.6 ksf=2761 kPa) from the Combined RCTS Tests of Specimen UTA-27-H.

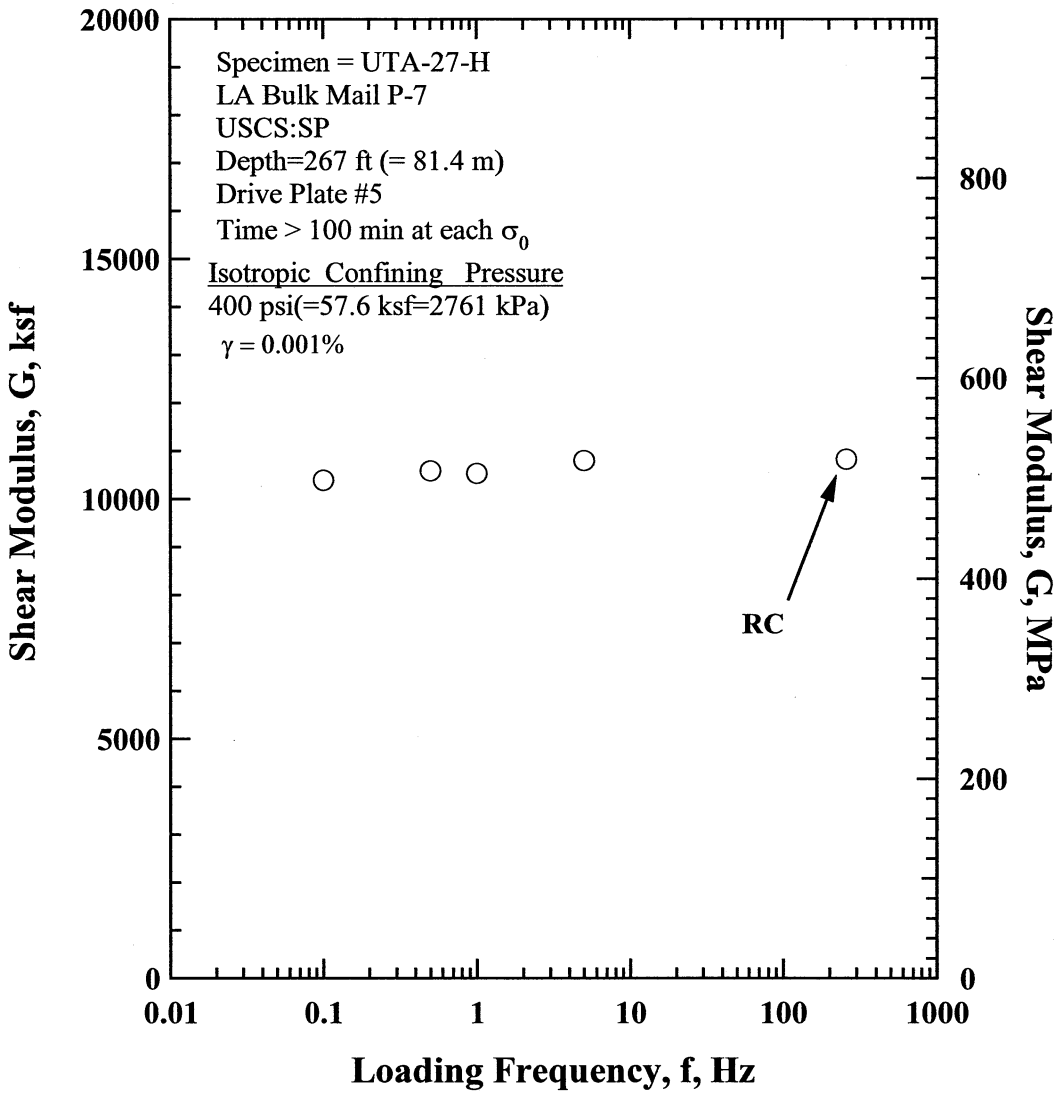

Figure O.19 Comparison of the Variation in Shear Modulus with Loading Frequency at an Isotropic Confining Pressure of 400 psi(=57.6 ksf=2761 kPa) from the Combined RCTS Tests of Specimen UTA-27-H.

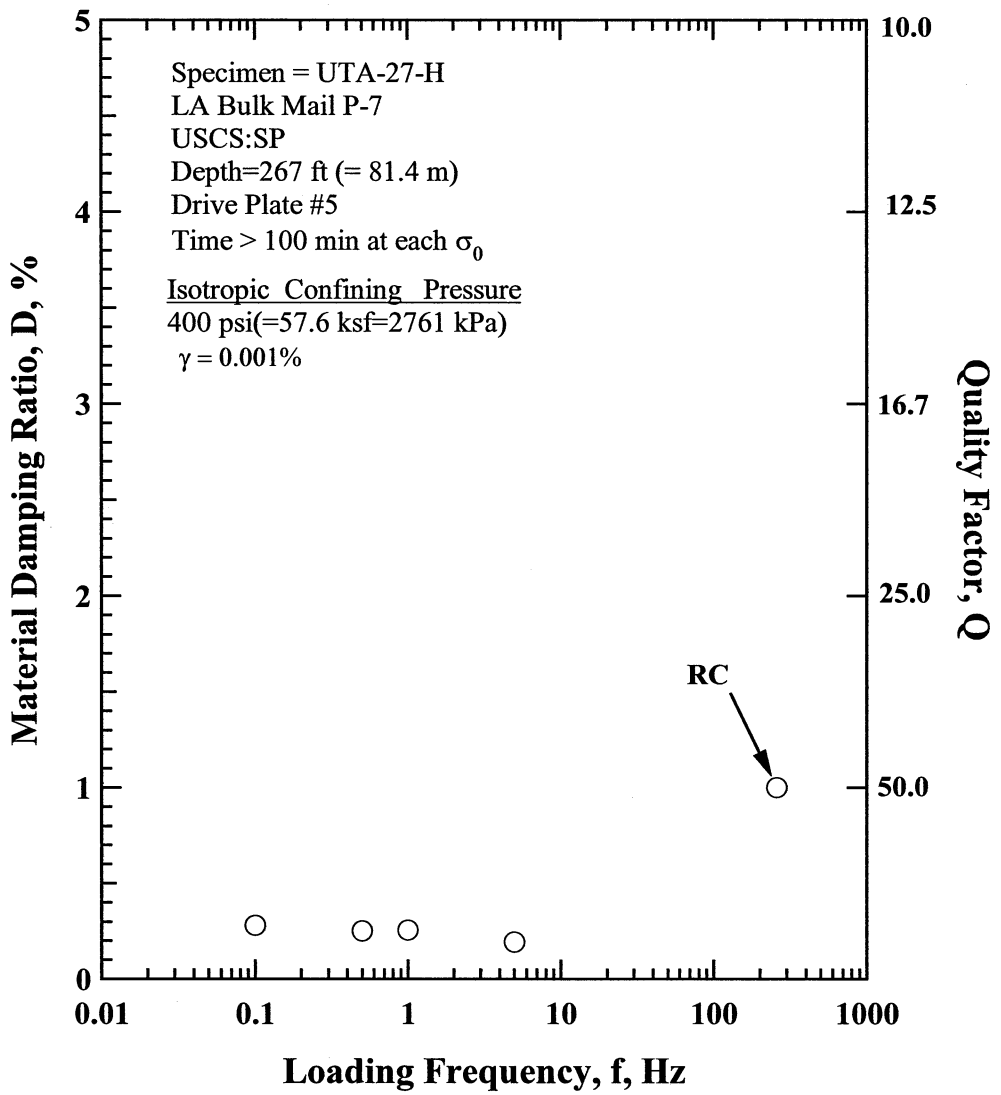

Figure O.20 Comparison of the Variation in Material Damping Ratio with Loading Frequency at an Isotropic Confining Pressure 400 psi(=57.6 ksf=2761 kPa) from the Combined RCTS Tests of Specimen UTA-27-H.

Table O.1 Variation in Low-Amplitude Shear Wave Velocity, Low-Amplitude Shear Modulus, Low-Amplitude Material Damping Ratio and Estimated Void Ratio with Isotropic Confining Pressure from RC Tests of Specimen UTA-27-H.

Effective Isotropic Confining Pressure, σ_o'			Low-Amplitude Shear Modulus, G_{max}		Low-Amplitude Shear Wave Velocity, Vs	Low-Amplitude Material Damping Ratio, D_{min}, %	Estimated Void Ratio, e
(psi)	(psf)	(kPa)	(ksf)	(MPa)	(fps)		
25	3600	172.6	2720	130.4	833	1.31	0.598
50	7200	345.2	3916	187.7	999	1.21	0.593
100	14400	690.3	5456	261.6	1178	1.12	0.586
200	28800	1380.7	7963	381.7	1420	1.09	0.575
400	57600	2761.3	10686	512.3	1640	1.05	0.556

Table O.2 Variation in Shear Modulus, Normalized Shear Modulus and Material Damping Ratio with Shearing Strain from RC Tests of Specimen UTA-27-H; Confining Pressure, σ_o' = 100 psi(=14.40 ksf=690 kPa).

Peak Shearing Strain, %	Shear Modulus, G, ksf	Normalized Shear Modulus, G/G_{max}	Average[+] Shearing Strain, %	Material Damping Ratio[x], D, %
8.72E-05	5563	1.00	8.18E-05	1.04
4.56E-05	5588	1.00	4.28E-05	1.02
1.71E-04	5546	1.00	1.61E-04	1.04
3.40E-04	5539	1.00	3.18E-04	1.09
6.63E-04	5538	1.00	6.18E-04	1.15
6.68E-04	5540	1.00	6.23E-04	1.13
1.20E-03	5481	0.99	1.12E-03	1.13
2.31E-03	5387	0.97	2.14E-03	1.28
4.21E-03	5236	0.94	3.84E-03	1.52
7.39E-03	5002	0.90	6.60E-03	1.88
7.57E-03	5002	0.90	6.76E-03	1.89
1.32E-02	4725	0.85	1.15E-02	2.31
2.20E-02	4349	0.78	1.81E-02	3.34
3.85E-02	3939	0.71	3.07E-02	3.94
5.78E-02	3598	0.65	4.13E-02	6.14

[+] Average Shearing Strain from the First Three Cycles of the Free Vibration Decay Curve

[x] Average Damping Ratio from the First Three Cycles of the Free Vibration Decay Curve

Table O.3 Variation in Shear Modulus, Normalized Shear Modulus and Material Damping Ratio with Shearing Strain from TS Tests of Specimen UTA-27-H; Confining Pressure, σ_o' =100 psi(=14.40 ksf=690 kPa).

First Cycle				Tenth Cycle			
Peak Shearing Strain, %	Shear Modulus, G, ksf	Normalized Shear Modulus, G/G_{max}	Material Damping Ratio, D, %	Peak Shearing Strain, %	Shear Modulus, G, ksf	Normalized Shear Modulus, G/G_{max}	Material Damping Ratio, D, %
1.58E-04	5424	1.00		1.56E-04	5492	1.00	0.62
3.17E-04	5411	1.00	0.57	3.15E-04	5454	1.00	0.62
6.35E-04	5406	1.00	0.49	6.33E-04	5430	0.99	0.57
1.29E-03	5331	0.98	0.63	1.28E-03	5350	0.98	0.64
2.62E-03	5254	0.97	0.94	2.62E-03	5262	0.96	0.88

Table O.4 Variation in Shear Modulus, Normalized Shear Modulus and Material Damping Ratio with Shearing Strain from RC Tests of Specimen UTA-27-H; Confining Pressure, σ_o' = 400 psi(=57.6 ksf=2761 kPa).

Peak Shearing Strain, %	Shear Modulus, G, ksf	Normalized Shear Modulus, G/G_{max}	Average[+] Shearing Strain, %	Material Damping Ratio[x], D, %
4.36E-05	10874	1.00	4.12E-05	0.91
2.22E-05	10875	1.00	2.09E-05	0.94
8.71E-05	10875	1.00	8.20E-05	0.98
1.74E-04	10875	1.00	1.64E-04	0.95
3.47E-04	10885	1.00	3.27E-04	0.98
6.40E-04	10875	1.00	6.02E-04	0.99
1.28E-03	10792	0.99	1.20E-03	1.01
2.45E-03	10706	0.98	2.29E-03	1.09
4.53E-03	10542	0.97	4.20E-03	1.24
8.38E-03	10295	0.95	7.69E-03	1.41
1.42E-02	9891	0.91	1.28E-02	1.78
2.54E-02	9339	0.86	2.23E-02	2.17

[+] Average Shearing Strain from the First Three Cycles of the Free Vibration Decay Curve

[x] Average Damping Ratio from the First Three Cycles of the Free Vibration Decay Curve

Table O.5 Variation in Shear Modulus, Normalized Shear Modulus and Material Damping Ratio with Shearing Strain from TS Tests of Specimen UTA-27-H; Confining Pressure, σ_o' =400 psi(=57.6 ksf=2761 kPa).

First Cycle				Tenth Cycle			
Peak Shearing Strain, %	Shear Modulus, G, ksf	Normalized Shear Modulus, G/G_{max}	Material Damping Ratio, D, %	Peak Shearing Strain, %	Shear Modulus, G, ksf	Normalized Shear Modulus, G/G_{max}	Material Damping Ratio, D, %
1.57E-04	10618	1.00	0.68	1.57E-04	10598	1.00	0.51
3.12E-04	10661	1.00	0.58	3.12E-04	10663	1.01	0.68
6.27E-04	10610	1.00	0.79	6.26E-04	10625	1.00	0.62
1.26E-03	10594	1.00	0.62	1.25E-03	10618	1.00	0.68

APPENDIX P

Specimen No. 15
UT Specimen ID: UTA-27-J

Gilroy #3 P-4
Depth = 182 ft (= 55.5m)
Soil Type: Clay (CL)

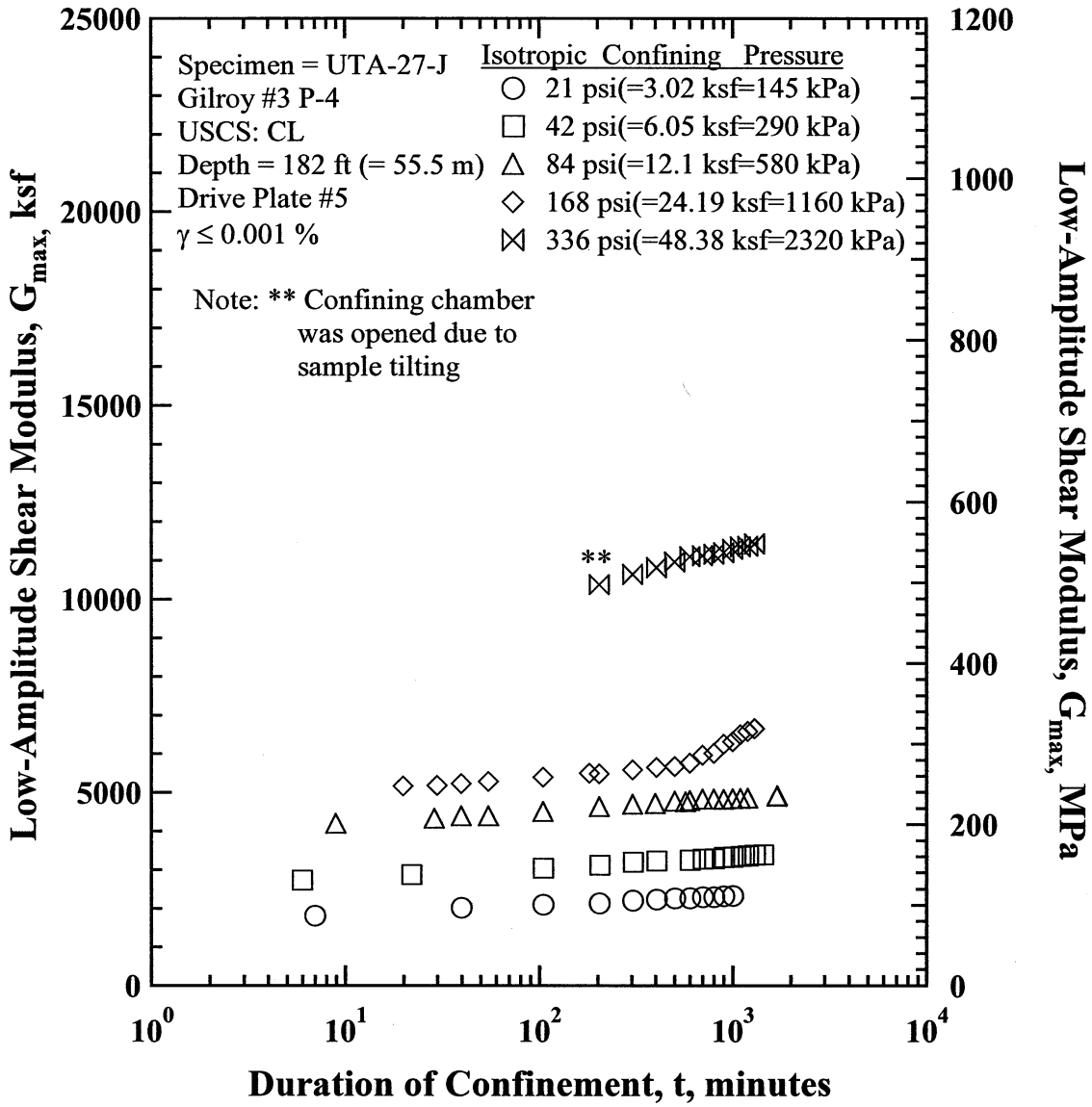

Figure P.1 Variation in Low-Amplitude Shear Modulus with Magnitude and Duration of Isotropic Confining Pressure from Resonant Column Tests of Specimen UTA-27-J.

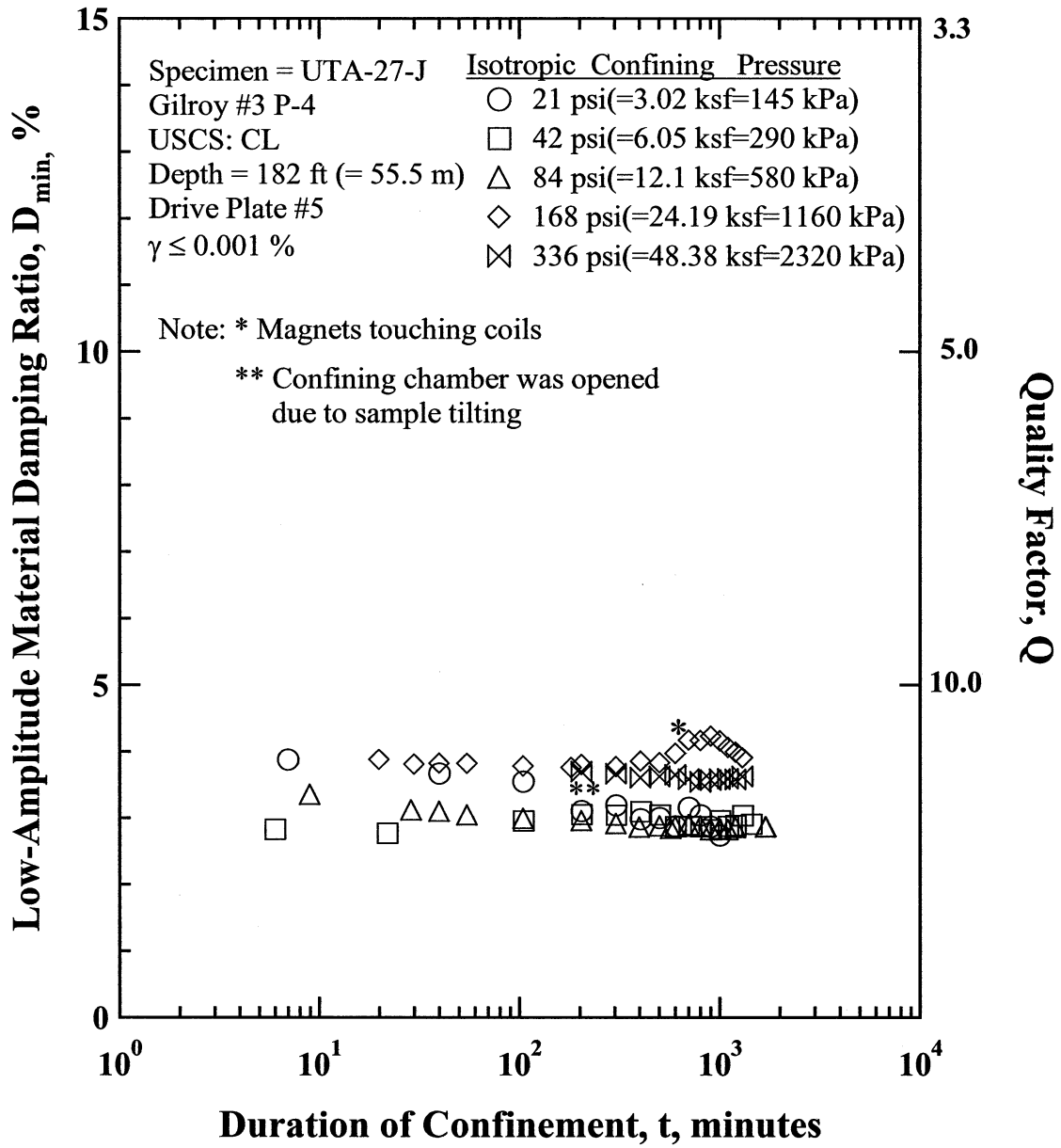

Figure P.2 Variation in Low-Amplitude Material Damping Ratio with Magnitude and Duration of Isotropic Confining Pressure from Resonant Column Tests of Specimen UTA-27-J

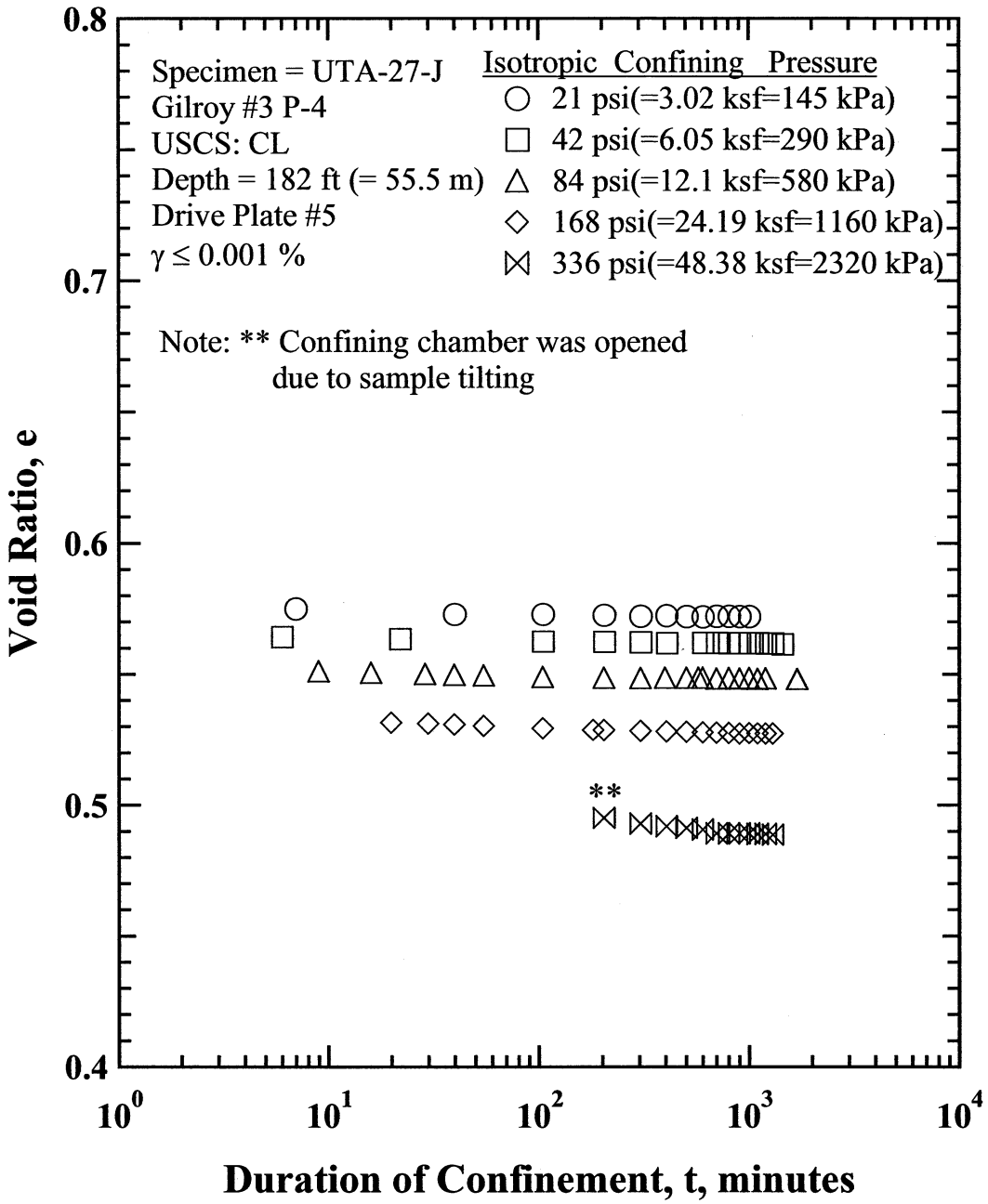

Figure P.3 Variation in Estimated Void Ratio with Magnitude and Duration of Isotropic Confining Pressure from Resonant Column Tests of Specimen UTA-27-J.

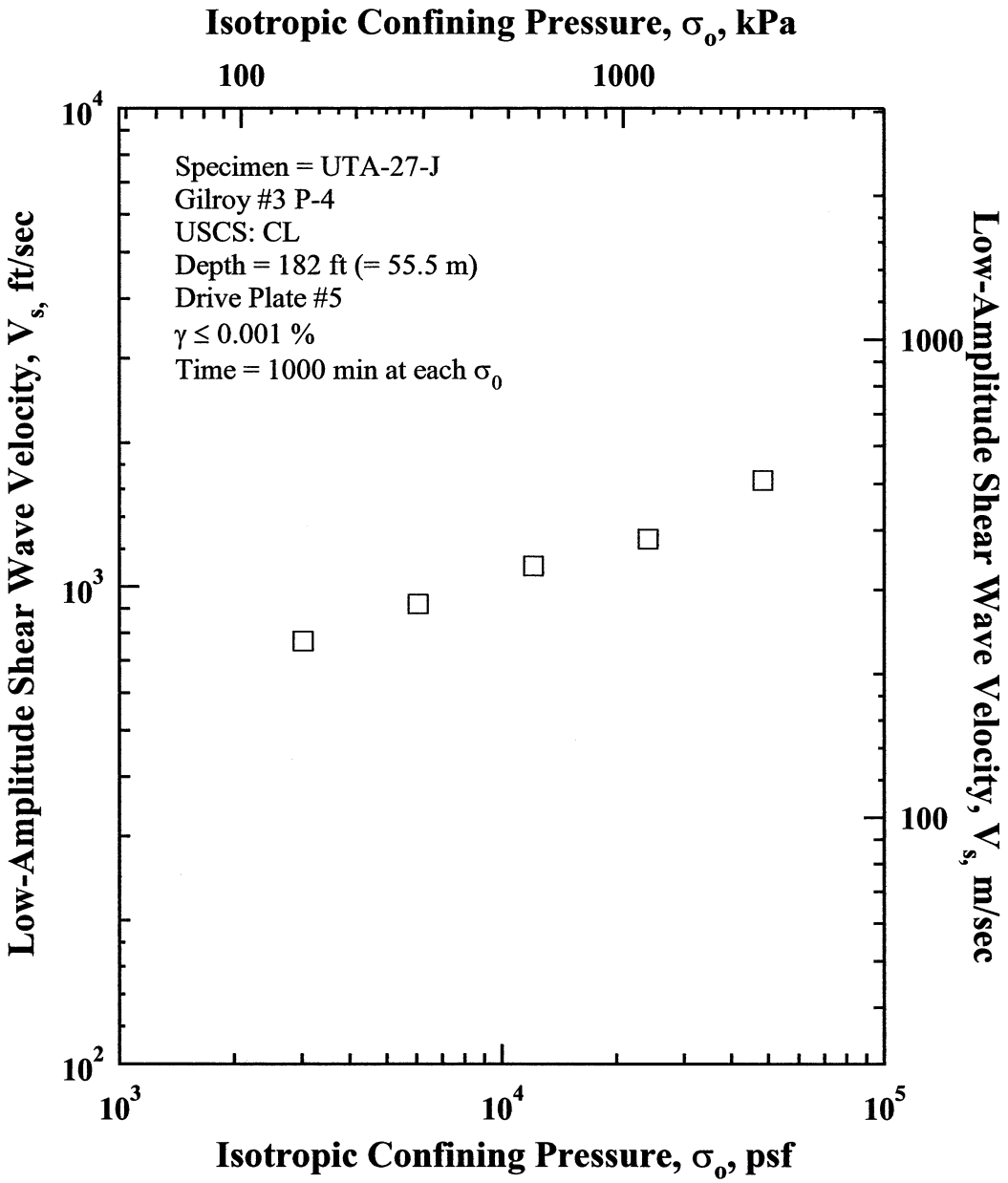

Figure P.4 Variation in Low-Amplitude Shear Wave Velocity with Isotropic Confining Pressure from Resonant Column Tests of Specimen UTA-27-J.

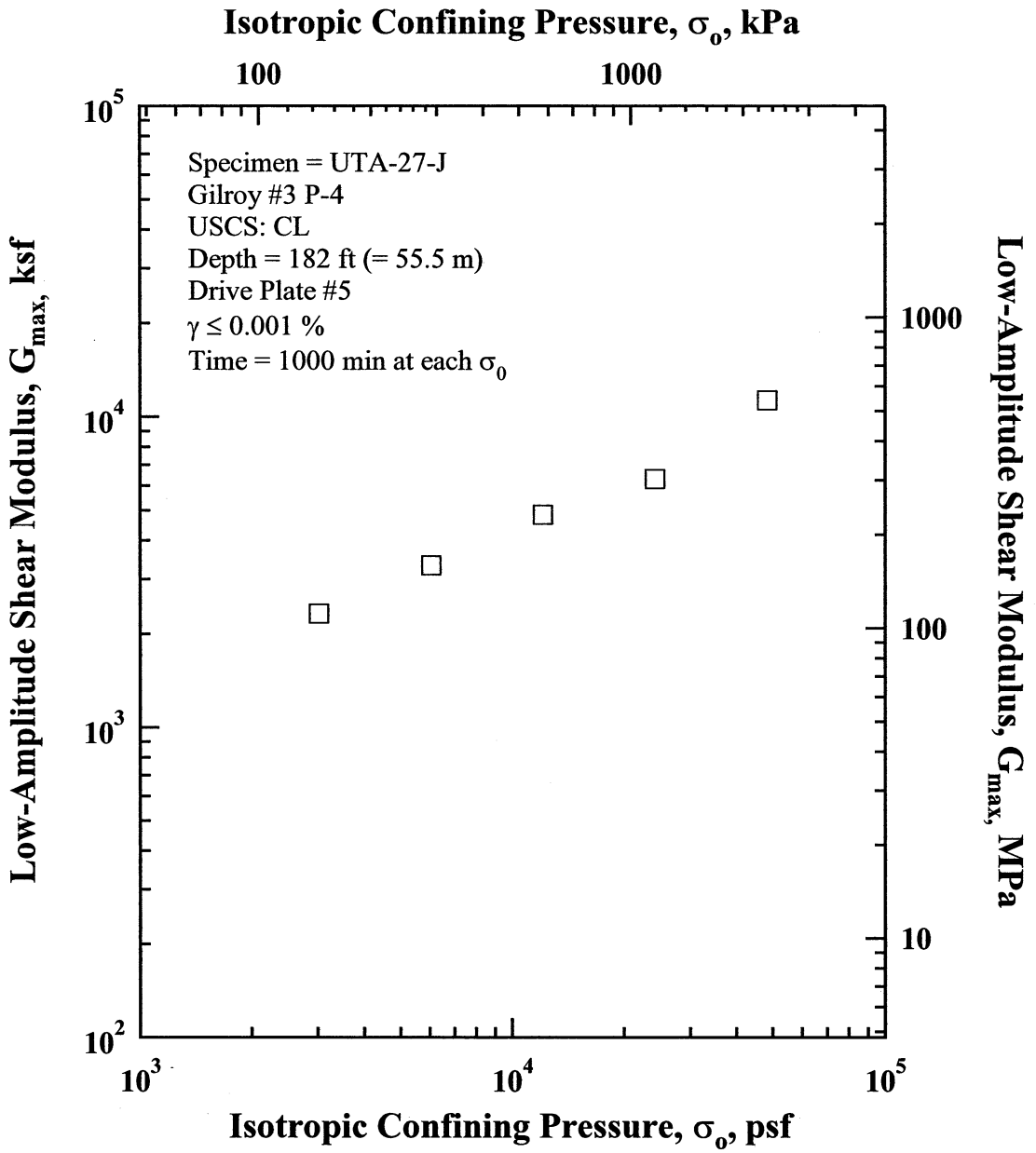

Figure P.5 Variation in Low-Amplitude Shear Modulus with Isotropic Confining Pressure from Resonant Column Tests of Specimen UTA-27-J.

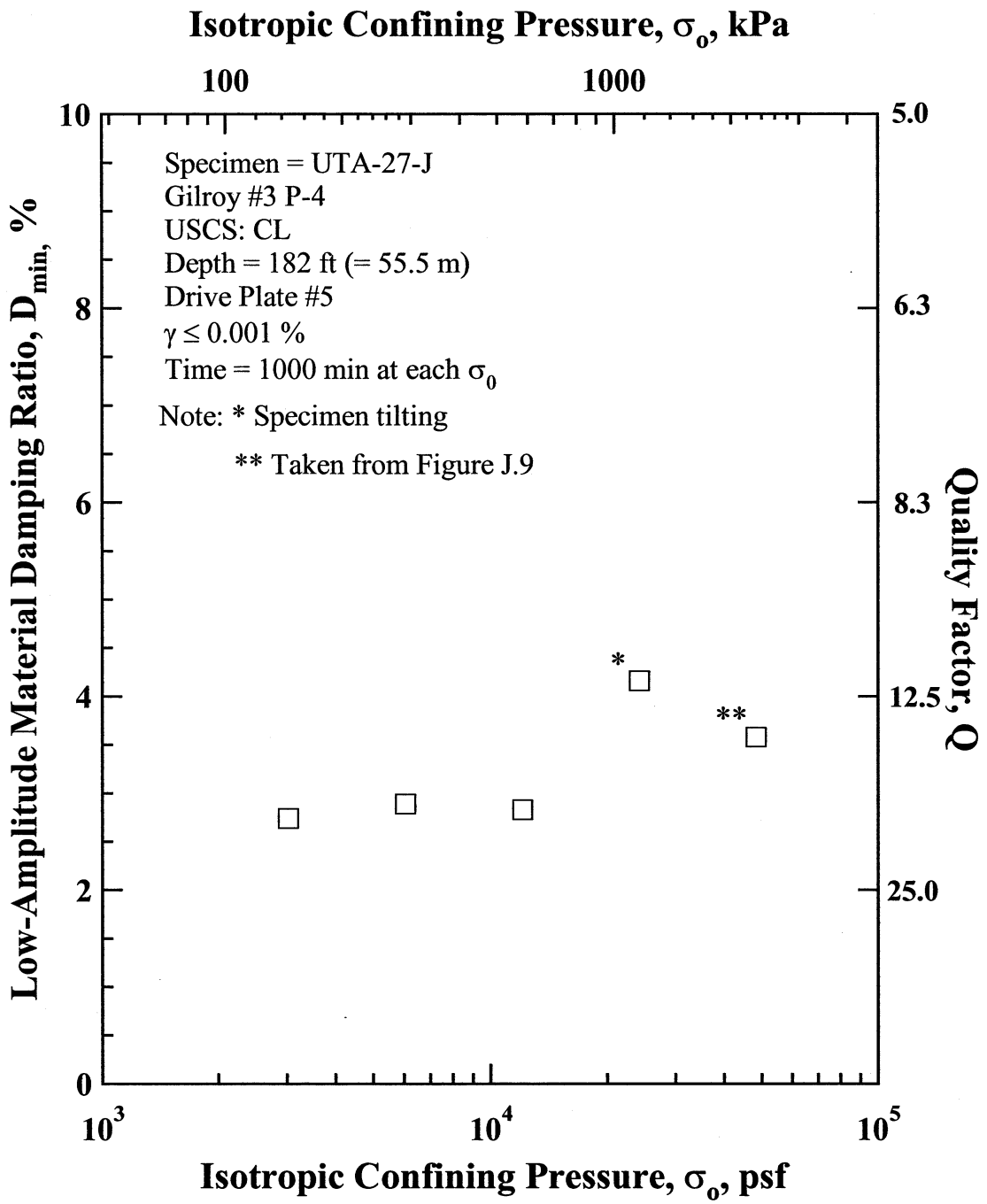

Figure P.6 Variation in Low-Amplitude Material Damping Ratio with Isotropic Confining Pressure from Resonant Column Tests of Specimen UTA-27-J.

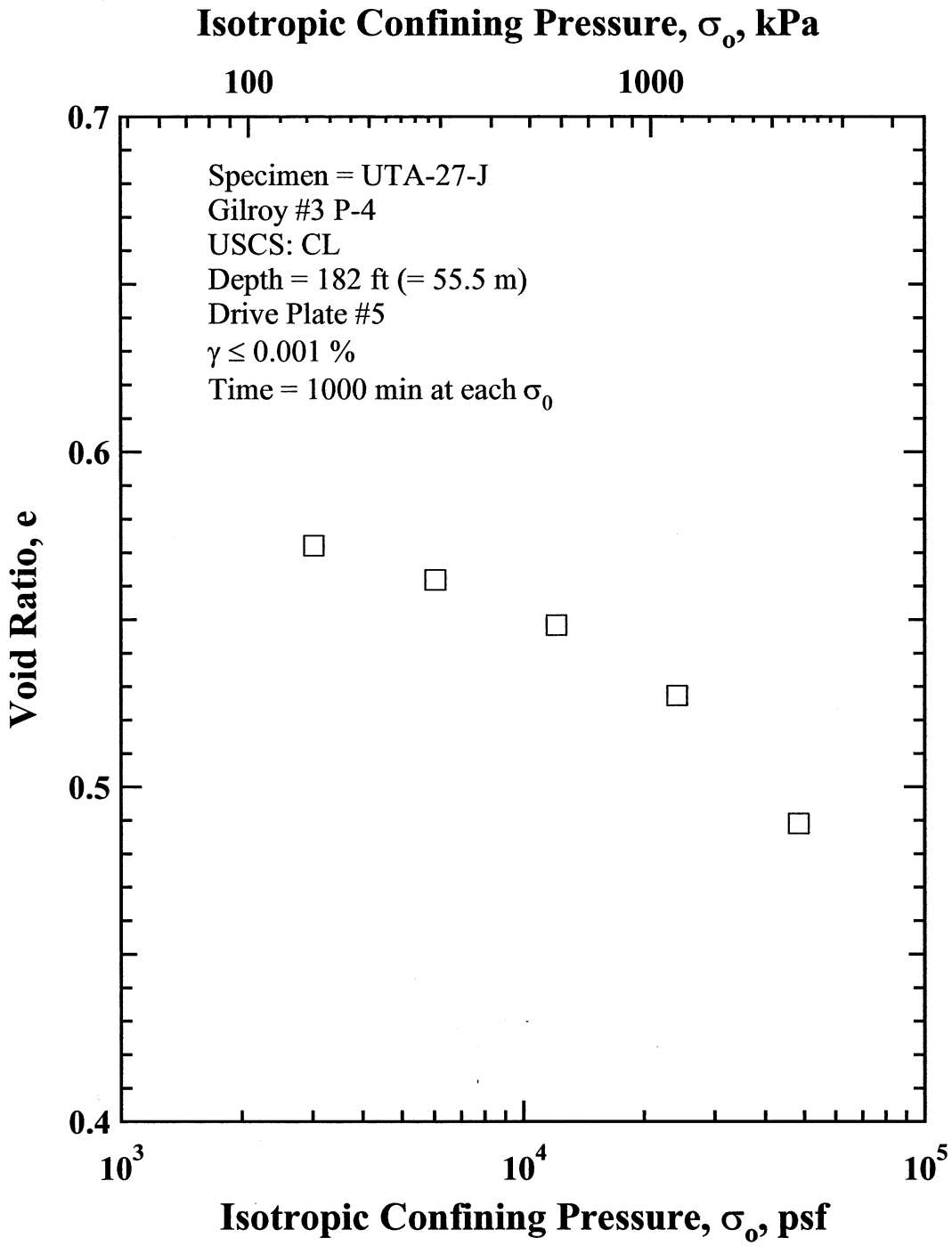

Figure P.7 Variation in Estimated Void Ratio with Isotropic Confining Pressure from Resonant Column Tests of Specimen UTA-27-J.

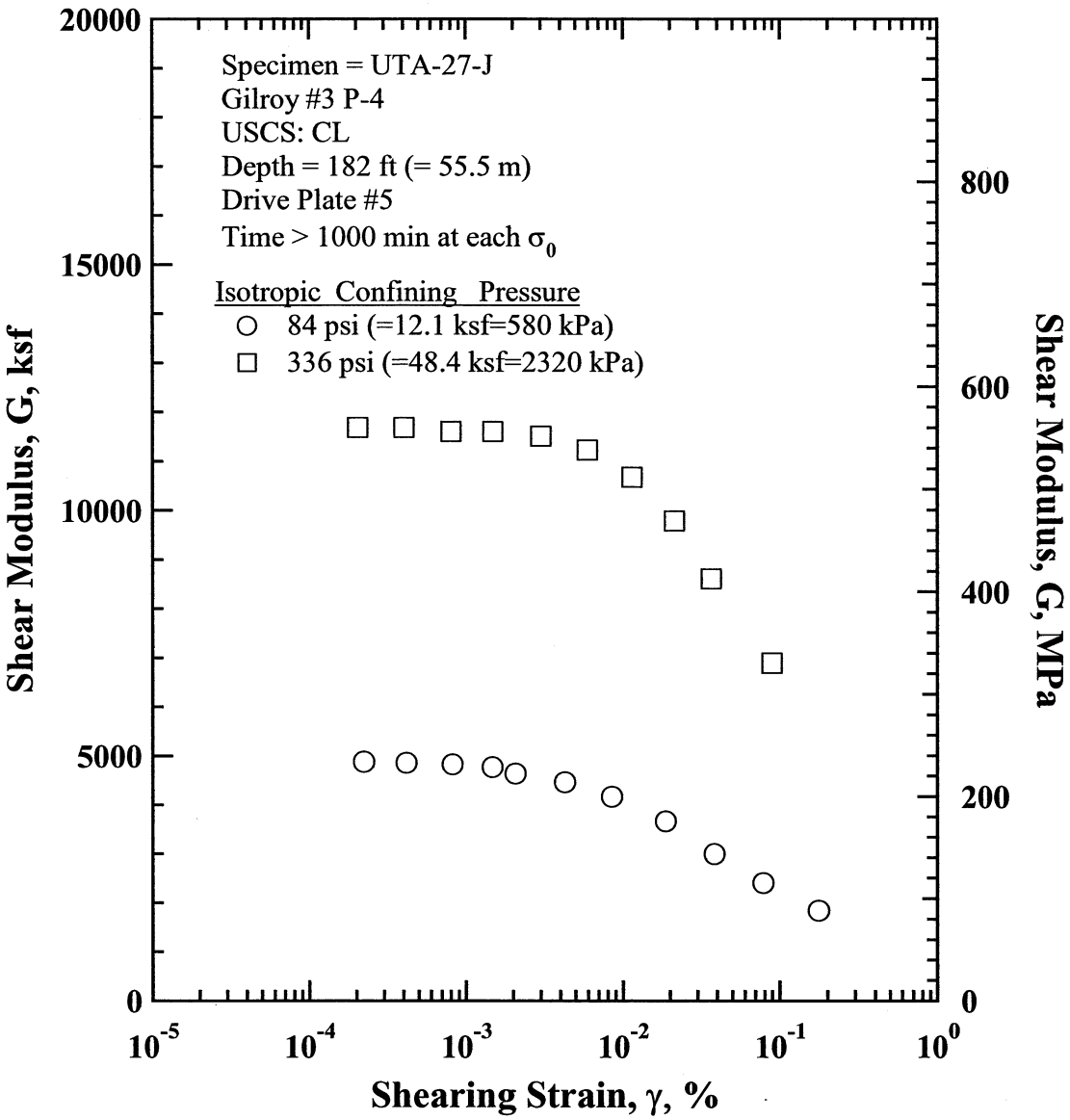

Figure P.8 Comparison of the Variation in Shear Modulus with Shearing Strain and Isotropic Confining Pressure from the Resonant Column Tests of Specimen UTA-27-J.

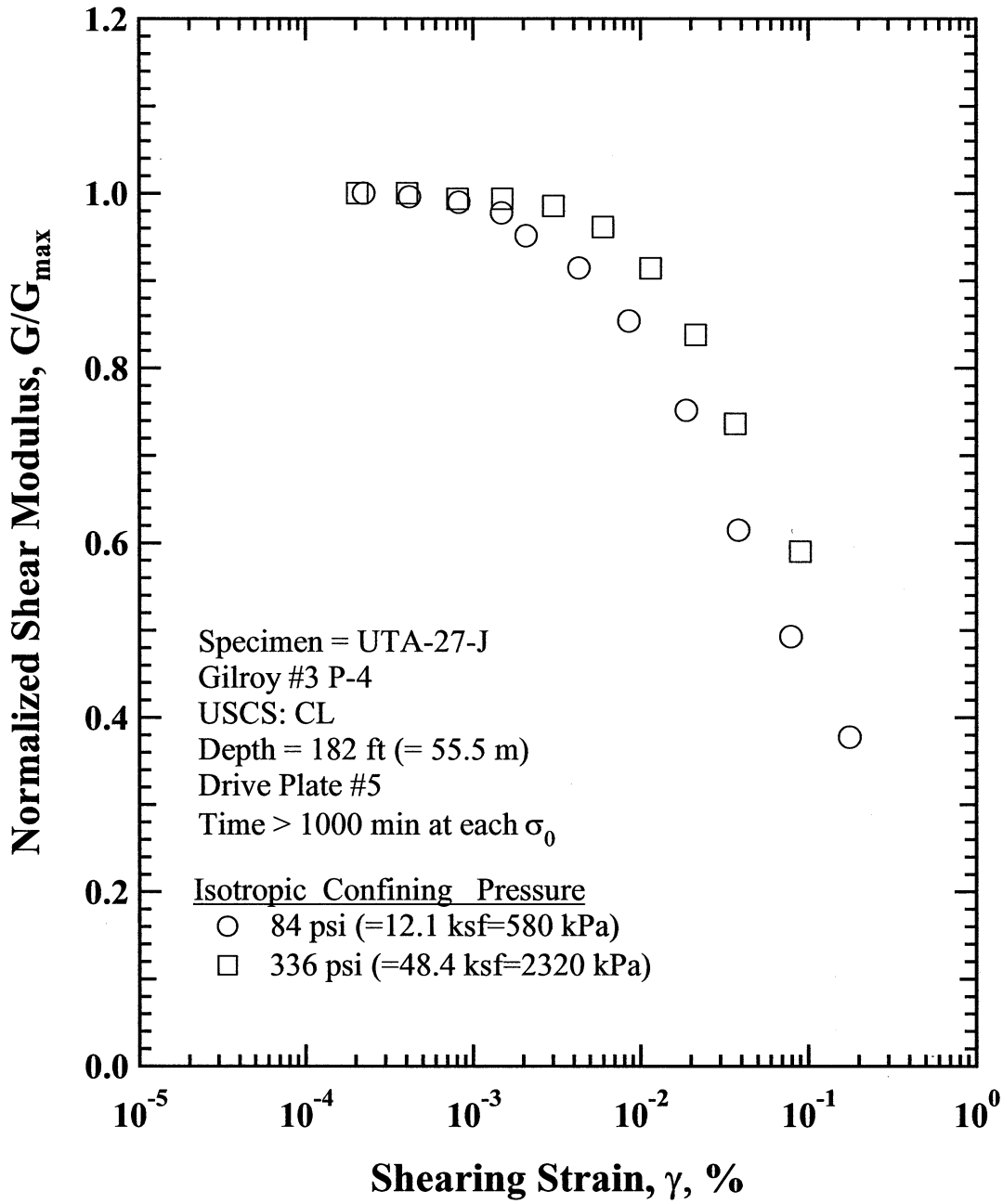

Figure P.9 Comparison of the Variation in Normalized Shear Modulus with Shearing Strain and Isotropic Confining Pressure from the Resonant Column Tests of Specimen UTA-27-J.

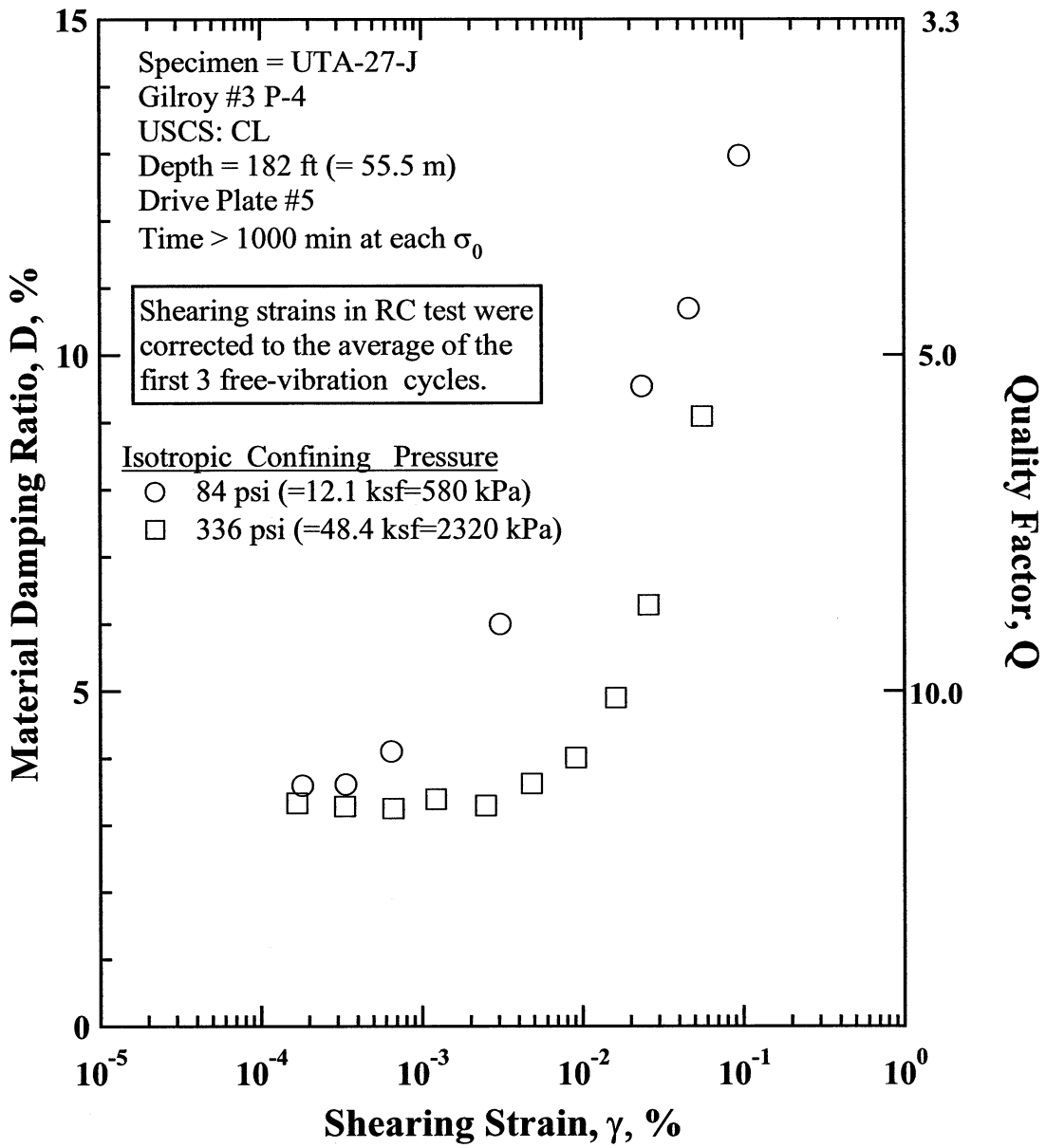

Figure P.10 Comparison of the Variation in Material Damping Ratio with Shearing Strain and Isotropic Confining Pressure from the Resonant Column Tests of Specimen UTA-27-J.

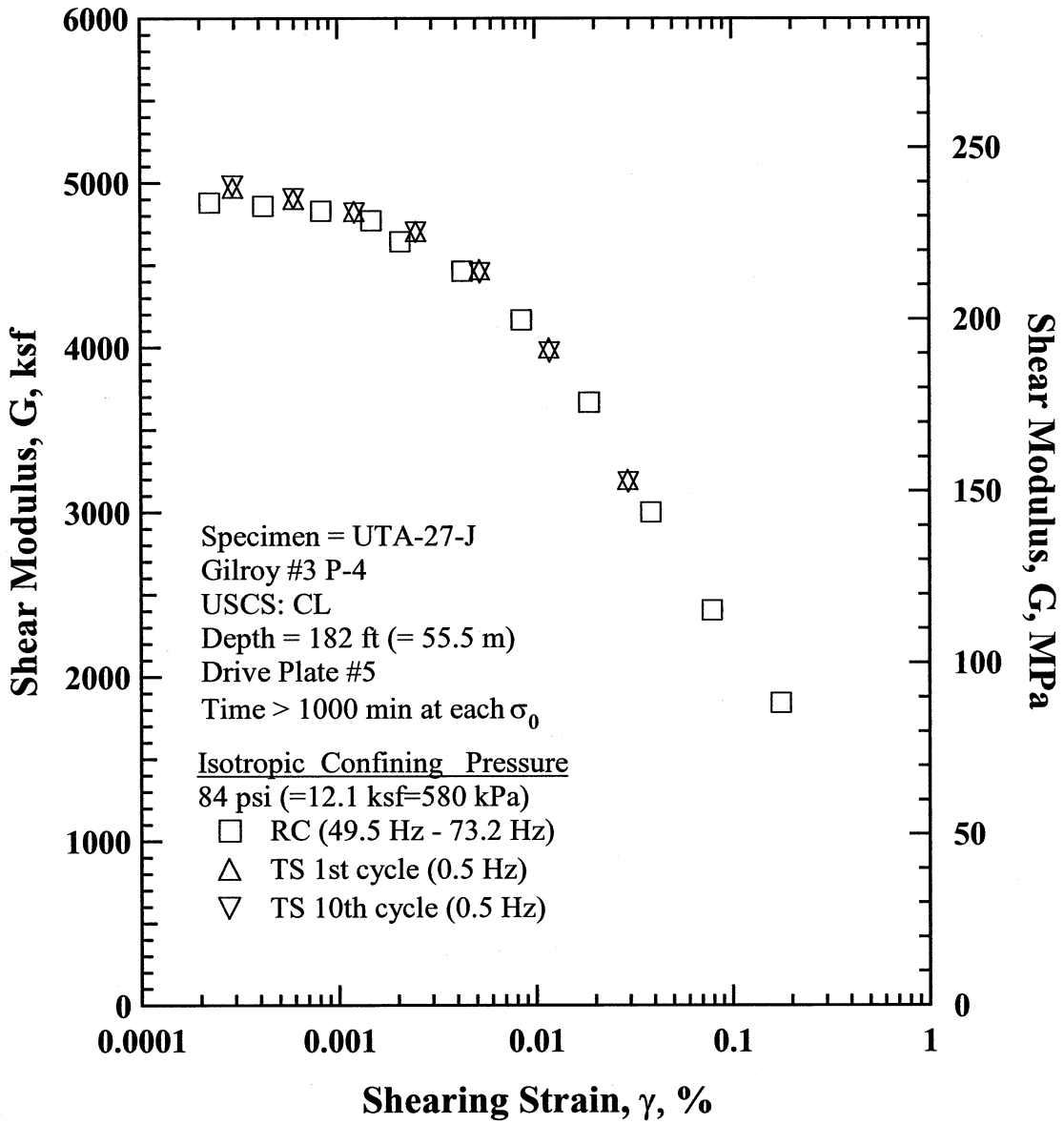

Figure P.11 Comparison of the Variation in Shear Modulus with Shearing Strain at an Isotropic Confining Pressure of 84 psi (=12.1 ksf=580 kPa) from the Combined RCTS Tests of Specimen UTA-27-J.

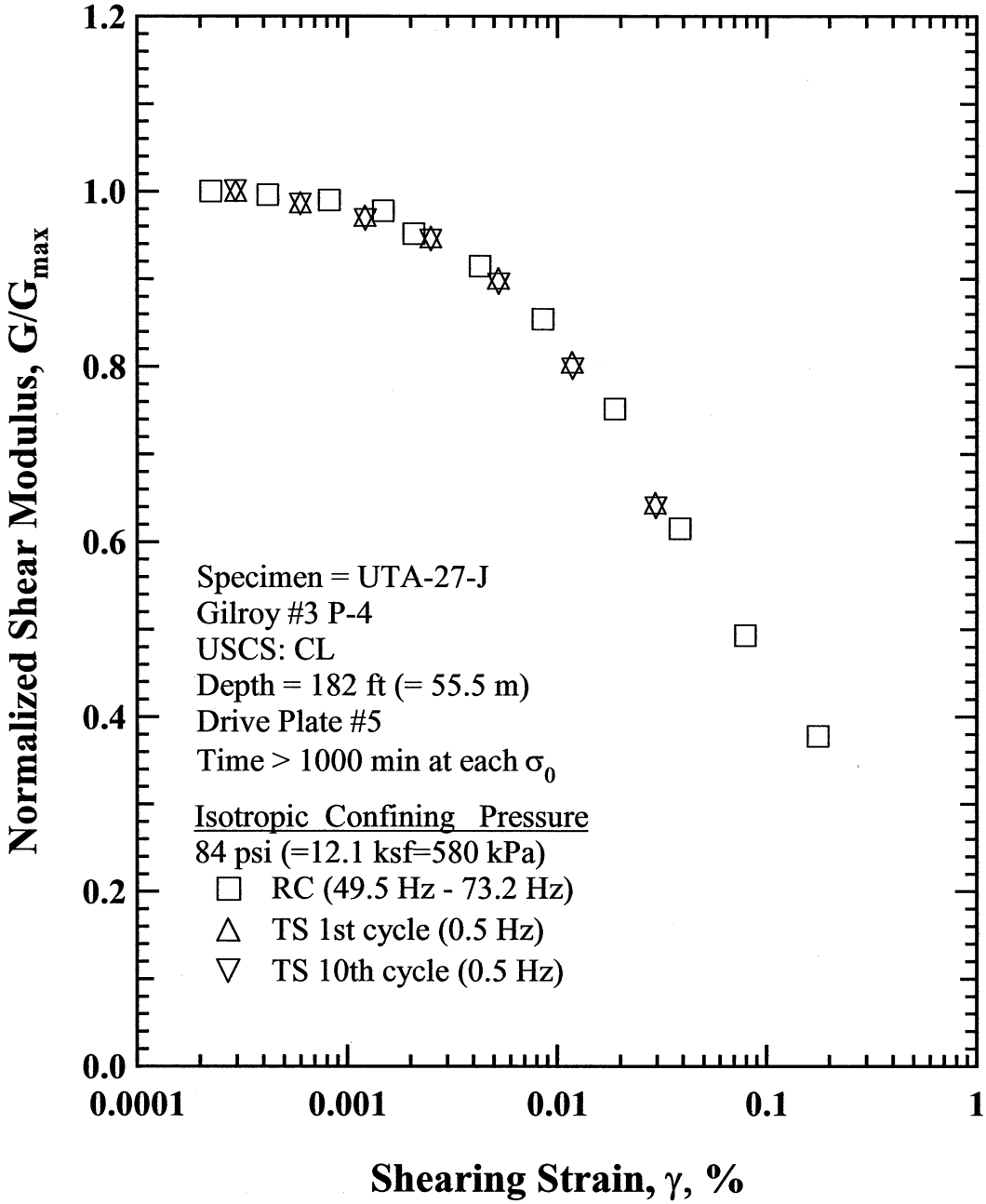

Figure P.12 Comparison of the Variation in Normalized Shear Modulus with Shearing Strain at an Isotropic Confining Pressure of 84 psi (=12.1 ksf=580 kPa) from the Combined RCTS Tests of Specimen UTA-27-J.

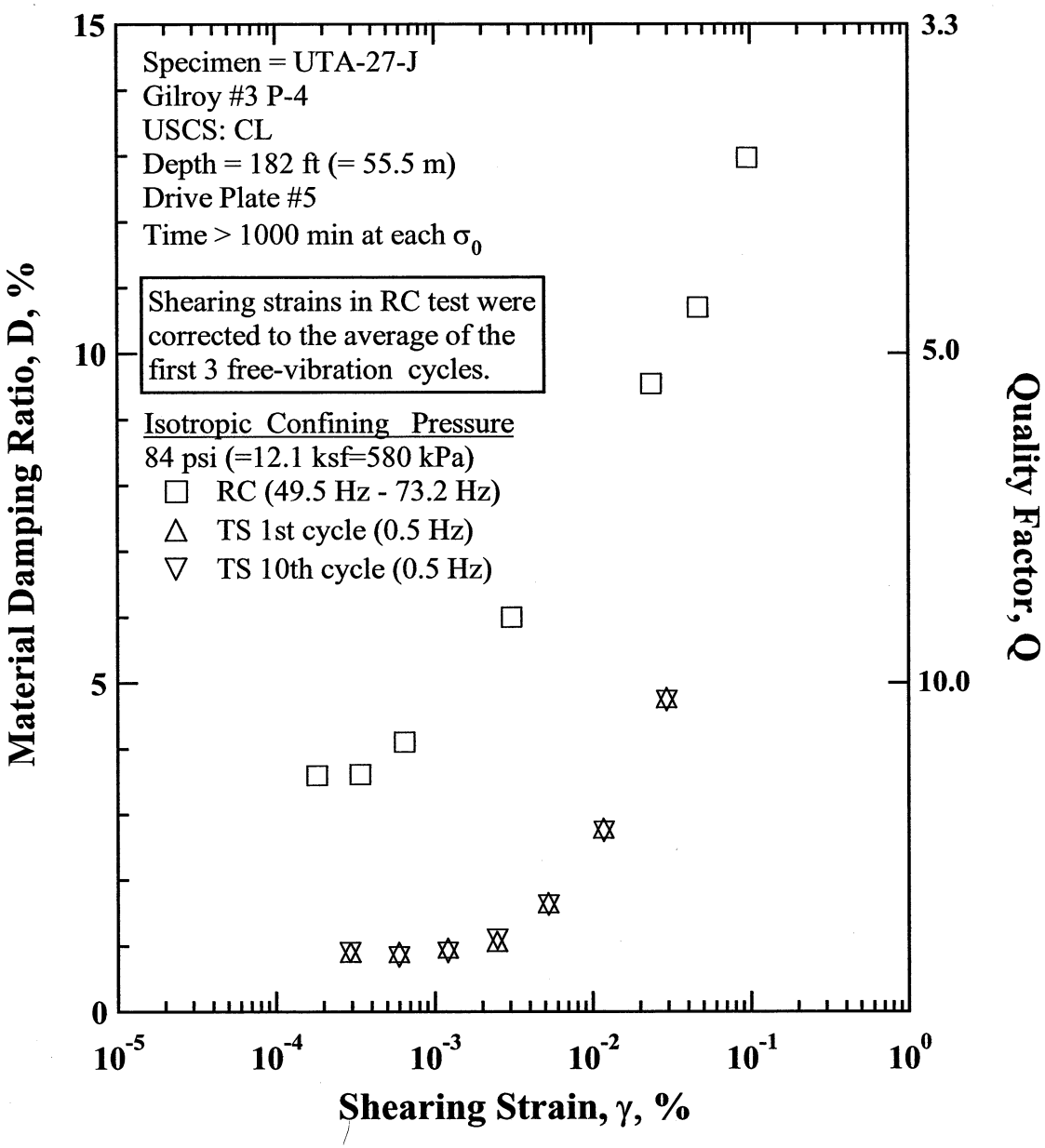

Figure P.13 Comparison of the Variation in Material Damping Ratio with Shearing Strain at an Isotropic Confining Pressure of 84 psi (=12.1 ksf=580 kPa) from the Combined RCTS Tests of Specimen UTA-27-J.

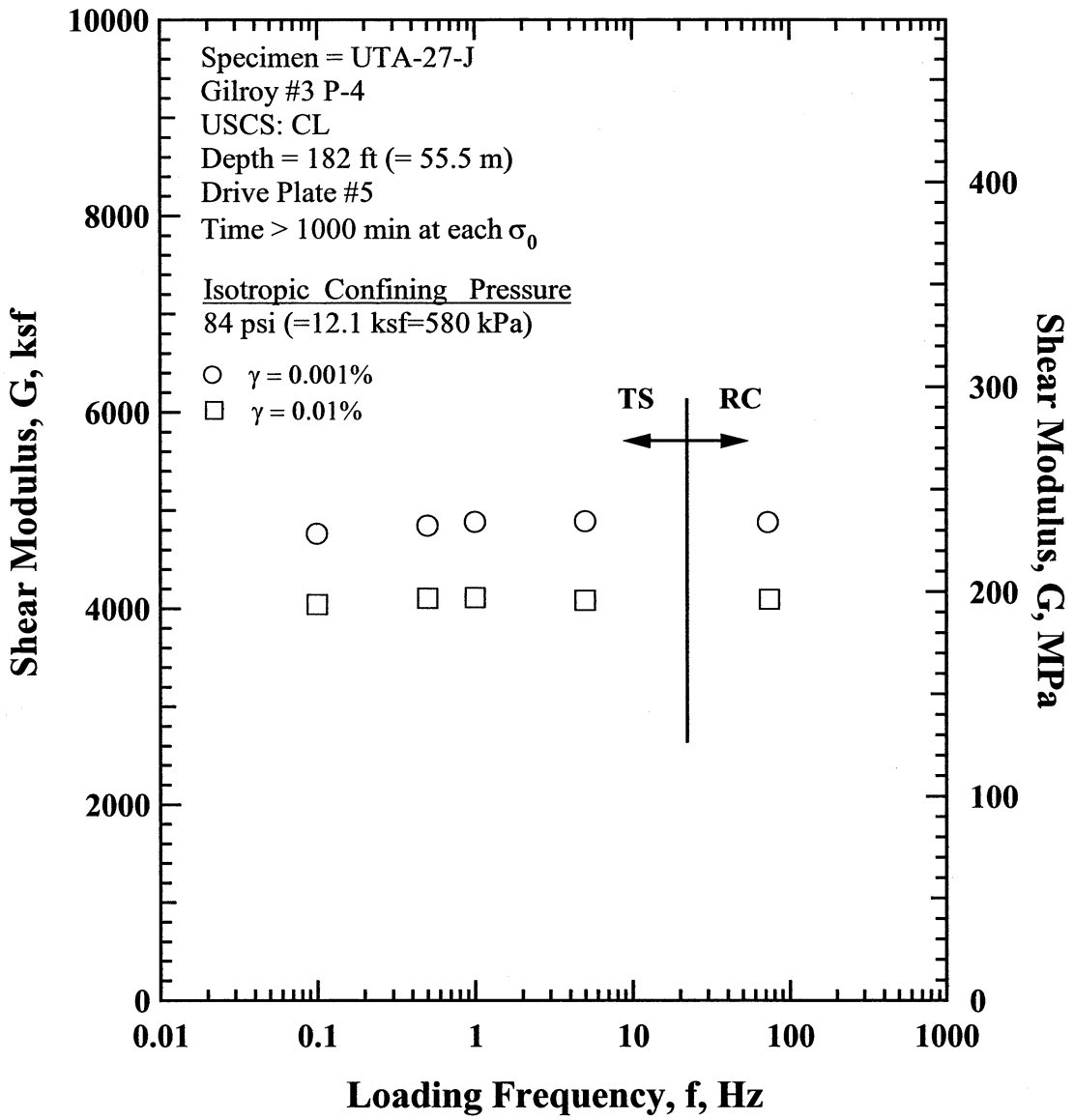

Figure P.14 Comparison of the Variation in Shear Modulus with Loading Frequency at an Isotropic Confining Pressure of 84 psi (=12.1 ksf=580 kPa) from the Combined RCTS Tests of Specimen UTA-27-J.

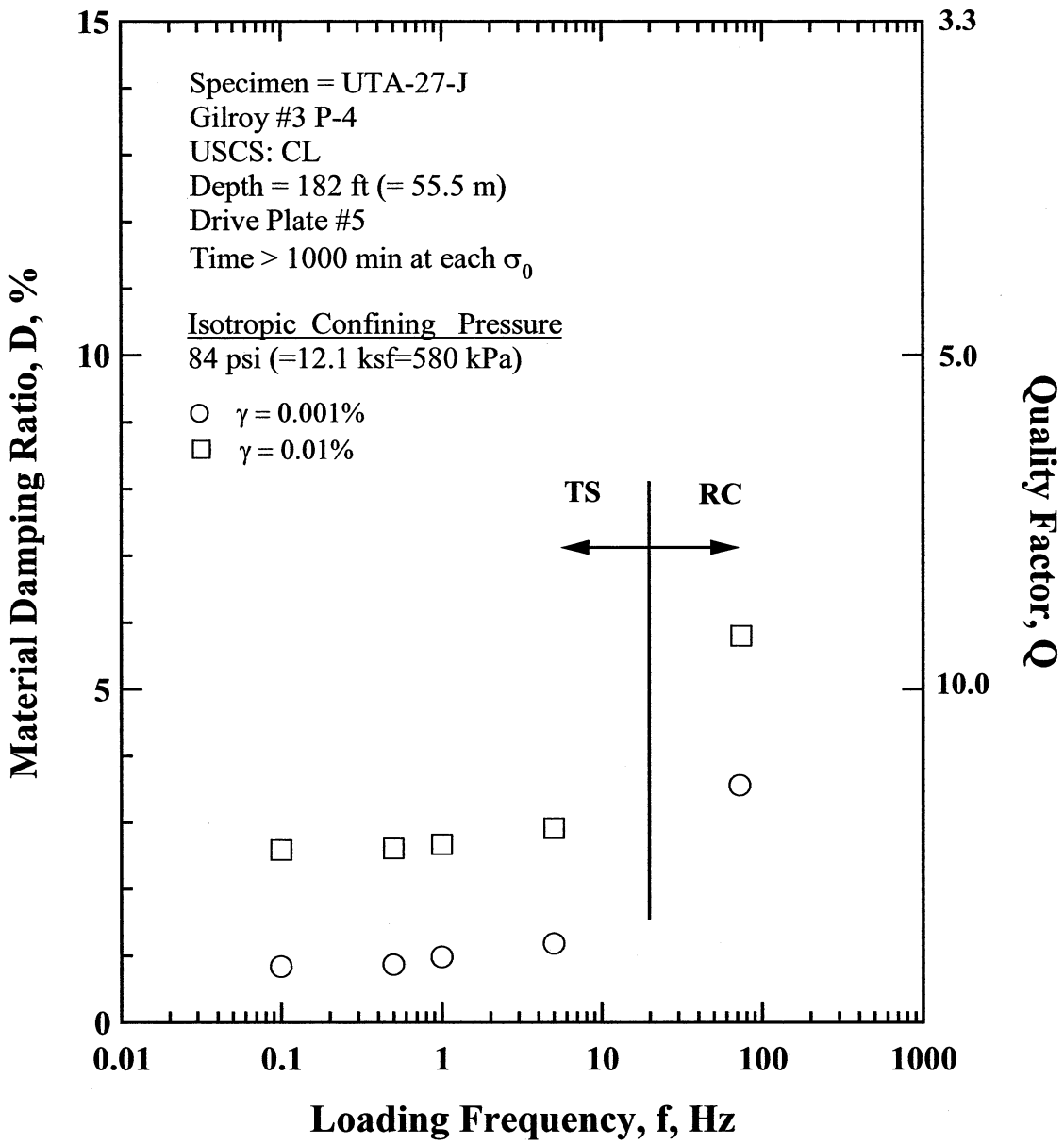

Figure P.15 Comparison of the Variation in Material Damping Ratio with Loading Frequency at an Isotropic Confining Pressure 84 psi (=12.1 ksf=580 kPa) from the Combined RCTS Tests of Specimen UTA-27-J.

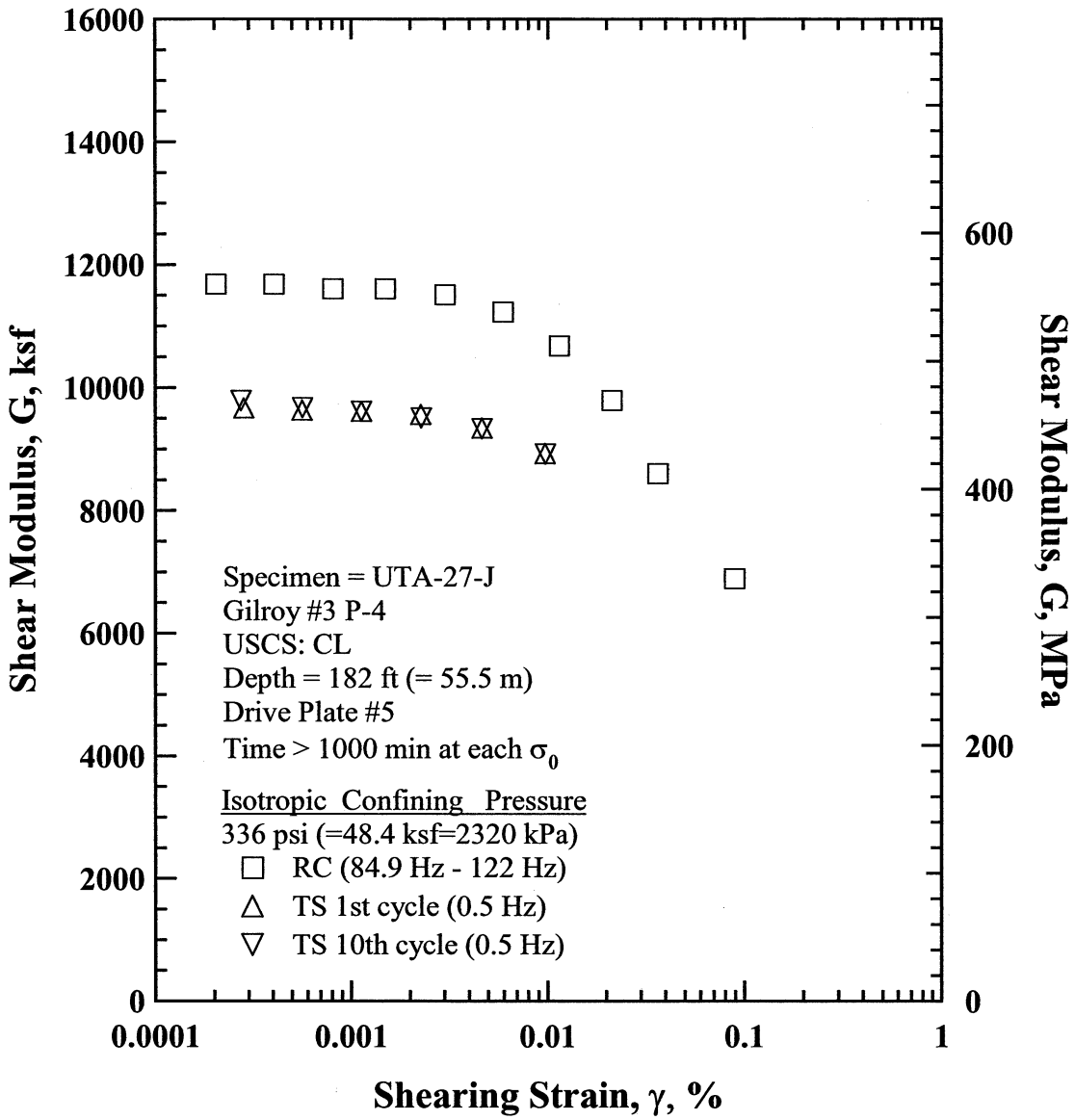

Figure P.16 Comparison of the Variation in Shear Modulus with Shearing Strain at an Isotropic Confining Pressure of 336 psi (=11.52 ksf=552 kPa) from the Combined RCTS Tests of Specimen UTA-27-J.

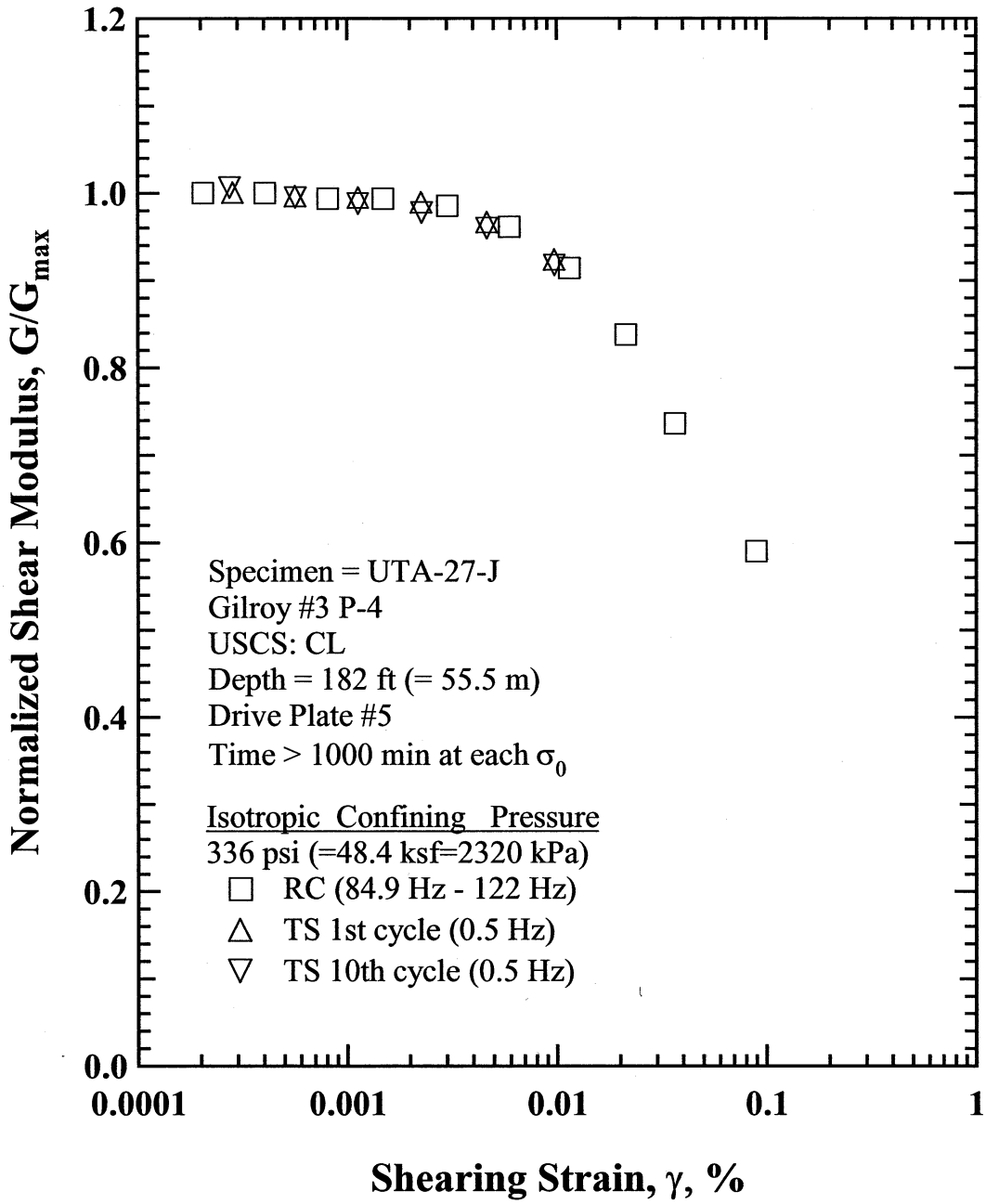

Figure P.17 Comparison of the Variation in Normalized Shear Modulus with Shearing Strain at an Isotropic Confining Pressure of 336 psi (=48.4 ksf=2320 kPa) from the Combined RCTS Tests of Specimen UTA-27-J.

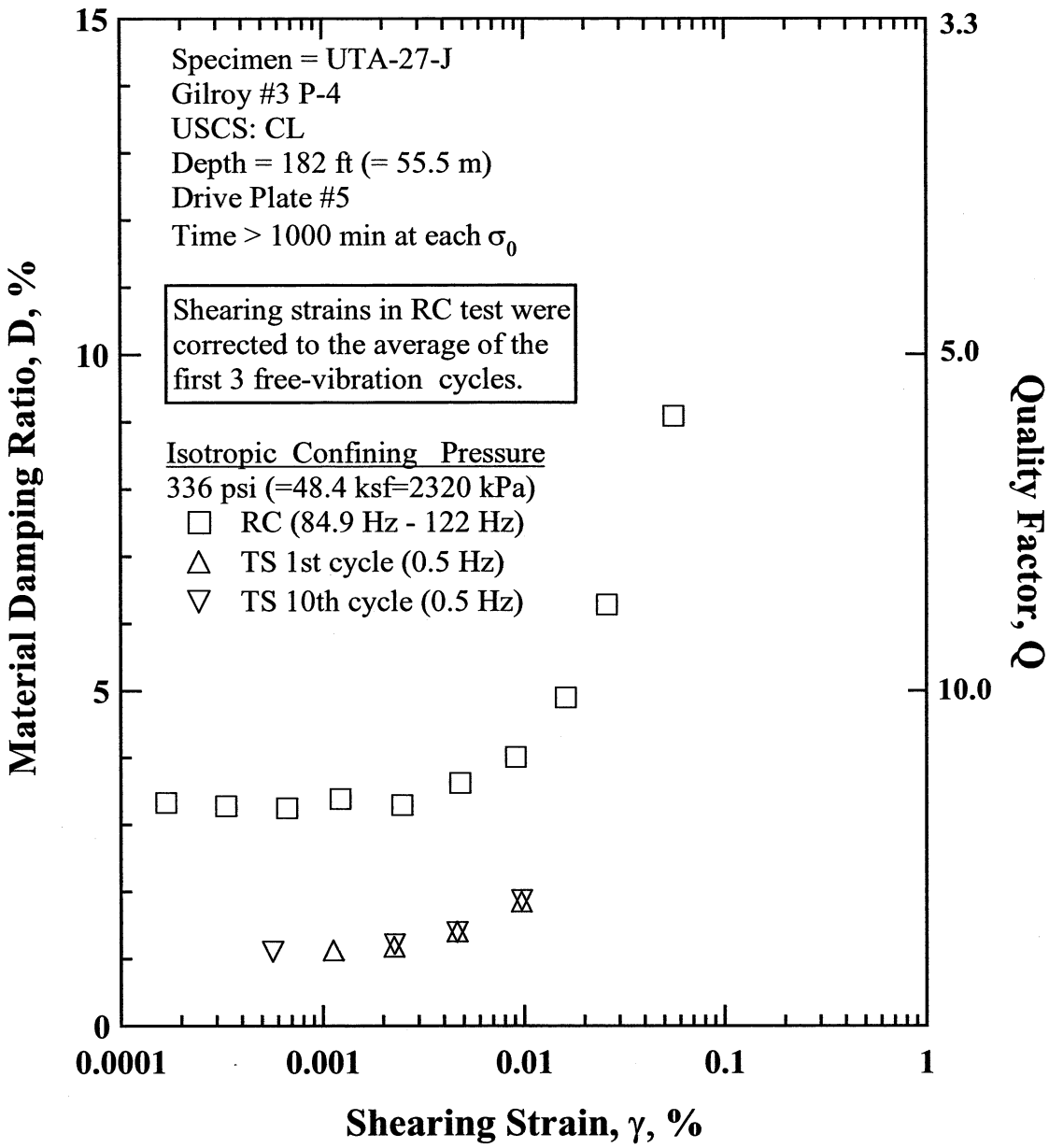

Figure P.18 Comparison of the Variation in Material Damping Ratio with Shearing Strain at an Isotropic Confining Pressure of 336 psi (=48.4 ksf=2320 kPa) from the Combined RCTS Tests of Specimen UTA-27-J.

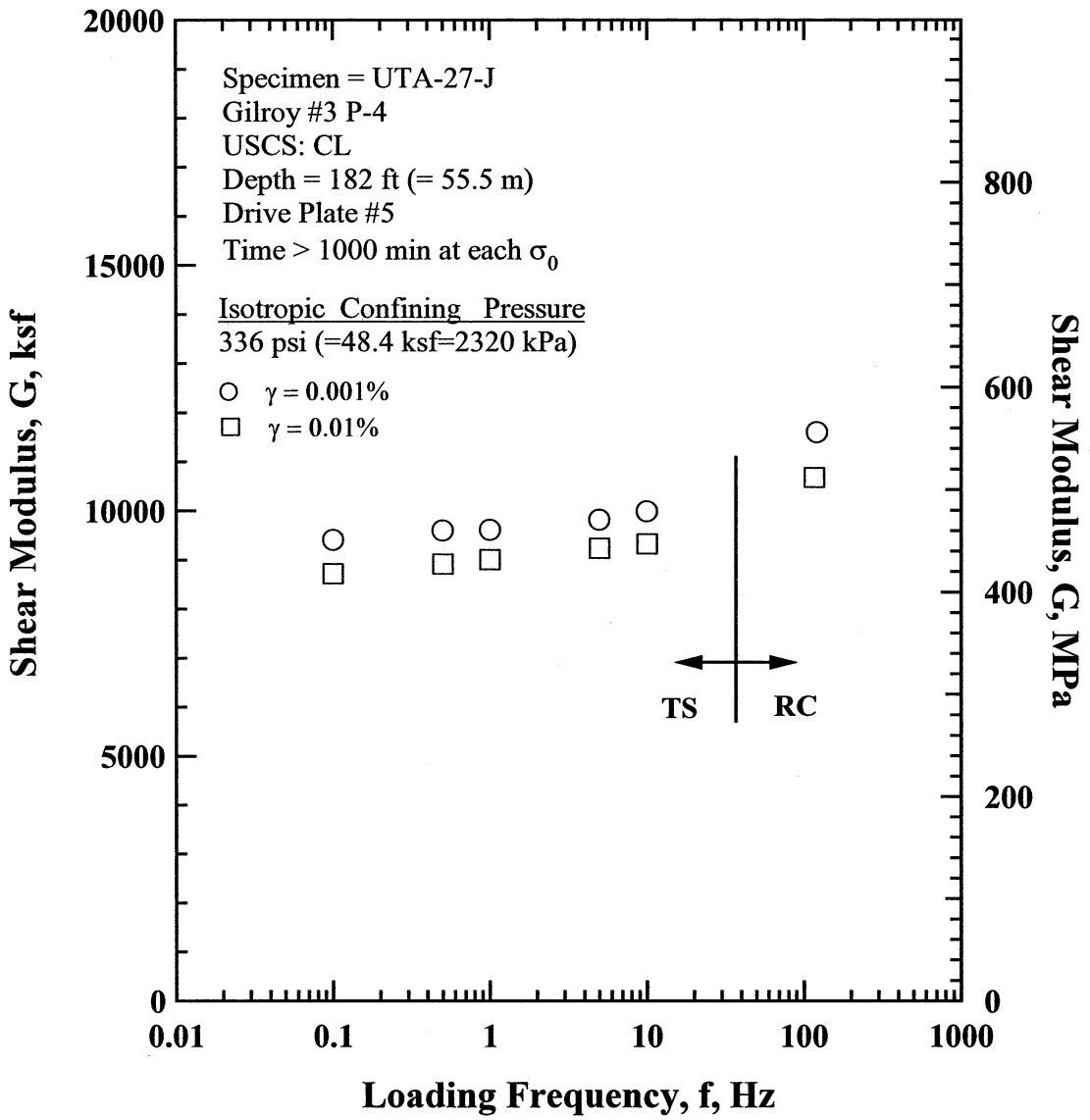

Figure P.19 Comparison of the Variation in Shear Modulus with Loading Frequency at an Isotropic Confining Pressure of 336 psi (=48.4 ksf=2320 kPa) from the Combined RCTS Tests of Specimen UTA-27-J.

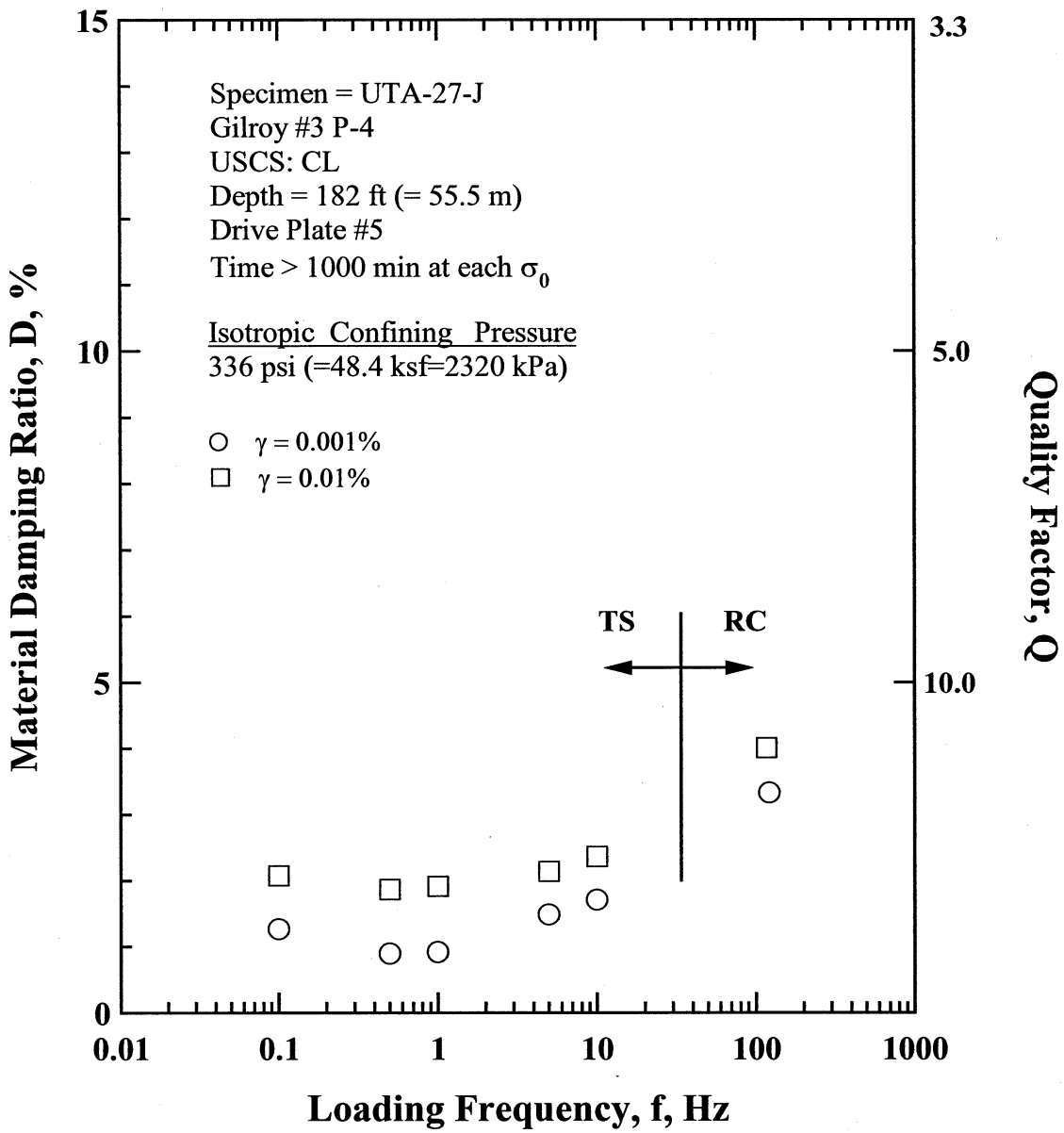

Figure P.20 Comparison of the Variation in Material Damping Ratio with Loading Frequency at an Isotropic Confining Pressure 336 psi (=48.4 ksf=2320 kPa) from the Combined RCTS Tests of Specimen UTA-27-J.

Table P.1 Variation in Low-Amplitude Shear Wave Velocity, Low-Amplitude Shear Modulus, Low-Amplitude Material Damping Ratio and Estimated Void Ratio with Isotropic Confining Pressure from RC Tests of Specimen UTA-27-J.

Effective Isotropic Confining Pressure, σ_o'			Low-Amplitude Shear Modulus, G_{max}		Low-Amplitude Shear Wave Velocity, Vs	Low-Amplitude Material Damping Ratio, Dmin	Estimated Void Ratio, e
(psi)	(psf)	(kPa)	(ksf)	(MPa)	(fps)	(%)	
21	3024	145.0	2324	111.4	769	2.74	0.572
42	6048	289.9	3327	159.5	919	2.89	0.562
84	12096	579.9	4834	231.7	1105	2.83	0.548
168	24192	1159.8	6310	302.5	1257	4.16	0.527
336	48384	2319.5	11282	540.9	1668	3.58	0.489

Table P.2 Variation in Shear Modulus, Normalized Shear Modulus and Material Damping Ratio with Shearing Strain from RC Tests of Specimen UTA-27-J; Confining Pressure, σ_o' = 84 psi(=12.1 ksf=580 kPa).

Peak Shearing Strain, %	Shear Modulus, G, ksf	Normalized Shear Modulus, G/G_{max}	Average[+] Shearing Strain, %	Material Damping Ratio[x], D, %
2.24E-04	4880	1.00	1.82E-04	3.60
4.18E-04	4860	1.01	3.39E-04	3.61
8.21E-04	4830	1.00	6.48E-04	4.10
1.48E-03	4770	1.00	1.48E-03	
2.07E-03	4642	1.00	2.07E-03	
4.29E-03	4463	0.98	3.08E-03	6.00
8.49E-03	4167	0.95	8.49E-03	
1.87E-02	3668	0.90	1.87E-02	
3.71E-02		0.81	3.71E-02	
3.84E-02	2999	0.69	2.37E-02	9.54
7.88E-02	2405	0.57	4.65E-02	10.70
1.76E-01	1843	0.40	9.57E-02	12.97

[+] Average Shearing Strain from the First Three Cycles of the Free Vibration Decay Curve

[x] Average Damping Ratio from the First Three Cycles of the Free Vibration Decay Curve

Table P.3 Variation in Shear Modulus, Normalized Shear Modulus and Material Damping Ratio with Shearing Strain from TS Tests of Specimen UTA-27-J; Confining Pressure, σ_o' = 84 psi(=12.1 ksf=580 kPa).

First Cycle				Tenth Cycle			
Peak Shearing Strain, %	Shear Modulus, G, ksf	Normalized Shear Modulus, G/G_{max}	Material Damping Ratio, D, %	Peak Shearing Strain, %	Shear Modulus, G, ksf	Normalized Shear Modulus, G/G_{max}	Material Damping Ratio, D, %
2.96E-04	4967	1.00	0.90	2.95E-04	4980	1.00	0.90
6.01E-04	4899	0.99	0.90	6.00E-04	4903	0.98	0.83
1.22E-03	4824	0.97	0.96	1.22E-03	4815	0.97	0.89
2.50E-03	4703	0.95	1.06	2.50E-03	4698	0.94	1.10
5.27E-03	4469	0.90	1.65	5.29E-03	4451	0.89	1.61
1.18E-02	3993	0.80	2.78	1.19E-02	3968	0.80	2.74
2.95E-02	3196	0.64	4.77	2.97E-02	3180	0.64	4.72

Table P.4 Variation in Shear Modulus, Normalized Shear Modulus and Material Damping Ratio with Shearing Strain from RC Tests of Specimen UTA-27-J; Confining Pressure, σ_o' = 336 psi(=48.4 ksf=2320 kPa).

Peak Shearing Strain, %	Shear Modulus, G, ksf	Normalized Shear Modulus, G/G_{max}	Average[+] Shearing Strain, %	Material Damping Ratio[x], D, %
2.04E-04	11681	1.00	1.68E-04	3.33
4.04E-04	11681	1.00	3.34E-04	3.28
8.06E-04	11606	0.99	6.66E-04	3.25
1.49E-03	11604	0.99	1.22E-03	3.39
3.02E-03	11510	0.99	2.49E-03	3.29
5.93E-03	11229	0.96	4.81E-03	3.62
1.14E-02	10678	0.91	9.08E-03	4.01
2.13E-02	9786	0.84	1.61E-02	4.90
3.65E-02	8602	0.74	2.59E-02	6.28
8.92E-02	6893	0.59	5.59E-02	9.09

[+] Average Shearing Strain from the First Three Cycles of the Free Vibration Decay Curve

[x] Average Damping Ratio from the First Three Cycles of the Free Vibration Decay Curve

Table P.5 Variation in Shear Modulus, Normalized Shear Modulus and Material Damping Ratio with Shearing Strain from TS Tests of Specimen UTA-27-J; Confining Pressure, σ_o' = 336 psi(=48.4 ksf=2320 kPa).

First Cycle				Tenth Cycle			
Peak Shearing Strain, %	Shear Modulus, G, ksf	Normalized Shear Modulus, G/G_{max}	Material Damping Ratio, D, %	Peak Shearing Strain, %	Shear Modulus, G, ksf	Normalized Shear Modulus, G/G_{max}	Material Damping Ratio, D, %
2.84E-04	9662	1.00		2.76E-04	9779	1.01	
5.66E-04	9623	1.00		5.69E-04	9668	0.99	1.10
1.13E-03	9605	0.99	1.12	1.13E-03	9603	0.99	
2.28E-03	9553	0.99	1.17	2.29E-03	9500	0.98	1.21
4.67E-03	9334	0.97	1.40	4.67E-03	9326	0.96	1.39
9.78E-03	8920	0.92	1.84	9.78E-03	8915	0.92	1.87

APPENDIX Q

Specimen No. 16
UT Specimen ID: UTA-27-K

Gilroy #3 P-5
Depth = 357 ft (= 108.8m)
Soil Type: Silt (ML)

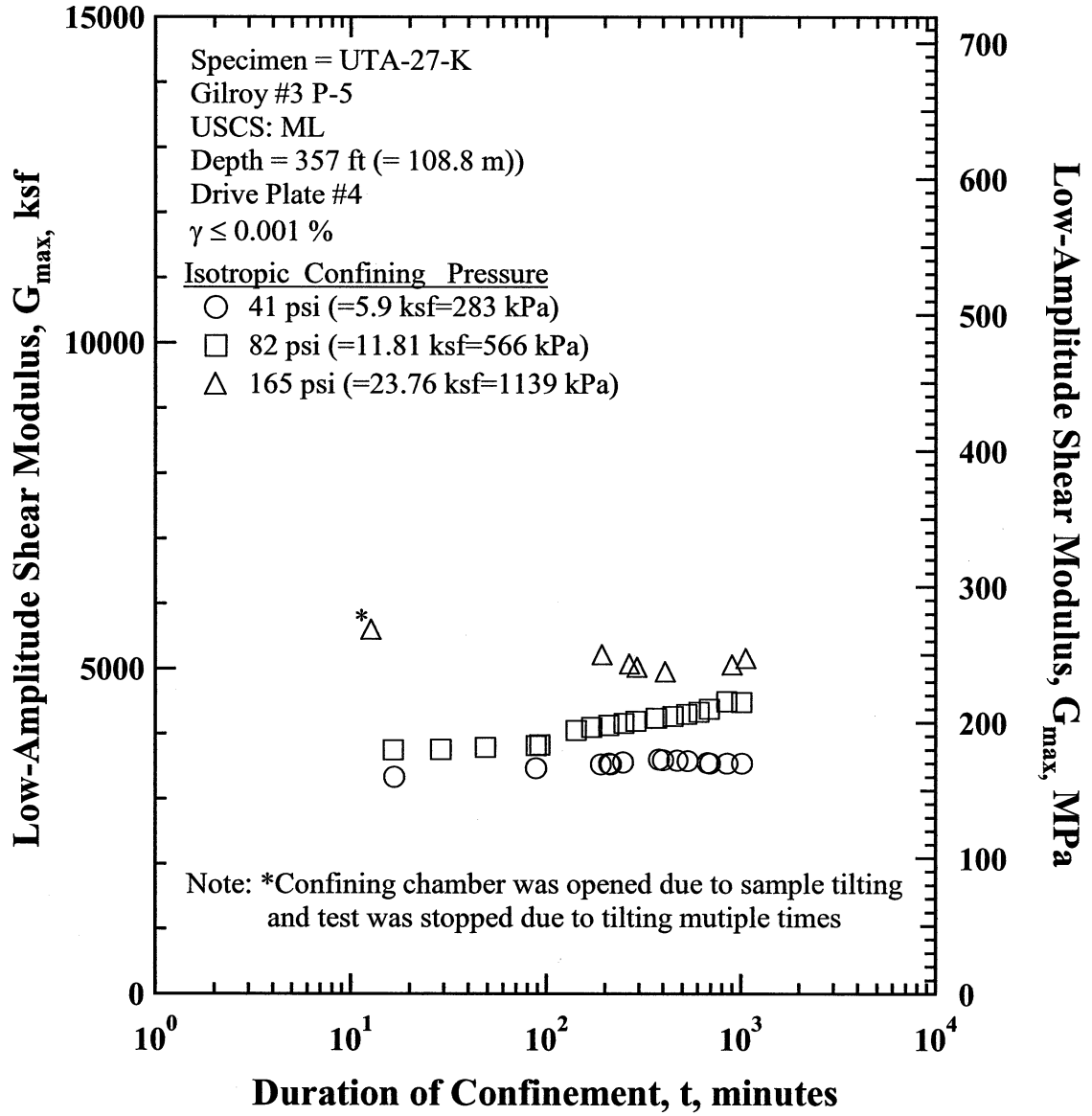

Figure Q.1 Variation in Low-Amplitude Shear Modulus with Magnitude and Duration of Isotropic Confining Pressure from Resonant Column Tests of Specimen UTA-27-K.

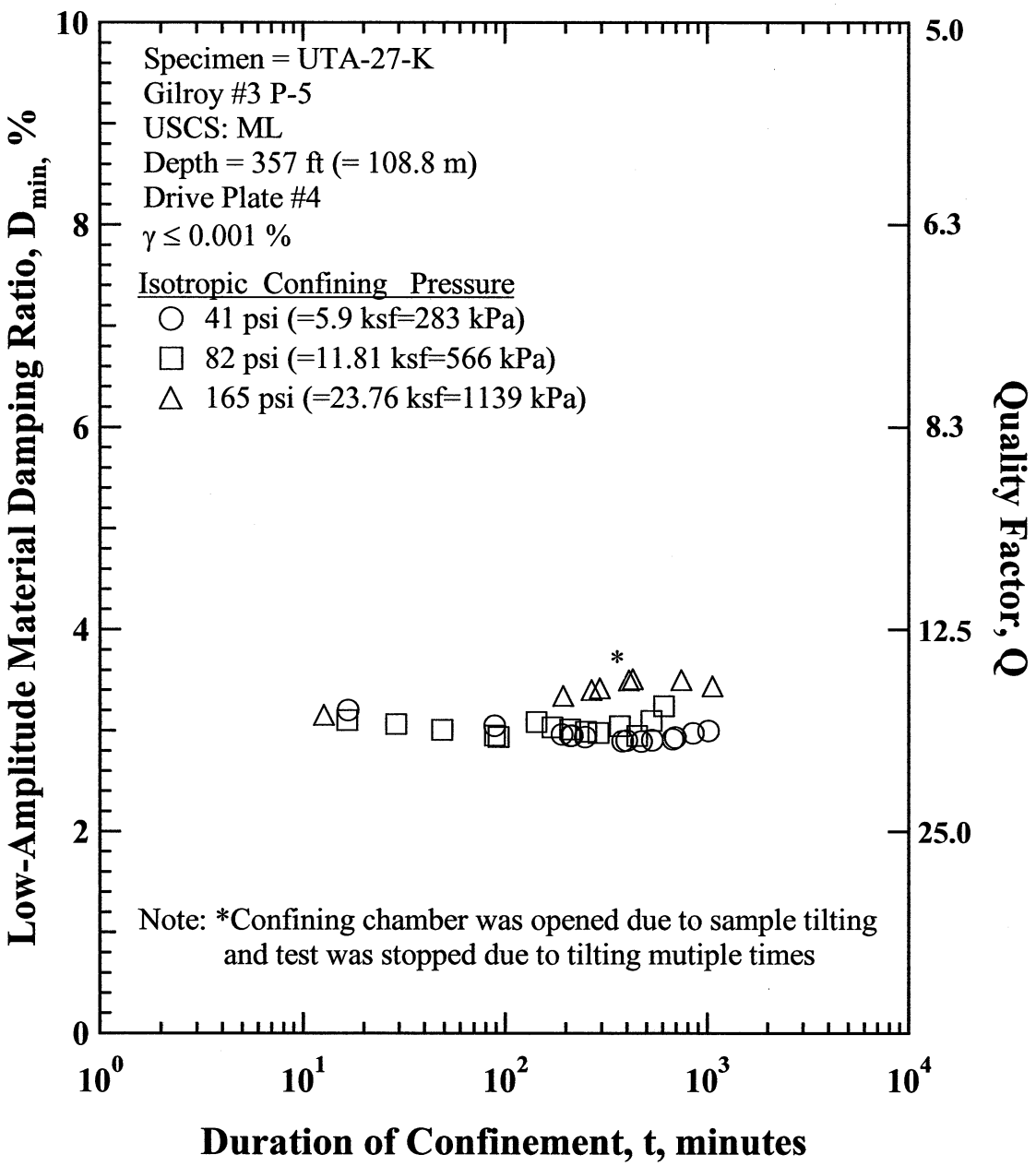

Figure Q.2 Variation in Low-Amplitude Material Damping Ratio with Magnitude and Duration of Isotropic Confining Pressure from Resonant Column Tests of Specimen UTA-27-K

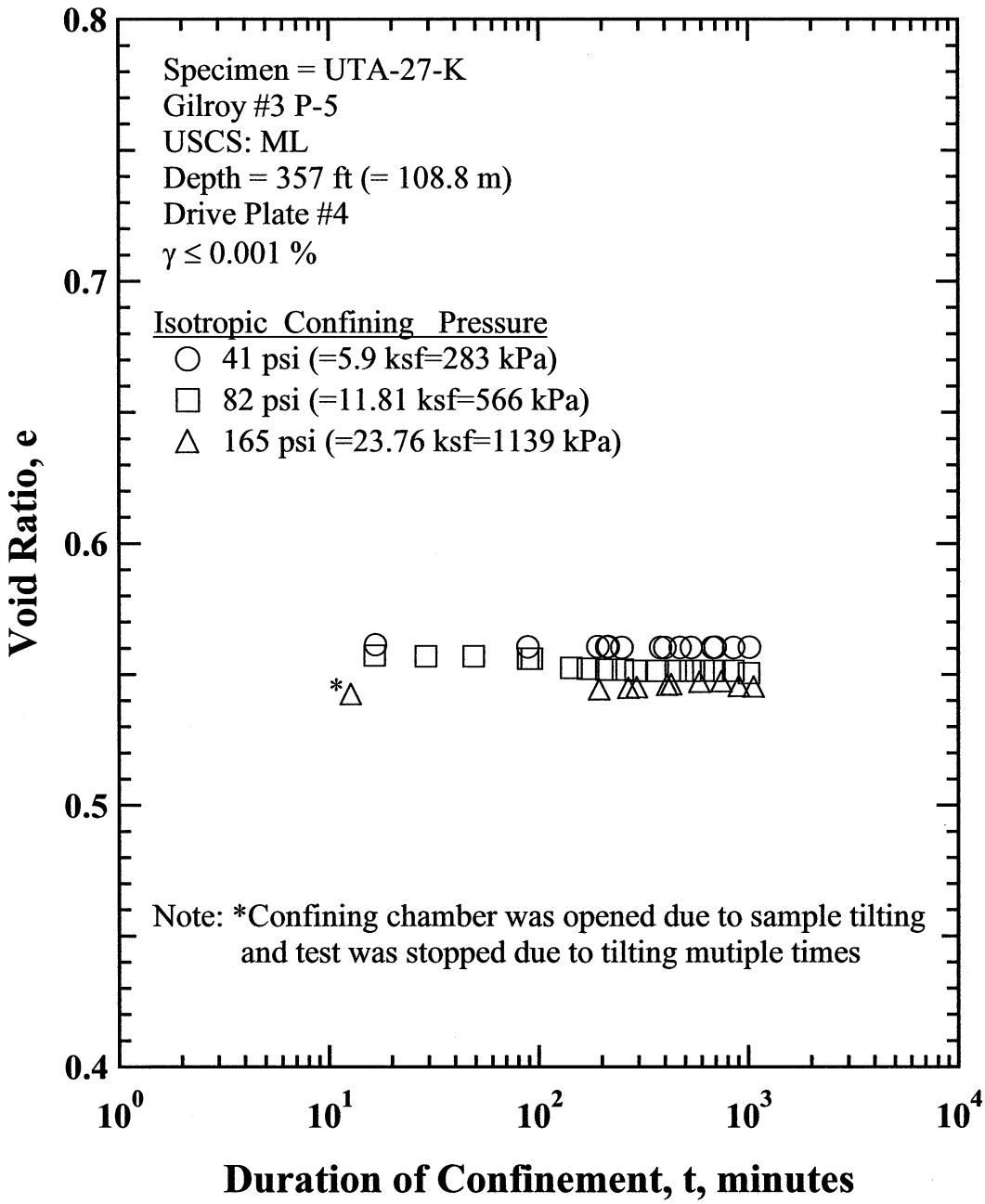

Figure Q.3 Variation in Estimated Void Ratio with Magnitude and Duration of Isotropic Confining Pressure from Resonant Column Tests of Specimen UTA-27-K.

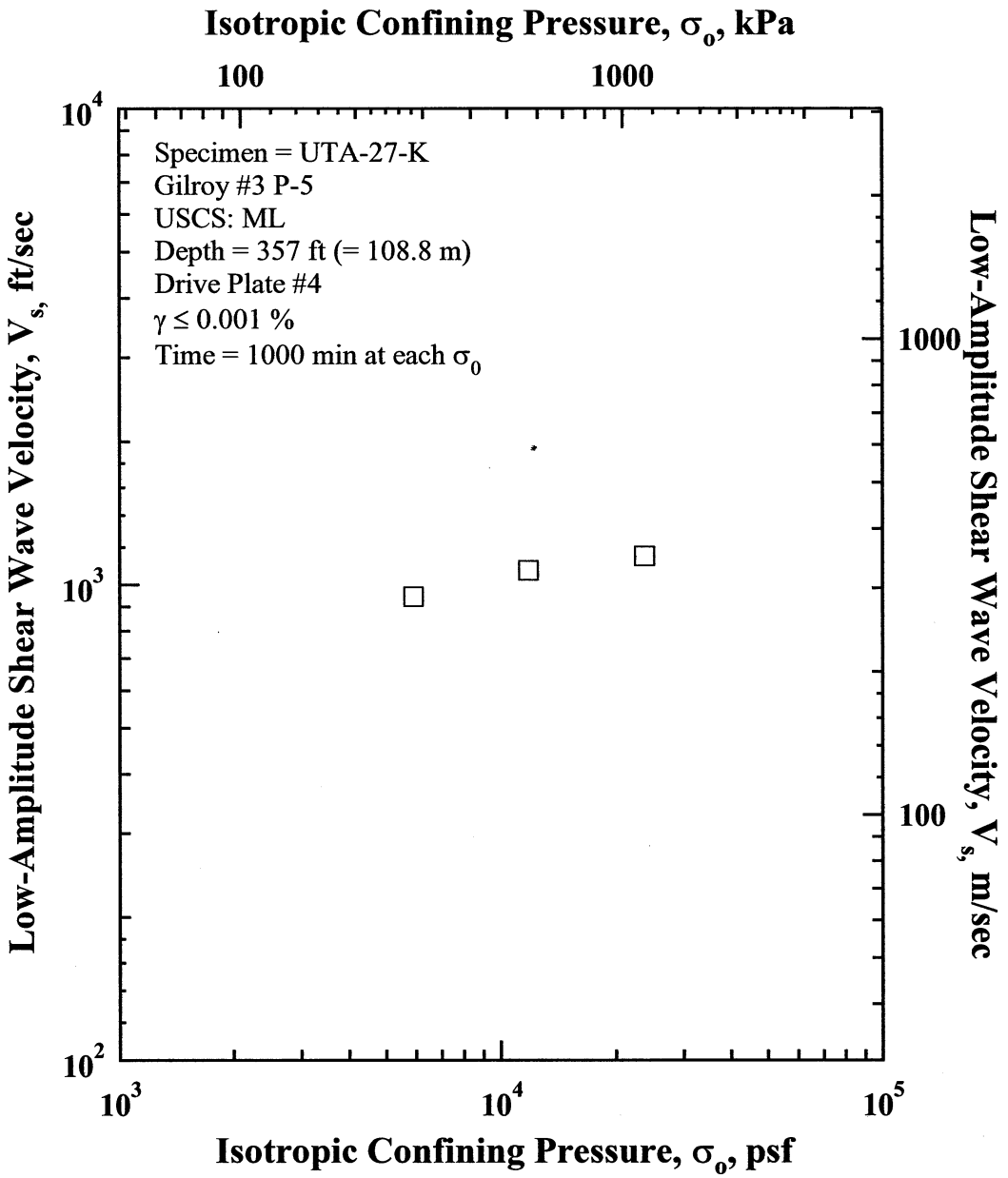

Figure Q.4 Variation in Low-Amplitude Shear Wave Velocity with Isotropic Confining Pressure from Resonant Column Tests of Specimen UTA-27-K.

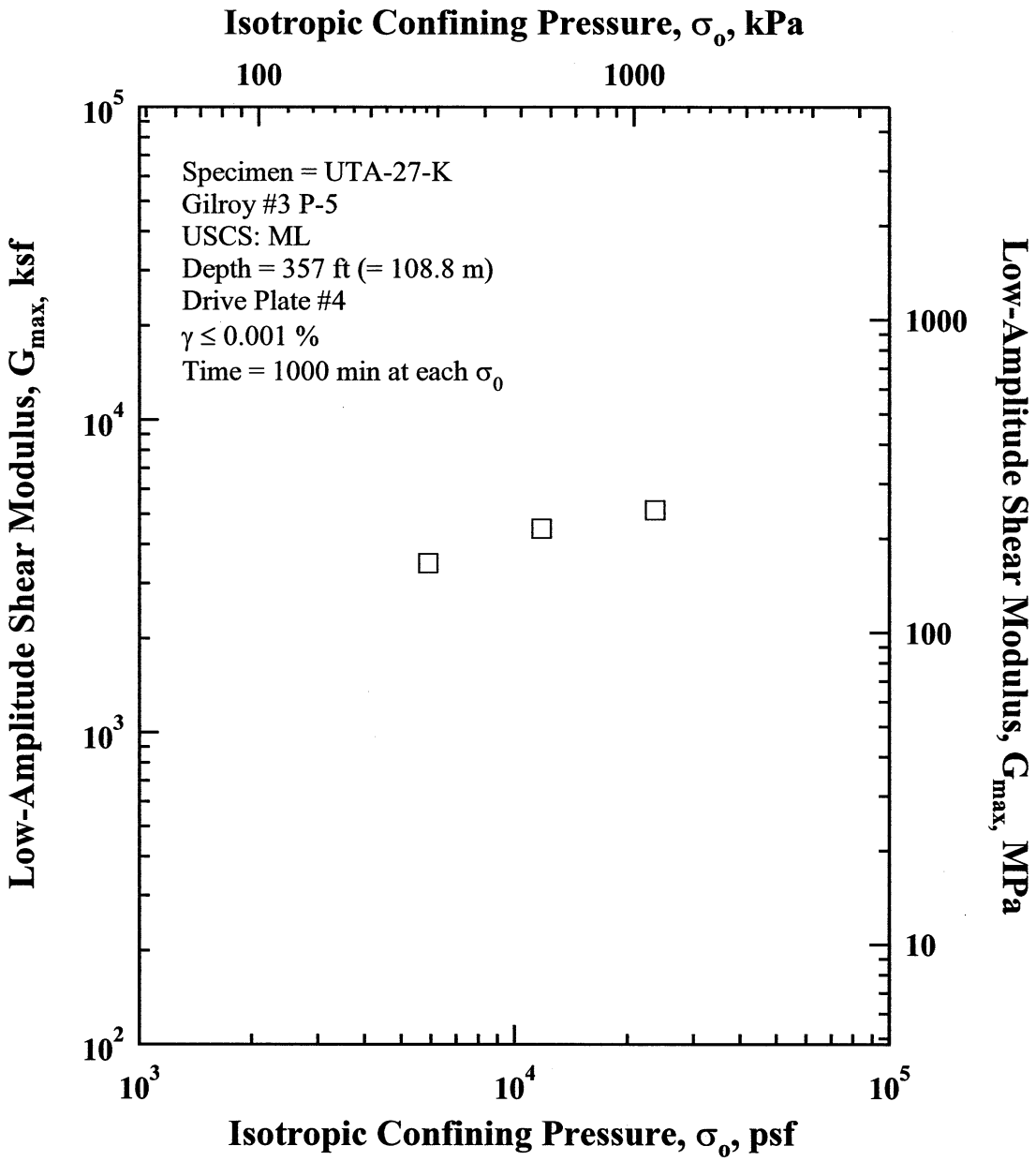

Figure Q.5 Variation in Low-Amplitude Shear Modulus with Isotropic Confining Pressure from Resonant Column Tests of Specimen UTA-27-K.

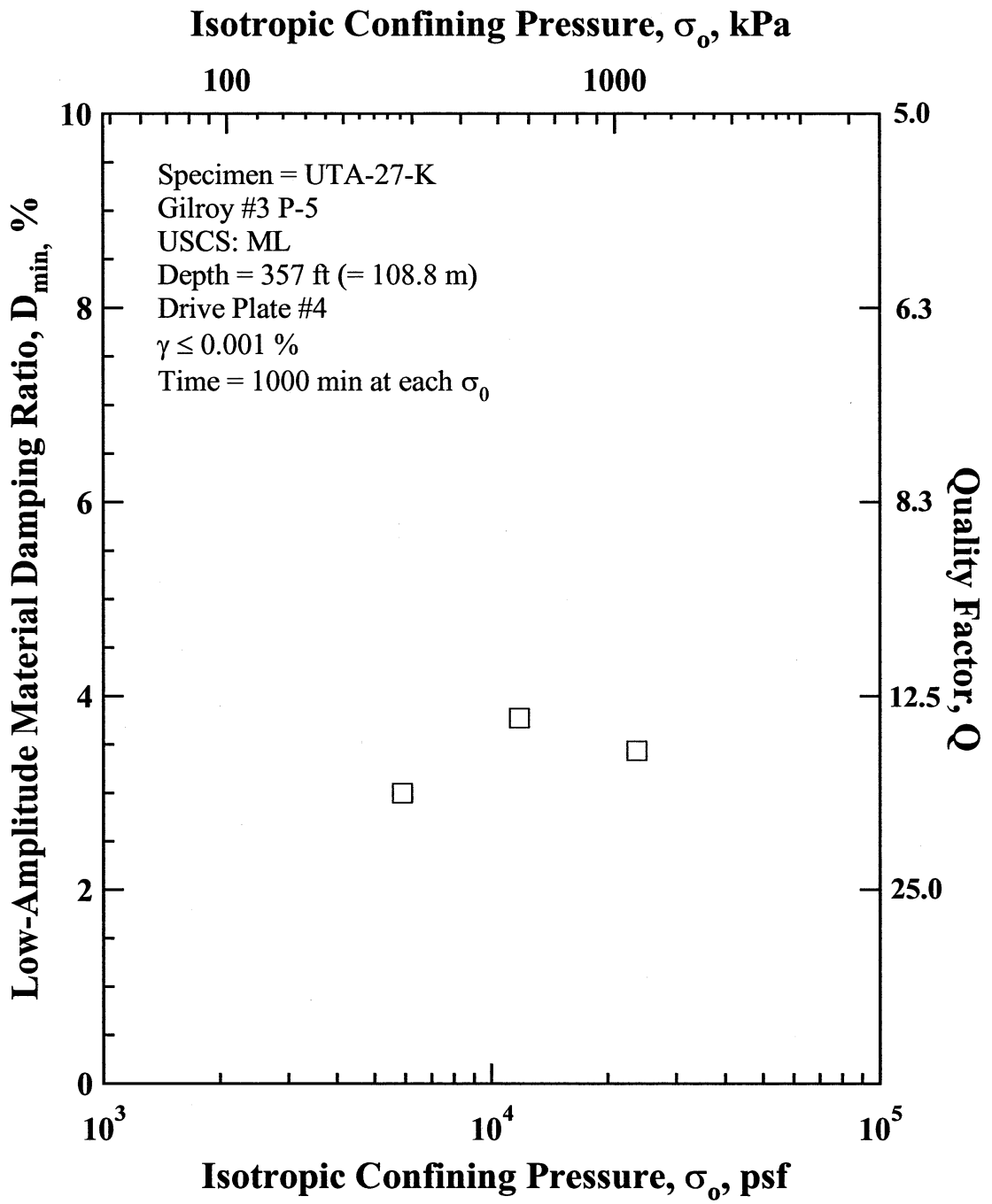

Figure Q.6 Variation in Material Damping Ratio with Isotropic Confining Pressure from Resonant Column Tests of Specimen UTA-27-K.

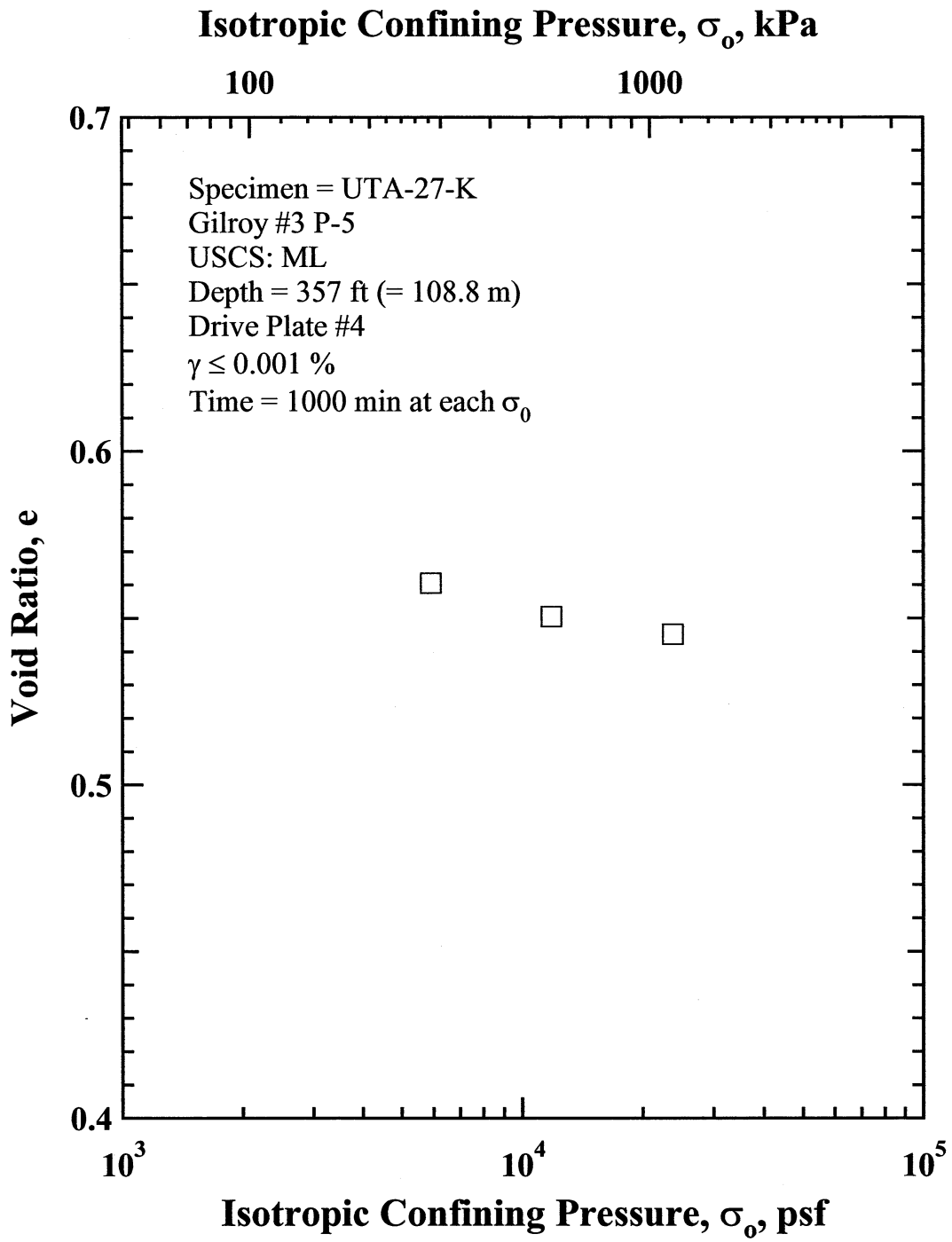

Figure Q.7 Variation in Estimated Void Ratio with Isotropic Confining Pressure from Resonant Column Tests of Specimen UTA-27-K.

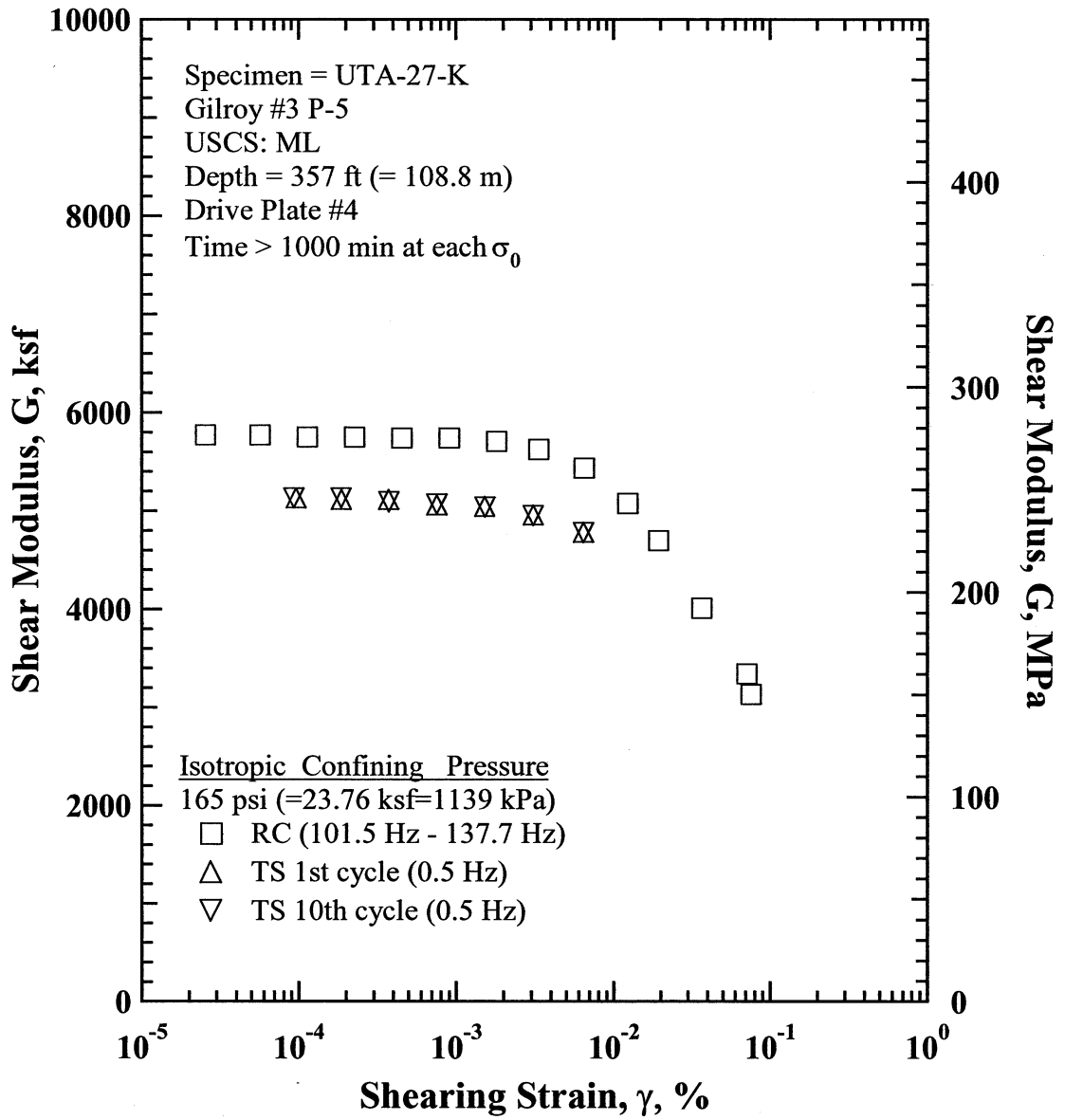

Figure Q.8 Comparison of the Variation in Shear Modulus with Shearing Strain at an Isotropic Confining Pressure of 165 psi (=23.76 ksf=1139 kPa) from the Combined RCTS Tests of Specimen UTA-27-K.

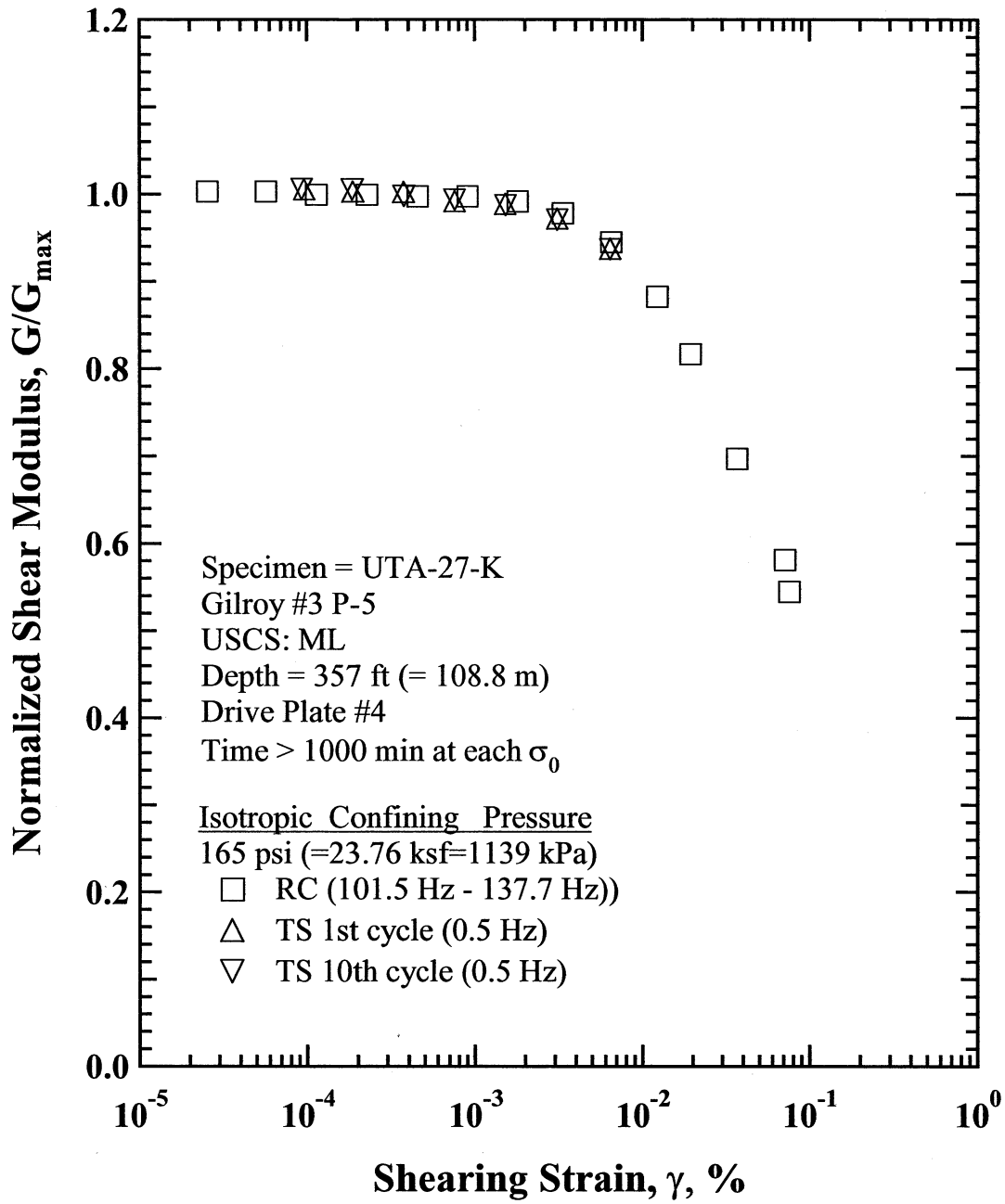

Figure Q.9 Comparison of the Variation in Normalized Shear Modulus with Shearing Strain at an Isotropic Confining Pressure of 165 psi (=23.76 ksf=1139 kPa) from the Combined RCTS Tests of Specimen UTA-27-K.

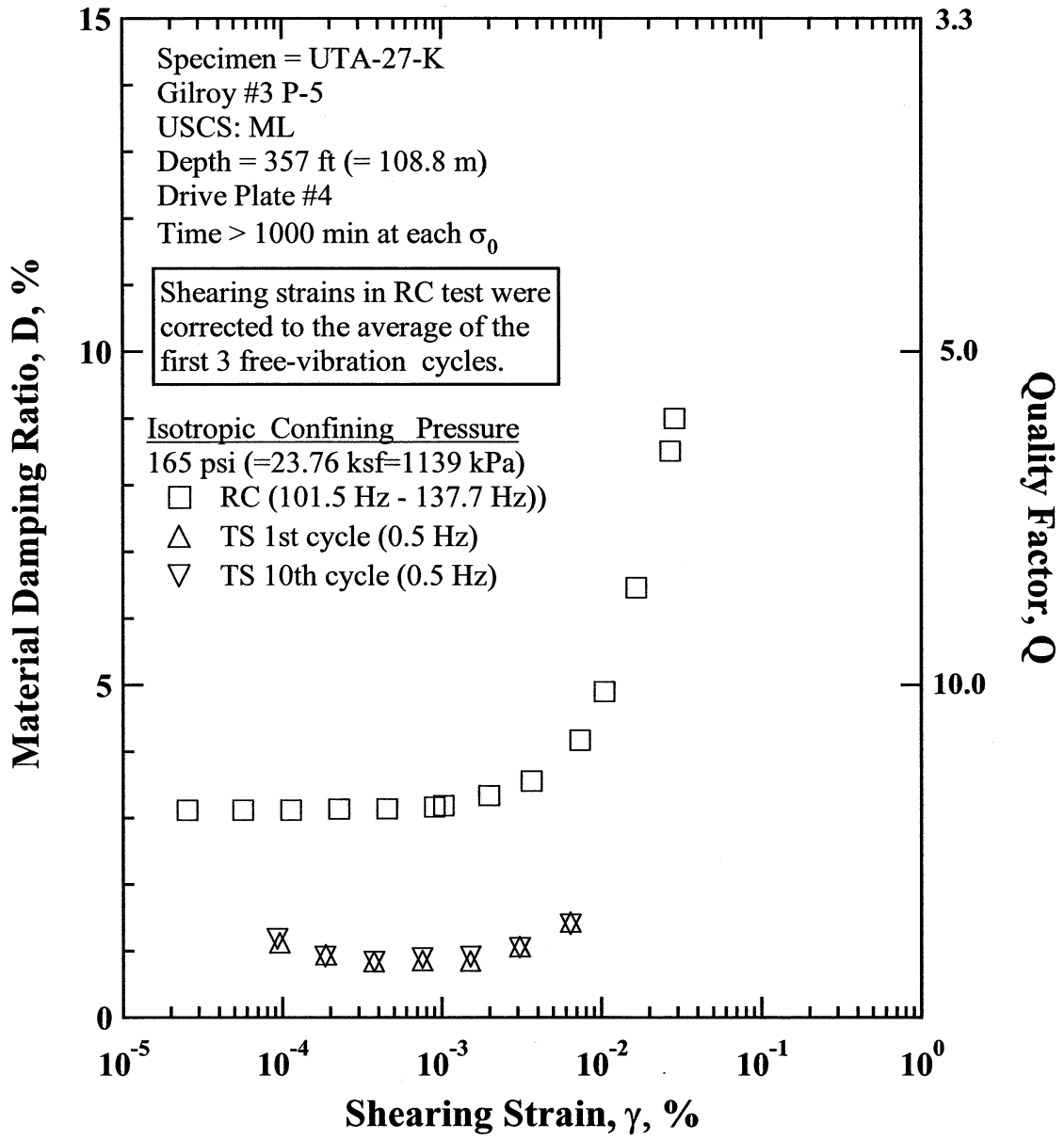

Figure Q.10 Comparison of the Variation in Material Damping Ratio with Shearing Strain at an Isotropic Confining Pressure of 165 psi (=23.76 ksf=1139 kPa) from the Combined RCTS Tests of Specimen UTA-27-K.

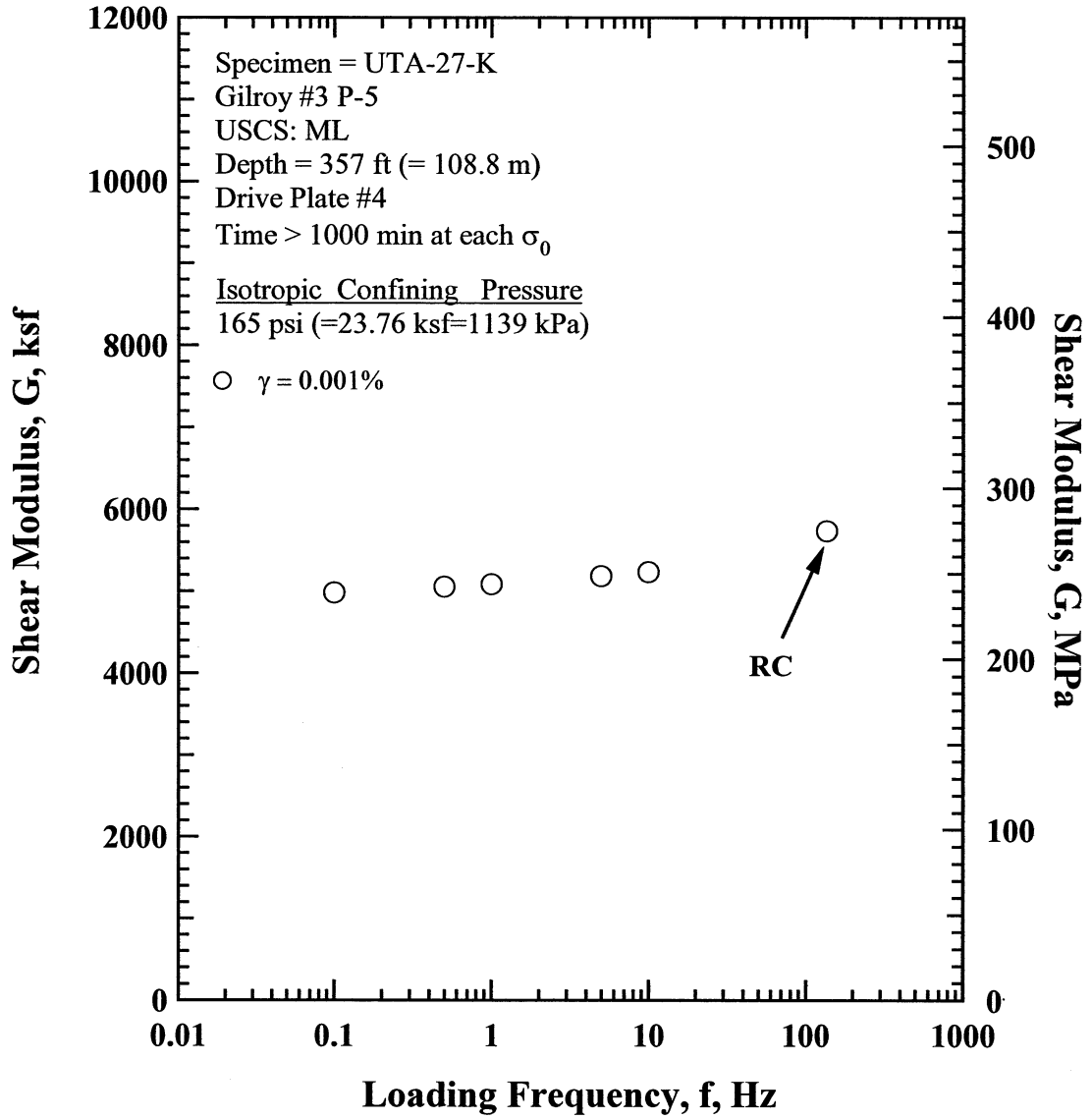

Figure Q.11 Comparison of the Variation in Shear Modulus with Loading Frequency at an Isotropic Confining Pressure of 165 psi (=23.76 ksf=1139 kPa) from the Combined RCTS Tests of Specimen UTA-27-K.

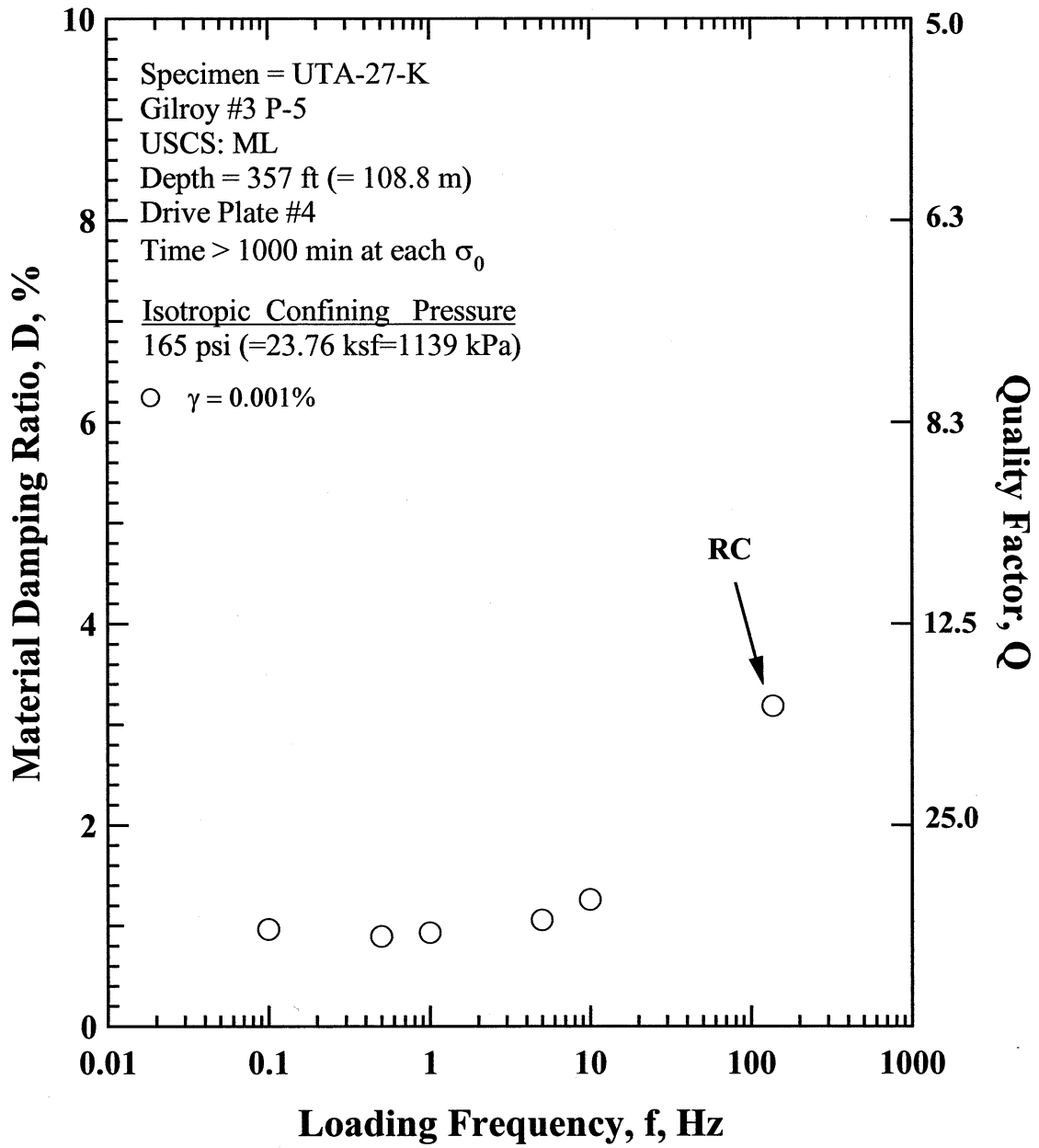

Figure Q.12 Comparison of the Variation in Material Damping Ratio with Loading Frequency at an Isotropic Confining Pressure 165 psi (=23.76 ksf=1139 kPa) from the Combined RCTS Tests of Specimen UTA-27-K.

Table Q.1 Variation in Low-Amplitude Shear Wave Velocity, Low-Amplitude Shear Modulus, Low-Amplitude Material Damping Ratio and Estimated Void Ratio with Isotropic Confining Pressure from RC Tests of Specimen UTA-27-K

Effective Isotropic Confining Pressure, σ_o'			Low-Amplitude Shear Modulus, G_{max}		Low-Amplitude Shear Wave Velocity, Vs	Low-Amplitude Material Damping Ratio, Dmin	Estimated Void Ratio, e
(psi)	(psf)	(kPa)	(ksf)	(MPa)	(fps)	(%)	
41	5904	283	3478	166.7	945	3.00	0.560
82	11808	566	4486	215.1	1072	3.77	0.550
165	23760	1139	5153	247.1	1149	3.43	0.545

Table Q.2 Variation in Shear Modulus, Normalized Shear Modulus and Material Damping Ratio with Shearing Strain from RC Tests of Specimen UTA-27-K; Confining Pressure, σ_o' =165 psi (=23.76 ksf=1139 kPa).

Peak Shearing Strain, %	Shear Modulus, G, ksf	Normalized Shear Modulus, G/G_{max}	Average[+] Shearing Strain, %	Material Damping Ratio[x], D, %
3.30E-06	5738	1.00	3.30E-06	3.01
7.85E-06	5749	1.00	7.85E-06	3.10
2.55E-05	5770	1.00	2.55E-05	3.12
5.66E-05	5770	1.00	5.66E-05	3.12
1.14E-04	5749	1.00	1.14E-04	3.12
2.27E-04	5749	1.00	2.27E-04	3.13
4.53E-04	5738	1.00	4.53E-04	3.14
9.05E-04	5738	1.00	9.05E-04	3.16
1.80E-03	5705	0.99	1.03E-03	3.18
3.34E-03	5626	0.98	1.99E-03	3.34
6.49E-03	5435	0.94	3.66E-03	3.55
1.23E-02	5076	0.88	7.36E-03	4.17
1.94E-02	4698	0.82	1.04E-02	4.90
3.67E-02	4010	0.70	1.66E-02	6.46
7.12E-02	3342	0.58	2.70E-02	8.51
7.55E-02	3132	0.54	2.88E-02	9.00

[+] Average Shearing Strain from the First Three Cycles of the Free Vibration Decay Curve

[x] Average Damping Ratio from the First Three Cycles of the Free Vibration Decay Curve

Table Q.3 Variation in Shear Modulus, Normalized Shear Modulus and Material Damping Ratio with Shearing Strain from TS Tests of Specimen UTA-27-K; Confining Pressure, σ_o' = 165 psi (=23.76 ksf=1139 kPa).

First Cycle				Tenth Cycle			
Peak Shearing Strain, %	Shear Modulus, G, ksf	Normalized Shear Modulus, G/G_{max}	Material Damping Ratio, D, %	Peak Shearing Strain, %	Shear Modulus, G, ksf	Normalized Shear Modulus, G/G_{max}	Material Damping Ratio, D, %
9.69E-05	5126	1.00	1.12	9.37E-05	5128	1.01	1.18
1.89E-04	5113	1.00	0.94	1.87E-04	5126	1.00	0.91
3.78E-04	5111	1.00	0.83	3.79E-04	5088	1.00	0.83
7.62E-04	5058	0.99	0.85	7.61E-04	5065	0.99	0.89
1.53E-03	5042	0.99	0.84	1.53E-03	5033	0.99	0.91
3.11E-03	4955	0.97	1.06	3.12E-03	4949	0.97	1.04
6.46E-03	4780	0.94	1.42	6.47E-03	4777	0.94	1.39

APPENDIX R

Specimen No. 17
UT Specimen ID: UTA-27-M

Lake Hughes P-1
Depth=6 ft (=1.83 m)
Soil Type: Silty Sand (SW-SM)

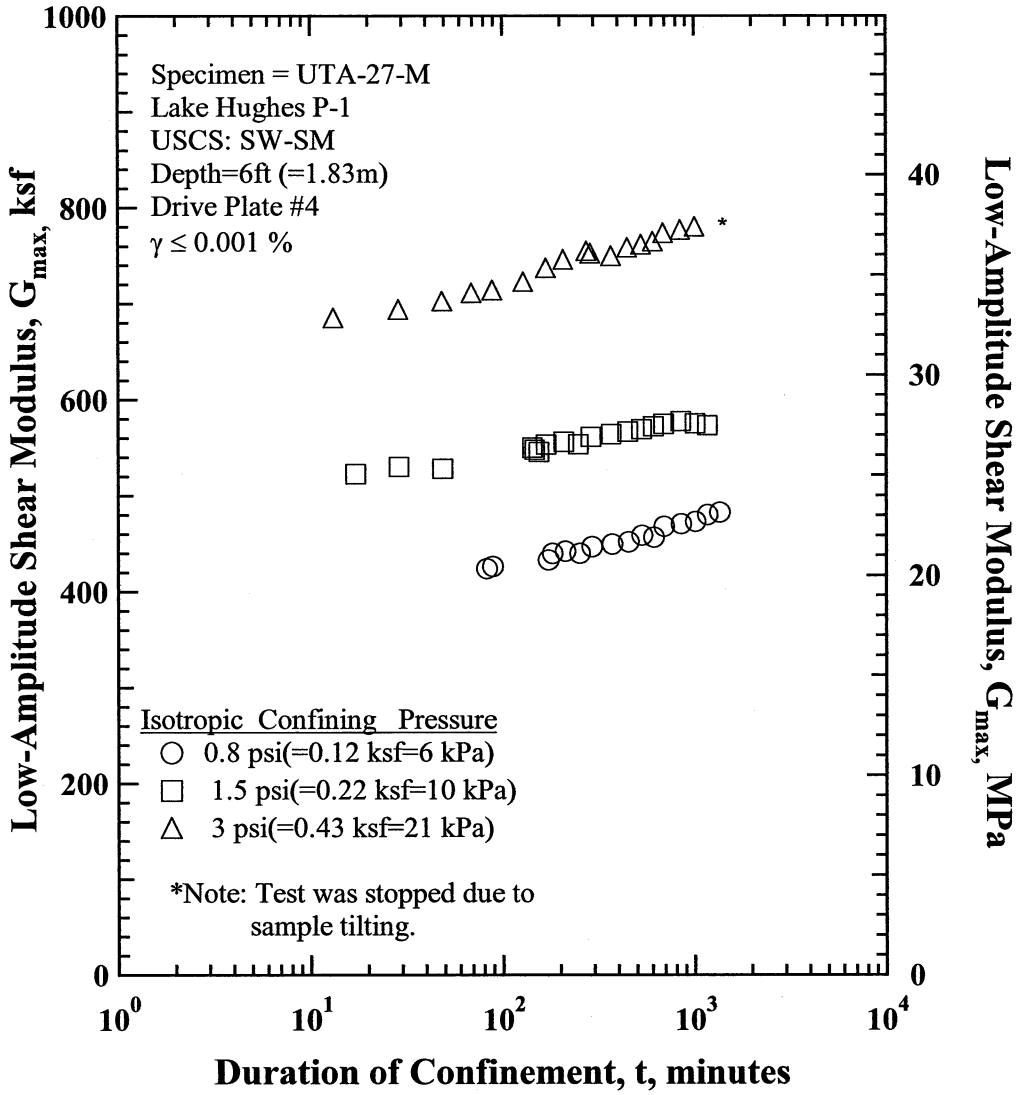

Figure R.1 Variation in Low-Amplitude Shear Modulus with Magnitude and Duration of Isotropic Confining Pressure from Resonant Column Tests of Specimen UTA-27-M.

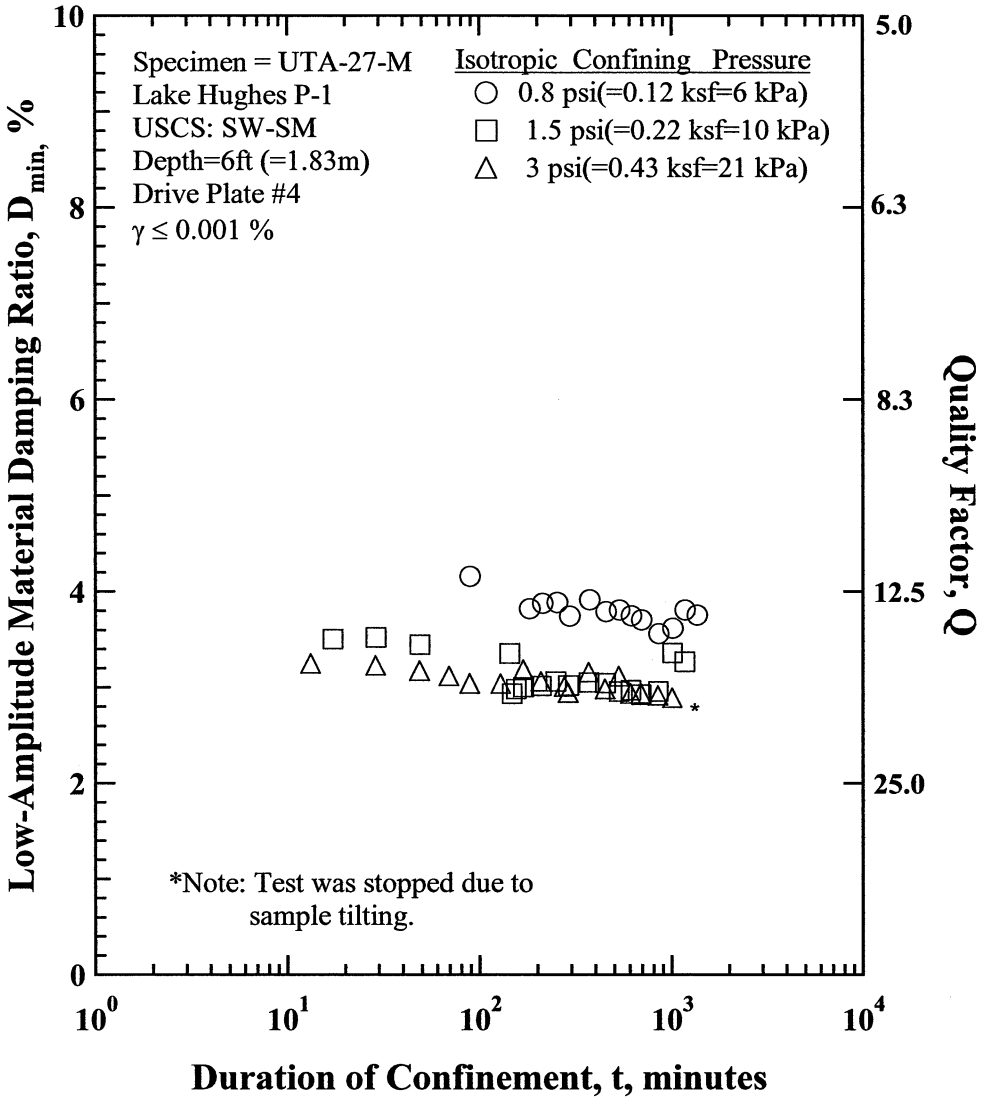

Figure R.2 Variation in Low-Amplitude Material Damping Ratio with Magnitude and Duration of Isotropic Confining Pressure from Resonant Column Tests of Specimen UTA-27-M

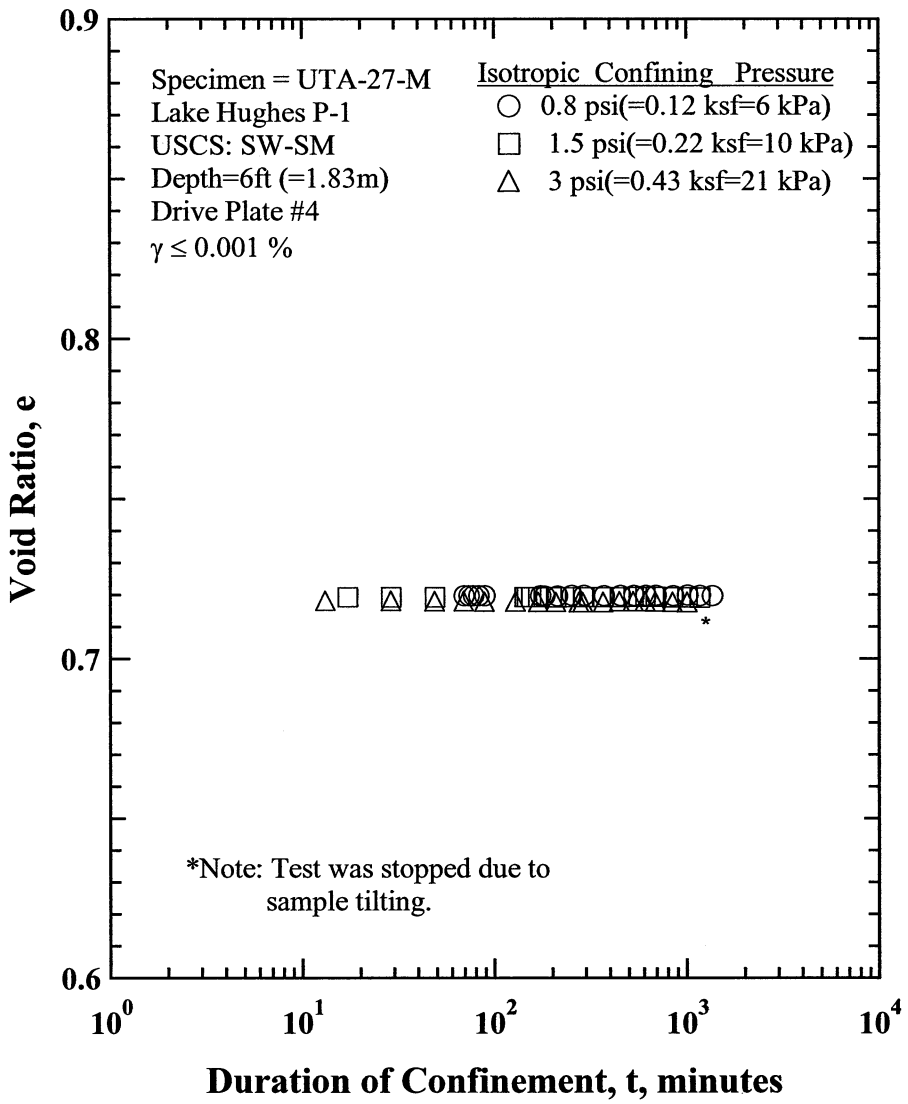

Figure R.3 Variation in Estimated Void Ratio with Magnitude and Duration of Isotropic Confining Pressure from Resonant Column Tests of Specimen UTA-27-M

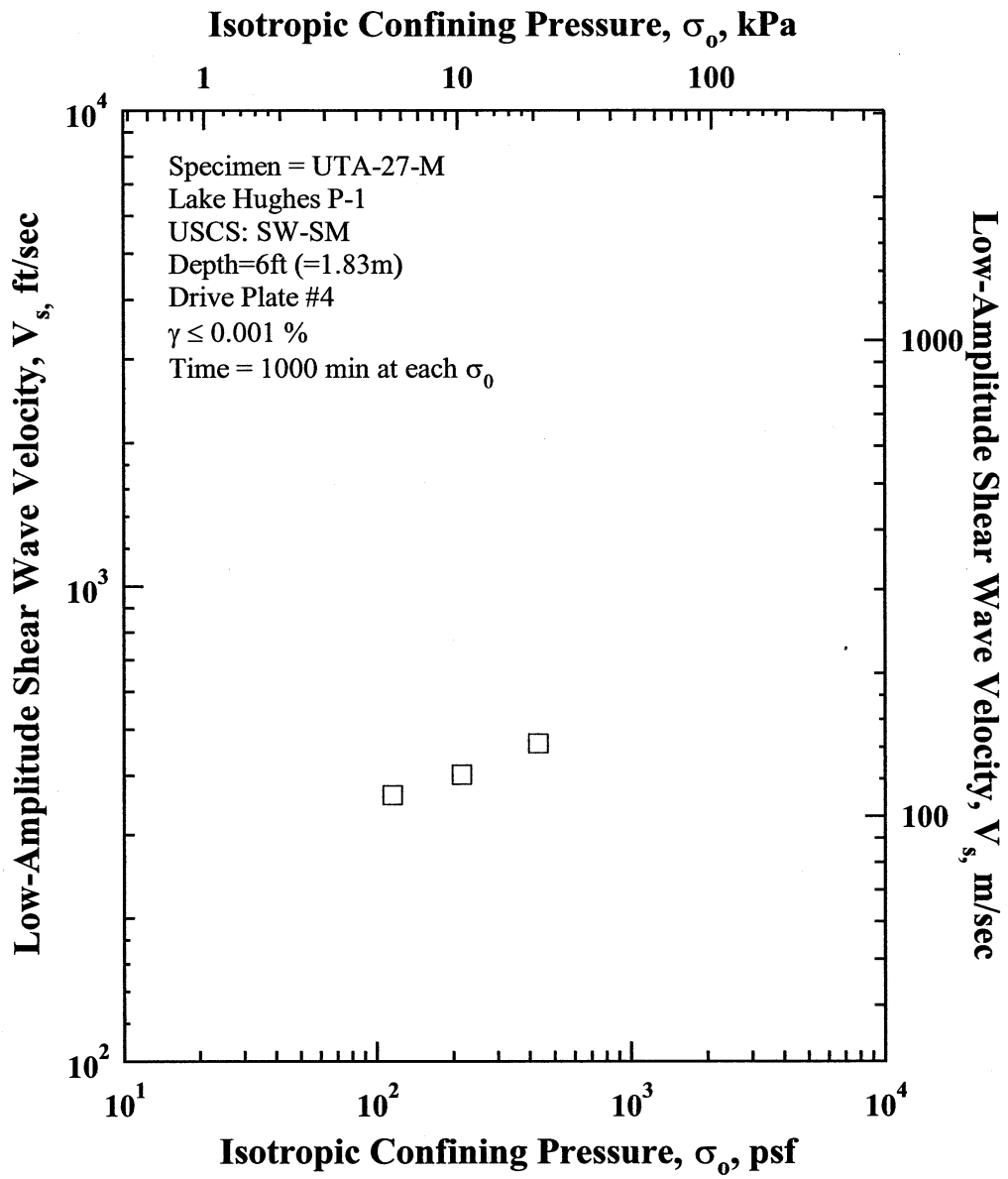

Figure R.4 Variation in Low-Amplitude Shear Wave Velocity with Isotropic Confining Pressure from Resonant Column Tests of Specimen UTA-27-M.

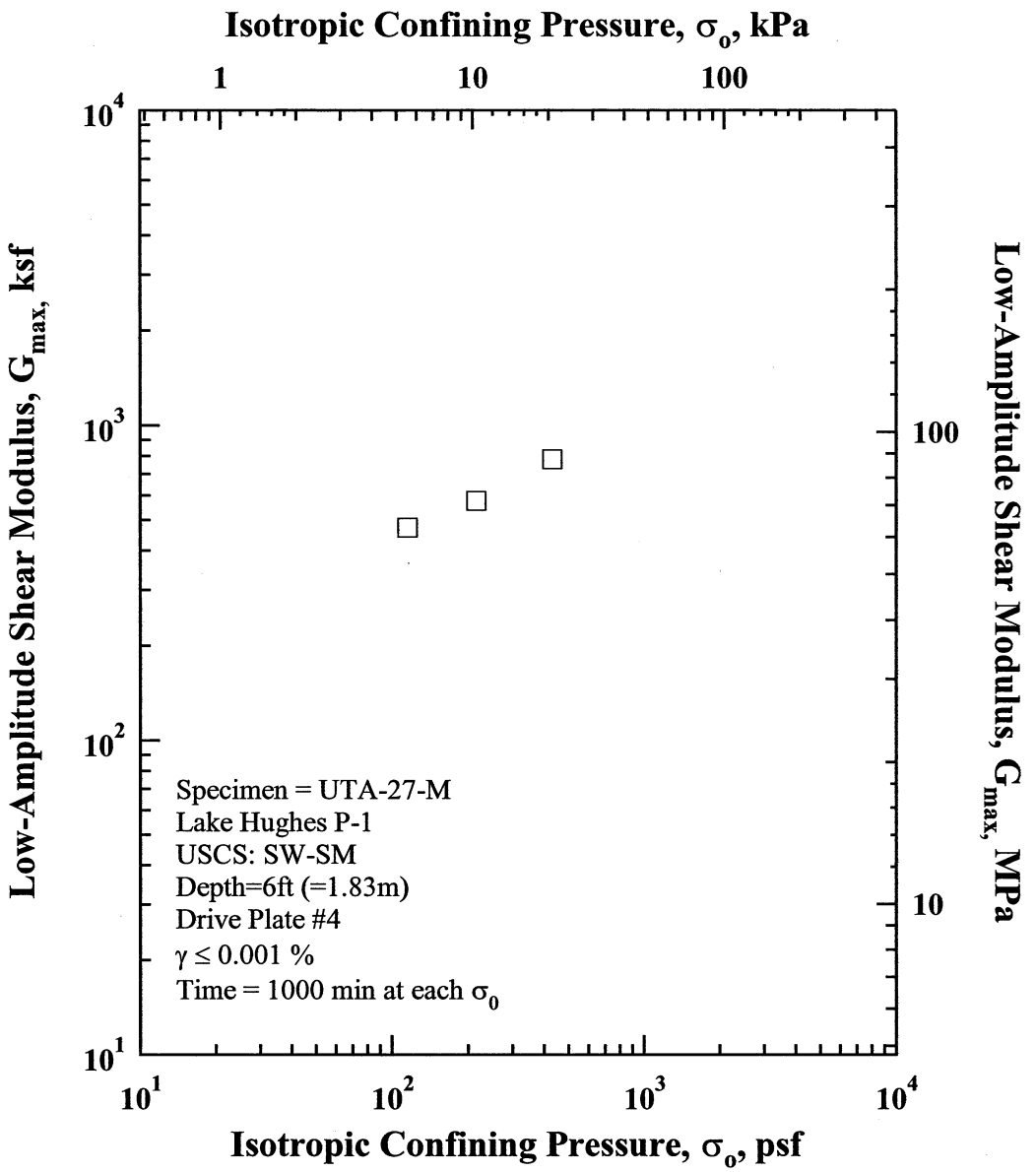

Figure R.5 Variation in Low-Amplitude Shear Modulus with Isotropic Confining Pressure from Resonant Column Tests of Specimen UTA-27-M.

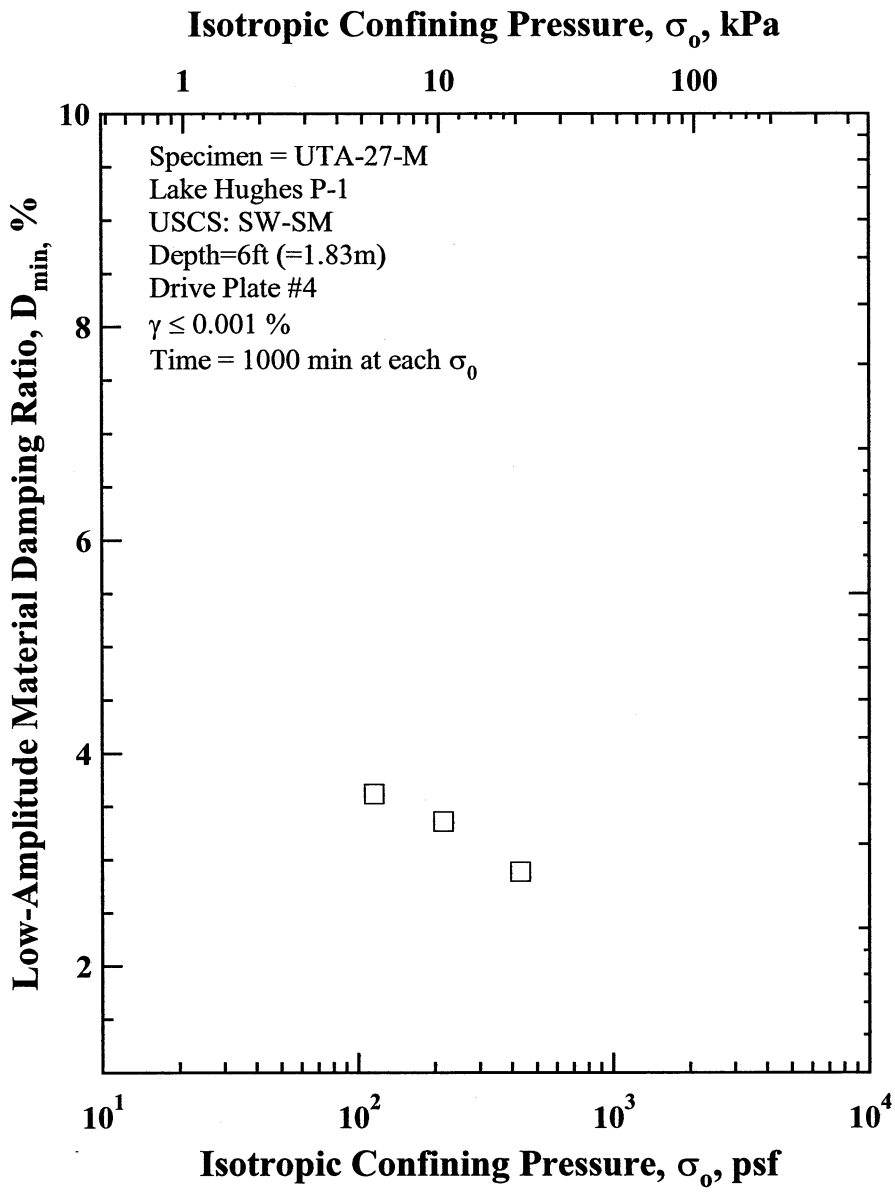

Figure R.6 Variation in Low-Amplitude Material Damping Ratio with Isotropic Confining Pressure from Resonant Column Tests of Specimen UTA-27-M.

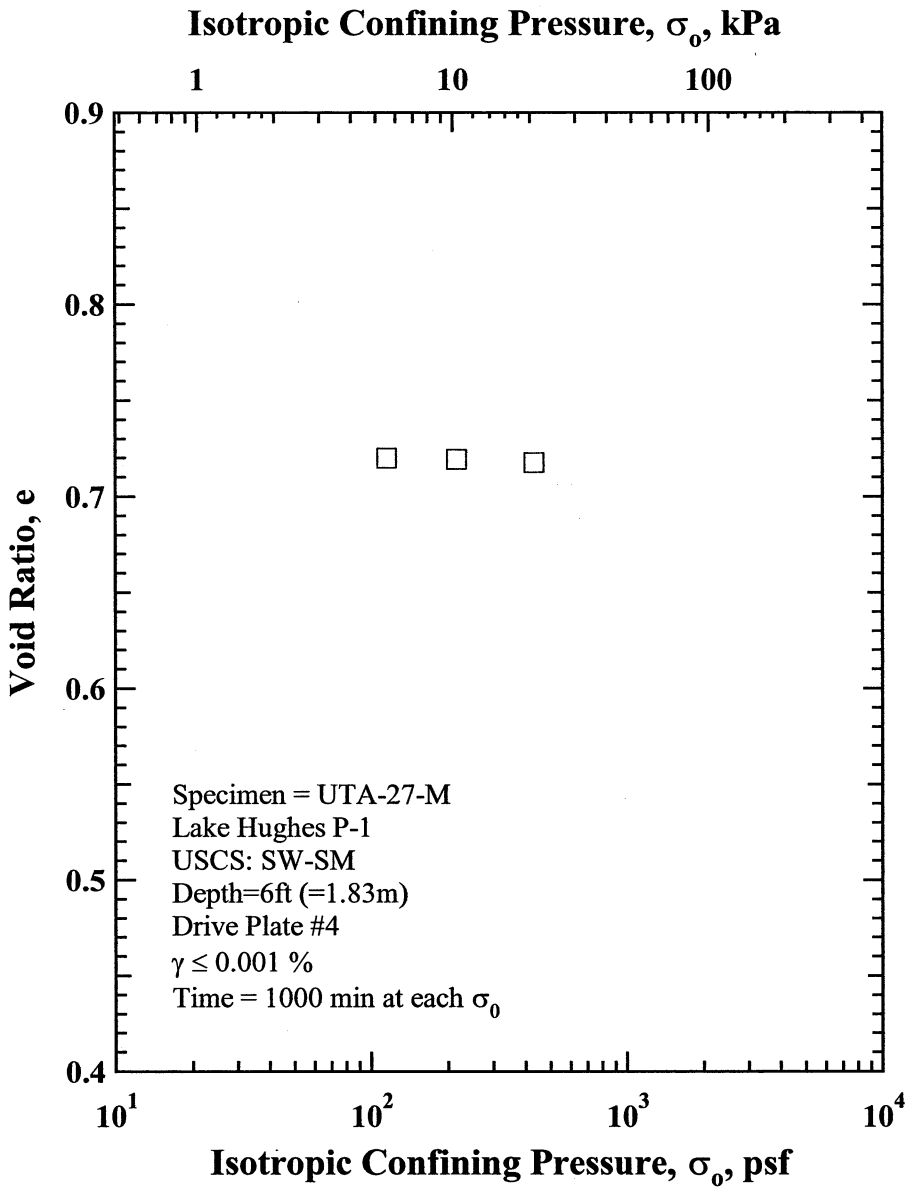

Figure R.7 Variation in Estimated Void Ratio with Isotropic Confining Pressure from Resonant Column Tests of Specimen UTA-27-M.

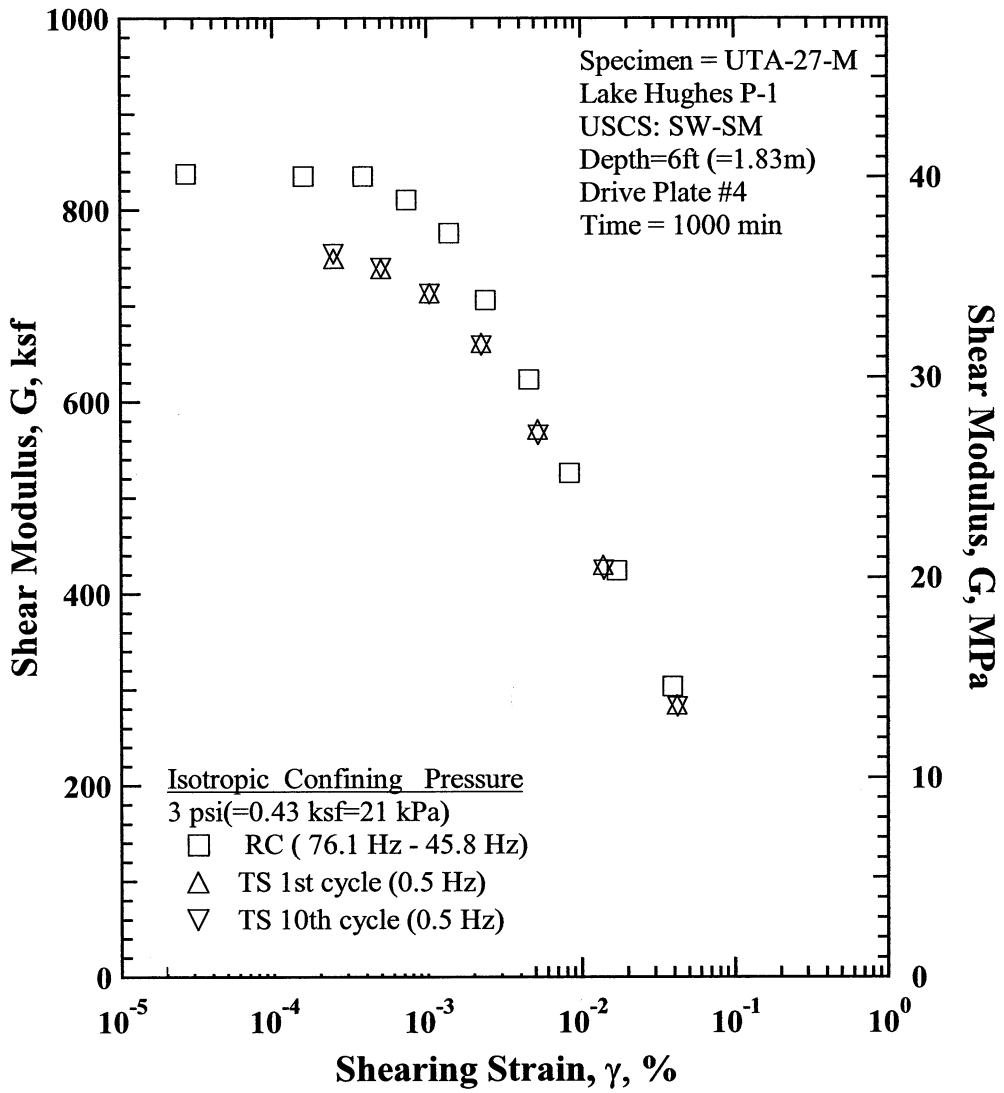

Figure R.8 Comparison of the Variation in Shear Modulus with Shearing Strain at an Isotropic Confining Pressure of 3 psi(=0.43 ksf=21 kPa) from the Combined RCTS Tests of Specimen UTA-27-M.

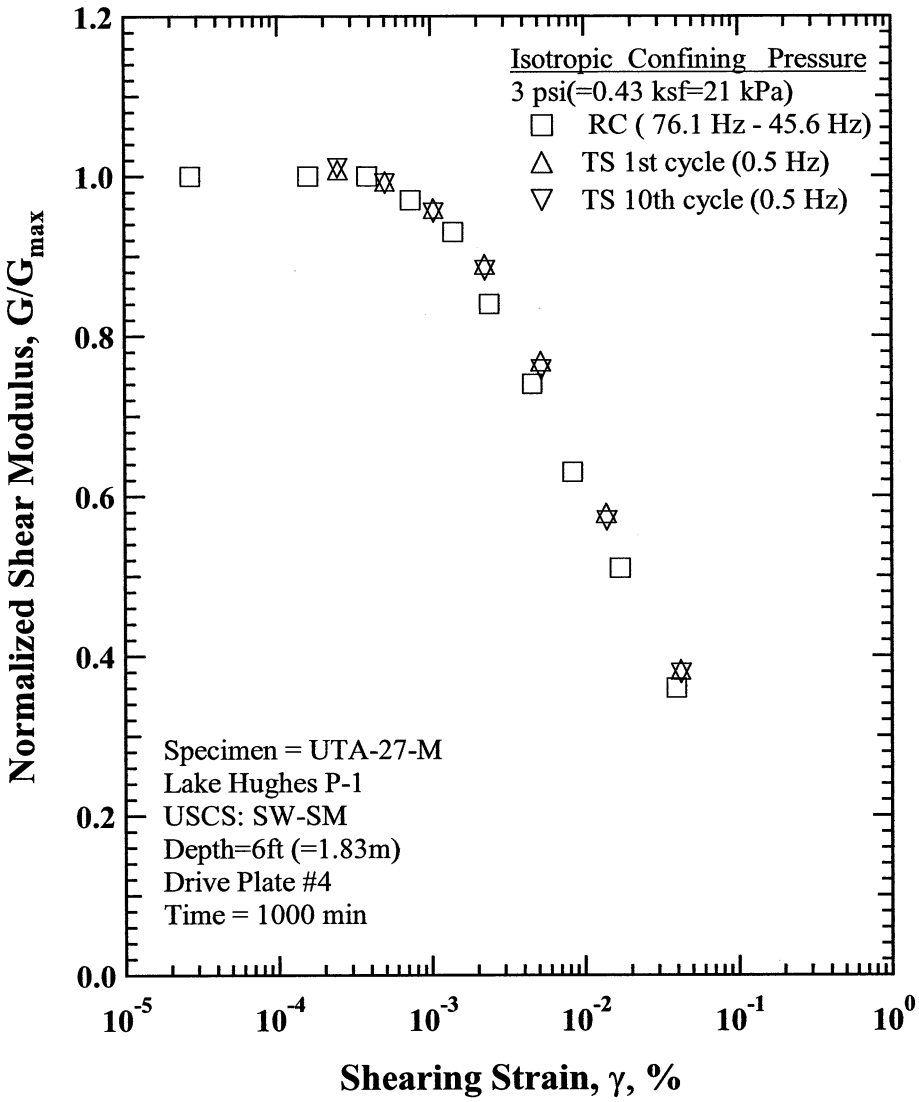

Figure R.9 Comparison of the Variation in Normalized Shear Modulus with Shearing Strain at an Isotropic Confining Pressure of 3 psi(=0.43 ksf=21 kPa) from the Combined RCTS Tests of Specimen UTA-27-M.

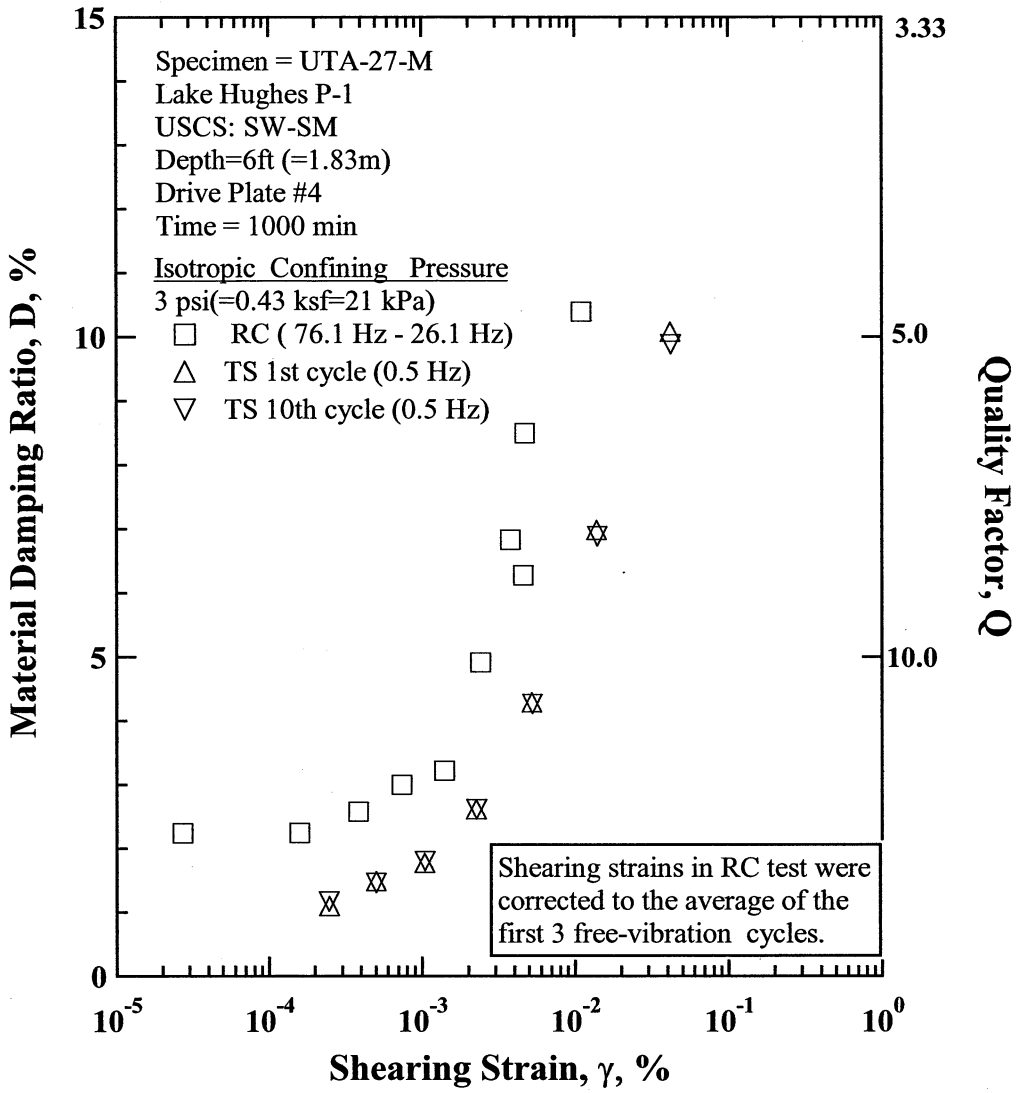

Figure R.10 Comparison of the Variation in Material Damping Ratio with Shearing Strain at an Isotropic Confining Pressure of 3 psi(=0.43 ksf=21 kPa) from the Combined RCTS Tests of Specimen UTA-27-M.

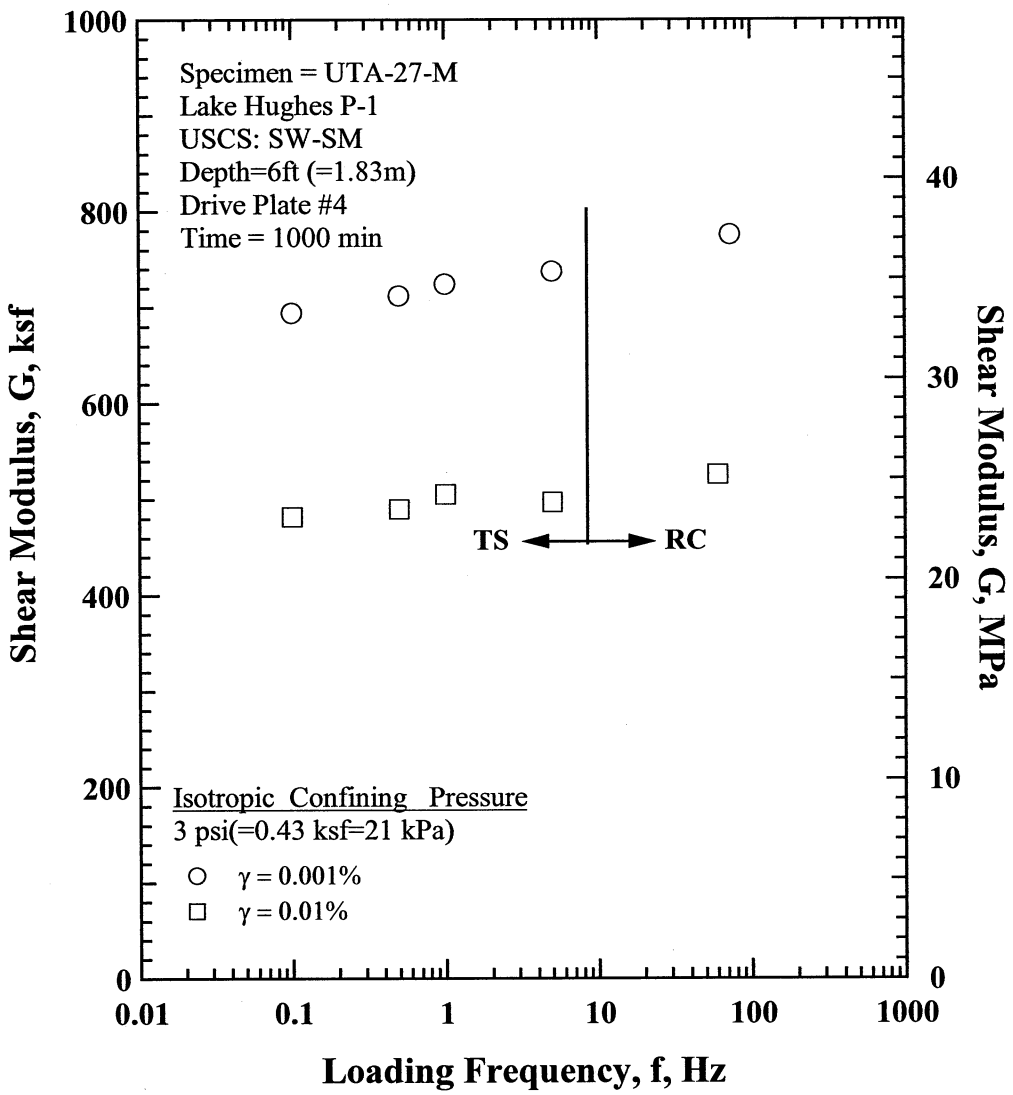

Figure R.11 Comparison of the Variation in Shear Modulus with Loading Frequency at an Isotropic Confining Pressure of 3 psi(=0.43 ksf=21 kPa) from the Combined RCTS Tests of Specimen UTA-27-M.

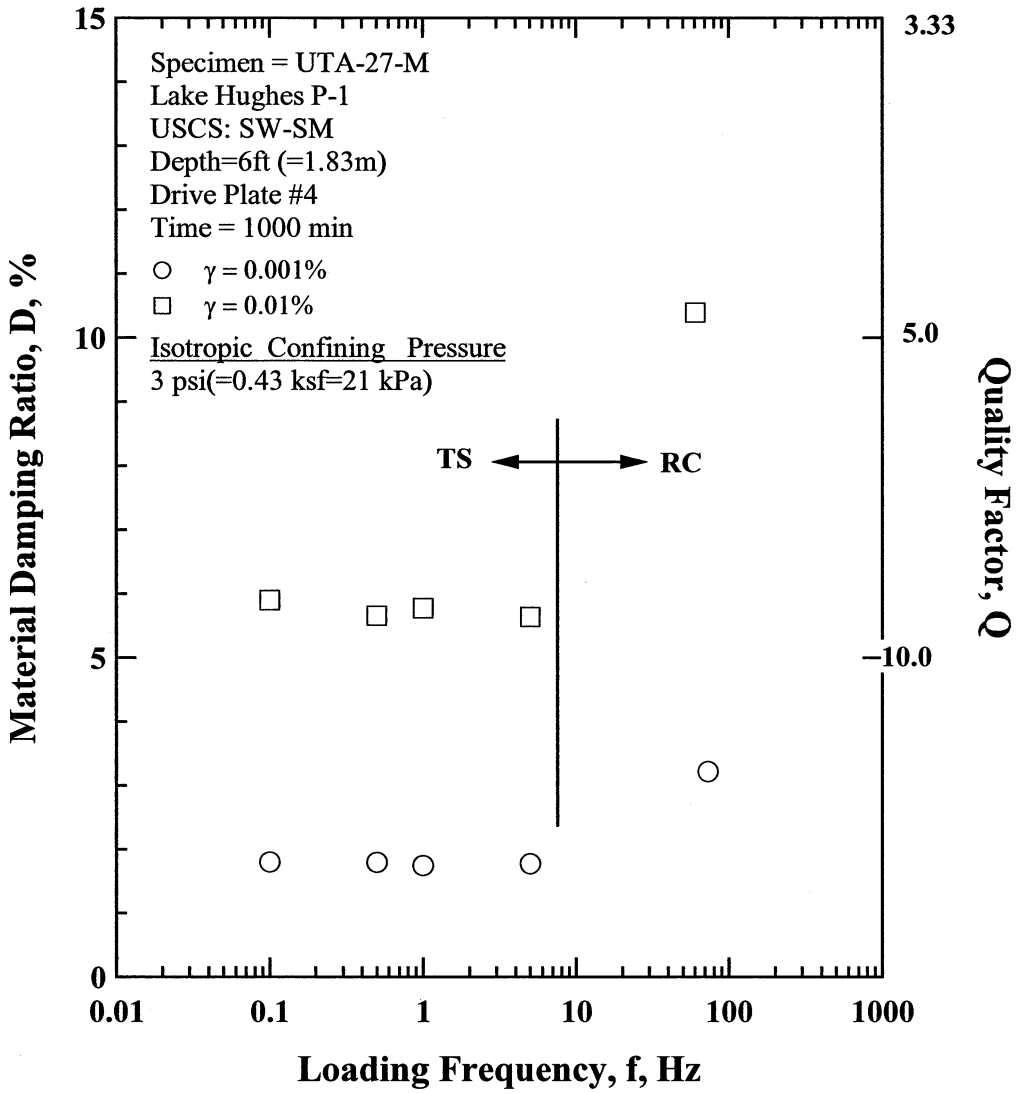

Figure R.12 Comparison of the Variation in Material Damping Ratio with Loading Frequency at an Isotropic Confining Pressure 3 psi(=0.43 ksf=21 kPa) from the Combined RCTS Tests of Specimen UTA-27-M.

Table R.1 Variation in Low-Amplitude Shear Wave Velocity, Low-Amplitude Shear Modulus, Low-Amplitude Material Damping Ratio and Estimated Void Ratio with Isotropic Confining Pressure from RC Tests of Specimen UTA-27-M

Effective Isotropic Confining Pressure, σ_o'			Low-Amplitude Shear Modulus, G_{max}		Low-Amplitude Shear Wave Velocity, Vs	Low-Amplitude Material Damping Ratio, Dmin	Estimated Void Ratio, e
(psi)	(psf)	(kPa)	(ksf)	(MPa)	(fps)	(%)	H
0.8	115	5.5	473	22.7	364	3.62	0.720
2	216	10.4	575	27.6	401	3.36	0.719
3	432	20.7	780	37.4	467	2.89	0.718

Table R.2 Variation in Shear Modulus, Normalized Shear Modulus and Material Damping Ratio with Shearing Strain from RC Tests of Specimen UTA-27-M; Confining Pressure, σ_o' =4 psi (=0.58 ksf=28 kPa).

Peak Shearing Strain, %	Shear Modulus, G, ksf	Normalized Shear Modulus, G/G_{max}	Average[+] Shearing Strain, %	Material Damping Ratio[x], D, %
2.71E-05	838	1.00	2.71E-05	2.24
1.58E-04	835	1.00	1.58E-04	2.25
3.84E-04	835	1.00	3.84E-04	2.58
7.39E-04	811	0.97	7.39E-04	3.00
1.40E-03	776	0.93	8.57E-04	3.10
2.40E-03	706	0.84	1.35E-03	4.21
4.58E-03	623	0.74	2.80E-03	5.46
8.39E-03	526	0.63	3.77E-03	6.83
1.70E-02	424	0.51	4.68E-03	8.50
3.93E-02	303	0.36	1.10E-02	10.39

[+] Average Shearing Strain from the First Three Cycles of the Free Vibration Decay Curve

[x] Average Damping Ratio from the First Three Cycles of the Free Vibration Decay Curve

Table R.3 Variation in Shear Modulus, Normalized Shear Modulus and Material Damping Ratio with Shearing Strain from TS Tests of Specimen UTA-27-M; Confining Pressure, σ_o' =4 psi (=0.58 ksf=28 kPa).

First Cycle				Tenth Cycle			
Peak Shearing Strain, %	Shear Modulus, G, ksf	Normalized Shear Modulus, G/G_{max}	Material Damping Ratio, D, %	Peak Shearing Strain, %	Shear Modulus, G, ksf	Normalized Shear Modulus, G/G_{max}	Material Damping Ratio, D, %
2.49E-04	749	1.01	1.10	2.48E-04	754	1.01	1.17
5.06E-04	738	0.99	1.49	5.05E-04	739	0.99	1.47
1.05E-03	713	0.96	1.78	1.05E-03	712	0.95	1.81
2.26E-03	661	0.89	2.61	2.27E-03	658	0.88	2.62
5.24E-03	571	0.77	4.29	5.29E-03	565	0.76	4.27
1.39E-02	429	0.58	6.99	1.41E-02	424	0.57	6.89
4.22E-02	284	0.38	10.08	4.25E-02	282	0.38	9.89

APPENDIX S

Specimen No. 18
UT Specimen ID: UTA-27-N

Joshua Tree P-7
Depth = 236ft (=71.9m)
Soil Type: Sand (SP)

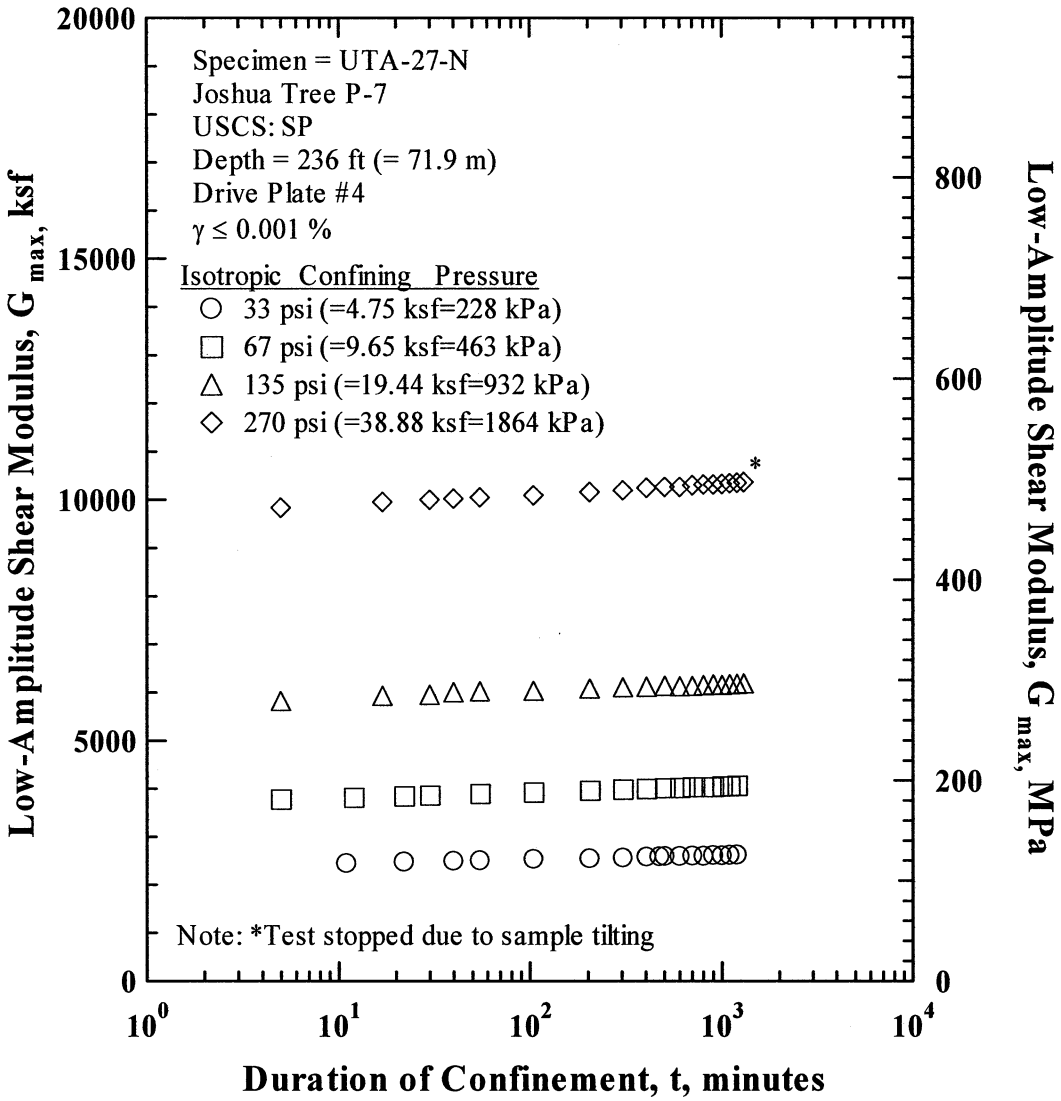

Figure S.1 Variation in Low-Amplitude Shear Modulus with Magnitude and Duration of Isotropic Confining Pressure from Resonant Column Tests of Specimen UTA-27-N.

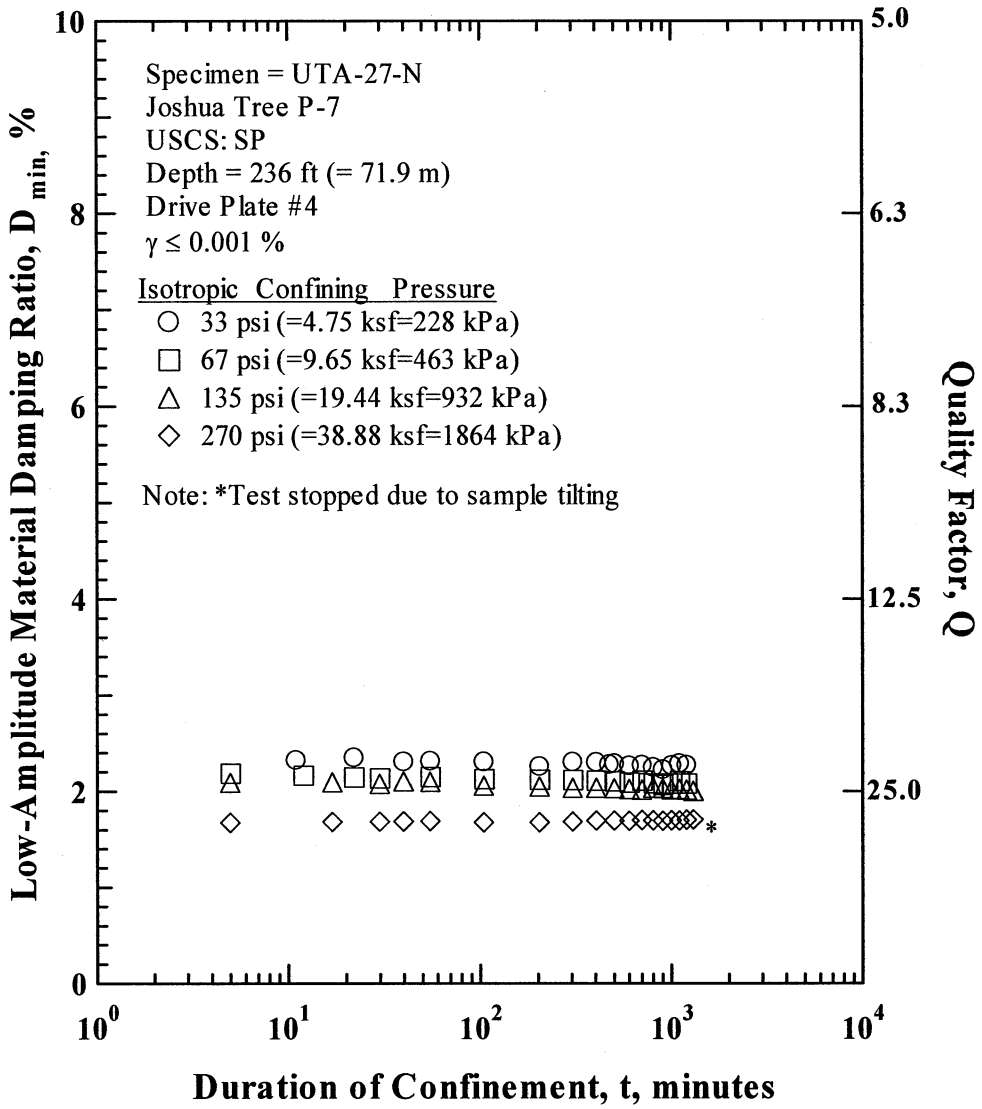

Figure S.2 Variation in Low-Amplitude Material Damping Ratio with Magnitude and Duration of Isotropic Confining Pressure from Resonant Column Tests of Specimen UTA-27-N

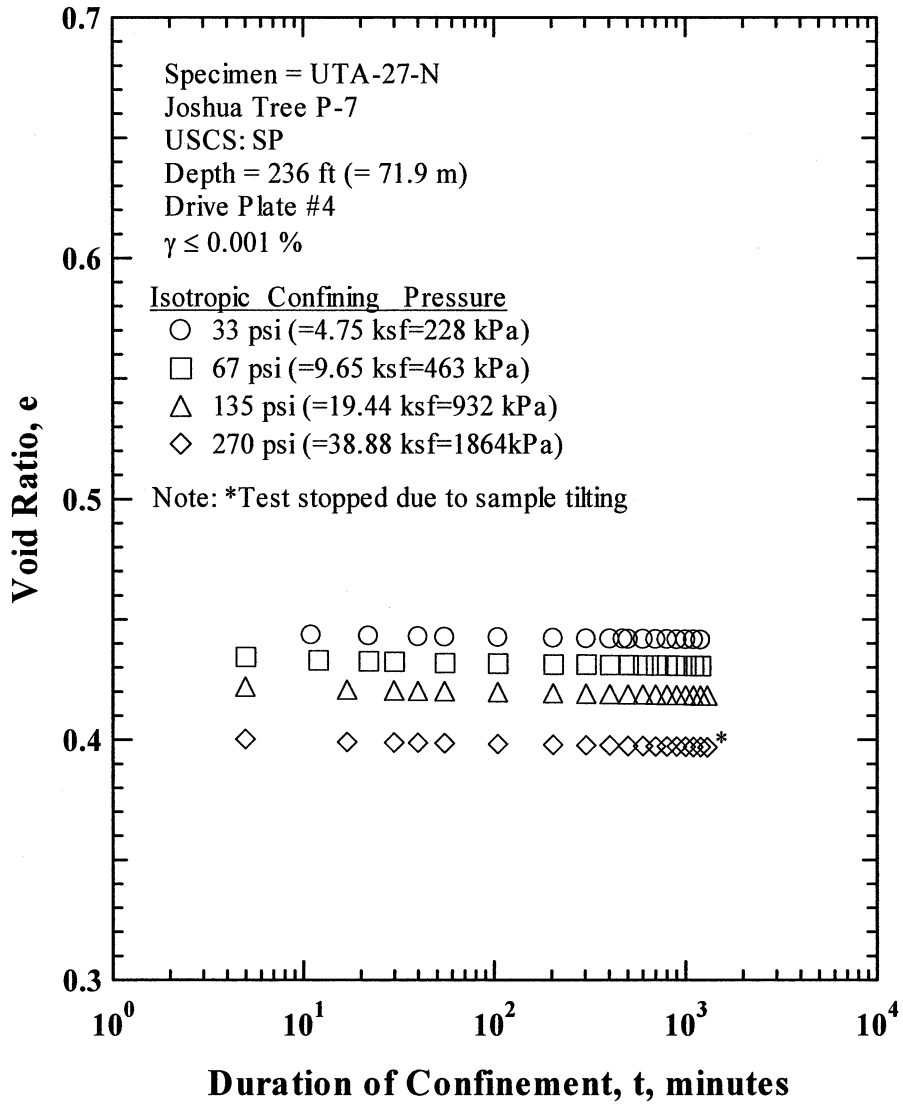

Figure S.3 Variation in Estimated Void Ratio with Magnitude and Duration of Isotropic Confining Pressure from Resonant Column Tests of Specimen UTA-27-N.

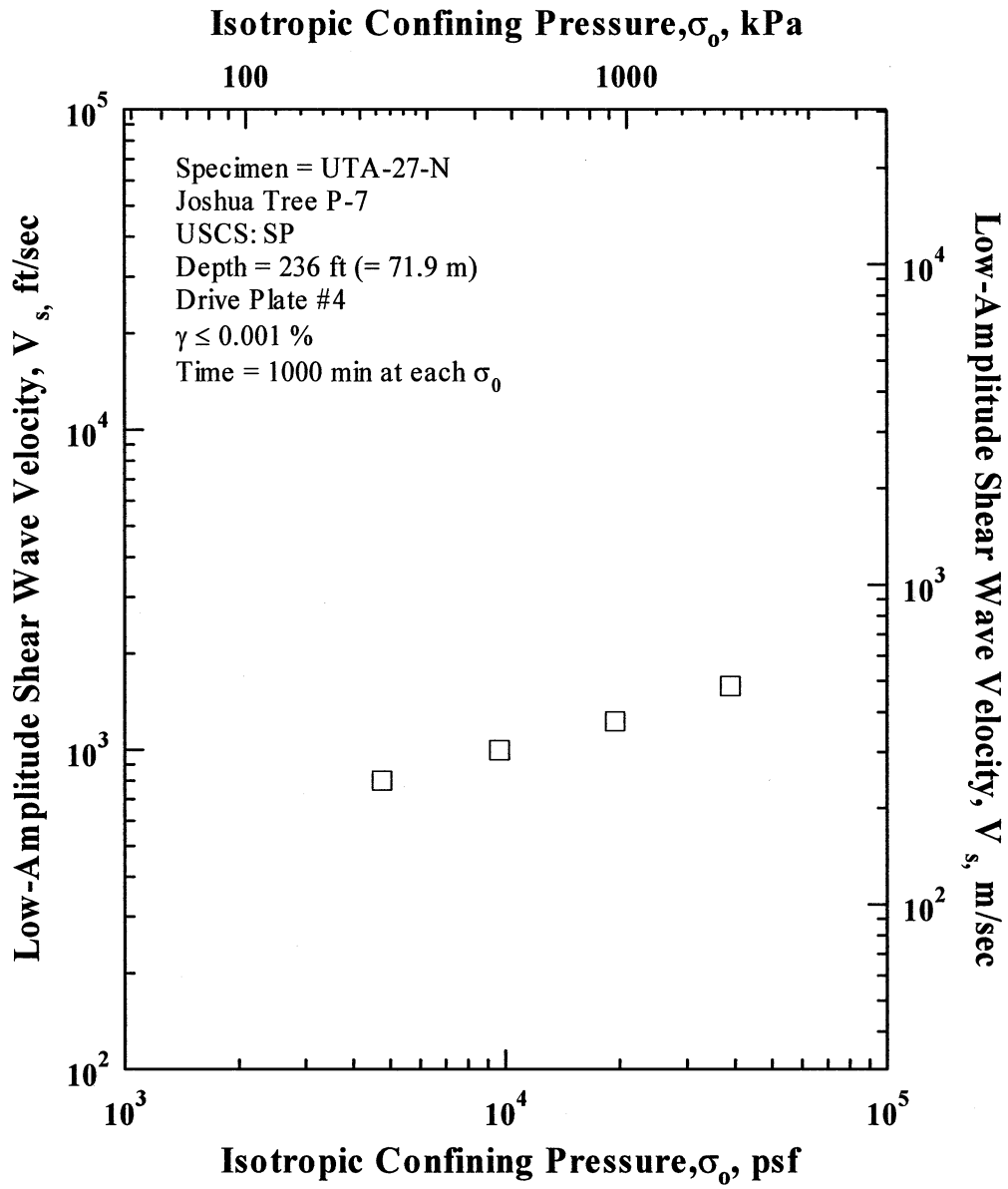

Figure S.4 Variation in Low-Amplitude Shear Wave Velocity with Isotropic Confining Pressure from Resonant Column Tests of Specimen UTA-27-N.

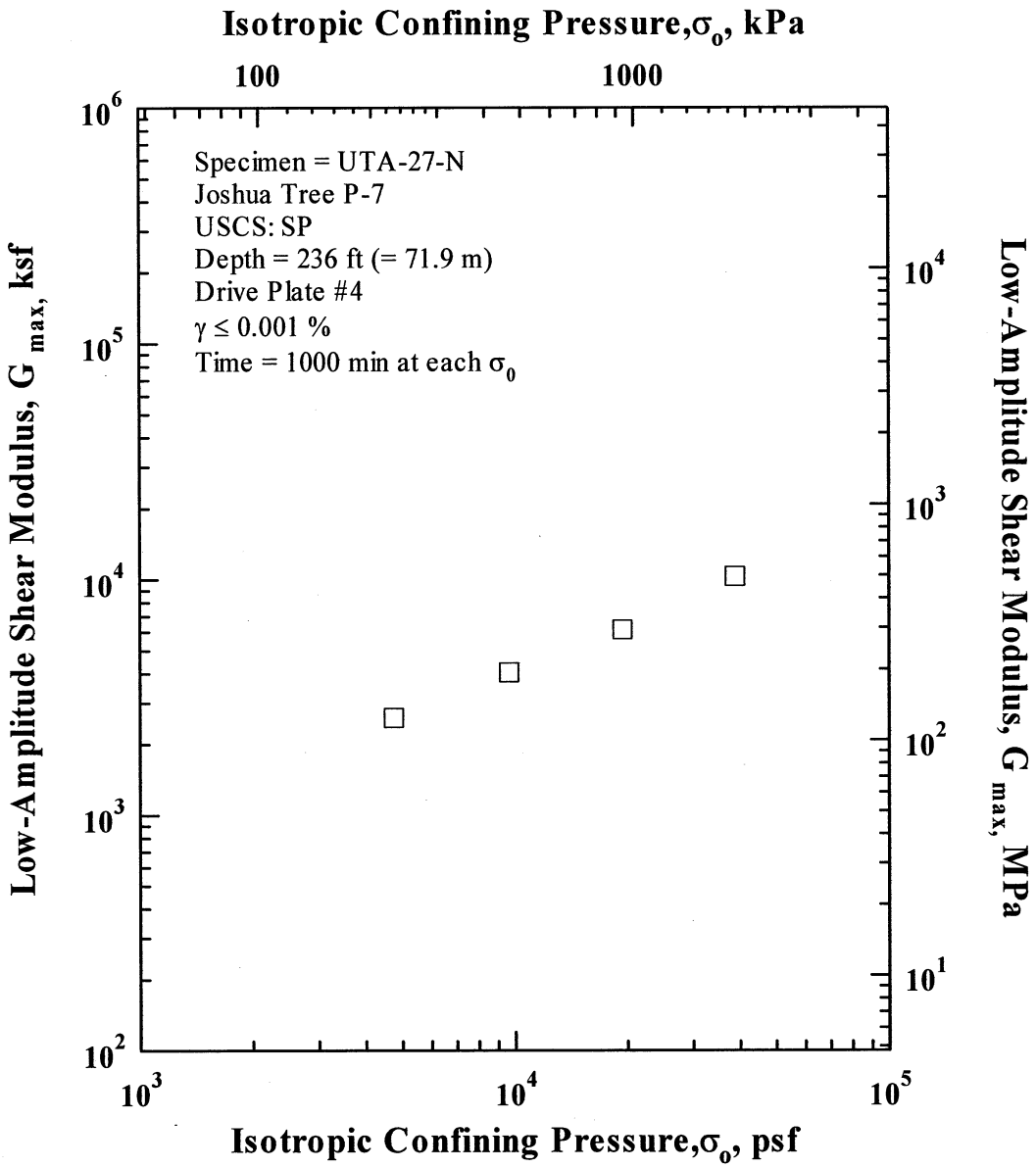

Figure S.5 Variation in Low-Amplitude Shear Modulus with Isotropic Confining Pressure from Resonant Column Tests of Specimen UTA-27-N.

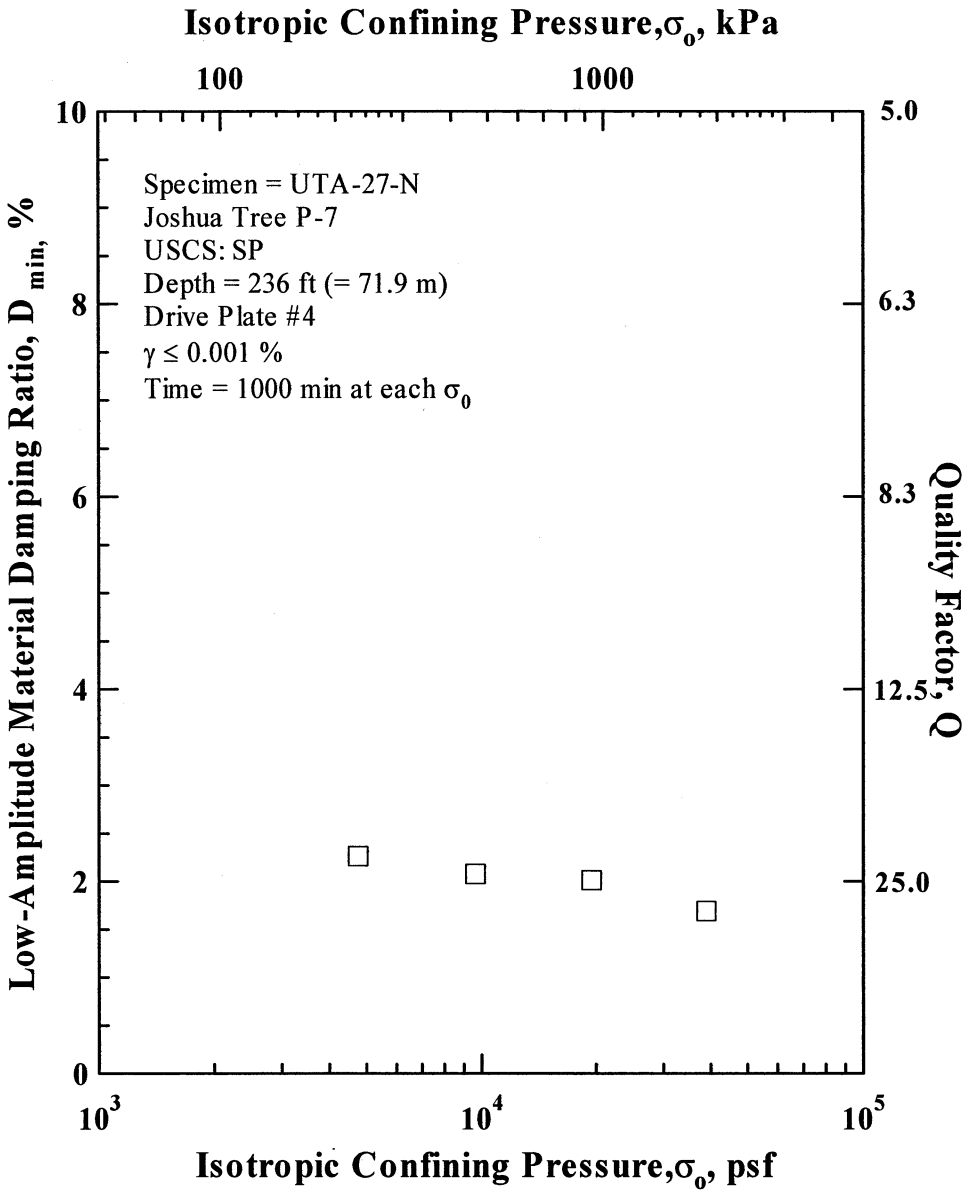

Figure S.6 Variation in Low-Amplitude Material Damping Ratio with Isotropic Confining Pressure from Resonant Column Tests of Specimen UTA-27-N.

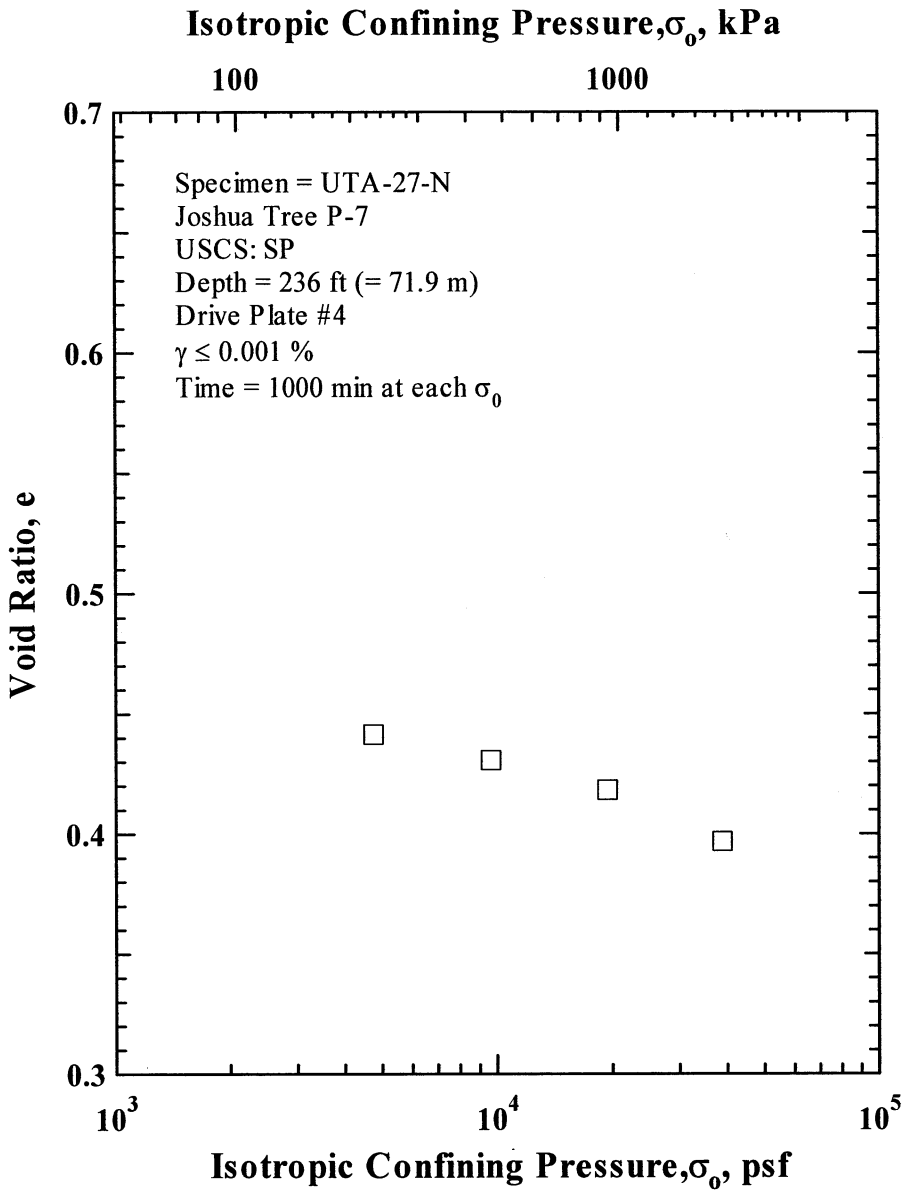

Figure S.7 Variation in Estimated Void Ratio with Isotropic Confining Pressure from Resonant Column Tests of Specimen UTA-27-N.

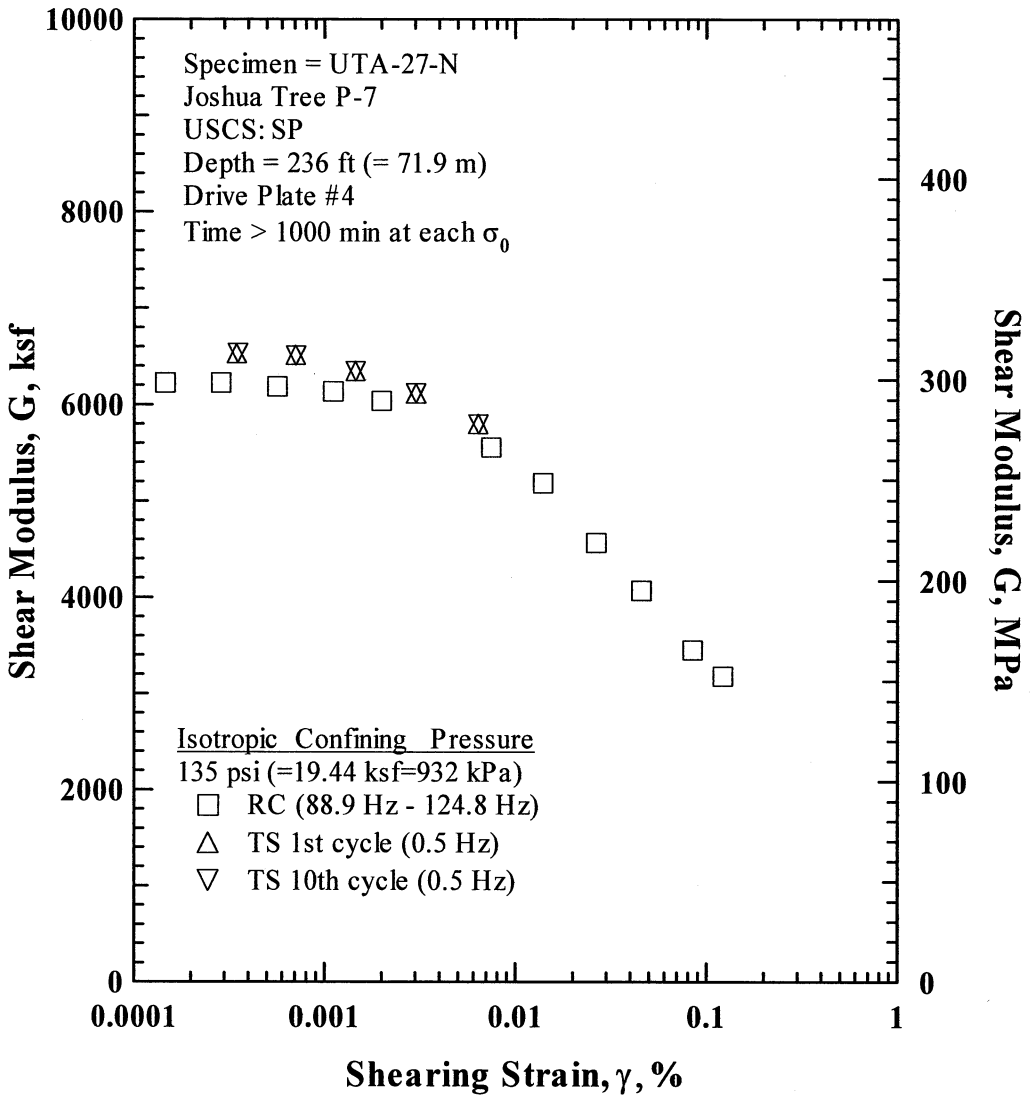

Figure S.8 Comparison of the Variation in Shear Modulus with Shearing Strain at an Isotropic Confining Pressure of 135 psi (=19.44 ksf=932 kPa) from the Combined RCTS Tests of Specimen UTA-27-N.

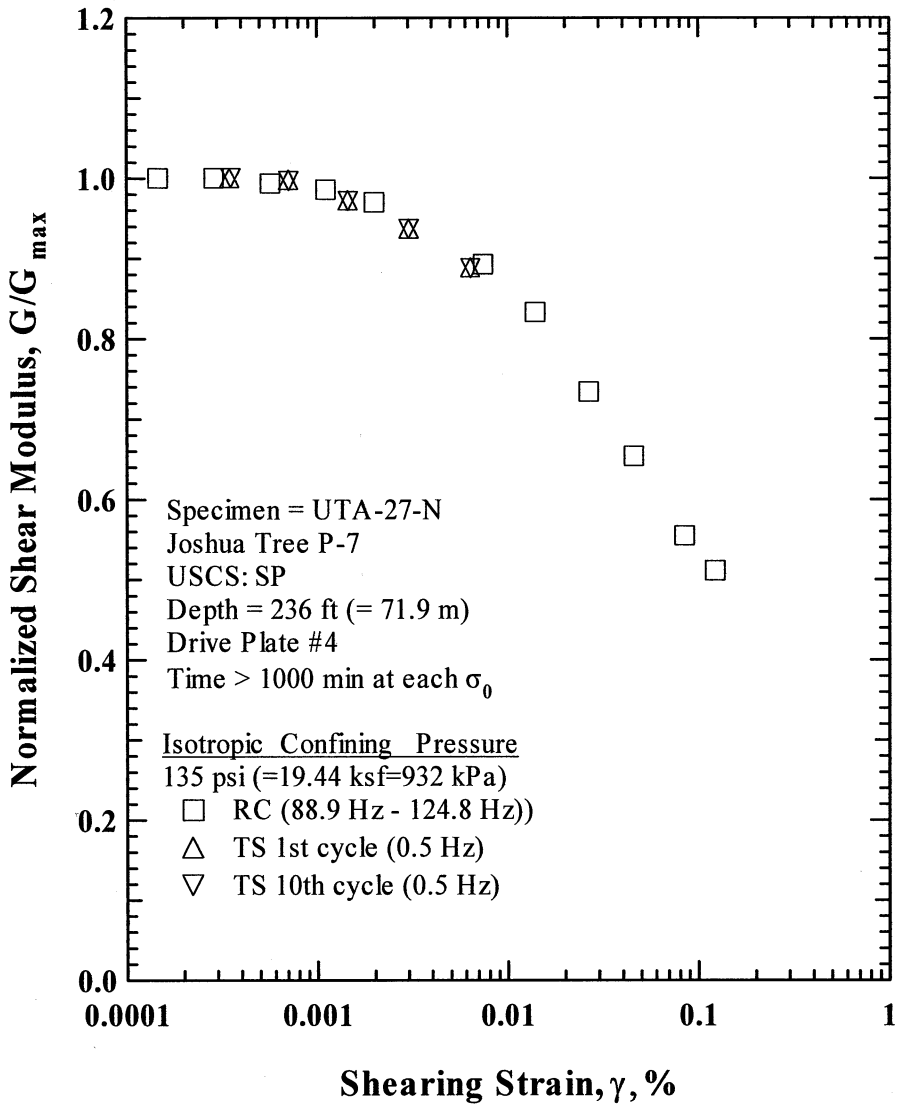

Figure S.9 Comparison of the Variation in Normalized Shear Modulus with Shearing Strain at an Isotropic Confining Pressure of 135 psi (=19.44 ksf=932 kPa) from the Combined RCTS Tests of Specimen UTA-27-N.

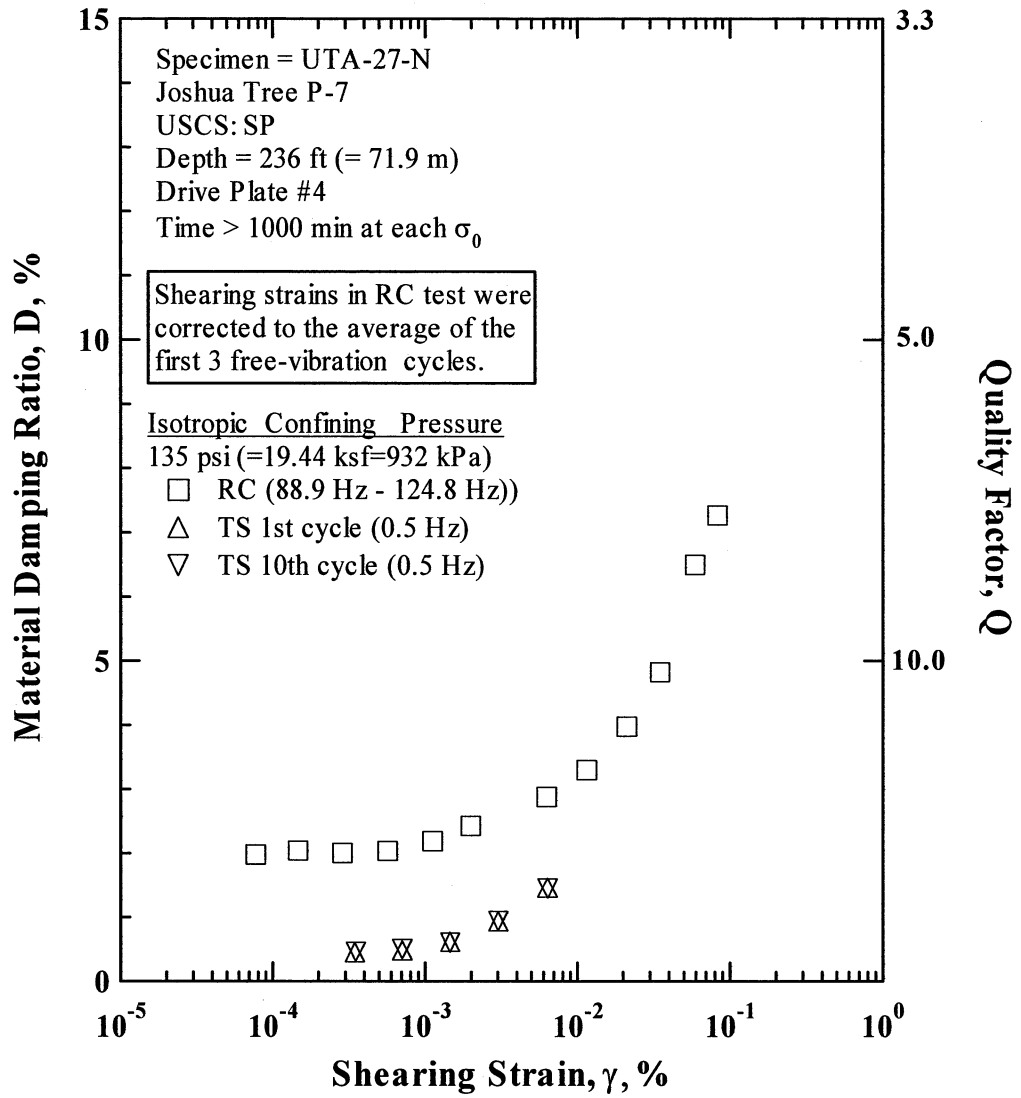

Figure S.10 Comparison of the Variation in Material Damping Ratio with Shearing Strain at an Isotropic Confining Pressure of 135 psi (=19.44 ksf=932 kPa) from the Combined RCTS Tests of Specimen UTA-27-N.

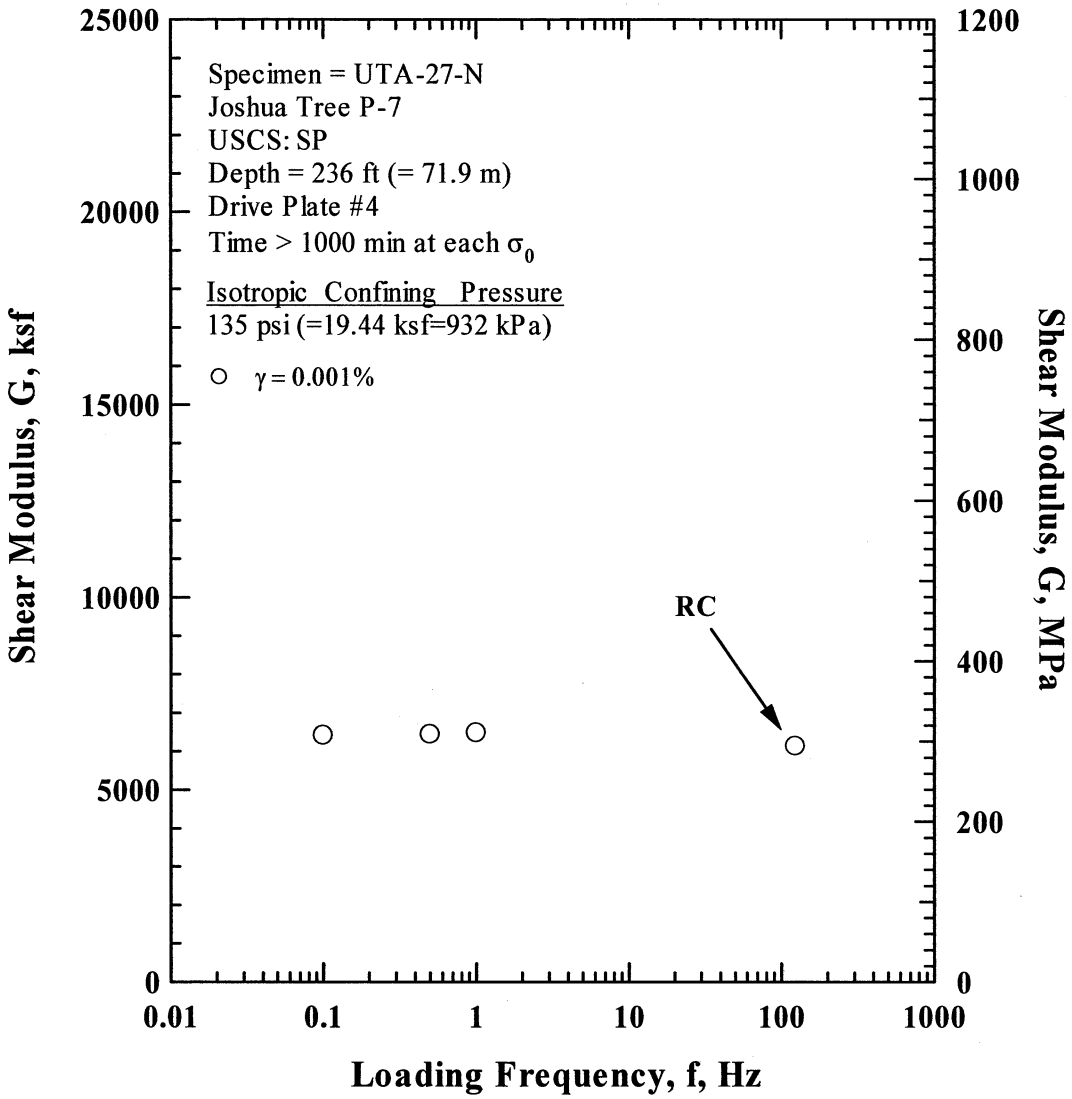

Figure S.11 Comparison of the Variation in Shear Modulus with Loading Frequency at an Isotropic Confining Pressure of 135 psi (=19.44 ksf=932 kPa) from the Combined RCTS Tests of Specimen UTA-27-N.

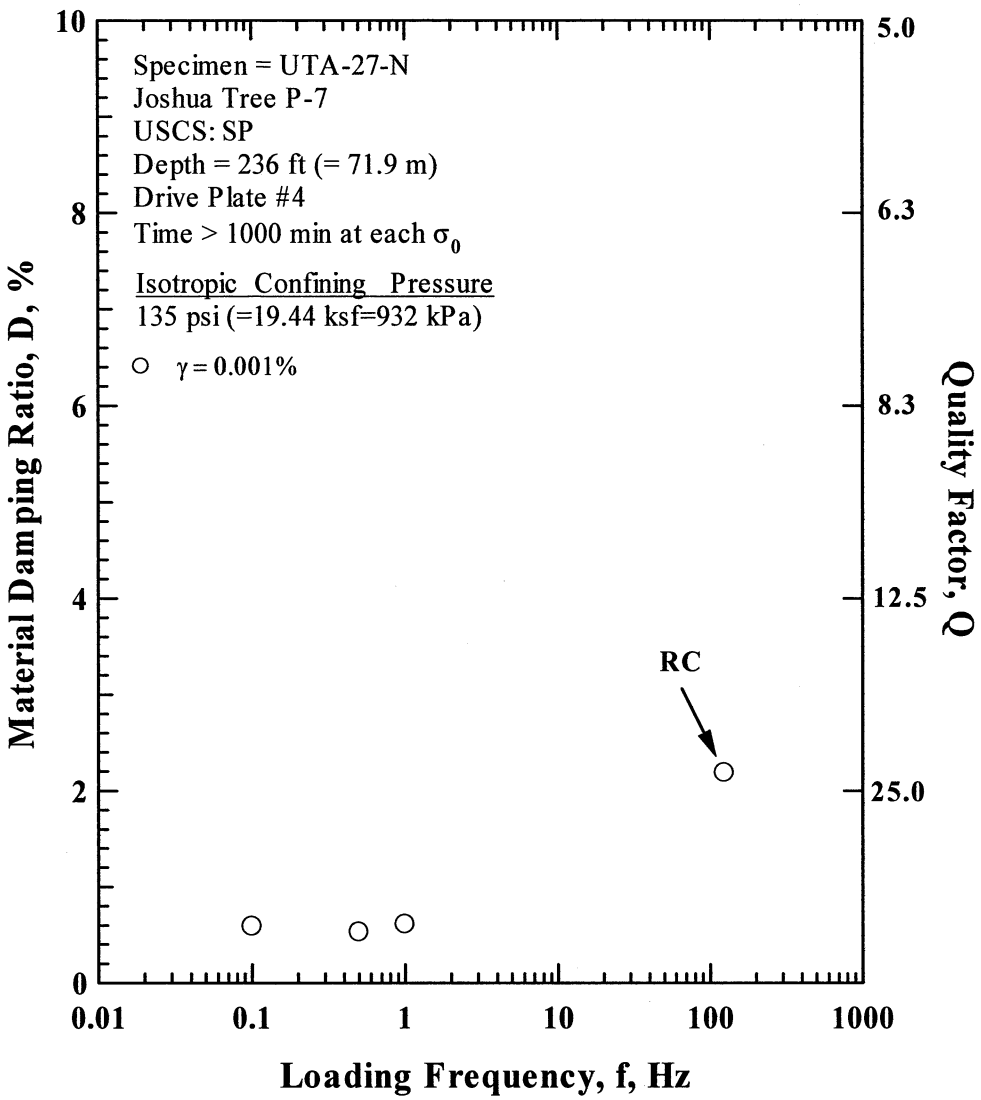

Figure S.12 Comparison of the Variation in Material Damping Ratio with Loading Frequency at an Isotropic Confining Pressure 135 psi (=19.44 ksf=932 kPa) from the Combined RCTS Tests of Specimen UTA-27-N.

Table S.1 Variation in Low-Amplitude Shear Wave Velocity, Low-Amplitude Shear Modulus, Low-Amplitude Material Damping Ratio and Estimated Void Ratio with Isotropic Confining Pressure from RC Tests of Specimen UTA-27-N

Effective Isotropic Confining Pressure, σ_o'			Low-Amplitude Shear Modulus, G_{max}		Low-Amplitude Shear Wave Velocity, Vs	Low-Amplitude Material Damping Ratio, Dmin	Estimated Void Ratio, e
(psi)	(psf)	(kPa)	(ksf)	(MPa)	(fps)	(%)	H
33	4752	228	2596	124.5	802	2.26	0.442
67	9648	463	4049	194.1	999	2.08	0.431
135	19440	932	6148	294.7	1227	2.01	0.418
270	38880	1864	10320	494.7	1582	1.69	0.397

Table S.2 Variation in Shear Modulus, Normalized Shear Modulus and Material Damping Ratio with Shearing Strain from RC Tests of Specimen UTA-27-N; Confining Pressure, σ_o' =135 psi (=19.44 ksf=932 kPa).

Peak Shearing Strain, %	Shear Modulus, G, ksf	Normalized Shear Modulus, G/G_{max}	Average[+] Shearing Strain, %	Material Damping Ratio[x], D, %
1.46E-04	6223	1.00	1.46E-04	2.04
7.73E-05	6222	1.00	7.73E-05	1.98
2.88E-04	6223	1.00	2.88E-04	2.01
5.68E-04	6184	0.99	5.68E-04	2.04
1.11E-03	6134	0.99	1.11E-03	2.19
1.99E-03	6036	0.97	1.99E-03	2.42
7.43E-03	5554	0.89	6.27E-03	2.88
1.39E-02	5184	0.83	1.15E-02	3.30
2.65E-02	4566	0.73	2.10E-02	3.98
4.57E-02	4069	0.65	3.48E-02	4.82
8.45E-02	3453	0.55	5.93E-02	6.49
1.22E-01	3180	0.51	8.29E-02	7.26

[+] Average Shearing Strain from the First Three Cycles of the Free Vibration Decay Curve

[x] Average Damping Ratio from the First Three Cycles of the Free Vibration Decay Curve

Table S.3 Variation in Shear Modulus, Normalized Shear Modulus and Material Damping Ratio with Shearing Strain from TS Tests of Specimen UTA-27-N; Confining Pressure, σ_o' =135 psi (=19.44 ksf=932 kPa).

First Cycle				Tenth Cycle			
Peak Shearing Strain, %	Shear Modulus, G, ksf	Normalized Shear Modulus, G/G_{max}	Material Damping Ratio, D, %	Peak Shearing Strain, %	Shear Modulus, G, ksf	Normalized Shear Modulus, G/G_{max}	Material Damping Ratio, D, %
3.49E-04	6523	1.00	0.44	3.55E-04	6525	1.00	0.45
7.11E-04	6509	1.00	0.47	7.12E-04	6501	1.00	0.50
1.46E-03	6341	0.97	0.61	1.46E-03	6338	0.97	0.59
3.03E-03	6109	0.94	0.93	3.03E-03	6108	0.94	0.93
6.40E-03	5795	0.89	1.45	6.41E-03	5789	0.89	1.44

APPENDIX T

Specimen No. 19
UT Specimen ID: UTA-27-O

Joshua Tree P-8
Depth = 328 ft (= 100 m)
Soil Type: Sand (SW)

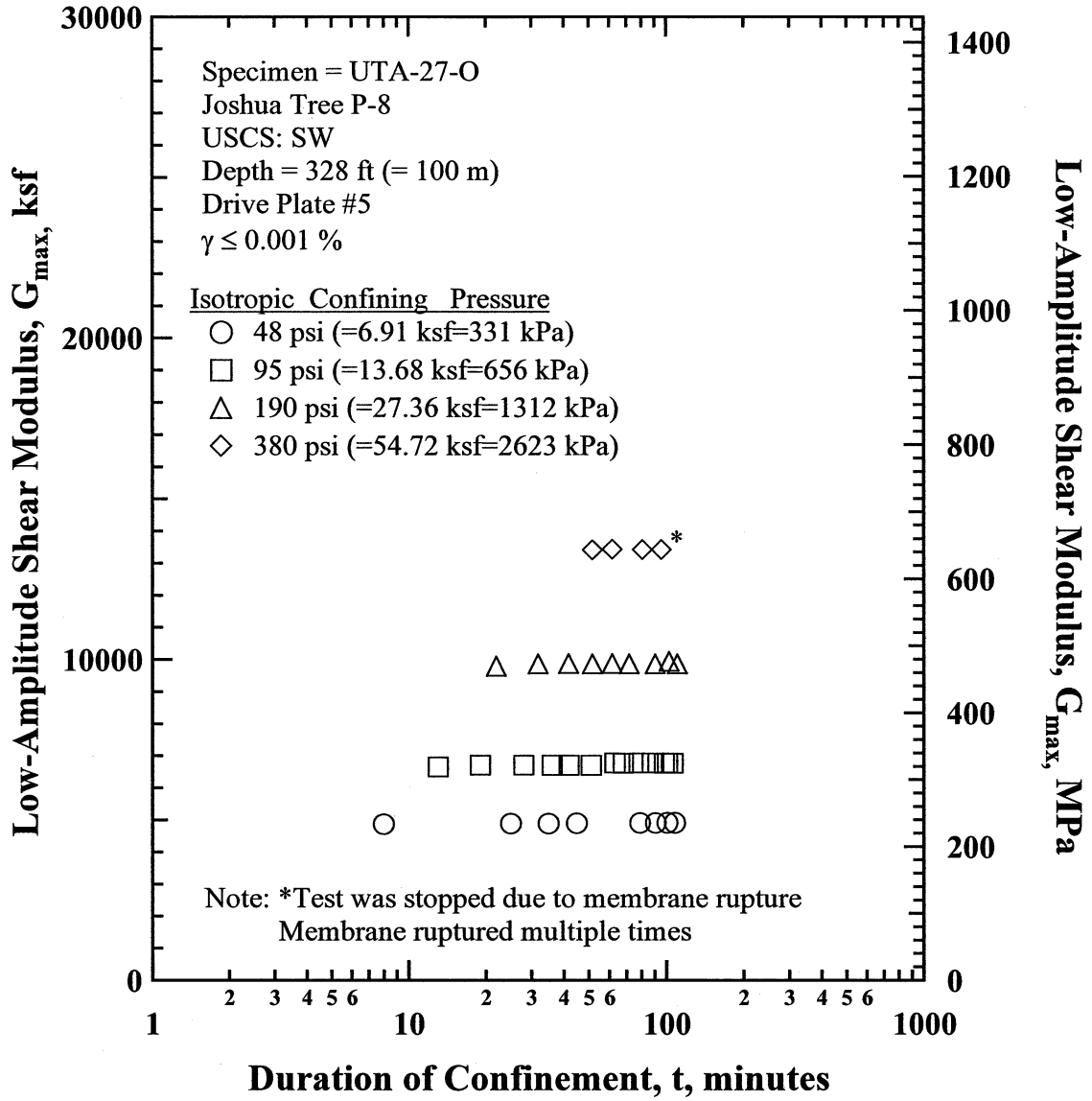

Figure T.1 Variation in Low-Amplitude Shear Modulus with Magnitude and Duration of Isotropic Confining Pressure from Resonant Column Tests of Specimen UTA-27-O.

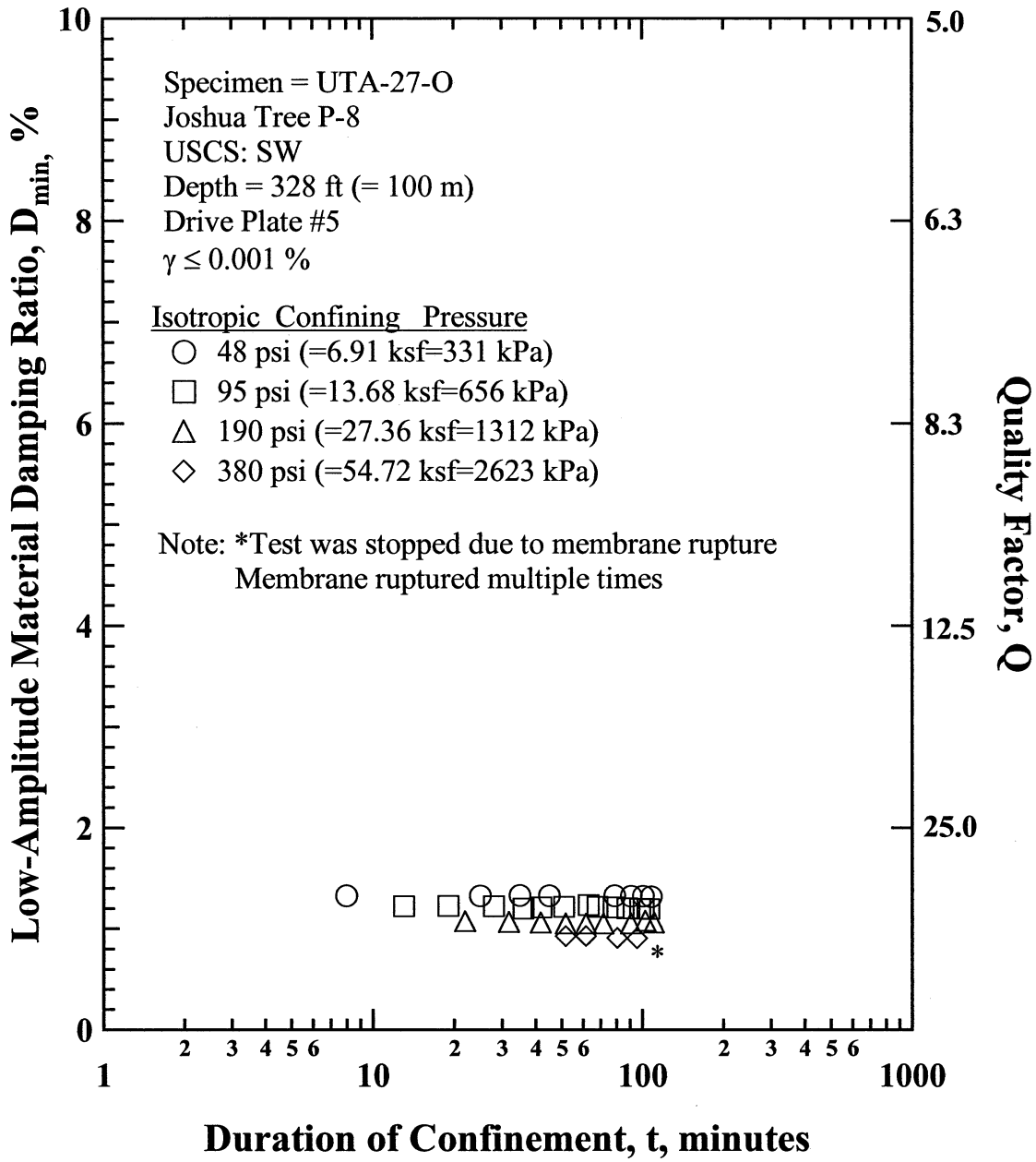

Figure T.2 Variation in Low-Amplitude Material Damping Ratio with Magnitude and Duration of Isotropic Confining Pressure from Resonant Column Tests of Specimen UTA-27-O

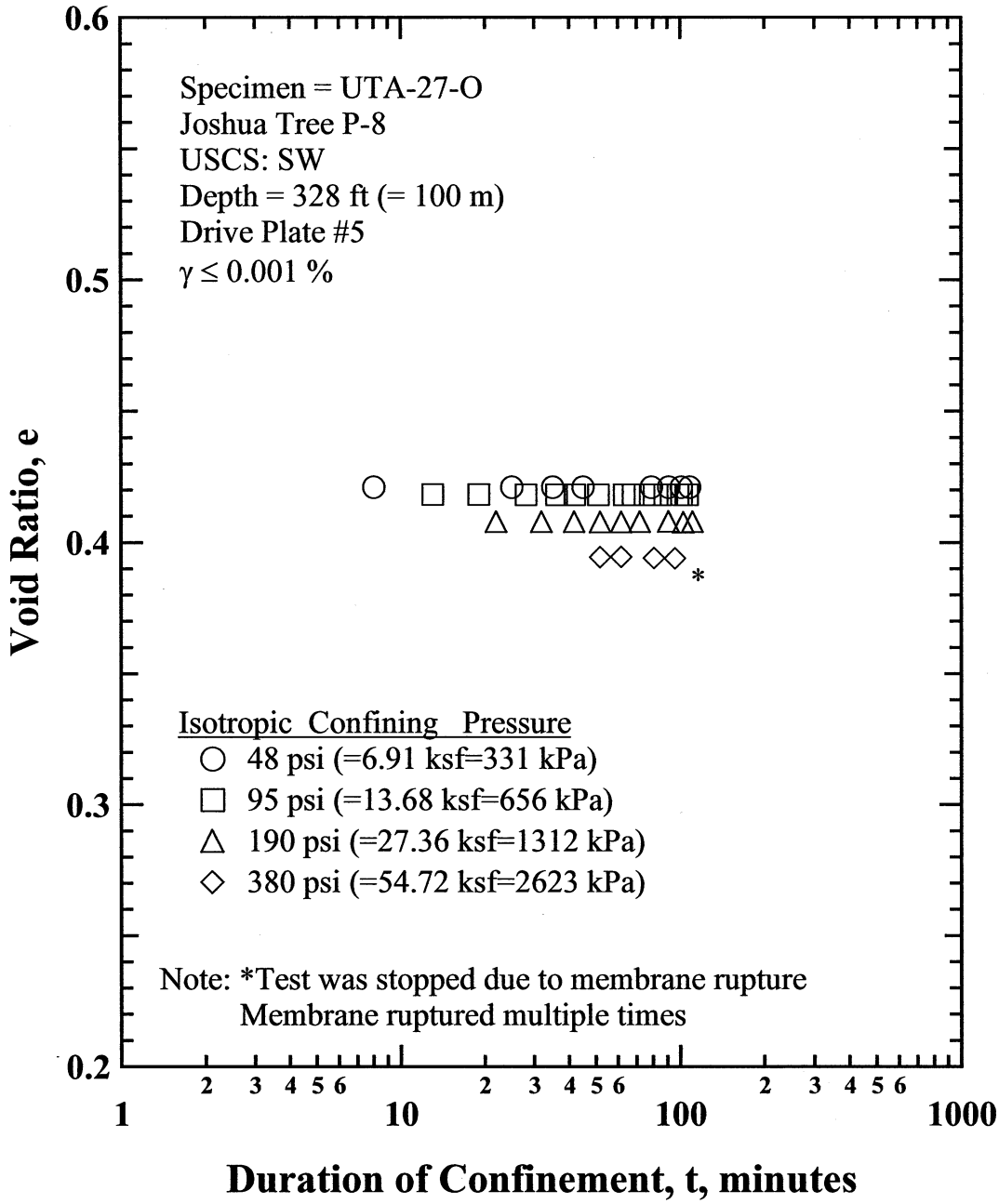

Figure T.3 Variation in Estimated Void Ratio with Magnitude and Duration of Isotropic Confining Pressure from Resonant Column Tests of Specimen UTA-27-O.

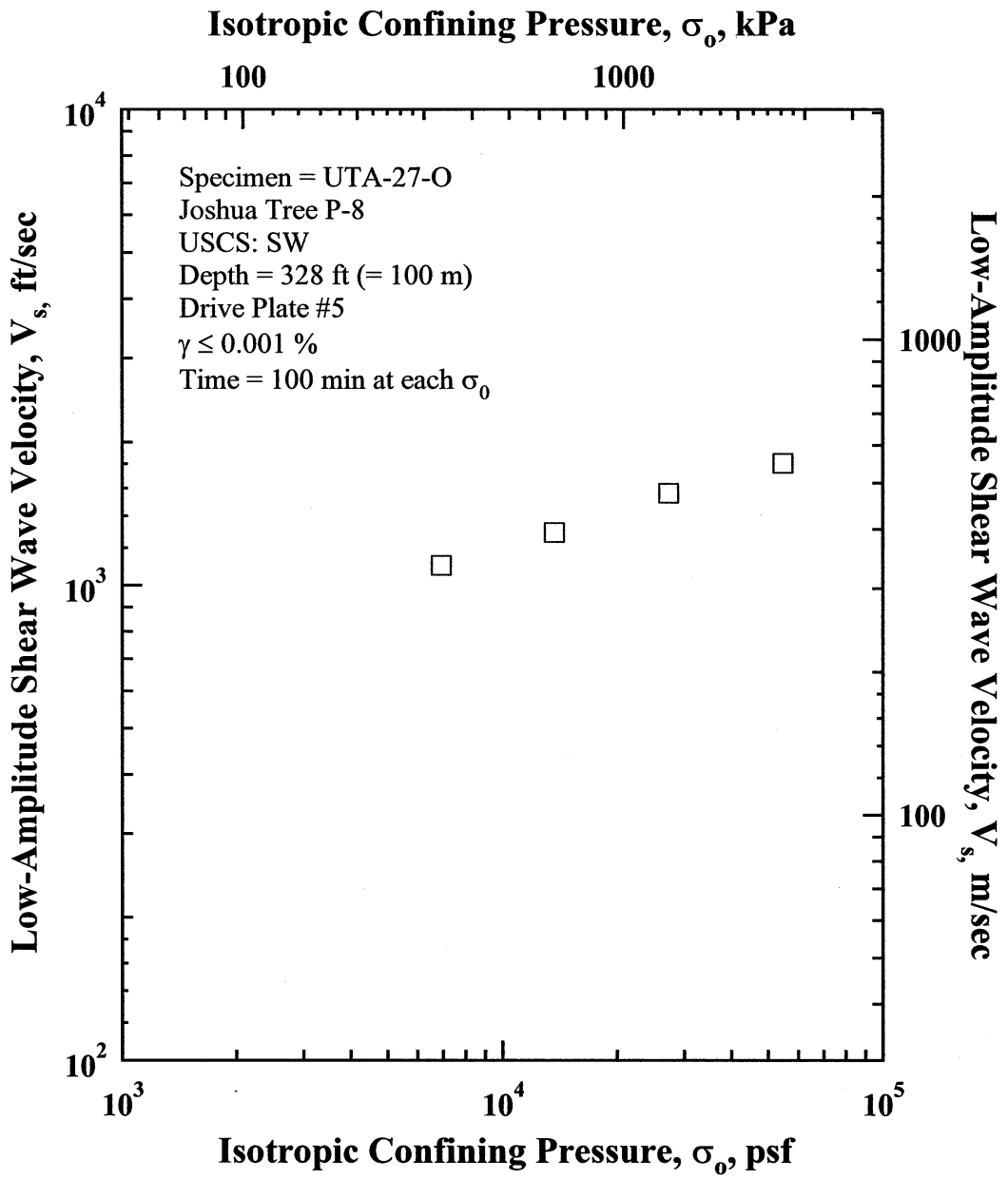

Figure T.4 Variation in Low-Amplitude Shear Wave Velocity with Isotropic Confining Pressure from Resonant Column Tests of Specimen UTA-27-O.

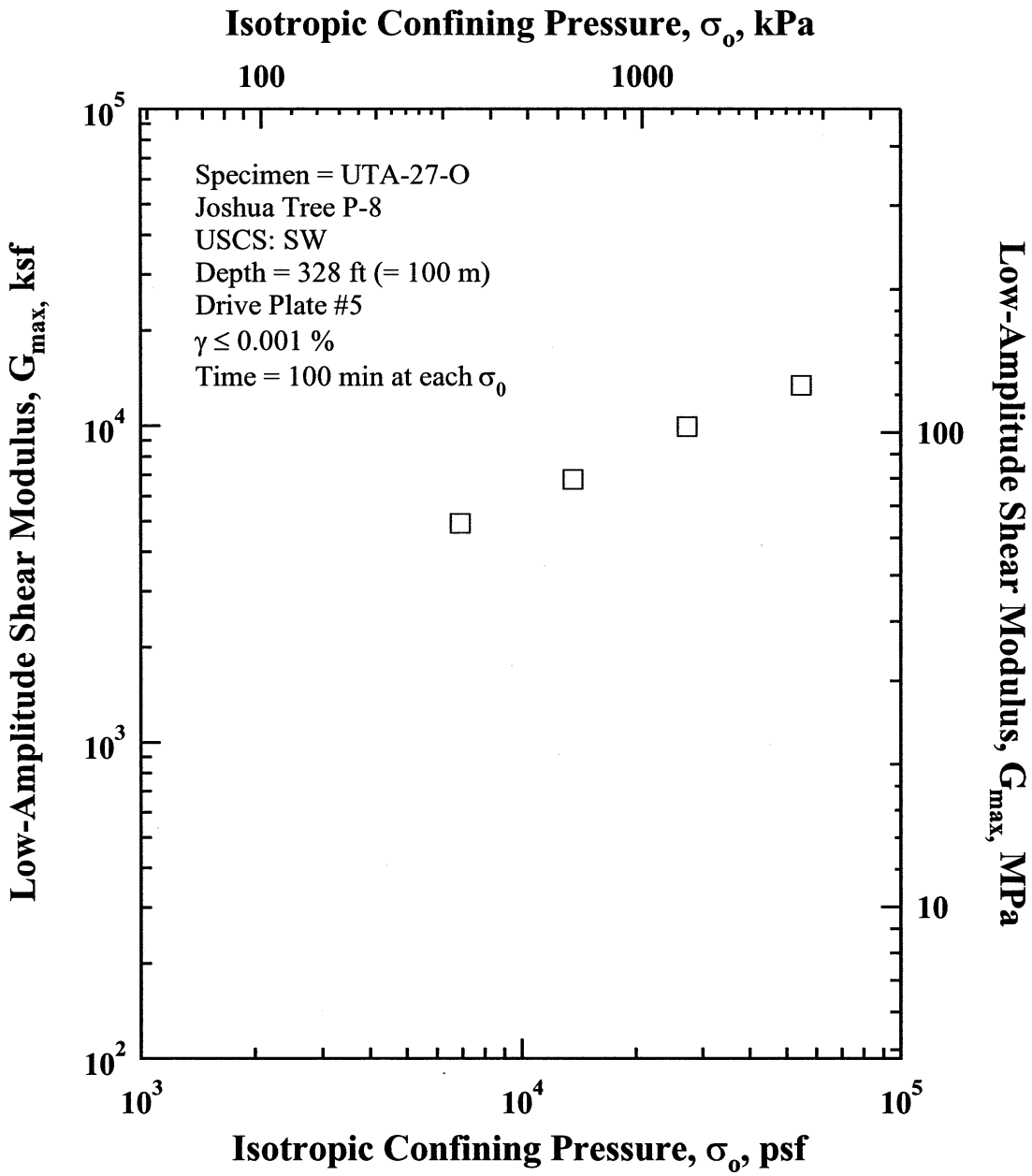

Figure T.5 Variation in Low-Amplitude Shear Modulus with Isotropic Confining Pressure from Resonant Column Tests of Specimen UTA-27-O.

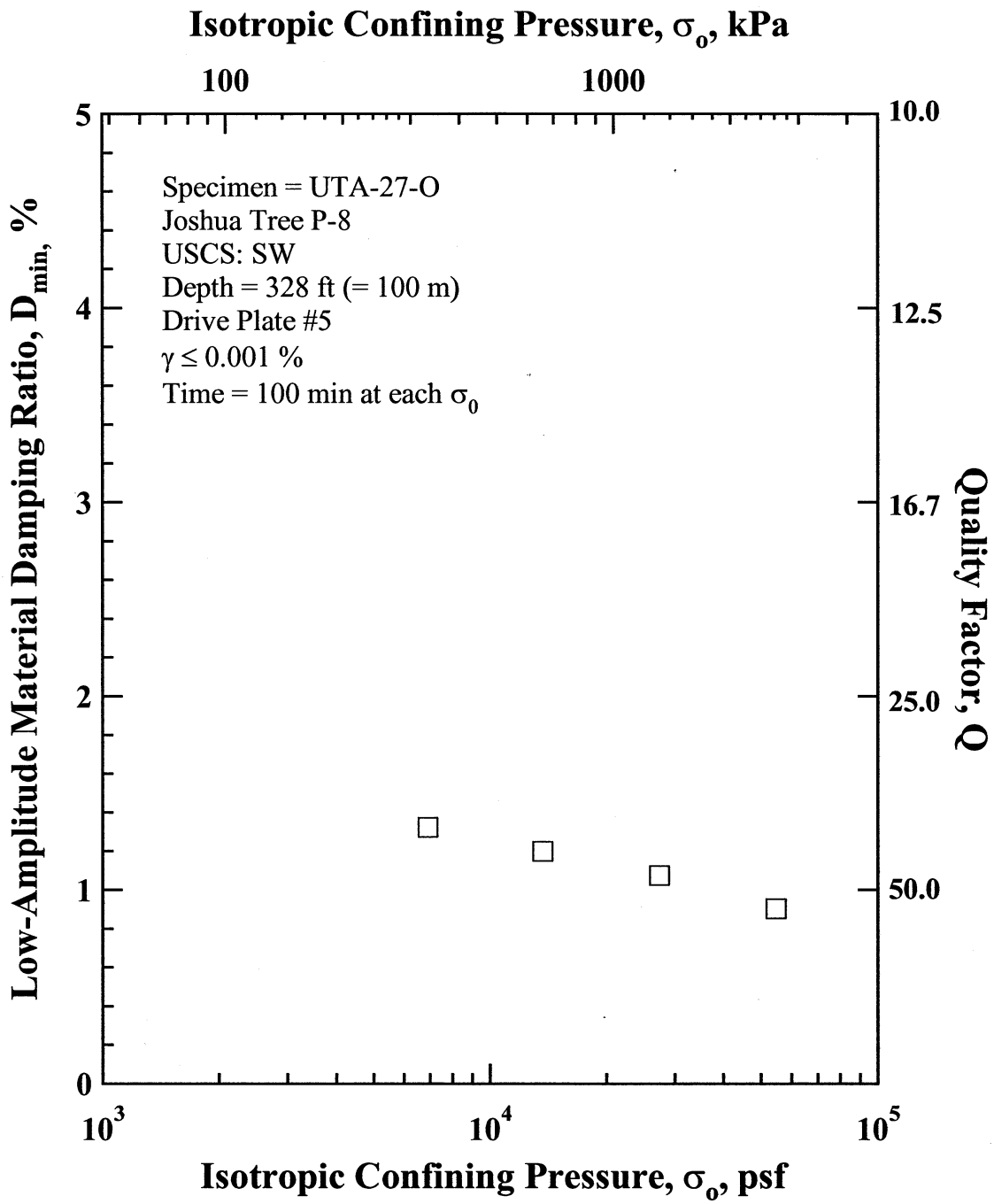

Figure T.6 Variation in Low-Amplitude Material Damping Ratio with Isotropic Confining Pressure from Resonant Column Tests of Specimen UTA-27-O.

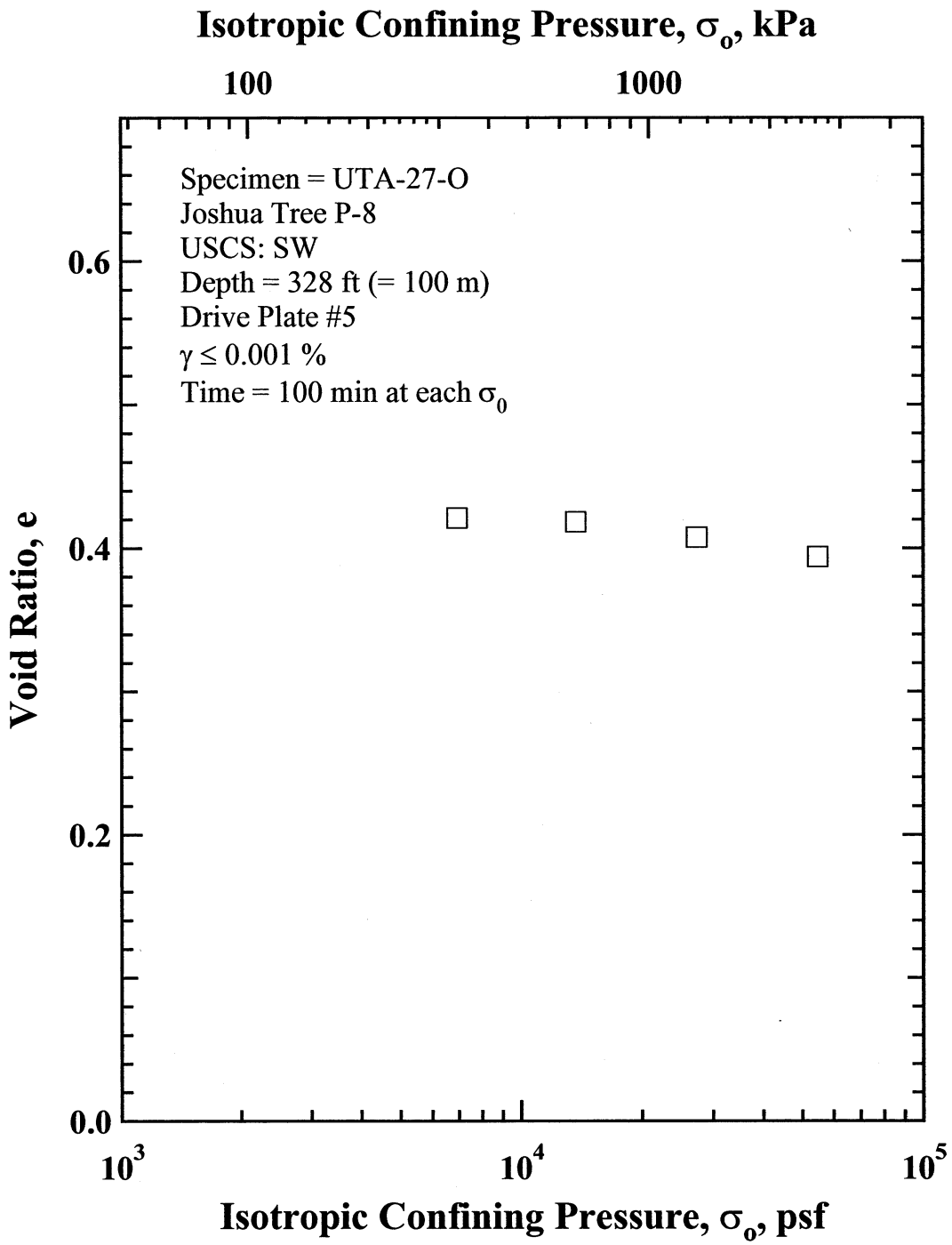

Figure T.7 Variation in Estimated Void Ratio with Isotropic Confining Pressure from Resonant Column Tests of Specimen UTA-27-O.

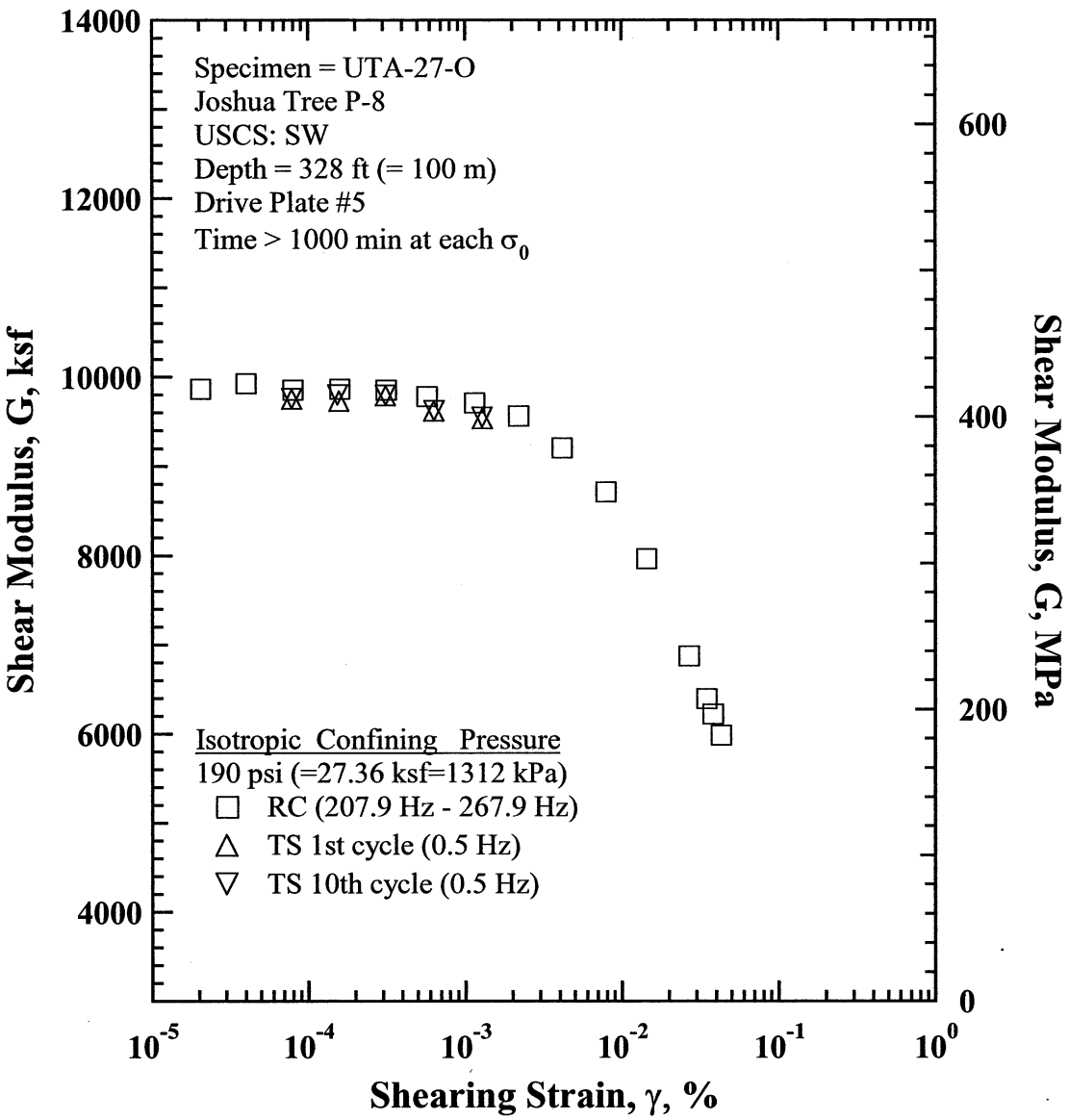

Figure T.8 Comparison of the Variation in Shear Modulus with Shearing Strain at an Isotropic Confining Pressure of 190 psi (=27.36 ksf=1312 kPa) from the Combined RCTS Tests of Specimen UTA-27-O.

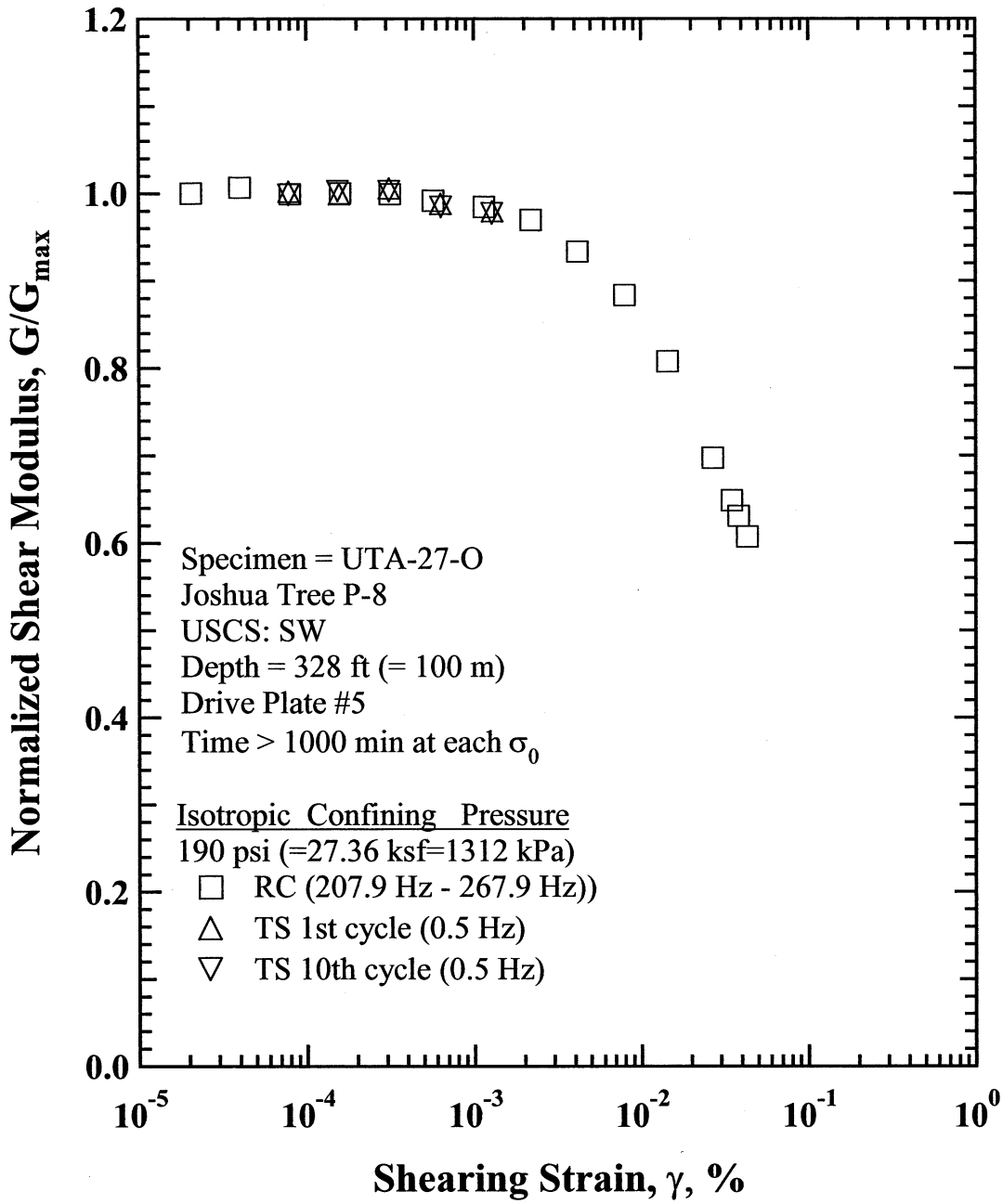

Figure T.9 Comparison of the Variation in Normalized Shear Modulus with Shearing Strain at an Isotropic Confining Pressure of 190 psi (=27.36 ksf=1312 kPa) from the Combined RCTS Tests of Specimen UTA-27-O.

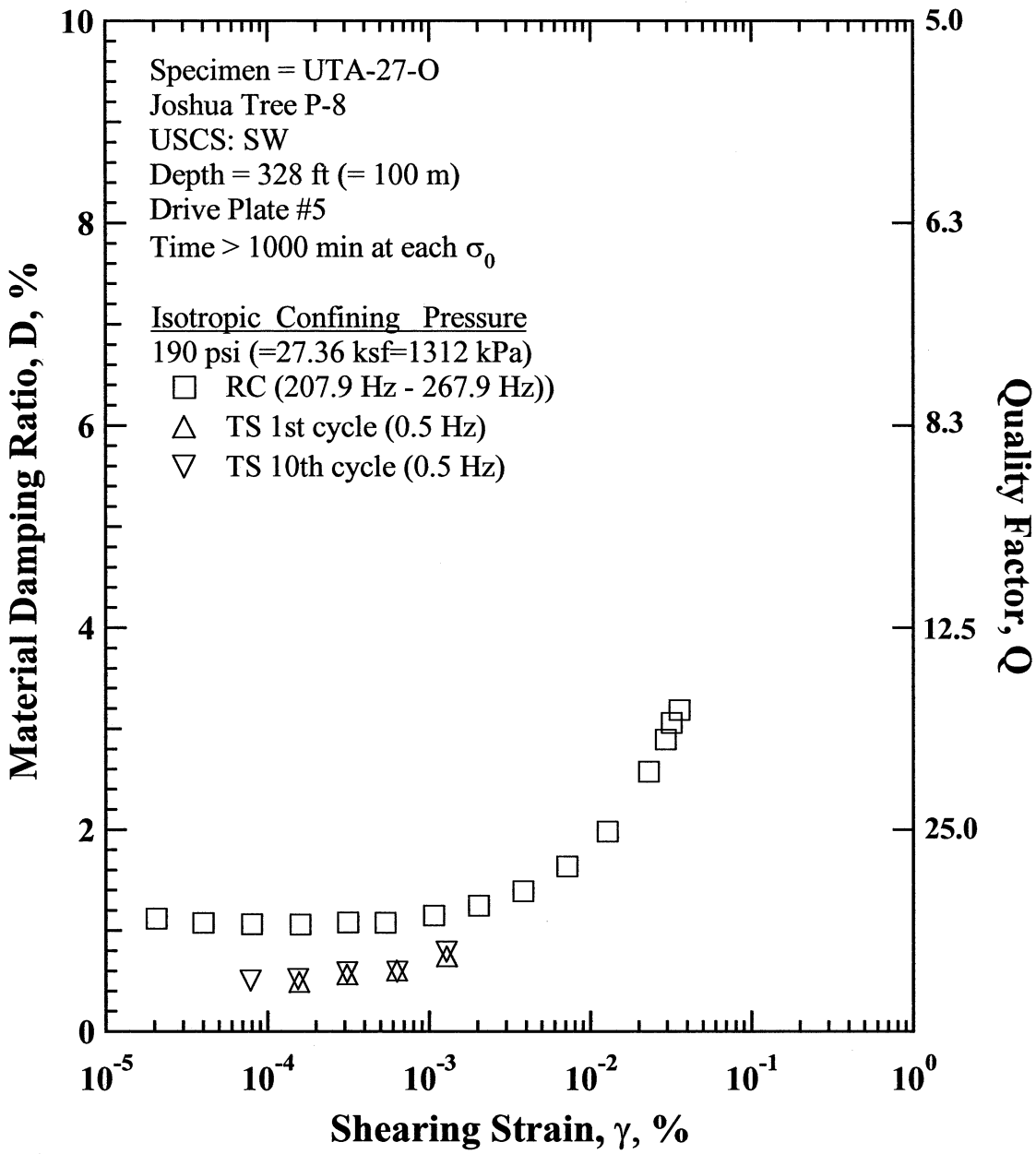

Figure T.10 Comparison of the Variation in Material Damping Ratio with Shearing Strain at an Isotropic Confining Pressure of 190 psi (=27.36 ksf=1312 kPa) from the Combined RCTS Tests of Specimen UTA-27-O.

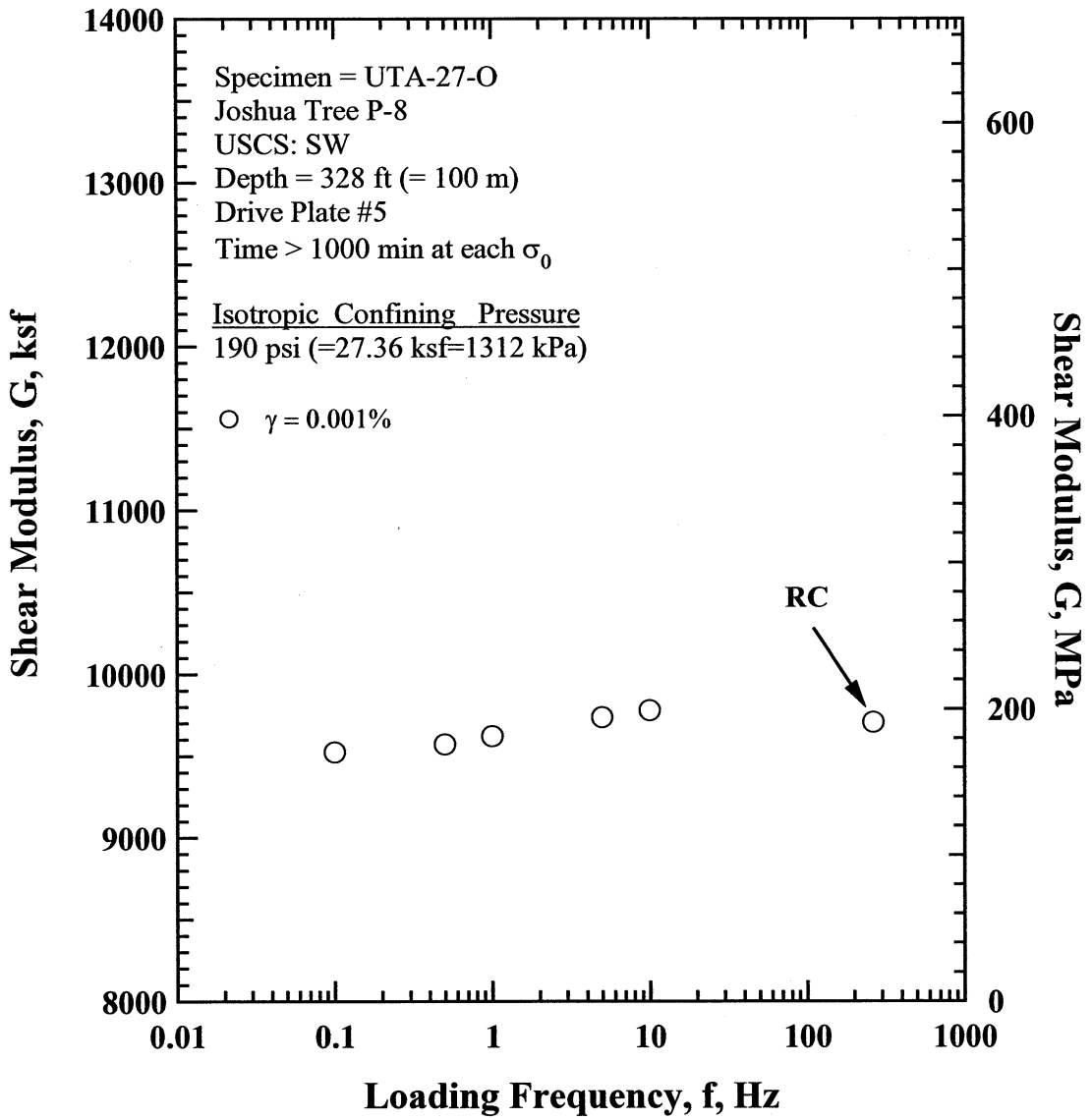

Figure T.11 Comparison of the Variation in Shear Modulus with Loading Frequency at an Isotropic Confining Pressure of 190 psi (=27.36 ksf=1312 kPa) from the Combined RCTS Tests of Specimen UTA-27-O.

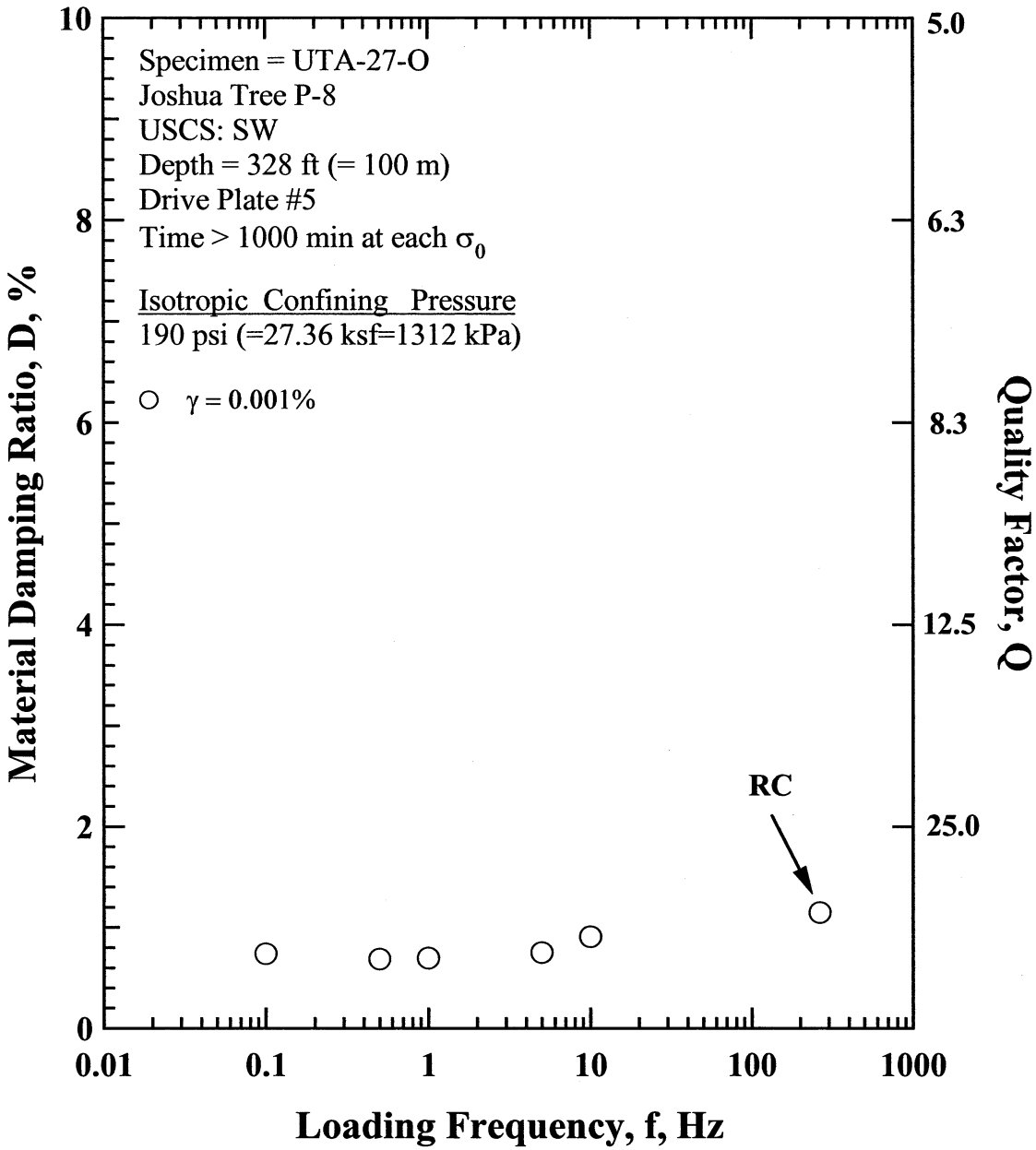

Figure T.12 Comparison of the Variation in Material Damping Ratio with Loading Frequency at an Isotropic Confining Pressure 190 psi (=27.36 ksf=1312 kPa) from the Combined RCTS Tests of Specimen UTA-27-O.

Table T.1 Variation in Low-Amplitude Shear Wave Velocity, Low-Amplitude Shear Modulus, Low-Amplitude Material Damping Ratio and Estimated Void Ratio with Isotropic Confining Pressure from RC Tests of Specimen UTA-27-Q

Effective Isotropic Confining Pressure, σ_o'			Low-Amplitude Shear Modulus, G_{max}		Low-Amplitude Shear Wave Velocity, Vs	Low-Amplitude Material Damping Ratio, Dmin	Estimated Void Ratio, e
(psi)	(psf)	(kPa)	(ksf)	(MPa)	(fps)	(%)	
48	6912	331	4915	235.6	1101	1.32	0.421
95	13680	656	6771	324.6	1291	1.20	0.418
190	27360	1312	9929	476.0	1560	1.07	0.408
380	54720	2623	13413	643.0	1807	0.90	0.394

Table T.2 Variation in Shear Modulus, Normalized Shear Modulus and Material Damping Ratio with Shearing Strain from RC Tests of Specimen UTA-27-Q; Confining Pressure, σ_o' =190 psi (=27.36 ksf=1312 kPa).

Peak Shearing Strain, %	Shear Modulus, G, ksf	Normalized Shear Modulus, G/G_{max}	Average[+] Shearing Strain, %	Material Damping Ratio[x], D, %
4.00E-05	9927	1.01	4.00E-05	1.07
2.05E-05	9863	1.00	2.05E-05	1.12
7.96E-05	9854	1.00	7.96E-05	1.06
1.59E-04	9864	1.00	1.59E-04	1.06
3.16E-04	9854	1.00	3.16E-04	1.08
5.73E-04	9781	0.99	5.37E-04	1.08
1.15E-03	9708	0.98	1.07E-03	1.15
2.19E-03	9562	0.97	2.03E-03	1.25
4.16E-03	9203	0.93	3.82E-03	1.39
7.92E-03	8712	0.88	7.17E-03	1.64
1.44E-02	7965	0.81	1.28E-02	1.98
2.69E-02	6877	0.70	2.31E-02	2.57
3.48E-02	6396	0.65	2.94E-02	2.89
3.82E-02	6221	0.63	3.19E-02	3.06
4.31E-02	5985	0.61	3.58E-02	3.19

[+] Average Shearing Strain from the First Three Cycles of the Free Vibration Decay Curve

[x] Average Damping Ratio from the First Three Cycles of the Free Vibration Decay Curve

Table T.3 Variation in Shear Modulus, Normalized Shear Modulus and Material Damping Ratio with Shearing Strain from TS Tests of Specimen UTA-27-Q; Confining Pressure, σ_o' = 190 psi (=27.36 ksf=1312 kPa).

First Cycle				Tenth Cycle			
Peak Shearing Strain, %	Shear Modulus, G, ksf	Normalized Shear Modulus, G/G_{max}	Material Damping Ratio, D, %	Peak Shearing Strain, %	Shear Modulus, G, ksf	Normalized Shear Modulus, G/G_{max}	Material Damping Ratio, D, %
7.89E-05	9748	1.00		7.89E-05	9753	1.00	0.50
1.58E-04	9725	1.00	0.49	1.55E-04	9797	1.00	0.52
3.14E-04	9785	1.01	0.56	3.14E-04	9795	1.00	0.58
6.39E-04	9615	0.99	0.60	6.40E-04	9619	0.98	0.59
1.30E-03	9528	0.98	0.74	1.29E-03	9546	0.98	0.79

APPENDIX U

Specimen No. 20
UT Specimen ID: UTA-27-P

Yermo P-6
Depth = 201ft (=61.3m)
Soil Type: Silty Sand (SM)

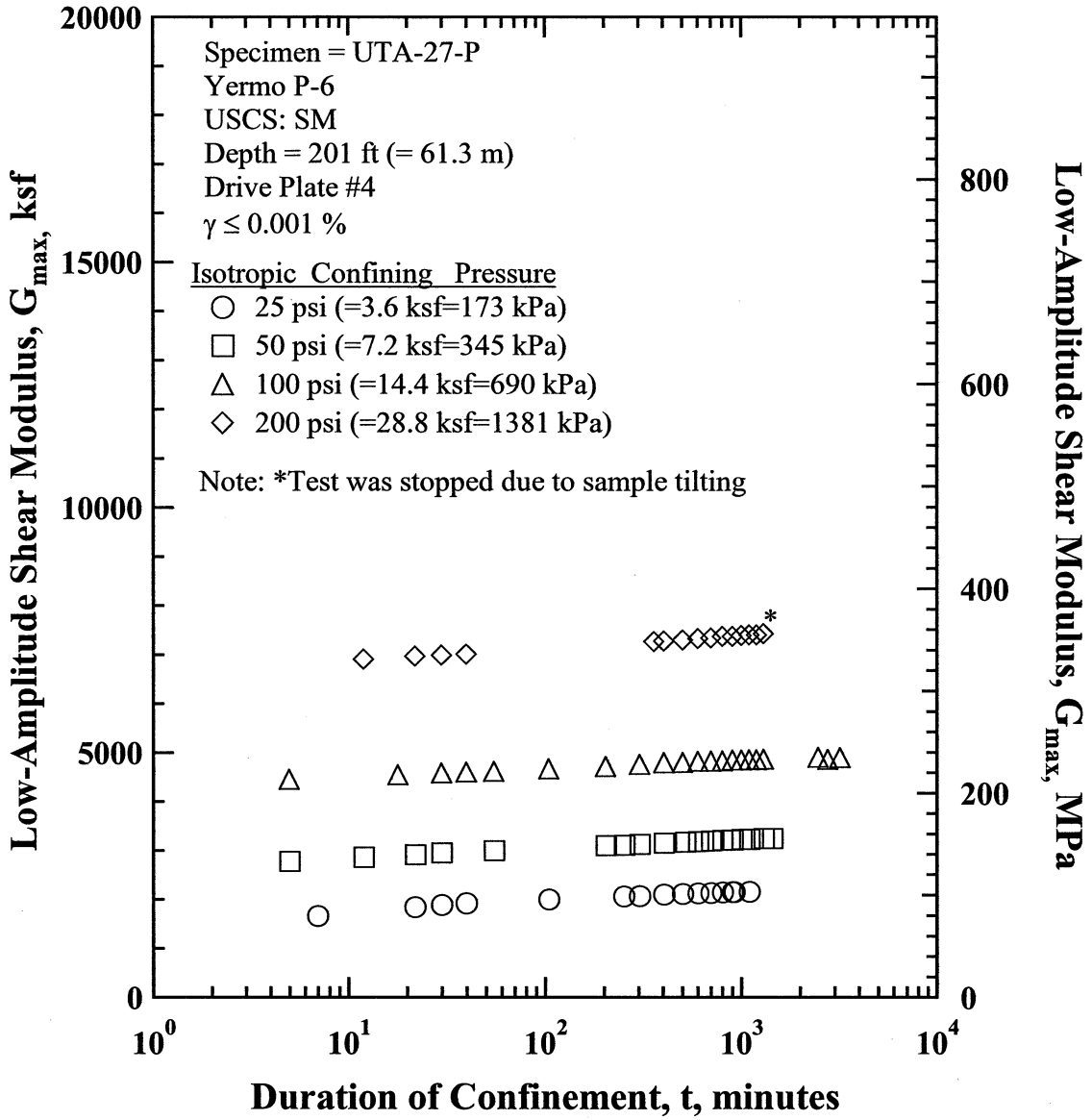

Figure U.1 Variation in Low-Amplitude Shear Modulus with Magnitude and Duration of Isotropic Confining Pressure from Resonant Column Tests of Specimen UTA-27-P.

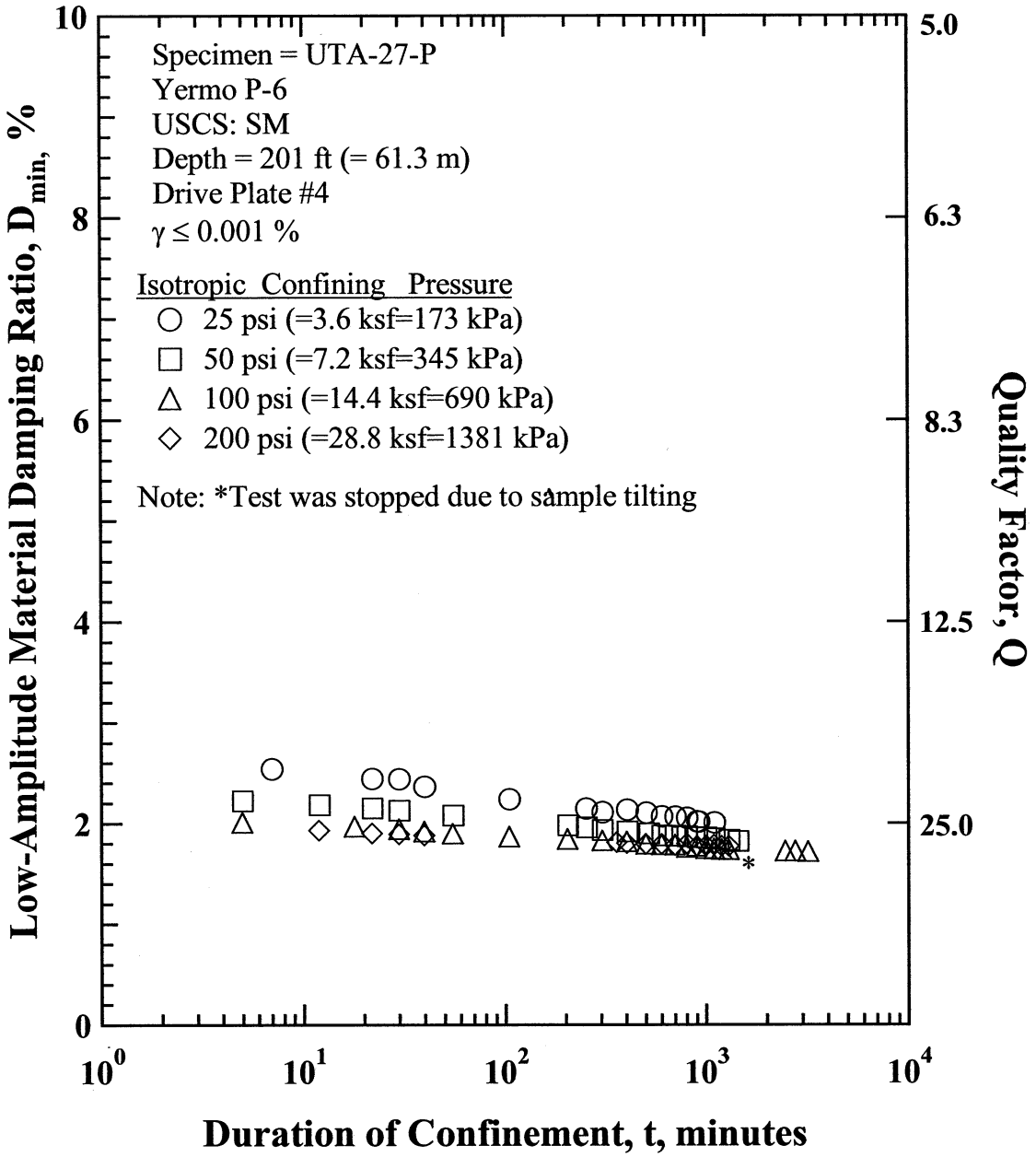

Figure U.2 Variation in Low-Amplitude Material Damping Ratio with Magnitude and Duration of Isotropic Confining Pressure from Resonant Column Tests of Specimen UTA-27-P

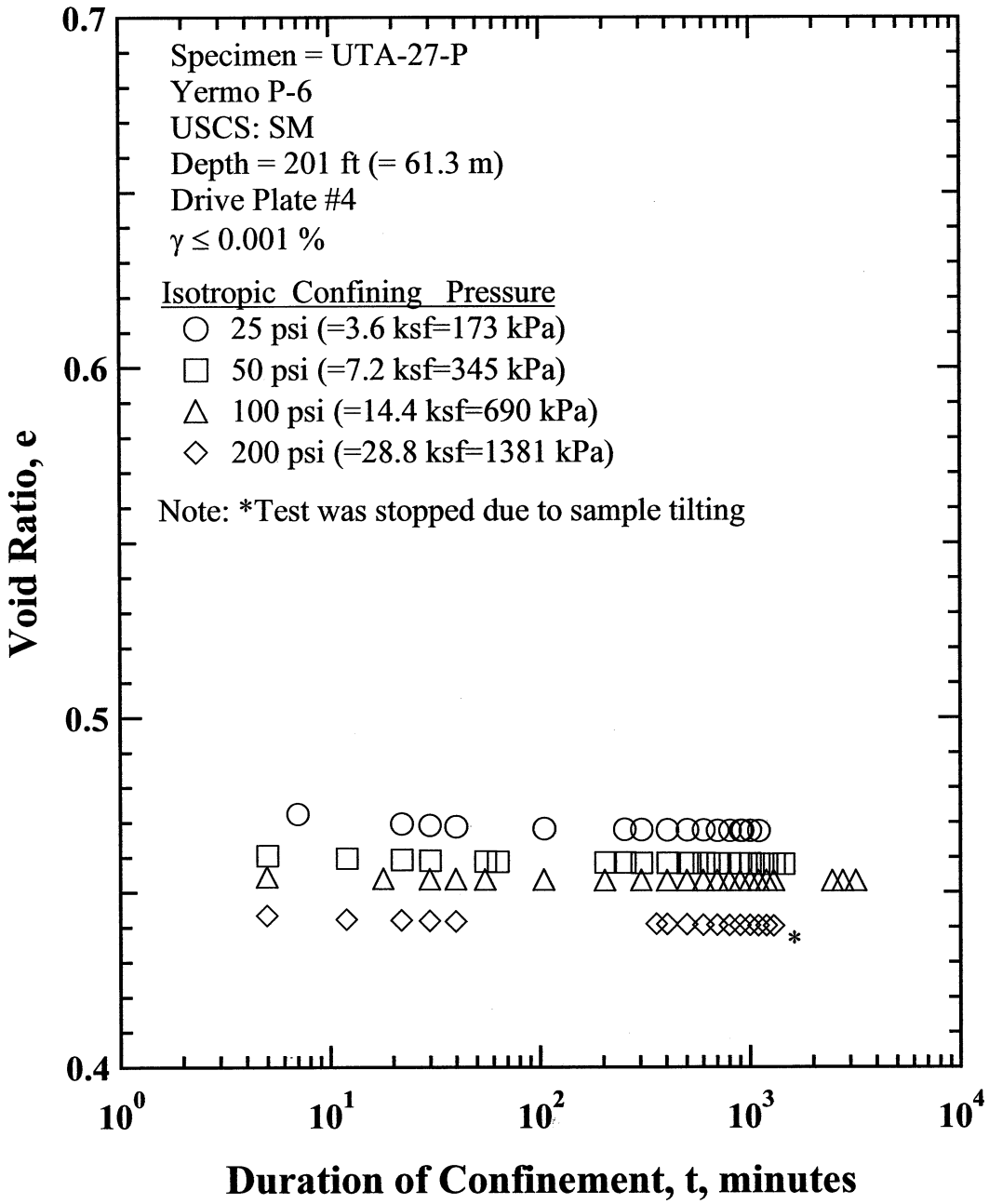

Figure U.3 Variation in Estimated Void Ratio with Magnitude and Duration of Isotropic Confining Pressure from Resonant Column Tests of Specimen UTA-27-P.

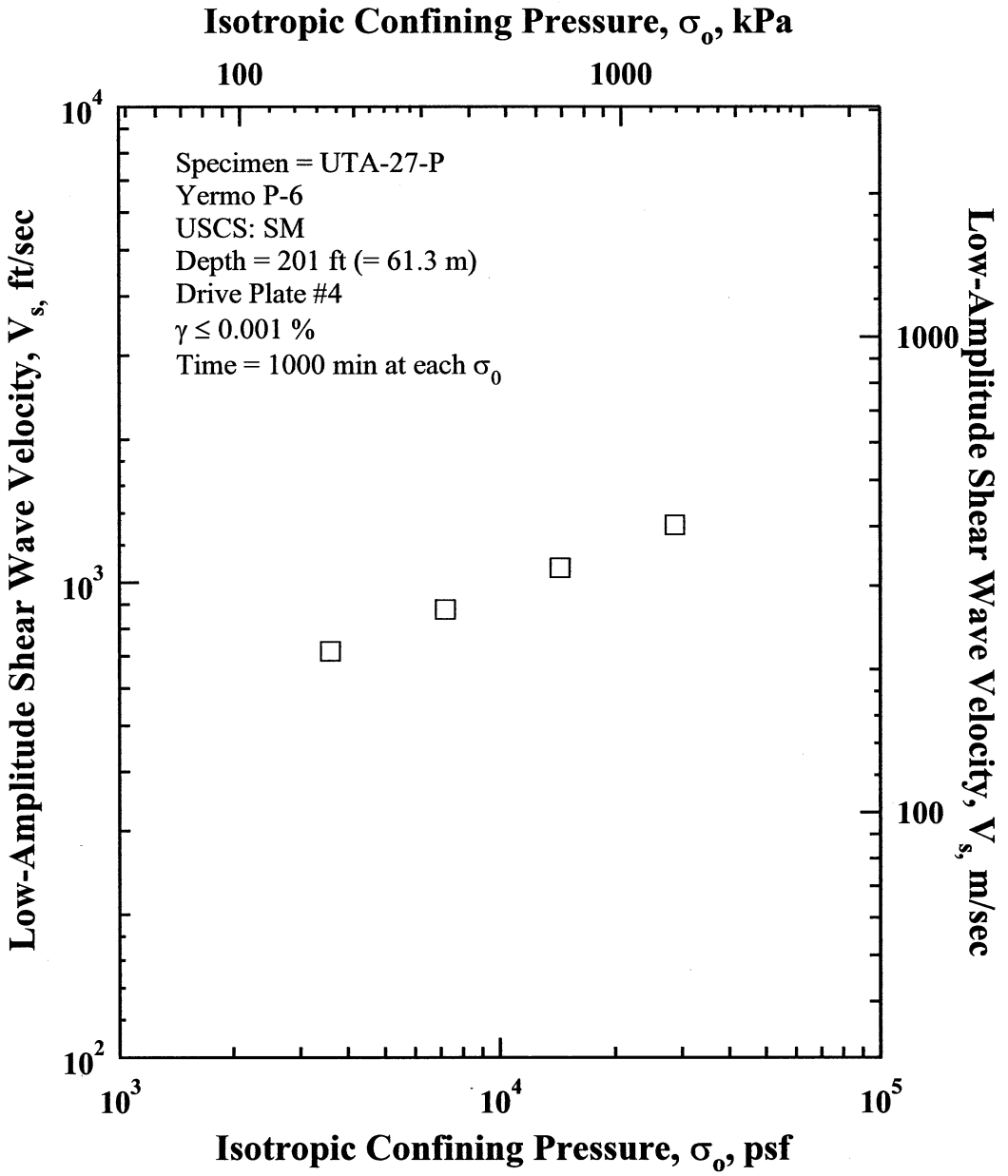

Figure U.4 Variation in Low-Amplitude Shear Wave Velocity with Isotropic Confining Pressure from Resonant Column Tests of Specimen UTA-27-P.

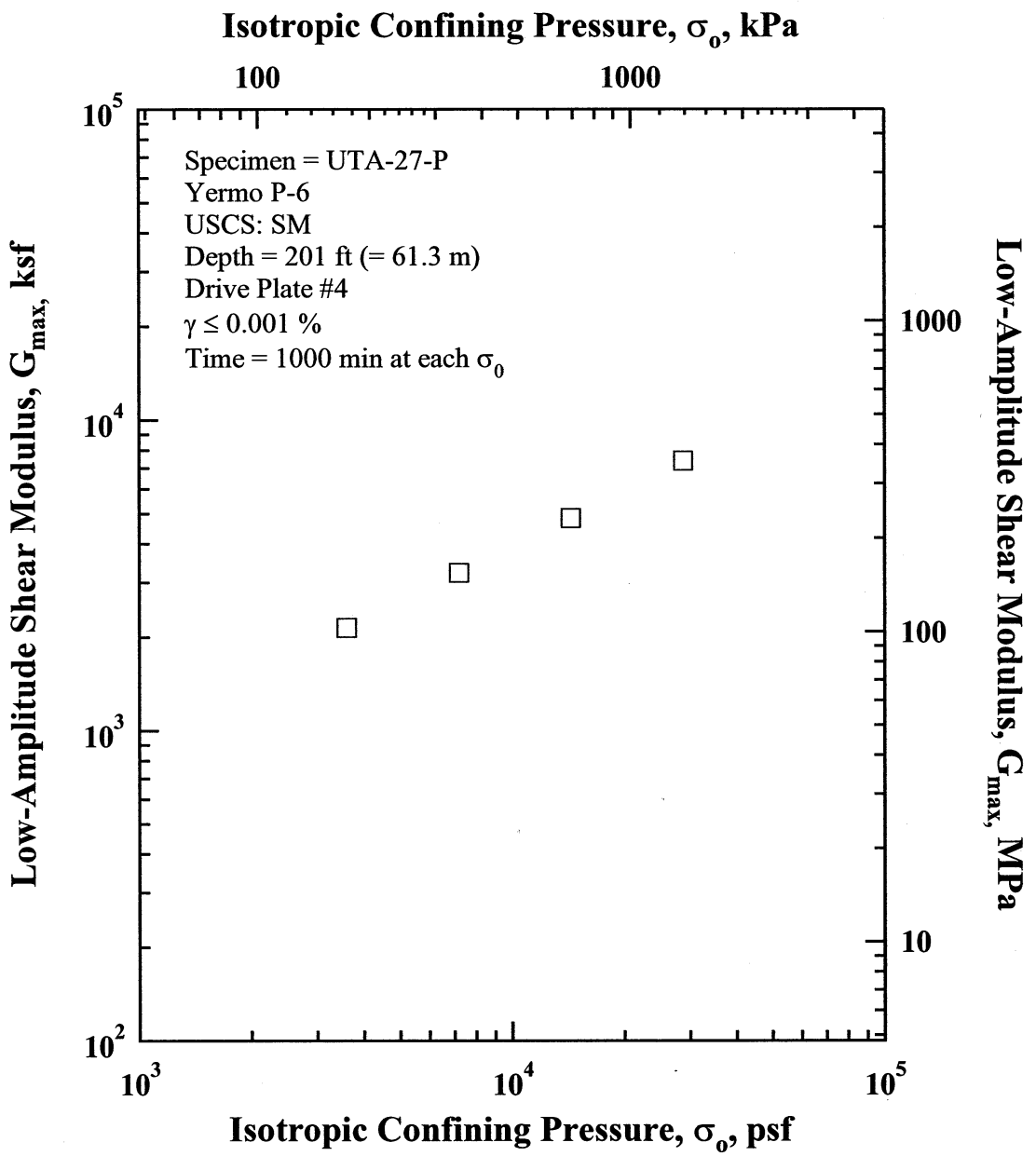

Figure U.5 Variation in Low-Amplitude Shear Modulus with Isotropic Confining Pressure from Resonant Column Tests of Specimen UTA-27-P.

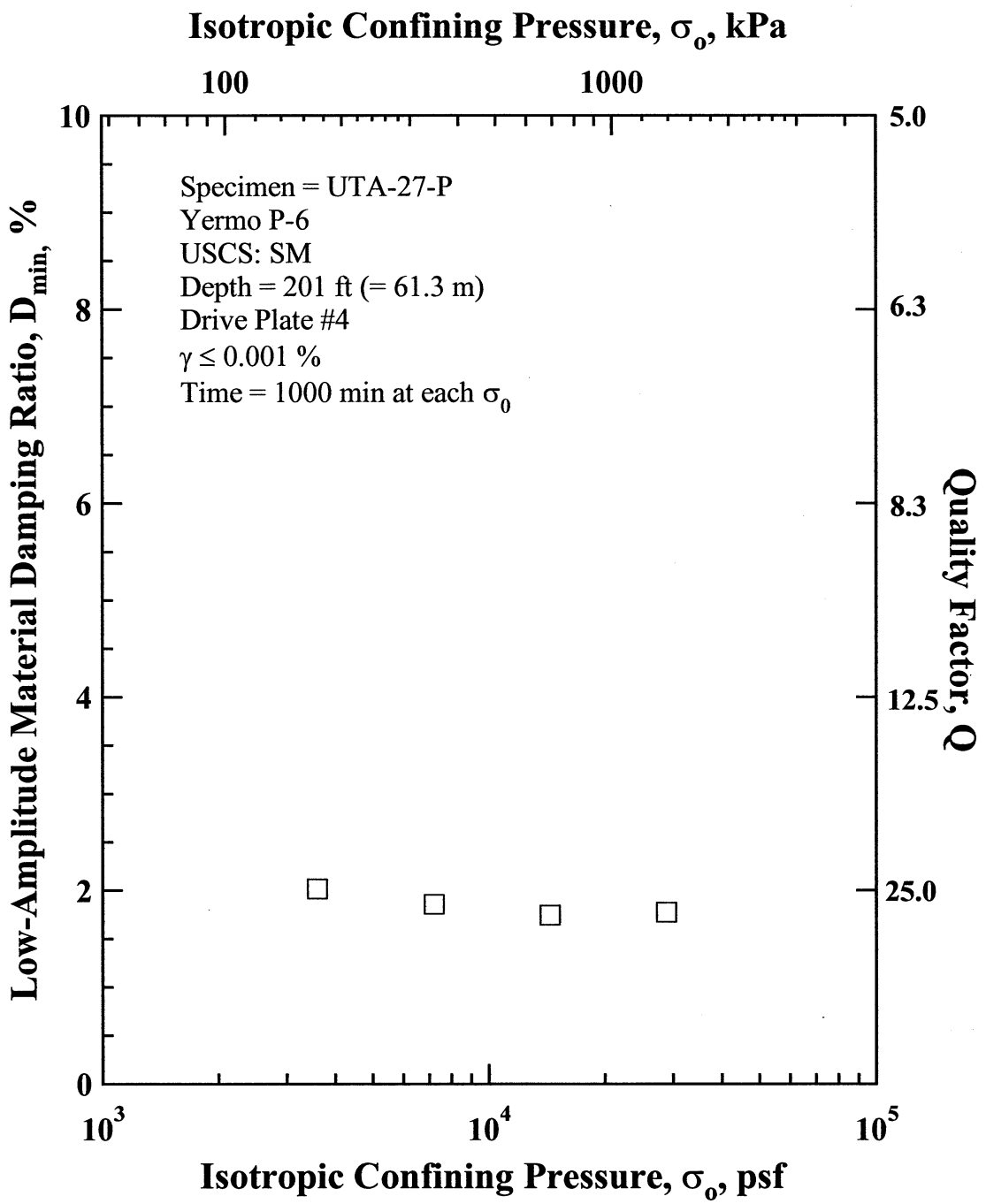

Figure U.6 Variation in Low-Amplitude Material Damping Ratio with Isotropic Confining Pressure from Resonant Column Tests of Specimen UTA-27-P.

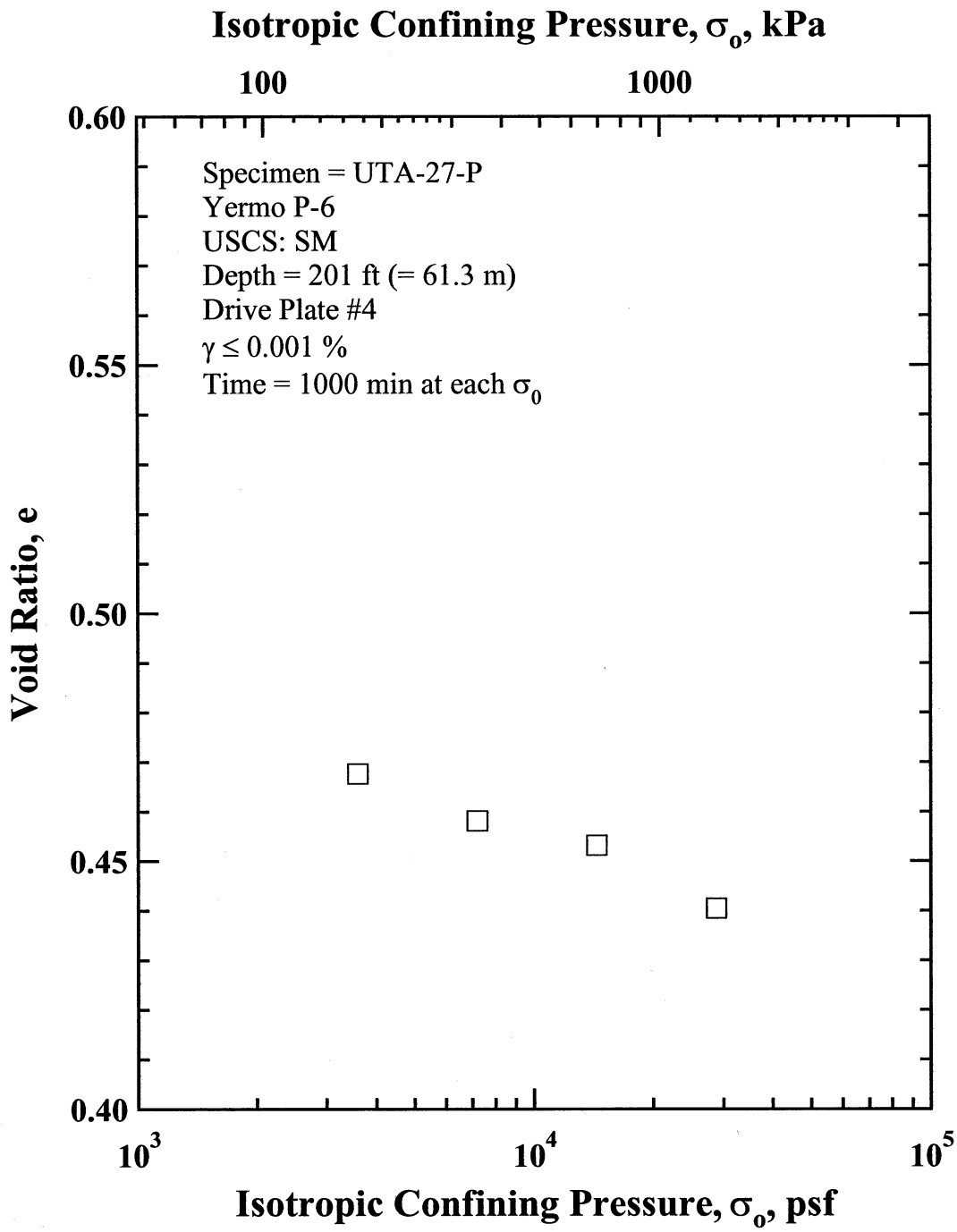

Figure U.7 Variation in Estimated Void Ratio with Isotropic Confining Pressure from Resonant Column Tests of Specimen UTA-27-P.

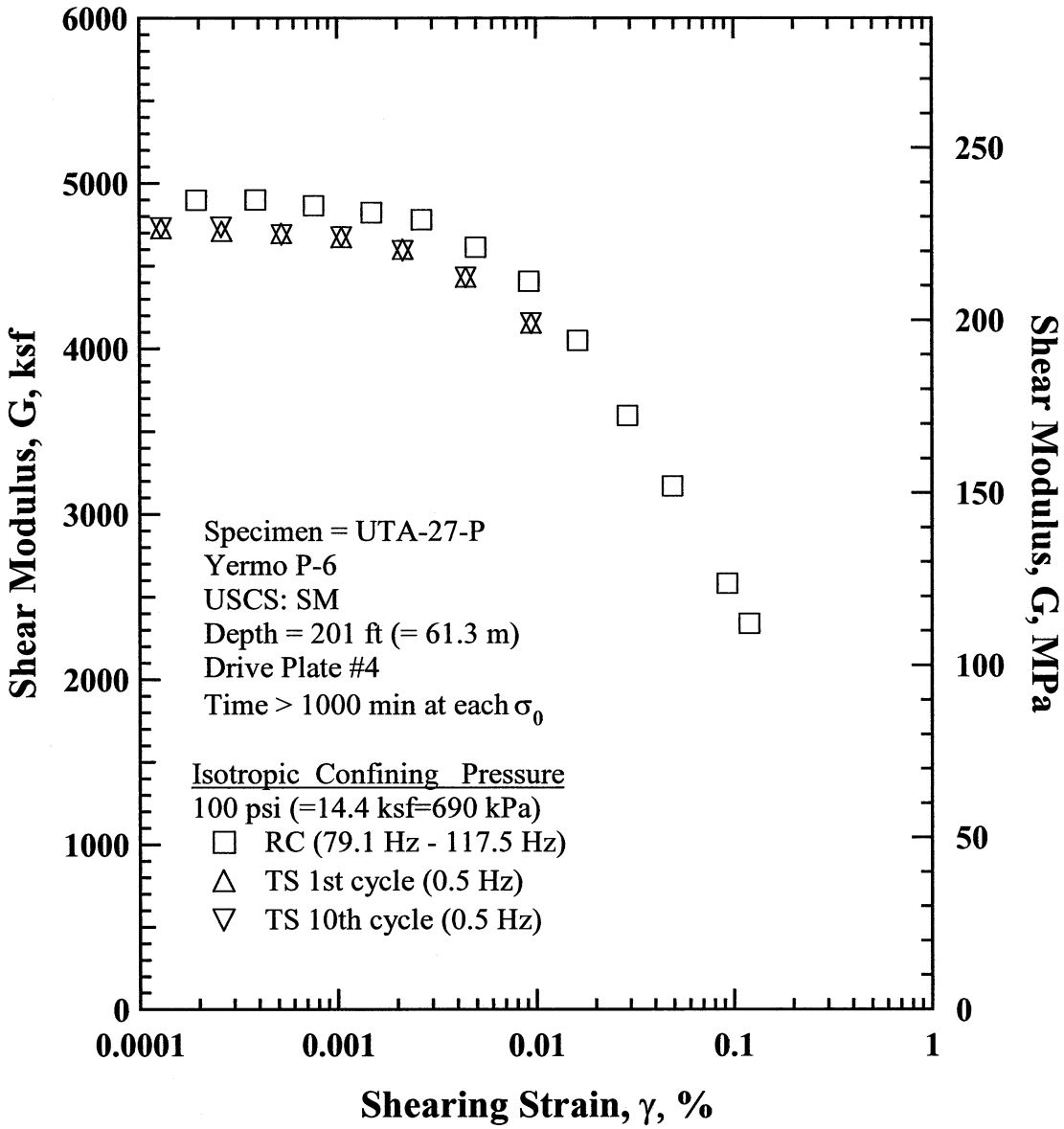

Figure U.8 Comparison of the Variation in Shear Modulus with Shearing Strain at an Isotropic Confining Pressure of 100 psi (=14.4 ksf=690 kPa) from the Combined RCTS Tests of Specimen UTA-27-P.

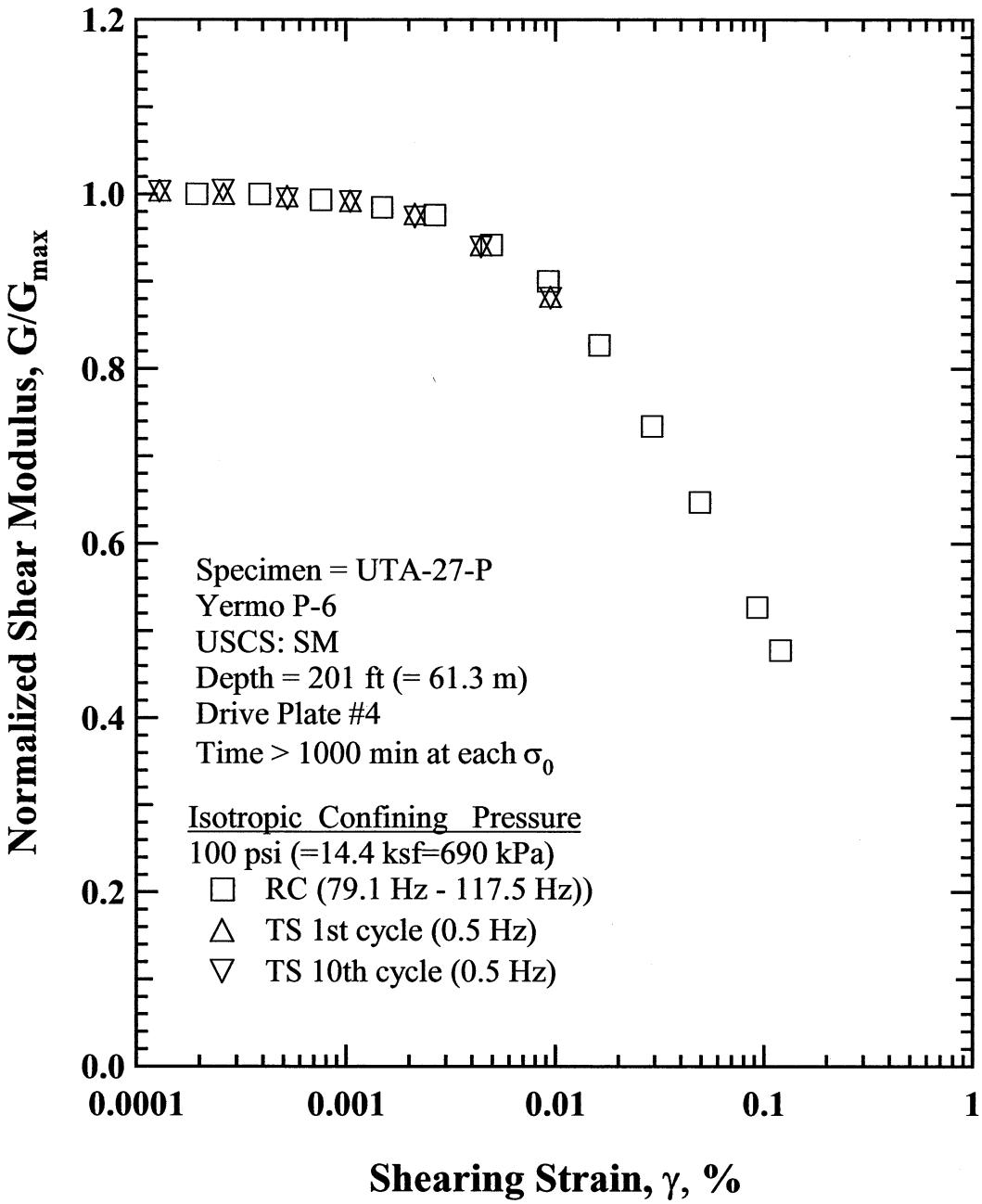

Figure U.9 Comparison of the Variation in Normalized Shear Modulus with Shearing Strain at an Isotropic Confining Pressure of 100 psi (=14.4 ksf=690 kPa) from the Combined RCTS Tests of Specimen UTA-27-P.

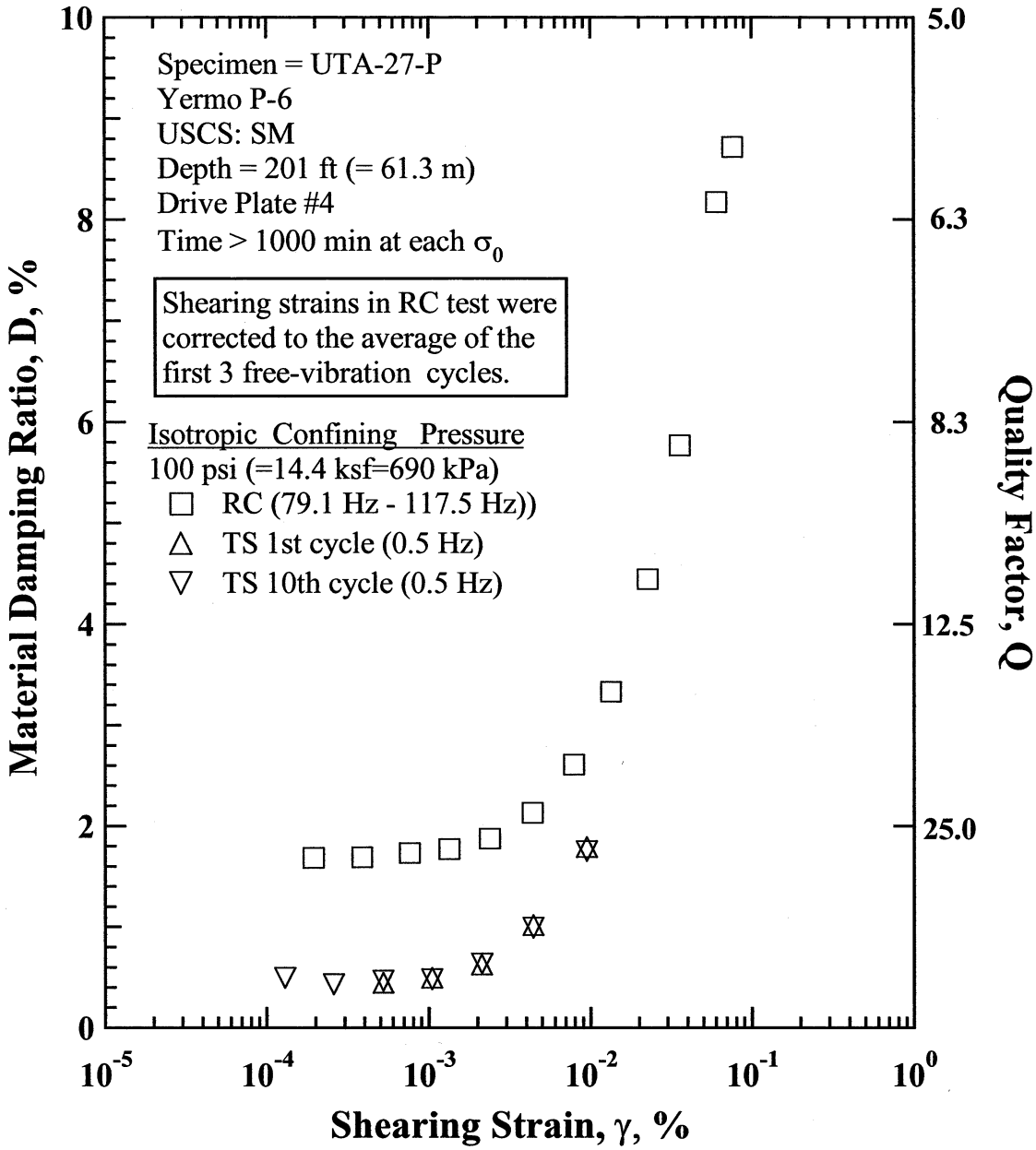

Figure U.10 Comparison of the Variation in Material Damping Ratio with Shearing Strain at an Isotropic Confining Pressure of 100 psi (=14.4 ksf=690 kPa) from the Combined RCTS Tests of Specimen UTA-27-P.

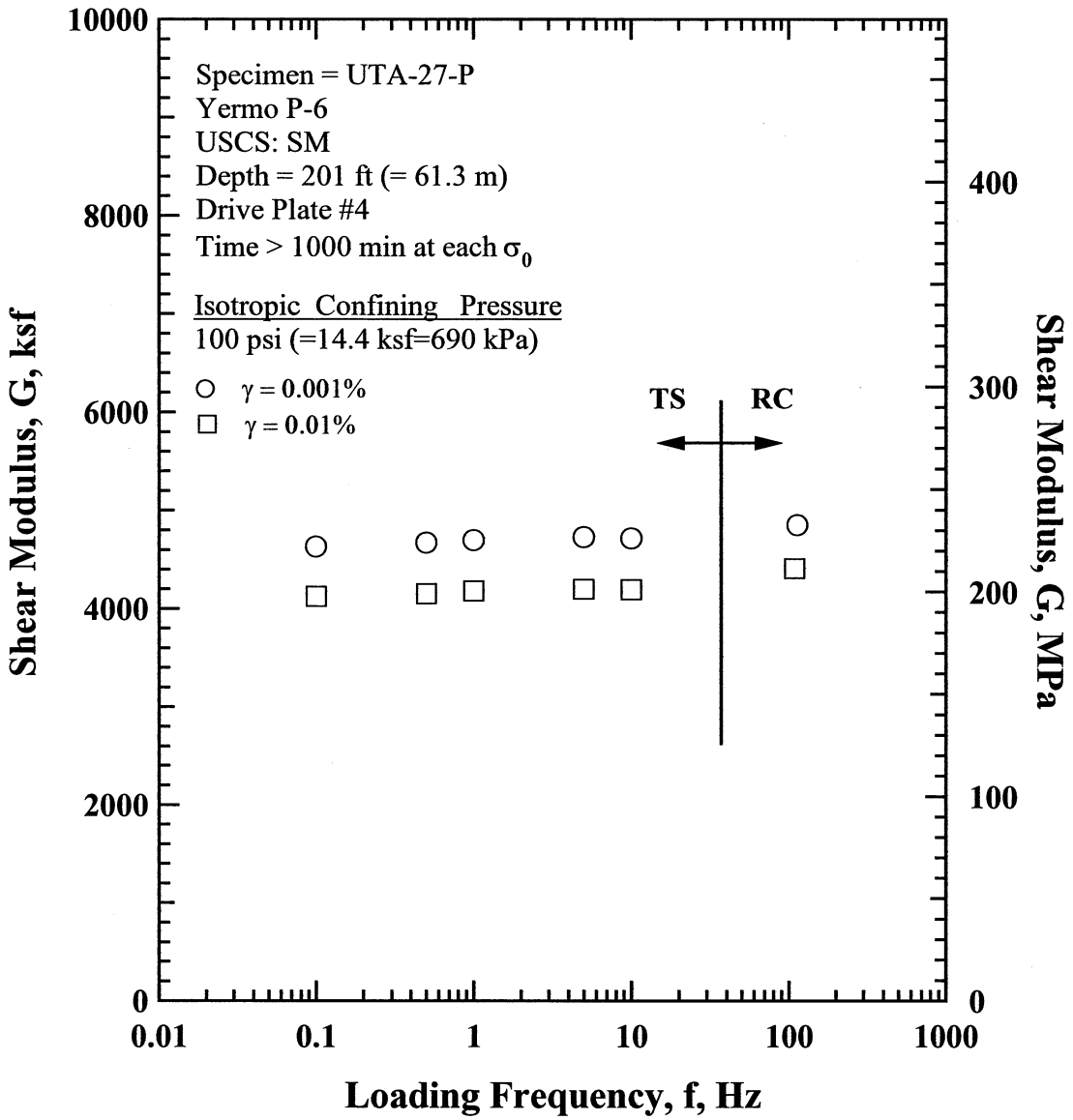

Figure U.11 Comparison of the Variation in Shear Modulus with Loading Frequency at an Isotropic Confining Pressure of 100 psi (=14.4 ksf=690 kPa) from the Combined RCTS Tests of Specimen UTA-27-P.

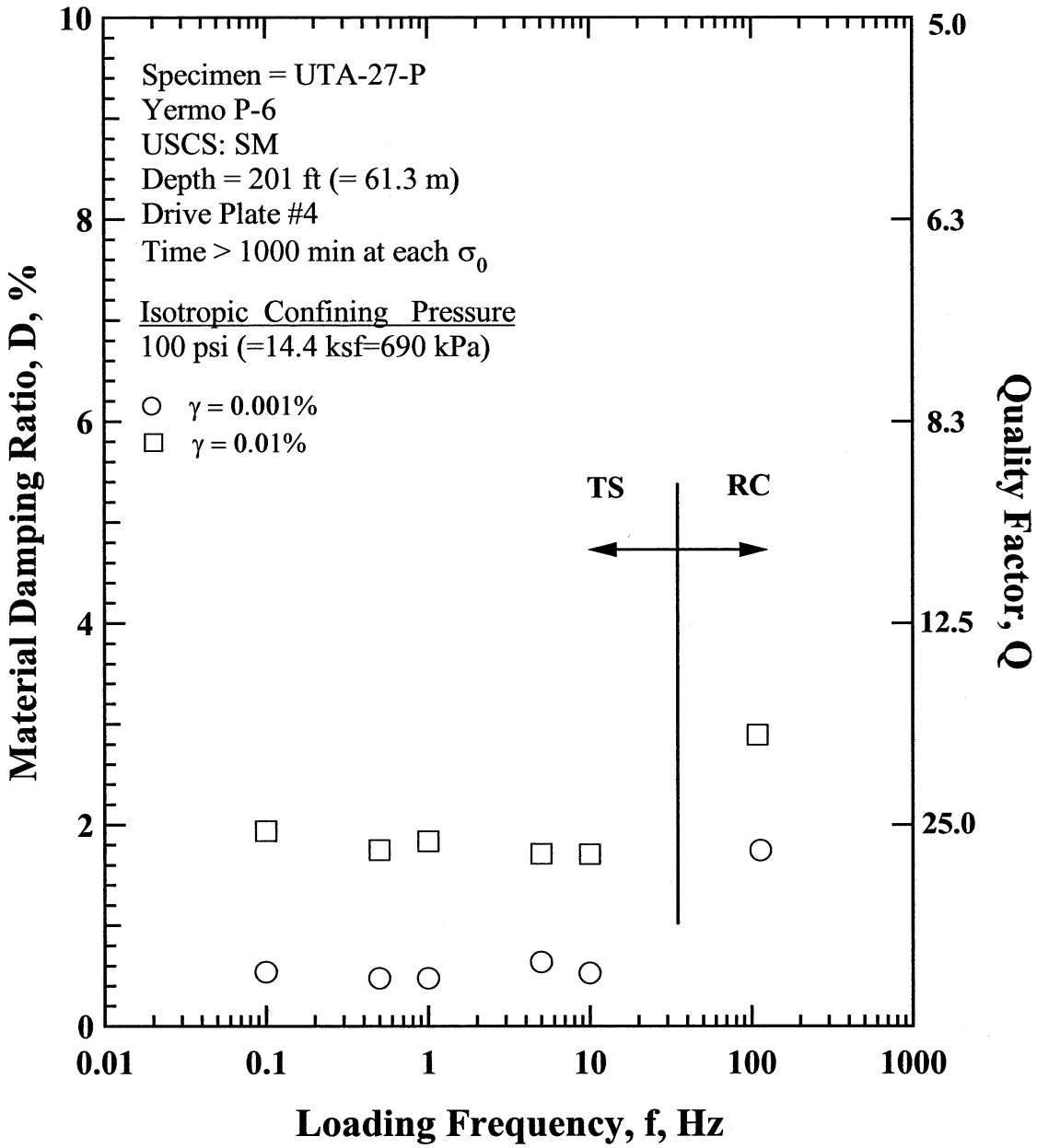

Figure U.12 Comparison of the Variation in Material Damping Ratio with Loading Frequency at an Isotropic Confining Pressure 100 psi (=14.4 ksf=690 kPa) from the Combined RCTS Tests of Specimen UTA-27-P.

Table U.1 Variation in Low-Amplitude Shear Wave Velocity, Low-Amplitude Shear Modulus, Low-Amplitude Material Damping Ratio and Estimated Void Ratio with Isotropic Confining Pressure from RC Tests of Specimen UTA-27-P.

Effective Isotropic Confining Pressure, σ_o'			Low-Amplitude Shear Modulus, G_{max}		Low-Amplitude Shear Wave Velocity, Vs	Low-Amplitude Material Damping Ratio, Dmin	Estimated Void Ratio, e
(psi)	(psf)	(kPa)	(ksf)	(MPa)	(fps)	(%)	
25	3600	173	2149	103.0	717	2.01	0.468
50	7200	345	3223	154.5	877	1.86	0.458
100	14400	690	4838	231.9	1073	1.74	0.453
200	28800	1381	7385	354.0	1323	1.77	0.440

Table U.2 Variation in Shear Modulus, Normalized Shear Modulus and Material Damping Ratio with Shearing Strain from RC Tests of Specimen UTA-27-P; Confining Pressure, σ_o' =100 psi (=14.4 ksf=690 kPa).

Peak Shearing Strain, %	Shear Modulus, G, ksf	Normalized Shear Modulus, G/G_{max}	Average^{+} Shearing Strain, %	Material Damping Ratio^{x}, D, %
1.94E-04	4899	1.00	1.94E-04	1.68
3.85E-04	4899	1.00	3.85E-04	1.69
7.60E-04	4865	0.99	7.60E-04	1.73
1.49E-03	4823	0.98	1.34E-03	1.77
2.66E-03	4780	0.98	2.38E-03	1.87
4.96E-03	4612	0.94	4.37E-03	2.13
9.19E-03	4408	0.90	7.87E-03	2.61
1.62E-02	4050	0.83	1.34E-02	3.33
2.90E-02	3597	0.73	2.25E-02	4.45
4.91E-02	3170	0.65	3.57E-02	5.77
9.29E-02	2581	0.53	6.05E-02	8.17
1.20E-01	2339	0.48	7.61E-02	8.72

$^{+}$ Average Shearing Strain from the First Three Cycles of the Free Vibration Decay Curve

^{x} Average Damping Ratio from the First Three Cycles of the Free Vibration Decay Curve

Table U.3 Variation in Shear Modulus, Normalized Shear Modulus and Material Damping Ratio with Shearing Strain from TS Tests of Specimen UTA-27-P; Confining Pressure, σ_o' = 100 psi (=14.4 ksf=690 kPa).

First Cycle				Tenth Cycle			
Peak Shearing Strain, %	Shear Modulus, G, ksf	Normalized Shear Modulus, G/G_{max}	Material Damping Ratio, D, %	Peak Shearing Strain, %	Shear Modulus, G, ksf	Normalized Shear Modulus, G/G_{max}	Material Damping Ratio, D, %
1.30E-04	4726	1.00		1.30E-04	4728	1.00	0.49
2.62E-04	4708	1.00		2.60E-04	4733	1.00	0.43
5.25E-04	4695	1.00	0.44	5.26E-04	4686	0.99	0.46
1.06E-03	4670	0.99	0.49	1.05E-03	4674	0.99	0.48
2.14E-03	4599	0.98	0.62	2.15E-03	4589	0.97	0.63
4.45E-03	4432	0.94	1.01	4.45E-03	4428	0.94	0.99
9.51E-03	4153	0.88	1.79	9.51E-03	4151	0.88	1.75

APPENDIX V

Specimen No. 21
UT Specimen ID: UTA-27-Q

Yermo P-7
Depth = 266ft (=81.1m)
Soil Type: Sand (SP)

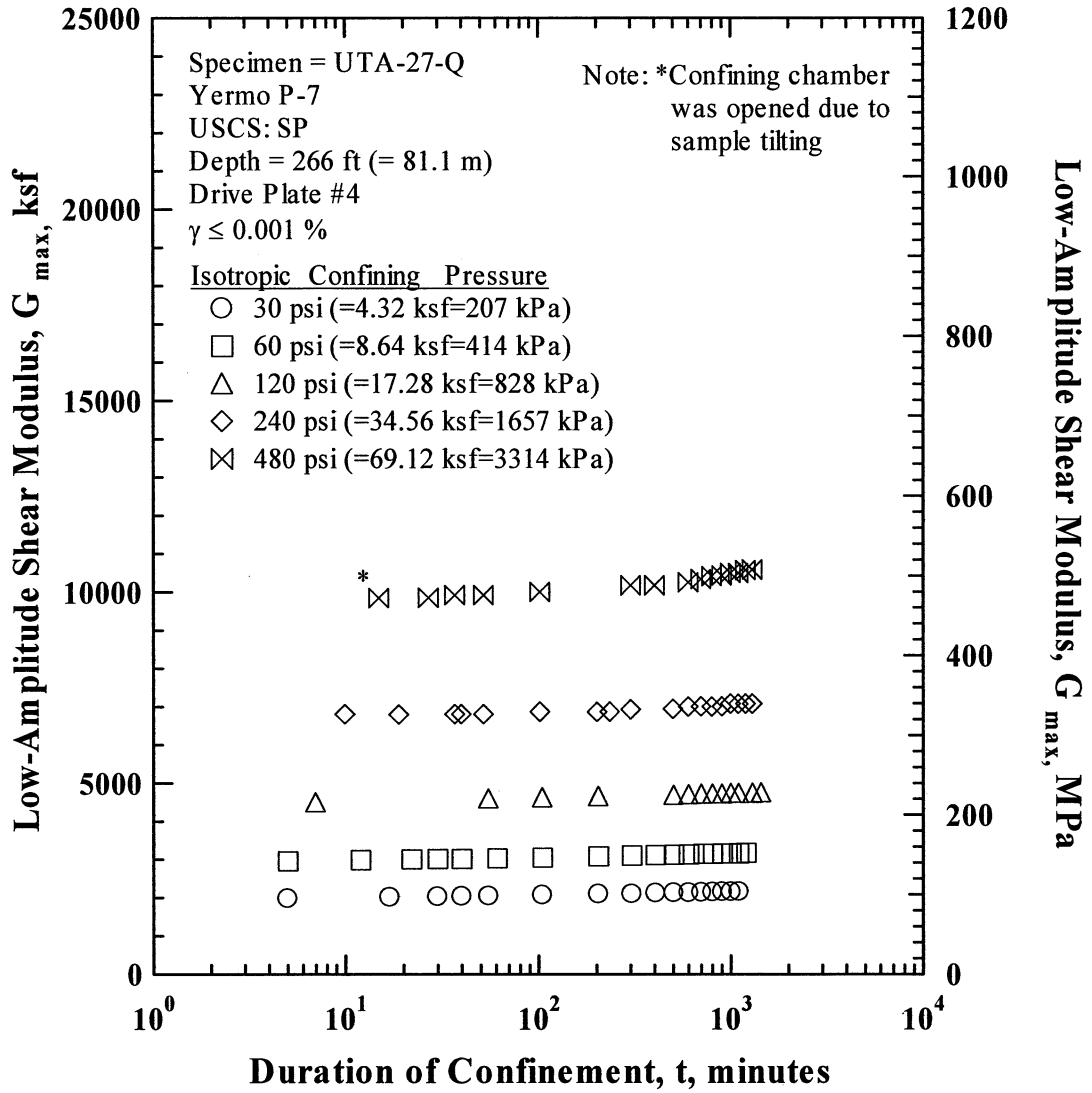

Figure S.1 Variation in Low-Amplitude Shear Modulus with Magnitude and Duration of Isotropic Confining Pressure from Resonant Column Tests of Specimen UTA-27-Q.

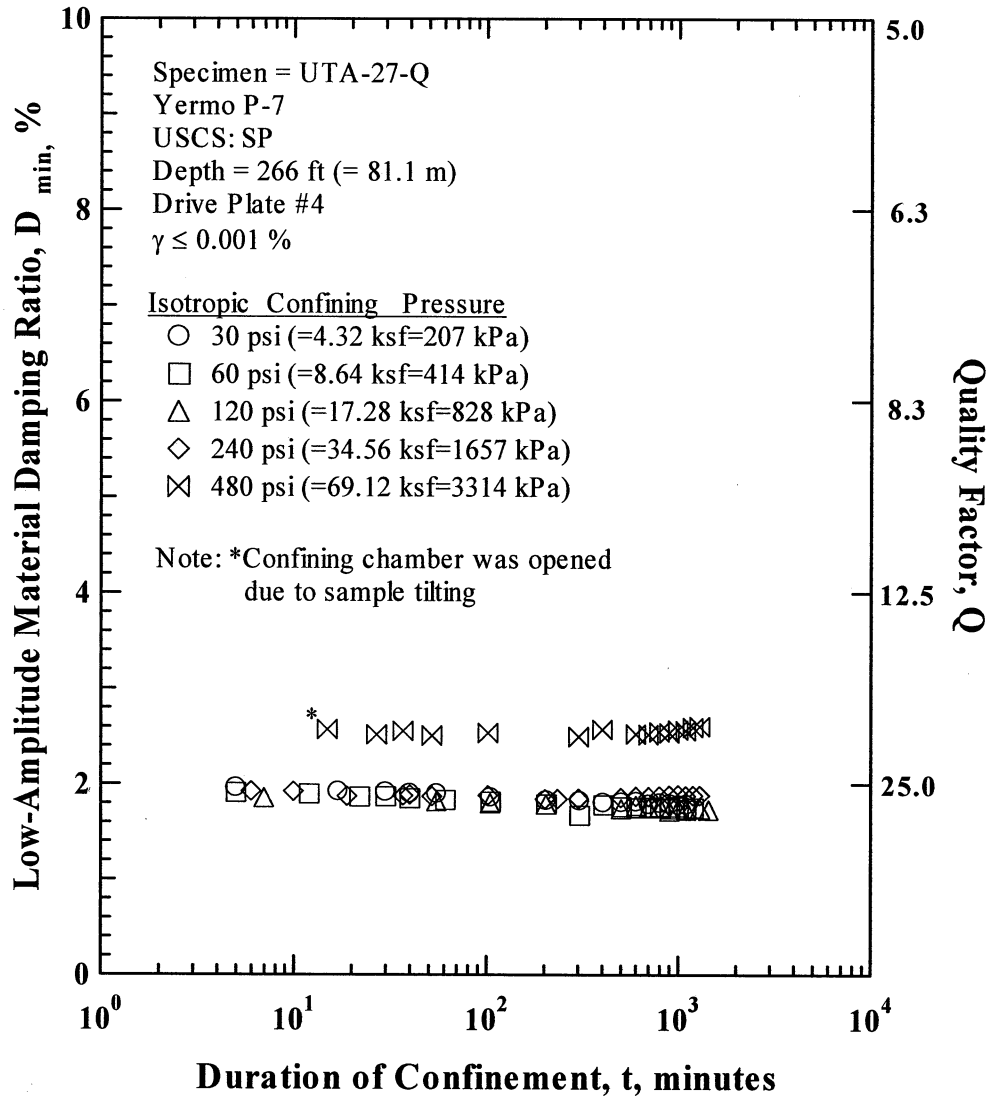

Figure S.2 Variation in Low-Amplitude Material Damping Ratio with Magnitude and Duration of Isotropic Confining Pressure from Resonant Column Tests of Specimen UTA-27-Q

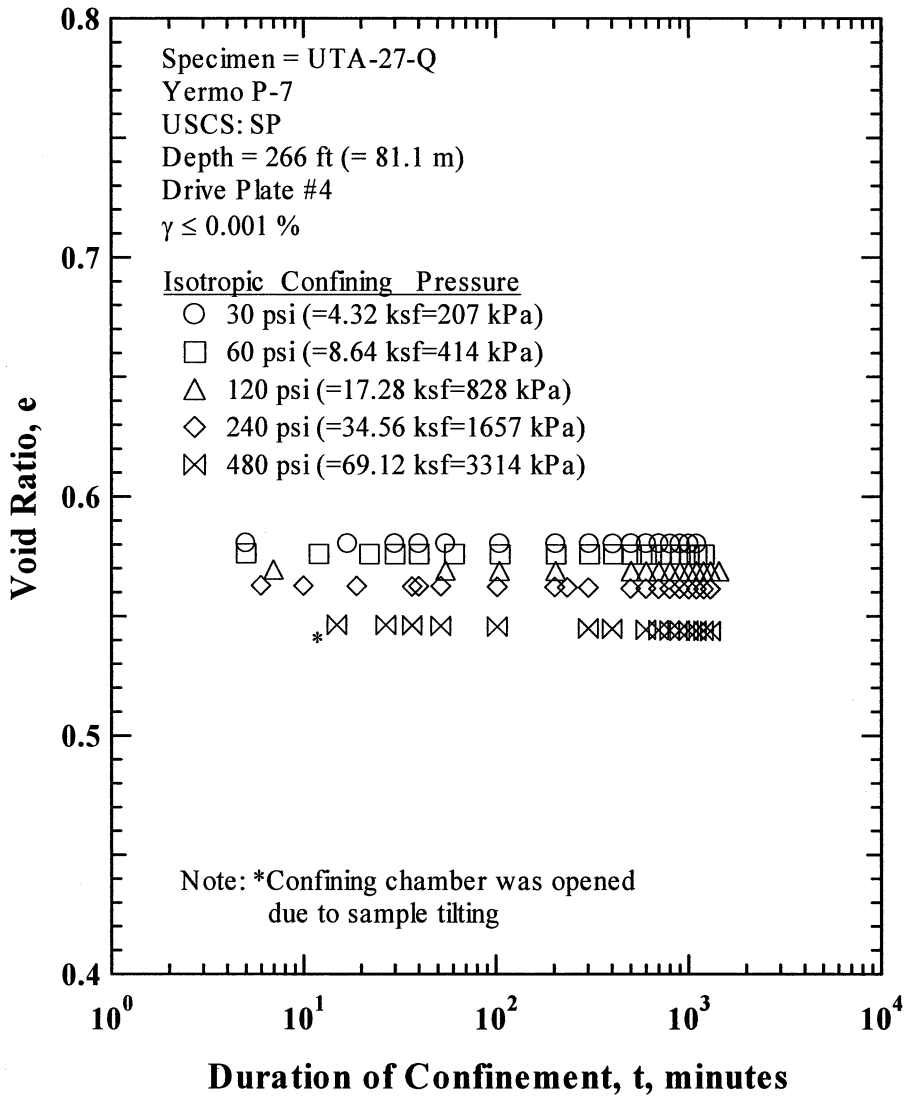

Figure S.3 Variation in Estimated Void Ratio with Magnitude and Duration of Isotropic Confining Pressure from Resonant Column Tests of Specimen UTA-27-Q.

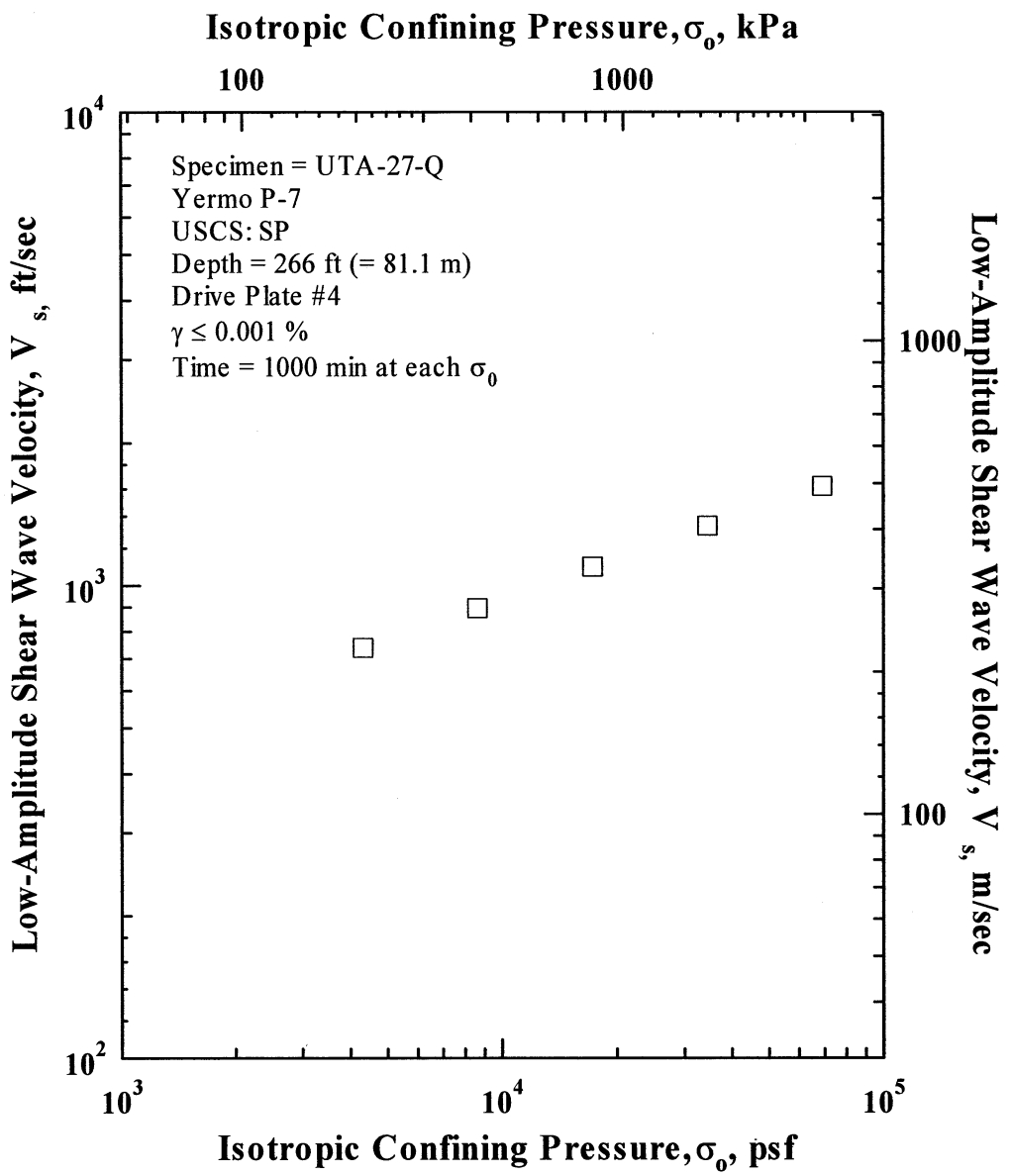

Figure S.4 Variation in Low-Amplitude Shear Wave Velocity with Isotropic Confining Pressure from Resonant Column Tests of Specimen UTA-27-Q.

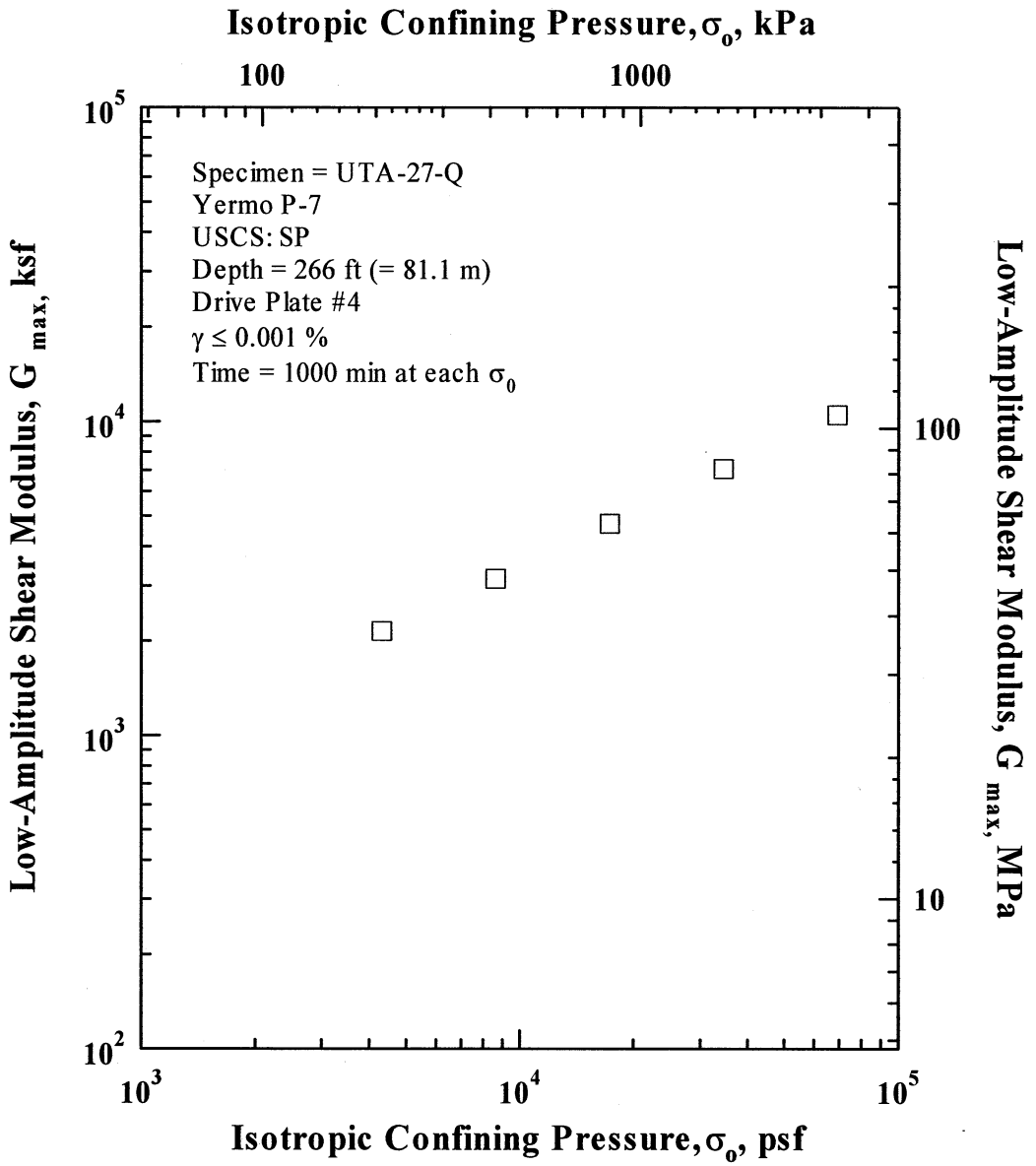

Figure S.5 Variation in Low-Amplitude Shear Modulus with Isotropic Confining Pressure from Resonant Column Tests of Specimen UTA-27-Q.

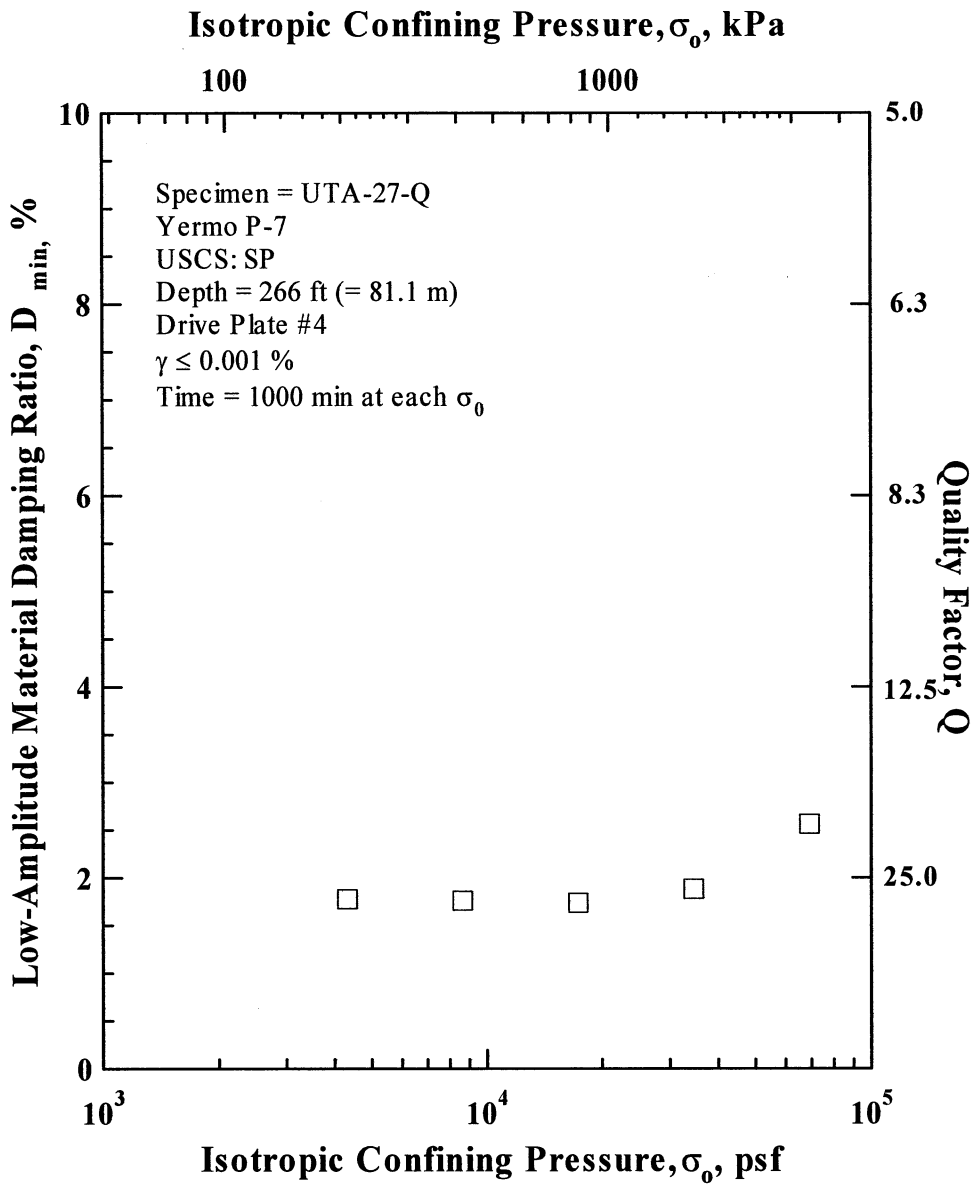

Figure S.6 Variation in Low-Amplitude Material Damping Ratio with Isotropic Confining Pressure from Resonant Column Tests of Specimen UTA-27-Q.

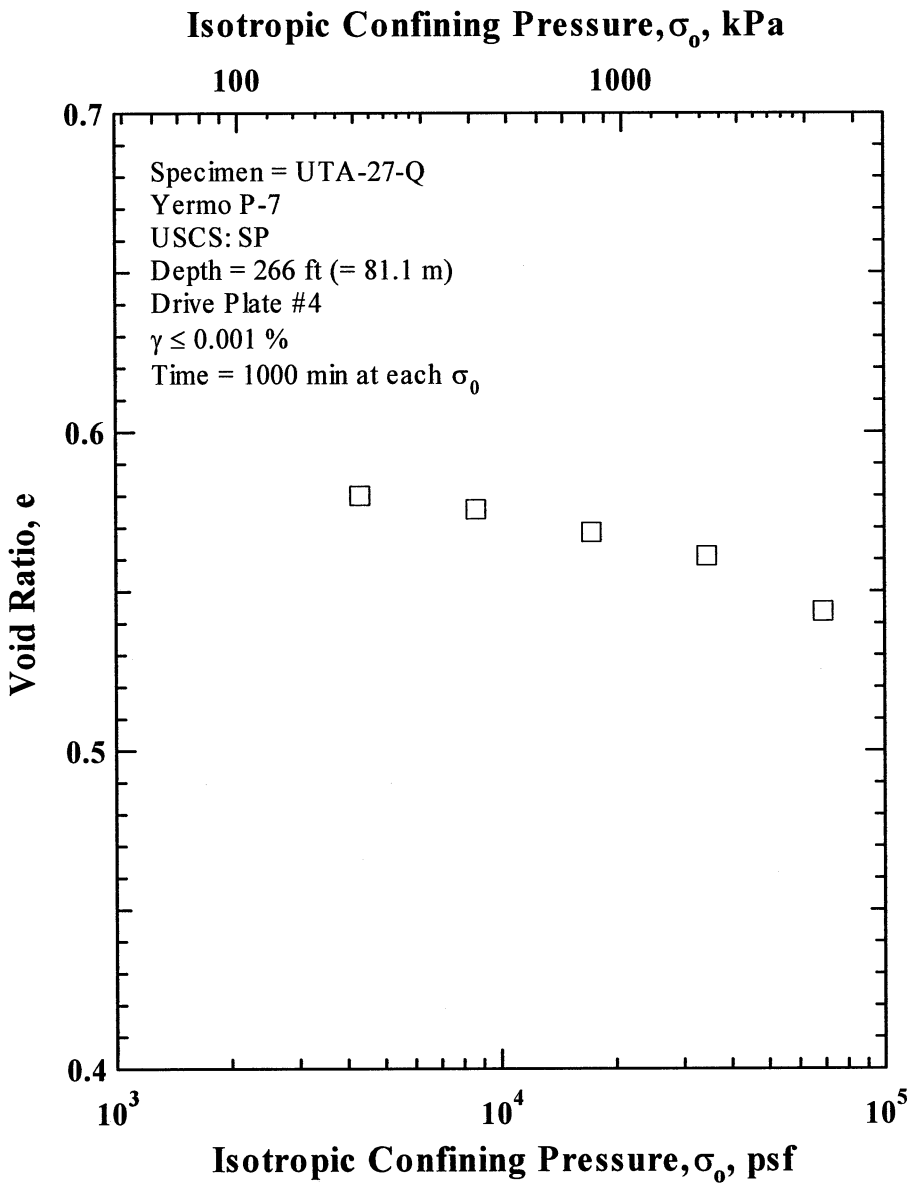

Figure S.7 Variation in Estimated Void Ratio with Isotropic Confining Pressure from Resonant Column Tests of Specimen UTA-27-Q.

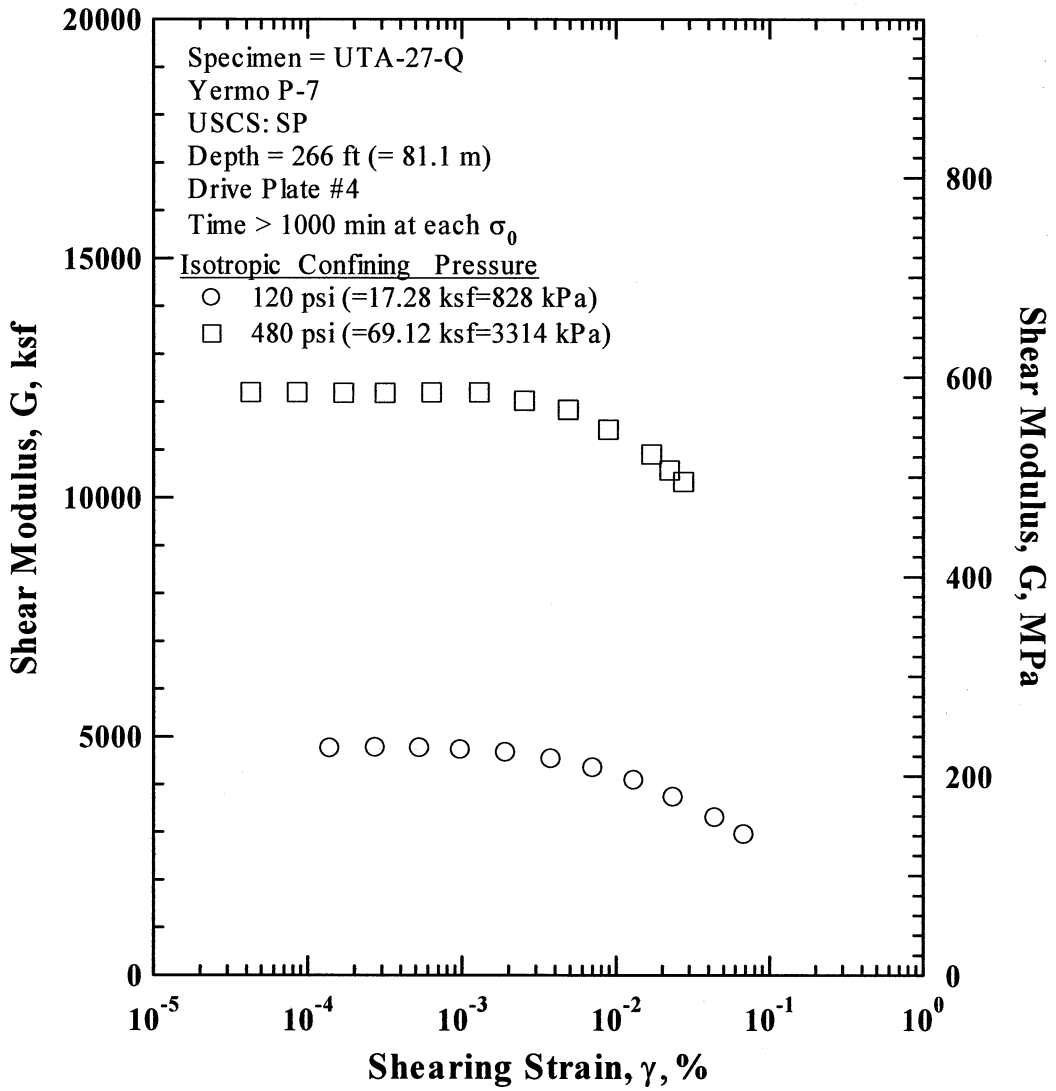

Figure S.8 Comparison of the Variation in Shear Modulus with Shearing Strain and Isotropic Confining Pressure from the Resonant Column Tests of Specimen UTA-27-Q.

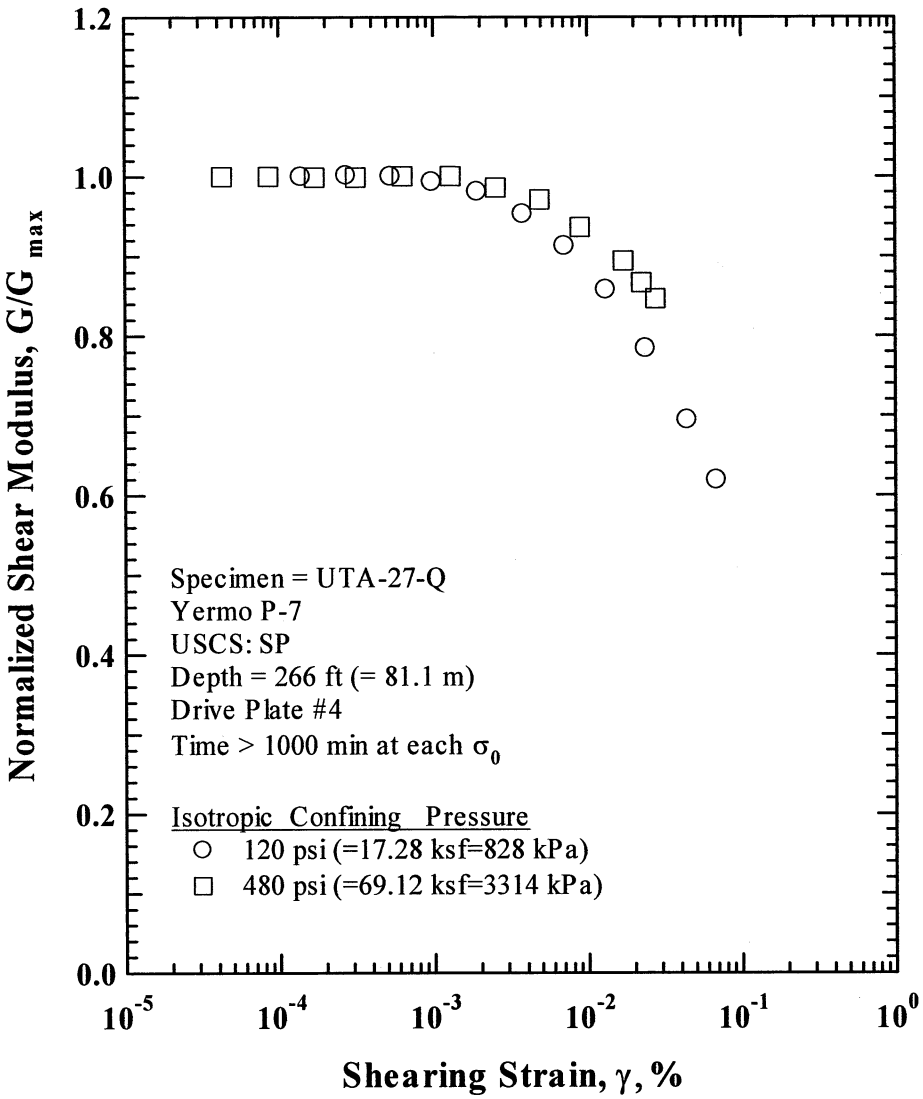

Figure S.9 Comparison of the Variation in Normalized Shear Modulus with Shearing Strain and Isotropic Confining Pressure from the Resonant Column Tests of Specimen UTA-27-Q.

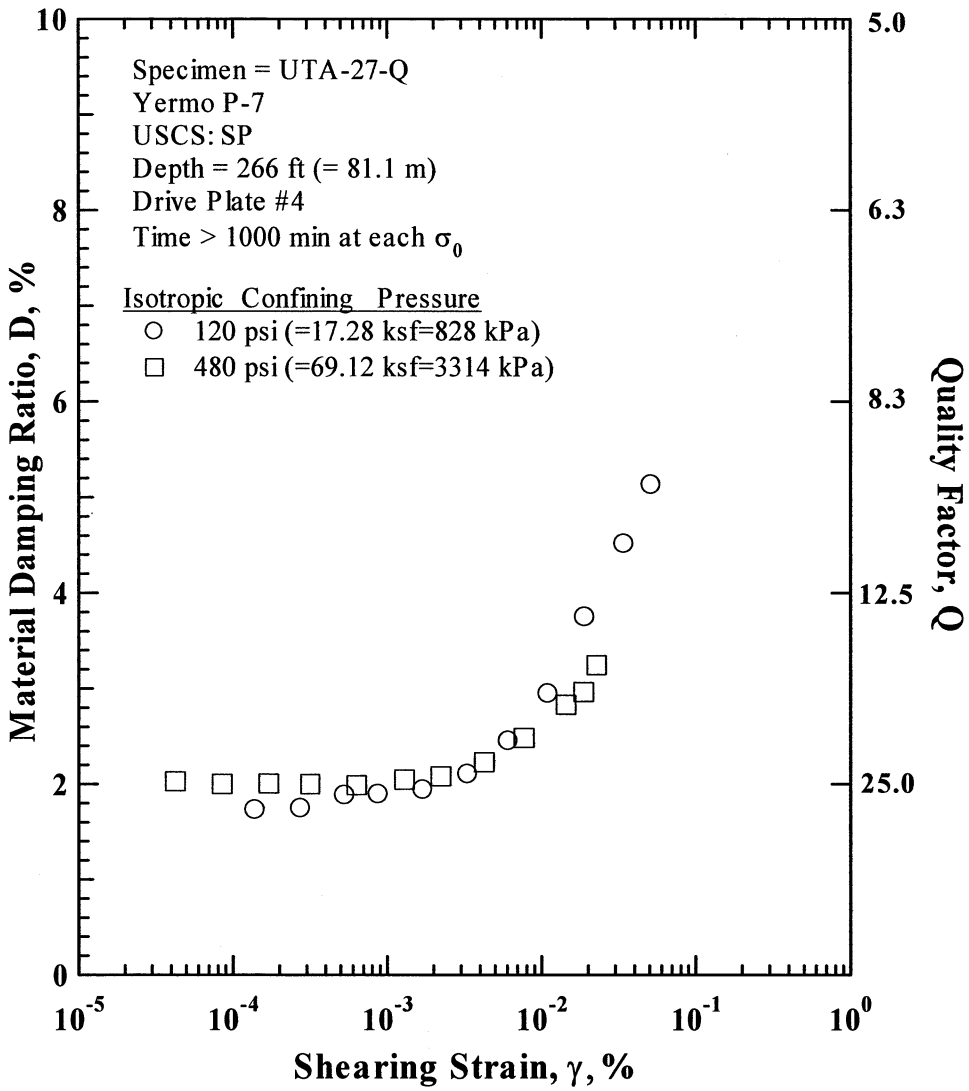

Figure S.10 Comparison of the Variation in Material Damping Ratio with Shearing Strain and Isotropic Confining Pressure from the Resonant Column Tests of Specimen UTA-27-Q.

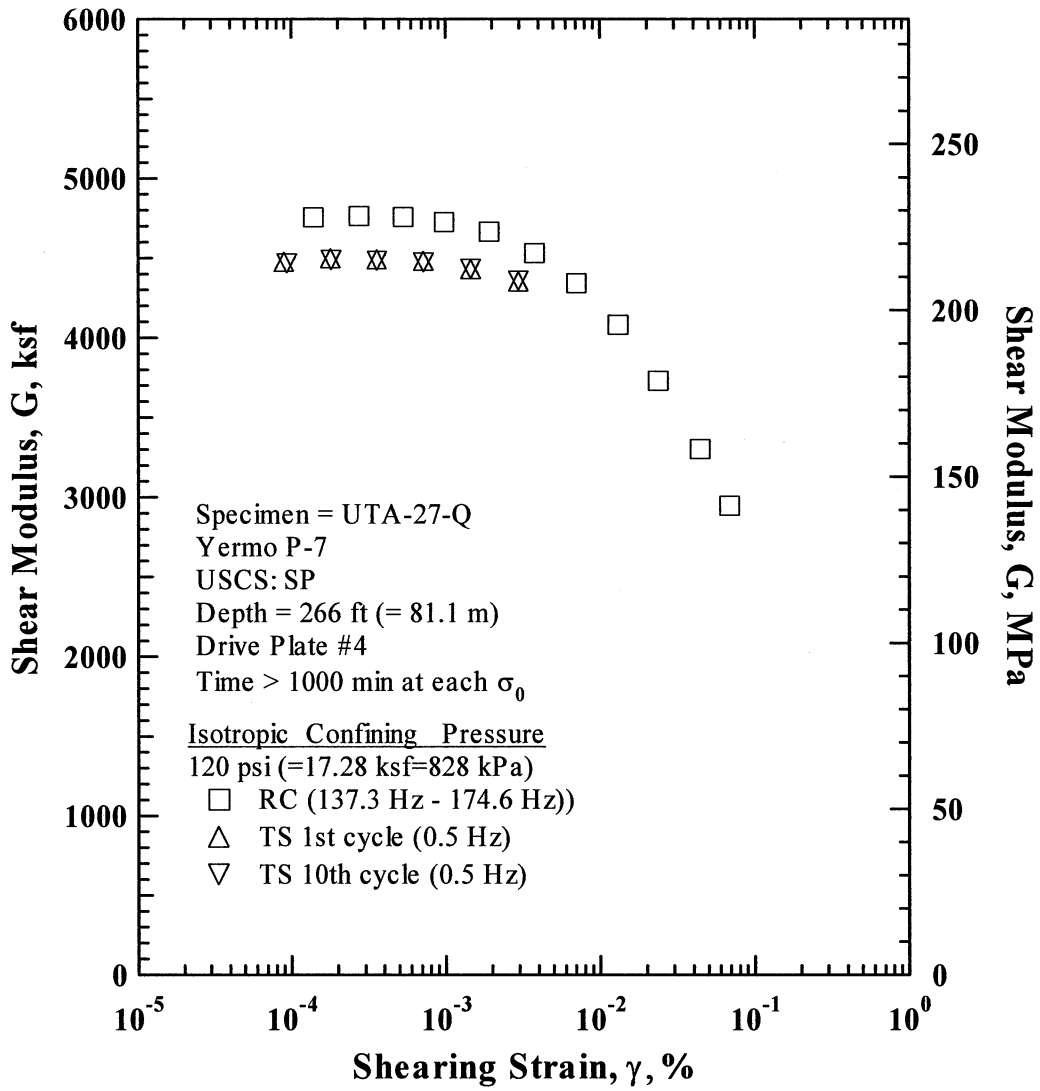

Figure S.11 Comparison of the Variation in Shear Modulus with Shearing Strain at an Isotropic Confining Pressure of 120 psi (=17.28 ksf=828 kPa) from the Combined RCTS Tests of Specimen UTA-27-Q.

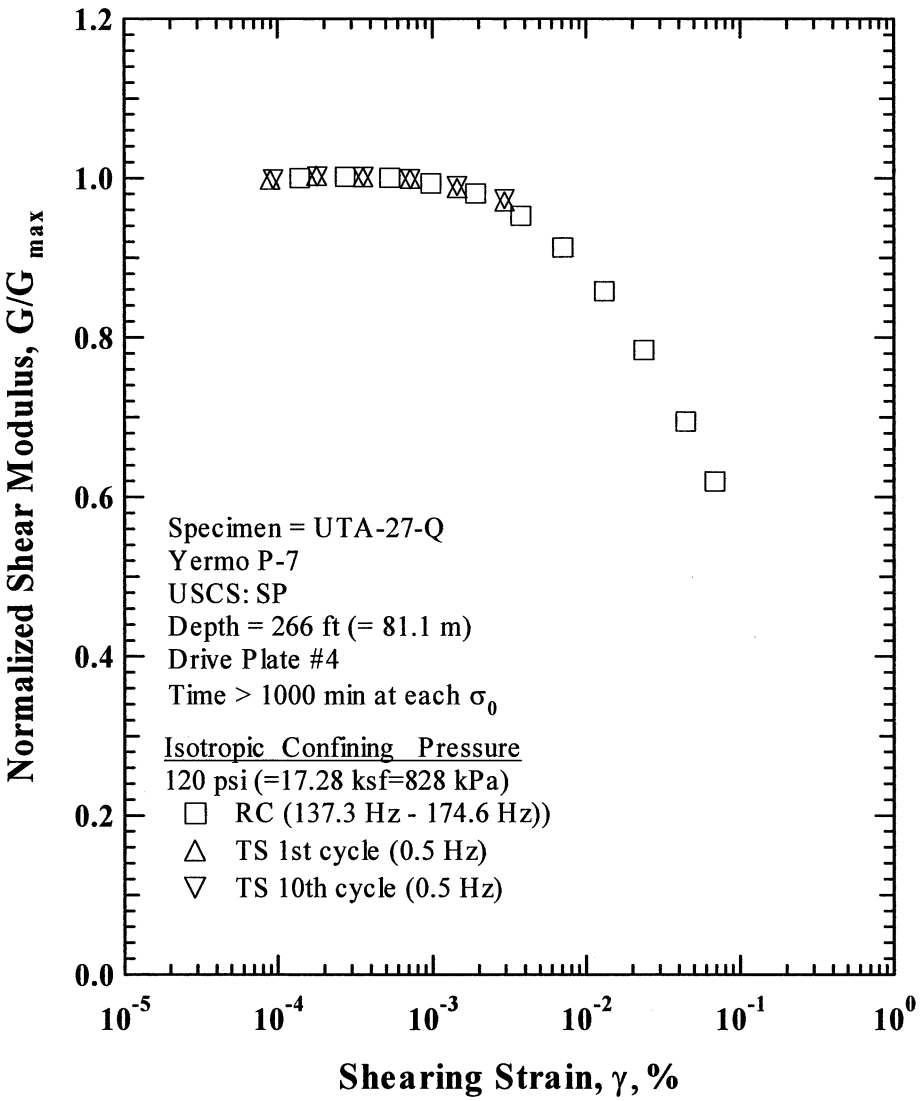

Figure S.12 Comparison of the Variation in Normalized Shear Modulus with Shearing Strain at an Isotropic Confining Pressure of 120 psi (=17.28 ksf=828 kPa) from the Combined RCTS Tests of Specimen UTA-27-Q.

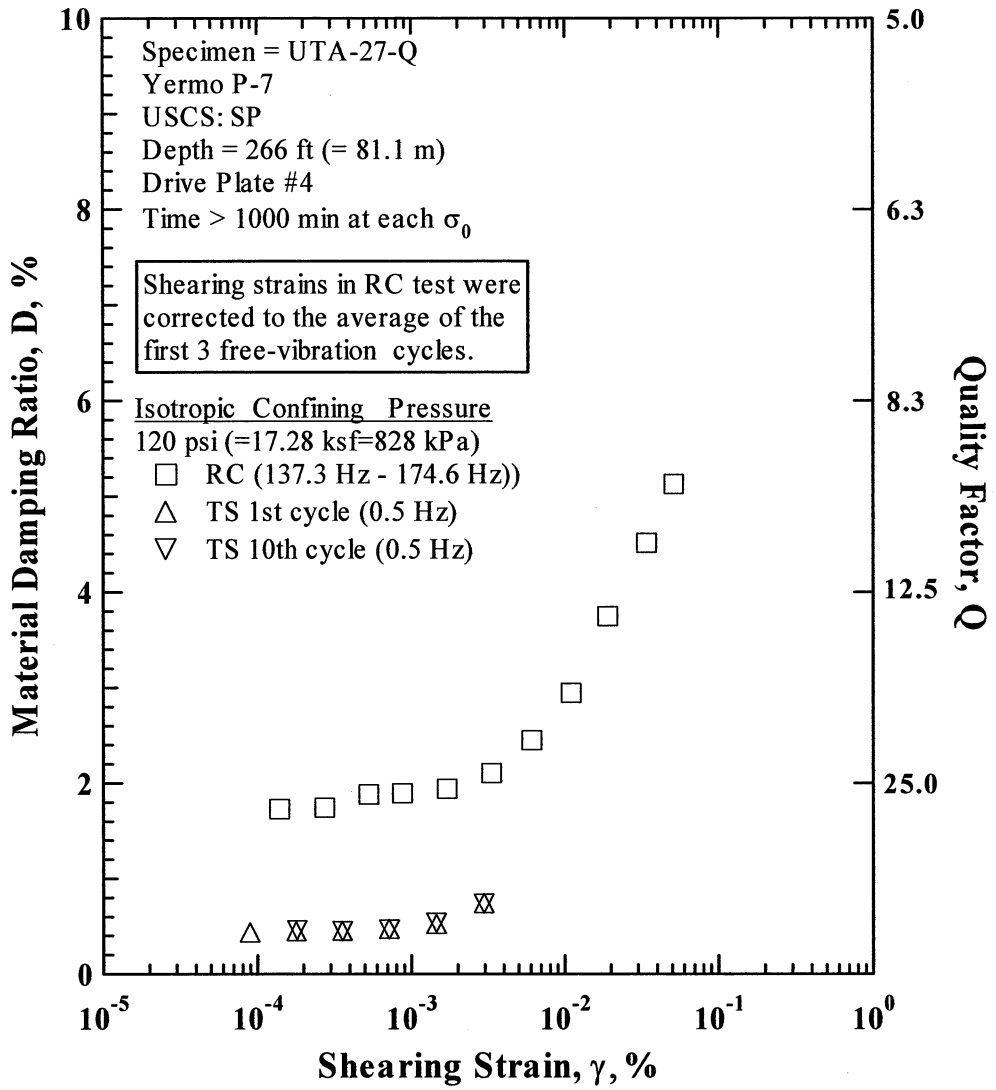

Figure S.13 Comparison of the Variation in Material Damping Ratio with Shearing Strain at an Isotropic Confining Pressure of 120 psi (=17.28 ksf=828 kPa) from the Combined RCTS Tests of Specimen UTA-27-Q.

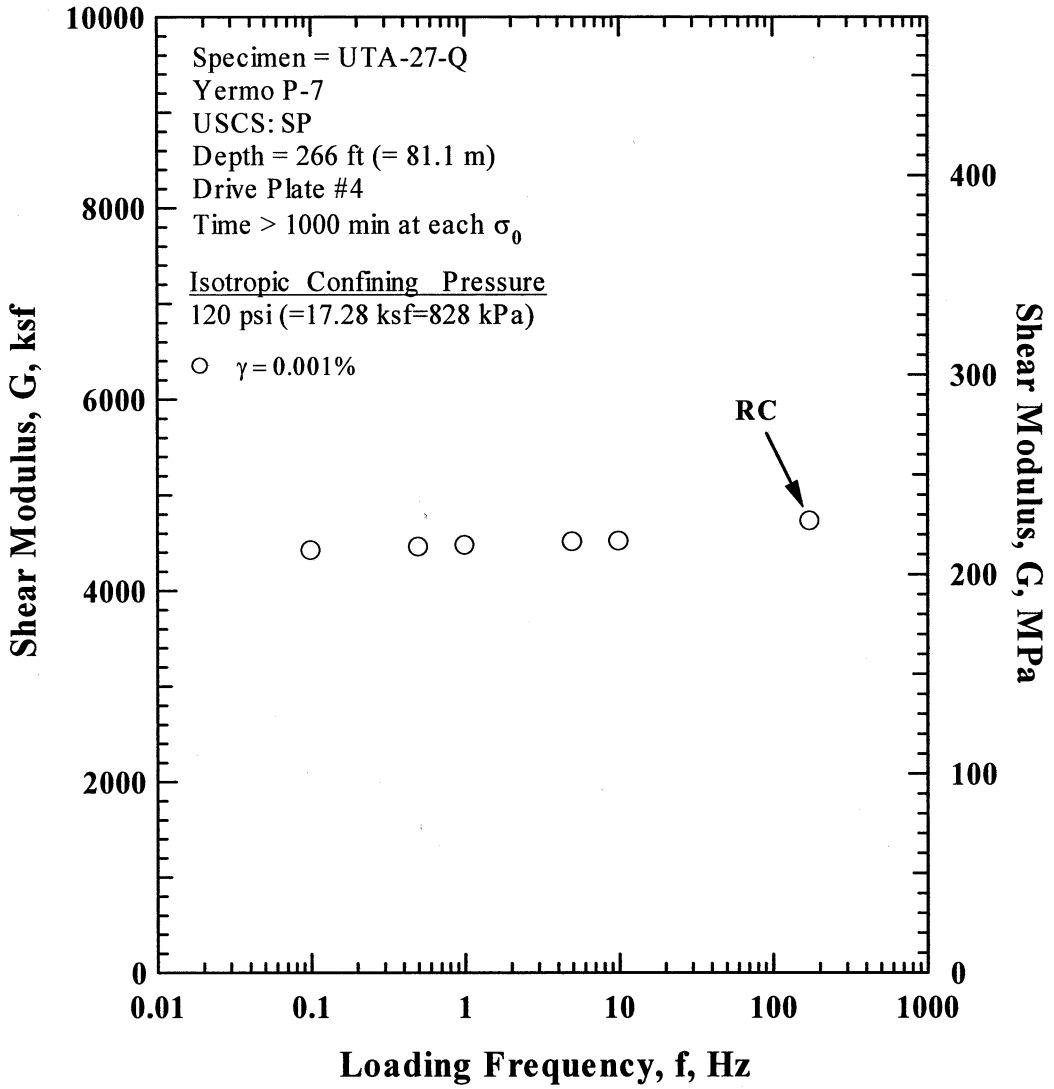

Figure S.14 Comparison of the Variation in Shear Modulus with Loading Frequency at an Isotropic Confining Pressure of 120 psi (=17.28 ksf=828 kPa) from the Combined RCTS Tests of Specimen UTA-27-Q.

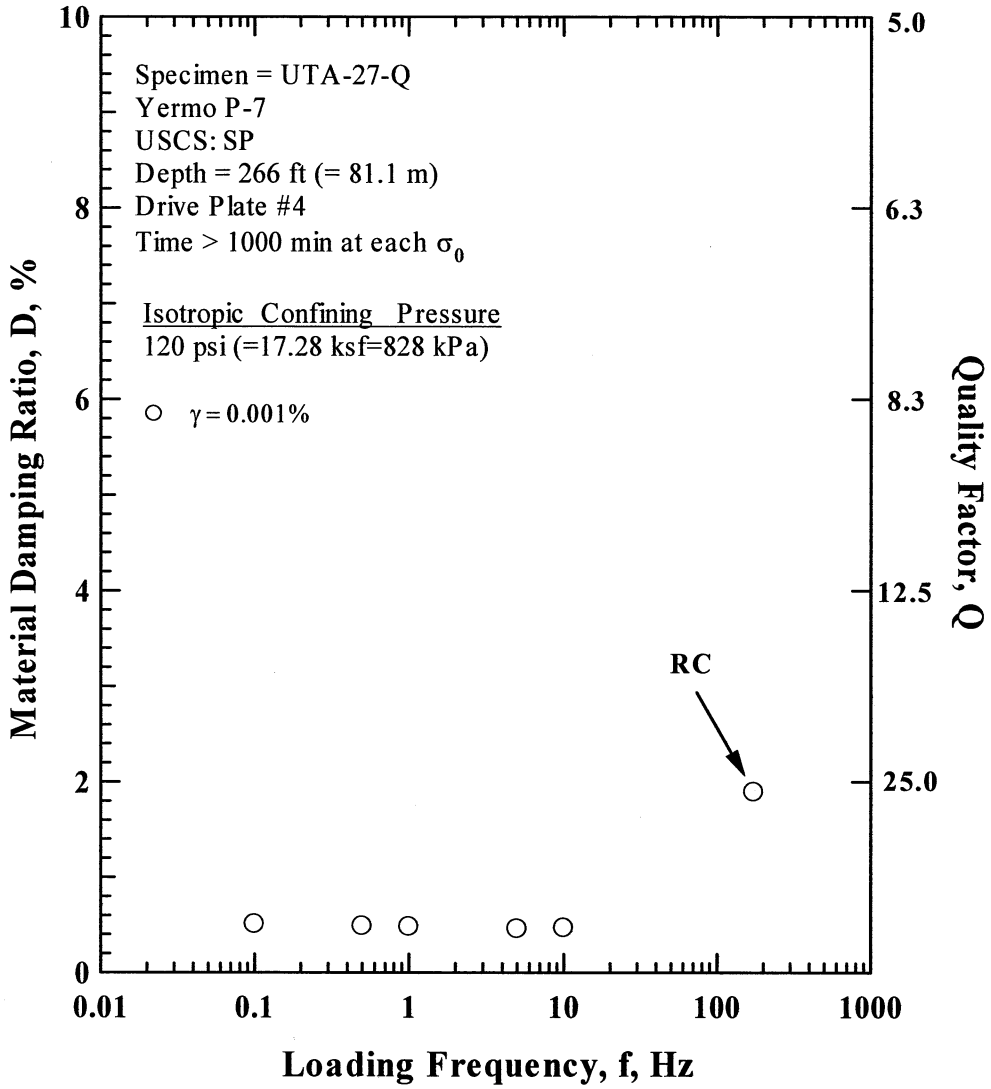

Figure S.15 Comparison of the Variation in Material Damping Ratio with Loading Frequency at an Isotropic Confining Pressure of 120 psi (=17.28 ksf=828 kPa) from the Combined RCTS Tests of Specimen UTA-27-Q.

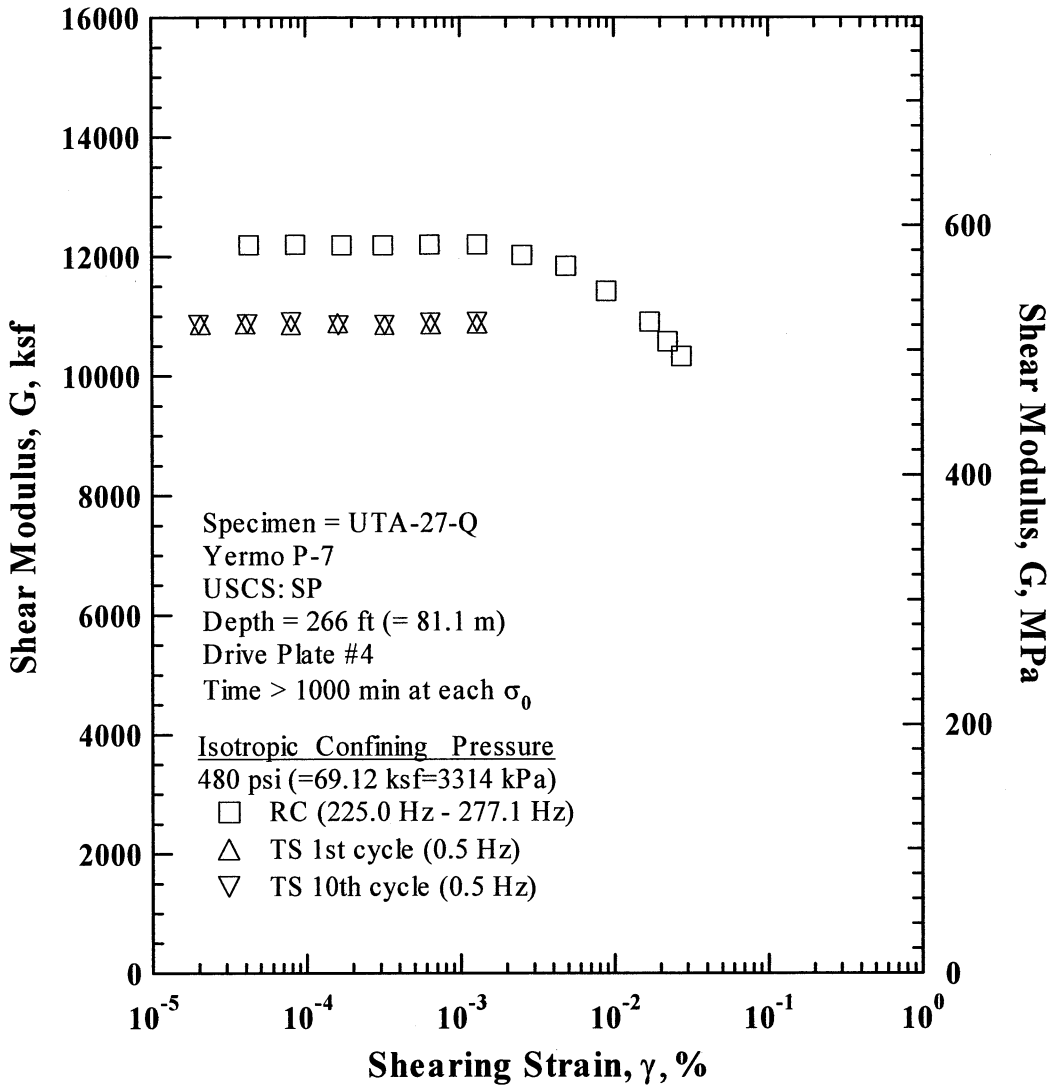

Figure S.16 Comparison of the Variation in Shear Modulus with Shearing Strain at an Isotropic Confining Pressure of 480 psi(=69.12 ksf=3314 kPa) from the Combined RCTS Tests of Specimen UTA-27-Q.

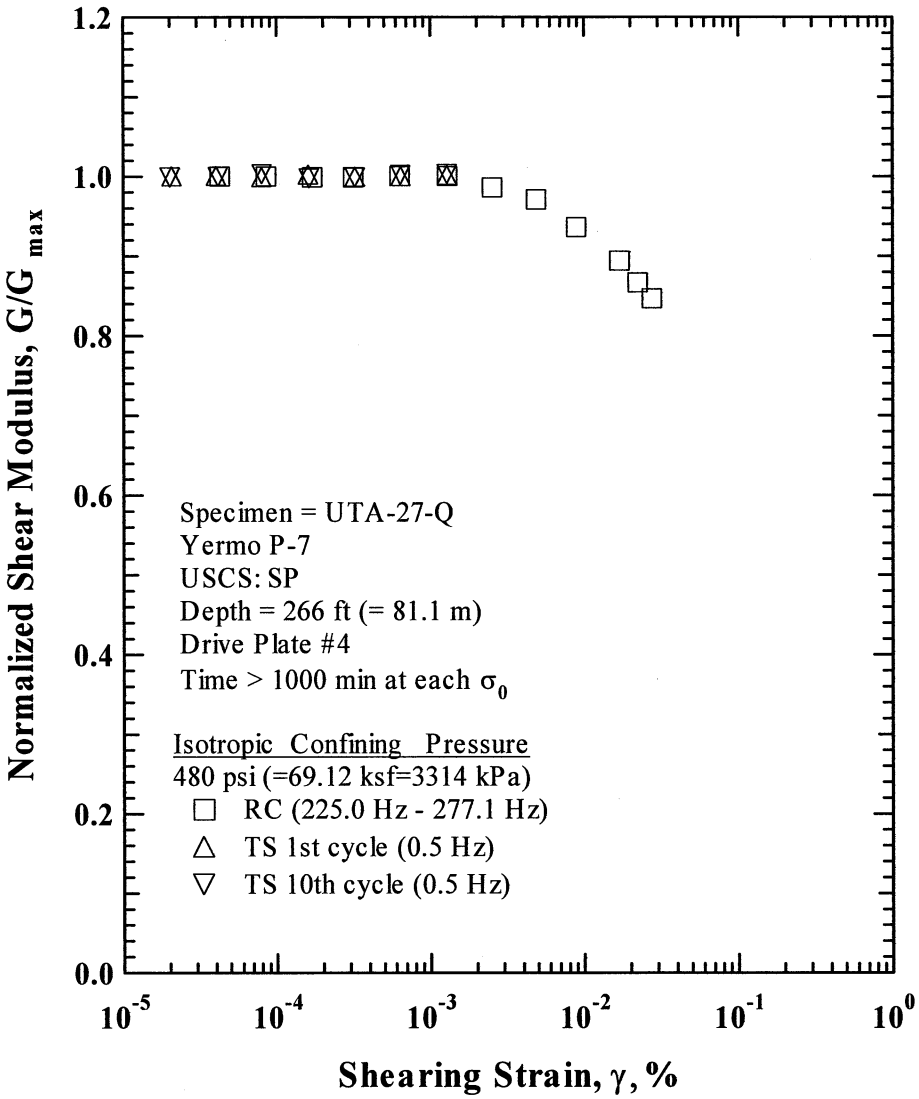

Figure S.17 Comparison of the Variation in Normalized Shear Modulus with Shearing Strain at an Isotropic Confining Pressure of 480 psi(=69.12 ksf=3314 kPa) from the Combined RCTS Tests of Specimen UTA-27-Q.

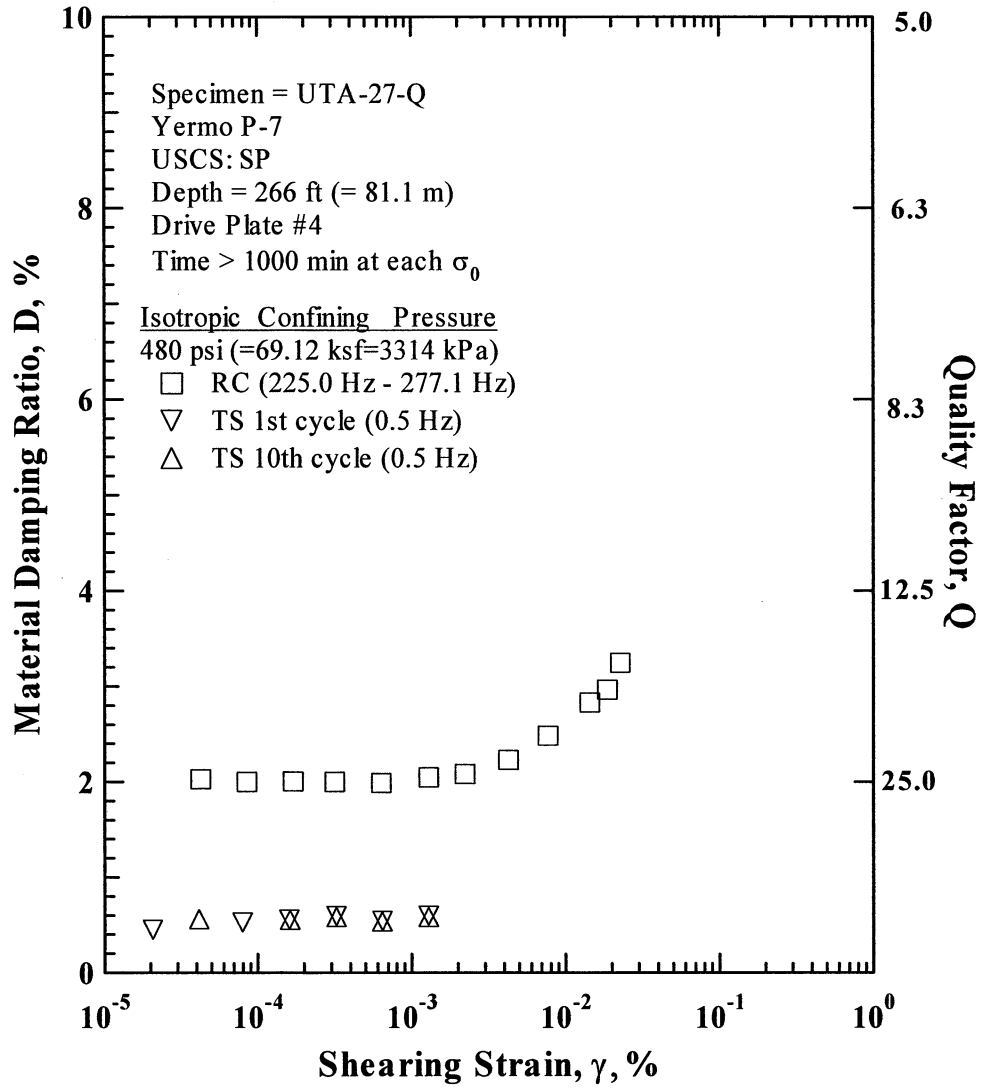

Figure S.18 Comparison of the Variation in Material Damping Ratio with Shearing Strain at an Isotropic Confining Pressure of 480 psi(=69.12 ksf=3314 kPa) from the Combined RCTS Tests of Specimen UTA-27-Q.

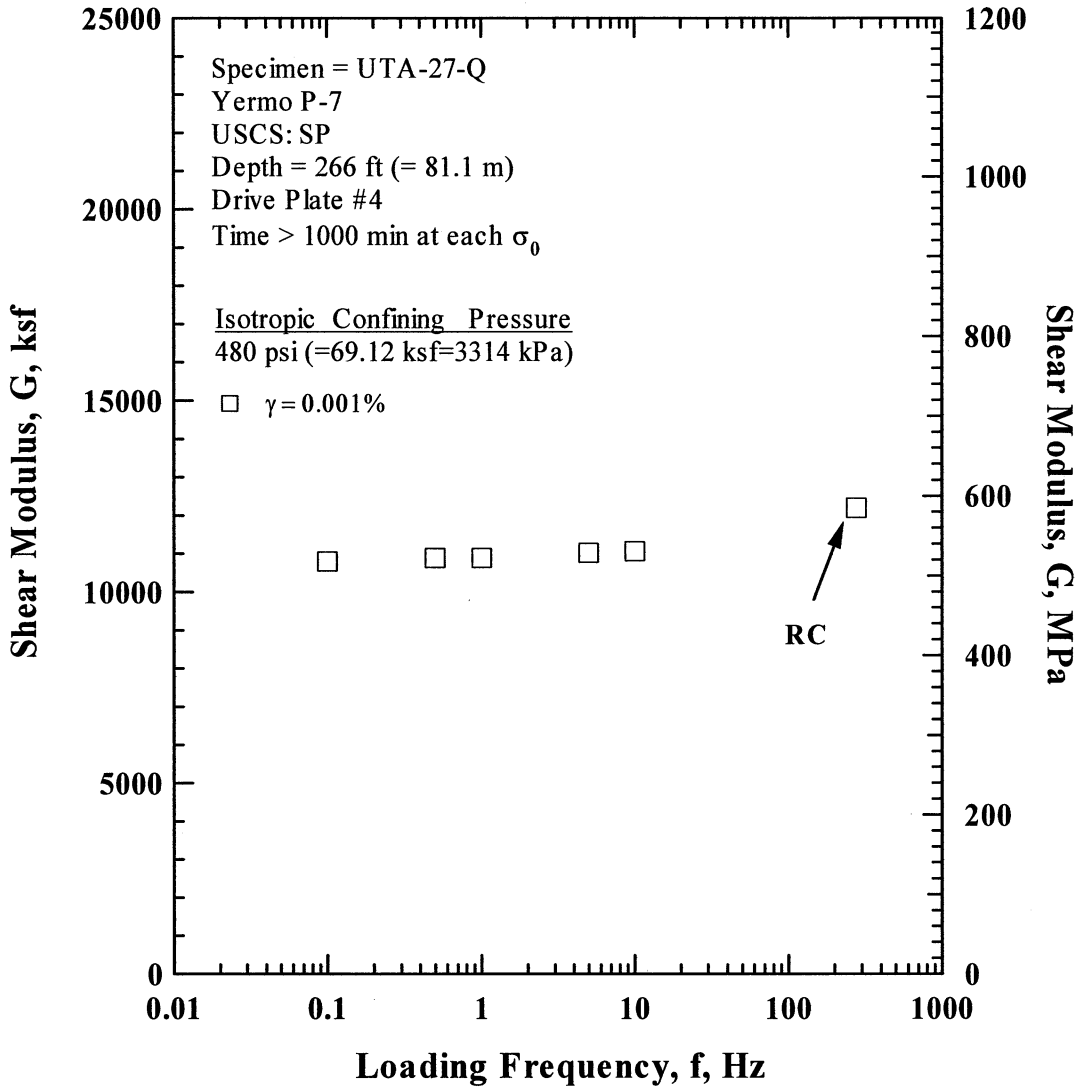

Figure S.19 Comparison of the Variation in Shear Modulus with Loading Frequency at an Isotropic Confining Pressure of 480 psi(=69.12 ksf=3314 kPa) from the Combined RCTS Tests of Specimen UTA-27-Q.

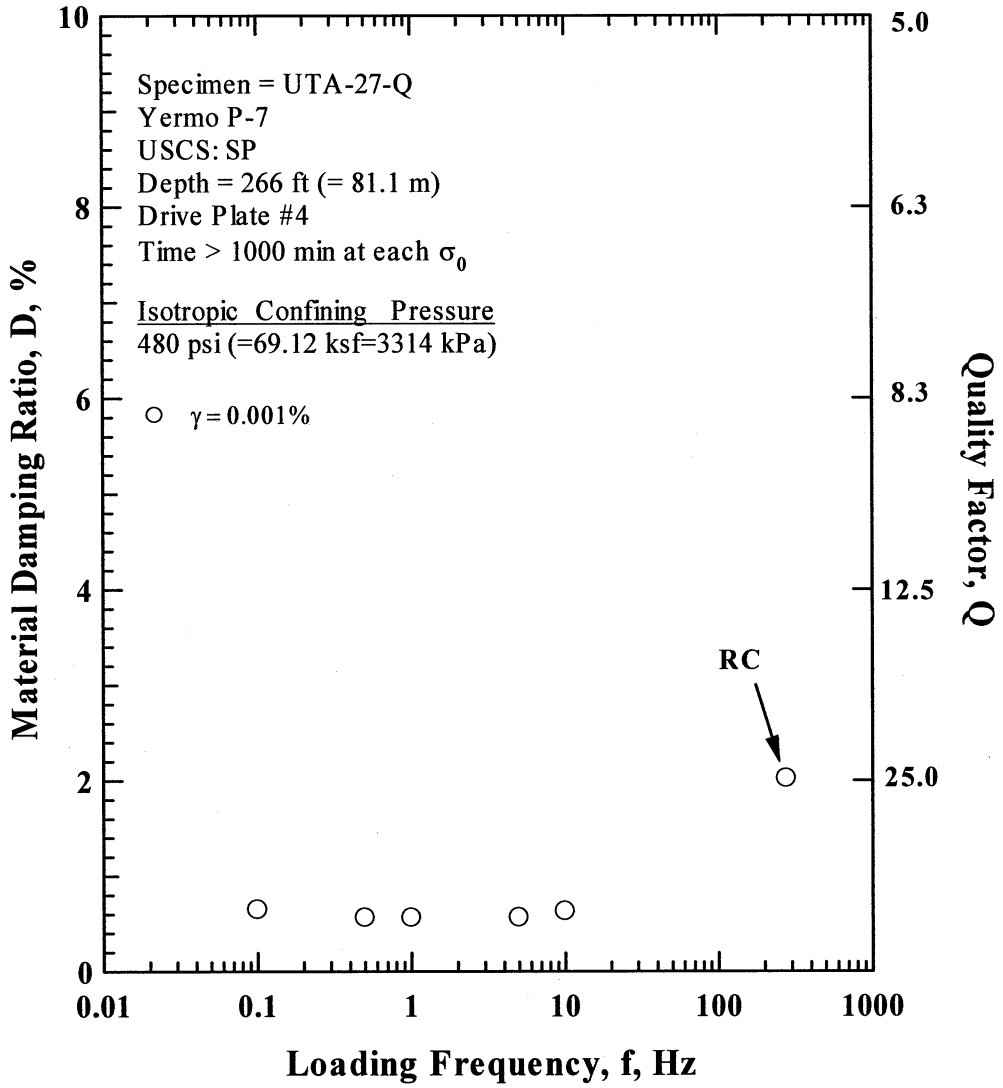

Figure S.20 Comparison of the Variation in Material Damping Ratio with Loading Frequency at an Isotropic Confining Pressure 480 psi(=69.12 ksf=3314 kPa) from the Combined RCTS Tests of Specimen UTA-27-Q.

Table V.1 Variation in Low-Amplitude Shear Wave Velocity, Low-Amplitude Shear Modulus, Low-Amplitude Material Damping Ratio and Estimated Void Ratio with Isotropic Confining Pressure from RC Tests of Specimen UTA-27-Q

Effective Isotropic Confining Pressure, σ_o'			Low-Amplitude Shear Modulus, G_{max}		Low-Amplitude Shear Wave Velocity, Vs	Low-Amplitude Material Damping Ratio, Dmin	Estimated Void Ratio, e
(psi)	(psf)	(kPa)	(ksf)	(MPa)	(fps)	(%)	
30	4320	207	2150	103.1	739	1.78	0.580
60	8640	414	3156	151.3	895	1.76	0.576
120	17280	828	4734	226.9	1095	1.74	0.569
240	34560	1657	7067	338.8	1336	1.88	0.561
480	69120	3314	10489	502.8	1622	2.56	0.544

Table V.2 Variation in Shear Modulus, Normalized Shear Modulus and Material Damping Ratio with Shearing Strain from RC Tests of Specimen UTA-27-Q ; Confining Pressure, σ_o' =120 psi (=17.28 ksf=828 kPa).

Peak Shearing Strain, %	Shear Modulus, G, ksf	Normalized Shear Modulus, G/G_{max}	Average^{+} Shearing Strain, %	Material Damping Ratio^{x}, D, %
1.39E-04	4756	1.00	1.39E-04	1.73
2.73E-04	4763	1.00	2.73E-04	1.75
5.32E-04	4758	1.00	5.32E-04	1.88
9.79E-04	4726	0.99	8.74E-04	1.89
1.91E-03	4666	0.98	1.70E-03	1.94
3.77E-03	4532	0.95	3.32E-03	2.10
7.06E-03	4342	0.91	6.10E-03	2.45
1.31E-02	4081	0.86	1.10E-02	2.94
2.37E-02	3730	0.78	1.90E-02	3.75
4.41E-02	3304	0.69	3.41E-02	4.51
6.85E-02	2947	0.62	5.13E-02	5.13

$^{+}$ Average Shearing Strain from the First Three Cycles of the Free Vibration Decay Curve

^{x} Average Damping Ratio from the First Three Cycles of the Free Vibration Decay Curve

Table V.3 Variation in Shear Modulus, Normalized Shear Modulus and Material Damping Ratio with Shearing Strain from TS Tests of Specimen UTA-27-Q ; Confining Pressure, σ_o' = 120 psi (=17.28 ksf=828 kPa).

First Cycle				Tenth Cycle			
Peak Shearing Strain, %	Shear Modulus, G, ksf	Normalized Shear Modulus, G/G_{max}	Material Damping Ratio, D, %	Peak Shearing Strain, %	Shear Modulus, G, ksf	Normalized Shear Modulus, G/G_{max}	Material Damping Ratio, D, %
9.00E-05	4474	1.00	0.43	9.40E-05	4465	1.00	
1.80E-04	4495	1.00	0.45	1.82E-04	4484	1.00	0.45
3.60E-04	4488	1.00	0.45	3.61E-04	4480	1.00	0.44
7.23E-04	4480	1.00	0.47	7.25E-04	4468	1.00	0.46
1.46E-03	4427	0.99	0.52	1.46E-03	4428	0.99	0.53
2.98E-03	4351	0.97	0.74	2.98E-03	4354	0.97	0.73

Table V.4 Variation in Shear Modulus, Normalized Shear Modulus and Material Damping Ratio with Shearing Strain from RC Tests of Specimen UTA-27-Q ; Confining Pressure, σ_o' = 480 psi (=69.12 ksf=3314 kPa).

Peak Shearing Strain, %	Shear Modulus, G, ksf	Normalized Shear Modulus, G/G_{max}	Average[+] Shearing Strain, %	Material Damping Ratio[x], D, %
4.24E-05	12197	1.00	4.24E-05	2.03
8.49E-05	12198	1.00	8.49E-05	2.00
1.70E-04	12186	1.00	1.70E-04	2.00
3.15E-04	12187	1.00	3.15E-04	2.00
6.34E-04	12200	1.00	6.34E-04	1.99
1.29E-03	12199	1.00	1.29E-03	2.05
2.52E-03	12024	0.99	2.22E-03	2.08
4.86E-03	11841	0.97	4.25E-03	2.23
8.90E-03	11421	0.94	7.67E-03	2.48
1.70E-02	10905	0.89	1.44E-02	2.83
2.23E-02	10575	0.87	1.87E-02	2.97
2.75E-02	10331	0.85	2.27E-02	3.24

[+] Average Shearing Strain from the First Three Cycles of the Free Vibration Decay Curve

[x] Average Damping Ratio from the First Three Cycles of the Free Vibration Decay Curve

Table V.5 Variation in Shear Modulus, Normalized Shear Modulus and Material Damping Ratio with Shearing Strain from TS Tests of Specimen UTA-27-Q ; Confining Pressure, σ_o' = 480 psi (=69.12 ksf=3314 kPa).

First Cycle				Tenth Cycle			
Peak Shearing Strain, %	Shear Modulus, G, ksf	Normalized Shear Modulus, G/G_{max}	Material Damping Ratio, D, %	Peak Shearing Strain, %	Shear Modulus, G, ksf	Normalized Shear Modulus, G/G_{max}	Material Damping Ratio, D, %
2.08E-05	10856	1.00	0.45	2.03E-05	10856	1.00	
4.05E-05	10863	1.00		4.17E-05	10863	1.00	0.56
8.01E-05	10846	1.00	0.52	8.03E-05	10897	1.00	
1.61E-04	10879	1.00	0.55	1.63E-04	10843	1.00	0.55
3.25E-04	10850	1.00	0.59	3.25E-04	10851	1.00	0.58
6.48E-04	10859	1.00	0.54	6.47E-04	10885	1.00	0.53
1.30E-03	10870	1.00	0.59	1.29E-03	10896	1.00	0.58

APPENDIX W

Specimen No. 22
UT Specimen ID: UTA-27-L

Halls Valley P-1
Depth = 7 ft (= 2.13m)
Soil Type: Clay (CL)

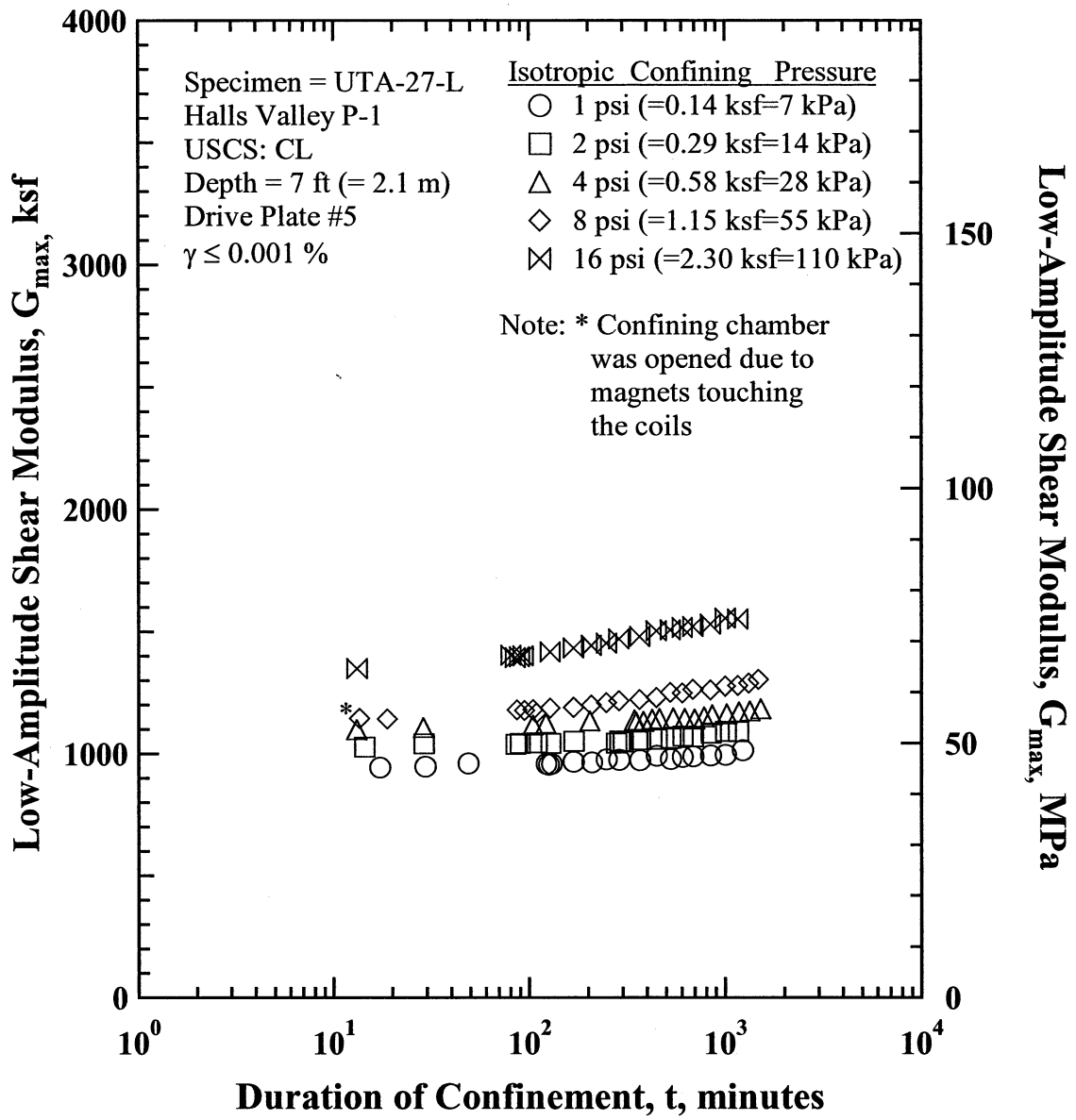

Figure W.1 Variation in Low-Amplitude Shear Modulus with Magnitude and Duration of Isotropic Confining Pressure from Resonant Column Tests of Specimen UTA-27-L.

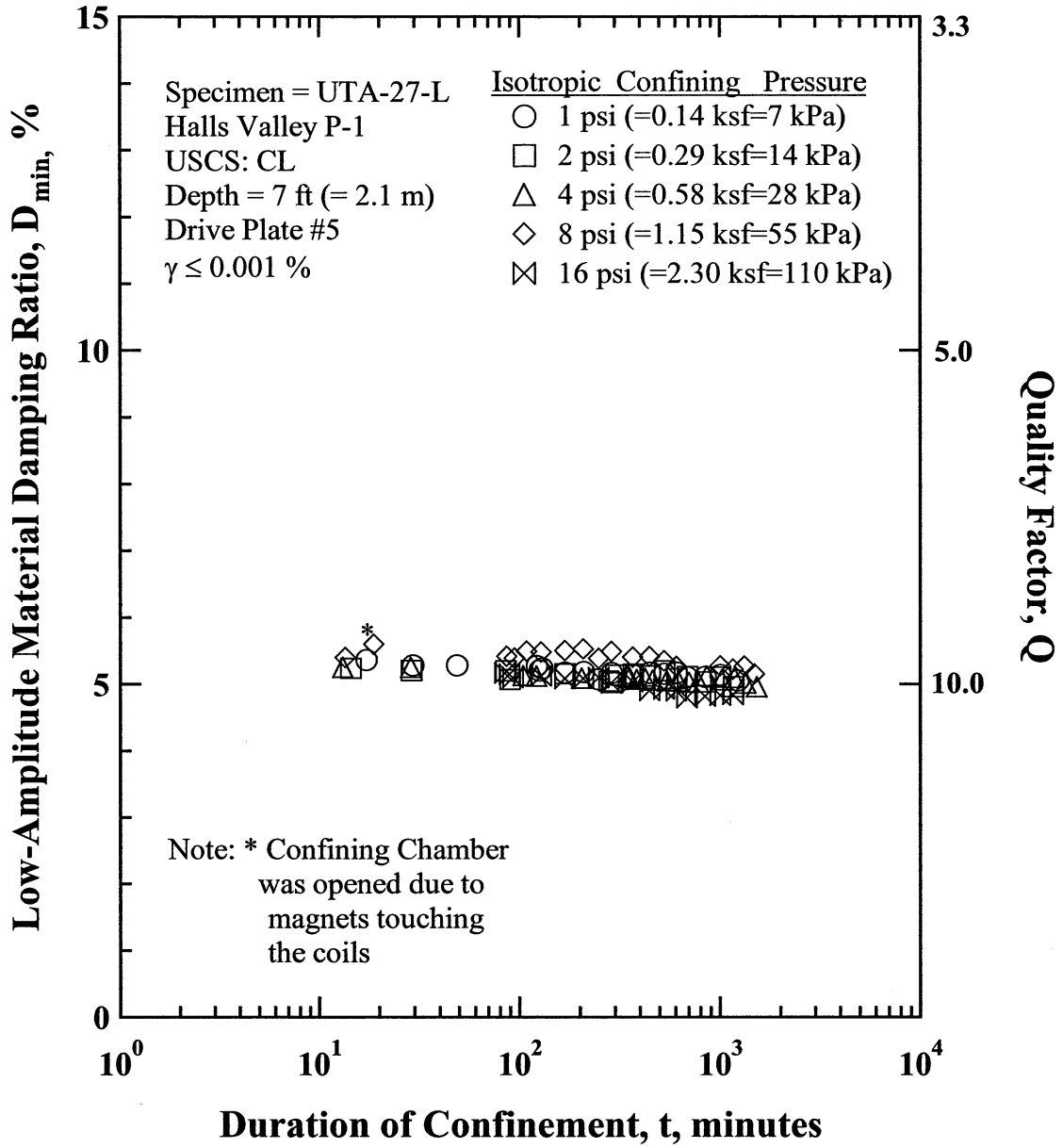

Figure W.2 Variation in Low-Amplitude Material Damping Ratio with Magnitude and Duration of Isotropic Confining Pressure from Resonant Column Tests of Specimen UTA-27-L

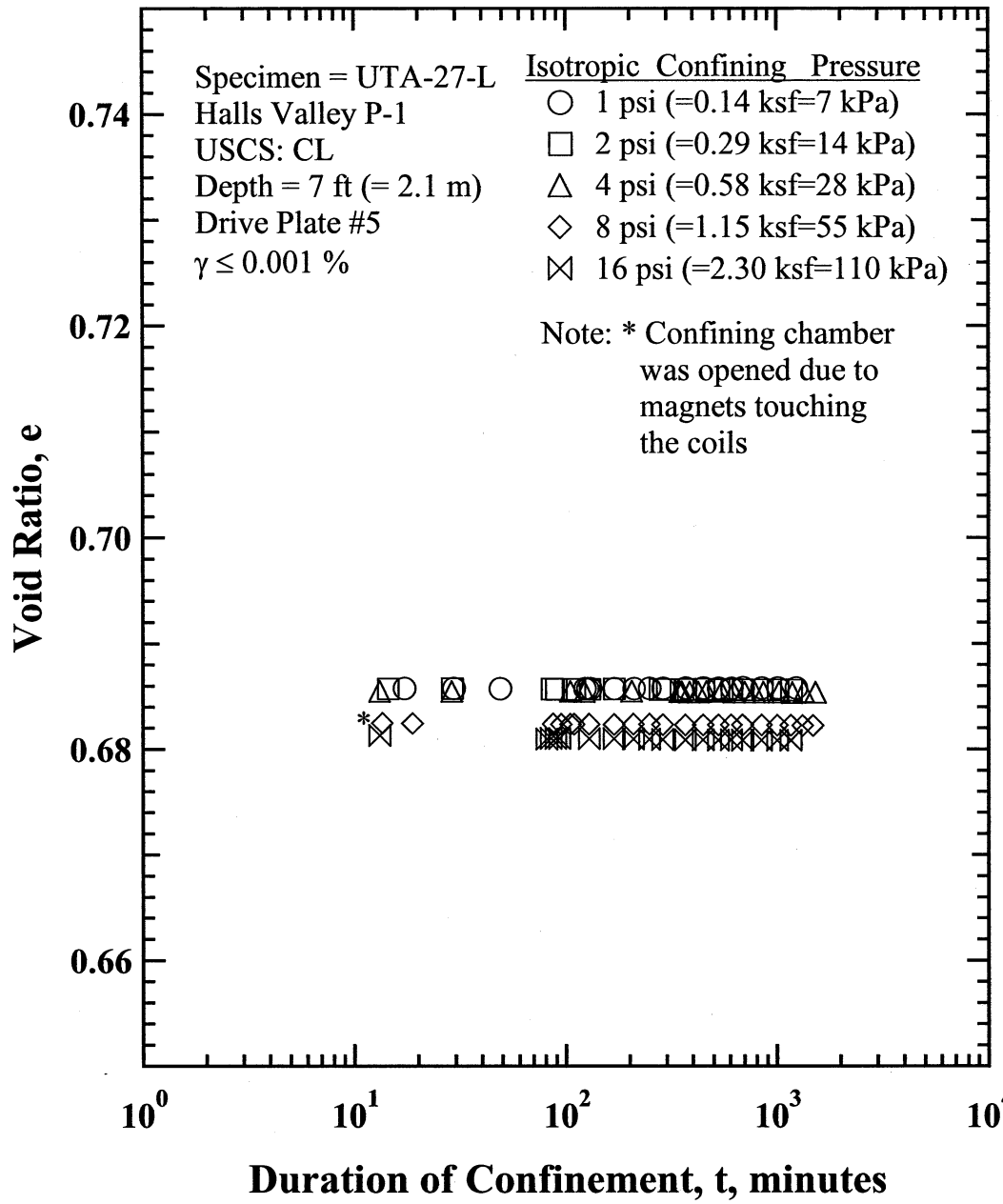

Figure W.3 Variation in Estimated Void Ratio with Magnitude and Duration of Isotropic Confining Pressure from Resonant Column Tests of Specimen UTA-27-L.

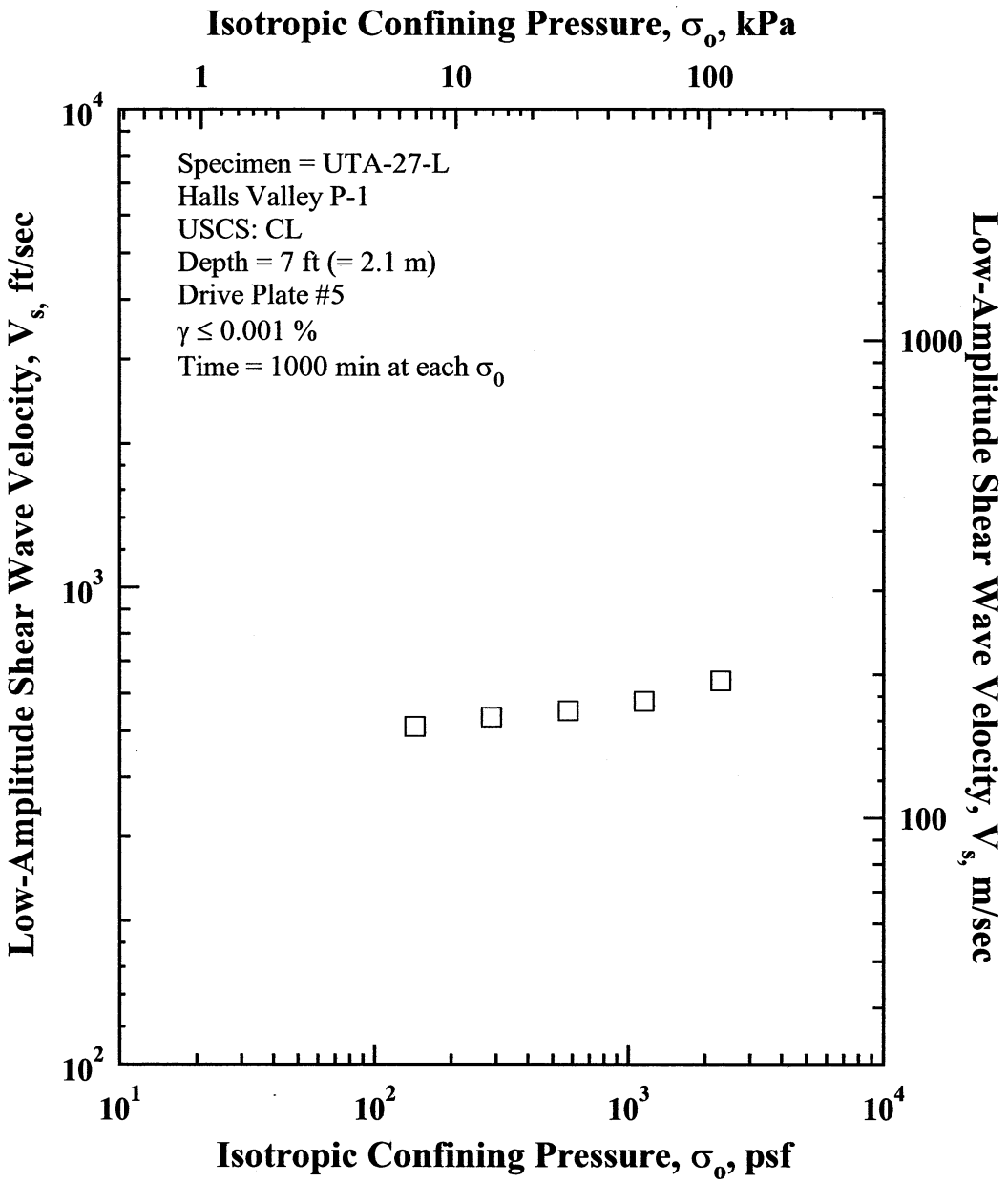

Figure W.4 Variation in Low-Amplitude Shear Wave Velocity with Isotropic Confining Pressure from Resonant Column Tests of Specimen UTA-27-L.

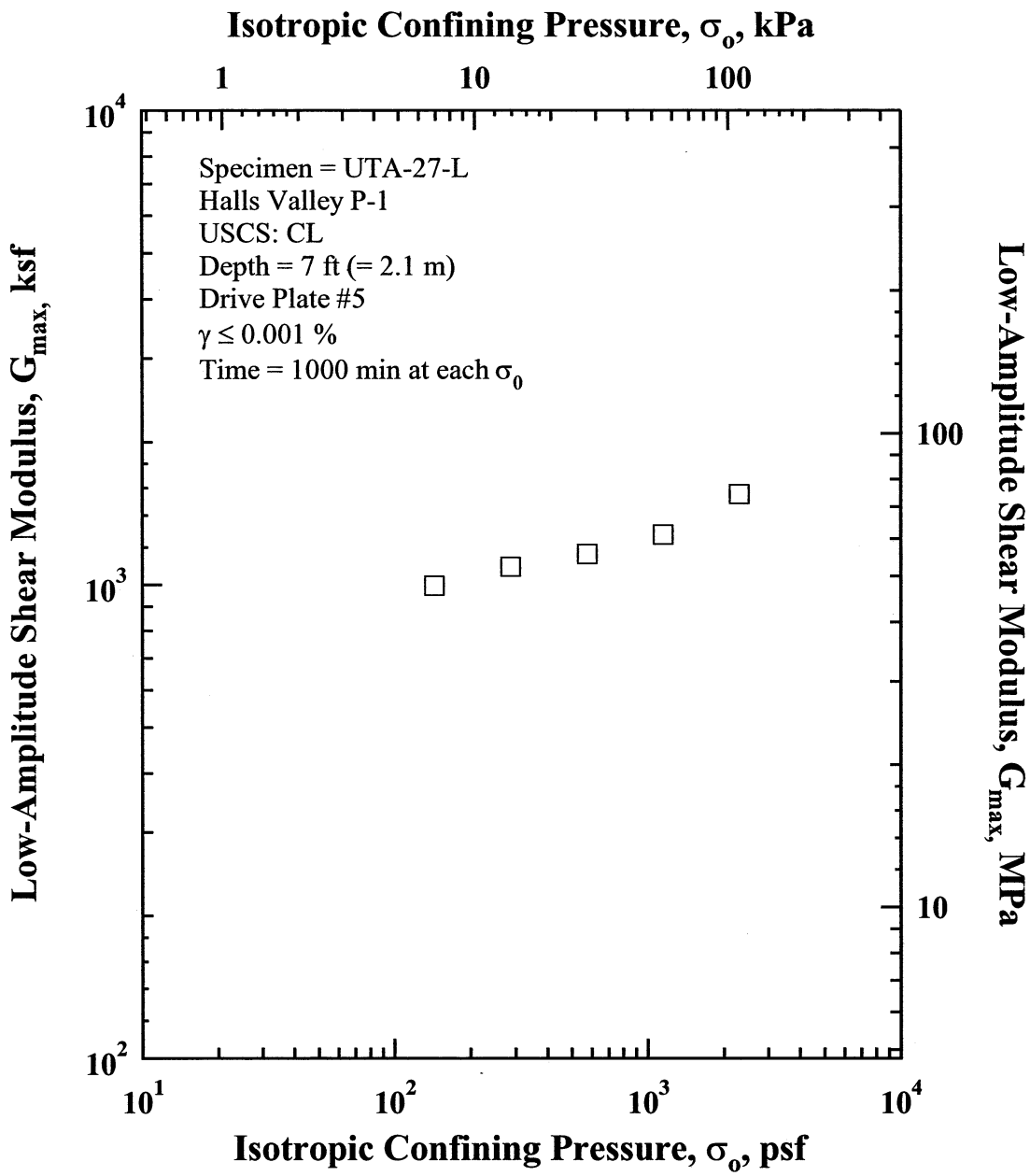

Figure W.5 Variation in Low-Amplitude Shear Modulus with Isotropic Confining Pressure from Resonant Column Tests of Specimen UTA-27-L.

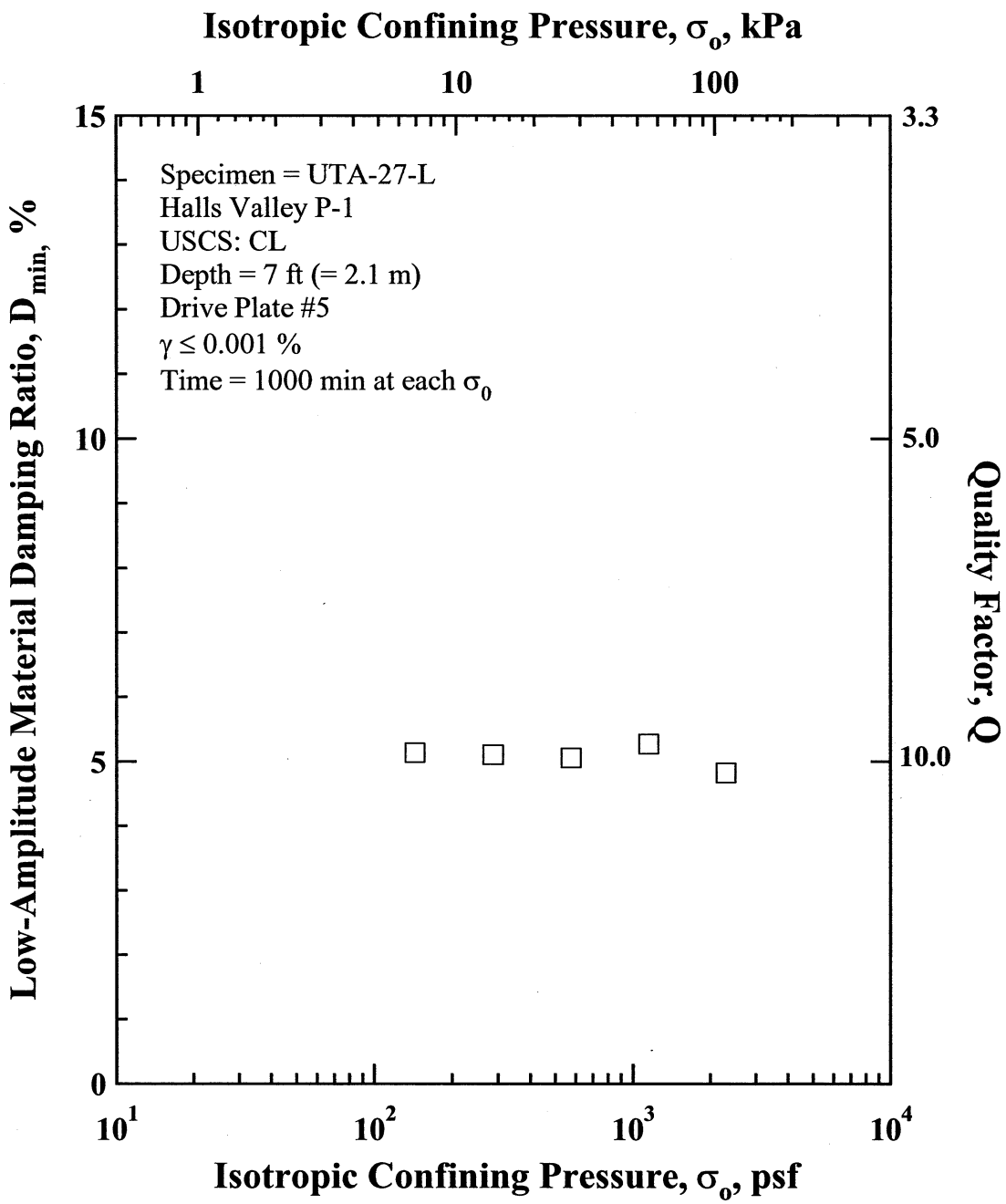

Figure W.6 Variation in Low-Amplitude Material Damping Ratio with Isotropic Confining Pressure from Resonant Column Tests of Specimen UTA-27-L.

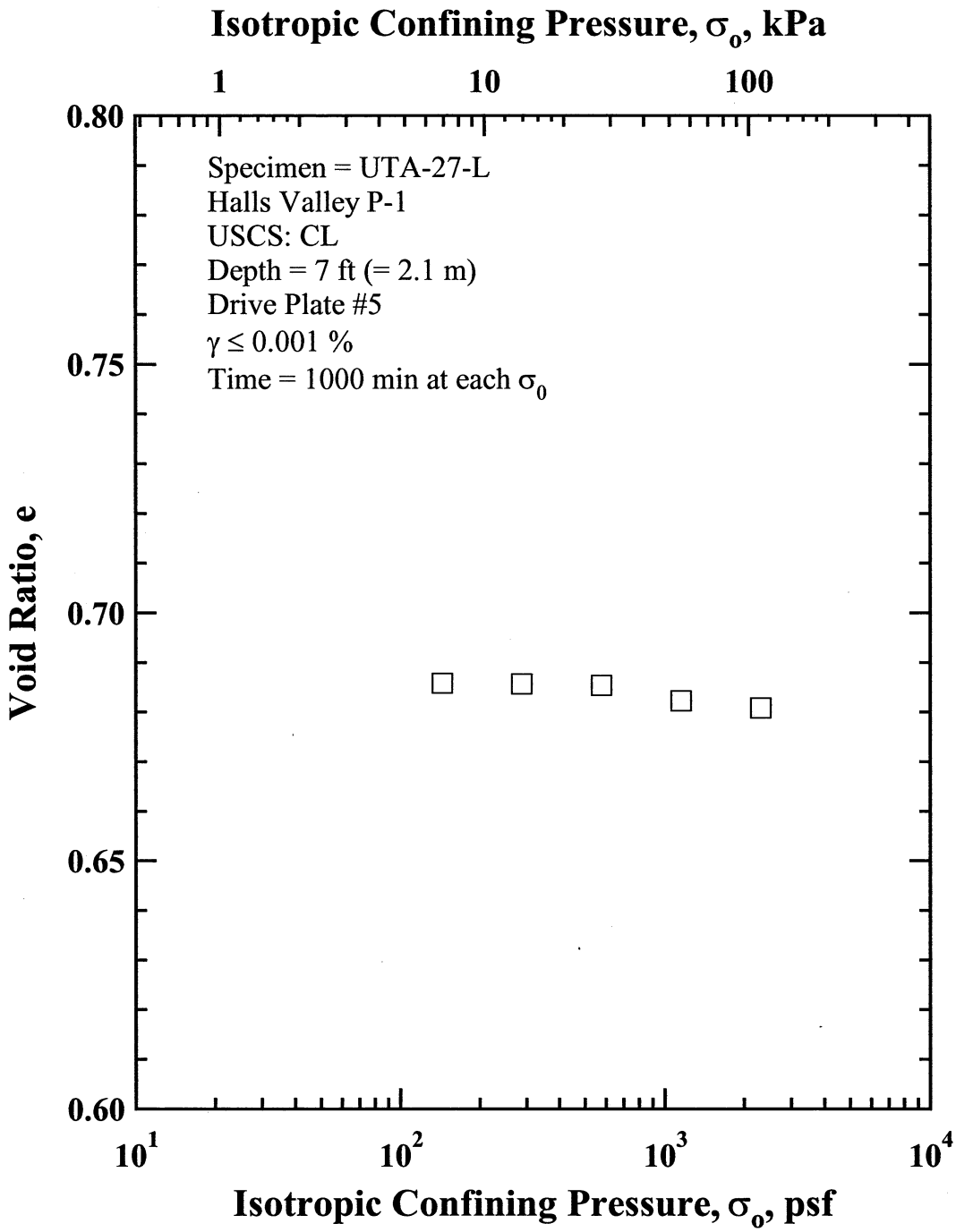

Figure W.7 Variation in Estimated Void Ratio with Isotropic Confining Pressure from Resonant Column Tests of Specimen UTA-27-L.

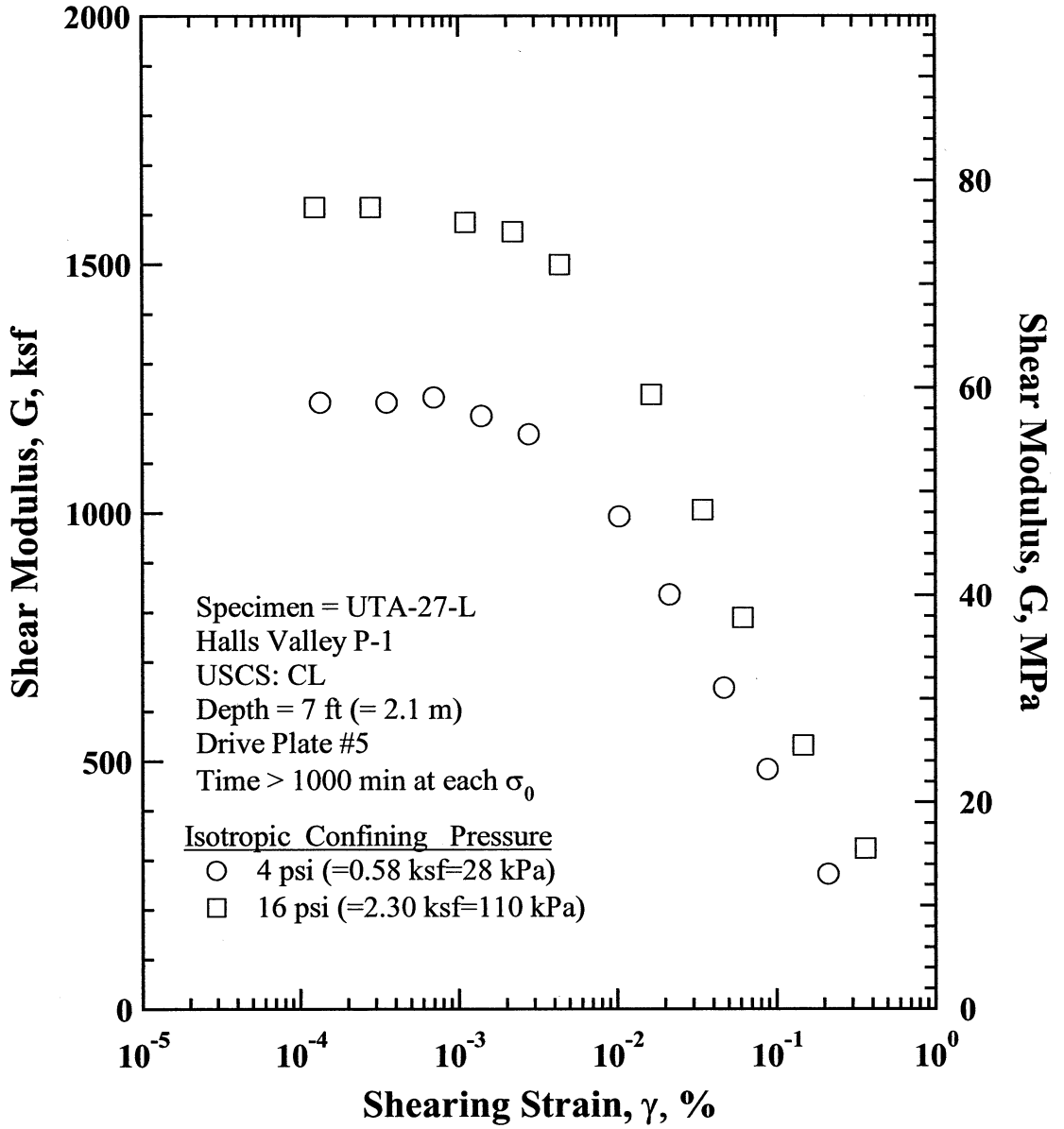

Figure W.8 Comparison of the Variation in Shear Modulus with Shearing Strain and Isotropic Confining Pressure from the Resonant Column Tests of Specimen UTA-27-L.

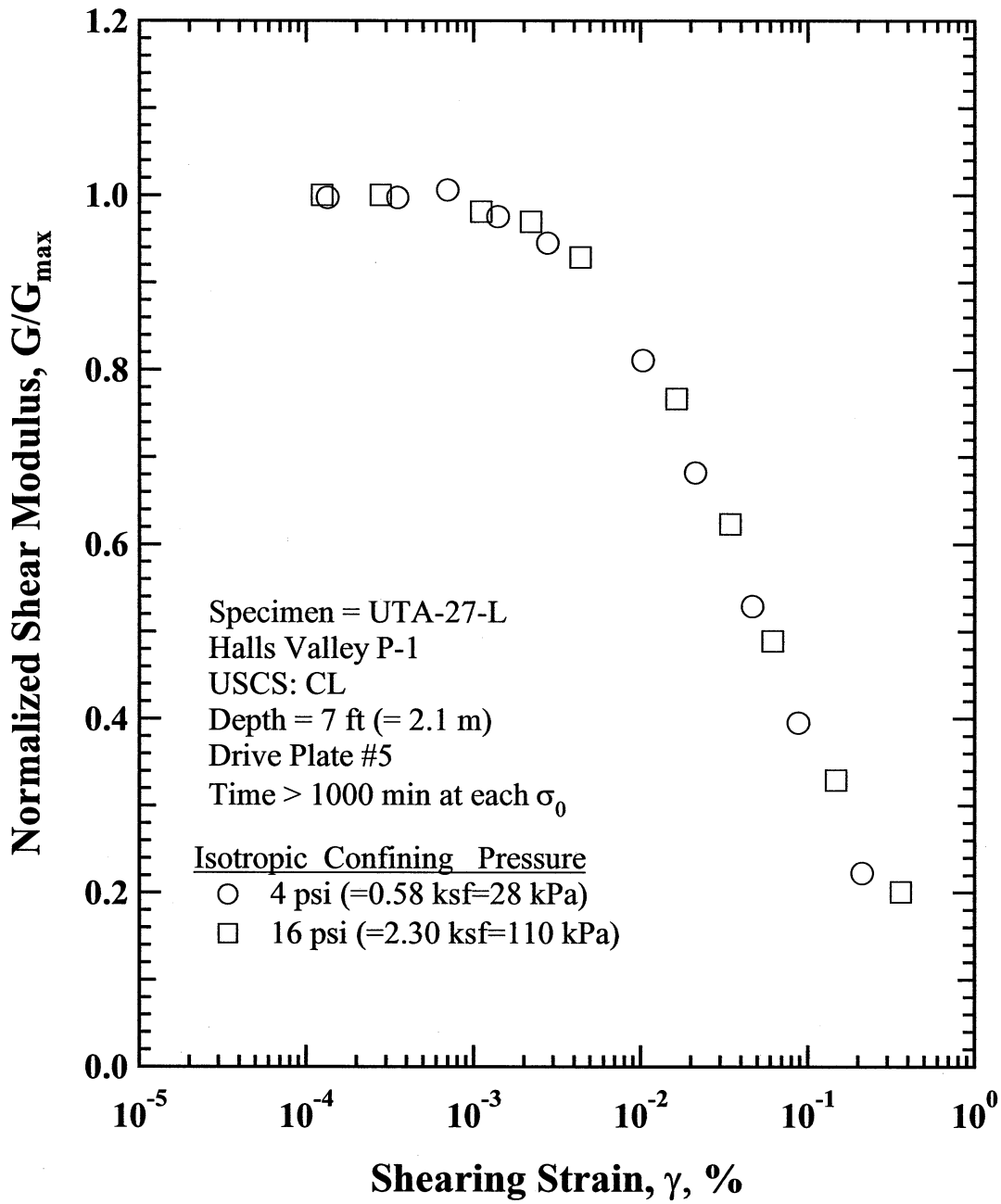

Figure W.9 Comparison of the Variation in Normalized Shear Modulus with Shearing Strain and Isotropic Confining Pressure from the Resonant Column Tests of Specimen UTA-27-L.

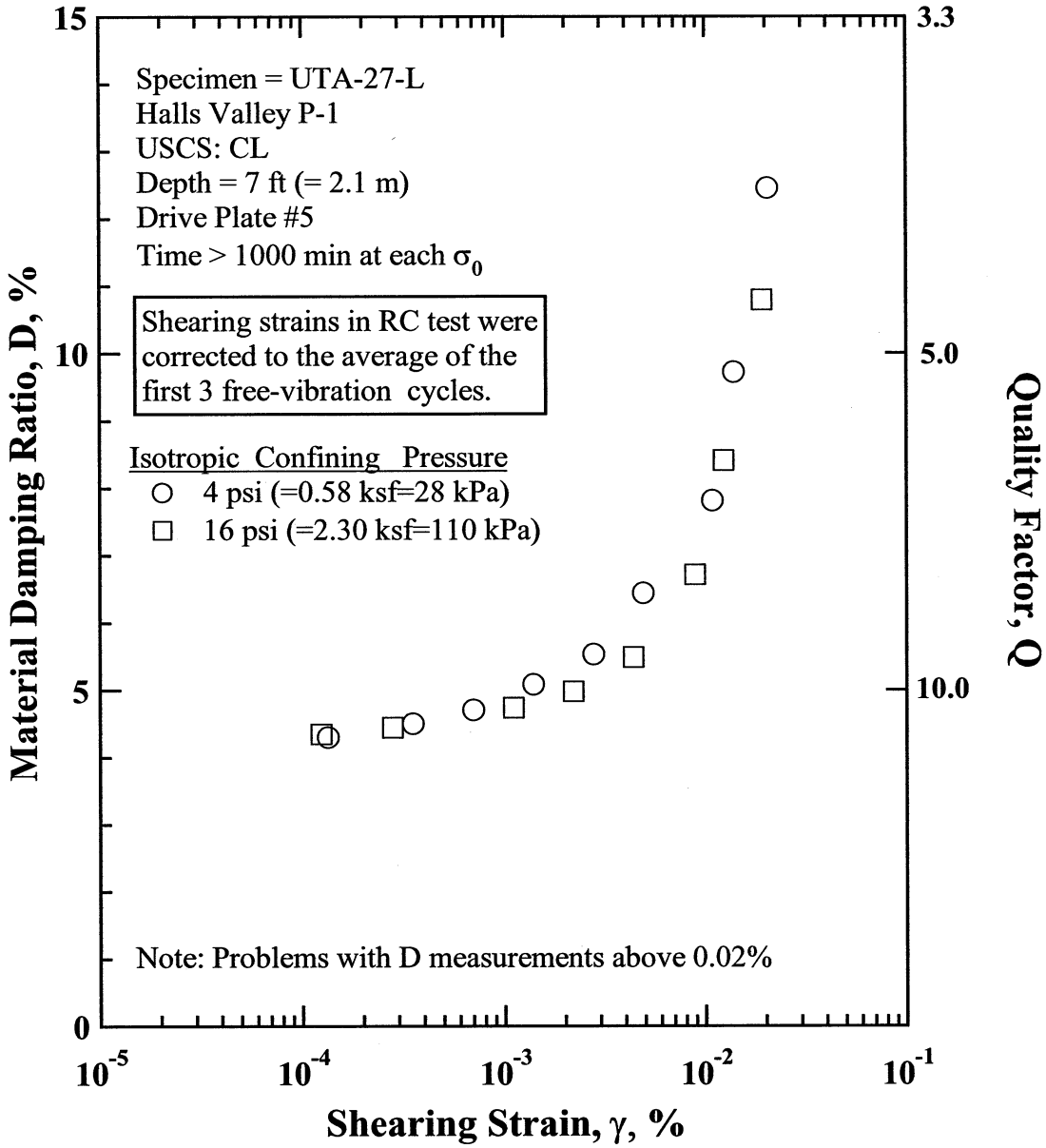

Figure W.10 Comparison of the Variation in Material Damping Ratio with Shearing Strain and Isotropic Confining Pressure from the Resonant Column Tests of Specimen UTA-27-L.

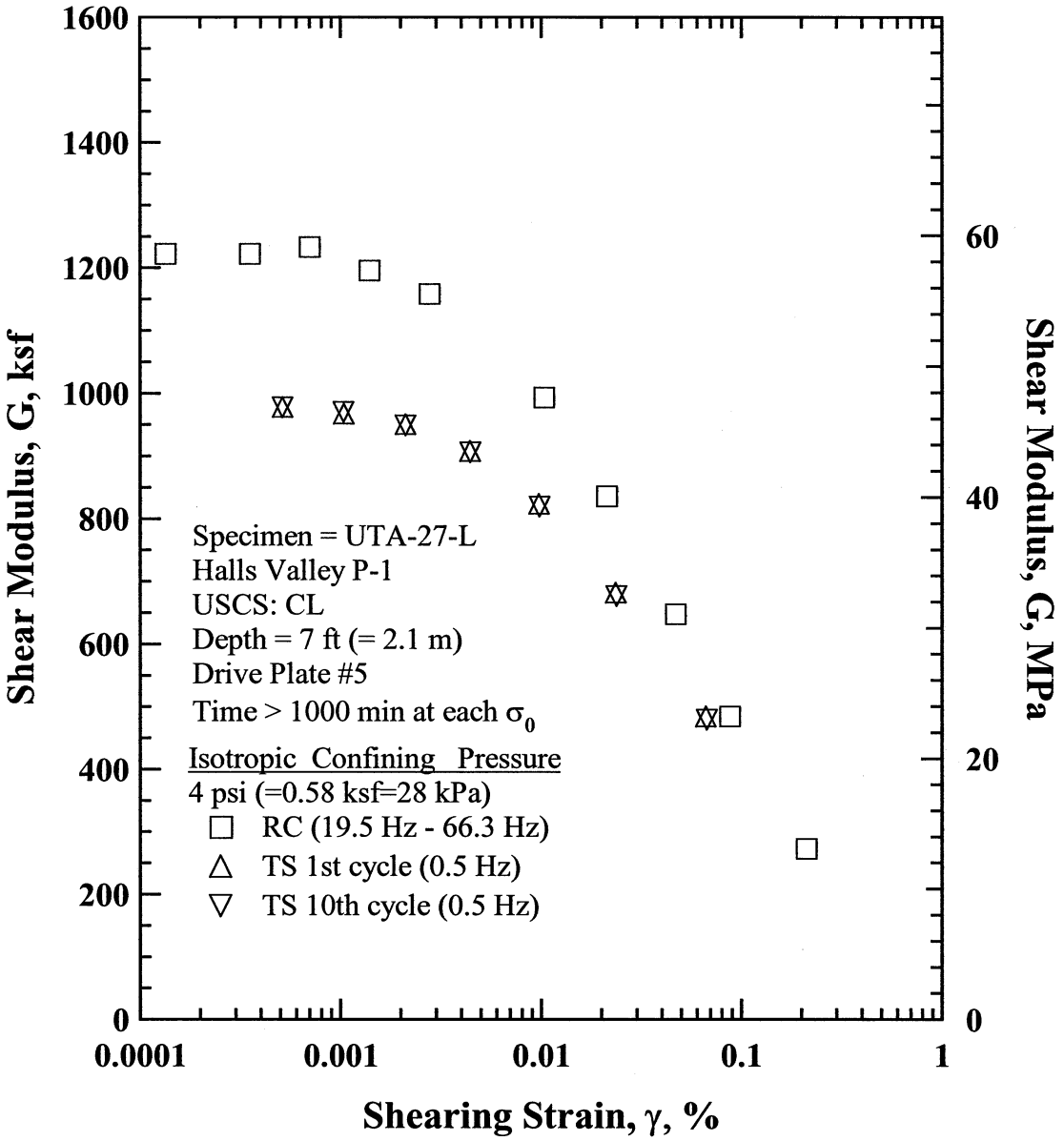

Figure W.11 Comparison of the Variation in Shear Modulus with Shearing Strain at an Isotropic Confining Pressure of 4 psi (=0.58 ksf=28 kPa) from the Combined RCTS Tests of Specimen UTA-27-L.

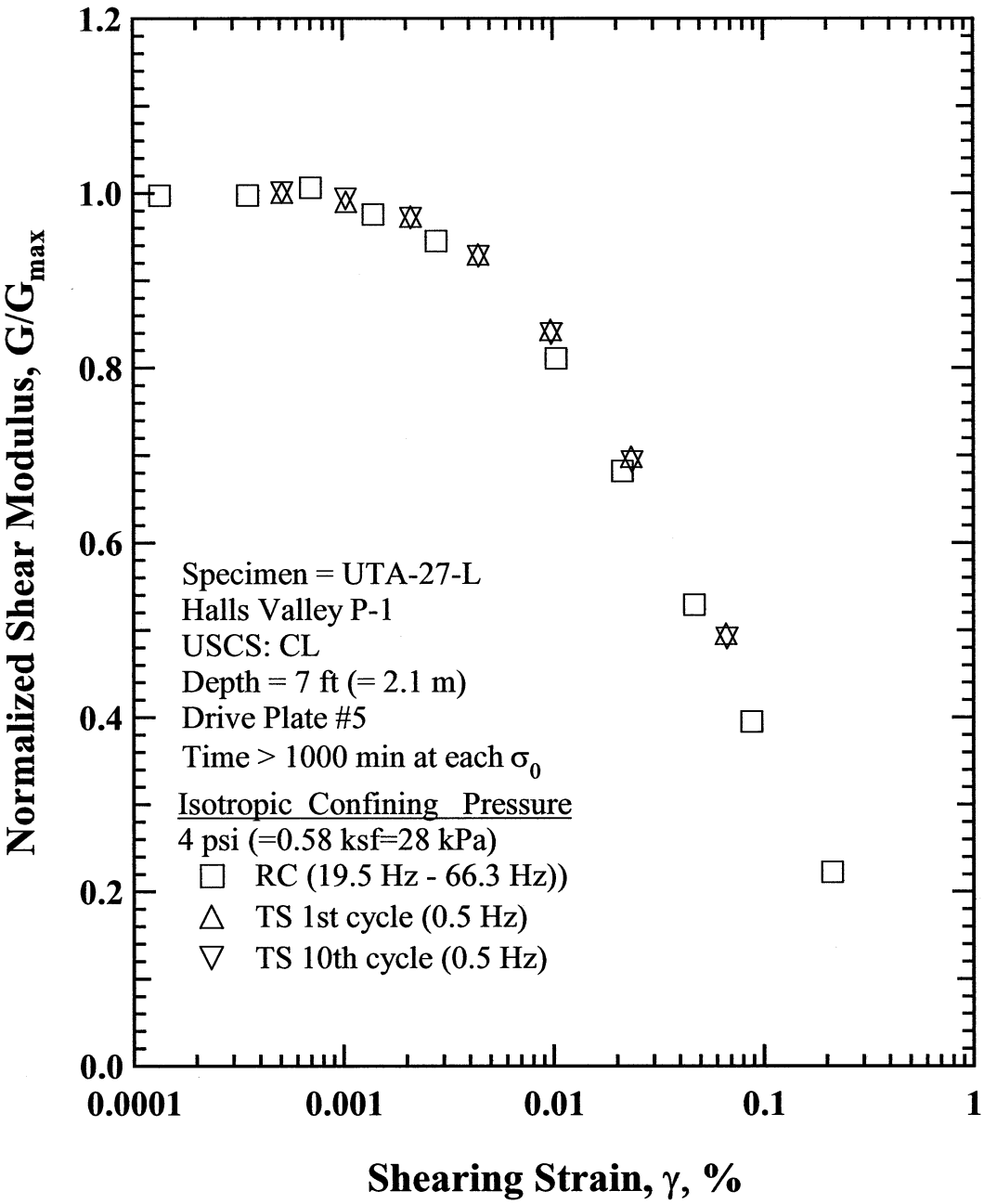

Figure W.12 Comparison of the Variation in Normalized Shear Modulus with Shearing Strain at an Isotropic Confining Pressure of 4 psi (=0.58 ksf=28 kPa) from the Combined RCTS Tests of Specimen UTA-27-L.

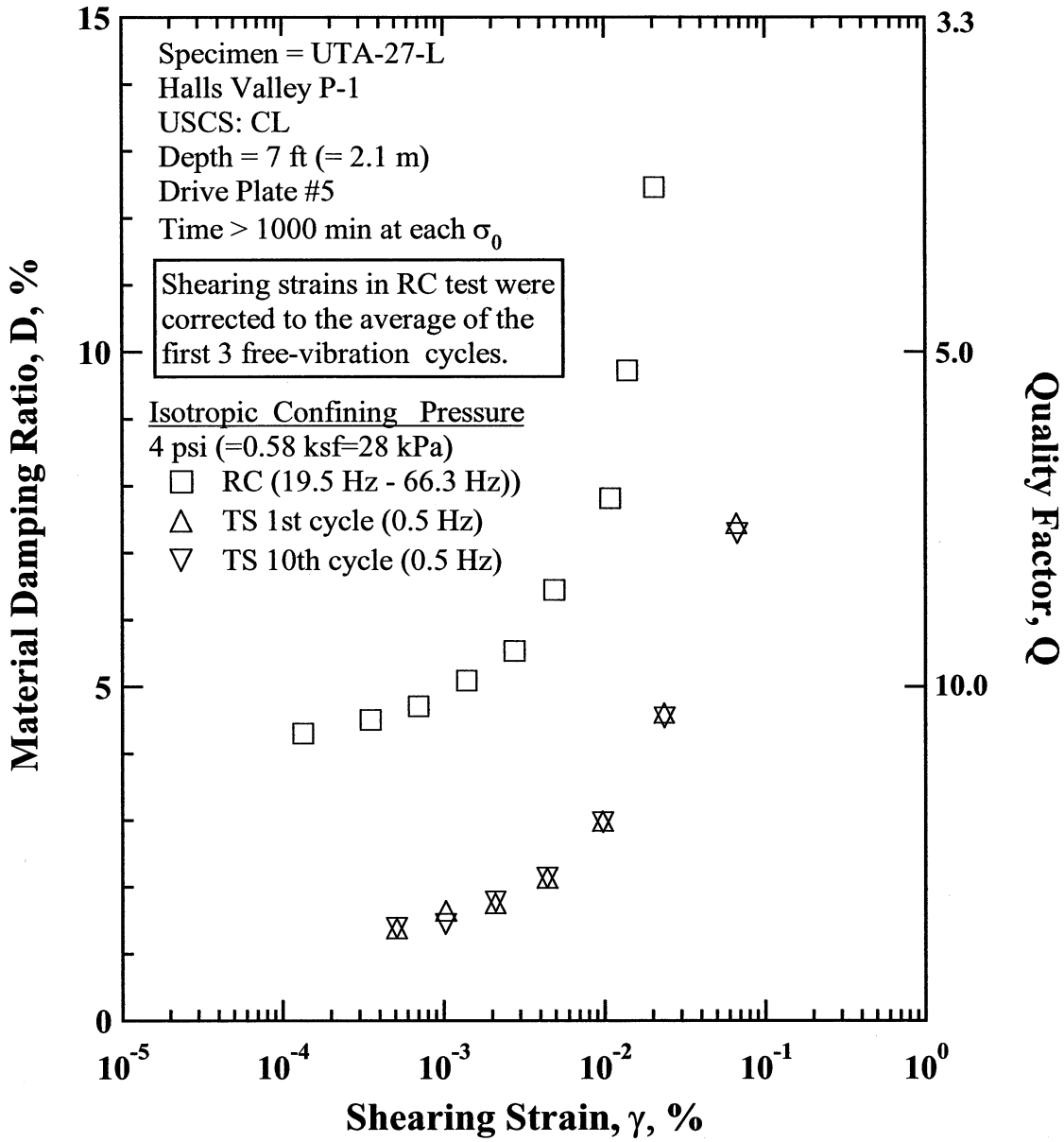

Figure W.13 Comparison of the Variation in Material Damping Ratio with Shearing Strain at an Isotropic Confining Pressure of 4 psi (=0.58 ksf=28 kPa) from the Combined RCTS Tests of Specimen UTA-27-L.

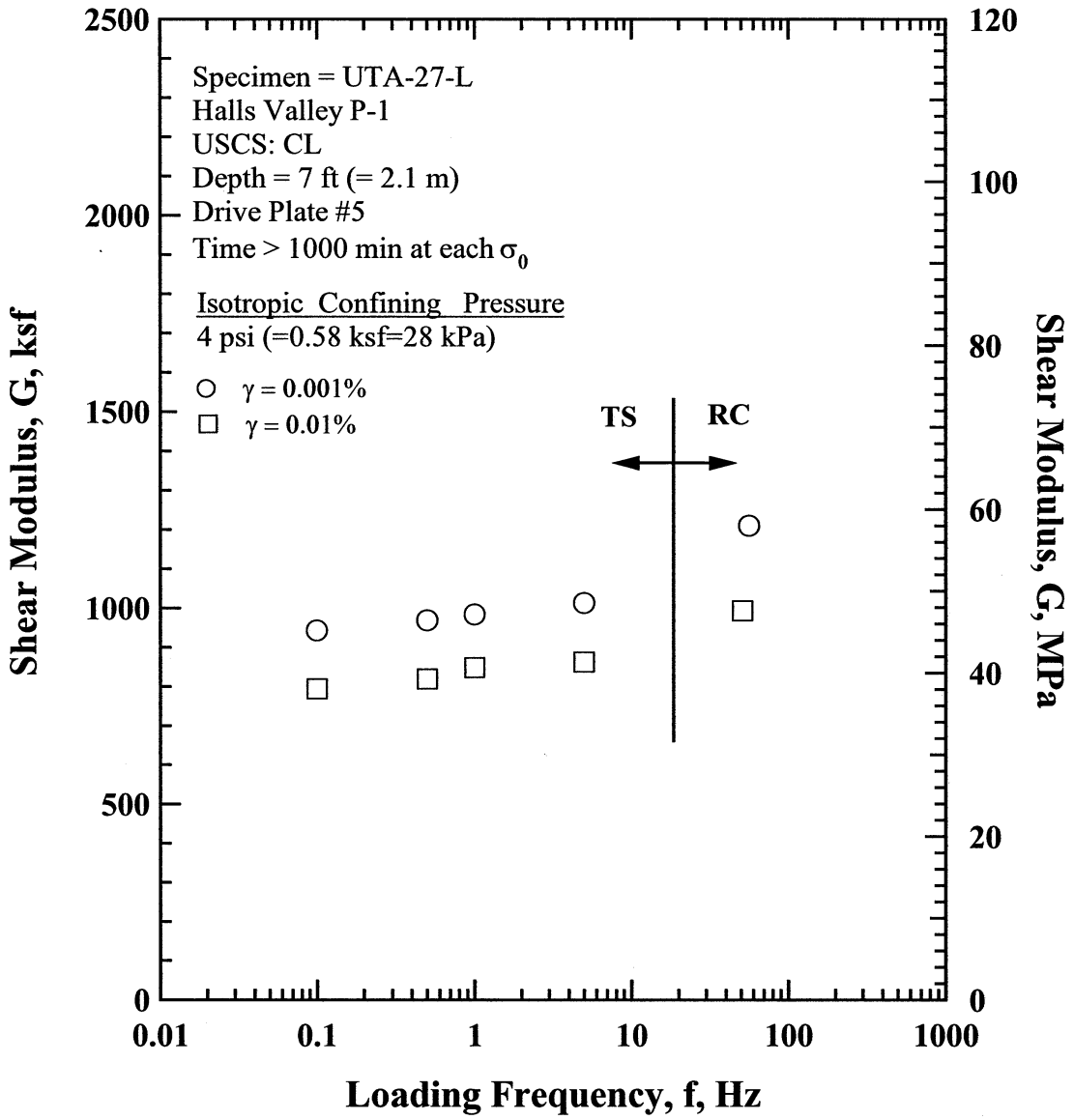

Figure W.14 Comparison of the Variation in Shear Modulus with Loading Frequency at an Isotropic Confining Pressure of 4 psi (=0.58 ksf=28 kPa) from the Combined RCTS Tests of Specimen UTA-27-L.

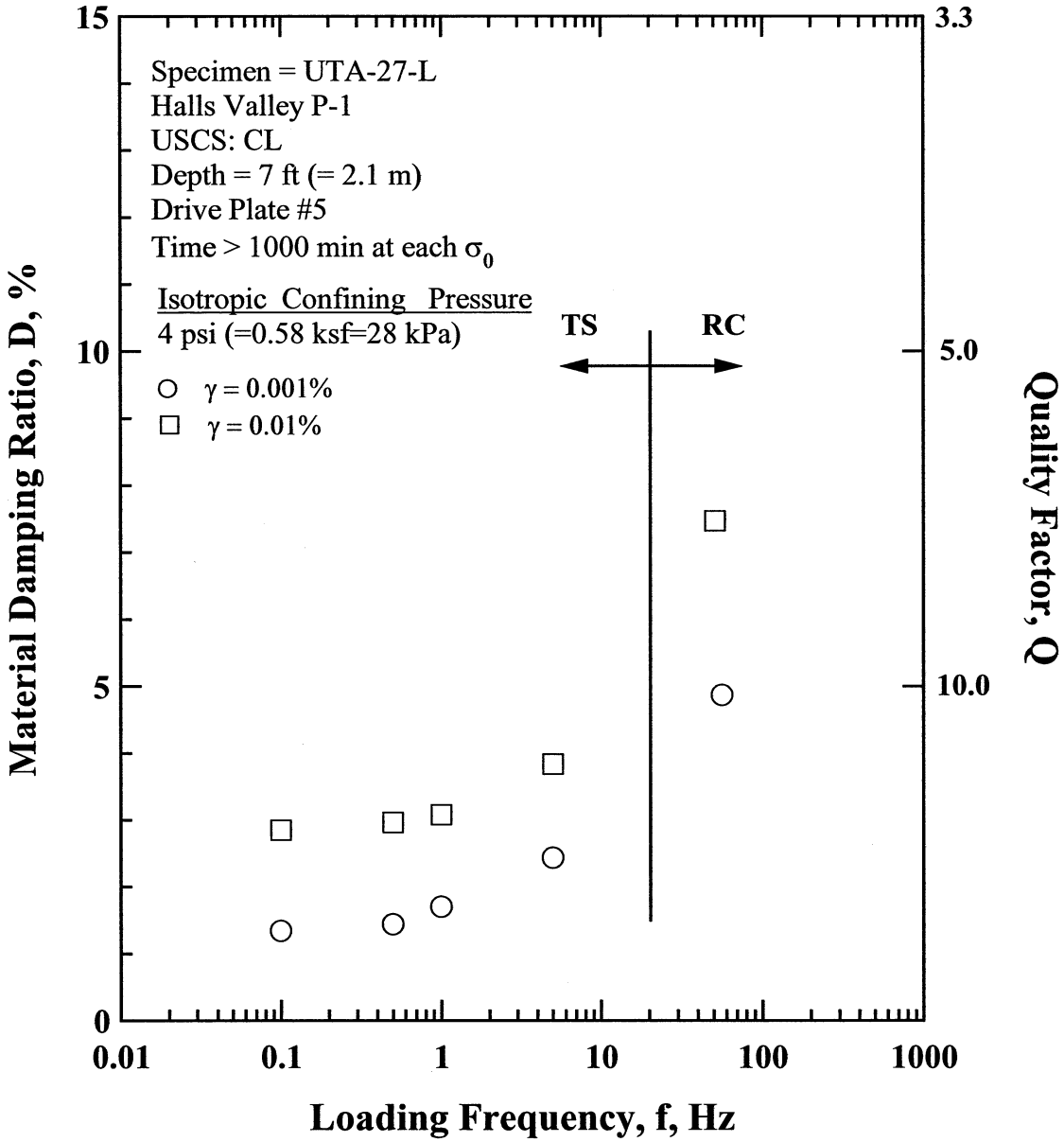

Figure W.15 Comparison of the Variation in Material Damping Ratio with Loading Frequency at an Isotropic Confining Pressure 4 psi (=0.58 ksf=28 kPa) from the Combined RCTS Tests of Specimen UTA-27-L.

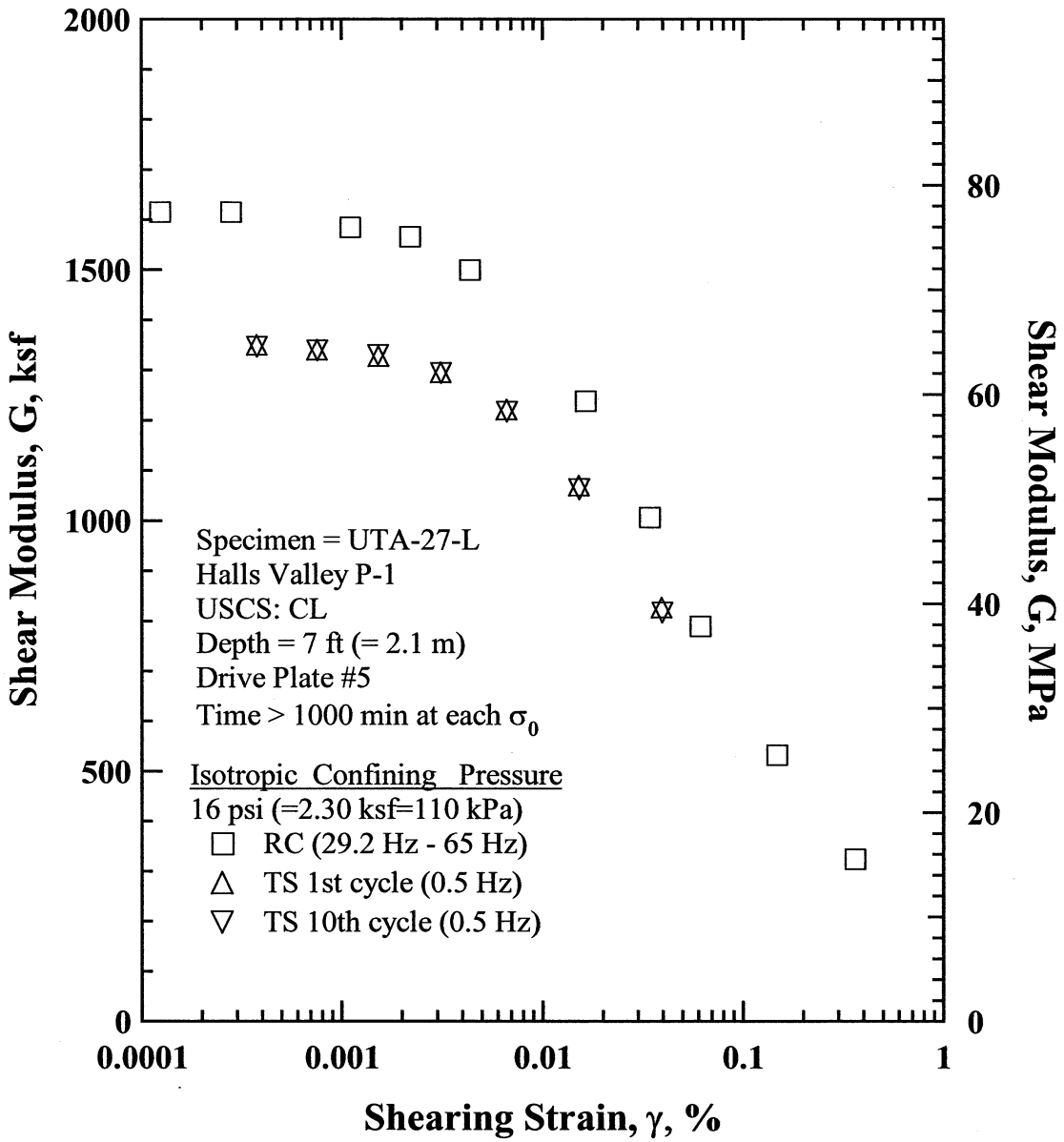

Figure W.16 Comparison of the Variation in Shear Modulus with Shearing Strain at an Isotropic Confining Pressure of 16 psi (=2.30 ksf=110 kPa) from the Combined RCTS Tests of Specimen UTA-27-L.

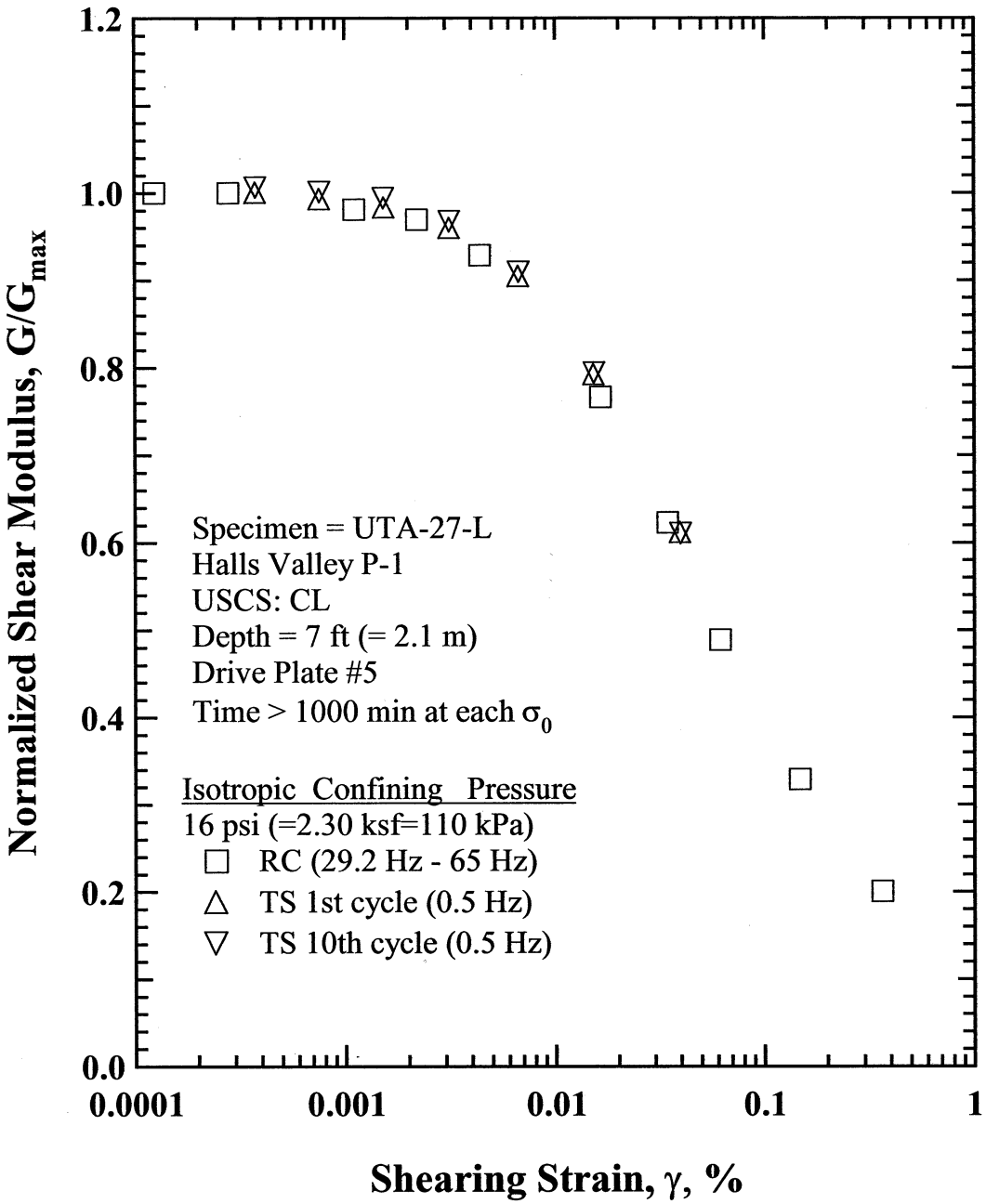

Figure W.17 Comparison of the Variation in Normalized Shear Modulus with Shearing Strain at an Isotropic Confining Pressure of 16 psi (=2.30 ksf=110 kPa) from the Combined RCTS Tests of Specimen UTA-27-L.

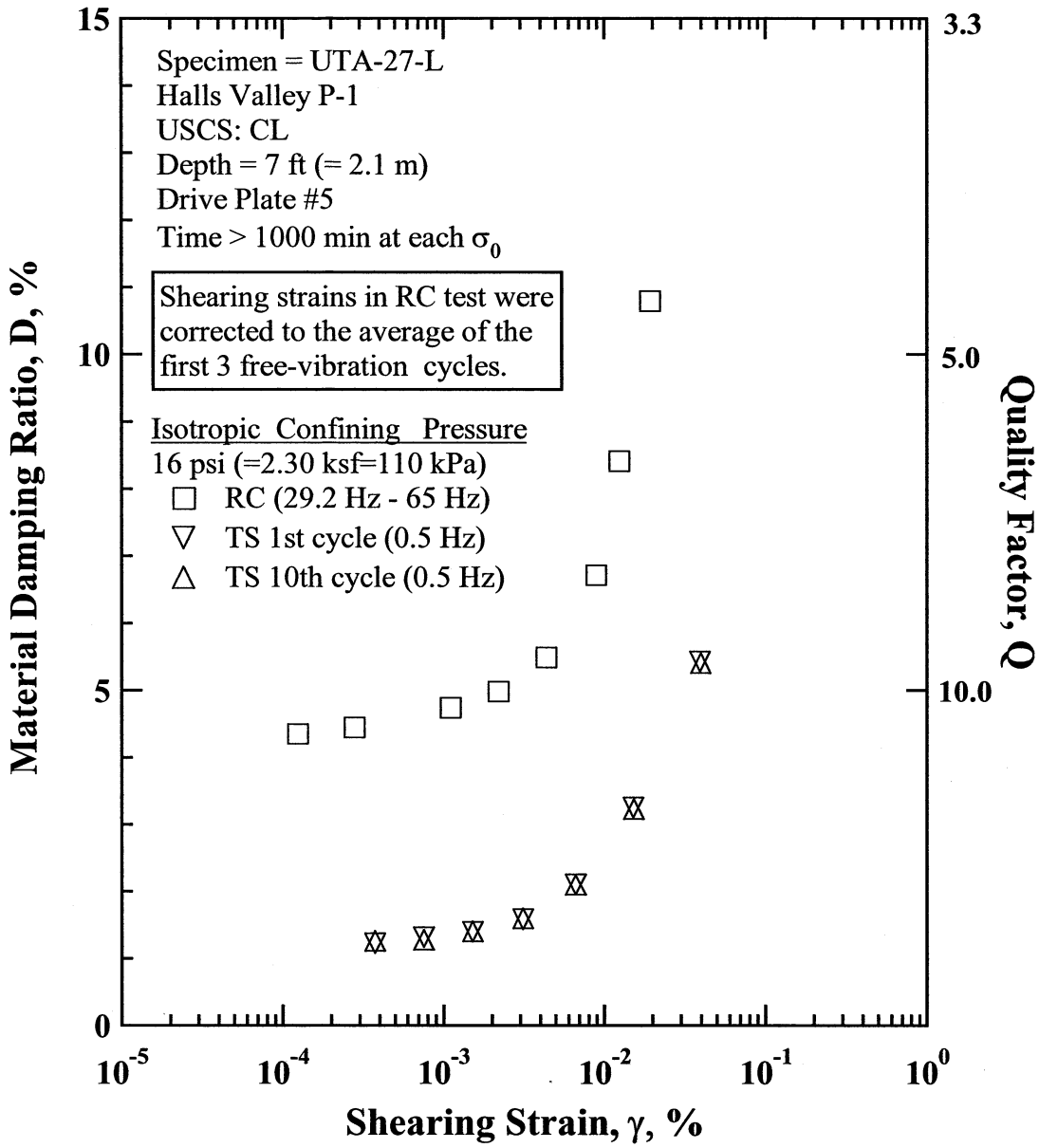

Figure W.18 Comparison of the Variation in Material Damping Ratio with Shearing Strain at an Isotropic Confining Pressure of 16 psi (=2.30 ksf=110 kPa) from the Combined RCTS Tests of Specimen UTA-27-L.

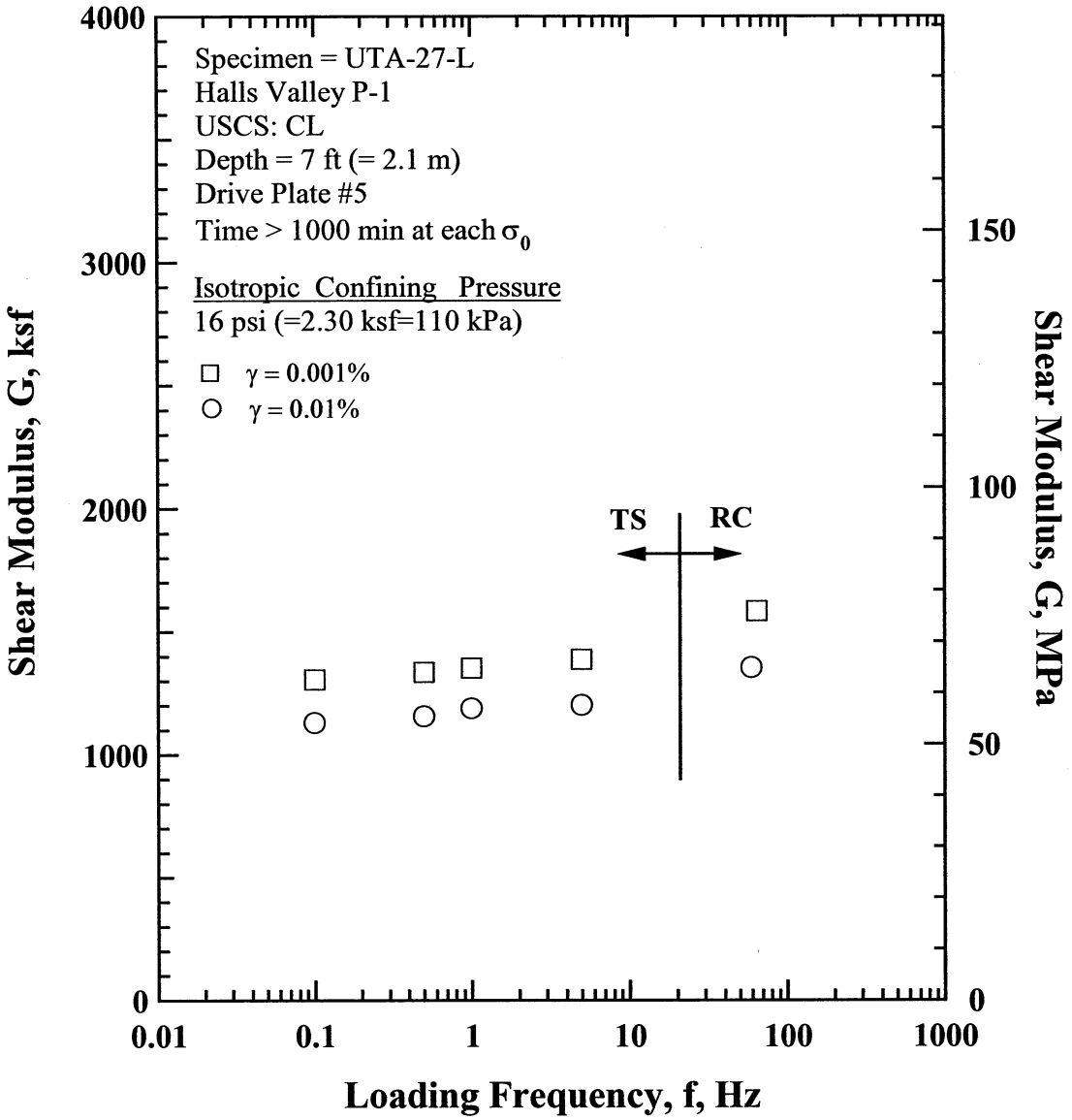

Figure W.19 Comparison of the Variation in Shear Modulus with Loading Frequency at an Isotropic Confining Pressure of 16 psi (=2.30 ksf=110 kPa) from the Combined RCTS Tests of Specimen UTA-27-L.

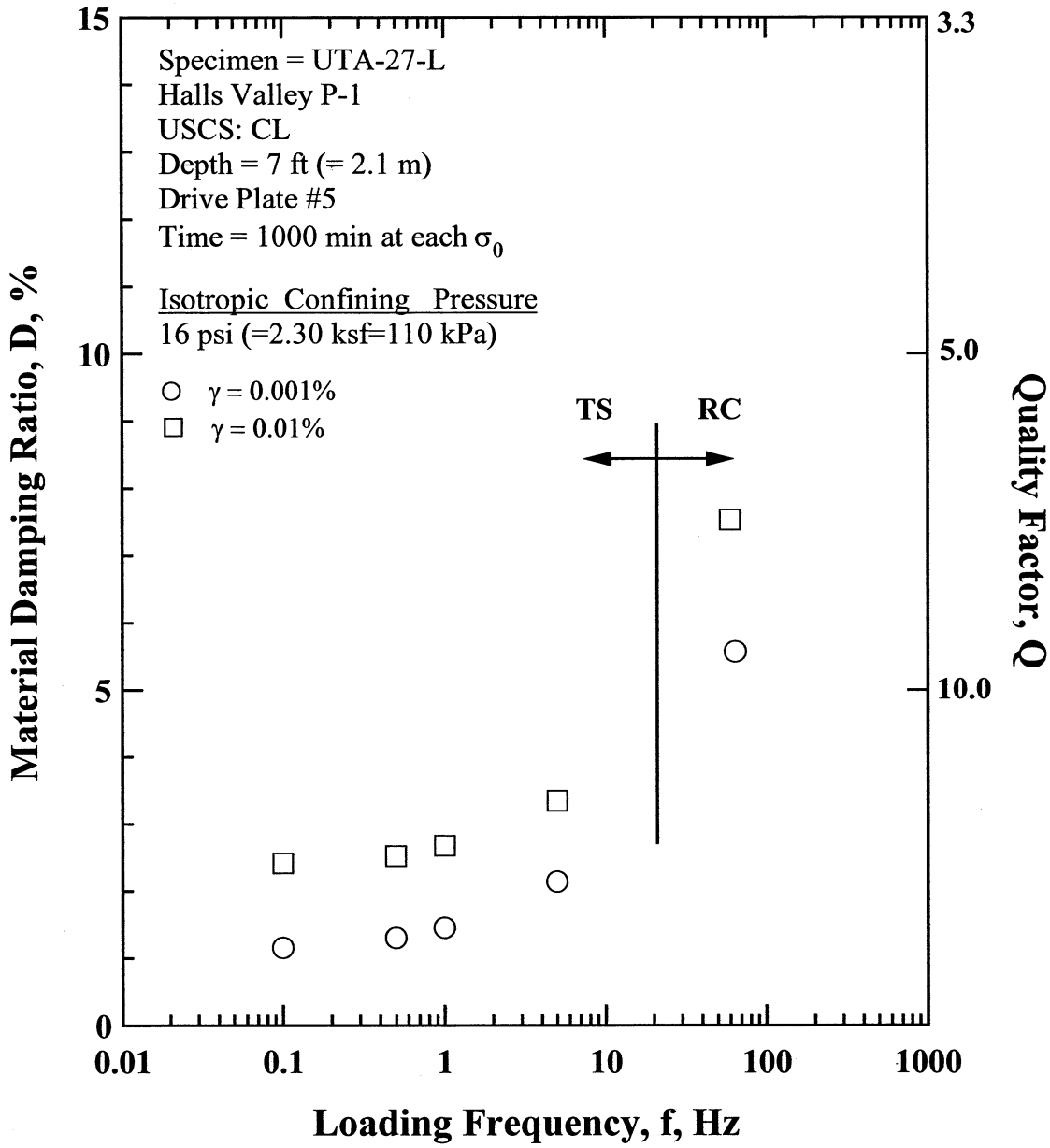

Figure W.20 Comparison of the Variation in Material Damping Ratio with Loading Frequency at an Isotropic Confining Pressure 16 psi (=2.30 ksf=110 kPa) from the Combined RCTS Tests of Specimen UTA-27-L.

Table W.1 Variation in Low-Amplitude Shear Wave Velocity, Low-Amplitude Shear Modulus, Low-Amplitude Material Damping Ratio and Estimated Void Ratio with Isotropic Confining Pressure from RC Tests of Specimen UTA-27-L.

Effective Isotropic Confining Pressure, σ_o'			Low-Amplitude Shear Modulus, G_{max}		Low-Amplitude Shear Wave Velocity, Vs	Low-Amplitude Material Damping Ratio, Dmin	Estimated Void Ratio, e
(psi)	(psf)	(kPa)	(ksf)	(MPa)	(fps)	(%)	
1	144	7	995	47.7	511	5.14	0.686
2	288	14	1092	52.3	535	5.11	0.686
4	576	28	1161	55.6	551	5.05	0.685
8	1152	55	1275	61.1	577	5.27	0.682
16	2304	110	1553	74.4	637	4.83	0.681

Table W.2 Variation in Shear Modulus, Normalized Shear Modulus and Material Damping Ratio with Shearing Strain from RC Tests of Specimen UTA-27-L; Confining Pressure, σ_o' =4 psi (=0.58 ksf=28 kPa).

Peak Shearing Strain, %	Shear Modulus, G, ksf	Normalized Shear Modulus, G/G_{max}	Average[+] Shearing Strain, %	Material Damping Ratio[x], D, %
1.34E-04	1222	1.00	1.34E-04	4.30
3.53E-04	1222	1.00	3.53E-04	4.51
7.00E-04	1233	1.01	7.00E-04	4.71
1.40E-03	1195	0.98	1.40E-03	5.09
2.78E-03	1158	0.94	2.78E-03	5.53
1.03E-02	993	0.81	4.90E-03	6.44
2.13E-02	836	0.68	1.09E-02	7.82
4.68E-02	648	0.53	1.39E-02	9.72
8.78E-02	484	0.39	2.05E-02	12.46
2.12E-01	273	0.22		

[+] Average Shearing Strain from the First Three Cycles of the Free Vibration Decay Curve

[x] Average Damping Ratio from the First Three Cycles of the Free Vibration Decay Curve

Table W.3 Variation in Shear Modulus, Normalized Shear Modulus and Material Damping Ratio with Shearing Strain from TS Tests of Specimen UTA-27-L; Confining Pressure, σ_o' =4 psi (=0.58 ksf=28 kPa).

First Cycle				Tenth Cycle			
Peak Shearing Strain, %	Shear Modulus, G, ksf	Normalized Shear Modulus, G/G_{max}	Material Damping Ratio, D, %	Peak Shearing Strain, %	Shear Modulus, G, ksf	Normalized Shear Modulus, G/G_{max}	Material Damping Ratio, D, %
5.15E-04	977	1.00	1.38	5.16E-04	977	1.00	1.38
1.04E-03	967	0.99	1.64	1.04E-03	970	0.99	1.44
2.12E-03	950	0.97	1.75	2.13E-03	948	0.97	1.78
4.44E-03	908	0.93	2.13	4.45E-03	905	0.93	2.13
9.80E-03	823	0.84	2.98	9.85E-03	819	0.84	2.97
2.37E-02	681	0.70	4.60	2.38E-02	676	0.69	4.53
6.67E-02	484	0.50	7.43	6.74E-02	479	0.49	7.29

Table W.4 Variation in Shear Modulus, Normalized Shear Modulus and Material Damping Ratio with Shearing Strain from RC Tests of Specimen UTA-27-L; Confining Pressure, σ_o' =16 psi (=2.30 ksf=110.45 kPa).

Peak Shearing Strain, %	Shear Modulus, G, ksf	Normalized Shear Modulus, G/G_{max}	Average[+] Shearing Strain, %	Material Damping Ratio[x], D, %
1.24E-04	1615	1.00	1.24E-04	4.35
2.79E-04	1615	1.00	2.79E-04	4.44
1.11E-03	1584	0.98	1.11E-03	4.74
2.20E-03	1566	0.97	2.20E-03	4.98
4.37E-03	1499	0.93	4.37E-03	5.49
1.64E-02	1238	0.77	8.91E-03	6.72
3.44E-02	1006	0.62	1.24E-02	8.41
6.14E-02	789	0.49	1.92E-02	10.79
1.47E-01	532	0.33		
3.63E-01	324	0.20		

[+] Average Shearing Strain from the First Three Cycles of the Free Vibration Decay Curve

[x] Average Damping Ratio from the First Three Cycles of the Free Vibration Decay Curve

Table W.5 Variation in Shear Modulus, Normalized Shear Modulus and Material Damping Ratio with Shearing Strain from TS Tests of Specimen UTA-27-L; Confining Pressure, σ_o' =16 psi (=2.30 ksf=110.45 kPa).

First Cycle				Tenth Cycle			
Peak Shearing Strain, %	Shear Modulus, G, ksf	Normalized Shear Modulus, G/G_{max}	Material Damping Ratio, D, %	Peak Shearing Strain, %	Shear Modulus, G, ksf	Normalized Shear Modulus, G/G_{max}	Material Damping Ratio, D, %
3.77E-04	1350	1.00	1.22	3.78E-04	1346	1.01	1.25
7.60E-04	1340	0.99	1.31	7.61E-04	1338	1.00	1.27
1.54E-03	1327	0.98	1.39	1.53E-03	1329	0.99	1.40
3.15E-03	1295	0.96	1.58	3.15E-03	1293	0.97	1.59
6.68E-03	1220	0.90	2.10	6.70E-03	1216	0.91	2.09
1.52E-02	1069	0.79	3.25	1.53E-02	1062	0.79	3.22
3.95E-02	825	0.61	5.42	4.00E-02	816	0.61	5.40

APPENDIX X

Specimen No. 23
UT Specimen ID: UTA-27-R

Halls Valley P-3
Depth = 52ft (=15.8m)
Soil Type: Clay (CH)

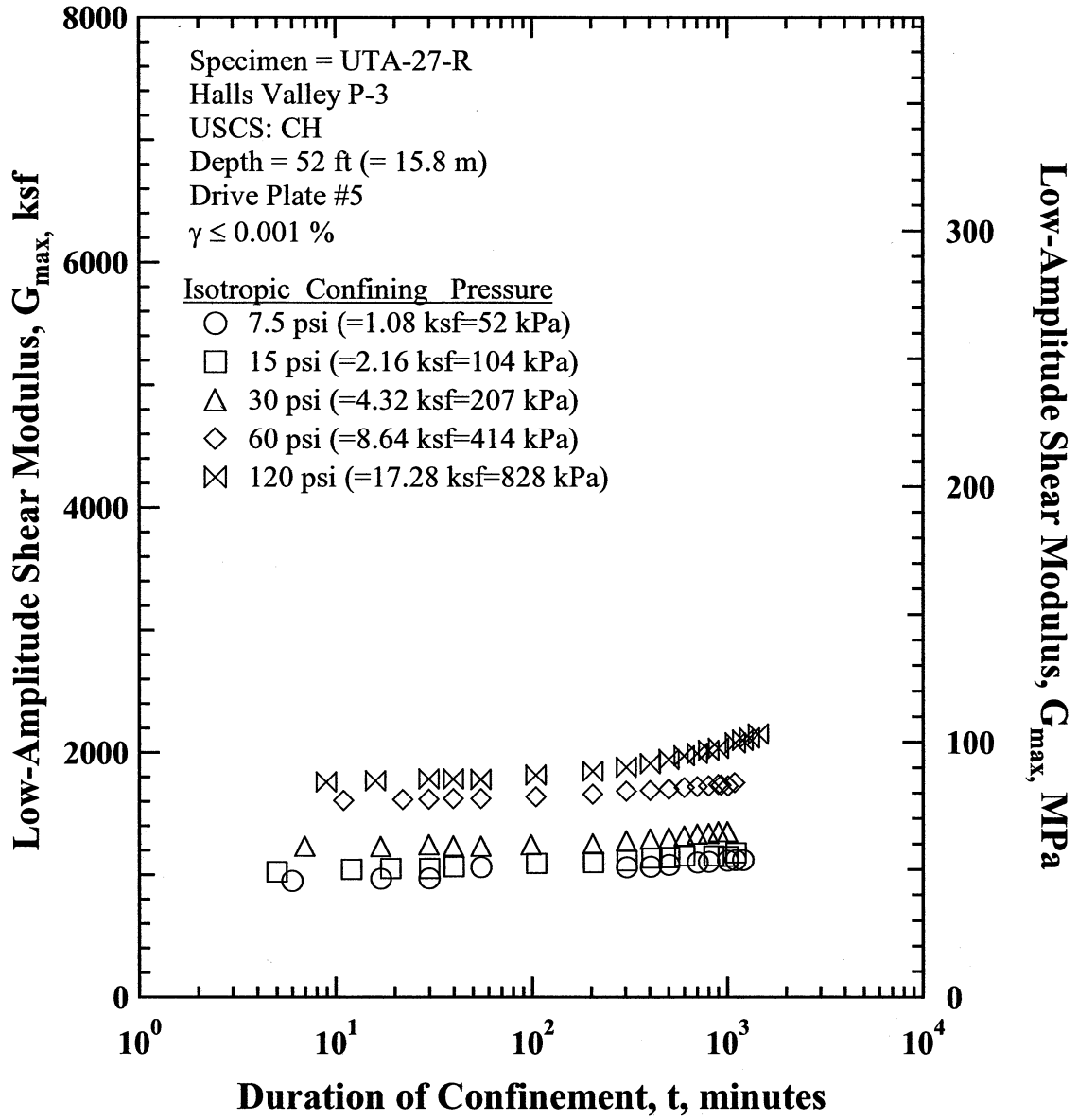

Figure X.1 Variation in Low-Amplitude Shear Modulus with Magnitude and Duration of Isotropic Confining Pressure from Resonant Column Tests of Specimen UTA-27-R.

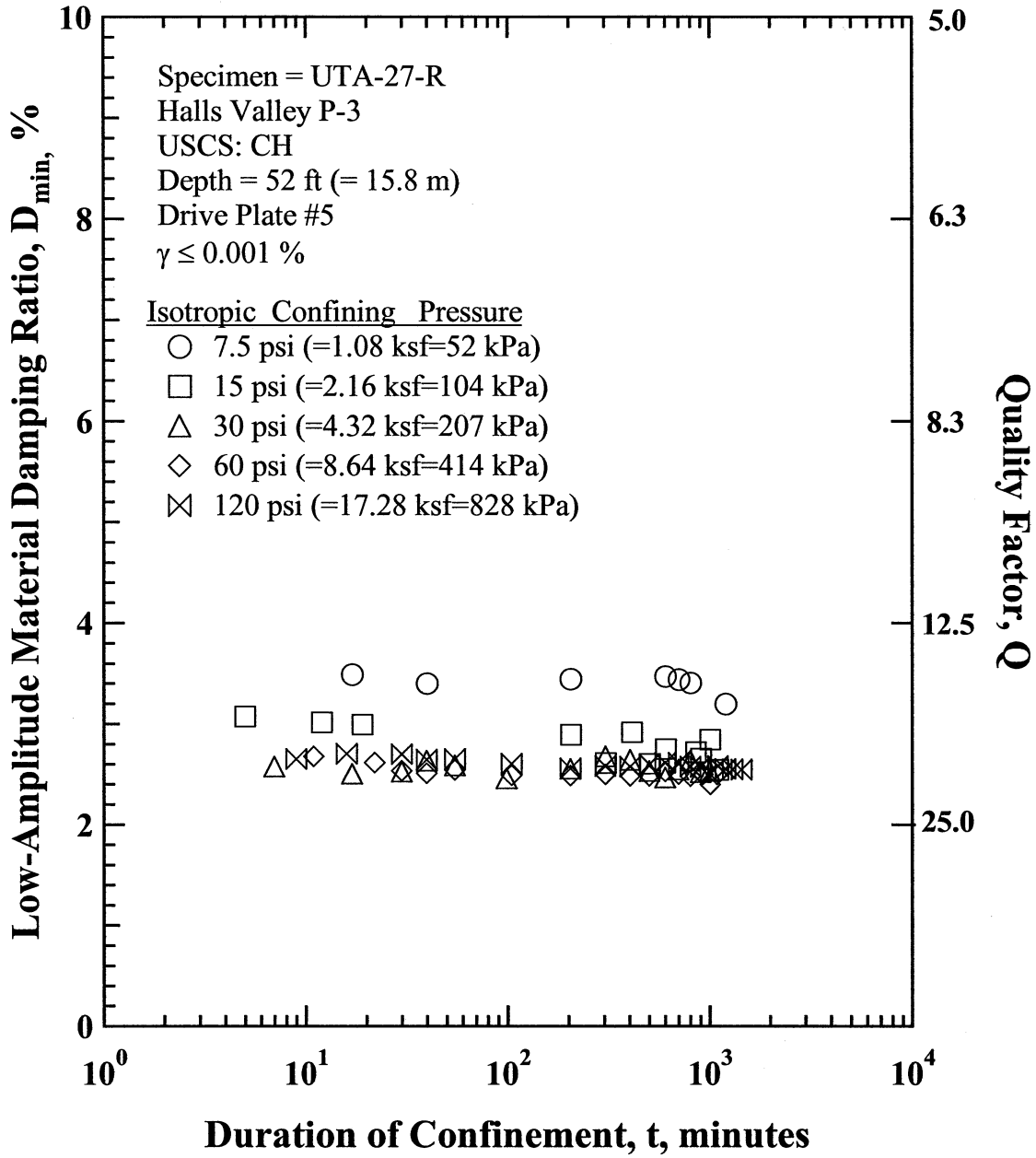

Figure X.2 Variation in Low-Amplitude Material Damping Ratio with Magnitude and Duration of Isotropic Confining Pressure from Resonant Column Tests of Specimen UTA-27-R

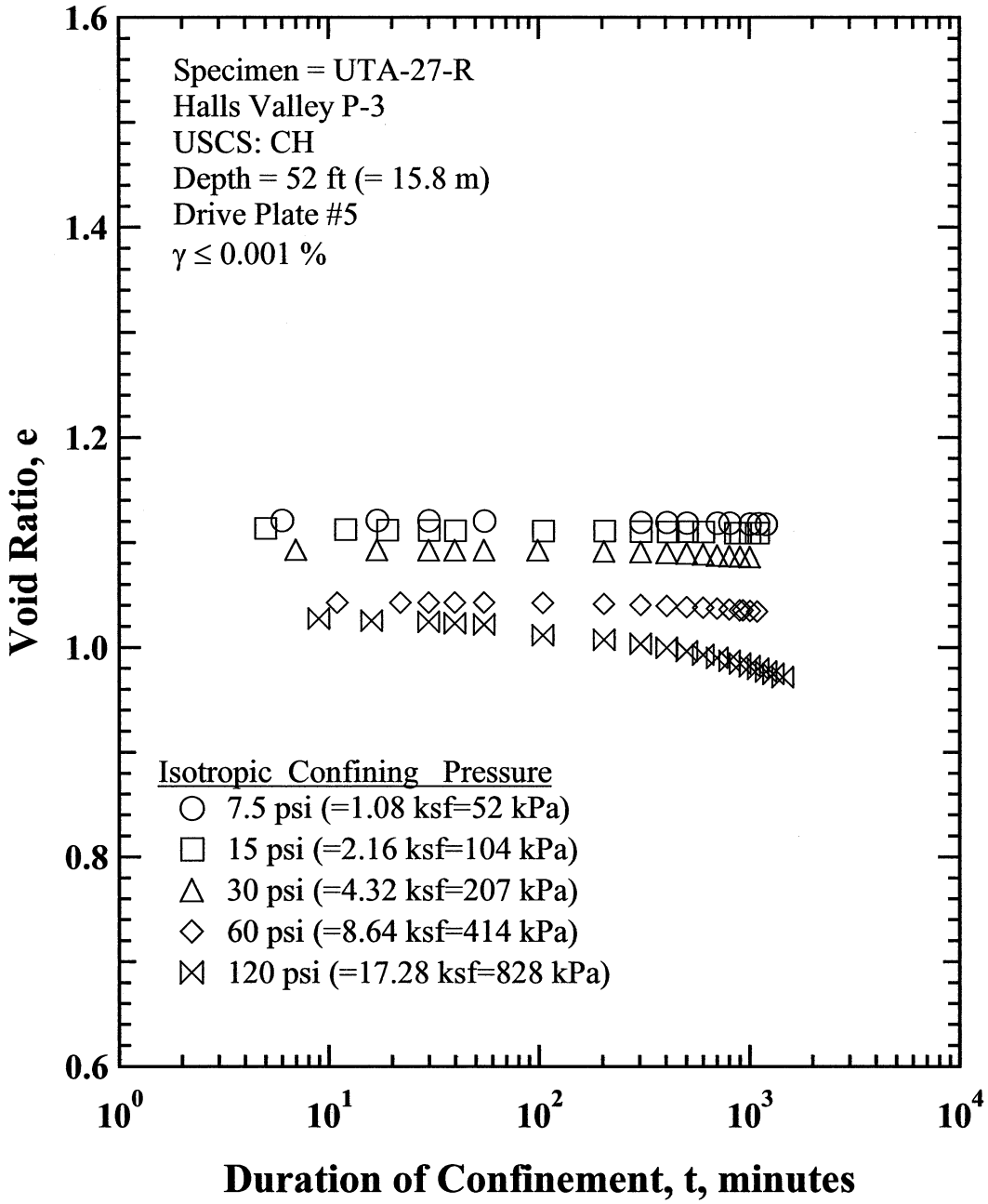

Figure X.3 Variation in Estimated Void Ratio with Magnitude and Duration of Isotropic Confining Pressure from Resonant Column Tests of Specimen UTA-27-R.

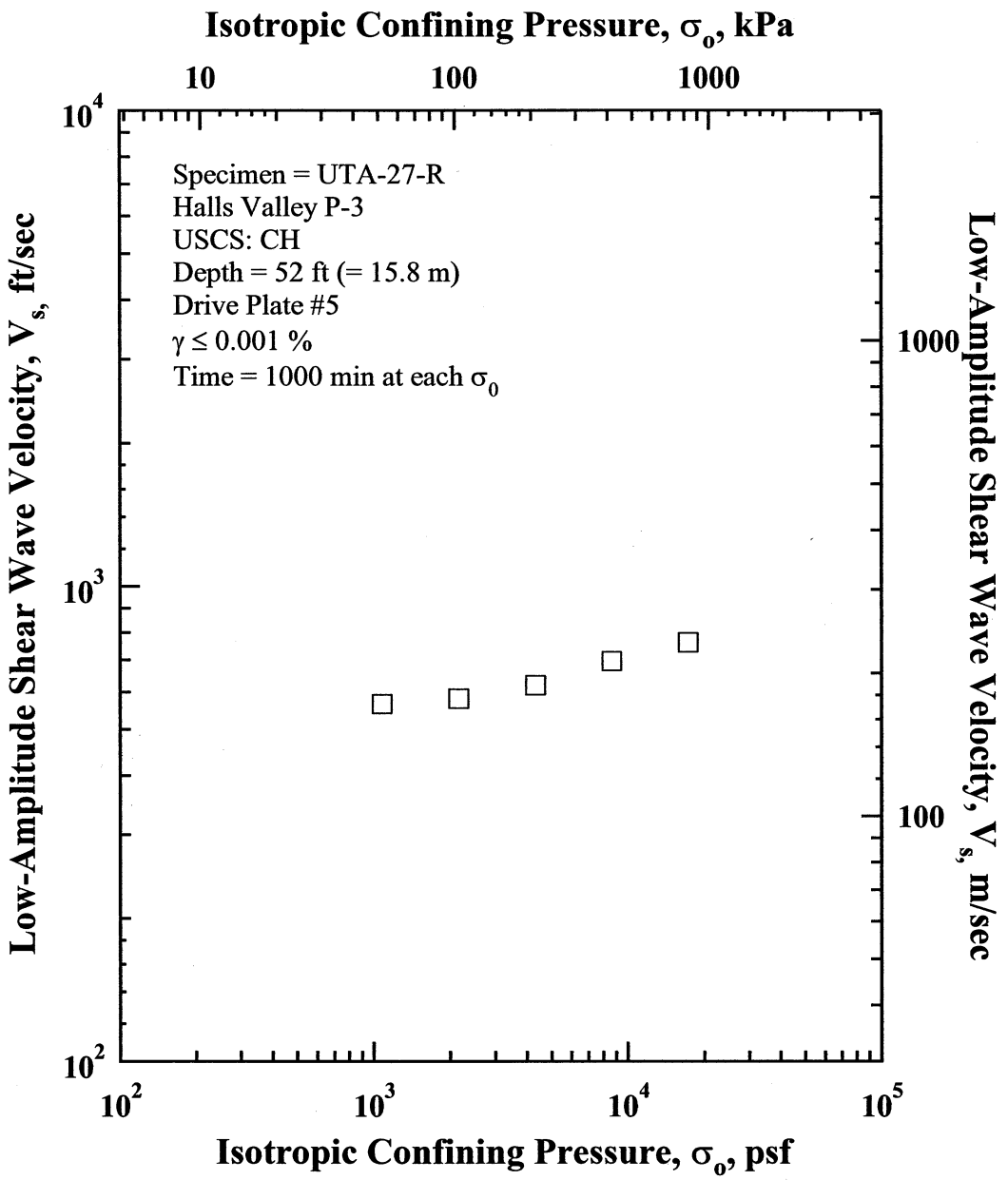

Figure X.4 Variation in Low-Amplitude Shear Wave Velocity with Isotropic Confining Pressure from Resonant Column Tests of Specimen UTA-27-R.

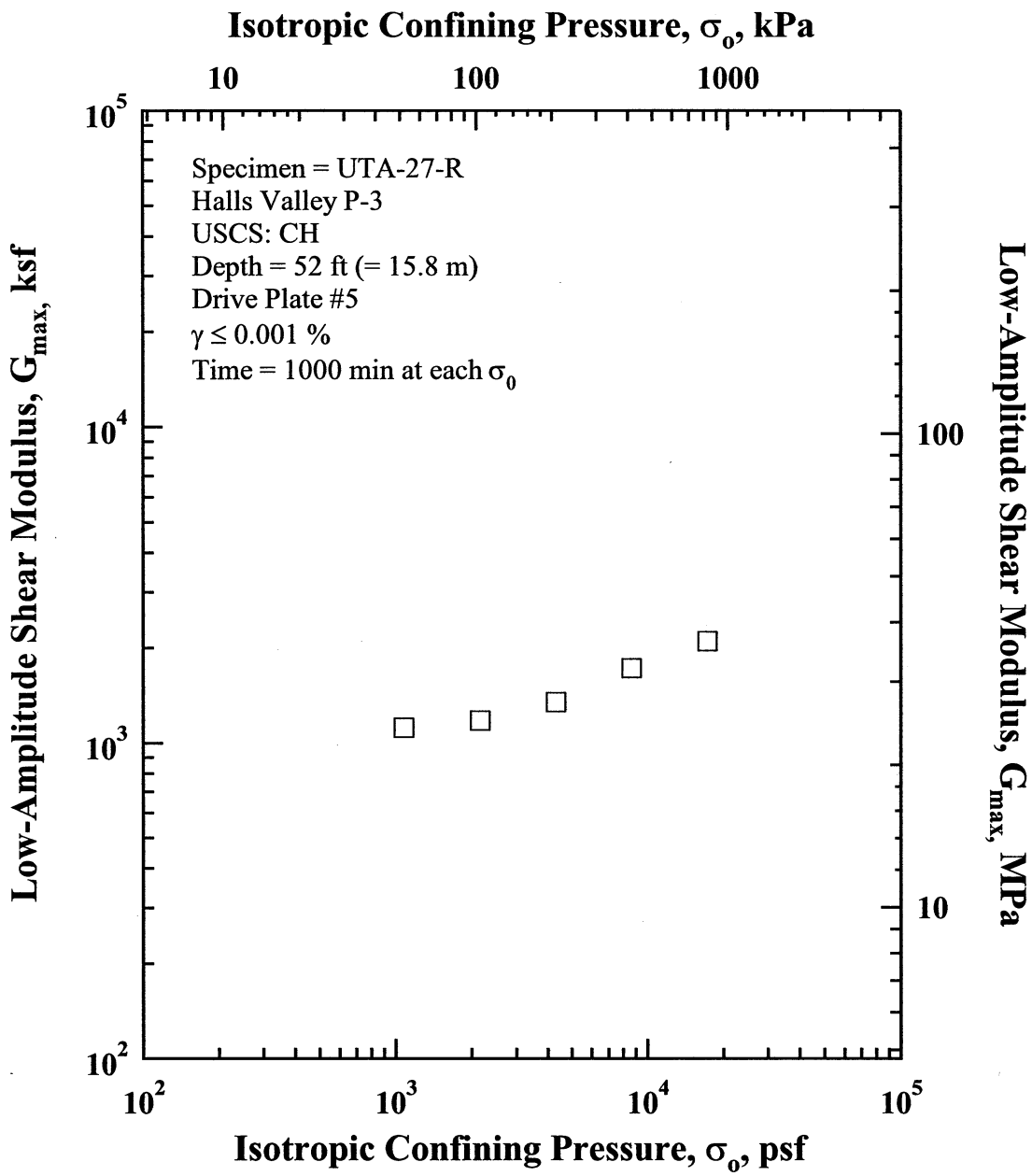

Figure X.5 Variation in Low-Amplitude Shear Modulus with Isotropic Confining Pressure from Resonant Column Tests of Specimen UTA-27-R.

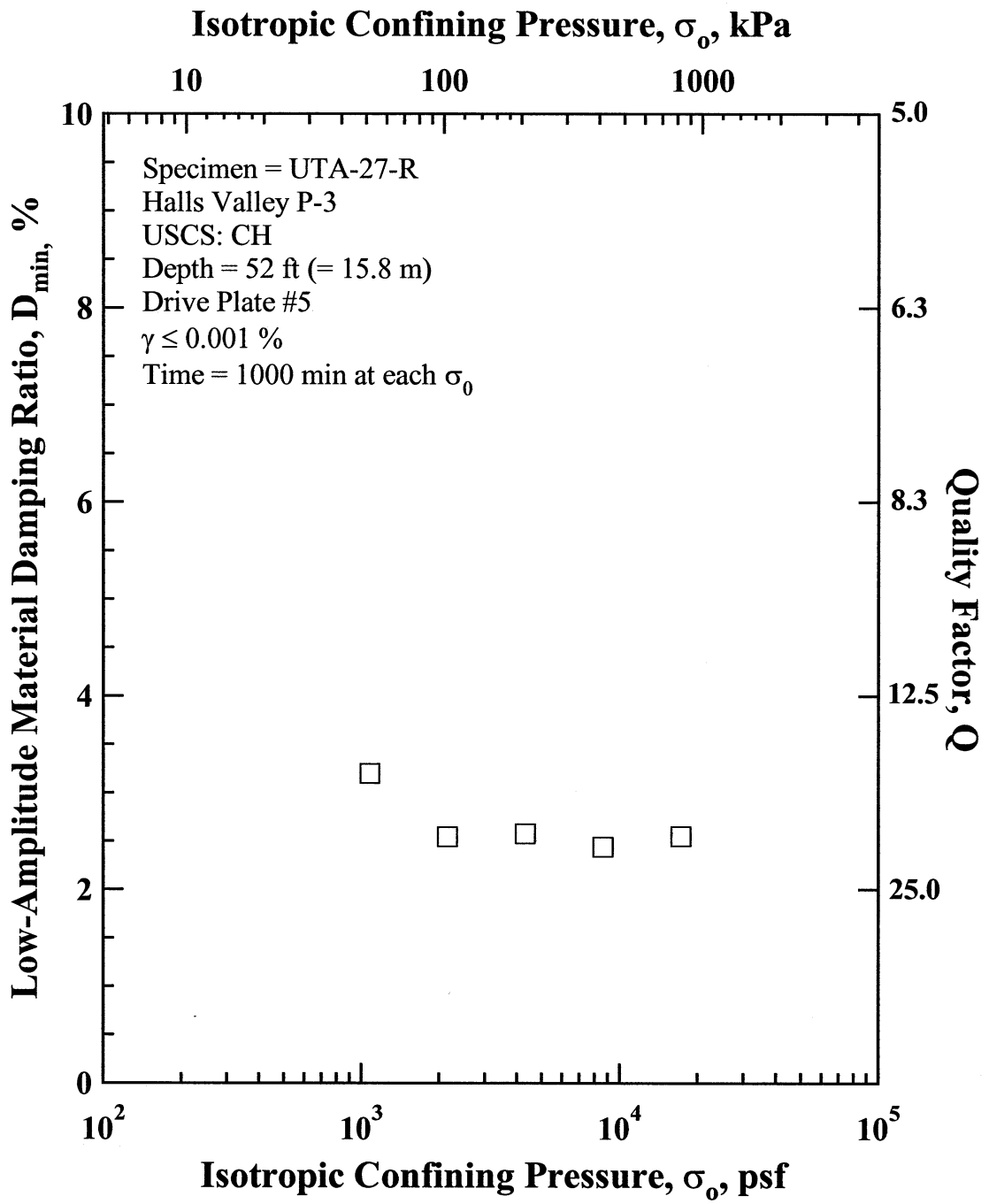

Figure X.6 Variation in Low-Amplitude Material Damping Ratio with Isotropic Confining Pressure from Resonant Column Tests of Specimen UTA-27-R.

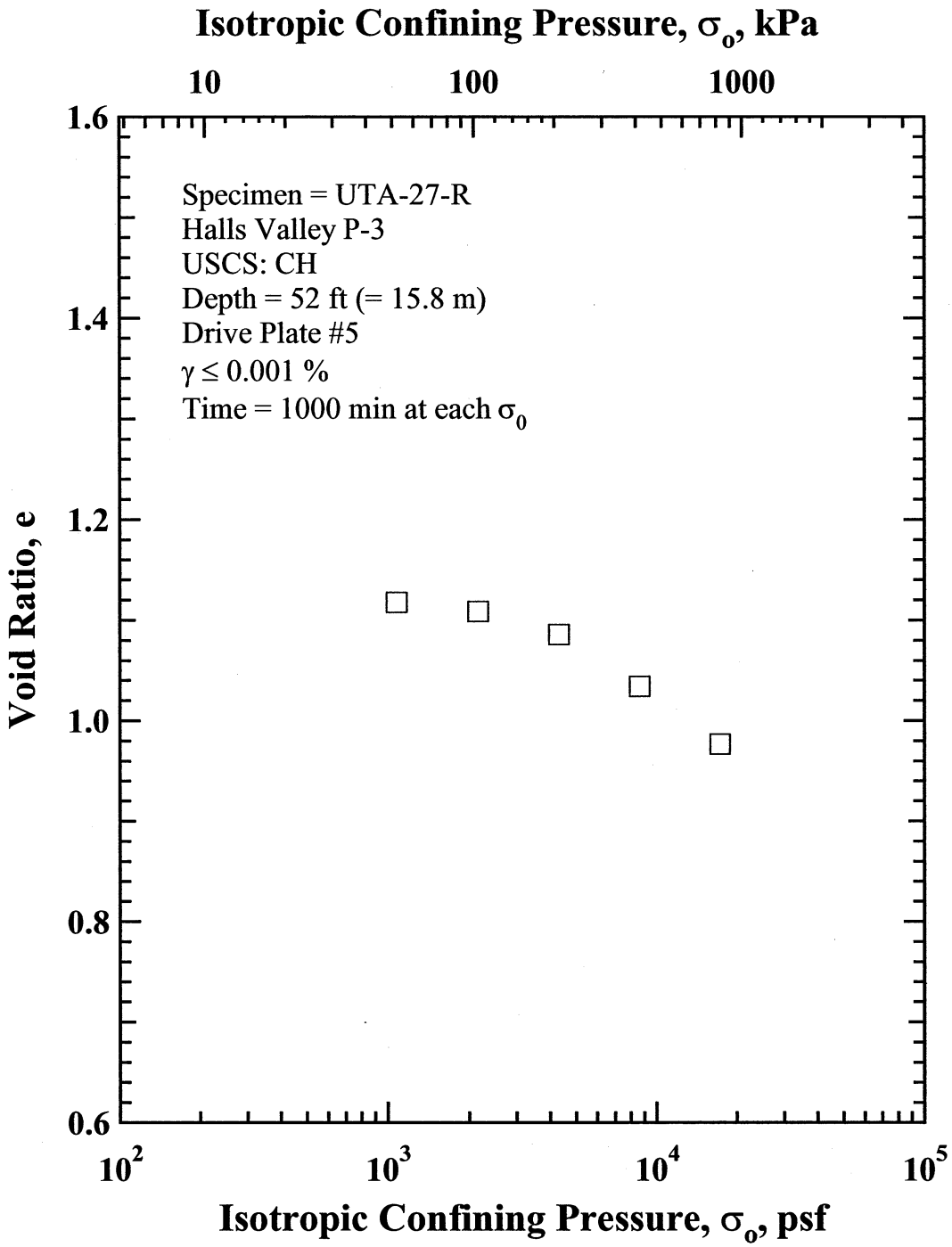

Figure X.7 Variation in Estimated Void Ratio with Isotropic Confining Pressure from Resonant Column Tests of Specimen UTA-27-R.

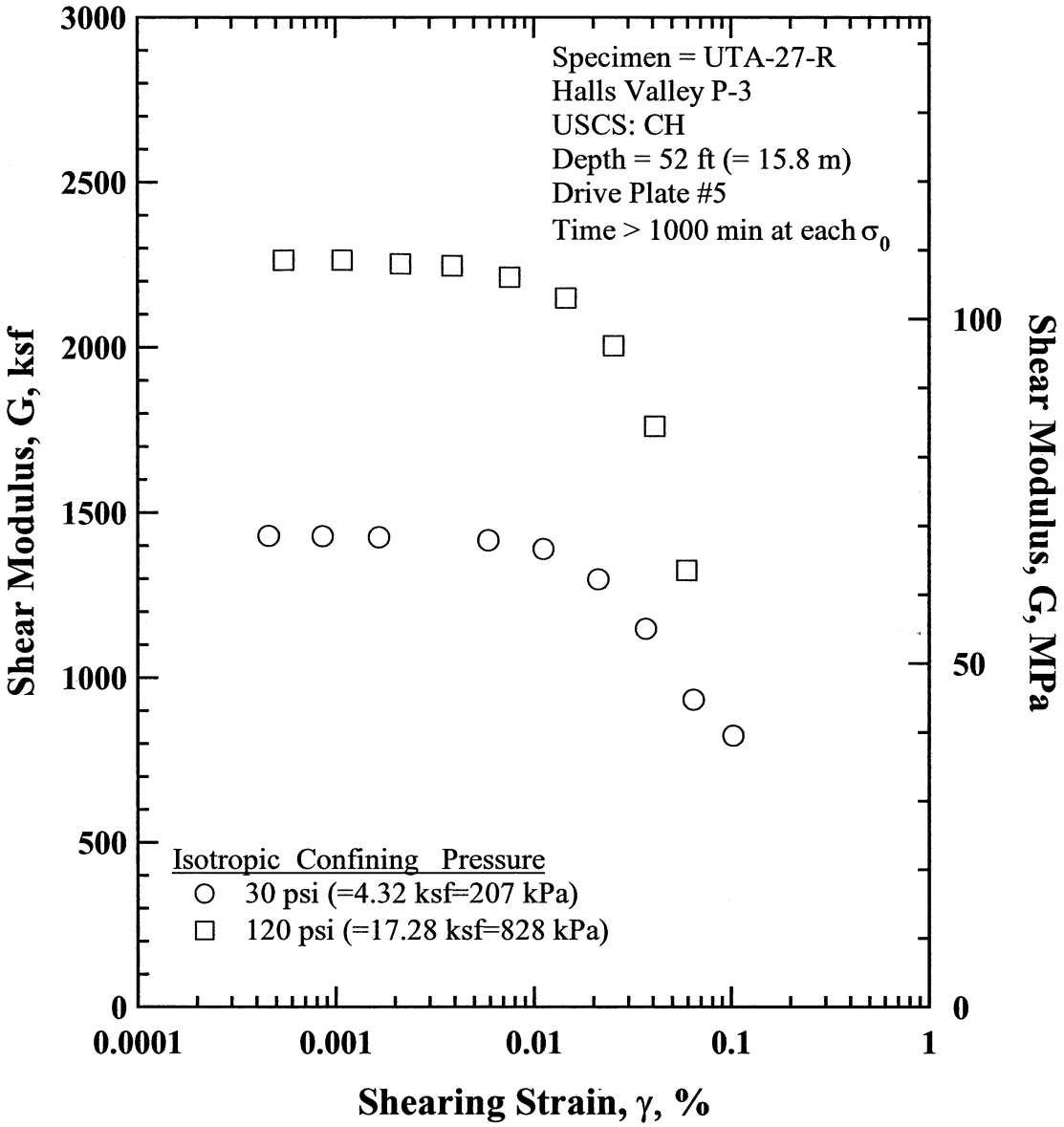

Figure X.8 Comparison of the Variation in Shear Modulus with Shearing Strain and Isotropic Confining Pressure from the Resonant Column Tests of Specimen UTA-27-R.

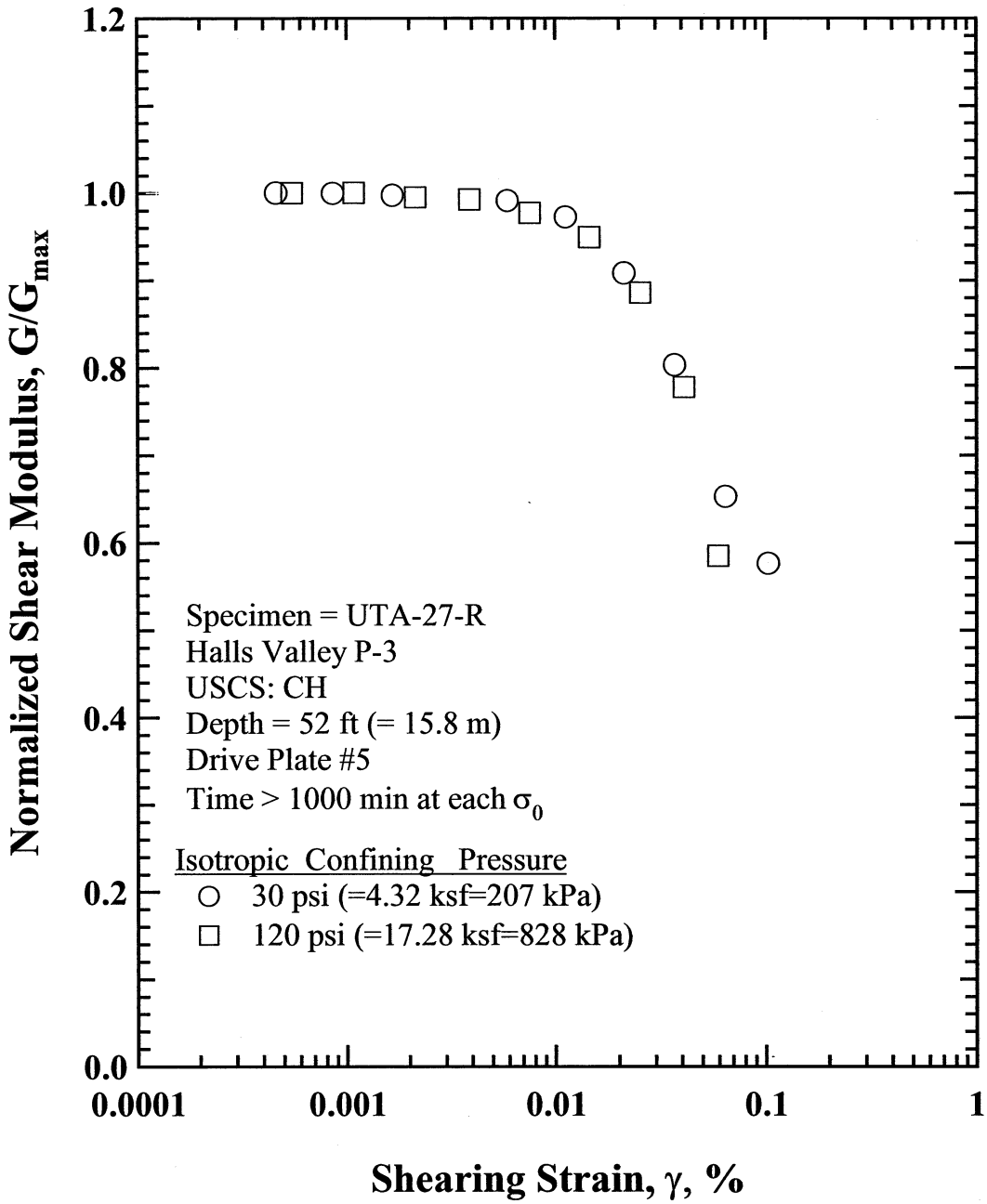

Figure X.9 Comparison of the Variation in Normalized Shear Modulus with Shearing Strain and Isotropic Confining Pressure from the Resonant Column Tests of Specimen UTA-27-R.

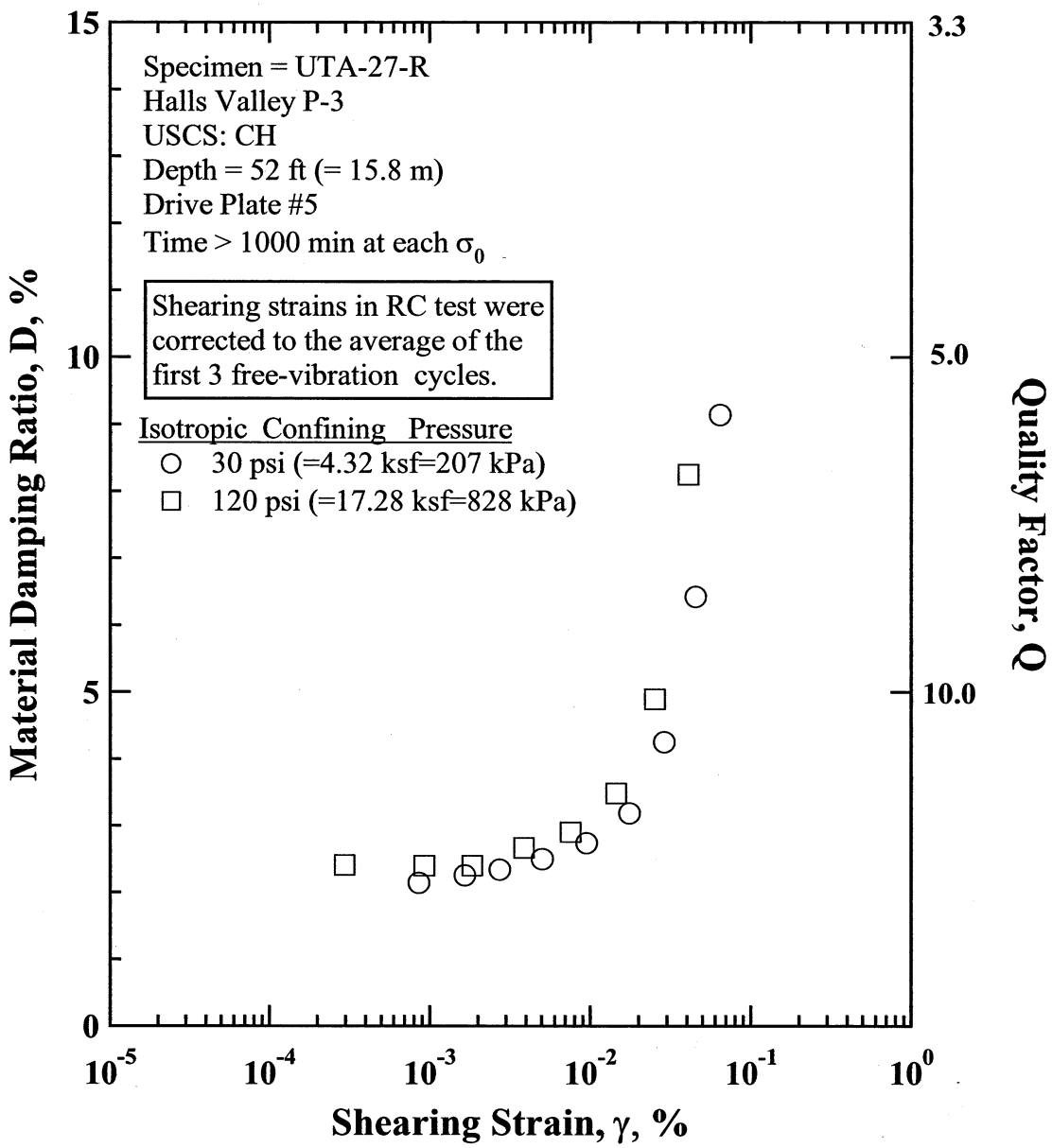

Figure X.10 Comparison of the Variation in Material Damping Ratio with Shearing Strain and Isotropic Confining Pressure from the Resonant Column Tests of Specimen UTA-27-R.

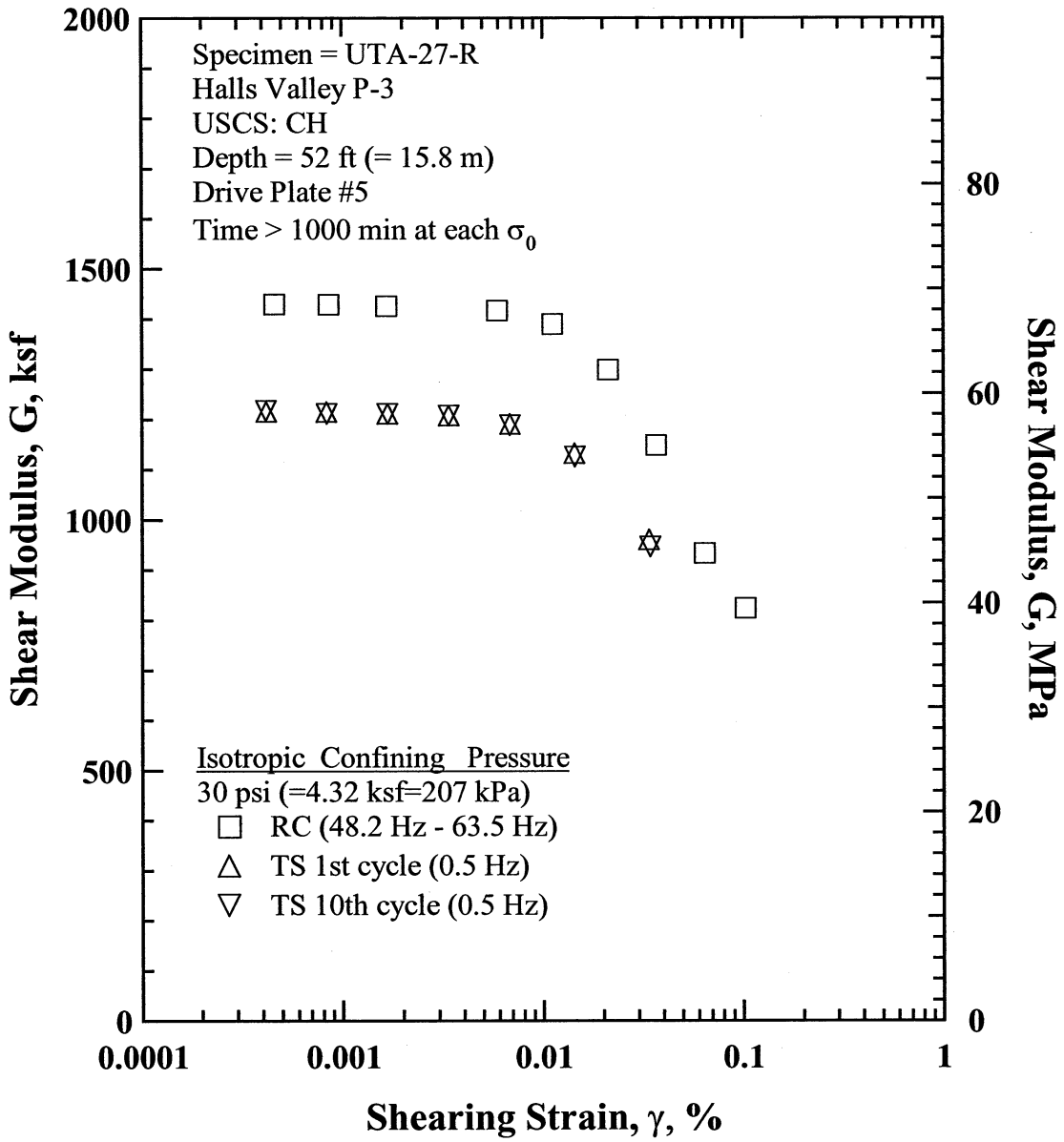

Figure X.11 Comparison of the Variation in Shear Modulus with Shearing Strain at an Isotropic Confining Pressure of 30 psi(=4.32 ksf=207 kPa) from the Combined RCTS Tests of Specimen UTA-27-R.

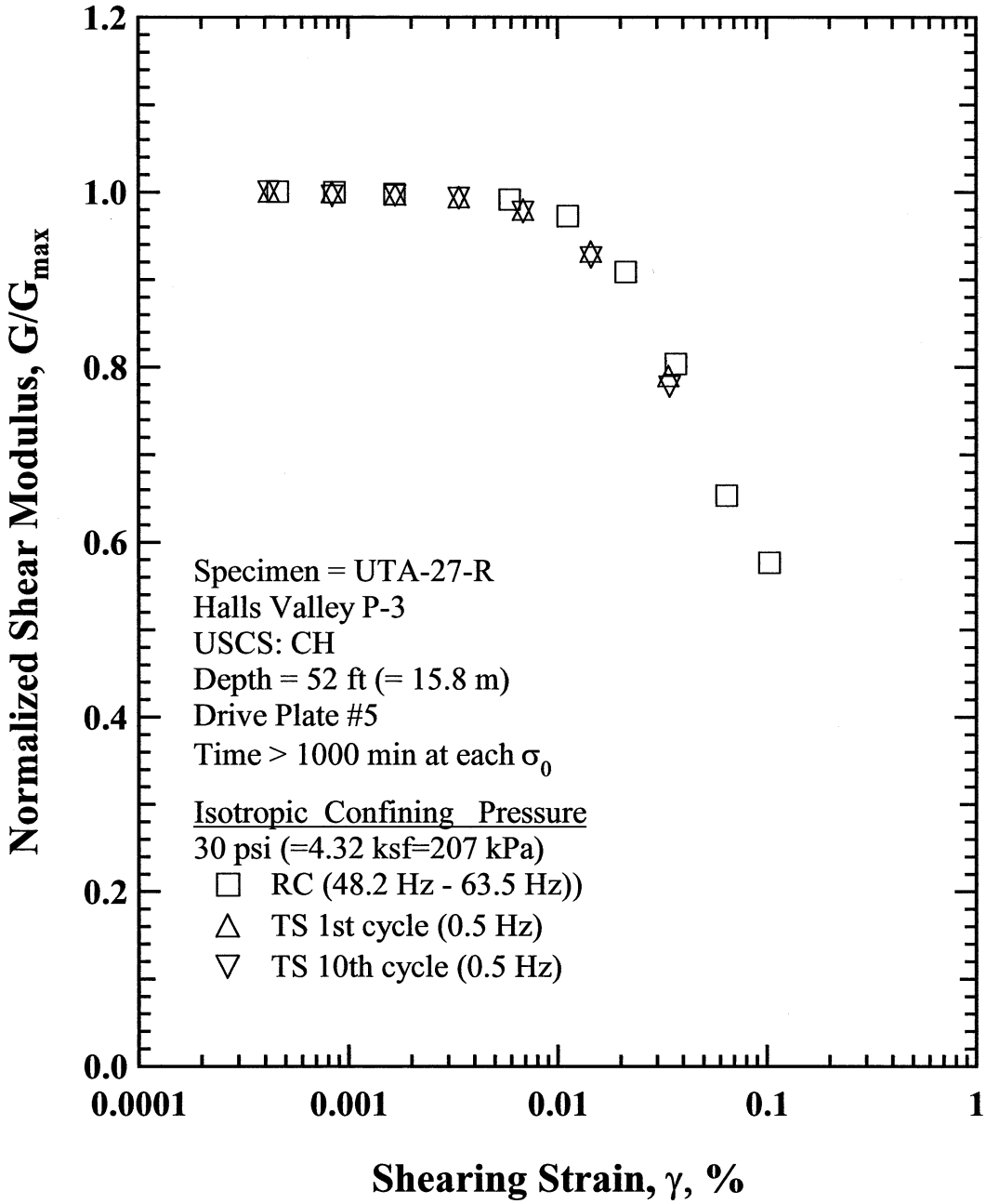

Figure X.12 Comparison of the Variation in Normalized Shear Modulus with Shearing Strain at an Isotropic Confining Pressure of 30 psi(=4.32 ksf=207 kPa) from the Combined RCTS Tests of Specimen UTA-27-R.

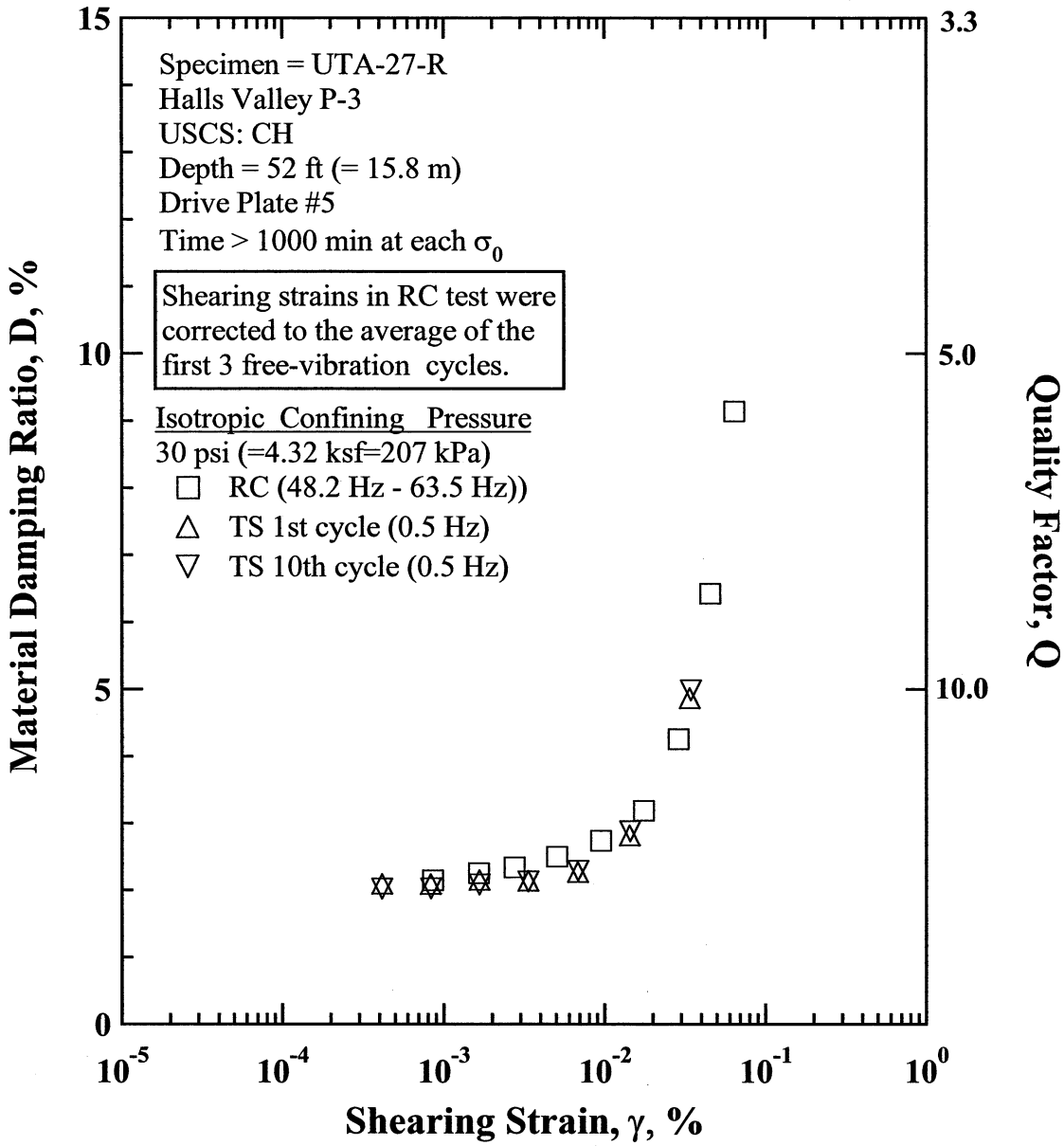

Figure X.13 Comparison of the Variation in Material Damping Ratio with Shearing Strain at an Isotropic Confining Pressure of 30 psi(=4.32 ksf=207 kPa) from the Combined RCTS Tests of Specimen UTA-27-R.

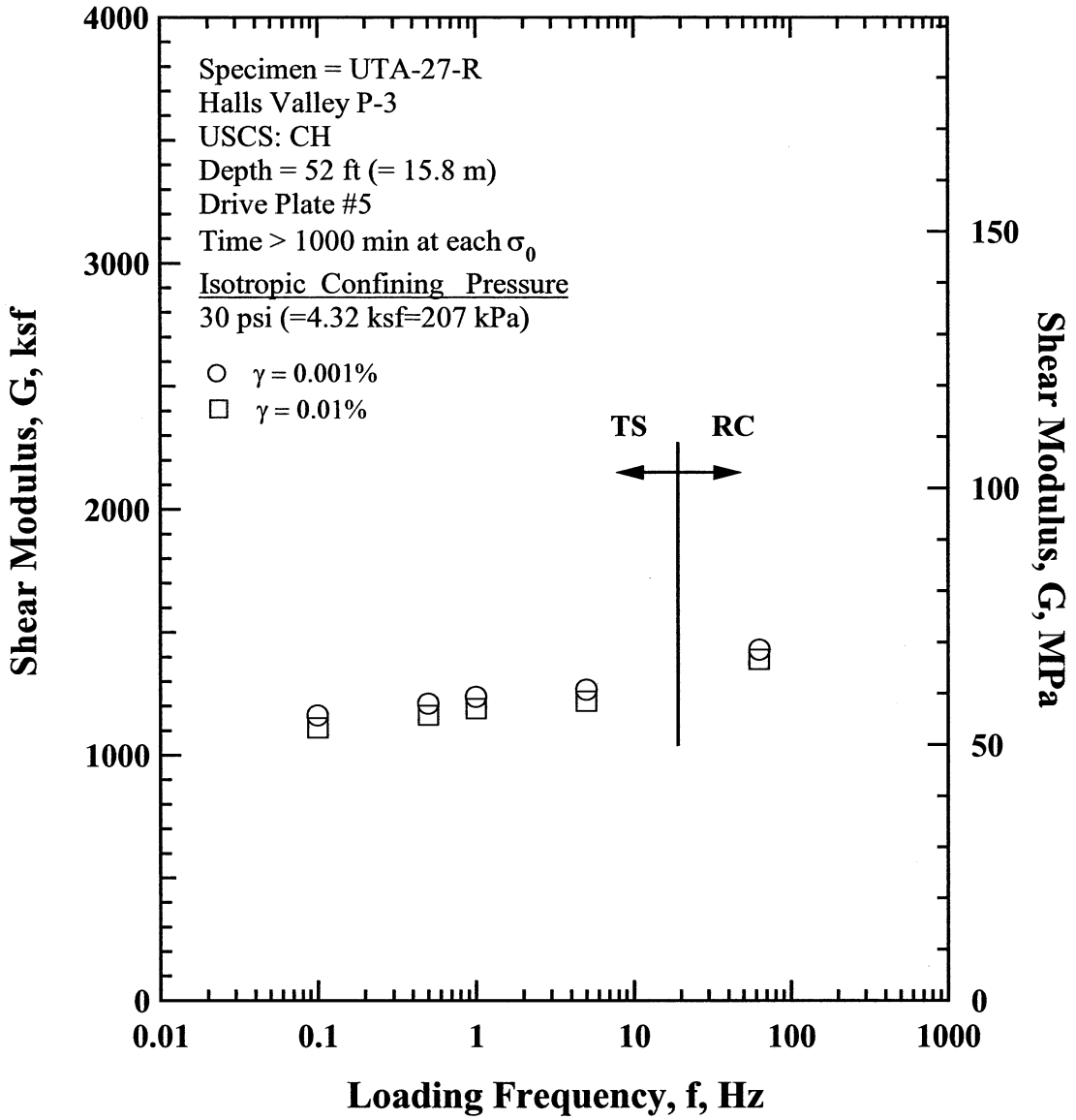

Figure X.14 Comparison of the Variation in Shear Modulus with Loading Frequency at an Isotropic Confining Pressure of 30 psi(=4.32 ksf=207 kPa) from the Combined RCTS Tests of Specimen UTA-27-R.

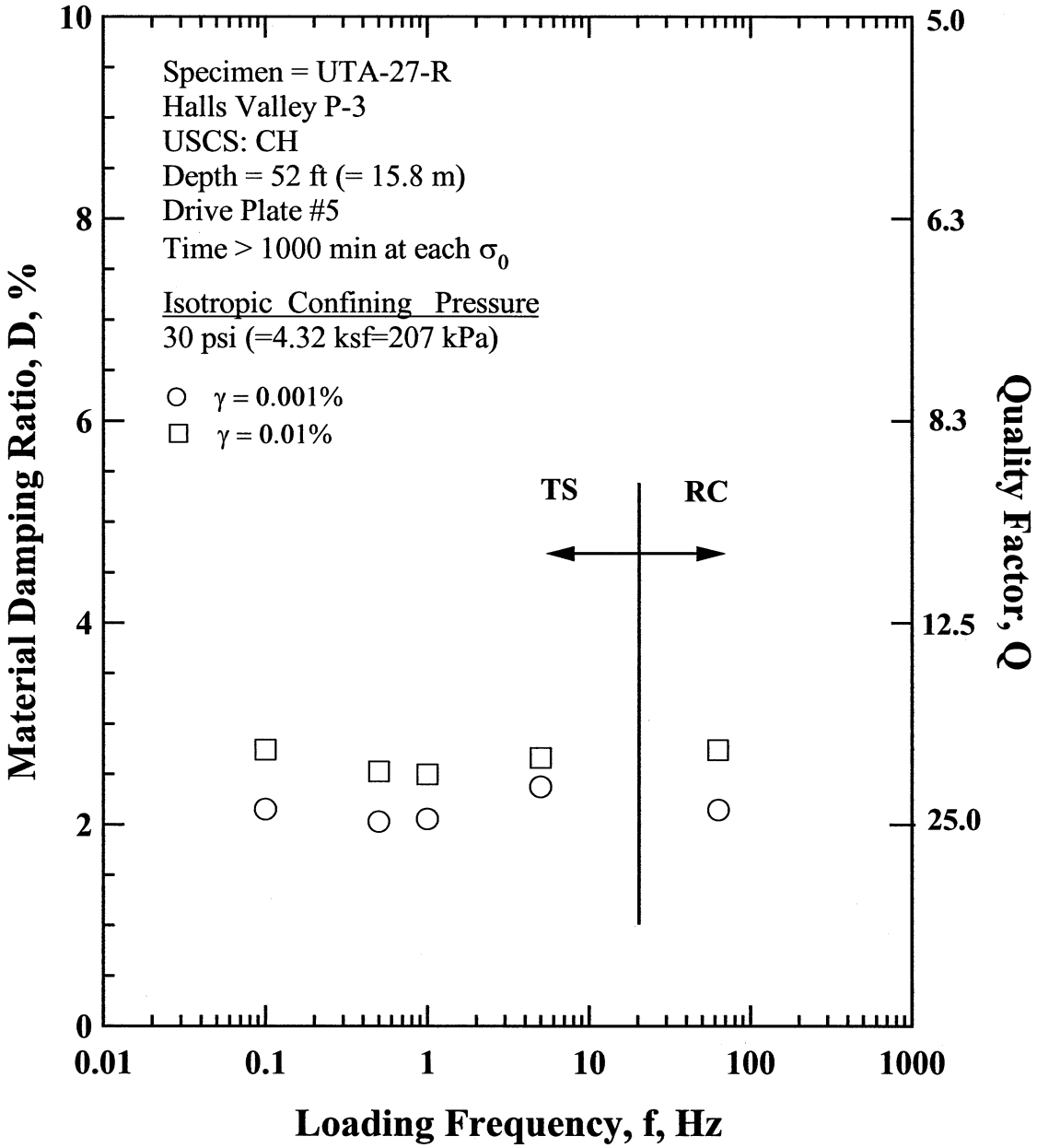

Figure X.15 Comparison of the Variation in Material Damping Ratio with Loading Frequency at an Isotropic Confining Pressure of 30 psi(=4.32 ksf=207 kPa) from the Combined RCTS Tests of Specimen UTA-27-R.

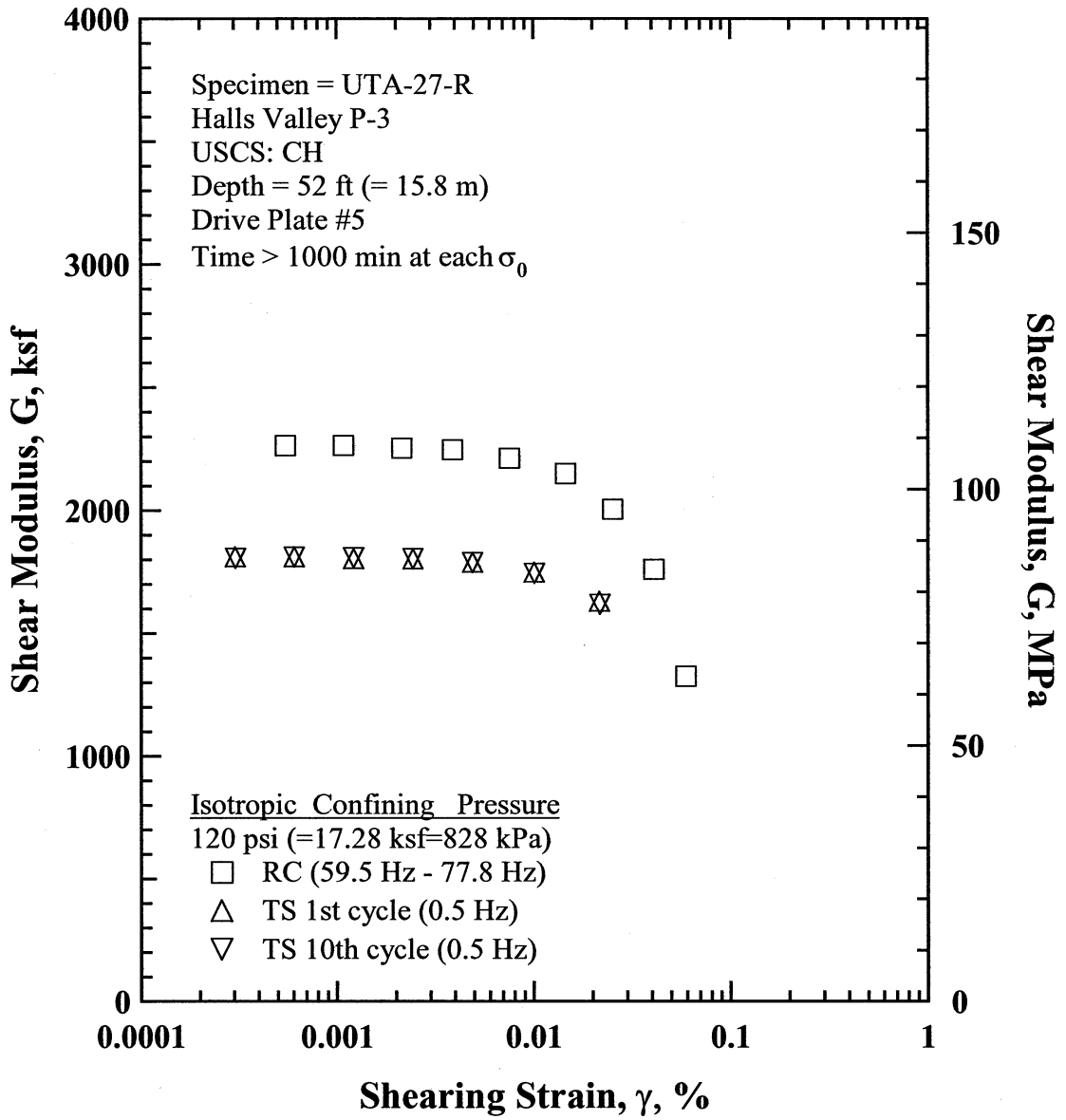

Figure X.16 Comparison of the Variation in Shear Modulus with Shearing Strain at an Isotropic Confining Pressure of 120 psi(=17.28 ksf=828 kPa) from the Combined RCTS Tests of Specimen UTA-27-R.

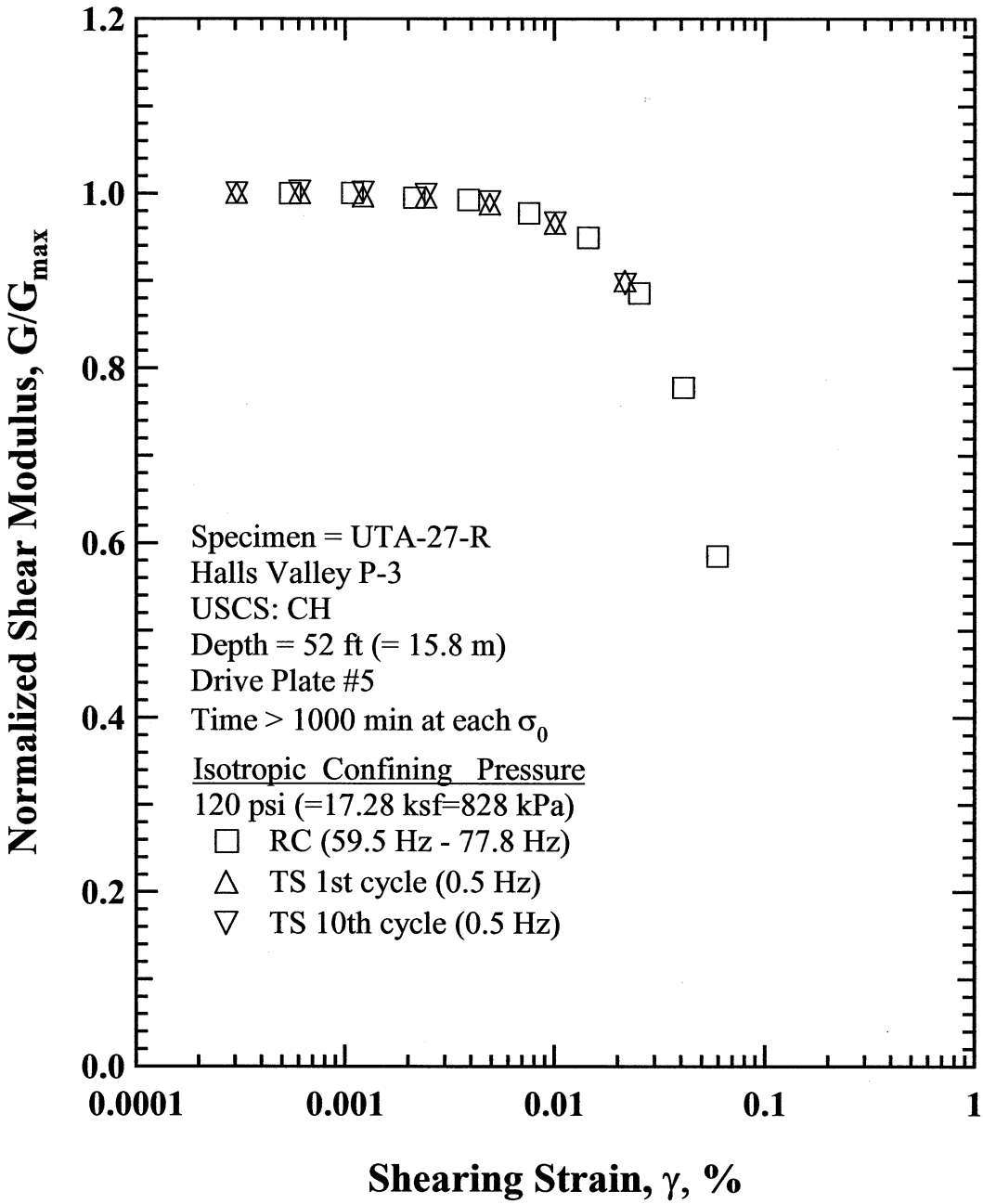

Figure X.17 Comparison of the Variation in Normalized Shear Modulus with Shearing Strain at an Isotropic Confining Pressure of 120 psi(=17.28 ksf=828 kPa) from the Combined RCTS Tests of Specimen UTA-27-R.

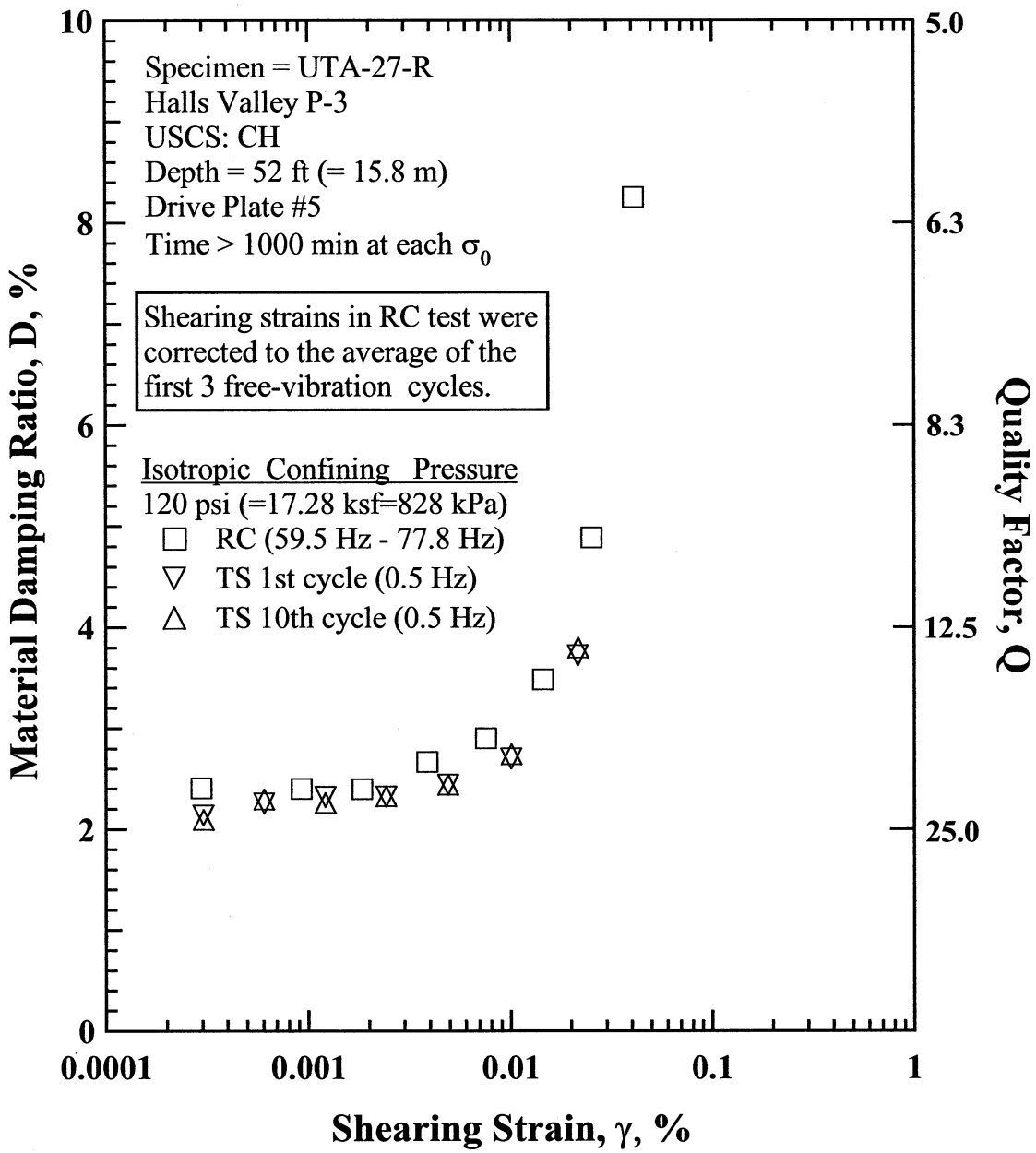

Figure X.18 Comparison of the Variation in Material Damping Ratio with Shearing Strain at an Isotropic Confining Pressure of 120 psi(=17.28 ksf=828 kPa) from the Combined RCTS Tests of Specimen UTA-27-R.

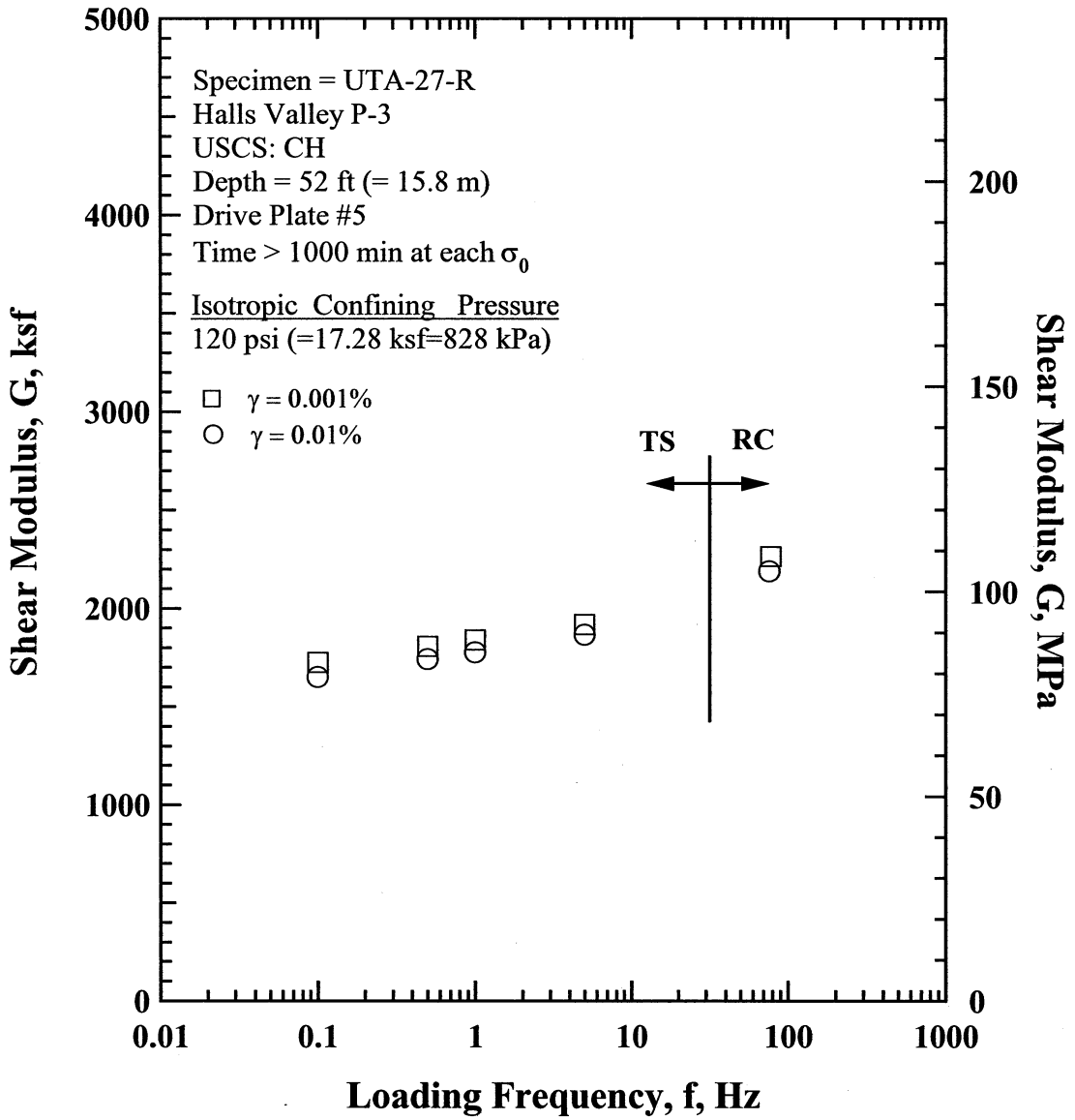

Figure X.19 Comparison of the Variation in Shear Modulus with Loading Frequency at an Isotropic Confining Pressure of 120 psi(=17.28 ksf=828 kPa) from the Combined RCTS Tests of Specimen UTA-27-R.

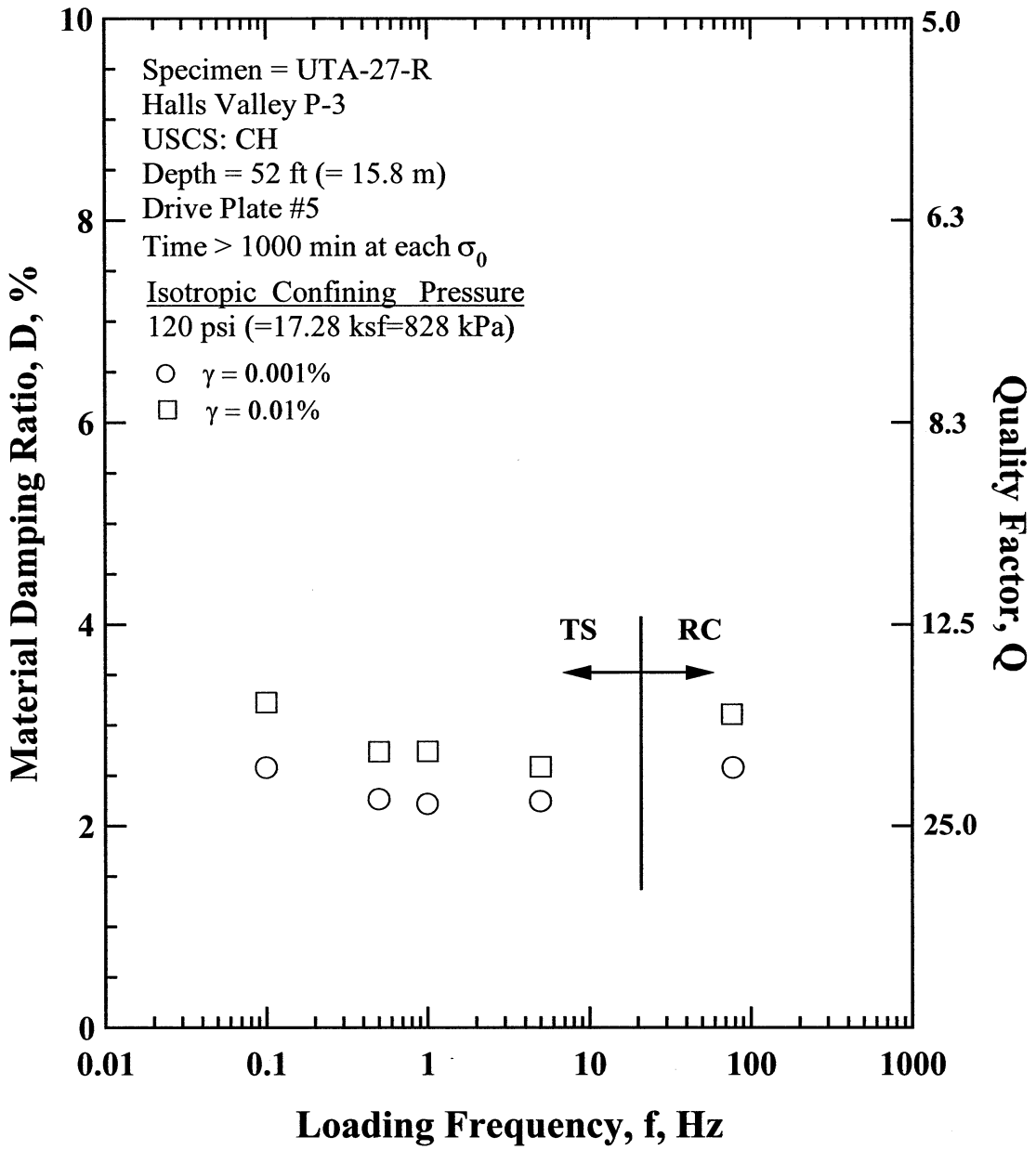

Figure X.20 Comparison of the Variation in Material Damping Ratio with Loading Frequency at an Isotropic Confining Pressure of 120 psi(=17.28 ksf=828 kPa) from the Combined RCTS Tests of Specimen UTA-27-R.

Table X.1 Variation in Low-Amplitude Shear Wave Velocity, Low-Amplitude Shear Modulus, Low-Amplitude Material Damping Ratio and Estimated Void Ratio with Isotropic Confining Pressure from RC Tests of Specimen UTA-27-R

Effective Isotropic Confining Pressure, σ_o'			Low-Amplitude Shear Modulus, G_{max}		Low-Amplitude Shear Wave Velocity, Vs	Low-Amplitude Material Damping Ratio, Dmin	Estimated Void Ratio, e
(psi)	(psf)	(kPa)	(ksf)	(MPa)	(fps)	(%)	
7.5	1080	52	1117	53.6	566	3.20	1.118
15	2160	104	1178	56.5	580	2.54	1.109
30	4320	207	1347	64.6	619	2.58	1.086
60	8640	414	1725	82.7	696	2.44	1.034
120	17280	828	2097	100.5	763	2.55	0.977

Table X.2 Variation in Shear Modulus, Normalized Shear Modulus and Material Damping Ratio with Shearing Strain from RC Tests of Specimen UTA-27-R ; Confining Pressure, σ_o' =30 psi (=4.32 ksf=207 kPa).

Peak Shearing Strain, %	Shear Modulus, G, ksf	Normalized Shear Modulus, G/G_{max}	Average[+] Shearing Strain, %	Material Damping Ratio[x], D, %
4.60E-04	1430	1.00	4.60E-04	
8.58E-04	1429	1.00	8.58E-04	2.15
1.66E-03	1426	1.00	1.66E-03	2.25
3.16E-03			2.75E-03	2.34
5.90E-03	1417	0.99	5.04E-03	2.50
1.12E-02	1390	0.97	9.49E-03	2.74
2.11E-02	1298	0.91	1.75E-02	3.19
3.69E-02	1148	0.80	2.89E-02	4.25
6.44E-02	933	0.65	4.53E-02	6.43
1.03E-01	824	0.58	6.43E-02	9.14

[+] Average Shearing Strain from the First Three Cycles of the Free Vibration Decay Curve

[x] Average Damping Ratio from the First Three Cycles of the Free Vibration Decay Curve

Table X.3 Variation in Shear Modulus, Normalized Shear Modulus and Material Damping Ratio with Shearing Strain from TS Tests of Specimen UTA-27-R ; Confining Pressure, σ_o' =30 psi (=4.32 ksf=207 kPa).

First Cycle				Tenth Cycle			
Peak Shearing Strain, %	Shear Modulus, G, ksf	Normalized Shear Modulus, G/G_{max}	Material Damping Ratio, D, %	Peak Shearing Strain, %	Shear Modulus, G, ksf	Normalized Shear Modulus, G/G_{max}	Material Damping Ratio, D, %
4.20E-04	1215	1.00	2.09	4.20E-04	1216	1.00	2.01
8.40E-04	1214	1.00	2.08	8.43E-04	1210	0.99	2.02
1.69E-03	1211	1.00	2.14	1.69E-03	1211	1.00	2.08
3.39E-03	1207	0.99	2.13	3.39E-03	1207	0.99	2.12
6.87E-03	1190	0.98	2.27	6.88E-03	1188	0.98	2.29
1.44E-02	1132	0.93	2.81	1.45E-02	1125	0.92	2.87
3.41E-02	959	0.79	4.86	3.46E-02	945	0.78	4.98

Table X.4 Variation in Shear Modulus, Normalized Shear Modulus and Material Damping Ratio with Shearing Strain from RC Tests of Specimen UTA-27-R ; Confining Pressure, σ_o' = 120 psi (=17.28 ksf=828 kPa).

Peak Shearing Strain, %	Shear Modulus, G, ksf	Normalized Shear Modulus, G/G_{max}	Average[+] Shearing Strain, %	Material Damping Ratio[x], D, %
5.48E-04	2264	1.00	2.96E-04	2.41
1.08E-03	2264	1.00	9.28E-04	2.40
2.14E-03	2253	1.00	1.85E-03	2.40
3.88E-03	2247	0.99	3.88E-03	2.67
7.54E-03	2213	0.98	7.54E-03	2.90
1.45E-02	2150	0.95	1.45E-02	3.48
2.52E-02	2005	0.89	2.52E-02	4.89
4.08E-02	1761	0.78	4.08E-02	8.25
5.94E-02	1325	0.59		

[+] Average Shearing Strain from the First Three Cycles of the Free Vibration Decay Curve

[x] Average Damping Ratio from the First Three Cycles of the Free Vibration Decay Curve

Table X.5 Variation in Shear Modulus, Normalized Shear Modulus and Material Damping Ratio with Shearing Strain from TS Tests of Specimen UTA-27-R ; Confining Pressure, σ_o' = 120 psi (=17.28 ksf=828 kPa).

First Cycle				Tenth Cycle			
Peak Shearing Strain, %	Shear Modulus, G, ksf	Normalized Shear Modulus, G/G_{max}	Material Damping Ratio, D, %	Peak Shearing Strain, %	Shear Modulus, G, ksf	Normalized Shear Modulus, G/G_{max}	Material Damping Ratio, D, %
3.05E-04	1811	1.00	2.14	3.06E-04	1804	1.00	2.09
6.09E-04	1810	1.00	2.25	6.10E-04	1808	1.00	2.29
1.22E-03	1803	1.00	2.32	1.22E-03	1806	1.00	2.26
2.45E-03	1802	1.00	2.32	2.45E-03	1802	1.00	2.32
4.94E-03	1787	0.99	2.44	4.94E-03	1787	0.99	2.44
1.01E-02	1747	0.96	2.70	1.01E-02	1743	0.97	2.74
2.17E-02	1628	0.90	3.72	2.19E-02	1616	0.90	3.79

APPENDIX Y

Specimen No. 24
UT Specimen ID: UTA-27-U

Saturn P-4
Depth= 100 ft (=30.5m)
Soil Type: Clay (CH)

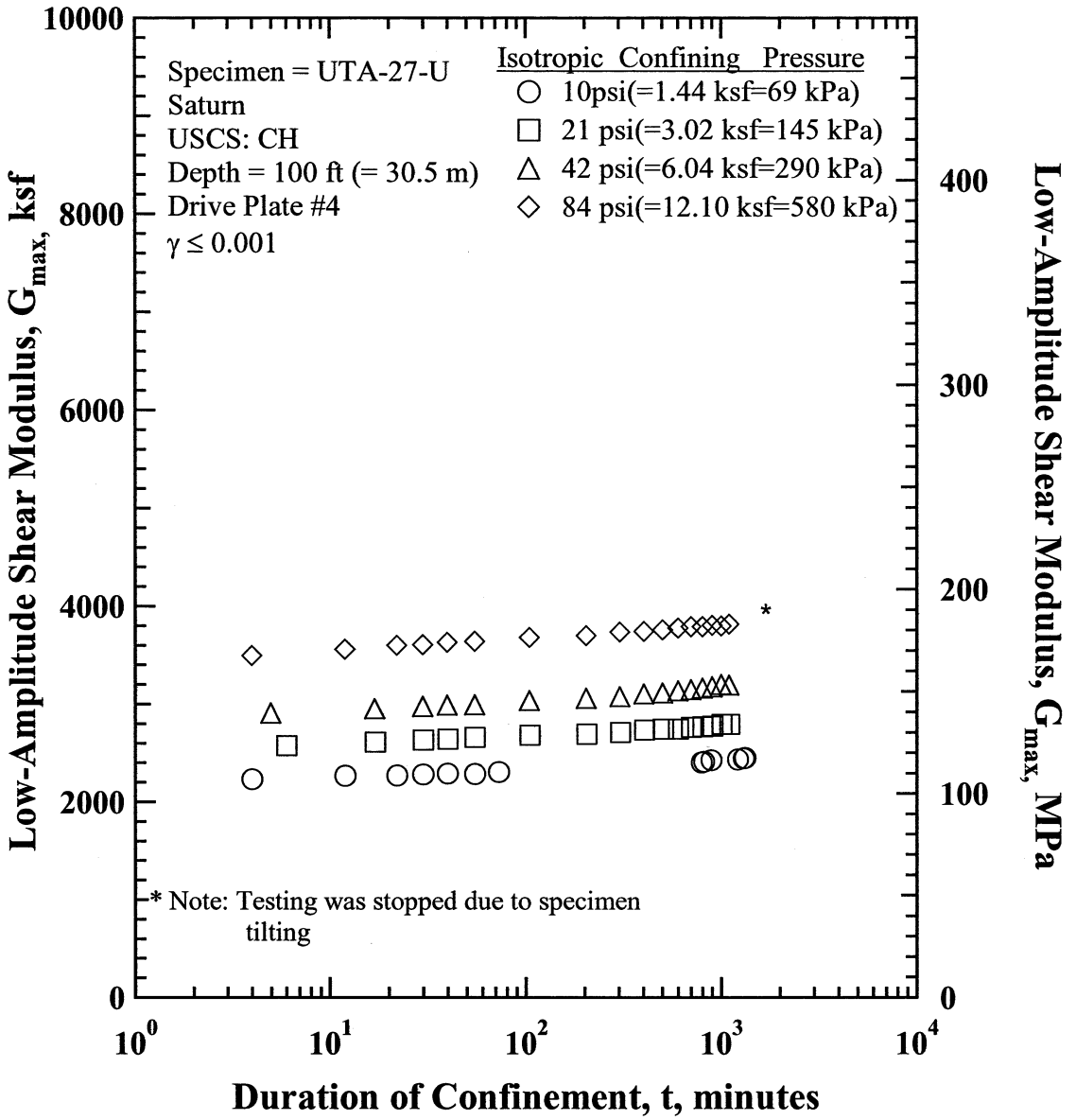

Figure Y.1 Variation in Low-Amplitude Shear Modulus with Magnitude and Duration of Isotropic Confining Pressure from Resonant Column Tests of Specimen UTA-27-U.

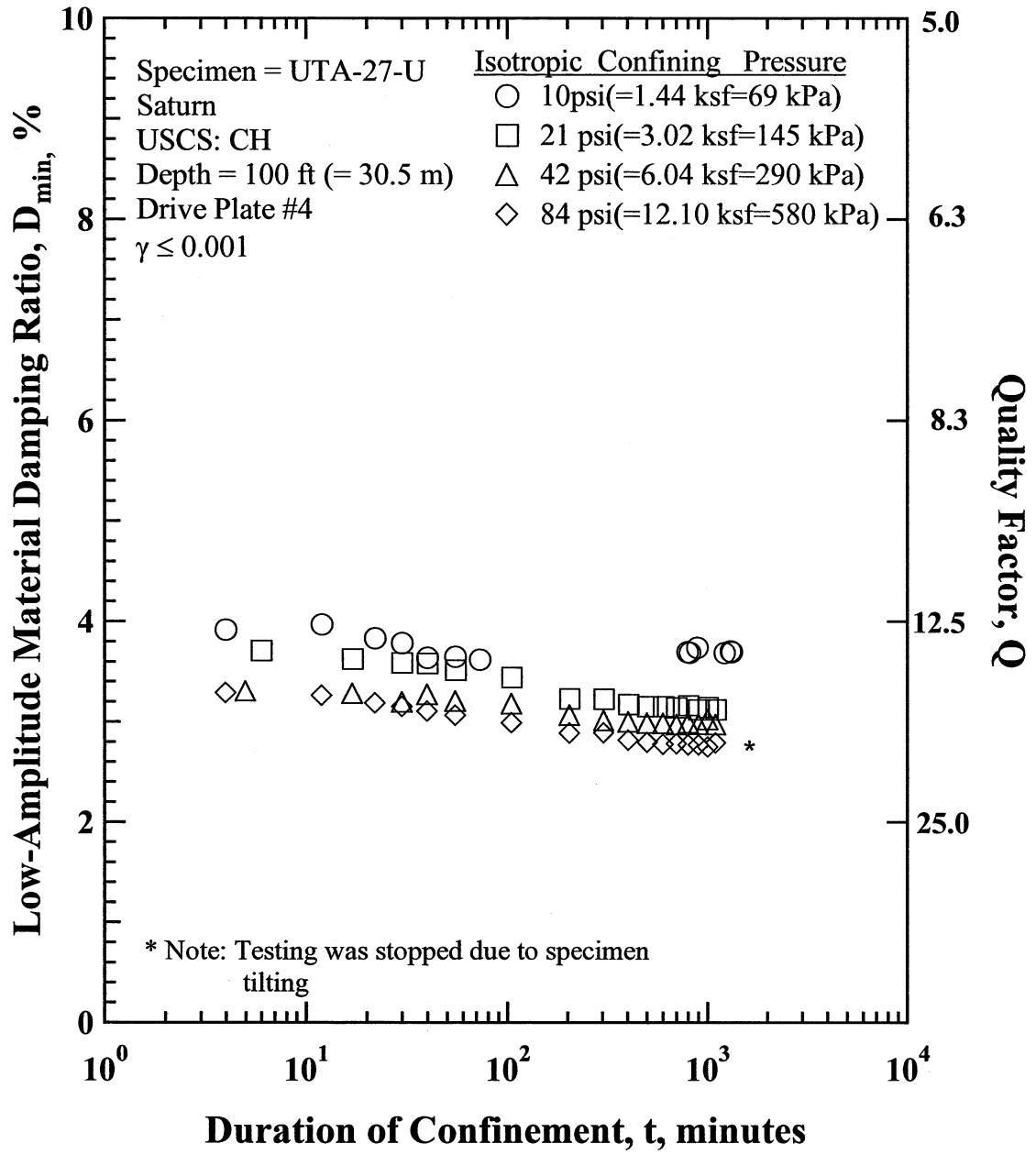

Figure Y.2 Variation in Low-Amplitude Material Damping Ratio with Magnitude and Duration of Isotropic Confining Pressure from Resonant Column Tests of Specimen UTA-27-U

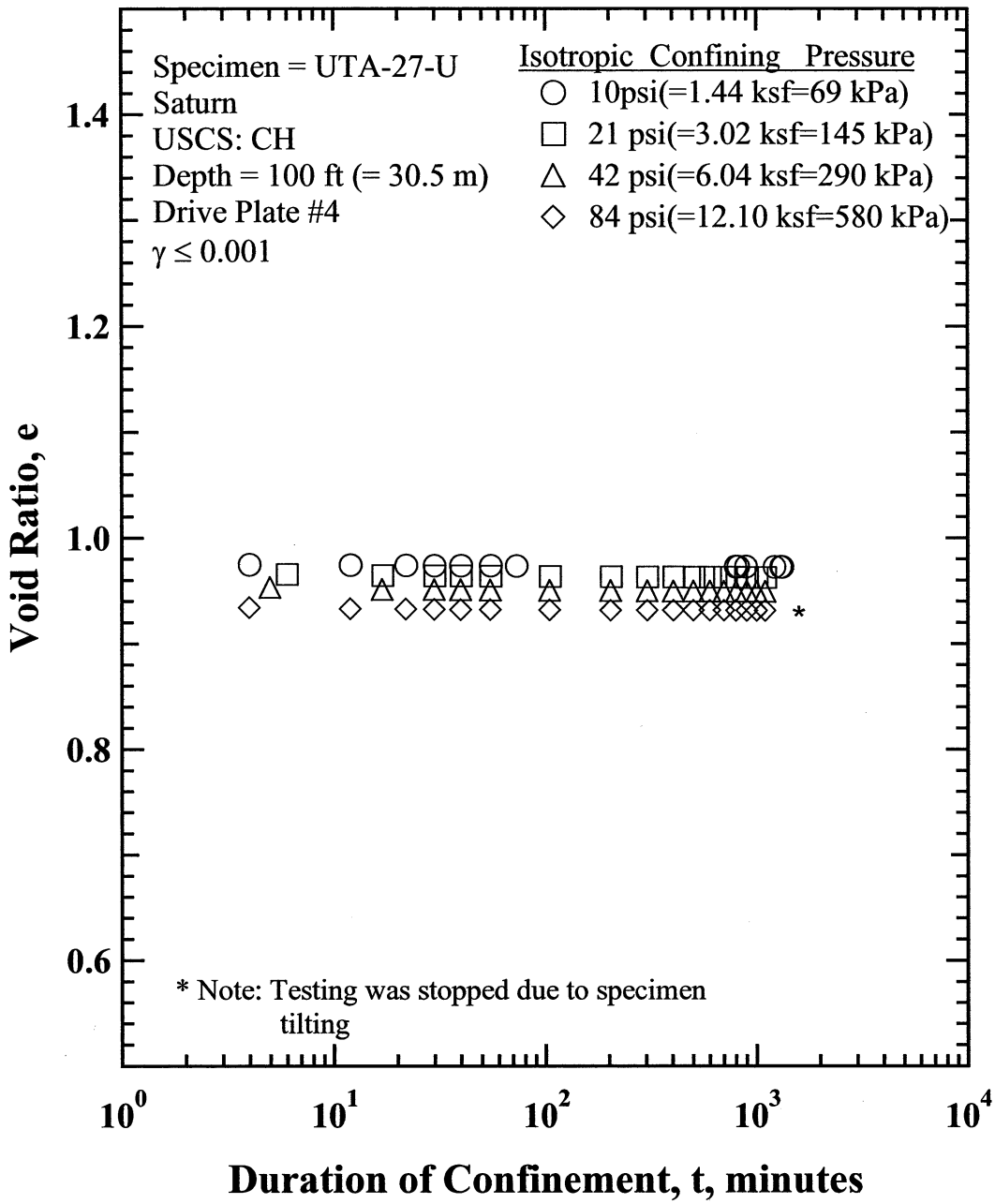

Figure Y.3 Variation in Estimated Void Ratio with Magnitude and Duration of Isotropic Confining Pressure from Resonant Column Tests of Specimen UTA-27-U

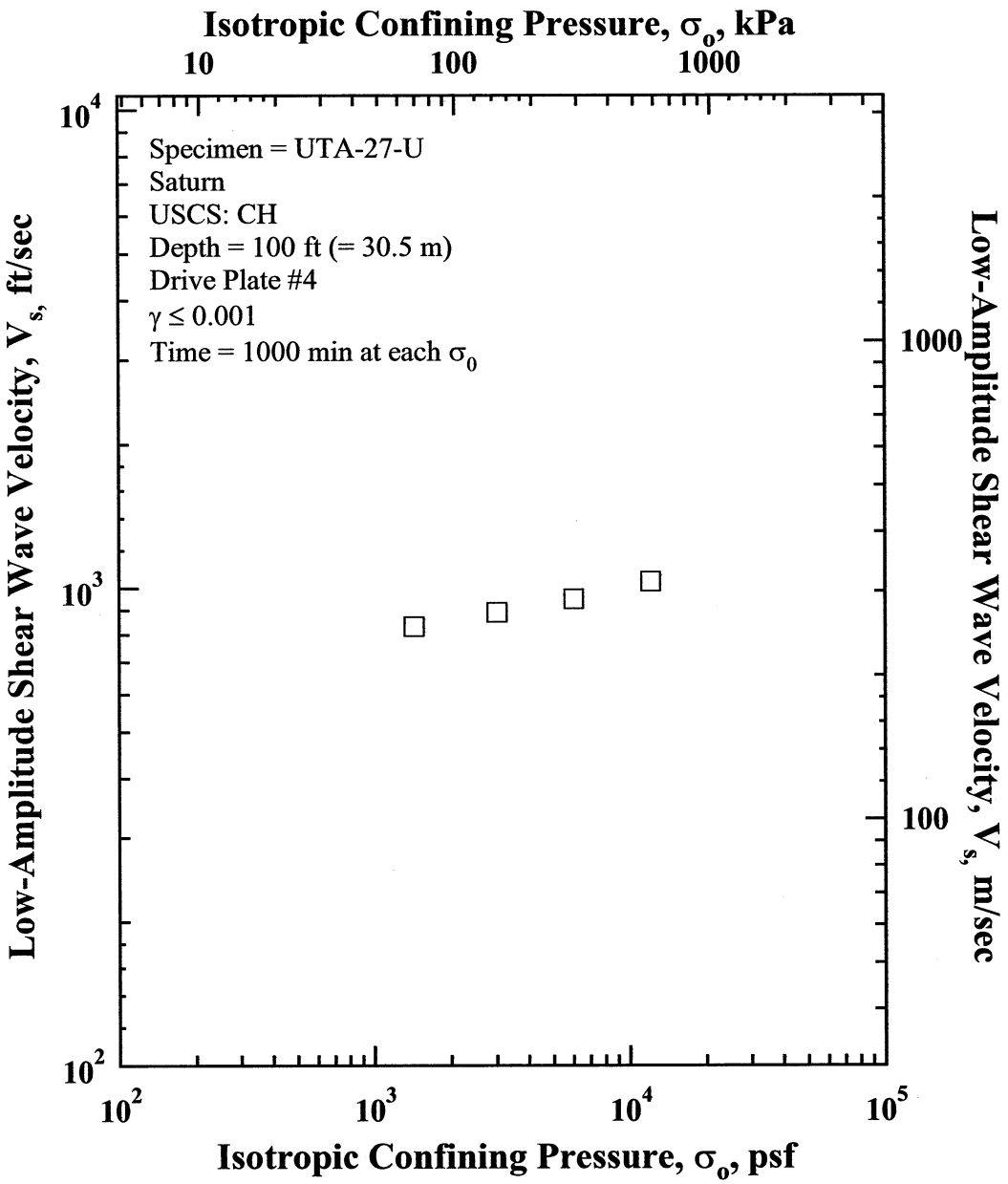

Figure Y.4 Variation in Amplitude Shear Wave Velocity with Isotropic Confining Pressure from Resonant Column Tests of Specimen UTA-27-U.

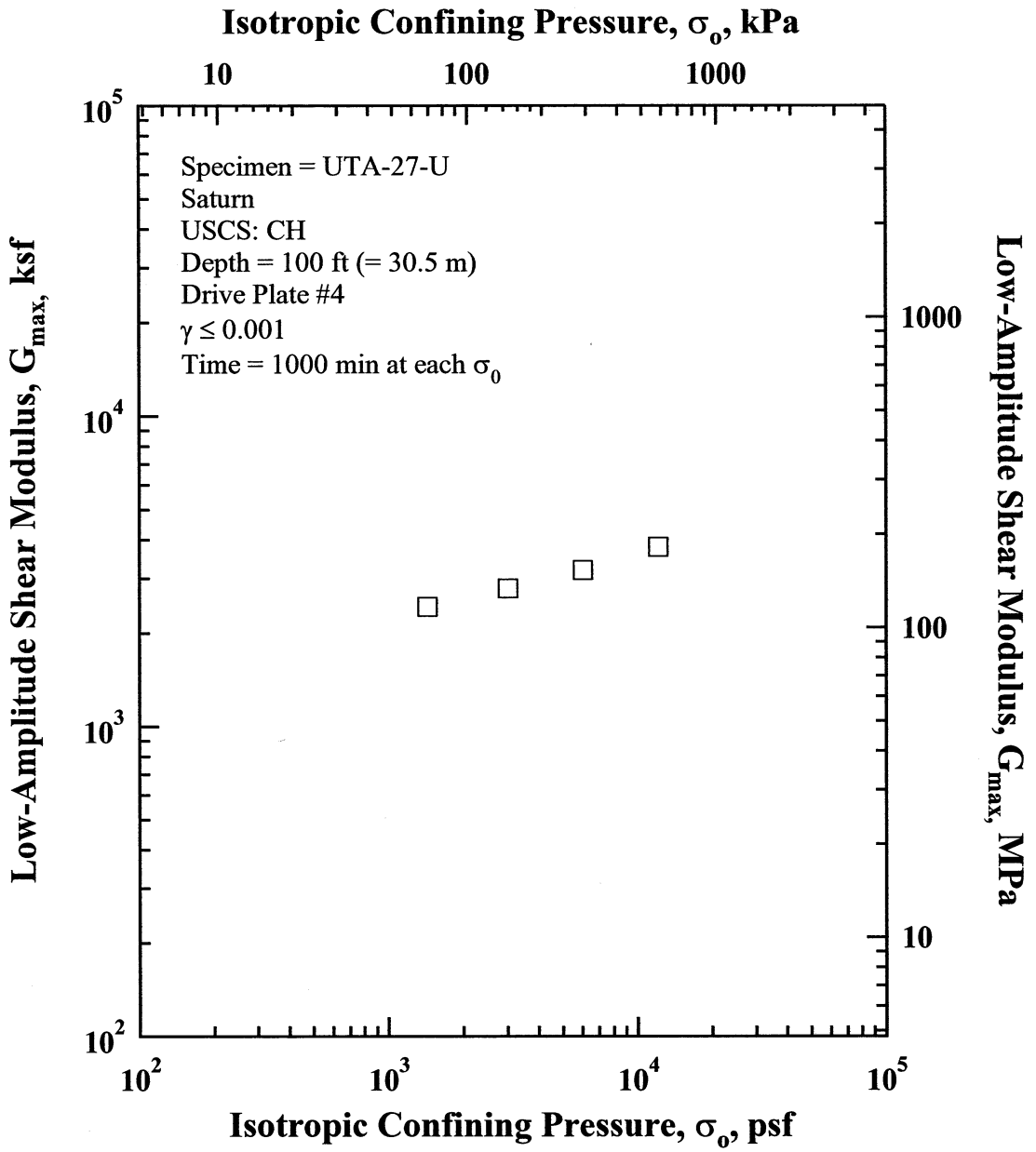

Figure Y.5 Variation in Low-Amplitude Shear Modulus with Isotropic Confining Pressure from Resonant Column Tests of Specimen UTA-27-U.

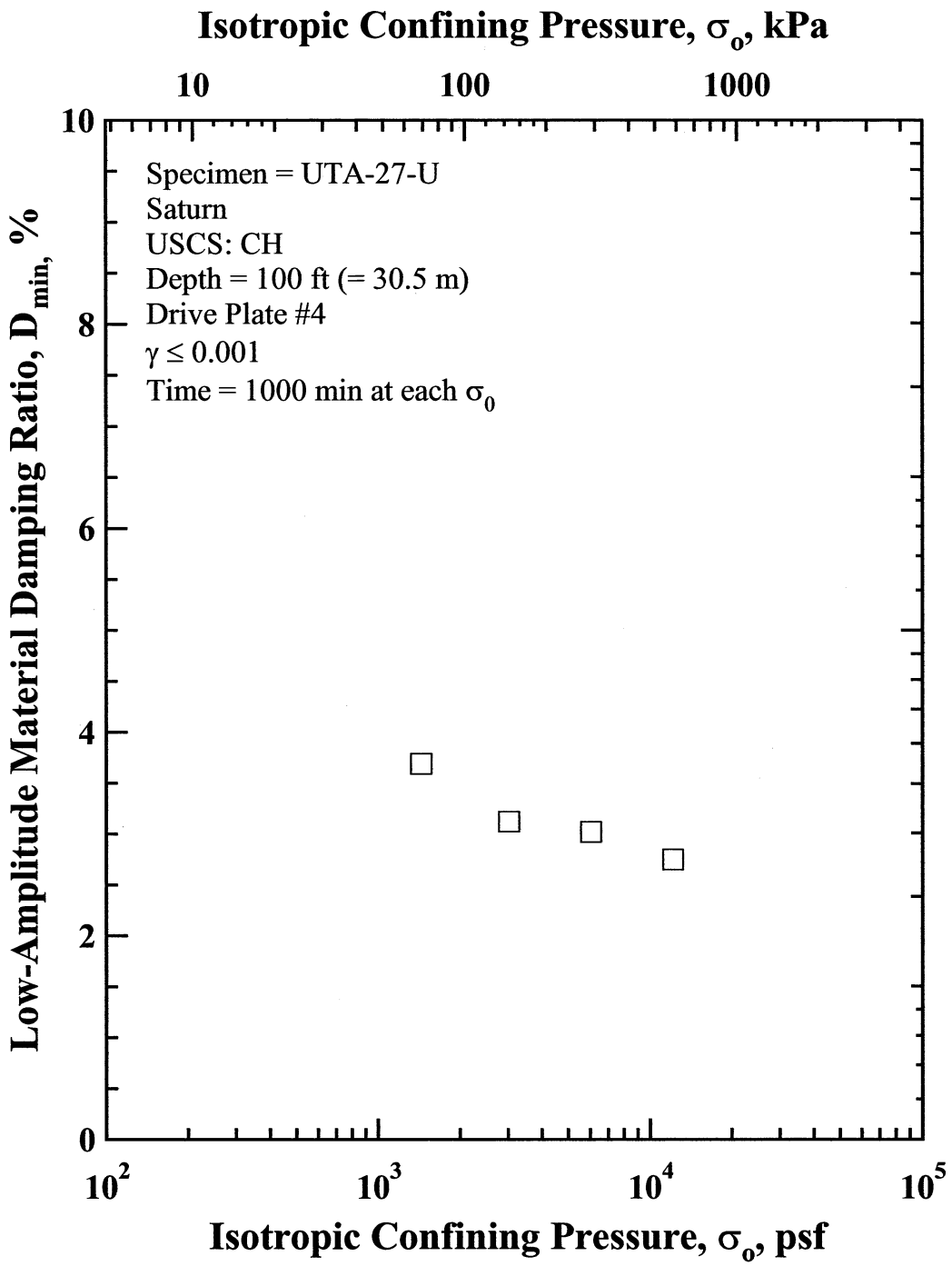

Figure Y.6 Variation in Amplitude Material Damping Ratio with Isotropic Confining Pressure from Resonant Column Tests of Specimen UTA-27-U.

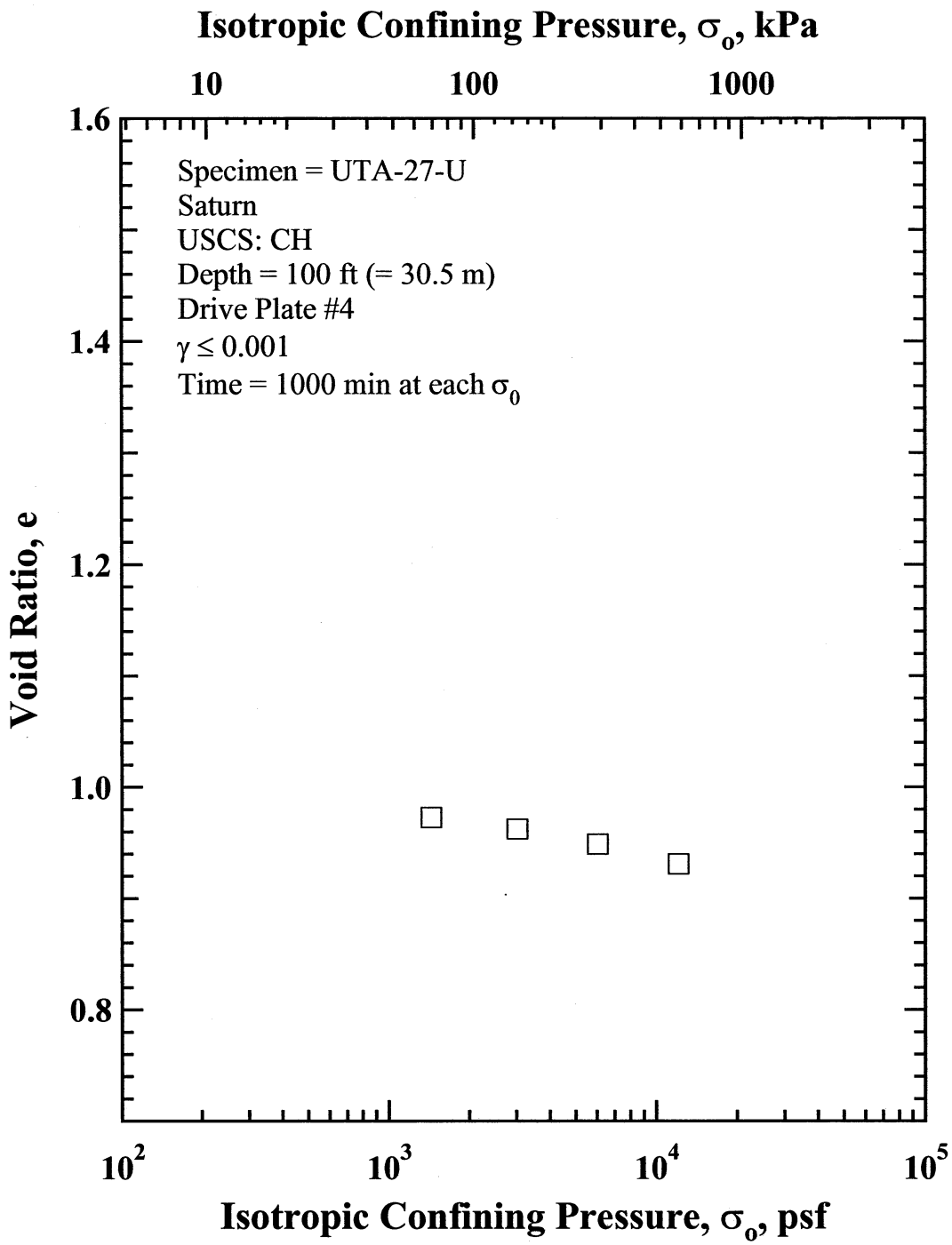

Figure Y.7 Variation in Estimated Void Ratio with Isotropic Confining Pressure from Resonant Column Tests of Specimen UTA-27-U.

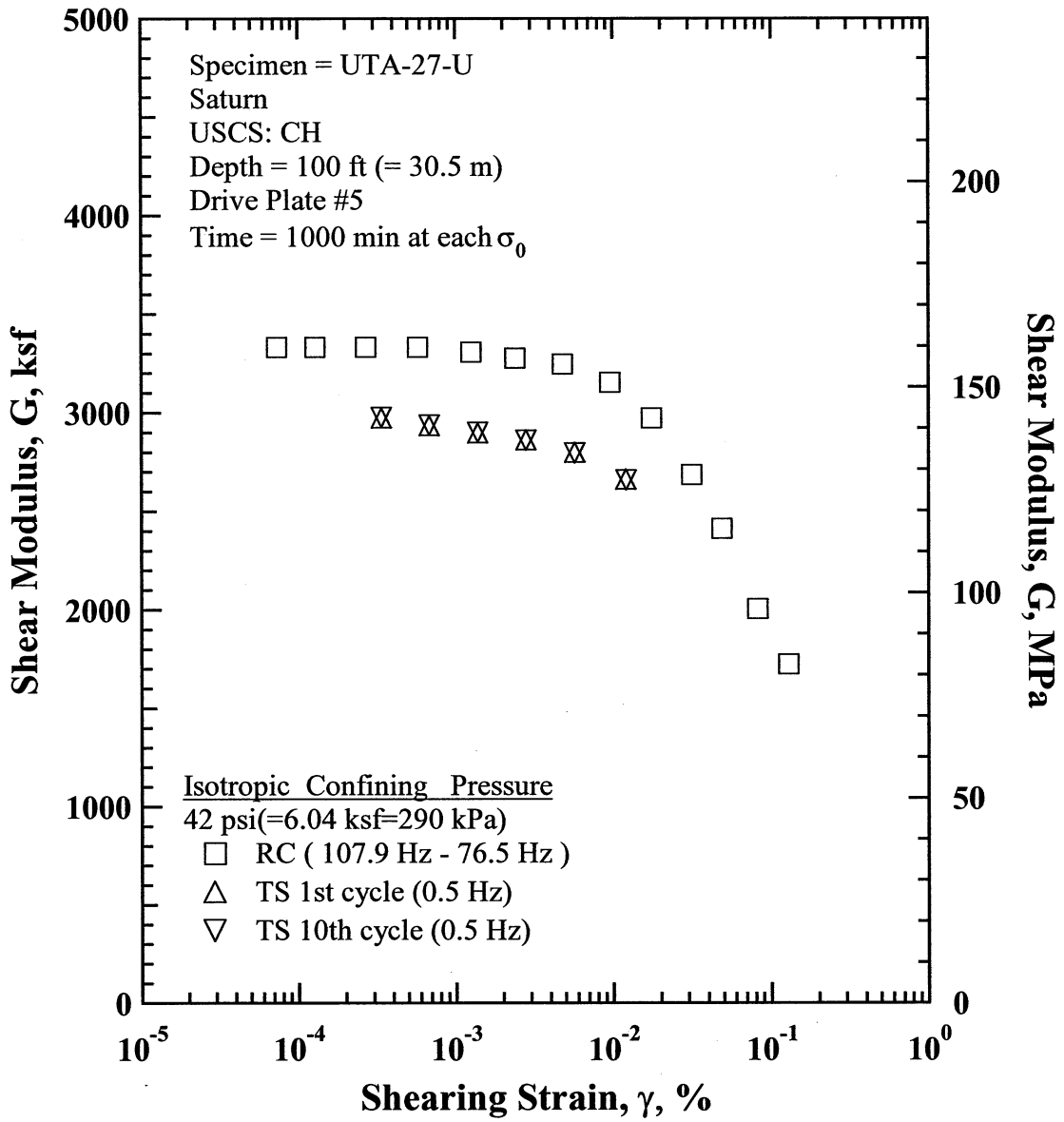

Figure Y.8 Comparison of the Variation in Shear Modulus with Shearing Strain at an Isotropic Confining Pressure of 42 psi(=6.04 ksf=290 kPa) from the Combined RCTS Tests of Specimen UTA-27-U.

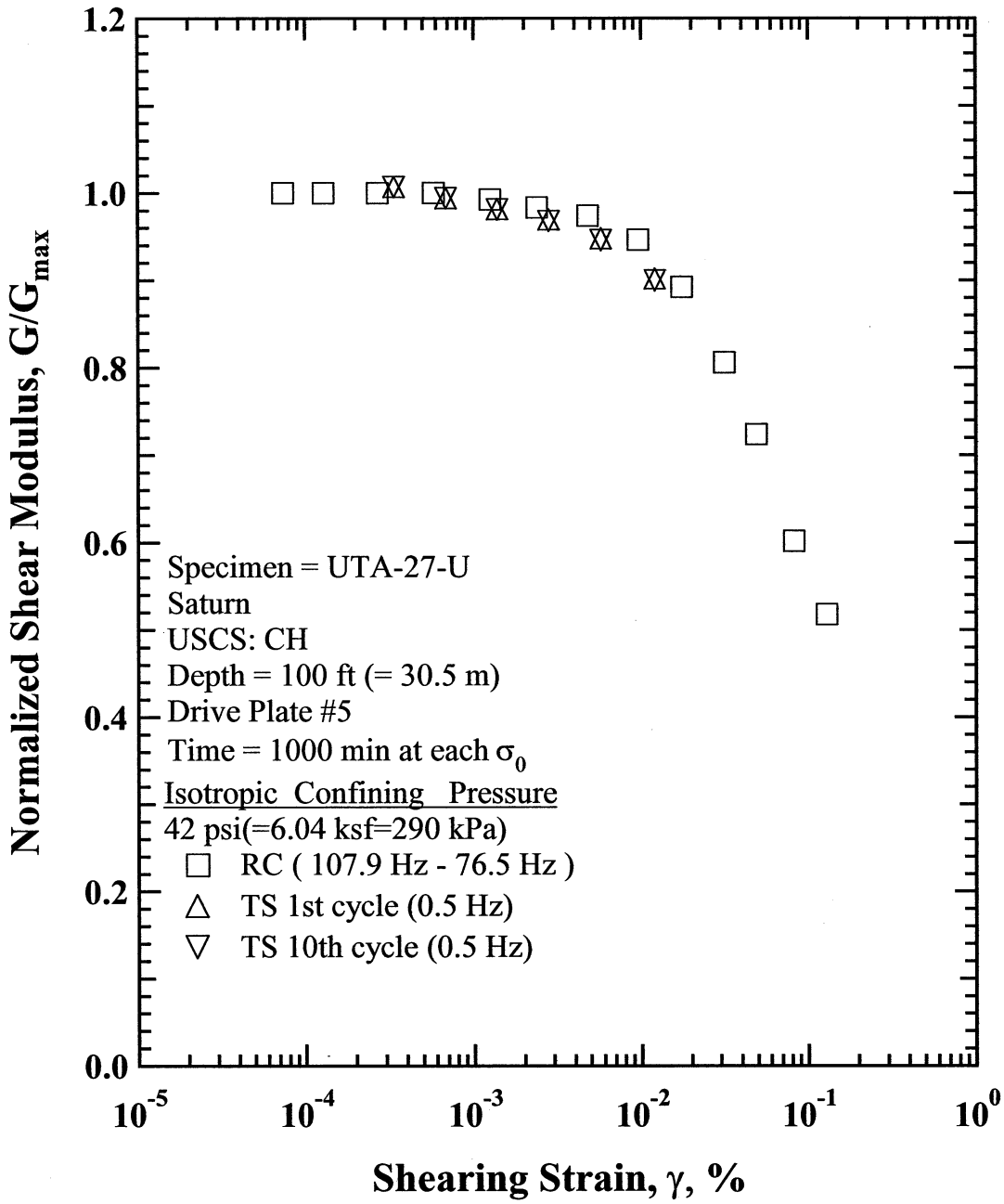

Figure Y.9 Comparison of the Variation in Normalized Shear Modulus with Shearing Strain at an Isotropic Confining Pressure of 42 psi(=6.04 ksf=290 kPa) from the Combined RCTS Tests of Specimen UTA-27-U.

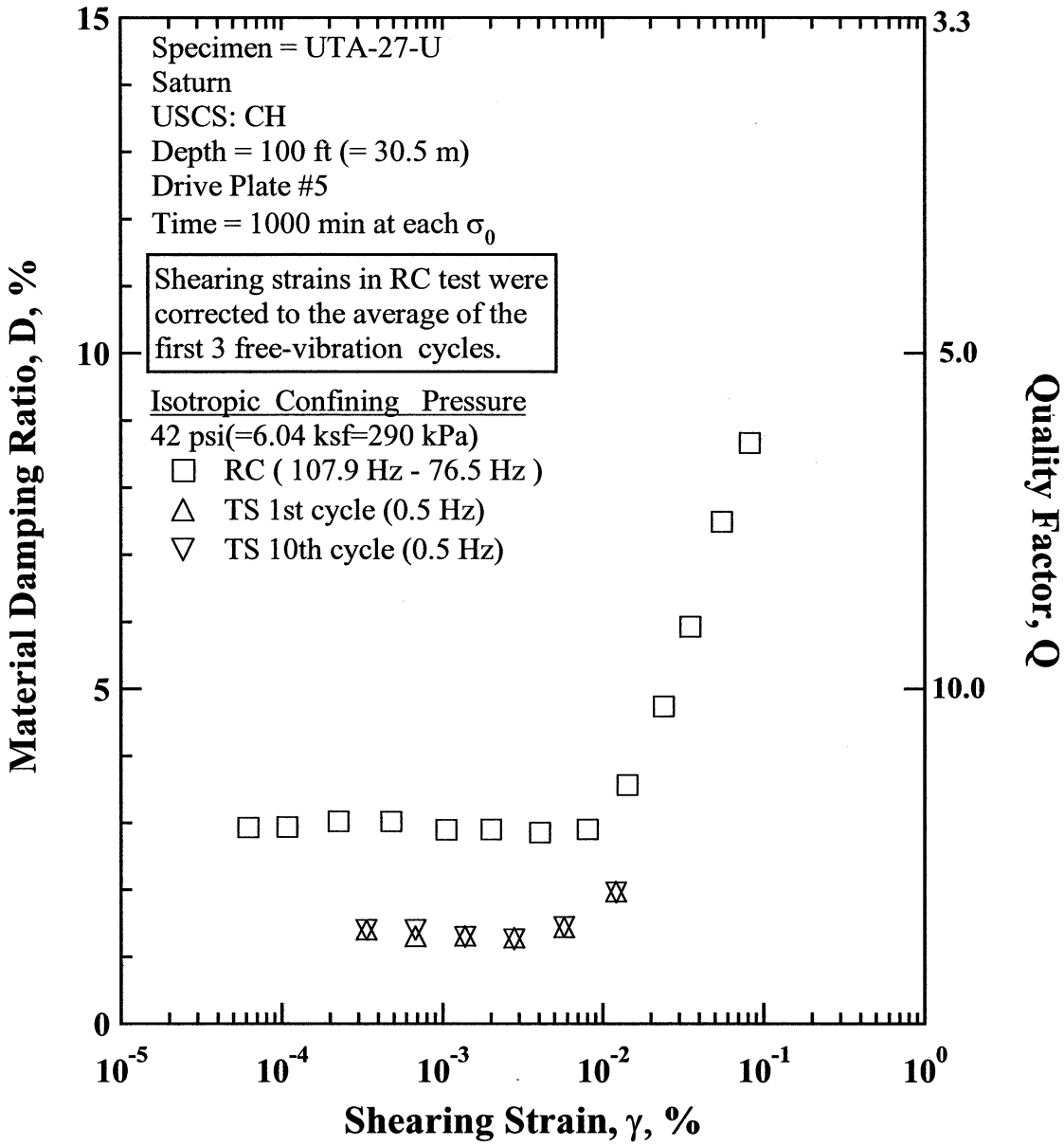

Figure Y.10 Comparison of the Variation in Material Damping Ratio with Shearing Strain at an Isotropic Confining Pressure of 42 psi(=6.04 ksf=290 kPa) from the Combined RCTS Tests of Specimen UTA-27-U.

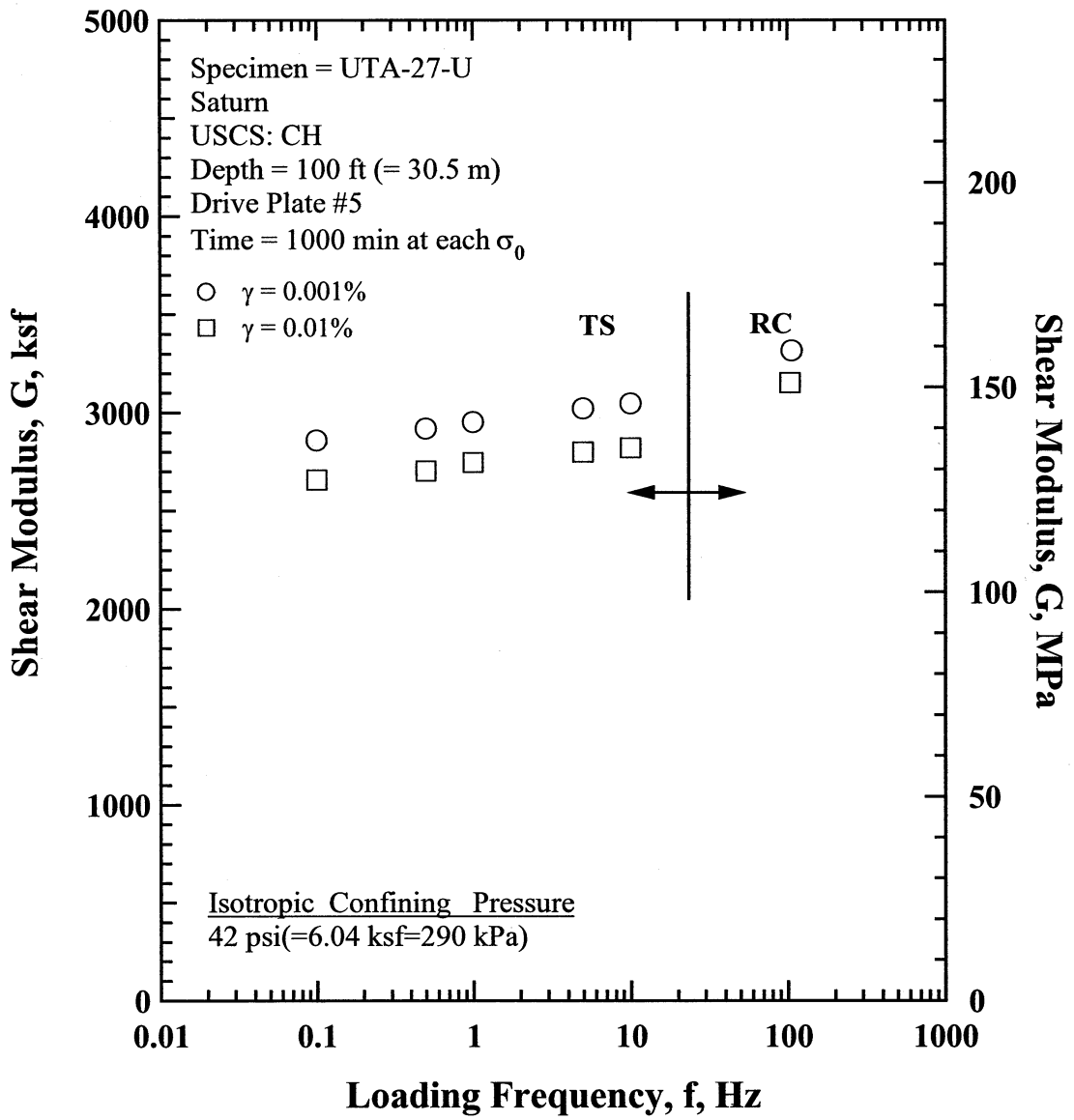

Figure Y.11 Comparison of the Variation in Shear Modulus with Loading Frequency at an Isotropic Confining Pressure of 42 psi(=6.04 ksf=290 kPa) from the Combined RCTS Tests of Specimen UTA-27-U.

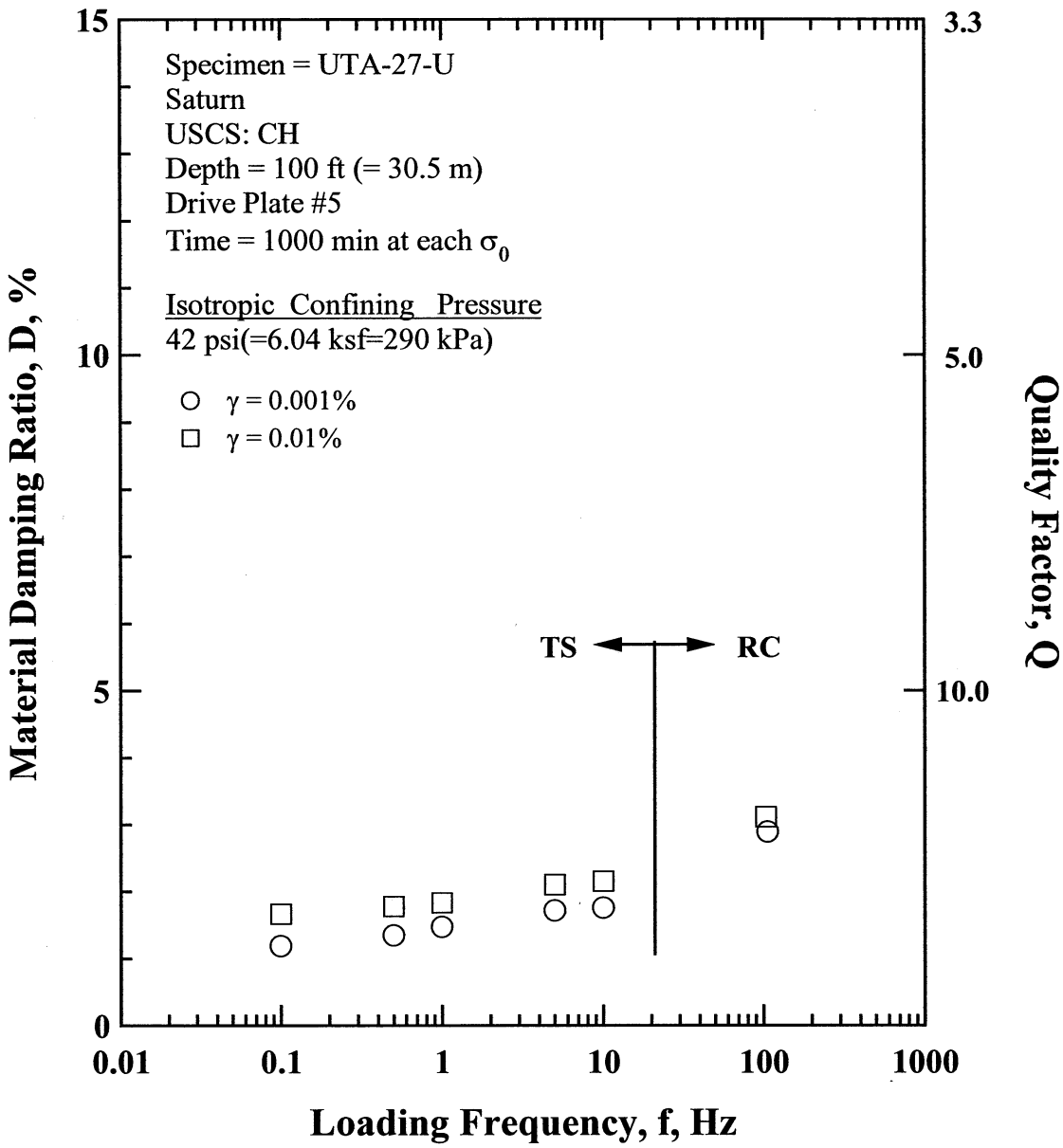

Figure Y.12 Comparison of the Variation in Material Damping Ratio with Loading Frequency at an Isotropic Confining Pressure 42 psi(=6.04 ksf=290 kPa from the Combined RCTS Tests of Specimen UTA-27-U.

Table Y.1 Variation in Low-Amplitude Shear Wave Velocity, Low-Amplitude Shear Modulus, Low-Amplitude Material Damping Ratio and Estimated Void Ratio with Isotropic Confining Pressure from RC Tests of Specimen UTA-27-U

Effective Isotropic Confining Pressure, σ_o'			Low-Amplitude Shear Modulus, G_{max}		Low-Amplitude Shear Wave Velocity, Vs	Low-Amplitude Material Damping Ratio, Dmin	Estimated Void Ratio, e
(psi)	(psf)	(kPa)	(ksf)	(MPa)	(fps)	(%)	
10.0	1440	69	2434	116.7	831	3.69	0.973
21	3024	145	2791	133.8	889	3.12	0.962
42	6048	290	3196	153.2	949	3.02	0.949
84	12096	580	3793	181.8	1032	2.75	0.931

Table Y.2 Variation in Shear Modulus, Normalized Shear Modulus and Material Damping Ratio with Shearing Strain from RC Tests of Specimen UTA-27-U ; Confining Pressure, σ_o' =42 psi (=6.04 ksf=290 kPa).

Peak Shearing Strain, %	Shear Modulus, G, ksf	Normalized Shear Modulus, G/G_{max}	Average^{+} Shearing Strain, %	Material Damping Ratio^{x}, D, %
7.35E-05	3332	1.00	6.18E-05	2.93
1.29E-04	3332	1.00	1.08E-04	2.94
2.70E-04	3332	1.00	2.26E-04	3.02
5.76E-04	3332	1.00	4.82E-04	3.02
1.25E-03	3307	0.99	1.05E-03	2.89
2.39E-03	3276	0.98	2.01E-03	2.90
4.79E-03	3244	0.97	4.05E-03	2.86
9.56E-03	3153	0.95	8.05E-03	2.90
1.75E-02	2973	0.89	1.42E-02	3.56
3.15E-02	2685	0.81	2.41E-02	4.74
4.88E-02	2412	0.72	3.52E-02	5.93
8.22E-02	2004	0.60	5.51E-02	7.49
1.29E-01	1724	0.52	8.21E-02	8.66

$^{+}$ Average Shearing Strain from the First Three Cycles of the Free Vibration Decay Curve

^{x} Average Damping Ratio from the First Three Cycles of the Free Vibration Decay Curve

Table Y.3 Variation in Shear Modulus, Normalized Shear Modulus and Material Damping Ratio with Shearing Strain from TS Tests of Specimen UTA-27-U ; Confining Pressure, σ_o' =42 psi (=6.04 ksf=290 kPa).

First Cycle				Tenth Cycle			
Peak Shearing Strain, %	Shear Modulus, G, ksf	Normalized Shear Modulus, G/G_{max}	Material Damping Ratio, D, %	Peak Shearing Strain, %	Shear Modulus, G, ksf	Normalized Shear Modulus, G/G_{max}	Material Damping Ratio, D, %
3.40E-04	2971	1.01	1.39	3.39E-04	2974	1.01	1.39
6.89E-04	2933	0.99	1.30	6.88E-04	2936	0.99	1.39
1.39E-03	2896	0.98	1.31	1.39E-03	2898	0.98	1.29
2.82E-03	2860	0.97	1.28	2.82E-03	2858	0.97	1.25
5.77E-03	2796	0.95	1.43	5.78E-03	2793	0.95	1.44
1.22E-02	2660	0.90	1.97	1.22E-02	2657	0.90	1.95

APPENDIX Z

Specimen No.25
UT Specimen ID: UTA-27-W

Obregon P-8
Depth = 101ft (=30.8m)
Soil Type: Clay (CH)

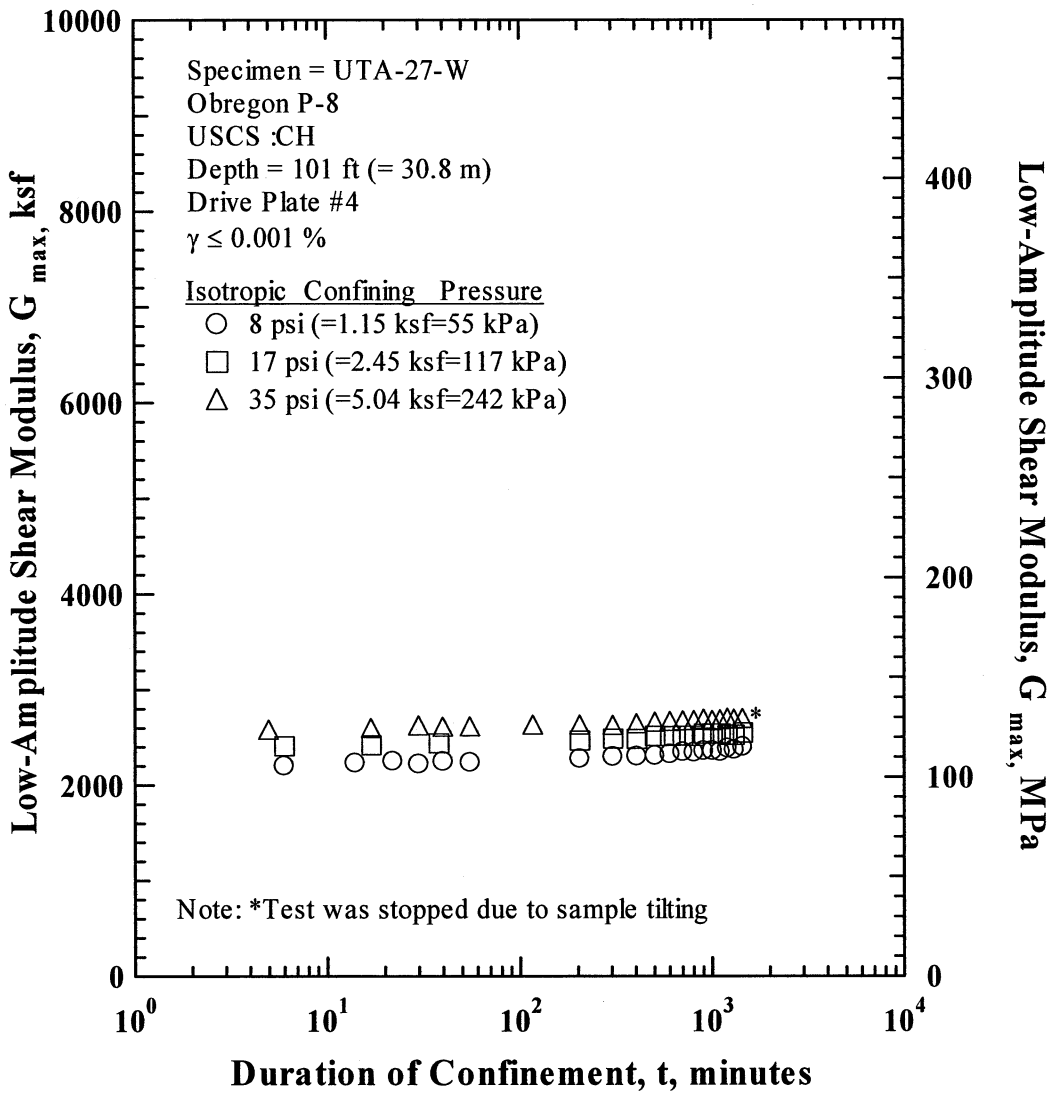

Figure Z.1 Variation in Low-Amplitude Shear Modulus with Magnitude and Duration of Isotropic Confining Pressure from Resonant Column Tests of Specimen UTA-27-W.

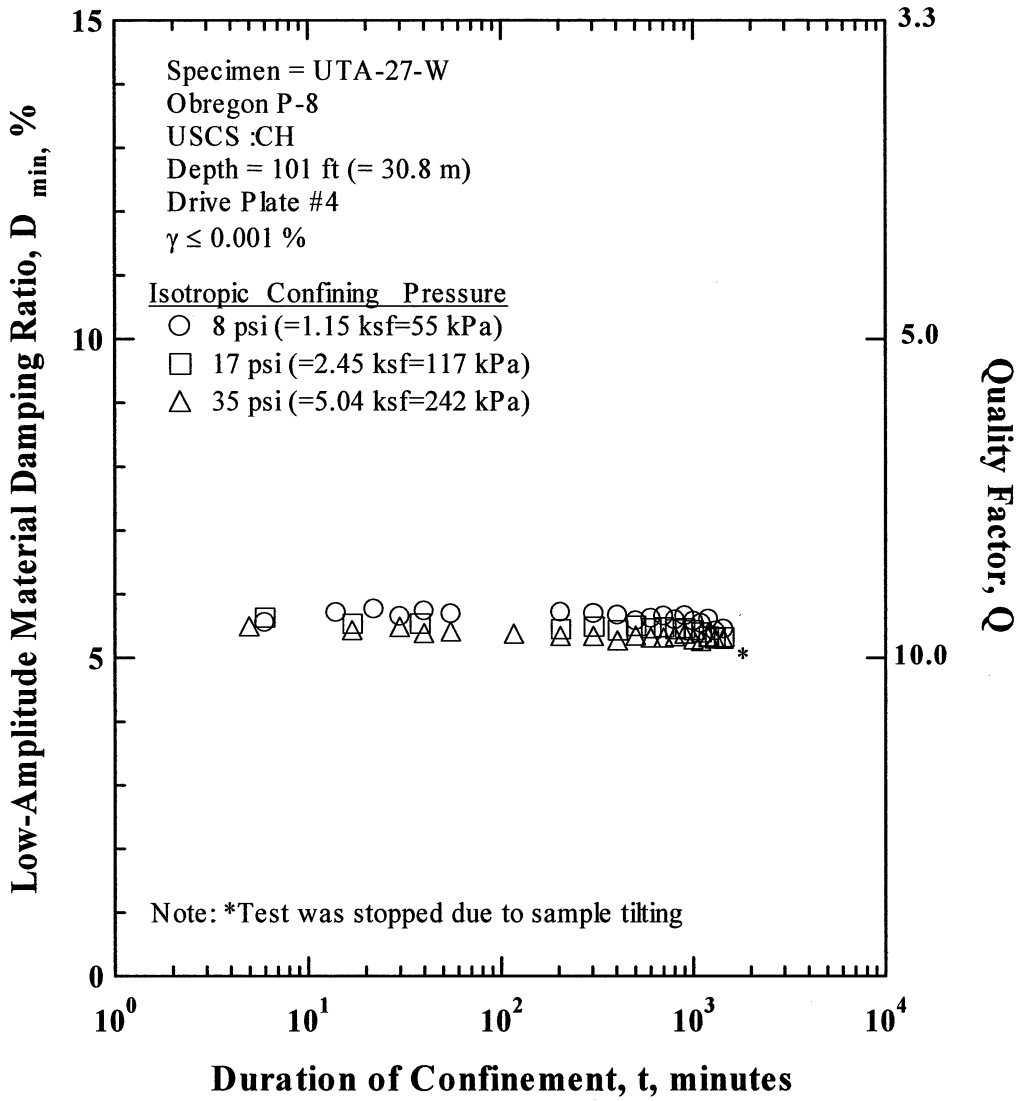

Figure Z.2 Variation in Low-Amplitude Material Damping Ratio with Magnitude and Duration of Isotropic Confining Pressure from Resonant Column Tests of Specimen UTA-27-W

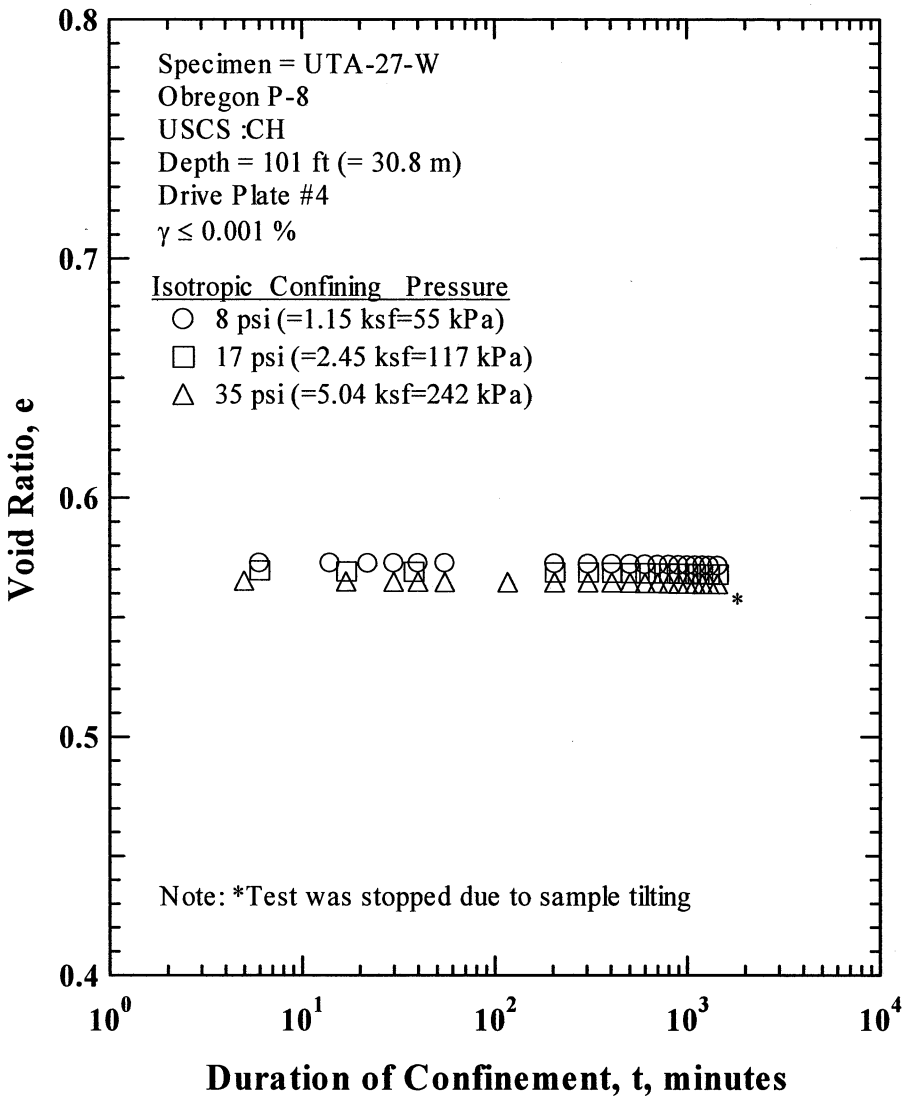

Figure Z.3 Variation in Estimated Void Ratio with Magnitude and Duration of Isotropic Confining Pressure from Resonant Column Tests of Specimen UTA-27-W.

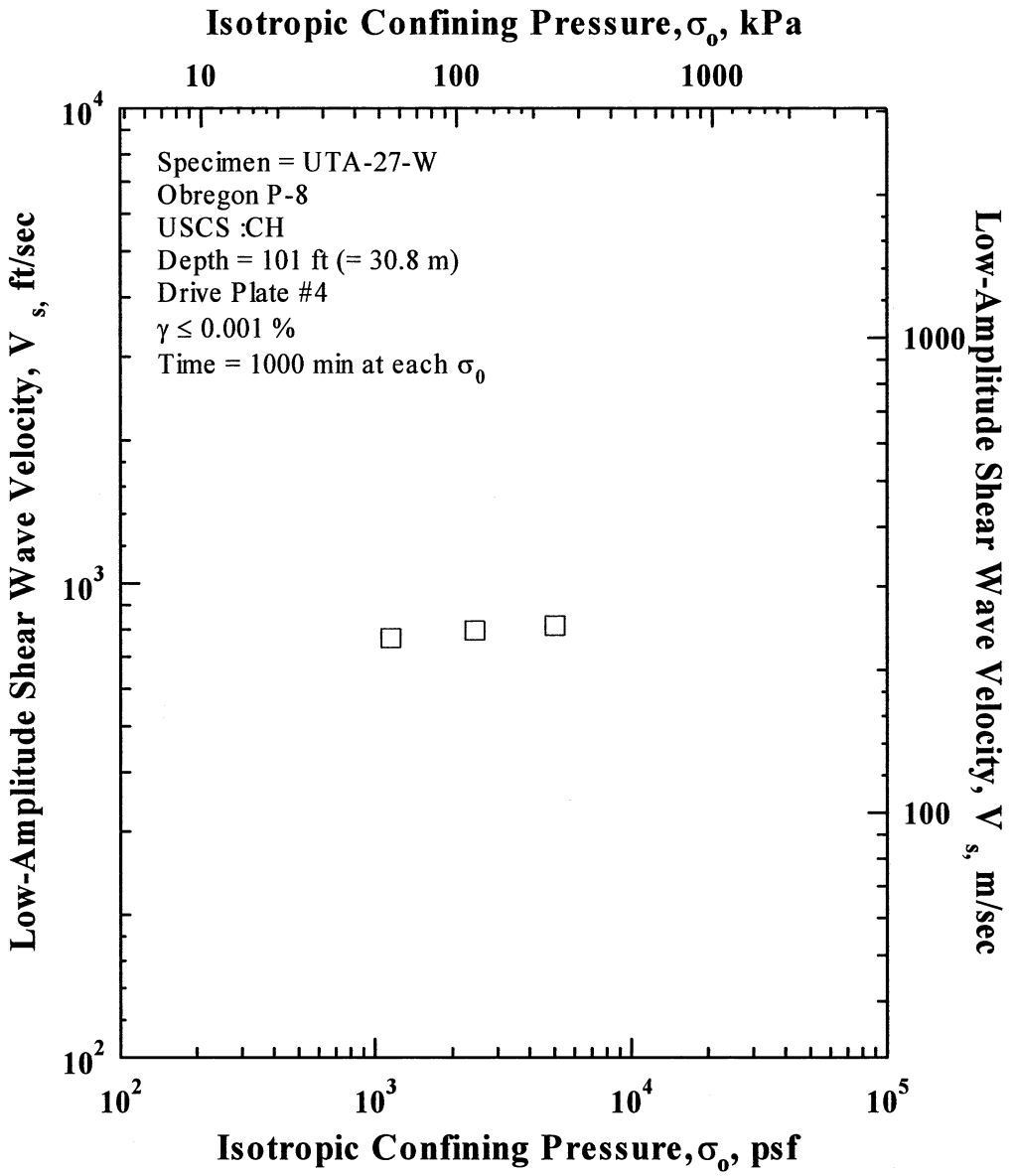

Figure Z.4 Variation in Low-Amplitude Shear Wave Velocity with Isotropic Confining Pressure from Resonant Column Tests of Specimen UTA-27-W.

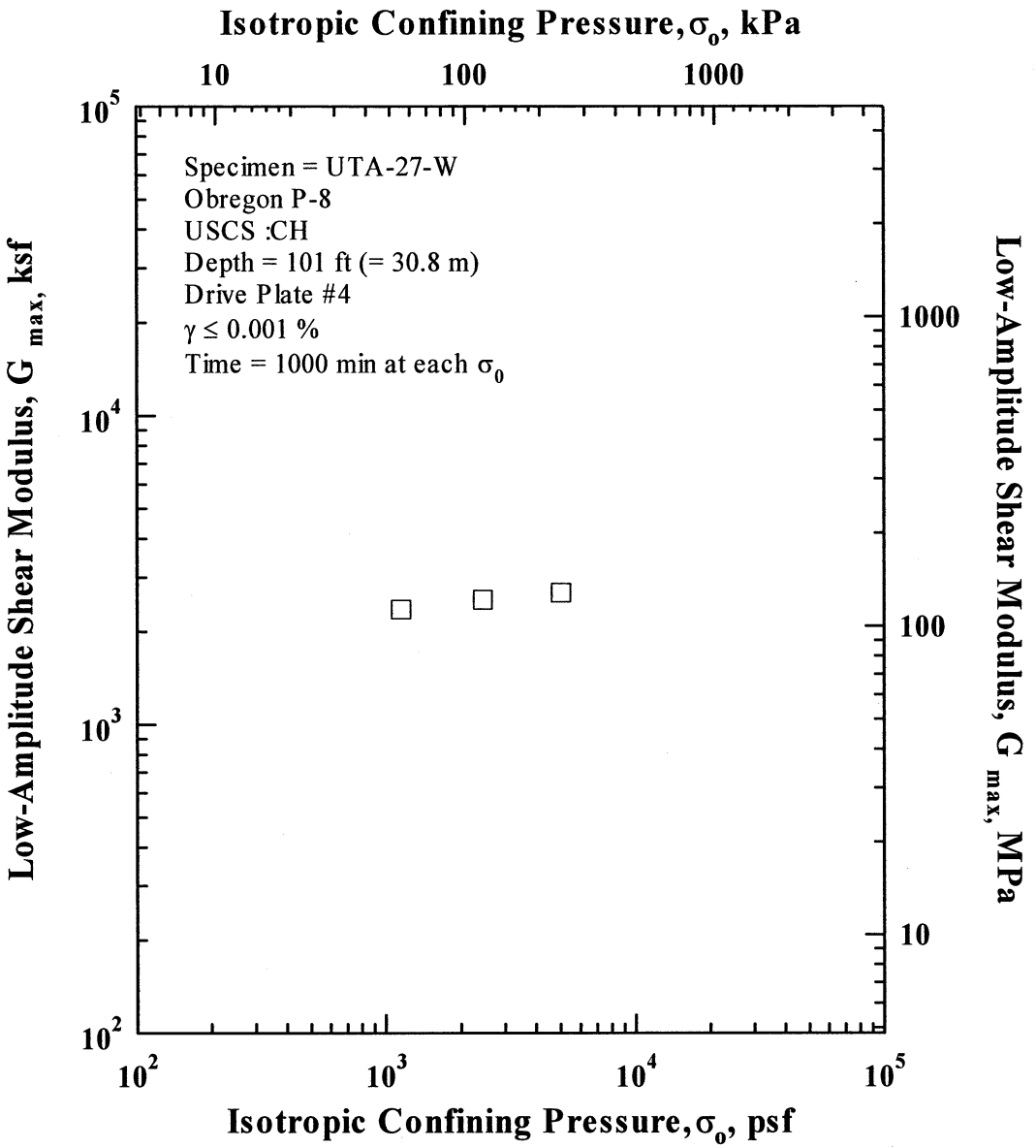

Figure Z.5 Variation in Low-Amplitude Shear Modulus with Isotropic Confining Pressure from Resonant Column Tests of Specimen UTA-27-W.

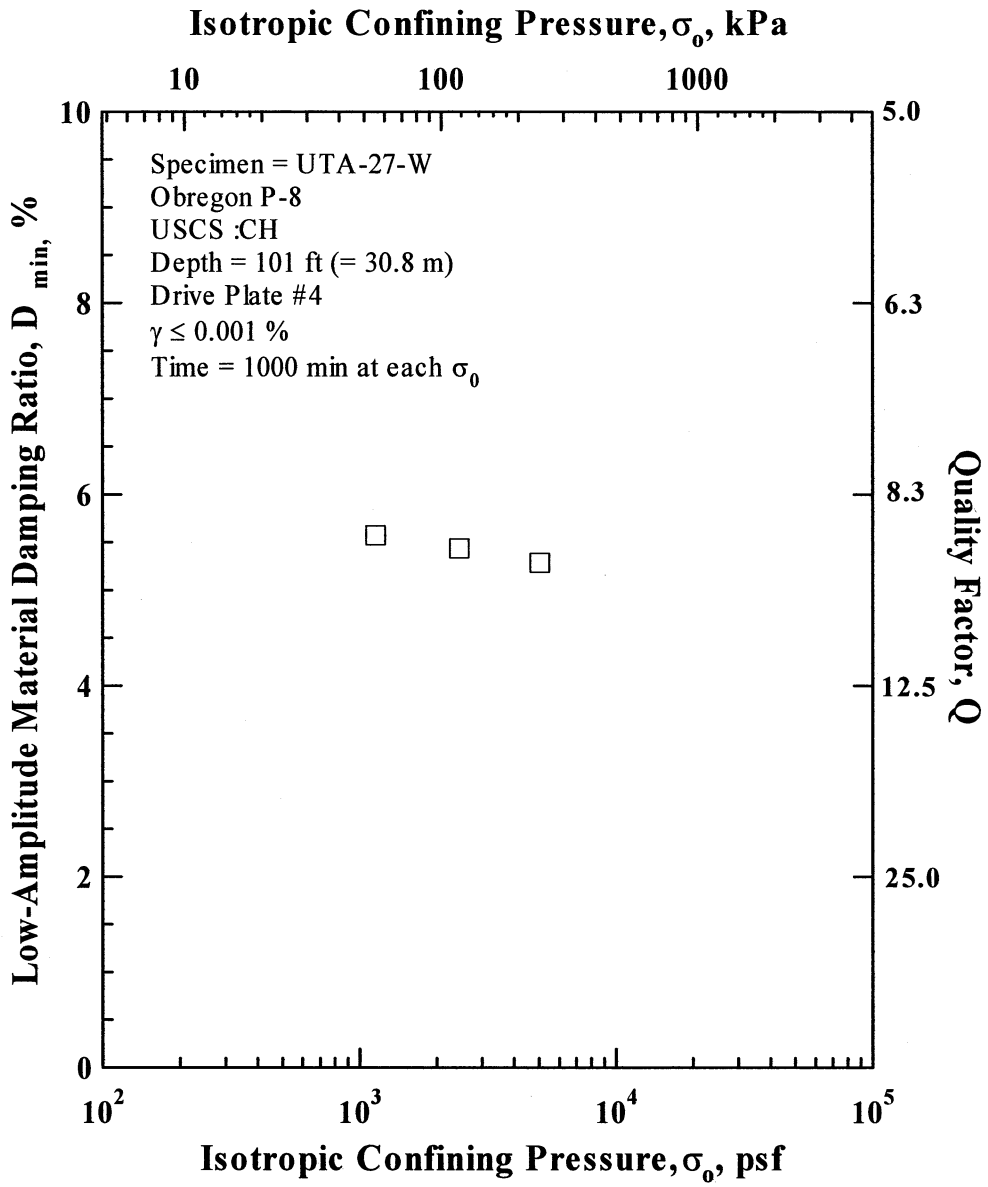

Figure Z.6 Variation in Low-Amplitude Material Damping Ratio with Isotropic Confining Pressure from Resonant Column Tests of Specimen UTA-27-W.

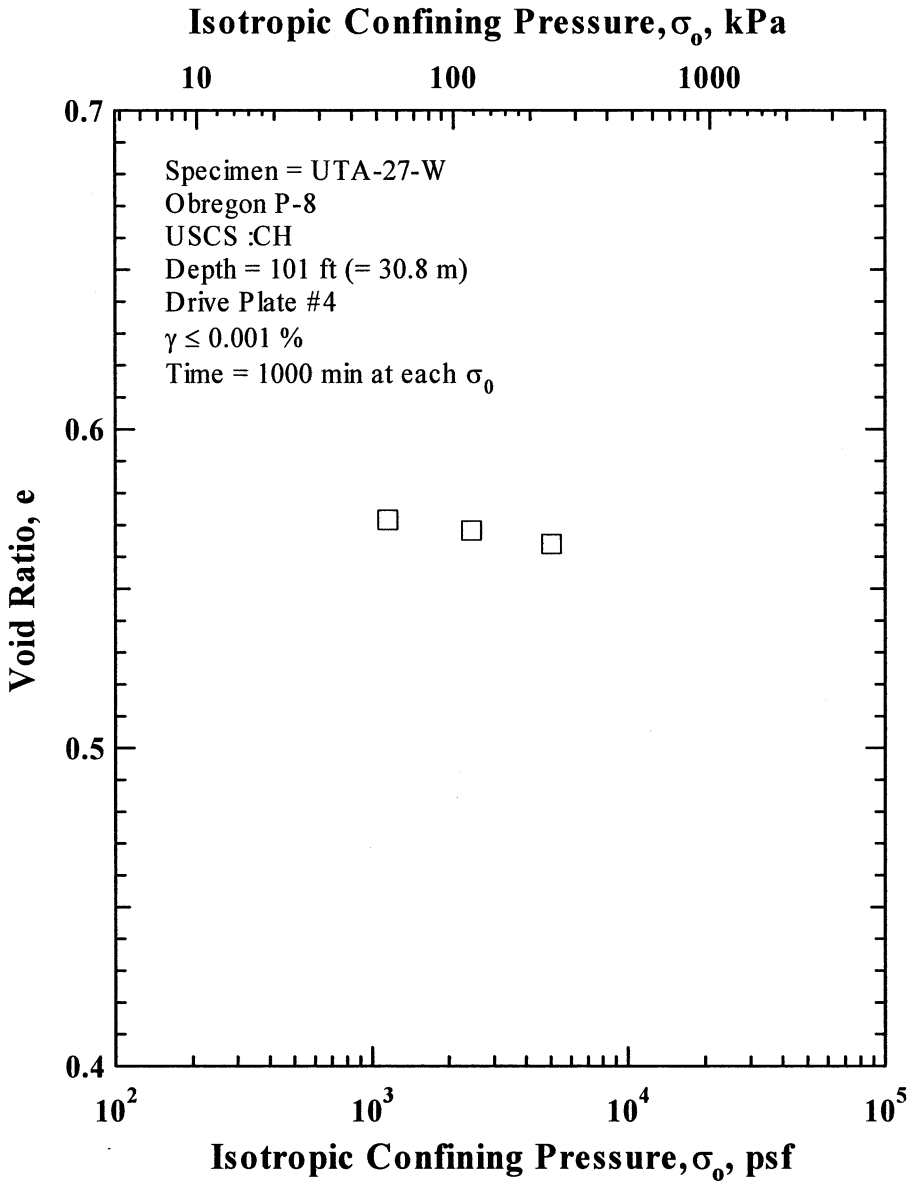

Figure Z.7 Variation in Estimated Void Ratio with Isotropic Confining Pressure from Resonant Column Tests of Specimen UTA-27-W.

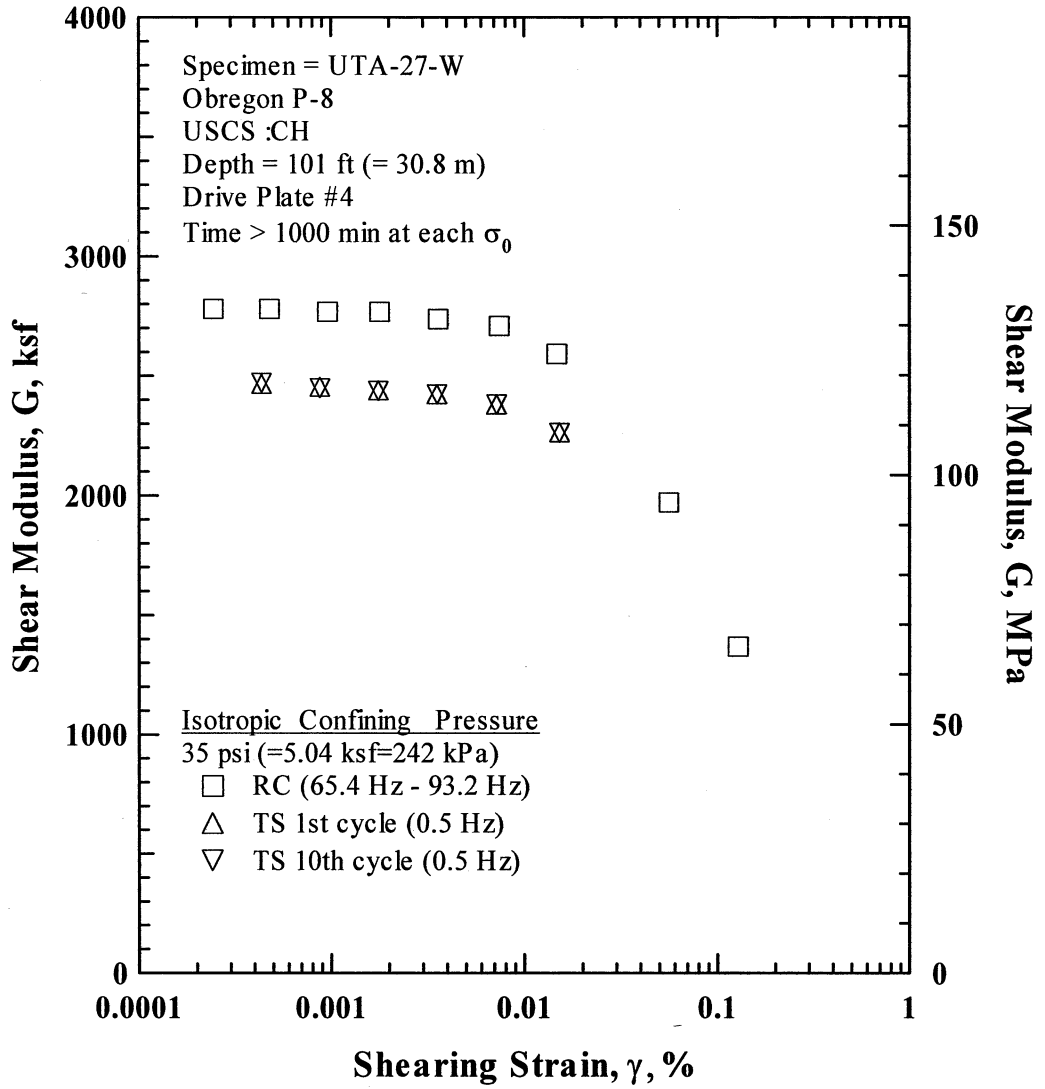

Figure Z.8 Comparison of the Variation in Shear Modulus with Shearing Strain at an Isotropic Confining Pressure of 35 psi (=5.04 ksf=242 kPa) from the Combined RCTS Tests of Specimen UTA-27-W.

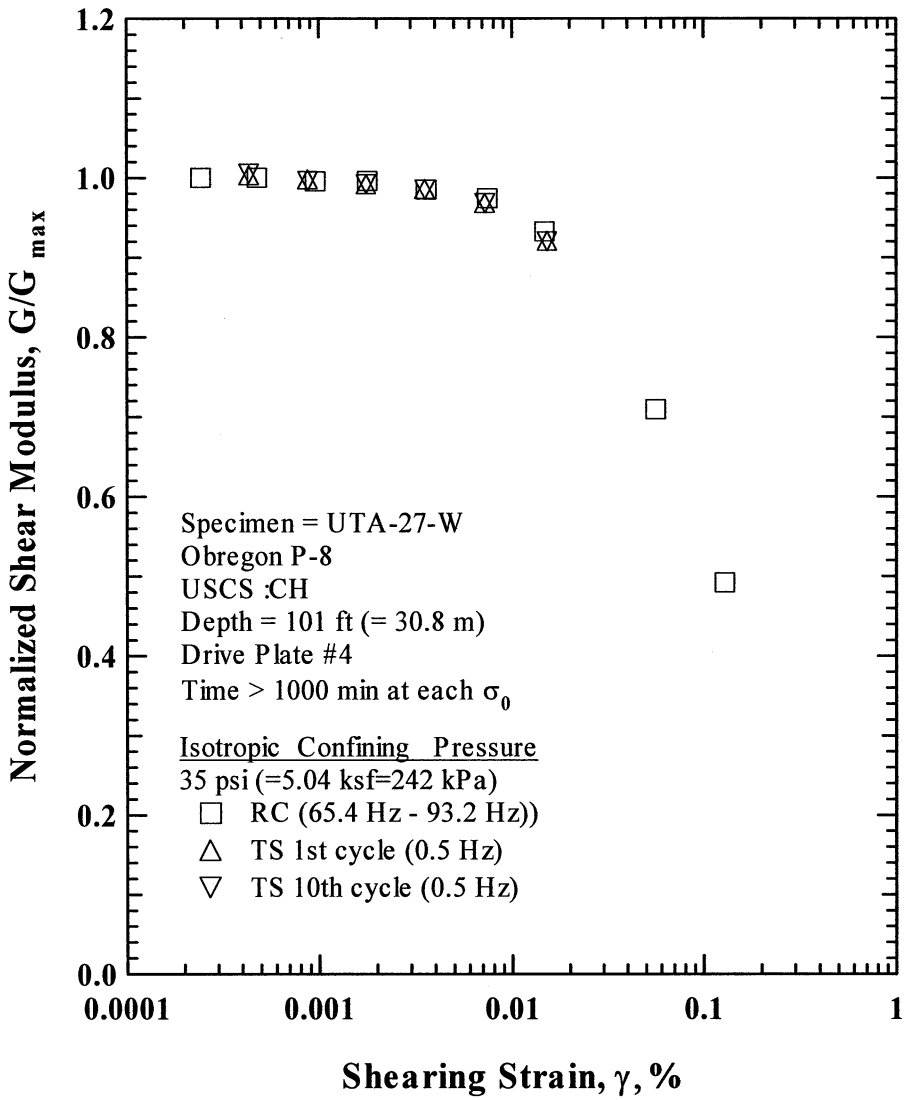

Figure Z.9 Comparison of the Variation in Normalized Shear Modulus with Shearing Strain at an Isotropic Confining Pressure of 35 psi (=5.04 ksf=242 kPa) from the Combined RCTS Tests of Specimen UTA-27-W.

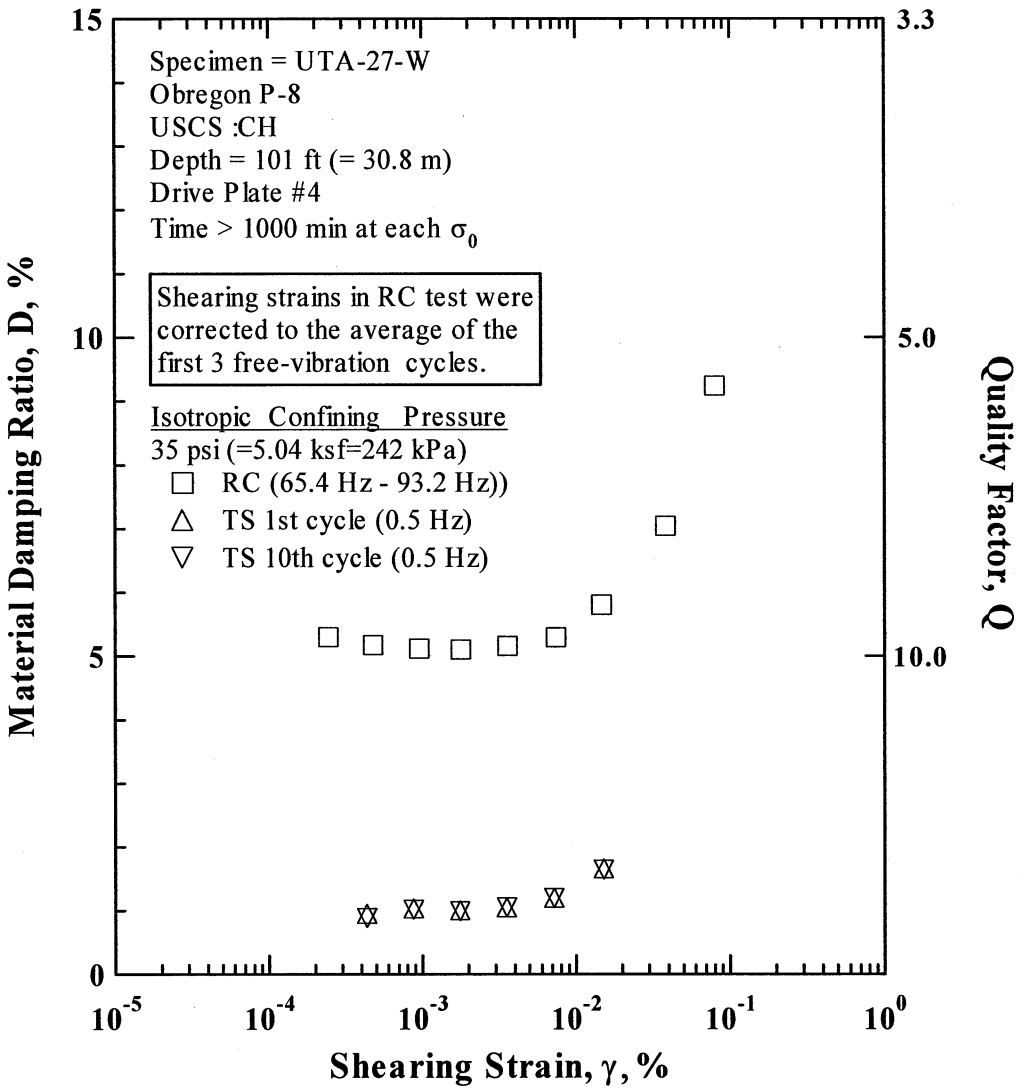

Figure Z.10 Comparison of the Variation in Material Damping Ratio with Shearing Strain at an Isotropic Confining Pressure of 35 psi (=5.04 ksf=242 kPa) from the Combined RCTS Tests of Specimen UTA-27-W.

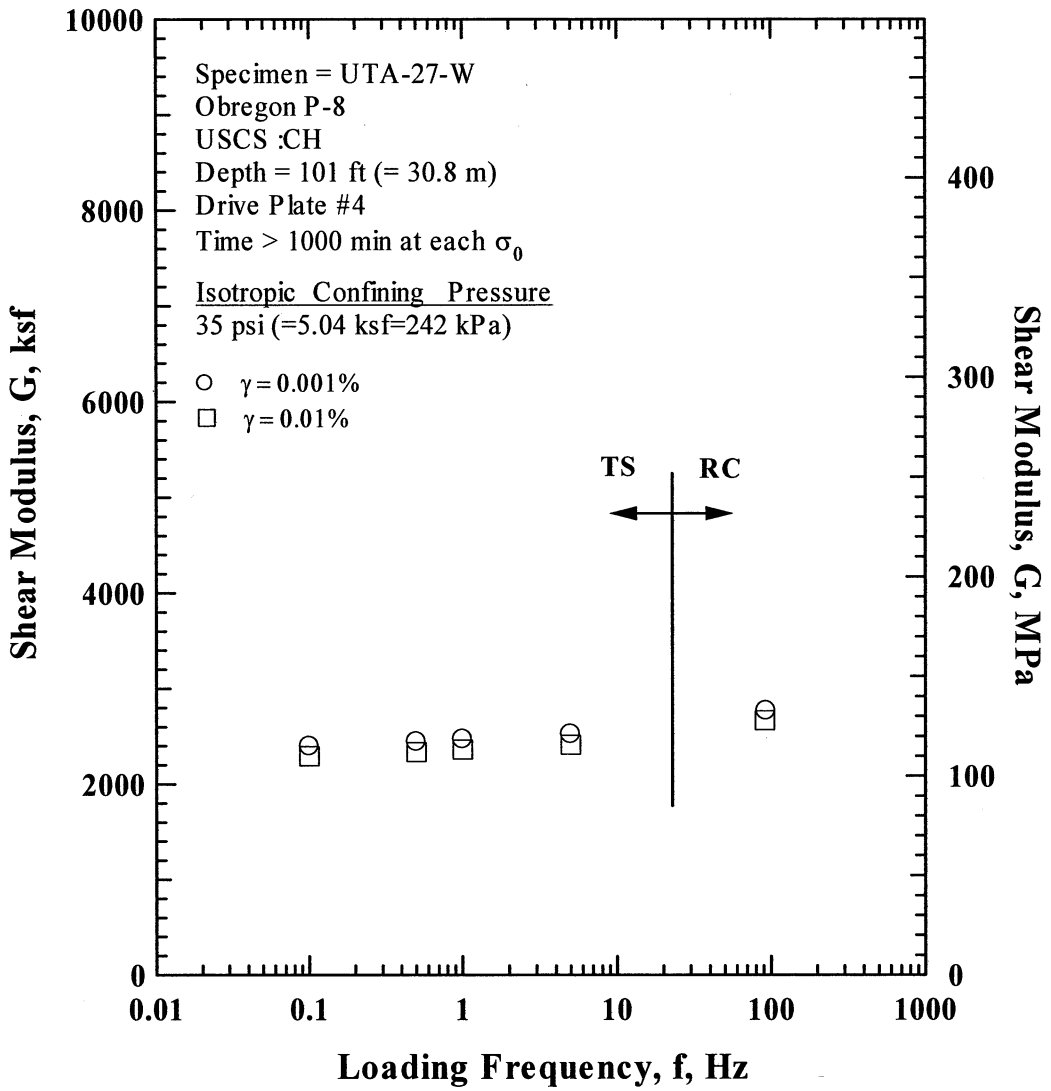

Figure Z.11 Comparison of the Variation in Shear Modulus with Loading Frequency at an Isotropic Confining Pressure of 35 psi (=5.04 ksf=242 kPa) from the Combined RCTS Tests of Specimen UTA-27-W.

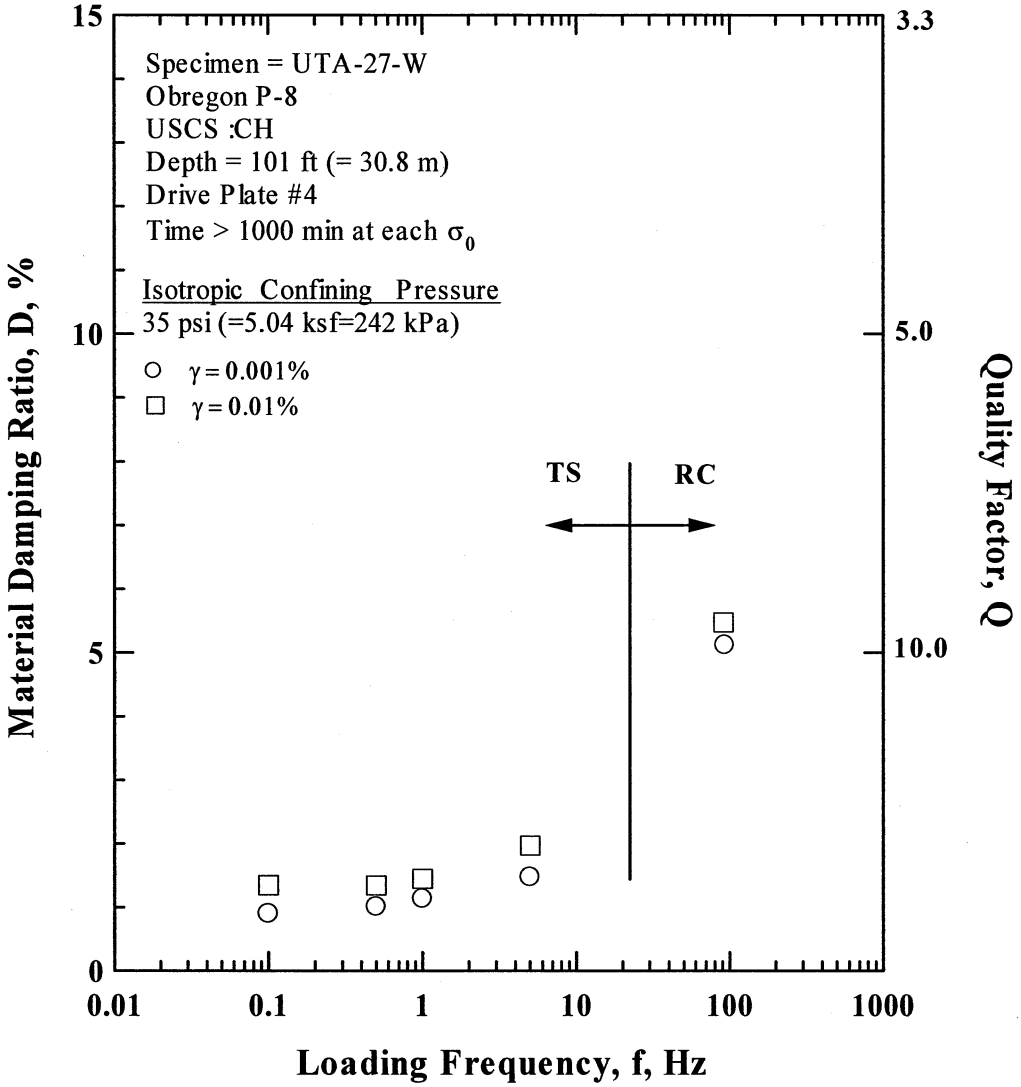

Figure Z.12 Comparison of the Variation in Material Damping Ratio with Loading Frequency at an Isotropic Confining Pressure 35 psi (=5.04 ksf=242 kPa) from the Combined RCTS Tests of Specimen UTA-27-W.

Table Z.1 Variation in Low-Amplitude Shear Wave Velocity, Low-Amplitude Shear Modulus, Low-Amplitude Material Damping Ratio and Estimated Void Ratio with Isotropic Confining Pressure from RC Tests of Specimen UTA-27-W.

Effective Isotropic Confining Pressure, σ_o'			Low-Amplitude Shear Modulus, G_{max}		Low-Amplitude Shear Wave Velocity, Vs	Low-Amplitude Material Damping Ratio, Dmin	Estimated Void Ratio, e
(psi)	(psf)	(kPa)	(ksf)	(MPa)	(fps)	(%)	
8	1152	55	2358	113.0	766	5.57	0.572
17	2448	117	2539	121.7	795	5.44	0.568
35	5040	242	2676	128.3	815	5.29	0.564

Table Z.2 Variation in Shear Modulus, Normalized Shear Modulus and Material Damping Ratio with Shearing Strain from RC Tests of Specimen UTA-27-W; Confining Pressure, σ_o' =35 psi (=5.04 ksf=242 kPa).

Peak Shearing Strain, %	Shear Modulus, G, ksf	Normalized Shear Modulus, G/G_{max}	Average^{+} Shearing Strain, %	Material Damping Ratio^{x}, D, %
2.44E-04	2779	1.00	2.44E-04	5.30
4.78E-04	2779	1.00	4.78E-04	5.17
9.58E-04	2767	1.00	9.58E-04	5.12
1.78E-03	2768	1.00	1.78E-03	5.10
3.59E-03	2738	0.99	3.59E-03	5.16
7.42E-03	2708	0.97	7.42E-03	5.30
1.47E-02	2592	0.93	1.47E-02	5.80
5.61E-02	1971	0.71	3.84E-02	7.04
1.28E-01	1368	0.49	7.99E-02	9.24

$^{+}$ Average Shearing Strain from the First Three Cycles of the Free Vibration Decay Curve

^{x} Average Damping Ratio from the First Three Cycles of the Free Vibration Decay Curve

Table Z.3 Variation in Shear Modulus, Normalized Shear Modulus and Material Damping Ratio with Shearing Strain from TS Tests of Specimen UTA-27-W; Confining Pressure, σ_o' =35 psi (=5.04 ksf=242 kPa).

First Cycle				Tenth Cycle			
Peak Shearing Strain, %	Shear Modulus, G, ksf	Normalized Shear Modulus, G/G_{max}	Material Damping Ratio, D, %	Peak Shearing Strain, %	Shear Modulus, G, ksf	Normalized Shear Modulus, G/G_{max}	Material Damping Ratio, D, %
4.37E-04	2464	1.00	0.94	4.37E-04	2468	1.00	0.88
8.80E-04	2452	1.00	1.03	8.82E-04	2446	1.00	1.01
1.77E-03	2438	0.99	1.00	1.77E-03	2436	0.99	0.98
3.56E-03	2422	0.99	1.04	3.56E-03	2420	0.98	1.04
7.24E-03	2379	0.97	1.19	7.25E-03	2378	0.97	1.19
1.53E-02	2262	0.92	1.65	1.53E-02	2260	0.92	1.64